PRINCIPLES of CLINICAL PHARMACOLOGY

SECOND EDITION

Arthur J. Atkinson, Jr., Darrell R. Abernethy,
Charles E. Daniels, Robert L. Dedrick
and Sanford P. Markey

PRINCIPLES OF CLINICAL PHARMACOLOGY

Second Edition

This page intentionally left blank

PRINCIPLES OF CLINICAL PHARMACOLOGY

Second Edition

Arthur J. Atkinson Jr., M.D.
NIH Clinical Center
Bethesda, MD 20892-1165

Darrell R. Abernethy, M.D., Ph.D.
National Institute on Aging
Geriatric Research Center
Laboratory of Clinical Investigation
Baltimore, MD 21224

Charles E. Daniels, R.Ph., Ph.D., FASHP
Skaggs School of Pharmacy and
Pharmaceutical Sciences
University of California, San Diego
San Diego, CA 92093-0657

Robert L. Dedrick, Ph.D.
Office of Research Services, OD, NIH
Division of Bioengineering and Physical Sciences
Bethesda, MD 20892

Sanford P. Markey, Ph.D.
National Institute of Mental Health, NIH
Laboratory of Neurotoxicology
Bethesda, MD 20892

ELSEVIER

Amsterdam • Boston • Heidelberg • London • New York
Oxford • Paris • San Diego • San Francisco • Singapore
Sydney • Tokyo

Academic Press is an imprint of Elsevier

Academic Press is an imprint of Elsevier
30 Corporate Drive, Suite 400, Burlington, MA 01803, USA
525 B Street, Suite 1900, San Diego, California 92101-4495, USA
84 Theobald's Road, London WC1X 8RR, UK

This book is printed on acid-free paper.

Library of Congress Cataloging-in-Publication Data
Application Submitted

British Library Cataloguing-in-Publication Data
A catalogue record for this book is available from the British Library.

ISBN 13: 978–0–12–369417–1
ISBN 10: 0–12–369417–5

For information on all Academic Press publications
visit our Web site at www.books.elsevier.com

Printed in the United States of America
06 07 08 09 10 9 8 7 6 5 4 3 2 1

Contents

This page intentionally left blank

Preface to the First Edition

The rate of introduction of new pharmaceutical products has increased rapidly over the past decade, and details learned about a particular drug become obsolete as it is replaced by newer agents. For this reason, we have chosen to focus this book on the principles that underlie the clinical use and contemporary development of pharmaceuticals. It is assumed that the reader will have had an introductory course in pharmacology and also some understanding of calculus, physiology and clinical medicine.

This book is the outgrowth of an evening course that has been taught for the past three years at the NIH Clinical Center[1]. Wherever possible, individuals who have lectured in the course have contributed chapters corresponding to their lectures. The organizers of this course are the editors of this book and we also have recruited additional experts to assist in the review of specific chapters. We also acknowledge the help of William A. Mapes in preparing much of the artwork. Special thanks are due Donna Shields, Coordinator for the ClinPRAT training program at NIH, whose attention to myriad details has made possible both the successful conduct of our evening course and the production of this book. Finally, we were encouraged and patiently aided in this undertaking by Robert M. Harington and Aaron Johnson at Academic Press.

[1] The lecture schedule and syllabus material for the current edition of the course are available on the Internet at: http://www.cc.nih.gov/ccc/principles

Preface to the Second Edition

Five years have passed since the first edition of *Principles of Clinical Pharmacology* was published. The second edition remains focused on the principles underlying the clinical use and contemporary development of pharmaceuticals. However, recent advances in the areas of pharmacogenetics, membrane transport, and biotechnology and in our understanding of the pathways of drug metabolism, mechanisms of enzyme induction, and adverse drug reactions have warranted the preparation of this new edition.

We are indebted to the authors from the first edition who have worked to update their chapters, but are sad to report that Mary Berg, author of the chapter on Pharmacological Differences between Men and Women, died on October 1, 2004. She was an esteemed colleague and effective advocate for studying sex differences in pharmacokinetics and pharmacodynamics. Fortunately, new authors have stepped in to prepare new versions of some chapters and to strengthen others. As with the first edition, most of the authors are lecturers in the evening course that has been taught for the past eight years at the National Institutes of Health (NIH) Clinical Center[1].

We also acknowledge the help of Cepha Imaging Pvt. Ltd. in preparing the new artwork that appears in this edition. Special thanks are due Donna Shields, Coordinator for the ClinPRAT training program at NIH, who has provided invaluable administrative support for both the successful conduct of our evening course and the production of this book. Finally, we are indebted to Tari Broderick, Keri Witman, Renske van Dijk, and Carl M. Soares at Elsevier for their help in bringing this undertaking to fruition.

[1] Videotapes and slide handouts for the NIH course are available on the Internet at: http://www.cc.nih.gov/ccc/principles and DVDs of the lectures also can be obtained from the American Society for Clinical Pharmacology and Therapeutics (Internet at http://www.ascpt.org/education/).

This page intentionally left blank

Contributors

Darrell R. Abernethy
National Institute on Aging
Geriatric Research Center
Laboratory of Clinical Investigation
Baltimore, MD 21224

Arthur J. Atkinson, Jr.
NIH Clinical Center
Bethesda, MD 20892-1165

Frank Balis
National Cancer Institute, NIH
Pharmacology and Experimental
Therapeutics Section
Bethesda, MD 20892

Mary J. Berg
Deceased

Leif Bertilsson
Karolinska Institutet
Department of Clinical Pharmacology
Karolinska University Hospital - Huddinge
S141 86 Stockholm
Sweden

Joseph S. Bertino, Jr.
Ordway Research Institute
Albany, NY 12208

Karim Anton Calis
NIH Clinical Center
Bethesda, MD 20892

Maylee Chen
Ordway Research Institute
Albany, NY 12208

Jerry M. Collins
Developmental Therapeutics Program
Division of Cancer Treatment and
Diagnosis
National Cancer Institute
Rockville, MD 20852

Charles E. Daniels
Skaggs School of Pharmacy and
Pharmaceutical Sciences
University of California, San Diego
San Diego, CA 92093-0657

Shannon Decker
Health Program Director
Greenebaum Cancer Center
University of Maryland
Baltimore, MD 21201-1595

Robert L. Dedrick
Office of Research Services, OD, NIH
Division of Bioengineering and
Physical Sciences
Bethesda, MD 20892

Marilynn C. Frederiksen
Northwestern University. School of Medicine
Department of Obstetrics and Gynecology
Chicago, IL 60611

David A. Flockhart
Professor of Medicine, Genetics and
Pharmacology
Division of Clinical Pharmacology
Indiana University School of Medicine
Indianapolis, IN 46250

David M. Foster
Seattle, WA 98112

Elizabeth Fox
Pharmacology and Experimental Therapeutics Section
Pediatric Oncology Branch
Bethesda, MD 20892

Pamela D. Garzone
Telik, Inc.
Drug Metabolism and Pharmacokinetics
Los Altos, CA 94024

Charles V. Grudzinskas
Center for Drug Development Science
University of California, San Francisco;
UC Washington Center
Washington, DC 20036

Nicholas H.G. Holford
University of Auckland
Department of Pharmacology and Clinical Pharmacology
School of Medicine
Grafton, Auckland
New Zealand

Lawrence J. Lesko
Food and Drug Administration
Office of Clinical Pharmacology and Biopharmaceuticals, CDER
Rockville, MD 20857

Sanford P. Markey
National Institute of Mental Health, NIH
Laboratory of Neurotoxicology
Bethesda, MD 20892

Raymond Miller
Pfizer Inc.
Ann Arbor Laboratories
Global Research and Development
Ann Arbor, MI 48105

Paul F. Morrison
Office of Research Services, OD, NIH
Division of Bioengineering and Physical Sciences
Bethesda, MD 20892

Diane R. Mould
Projections Research, Inc.
Phoenixville, PA 19460

Anne N. Nafziger
Ordway Research Institute
Albany, NY 12208

Carl C. Peck
Center for Drug Development Science
University of California, San Francisco, CA;
UC Washington Center
Washington, DC 20036

Scott R. Penzak
NIH Clinical Center
Clinical Pharmacokinetics Research Lab.
NIH Clinical Center Pharmacy Department
Bethesda, MD 20892

Peter C. Preusch
National Institute of General Medical Sciences, NIH
Pharmacology, Physiology and Biological Chemistry Division
Bethesda, MD 20892-6200

Marcus M. Reidenberg
Scarsdale, NY 10583

Sarah M. Robertson
NIH Clinical Center
Pharmacy Department
Bethesda, MD 20892

Paul Edward Rolan
Department of Clinical and Experimental Pharmacology
Medical School
University of Adelaide SA 5005
Australia
ICON - Medeval
Clinical Pharmacology
Manchester Science Park, Manchester
United Kingdom

Chandrahas G. Sahajwalla
Food and Drug Administration
Office of Clinical Pharmacology and Biopharmaceuticals, CDER
Rockville, MD 20857

Edward A. Sausville
Associate Director for Clinical Research
Greenebaum Cancer Center
University of Maryland
Baltimore, MD 21201-1595

Emil N. Sidawy
Shady Grove Adventist Hospital
Rockville, Maryland

Elizabeth Soyars Lowe
AstraZeneca Pharmaceuticals
Wilmington, DE 19850

Catherine S. Stika
Northwestern Un. School of Medicine
Chicago, IL 60611

Gregory M. Susla
VHA Consulting Services, Inc.
Frederick, MD 21704

Chris H. Takimoto
Institute for Drug Development
Cancer Therapy and Research Center
San Antonio, TX 78245-3217

Michael J. Wick
Institute for Drug Development
Cancer Therapy and Research
Center
San Antonio, TX 78245-3217

Lind R. Young
Department of Pharmacy Services
Carilion Medical Center
Roanoke, Virginia

This page intentionally left blank

CHAPTER

1

Introduction to Clinical Pharmacology

ARTHUR J. ATKINSON, JR.
Clinical Center, National Institutes of Health, Bethesda, Maryland

Fortunately a surgeon who uses the wrong side of the scalpel cuts his own fingers and not the patient; if the same applied to drugs they would have been investigated very carefully a long time ago.

Rudolph Bucheim
Beitrage zur Arzneimittellehre, 1849 (1)

BACKGROUND

Clinical pharmacology can be defined as the study of drugs in humans. Clinical pharmacology often is contrasted with basic pharmacology. Yet *applied* is a more appropriate antonym for *basic* (2). In fact, many basic problems in pharmacology can only be studied in humans. This text will focus on the basic principles of clinical pharmacology. Selected applications will be used to illustrate these principles, but no attempt will be made to provide an exhaustive coverage of applied therapeutics. Other useful supplementary sources of information are listed at the end of this chapter.

Leake (3) has pointed out that pharmacology is a subject of ancient interest but is a relatively new science. Reidenberg (4) subsequently restated Leake's listing of the fundamental problems with which the science of pharmacology is concerned:

1. The relationship between dose and biological effect.
2. The localization of the site of action of a drug.
3. The mechanism(s) of action of a drug.
4. The absorption, distribution, metabolism, and excretion of a drug.
5. The relationship between chemical structure and biological activity.

These authors agree that pharmacology could not evolve as a scientific discipline until modern chemistry provided the chemically pure pharmaceutical products that are needed to establish a quantitative relationship between drug dosage and biological effect.

Clinical pharmacology has been termed a bridging discipline because it combines elements of classical pharmacology with clinical medicine. The special competencies of individuals trained in clinical pharmacology have equipped them for productive careers in academia, the pharmaceutical industry, and governmental agencies, such as the National Institutes of Health (NIH) and the Food and Drug Administration (FDA). Reidenberg (4) has pointed out that clinical pharmacologists are concerned both with the optimal use of existing medications and with the scientific study of drugs in humans. The latter area includes both evaluation of the safety and efficacy of currently available drugs and development of new and improved pharmacotherapy.

Optimizing Use of Existing Medicines

As the opening quote indicates, the concern of pharmacologists for the safe and effective use of medicine can be traced back at least to Rudolph Bucheim (1820–1879), who has been credited with

establishing pharmacology as a laboratory-based discipline (1). In the United States, Harry Gold and Walter Modell began in the 1930s to provide the foundation for the modern discipline of clinical pharmacology (5). Their accomplishments include the invention of the double-blind design for clinical trials (6), the use of effect kinetics to measure the absolute bioavailability of digoxin and characterize the time course of its chronotropic effects (7), and the founding of *Clinical Pharmacology and Therapeutics.*

Few drugs have focused as much public attention on the problem of adverse drug reactions as did thalidomide, which was first linked in 1961 to catastrophic outbreaks of phocomelia by Lenz in Germany and McBride in Australia (8). Although thalidomide had not been approved at that time for use in the United States, this tragedy prompted passage in 1962 of the Harris–Kefauver Amendments to the Food, Drug, and Cosmetic Act. This act greatly expanded the scope of the FDA's mandate to protect the public health. The thalidomide tragedy also provided the major impetus for developing a number of NIH-funded academic centers of excellence that have shaped contemporary clinical pharmacology in this country. These U.S. centers were founded by a generation of vigorous leaders, including Ken Melmon, Jan Koch-Weser, Lou Lasagna, John Oates, Leon Goldberg, Dan Azarnoff, Tom Gaffney, and Leigh Thompson. Collin Dollery and Folke Sjöqvist established similar programs in Europe. In response to the public mandate generated by the thalidomide catastrophe, these leaders quickly reached consensus on a number of theoretically preventable causes that contribute to the high incidence of adverse drug reactions (5). These causes include the following failures of approach:

1. Inappropriate polypharmacy.
2. Failure of prescribing physicians to establish and adhere to clear therapeutic goals.
3. Failure of medical personnel to attribute new symptoms or changes in laboratory test results to drug therapy.
4. Lack of priority given to the scientific study of adverse drug reaction mechanisms.
5. General ignorance of basic and applied pharmacology and therapeutic principles.

The important observations also were made that, unlike the teratogenic reactions caused by thalidomide, most adverse reactions encountered in clinical practice occurred with commonly used, rather than newly introduced, drugs, and were dose related, rather than idiosyncratic (9, 10).

Recognition of the considerable variation in response of patients treated with standard drug doses provided the impetus for the development of laboratory methods to measure drug concentrations in patient blood samples (10). The availability of these measurements also made it possible to apply pharmacokinetic principles to routine patient care. Despite these advances, *serious adverse drug reactions* (defined as those adverse drug reactions that require or prolong hospitalization, are permanently disabling, or result in death) have been estimated to occur in 6.7% of hospitalized patients (11). Although this figure has been disputed, the incidence of adverse drug reactions probably is still higher than is generally recognized (12). In addition, the majority of these adverse reactions continue to be caused by drugs that have been in clinical use for a substantial period of time (5).

The fact that most adverse drug reactions occur with commonly used drugs focuses attention on the last of the preventable causes of these reactions: the training that prescribing physicians receive in pharmacology and therapeutics. Bucheim's comparison of surgery and medicine is particularly apt in this regard (5). Most U.S. medical schools provide their students with only a single course in pharmacology that traditionally is part of the second-year curriculum, when students lack the clinical background that is needed to support detailed instruction in therapeutics. In addition, Sjöqvist (13) has observed that most academic pharmacology departments have lost contact with drug development and pharmacotherapy. As a result, students and residents acquire most of their information about drug therapy in a haphazard manner from colleagues, supervisory house staff and attending physicians, pharmaceutical sales representatives, and whatever independent reading they happen to do on the subject. This unstructured process of learning pharmacotherapeutic technique stands in marked contrast to the rigorously supervised training that is an accepted part of surgical training, in which instantaneous feedback is provided whenever a retractor, let alone a scalpel, is held improperly.

Evaluation and Development of Medicines

Clinical pharmacologists have made noteworthy contributions to the evaluation of existing medicines and development of new drugs. In 1932, Paul Martini published a monograph entitled *Methodology of Therapeutic Investigation* that summarized his experience in scientific drug evaluation and probably entitles him to be considered the "first clinical pharmacologist" (14). Martini described the use of placebos, control groups, stratification, rating scales, and the "n of 1" trial design, and emphasized the need to estimate the adequacy of sample size and to establish

baseline conditions before beginning a trial. He also introduced the term "clinical pharmacology." Gold (6) and other academic clinical pharmacologists also have made important contributions to the design of clinical trials. More recently, Sheiner (15) outlined a number of improvements that continue to be needed in the use of statistical methods for drug evaluation, and asserted that clinicians must regain control over clinical trials in order to ensure that the important questions are being addressed.

Contemporary drug development is a complex process that is conventionally divided into preclinical research and development and a number of clinical development phases, as shown in Figure 1.1 for drugs licensed by the United States Food and Drug Administration (16). After a drug candidate is identified and put through *in vitro* screens and animal testing, an Investigational New Drug application (IND) is submitted to the FDA. When the IND is approved, Phase I clinical development begins with a limited number of studies in healthy volunteers or patients. The goal of these studies is to establish a range of tolerated doses and to characterize the drug candidate's pharmacokinetic properties and initial toxicity profile. If these results warrant further development of the compound, short-term Phase II studies are conducted in a selected group of patients to obtain evidence of therapeutic efficacy and to explore patient therapeutic and toxic responses to several dose regimens. These dose-response relationships are used to design longer Phase III trials to confirm therapeutic efficacy and document safety in a larger patient population. The material obtained during preclinical and clinical development is then incorporated in a New Drug Application (NDA) that is submitted to the FDA for review. The FDA may request clarification of study results or further studies before the NDA is approved and the drug can be marketed. Adverse drug reaction monitoring and reporting is mandated after NDA approval. Phase IV studies conducted after NDA approval, may include studies to support FDA licensing for additional therapeutic indications or "over-the-counter" (OTC) sales directly to consumers.

Although the expertise and resources needed to develop new drugs is primarily concentrated in the pharmaceutical industry, clinical investigators based in academia have played an important catalytic role in championing the development of a number of drugs (17). For example, dopamine was first synthesized in 1910 but the therapeutic potential of this compound was not recognized until 1963 when Leon Goldberg and his colleagues provided convincing evidence that dopamine mediated vasodilation by binding to a previously undescribed receptor (18).

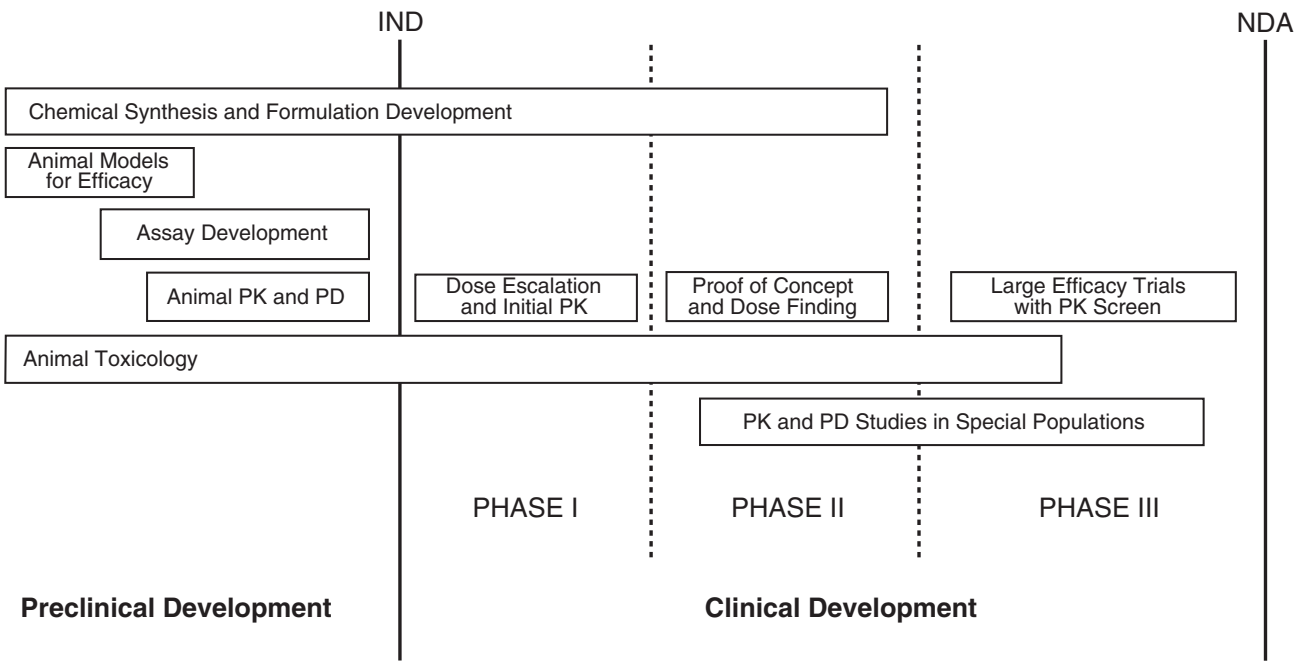

FIGURE 1.1 The process of new drug development in the United States. (PK indicates pharmacokinetic studies; PD indicates studies of drug effect or pharmacodynamics). Further explanation is provided in the text. (Modified from Peck CC *et al*. Clin Pharmacol Ther 1992;51:465–73.)

These investigators subsequently demonstrated the clinical utility of intravenous dopamine infusions in treating patients with hypotension or shock unresponsive to plasma volume expansion. This provided the basis for a small pharmaceutical firm to bring dopamine to market in the early 1970s.

Academically based clinical pharmacologists have a long tradition of interest in drug metabolism. Drug metabolism generally constitutes an important mechanism by which drugs are converted to inactive compounds that usually are more rapidly excreted than is the parent drug. However, some drug metabolites have important pharmacologic activity. This was first demonstrated in 1935 when the antibacterial activity of prontosil was found to reside solely in its metabolite, sulfanilamide (19). Advances in analytical chemistry over the past 30 years have made it possible to measure on a routine basis plasma concentrations of drug metabolites as well as parent drugs. Further study of these metabolites has demonstrated that several of them have important pharmacologic activity that must be considered for proper clinical interpretation of plasma concentration measurements (20). In some cases, clinical pharmacologists have demonstrated that drug metabolites have pharmacologic properties that make them preferable to marketed drugs.

For example, when terfenadine (Seldane), the prototype of nonsedating antihistamine drugs, was reported to cause *torsades de pointes* and fatality in patients with no previous history of cardiac arrhythmia, Woosley and his colleagues (21) proceeded to investigate the electrophysiologic effects of both terfenadine and its carboxylate metabolite (Figure 1.2). These investigators found that terfenadine, like quinidine, an antiarrhythmic drug with known propensity to cause *torsades de pointes* in susceptible individuals, blocked the delayed rectifier potassium current. However, terfenadine carboxylate, which actually accounts for most of the observed antihistaminic effects when patients take terfenadine, was found to be devoid of this proarrhythmic property. These findings provided the impetus for commercial development of the carboxylate metabolite as a safer alternative to terfenadine. This metabolite is now marketed as fexofenadine (Allegra).

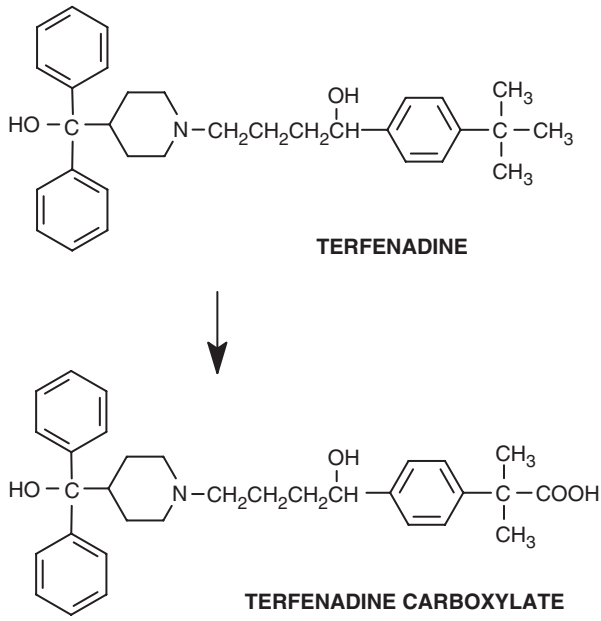

FIGURE 1.2 Chemical structures of terfenadine and its carboxylate metabolite. The acid metabolite is formed by oxidation of the *t*-butyl side chain of the parent drug.

PHARMACOKINETICS

Pharmacokinetics is defined as the quantitative analysis of the processes of drug absorption, distribution, and elimination that determine the time course of drug action. *Pharmacodynamics* deals with the mechanism of drug action. Hence, pharmacokinetics and pharmacodynamics constitute two major subdivisions of pharmacology.

Since as many as 70 to 80% of adverse drug reactions are dose related (9), our success in preventing these reactions is contingent on our grasp of the principles of pharmacokinetics that provide the scientific basis for dose selection. This becomes critically important when we prescribe drugs that have a narrow therapeutic index. Pharmacokinetics is inescapably mathematical. Although 95% of pharmacokinetic calculations required for clinical application are simple algebra, some understanding of calculus is required to fully grasp the principles of pharmacokinetics.

Concept of Clearance

Because pharmacokinetics comprises the first few chapters of this book and figures prominently in subsequent chapters, we will pause here to introduce the clinically most important concept in pharmacokinetics: the concept of *clearance*. In 1929, Möller *et al.* (22) observed that, above a urine flow rate of 2 mL/min, the rate of urea excretion by the kidneys is proportional to the amount of urea in a constant volume of blood. They introduced the term "clearance" to describe this constant and defined urea clearance as the volume of blood that one minute's excretion serves to clear of urea. Since then, creatinine clearance has

become the routine clinical measure of renal functional status, and the following equation is used to calculate creatinine clearance (CL_{CR}):

$$CL_{CR} = UV/P$$

where U is the concentration of creatinine excreted over a certain period of time in a measured volume of urine (V) and P is the serum concentration of creatinine. This is really a first-order differential equation, since UV is simply the rate at which creatinine is being excreted in urine (dE/dt). Hence,

$$dE/dt = CL_{CR} \cdot P$$

If instead of looking at the rate of creatinine excretion in urine, we consider the rate of change of creatinine in the body (dX/dt), we can write the following equation:

$$dX/dt = I - CL_{CR} \cdot P$$

Here I is the rate of *synthesis* of creatinine in the body and $CL_{CR} \cdot P$ is the rate of creatinine *elimination*. At steady state, these rates are equal and there is no change in the total body content of creatinine ($dX/dt = 0$), so:

$$P = I/CL_{CR} \tag{1.1}$$

This equation explains why it is hazardous to estimate the status of renal function solely from serum creatinine results in patients who have a reduced muscle mass and a decline in creatinine synthesis rate. For example, creatinine synthesis rate may be substantially reduced in elderly patients, so it is not unusual for serum creatinine concentrations to remain within normal limits, even though renal function is markedly impaired.

Clinical Assessment of Renal Function

In routine clinical practice, it is not practical to collect the urine samples that are needed to measure creatinine clearance directly. However, creatinine clearance in adult patients can be estimated either from a standard nomogram or from equations such as that proposed by Cockcroft and Gault (23). For men, creatinine clearance can be estimated from this equation as follows:

$$CL_{CR}\,(\text{mL/min}) = \frac{(140 - \text{age})(\text{weight in kg})}{72(\text{serum creatinine in mg/dL})} \tag{1.2}$$

For women, this estimate should be reduced by 15%. While this equation estimates creatinine clearance well, creatinine clearance overestimates true glomerular filtration rate (GFR) as measured by inulin clearance because creatinine is secreted by the renal tubule in addition to being filtered at the glomerulus (24). The overestimation increases as GFR declines from 120 to 10 mL/min/1.73 m^2, ranging from a 10–15% overestimation with normal GFR to a 140% overestimation when GFR falls below 10 mL/min. Serum creatinine does not start to rise until GFR falls to 50 mL/min because increasing tubular secretion of creatinine offsets the decline in its glomerular filtration. The Cockcroft and Gault equation also overestimates glomerular filtration rate in patients with low creatinine production due to cirrhosis or cachexia and may be misleading in patients with anasarca or rapidly changing renal function. In these situations, accurate estimates of creatinine clearance can only be obtained by actually measuring urine creatinine excretion rate in a carefully timed urine specimen. By comparing Equation 1.1 with Equation 1.2, we see that the terms $(140 - age)(weight\ in\ kg)/72$ simply provide an estimate of the creatinine formation rate in an individual patient.

The Cockcroft and Gault equation cannot be used to estimate creatinine clearance in pediatric patients because muscle mass has not reached the adult proportion of body weight. Therefore, Schwartz and colleagues (25, 26) developed the following equation to predict creatinine clearance in these patients:

$$CL_{CR}\,(\text{mL/min/1.73 m}^2) = \frac{k \cdot L\ (\text{in cm})}{\text{plasma creatinine in mg/dL}}$$

where L is body length and k varies by age and sex as follows:

Neonates to children 1 year of age:	$k = 0.45$
Children 1–13 years of age:	$k = 0.55$
Females 13–20 years of age:	$k = 0.57$
Males 13–20 years of age:	$k = 0.70$

From the standpoint of clinical pharmacology, the utility of using the Cockcroft and Gault equation, or other methods, to estimate creatinine clearance stems from the fact that these estimates can alert healthcare workers to the presence of impaired renal function in patients whose creatinine formation rate is reduced. As discussed in Chapter 5, creatinine clearance estimates also can be used to guide dose adjustment in these patients.

Dose-Related Toxicity Often Occurs When Impaired Renal Function is Unrecognized

Failure to appreciate that a patient has impaired renal function is a frequent cause of dose-related

TABLE 1.1 Status of Renal Function in 44 Patients with Digoxin Toxicity[a]

Serum creatinine (mg/dL)	No. of patients with CL_{CR} of		Percentage of group
	50 mL/min	<50 mL/min	
1.7	4	19	52%
>1.7	0	21	48%

[a]Data from Piergies AA, Worwag EM, Atkinson AJ Jr. Clin Pharmacol Ther 1994;55:353–8.

adverse drug reactions with digoxin and other drugs that normally rely primarily on the kidneys for elimination. As shown in Table 1.1, an audit of patients with high plasma concentrations of digoxin (≥3.0 ng/mL) demonstrated that 19, or 43%, of 44 patients with digoxin toxicity had serum creatinine concentrations within the range of normal values, yet had estimated creatinine clearances less than 50 mL/min (27). Hence, assessment of renal function is essential if digoxin and many other drugs are to be used safely and effectively, and is an important prerequisite for the application of clinical pharmacologic principles to patient care.

Decreases in renal function are particularly likely to be unrecognized in older patients whose creatinine clearance declines as a consequence of aging rather than of overt kidney disease. It is for this reason that the Joint Commission on Accreditation of Healthcare Organizations has placed the estimation or measurement of creatinine clearance in patients 65 years of age or older at the top of its list of indicators for monitoring the quality of medication use (28). Unfortunately, healthcare workers have considerable difficulty in using standard equations to estimate creatinine clearance in their patients and this is done only sporadically, so routine provision of these estimates is probably something that is best performed by a computerized laboratory reporting system (29). In fact, computer-generated estimates of creatinine clearance have been incorporated into a computerized prescriber order entry system and have been shown to provide decision support that has significantly improved drug prescribing for patients with impaired renal function (30).

REFERENCES

1. Holmstedt B, Liljestrand G. Readings in pharmacology. Oxford: Pergamon; 1963.
2. Reidenberg MM. Attitudes about clinical research. Lancet 1996;347:1188.
3. Leake CD. The scientific status of pharmacology. Science 1961;134:2069–79.
4. Reidenberg MM. Clinical pharmacology: The scientific basis of therapeutics. Clin Pharmacol Ther 1999;66:2–8.
5. Atkinson AJ Jr, Nordstrom K. The challenge of in-hospital medication use: An opportunity for clinical pharmacology. Clin Pharmacol Ther 1996;60:363–7.
6. Gold H, Kwit NT, Otto H. The xanthines (theobromine and aminophylline) in the treatment of cardiac pain. JAMA 1937;108:2173–9.
7. Gold H, Catell McK, Greiner T, Hanlon LW, Kwit NT, Modell W, Cotlove E, Benton J, Otto HL. Clinical pharmacology of digoxin. J Pharmacol Exp Ther 1953;109:45–57.
8. Taussig HB. A study of the German outbreak of phocomelia: The thalidomide syndrome. JAMA 1962;180:1106–14.
9. Melmon KL. Preventable drug reactions — causes and cures. N Engl J Med 1971;284:1361–8.
10. Koch-Weser J. Serum drug concentrations as therapeutic guides. N Engl J Med 1972;287:227–31.
11. Lazarou J, Pomeranz BH, Corey PN. Incidence of adverse drug reactions in hospitalized patients: A meta-analysis of prospective studies. JAMA 1998;279:1200–5.
12. Bates DW. Drugs and adverse drug reactions. How worried should we be? JAMA 1998;279:1216–7.
13. Sjöqvist F. The past, present and future of clinical pharmacology. Eur J Clin Pharmacol 1999;55:553–7.
14. Shelley JH, Baur MP. Paul Martini: The first clinical pharmacologist? Lancet 1999;353:1870–73.
15. Sheiner LB. The intellectual health of clinical drug evaluation. Clin Pharmacol Ther 1991;50:4–9.
16. Peck CC, Barr WH, Benet LZ, Collins J, Desjardins RE, Furst DE, Harter JG, Levy G, Ludden T, Rodman JH, Santhanan L, Schentag JJ, Shah VP, Sheiner LB, Skelly JP, Stanski DR, Temple RJ, Viswanathan CT, Weissinger J, Yacobi A. Opportunities for integration of pharmacokinetics, pharmacodynamics, and toxicokinetics in rational drug development. Clin Pharmacol Ther 1992;51:465–73.
17. Flowers CR, Melmon KL. Clinical investigators as critical determinants in pharmaceutical innovation. Nature Med 1997;3:136–43.
18. Goldberg LI. Cardiovascular and renal actions of dopamine: Potential clinical applications. Pharmacol Rev 1972;24:1–29.
19. Tréfouël J, Tréfouël Mme J, Nitti F, Bouvet D. Activité du *p*-aminophénylsulfamide sur les infections streptococciques expérimentales de la souris et du lapin. Compt Rend Soc Biol (Paris) 1935;120:756–8.
20. Atkinson AJ Jr, Strong JM. Effect of active drug metabolites on plasma level-response correlations. J Pharmacokinet Biopharm 1977;5:95–109.
21. Woosley RL, Chen Y, Freiman JP, Gillis RA. Mechanism of the cardiotoxic actions of terfenadine. JAMA 1993;269:1532–6.
22. Möller E, McIntosh JF, Van Slyke DD. Studies of urea excretion. II. Relationship between urine volume and the rate of urea excretion in normal adults. J Clin Invest 1929;6:427–65.
23. Cockroft DW, Gault MH. Prediction of creatinine clearance from serum creatinine. Nephron 1976; 16:31–41.

24. Bauer JH, Brooks CS, Burch RN. Clinical appraisal of creatinine clearance as a measurement of glomerular filtration rate. Am J Kidney Dis 1982;2:337–46.
25. Schwartz GJ, Feld LG, Langford DJ. A simple estimate of glomerular filtration rate in full-term infants during the first year of life. J Pediatr 1984;104:849–54.
26. Schwartz GJ, Gauthier B. A simple estimate of glomerular filtration rate in adolescent boys. J Pediatr 1985;106:522–6.
27. Piergies AA, Worwag EM, Atkinson AJ Jr. A concurrent audit of high digoxin plasma levels. Clin Pharmacol Ther 1994;55:353–8.
28. Nadzam DM. A systems approach to medication use. In: Cousins DM, ed. Medication use. Oakbrook Terrace, IL: Joint Commission on Accreditation of Healthcare Organizations; 1998. p. 5–17.
29. Smith SA. Estimation of glomerular filtration rate from the serum creatinine concentration. Postgrad Med 1988;64:204–8.
30. Chertow GM, Lee J, Kuperman GJ, Burdick E, Horsky J, Seger DL, Lee R, Mekala A, Song J, Komaroff AL, Bates DW. Guided medication dosing for inpatients with renal insufficiency. JAMA 2001;286:2839–44.

Additional Sources of Information

General

Bruton LL, Lazo JS, Parker KL, editors. Goodman & Gilman's The pharmacological basis of therapeutics. 11th ed. New York: McGraw-Hill; 2006.

This is the standard reference textbook of pharmacology. It contains good introductory presentations of the general principles of pharmacokinetics, pharmacodynamics, and therapeutics. Appendix II contains a useful tabulation of the pharmacokinetic properties of many commonly-used drugs.

Hardman JG, Limbird LE, Gilman AG, eds. Goodman & Gilman's The pharmacological basis of therapeutics. 10th ed. New York: McGraw-Hill; 2001.

This is the standard reference textbook of pharmacology. It contains good introductory presentations of the general principles of pharmacokinetics, pharmacodynamics, and therapeutics. Appendix II contains a useful tabulation of the pharmacokinetic properties of many commonly-used drugs.

Carruthers SG, Hoffman BB, Melmon KL, Nierenberg DW, eds. Melmon and Morrelli's Clinical pharmacology. 4th ed. New York: McGraw-Hill; 2000.

This is the classic textbook of clinical pharmacology, with introductory chapters devoted to general principles and subsequent chapters covering different therapeutic areas. A final section is devoted to core topics in clinical pharmacology.

Pharmacokinetics

Gibaldi M, Perrier D. Pharmacokinetics. 2nd ed. New York: Marcel Dekker; 1982.

This is a standard reference in pharmacokinetics and is the one most often cited in the "methods section" of papers that are published in journals covering this area.

Rowland M, Tozer TN. Clinical pharmacokinetics concepts and applications. 3rd ed. Baltimore: Williams & Wilkins; 1995.

This is a well-written book that is very popular as an introductory text.

Drug Metabolism

Pratt WB, Taylor P, eds. Principles of drug action: The basis of pharmacology. 3rd ed. New York: Churchill Livingstone; 1990.

This book is devoted to basic principles of pharmacology and has good chapters on drug metabolism and pharmacogenetics.

Drug Therapy in Special Populations

Evans WE, Schentag JJ, Jusko WJ, eds. Applied pharmacokinetics: Principles of therapeutic drug monitoring. 3rd ed. Vancouver, WA: Applied Therapeutics; 1992.

This book contains detailed information that is useful for individualizing dose regimens of a number of commonly used drugs.

Drug Development

Spilker B. Guide to clinical trials. Philadelphia: Lippincott-Raven; 1996.

This book contains detailed discussions of many practical topics that are relevant to the process of drug development.

Yacobi A, Skelly JP, Shah VP, Benet LZ, eds. Integration of pharmacokinetics, pharmacodynamics, and toxicokinetics in rational drug development. New York: Plenum; 1993.

This book describes how the basic principles of clinical pharmacology currently are being applied in the process of drug development.

Journals

Clinical Pharmacology and Therapeutics
British Journal of Clinical Pharmacology
Journal of Pharmaceutical Sciences
Journal of Pharmacokinetics and Biopharmaceutics

Web Sites

American Society for Clinical Pharmacology and Therapeutics (ASCPT): http://www.ascpt.org/
The American Board of Clinical Pharmacology (ABCP): http://www.abcp.net/

This page intentionally left blank

PART

I

PHARMACOKINETICS

This page intentionally left blank

CHAPTER

2

Clinical Pharmacokinetics

ARTHUR J. ATKINSON, JR.
Clinical Center, National Institutes of Health, Bethesda, Maryland

Pharmacokinetics is an important tool that is used in the conduct of both basic and applied research, and is an essential component of the drug development process. In addition, pharmacokinetics is a valuable adjunct for prescribing and evaluating drug therapy. For most clinical applications, pharmacokinetic analyses can be simplified by representing drug distribution within the body by a *single compartment* in which drug concentrations are uniform (1). Clinical application of pharmacokinetics usually entails relatively simple calculations, carried out in the context of what has been termed the *target concentration strategy*. We shall begin by discussing this strategy.

THE TARGET CONCENTRATION STRATEGY

The rationale for measuring concentrations of drugs in plasma, serum, or blood is that *concentration-response* relationships are often less variable than are *dose-response* relationships (2). This is true because individual variation in the processes of drug absorption, distribution, and elimination affects dose-response relationships, but not the relationship between free (nonprotein-bound) drug concentration in plasma water and intensity of effect (Figure 2.1).

Because most adverse drug reactions are dose related, therapeutic drug monitoring has been advocated as a means of improving therapeutic efficacy and reducing drug toxicity (3). Drug level monitoring is most useful when combined with pharmacokinetic-based dose selection in an integrated management plan, as outlined in Figure 2.2. This approach to drug dosing has been termed the *target concentration strategy*.

The rationale of therapeutic drug monitoring was first elucidated over 75 years ago when Otto Wuth recommended monitoring bromide levels in patients treated with this drug (4). More widespread clinical application of the target concentration strategy has been possible only because major advances have been made over the past 35 years in developing analytical methods capable of routinely measuring drug concentrations in patient serum, plasma, or blood samples, and because of increased understanding of basic pharmacokinetic principles (5).

Monitoring Serum Concentrations of Digoxin as an Example

Given the advanced state of modern chemical and immunochemical analytical methods, the greatest current challenge is the establishment of the range of drug concentrations in blood, plasma, or serum that correlate reliably with therapeutic efficacy or toxicity. This challenge is exemplified by the results shown in Figure 2.3 that are taken from the attempt by Smith and Haber (6) to correlate serum digoxin levels with clinical manifestations of toxicity. A maintenance dose of 0.25 mg/day is usually prescribed for patients with apparently normal renal function, and this corresponds to a steady-state pre-dose digoxin level of 1.4 ng/mL when measured by the immunoassays

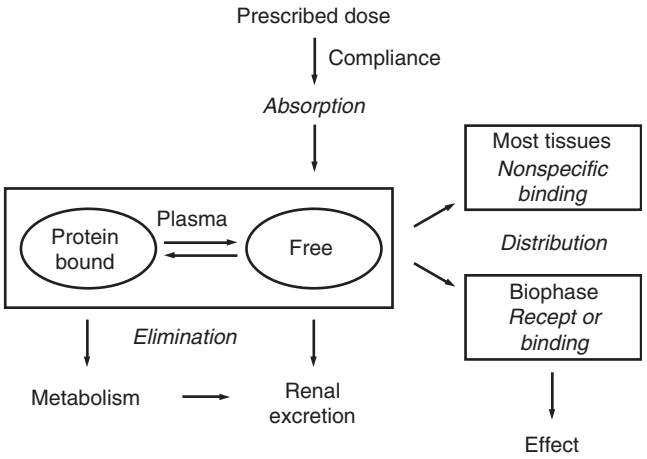

FIGURE 2.1 Diagram of factors that account for variability in observed effects when standard drug doses are prescribed. Some of this variability can be compensated for by using plasma concentration measurements to guide dose adjustments.

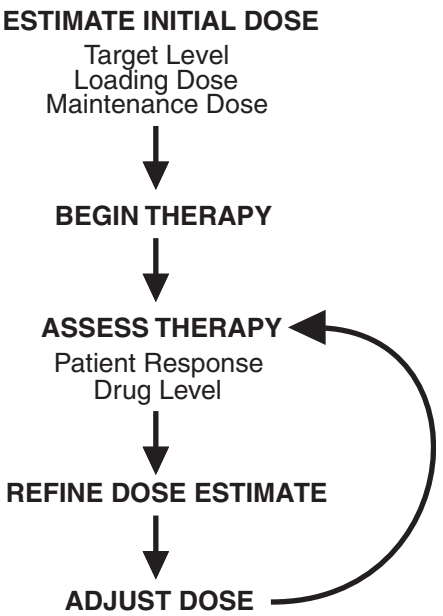

FIGURE 2.2 Target concentration strategy in which pharmacokinetics and drug level measurements are integral parts of a therapeutic plan that extends from initial drug dose estimation to subsequent patient monitoring and dose adjustment.

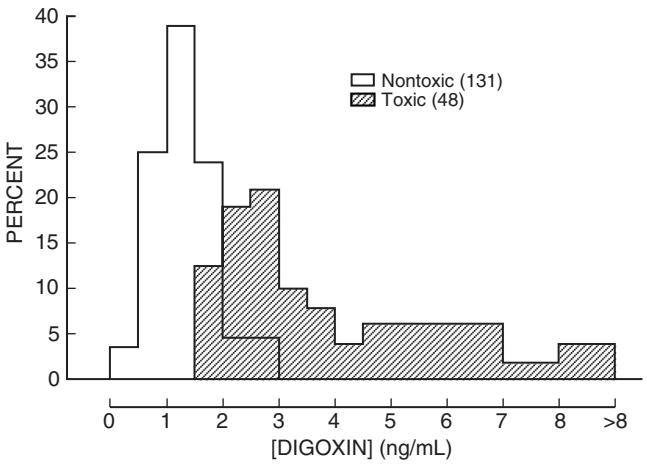

FIGURE 2.3 Superimposed frequency histograms in which serum digoxin concentrations are shown for 131 patients without digoxin toxicity and 48 patients with electrocardiographic evidence of digoxin toxicity. (Reproduced with permission from Smith TW, Haber E. J Clin Invest 1970;49:2377–86.)

that were initially marketed. It can be seen that no patient with digoxin levels below 1.6 ng/mL was toxic and that all patients with digoxin levels above 3.0 ng/mL had evidence of digoxin intoxication. However, there is a large intermediate range between 1.6 and 3.0 ng/mL in which patients could be either nontoxic or toxic.

Additional clinical information is often necessary to interpret drug concentration measurements that are otherwise equivocal. Thus, Smith and Haber found that all toxic patients with serum digoxin levels less than 2.0 ng/mL had coexisting coronary heart disease, a condition known to predispose the myocardium to the toxic effects of this drug. Conversely, 4 of the 10 nontoxic patients with levels above 2.0 ng/mL were being treated with antiarrhythmic drugs that might have suppressed electrocardiographic evidence of digoxin toxicity. Accordingly, laboratory reports of digoxin concentration have traditionally been accompanied by the following guidelines:

Usual therapeutic range:	0.8–1.6 ng/mL
Possibly toxic levels:	1.6–3.0 ng/mL
Probably toxic levels:	>3.0 ng/mL

Despite the ambiguity in interpreting digoxin level results, it was demonstrated in a controlled study that routine availability of digoxin concentration measurements markedly reduced the incidence of toxic reactions to this drug (7).

The traditional digoxin serum level recommendations were based largely on studies in which digoxin toxicity or intermediate inotropic endpoints were measured, and the challenge of establishing an appropriate range for optimally effective digoxin serum concentrations is a continuing one (8). Control of ventricular rate serves as a useful guide for digoxin dosing in patients with atrial fibrillation, but dose recommendations are evolving for treating congestive heart failure patients who remain in normal sinus rhythm. Recent studies have focused on the long-term clinical outcome of patients with chronic heart failure. The Digitalis Investigation Group trial, in which nearly 1000 patients were enrolled, concluded that,

compared to placebo, digoxin therapy decreases the need for hospitalization and reduces the incidence of death from congestive heart failure, but not overall mortality (9). Post hoc analysis of these data indicated that all-cause mortality was only lessened in men whose serum digoxin concentrations ranged from 0.5 to 0.9 ng/mL (10). Higher levels were associated with progressively greater mortality and did not confer other clinical benefit. Retrospective analysis of the data from this study suggested that digoxin therapy is associated with increased all-cause mortality in women (11), but inadequate serum concentration data were obtained to identify a dose range that might be beneficial (10). These findings are consistent with the view that the therapeutic benefits of digoxin relate more to its sympathoinhibitory effects, which are obtained when digoxin serum concentrations reach 0.7 ng/mL, than to its inotropic action, which continues to increase with higher serum levels (8). As a result of these observations, the proposal has been made that optimally therapeutic digoxin concentrations should lie within the range of 0.5–0.8 ng/mL. Based on the pharmacokinetic properties of digoxin, one would expect levels in this range to be obtained with a daily dose of 0.125 mg. However, there is an unresolved paradox in the Digoxin Investigation Group trial in that most patients with serum digoxin levels in this range were presumed to be taking a 0.25-mg daily digoxin dose (9).

General Indications for Drug Concentration Monitoring

Unfortunately, controlled studies documenting the clinical benefit of drug concentration monitoring are limited. In addition, one could not justify concentration monitoring all prescribed drugs even if this technical challenge could be met. Thus, drug concentration monitoring is most helpful for drugs that have a low therapeutic index and that have no clinically observable effects that can be easily monitored to guide dose adjustment. Generally accepted indications for measuring drug concentrations are as follows:

1. To evaluate concentration-related toxicity:
   - Unexpectedly slow drug elimination
   - Accidental or purposeful overdose
   - Surreptitious drug taking
   - Dispensing errors
2. To evaluate lack of therapeutic efficacy:
   - Patient noncompliance with prescribed therapy
   - Poor drug absorption
   - Unexpectedly rapid drug elimination
3. To ensure that the dose regimen is likely to provide effective prophylaxis.
4. To use pharmacokinetic principles to guide dose adjustment.

Despite these technical advances, adverse reactions still occur frequently with digoxin, phenytoin, and many other drugs for which drug concentration measurements are routinely available. The persistence in contemporary practice of dose-related toxicity with these drugs most likely reflects inadequate understanding of basic pharmacokinetic principles. This is illustrated by the following case history (5):

> In October, 1981, a 39-year-old man with mitral stenosis was hospitalized for mitral valve replacement. He had a history of chronic renal failure resulting from interstitial nephritis and was maintained on hemodialysis. His mitral valve was replaced with a prosthesis and digoxin therapy was initiated postoperatively in a dose of 0.25 mg/day. Two weeks later, he was noted to be unusually restless in the evening. The following day, he died shortly after he received his morning digoxin dose. Blood was obtained during an unsuccessful resuscitation attempt, and the measured plasma digoxin concentration was 6.9 ng/mL.

CONCEPTS UNDERLYING CLINICAL PHARMACOKINETICS

Pharmacokinetics provides the scientific basis of dose selection, and the process of dose regimen design can be used to illustrate with a single-compartment model the basic concepts of *apparent distribution volume* (V_d), *elimination half-life* ($t_{1/2}$) and *elimination clearance* (CL_E). A schematic diagram of this model is shown in Figure 2.4, along with the two primary pharmacokinetic parameters of distribution volume and elimination clearance that characterize it.

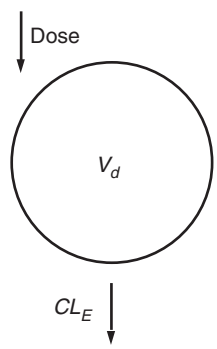

FIGURE 2.4 Diagram of a single-compartment model in which the primary kinetic parameters are the apparent distribution volume of the compartment (V_d) and the elimination clearance (CL_E).

Initiation of Drug Therapy (Concept of Apparent Distribution Volume)

Sometimes drug treatment is begun with a loading dose to produce a rapid therapeutic response. Thus, a patient with atrial fibrillation might be given a 0.75-mg intravenous loading dose of digoxin as initial therapy to control ventricular rate. The expected plasma concentrations of digoxin are shown in Figure 2.5. Inspection of this figure indicates that the log plasma-concentration-vs.-time curve eventually becomes a straight line. This part of the curve is termed the *elimination phase*. By extrapolating this elimination-phase line back to time zero, we can estimate the plasma concentration (C_0) that would have occurred if the loading dose were instantaneously distributed throughout the body. Measured plasma digoxin concentrations lie above the back-extrapolated line for several hours because distribution equilibrium actually is reached only slowly after a digoxin dose is administered. This part of the plasma-level-vs.-time curve is termed the *distribution phase*. This phase reflects the underlying *multicompartmental* nature of digoxin distribution from the intravascular space to peripheral tissues.

As shown in Figure 2.5, the back-extrapolated estimate of C_0 can be used to calculate the apparent volume ($V_{d(extrap)}$) of a hypothetical single compartment into which digoxin distribution occurs:

$$V_{d(extrap)} = \text{Loading dose}/C_0 \qquad (2.1)$$

In this case, the apparent distribution volume of 536 L is much larger than is anatomically possible. This apparent anomaly occurs because digoxin has a much higher binding affinity for tissues than for plasma, and the apparent distribution volume is the volume of *plasma* that would be required to provide the observed dilution of the loading dose. Despite this apparent anomaly, the concept of distribution volume is clinically useful because it defines the relationship between plasma concentration and the total amount of drug in the body. Further complexity arises from the fact that $V_{d(extrap)}$ is only one of three different distribution volume estimates that we will encounter. Because the distribution process is neglected in calculating this volume, it represents an overestimate of the sum of the volumes of the individual compartments involved in drug distribution.

The time course of the myocardial effects of digoxin parallels its concentration profile in peripheral tissues (Figure 2.5), so there is a delay between the attainment of peak plasma digoxin concentrations and the observation of maximum inotropic and chronotropic effects. The range of therapeutic and toxic digoxin concentrations has been estimated from observations made during the elimination phase, so blood should not be sampled for digoxin assay until distribution equilibrium is nearly complete. In clinical practice, this means waiting for at least 6 hours after a digoxin dose has been administered. In an audit of patients with measured digoxin levels of 3.0 ng/mL or more, it was

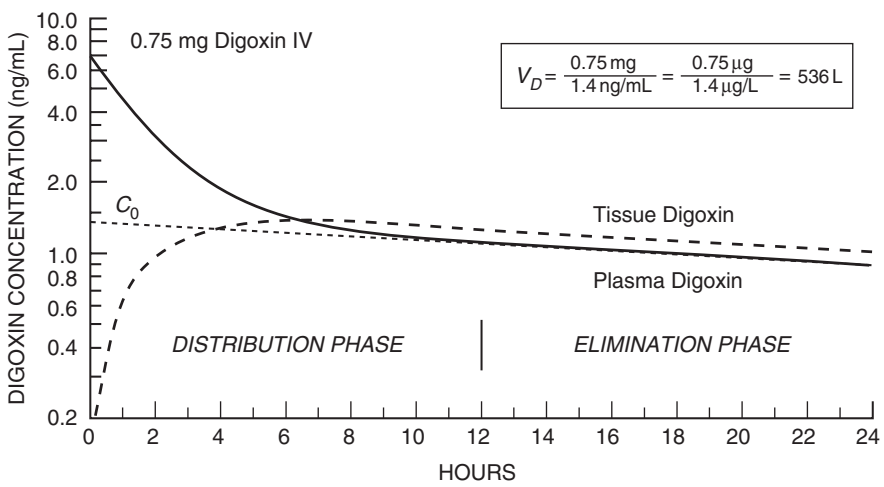

FIGURE 2.5 Simulation of plasma (*solid line*) and tissue (*heavy dashed line*) digoxin concentrations after intravenous administration of a 0.75-mg loading dose to a 70-kg patient with normal renal function. C_0 is estimated by back extrapolation (*dotted line*) of elimination-phase plasma concentrations. V_d is calculated by dividing the administered drug dose by this estimate of C_0, as shown. Tissue concentrations are referenced to the apparent distribution volume of a peripheral compartment that represents tissue distribution. (Reproduced with permission from Atkinson AJ Jr, Kushner W. Annu Rev Pharmacol Toxicol 1979;19:105–27.)

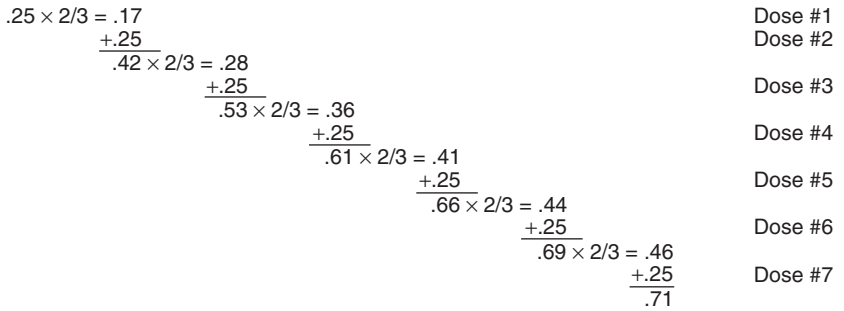

SCHEME 2.1

found that nearly one-third of these levels were not associated with toxicity but reflected procedural error, in that blood was sampled less than 6 hours after digoxin administration (12).

For other drugs, such as thiopental (13) or lidocaine (14), the locus of pharmacologic action (termed the *biophase* in classical pharmacology) is in rapid kinetic equilibrium with the intravascular space. The distribution phase of these drugs represents their somewhat slower distribution from intravascular space to pharmacologically inert tissues, such as skeletal muscle, and serves to shorten the duration of their pharmacologic effects when single doses are administered. Plasma levels of these drugs reflect therapeutic and toxic effects throughout the dosing interval and blood can be obtained for drug assay without waiting for the elimination phase to be reached.

Continuation of Drug Therapy (Concepts of Elimination Half-Life and Clearance)

After starting therapy with a loading dose, maintenance of a sustained therapeutic effect often necessitates administering additional drug doses to replace the amount of drug that has been excreted or metabolized. Fortunately, the elimination of most drugs is a *first-order* process in that the rate of drug elimination is directly proportional to the drug concentration in plasma.

Elimination Half-Life

It is convenient to characterize the elimination of drugs with first-order elimination rates by their *elimination half-life*, the time required for half an administered drug dose to be eliminated. If drug elimination half-life can be estimated for a patient, it is often practical to continue therapy by administering half the loading dose at an interval of one elimination half-life. In this way, drug elimination can be balanced by drug administration and a steady state maintained from the onset of therapy. Because digoxin has an elimination half-life of 1.6 days in patients with normal renal function, it is inconvenient to administer digoxin at this interval. When renal function is normal, it is customary to initiate maintenance therapy by administering daily digoxin doses equal to one-third of the required loading dose.

Another consequence of first-order elimination kinetics is that a constant fraction of total body drug stores will be eliminated in a given time interval. Thus, if there is no urgency in establishing a therapeutic effect, the loading dose of digoxin can be omitted and 90% of the eventual steady-state drug concentration will be reached after a period of time equal to 3.3 elimination half-lives. This is referred to as the *Plateau Principle.* The classical derivation of this principle is provided later in this chapter, but for now brute force will suffice to illustrate this important concept. Suppose that we elect to omit the 0.75-mg digoxin loading dose shown in Figure 2.5 and simply begin therapy with a 0.25-mg/day maintenance dose. If the patient has normal renal function, we can anticipate that one-third of the total amount of digoxin present in the body will be eliminated each day and that two-thirds will remain when the next daily dose is administered. As shown in Scheme 2.1, the patient will have digoxin body stores of 0.66 mg just after the fifth daily dose (3.3 × 1.6 day half-life = 5.3 days), and this is 88% of the total body stores that would have been provided by a 0.75-mg loading dose.

The solid line in Figure 2.6 shows ideal matching of digoxin loading and maintenance doses. When the digoxin loading dose (called the *digitalizing dose* in clinical practice) is omitted, or when the loading dose and maintenance dose are not matched appropriately, steady-state levels are reached only asymptotically. However, the most important concept that this figure demonstrates is that *the eventual steady-state level is determined only by the maintenance dose*, regardless

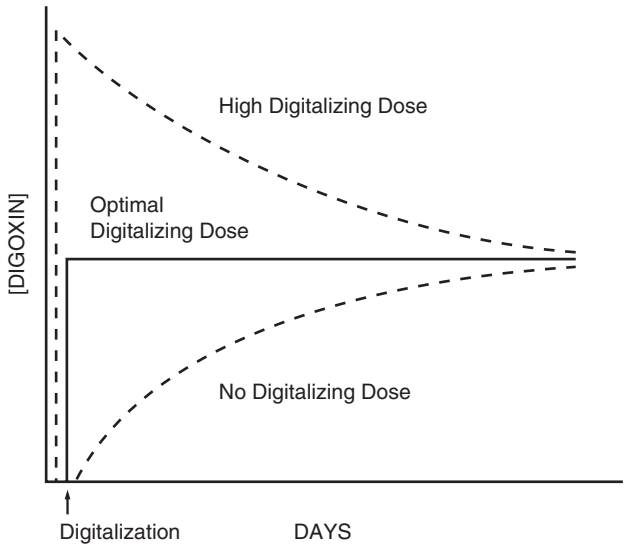

FIGURE 2.6 Expected digoxin plasma concentrations after administering perfectly matched loading and maintenance doses (*solid line*), no initial loading dose (*bottom dashed line*), or a loading dose that is large in relation to the subsequent maintenance dose (*upper dashed line*).

of the size of the loading dose. Selection of an inappropriately high digitalizing dose only subjects patients to an interval of added risk without achieving a permanent increase in the extent of digitalization. Conversely, when a high digitalizing dose is required to control ventricular rate in patients with atrial fibrillation or flutter, a higher than usual maintenance dose also will be required.

Elimination Clearance

Just as creatinine clearance is used to quantitate the renal excretion of creatinine, the removal of drugs eliminated by first-order kinetics can be defined by an *elimination clearance* (CL_E). In fact, elimination clearance is the primary pharmacokinetic parameter that characterizes the removal of drugs that are eliminated by first-order kinetics. When drug administration is by intravenous infusion, the eventual steady-state concentration of drug in the body (C_{ss}) can be calculated from the following equation, where the drug infusion rate is given by I:

$$C_{ss} = I/CL_E \tag{2.2}$$

When intermittent oral or parenteral doses are administered at a dosing interval, τ, the corresponding equation is

$$\overline{C}_{ss} = \frac{\text{Dose}/\tau}{CL_E} \tag{2.3}$$

where $\overline{C}_{ss}$is the mean concentration during the dosing interval. Under conditions of intermittent administration, there is a continuing periodicity in maximum ("peak") and minimum ("trough") drug levels so that only a quasi-steady state is reached. However, unless particular attention is directed to these peak and trough levels, no distinction generally is made in clinical pharmacokinetics between the true steady state that is reached when an intravenous infusion is administered continuously and the quasi-steady state that results from intermittent administration.

Since there is a directly proportionate relationship between administered drug dose and steady-state plasma level, Equations 2.2 and 2.3 provide a straightforward guide to dose adjustment for drugs that are eliminated by first-order kinetics. Thus, to double the plasma level, the dose simply should be doubled. Conversely, to halve the plasma level, the dose should be halved. It is for this reason that Equations 2.2 and 2.3 are the most clinically important pharmacokinetic equations. Note that, as is apparent from Figure 2.6, these equations also stipulate that the steady-state level is determined only by the maintenance dose and elimination clearance. The loading dose does not appear in the equations and does not influence the eventual steady-state level.

In contrast to elimination clearance, elimination half-life ($t_{1/2}$) is not a primary pharmacokinetic parameter because it is determined by distribution volume as well as by elimination clearance.

$$t_{1/2} = \frac{0.693 V_{d(area)}}{CL_E} \tag{2.4}$$

The value of V_d in this equation is not $V_{d(extrap)}$ but instead it represents a second estimate of distribution volume, referred to as $V_{d(area)}$ or $V_{d(\beta)}$ that generally is estimated from measured elimination half-life and clearance. The similarity of these two estimates of distribution volume reflects the extent to which drug distribution is accurately described by a single-compartment model, and obviously varies from drug to drug (15).

Figure 2.7 illustrates how differences in distribution volume affect elimination half-life and peak and trough plasma concentrations when the same drug dose is given to two patients with the same elimination clearance. If these two hypothetical patients were given the same nightly dose of a sedative-hypnotic drug for insomnia, $\overline{C}_{ss}$ would be the same for both. However, the patient with the larger distribution volume might not obtain sufficiently high plasma levels to fall asleep in the evening, and might have a plasma

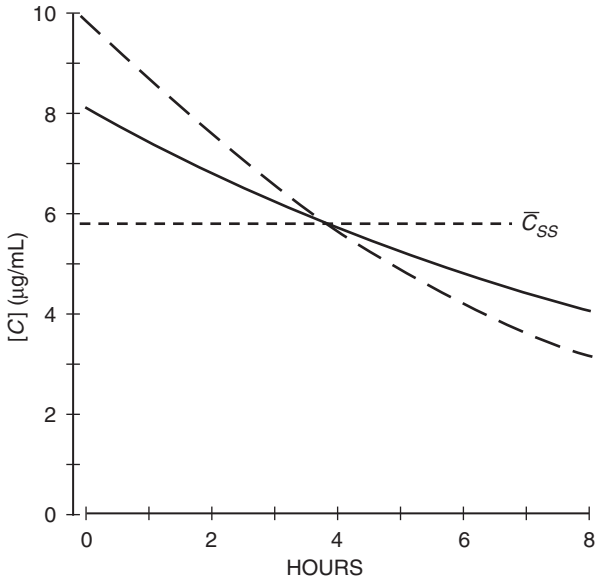

FIGURE 2.7 Plasma concentrations after repeated administration of the same drug dose to two hypothetical patients whose elimination clearance is the same but whose distribution volumes differ. The patients have the same $\overline{C}_{ss}$ but the larger distribution volume results in lower peak and higher trough plasma levels (*solid line*) than when the distribution volume is smaller (*dashed line*).

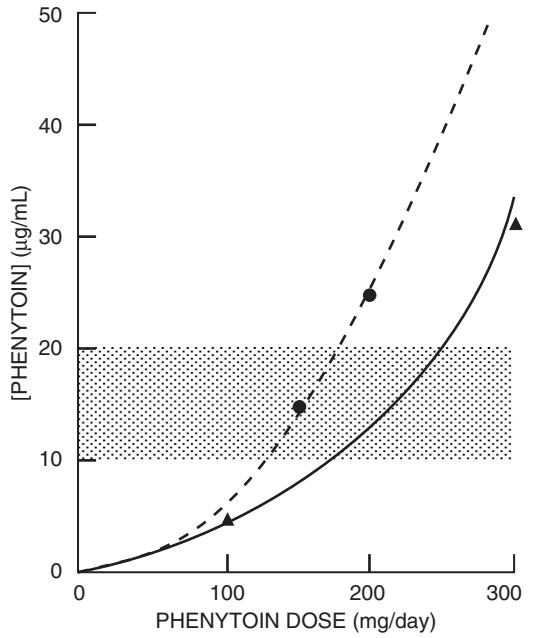

FIGURE 2.9 The lines show the relationship between dose and steady-state plasma phenytoin concentrations predicted for two patients who became toxic after initial treatment with 300 mg/day. Measured steady-state plasma concentrations are shown by the circles and triangles. The shaded area shows the usual range of therapeutically effective phenytoin plasma concentrations. (Reproduced with permission from Atkinson AJ Jr. Med Clin North Am 1974;58:1037–49.)

level that was high enough to cause drowsiness in the morning.

Drugs Not Eliminated by First-Order Kinetics

Unfortunately, the elimination of some drugs does not follow first-order kinetics. For example, the primary pathway of phenytoin elimination entails initial metabolism to form 5-(parahydroxyphenyl)-5-phenylhydantoin (*p*-HPPH), followed by glucuronide conjugation (Figure 2.8). The metabolism of this drug is not first order but follows *Michaelis–Menten* kinetics because the microsomal enzyme system that forms *p*-HPPH is partially saturated at phenytoin concentrations of 10–20 μg/mL that are therapeutically effective. The result is that phenytoin plasma concentrations rise hyperbolically as dosage is increased (Figure 2.9).

For drugs eliminated by first-order kinetics, the relationship between dosing rate and steady-state plasma concentration is given by rearranging Equation 2.3 as follows:

$$\text{Dose}/\tau = CL_E \cdot \overline{C}_{ss} \qquad (2.5)$$

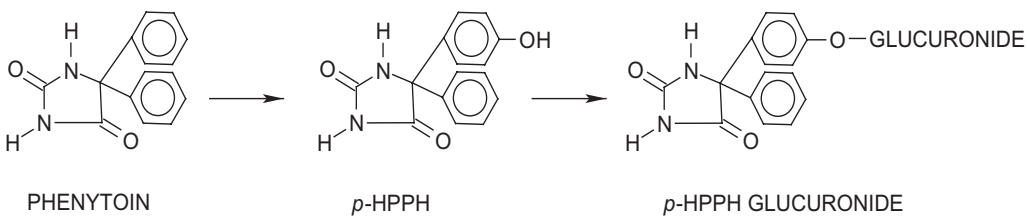

FIGURE 2.8 Metabolism of phenytoin to form *p*-HPPH and *p*-HPPH glucuronide. The first step in this enzymatic reaction sequence is rate limiting and follows Michaelis–Menten kinetics, showing progressive saturation as plasma concentrations rise within the range that is required for anticonvulsant therapy to be effective.

The corresponding equation for phenytoin is

$$\text{Dose}/\tau = \frac{V_{max}}{K_m + \overline{C}_{ss}} \cdot \overline{C}_{ss} \tag{2.6}$$

where V_{max} is the maximum rate of drug metabolism and K_m is the apparent Michaelis–Menten constant for the enzymatic metabolism of phenytoin.

Although phenytoin plasma concentrations show substantial interindividual variation when standard doses are administered, they average 10 μg/mL when adults are treated with a 300-mg total daily dose, but rise to an average of 20 μg/mL when the dose is increased to 400 mg (15). This nonproportional relationship between phenytoin dose and plasma concentration complicates patient management and undoubtedly contributes to the many adverse reactions that are seen in patients treated with this drug. Although several pharmacokinetic approaches have been developed for estimating dose adjustments, it is safest to change phenytoin doses in small increments and to rely on careful monitoring of clinical response and phenytoin plasma levels. The pharmacokinetics of phenytoin were studied in both patients shown in Figure 2.9 after they became toxic when treated with the 300-mg/day dose that is routinely prescribed as initial therapy for adults (16). The figure demonstrates that the entire therapeutic range is traversed in these patients by a dose increment of less than 100 mg/day.

Even though many drugs in common clinical use are eliminated by drug-metabolizing enzymes, relatively few of them have Michaelis–Menten elimination kinetics (e.g., aspirin and ethyl alcohol). The reason for this is that K_m for most drugs is much greater than $\overline{C}_{ss}$. Hence for most drugs, $\overline{C}_{ss}$ can be ignored in the denominator of Equation 2.6, and this equation reduces to

$$\text{Dose}/\tau = \frac{V_{max}}{K_m} \cdot \overline{C}_{ss}$$

where the ratio V_{max}/K_m is equivalent to CL_E in Equation 2.5. Thus, for most drugs, a change in dose will change steady-state plasma concentrations proportionately, a property that is termed *dose proportionality*.

MATHEMATICAL BASIS OF CLINICAL PHARMACOKINETICS

In the following sections we will review the mathematical basis of some of the important relationships that are used when pharmacokinetic principles are applied to the care of patients. The reader also is referred to other literature sources that may be helpful (1, 15, 17).

First-Order Elimination Kinetics

For most drugs, the amount of drug eliminated from the body during any time interval is proportional to the total amount of drug present in the body. In pharmacokinetic terms, this is called *first-order* elimination and is described by the equation

$$dX/dt = -kX \tag{2.7}$$

where X is the total amount of drug present in the body at any time (t) and k is the elimination rate constant for the drug. This equation can be solved by separating variables and direct integration to calculate the amount of drug remaining in the body at any time after an initial dose.

Separating variables:

$$dX/X = -k\,dt$$

Integrating from zero time to time = t:

$$\int_{X_0}^{X} dX/X = -k \int_0^t dt$$

$$\ln X\Big|_{X_0}^{X} = -kt\Big|_0^t$$

$$\ln \frac{X}{X_0} = -kt \tag{2.8}$$

$$X = X_0 e^{-kt} \tag{2.9}$$

Although these equations deal with total amounts of drug in the body, the equation $C = X/V_d$ provides a general relationship between X and drug concentration (C) at any time after the drug dose is administered. Therefore, C can be substituted for X in Equations 2.7 and 2.8 as follows:

$$\ln \frac{C}{C_0} = -kt \tag{2.10}$$

$$C = C_0 e^{-kt} \tag{2.11}$$

Equation 2.10 is particularly useful since it can be rearranged in the form of the equation for a straight line ($y = mx + b$) to give

$$\ln C = -kt + \ln C_0 \tag{2.12}$$

Now when data are obtained after administration of a single drug dose and C is plotted on base 10 semilogarithmic graph paper, a straight line is obtained with 0.434 times the slope equal to k ($\log x/\ln x = 0.434$) and an intercept on the ordinate of C_0. In practice C_0 is never measured directly because some time is needed for the injected drug to distribute throughout body fluids. However, C_0 can be estimated by back-extrapolating the straight line given by Equation 2.12 (Figure 2.5).

Concept of Elimination Half-Life

If the rate of drug distribution is rapid compared with rate of drug elimination, the terminal exponential phase of a semilogarithmic plot of drug concentrations vs time can be used to estimate the elimination half-life of a drug, as shown in Figure 2.10. Because Equation 2.10 can be used to estimate k from any two concentrations that are separated by an interval t, it can be seen from this equation that when $C_2 = 1/2C_1$,

$$\ln 1/2 = -kt_{1/2}$$

$$\ln 2 = kt_{1/2}$$

So,

$$t_{1/2} = \frac{0.693}{k} \quad \text{and} \quad k = \frac{0.693}{t_{1/2}} \tag{2.13}$$

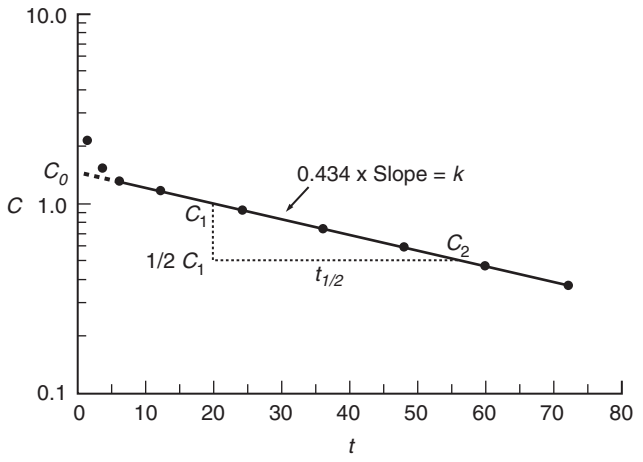

FIGURE 2.10 Plot of drug concentrations vs. time on semilogarithmic coordinates. Back extrapolation (*dashed line*) of the elimination-phase slope (*solid line*) provides an estimate of C_0. The elimination half-life ($t_{1/2}$) can be estimated from the time required for concentrations to fall from some point on the elimination-phase line (C_1) to $C_2 = \frac{1}{2}C_1$, as shown by the dotted lines. In the case of digoxin, C would be in units of ng/mL and t in hours.

For digoxin, $t_{1/2}$ is usually 1.6 days for patients with normal renal function and $k = 0.43$ day^{-1} ($0.693/1.6 = 0.43$). As a practical point, it is easier to estimate $t_{1/2}$ from a graph such as Figure 2.10 and to then calculate k from Equation 2.13, than to estimate k directly from the slope of the elimination-phase line.

Relationship of k to Elimination Clearance

In Chapter 1, we pointed out that the creatinine clearance equation

$$CL_{CR} = UV/P$$

could be rewritten in the form of the following first-order differential equation:

$$dX/dt = -CL_{CR} \cdot P$$

If this equation is generalized by substituting CL_E for CL_{CR}, it can be seen from Equation 2.7 that, since $P = X/V_d$,

$$k = \frac{CL_E}{V_d} \tag{2.14}$$

Equation 2.4 was derived by substituting CL_E/V_d for k in Equation 2.13. Although V_d and CL_E are the two primary parameters of the single-compartment model, confusion arises because k is initially calculated from experimental data. However, k is influenced by changes in distribution volume as well as clearance and does not reflect just changes in drug elimination.

Cumulation Factor

In the steady-state condition, the rate of drug administration is exactly balanced by the rate of drug elimination. Gaddum (18) first demonstrated that the maximum and minimum drug levels that are expected at steady state (quasi-steady state) can be calculated for drugs that are eliminated by first-order kinetics. Assume that just maintenance doses of a drug are administered without a loading dose (Figure 2.6, lowest curve). Starting with Equation 2.9,

$$X = X_0\, e^{-kt}$$

where X_0 is the maintenance dose and X is the amount of drug remaining in the body at time t. If τ is the dosing interval, let

$$p = e^{-k\tau}$$

Therefore, just before the second dose,

$$X_{1(min)} = X_0 p$$

Just after the second dose,

$$X_{2(max)} = X_0 + X_0 p = X_0(1 + p)$$

Similarly, after the third dose,

$$X_{3(max)} = X_0 + X_0 p + X_0 p^2 = X_0(1 + p + p^2)$$

and after the nth dose,

$$X_{n(max)} = X_0(1 + p + \cdots + p^{n-1})$$

or,

$$X_{n(max)} = X_0 \frac{(1 - p^n)}{(1 - p)}$$

Since $p < 1$, as $n \to \infty, p^n \to 0$. Therefore,

$$X_{\infty(max)} = X_0/(1 - p)$$

or, substituting for p,

$$X_{\infty(max)} = \frac{X_0}{\left(1 - e^{-k\tau}\right)}$$

The value of X_∞ is the maximum *total body content* of the drug that is reached during a dosing interval at steady state. The maximum *concentration* is determined by dividing this value by V_d. The *minimum* value is given by multiplying either of these maximum values by $e^{-k\tau}$.

Note that the respective maximum and minimum drug concentrations after the first dose are

$$\text{Maximum:} \quad C_0$$

$$\text{Minimum:} \quad C_0 e^{-k\tau}$$

The expected steady-state counterparts of these initial concentration values can be estimated by multiplying them by the *cumulation factor* (*CF*):

$$CF = \frac{1}{1 - e^{-kt}} \tag{2.15}$$

Plateau Principle

Although the time required to reach steady state cannot be calculated explicitly, the time required to reach *any specified fraction of the eventual steady state* can be estimated. For dosing regimens in which drugs are administered at a constant interval, Gaddum (18) showed that the number of drug doses (n) required to reach a fraction (f) of the eventual steady-state amount of drug in the body can be calculated as follows:

$$f = \frac{X_n}{X_\infty} = \frac{X_0\left(1 - p^n\right)}{\left(1 - p\right)} \cdot \frac{\left(1 - p\right)}{X_0} = 1 - p^n \tag{2.16}$$

In clinical practice, $f = 0.90$ is usually a reasonable approximation of eventual steady state. Substituting this value into Equation 2.16 and solving for n,

$$0.90 = 1 - e^{-nk\tau}$$

$$e^{-nk\tau} = 0.1$$

$$n = -\frac{\ln\ 0.1}{k\tau}$$

$$n = \frac{2.3}{k\tau}$$

From Equation 2.13,

$$k = 0.693/t_{1/2}$$

Therefore, the time needed to reach 90% of steady state is $n\tau = 3.3t_{1/2}$ and the corresponding number of doses is

$$n = 3.3t_{1/2} \tag{2.17}$$

Not only are drug accumulation greater and steady-state drug levels higher in patients with a prolonged elimination half-life, but also, an important consequence of Equation 2.17 is that it takes these patients longer to reach steady state. For example, the elimination half-life of digoxin in patients with normal renal function is 1.6 days, so that 90% of the expected steady state is reached in 5 days when daily doses of this drug are administered. However, the elimination half-life of digoxin is approximately 4.3 days in functionally anephric patients, such as the one described in the previous case history, and 14 days would be required to reach 90% of the expected steady state. This explains why this patient's adverse reaction occurred 2 weeks after starting digoxin therapy.

Application of Laplace Transforms to Pharmacokinetics

The Laplace transformation method of solving differential equations falls into the area of *operational calculus* that is finding increasing utility in pharmacokinetics. Operational calculus was invented by an English engineer, Sir Oliver Heaviside (1850–1925), who had an intuitive grasp of mathematics (19). Although Laplace provided the theoretical basis for the method, some of Sir Oliver's intuitive contributions remain (e.g., the Heaviside Expansion Theorem utilized in Chapter 3). The idea of operational mathematics and Laplace transforms perhaps is best understood by comparison with the use of logarithms to perform arithmetic operations. This comparison is diagrammed in the flowcharts shown in Scheme 2.2.

Just as there are tables of logarithms, there are tables to aid the mathematical process of obtaining Laplace transforms ($\mathcal{L}$) and inverse Laplace transforms ($\mathcal{L}^{-1}$). Laplace transforms can also be calculated directly from the integral:

$$\mathcal{L}[F(t)] = f(s) = \int_0^\infty F(t)\, e^{-st} dt$$

We can illustrate the application of Laplace transforms by using them to solve the simple differential equation that we have used to describe the single-compartment model (Equation 2.7). Starting with this equation,

$$dX/dt = -kX$$

we can use a table of Laplace transform operations (Appendix I) to take Laplace transforms of each side of this equation to create the *subsidiary equation*:

For X on the right side of the equation:

$$\mathcal{L}F(t) = f(s)$$

For dX/dt on the left side of the equation:

$$\mathcal{L}F'(t) = sf(s) - F(0)$$

Since $F(0)$ represents the *initial condition*, in this case the amount of drug in the model compartment at time zero, X_0, the subsidiary equation can be written

$$sf(s) - X_0 = -kf(s)$$

This can be rearranged to give

$$(s + k)f(s) = X_0$$

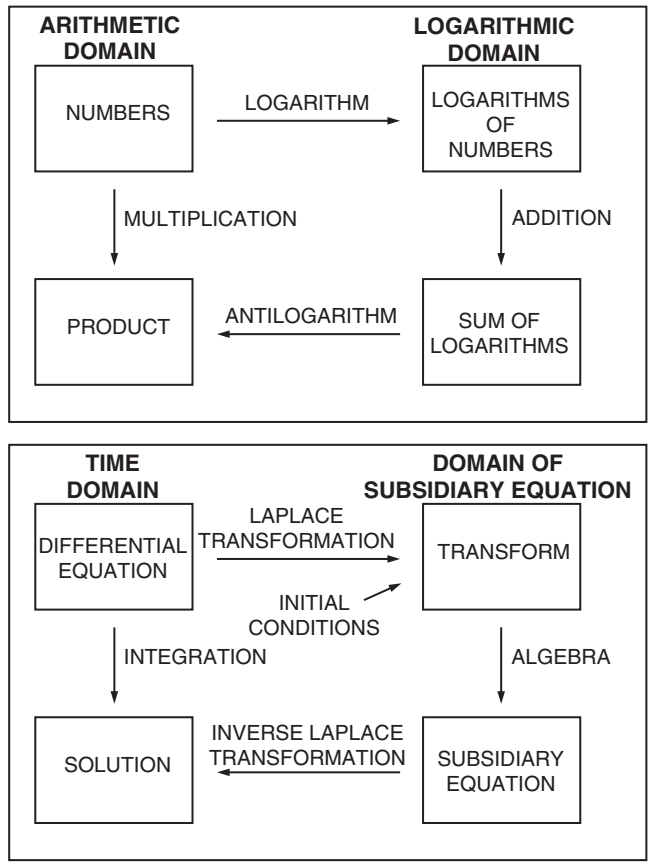

SCHEME 2.2

Or,

$$f(s) = X_0/(s + k)$$

A table of *inverse Laplace transforms* indicates

$$\mathcal{L}^{-1}\frac{1}{s - a} = e^{at}$$

Therefore, the solution to the differential equation is

$$X = X_0 e^{-kt}$$

and this is the same result that we obtained as Equation 2.9.

In other words, the Laplace operation transforms the differential equation from the time domain to another functional domain represented by the subsidiary equation. After algebraic simplification of this subsidiary equation, the inverse transformation is used to return the solved equation to the time domain.

We have selected a simple example to illustrate the use of Laplace transform methods. A more advanced application is given in the next chapter, in which equations are derived for a two-compartment model. It will be shown subsequently that Laplace transform methods also are helpful in pharmacokinetics when convolution/deconvolution methods are used to characterize drug absorption processes.

REFERENCES

1. Atkinson AJ Jr, Kushner W. Clinical pharmacokinetics. Annu Rev Pharmacol Toxicol 1979;19:105–27.
2. Atkinson AJ Jr, Reidenberg MM, Thompson WL. Clinical Pharmacology. In: Greenberger N, ed. MKSAP VI Syllabus. Philadelphia: Am Col Phys; 1982. p. 85–96.
3. Koch-Weser J. Serum drug concentrations as therapeutic guides. N Engl J Med 1972;287:227–31.
4. Wuth O. Rational bromide treatment: New methods for its control. JAMA 1927;88:2013–17.
5. Atkinson AJ Jr, Ambre JJ. Kalman and Clark's drug assay: The strategy of therapeutic drug monitoring. 2nd ed. New York: Masson; 1984.
6. Smith TW, Haber E. Digoxin intoxication: The relationship of clinical presentation to serum digoxin concentration. J Clin Invest 1970;49:2377–86.
7. Duhme DW, Greenblatt DJ, Koch-Weser J. Reduction of digoxin toxicity associated with measurement of serum levels. Ann Intern Med 1974;80:516–9
8. Adams KF Jr, Gheorghiade M, Uretsky BF, Patterson JH, Schwartz TA, Young JB. Clinical benefits of low serum digoxin concentrations in heart failure. J Am Coll Cardiol 2002;39:946–53.
9. The Digitalis Investigation Group. The effect of digoxin on mortality and morbidity in patients with heart failure. N Engl J Med 1997;336:525–33.
10. Rathore SS, Curtis JP, Wang Y, Bristow MR, Krumholz HM. Association of serum digoxin concentration and outcomes in patients with heart failure. JAMA 2003;289:871–8.
11. Rathore SS, Wang W, Krumholz HM. Sex-based differences in the effect of digoxin for the treatment of heart failure. N Engl J Med 2002;347:1403–11.
12. Piergies AA, Worwag EW, Atkinson AJ Jr. A concurrent audit of high digoxin plasma levels. Clin Pharmacol Ther 1994;55:353–8.
13. Goldstein A, Aronow L. The durations of action of thiopental and pentobarbital. J Pharmacol Exp Ther 1960;128:1–6.
14. Benowitz N, Forsyth RP, Melmon KL, Rowland M. Lidocaine disposition kinetics in monkey and man. I. Prediction by a perfusion model. Clin Pharmacol Ther 1974;16:87–98.
15. Gibaldi M, Perrier D. Pharmacokinetics. 2nd ed. New York: Marcel Dekker; 1982. p. 199–219.
16. Atkinson AJ Jr. Individualization of anticonvulsant therapy. Med Clin North Am 1974;58:1037–49.
17. Rowland M, Tozer TN. Clinical pharmacokinetics: Concepts and applications. 3rd ed. Baltimore: Lea & Febiger, 1994.
18. Gaddum JH. Repeated doses of drugs. Nature 1944;153:494.
19. Van Valkenberg ME. The Laplace transformation. In: Network analysis. Englewood Cliffs (NJ): Prentice-Hall;1964. p. 159–81.

STUDY PROBLEMS

Select the *one* lettered answer or statement completion that is BEST. It may be helpful to carry out dimensional analysis by including units in your calculations. Answers are provided in Appendix II.

1. A 35-year-old woman is being treated with gentamicin for a urinary tract infection. The gentamicin plasma level is 4 μg/mL shortly after initial intravenous administration of an 80-mg dose of this drug. The distribution volume of gentamicin is:

   A. 5 L
   B. 8 L
   C. 10 L
   D. 16 L
   E. 20 L

2. A 58-year-old man is hospitalized in cardiac intensive care following an acute myocardial infarction. He has had recurrent episodes of ventricular tachycardia that have not responded to lidocaine, and an intravenous infusion of procainamide will now be administered. The patient weighs 80 kg and expected values for his procainamide distribution volume and elimination half-life are 2.0 L/kg and 3 hours, respectively.

   What infusion rate will provide a steady-state plasma procainamide level of 4.0 μg/mL?

   A. 2.5 mg/min
   B. 5.0 mg/min
   C. 7.5 mg/min
   D. 10.0 mg/min
   E. 12.5 mg/min

3. A patient with peritonitis is treated with gentamicin, 80 mg every 8 hours. Plasma gentamicin levels are measured during the first dosing interval. The gentamicin plasma level is 10 μg/mL at its peak after initial intravenous administration of this drug, and is 5 μg/mL when measured 5 hours later.

   The cumulation factor can be used to predict an expected steady-state peak level of:

   A. 10 μg/mL
   B. 12 μg/mL
   C. 15 μg/mL
   D. 18 μg/mL
   E. 20 μg/mL

4. A 20-year-old man is hospitalized after an asthmatic attack precipitated by an upper respiratory infection and fails to respond in the emergency room to two subcutaneously injected doses of epinephrine. The patient has not been taking theophylline-containing medications for the past 6 weeks. He weighs 60 kg and you estimate that his apparent volume of theophylline distribution is 0.45 L/kg. Bronchodilator therapy includes a 5.6-mg/kg loading dose of aminophylline, infused intravenously over 20 min, followed by a maintenance infusion of 0.63 mg/kg per hour (0.50 mg/kg per hour of theophylline). Forty-eight hours later, the patient's respiratory status has improved. However, he has nausea and tachycardia, and his plasma theophylline level is 24 μg/mL.

   For how long do you expect to suspend theophylline administration in order to reach a level of 12 μg/mL before restarting the aminophylline infusion at a rate of 0.31 mg/kg per hour?

   A. 5 hours
   B. 10 hours
   C. 15 hours
   D. 20 hours
   E. 25 hours

5. Digitoxin has an elimination half-life of approximately 7 days and its elimination is relatively unaffected by decreased renal function. For this latter reason, the decision is made to use this drug to control ventricular rate in a 60-year-old man with atrial fibrillation and a creatinine clearance of 25 mL/min.

   If no loading dose is administered and a maintenance dose of 0.1 mg/day is prescribed, how many days would be required for digitoxin levels to reach 90% of their expected steady-state value?

   A. 17 days
   B. 19 days
   C. 21 days
   D. 23 days
   E. 24 days

6. A 75-year-old man comes to your office with anorexia and nausea. Five years ago he was found to have congestive heart failure that responded to treatment with a thiazide diuretic and an angiotensin-converting enzyme inhibitor. Three years ago digoxin was added to the regimen in a dose of 0.25 mg/day. This morning he omitted his digoxin dose. On hospital admission, electrocardiographic monitoring shows frequent bigeminal extrasystoles and the patient's plasma digoxin level is 3.2 ng/mL. Twenty-four hours later, the digoxin level is 2.7 ng/mL. At that time you decide that it would be appropriate to let the digoxin level fall to 1.6 ng/mL before restarting a daily digoxin dose of 0.125 mg.

   For how many *more* days do you anticipate having to withhold digoxin before your target level of 1.6 ng/mL is reached?

   A. 2 days
   B. 3 days
   C. 4 days
   D. 5 days
   E. 6 days

7. A 50-year-old man is being treated empirically with gentamicin and a cephalosporin for pneumonia. The therapeutic goal is to provide a maximum gentamicin level of *more than* 8 μg/mL 1 hour after intravenous infusion, and a minimum concentration, just before dose administration, of *less than* 1 μg/ml. His estimated plasma gentamicin clearance and elimination half-life are 100 mL/min and 2 hours, respectively. Which of the following dosing regimens is appropriate?

   A. 35 mg every 2 hours
   B. 70 mg every 4 hours
   C. 90 mg every 5 hours
   D. 110 mg every 6 hours
   E. 140 mg every 8 hours

8. You start a 19-year-old man on phenytoin in a dose of 300 mg/day to control generalized (grand mal) seizures. Ten days later, he is brought to an emergency room following a seizure. His phenytoin level is found to be 5 μg/mL and the phenytoin dose is increased to 600 mg/day. Two weeks later, he returns to your office complaining of drowsiness and ataxia. At that time his phenytoin level is 30 μg/mL.

   Assuming patient compliance with previous therapy, which of the following dose regimens should provide a phenytoin plasma level of 15 μg/mL (therapeutic range: 10–20 μg/mL)?

   A. 350 mg/day
   B. 400 mg/day
   C. 450 mg/day
   D. 500 mg/day
   E. 550 mg/day

This page intentionally left blank

CHAPTER

3

Compartmental Analysis of Drug Distribution

ARTHUR J. ATKINSON, JR.
Clinical Center, National Institutes of Health, Bethesda, Maryland

Drug distribution can be defined as the postabsorptive transfer of drug from one location in the body to another. Absorption after various routes of drug administration is not considered part of the distribution process and is dealt with separately. In most cases, the process of drug distribution is symmetrically reversible and requires no input of energy. However, there is increasing awareness that receptor-mediated endocytosis and carrier-mediated active transport also play important roles in either increasing or limiting the extent of drug distribution. The role of these processes in drug distribution will be considered in Chapter 14.

PHYSIOLOGICAL SIGNIFICANCE OF DRUG DISTRIBUTION VOLUMES

Digoxin is typical of most drugs in that its distribution volume, averaging 536 L in 70-kg subjects with normal renal function, is not readily interpreted by reference to physiologically defined fluid spaces. However, some drugs and other compounds appear to have distribution volumes that are physiologically identifiable. Thus, the distribution volumes of inulin, quaternary neuromuscular blocking drugs, and, initially, aminoglycoside antibiotics approximate expected values for extracellular fluid space (ECF). The distribution volumes of urea, antipyrine, ethyl alcohol, and caffeine also can be used to estimate total body water (TBW) (1).

Binding to plasma proteins affects drug distribution volume estimates. Initial attempts to explain the effects of protein binding on drug distribution were based on the assumption that the distribution of these proteins was confined to the intravascular space. However, "plasma" proteins distribute throughout ECF, so the distribution volume of even highly protein-bound drugs exceeds plasma volume and approximates ECF in many cases (1). For example, thyroxine is 99.97% protein bound and its distribution volume of 0.15 L/kg (2) approximates recent ECF estimates of 0.16 ± 0.01 L/kg made with inulin (3). Distribution volumes are usually larger than ECF for uncharged drugs that are less tightly protein bound to plasma proteins. Theophylline is a methylxanthine, similar to caffeine, and its nonprotein-bound, or free, fraction distributes in TBW. The fact that theophylline is normally 40% bound to plasma proteins accounts for the findng that its 0.5 L/kg apparent volume of distribution is intermediate between expected values for ECF and TBW (Figure 3.1). The impact on distribution volume (V_d) of changes in the extent of theophylline binding to plasma proteins can be estimated from the following equation:

$$V_d = \text{ECF} + f_u(\text{TBW} - \text{ECF}) \qquad (3.1)$$

where f_u is the fraction of unbound theophylline that can be measured in plasma samples (4). An additional correction has been proposed to account for the fact that interstitial fluid protein concentrations are

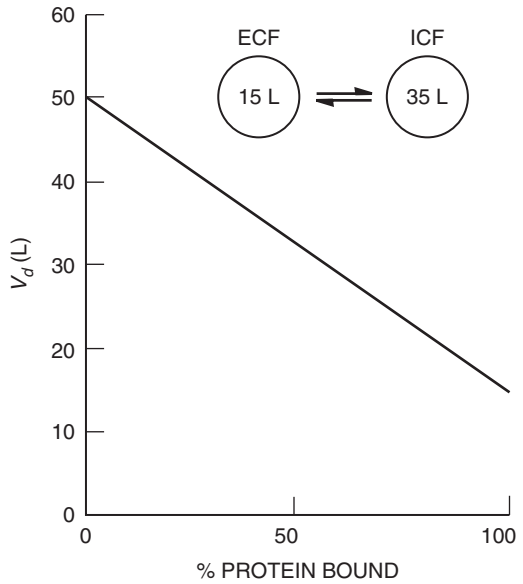

FIGURE 3.1 Analysis of theophylline V_d in terms of protein binding, ECF, and intracellular fluid (ICF) components of TBW in a hypothetical 70-kg subject. Theophylline is normally 40% bound, so its V_d approximates 35 L or 0.5 L/kg. (Reproduced with permission from Atkinson AJ Jr, Ruo TI, Frederiksen MC. Trends Pharmacol Sci 1991;12:96–101.)

less than those in plasma (5). However, this correction does not account for the heterogeneous nature of interstitial fluid composition and entails additional complexity that may not be warranted (1).

Many drugs have distribution volumes that exceed expected values for TBW, or are considerably larger than ECF despite extensive binding to plasma proteins. The extensive tissue binding of these drugs increases the apparent distribution volume that is calculated by reference to drug concentrations measured in plasma water. By modifying Equation 3.1 as follows,

$$V_d = \text{ECF} + \Phi f_u(\text{TBW} - \text{ECF}) \qquad (3.2)$$

published kinetic data can be used to estimate the tissue-binding affinity (Φ) of these drugs.

For many drugs, the extent of tissue binding is related to their lipophilicity. Although the octanol/water partition coefficient (P_{oct}) measured at pH 7.4 is the *in vitro* parameter traditionally used to characterize lipophilicity and is appropriate for neutral compounds, this coefficient fails to take into account the fact that many acidic and basic drugs are ionized at physiological pH. Because only an unionized drug generally partitions into tissues, a distribution coefficient (D_{oct}) is thought to provide a better correlation with the extent to which a drug distributes into tissues (6). Thus, for drugs that are monoprotic bases,

$$\log D_{oct} = \log P_{oct} + \left[1/\left(1 + 10^{\text{p}K_a - \text{pH}}\right)\right]$$

where pK_a is the dissociation constant of the drug. For monoprotic acids, the exponent in this equation becomes pH$-$pK_a. In Figure 3.2, published experimentally determined values for log D_{oct} are compared with estimates of log Φ. Equation 3.2 was rearranged to calculate Φ from literature values for f_u and distribution volume (7, 8), and from estimates of ECF (0.16 L/kg) and TBW (0.65 L/kg) that were obtained from a study of inulin and urea distribution kinetics (3).

Since the parameters f_u and D_{oct} can be obtained by *in vitro* measurements, Lombardo *et al.* (8) have used the reverse of this type of approach to predict drug distribution volume in humans in order to evaluate its utility in compound optimization and selection during the early stages of drug development. Although this approach would not be expected to provide an accurate prediction of the distribution volume of drugs that bind to specific subcellular components, this is not necessarily the case. For example, digoxin incorporates a steroid molecule (aglycone) but is relatively polar because three glycoside (sugar) groups are attached to it. It is a neutral compound and has an octanol/water partition coefficient of 18, but also binds very tightly to the enzyme Na/K-ATPase that is present in most body tissues. Since digoxin is only 25% bound to plasma proteins ($f_u = 0.75$), Equation 3.2 can be used to estimate that a 536 L distribution volume of this drug corresponds to a Φ value of 20.4, consistent with the relationship between lipophilicity and tissue partitioning shown in Figure 3.2. However, an important consequence of the specificity

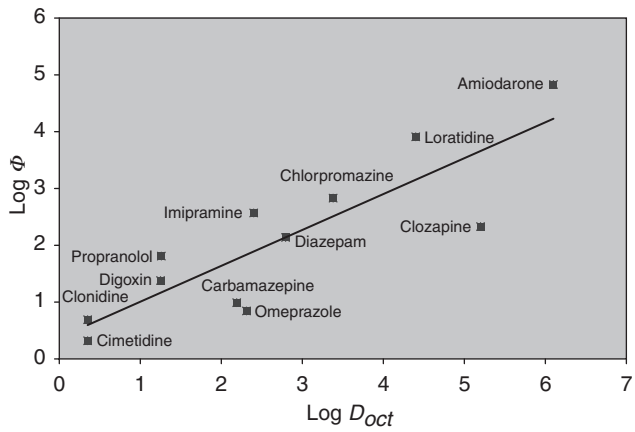

FIGURE 3.2 Relationship between lipophilicity, estimated from D_{oct}, and tissue/plasma partition ratio (Φ) for several commonly used drugs.

of this binding is that digoxin can be displaced from its Na/K-ATPase binding sites by concurrent administration of quinidine, causing a decrease in digoxin distribution volume (9). As discussed in Chapter 5, Sheiner *et al.* (10) also have shown that elevations in serum creatinine concentration, resulting from impaired renal function, are associated with decreases in digoxin distribution volume. This presumably reflects the same impairment in Na/K-ATPase activity that makes these patients more susceptible to toxicity when digoxin levels are $\geq$3.0 ng/mL (11).

PHYSIOLOGICAL BASIS OF MULTICOMPARTMENTAL MODELS OF DRUG DISTRIBUTION

Basis of Multicompartmental Structure

In 1937, Teorell (12) first used a multicompartmental system to model the kinetics of drug distribution. The two body distribution compartments of his model consisted of a central compartment corresponding to intravascular space and a peripheral compartment representing nonmetabolizing body tissues. Drug elimination was modeled as proceeding from the central compartment. Drug transfer between compartments is characterized by *intercompartmental clearance*, a term coined by Sapirstein *et al.* (13) to describe the volume-independent parameter that quantifies the rate of analyte transfer between the compartments of a kinetic model. Thus, elimination clearance and intercompartmental clearance share the property of volume independence in that they are not affected by changes in compartment volume.

Although more can be learned about the process of drug distribution when the physiological identity of the model compartments can be established, most models used in pharmacokinetics are simply mathematical models that are developed without regard to underlying physiology (14). The number of model compartments is defined by analysis of experimental data and corresponds to the number of exponential phases present in the plot of plasma levels vs. time. In contrast to Teorell's model, the central compartment of most two-compartment models often exceeds expected values for intravascular space, and three-compartment models are required to model the kinetics of many other drugs. The situation has been further complicated by the fact that some drugs have been analyzed with two-compartment models on some occasions and with three-compartment models on others. To some extent, these discrepancies reflect differences in experimental design. Particularly for rapidly distributing drugs, a tri-exponential plasma-level-vs.-time curve is likely to be observed only when the drug is administered by rapid intravenous injection and blood samples are obtained frequently in the immediate postinjection period.

The central compartment of a pharmacokinetic model usually is the only one that is directly accessible to sampling. When attempting to identify this compartment as intravascular space, the erythrocyte/plasma partition ratio must be incorporated in comparisons of central compartment volume with expected blood volume if plasma levels, rather than whole blood levels, are used for pharmacokinetic analysis. Models in which the central compartment corresponds to intravascular space are of particular interest because the process of distribution from the central compartment then can be identified as transcapillary exchange (Figure 3.3). In three-compartment models of this type, it might be tempting to conclude that the two peripheral compartments were connected in series (*catenary* model) and represented interstitial fluid space and intracellular water. Urea is a marker of TBW and the kinetics of its distribution could be analyzed with a three-compartment catenary model of this type. On the other hand, a three-compartment model is also required to model distribution of inulin from a central compartment that corresponds to plasma volume. This implies that interstitial fluid is kinetically heterogeneous and suggests that the

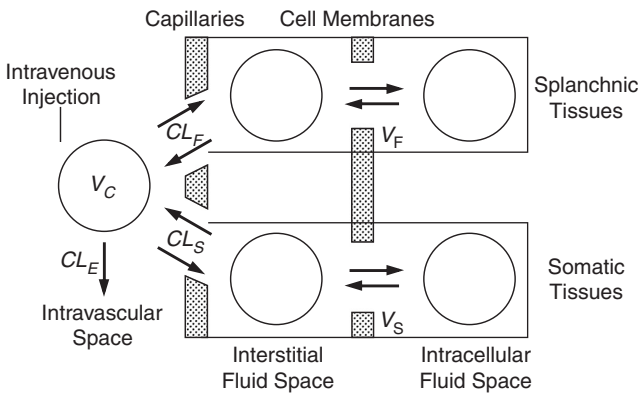

FIGURE 3.3 Multicompartmental model of the kinetics of inulin and urea distribution and elimination. After injection into a central compartment corresponding to intravascular space (V_C), both compounds distribute to rapidly (V_F) and slowly (V_S) equilibrating peripheral compartments (*rectangles*), at rates of transcapillary exchange that are characterized by intercompartmental clearances CL_F and CL_S. These peripheral compartments contain both interstitial and intracellular fluid components but transfer of urea between them is too rapid to be distinguished kinetically. Inulin is limited in its distribution to the interstitial fluid components of the peripheral compartments. (Reproduced with permission from Odeh YK, Wang Z, Ruo TI, Wang T, Frederiksen MC, Pospisil PA, Atkinson AJ Jr. Clin Pharmacol Ther 1993;53:419–25.)

mammillary system shown in Figure 3.3 represents the proper configuration for modeling both inulin and urea distribution kinetics (1, 3).

The proposed physiological basis for this model is that transfer of relatively small polar compounds, such as urea and inulin, occurs rapidly across fenestrated and discontinuous capillaries that are located primarily in the splanchnic vascular bed, but proceeds more slowly through the interendothelial cell junctions of less porous capillaries that have a continuous basement membrane and are located primarily in skeletal muscle and other somatic tissues. Direct evidence to support this proposal has been provided by kinetic studies in which the volume of the rapidly equilibrating compartment was found to be reduced in animals whose spleen and lower intestine had been removed (15). Indirect evidence also has been provided by a study of the distribution and pharmacologic effects of *insulin*, a compound with molecular weight and extracellular distribution characteristics similar to those of *inulin*. As shown in Figure 3.4, insulin distribution kinetics were analyzed together with the rate of glucose utilization needed to stabilize plasma glucose concentrations (glucose clamp) (16). Since changes in the rate of glucose infusion paralleled the rise and fall of insulin concentrations in the slowly equilibrating peripheral compartment, it was inferred that this compartment is largely composed of skeletal muscle. This *pharmacokinetic–pharmacodynamic* (PK–PD) study is also of interest because it illustrates one of the few examples in which a distribution compartment can be plausibly identified as the site of drug action or *biophase*.

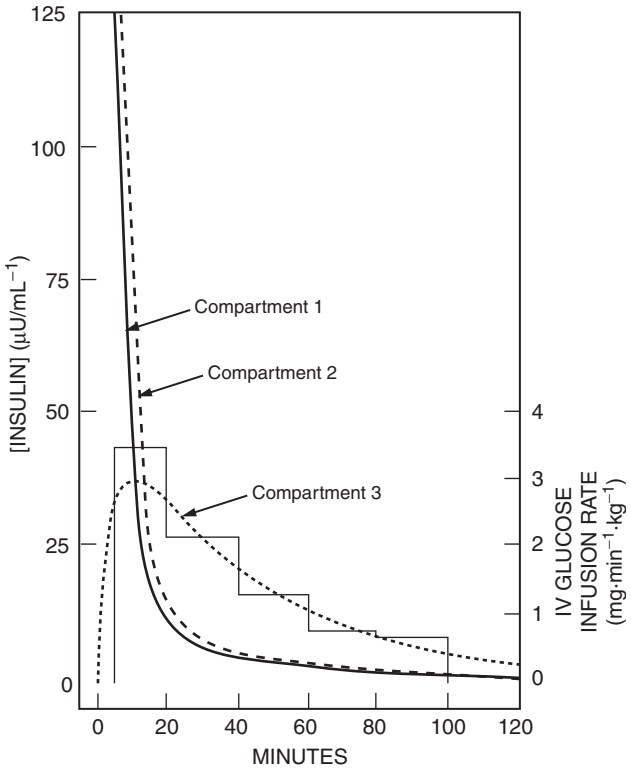

FIGURE 3.4 Measured plasma concentrations of insulin in compartment 1 (intravascular space) after intravenous injection of a 25-mU/kg dose, and computer-derived estimates of insulin concentration in presumed splanchnic (compartment 2) and somatic (compartment 3) components of interstitial fluid space. The bar graph indicates the glucose infusion rate needed to maintain blood glucose concentrations at the basal level. (Reproduced with permission from Sherwin RS, Kramer KJ, Tobin JD, Insel PA, Liljenquist JE, Berman M, Andres R. J Clin Invest 1974;53:1481–92.)

Mechanisms of Transcapillary Exchange

At this time, the physiological basis for the transfer of drugs and other compounds between compartments can only be inferred for mammillary systems in which the central compartment represents intravascular space and intercompartmental clearance can be equated with transcapillary exchange. In the case of inulin and urea, intercompartmental clearance (CL_I) can be analyzed in terms of the rate of blood flow (Q) through exchanging capillary beds and the permeability coefficient–surface area product ($P \cdot S$) characterizing diffusion through capillary fenestrae (primarily in splanchnic capillary beds) or small pores (primarily in somatic capillary beds). The following permeability-flow equation,[1] used by Renkin (17) for analyzing transcapillary exchange in an isolated perfused hind limb preparation,

$$CL_I = Q\left(1 - e^{-P \cdot S/Q}\right) \tag{3.3}$$

to be the first to have applied this equation to the transcapillary exchange of nongaseous solutes. He was guided in this effort by Christian Bohr's derivation of the equation in the context of pulmonary gas exchange (Skand Arch Physiol 1909;22:221–80). Seymour Kety based his derivation of the equation on Bohr's prior work and also applied it to pulmonary gas exchange (Pharmacol Rev 1951;3:1–41). Renkin's derivation was not published along with his original paper (17) but was archived by the American Documentation Institute (document 4648) and serves as the basis for the derivation published in reference 18. A final independent derivation was published by Christian Crone (Acta Physiol Scand 1963;54:292–305). Renkin concludes that the equation could be eponymously termed the *Bohr/Kety/Renkin/Crone Equation* but prefers to simply refer to it as the *flow-diffusion equation* (Renkin EM. Personal communication. December 10, 1999).

[1] There is a long history behind attempts to analyze transcapillary exchange in terms of its blood flow and diffusional permeability components. Eugene Renkin appears

subsequently was adapted to multicompartmental pharmacokinetic models (18). Because CL_I is replaced by two terms, Q and $P \cdot S$, it is necessary to study both inulin and urea distribution kinetics simultaneously. In order to estimate all the parameters characterizing the transcapillary exchange of these compounds, it is also necessary to assume that the ratio of their $P \cdot S$ values is the same as the ratio of their free water diffusion coefficients. However, when this is done, there is good agreement between the sum of blood flows to the peripheral compartments and independent measures of cardiac output (1, 3).

Although this approach seems valid for small, uncharged molecules, molecular charge appears to slow transcapillary exchange. Large molecular size also retards transcapillary exchange (19). Molecules considerably larger than inulin are probably transported through small-pore capillaries by convection rather than by diffusion (Figure 3.5). Conversely, very lipid-soluble compounds appear to pass directly though capillary walls at rates limited only by blood flow ($P \cdot S \gg Q$). Even though theophylline is a relatively polar compound, its transcapillary exchange is also blood-flow limited and presumably occurs by carrier-mediated facilitated diffusion (20). This leads to the classification shown in Table 3.1.

Although there have been few studies designed to interpret actual drug distribution results in physiological terms, a possible approach is to administer the drug under investigation along with reference compounds such as inulin and urea. This experimental design was used to show that theophylline distributed from intravascular space to two peripheral compartments that had intercompartmental clearances corresponding to the blood flow components of urea and inulin transcapillary exchange (20). It also should be emphasized that conventional kinetic studies do not have the resolving power to identify distribution to smaller

TABLE 3.1 Classification of Transcapillary Exchange Mechanisms

1. Diffusive transfer of small molecules (<6000 Da)
   - Transferred at rates proportional to their free water diffusion coefficients
     - Polar, uncharged compounds (e.g., urea, inulin)
   - Transferred more slowly than predicted from free water diffusion coefficients
     - Highly charged compounds (e.g., quaternary skeletal muscle relaxants)
     - Compounds with intermediate polarity that interact with capillary walls (e.g., procainamide)
   - Transferred more rapidly than predicted from free water diffusion coefficients
     - Highly lipid-soluble compounds that freely penetrate endothelial cells (e.g., anesthetic gases)
     - Compounds transferred by carrier-mediated facilitated diffusion (e.g., theophylline)
2. Convective transfer of large molecules (>50,000 Da)

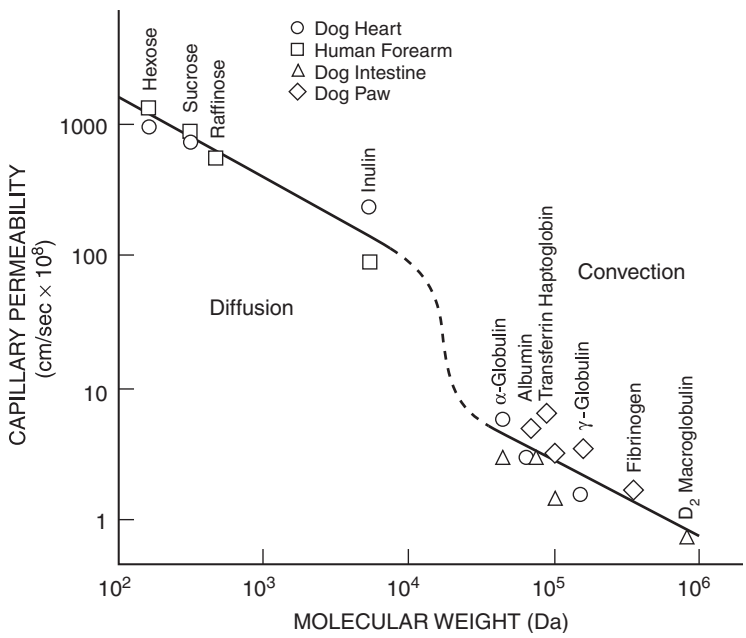

FIGURE 3.5 Plot of capillary permeability vs. molecular weight. (Reproduced with permission from Dedrick RL, Flessner MF. Prog Clin Biol Res 1989;288:429–38.)

but pharmacologically important regions such as the brain, in which transcapillary exchange is limited by tight junctions or by carrier-mediated active transport (e.g., P-glycoprotein).

CLINICAL CONSEQUENCES OF DIFFERENT DRUG DISTRIBUTION PATTERNS

As pointed out in Chapter 2, the process of drug distribution can account for both the slow onset of pharmacologic effect of some drugs (e.g., digoxin) and the termination of pharmacologic effect after bolus intravenous injection of others (e.g., lidocaine and thiopental). When theophylline was introduced in the 1930s, it was often administered by rapid intravenous injection to asthmatic patients. It was only after several fatalities were reported that the current practice was adopted of initiating therapy with a slow intravenous infusion. Nonetheless, excessively rapid intravenous administration of theophylline still contributes to the frequency of serious adverse reactions to this drug (21). The rapidity of carrier-mediated theophylline distribution to the brain and heart probably contributes to the infusion-rate dependency of these serious adverse reactions.

The impact of physiological changes on drug distribution kinetics has not been studied extensively. For example, it is known that pregnancy alters the elimination kinetics of many drugs. But physiological changes in body fluid compartment volumes and protein binding also affect drug distribution in pregnant subjects. As discussed in Chapter 22, Equation 3.1 has been used to correlate pregnancy-associated changes in theophylline distribution with this altered physiology (4). As described in Chapter 6, changes in intercompartmental clearance occur during hemodialysis and have important effects on the extent of drug removal during this procedure.

For most drugs whose plasma-level-vs.-time curve demonstrates more than one exponential phase, the terminal phase primarily, but not entirely, reflects the process of drug elimination, and the initial phase or phases primarily reflect the process of drug distribution. However, the sequence of *distribution* and *elimination phases* is reversed for some drugs, and these drugs are said to exhibit *"flip-flop" kinetics*. For example, Schentag and colleagues (22) have shown that the elimination phase precedes the distribution phase of gentamicin, an aminoglycoside antibiotic, and accounts for the long terminal half-life that is seen after a course of therapy (Figure 3.6). In this case, the central compartment of drug distribution probably corresponds to ECF. In one of the few studies in which drug concentrations were actually measured in human tissues, Schentag *et al.* (23) demonstrated that the kidneys account for the largest fraction of drug in the peripheral compartment. Although aminoglycosides are highly charged and do not passively diffuse across mammalian cell membranes, they are taken up by proximal renal tubular cells by a receptor-mediated

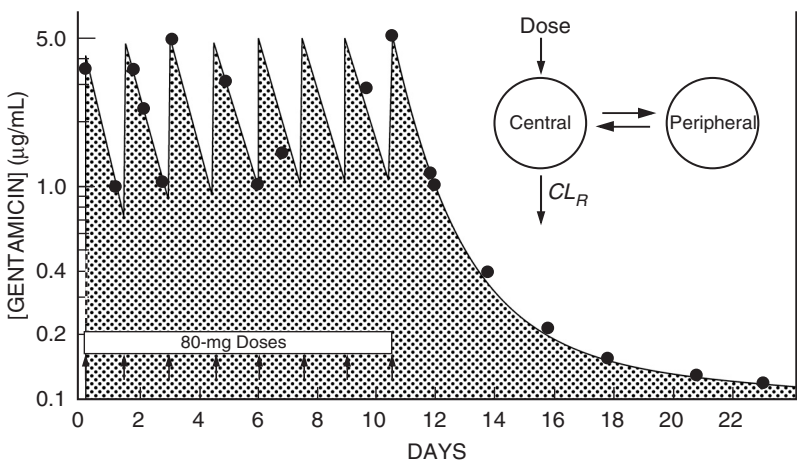

FIGURE 3.6 Serum gentamicin concentrations measured in a patient during and after a 10.5-day course of therapy (80 mg every 36 hrs). Data were analyzed with the two-compartment model shown in the figure. The half-life of serum levels during therapy is primarily reflective of renal elimination. The terminal half-life seen after therapy was stopped is the actual distribution phase. (Reproduced with permission from Schentag JJ, Jusko WJ, Plaut ME, Cumbo TJ, Vance JW, Abrutyn E. JAMA 1977;238:327–9.)

endocytic mechanism in which megalin serves as the endocytic receptor (24). The observation that the nephrotoxicity of aminoglycosides is less with intermittent than with continuous administration of the same total antibiotic dose (25) reflects the fact that their uptake by proximal renal tubule cells becomes saturated at the higher glomerular ultrafiltrate concentrations achieved with intermittent dosing (26). This also supports the rationale for once-daily rather than thrice-daily aminoglycoside dosing. Even when similar dose regimens are employed, the extent of tissue distribution is much greater in patients who have nephrotoxic reactions to gentamicin than it is in those whose renal function remains intact (Figure 3.7) (27).

In technical terms, we can say that the approximation of a single-compartment model represents *misspecification* of what is really a two-compartment system for gentamicin. However, the distribution phase for this drug is not even apparent until therapy is stopped. Nonetheless, the extent to which peak and/or trough levels rise during repetitive dosing can be used to provide an important clue to extensive gentamicin accumulation in the "tissue" compartment. Most clinical pharmacokinetic calculations are made with the initial assumption that gentamicin distributes in a single compartment that roughly corresponds to ECF. If the dose and dose interval are kept constant, steady-state peak and trough levels can be predicted simply by multiplying initial peak and trough levels by the *cumulation factor* (*CF*). As derived in Chapter 2,

$$CF = 1/(1 - e^{-k\tau}) \tag{3.4}$$

where k is $\ln 2/t_{1/2}$ and τ is the dosing interval. If peak and trough levels initially rise more rapidly than predicted from Equation 3.4, this reflects fact that substantial drug is accumulating in the "tissue" compartment. Of course, deterioration in renal function can also cause gentamicin peak and trough levels to increase, but usually this occurs after five or more days of therapy.

An important point about drugs that exhibit flip-flop kinetics is that the terminal exponential phase usually is reached only when plasma drug levels are subtherapeutic. For this reason, the half-life corresponding to this terminal exponential phase (greater than 4 days in the example shown in Figure 3.7) cannot be used in selecting an appropriate dosing interval. If the actual extent of drug accumulation is known from the ratio of steady-state/initial plasma levels, the observed cumulation factor (CF_{obs}) during repetitive dosing can be used to estimate an effective elimination

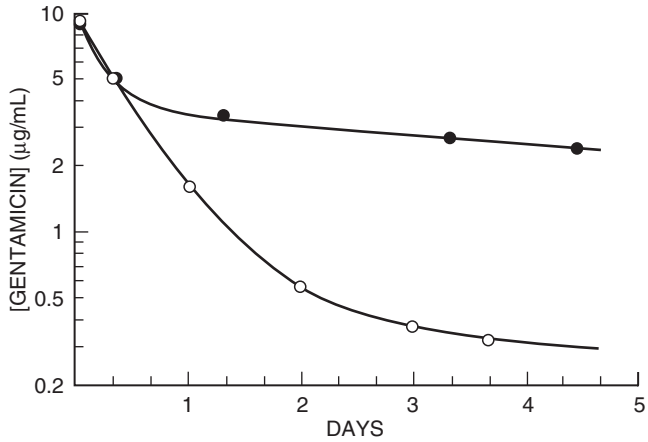

FIGURE 3.7 Decline in serum gentamicin concentrations after therapy was stopped in a patient with nephrotoxicity (•) and a patient who did not have this adverse reaction (○). Both patients had been treated with gentamicin at an 8-hour dosing interval and had nearly identical elimination-phase half-lives and peak and trough levels. (Reproduced with permission from Colburn WA, Schentag JJ, Jusko WJ, Gibaldi M. J Pharmacokinet Biopharm 1978;6:179–86.)

rate constant (k_{eff}) by rearranging Equation 3.4 to the form

$$k_{\text{eff}} = \frac{1}{\tau} \ln \left(\frac{CF_{obs}}{CF_{obs} - 1} \right)$$

and the effective half-life ($t_{1/2eff}$) can be calculated as

$$t_{1/2eff} = \ln 2/k_{eff}$$

The effective half-life can then be used to design dose regimens for drugs that have a terminal exponential phase representing the disposition of only a small fraction of the total drug dose (28).

ANALYSIS OF EXPERIMENTAL DATA

Derivation of Equations for a Two-Compartment Model

After rapid intravenous injection, sequentially measured plasma levels may follow a pattern similar to that shown by the solid circles in Figure 3.8. For most drugs, the elimination phase is reached when the data points fall on the line marked "β." The distribution phase occurs prior to that time. In this case, the curve contains two exponential phases and can be described by the following sum-of-exponentials *data equation*:

$$C = A'e^{-\alpha t} + B'e^{-\beta t} \tag{3.5}$$

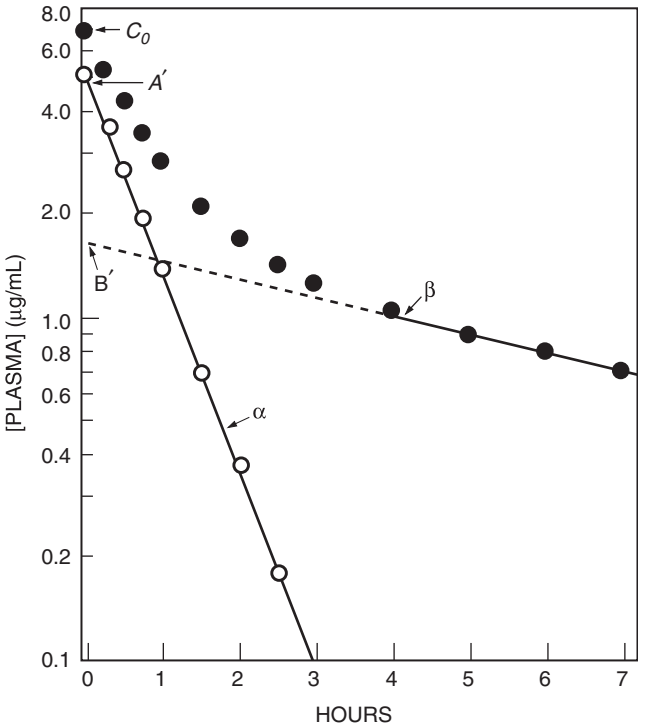

FIGURE 3.8 "Curve-peeling" technique used to estimate the coefficients and exponents of Equation 3.5. Data points (•) are plotted on semilogarithmic coordinates and the points for the α-curve (○) are obtained by subtracting back-extrapolated β-curve values from the experimental data.

where A', B', α, and β are the back-extrapolated intercepts and slopes shown in the figure. The drug concentration in the central compartment at time zero (C_0) equals the sum of $A' + B'$. For convenience in the derivation that follows, we normalize the values of these intercepts:

$$A = A'V_1/C_0V_1 = A'/C_0$$

$$B = B'V_1/C_0V_1 = B'/C_0$$

Since $A + B = 1$, the administered dose also has a normalized value of 1.

Because there are two exponential terms in the data equation, the data are consistent with a two-compartment model. The assumption usually is made that both intravenous administration and subsequent drug elimination proceed via the central compartment. Accordingly, the model is drawn as shown in Figure 3.9. We are interested in obtaining values for the parameters of this model in terms of the parameters of the data equation (Equation 3.5). Whereas the data equation is written in the concentration units of the data, the equations for the model shown in Figure 3.9 usually are developed in terms of the amounts of

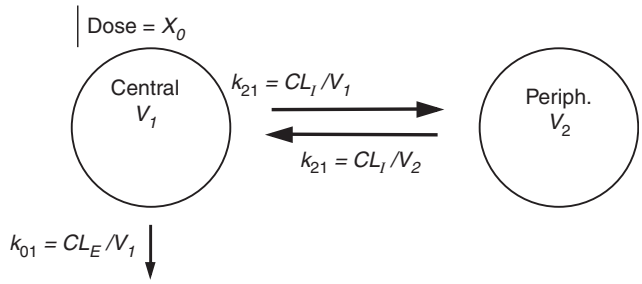

FIGURE 3.9 Schematic drawing of a two-compartment model with central and peripheral (Periph.) compartments. The number of primary model parameters (V_1, V_2, CL_E, and CL_I) that can be identified from the data cannot exceed the total number of coefficients and exponents in the data equation.

drug in each compartment (X_1 and X_2), the micro-rate constants describing drug transfer between or out of compartments (*ks*), and a single drug dose (X_0). The model can be described in terms of two first-order linear differential equations (*model equations*):

$$dX_1/dt = -k_{01}X_1 - k_{21}X_1 + k_{12}X_2$$

$$dX_2/dt = k_{21}X_1 - k_{12}X_2$$

Combining terms,

$$dX_1/dt = -(k_{01} + k_{21})X_1 + k_{12}X_2$$

$$dX_2/dt = k_{21}X_1 - k_{12}X_2$$

Laplace transforms can be used to transform this system of linear differential equations in the time domain into a system of linear equations in the Laplace domain. From the table of Laplace operations (Appendix I) we obtain

$$sX_1 - X_1(0) = -\left(k_{01} + k_{21}\right)X_1 + k_{12}X_2$$

$$sX_2 - X_2(0) = k_{21}X_1 - k_{12}X_2$$

If a single drug dose is injected intravenously, the entire administered dose is initially in compartment 1 and, because of normalization, $X_1(0)$ equals 1. The amount of drug in compartment 2 at zero time [$X_2(0)$] is 0. We can now write the following nonhomogeneous linear equations:

$$\left(s + k_{01} + k_{21}\right)X_1 - k_{12}X_2 = 1$$

$$-k_{21}X_1 + \left(s + k_{12}\right)X_2 = 0$$

The method of determinants (Cramer's Rule) can be used to solve the equations for each model compartment. However, we will focus only on the solution

for the central compartment, which is the one usually sampled for concentration measurements.

$$X_1 = \frac{\begin{vmatrix} 1 & -k_{12} \\ 0 & s+k_{12} \end{vmatrix}}{\begin{vmatrix} s+k_{01}+k_{21} & -k_{12} \\ -k_{21} & s+k_{12} \end{vmatrix}}$$

$$X_1 = \frac{s+k_{12}}{s^2 + (k_{01}+k_{21}+k_{12})\, s + k_{01}k_{12}} \tag{3.6}$$

This solution is in the form of a quotient of two polynomials, $P(s)/Q(s) \cdot Q(s)$ can be expressed in terms of its factors as follows:

$$X_1 = \frac{s+k_{12}}{(s+\alpha)\,(s+\beta)}$$

where the roots of the polynomial $Q(s)$ are $R_1 = -\alpha$ and $R_2 = -\beta$. The Heaviside Expansion Theorem states,

$$X_i = \sum_{i=1}^{n} \frac{P(R_i)}{Q'(R_i)}\, e^{R_i t}$$

Since

$$Q(s) = s^2 + (\alpha+\beta)\, s + \alpha\beta \tag{3.7}$$

$$Q'(s) = 2s + \alpha + \beta$$

Therefore,

$$X_1 = \frac{k_{12}-\alpha}{-2\alpha+\alpha+\beta} e^{-\alpha t} + \frac{k_{12}-\beta}{-2\beta+\alpha+\beta} e^{-\beta t}$$

$$X_1 = \frac{k_{12}-\alpha}{\beta-\alpha} e^{-\alpha t} + \frac{k_{12}-\beta}{\alpha-\beta} e^{-\beta t} \tag{3.8}$$

In order to estimate the model parameters from the data equation, we also need to specify the rate of drug elimination from the central compartment (V_1). The rate of elimination from this compartment, dE/dt, is given by the equation

$$dE/dt = k_{01} X_1$$

So total elimination is

$$E = k_{01} \int_0^\infty X_1\, dt$$

Since E equals the administered dose, which has been normalized to 1,

$$k_{01} = \frac{1}{\int_0^\infty X_1\, dt} \tag{3.9}$$

If X_1 is written in the form of the data equation (Equation 3.5),

$$X_1 = Ae^{-\alpha t} + Be^{-\beta t} \tag{3.10}$$

We obtain

$$\int_0^\infty X_1\, dt = -(A/\alpha)e^{-\alpha t} - (B/\beta)e^{-\beta t} \Big|_0^\infty$$

$$= A/\alpha + B/\beta$$

Substituting this result into Equation 3.9,

$$\boxed{k_{01} = \frac{1}{A/\alpha + B/\beta}} \tag{3.11}$$

By comparing Equations 3.6 and 3.7, it is apparent that,

$$Q(s) = s^2 + (k_{01}+k_{21}+k_{12})s + k_{01}k_{12}$$

So, from Equation 3.7,

$$\alpha + \beta = k_{01} + k_{21} + k_{12} \tag{3.12}$$

$$\alpha\beta = k_{01}k_{12} \tag{3.13}$$

Rearranging Equation 3.13,

$$k_{12} = \frac{\alpha\beta}{k_{01}}$$

Substituting for k_{01} as defined by Equation 3.11,

$$\boxed{k_{12} = \beta A + \alpha B} \tag{3.14}$$

Equation 3.12 can be rearranged to give

$$k_{21} = \alpha + \beta - k_{01} - k_{12}$$

$$= \alpha + \beta - \frac{\alpha\beta}{k_{12}} - k_{12}$$

$$= -\frac{k_{12}^2 - (\alpha+\beta)k_{12} + \alpha\beta}{k_{12}}$$

$$= -\frac{(k_{12}-\alpha)(k_{12}-\beta)}{k_{12}}$$

by comparing Equations 3.8 and 3.10,

$$A = \frac{k_{12} - \alpha}{\beta - \alpha}$$

so,

$$k_{12} - \alpha = -A(\alpha - \beta)$$

and

$$B = \frac{k_{12} - \beta}{\alpha - \beta}$$

so,

$$k_{12} - \beta = B(\alpha - \beta)$$

Therefore,

$$\boxed{k_{21} = \frac{AB(\alpha - \beta)^2}{k_{12}}} \qquad (3.15)$$

These techniques also can be applied to develop equations for three-compartment and other commonly used pharmacokinetic models.

Calculation of Rate Constants and Compartment Volumes from Data

Values for the data equation parameters can be obtained by the technique of "curve peeling" that was illustrated in Figure 3.8. After plotting the data, the first step is to identify the terminal exponential phase of the curve, in this case termed the *β-phase*, and then back-extrapolate this line to obtain the ordinate intercept (B'). It is easiest to calculate the value of β by first calculating the half-life of this phase. The value for β then can be estimated from the relationship $\beta = \ln 2/t_{1/2\beta}$. The next step is to subtract the corresponding value on the back-extrapolated β-phase line from each of the data point values obtained during the previous exponential phase. This generates the α-line from which the α-slope and A' intercept can be estimated.

After calculating the normalized intercept values A and B, the rate constants for the model can be obtained from Equations 3.11, 3.14, and 3.15. The volume of the central compartment is calculated from the ratio of the administered dose to the back-extrapolated value for C_0 (which equals $A' + B'$) as follows:

$$V_1 = \frac{\text{Dose}}{C_0}$$

Since $k_{21} = CL_I/V_1$, and $k_{12} = CL_I/V_2$,

$$k_{21}V_1 = k_{12}V_2$$

and

$$V_2 = V_1(k_{21}/k_{12})$$

The sum of V_1 and V_2 is termed the apparent volume of distribution at steady state ($V_{d(ss)}$) and is the third distribution volume that we have described. Note also that $CL_I = k_{21}V_1 = k_{12}V_2$.

Even though computer programs now are used routinely for pharmacokinetic analysis, most require initial estimates of the model parameters. As a result of the least-squares fitting procedures employed, these computer programs generally yield the most satisfactory results when the technique of curve peeling is used to make reasonably accurate initial estimates of parameter values.

Different Estimates of Apparent Volume of Distribution

The three estimates of distribution volume that we have encountered have slightly different properties (24). Of the three, $V_{d(ss)}$ has the strongest physiologic rationale for multicompartment systems of drug distribution. It is independent of the rate of both drug distribution and elimination, and is the volume that is referred to in Equations 3.1 and 3.2. On the other hand, estimates of $V_{d(area)}$ are most useful in clinical pharmacokinetics, since it is this volume that links elimination clearance to elimination half-life in the equation

$$t_{1/2} = \frac{0.693V_{d(area)}}{CL_E}$$

Because the single-compartment model implied by this equation makes no provision for the contribution of intercompartmental clearance to elimination half-life, estimates of $V_{d(area)}$ are larger than $V_{d(ss)}$.

Estimates of $V_{d(extrap)}$ are also based on a single-compartment model in which drug distribution is assumed to be infinitely fast. However, slowing of intercompartmental clearance reduces estimates of B', the back-extrapolated β-curve intercept in Figure 3.8, to a greater extent than it prolongs elimination half-life. As a result, $V_{d(extrap)}$ calculated from the equation

$$V_{d(extrap)} = \text{Initial dose}/B'$$

is even larger than $V_{d(area)}$. Thus, when the plasma-level-vs.-time curve includes more than a single

exponential component, the relationship of the three distribution volume estimates to each other is

$$V_{d(extrap)} > V_{d(area)} > V_{d(ss)}$$

REFERENCES

1. Atkinson AJ Jr, Ruo TI, Frederiksen MC. Physiological basis of multicompartmental models of drug distribution. Trends Pharmacol Sci 1991;12:96–101.
2. Larsen PR, Atkinson AJ Jr, Wellman HN, Goldsmith RE. The effect of diphenylhydantoin on thyroxine metabolism in man. J Clin Invest 1970;49:1266–79.
3. Odeh YK, Wang Z, Ruo TI, Wang T, Frederiksen MC, Pospisil PA, Atkinson AJ Jr. Simultaneous analysis of inulin and $^{15}N_2$-urea kinetics in humans. Clin Pharmacol Ther 1993;53:419–25.
4. Frederiksen MC, Ruo TI, Chow MJ, Atkinson AJ Jr. Theophylline pharmacokinetics in pregnancy. Clin Pharmacol Ther 1986;40:321–8.
5. Øie S, Tozer TN. Effect of altered plasma protein binding on apparent volume of distribution. J Pharm Sci 1979;68:1203–5.
6. Lombardo F, Shalaeva MY, Tupper KA, Gao F. $ElogD_{oct}$: A tool for lipophilicity determination in drug discovery. 2. Basic and neutral compounds. J Med Chem 2001;44:2490–7.
7. Thummel KE, Shen DD. Design and optimization of dosage regimens: Pharmacokinetic data. In: Hardman JG, Limbird LE, Gilman AG, eds. Goodman & Gilman's The pharmacological basis of therapeutics. 10th ed. New York: McGraw-Hill; 2001. p. 1924–2023.
8. Lombardo F, Obach RS, Shalaeva MY, Gao F. Prediction of human volume of distribution values for neutal and basic drugs. 2. Extended data set and leave-class-out statistics. J Med Chem 2004;47:1242–50.
9. Hager WD, Fenster P, Mayersohn M, Perrier D, Graves P, Marcus FI, Goldman S. Digoxin–quinidine interaction: Pharmacokinetic evaluation. N Engl J Med 1979;300:1238–41.
10. Sheiner LB, Rosenberg B, Marathe VV. Estimation of population characteristics of pharmacokinetic parameters from routine clinical data. J Pharmacokinet Biopharm 1977;5:445–79.
11. Piergies AA, Worwag EW, Atkinson AJ Jr. A concurrent audit of high digoxin plasma levels. Clin Pharmacol Ther 1994;55:353–8.
12. Teorell T. Kinetics of distribution of substances administered to the body: I. The extravascular modes of administration. Arch Intern Pharmacodyn 1937;57:205–25.
13. Sapirstein LA, Vidt DG, Mandel MJ, Hanusek G. Volumes of distribution and clearances of intravenously injected creatinine in the dog. Am J Physiol 1955;181:330–6.
14. Berman M. The formulation and testing of models. Ann NY Acad Sci 1963;108:192–4.
15. Sedek GS, Ruo TI, Frederiksen MC, Frederiksen JW, Shih S-R, Atkinson AJ Jr. Splanchnic tissues are a major part of the rapid distribution spaces of inulin, urea and theophylline. J Pharmacol Exp Ther 1989;251:963–9.
16. Sherwin RS, Kramer KJ, Tobin JD, Insel PA, Liljenquist JE, Berman M, Andres R. A model of the kinetics of insulin in man. J Clin Invest 1974; 53:1481–92.
17. Renkin EM. Effects of blood flow on diffusion kinetics in isolated perfused hindlegs of cats: A double circulation hypothesis. Am J Physiol 1953;183:125–36.
18. Stec GP, Atkinson AJ Jr. Analysis of the contributions of permeability and flow to intercompartmental clearance. J Pharmacokinet Biopharm 1981;9:167–80.
19. Dedrick RL, Flessner MF. Pharmacokinetic considerations on monoclonal antibodies. Prog Clin Biol Res 1989;288:429–38.
20. Belknap SM, Nelson JE, Ruo TI, Frederiksen MC, Worwag EM, Shin S-G, Atkinson AJ Jr. Theophylline distribution kinetics analyzed by reference to simultaneously injected urea and inulin. J Pharmacol Exp Ther 1987;243:963–9.
21. Camarta SJ, Weil MH, Hanashiro PK, Shubin H. Cardiac arrest in the critically ill. I. A study of predisposing causes in 132 patients. Circulation 1971;44:688–95.
22. Schentag JJ, Jusko WJ, Plaut ME, Cumbo TJ, Vance JW, Abrutyn E. Tissue persistence of gentamicin in man. JAMA 1977;238:327–9.
23. Schentag JJ, Jusko WJ, Vance JW, Cumbo TJ, Abrutyn E, DeLattre M, Gerbracht LM. Gentamicin disposition and tissue accumulation on multiple dosing. J Pharmacokinet Biopharm 1977;5:559–77.
24. Nagai J, Takano M. Molecular aspects of renal handling of aminoglycosides and strategies for preventing the nephrotoxicity. Drug Metab Pharmacokinet 2004;19:159–79.
25. Reiner NE, Bloxham DD, Thompson WL. Nephrotoxicity of gentamicin and tobramycin given once daily or continuously in dogs. J Antimicrob Chemother 1978;4(suppl A):85–101.
26. Verpooten GA, Giuliano RA, Verbist L, Eestermans G, De Broe ME. Once-daily dosing decreases renal accumulation of gentamicin and netilmicin. Clin Pharmacol Ther 1989;45:22–7.
27. Colburn WA, Schentag JJ, Jusko WJ, Gibaldi M. A model for the prospective identification of the prenephrotoxic state during gentamicin therapy. J Pharmacokinet Biopharm 1978;6:179–86.
28. Boxenbaum H, Battle M. Effective half-life in clinical pharmacology. J Clin Pharmacol 1995;35:763–66.
29. Gibaldi M, Perrier D. Pharmacokinetics. 2nd ed. New York: Marcel Dekker; 1982. p. 199–219.

STUDY PROBLEMS

1. Single-dose and steady-state multiple-dose plasma-level-vs.-time profiles of tolrestat, an aldose reductase inhibitor, were compared. The terminal exponential-phase half-life was 31.6 hours at the conclusion of multiple-dose therapy administered at a 12-hour dosing interval. However, there was little apparent increase in plasma concentrations with repetitive dosing, and the cumulation factor, based

on the area under the plasma concentration-vs.-time curve measurements, was only 1.29. Calculate the effective half-life for this drug. (*Reference*: Boxenbaum H, Battle M. Effective half-life in clinical pharmacology. J Clin Pharmacol 1995;35:763–6.)

2. The following data were obtained in a Phase I dose-escalation tolerance study after administering a 100-mg bolus of a new drug to a healthy volunteer:

Plasma Concentration Data

Time (hr)	[Plasma] (μg/mL)
0.10	6.3
0.25	5.4
0.50	4.3
0.75	3.5
1.0	2.9
1.5	2.1
2.0	1.7
2.5	1.4
3.0	1.3
4.0	1.1
5.0	0.9
6.0	0.8
7.0	0.7

   a. Use two-cycle, semilogarithmic graph paper to estimate α, β, A, and B by the technique of curve peeling.
   b. Draw a two-compartment model with elimination proceeding from the central compartment (V_1). Use Equations 3.11, 3.14, and 3.15 to calculate the rate constants for this model.
   c. Calculate the central compartment volume and the elimination and intercompartmental clearances for this model.
   d. Calculate the volume for the peripheral compartment for the model. Sum the central and peripheral compartment volumes to obtain $V_{d(ss)}$ and compare your result with the volume estimates, $V_{d(extrap)}$ and $V_{d(area)}$, that are based on the assumption that the β-slope represents elimination from a one-compartment model. Comment on your comparison.

CHAPTER

4

Drug Absorption and Bioavailability

ARTHUR J. ATKINSON, JR.
Clinical Center, National Institutes of Health, Bethesda, Maryland

DRUG ABSORPTION

The study of drug absorption is of critical importance in developing new drugs and in establishing the therapeutic equivalence of new formulations or generic versions of existing drugs. A large number of factors can affect the rate and extent of absorption of an oral drug dose. These are summarized in Figure 4.1.

Biopharmaceutic factors include drug solubility and formulation characteristics that impact the rate of drug disintegration and dissolution. From the physiologic standpoint, passive nonionic diffusion is the mechanism by which most drugs are absorbed once they are in solution. However, attention also has been focused on the role that specialized small-intestine transport systems play in the absorption of some drugs (1). Thus, levodopa, α-methyldopa, and baclofen are amino acid analogs that are absorbed from the small intestine by the large neutral amino acid (LNAA) transporter. Similarly, some amino-β-lactam antibiotics, captopril, and other angiotensin-converting enzyme inhibitors are absorbed via an oligopeptide transporter (PEPT-1), and salicylic acid and pravastatin via a monocarboxylic acid transporter.

Absorption by passive diffusion is largely governed by the molecular size and shape, degree of ionization, and lipid solubility of a drug. Classical explanations of the rate and extent of drug absorption have been based on the pH-partition hypothesis. According to this hypothesis, weakly acidic drugs are largely unionized and lipid soluble in acid medium, and hence should be absorbed best by the stomach. Conversely, weakly basic drugs should be absorbed primarily from the more alkaline contents of the small intestine. Absorption would not be predicted for drugs that are permanently ionized, such as quaternary ammonium compounds. In reality, the stomach does not appear to be a major site for the absorption of even acidic drugs. The surface area of the intestinal mucosa is so much greater than that of the stomach that this more than compensates for the decreased absorption rate per unit area. Table 4.1 shows results that were obtained when the stomach and small bowel of rats were perfused with solutions of aspirin at two different pH values (2). Even at a pH of 3.5, gastric absorption of aspirin makes only a small contribution to the observed serum level, and the rate of gastric absorption of aspirin is less than the rate of intestinal absorption even when normalized to organ protein content. Furthermore, it is a common misconception that the pH of resting gastric contents is always 1 to 2 (3). Values exceeding pH 7 may occur after meals, and achlorhydria is common in the elderly.

Since absorption from the stomach is poor, the rate of gastric emptying becomes a prime determinant of the rate of drug absorption. Two patterns of gastric motor activity have been identified that reflect whether the subject is fed or fasting (4, 5). Fasting motor activity has a cyclical pattern. Each cycle lasts 90 to 120 minutes and consists of the following four phases:

Phase 1: A period of quiescence lasting approximately 60 minutes.
Phase 2: A 40-minute period of persistent but irregular contractions that increase in intensity as the phase progresses.

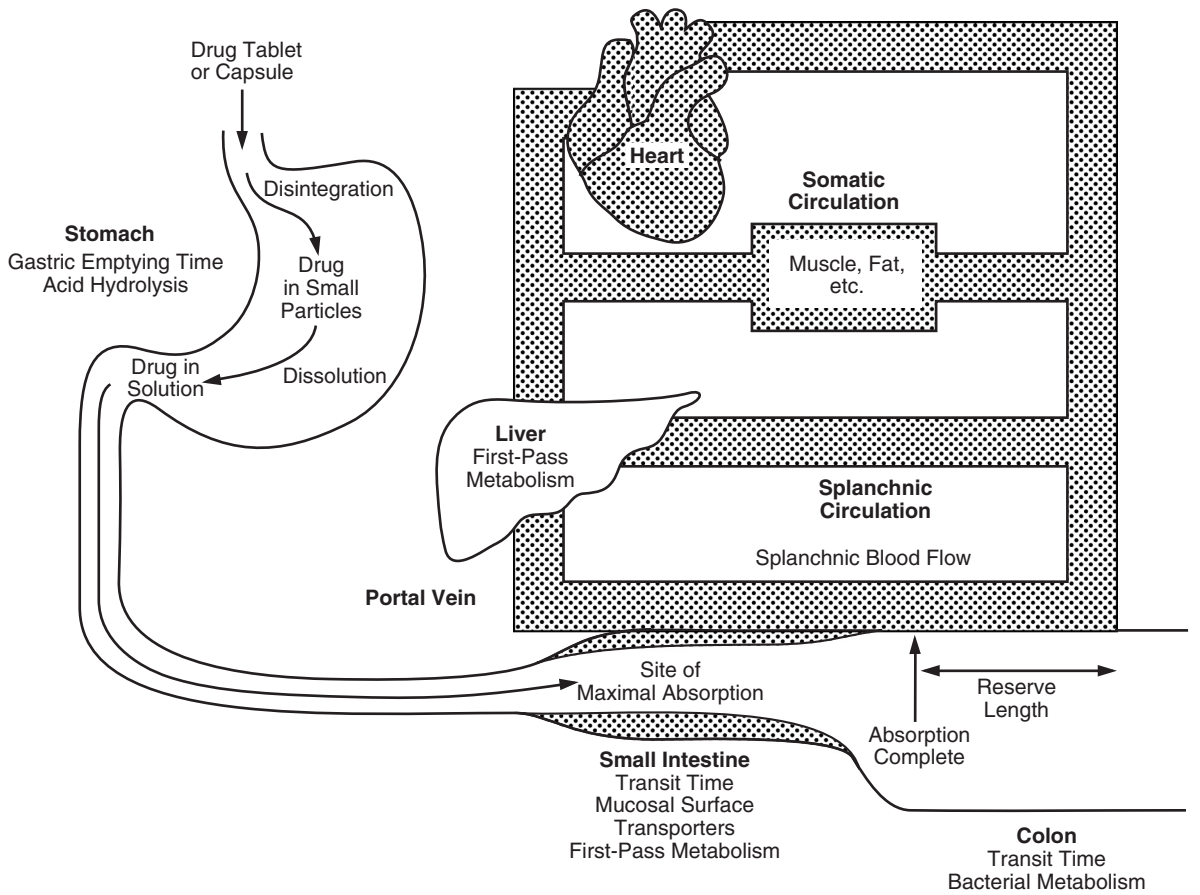

FIGURE 4.1 Summary of biopharmaceutic and physiologic processes that affect the rate and extent of absorption of an orally administered drug dose. Further explanation is provided in the text.

Phase 3: A short burst of intense contractions that are propagated distally from the stomach to the terminal ileum. These have been termed migrating motor complexes (MMCs), or "housekeeper waves."

Phase 4: A short period of transition with diminished contractile activity.

After feeding, the MMCs are inhibited and there is uncoupling of proximal and distal gastric motility such that the resting tone of the antrum is decreased. However, solid food stimulates intense and sustained antral contractions that reduce the particle size of gastric contents. The pylorus is partially constricted and, although liquids and particles less than 1 mm in diameter can pass through to the small bowel, larger particles are retained in the stomach. Studies employing γ-scintigraphy have confirmed that, as a result of these patterns of motor activity, a tablet taken in the fasting state will generally leave the stomach in less than two hours but may be retained in the stomach for more than ten hours if taken following a heavy meal (6).

Slow gastric emptying may not only retard drug absorption but, in some cases, may lead to less complete drug absorption as well. Thus, penicillin is degraded under acid conditions and levodopa is decarboxylated by enzymes in the gastric mucosa. Accordingly, patients should be advised to take these medications before meals. On the other hand, the prolonged gastric residence time that follows feeding may be needed to optimize the bioavailability of saquinavir and other drugs that are either poorly soluble or prepared in formulations that have a slow rate of

TABLE 4.1 Aspirin (ASA) Absorption from Simultaneously Perfused Stomach and Small Intestine[a]

pH	ASA absorption (μmol/100 mg protein/hr)		ASA serum level (mg/100 mL)
	Stomach	Small bowel	
3.5	346	469	20.6
6.5	0	424	19.7

[a]Data from Hollander D, Dadugalza VD, Fairchild PA. J Lab Clin Med 1981;98:591–8.

disintegration (7). Concurrent administration of drugs that modify gastric motility may also affect drug absorption. Hence, metaclopramide stimulates gastric emptying and has been shown to increase the rate of acetaminophen absorption, whereas propantheline delays gastric emptying and retards acetaminophen absorption (8).

Transit through the small intestine is more rapid than generally has been appreciated. Small-intestinal transit time averages 3 ± 1 hours ($\pm$SE), is similar for large and small particles, and is not appreciably affected by fasting or fed state (6). Rapid transit through the small intestine may reduce the bioavailability of compounds that either are relatively insoluble or are administered as extended release formulations that have an absorption window with little reserve length. *Reserve length* is defined as the anatomical length over which absorption of a particular drug can occur, less the length at which absorption is complete (Figure 4.1) (9). Digoxin is an important example of a compound that has marginal reserve length. Consequently, the extent of absorption of one formulation of this drug is influenced by small bowel motility, being decreased when coadministered with metoclopramide and increased when an atropinic was given shortly before the digoxin dose (10).

Administered drug also may be lost in transit through the intestine. Thus, digoxin is metabolized to inactive dihydro compounds by *Eubacterium lentum*, a constituent of normal bacterial flora in some individuals (11). In addition to their effects on gastrointestinal motility, drug–drug and food–drug interactions can have a direct effect on drug absorption (12). These interactions are discussed in Chapter 15. Mucosal integrity of the small intestine also may affect the bioavailability of drugs that have little reserve length. Thus, the extent of digoxin absorption was found to be less than one-third of normal in patients with D-xylose malabsorption due to sprue, surgical resection of the small intestine, or intestinal hypermotility (13). Splanchnic blood flow is another factor that can affect the rate and extent of drug absorption (14), but only a few clinical studies have been designed to demonstrate its significance (15).

Once absorbed, drugs can be metabolized before reaching the systemic circulation, either in their first pass through the intestinal mucosa or after delivery by the portal circulation to the liver. Hepatic first-pass metabolism of a number of drugs has been well studied and in many cases reflects the activity of cytochrome P450 enzymes (16). Cytochrome P450 (CYP) 3A4 plays the major role in the intestinal metabolism of drugs and other xenobiotics, and is strategically placed at the apex of intestinal villi (17). Studies in anhepatic patients have demonstrated that intestinal CYP3A4 may account for as much as half of the first-pass metabolism of cyclosporine that normally is observed (18).

P-Glycoprotein, an efflux transporter that shares considerable substrate specificity with CYP3A4, is also localized on the luminal membrane of intestinal epithelial cells, and may act in concert with intestinal CYP3A4 to reduce the net absorption of a variety of lipophilic drugs (19). Marzolini *et al*. (20) recently compiled a list of drugs that are P-glycoprotein substrates, and some of these are listed in Table 4.2 along

TABLE 4.2 Extent of Absorption (F) of Some P-Glycoprotein Substrates [a]

>70% Absorption		30–70% Absorption		<30% Absorption	
Drug	***F* (%)**	**Drug**	***F* (%)**	**Drug**	***F* (%)**
Phenobarbital	100	Digoxin	70	Cyclosporine	28
Levofloxacin	99	Indinavir	65	Tacrolimus	25
Methadone	92	Ondanseton	62	Morphine	24
Phenytoin	90	Cimetidine	60	Verapamil	22
Methylprednisolone	82	Clarithromycin	55	Nicardipine	18
Tetracycline	77	Itraconazole	55	Sirolimus	15
		Etoposide	52	Saquinavir	13
		Amitriptyline	48	Atorvastatin	12
		Amiodarone	46	Paclitaxel	10
		Diltiazem	38	Doxorubicin	5
		Losartan	36		
		Erythromycin	35		
		Chlorpromazine	32		

[a] Underlined drugs are also substrates for CYP3A4.

with the extent to which they are absorbed after oral administration (21). The underlined names indicate drugs that also are known to be CYP3A4 substrates. As expected, many of these drugs are poorly absorbed. However, what is surprising is that the absorption of some P-glycoprotein substrate drugs exceeds 70%. In part, this can be explained by the fact that some drugs reach millimolar concentrations in the intestinal lumen that exceed the Michaelis–Menten constant of P-glycoprotein, thus saturating this transport mechanism (19). This is particularly likely to occur with drugs (such as indinavir) that are administered in greater than 100-mg doses. In addition, P-glycoprotein transport is nondestructive, so, provided there is adequate reserve length, some of the drug that is extruded by P-glycoprotein in the proximal small intestine may be reabsorbed distally, as shown in Figure 4.2. On the other hand, repeated exposure to metabolism in the intestinal mucosa would further reduce the absorption of drugs that also are CYP3A4 substrates (19).

Morphine, organic nitrates, propranolol, lidocaine, and cyclosporine are some commonly used drugs that have extensive first-pass metabolism or intestinal P-glycoprotein transport. As a result, effective oral doses of these drugs are substantially higher than are intravenously administered doses. Despite the therapeutic challenge posed by presystemic elimination of orally administered drugs, first-pass metabolism provides important protection from some potentially noxious dietary xenobiotics. Thus, hepatocytes contain monamine oxidase that inactivates tyramine present in Chianti wine and in cheddar and other aged cheeses. Patients treated with monamine oxidase inhibitors lack this protective barrier, and tyramine in foods and beverages can reach the systemic circulation, causing norepinephrine release from sympathetic ganglia and potentially fatal hypertensive crises (22). On the other hand, first-pass sulfation of swallowed isoproterenol minimizes the systemic side effects experienced by patients using isoproterenol nebulizers.

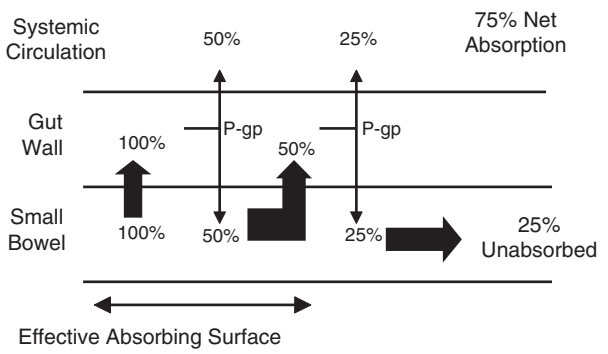

FIGURE 4.2 Possible explanation for >70% absorption of some P-glycoprotein (P-gp) substrates that have a reserve length that permits repeated absorption opportunities.

BIOAVAILABILITY

Bioavailability is the term most often used to characterize drug absorption. This term has been defined as the relative amount of a drug administered in a pharmaceutical product that enters the systemic circulation in an unchanged form, and the rate at which this occurs (23). Implicit in this definition is the concept that a comparison is being made. If the comparison is made between an oral and an intravenous formulation of a drug, which by definition has 100% bioavailability, the *absolute bioavailability* of the drug is measured. If the comparison is made between two different oral formulations, then the *relative bioavailability* of these formulations is determined. As shown in Figure 4.3, three indices of drug bioavailability usually are estimated: the maximum drug concentration in plasma (C_{max}), the time needed to reach this maximum (t_{max}), and the area under the plasma or serum-concentration-vs.-time curve (*AUC*). Generally there is also an initial lag period (t_{lag}) that occurs before drug concentrations are measurable in plasma.

The *AUC* measured after administration of a drug dose is related to the extent of drug absorption in the following way. Generalizing from the analysis of creatinine clearance that we presented in Chapter 1, the first-order differential equation

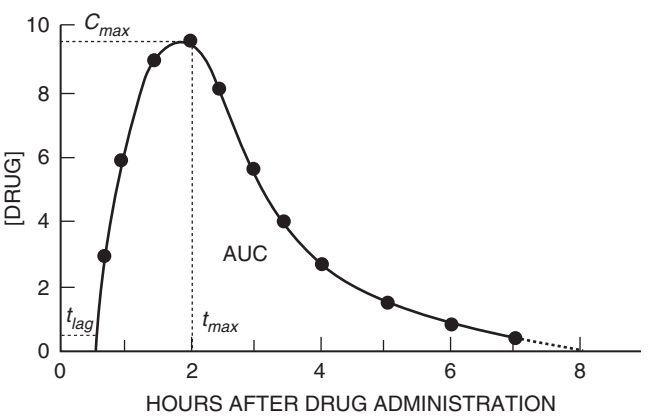

FIGURE 4.3 Hypothetical plasma concentration-vs.-time curve after a single oral drug dose. Calculation of the area under the plasma level-vs.-time curve (*AUC*) requires extrapolation of the elimination-phase curve beyond the last measurable plasma concentration, as shown by the dotted line.

describing rate of drug elimination from a single-compartment model is

$$dE/dt = CL \cdot C$$

where dE/dt is the rate of drug elimination, CL is the elimination clearance, and C is the concentration of drug in the compartment. Separating variables and integrating yields the result

$$E = CL \int_0^\infty C\,dt \tag{4.1}$$

where E is the total amount of drug eliminated in infinite time. By mass balance, E must equal the amount of the drug dose that is absorbed. The integral is simply the AUC. Thus, for an oral drug dose (D_{oral}),

$$D_{oral} \cdot F = CL \cdot AUC_{oral} \tag{4.2}$$

where F is the fraction of the dose that is absorbed and AUC_{oral} is the AUC resulting from the administered oral dose.

Absolute Bioavailability

In practice, absolute bioavailability most often is measured by sequentially administering single intravenous and oral doses (D_{IV} and D_{oral}) of a drug and comparing their respective $AUCs$. Extent of absorption of the oral dose can be calculated by modifying Equation 4.2 as follows:

$$\%\,\text{Absorption} = \frac{CL \cdot D_{IV} \cdot \text{AUC}_{oral}}{CL \cdot \text{D}_{oral} \cdot \text{AUC}_{IV}} \times 100$$

$$= \frac{D_{IV} \cdot \text{AUC}_{oral}}{D_{oral} \cdot \text{AUC}_{IV}} \times 100$$

A two-formulation, two-period, two-sequence crossover design is usually used to control for administration sequence effects. $AUCs$ frequently are estimated using the linear trapezoidal method, the log trapezoidal method, or a combination of the two (24). Alternatively, bioavailability can be assessed by comparing the amounts of unmetabolized drug recovered in the urine after giving the drug by the intravenous and oral routes. This follows directly from Equation 4.1, since urinary excretion accounts for a constant fraction of total drug elimination when drugs are eliminated by first-order kinetics.

In either case, the assumption usually is made that the elimination clearance of a drug remains the same in the interval between drug doses. This problem can be circumvented by administering an intravenous dose of the stable-isotope-labeled drug intravenously at the same time that the test formulation of unlabeled drug is given orally. Although the feasibility of this technique was first demonstrated in normal subjects (25), the method entails only a single study and set of blood samples and is ideally suited for the evaluation of drug absorption in patients, as shown in Figure 4.4 (15).

In this case, a computer program employing a least-squares fitting algorithm was used to analyze that data in terms of the pharmacokinetic model shown

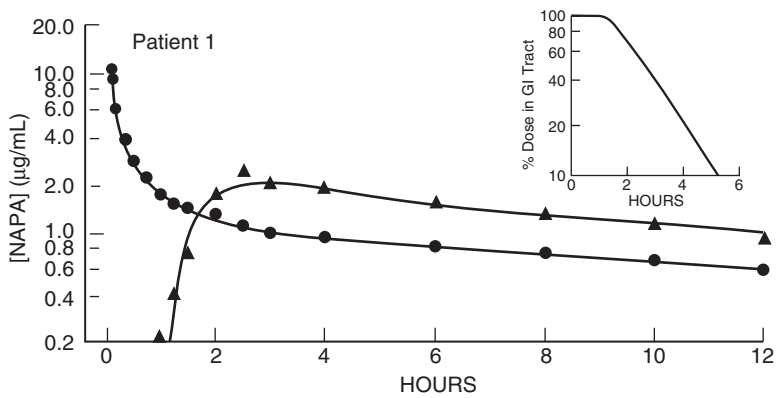

FIGURE 4.4 Kinetic analysis of plasma concentrations resulting from the intravenous injection of NAPA-^{13}C (•) and the simultaneous oral administration of a NAPA tablet (▲). The solid lines are a least-squares fit of the measured concentrations shown by the data points. The calculated percentage of the oral dose remaining in the gastrointestinal (GI) tract is plotted in the insert. (Reproduced with permission from Atkinson AJ, Jr. *et al*. Clin Pharmacol Ther 1989;46:182–9.)

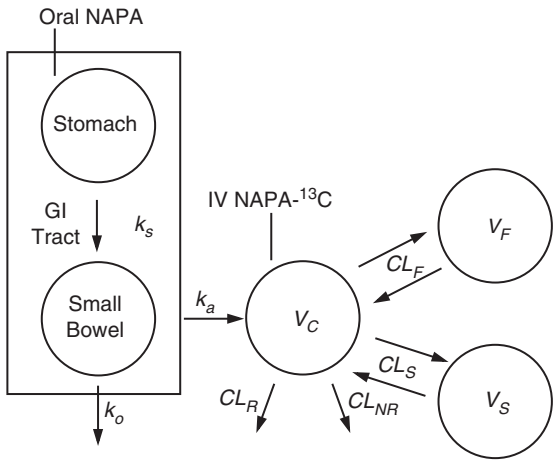

FIGURE 4.5 Multicompartment system used to model the kinetics of NAPA absorption, distribution, and elimination. NAPA labeled with ^{13}C was injected intravenously (IV) to define the kinetics of NAPA disposition. NAPA distribution from intravascular space (V_C) to fast (V_F) and slow (V_S) equilibrating peripheral compartments is characterized by the intercompartmental clearances CL_F and CL_S. NAPA is cleared from the body by both renal (CL_R) and nonrenal (CL_{NR}) mechanisms. A NAPA tablet was administered orally with the intravenous dose to analyze the kinetics of NAPA absorption from the gastrointestinal (GI) tract. After an initial delay that consisted of a time lag (not shown) and presumed delivery of NAPA to the small bowel (k_s), the rate and extent of NAPA absorption were determined by k_a and k_o, as described in the text. (Reproduced with permission from Atkinson AJ, Jr. *et al*. Clin Pharmacol Ther 1989;46:182–9.)

in Figure 4.5. The extent of *N*-acetylprocainamide (NAPA) absorption was calculated from model parameters representing the absorption rate (k_a) and nonabsorptive loss (k_o) from the gastrointestinal tract, as follows:

$$\% \text{ Absorption} = \frac{k_a}{k_a + k_o} \times 100$$

The extent of absorption also was assessed by comparing the 12-hour urine recovery of NAPA and NAPA-^{13}C. A correction was made to the NAPA recovery to compensate for the lag in NAPA absorption that was observed after the oral dose was administered. The results of these two methods of assessing extent of absorption are compared in Table 4.3. The discrepancy was less than 2% for all but one of the subjects.

Slow and incomplete absorption of procainamide has been reported in patients with acute myocardial infarction, and has been attributed to decreased splanchnic blood flow (26). Decreased splanchnic blood flow also may reduce the bioavailability of NAPA, the acetylated metabolite of procainamide. Although an explicit relationship between CL_F and k_a is not shown in Figure 4.5, splanchnic blood flow is proposed as a major determinant of CL_F, and it is noteworthy that the extent of NAPA absorption in patients was well correlated with CL_F estimates ($r = 0.89$, $p = 0.045$). This illustrates how a model-based approach can provide important insights into patient factors affecting drug absorption.

TABLE 4.3 Comparison of Bioavailability Estimates

Patient number	Kinetic analysis (%)	NAPA recovery in urine[a] (%)
1	66.1	65.9
2	92.1	92.1
3	68.1	69.9
4	88.2	73.1
5	75.7	75.6

[a]Corrected for absorption lag time.

Relative Bioavailability

If the bioavailability comparison is made between two oral formulations of a drug, then their relative bioavailability is measured. Two formulations generally are regarded as being *bioequivalent* if the 90% confidence interval of the ratios of the population average estimates of *AUC* and C_{max} for the test and reference formulations lie within a preestablished bioequivalence limit, usually 80–125% (27). Bioequivalence studies are needed during clinical investigation of a new drug product in order to ensure that different clinical trial batches and formulations have similar performance characteristics. They also are required when significant manufacturing changes occur after drug approval. Following termination of marketing exclusivity, generic drugs that are introduced are expected to be bioequivalent to the innovator's product. Population average metrics of the test and reference formulations have traditionally been compared to calculate an *average bioequivalence*. However, more sophisticated statistical approaches have been advocated to compare full population distributions or estimate intraindividual differences in bioequivalence (27).

Although *therapeutic equivalence* is assured if two formulations are bioequivalent, the therapeutic equivalence of two bioinequivalent formulations can be judged only within a specific clinical context (23). Thus, if we ordinarily treat streptococcal throat infections with a 10-fold excess of penicillin, a formulation having half the bioavailability of the usual formulation would be therapeutically equivalent, since it still would provide a 5-fold excess of antibiotic.

On the other hand, bioinequivalence of cyclosporine formulations, and of other drugs that have a narrow therapeutic index, could have serious therapeutic consequences.

In Vitro Prediction of Bioavailability

The introduction of combinatorial chemistry and high throughput biological screens has placed increasing stress on the technology that traditionally has been used to assess bioavailability. Insufficient time and resources are available to conduct formal *in vivo* kinetic studies for each candidate compound that is screened. Consequently, there is a clear need to develop *in vitro* methods that can be integrated into biological screening processes as reliable predictors of bioavailability. For reformulation of some immediate-release compounds it even is possible that *in vitro* data will suffice and that the requirement for repeated *in vivo* studies can be waived (28).

An important part of this development effort has been the establishment of a theoretical basis for drug classification that focuses on three critical biopharmaceutical properties: drug solubility relative to drug dose, dissolution rate of the drug formulation, and the intestinal permeability of the drug (29). Drug solubility can be measured *in vitro* and related to the volume of fluid required to dissolve the drug dose completely. *In vitro* dissolution tests have been standardized and are widely used for manufacturing quality control and in the evaluation of new formulations and generic products. However, proper selection of the apparatus and dissolution medium for these tests needs to be based on the physical chemistry of the drug and on the dosage form being evaluated (30). For immediate release products, a dissolution specification of 85% dissolved in less than 15 minutes has been proposed as sufficient to exclude decreases in bioavailability due to dissolution-rate limitations. Based on these considerations, the following biopharmaceutic drug classification has been established (29).

Class I — High solubility–high permeability drugs: Drugs in this class are well absorbed but their bioavailability may be limited either by first-pass metabolism or by P-glycoprotein-mediated efflux from the intestinal mucosa. *In vitro–in vivo* correlations of dissolution rate with the rate of drug absorption are expected if dissociation is slower than gastric emptying rate. If dissociation is sufficiently rapid, gastric emptying will limit absorption rate.

Class II — Low solubility–high permeability drugs: Poor solubility may limit the extent of absorption of high drug doses. The rate of absorption is limited by dissolution rate and generally is slower than for drugs in Class I. *In vitro–in vivo* correlations are tenuous in view of the many formulation and physiological variables that can affect the dissolution profile.

Class III — High solubility–low permeability drugs: Intestinal permeability limits both the rate and extent of absorption for this class of drugs and intestinal reserve length is marginal. Bioavailability is expected to be variable but, if dissolution is 85% complete in less than 15 minutes, this variability will reflect differences in physiological variables such as intestinal permeability and intestinal transit time.

Class IV — Low solubility–low permeability drugs: Effective oral delivery of this class of drugs presents the most difficulties, and reliable *in vitro–in vivo* correlations are not expected.

The rapid evaluation of the intestinal membrane permeability of drugs represents a continuing challenge. Human intubation studies have been used to measure jejeunal effective permeability of a number of drugs, and these measurements have been compared with the extent of drug absorption. It can be seen from Figure 4.6 that the expected fraction absorbed exceeds 95% for drugs with a jejeunal permeability of more than 2–4 $\times 10^{-4}$ cm/sec (29).

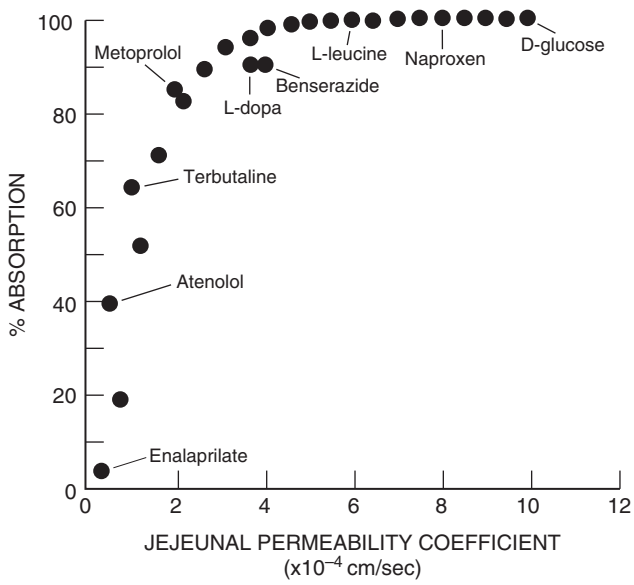

FIGURE 4.6 Relationship between jejeunal permeability measured by intestinal intubation and extent of absorption of a series of compounds. (Reproduced with permission from Amidon GL, Lennerås H, Shah VP, Crison JR. Pharm Res 1995;12:413–20.)

Although human intubation studies are even more laborious than formal assessment of absolute bioavailability, they have played an important role in validating *in vitro* methods that have been developed. The most commonly used *in vitro* method is based on measurement of drug transfer across a monolayer of cultured Caco-2 cells derived from a human colorectal carcinoma. Artursson and Karlsson (31) found that the apparent permeability of 20 drugs measured with the Caco-2 cell model was well correlated with the extent of drug absorption in human subjects, and that drugs with permeability coefficients exceeding 1×10^{-6} cm/sec were completely absorbed (Figure 4.7).

However, Caco-2 cells, being derived from colonic epithelium, have less paracellular permeability than does jejeunal mucosa, and the activity of drug-metabolizing enzymes, transporters, and efflux mechanisms in these cells does not always reflect what is encountered *in vivo*. In addition, the Caco-2 cell model provides no assessment of the extent of hepatic first-pass metabolism. Despite these shortcomings, this *in vitro* model has been useful in accelerating biological screening programs and further methodological improvements can be expected (32).

The ability of combinatorial chemistry to synthesize large numbers of compounds has stimulated interest in developing *in silico* methods that can predict bioavailability as part of the drug discovery process. Current computational methods can provide separate estimates of the solubility and intestinal permeability of candidate drug molecules even before they are synthesized (33). However, this approach has not yet been perfected, and the computational requirement of the most sophisticated models makes them suitable only for lead compound optimization. In addition, physiologically based models of the absorption milieu of different intestinal tract segments may be required to provide a more accurate estimate of the absorption of some drugs. The utility of this pharmacokinetic approach has been demonstrated in a study of the dose-dependent absorption of ganciclovir (34).

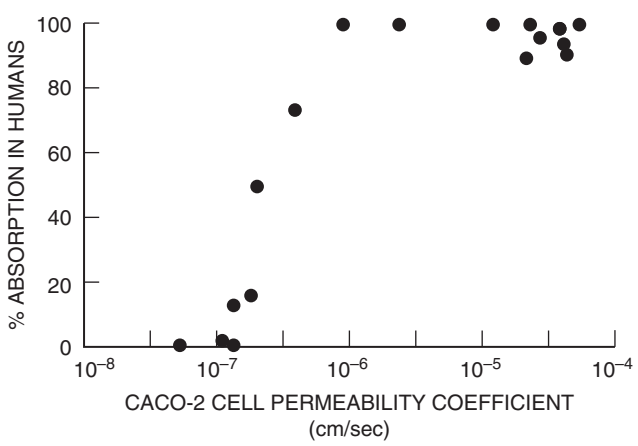

FIGURE 4.7 Relationship for a series of 20 compounds between apparent permeability coefficients in a Caco-2 cell model and the extent of absorption after oral administration to humans. (Reproduced with permission from Artursson P, Karlsson J. Biochem Biophys Res Commun 1991;175:880–5.)

KINETICS OF DRUG ABSORPTION AFTER ORAL ADMINISTRATION

After drug administration by the oral route, some time passes before any drug appears in the systemic circulation. This lag time (t_{lag}) reflects the time required for disintegration and dissolution of the drug product, and the time for the drug to reach the absorbing surface of the small intestine. After this delay, the plasma-drug-concentration-vs.-time curve shown in Figure 4.3 reflects the combined operation of the processes of drug absorption and of drug distribution and elimination. The peak concentration, $C_{\max}$, is reached when drug entry into the systemic circulation no longer exceeds drug removal by distribution to tissues, metabolism, and excretion. Thus, drug absorption is not completed when C_{max} is reached.

In Chapters 2 and 3 we analyzed the kinetic response to a bolus injection of a drug, an input that can be represented by a single impulse. Similarly, the input resulting from administration of an oral or intramuscular drug dose, or a constant intravenous infusion, can be regarded as a series of individual impulses, $G(\theta)\ d\theta$, where $G(\theta)$ describes the rate of absorption over a time increment between θ and $\theta + d\theta$. If the system is linear and the parameters are time invariant (35), we can think of the plasma response $[X(t)]$ observed at time t as resulting from the sum or integral over each absorption increment occurring at prior time θ $[G(\theta)\, d\theta, \text{where}\, 0 \leq \theta \leq t]$ reduced by the fractional drug disposition that occurs between θ and $t[H(t - \theta)]$, that is:

$$X(t) = \int_0^t G(\theta) \cdot H(t - \theta)\, d\theta$$

The function $H(t)$ describes drug disposition after intravenous bolus administration of a unit dose at time t. The interplay of these functions and associated physiological processes is represented schematically in Figure 4.8. This expression for $X(t)$ is termed the

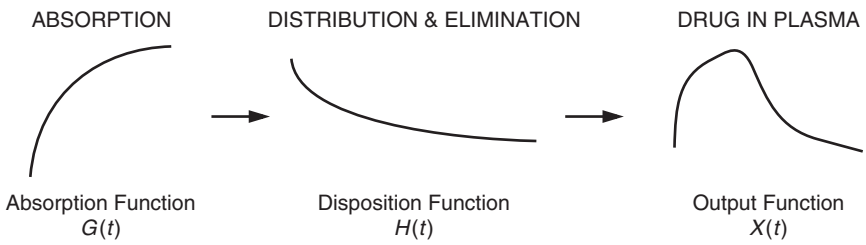

FIGURE 4.8 The processes of drug absorption and disposition (distribution and elimination) interact to generate the observed time course of drug in the body. Similarly, the output function can be represented as an interaction between absorption and disposition functions.

convolution of $G(t)$ and $H(t)$ and can be represented as

$$X(t) = G(t) * H(t)$$

where the operation of convolution is denoted by the symbol $*$. The operation of convolution in the time domain corresponds to multiplication in the domain of the subsidiary algebraic equation given by Laplace transformation. Thus, in Laplace transform notation,

$$x(s) = g(s) \cdot h(s)$$

In the disposition model shown in Figure 4.9, the kinetics of drug distribution and elimination are represented by a single compartment with first-order elimination as described by the equation

$$dH/dt = -kH$$

Since

$$\mathcal{L}F(t) = f(s)$$

and

$$\mathcal{L}F'(t) = sf(s) - F_0$$

then

$$sh(s) - H_0 = -k\,h(s)$$

H_0 is a unit impulse function, so $h(s)$ is given by

$$h(s) = \frac{1}{s+k} \tag{4.3}$$

Although the absorption process is quite complex, it often follows simple first-order kinetics. To obtain the appropriate absorption function, consider absorption under circumstances where there is no elimination (36). This can be diagrammed as shown in Figure 4.10. In this absorption model, drug disappearance from the gut is described by the equation

$$dM/dt = -aM$$

So,

$$M = M_0 e^{-at}$$

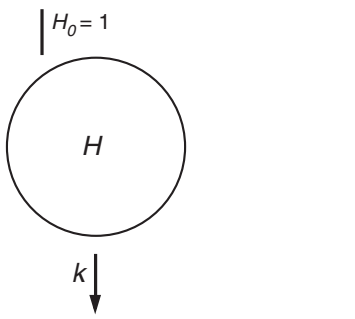

FIGURE 4.9 Disposition model representing the elimination of a unit impulse drug dose ($H_0 = 1$) from a single body compartment. Drug in this compartment (H) is removed as specified by the first-order elimination rate constant k.

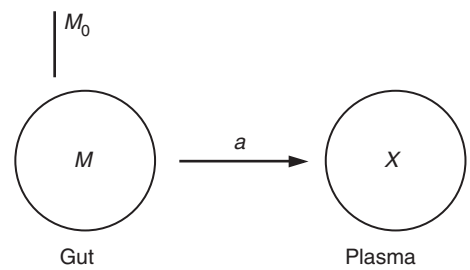

FIGURE 4.10 Model representing the absorption of a drug dose (M_0) from a gut compartment to a plasma compartment. The first-order absorption constant a determines the rate at which drug remaining in the gut (M) is transferred to plasma (X).

But the rate of drug appearance in plasma is

$$dX/dt = aM$$

The absorption function is defined as this rate, so $G(t)$ is

$$G(t) = aM_0e^{-at}$$

By definition,

$$g(s) = \int_0^\infty G(t)e^{-st}\,dt$$

So,

$$g(s) = aM_0 \int_0^\infty e^{-at}e^{-st}\,dt$$

$$g(s) = -\frac{aM_0}{s+a}e^{-(s+a)t}\Big|_0^\infty$$

Therefore,

$$g(s) = \frac{aM_0}{s+a} \tag{4.4}$$

Multiplication of Equations 4.3 and 4.4 gives

$$x(s) = g(s)\cdot h(s) = \frac{aM_0}{s+a}\cdot\frac{1}{s+k}$$

and

$$X(t) = \mathcal{L}^{-1}\frac{aM_0}{(s+a)(s+k)}$$

The table of inverse Laplace transforms shows that there are two solutions for this equation. Usually, $a \neq k$ and

$$X(t) = \frac{aM_0}{k-a}\left(e^{-at} - e^{-kt}\right) \tag{4.5}$$

In the special case, where $a = k$,

$$X(t) = aM_0t\,e^{-kt} \tag{4.6}$$

Time to Peak Level

The time needed to reach the peak level (t_{max}) can be determined by differentiating $X(t)$. For $a \neq k$,

$$X'(t) = \left[\frac{aM_0}{k-a}\right]\left(-ae^{-at} + ke^{-kt}\right)$$

At the peak level, $X'(t) = 0$. Therefore,

$$ke^{-kt_{max}} = ae^{-at_{max}} \tag{4.7}$$

$$a/k = e^{(a-k)t_{max}}$$

and

$$t_{max} = \frac{1}{a-k}\ln(a/k) \tag{4.8}$$

The absorption half-life is another kinetic parameter that can be calculated as $\ln 2/a$.

Value of Peak Level

The value of the peak level (C_{max}) can be estimated by substituting the value for t_{max} back into the equation for $X(t)$ For a $\neq k$, we can use Equation 4.7 to obtain

$$e^{-at_{max}} = \frac{k}{a}e^{-k_{max}}$$

Substituting this result into Equation 4.5

$$X_{max} = \frac{aM_0}{k-a}\left(\frac{k}{a} - 1\right)e^{-kt_{max}}$$

Hence

$$X_{max} = M_0e^{-kt_{max}}$$

But from Equation 4.8,

$$-kt_{max} = \frac{k}{k-a}\ln(a/k)$$

So,

$$e^{-kt_{max}} = (a/k)^{k/(k-a)}$$

Therefore,

$$X_{max} = M_0(a/k)^{k/(k-a)} \tag{4.9}$$

The maximum plasma concentration would then by given by $C_{max} = X_{max}/V_d$, where V_d is the distribution volume. It can be seen from Equations 4.8 and 4.9 that C_{max} and t_{max} are complex functions of both the absorption rate, a, and the elimination rate, k, of a drug.

Use of Convolution/Deconvolution to Assess *In Vitro–In Vivo* Correlations

Particularly for extended-release formulations, the simple characterization of drug absorption in terms of *AUC*, C_{max}, and t_{max} is inadequate and a more comprehensive comparison of *in vitro* test results with *in vivo* drug absorption is needed (37). Both $X(t)$, the output function after oral absorption, and $H(t)$, the disposition function, can be obtained from experimental data, and the absorption function, $G(t)$, can be estimated by the process of *deconvolution*. This process is the inverse of convolution and, in the Laplace domain, $g(s)$ can be obtained by dividing the transform of the output function, $x(s)$, by the transform of the disposition function, $h(s)$:

$$g(s) = x(s)/h(s)$$

Since this approach requires that $X(t)$ and $H(t)$ be defined by explicit functions, deconvolution is usually performed using numerical methods (38). Alternatively, the absorption function can be obtained from a pharmacokinetic model, as shown by the insert in Figure 4.4 (15). Even when this approach is taken, numerical deconvolution methods may be helpful in developing the appropriate absorption model (25). As a second step in the analysis, linear regression commonly is used to compare the time course of drug absorption with dissolution test results at common time points, as shown in Figure 4.11 (39). The linear relationship in this figure, with a slope and a coefficient of determination (R^2) of nearly one, would be expected primarily for Class I drugs. The nonzero intercept presumably reflects the time lag in gastric emptying.

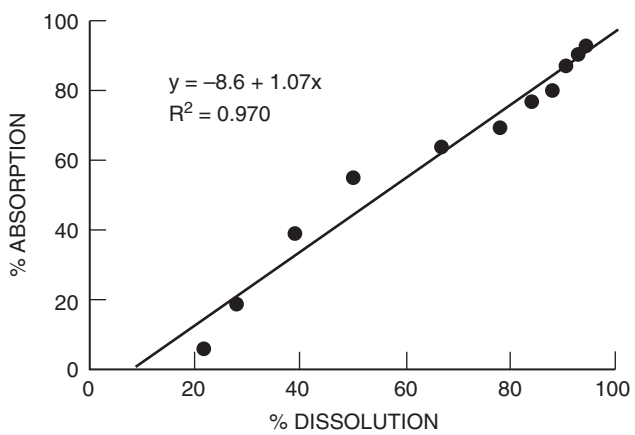

FIGURE 4.11 Linear regression comparing the extent of drug dissolution and oral absorption at common time points. (Reproduced with permission from Rackley RJ. Examples of *in vitro–in vivo* relationships with a diverse range of quality. In: Young D, Devane JG, Butler J, eds. *In vitro–in vivo* correlations. New York: Plenum Press; 1997. p. 1–15.)

Another approach is to convolute a function representing *in vitro* dissolution with the disposition function in order to predict the plasma-level-vs.-time curve following oral drug administration. Obviously, correlations will be poor if there is substantial first-pass metabolism of the drug or if *in vivo* conditions, such as rapid intestinal transit that results in inadequate reserve length, are not reflected in the dissolution test system.

REFERENCES

1. Tsuji A, Tamai I. Carrier-mediated intestinal transport of drugs. Pharm Res 1996;13:963–77.
2. Hollander D, Dadugalza VD, Fairchild PA. Intestinal absorption of aspirin: Influence of pH, taurocholate, ascorbate, and ethanol. J Lab Clin Med 1981; 98:591–8.
3. Meldrum SJ, Watson BW, Riddle HC, Sladen GE. pH profile of gut as measured by radiotelemetry capsule. Br Med J 1972;2:104–6.
4. Wilding IR, Coupe AJ, Davis SS. The role of γ-scintigraphy in oral drug delivery. Adv Drug Del Rev 1991;7:87–117.
5. Rees WDW, Brown CM. Physiology of the stomach and duodenum. In: Haubrich WS, Schaffner F, Berk JE, eds. Bockus gastroenterology. Philadelphia: WB Saunders; 1995. p. 582–614.
6. Davis SS, Hardy JG, Fara JW. Transit of pharmaceutical dosage forms through the small intestine. Gut 1986;27:886–92.
7. Kenyon CJ, Brown F, McClelland, Wilding IR. The use of pharmacoscintigraphy to elucidate food effects observed with a novel protease inhibitor (saquinavir). Pharm Res 1998;15:417–22.
8. Nimmo I, Heading RC, Tothill P, Prescott LF. Pharmacological modification of gastric emptying: Effects of propantheline and metclopromide on paracetamol absorption. Br Med J 1973;1:587–9.
9. Higuchi WI, Ho NFH, Park JY, Komiya I. Rate-limiting steps in drug absorption. In: Prescott LF, Nimmo WS, eds. Drug absorption. Sydney: ADIS Press; 1981. p. 35–60.
10. Manninen V, Melin J, Apajalahti A, Karesoja M. Altered absorption of digoxin in patients given propantheline and metoclopramide. Lancet 1973; 1:398–9.
11. Dobkin JF, Saha JR, Butler VP Jr, Neu HC, Lindenbaum J. Digoxin-inactivating bacteria: Identification in human gut flora. Science 1983;220:325–7.
12. Welling PG. Interactions affecting drug absorption. Clin Pharmacokinet 1984;9:404–34
13. Heizer WD, Smith TW, Goldfinger SE. Absorption of digoxin in patients with malabsorption syndromes. N Engl J Med 1971;285:257–9.
14. Winne D. Influence of blood flow on intestinal absorption of xenobiotics. Pharmacology 1980; 21:1–15.

15. Atkinson AJ Jr, Ruo TI, Piergies AA, Breiter HC, Connelly TJ, Sedek GS, Juan D, Hubler GL, Hsieh A-M. Pharmacokinetics of *N*-acetylprocainamide in patients profiled with a stable isotope method. Clin Pharmacol Ther 1989;46:182–9.
16. Watkins PB. Drug metabolism by cytochromes P450 in the liver and small bowel. Gastroenterol Clin N Am 1992;21:511–26.
17. Doherty MM, Charman WN. The mucosa of the small intestine. How clinically relevant as an organ of drug metabolism? Clin Pharmacokinet 2002;41:235–53.
18. Kolars JC, Merion RM, Awni WM, Watkins PB. First-pass metabolism of cyclosporine by the gut. Lancet 1991;338:1488–90.
19. Lin JH. Drug–drug interaction mediated by inhibition and induction of P-glycoprotein. Adv Drug Deliv Rev 2003;55:53–81.
20. Marzolini C, Paus E, Buclin T, Kim R. Polymorphisms in human MDR1 (P-glycoprotein): Recent advances and clinical relevance. Clin Pharmacol Ther 2004;75:13–33.
21. Thummel KE, Shen DD. Design and optimization of dosage regimens: Pharmacokinetic data. In: Hardman JG, Limbird LE, Gilman AG, eds. Goodman & Gilman's The pharmacological basis of therapeutics. 10th ed. New York: McGraw-Hill; 2001. p. 1924–2023.
22. Lippman SB, Nash K. Monamine oxidase inhibitor update. Potential adverse food and drug interactions. Drug Saf 1990;5:195–204.
23. Koch-Weser J. Bioavailability of drugs. N Engl J Med 1974;291:233–7, 503–6.
24. Yeh KC, Kwan KC. A comparison of numerical integrating algorithms by trapezoidal, Lagrange, and spline approximation. J Pharmacokinet Biopharm 1978;6:79–98.
25. Strong JM, Dutcher JS, Lee W-K, Atkinson AJ Jr. Absolute bioavailability in man of *N*-acetylprocainamide determined by a novel stable isotope method. Clin Pharmacol Ther 1975;18:613–22.
26. Koch-Weser J. Pharmacokinetics of procainamide in man. Ann NY Acad Sci 1971;179:370–82.
27. Patnaik, RN, Lesko LJ, Chen ML, Williams RL. The FDA Individual Bioequivalence Working Group. Individual bioequivalence: New concepts in the statistical assessment of bioequivalence metrics. Clin Pharmacokinet 1997;33:1–6.
28. Biopharmaceutic Classification Working Group, Biopharmaceutics Coordinating Committee, CDER. Waiver of *in vivo* bioavailability and bioequivalence studies for immediate-release solid oral dosage forms based on a biopharmaceutics classification system. Guidance for Industry, Rockville: FDA; 2000. (Internet at http://www.fda.gov/cder/guidance/index.htm.)
29. Amidon GL, Lennerås H, Shah VP, Crison JR. A theoretical basis for a biopharmaceutic drug classification: The correlation of *in vitro* drug product dissolution and *in vivo* bioavailability. Pharm Res 1995;12:413–20.
30. Rohrs BR, Skoug JW, Halstead GW. Dissolution assay development for *in vitro–in vivo* correlations: Theory and case studies. In: Young D, Devane JG, Butler J, eds. *In vitro–in vivo* correlations. New York: Plenum Press; 1997. p. 17–30.
31. Artursson P, Karlsson J. Correlation between oral drug absorption in humans and apparent drug permeability coefficients in human intestinal epithelial (Caco-2) cells. Biochem Biophys Res Commun 1991;175:880–5.
32. Artursson P, Borchardt RT. Intestinal drug absorption and metabolism in cell cultures: Caco-2 and beyond. Pharm Res 1997;14:1655–8.
33. Stenberg P, Bergström CAS, Luthman K, Artursson P. Theoretical predictions of drug absorption in drug discovery and development. Clin Pharmacokinet 2002;41:877–99.
34. Norris DA, Leesman GD, Sinko PJ, Grass GM. Development of predictive pharmacokinetic simulation models for drug discovery. J Control Release 2000;65:55–62.
35. Sokolnikoff IS, Redheffer RM. Mathematics of physics and modern engineering. 2nd ed. New York: McGraw-Hill; 1966. p. 224.
36. Atkinson AJ Jr, Kushner W. Clinical pharmacokinetics. Annu Rev Pharmacol Toxicol 1979;19:105–27.
37. Langenbucher F, Mysicka J. *In vitro* and *in vivo* deconvolution assessment of drug release kinetics from oxprenolol Oros preparations. Br J Clin Pharmacol 1985;19:151S–62S.
38. Vaughan DP, Dennis M. Mathematical basis of point-area deconvolution method for determining *in vivo* input functions. J Pharm Sci 1978;67:663–5.
39. Rackley RJ. Examples of *in vitro–in vivo* relationships with a diverse range of quality. In: Young D, Devane JG, Butler J, eds. *In vitro–in vivo* correlations. New York: Plenum Press; 1997. p. 1–15.

STUDY PROBLEMS

1. An approach that has been used during drug development to measure the absolute bioavailability of a drug is to administer an initial dose intravenously in order to estimate the area under the plasma-level-vs.-time curve from zero to infinite time (AUC). Subjects then are begun on oral therapy. When steady state is reached, the AUC during a dosing interval ($AUC_{0\rightarrow\tau}$) is measured. The extent of absorption of the oral formulation is calculated from the following equation:

$$\%\ \text{Absorption} = \frac{D_{IV} \cdot AUC_{0\rightarrow\tau(oral)}}{D_{oral} \cdot AUC_{IV}} \times 100$$

   This approach requires AUC to equal $AUC_{0\rightarrow\tau}$ if the same doses are administered intravenously and orally and the extent of absorption is 100%. Derive the proof for this equality.
2. When a drug is administered by constant intravenous administration, this zero-order input can be represented by a "step function." Derive the appropriate absorption function and convolute it with the disposition function to obtain the output function.

(*Clue:* Remember that the absorption function is the *rate* of drug administration.)

3. A 70-kg patient is treated with an intravenous infusion of lidocaine at a rate of 2 mg/min. Assume a single-compartment distribution volume of 1.9 L/kg and an elimination half-life of 90 minutes.
   a. Use the output function derived in Problem 2 to predict the expected steady-state plasma lidocaine concentration.
   b. Use this function to estimate the time required to reach 90% of this steady-state level.
   c. Express this 90% equilibration time in terms of number of elimination half-lives.

This page intentionally left blank

CHAPTER

5

Effects of Renal Disease on Pharmacokinetics

ARTHUR J. ATKINSON, JR.[1] **AND MARCUS M. REIDENBERG** [2]

[1]*Clinical Center, National Institutes of Health, Bethesda, Maryland*
[2]*Weill Medical College of Cornell University, New York, New York*

A 67-year-old man had been functionally anephric, requiring outpatient hemodialysis for several years. He was hospitalized for revision of his arteriovenous shunt and postoperatively complained of symptoms of gastroesophageal reflux. This complaint prompted institution of cimetidine therapy. In view of the patient's impaired renal function, the usually prescribed dose was reduced by half. Three days later, the patient was noted to be confused. An initial diagnosis of dialysis dementia was made and the family was informed that dialysis would be discontinued. On teaching rounds, the suggestion was made that cimetidine be discontinued. Two days later the patient was alert and was discharged from the hospital to resume outpatient hemodialysis therapy.

Although drugs are developed to treat patients who have diseases, relatively little attention has been given to the fact that these diseases themselves exert important effects that affect patient response to drug therapy. Accordingly, the case presented here is an example from the past that illustrates a therapeutic problem that persists today. In the idealized scheme of contemporary drug development that was shown in Figure 1.1 (Chapter 1), the pertinent information would be generated in pharmacokinetic–pharmacodynamic (PK–PD) studies in special populations that are carried out concurrently with Phase II and Phase III clinical trials (1). Additional useful information can be obtained by using population pharmacokinetic methods to analyze data obtained in the large-scale Phase III trials themselves (2). However, a review of labeling in the *Physician's Desk Reference* indicates that there often is scant information available to guide dose selection for individual patients (3).

Illness, aging, sex, and other patient factors may have important effects on *pharmacodynamic* aspects of patient response to drugs. For example, patients with advanced pulmonary insufficiency are particularly sensitive to the respiratory depressant effects of narcotic and sedative drugs. In addition, these patient factors may affect the *pharmacokinetic* aspects of drug elimination, distribution, and absorption. In this regard, renal impairment has been estimated to account for one-third of the prescribing errors resulting from inattention to patient pathophysiology (4). Even when the necessary pharmacokinetic and pharmacodynamic information is available, appropriate dose adjustments often are not made for patients with impaired renal function because assessment of this function usually is based solely on serum creatinine measurements without concomitant estimation of creatinine clearance (5).

Because there is a large population of functionally anephric patients who are maintained in relatively stable condition by hemodialysis, a substantial number of pharmacokinetic studies have been carried out in these individuals. Patients with intermediate levels of impaired renal function have not been studied to the same extent, but studies in these patients are recommended in current FDA guidelines (5).

EFFECTS OF RENAL DISEASE ON DRUG ELIMINATION

The effects of decreased renal function on drug elimination have been examined most extensively. This is appropriate, since only elimination clearance (CL_E) and drug dose determine the steady-state concentration of drug in the body (C_{ss}). This is true whether the drug is given by constant intravenous infusion (I), in which case:

$$C_{ss} = I/CL_E \tag{5.1}$$

or by intermittent oral or parenteral doses, in which case the corresponding equation is:

$$\overline{C}_{ss} = \frac{\text{Dose}/\tau}{CL_E} \tag{5.2}$$

where $\overline{C}_{ss}$ is the mean concentration during the dosing interval τ.

For many drugs, CL_E consists of additive renal (CL_R) and nonrenal (CL_{NR}) components, as indicated by the following equation:

$$CL_E = CL_R + CL_{NR} \tag{5.3}$$

Nonrenal clearance is usually equated with drug metabolism, but also could include hemodialysis and other methods of drug removal. In fact, even the metabolic clearance of a drug frequently consists of additive contributions from several parallel metabolic pathways. The characterization of drug metabolism by a clearance term usually is appropriate, since the metabolism of most drugs can be described by first-order kinetics within the range of therapeutic drug concentrations.

Dettli (7) proposed that the additive property of *elimination rate constants* representing parallel elimination pathways provides a way of either using Equation 5.3 or constructing nomograms to estimate the dose reductions that are appropriate for patients with impaired renal function. This approach also can be used to estimate *elimination clearance*, as illustrated for cimetidine in Figure 5.1. In implementing this approach, creatinine clearance (CL_{CR}) usually is estimated in adults from the Cockcroft and Gault equation (Equation 1.2) (9), and in pediatric patients from other simple equations, as discussed in Chapter 1. Although a more accurate prediction method has been proposed for estimating creatinine clearance in adults (10), its increased complexity has deterred its widespread adoption. Calculations or nomograms for many drugs can be made after consulting tables in Appendix II of Goodman and Gilman (11) or other reference sources to obtain values of CL_E and the fractional dose eliminated by renal excretion (percentage urinary excretion) in normal subjects.

Schentag *et al.* (12) obtained slightly lower estimates of cimetidine percentage urinary excretion in normal subjects and of CL_E in patients with duodenal ulcer and in older normal subjects than is shown in Figure 5.1, which is based on reports by previous investigators who studied only young subjects (13). Nonetheless, there is apparent internal discrepancy in the labeling for cimetidine. Under "Dosage Adjustment for Patients with Impaired Renal Function," the label states that, "Patients with creatinine clearance less than 30 cc/min who are being treated for prevention of upper gastrointestinal bleeding should receive half the recommended dose." However, under

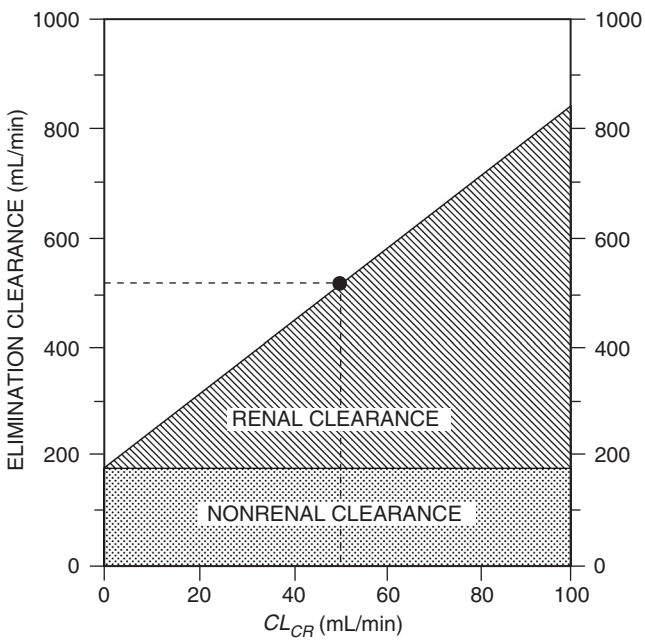

FIGURE 5.1 Nomogram for estimating cimetidine elimination clearance (CL_E) for a 70-kg patient with impaired renal function. The right-hand ordinate indicates cimetidine CL_E measured in young adults with normal renal function, and the left-hand ordinate indicates expected cimetidine CL_E in a functionally anephric patient, based on the fact that 23% of an administered dose is eliminated by nonrenal routes in normal subjects. The heavy line connecting these points can be used to estimate cimetidine CL_E from creatinine clearance (CL_{CR}). For example, a 70-kg patient with CL_{CR} of 50 mL/min (•) would be expected to have a cimetidine CL_E of 517 mL/min, and to respond satisfactorily to doses that are 60% of those recommended for patients with normal renal function. (Reproduced with permission from Atkinson AJ Jr, Craig RM. Therapy of peptic ulcer disease. In: Molinoff PB, ed. Peptic ulcer disease. Mechanisms and management. Rutherford, NJ: Healthpress Publishing Group, Inc.; 1990. p. 83–112.)

"Pharmacokinetics" the label indicates that "following I.V. or I.M. administration, approximately 75% of the drug is recovered from the urine after 24 hours as the parent compound" (14). Since only one-fourth of the dose is eliminated by nonrenal mechanisms, it can be expected that functionally anephric patients who receive half the usual cimetidine dose, such as the man in the case presented at the beginning of this chapter, will have potentially toxic blood levels that are twice those recommended for patients with normal renal function.

When dose adjustments are needed for patients with impaired renal function, they can be made by reducing the drug dose or by lengthening the dosing interval. Either approach, or a combination of both, may be employed in practice. For example, once the expected value for CL_E has been estimated, the daily drug dose can be reduced in proportion to the quotient of the expected clearance divided by the normal clearance. This will maintain the average drug concentration at the usual level, regardless of whether the drug is administered by intermittent doses or by continuous infusion. On the other hand, it is often convenient to administer doses of drugs that have a short elimination half-life at some multiple of their elimination half-life. The multiple that is used is determined by the therapeutic index of the drug. The expected half-life can be calculated from the following equation:

$$t_{1/2} = \frac{0.693 V_{d(area)}}{CL_E} \tag{5.4}$$

and the usual dose can be administered at an interval equal to the same multiple of the increased half-life. Dose-interval adjustment is usually necessary when safety and efficacy concerns specify a target range for both peak and trough plasma levels or when selection of drug doses is limited.

The reliability of the Dettli method of predicting drug clearance depends on two critical assumptions:

1. The nonrenal clearance of the drug remains constant when renal function is impaired.
2. CL_E declines in a linear fashion with CL_{CR}.

There are several important exceptions to the first assumption that will be considered when we discuss the effects of impaired renal function on drug metabolism. Nonetheless, this approach is widely used for individualizing drug dosage for patients with impaired renal function. In addition, Equations 5.3 and 5.4 provide a useful tool for hypothesis generation during drug development when pharmacokinetic studies are planned for subjects with impaired renal function.

TABLE 5.1 Important Mechanisms of Renal Elimination of Drugs

I. Glomerular filtration

- Affects all drugs and metabolites of appropriate molecular size
- Influenced by protein binding (f_u = free fraction)
  Drug filtration rate = GFR × f_u × [drug]

II. Renal tubular secretion

- Not influenced by protein binding
- May be affected by competition with other drugs, etc.
  Examples:
  Active drugs: Acids — penicillin
  Bases — procaine amide
  Metabolites: Glucuronides, hippurates, etc.

III. Reabsorption by nonionic diffusion

- Affects weak acids and weak bases
- Only important if excretion of free drug is major elimination path
  Examples:
  Weak acids: Phenobarbital
  Weak bases: Quinidine

IV. Active reabsorption

- Affects ions, not proved for other drugs
  Examples:
  Halides: Fluoride, bromide
  Alkaline metals: Lithium

Mechanisms of Renal Handling of Drugs

Important mechanisms involved in the renal excretion and reabsorption of drugs have been reviewed by Reidenberg (15) and are shown in Table 5.1.

Excretion Mechanisms

Glomerular filtration affects all drugs of small molecular size and is *restrictive* in the sense that it is limited by drug binding to plasma proteins. On the other hand, renal tubular secretion is *nonrestrictive* since both protein-bound and free drug concentrations in plasma are available for elimination. In fact, the proximal renal tubular secretion of *p*-aminohippurate is rapid enough that its elimination clearance is used to estimate renal blood flow. There are many proteins in renal tubular cells that actively transport compounds against a concentration gradient. In addition to P-glycoprotein and six multiple drug resistance proteins, five known cation and nine organic anion transporters have been identified (16). Transporters involved in drug secretion are located both at the basolateral membrane of renal tubule cells, where they

transport drugs from blood into these cells, and at the brush border membrane, where they transport drugs into proximal tubular urine. Despite the progress that has been made in cloning these transporters and in establishing their binding affinities for various drugs, more work needs to be done before it will be possible to identify which transporters are actually responsible for the renal secretion of a given drug.

Competition by drugs for renal tubular secretion is an important cause of drug–drug interactions. Inhibitors of P-glycoprotein slow this renal tubular pathway. Anionic drugs compete with other anionic drugs for these active transport pathways, as do cationic drugs for their pathways. When two drugs secreted by the same pathway are given together, the renal clearance of each will be less than when either drug is given alone. Methotrexate is a clinically important example of an anionic drug that is actively secreted by renal tubular cells. Its renal clearance is halved when salicylate is coadministered with it (17).

Reabsorption Mechanisms

Net drug elimination also may be affected by drug reabsorption in the distal nephron, primarily by nonionic passive diffusion. Because only the nonionized form of a drug can diffuse across renal tubule cells, the degree of reabsorption of a given drug depends on its degree of ionization at a given urinary pH. For this reason, sodium bicarbonate is administered to patients with salicylate or phenobarbital overdose in order to raise urine pH, thereby increasing the ionization and minimizing the reabsorption of these acidic drugs. This therapeutic intervention also reduces reabsorption by increasing urine flow. Lithium and bromide are perhaps the only two drugs that are reabsorbed by active transport mechanisms. Present evidence suggests that lithium is reabsorbed at the level of the proximal tubule by a Na^+/H^+ exchanger (NHE-3) at the brush border and extruded into the blood by Na/K-ATPase and sodium bicarbonate cotransporter located at the basolateral membrane (18).

Renal Metabolism

The kidney plays a major role in the clearance of insulin from the systemic circulation, removing approximately 50% of endogenous insulin and a greater proportion of insulin administered to diabetic patients (19). Insulin is filtered at the glomerulus and reabsorbed by proximal tubule cells, where it is degraded by proteolytic enzymes. Insulin requirements are markedly reduced in diabetic patients with impaired renal function. Imipenem and perhaps other peptides, peptidomimetics, and small proteins are also filtered at the glomerulus and subsequently metabolized by proximal renal tubule cell proteases (20). Cilastatin, an inhibitor of proximal tubular dipeptidases, is coadministered with imipenem to maintain the clinical effectiveness of this antibiotic.

Analysis and Interpretation of Renal Excretion Data

Renal tubular mechanisms of excretion and reabsorption can be analyzed by stop-flow and other standard methods used in renal physiology, but detailed studies are seldom performed. For most drugs, all that has been done has been to correlate renal drug clearance with the reciprocal of serum creatinine or with creatinine clearance. Even though creatinine clearance primarily reflects glomerular filtration rate, it serves as a rough guide to the renal clearance of drugs that have extensive renal tubular secretion or reabsorption. This is a consequence of the glomerulo-tubular balance that is maintained in damaged nephrons by intrinsic tubule and peritubular capillary adaptations that parallel reductions in single nephron glomerular filtration rate (21). For this reason, CL_E usually declines fairly linearly with reductions in CL_{CR}. However, some discrepancies can be expected. For example, Reidenberg *et al.* (22) have shown that renal secretion of some basic drugs declines with aging more rapidly than does glomerular filtration rate. Also, studies with *N*-1-methylnicotinamide, an endogenous marker of renal tubular secretion, have demonstrated some degree of glomerulo-tubular imbalance in patients with impaired renal function (23).

Despite the paucity of detailed studies, it is possible to draw some general mechanistic conclusions from renal clearance values:

- If renal clearance *exceeds* drug filtration rate (Table 5.1), there is net renal tubular secretion of the drug.
- If renal clearance *is less than* drug filtration rate, there is net renal tubular reabsorption of the drug.

Effects of Impaired Renal Function on Nonrenal Metabolism

Most drugs are not excreted unchanged by the kidneys but first are biotransformed to metabolites that then are excreted. Renal failure not only may retard the excretion of these metabolites, which in some cases have important pharmacologic activity, but, in some cases, alters the nonrenal as well as the renal metabolic clearance of drugs (15, 24). The impact of impaired renal function on drug metabolism is dependent on the metabolic pathway, as indicated in Table 5.2. In most

TABLE 5.2 Effect of Renal Disease on Drug Metabolism

Type of metabolism	Effect
I. Oxidations	Normal or increased
Example: Phenytoin	
II. Reductions	Slowed
Example: Hydrocortisone	
III. Hydrolyses	
• Plasma esterase	Slowed
Example: Procaine	
• Plasma peptidase	Normal
Example: Angiotensin	
• Tissue peptidase	Slowed
Example: Insulin	
IV. Syntheses	
• Glucuronide formation	Normal
Example: Hydrocortisone	
• Acetylation	Slowed
Example: Procainamide	
• Glycine conjugation	Slowed
Example: *p*-Aminosalicylic acid	
• O-Methylation	Normal
Example: Methyldopa	
• Sulfate conjugation	Normal
Example: Acetaminophen	

cases, it is unclear how much impairment in renal function needs to be present before drug metabolism is affected. However, clinical experience suggests, for example, that creatinine clearance must fall below 25 mL/min before the acetylation rate of procainamide is impaired.

EFFECTS OF RENAL DISEASE ON DRUG DISTRIBUTION

Impaired renal function is associated with important changes in the binding of some drugs to *plasma proteins*. In some cases the *tissue binding* of drugs is also affected.

Plasma Protein Binding of Acidic Drugs

Reidenberg and Drayer (25) have stated that protein binding in serum from uremic patients is decreased for every acidic drug that has been studied. Most acidic drugs bind to the bilirubin binding site on albumin, but there are also different binding sites that play a role. The reduced binding that occurs when renal function is impaired has been variously attributed to reductions in serum albumin concentration, structural changes in the binding sites, or displacement of drugs from albumin binding sites by organic molecules that accumulate in uremia. As described in Chapter 3, reductions in the protein binding of acidic drugs result in increases in their distribution volume. In addition, the elimination clearance of *restrictively eliminated* drugs is increased. However, protein binding changes do not affect distribution volume or clearance estimates when they are referenced to unbound drug concentrations. For restrictively eliminated drugs, the term *intrinsic clearance* is used to describe the clearance that would be observed in the absence of any protein binding restrictions. As discussed in Chapter 7, the clearance of restrictively eliminated drugs, when referenced to total drug concentrations, simply equals the product of the unbound fraction of drug (f_u) and this intrinsic clearance (CL_{int}):

$$CL = f_u \cdot CL_{int} \tag{5.5}$$

Phenytoin is an acidic, restrictively eliminated drug that can be used to illustrate some of the changes in drug distribution and elimination that occur in patients with impaired renal function. In patients with normal renal function, 92% of the phenytoin in plasma is protein bound. However, the percentage that is unbound or "free" rises from 8% in these individuals to 16%, or more, in hemodialysis-dependent patients. In a study comparing phenytoin pharmacokinetics in normal subjects and uremic patients, Odar-Cederlöf and Borgå (26) administered a single low dose of this drug so that first-order kinetics were approximated. The results shown in Table 5.3 can be inferred from their study. The uremic patients had an increase in distribution volume that was consistent with the observed decrease in phenytoin binding to plasma proteins. The threefold increase in hepatic clearance that was observed in these patients also was primarily the result of decreased phenytoin protein binding. Although intrinsic hepatic clearance also appeared to be increased in the uremic patients, the difference did not reach statistical significance at the $P = 0.05$ level.

TABLE 5.3 Effect of Impaired Renal Function on Phenytoin Kinetics

Parameter	Normal subjects (n = 4)	Uremic patients (n = 4)
Percentage unbound (f_u)	12%	26%
Distribution volume ($V_{d(area)}$)	0.64 L/kg	1.40 L/kg
Hepatic clearance (CL_H)	2.46 L/hr	7.63 L/hr
Intrinsic clearance (CL_{int})	20.3 L/hr	29.9 L/hr

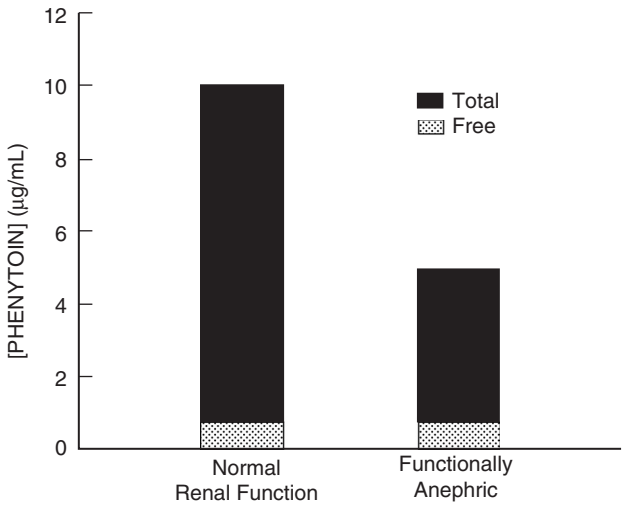

FIGURE 5.2 Comparison of free and total plasma phenytoin levels in a patient with normal renal function and in a functionally anephric patient; both are treated with a 300-mg daily phenytoin dose and have identical CL_{int}. Although free phenytoin levels are 0.8 μg/mL in both patients, phenytoin is only 84% bound (16% free) in the functionally anephric patient, compared to 92% bound (8% free) in the patient with normal renal function. For that reason, total phenytoin levels in the functionally anephric patient are only 5 μg/mL, whereas they are 10 μg/mL in the patient with normal renal function.

A major problem arises in clinical practice when only total (protein bound + free) phenytoin concentrations are measured and used to guide therapy of patients with severely impaired renal function. The decreases in phenytoin binding that occur in these patients result in commensurate decreases in total plasma levels (Figure 5.2). Even though therapeutic and toxic pharmacologic effects are correlated with unbound rather than total phenytoin concentrations in plasma, the decrease in total concentrations can mislead physicians to increase phenytoin doses inappropriately. Fortunately, rapid ultrafiltration procedures are available that make it possible to measure free phenytoin concentrations in these patients on a routine basis.

Plasma Protein Binding of Basic and Neutral Drugs

The protein binding of basic drugs tends to be normal or only slightly reduced (25). In some cases, this may reflect the facts that these drugs bind to α_1–acid glycoprotein and that concentrations of this glycoprotein are higher in hemodialysis-dependent patients than in patients with normal renal function.

Tissue Binding of Drugs

The distribution volume of some drugs also can be altered when renal function is impaired. As described in Chapter 3, Sheiner *et al.* (27) have shown that impaired renal function is associated with a decrease in digoxin distribution volume that is described by the following equation:

$$V_d(\text{in L}) = 3.84 \cdot \text{weight (in kg)} + 3.12\ CL_{CR}\ (\text{in mL/min})$$

This presumably reflects a reduction in tissue levels of Na/K-ATPase, an enzyme that represents a major tissue-binding site for digoxin (28). In other cases in which distribution volume is decreased in patients with impaired renal function, the relationship between the degree of renal insufficiency and reduction in distribution volume has not been characterized nor have plausible mechanisms been proposed.

EFFECTS OF RENAL DISEASE ON DRUG ABSORPTION

The bioavailability of most drugs that have been studied has not been found to be altered in patients with impaired renal function. However, the absorption of D-xylose, a marker compound used to evaluate small intestinal absorptive function, was slowed (absorption rate constant: 0.555 hr^{-1} vs. 1.03 hr^{-1}) and less complete (percentage dose absorbed: 48.6% vs. 69.4%) in patients with chronic renal failure than in normal subjects (29). Although these results were statistically significant, there was considerable interindividual variation in both patients and normal subjects. This primary absorptive defect may explain the fact that patients with impaired renal function have *reduced* bioavailability of furosemide (30) and pindolol (31). However, it also is possible that impaired renal function will result in *increased* bioavailability of drugs exhibiting first-pass metabolism when the function of drug-metabolizing enzymes is compromised. Studies with orally administered propranolol have suggested this, but absolute bioavailability was not measured (32).

The paucity of reliable bioavailability data in patients with impaired renal function underscores the cumbersome nature of most absolute bioavailability studies in which oral and intravenous drug doses are administered on two separate occasions. The validity of this approach rests on the assumption that the kinetics of drug distribution and elimination remain

unchanged in the interval between the two studies, an assumption that obviously is more tenuous for patients than for normal subjects. As discussed in Chapter 4, these shortcomings can be overcome by conducting a single study in which an intravenous formulation of the stable isotope-labeled drug is administered simultaneously with the oral drug dose (33).

The simultaneous administration technique was used to study a 64-year-old man with a creatinine clearance of 79 mL/min who was started on *N*-acetylprocainamide (NAPA) therapy for ventricular arrhythmias (see Figure 4.4). The oral NAPA dose was 66% absorbed in this patient, compared to 91.6 ± 9.2% when this method was used to assess NAPA absorption in normal subjects. Although this approach is ideally suited for studies of drug absorption in various patient populations, the required additional chemical synthesis of stable isotope-labeled drug and mass spectrometric analysis of patient samples have precluded its widespread adoption.

REFERENCES

1. Yacobi A, Batra VK, Desjardins RE, Faulkner RD, Nicolau G, Pool WR, Shah A, Tonelli AP. Implementation of an effective pharmacokinetics research program in industry. In: Yacobi A, Skelly JP, Shah VP, Benet LZ, eds. Integration of pharmacokinetics, pharmacodynamics, and toxicokinetics in rational drug development. New York: Plenum; 1993. p.125–35.
2. Peck CC. Rationale for the effective use of pharmacokinetics and pharmacodynamics in early drug development. In: Yacobi A, Skelly JP, Shah VP, Benet LZ, eds. Integration of pharmacokinetics, pharmacodynamics, and toxicokinetics in rational drug development. New York: Plenum; 1993. p.1–5.
3. Spyker DA, Harvey ED, Harvey BE, Harvey AM, Rumack BH, Peck CC, Atkinson AJ Jr, Woosley RL, Abernethy DR, Cantilena LR. Assessment and reporting of clinical pharmacology information in drug labeling. Clin Pharmacol Ther 2000;67:196–200.
4. Lesar TS, Briceland L, Stein DS. Factors related to errors in medication prescribing. JAMA 1997; 277:312–7.
5. Piergies AA, Worwag EM, Atkinson AJ Jr. A concurrent audit of high digoxin plasma levels. Clin Pharmacol Ther 1994;55:353–8.
6. CDER, CBER. Pharmacokinetics in patients with impaired renal function —- study design, data analysis, and impact on dosing and labeling. Guidance for Industry, Rockville: FDA; 1998. (Internet at http://www.fda.gov/cder/guidance/index.htm.)
7. Dettli L. Individualization of drug dosage in patients with renal disease. Med Clin North Am 1974; 58:977–85.
8. Atkinson AJ Jr, Craig RM. Therapy of peptic ulcer disease. In: Molinoff PB, ed. Peptic ulcer disease. Mechanisms and management. Rutherford, NJ: Healthpress Publishing Group, Inc.; 1990. p. 83–112.
9. Cockroft DW, Gault MH. Prediction of creatinine clearance from serum creatinine. Nephron 1976; 16:31–41.
10. Levey AS, Bosch JP, Breyer Lewis J, Greene T, Rogers N, Roth D. A more accurate method to estimate glomerular filtration rate from serum creatinine: A new prediction equation. Ann Intern Med 1999;130:461–70.
11. Thummel KE, Shen DD. Design and optimization of dosage regimens: Pharmacokinetic data. In: Hardman JG, Limbird LE, Gilman AG, eds. Goodman & Gilman's The pharmacological basis of therapeutics. 10th ed. New York: McGraw-Hill; 2001. p. 1924–2023.
12. Schentag JJ, Cerra FB, Calleri GM, Leising ME, French MA, Bernhard H. Age, disease, and cimetidine disposition in healthy subjects and chronically ill patients. Clin Pharmacol Ther 1981;29:737–43.
13. Grahnén A, von Bahr C, Lindström B, Rosén A. Bioavailability and pharmacokinetics of cimetidine. Eur J Clin Pharmacol 1979;16:335–40.
14. Physician's Desk Reference. 59th ed. Montvale, NJ: Medical Economics; 2005. p. 1626–9.
15. Reidenberg MM. Renal function and drug actions. Philadelphia: Saunders; 1971.
16. Dresser MJ, Leabman MK, Giacomini KM. Transporters involved in the elimination of drugs in the kidney: Organic anion transporters and organic cation transporters. J Pharm Sci 2001;90:397–421.
17. Liegler DG, Henderson ES, Hahn MA, Oliverio VT. The effect of organic acids on renal clearance of methotrexate in man. Clin Pharmacol Ther 1969;10:849–57.
18. Ng LL, Quinn PA, Baker F, Carr SJ. Red cell Na^+/Li^+ countertransport and Na^+/H^+ exchanger isoforms in human proximal tubules. Kidney Int 2000;58:229–35.
19. Duckworth WC, Bennett RG, Hamel FG. Insulin degradation: Progress and potential. Endocr Rev 1998;19:608–24.
20. Brater DC. Measurement of renal function during drug development. Br J Clin Pharmacol 2002;54:87–95.
21. Brenner BM. Nephron adaptation to renal injury or ablation. Am J Physiol 1985;249:F324–37.
22. Reidenberg MM, Camacho M, Kluger J, Drayer DE: Aging and renal clearance of procainamide and acetylprocainamide. Clin Pharmacol Ther 1980;28:732–5.
23. Maiza A, Waldek S, Ballardie FW, Daley-Yates PT. Estimation of renal tubular secretion in man, in health and disease, using endogenous *N*-1-methylnicotinamide. Nephron 1992;60:12–6.
24. Reidenberg MM. The biotransformation of drugs in renal failure. Am J Med 1977;62:482–5.
25. Reidenberg MM, Drayer DE. Alteration of drug-protein binding in renal disease. Clin Pharmacokinet 1984;9(suppl 1):18–26.
26. Odar-Cederlöf I, Borgå O. Kinetics of diphenylhydantoin in uremic patients: Consequences of decreased plasma protein binding. Eur J Clin Pharmacol 1974;7:31–7.

27. Sheiner LB, Rosenberg B, Marathe VV. Estimation of population characteristics of pharmacokinetic parameters from routine clinical data. J Pharmacokinet Biopharm 1977;5:445–79.
28. Aronson JK, Grahame-Smith DG. Altered distribution of digoxin in renal failure —- a cause of digoxin toxicity? Br J Clin Pharmacol 1976;3:1045–51.
29. Craig RM, Murphy P, Gibson TP, Quintanilla A, Chao GC, Cochrane C, Patterson A, Atkinson AJ Jr. Kinetic analysis of D-xylose absorption in normal subjects and in patients with chronic renal failure. J Lab Clin Med 1983;101:496–506.
30. Huang CM, Atkinson AJ Jr, Levin M, Levin NW, Quintanilla A. Pharmacokinetics of furosemide in advanced renal failure. Clin Pharmacol Ther 1974;16:659–66.
31. Chau NP, Weiss YA, Safar ME, Lavene DE, Georges DR, Milliez P. Pindolol availability in hypertensive patients with normal and impaired renal function. Clin Pharmacol Ther 1977;22:505–10.
32. Bianchetti G, Graziani G, Brancaccio D, Morganti A, Leonetti G, Manfrin M, Sega R, Gomeni R, Ponticelli C, Morselli PL. Pharmacokinetics and effects of propranolol in terminal uraemic patients and in patients undergoing regular dialysis treatment. Clin Pharmacokinet 1976;1:373–84.
33. Atkinson AJ Jr, Ruo TI, Piergies AA, Breiter HC, Connely TJ, Sedek GS, Juan D, Hubler GL, Hsieh A-M. Pharmacokinetics of *N*-acetylprocainamide in patients profiled with a stable isotope method. Clin Pharmacol Ther 1989;46:182–9.

STUDY PROBLEM

The following pharmacokinetic data for *N*-acetylprocainamide (NAPA) were obtained in a Phase I study[1] in which procainamide and NAPA kinetics were compared in volunteers with normal renal function:

Elimination half-life:	6.2 hr
Elimination clearance:	233 mL/min
% Renal excretion:	85.5%

a. Use these results to predict the elimination half-life of NAPA in functionally anephric patients, assuming that nonrenal clearance is unchanged in these individuals.
b. Create a nomogram similar to that shown in Figure 5.1 to estimate the elimination clearance of NAPA that would be expected for a patient with a creatinine clearance of 50 mL/min. Assume that a creatinine clearance of 100 mL/min is the value for individuals with normal renal function.
c. If the usual starting dose of NAPA is 1 g every 8 hours in patients with normal renal function, what would be the equivalent dosing regimen for a patient with an estimated creatinine clearance of 50 mL/min if the dose is decreased but the 8-hour dosing interval is maintained?
d. If the usual starting dose of NAPA is 1 g every 8 hours in patients with normal renal function, what would be the equivalent dosing regimen for a patient with an estimated creatinine clearance of 50 mL/min if the 1-g dose is maintained but the dosing interval is increased?

[1] Dutcher JS, Strong JM, Lucas SV, Lee W-K, Atkinson AJ Jr. Procainamide and *N*-acetylprocainamide kinetics investigated simultaneously with stable isotope methodology. Clin Pharmacol Ther 1977;22:447–57.

CHAPTER

6

Pharmacokinetics in Patients Requiring Renal Replacement Therapy

ARTHUR J. ATKINSON, JR.[1] **AND GREGORY M. SUSLA**[2]
[1]*Clinical Center, National Institutes of Health, Bethesda, Maryland,*
[2]*VHA Consulting Services, Frederick, Maryland*

Although measurements of drug recovery in the urine enable reasonable characterization of the renal clearance of most drugs, analysis of drug elimination by the liver is hampered by the types of measurements that can be made in routine clinical studies. Hemodialysis and hemofiltration are considered at this point in the text because they provide an unparalleled opportunity to measure blood flow to the eliminating organ, drug concentrations in blood entering and leaving the eliminating organ, and recovery of eliminated drug in the dialysate or ultrafiltrate. The measurements that can be made in analyzing drug elimination by different routes are compared in Table 6.1.

Hemodialysis is an area of long-standing interest to pharmacologists. The pioneer American pharmacologist, John Jacob Abel, can be credited with designing the first artificial kidney (1). He conducted extensive studies in dogs to demonstrate the efficacy of hemodialysis in removing poisons and drugs. European scientists were the first to apply this technique to humans, and Kolff sent a rotating-drum artificial kidney to the United States when the Second World War ended (2, 3). Repetitive use of hemodialysis for treating patients with chronic renal failure finally was made possible by the development of techniques for establishing long-lasting vascular access in the 1960s. By the late 1970s, continuous peritoneal dialysis had become a therapeutic alternative for these patients and offered the advantages of simpler, non-machine-dependent home therapy and less hemodynamic stress (4). In 1977, continuous arteriovenous hemofiltration (CAVH) was introduced as a method for removing fluid from diuretic-resistant patients, whose hemodynamic instability made them unable to tolerate conventional intermittent hemodialysis (5). Since then, this and related techniques have become the preferred treatment modality for critically ill patients with acute renal failure. Several variations of these techniques have been developed that use hemodialysis and/or hemofiltration to remove both solutes and fluid, and some of these are listed in Table 6.2 (6). All of these methods can affect pharmacokinetics, but we will focus on conventional intermittent hemodialysis and selected aspects of continuous renal replacement therapy in this chapter.

KINETICS OF INTERMITTENT HEMODIALYSIS

Solute Transfer across Dialyzing Membranes

In Abel's artificial kidney, blood flowed through a hollow cylinder of dialyzing membrane that was immersed in a bath of dialysis fluid. However, in modern hollow-fiber dialysis cartridges, there is a continuous countercurrent flow of dialysate along the outside of the dialyzing membrane that maximizes the concentration gradient between blood and dialysate. Mass transfer across the dialyzing membrane occurs

TABLE 6.1 Measurements Made in Assessing Drug Elimination by Different Routes

Measurements	Renal elimination	Hepatic elimination	Hemodialysis
Blood flow	+[a]	+[a]	+
Afferent blood concentration	+	+	+
Efferent blood concentration	0	0	+
Recovery of eliminated drug	+	0	+

[a] Not actually measured in routine pharmacokinetic studies.

by diffusion and ultrafiltration. The rate of transfer has been analyzed with varying sophistication by a number of investigators (7). A simple approach is that taken by Eugene Renkin, who neglected ultrafiltration and nonmembrane diffusive resistance and likened this transfer process to mass transfer across capillary walls (see Chapter 3) (8). Renkin expressed dialysis clearance (CL_D) as

$$CL_D = Q(1 - e^{-P \cdot S/Q}) \tag{6.1}$$

where Q is blood flow through the dialyzer and $P \cdot S$ is the permeability coefficient–surface area product of the dialyzing membrane, defined by Fick's First Law of Diffusion as

$$P \cdot S = DA/\lambda$$

In this equation, A is the surface area, λ is the thickness of the dialyzing membrane, and D is the diffusivity of a given solute in the dialyzing membrane. Solute diffusivity is primarily determined by molecular weight.

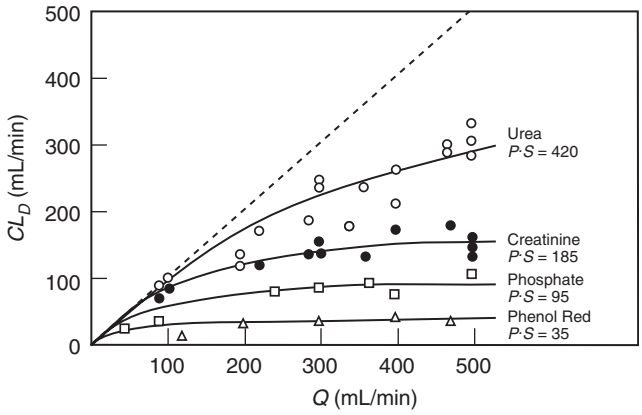

FIGURE 6.1 Plot of dialysis clearance (CL_D) vs. dialyzer blood flow (Q). The theoretical curves were fit to experimental data points to obtain estimates of the permeability coefficient–surface area product ($P{\cdot}S$) for each solute. Flow-limited clearance is indicated by the dashed line. The data were generated with a Kolff–Brigham type hemodialysis apparatus. (Reproduced with permission from Renkin EM. Tr Am Soc Artific Organs 1956;2:102–5.)

Nonspherical molecular shape also may affect the diffusivity of larger molecules.

Renkin used Equation 6.1 to estimate permeability coefficients for several solutes from flow and clearance measurements made on the Kolff–Brigham artificial kidney (Figure 6.1). This theoretical analysis seems reasonably consistent with the experimental results. In the Figure, the dashed line indicates a flow limitation to transport because clearance can never exceed dialyzer blood flow, a result that is obvious from inspection of Equation 6.1 (i.e., $e^{-P \cdot S/Q}$ is never less than 0).

An analysis of relative dialysis clearance and dialyzer permeability coefficient–surface area products that was made for the closely related compounds procainamide (PA) and *N*-acetylprocainamide (NAPA) is summarized in Table 6.3. Dialyzer clearance measurements of PA (CL_{PA}) and NAPA (CL_{NAPA})

TABLE 6.2 Summary of Selected Renal Replacement Therapies

Procedure	Abbreviation	Diffusion	Convection	Vascular access	Replacement fluid
Intermittent hemodialysis	HD	++++	+	Fistula or vein–vein	No
Intermittent high-flux dialysis	HFD	+++	++	Fistula or vein–vein	No
Continuous ambulatory peritoneal dialysis	CAPD	++++	+	None	No
Continuous arteriovenous hemofiltration	CAVH	0	++++	Artery–vein	Yes
Continuous venovenous hemofiltration	CVVH	0	++++	Vein–vein	Yes
Continuous arteriovenous hemodialysis	CAVHD	++++	+	Artery–vein	Yes
Continuous venovenous hemodialysis	CVVHD	++++	+	Vein–vein	Yes
Continuous arteriovenous hemodiafiltration	CAVHDF	+++	+++	Artery–vein	Yes
Continuous venovenous hemodiafiltration	CVVHDF	+++	+++	Vein–vein	Yes

TABLE 6.3 Dialyzer Permeability Coefficient–Surface Area Products for PA and NAPA[a]

Column	CL_{PA} (mL/min)	CL_{NAPA} (mL/min)	$P \cdot S_{PA}$ (mL/min)	$P \cdot S_{NAPA}$ (mL/min)	Ratio $P \cdot S_{PA}/P \cdot S_{NAPA}$
Dow 4	79.9	55.3	102.0	64.7	1.58
Dow 5	114.6	89.9	170.2	119.4	1.43
Gambro 17	50.8	33.3	58.6	36.4	1.61
Ultra-flow II	78.5	63.8	99.7	76.8	1.30
Ultra-flow 145	63.4	50.4	76.3	58.1	1.31
Vivacell	37.1	27.8	41.0	29.9	1.37
Ex 23	50.4	50.4	58.1	58.1	1.00
Ex 25	71.6	62.6	88.6	75.1	1.18
Ex 29	81.4	78.0	104.5	98.9	1.06
Ex 55	51.8	53.9	60.0	62.8	0.93
			Mean ± SD:		1.28 ± 0.23

[a] Clearance data obtained by Gibson TP *et al.* (9), with dialyzer blood flow set at 200 (mL/min) and single-pass dialysate flow at 400 mL/min.

made by Gibson *et al.* (9) were used together with Equation 6.1 to calculate $P \cdot S$ values for PA ($P \cdot S_{PA}$) and NAPA ($P \cdot S_{NAPA}$). The ratio of these $P \cdot S$ values is also shown, since this ratio indicates the relative diffusivity of PA and NAPA. The utility of Renkin's approach is confirmed by the fact that the mean $P \cdot S$ ratio of 1.28 ± 0.23 (± SD) is in close agreement with the diffusion coefficient ratio of 1.23 that was obtained for PA and NAPA by the porous-plate method of McBain and Liu (10).

Calculation of Dialysis Clearance

Currently, the efficiency of hemodialysis is expressed in terms of *dialysis clearance*. Dialysis clearance (CL_D) is usually estimated from the Fick equation as follows:

$$CL_D = Q\left[\frac{A - V}{A}\right] \tag{6.2}$$

where A is the solute concentration entering (arterial) and V is the solute concentration leaving (venous) the dialyzer. The terms in brackets collectively describe what is termed the *extraction ratio* (E). As a general principle, clearance from an eliminating organ can be thought of as the product of organ blood flow and extraction ratio.

Single-pass dialyzers are now standard for patient care and clearance calculations suffice for characterizing their performance. However, recirculating dialyzers were used in the early days of hemodialysis. Dialysis bath solute concentration (Bath) had to be considered in describing the performance of recirculating dialyzers and was included in the equation for calculating *dialysance* (D), as shown in the following equation (7):

$$D = Q\left[\frac{A - V}{A - \text{Bath}}\right]$$

Considerable confusion surrounds the proper use of Equation 6.2 to calculate dialysis clearance. There is general agreement that *blood clearance* is calculated when Q is set equal to blood flow and A and V are expressed as blood concentrations. In conventional practice, *plasma clearance* is obtained by setting Q equal to plasma flow and expressing A and V as plasma concentrations. In fact, this estimate of plasma clearance is only the same as plasma clearance calculated by standard pharmacokinetic techniques when the solute is totally excluded from red blood cells.

This dilemma is best avoided by calculating dialysis clearance using an equation that is analogous to the equation used to determine renal clearance:

$$CL_P = \frac{C_D \cdot Vol_D}{P \cdot t} \tag{6.3}$$

where the amount of drug recovered by dialysis is calculated as the product of the drug concentration in dialysate (C_D) and total volume of dialysate (Vol_D) collected during the dialysis time (t), and P is the average concentration of drug in plasma entering the dialyzer. The term *recovery clearance* has been coined for this clearance estimate, and it is regarded as the "gold standard" of dialysis clearance estimates (11).

Equation 6.3 provides an estimate of dialysis plasma clearance (CL_P) that is *pharmacokinetically consistent* with estimates of elimination and intercompartmental clearance that are based on plasma concentration measurements. On the other hand, if the average drug concentration in blood entering the dialyzer (B) is substituted for P, a valid estimate of blood clearance (CL_B) is obtained:

$$CL_B = \frac{C_D \cdot Vol_D}{B \cdot t} \tag{6.4}$$

We can use these recovery clearances to examine the *effective* flow of plasma (Q_{EFF}) that is needed if Equation 6.2 is to yield an estimate of dialysis clearance that is consistent with the corresponding recovery clearance value. Since $CL_B = Q_B E$, it follows from Equation 6.4 that:

$$\frac{C_D \cdot Vol_D}{B \cdot t} = Q_B E$$

Rearranging,

$$\frac{C_D \cdot Vol_D}{E \cdot t} = Q_B B$$

But from Equation 6.3,

$$\frac{C_D \cdot Vol_D}{t} = CL_P P$$

Therefore,

$$CL_P/E = Q_B \cdot B/P$$

However,

$$CL_P = Q_{EFF} \cdot E$$

Therefore,

$$Q_{EFF} = Q_B \cdot B/P$$

For drugs like NAPA that partition preferentially into red blood cells and are fully accessible to the dialyzer from both plasma and erythrocytes, the effective plasma flow will not be less than but will *exceed* measured blood flow (12).

Some authorities argue that it is improper to combine organ *blood* flow and *plasma* concentrations in Equation 6.2 (7, 11). However, in many cases the ratio of red cell/plasma drug concentrations remains constant over a wide concentration range so the same estimate of extraction ratio is obtained regardless of whether plasma concentrations or blood concentrations are measured.

As shown in Figure 6.2, pharmacokinetic models can be constructed that incorporate all the measurements made during hemodialysis (12). For this purpose it is convenient to rearrange Equation 6.2 to the form

$$V = [(Q_{PK} - CL_D)/Q_{PK}] \cdot A \qquad (6.5)$$

where Q_{PK} is the pharmacokinetically calculated flow of blood or plasma through the dialysis machine. Since CL_D is calculated from the recovery of drug in dialysis bath fluid, an estimate of Q_{PK} can be obtained from the observed ratio of V/A (Equation 6.5 and Figure 6.2).

In a study of NAPA hemodialysis kinetics, blood flow measured through the dialyzer averaged 195 mL/min (12). When evaluated by paired t test this was significantly less than Q_{PK}, which averaged 223 mL/min. However, Q_{PK} was similar to estimates of Q_{EFF}, which averaged 217 mL/min. In this case

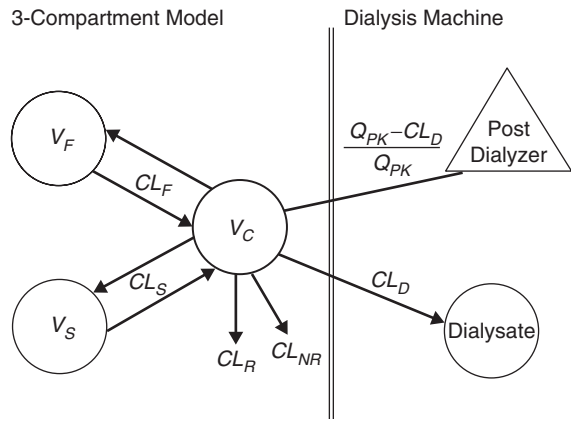

FIGURE 6.2 Multicompartmental system for modeling pharmacokinetics during hemodialysis. Drug is delivered to the dialysis machine from the central compartment (V_C) and represents A in the Fick equation. The dialysis machine is modeled by a compartment representing drug recovery in dialysis bath fluid and a proportionality (*triangle*) representing the drug concentration in blood returning to the patient.

NAPA concentrations in erythrocytes were 1.5 times as high as in plasma, and this preferential distribution of drug into red blood cells enhanced drug removal by hemodialysis. Unfortunately, most hemodialysis studies have not incorporated the full range of readily available measurements in an integrated pharmacokinetic analysis.

Patient Factors Affecting Hemodialysis of Drugs

Because elimination clearances are additive, total solute clearance during hemodialysis (CL_T) can be expressed as the sum of dialysis clearance (CL_D), and the patient's renal clearance (CL_R) and nonrenal clearance (CL_{NR}):

$$CL_T = CL_D + CL_R + CL_{NR} \qquad (6.6)$$

When CL_D is small relative to the sum of CL_R and CL_{NR}, hemodialysis can be expected to have little impact on the overall rate of drug removal. The extent of drug binding to plasma proteins is the most important patient factor affecting dialysis clearance, and in that sense dialysis clearance is restrictive. However, partitioning into erythrocytes has been shown to enhance rather than retard the clearance of at least some drugs. A large distribution volume also reduces the fraction of total body stores of a drug that can be removed by hemodialysis, and limits the effect of hemodialysis on shortening drug elimination half-life,

since:

$$t_{1/2} = \frac{0.693\, V_d}{CL_T}$$

Finally, there are significant hemodynamic changes during hemodialysis that not only may affect the extent of drug removal by this procedure but also may have an important impact on patient response.

Hemodynamic Changes during Dialysis

Few studies of pharmacokinetics during hemodialysis have utilized the recovery method of calculating dialysis clearance that is necessary to evaluate the impact of hemodynamic changes that may affect the efficiency of this procedure. The decrease in both A and V drug concentrations that occurs during hemodialysis is generally followed by a postdialysis rebound, as shown for NAPA in Figure 6.3. However, if no change in drug distribution is assumed, two discrepancies are likely to be encountered when the recovery method is incorporated in an integrated analysis of hemodialysis kinetics:

1. The total amount of drug recovered from the dialysis fluid is less than would be expected from the drop in plasma concentrations during hemodialysis.
2. The extent of the rebound in plasma levels is less than would be anticipated.

The only single parameter change that can resolve these discrepancies is a reduction in the intercompartmental clearance for the slowly equilibrating compartment (CL_S). This is illustrated in the bottom panel of Figure 6.3, and in this study the extent of reduction in CL_S was found to average 77% during hemodialysis (12). This figure also shows that a reduction in CL_S persisted for some time after hemodialysis was completed.

The hemodynamic basis for these changes in CL_S was investigated subsequently in a dog model (13). Urea and inulin were used as probes and were injected simultaneously 2 hours before dialysis. The pharmacokinetic model shown in Figure 6.2 was used for

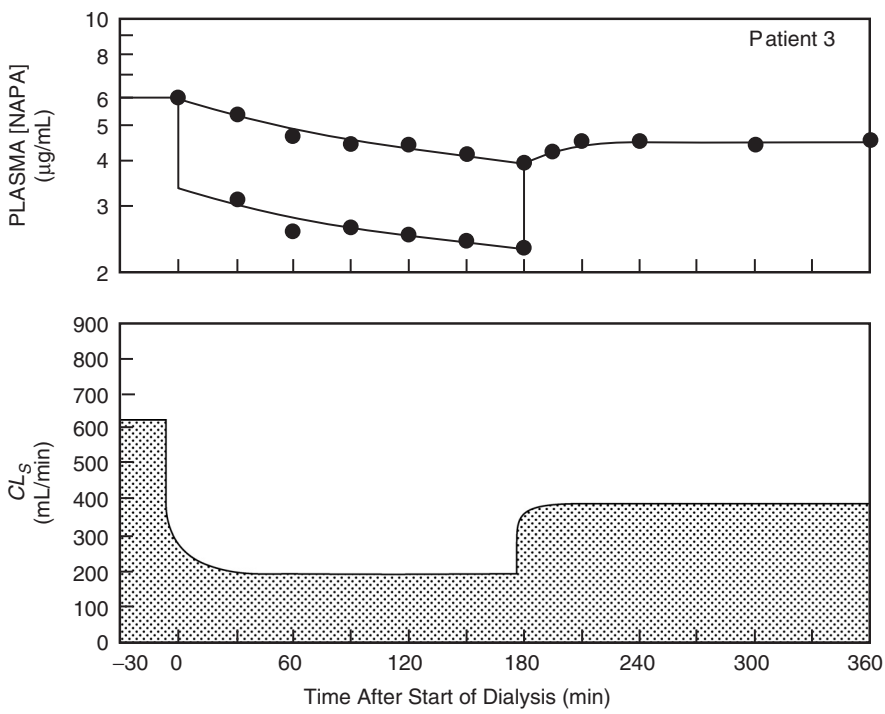

FIGURE 6.3 Computer-fitted curves from pharmacokinetic analysis of NAPA plasma concentrations (•) measured before, during, and after hemodialysis. NAPA plasma concentrations entering (*A*) and leaving (*V*) the artificial kidney are shown during dialysis. The bottom panel shows changes occurring in slow compartment intercompartmental clearance (CL_S) during and after dialysis. (Reproduced with permission from Stec GP, Atkinson AJ Jr, Nevin MJ, Thenot J-P, Gibson TP, Ivanovich P, del Greco F. Clin Pharmacol Ther 1979;26:618–28.)

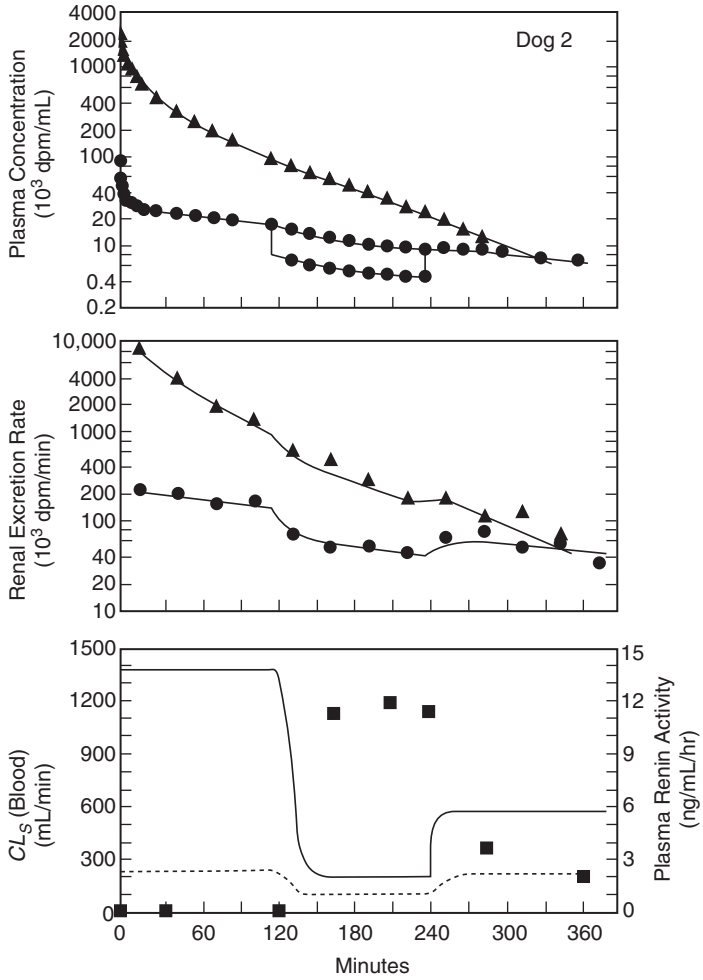

FIGURE 6.4 Kinetic analysis of urea ^{14}C (•) and inulin ^{3}H (▲) plasma concentrations (*upper panel*) and renal excretion rates (*middle panel*) before, during, and after dialysis of a dog with intact kidneys. Inulin was not dialyzable but urea concentrations entering and leaving the dialyzer are both shown. The bottom panel shows CL_S estimates for urea (—) and inulin (- - -), and measured plasma renin activity (■). (Reproduced with permission from Bowsher DJ, Krejcie TC, Avram MJ, Chow MJ, del Greco F, Atkinson AJ Jr. J Lab Clin Med 1985;105:489–97.)

data analysis and representative results are shown in Figure 6.4. During hemodialysis, CL_S for urea and inulin fell on average to 19 and 63% of their respective predialysis values and it was estimated that the efficiency of urea removal was reduced by 10%. In the 2 hours after dialysis, urea CL_S averaged only 37% of predialysis values but returned to its predialysis level for inulin. Compartmental blood flow and permeability coefficient–surface area products of the calculated intercompartmental clearances were calculated as described in Chapter 3 from the permeability-flow equation derived by Renkin (14). During and after dialysis, blood flow to the slow equilibrating compartment (Q_S) on average was reduced to 10 and 20%, respectively, of predialysis values. The permeability coefficient–surface area product did not change significantly. There were no changes in either fast compartment blood flow or permeability coefficient–surface area product. Measurements of plasma renin activity in these dogs with intact kidneys (lower panel of Figure 6.4) suggest that these hemodynamic changes, both during and after hemodialysis, were mediated at least in part by the renin–angiotensin system.

Since the slow equilibrating compartment is largely composed of skeletal muscle, it is not surprising that

the hemodynamic changes associated with hemodialysis result in the skeletal muscle cramps that have been estimated to complicate more than 20% of hemodialysis sessions. Plasma volume contraction appears to be the initiating event that triggers blood pressure homeostatic responses. Those patients who are particularly prone to cramps appear to have a sympathetic nervous system response to this volume stress that is not modulated by activation of a normal renin–angiotensin system (15).

KINETICS OF CONTINUOUS RENAL REPLACEMENT THERAPY

Hemofiltration is a prominent feature of many continuous renal replacement therapies (Table 6.2). However, continuous hemodialysis can also be employed to accelerate solute removal (16). The contribution of both processes to extracorporeal drug clearance will be considered separately in the context of continuous renal replacement therapy.

Clearance by Continuous Hemofiltration

Hemofiltration removes solutes by convective mass transfer down a hydrostatic pressure gradient (17, 18). As plasma water passes through the hemofilter membrane, solute is carried along by solvent drag. Convective mass transfer thus mimics the process of glomerular filtration. The pores of hemofilter membranes are larger than those of dialysis membranes and permit passage of solutes having a molecular weight of up to 50 kDa. Accordingly, a wider range of compounds will be removed by hemofiltration than by hemodialysis. Since large volumes of fluid are removed, fluid replacement solutions need to be administered at rates exceeding 10 L/day (19). This fluid can be administered either before (predilution mode) or after (postdilution mode) the hemofilter. In contemporary practice, roller pumps are used to generate the hydrostatic driving force for ultrafiltration, and the need for arterial catheterization has been obviated by the placement of double-lumen catheters into a large vein (18).

Albumin and other drug-binding proteins do not pass through the filtration membrane, so only unbound drug in plasma water is removed by ultrafiltration. In addition, albumin and other negatively charged plasma proteins exert a Gibbs–Donnan effect that retards the transmembrane convection of some polycationic drugs, such as gentamicin (20, 21). The situation with regard to erythrocyte drug binding is less clear. Although predilution reduces the efficiency of solute removal because solute concentrations in the hemofilter are less than in plasma water (22), it has been reported that net urea removal is enhanced when replacement fluid is administered in the predilution mode, because it can diffuse down its concentration gradient from red blood cells into the diluted plasma water before reaching the hemofilter (19).

The extent to which a solute is carried in the ultrafiltrate across a membrane is characterized by its *sieving coefficient* (*SC*). An approximate equation for calculating sieving coefficients is

$$SC = UF/A \tag{6.7}$$

where *UF* is the solute concentration in the ultrafiltrate and *A* is the solute concentration in plasma water entering the hemofilter (23). The convective clearance of solute across an ultrafilter (CL_{UF}) is given by the product of *SC* and the rate at which fluid crosses the ultrafilter (*UFR*):

$$CL_{UF} = SC \cdot UFR \tag{6.8}$$

Since *UFR* cannot exceed blood flow through the hemofilter, that establishes the theoretical upper limit for CL_{UF}. The major determinants of *SC* are molecular size and the unbound fraction of a compound in plasma water. Values of *SC* may range from 0, for macromolecules that do not pass through the pores of the hemofilter membrane, to 1, for small-molecule drugs that are not protein bound. Although less information has been accumulated about the ultrafiltration clearance of drugs than about their dialysis clearance, in many cases the unbound fraction of drug in plasma water can be used to approximate *SC*.

Measured values of *SC* and fraction of unbound drug in plasma (f_u) are compared for several drugs in Figure 6.5. Values of f_u and *SC* were taken from data published by Golper and Marx (21) with the following exceptions. For both theophylline and phenytoin, measurements of f_u are much higher in serum from uremic patients than in serum from normal subjects and agree more closely with experimental values of *SC*. Accordingly, uremic patient f_u values for theophylline (24) and phenytoin (25) were chosen for the figure, as well as values of *SC* that were obtained in clinical studies of ceftazidime (26), ceftriaxone (27), ciprofloxacin (28), cyclosporine (29), and phenytoin (25). The fact that *SC* values for gentamicin and vancomycin are less than expected on the basis of their protein binding reflects the retarding Gibbs–Donnan effect referred to previously (20, 21). On the other hand, *SC* values for cyclosporine and ceftazidime are considerably greater than expected from f_u measurements. Hence, factors

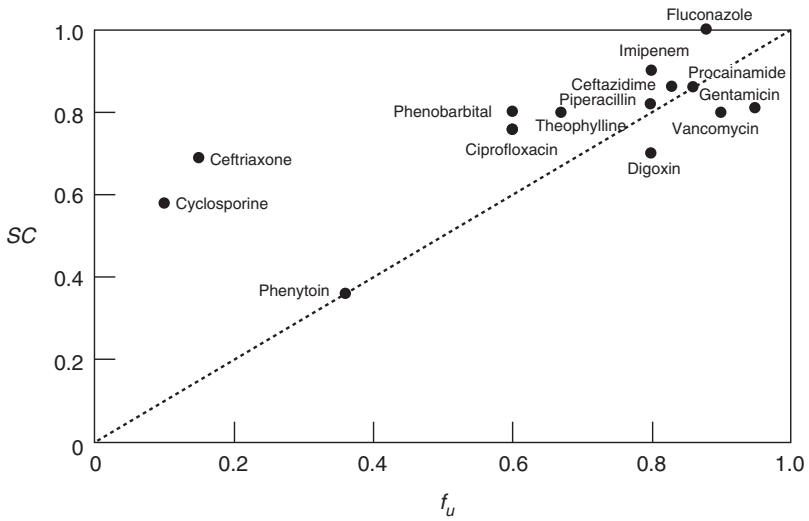

FIGURE 6.5 Relationship between free fraction (f_u) and hemofiltration sieving coefficient (*SC*) for selected drugs. The line of identity (*dashed line*) indicates what would be expected if *SC* were equal to f_u. (See text for further details.)

other than plasma protein binding may affect the sieving of some drugs during hemofiltration (30).

Clearance by Continuous Hemodialysis

Some of the renal replacement therapies listed in Table 6.2 incorporate continuous hemodialysis, or a combination of continuous hemofiltration and hemodialysis. Continuous hemodialysis differs importantly from conventional intermittent hemodialysis in that the flow rate of dialysate is much lower than is countercurrent blood flow through the dialyzer. As a result, concentrations of many solutes in dialysate leaving the dialyzer (C_D) will have nearly equilibrated with their plasma concentrations in blood entering the dialyzer (C_P) (16, 31). The extent to which this equilibration is complete is referred to as the dialysate saturation (S_D) and is calculated as the following ratio:

$$S_D = C_D / C_P$$

In contrast with intermittent hemodialysis in which dialyzer blood flow is rate limiting, diffusive drug clearance during continuous renal replacement therapy is limited by dialysate flow (Q_D), which typically is only 25 mL/min. Accordingly, diffusive drug clearance (CL_D) is calculated from the equation:

$$CL_D = Q_D \cdot S_D \tag{6.9}$$

Equation 6.9 is a nonmechanistic description of clearance that does not incorporate the factors of molecular size or protein binding that account for incomplete equilibration of plasma and dialysate solute concentrations. Dialysate saturation also becomes progressively less complete as dialysate flow approaches blood flow (16).

Extracorporeal Clearance during Continuous Renal Replacement Therapy

Extracorporeal clearance during continuous renal replacement therapy (CL_{EC}) can be regarded as the sum of convective and hemodialytic clearance (16, 31):

$$CL_{EC} = SC \cdot UFR + Q_D \cdot S_D \tag{6.10}$$

Because solute diffusivity decreases with increasing molecular weight, diffusion becomes relatively inefficient even with large-pore hemofilter membranes and convection becomes the primary mechanism involved in the extracorporeal clearance of vancomycin (MW: 1448Da) and other high molecular weight drugs (22). Unfortunately, ultrafiltration rate (*UFR*) tends to decrease with time, falling rather rapidly during the first 6 hours of therapy and reaching about half of its original value in approximately 20 hours (16). Conversely, drug adsorption to the dialyzer membrane may decrease during therapy, resulting in an increase in the sieving coefficient (*SC*) (32). For these reasons, estimates of extracorporeal drug clearance during continuous renal replacement therapy are most reliable when made from measurements of drug recovery in dialysate, as discussed for conventional

hemodialysis. Where the total volume of dialysate recovered during the treatment time (t) is V_{UF}, extracorporeal clearance of drug from plasma can be calculated as follows:

$$CL_{EC} = \frac{C_D \cdot V_{UF}}{C_P \cdot t} \tag{6.11}$$

By analogy with Equation 6.6, the contribution of CL_{EC} to total solute clearance during continuous renal replacement therapy is given by

$$CL_T = CL_{EC} + CL_R + CL_{NR} \tag{6.12}$$

CLINICAL CONSIDERATIONS

From the clinical standpoint, the two main pharmacokinetic considerations regarding renal replacement therapy deal with the use of these therapeutic modalities to treat drug toxicity and, more frequently, the need to administer supplemental drug doses to patients whose impaired renal function necessitates intervention. The factors that determine the extent of drug removal by renal replacement therapy are summarized in Table 6.4. As yet, there has been no attempt to analyze the interaction of all these factors with sufficient rigor to provide precise guidelines for clinical practice. However, extensive protein binding and large distribution volume are the most important factors limiting the extent to which most drugs are removed by hemodialysis or hemofiltration. Accordingly, neither conventional intermittent hemodialysis nor continuous renal replacement therapy will significantly enhance the removal of drugs such as phenytoin, which is extensively bound to plasma proteins, or digoxin, which has a large distribution volume.

TABLE 6.4 Factors Affecting the Extent of Drug Removal by Renal Replacement Therapy

Characteristics of hemodialysis or hemofiltration
• Extracorporeal clearance ($CL_{EC} = CL_D + CL_{UF}$)
• Duration of hemodialysis or hemofiltration
Patient characteristics
• Distribution volume of drug
• Drug binding to plasma proteins
• Drug partitioning into erythrocytes
• Reduction in intercompartmental clearance

Reduction in intercompartmental clearance during hemodialysis may result in a greater than expected decrease in drug concentrations in plasma and rapidly equilibrating tissues, since hemodynamic changes during hemodialysis may effectively sequester a substantial amount of drug in skeletal muscle. This tourniquet-like effect, and its persistence in the postdialysis period, may be useful in treating patients with central nervous system or cardiovascular toxic reactions to drugs (33). Although intercompartmental clearance has not been studied during continuous renal replacement therapy, these modalities produce less hemodynamic instability and would be expected to provoke a smaller cardiovascular homeostatic response.

Drug Dosing Guidelines for Patients Requiring Renal Replacement Therapy

Drug doses need to be increased or supplemented for patients requiring renal replacement therapy only if CL_{EC}, representing extracorporeal clearance from either intermittent hemodialysis or continuous renal replacement therapy, is substantial when compared to $CL_R + CL_{NR}$ (Equation 6.12). Levy (34) has proposed that supplementation is needed only when CL_{EC} is greater than 30% of $CL_R + CL_{NR}$. Several approaches will be considered that can be used to make appropriate drug dose adjustments for patients requiring renal replacement therapy.

Perhaps the simplest approach is to guide dosage using standard reference tables, such as those published by Aronoff and colleagues (35). These tables are based on published literature and suggest drug dose reductions for patients with various levels of renal impairment, as well as for patients requiring conventional hemodialysis, chronic ambulatory peritoneal dialysis, and continuous renal replacement therapy. Although fewer data are available for patients treated with continuous renal replacement therapy than for those treated with conventional intermittent hemodialysis, *UFR* generally ranges from 10 to 16 mL/min during hemofiltration without extracorporeal blood pumping and from 20 to 30 mL/min when blood pumps are used (21). Accordingly, for many drugs, the dose recommendation for patients treated with continuous renal replacement therapy is considered simply to be that which is appropriate for patients with a glomerular filtration rate of 10–50 mL/min.

A second approach is to calculate supplemental doses to replace drug lost during hemodialysis or continuous renal replacement therapy by directly measuring drug loss by extracorporeal removal or by

estimating this loss from drug levels measured in plasma (21, 23). It is relatively easy to make repeated plasma level measurements of some drugs, and to use these to refine supplemental dose estimates. In this case, the supplemental dose (D_{sup}) can be estimated from a plasma level measured at the conclusion of dialysis, or at a convenient interval during continuous renal replacement therapy ($C_{measured}$):

$$D_{sup} = \left(C_{target} - C_{measured}\right) V_d \tag{6.13}$$

When used in the setting of intermittent hemodialysis, this method is likely to overestimate the supplemental dose that is needed, because drug redistribution to the intravascular space from the periphery is slowed by the marked hemodynamic changes that occur during hemodialysis and persist for some time afterwards (12). For example, Pollard *et al.* (36) reported that the postdialysis rebound in serum vancomycin concentrations following high-flux hemodialysis ranged from 19 to 60% of the intradialytic concentration drop and did not peak for an average of 6 hours (range: 1–12 hr). Although the most reliable estimate of extracorporeal drug loss is based on actual measurement of the drug that is removed in dialysate, it is often inconvenient to measure large volumes of dialysate, and many routine drug assay laboratories are not prepared to assay drug concentrations in this fluid. On the other hand, Equation 6.13 provides a reasonably reliable guide to drug dosing during continuous renal replacement therapy because hemodynamic changes are minimized and the rate of drug removal by these modalities is usually less than the rate of drug redistribution from the periphery.

A third approach is to use the principles discussed previously to calculate a maintenance dose multiplication factor (*MDMF*) that can be used to augment the dose that would be appropriate in the absence of renal replacement therapy (32). For continuous renal replacement therapy, *MDMF* is given simply by the following ratio of clearances:

$$MDMF = \frac{CL_{EC} + CL_R + CL_{NR}}{CL_R + CL_{NR}} \tag{6.14}$$

The relative time on (t_{ON}) and off (t_{OFF}) extracorporeal therapy during a dosing interval also must be taken into account for conventional hemodialysis and other intermittent interventions. In this situation:

$$MDMF = \frac{\left(CL_{EC} + CL_R + CL_{NR}\right) t_{ON} + \left(CL_R + CL_{NR}\right) t_{OFF}}{\left(CL_R + CL_{NR}\right)\left(t_{ON} + t_{OFF}\right)}$$

$$MDMF = \left(\frac{CL_{EC}}{CL_R + CL_{NR}}\right)\left(\frac{t_{ON}}{t_{ON} + t_{OFF}}\right) + 1 \tag{6.15}$$

Estimates of *MDMF* for several drugs are listed in Table 6.5. With the exception of vancomycin, baseline drug clearance values for functionally anephric patients (CL_{aneph}) are taken from either the intermittent hemodialysis or the continuous renal replacement references that are cited. In the first 2 weeks after the onset of acute renal failure, vancomycin CL_{aneph} falls from approximately 40 mL/min to the value of 6.0 mL/min that is found in patients with chronic renal failure (37). This latter value is included in Table 6.5

TABLE 6.5 Estimated Drug Dosing Requirements for Patients Requiring Renal Replacement Therapy[a]

		Intermittent hemodialysis				Continuous renal replacement therapy							
Drug	$CL_{(aneph)}$ (mL/min)	Mode	CL_D (mL/min)	*MDMF*	Ref.	Mode	*SC*	*UFR* (mL/min)	CL_{UF} (mL/min)	CL_{HD} (mL/min)	CL_{EC} (mL/min)	*MDMF*	Ref.
Ceftazidime	11.2	HD	43.6	1.6	38	CAVHD	0.86	7.5	6.5	6.6	13.1	2.2	26
Ceftriazone	7.0	HD	11.8	1.0	39	CVVH	0.69	24.1	16.6	—	16.6	3.4	27
Ciprofloxacin	188[b]	HD	40.0	1.0	40	CAVHD/ CVVHD	0.76	7.2	4.8	7.3	12.1	2.4	28
Cyclosporine	463	HD	0.31	1.0	41	CAVH	0.58	4.4	2.6	—	2.6	1.0	29
Gentamicin	15.3	HFD	116	2.0	42	CAVHD	—	—	—	—	5.2	1.3	47
Phenytoin	83[c]	HD	12.0	1.0	43	CAVH	0.36	2.8	1.0	—	1.0	1.0	25
Theophylline	57.4	HD	77.9	1.1	44	CAVHD	—	—	23.3	—	23.3	1.4	46
Vancomycin	6	HFD	106	3.9	45	CVVH	0.89	26.2	23.3	—	23.3	4.9	48

[a] See Table 6.2 for mode abbreviations; *MDMF*, maintenance dose multiplication factor.
[b] Calculated from CL/F, with F assumed to be 60% as in normals.
[c] Elimination of this drug follows Michaelis–Menten kinetics. Apparent clearance will be lower when plasma levels are higher than those obtained in this study.

(the abbreviations used for treatment modality were defined in Table 6.2). In the studies of intermittent hemodialysis, CL_{EC} was calculated by the recovery method except for the studies of ceftazidime (38), ceftriaxone (39), and ciprofloxacin (40), in which this clearance was estimated from the reduction in elimination half-life during dialysis. Equation 6.15 was used to estimate *MDMF* for a dialysis time of 4 hours during a single 24-hour period. In the studies of continuous renal replacement therapy, CL_{EC} was calculated from drug recovery in ultrafiltrate/dialysate in all but the case report of theophylline removal by continuous arteriovenous hemodialysis (CAVHD) (46). In this study, CL_{EC} was estimated from the change in theophylline clearance before and during extracorporeal therapy. Dialysate flow also was not specified in this report. However, the CL_{EC} values for ceftazidime (26), ciprofloxacin (28), and gentamicin (47) all were obtained with a dialysate flow rate of 1 L/hr. Estimates of *MDMF* were made from Equation 6.14.

It is apparent from Table 6.5 that drug dose adjustments generally are required more frequently for patients receiving continuous renal replacement therapy than for those requiring intermittent hemodialysis. In addition, it is evident that drug dosing need not be altered with any modality for phenytoin, cyclosporine, and other drugs that are extensively bound to plasma proteins. As in treating other patients with impaired renal function, maintenance drug doses for patients receiving renal replacement therapy can be adjusted by increasing the dosing interval as well as by reducing the drug dose. An estimate of the increased dosing interval (τ') can be made by dividing the maintenance dosing interval (τ) by *MDMF* (32). Finally, it should be noted that plasma level measurements of gentamicin, theophylline, and vancomycin are routinely available and can be used to provide a more accurate assessment of dosing requirements when these drugs are used to treat patients requiring renal replacement therapy.

Extracorporeal Therapy of Patients with Drug Toxicity

Intensive supportive therapy is all that is required for most patients suffering from dose-related drug toxicity, and drug removal by extracorporeal methods generally is indicated only for those patients whose condition deteriorates despite institution of these more conservative measures (49). However, a decision to intervene with extracorporeal therapy may be prompted by other clinical and pharmacologic considerations that are listed in Table 6.6. For example, most intoxications with phenobarbital can be managed by a combination of supportive care and minimization of renal tubular reabsorption of this drug by forced diuresis and urine alkalinization. However, extracorporeal therapy is indicated if the serum phenobarbital level exceeds 100 μg/mL (49).

TABLE 6.6 Considerations for Extracorporeal Treatment of Drug Intoxications

General clinical considerations
• Clinical deterioration despite intensive supportive therapy
• Severe intoxication indicated by depression of midbrain function or measured plasma or serum level
• Condition complicated by pneumonia, sepsis, or other coexisting illness
Pharmacologic considerations
• Extracorporeal intervention can increase drug elimination significantly
• Drug clearance is slow due to pharmacologic properties of intoxicant or patient's impaired renal or hepatic function
• Intoxicant has a toxic metabolite or has toxic effects that are delayed

A number of low molecular weight alcohols are converted to toxic metabolites. For example, methanol is converted by hepatic alcohol dehydrogenase to formaldehyde and formic acid, which cause metabolic acidosis and retinal injury (50, 51). Clinical evidence of this toxicity is delayed for 12 to 18 hours, providing a therapeutic window for inhibiting methanol metabolism. Ethyl alcohol has traditionally been used to competitively inhibit alcohol dehydrogenase. However, ethyl alcohol must be infused continuously in large fluid volumes that may be deleterious, exhibits Michaelis–Menten elimination kinetics that make appropriate drug dosing difficult, and depresses the central nervous system, thus complicating patient evaluation. Fomepizole (4-methylpyrazole) is a more effective inhibitor of alcohol dehydrogenase that can be administered at a convenient interval and does not depress the central nervous system (51). Accordingly, it has replaced ethyl alcohol as the standard of care in managing patients who have ingested either methanol or ethylene glycol. Despite this therapeutic advance, hemodialysis, which effectively removes both methanol and its toxic metabolites, continues to be indicated when plasma or serum methanol levels exceed 50 mg/dL (49, 51). Because clinical risk is more specifically related to the presence of serum formate, formate levels in excess of 20 mg/dL also may be helpful in indicating the need for hemodialysis (52).

Although hemodialysis is effective in removing phenobarbital, methanol, and other low molecular weight compounds that have a relatively small distribution volume and are not extensively

protein bound, the technique of hemoperfusion has greater efficiency in treating patients with a wide range of intoxications (49, 50). Hemoperfusion entails passage of blood in an extracorporeal circuit through a sorbent column of activated charcoal or resin. Because hemoperfusion relies on the physical process of adsorption and the blood comes in direct contact with sorbent particles, it is not limited in its efficiency by protein binding, and compounds with molecular masses as high as 40 kDa can be adsorbed. Several common intoxicants are listed in Table 6.7 along with the relative efficiency with which they can be removed by hemodialysis and hemoperfusion. Additional practical considerations are that only hemodialysis may be available in certain clinical settings and that hemodialysis also provides an opportunity to correct acidosis and electrolyte imbalances that may occur with some intoxications.

Complications of hemoperfusion include platelet and leukocyte depletion, hypocalcemia, and a mild reduction in body temperature (50). In many cases, these complications are outweighed by the fact that intoxicants are removed more rapidly by hemoperfusion than by hemodialysis. However, an additional consideration is that hemoperfusion clearance tends to decline during therapy as column efficiency declines, presumably reflecting saturation of adsorbent sites (53). In addition, intercompartmental clearance from skeletal muscle and other slowly equilibrating tissues can limit the extent of drug removal by hemoperfusion and result in a rebound of blood levels and possible toxicity at the conclusion of this procedure (54). In some instances, alternative therapies have been developed that are even more efficient than hemoperfusion. For example, digoxin-specific antibody fragments (Fab) now are available for treating severe intoxication with either digoxin or digitoxin (55). In most patients, initial improvement is observed within 1 hour of Fab administration and toxicity is resolved completely within 4 hours.

TABLE 6.7 Comparison of Hemodialysis and Hemoperfusion Efficiency[a]

Intoxicant	Hemodialysis	Charcoal hemoperfusion	Resin hemoperfusion
Acetaminophen	++[b]	++	+++
Acetylsalicylic acid	++	++	—
Amobarbital	++	++	+++
Phenobarbital	++	++	+++
Theophylline	++	+++	+++
Tricyclic antidepressants	++	++	+++

[a] Calculated for blood flow of 200 mL/min [based on data from Winchester JF (50)].

[b] ++; Extraction ratio 0.2–0.5; +++, extraction ratio >0.5.

REFERENCES

1. Abel JJ, Rowntree LG, Turner BB. On the removal of diffusible substances from the circulating blood of living animals by dialysis. J Pharmacol Exp Ther 1914;5:275–317.
2. Kolff WJ. First clinical experience with the artificial kidney. Ann Intern Med 1965;62:608–19.
3. Uribarri J. Past, present and future of end-stage renal disease therapy in the United States. Mt Sinai J Med 1999;66:14–9.
4. Baillie GR, Eisele G. Continuous ambulatory peritoneal dialysis: A review of its mechanics, advantages, complications, and areas of controversy. Ann Pharmacother 1992;26:1409–20.
5. Kramer P, Wigger W, Rieger J, Matthaei D, Scheler F. Arteriovenous haemofiltration: A new and simple method for the treatment of overhydrated patients resistant to diuretics. Klin Wochenschr 1977;55:1121–2.
6. Ronco C, Bellomo R. Continuous renal replacement therapies: The need for a standard nomenclature. Contrib Nephrol 1995;116:28–33.
7. Henderson LW. Hemodialysis: Rationale and physical principles. In: Brenner BM, Rector FC Jr, eds. The kidney. Philadelphia: WB Saunders; 1976. p. 1643–71.
8. Renkin EM. The relation between dialysance, membrane area, permeability and blood flow in the artificial kidney. Tr Am Soc Artific Organs 1956;2:102–5.
9. Gibson TP, Matusik E, Nelson LD, Briggs WA. Artificial kidneys and clearance calculations. Clin Pharmacol Ther 1976;20:720–6.
10. McBain JW, Liu TH. Diffusion of electrolytes, nonelectrolytes and colloidal electrolytes. J Am Chem Soc 1931;53:59–74.
11. Gibson TP. Problems in designing hemodialysis drug studies. Pharmacotherapy 1985;5:23–9.
12. Stec GP, Atkinson AJ Jr, Nevin MJ, Thenot J-P, Ruo TI, Gibson TP, Ivanovich P, del Greco F. *N*-Acetylprocainamide pharmacokinetics in functionally anephric patients before and after perturbation by hemodialysis. Clin Pharmacol Ther 1979;26:618–28.
13. Bowsher DJ, Krejcie TC, Avram MJ, Chow MJ, del Greco F, Atkinson AJ Jr. Reduction in slow intercompartmental clearance of urea during dialysis. J Lab Clin Med 1985;105:489–97.
14. Renkin EM. Effects of blood flow on diffusion kinetics in isolated perfused hindlegs of cats: A double circulation hypothesis. Am J Physiol 1953;183:125–36.
15. Sidhom OA, Odeh YK, Krumlovsky FA, Budris WA, Wang Z, Pospisil PA, Atkinson AJ Jr. Low dose prazosin in patients with muscle cramps during hemodialysis. Clin Pharmacol Ther 1994;56:445–51.

16. Sigler MH, Teehan BP, Van Valceknburgh D. Solute transport in continuous hemodialysis: A new treatment for acute renal failure. Kidney Int 1987;32:562–71.
17. Bressolle F, Kinowski J-M, de la Coussaye JE, Wynn N, Eledjam J-J, Galtier M. Clinical pharmacokinetics during continuous haemofiltration. Clin Pharmacokinet 1994;26:457–71.
18. Meyer MM. Renal replacement therapies. Critical Care Clin 2000;16:29–58.
19. Golper TA. Continuous arteriovenous hemofiltration in acute renal failure. Am J Kidney Dis 1985; 6:373–386.
20. Golper TA, Saad A-MA. Gentamicin and phenytoin *in vitro* sieving characteristics through polysulfone hemofilters: Effect of flow rate, drug concentration and solvent systems. Kidney Int 1986;30:937–43.
21. Golper TA, Marx MA. Drug dosing adjustments during continuous renal replacement therapies. Kidney Int 1998;53(suppl 66):S165–8.
22. Clark WR, Ronco C. CRRT efficiency and efficacy in relation to solute size. Kidney Int 1999;56 (suppl 72):S3–7.
23. Golper TA, Wedel SK, Kaplan AA, Saad A-M, Donta ST, Paganini EP. Drug removal during continuous arteriovenous hemofiltration: Theory and clinical observations. Int J Artif Organs 1985;8:307–12.
24. Vanholder R, Van Landschoot N, De Smet R, Schoots A, Ringoir S. Drug protein binding in chronic renal failure: Evaluation of nine drugs. Kidney Int 1988;33:996–1004.
25. Lau AH, Kronfol NO. Effect of continuous hemofiltration on phenytoin elimination. Ther Drug Monitor 1994;16:53–7.
26. Davies SP, Lacey LF, Kox WJ, Brown EA. Pharmacokinetics of cefuroxime and ceftazidime in patients with acute renal failure treated by continuous arteriovenous haemodialysis. Nephrol Dial Transplant 1991; 6:971–6.
27. Kroh UF, Lennartz H, Edwards DJ, Stoeckel K. Pharmacokinetics of ceftriaxone in patients undergoing continuous veno-venous hemofiltration. J Clin Pharmacol 1996;36:1114–9.
28. Davies SP, Azadian BS, Kox WJ, Brown EA. Pharmacokinetics of ciprofloxacin and vancomycin in patients with acute renal failure treated by continuous haemodialysis. Nephrol Dial Transplant 1992;7:848–54.
29. Cleary JD, Davis G, Raju S. Cyclosporine pharmacokinetics in a lung transplant patient undergoing hemofiltration. Transplantation 1989;48:710–2.
30. Lau AH, Pyle K, Kronfol NO, Libertin CR. Removal of cephalosporins by continuous arteriovenous ultrafiltration (CAVU) and hemofiltration (CAVH). Int J Artif Organs 1989;12:379–83.
31. Schetz M, Ferdinande P, Van den Berghe G, Verwaest C, Lauwers P. Pharmacokinetics of continuous renal replacement therapy. Intensive Care Med 1995;21:612–20.
32. Reetze-Bonorden P, Böhler J, Keller E. Drug dosage in patients during continuous renal replacement therapy: Pharmacokinetic and therapeutic considerations. Clin Pharmacokinet 1993;24;362–79.
33. Atkinson AJ Jr, Krumlovsky FA, Huang CM, del Greco F. Hemodialysis for severe procainamide toxicity. Clinical and pharmacokinetic observations. Clin Pharmacol Ther 1976;20:585–92.
34. Levy G. Pharmacokinetics in renal disease. Am J Med 1977;62:461–5.
35. Aronoff GR, Berns JS, Brier ME, Golper TA, Morrison G, Singer I, Swan SK, Bennett WM. Drug prescribing in renal failure: Dosing guidelines for adults. 4th ed. Philadelphia: American College of Physicians;1999.
36. Pollard TA, Lampasona V, Akkerman S, Tom K, Hooks MA, Mullins RE, Maroni BJ. Vancomycin redistribution: Dosing recommendations following high-flux hemodialysis. Kid Int 1994;45:232–7.
37. Macias WL, Mueller BA, Scarim KS. Vancomycin pharmacokinetics in acute renal failure: Preservation of nonrenal clearance. Clin Pharmacol Ther 1991; 50:688–94.
38. Ohkawa M, Nakashima T, Shoda R, Ikeda A, Orito M, Sawaki M, Sugata T, Shimamura M, Hirano S, Okumura K. Pharmacokinetics of ceftazidime in patients with renal insufficiency and in those undergoing hemodialysis. Chemotherapy 1985; 31:410–6.
39. Ti T-Y, Fortin L, Kreeft JH, East DS, Ogilvie RI, Somerville PJ. Kinetic disposition of intravenous ceftriaxone in normal subjects and patients with renal failure on hemodialysis or peritoneal dialysis. Antimicrob Agents Chemother 1984;25:83–7.
40. Singlas E, Taburet AM, Landru I, Albin H, Ryckelinck JP. Pharmacokinetics of ciprofloxacin tablets in renal failure; influence of haemodialysis. Eur J Clin Pharmacol 1987;31:589–93.
41. Venkataramanan R, Ptachcinski RJ, Burckart GJ, Yang SL, Starzl TE, van Theil DH. The clearance of cyclosporine by hemodialysis. J Clin Pharmacol 1984;24:528–31.
42. Amin NB, Padhi ID, Touchette MA, Patel RV, Dunfee TP, Anandan JV. Characterization of gentamicin pharmacokinetics in patients hemodialyzed with high-flux polysulfone membranes. Am J Kidney Dis 1999;34:222–7.
43. Martin E, Gambertoglio JG, Adler DS, Tozer TN, Roman LA, Grausz H. Removal of phenytoin by hemodialysis in uremic patients. JAMA 1977; 238:1750–3.
44. Kradjan WA, Martin TR, Delaney CJ, Blair AD, Cutler RE. Effect of hemodialysis on the pharmacokinetics of theophylline in chronic renal failure. Nephron 1982;32:40–44.
45. Touchette MA, Patel RV, Anandan JV, Dumler F, Zarowitz BJ. Vancomycin removal by high-flux polysulfone hemodialysis membranes in critically ill patients with end-stage renal disease. Am J Kidney Dis 1995;26:469–74.
46. Urquhart R, Edwards C. Increased theophylline clearance during hemofiltration. Ann Pharmacother 1995;29:787–8.
47. Ernest D, Cutler DJ. Gentamicin clearance during continuous arteriovenous hemodiafiltration. Crit Care Med 1992;20:586–9.
48. Boereboom FTJ, Ververs FFT, Blankestijn PJ, Savelkoul THE, van Dijk A. Vancomycin clearance during continuous venovenous haemofiltration in critically ill patients. Intensive Care Med 1999;25:1100–4.

49. Blye E, Lorch J, Cortell S. Extracorporeal therapy in the treatment of intoxication. Am J Kidney Dis 1984;3:321–38.
50. Winchester JF. Active methods for detoxification. In: Haddad LM, Shannon MW, Winchester JF, eds. Clinical management of poisoning and drug overdose. 3rd ed. Philadelphia: WB Saunders; 1998. p. 175–88.
51. Mycyk MB, Leikin JB. Antidote review: Fomepizole for methanol poisoning. Am J Ther 2003;10:68–70.
52. Osterloh JD, Pond SM, Grady S, Becker CE. Serum formate concentrations in methanol intoxication as a criterion for hemodialysis. Ann Intern Med 1986;104:200–3.
53. Shah G, Nelson HA, Atkinson AJ Jr, Okita GT, Ivanovich P, Gibson TP. Effect of hemoperfusion on the pharmacokinetics of digitoxin in dogs. J Lab Clin Med 1979;93:370–80.
54. Gibson TP, Atkinson AJ Jr. Effect of changes in intercompartment rate constants on drug removal during hemoperfusion. J Pharm Sci 1978;67:1178–9.
55. Antman E, Wenger TL, Butler VP Jr, Haber E, Smith TW. Treatment of 150 cases of life-threatening digitalis intoxication with digoxin-specific Fab antibody fragments: Final report of a multicenter study. Circulation 1990;81:1744–52.

CHAPTER

7

Effect of Liver Disease on Pharmacokinetics

GREGORY M. SUSLA[1] AND ARTHUR J. ATKINSON, JR.[2]

[1]*VHA Consulting Services, Frederick, Maryland,*
[2]*Clinical Center, National Institutes of Health, Bethesda, Maryland*

HEPATIC ELIMINATION OF DRUGS

Hepatic clearance (CL_H) may be defined as the volume of blood perfusing the liver that is cleared of drug per unit time. Usually, hepatic clearance is equated with nonrenal clearance and is calculated as total body clearance (CL_E) minus renal clearance (CL_R):

$$CL_H = CL_E - CL_R \tag{7.1}$$

Accordingly, these estimates may include a component of extrahepatic nonrenal clearance.

The factors that affect hepatic clearance include blood flow to the liver (Q), the fraction of drug not bound to plasma proteins (f_u), and intrinsic clearance (CL_{int}) (1, 2). Intrinsic clearance is simply the hepatic clearance that would be observed in the absence of blood flow and protein binding restrictions. As discussed in Chapter 2, hepatic clearance usually can be considered to be a first-order process. In those cases, intrinsic clearance represents the ratio of V_{max}/K_m, and this relationship has been used as the basis for correlating *in vitro* studies of drug metabolism with *in vivo* results (3). However, for phenytoin and several other drugs, the Michaelis–Menten equation is needed to characterize intrinsic clearance.

The well-stirred model, shown in Figure 7.1, is the model of hepatic clearance that is used most commonly in pharmacokinetics. If we apply the Fick equation (see Chapter 6) to this model, hepatic clearance can be defined as follows (2):

$$CL_H = Q\left[\frac{C_a - C_v}{C_a}\right] \tag{7.2}$$

The ratio of concentrations defined by the terms within the brackets is termed the *extraction ratio (ER)*. An expression for the extraction ratio also can be obtained by applying the following mass balance equation to the model shown in Figure 7.1:

$$V(dC_a/dt) = QC_a - QC_v - f_u CL_{int} C_v$$

At steady state,

$$Q(C_a - C_v) = f_u CL_{int} C_v \tag{7.3}$$

Also,

$$QC_a = \left(Q + f_u CL_{int}\right) C_v \tag{7.4}$$

since

$$ER = \frac{C_a - C_v}{C_a}$$

Equation 7.3 can be divided by Equation 7.4 to define extraction ratio in terms of Q, f_u, and CL_{int}:

$$ER = \frac{f_u CL_{int}}{Q + f_u CL_{int}} \tag{7.5}$$

By substituting this expression for extraction ratio into Equation 7.2, hepatic clearance can be expressed as

$$CL_H = Q\left[\frac{f_u CL_{int}}{Q + f_u CL_{int}}\right] \tag{7.6}$$

Two limiting cases arise when $f_u CL_{int} << Q$ and when $f_u CL_{int} >> Q$ (2). In the former instance

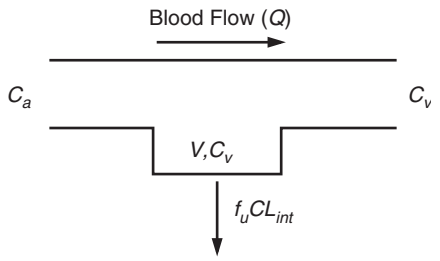

FIGURE 7.1 The well-stirred model of hepatic clearance, in which the liver is viewed as a single compartment having a volume (V) and blood flow (Q). Drug concentrations reaching the liver via the hepatic artery and portal vein are designated by C_a, and those in emergent hepatic venous blood by C_v. Drug concentrations within the liver are considered to be in equilibrium with those in emergent venous blood. Intrinsic clearance (CL_{int}) acts to eliminate the fraction of drug not bound to plasma proteins (f_u).

Equation 7.5 can be simplified to

$$CL_H = f_u CL_{int} \tag{7.7}$$

Hepatic clearance is termed *restrictive* in this case, since it is limited by protein binding. This situation is analogous to the elimination of drugs by glomerular filtration. Drugs that are restrictively eliminated have extraction ratios < 0.3.

When $f_u CL_{int} >> Q$, Equation 7.5 can be reduced to

$$CL_H = Q \tag{7.8}$$

In this case, hepatic clearance is *flow limited*, similar to the renal tubular excretion of *p*-aminohippurate. Because protein binding does not affect their clearance, drugs whose hepatic clearance is flow limited are said to be *nonrestrictively* eliminated and have extraction ratios > 0.7.

In addition to the well-stirred model that is the basis for Equation 7.6, several other kinetic models of hepatic clearance have been developed (4). However, the following discussion will be based on the relationships defined by Equation 7.6, and the limiting cases represented by Equations 7.7 and 7.8.

Restrictively Metabolized Drugs (ER < 0.3)

The product of f_u and CL_{int} is small relative to liver blood flow (usually about 1500 mL/min) for drugs that are restrictively metabolized. Although the extraction ratio of these drugs is less than 0.3, hepatic metabolism often constitutes their principal pathway of elimination and they frequently have long elimination-phase half-lives (e.g., diazepam: $t_{1/2} = 43$ hr). The hepatic clearance of these drugs is affected by changes in their binding to plasma proteins, by induction or inhibition of hepatic drug-metabolizing enzymes, and by age, nutrition, and pathological factors. However, as indicated by Equation 7.7, their hepatic clearance is not affected significantly by changes in hepatic blood flow.

Effect of Changes in Protein Binding on Hepatic Clearance

It usually is assumed that the free drug concentration in blood is equal to the drug concentration to which hepatic drug-metabolizing enzymes are exposed. Although protein binding would not be anticipated to change hepatic clearance significantly for restrictively metabolized drugs that have $f_u > 80\%$, displacement of highly bound ($f_u < 20\%$) drugs from their plasma protein binding sites will result in a significant increase in their hepatic clearance. However, steady-state concentrations of unbound drug will be unchanged as long as there is no change in CL_{int}. This occurs in some drug interactions, as diagrammed in Figure 7.2. This situation also is encountered in pathological conditions in which plasma proteins or plasma protein binding is decreased, as described in Chapter 5 for phenytoin kinetics in patients with impaired renal function. Since pharmacological effects

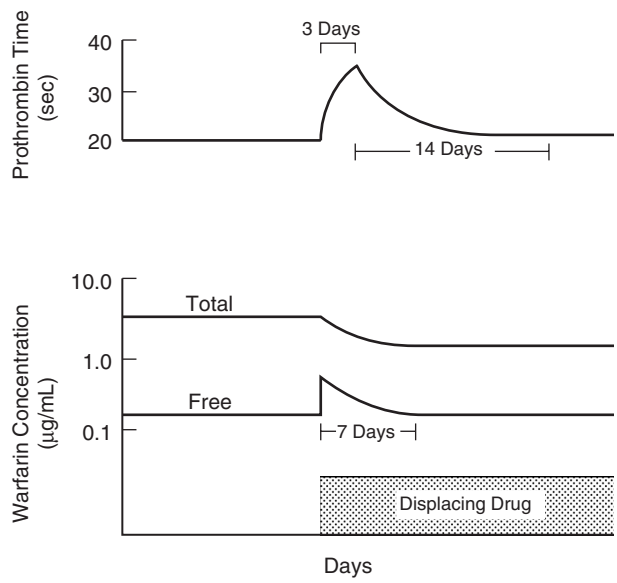

FIGURE 7.2 Time course of an interaction in which warfarin, a restrictively metabolized drug, is displaced from its plasma protein binding sites. Although free warfarin concentrations rise initially as a result of the interaction, they subsequently return to preinteraction levels. As a result, the increase in prothrombin time is only transient. Because f_u is increased, total (bound plus free) warfarin levels remain depressed as long as treatment with the displacing drug is continued. (Reproduced with permission from Atkinson AJ Jr, Reidenberg MM, Thompson WL. Clinical pharmacology. In: Greenberger N, ed. MKSAP VI Syllabus. Philadelphia: American College of Physicians; 1982. p. 85–96.)

are related to concentrations of unbound drug, pure displacement-type drug interactions put patients at risk for only a brief period of time. Similarly, dose adjustments are not needed for patients whose protein binding is impaired. In fact, as pointed out in Chapter 5, measurement of total rather than unbound drug levels in these patients actually may lead to inappropriate dose increases.

Effect of Changes in Intrinsic Clearance on Hepatic Drug Clearance

Both hepatic disease and drug interactions can alter the intrinsic clearance of restrictively eliminated drugs. Drug interactions will be considered in more detail in Chapter 15. The effects of liver disease on drug elimination will be discussed in the following sections. Although a number of probe drugs have been used to characterize hepatic clearance, analysis of the factors influencing the intrinsic clearance of drugs is hampered by the fact that, in contrast to the use of creatinine clearance to assess renal function, there are no simple measures that can be applied on a routine clinical basis to assess hepatic clearance.

Drugs with an Intermediate Extraction Ratio (0.3 < ER < 0.7)

Few drugs exhibit an intermediate extraction ratio. Evaluation of the hepatic clearance of these drugs requires consideration of all of the parameters included in Equation 7.6. Disease-associated or drug-induced alterations in protein binding, hepatic blood flow, or intrinsic clearance may alter hepatic clearance significantly.

Nonrestrictively Metabolized Drugs (ER > 0.70)

The product of f_u and CL_{int} is large relative to liver blood flow for drugs that are nonrestrictively metabolized. These drugs characteristically have short elimination-phase half-lives (e.g., propranolol: $t_{1/2} = 3.9$ hr), and changes in hepatic blood flow have a major effect on their hepatic clearance (Equation 7.8). Accordingly, hemodynamic changes, such as congestive heart failure, that reduce liver blood flow will reduce the hepatic clearance of these drugs and may necessitate appropriate adjustments in intravenous dosage. Changes in hepatic blood flow will also affect the first-pass metabolism of oral doses of nonrestrictively metabolized drugs, but the effects of this on patient exposure are not intuitively obvious.

First-Pass Metabolism

Because nonrestrictively metabolized drugs have an extraction ratio that exceeds 0.7, they undergo extensive first-pass metabolism, which reduces their bioavailability after oral administration (Chapter 4). If there is no loss of drug due to degradation or metabolism within the gastrointestinal tract or to incomplete absorption, the relationship between bioavailability (F) and extraction ratio is given by the following equation:

$$F = 1 - ER \tag{7.9}$$

Because Equation 7.8 implies that $ER = 1$ for nonrestrictively metabolized drugs, yet the oral route of administration can be used for many drugs in this category (e.g., $F > 0$ for morphine and propranolol), it is apparent that Equation 7.9 represents only a rough approximation. By using Equation 7.5 to substitute for ER in Equation 7.9, we obtain a more precise estimate of the impact of first-pass metabolism on bioavailability:

$$F = \frac{Q}{Q + f_u CL_{int}} \tag{7.10}$$

Considering the case in which a drug is eliminated only by hepatic metabolism, Equation 4.2 from Chapter 4 can be rewritten as follows:

$$D_{oral} \cdot F = CL_H \cdot AUC_{oral}$$

Using Equations 7.6 and 7.10 to substitute, respectively, for CL_H and F yields the result that

$$D_{oral} = f_u CL_{int} \cdot AUC_{oral} \tag{7.11}$$

It can be seen from Equation 7.11 that oral doses of nonrestrictively metabolized drugs should not need to be adjusted in response to changes in hepatic blood flow. Equation 7.11 also forms the basis for using AUC_{oral} measurements to calculate so-called "oral clearance'' as an estimate of $f_u CL_{int}$. However, if renal excretion contributes to drug elimination, it will reduce AUC_{oral} and lead to overestimation of $f_u CL_{int}$ unless the contribution of renal clearance is accounted for (2).

Biliary Excretion of Drugs

Relatively few drugs are taken up by the liver and without further metabolism excreted into bile, which, as an aqueous solution, generally favors excretion of more water-soluble compounds (5). On the other hand,

many polar drug metabolites, such as glucuronide conjugates, undergo biliary excretion. In order for compounds to be excreted in bile they must first pass the fenestrated endothelium that lines the hepatic sinusoids, then cross both the luminal and canalicular membrane surfaces of hepatocytes. Passage across these two hepatocyte membrane surfaces often is facilitated by active transport systems, which will be discussed in Chapter 14. Consequently, chemical structure, polarity, and molecular weight are important determinants of the extent to which compounds are excreted in bile. In general, polar compounds with a molecular weight range of 500 to 600 Da are excreted in bile, whereas those with a lower molecular weight tend to be eliminated preferentially by renal excretion. However, 5-fluorouracil has a molecular weight of only 130 Da, yet is excreted in bile with a bile/plasma concentration ratio of 2.0 (6). Nonetheless, biliary excretion of parent drug and metabolites accounts for only 2–3% of the elimination of an administered 5-fluorouracil dose in patients with normal renal function (7).

Compounds that enhance bile production stimulate biliary excretion of drugs normally eliminated by this route, whereas biliary excretion of drugs will be decreased by compounds that decrease bile flow or by pathophysiologic conditions that cause cholestasis (8). Route of administration may also influence the extent of drug excretion into bile. Oral administration may cause a drug to be extracted by the liver and excreted into bile to a greater degree than if the intravenous route were used.

Enterohepatic Circulation

Drugs excreted into bile traverse the biliary tract to reach the small intestine, where they may be reabsorbed (5). Drug metabolites that reach the intestine also may be converted back to the parent drug and be reabsorbed. This is particularly true for some glucuronide conjugates that are hydrolyzed by β-glucuronidase present in intestinal bacteria. The term *enterohepatic circulation* refers to this cycle in which a drug or metabolite is excreted in bile and then reabsorbed from the intestine either as the metabolite or after conversion back to the parent drug. Thus, enterohepatic cycling of a drug increases its bioavailability, as assessed from the area under the plasma-level-vs.-time curve, and prolongs its elimination-phase half-life.

Studies in animals have demonstrated that biliary clearance actually may exceed plasma clearance for some drugs and in species with extensive enterohepatic circulation (9). Interruption of enterohepatic circulation reduces both the area under the plasma-level-vs.-time curve and the elimination-phase half-life. Enterohepatic circulation also increases the total exposure of the intestinal mucosa to potentially toxic drugs. Thus, the intestinal toxicity of indomethacin is most marked in those species that have a high ratio of biliary to renal drug excretion (9).

Enterohepatic circulation may result in a second peak in the plasma-level-vs.-time curve as shown in Figure 7.3A. The occurrence of this large peak of drug concentration in intestinal fluid appears to reflect intermittent gallbladder contraction and pulsatile delivery of drug-containing bile to the intestine, because this double-peak phenomenon is not encountered in animal species that lack a gallbladder (10). Realistic pharmacokinetic modeling of this process entails incorporation of a variable lag-time interval that can reflect intermittent gallbladder emptying, as in Figure 7.3B. Cimetidine is typical of many drugs that undergo enterohepatic circulation, in that secondary plasma concentration peaks occur after oral, but not intravenous, administration (11). These secondary peaks were seen after meals in individuals who were given cimetidine while fasting but were allowed subsequent food intake that presumably triggered gallbladder contraction and the discharge of drug-containing bile into the small intestine. Secondary peaks were not seen when cimetidine was administered intravenously or coadministered orally with food. On the other hand, ranitidine differs from cimetidine and is unusual in that secondary peaks occur after both intravenous and oral administration to fasting patients who subsequently were fed, as shown in Figure 7.3A (12). This difference reflects the fact that cimetidine reaches the bile from the liver primarily during first-pass transit via the portal circulation (k_1 in Figure 7.3B), whereas there is substantial hepatic uptake of ranitidine from the systemic circulation (k_2, in Figure 7.3B).

EFFECTS OF LIVER DISEASE ON PHARMACOKINETICS

Liver disease in humans encompasses a wide range of pathological disturbances that can lead to a reduction in liver blood flow, extrahepatic or intrahepatic shunting of blood, hepatocyte dysfunction, quantitative and qualitative changes in serum proteins, and changes in bile flow. Different forms of hepatic disease may produce different alterations in drug absorption, disposition, and pharmacologic effect. The pharmacokinetic or pharmacodynamic consequences of a specific hepatic disease may differ

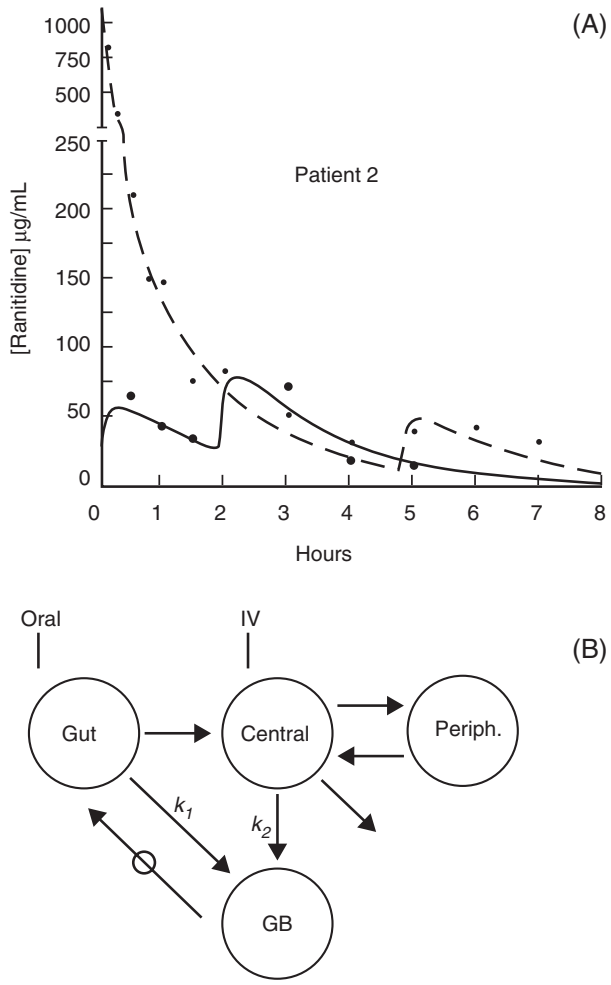

FIGURE 7.3 (A) Pharmacokinetic analysis of secondary plasma concentration peaks following the oral and intravenous administration of 20-mg doses of ranitidine to a healthy subject. The lines are based on the pharmacokinetic model (B) and represent a least-squares fit of the plasma concentrations measured after the intravenous (*dashed line*) and oral (*solid line*) doses. (B) Pharmacokinetic model used for the analysis of the enterohepatic cycling of cimetidine and ranitidine. Drug enters the gallbladder via the liver, for which a separate compartment is not required, either during first-pass transit from the gut via the portal circulation (k_1) or directly from the systemic circulation (k_2). The irregular discharge of drug-containing bile from the gallbladder is indicated by the arrow (⊸) going from gallbladder (GB) to gut. Drug distribution within the body is modeled as a two-compartment system. (Reproduced with permission from Miller R. J Pharm Sci 1984;73:1376–9.)

among individuals or even within a single individual over time. Each of the major determinants of hepatic clearance, CL_{int}, f_u, Q, and vascular architecture may be independently altered.

Although there are numerous causes of hepatic injury, it appears that the hepatic response to injury is a limited one and that the functional consequences are determined more by the extent of the injury than by the cause. At this time there is no generally available test that can be used to correlate changes in drug absorption and disposition with the degree of hepatic impairment.

Acute Hepatitis

Acute hepatitis is an inflammatory condition of the liver that is caused by viruses or hepatotoxins. In acute viral hepatitis, inflammatory changes in the hepatocyte are generally mild and transient, although they can be chronic (chronic active hepatitis) and severe, resulting in cirrhosis or death. Blaschke and Williams and their colleagues (12–15) have conducted informative studies of the effects of acute viral hepatitis on drug disposition. These investigators used a longitudinal study design in which each of a small number of patients was studied initially during the time that they had acute viral hepatitis and subsequently after recovery (Table 7.1). The drugs that were administered included phenytoin (12), tolbutamide (13), warfarin (14), and lidocaine (15). The most consistent significant finding was that the plasma protein binding of both phenytoin and tolbutamide was reduced during acute hepatitis. For both drugs, this was partly attributed to drug displacement from protein binding sites by elevated bilirubin levels. As a result of these changes, the distribution volume of phenytoin increased slightly during hepatitis (see Chapter 3). Although no significant change was noted in the average values of either phenytoin CL_H or CL_{int}, CL_{int} was reduced by approximately 50% in the two patients with the greatest evidence of hepatocellular damage. On the other hand, the reduction in tolbutamide binding to plasma proteins had no observable effect on distribution volume or CL_{int} but did result in an increase in CL_H. No consistent changes were observed in warfarin kinetics during acute viral hepatitis. However, prothrombin time was prolonged to a greater extent than expected in two of the five patients, reflecting impaired synthesis of Factor VII. Lidocaine kinetics also were not altered consistently during acute viral hepatitis, although clearance decreased in four of the six patients who were studied.

In general, drug elimination during acute viral hepatitis is either normal or only moderately impaired. Observed changes tend to be variable and related to the extent of hepatocellular damage incurred. If the acute hepatitis resolves, drug disposition returns to normal. Drug elimination is likely to be impaired most significantly in patients who develop chronic hepatitis B virus-related liver disease, but even then only late in the evolution of this disease (16). This stands in marked contrast to the severity of

TABLE 7.1 Pharmacokinetics of Some Drugs during and after Acute Viral Hepatitis

	f_u		V_d		CL_H		CL_{int}		
Drug	During	After	During L/kg	After (L/kg)	During (mL/hr/kg)	After (mL/hr/kg)	During (mL/hr/kg)	After (mL/hr/kg)	Ref.
Phenytoin[a]	0.126[b]	0.099	0.68[b]	0.63	0.0430	0.0373	0.352	0.385	12
Tolbutamide	0.087[b]	0.068	0.15	0.15	26[b]	18	300	260	13
Warfarin	0.012	0.012	0.09	0.21	6.1	6.1	519	514	14
Lidocaine	0.56	0.49	3.1	2.0	13.0	20.0	23.2[c]	40.8[c]	15

[a] A low dose of phenytoin was administered so that first-order kinetics would be approximated.
[b] Difference in studies during and after recovery from acute viral hepatitis was significant at $P < 0.05$ by paired t-test.
[c] Protein binding results for individual patients were not given, so CL_{int} was estimated from average values.

acute hepatitis that can be caused by hepatotoxins. For example, Prescott and Wright (17) found that liver damage can occur within 2 to 3 hours after ingestion of an acetaminophen overdose. The elimination-phase half-life of acetaminophen averaged only 2.7 hours in patients without liver damage, but ranged from 4.3 to 7.7 hours (mean = 5.8 hr) in four patients with liver damage and from 4.3 to 13.9 hours (mean = 7.7 hr) in three patients with both liver and kidney damage resulting from acetaminophen toxicity. These authors observed that a fatal outcome was likely in patients whose acetaminophen elimination half-life exceeded 10 to 12 hours.

Chronic Liver Disease and Cirrhosis

Chronic liver disease is usually secondary to chronic alcohol abuse or chronic viral hepatitis. Alcoholic liver disease is most common and begins with the accumulation of fat vacuoles within hepatocytes and hepatic enlargement. There is a decrease in cytochrome P450 content per weight of tissue, but this is compensated for by the increase in liver size so that drug metabolism is not impaired (18). Alcoholic fatty liver may be accompanied or followed by alcoholic hepatitis, in which hepatocyte degeneration and necrosis become evident. In neither of these conditions is there significant diversion of blood flow past functioning hepatocytes by functional or anatomic shunts.

Cirrhosis occurs most frequently in the setting of alcoholic liver disease and represents the final common pathway of a number of chronic liver diseases. The development of cirrhosis is characterized by the appearance of fibroblasts and collagen deposition. This is accompanied by a reduction in liver size and the formation of nodules of regenerated hepatocytes. As a result, total liver content of cytochrome P450 is reduced in these patients. Initially, fibroblasts deposit collagen fibrils in the sinusoidal space, including the space of Disse (18). Collagen deposition not only produces characteristic bands of connective scar tissue but also forms a basement membrane devoid of microvilli along the sinusoidal surface of the hepatocyte. The collagen barrier between the hepatocyte and sinusoid, in conjunction with alterations in the sinusoidal membrane of the hepatocyte, results in functional shunting of blood past the remaining hepatocyte mass. This can interfere significantly with the hepatic uptake of oxygen, nutrients, and plasma constituents, including drugs and metabolites.

The deposition of fibrous bands also disrupts the normal hepatic vascular architecture and increases vascular resistance and portal venous pressure. This reduces portal venous flow that normally accounts for 70% of total liver blood flow (19). However, the decrease in portal venous flow is compensated for by an increase in hepatic artery flow, so that total blood flow reaching the liver is maintained at the normal value of 18 mL/min · kg in patients with either chronic viral hepatitis or cirrhosis (20). The increase in portal venous pressure also leads to the formation of extrahepatic and intrahepatic shunts. Extrahepatic shunting occurs through the extensive collateral network that connects the portal and systemic circulations (19). Important examples include collaterals at the gastroesophageal junction, which can dilate to form varices, and the umbilical vein. In a study of cirrhotic patients with bleeding esophageal varices, an average of 70% of mesenteric and 95% of splenic blood flow was found to be diverted through extrahepatic shunts (21). Intrahepatic shunting results both from intrahepatic vascular anastamoses that bypass hepatic sinusoids and from the functional sinusoidal barrier caused by collagen deposition. Iwasa *et al*. (20) found that the combination of anatomic and functional intrahepatic shunting averaged 25% of total liver blood flow in normal subjects, but was increased to 33% in patients with chronic viral hepatitis and to 52% in cirrhotic patients.

Pharmacokinetic Consequences of Liver Cirrhosis

The net result of chronic hepatic disease that leads to cirrhosis is that pathophysiologic alterations may result in both decreased hepatocyte function, with as much as a 50% decrease in cytochrome P450 content, and/or shunting of blood away from optimally functioning hepatocytes. Accordingly, cirrhosis affects drug metabolism more than does any other form of liver disease. In fact, cirrhosis may decrease the clearance of drugs that are nonrestrictively eliminated in subjects with normal liver function, to the extent that it no longer approximates hepatic blood flow but is influenced to a greater extent by hepatic intrinsic clearance (22). By reducing first-pass hepatic metabolism, cirrhosis also may cause a clinically significant increase in the extent to which nonrestrictively eliminated drugs are absorbed.

Influence of Portosystemic Shunting

When portosystemic shunting is present, total hepatic blood flow (Q) equals the sum of perfusion flow (Q_p) and shunt flow (Q_s). Portocaval shunting will impair the efficiency of hepatic extraction and reduce the extraction ratio, as indicated by the following modification of Equation 7.5 (23).

$$ER = \frac{f_u CL_{int}}{Q + f_u CL_{int}} \cdot \frac{Q_p}{Q} \tag{7.12}$$

The corresponding impact on hepatic clearance is given by the following equation:

$$CL_H = Q_p \left[\frac{f_u CL_{int}}{Q + f_u CL_{int}} \right] \tag{7.13}$$

Because Q and Q_p are both reduced in patients with severe cirrhosis, in whom portocaval shunting is most pronounced, hepatic clearance will be reduced more for nonrestrictively than for restrictively metabolized drugs.

Similarly, restrictively metabolized drugs exhibit little first-pass metabolism even in patients with normal liver function, so portocaval shunting will have little impact on drug bioavailability. On the other hand, portocaval shunting will decrease the extraction ratio and increase the bioavailability of nonrestrictively metabolized drugs as follows:

$$F = 1 - \frac{f_u CL_{int}}{Q + f_u CL_{int}} \cdot \frac{Q_p}{Q} \tag{7.14}$$

For example, if the extraction ratio of a completely absorbed but nonrestrictively metabolized drug decreases from 0.95 to 0.90, the bioavailability will double from 0.05 to 0.10. Because this increase in absorption is accompanied by a decrease in elimination clearance, total exposure following oral administration of nonrestrictively eliminated drugs will increase to an even greater extent than will the increase in bioavailability, as shown in Table 7.2 for meperidine (24), pentazocine (24), and propranolol (25). Cirrhosis also is associated with a reduction in propranolol binding to plasma proteins, so this also contributes to the increased exposure following either intravenous or oral doses of this drug (see the following section). Accordingly, the relative exposure estimates for propranolol in Table 7.2 are based on comparisons of area under the plasma-level-vs.-time curve of non-protein-bound plasma concentrations. The increase in drug exposure resulting from these changes may cause unexpected increases in intensity of pharmacologic response or in toxicity when the usual doses of these drugs are prescribed for patients with liver disease.

TABLE 7.2 Impact of Cirrhosis on Bioavailability and Relative Exposure to Doses of Nonrestrictively Eliminated Drugs

	Absolute bioavailability		Relative exposure (Cirrhotics/control)		
Drug	Controls (%)	Cirrhotics (%)	IV	Oral	Ref.
Meperidine	48	87	1.6	3.1	24
Pentazocine	18	68	2.0	8.3	24
Propranolol	38	54	1.5[a]	2.0[a]	25

[a] These estimates also incorporate the 55% increase in propranolol free fraction that was observed in cirrhotic patients.

Consequences of Decreased Protein Binding

Hypoalbuminemia frequently accompanies chronic liver disease and may reduce drug binding to plasma proteins (26). In addition, endogenous substances such as bilirubin and bile acids accumulate and may displace drugs from protein binding sites. Reductions in protein binding will tend to increase the hepatic clearance of restrictively metabolized drugs. For drugs that have low intrinsic clearance and tight binding to plasma proteins, it is possible that liver disease results in a decrease in CL_{int} but also an increase in f_u. The resultant change in hepatic clearance will depend on changes in both these parameters. Thus, hepatic disease generally produces no change in warfarin clearance, a decrease in diazepam clearance, and

an increase in tolbutamide clearance. However, as discussed in Chapter 5, unbound drug concentrations will not be affected by decreases in the protein binding of restrictively metabolized drugs. Therefore, no dosage alterations are required for these drugs when protein binding is the only parameter that is changed.

Although reduced protein binding will not affect the clearance or total (bound plus free) plasma concentration of nonrestrictively eliminated drugs, it will increase the plasma concentration of free drug. This may increase the intensity of the pharmacological effect that is observed at a given total drug concentration (26). Therefore, even in the absence of changes in other pharmacokinetic parameters, a reduction in the plasma protein binding of nonrestrictively eliminated drugs will necessitate a corresponding reduction in drug dosage.

As previously discussed in the context of renal disease (Chapter 5), reduced protein binding will increase the distribution volume referenced to total drug concentrations and this will tend to increase elimination-phase half-life (26).

Consequences of Hepatocellular Changes

The liver content of cytochrome P450 enzymes is decreased in patients with cirrhosis. In these patients, intrinsic clearance is the main determinant of the systemic clearance of lidocaine and indocyanine green, two drugs that have nonrestrictive metabolism in subjects with normal liver function. However, cirrhosis does not reduce the function of different drug-metabolizing enzymes uniformly. As can be seen from the results of the two *in vitro* studies summarized in Table 7.3, CYP1A2 content is consistently reduced in cirrhosis (27, 28). Significant reductions in CYP2E1 and CYP3A also have been found by some investigators. Although CYP2C19 appears to be somewhat more resilient in these *in vitro* studies, content of this enzyme was markedly reduced in patients with cholestatic types of cirrhosis (28). More recent studies in patients with liver disease, in whom the presence or absence of cholestasis was not noted, have indicated that clearance of *S*-mephenytoin, a CYP2C19 probe, was decreased by 63% in cirrhotic patients with mild cirrhosis and by 96% in patients with moderate cirrhosis (29). On the other hand, administration of debrisoquine to these patients indicated normal function of CYP2D6. Glucuronide conjugation of morphine, and presumably of other drugs, is relatively well preserved in patients with mild and moderate cirrhosis, but morphine clearance was 59% reduced in patients whose cirrhosis was severe enough to have caused previous hepatic encephalopathy (30).

TABLE 7.3 Differential Alterations of Cytochrome P450 Enzyme Content in Cirrhosis

Enzyme	Representative substrate	Change in cirrhosis	
		Guengerich and Turvy (27)	George et al. (28)
CYP1A2	Theophylline	↓ 53%[a]	↓ 71%[b]
CYP2C19	Omeprazole	↑ 95%	↓ 43%
CYP2E1	Acetaminophen	↓ 59%[a]	↓ 19%
CYP3A	Midazolam	↓ 47%	↓ 75%[c]

[a] $P < 0.05$.
[b] $P < 0.005$.
[c] $P < 0.0005$.

USE OF THERAPEUTIC DRUGS IN PATIENTS WITH LIVER DISEASE

A number of clinical classification schemes and laboratory measures have been proposed as a means of guiding dose adjustments in patients with liver disease, much as creatinine clearance has been used to guide dose adjustments in patients with impaired renal function. The Pugh modification of Child's classification of liver disease severity (Table 7.4) is the classification scheme that is used most commonly in studies designed to formulate drug dosing recommendations for patients with liver disease (31, 32). Because patients with only mild or moderately severe liver disease usually are enrolled in these studies, there are relatively few data from patients with severe liver disease, in whom both pharmacokinetic changes and altered pharmacologic response are expected to be most pronounced. The administration of narcotic, sedative, and psychoactive drugs to patients with severe liver disease is particularly hazardous because these drugs have the potential to precipitate life-threatening hepatic encephalopathy.

Effects of Liver Disease on the Hepatic Elimination of Drugs

Equation 7.13 emphasizes the central point that changes in perfusion and protein binding, as well as intrinsic clearance, will affect the hepatic clearance of a number of drugs. The intact hepatocyte theory has been proposed as a means of simplifying this complexity (33). This theory is analogous to the intact nephron theory (see Chapter 5) in that it assumes that the increase in portocaval shunting parallels the loss of functional cell mass, and that the reduced mass

TABLE 7.4 Pugh Modification of Child's Classification of Liver Disease Severity[a]

Assessment parameters	Assigned score		
	1 Point	2 Points	3 Points
Encephalopathy grade	0	1 or 2	3 or 4
Ascites	Absent	Slight	Moderate
Bilirubin (mg/dL)	1–2	2–3	>3
Albumin (g/dL)	>3.5	2.8–3.5	<2.8
Prothrombin Time (seconds > control)	1–4	4–10	>10
Classification of clinical severity			
Clinical severity	Mild	Moderate	Severe
Total points	5–6	7–9	>9

Encephalopathy grade

Grade 0: Normal consciousness, personality, neurological examination, EEG

Grade 1: Restless, sleep disturbed, irritable/agitated, tremor, impaired handwriting, 5-cps waves on EEG

Grade 2: Lethargic, time-disoriented, inappropriate, asterixis, ataxia, slow triphasic waves on EEG

Grade 3: Somnolent, stuporous, place-disoriented, hyperactive reflexes, rigidity, slower waves on EEG

Grade 4: Unrousable coma, no personality/behavior, decerebrate, slow (2–3 cps) delta waves on EEG

[a] Adapted from Pugh *et al.* Br J Surg 1973;60:646–9 (31), and CDER, CBER. Guidance for industry. Rockville, MD: FDA; 2003 (32). (Internet at http://www.fda.gov/cder/guidance/index.htm.)

of normally functioning liver cells is perfused normally. Other theories have been proposed to account for the effects of chronic liver disease on hepatic drug clearance and it currently is not clear which, if any, of these theories is most appropriate (34). However, what is apparent from studies in patients with significantly impaired liver function is that the intrinsic clearance of some drugs that normally are nonrestrictively metabolized is reduced to the extent that $f_u CL_{int}$ now becomes rate limiting and clearance is no longer approximated by hepatic perfusion rate (22). It also is apparent from Equation 7.14 that the presence of portosystemic shunting and hepatocellular damage will significantly increase the bioavailability of drugs that normally have extensive first-pass hepatic metabolism.

Correlation of Laboratory Tests with Drug Metabolic Clearance

Bergquist *et al.* (35) presented examples in which several laboratory tests that are commonly used to assess liver function provide a more reliable indication of impaired drug metabolic clearance than does the Child–Pugh clinical classification scheme (Table 7.5). Serum albumin concentrations were of greatest predictive value for two of the drugs shown in the table. However, this marker was not correlated with the hepatic clearance of lansoprazole, and a combination of all three laboratory tests was better correlated with hepatic clearance of atorvastatin than was serum albumin alone. Serum concentrations of aspartate aminotransferase (AST) or alanine transaminase (ALT) were not correlated with hepatic drug clearance, as might be expected from the fact that these enzymes reflect hepatocellular damage rather than hepatocellular function.

TABLE 7.5 Correlation of Laboratory Test Results with Impaired Hepatic Clearance[a]

Drug	Enzyme(s)	Laboratory test		
		Albumin	PT[b]	Bilirubin
"A"	CYP2C9	X		
"B"	Not given	X		
Atorvastatin	CYP3A4	X	X	X
Lansoprazole	CYP3A4 + CYP 2C19		X	

[a] Data from Bergquist *et al.* Clin Pharmacol Ther 1999;62: 365–76 (35).
[b] Prothrombin time.

Use of Probe Drugs to Characterize Hepatic Drug Clearance

A number of probe drugs have been administered to normal subjects and to patients to evaluate hepatic clearance. Quantitative liver function tests using probe drugs can be categorized as either specific for a given metabolic pathway or as more generally reflective of hepatic metabolism, perfusion, or biliary function. An example of the latter category is the *aminopyrine breath test*, which is a broad measure of hepatic microsomal drug metabolism, since aminopyrine is metabolized by at least six cytochrome P450 enzymes (36). Other tests in this category are the *galactose elimination test*, to measure cytosolic drug metabolism; *sorbitol clearance*, to measure liver parenchymal perfusion; and *indocyanine green clearance*, reflecting both parenchymal perfusion and biliary secretory capacity. Figure 7.4 illustrates the relationship between the degree of impairment in these tests and the Child–Pugh class of liver disease severity in patients with chronic hepatitis B and C (37). These results indicate that hepatic metabolic capacity is impaired before portosystemic shunting becomes prominent in the pathophysiology of chronic viral hepatitis. However, these nonspecific tests are, by their nature, of limited value in predicting the clearance of a specific drug in an individual patient.

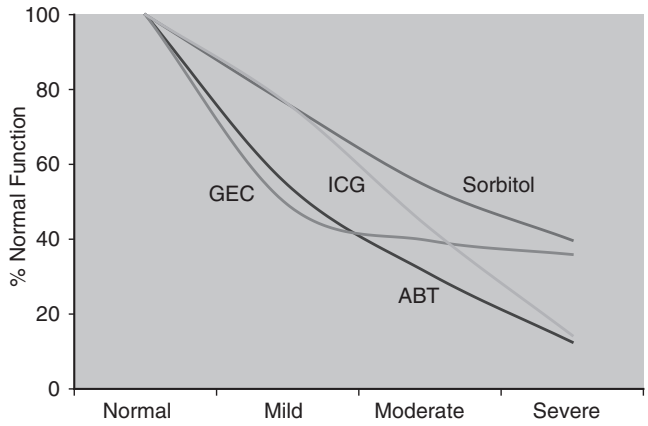

FIGURE 7.4 Relationship between Child–Pugh stages of liver disease severity and extent of impairment in antipyrine breath test (ABT), galactose elimination capacity (GEC), sorbitol clearance, and indocyanine green clearance (ICG). (Adapted from data published by Herold C, Heinz R, Niedobitek G *et al*. Liver 2001;21:260–5.)

The monoethylglycinexylidide (MEGX) test is an example of a test that specifically evaluates the function of a single metabolic pathway. In this test, a 1-mg/kg dose of lidocaine is administered intravenously and plasma concentrations of its N-dealkylated metabolite, MEGX, are measured either 15 or 30 minutes later. Testa *et al*. (38) found that a 30-minute post-dose MEGX concentration of 50 ng/ml provided the best discrimination between chronic hepatitis and cirrhosis (sensitivity, 93.5%; specificity, 76.9%). These authors concluded that both hepatic blood flow and the enzymatic conversion of lidocaine to MEGX, initially thought to be mediated by CYP3A4 but subsequently shown to be due primarily to CYP1A2 (39), were well preserved in patients with mild and moderate chronic hepatitis. However, MEGX levels fell significantly in patients with cirrhosis and were well correlated with the clinical stage of cirrhosis, as shown in Figure 7.5. Morphine, *S*-mephenytoin, debrisoquin, and erythromycin have been used as selective probes to evaluate, respectively, glucuronidation and the CYP2C19, CYP2D6, and CYP3A4 metabolic pathways in patients with different Child–Pugh classes of liver disease severity, and these results are included in Figure 7.5 (29, 30, 38, 40). To increase the efficiency of evaluating specific drug metabolic pathways, the strategy has been developed of simultaneously administering a combination of probes (41). As many as five probe drugs have been administered in this fashion to provide a profile of CYP1A2, CYP2E1, CYP3A, CYP2D6, CYP2C19, and *N*-acetyltransferase activity (42). The method was evaluated to exclude the possibility of a significant metabolic interaction between the individual probes. Although a number of different versions of the cocktail approach have been described, these all are too cumbersome for routine clinical use (43). In addition, even when the metabolic pathway for a given drug is known, prediction of hepatic drug clearance in individual patients is complicated by the effects of pharmacogenetic variation and drug interactions.

Effects of Liver Disease on the Renal Elimination of Drugs

Drug therapy in patients with advanced cirrhosis is further complicated by the fact that renal blood flow and glomerular filtration rate are frequently depressed in these patients in the absence of other known causes of renal failure. This condition, termed the *hepatorenal syndrome*, occurs in a setting of vasodilation of the splanchnic circulation that results in underfilling of the systemic circulation. This activates pressor responses, causing marked vasoconstriction of the renal circulation (44). The functional nature of this syndrome is indicated by the observations that it reverses following successful liver transplantation and is not accompanied by significant histological evidence of kidney damage.

Ginès *et al.* (45) monitored 234 patients with cirrhosis, ascites, and a glomerular filtration rate (GFR) of more than 50 mL/min. These authors found that the hepatorenal syndrome developed within 1 year in 18%, and within 5 years in 39%, of these

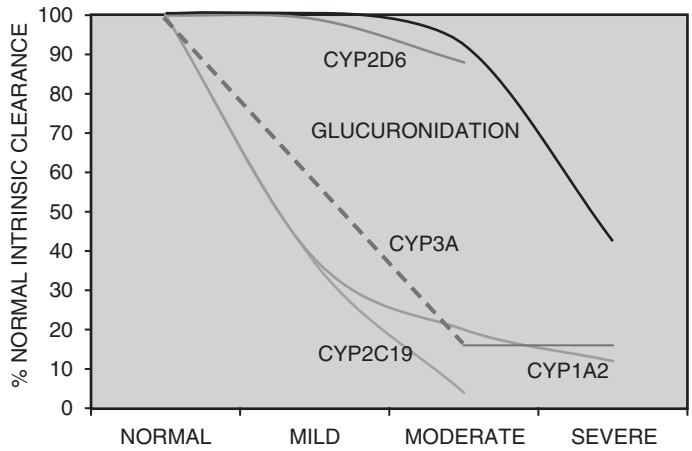

FIGURE 7.5 Schematic diagram showing the relationship between Child–Pugh stages of liver disease severity and the intrinsic clearance of drugs mediated by specific cytochrome P450 metabolic pathways. Estimates for glucuronidation (30), CYP2D6 (29), CYP1A2 (38), CYP3A4 (40), and CYP2C19 (29) pathways are based on the literature sources. The erythromycin breath test was used to assess hepatic CYP3A in a study in which no patients with mild liver disease were included, and results in patients with moderate and severe liver disease were combined.

patients. Although the Pugh score was of no predictive value, high plasma renin activity, low serum sodium concentrations, and small liver size were independent predictors of the onset of this syndrome. Baseline GFR also was of predictive value, but serum creatinine and creatinine clearance, either measured or calculated from the Cockcroft and Gault equation (Chapter 1), overestimated renal function in this group of patients (46). This overestimation reflects the fact that the rate of creatinine synthesis is depressed in these patients, so serum creatinine concentrations may remain within the normal range even when inulin clearance decreases to as low as 10 mL/min. As a result, many patients with cirrhosis and ascites have a normal serum creatinine concentration but a GFR of less than 60 mL/min.

The need for caution in estimating drug dosage for patients with the hepatorenal syndrome is exemplified by carbenicillin, an antipseudomonal, semisynthetic penicillin that is excreted primarily by the kidneys, with biliary excretion normally accounting for less than 20% of total elimination. The decline in renal function that is associated with severe liver disease prolongs the elimination half-life of this drug from 1 hour in subjects with normal renal and liver function to approximately 24 hours (47). Although studies in patients with hepatorenal syndrome were not reported, similar half-life prolongations have been described in patients with combined renal and hepatic functional impairment who were treated with the newer but pharmacokinetically similar antipseudomonal penicillins piperacillin (48) and mezlocillin (49). Consequently, it is advisable to consider reducing doses even for drugs that are eliminated to a significant extent by renal excretion when treating patients with cirrhosis that is severe enough to be accompanied by ascites.

Effects of Liver Disease on Patient Response

The relationship between drug concentration and response also can be altered in patients with advanced liver disease. Of greatest concern is the fact that customary doses of sedatives may precipitate the disorientation and coma that are characteristic of portal-systemic or hepatic encephalopathy. Experimental hepatic encephalopathy is associated with increased γ-aminobutyric acid-mediated inhibitory neurotransmission, and there has been some success in using the benzodiazepine antagonist flumazenil to reverse this syndrome (50). This provides a theoretical basis for the finding that brain hypersensitivity, as well as impaired drug elimination, is responsible for the exaggerated sedative response to diazepam that is exhibited by some patients with chronic liver disease (51). Bakti *et al*. (52) conducted a particularly well-controlled

demonstration of benzodiazepine hypersensitivity by showing that central nervous system (CNS) performance in cirrhotic patients was impaired when compared to subjects with normal liver function at a time when plasma concentrations of unbound triazolam were the same in both groups. Changes in the cerebrospinal fluid (CSF)/serum concentration ratio of cimetidine have been reported in patients with liver disease, suggesting an increase in blood–brain barrier permeability that also could make these patients more sensitive to the adverse CNS effects of a number of other drugs (53).

Although cirrhotic patients frequently are treated with diuretic drugs to reduce ascites, they exhibit a reduced responsiveness to loop diuretics that cannot be overcome by administering larger doses. This presumably is related to the pathophysiology of increased sodium retention that contributes to the development of ascites (54). In addition, decreases in renal function, which are often unrecognized in these patients (46), may lead to decreased delivery of loop diuretics to their renal tubular site of action. Because hyperaldosteronism is prevalent in these patients and spironolactone is not dependent on glomerular filtration for efficacy, it should be the mainstay of diuretic therapy in this clinical setting (55).

When diuretic therapy does result in effective fluid removal in cirrhotic patients, it is associated with a very high incidence of adverse reactions. In one study of diuretic therapy in cirrhosis, furosemide therapy precipitated the hepatorenal syndrome in 12.8%, and hepatic coma in 11.6%, of the patients (56). Although daily doses of this drug did not differ, patients who had adverse drug reactions received total furosemide doses that averaged 1384 mg, whereas patients without adverse reactions received lower total doses that averaged 743 mg. Accordingly, when spironolactone therapy does not provide an adequate diuresis, only small frequent doses of loop diuretics should be added to the spironolactone regimen (55). Cirrhotic patients also appear to be at an increased risk of developing acute renal failure after being treated with angiotensin-converting enzyme inhibitors and nonsteroidal anti-inflammatory drugs (57).

Modification of Drug Therapy in Patients with Liver Disease

It is advisable to avoid using certain drugs in patients with advanced liver disease. For example, angiotensin-converting enzyme inhibitors and nonsteroidal anti-inflammatory drugs should be avoided because of their potential to cause acute renal failure. Paradoxically, administration of captopril to cirrhotic patients with ascites actually impairs rather than promotes sodium excretion (58). Since coagulation disorders are common in patients with advanced cirrhosis, alternatives should be sought for therapy with β-lactam antibiotics that contain the *N*-methylthiotetrazole side chain (e.g., cefotetan), which inhibits γ-carboxylation of vitamin K–dependent clotting factors (57).

It also is prudent to reduce the dosage of a number of other drugs that frequently are used to treat patients with liver disease (59). Particular attention has been focused on drugs whose clearance is significantly impaired in patients with moderate hepatic impairment, as assessed in Table 7.4 (32). Even greater caution should be exercised in using these drugs to treat patients with severely impaired liver function. Table 7.6 lists several drugs whose dose should be reduced by 50% in treating patients with moderate hepatic impairment. Most of the drugs in this table have first-pass metabolism that is greater than 50% in normal subjects but is substantially reduced when liver function is impaired. Drug exposure to standard doses is further increased by what is generally a substantial decrease in elimination clearance. Although not routinely evaluated in most studies of patients with liver disease, drug binding to plasma proteins also may be reduced in these patients and may contribute to exaggerated responses to nonrestrictively

TABLE 7.6 Some Drugs Requiring at Least a 50% Dose Reduction in Patients with Moderate Cirrhosis

		Parameter values or changes in cirrhosis			
Drug	***F* (%)**	***F* (%)**	**Clearance**	f_u	**Ref.**
Analgesic drugs					
Morphine	47	100	↓ 59%	—	30
Meperidine	47	91	↓ 46%	—	24
Pentazocine	17	71	↓ 50%	—	24
Cardiovascular drugs					
Propafenone	21	75	↓ 24%	↑ 213%	60
Verapamil	22	52	↓ 51%	No change	61
Nifedipine	51	91	↓ 60%	↑ 93%	62
Nitrendipine	40	54	↓ 34%	↑ 43%	63
Nisoldipine	4	15	↓ 42%	—	64
Losartan	33	66	↓ 50%	—	65–67
Other					
Omeprazole	56	98	↓ 89%	—	68
Tacrolimus	27	36	↓ 72%	—	69, 70

metabolized drugs. Formation of pharmacologically active metabolites is another complicating factor that deserves consideration. For example, losartan has an active metabolite, EXP3174, that is primarily responsible for the extent and duration of pharmacological effect in patients treated with this drug (65). Although standard doses produce plasma concentrations of losartan that are four to five times higher in patients with cirrhosis than are those observed in normal subjects, plasma levels of EXP3174 are only increased by a factor of 1.5 to 2.0 (67). This provided the rationale for reducing the usual losartan dose by only half in a trial in which this drug was used to reduce portal pressure in patients with cirrhosis and esophageal varices (71).

REFERENCES

1. Rowland M, Benet LZ, Graham GG. Clearance concepts in pharmacokinetics. J Pharmacokinet Biopharm 1973;1:123–36.
2. Wilkinson GR, Shand DG. A physiological approach to hepatic drug clearance. Clin Pharmacol Ther 1975;18:377–90.
3. Rane A, Wilkinson GR, Shand DG. Prediction of hepatic extraction ratio from *in vitro* measurement of intrinsic clearance. J Pharmacol Exp Ther 1977;200:420–4.
4. Roberts MS, Donaldson JD, Rowland M. Models of hepatic elimination: Comparison of stochastic models to describe residence time distributions and to predict the influence of drug distribution, enzyme heterogeneity, and systemic recycling on hepatic elimination. J Pharmacokinet Biopharm 1988;16:41–83.
5. Roberts MS, Magnusson BM, Burczynski FJ, Weiss M. Enterohepatic circulation: Physiological, pharmacokinetic and clinical implications. Clin Pharmacokinet 2002;41:751–90.
6. Rollins DE, Klaassen CD. Biliary excretion of drugs in man. Clin Pharmacokinet 1979;4:368–79.
7. Heggie GD, Sommadossi J-P, Cross DS, Huster WJ, Diasio RB. Clinical pharmacokinetics of 5-fluorouracil and its metabolites in plasma, urine, and bile. Cancer Res 1987;47:2203–6.
8. Siegers C-P, Bumann D. Clinical significance of the biliary excretion of drugs. Prog Pharmacol Clin Pharmacol 1991;8:537–49.
9. Duggan DE, Hooke KF, Noll RM, Kwan KC. Enterohepatic circulation of indomethacin and its role in intestinal irritation. Biochem Pharmacol 1975;24:1749–54.
10. Veng Pedersen P, Miller R. Pharmacokinetics and bioavailability of cimetidine in humans. J Pharm Sci 1980;69:394–8.
11. Miller R. Pharmacokinetics and bioavailability of ranitidine in humans. J Pharm Sci 1984;73:1376–9.
12. Blaschke TF, Meffin PJ, Melmon KL, Rowland M. Influence of acute viral hepatitis on phenytoin kinetics and protein binding. Clin Pharmacol Ther 1975;17:685–91.
13. Williams RL, Blaschke TF, Meffin PJ, Melmon KL, Rowland M. Influence of acute viral hepatitis on disposition and plasma binding of tolbutamide. Clin Pharmacol Ther 1977;21:301–9.
14. Williams RL, Schary WL, Blaschke TF, Meffin PJ, Melmon KL, Rowland M. Influence of acute viral hepatitis on disposition and pharmacologic effect of warfarin. Clin Pharmacol Ther 1976;20:90–7.
15. Williams RL, Blaschke TF, Meffin PJ, Melmon KL, Rowland M. Influence of viral hepatitis on the disposition of two compounds with high hepatic clearance: Lidocaine and indocyanine green. Clin Pharmacol Ther 1976;20:290–9.
16. Villeneuve JP, Thibeault MJ, Ampelas M, Fortunet-Fouin H, LaMarre L, Côtè J, Pomier-Layrargues G, Huet P-M. Drug disposition in patients with HB_sAg-positive chronic liver disease. Dig Dis Sci 1987;32:710–4.
17. Prescott LF, Wright N. The effects of hepatic and renal damage on paracetamol metabolism and excretion following overdosage. A pharmacokinetic study. Br J Pharmacol 1973;49:602–13.
18. Sotaniemi EA, Niemelä O, Risteli L, Stenbäck F, Pelkonen RO, Lahtela JT, Risteli J. Fibrotic process and drug metabolism in alcoholic liver disease. Clin Pharmacol Ther 1986;40:46–55.
19. Boyer TD, Henderson JM. Portal hypertension and bleeding esophageal varices. In: Zakim D, Boyer TD, eds. Hepatology: A textbook of liver disease. 4th ed. Philadelphia: WB Saunders; 2003. p. 581–629.
20. Iwasa M, Nakamura K, Nakagawa T, Watanabe S, Katoh H, Kinosada Y, Maeda H, Habara J, Suzuki S. Single photon emission computed tomography to determine effective hepatic blood flow and intrahepatic shunting. Hepatology 1995;21:359–65.
21. Lebrec D, Kotelanski B, Cohn JN. Splanchnic hemodynamics in cirrhotic patients with esophageal varices and gastrointestinal bleeding. Gastroenterology 1976;70:1108–11.
22. Huet P-M, Villeneuve J-P. Determinants of drug disposition in patients with cirrhosis. Hepatology 1983;3:913–8.
23. McLean A, du Souich P, Gibaldi M. Noninvasive kinetic approach to the estimation of total hepatic blood flow and shunting in chronic liver disease — a hypothesis. Clin Pharmacol Ther 1979;25:161–6.
24. Neal EA, Meffin PJ, Gregory PB, Blaschke TF. Enhanced bioavailability and decreased clearance of analgesics in patients with cirrhosis. Gastroenterology 1979;77:96–102.
25. Wood AJJ, Kornhauser DM, Wilkinson GR, Shand DG, Branch RA. The influence of cirrhosis on steady-state blood concentrations of unbound propranolol after oral administration. Clin Pharmacokinet 1978;3:478–87.
26. Blaschke TF. Protein binding and kinetics of drugs in liver diseases. Clin Pharmacokinet 1977;2:32–44.
27. Guengerich FP, Turvy CG. Comparison of levels of several human microsomal cytochrome P-450 enzymes and epoxide hydrolase in normal and disease states using immunochemical analysis of surgical liver samples. J Pharmacol Exp Ther 1991;256:1189–94.

28. George J, Murray M, Byth K, Farrell GC. Differential alterations of cytochrome P450 proteins in livers from patients with severe chronic liver disease. Hepatology 1995;21:120–8.
29. Adedoyin A, Arns PA, Richards WO, Wilkinson GR, Branch RA. Selective effect of liver disease on the activities of specific metabolizing enzymes: Investigation of cytochromes P450 2C19 and 2D6. Clin Pharmacol Ther 1998;64:8–17.
30. Hasselström J, Eriksson S, Persson A, Rane A, Svensson O, Säwe J. The metabolism and bioavailability of morphine in patients with severe liver cirrhosis. Br J Clin Pharmacol 1990;29:289–97.
31. Pugh RNH, Murray-Lyon IM, Dawson JL, Pietroni MC, Williams R. Transection of the oesophagus for bleeding oesophageal varices. Br J Surg 1973;60: 646–9.
32. CDER, CBER. Pharmacokinetics in patients with impaired hepatic function: Study design, data analysis, and impact on dosing and labeling. Guidance for industry. Rockville, MD: FDA; 2003. (Internet at http://www.fda.gov/cder/guidance/index.htm.)
33. Wood AJJ, Villeneuve JP, Branch RA, Rogers LW, Shand DG. Intact hepatocyte theory of impaired drug metabolism in experimental cirrhosis in the rat. Gastroenterology 1979;76:1358–62.
34. Tucker GT. Alteration of drug disposition in liver impairment. Br J Clin Pharmacol 1998;46:355.
35. Bergquist C, Lindergård J, Salmonson T. Dosing recommendations in liver disease. Clin Pharmacol Ther 1999;66:201–4.
36. Engel G, Hofmann U, Heidemann H, Cosme J, Eichelbaum M. Antipyrine as a probe for human oxidative drug metabolism: Identification of the cytochrome P450 enzymes catalyzing 4-hydroxyantipyrine, 3-hydroxymethylantipyrine, and norantipyrine formation. Clin Pharmacol Ther 1996;59:613–23.
37. Herold C, Heinz R, Niedobitek G, Schneider T, Hahn EG, Schuppan D. Quantitative testing of liver function in relation to fibrosis in patients with chronic hepatitis B and C. Liver 2001;21:260–5.
38. Testa R, Caglieris S, Risso D, Arzani L, Campo N, Alvarez S, Giannini E, Lantieri PB, Celle G. Monoethylglycinexylidide formation measurement as a hepatic function test to assess severity of chronic liver disease. Am J Gastroenterol 1997;92:2268–73.
39. Orlando R, Piccoli P, De Martin S, Padrini R, Floreani M, Palatini P. Cytochrome P50 1A2 is a major determinant of lidocaine metabolism *in vivo*: Effects of liver function. Clin Pharmacol Ther 2004;75:80–8.
40. Lown K, Kolars J, Turgeon K, Merion R, Wrighton SA, Watkins PB. The erythromycin breath test selectively measures P450IIIA in patients with severe liver disease. Clin Pharmacol Ther 1992;51:229–38.
41. Breimer DD, Schellens JHM. A 'cocktail' strategy to assess *in vivo* oxidative drug metabolism in humans. Trends Pharmacol Sci 1990;11:223–5.
42. Frye RF, Matzke GR, Adedoyin A, Porter JA, Branch RA. Validation of the five-drug "Pittsburgh cocktail" approach for assessment of selective regulation of drug-metabolizing enzymes. Clin Pharmacol Ther 1997;62:365–76.
43. Tanaka E, Kurata N, Yasuhara H. How useful is the "cocktail approach" for evaluating human hepatic drug metabolizing capacity using cytochrome P450 phenotyping probes *in vivo*? J Clin Pharm Ther 2003;28:157–65.
44. Ginès P, Guevara M, Arroyo V, Rodés J. Hepatorenal syndrome. Liver 2003;362:1819–27.
45. Ginès A, Escorsell A, Ginès P, Saló J, Jiménez W, Inglada L, Navasa M, Clària J, Mimola A, Arroyo V, Rodés J. Incidence, predictive factors, and prognosis of the hepatorenal syndrome in cirrhosis with ascites. Gastroenterology 1993;105:229–36.
46. Papadakis MA, Arieff AI. Unpredictability of clinical evaluation of renal function in cirrhosis: Prospective study. Am J Med 1987;82:945–52.
47. Hoffman TA, Cestero R, Bullock WE. Pharmacodynamics of carbenicillin in hepatic and renal failure. Ann Intern Med 1970;73:173–8.
48. Green L, Dick JD, Goldberger SP, Anelopulos CM. Prolonged elimination of piperacillin in a patient with renal and liver failure. Drug Intell Clin Pharm 1985;19:427–9.
49. Cooper BE, Nester TJ, Armstrong DK, Dasta JF. High serum concentrations of mezlocillin in a critically ill patient with renal and hepatic dysfunction. Clin Pharm 1986;5:764–6.
50. Ferenci P, Grimm G, Meryn S, Gangl A. Successful long-term treatment of portal–systemic encephalopathy by the benzodiazepine antagonist flumazenil. Gastroenterology 1989;96:240–3.
51. Branch RA, Morgan MH, James J, Read AE. Intravenous administration of diazepam in patients with chronic liver disease. Gut 1976;17:975–83.
52. Bakti G, Fisch HU, Karlaganis G, Minder C, Bircher J. Mechanism of the excessive sedative response of cirrhotics to benzodiazepines: Model experiments with triazolam. Hepatology 1987;7:629–38.
53. Schentag JJ, Cerra FB, Calleri GM, Leising ME, French MA, Bernhard H. Age, disease, and cimetidine disposition in healthy subjects and chronically ill patients. Clin Pharmacol Ther 1981;29:737–43.
54. Brater DC. Resistance to loop diuretics: Why it happens and what to do about it. Drugs 1985;30: 427–43.
55. Brater DC. Use of diuretics in cirrhosis and nephrotic syndrome. Semin Nephrol 1999;19:575–80.
56. Naranjo CA, Pontigo E, Valdenegro C, González G, Ruiz I, Busto U. Furosemide-induced adverse reactions in cirrhosis of the liver. Clin Pharmacol Ther 1979;25:154–60.
57. Westphal J-F, Brogard J-M. Drug administration in chronic liver disease. Drug Safety 1997;17:47–73.
58. Daskalopoulos G, Pinzani M, Murray N, Hirschberg R, Zipser RD. Effects of captopril on renal function in patients with cirrhosis and ascites. J Hepatol 1987;4:330–6.
59. Rodighiero V. Effects of liver disease on pharmacokinetics: An update. Clin Pharmacokinet 1999;37:399–431.
60. Lee JT, Yee Y-G, Dorian P, Kates RE. Influence of hepatic dysfunction on the pharmacokinetics of propafenone. J Clin Pharmacol 1987;27:384–9.
61. Somogyi A, Albrecht M, Kliems G, Schäfer K, Eichelbaum M. Pharmacokinetics, bioavailability and

ECG response of verapamil in patients with liver cirrhosis. Br J Clin Pharmacol 1981;12:51–60.
62. Kleinbloesem CH, van Harten J, Wilson JPH, Danhof M, van Brummelen P, Breimer DD. Nifedipine: Kinetics and hemodynamic effects in patients with liver cirrhosis after intravenous and oral administration. Clin Pharmacol Ther 1986;40:21–8.
63. Dylewicz P, Kirch W, Santos SR, Hutt HJ, Mönig H, Ohnhaus EE. Bioavailability and elimination of nitrendipine in liver disease. Eur J Clin Pharmacol 1987;32:563–8.
64. van Harten J, van Brummelen P, Wilson JHP, Lodewijks MTM, Breimer DD. Nisoldipine: Kinetics and effects on blood pressure in patients with liver cirrhosis after intravenous and oral administration. Eur J Clin Pharmacol 1988;34:387–94.
65. Lo M-W, Goldberg MR, McCrea JB, Lu H, Furtek CI, Bjornsson TD. Pharmacokinetics of losartan, an angiotensin II receptor antagonist, and its active metabolite EXP3174 in humans. Clin Pharmacol Ther 1995;58:641–9.
66. Goa KL, Wagstaff AJ. Losartan potassium. A review of its pharmacology, clinical efficacy and tolerability in the management of hypertension. Drugs 1996;51:820–45.
67. McIntyre M, Caffe SE, Michalak RA, Reid JL. Losartan, an orally active angiotensin (AT1) receptor antagonist: A review of its efficacy and safety in essential hypertension. Pharmacol Ther 1997;74:181–94.
68. Andersson T, Olsson R, Regårdh C-G, Skänberg I. Pharmacokinetics of [^{14}C]omeprazole in patients with liver cirrhosis. Clin Pharmacokinet 1993;24:71–8.
69. Venkataramanan R, Jain A, Cadoff E, Warty V, Iwasaki K, Nagase K, Drajack A, Imventarza O, Todo S, Fung JJ, Starzl TE. Pharmacokinetics of FK 506: Preclinical and clinical studies. Transplant Proc 1990;22(suppl 1): 52–6.
70. Jain AB, Venkataramanan R, Cadoff E, Fung JJ, Todo S, Krajack A, Starzl TE. Effect of hepatic dysfunction and T tube clamping on FK 506 pharmacokinetics and trough concentrations. Transplant Proc 1990;22(suppl 1):57–9.
71. Schneider AW, Kalk JF, Klein CP. Effect of losartan, and angiotensin II receptor antagonist, on portal pressure in cirrhosis. Hepatology 1999;29:334–9.

This page intentionally left blank

CHAPTER

8

Noncompartmental versus Compartmental Approaches to Pharmacokinetic Analysis

DAVID M. FOSTER
University of Washington, Seattle, Washington

INTRODUCTION

From previous chapters, it is clear that the evaluation of pharmacokinetic parameters is an essential part of understanding how drugs function in the body. To estimate these parameters, studies are undertaken in which transient data are collected. These studies can be conducted in animals at the preclinical level, through all stages of clinical trials, and can be data rich or sparse. No matter what the situation, there must be some common means by which to communicate the results of the experiments. Pharmacokinetic parameters serve this purpose. Thus, in the field of pharmacokinetics, the definitions and formulas for the parameters must be agreed upon, and the methods used to calculate them understood. This understanding includes assumptions and domains of validity, for the utility of the parameter values depends upon them. This chapter focuses on the assumptions and domains of validity for the two commonly used methods — noncompartmental and compartmental analysis. Compartmental models have been presented in earlier chapters. This chapter expands upon this, and presents a comparison of the two methods.

Pharmacokinetic parameters fall basically into two categories. One category is qualitative or descriptive in that the parameters are observational, requiring no formula for calculation. Examples would include the maximal observed concentration of a drug or the amount of drug excreted in the urine during a given time period. The other category is quantitative. Quantitative parameters require a mathematical formalism for calculation. Examples here would include mean residence times, clearance rates, and volumes of distribution. Estimation of terminal slopes would also fall into this category. This chapter is concerned only with parameters requiring a mathematical formalism.

The quantitative parameters require not only a mathematical formalism but also data from which to estimate them. As noted, the two most common methods used for pharmacokinetic estimation are noncompartmental and compartmental analysis. A comparison of the two methods has been given by Gillespie (1). Comparisons regarding the two methodologies as applied to metabolic studies have been provided by DiStefano III (2) and Cobelli and Toffolo (3). Covell *et al.* (4) have made an extensive theoretical comparison of the two methods.

Under what circumstances can the two methods be used to estimate the pharmacokinetic parameters of interest? The answer to this question is the subject of this chapter. To begin, one must start with a definition of kinetics, since it is through this definition that one can introduce mathematical and statistical analyses to study the dynamic characteristics of a system. This can be used to define specific parameters of interest that can be estimated from data. From the definition of kinetics, the types of equations that can be used to provide a mathematical description of the system can be given. The assumptions underlying

noncompartmental analysis and estimation techniques for the different parameters for different experimental input–output configurations can then be discussed. One can then move to compartmental analysis and understand that the models set in full generality are very difficult to solve. With appropriate assumptions that are commonly made in pharmacokinetic studies, a simpler set of compartmental models will evolve. These models are easy to solve, and it will be seen that all parameters estimated using noncompartmental analysis can be recovered from these compartmental models. Under conditions when the two methods should, in theory, yield the same estimates, differences can be attributed to the numerical techniques used (e.g., sums of exponentials vs trapezoidal integration). With this knowledge, the circumstances under which the two methods will provide the same or different estimates of the pharmacokinetic parameters can be discussed. Thus, it is not the point of this chapter to favor one method over another; rather, the intent is to describe the assumptions and consequences of using either method.

Most of the theoretical details of the material covered in this chapter can be found in Covell *et al.* (4), Jacquez and Simon (5), and Jacquez (6). Of particular importance to this chapter is the material covered in Covell *et al.* (4) in which the relationships between the calculation of kinetic parameters from statistical moments and the same parameters calculated from the rate constants of a linear, constant-coefficient compartmental model are derived. Jacquez and Simon (5) discuss in detail the mathematical properties of systems that depend upon local mass balance; this forms the basis for understanding compartmental models and the simplifications that result from certain assumptions about a system under study. Berman (7) gives examples using metabolic turnover data, while the examples provided in Gibaldi and Perrier (8) and Rowland and Tozer (9) are more familiar to clinical pharmacologists.

KINETICS, PHARMACOKINETICS, AND PHARMACOKINETIC PARAMETERS

Kinetics and the Link to Mathematics

Substances in a biological system are constantly undergoing change. These changes can include transport (e.g., transport via the circulation or transport into or out from a cell) or transformation (e.g., biochemically changing from one substance to another). These changes and the concomitant outcomes form the basis for the system in which the substance interacts. How can one formalize these changes, and, once formalized, how can one describe their quantitative nature? Dealing with these questions involves an understanding and utilization of concepts related to kinetics.

The *kinetics* of a substance in a biological system are its spatial and temporal distribution in that system. The kinetics are the result of several complex events, including entry into the system, subsequent distribution (which may entail circulatory dynamics), transport into and from cells, and elimination (which usually requires biochemical transformations). Together these events characterize the substance and the system in which it resides.

While the substance can be an element such as calcium or zinc, or a compound such as amino acids, proteins, or sugars that exist normally in the body, in this chapter, it will be assumed to be a drug that is not normally present in the system. Thus, in this chapter, the *pharmacokinetics* of a drug is defined as its spatial and temporal distribution in a system. Unlike substances normally present, input of drugs into the system occurs only from exogenous sources. In addition, unless otherwise noted, the system under consideration will be the whole body. It should be noted that this definition of pharmacokinetics differs somewhat from the more conventional definition given in Chapter 1. The reason for this is seen in the following section.

From the spatial component of the definition, location in the system is important. From the temporal component of the definition, it follows that the amount of substance at a specific location is changing with time. The combination of these temporal and spatial components leads to partial derivatives,

$$\frac{\partial}{\partial t}, \frac{\partial}{\partial x}, \frac{\partial}{\partial y}, \frac{\partial}{\partial z} \tag{8.1}$$

which, mathematically, reflect change in time and space. Here t is time, and a three-dimensional location in the system is represented by the coordinates (x, y, z).

If one chooses to use partial derivatives to describe drug kinetics in the body, then expressions for each of $\partial/\partial t, \partial/\partial x, \partial/\partial y$, and $\partial/\partial z$ must be written. That is, a system of partial differential equations must be specified. Writing these equations involves a knowledge of physical chemistry, irreversible thermodynamics, and circulatory dynamics. Such equations will incorporate parameters that can be either deterministic (known) or stochastic (contain statistical uncertainties). Although such equations can be written for specific systems, defining and then estimating the unknown parameters

is in most cases impossible because of the difficulty in obtaining sufficient data to resolve the spatial components of the system. In pharmacokinetic applications, partial differential equations are used to describe distributed systems models. Such models are discussed in Chapter 9.

How does one resolve the difficulty associated with partial differential equations? The most common way is to reduce the system into a finite number of components. This can be accomplished by lumping together processes based upon time or location, or a combination of the two. One thus moves from partial derivatives to ordinary derivatives, where space is not taken directly into account. This reduction in complexity results in the compartmental models discussed later in this chapter. The same lumping process also forms the basis for the noncompartmental models discussed in the next section, although the reduction is much simpler than for compartmental models.

One can now appreciate why conventional definitions of pharmacokinetics are a little different from the definition given here. The conventional definitions make references to events other than temporal and spatial distribution. These events are, in fact, consequences of a drug's kinetics, and thus the two should be separated. The processes of drug absorption, distribution, metabolism, and elimination relate to parameters that can only be estimated from a mathematical model describing the kinetics of the drug. The point is that, to understand the mathematical basis of pharmacokinetic parameter estimation, it is necessary to keep in mind the separation between kinetics per se and the use of data to estimate pharmacokinetic parameters.

Using the definition of pharmacokinetics given in terms of spatial and temporal distributions, one can easily progress to a description of the underlying assumptions and mathematics of noncompartmental and compartmental analysis, and, from there, proceed to the processes involved in estimating the pharmacokinetic parameters. This will permit a better understanding of the domain of validity of noncompartmental vs compartmental parameter estimation.

Pharmacokinetic Parameters

What is desired from the pharmacokinetic parameters is a quantitative measure of how a drug behaves in the system. To estimate these parameters, one must design an experiment to collect transient data that can then be used to estimate the parameters of interest.

To design such an experiment, the system must contain at least one *accessible pool*; that is, the system must contain a "pool" that is available for drug input and data collection. As we will see, this pool must have certain properties. If the system contains an accessible pool, this implies that parts of the system are not accessible for test input and/or data collection. This divides the system into accessible and nonaccessible pools. A drug (or drug metabolite) in this pool interacts with other components of the system. The difference between noncompartmental and compartmental models is the way in which the nonaccessible portion of the system is described.

The pharmacokinetic parameters defined in the following section characterize both the accessible pool and the system parameters — that is, parameters that characterize the accessible and nonaccessible pools together. This situation is illustrated by the two models shown in Figure 8.1. For example, Figure 8.1A could describe the situation where plasma is the accessible pool and is used for both drug input and sampling. Figure 8.1B accommodates extravascular input (e.g., oral dosing or intramuscular injection) followed by the collection of serial blood samples, but it can also accommodate the situation where the input is intravascular and only urine samples are collected. Thus, the schematic in Figure 8.1 describes the experimental situation for most pharmacokinetic studies.

Accessible Pool Parameters

The pharmacokinetic parameters descriptive of the accessible pool are as follows (these definitions apply

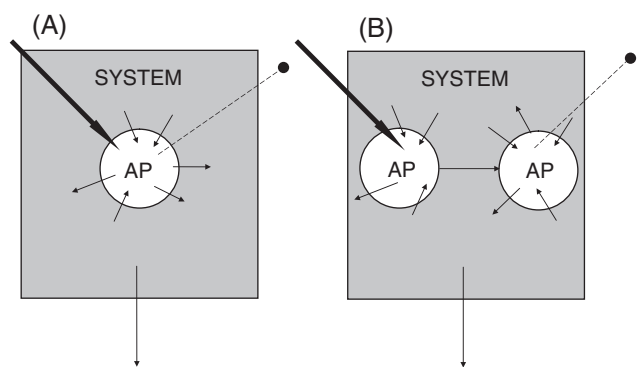

FIGURE 8.1 (A) A system in which an accessible pool (AP) is available for test input (*bold arrow*) and sampling (*dashed line with bullet*). Loss of material from the system is indicated by the arrow leaving the system box. Material exchanging between the accessible pool and the rest of the system is indicated by the small arrows leaving and entering the accessible pool. The pharmacokinetic parameters estimated from kinetic data characterize the accessible pool and the system in which the accessible pool is embedded. (B) A system in which there are two accessible pools, one that is available for test input (*bold arrow*) and a second that is available for sampling (*dashed line with bullet*); the test input is transported to the second accessible pool as indicated by the transfer arrow. Other transfer arrows are as explained in (A).

to both noncompartmental and compartmental models; how they relate to the situation where there are two accessible pools will be discussed for the individual cases):

Volume of distribution: V_a (units: volume). The volume of the accessible pool is a volume in which the drug, upon introduction into the system, intermixes uniformly (kinetically homogeneous) and instantaneously.

Clearance rate: CL_a(units: volume/time). This is the rate at which the accessible pool is irreversibly cleared of drug per unit time.

Elimination rate constant: k_e (units: 1/time). This is the fraction of drug that is irreversibly cleared from the accessible pool per unit time. (In some literature, this is referred to as the fractional clearance or fractional catabolic rate.)

Mean residence time: MRT_a (units: time). This is the average time a drug spends in the accessible pool during all passages through the system before being irreversibly cleared.

System Parameters

The pharmacokinetic parameters descriptive of the system are as follows (although these definitions apply to both noncompartmental and compartmental models, some modification will be needed for two accessible pool models as well as compartmental models):

Total equivalent volume of distribution: V_{tot} (units: volume). This is the total volume of the system seen from the accessible pool; it is the volume in which the total amount of drug would be distributed, assuming the concentration of material throughout the system is uniform and equal to the concentration in the accessible pool.

System mean residence time: MRT_s (units: time). This is the average time the drug spends in the system before leaving the system for the last time.

Mean residence time outside the accessible pool: MRT_o (units: time). This is the average time the drug spends outside the accessible pool before leaving the system for the last time.

Bioavailability: F (units: dimensionless). This is the fraction of drug that appears in a second accessible pool following administration in a first accessible pool.

Absorption rate constant: k_a (units: 1/time). This is the fraction of drug that appears per unit time in a second accessible pool following administration in a first accessible pool.

Moments

Moments of a function will play an essential role in estimating specific pharmacokinetic parameters. The modern use of moments in the analysis of pharmacokinetic data and the notions of noncompartmental or integral equation analysis can be traced to Yamaoka *et al.* (10), although these authors correctly point out that the formulas were known since the late 1930s.

The moments of a function are defined as follows (how they are used will be described later): Suppose $C(t)$ is a real-valued function defined on the interval $[0, \infty]$; in this chapter, $C(t)$ will be used to denote a functional description of a set of pharmacokinetic data. The zeroth, first, and second moments of $C(t)$, denoted S_0, S_1, and S_2, are defined

$$S_0 = \int_0^\infty C(t)\,dt = AUC \tag{8.2}$$

$$S_1 = \int_0^\infty t \cdot C(t)\,dt = AUMC \tag{8.3}$$

$$S_2 = \int_0^\infty t^2 \cdot C(t)\,dt \tag{8.4}$$

In these equations, the first and second moments, S_0 and S_1, are also defined, respectively, as *AUC*, "area under the curve," and *AUMC*, "area under the first moment curve." *AUC* was introduced in the discussion of bioavailability in Chapter 4, and it and *AUMC* are the more common expressions in pharmacokinetics and will be used in the following discussions. The second moment, S_2, is rarely used and will not be discussed in this chapter.

The following discussion will describe how *AUC* and *AUMC* are estimated, how they are used to estimate specific pharmacokinetic parameters (including the assumptions), and what their relationship is to specific pharmacokinetic parameters estimated from compartmental models. Both moments, however, are used for other purposes. For example, *AUC* acts as a surrogate for exposure, and values of *AUC* from different dose levels of a drug have been used to justify assumptions of pharmacokinetic linearity. These uses will not be reviewed.

NONCOMPARTMENTAL ANALYSIS

Noncompartmental Model

The noncompartmental model provides a framework to introduce and use statistical moment analysis

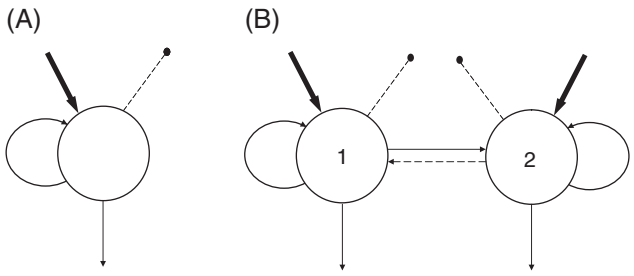

FIGURE 8.2 The single (A) and two (B) accessible pool models. See text for explanation.

to estimate pharmacokinetic parameters. There are basically two forms of the noncompartmental model: the single accessible pool model and the two accessible pool model. These are schematized in Figure 8.2.

What is the relationship between the situation described in Figure 8.1 and the two models shown in Figure 8.2? Consider first the single accessible pool model shown in Figure 8.2A. The accessible pool here, denoted by the circle into which drug is input (*bold arrow*) and from which samples are taken (*dotted line with bullet*), is the same as that shown in the model depicted in Figure 8.1A. The entire interaction of the accessible pool with the rest of the system is indicated by the looped arrow leaving and returning to the accessible pool. This is called the *recirculation-exchange* arrow, and encompasses all interactions the drug has in the system outside of the accessible pool. Notice that a drug introduced into this pool has two routes by which it can leave the accessible pool. One is via recirculation-exchange, and the other is via irreversible loss, denoted by the arrow leaving the accessible pool. As indicated in Figure 8.2A, drug can only enter and leave the accessible pool. Drug can neither enter nor leave the system along the recirculation-exchange arrow. This is called the equivalent sink and source constraint, and is fundamental in understanding the domain of validity of the pharmacokinetic parameters estimated from this model (2). The single accessible pool model is used primarily when the accessible pool is plasma, and the drug is administered directly into plasma.

The situation depicted in Figure 8.2B, the two accessible pool model, derives in a similar fashion from the model shown in Figure 8.1B. The difference between the single and two accessible pool models is as follows: While both pools have recirculation-exchange arrows, material can flow from pool 1 to pool 2. This model is used to describe extravascular drug input, or the situation in which either plasma concentrations of a drug and its metabolite are measured or both plasma and urine data are collected.

Note that there is a dashed arrow from pool 2 to pool 1 in Figure 8.2B. This indicates that exchange can occur in this direction also. Although analysis of this exchange is frequently incorporated in metabolic kinetic studies, there are relatively few examples in pharmacokinetics in which this has been studied. It is essential to note that this arrow is not equivalent to an arrow in a multicompartmental model! This arrow represents transfer of material from pool 1 to pool 2 by whatever routes exist, and can be a composite of many activities, including delays.

The two accessible pool model accommodates a more complex experimental format than does the single pool model. For example, one could have inputs into both pools, and samples from both as well. However, in most pharmacokinetic studies with the two accessible pool model, pool 2 is plasma and input is only into pool 1. In this situation, the pharmacokinetic parameters depend on bioavailability and can only be estimated up to a proportionality constant, as is the case with so-called *oral clearance* (CL/F), referred to as *relative clearance* in this chapter.

Kinetic Parameters of the Noncompartmental Model

The kinetic parameters of the noncompartmental model are those defined previously for the accessible pool and system. However, the formulas depend upon the experimental protocol, especially on the mode of drug administration. In this chapter, only the canonical inputs will be considered, such as an intravenous bolus (or multiple boluses) or constant infusion (or multiple constant infusions). References will be given for those interested in more complex protocols.

The relationships among the accessible pool parameters in the noncompartmental model are given in the following equations:

$$k_e = CL_a / V_a \tag{8.5}$$

$$MRT_a = 1/k_e \tag{8.6}$$

Equation 8.5 can be rearranged to yield

$$k_e \cdot V_a = CL_a \tag{8.5}$$

In addition, Equations 8.5 and 8.6 can be combined to yield the more familiar

$$V_a = MRT_a \cdot CL_a \tag{8.7}$$

The relationships among the system parameters for the noncompartmental model are

$$V_{tot} = MRT_s \cdot CL_a \tag{8.8}$$

$$MRT_o = MRT_s - MRT_a \tag{8.9}$$

The Single Accessible Pool Model

Assume a single bolus injection of drug whose amount is denoted by d or a constant infusion of drug whose infusion rate is u over the time domain $[0, t]$. Then,

	Bolus	**Infusion**	
V_a	$\dfrac{d}{C(0)}$	$\dfrac{u}{\dot{C}(0)}$	(8.10)
CL_a	$\dfrac{d}{AUC}$	$\dfrac{u}{\overline{C}}$	(8.11)
MRT_s	$\dfrac{AUMC}{AUC}$	$\dfrac{\int_0^\infty [\overline{C} - C(t)]\,dt}{\overline{C}}$	(8.12)

In these formulas, $C(0)$ is the concentration of drug in the system at time zero, $\dot{C}(0)$ is the first derivative of $C(t)$ evaluated at time zero, and $\overline{C}$ is the steady-state value for the concentration of drug in the accessible pool following a constant infusion into that pool. The remaining single accessible pool parameters, k_e, V_{tot}, and MRT_o can be calculated for either method of input using Equations 8.5, 8.6, and 8.9.

Although these formulas are for the single-input format, formulas also exist for generic inputs, including multiple boluses or infusions. If $u(t)$ is a generic input function, the formulas for V_a, CL_a, and MRT_s are

$$V_a = \frac{u(0)}{\dot{C}(0)} \tag{8.13}$$

$$CL_a = \frac{\int_0^\infty u(t)\,dt}{AUC} \tag{8.14}$$

$$MRT_s = \frac{\int_0^\infty t \cdot C(t)\,dt}{AUC} - \frac{\int_0^\infty t \cdot u(t)\,dt}{\int_0^\infty u(t)\,dt} \tag{8.15}$$

What is the origin of these formulas? That is, how are Equations 8.10–8.12 and 8.13–8.15 obtained? The answer is not obvious. Weiss (11) presents an excellent description of mean residence times and points out that, besides an accessible pool that must be available for test input and measurement, the system must be linear and time invariant for the equations to be valid. (The notions of linearity and time invariance will be discussed in more detail later.) For a formal derivation of these equations, the reader is referred to Weiss (11), Covell *et al.* (4), or Cobelli *et al.* (12). An understanding of the derivations is absolutely essential to understanding the domain of validity of the pharmacokinetic parameters obtained by noncompartmental methods, no matter what method of evaluating the integrals or extrapolations is employed.

The Two Accessible Pool Model

The two accessible pool model presents problems in estimating the pharmacokinetic parameters characterizing this situation. This is largely because the desired parameters, such as clearance, volumes, and residence times, cannot be estimated from a single-input–single-output experiment with input into the first pool and samples from the second pool. To deal with this situation, recall first the notion of absolute bioavailability originally discussed in Chapter 4. Let D_{oral} be the total dose of drug input into the first accessible pool, and let D_{IV} be the dose into the second accessible pool, assumed to be intravascular space. Let $AUC\{2\}$ be the area under the concentration–time curve in the second accessible pool following the dose D_{oral} (this is AUC_{oral} in the notation of Chapter 4), and let AUC_{IV} be the area under the concentration–time curve in the second accessible pool following the bolus dose D_{IV} (in a separate experiment). The absolute bioavailability is defined

$$F = \frac{AUC\{2\}}{AUC_{IV}} \cdot \frac{D_{IV}}{D_{oral}} \tag{8.16}$$

The following parameters can be calculated from data following a bolus injection into the first accessible pool. Let $CL\{2\}$ and $V\{2\}$, respectively, be the clearance from and volume of the second accessible pool, and let $CL\{2, \text{rel}\}$ and $V\{2, \text{rel}\}$ be the relative clearance from and volume of the second accessible pool. Then

$$MRT\{2, 1\} = \frac{\int_0^\infty tC\{2\}(t)\,dt}{\int_0^\infty C\{2\}(t)\,dt} \tag{8.17}$$

$$CL\{2, \text{rel}\} = \frac{CL\{2\}}{F} = \frac{D_{oral}}{AUC\{2\}} \tag{8.18}$$

$$V\{2, \text{rel}\} = \frac{V\{2\}}{F} = CL\{2, \text{rel}\} \cdot MRT\{2, 1\} \tag{8.19}$$

$MRT\{2, 1\}$ is the mean residence time of drug in the second accessible pool following introduction of drug into the first accessible pool.

Clearly this situation is not as rich in information as the single accessible pool situation. Of course, the parameters $CL\{2\}$ and $V\{2\}$ can be calculated in the event that F is known or when a separate intravenous dose is administered. Information on other input formats or the situation when there is a two-input–four-output experiment can be found in Cobelli *et al.* (12).

Estimating the Kinetic Parameters of the Noncompartmental Model

For the canonical input of drug, what information is needed? For the bolus input, an estimate of the drug concentration at time zero, $C(0)$, is needed in order to estimate V_a. For a constant infusion of drug, an estimate of $\dot{C}(0)$ is needed to estimate V_a, and an estimate of the plateau concentration, $\overline{C}$, is needed to estimate clearance and the system mean residence time.

The most important estimates, however, involve *AUC* and *AUMC*. These integrals are from time zero to time infinity whereas an experiment has only a finite time domain $[0, t_n]$, where t_n is the time of the last measurable datum. In addition, it is rarely the case that the first datum is obtained at time zero. Hence, assuming that the time of the first measurable datum is t_1, one must partition the integral as follows to estimate *AUC* and *AUMC*:

$$AUC = \int_0^\infty C(t)\,dt = \int_0^{t_1} C(t)\,dt + \int_{t_1}^{t_n} C(t)\,dt + \int_{t_n}^\infty C(t)\,dt \tag{8.20}$$

$$AUMC = \int_0^\infty t \cdot C(t)\,dt = \int_0^{t_1} t \cdot C(t)\,dt + \int_{t_1}^{t_n} t \cdot C(t)\,dt + \int_{t_n}^\infty t \cdot C(t)\,dt \tag{8.21}$$

Estimating AUC and AUMC Using Sums of Exponentials

For the single accessible pool model, following a bolus injection of amount D into the pool, the pharmacokinetic data can be described by a sum of exponentials equation of the general form shown in Equation 8.22:

$$C(t) = A_1 e^{-\lambda_1 t} + \cdots + A_n e^{-\lambda_n^t} \tag{8.22}$$

In this, and subsequent equations, the A_i are called *coefficients* and the λ_i are *exponentials* (in mathematical parlance, they are called *eigenvalues*). Following a constant infusion into the accessible pool, Equation 8.22 changes to Equation 8.23 with the restriction that the sum of the coefficients equals zero, reflecting the fact that no drug is present in the system at time zero.

$$C(t) = A_0 + A_1 e^{-\lambda_1 t} + \cdots + A_n e^{-\lambda_n^t} \tag{8.23}$$

$$A_0 + A_1 + \cdots + A_n = 0$$

What is the advantage of using sums of exponentials to describe pharmacokinetic data in the situation of the single accessible pool model following a bolus injection or constant infusion? The reason is that the integrals required to estimate the pharmacokinetic parameters are very easy to calculate!

For the bolus injection, from Equation 8.22,

$$AUC = \int_0^\infty C(t)\,dt = \frac{A_1}{\lambda_1} + \cdots + \frac{A_n}{\lambda_n} \tag{8.24}$$

$$AUMC = \int_0^\infty t \cdot C(t)\,dt = \frac{A_1}{\lambda_1^2} + \cdots + \frac{A_n}{\lambda_n^2} \tag{8.25}$$

In addition, for the bolus injection,

$$C(0) = A_1 + \cdots + A_n \tag{8.26}$$

provides an estimate for $C(0)$. Thus, with a knowledge of the amount of drug in the bolus, D, all pharmacokinetic parameters can be estimated.

For the constant infusion, the steady-state concentration, $\overline{C}$, can be seen from Equation 8.23 to equal A_0. An estimate for $\dot{C}(0)$ can be obtained,

$$\dot{C}(0) = -A_1\lambda_1 - \cdots - A_n\lambda_n \tag{8.27}$$

and since the estimate for $\overline{C}$ is A_0,

$$\int_0^\infty [\overline{C} - C(t)]\,dt = \frac{A_1}{\lambda_1} + \cdots + \frac{A_n}{\lambda_n} \tag{8.28}$$

Thus, all the pharmacokinetic parameters for the constant infusion can easily be estimated.

An advantage of using sums of exponentials is that error estimates for all the pharmacokinetic parameters can also be obtained as part of the fitting process; this is not the case for most of the so-called numerical techniques (see the following section). In addition, for multiple inputs (i.e., multiple boluses or infusions), sums of exponentials can be used over each experimental time period for a specific bolus or infusion, recognizing that the exponentials, the λ_i, remain the same. The reason is that the exponentials are system parameters and do not depend on a particular mode of introducing drug into the system (13).

Estimating AUC and AUMC Using Other Functions

While sums of exponentials may seem the logical function to use to describe $C(t)$ and hence to estimate *AUC* and *AUMC*, the literature is full of other recommendations for estimating *AUC* and *AUMC* [see, for example, Yeh and Kwan (14) or Purves (15)]. These include the trapezoidal rule or the log-trapezoidal rule or a combination of the two, splines, and Lagrangians, among others. All result in formulas for calculations over the time domain of the data, and are left with the problem of estimating the integrals $\int_{t_n}^{\infty} C(t)\,dt$ and $\int_{t_n}^{\infty} t \cdot C(t)\,dt$. The problem of estimating $\int_0^{t_1} C(t)\,dt$ and $\int_0^{t_1} t \cdot C(t)\,dt$, and estimating a value for $C(0)$, $\dot{C}(0)$, or $\overline{C}$, is rarely discussed.

There are two problems with this approach. First, estimating *AUMC* is very difficult. While one hopes that the experiment has been designed so that $\int_{t_n}^{\infty} C(t)\,dt$ contributes 5% or less to *AUC*, $\int_{t_n}^{\infty} t \cdot C(t)\,dt$ can contribute as much as 50% or more to *AUMC*. Hence estimates of *AUMC* are subject to large errors. The second problem is that it is extremely difficult to obtain error estimates for *AUC* and *AUMC* that will translate into error estimates for the pharmacokinetic parameters derived from them. As a result, it is normal practice in individual studies to ignore error estimates for these parameters, and hence the pharmacokinetic parameters that rely upon them. One tries to circumvent the statistical nature of the problem by conducting repeated studies and basing the statistics on averages and standard errors of the mean.

Estimating $\int_{t_1}^{t_n} C(t)\,dt$ and $\int_{t_1}^{t_n} t \cdot C(t)\,dt$

In what follows, some comments will be made on the commonly used functional approaches to estimating $\int_{t_1}^{t_n} C(t)\,dt$ and $\int_{t_n}^{\infty} t \cdot C(t)\,dt$ (i.e., the trapezoidal rule, or a combination of the trapezoidal and log-trapezoidal rule) (15, 16). Other methods such as splines and Lagrangians will not be discussed. The interested reader is referred to Yeh and Kwan (14) and Purves (15).

Suppose $[(y_{obs}(t_i), t_i)]_{i=1}^{n}$ is a set of pharmacokinetic data. For example, this can be n plasma samples starting with the first measurable sample being at time t_1 and the last measurable sample at time t_n. If $[t_{i-1}, t_i]$ is the ith interval, then the *AUC* and *AUMC* for this interval calculated using the trapezoidal rule are

$$AUC_{i-1}^{i} = \frac{1}{2}(y_{obs}(t_i) + y_{obs}(t_{i-1})(t_i - t_{i-1})) \tag{8.29}$$

$$AUMC_{i-1}^{i} = \frac{1}{2}(t_i \cdot y_{obs}(t_i) + t_{i-1} \cdot y_{obs}(t_{i-1})(t_i - t_{i-1})) \tag{8.30}$$

For the log-trapezoidal rule, the formulas are

$$AUC_{i-1}^{i} = \frac{1}{\ln\left[y_{obs}(t_i)/y_{obs}(t_{i-1})\right]} \times (y_{obs}(t_i) + y_{obs}(t_{i-1})(t_i - t_{i-1})) \tag{8.31}$$

$$AUMC_{i-1}^{i} = \frac{1}{\ln\left[y_{obs}(t_i)/y_{obs}(t_{i-1})\right]} \times (t_i \cdot y_{obs}(t_i) + t_{i-1}.y_{obs}(t_{i-1})(t_i - t_{i-1})) \tag{8.32}$$

One method by which *AUC* and *AUMC* can be estimated from t_1 to t_n is to use the trapezoidal rule and add up the individual terms AUC_{i-1}^{i} and $AUMC_{i-1}^{i}$. If one chooses this approach, then it is possible to obtain an error estimate for *AUC* and *AUMC* using the method proposed by Katz and D'Argenio (17). Other approaches use a combination of the trapezoidal and log-trapezoidal formulas. The idea here is that the trapezoidal approximation is a good approximation when $y_{obs}\ (t_i) \geq y_{obs}\ (t_{i-1})$ (i.e., when the data are rising), and the log-trapezoidal rule is a better approximation when $y_{obs}(t_i) \prec y_{obs}(t_{i-1})$ (i.e., the data are falling). The rationale is that the log-trapezoidal formula takes into account some of the curvature in the falling portion of the curve. If a combination of the two formulas is used, it is not possible to obtain an error estimate for *AUC* and *AUMC* from t_1 to t_n using the quadrature method of Katz and D'Argenio.

The software system WinNonlin (18) uses a combination of the trapezoidal and log-trapezoidal formulas to estimate *AUC* and *AUMC*, and the formulas resulting from them. As a result, no statistical information is available.

Extrapolating from t_n to Infinity

One now has to deal with estimating $\int_{t_n}^{\infty} C(t)\,dt$ and $\int_{t_n}^{\infty} t \cdot C(t)\,dt$. The most common way to estimate these integrals is to assume that the data decay monoexponentially beyond the last measurement at time t_n. Such a function can be written

$$y(t) = A_z e^{-\lambda_z t} \tag{8.33}$$

Here the exponent λ_z characterizes the terminal decay and is used to calculate the half-life of the terminal decay

$$t_{z,1/2} = \frac{\ln(2)}{\lambda_z} \tag{8.34}$$

Estimates for the integrals can be based on the last datum [i.e., assuming the monoexponential decay is from the last datum y_{obs} (t_n)]:

$$AUC_{\text{extrap-dat}} = \int_{t_n}^{\infty} C(t)\, dt = \frac{y_{obs}(t_n)}{\lambda_z} \tag{8.35}$$

$$AUMC_{\text{extrap-dat}} = \int_{t_n}^{\infty} t \cdot C(t)\, dt = \frac{t_n \cdot y_{obs}(t_n)}{\lambda_z} + \frac{y_{obs}(t_n)}{\lambda_z^2} \tag{8.36}$$

or from the model calculated "last datum":

$$AUC_{\text{extrap-calc}} = \int_{t_n}^{\infty} C(t)\, dt = \frac{A_z e^{-\lambda_z t_n}}{\lambda_z} \tag{8.37}$$

$$\text{AUMC}_{\text{extrap-calc}} = \int_{t_n}^{\infty} t \cdot C(t)\, dt = \frac{t_n \cdot A_z e^{-\lambda_z t_n}}{\lambda_z} + \frac{A_z e^{-\lambda_z t_n}}{\lambda_z^2} \tag{8.38}$$

There are a variety of ways that one can estimate λ_z. Most rely on the fact that the last two or three data decay exponentially, and thus Equation 8.33 can be fitted to these data. Various options for including or excluding other data have been proposed [e.g., Gabrielsson and Weiner (16), Marino *et al.* (19)]. These will not be discussed here. What is certain is that all parameters and area estimates will have statistical information, since they are obtained by fitting Equation 8.33 to the data.

It is of interest to note that an estimate for λ_z could differ from λ_n, the terminal slope of a multiexponential function describing the pharmacokinetic data. The reason is that all data are considered in estimating λ_n as opposed to a finite (terminal) subset used to estimate λ_z. Thus, a researcher checking both methods should not be surprised if there are slight differences.

Estimating AUC and AUMC from 0 to Infinity

Estimating *AUC* and *AUMC* from zero to infinity is now simply a matter of adding the two components (i.e., the *AUC* and *AUMC*) over the time domain of the data and the extrapolation from the last datum to infinity. The zero-time value is handled in a number of ways. For the bolus injection, it can be estimated using a modification of the methodology used to estimate λ_z. In this way, statistical information on $C(0)$ would be available. Otherwise, if an arbitrary value is assigned, no such information is available.

Error estimates for the pharmacokinetic parameters will be available only if error estimates for *AUC* and *AUMC* are calculated. In general, this will not be the case when numerical formulas are used over the time domain of the data. Performing studies on several individuals and obtaining averages and standard errors of the mean on these individuals essentially begs the question. With all the limitations, it is somewhat surprising that sums of exponentials are not used as the function of choice, especially since the canonical inputs, boluses and infusions, are the most common ways to introduce a drug into the system.

COMPARTMENTAL ANALYSIS

Definitions and Assumptions

As noted earlier in this chapter, it is very difficult to use partial differential equations to describe the kinetics of a drug. A convenient way to deal with this situation is to lump portions of the system into discrete entities and then discuss movement of material among these entities. These lumped portions of the system essentially contain the same material, whose kinetics share a similar time frame. Thus, the lumping is a combination of known physiology and biochemistry on the one hand, and the time frame of a particular experiment on the other.

Compartmental models are the mathematical result of such lumping. A *compartment* is an amount of material that is kinetically homogeneous. *Kinetic homogeneity* means that material introduced into a compartment mixes instantaneously, and that each particle in the compartment has the same probability as all other particles in the compartment of leaving the compartment along the various exit pathways from the compartment. A *compartmental model* consists of a finite number of compartments with specified interconnections, inputs, and losses.

Let $X_i(t)$ be the mass of a drug in the ith compartment. The notation for input, loss, and transfers is summarized in Figure 8.3. Because this notation describes the compartment in full generality, it is a little different from that used in earlier chapters. This difference is necessary to understand how one passes to the linear compartmental model. In Figure 8.3, the rate constants describe mathematically the mass transfer of material among compartments interacting with the ith compartment (F_{ji} is the transfer of material from compartment i to compartment j, F_{ij} is the transfer of material from compartment j to compartment i), the new input F_{i0} (this corresponds to X_0 in Chapter 4), and loss to the environment F_{0i} from compartment i. The mathematical expression describing the rate of

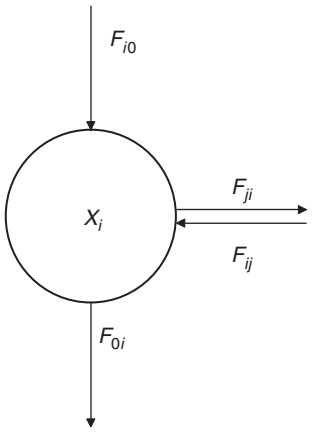

FIGURE 8.3 The *i*th compartment of an *n*-compartment model. See text for explanation.

change for $X_i(t)$ is derived from the mass balance equation:

$$\frac{dX_i(t)}{dt}=\frac{dX_i}{dt}=\sum_{\substack{j=0\\ j\neq i}}^{n} F_{ij}-\sum_{\substack{j=0\\ j\neq i}}^{n} F_{ji} \tag{8.39}$$

There are several important features to understand about the F_{ij} that derive from the fact that the compartmental model is being used to describe a biological system, and hence conservation of mass must be obeyed. First, the F_{ij} must be nonnegative for all times t (assumed to be between time zero and infinity). In fact, the F_{ij} can be either stochastic (have uncertainty associated with them) or deterministic (the form known exactly). In this chapter, the F_{ij} will be assumed to be deterministic but can be functions of the X_i and/or time t. [Readers interested in stochastic compartmental models can find references to numerous articles in Covell *et al.* (4)]. Second, as pointed out by Jacquez and Simon (5), if $X_i=0$, then $F_{ji}=0$ for all $j \neq i$ and hence $dX_i/dt \geq 0$. An important consequence of this, as shown by these authors, is that the F_{ji}, with the exception of $F_{i0,}$ which remains unchanged, can be written

$$F_{ji}(\vec{X},\vec{p}s,t)=k_{ji}(\vec{X},\vec{p},t)\cdot X_i(t) \tag{8.40}$$

The function F_{i0} is either a constant or a function of t alone. The k_{ji} written in this format are called the *fractional transfer functions*. Equation 8.40 is a subtle but important step in moving from the general compartment model to the linear, constant-coefficient model because it shows explicitly that the fractional transfers can be functions and not necessarily constants, and that, as functions, the mass terms can be split out from the fractional transfer term. In Equation 8.40, $\mathbf{X}=(X_1,\ldots,X_n)$ is a notation for compartmental masses (mathematically it is called a vector), $\mathbf{p}$ is a descriptor of other elements such as blood flow, pH, and temperature that control the system, and t is time. Written in this format, Equation 8.39 becomes

$$\frac{dX_i}{dt}=-\left[\sum_{\substack{j=0\\ j\neq i}}^{n} k_{ji}(\vec{X},\vec{p},t)\right]X_i(t)+\sum_{\substack{j=1\\ j\neq i}}^{n} k_{ij}(\vec{X},\vec{p},t)X_j(t)+F_{i0} \tag{8.41}$$

Define

$$k_{ii}(\vec{X},\vec{p},t)=-\left[\sum_{\substack{j=0\\ j\neq i}}^{n} k_{ji}(\vec{X},\vec{p},t)\right] \tag{8.42}$$

and write

$$K(\mathbf{X},\mathbf{p},t)=\begin{bmatrix} k_{11} & k_{12} & \cdots & k_{1n}\\ k_{21} & k_{22} & \cdots & k_{2n}\\ \vdots & \vdots & \ddots & \vdots\\ k_{n1} & k_{n2} & \cdots & k_{nn}\end{bmatrix} \tag{8.43}$$

where in Equation 8.43 the individual terms of the matrix, for convenience, do not contain the $(\vec{X},\vec{p},t)$. The matrix $K(\vec{X},\vec{p},t)$ is called the *compartmental matrix*. This matrix is key to deriving many kinetic parameters, and in making the link between compartmental and noncompartmental analysis.

There are several reasons for going first to this level of generality for the *n*-compartment model. First, it points out clearly that the theories of noncompartmental and compartmental models are very different. While the theory underlying noncompartmental models relies more on statistical theory, especially in developing residence time concepts [see, e.g., Weiss (11)], the theory underlying compartmental models is really the theory of ordinary, first-order differential equations in which, because of the nature of the compartmental model applied to biological applications, there are special features in the theory. These are reviewed in detail in Jacquez and Simon (5), who also refer to the many texts and research articles on the subject.

Second, this gets at the complexity involved in postulating the structure of a compartmental model to

describe the kinetics of a particular drug. As illustrated by the presentation in Chapter 3, it is very difficult to postulate a model structure in which the model compartments have physiological relevance as opposed simply to representing the mathematical construct X_i, especially when one is dealing with the single-input–single-output experiment. Although the most general compartmental model must be appreciated in its potential application to the interpretation of kinetic data, the fact is that such complex models are not often used. Thus, the most common models are the linear, constant-coefficient compartmental models described in the next section. In this discussion, it also will be assumed that all systems are open (i.e., drug introduced into the system will eventually leave the system). This means that some special situations discussed by Jacquez and Simon (5) do not have to be considered (i.e., compartmental models with submodels from which material cannot escape).

Linear, Constant-Coefficient Compartmental Models

Suppose the compartmental matrix is a constant matrix (i.e., all k_{ij} are constants). In this situation, one can write K instead of $K(\vec{X},\vec{p},t)$ to indicate that the elements of the matrix no longer depend on $(\vec{X},\vec{p},t)$. As will be seen, there are several important features of the K matrix that will be used in recovering pharmacokinetic parameters of interest. In addition, as described in Jacquez and Simon (5) and Covell *et al.* (4), the solution to the compartmental equations (a system of linear, constant-coefficient equations) involves sums of exponentials.

What is needed for the compartmental matrix to be constant? Recall that the individual elements of the matrix k_{ij} $(\vec{X},\vec{p},t)$ are functions of several variables. For the k_{ij} $(\vec{X},\vec{p},t)$ to be constant, $\vec{X}$ and $\vec{p}$ must be constant (actually this assumption can be relaxed, but for purposes of this discussion, constancy will be assumed), and the k_{ij} $(\vec{X},\vec{p},t)$ cannot depend explicitly on time (i.e., the k_{ij} $(\vec{X},\vec{p},t)$ are time invariant). Notice with this concept that the time invariant k_{ij} $(\vec{X},\vec{p},t)$ can assume different values, depending upon the constant values for $\vec{X}$ and $\vec{p}$. This leads naturally to the concept of the steady state.

Under what circumstances are compartmental models linear, constant coefficient? This normally depends upon a particular experimental design. The reason is that most biological systems, including those in which drugs are analyzed, are inherently nonlinear. However, the assumption of linearity holds reasonably well over the dose range studied for most drugs, and most pharmacokinetic studies have been carried out under stable conditions of minimal physiological perturbation.

Parameters Estimated from Compartmental Models

Experimenting on Compartmental Models: Input and Measurements

In postulating a compartmental model such as that shown in Figure 8.4A, one is actually making a statement concerning how the system is believed to behave. To know if a particular model structure can predict the behavior of a drug in the body, one must be able to obtain kinetic data from which the parameters characterizing the system of differential equations can be estimated; the model predictions can then be compared against the data. Experiments are designed to generate the data; the experiment must then be reproduced on the model. This is done by specifying inputs and samples, as shown in Figure 8.4B. More specifically, the input specifies the F_{i0} terms in the differential equations, and the samples provide the measurement equations that link the model's predictions, which are normally in units of drug mass, with the samples, which are usually in concentration units.

To emphasize this point, once a model structure is postulated, the compartmental matrix is known, since it depends only upon the transfers and losses. The input, the F_{i0}, comes from the experimental input and thus is determined by the investigator. In addition, the units of the differential equation (i.e., the units of the X_i) are determined by the units of the input. The point is that if the parameters of the model can be estimated from the data from a particular experimental design [i.e., if the model is *a priori* identifiable; see

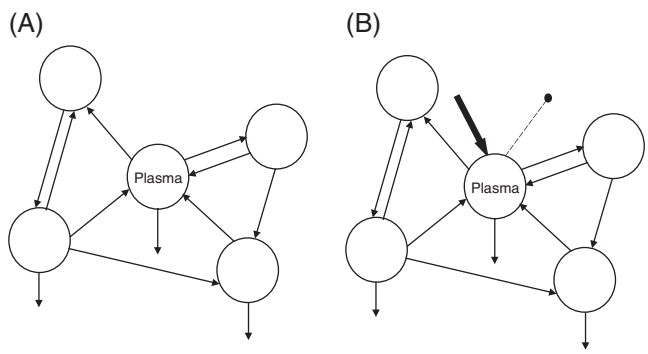

FIGURE 8.4 (A) A compartmental model of drug behavior in the body. (B) An experimental protocol on (A), showing drug administration (*bold arrow*) and plasma sampling (*dashed line with bullet*).

Carson *et al.* (20), Cobelli *et al.* (12)], then the specific form of the input is not important. Thus, the data from a bolus injection or constant infusion should be equally rich from an information point of view.

The final point to make in dealing with experiments on the model relates to the measurement variable(s). The units of the X_i are determined by the experimental input vector, and are usually mass. The units of the data are normally concentration. No matter what the units of the data, there must be a measurement equation linking the X_i involved in the measurement with the data. For example, if the measurement was taken from compartment 1 and the units of the data are concentration, one would need to write the measurement equation

$$C_1(t) = X_1/V_1 \tag{8.44}$$

Here V_1 is the volume of compartment 1, and is a parameter to be estimated from the data.

Clearly, once a compartmental structure is postulated, there are many experimental protocols and measurement variables that can be accommodated. One just needs to be sure that the parameters characterizing the compartmental matrix, K, and the parameters characterizing the measurement variables can be estimated from the data generated by the experiment.

Nonlinearities in Compartmental Models

Some fractional transfer functions of compartmental models may actually be functions, (i.e., the model may actually be nonlinear). The most common example is when a transfer or loss is saturable. Here a Michaelis–Menten type of transfer function can be defined, as was shown in Chapter 2 for the elimination of phenytoin. In this case, loss from compartment 1 is concentration dependent and saturable, and one can write

$$CL_1 = k_{01} \cdot V_1 = \frac{V_{max}}{K_m + C_1} \tag{8.45}$$

where V_{max} and K_m are parameters that can be estimated from the pharmacokinetic data. In the differential equation dX_1/dt, this will result in the term

$$-k_{01} \cdot X_1 = -\frac{V_{max}}{K_m + C_1} \cdot C_1 \tag{8.46}$$

Another example of a function-dependent transfer function was given in Chapter 6, in which hemodynamic changes during and after hemodialysis reduce intercompartmental clearance between the intravascular space and a peripheral compartment, as shown in Figure 6.3.

If one has pharmacokinetic data and knows that the situation calls for nonlinear kinetics, then compartmental models, no matter how difficult to postulate, are really required. Noncompartmental models cannot deal with the time-varying situation.

Calculating Model Parameters from a Compartmental Model

Realizing the full generality of the compartmental model, consider now only the limited situation of linear, constant-coefficient models. What parameters can be calculated from a model? The answer to this question can be addressed in the context of Figure 8.5.

Model Parameters

Once a specific multicompartmental structure has been developed to explain the pharmacokinetics of a particular drug, the parameters characterizing this model are the components of the compartmental matrix, K, and the volume parameters associated with the individual measurements. The components of the compartmental matrix are the rate constants k_{ij}.

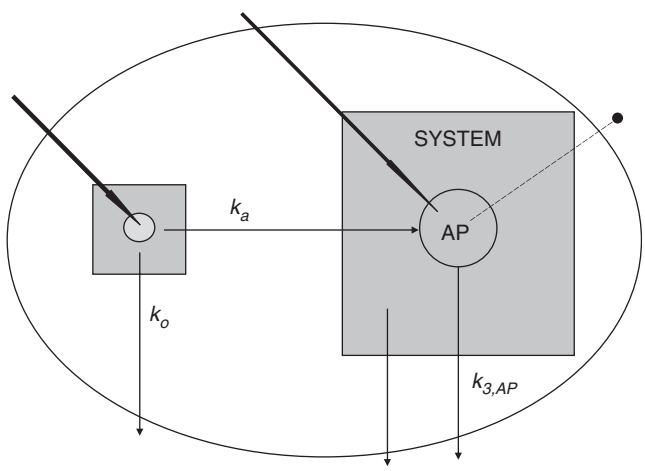

FIGURE 8.5 The system model shown on the right contains an accessible pool embedded in an arbitrary multicompartmental model, indicated by the shaded box. The drug can be introduced directly into this pool, as indicated by the bold arrow. The drug can also be introduced into a second compartment, indicated by the circle in the small, shaded box on the left. Drug can move from this compartment, as denoted by the arrow passing from the small, shaded box, through the large box, into the accessible pool. The rate is denoted k_a. Material also can be lost from the small box; this is denoted k_o. Finally, material has two ways by which it can leave the system. One is directly from the accessible pool, $k_{e,AP}$, and the other is from nonaccessible pools, denoted by the arrow leaving the large box. That both small and large boxes exist in a larger system is denoted by the ellipse surrounding the individual components of the system. See text for additional explanation.

Together, these comprise the primary *mathematical* parameters of the model. The primary *physiological* parameters of clearance and distribution volume are secondary from a mathematical standpoint. For this reason, the mathematical parameters of compartmental models need to be reparameterized in order to recover these physiological parameters (e.g., see Figure 3.8). Although this works relatively well for simple models, it becomes a very difficult exercise once one moves to more complex models.

The next question is whether the parameters characterizing a model can be estimated from a set of pharmacokinetic data. The answer to this question has two parts. The first is called *a priori identifiability*. This answers the question, "given a particular model structure and experimental design, if the data are 'perfect,' can the model parameters be estimated?" The second part is *a posteriori identifiability*. This answers the question, "given a particular model structure and a set of pharmacokinetic data, can the model parameters be estimated within a reasonable degree of statistical precision?"

A priori identifiability is a critical part of model development. While the answer to the question for many of the simpler models used in pharmacokinetics is well known, the general answer, even for linear, constant-coefficient models, is more difficult (12). Figure 8.6 illustrates the situation with some specific model structures (A–F); the interested reader is referred to Cobelli *et al*. (12) for precise details. Model A is a standard two-compartment model with input and sampling from a "plasma" compartment. There are three k_{ij} and a volume term to be estimated. This model can be shown to be *a priori* identifiable. Model B has four k_{ij} and a volume term to be estimated. These parameters cannot be estimated from a single set of pharmacokinetic data, no matter how information rich they are. In fact, there are an infinite number of values for the k_{ij} and volume term that will produce the same fit of the data. If one insists on using this model structure, then some constraint will have to be placed on the parameters, such as fixing the volume or defining a relationship among the k_{ij}. Model C, while *a priori* identifiable, will have a different compartmental matrix from that of model A, and hence, as discussed previously, some of the pharmacokinetic parameters will be different for the two models.

Two commonly used three-compartment models are shown in Figures 8.6D and E. Of the two peripheral compartments, one exchanges rapidly and one changes slowly with the central compartment. Model D is *a priori* identifiable while model E is not. Model E will have two different compartmental matrices that will produce the same fit of the data. The reason is that the loss is from a peripheral compartment. Finally, model F, a model very commonly used to describe the pharmacokinetics of drug absorption, is not *a priori* identifiable. Again, there are two values for the compartmental K matrix that will produce the same fit to the data.

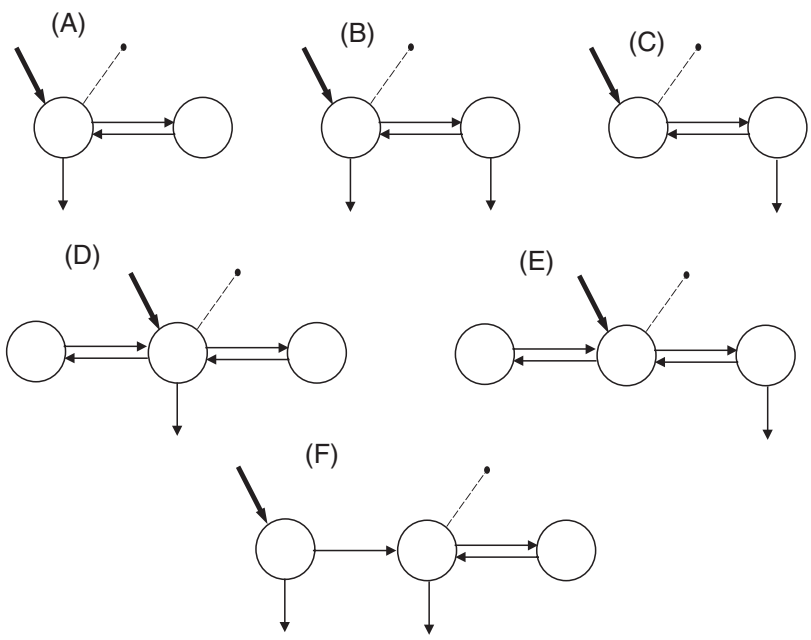

FIGURE 8.6 Examples of multicompartmental models. See text for explanation.

A posteriori identifiability is linked to the theory of optimization in mathematics because one normally uses a software package that has an optimization (data-fitting) capability in order to estimate parameter values for a multicompartmental model from a set of pharmacokinetic data. One obtains an estimate for the parameter values, an estimate for their errors, and a value for the correlation (or covariance) matrix. The details of optimization and how to deal with the output from an optimization routine are beyond the scope of this chapter, and the interested reader is referred to Cobelli *et al.* (12). The point to be made here is that the output from these routines is crucial in assessing the goodness-of-fit — that is, how well the model performs when compared to the data — since inferences about a drug's pharmacokinetics will be made from these parameter values.

Residence Time Calculations

The notion of residence times can be very important in assessing the pharmacokinetics of a drug. The information about residence times available from a linear, constant-coefficient compartmental model is very rich, and will be reviewed in the following comments.

Residence time calculations are a direct result of manipulating the compartmental matrix K. Let $\Theta = -K^{-1}$ be the negative inverse of the compartmental matrix, and let ϑ_{ij} be the ijth element of Θ. The matrix Θ is called the *mean residence time* matrix. The following information given concerning the interpretation of this matrix comes from Covell *et al.* (4) and Cobelli *et al.* (12). Further detail is beyond the scope of this chapter, and the interested reader is directed to these two references.

As explained in Covell *et al.* (4) and Cobelli *et al.* (12), the elements of the mean residence time matrix have important probabilistic interpretations. First, the generic element ϑ_{ij} represents the average time a drug particle entering the system in compartment j spends in compartment i before irreversibly leaving the system by any route. Second, the ratio $\vartheta_{ij}/\vartheta_{ii}$, $i \neq j$, equals the probability that a drug particle in compartment j will eventually reach compartment i. Finally, if a compartmental model has loss from a single compartment only, say, compartment 1, then it can be shown that $k_{01} = 1/\vartheta_{11}$. Clearly, if one is analyzing pharmacokinetic data using compartmental models in which the K matrix is constant, this information can be critical in assessing the behavior of a particular drug.

However, more can be said about the ϑ_{ij} that is important in comparing compartmental and noncompartmental models. Suppose there is a generic input into compartment 1 only, F_{10} (remember, in this situation F_{10} can be a function). Then it can be shown that the area under $X_i(t)$, the drug mass in the ith compartment, equals

$$\int_0^\infty X_i(t)\, dt = \vartheta_{i1} \int_0^\infty F_{10}\, dt \tag{8.47}$$

whence

$$\vartheta_{i1} = \frac{\int_0^\infty X_i(t)\, dt}{\int_0^\infty F_{10}\, dt} \tag{8.48}$$

More generally, suppose F_{j0} is an arbitrary input into compartment j, and $X_i^j(t)$ is the amount of drug in compartment i following an initial administration in compartment j. Then

$$\vartheta_{ij} = \frac{\int_0^\infty X_i^j(t)\, dt}{\int_0^\infty F_{j0}\, dt} \tag{8.49}$$

This equation shows that ϑ_{ij} equals the area under the model predicted drug mass curve in compartment i resulting from an input compartment j, normalized to the dose.

The use of the mean residence time matrix can be a powerful tool in pharmacokinetic analysis with a compartmental model, especially if one is dealing with a model of the system in which physiological and/or anatomical correlates are being assigned to specific compartments (2). Modeling software tools such as SAAM II (21) automatically calculate the mean residence time matrix from the compartmental matrix, making the information easily available.

NONCOMPARTMENTAL VERSUS COMPARTMENTAL MODELS

In comparing noncompartmental with compartmental models, it should now be clear that this is not a question of declaring one method better than the other. It is a question of (1) what information is desired from the data and (2) what is the most appropriate method to obtain this information. It is hoped that the reader of this chapter will be enabled to make an informed decision on this issue.

This discussion will rely heavily on the following sources. First, the publications of DiStefano and Landaw (22, 23) deal with issues related to compartmental versus single accessible pool noncompartmental models. Second, Cobelli and Toffolo (3) discuss the two accessible pool noncompartmental model. Finally, Covell *et al.* (4) provide the theory to demonstrate the link between noncompartmental and compartmental models in estimating the pharmacokinetic parameters.

Models of Data vs Models of System

Suppose one has a set of pharmacokinetic data. The question is how to obtain information from the data related to the disposition of the drug in question. DiStefano and Landaw (22) deal with this question by making the distinction between models of data and models of system. Understanding this distinction is useful in understanding the differences between compartmental and noncompartmental models.

As discussed, the noncompartmental model divides the system into two components: an accessible pool and nonaccessible pools. The kinetics of the nonaccessible pools are lumped into the recirculation-exchange arrows. From this, as has been discussed, we can estimate pharmacokinetic parameters describing the accessible pool and system.

What happens in the compartmental model framework? Here the most common way to deal with pharmacokinetic data is to fit them first by a sum of exponentials, since, in a linear, constant-coefficient system, the number of exponential phases in the plasma level-vs-time curve equals the number of compartments in the model.

Consider the situation in which plasma data are obtained following a bolus injection of the drug. Then the data can be described by

$$C(t) = A_1 e^{-\lambda_1 t} + A_2 e^{-\lambda_2 t} \tag{8.50}$$

These data can be equally well fitted by the standard two-compartment model shown in Figure 8.7A. While this model and Equation 8.50 will produce an identical fit to the data, and while, as seen in the following, all pharmacokinetic parameters recovered from this model will equal those calculated using the noncompartmental formulas, the model serves only as a descriptor of the data. That is, no comment is being made about a physiological, biochemical, and/or anatomical significance to the extravascular compartment 2. This is what DiStefano and Landaw would call a model of data, because little to nothing is being said about the system into which the drug is administered.

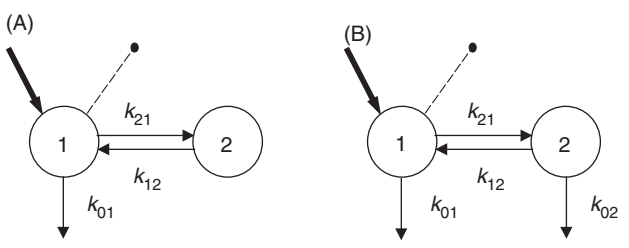

FIGURE 8.7 Two two-compartment models in which drug is administered intravenously into compartment 1; samples are taken from this compartment. See text for explanation.

Suppose, on the other hand, additional information is known about the disposition of the drug. For example, suppose it is known that a major tissue in the body is where virtually all of the drug is taken up extravascularly, and that it is known from independent experiments approximately what fraction of the drug is metabolized in that compartment. Now, given that the plasma data can be fitted by a sum of two exponentials, one can start to develop a system model for the drug. In particular, one can write an equation in which the loss rate constants k_{01} and k_{02} are related through a knowledge of how much of the drug is metabolized in the tissue; compartment 2 can thus be associated with the tissue.

It is interesting how people react to such modeling techniques. First, one has used the fact that the data support a two-compartment model, and the fact that a relationship between the loss rate constants can be written based upon *a priori* knowledge. A physiological significance can thus be associated with the compartments and the k_{ij} that goes beyond the model of data just discussed. A criticism of such a statement is that the model does not contain all elements of the system in which the drug is known to interact. If this critique is justified, then one has to design a new experiment to uncover information on these parts of the system. One may have to change the sampling schedule to resolve more components in the data, or one may have to design a different series of input–output experiments. One even may have to conduct a study in which marker compounds for known physiological spaces are coadministered with the study drug (24).

This is not a shortcoming of the modeling approach, but illustrates how a knowledge of compartmental modeling can be a powerful tool for understanding the pharmacokinetics of a drug. Such an understanding is not available from noncompartmental models or when compartmental models are used only as models of data. Thus, predicting detailed events in nonaccessible portions of the system model is the underlying rationale for developing models of systems, remembering, of course, that such predictions are only as good as the assumptions in the model.

Equivalent Sink and Source Constraints

When are the parameter estimates from the noncompartmental model equal to those from a linear, constant-coefficient compartmental model? As DiStefano and Landaw (22) explain, they are equal when the equivalent sink and source constraints are valid. The equivalent source constraint means that all

drug enters the same accessible pools; this is almost universally the case in pharmacokinetic studies. The equivalent sink constraint means that irreversible loss of drug can occur only from the accessible pools. If any irreversible loss occurs from the nonaccessible part of the system, this constraint is not valid. For the single accessible pool model, for example, the system mean residence time and the total equivalent volume of distribution will be underestimated (22).

The equivalent sink constraint is illustrated in Figure 8.8. In Figure 8.8A, the constraint holds and hence the parameters estimated from either the noncompartmental model (*left*) or the multicompartmental model (*right*) will be equal. If the multicompartmental model is a model of the system, then, of course, the information about the drug's disposition will be much richer, since many more specific parameters can be estimated to describe each compartment.

In Figure 8.8B, the constraint is not satisfied, and the noncompartmental model is not appropriate. As previously described, if used, it will underestimate certain pharmacokinetic parameters. On the other hand, the multicompartmental model shown on the right can account for sites of loss from nonaccessible compartments, providing a richer source of information about the drug's disposition.

Recovering Pharmacokinetic Parameters from Compartmental Models

Assume a linear, constant-coefficient compartmental model in which compartment 1 is the accessible compartment into which the drug is administered and from which samples are taken. Following a bolus injection of the drug, the volume V_1 will be estimated as a parameter of the model. V_1 thus will correspond to V_a for the noncompartmental model. The clearance rate from compartment 1, CL_1, is equal to the product of V_1 and k_{01}:

$$CL_1 = V_1 \cdot k_{01} \tag{8.51}$$

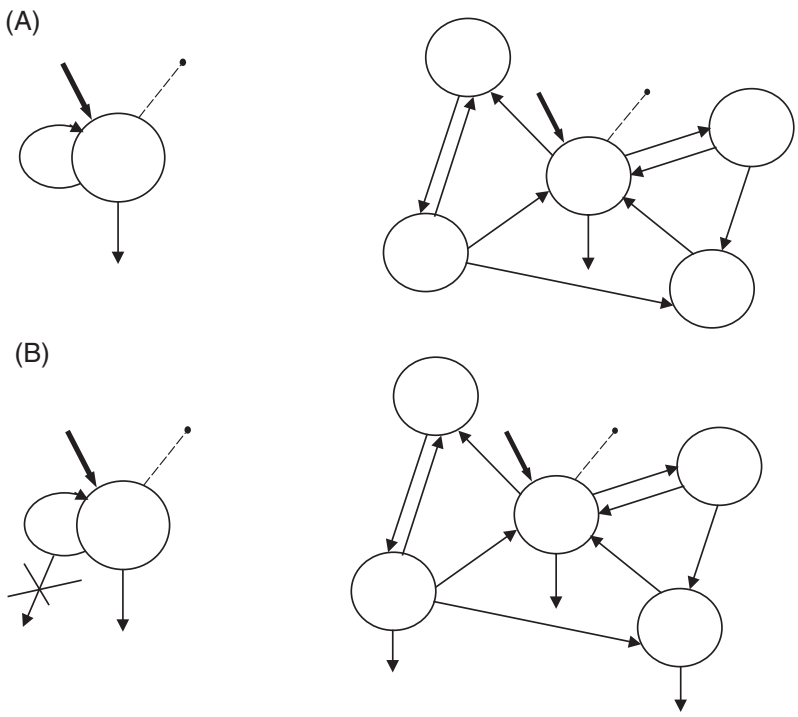

FIGURE 8.8 (A) A single accessible pool model (*left*) and a multicompartmental model showing a structure for the recirculation-exchange arrow (*right*). (B) A single accessible pool model with an irreversible loss from the recirculation-exchange arrow (*left*) and a multicompartmental model showing a structure for the recirculation-exchange arrow that includes loss from peripheral compartments (*right*). See text for additional explanation.

If the only loss is from compartment 1, then k_{01} equals k_e, and one has

$$CL_a = CL_1 = V_1 \cdot k_{01} = V_a \cdot k_e \tag{8.52}$$

showing the equivalence of the two methods. From the residence time matrix,

$$\vartheta_{11} = \frac{\int_0^\infty X_1(t)\, dt}{d} = k_{01} \tag{8.53}$$

hence, the mean residence time in compartment 1, MRT_1, equals the reciprocal of k_{01}. Again, if the only loss from the system is via compartment 1, then MRT_1 equals MRT_a.

Similar results hold for the constant infusion or generic input. In other words, the parameters can be shown to be equal if the equivalent sink and source constraints are valid. Again, the interested reader is referred to Cobelli and Toffolo (3) or Covell *et al.* (4) for details and for consideration of the situation in which the equivalent source and sink constraints are not valid.

CONCLUSION

In conclusion, noncompartmental models and linear, constant-coefficient models have different domains of validity. When the domains are identical, then the pharmacokinetic parameters estimated by either method should, in theory, be equal. If they are not, then differences are due to the methods used to estimate them.

Information provided in this chapter should make it easier for a researcher to choose a particular method and to have greater confidence in evaluating reported results of pharmacokinetic analyses.

REFERENCES

1. Gillespie WR. Noncompartmental versus compartmental modeling in clinical pharmacokinetics. Clin Pharmacokinet 1991;20:253–62.
2. DiStefano JJ III. Noncompartmental versus compartmental analysis: Some bases for choice. Am J Physiol 1982;243:R1–6.
3. Cobelli C, Toffolo G. Compartmental versus noncompartmental modeling for two accessible pools. Am J Physiol 1984;247:R488–96.
4. Covell DG, Berman M, DeLisi C. Mean residence time — Theoretical development, experimental determination, and practical use in tracer analysis. Math. Biosci. 1984;72:213–244.
5. Jacquez JA, Simon CP. Qualitative theory of compartmental systems. SIAM Rev 1993:35;43–79.
6. Jacquez JA. Compartmental analysis in biology and medicine. 3rd ed. Ann Arbor, MI: BioMedware; 1996.
7. Berman M. Kinetic analysis of turnover data. Prog Biochem Pharmacol 1979;15:67–108.
8. Gibaldi M, Perrier D. Pharmacokinetics. 2nd ed. New York: Marcel Dekker; 1982.
9. Rowland M, Tozer TN. Clinical pharmacokinetics: Concepts and applications. 3rd ed. Baltimore, MD: Williams & Wilkins; 1995
10. Yamaoka K, Nakagawa T, Uno T. Statistical moments in pharmacokinetics. J Pharmacokinet Biopharm 1978;6:547–58.
11. Weiss M. The relevance of residence time theory to pharmacokinetics. Eur J Clin Pharmacol 1992;43:571–9.
12. Cobelli C, Foster DM, Toffolo G. Tracer kinetics in biomedical research: From data to model. New York: Kluwer Academic/Plenum Publishers; 2000.
13. Berman M, Schonfeld R. Invariants in experimental data on linear kinetics and the formulation of models. J Appl Physics 1956;27:1361–70.
14. Yeh KC, Kwan KC. A comparison of numerical integration algorithms by trapezoidal, Lagrange and spline approximation. J Pharmacokinet Biopharm. 1978;6:79–98.
15. Purves RD. Optimum numerical integration methods for estimation of area-under-the-curve and area-under-the-moment-curve. J Pharmacokinet Biopharm 1992;20:211–26.
16. Gabrielsson J, Weiner D. Pharmacokinetic/pharmacodymanic data analysis: Concepts and applications. 2nd ed. Stockholm: The Swedish Pharmaceutical Press; 1997.
17. Katz D, D'Argenio DZ. Experimental design for estimating integrals by numerical quadrature, with applications to pharmacokinetic studies. Biometrics 1983;39:621–28.
18. User's guide for version 1.5 of WinNonlin. Apex, NC: Scientific Consulting; 1997.
19. Marino AT, DiStefano JJ III, Landaw EM. DIMSUM: An expert system for multiexponential model discrimination. Am J Physiol 1992;262:E546–56.
20. Carson ER, Cobelli C, Finkelstein L. Mathematical modeling of metabolic and endocrine systems. Model formulation, identification and validation. New York: Wiley; 1983.
21. SAAM II User guide. Seattle, WA: SAAM Institute; 1998.
22. DiStefano JJ III, Landaw EM. Multiexponential, multicompartmental and noncompartmental modeling I: Methodological limitations and physiological interpretations. Am J Physiol 1984;246:R651–64.
23. Landaw EM, DiStefano JJ III. Multiexponential, multicompartmental and noncompartmental modeling II. Data analysis and statistical considerations. Am J Physiol 1984;246:R665–76.
24. Belknap SM, Nelson JE, Ruo TI, Frederiksen MC, Worwag EM, Shin S-G, Atkinson AJ Jr. Theophylline distribution kinetics analyzed by reference to simultaneously injected urea and inulin. J Pharmacol Exp Ther 1987;243:963–9.

This page intentionally left blank

CHAPTER

9

Distributed Models of Drug Kinetics

PAUL F. MORRISON
Office of Research Services, National Institutes of Health, Bethesda, Maryland

INTRODUCTION

The hallmark of distributed models of drug kinetics is their ability to describe not only the time dependence of drug distribution in tissue but also its detailed spatial dependence. Previous discussion has mostly revolved around methods meant to characterize the time history of a drug in one or more spatially homogeneous compartments. In these earlier approaches, the end results of pharmacokinetic modeling were time-dependent concentrations, *C(t)*, of the drug or metabolite of interest for each body compartment containing one or more organs or tissue types. In these situations, the agent is also delivered homogeneously and reaches a target organ, either via blood capillaries whose distribution is assumed to be homogeneous throughout the organ, or via infusion directly into that organ, followed by instantaneous mixing with the extravascular space. In contrast, distributed pharmacokinetic models require that neither the tissue architecture nor the delivery source be uniform throughout the organ. The end results of this type of modeling are organ concentration functions (for each drug or metabolite) that depend on two independent variables, one describing spatial dependence and the other describing time dependence — that is, $C(\vec{r},t)$, where $\vec{r}$ is a spatial vector to a given location in an organ. As might be expected, the pharmacokinetic analysis and equations needed to incorporate spatial dependence in this function require a more complicated formalism than that used previously with compartment models.

It is the goal of this chapter to describe the general principles behind distributed models and to provide an introduction to the formalisms employed with them. Emphasis will be placed on the major physiological, metabolic, and physical factors involved. Following this, we will present several examples where distributed kinetic models are necessary. These will include descriptions of drug delivery to the tissues forming the boundaries of the peritoneal cavity following intraperitoneal infusion, to the brain tissues comprising the ventricular walls following intraventricular infusion, and to the parenchymal tissue of the brain following direct interstitial infusion. The chapter will end by identifying still other applications where distributed kinetic models are required.

CENTRAL ISSUES

The central issue with distributed models is to answer the question, "What is the situation that leads to a spatially dependent distribution of drug in a tissue and how is this distribution described quantitatively?"

The situation leading to spatial dependence involves the delivery of an agent to a tissue from a geometrically nonuniform source followed by movement of the agent away from the source along a path on which local clearance or binding mechanisms deplete it, thus causing its concentration to vary with location. Several modes of drug delivery lead to this situation. The most common is the delivery of an agent from a spatially restricted source to a homogeneous tissue. One such example is the slow infusion of drugs directly into the interstitial space of tissues

via implanted needles or catheters. The infused drug concentration decreases due to local clearances as the drug moves out radially from the catheter tip. Another example is the delivery of drugs from solutions bathing the surface of a target organ, in which the drug concentration decreases with increasing penetration depth and residence time in the tissue. Modes of drug delivery in which either the source or target tissue are nonuniform are also encountered. One such example is the intravenous delivery of drugs to tumor tissue. In this case, especially in larger tumors, the distribution of capillaries is often highly heterogeneous and microvasculature is completely absent in the necrotic core. Certain tumors are also characterized by cystic inclusions and channeling through the interstitial space, all of which lead to drug concentrations that are spatially dependent throughout the target tissue. Still another example is the intravenous delivery of very tightly binding proteins (e.g., high-affinity antibody conjugates) to a homogeneous tissue. In this case, the concentration of protein between adjacent capillaries often exhibits a spatially dependent profile, even though the capillary bed itself is homogeneously distributed. Such profiles arise because the tight binding causes the concentration fronts, spreading out from capillaries into the space between them, to be extremely steep; if intravascular concentrations are sufficiently low relative to binding capacity, these fronts may move slowly, thus producing time-dependent spatial concentration profiles (1).

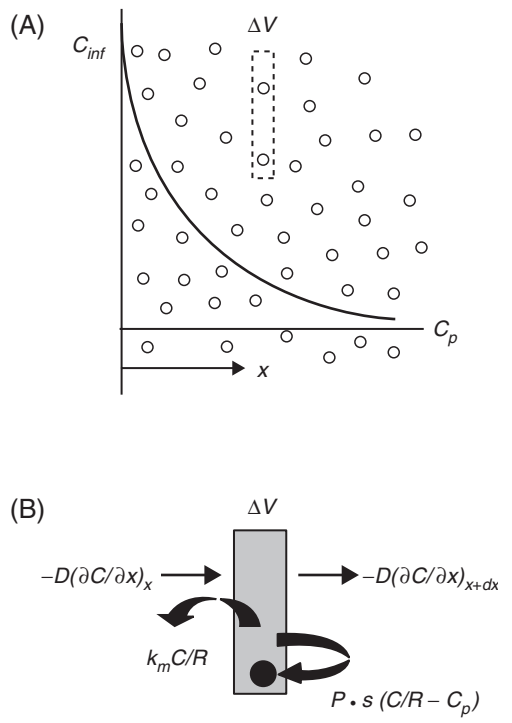

FIGURE 9.1 (A) Representative concentration profile that develops in tissue when delivering a drug across a fluid–tissue interface. Differential volume element ΔV is indicated by the rectangle, and circles denote capillaries; C_{inf} is the concentration of infusate solution in contact with the tissue surface and C_p is the plasma concentration. (B) Elements contributing to the mass balance over ΔV. On the left, $-D(\partial C/\partial x)_x$ is the diffusive (Fickian) flux entering the volume element at x; $-D(\partial C/\partial x)_{x+dx}$ (right) is the outgoing flux at $x + dx$. Other terms denote the metabolic rate constant (k_m) and microvascular permeability coefficient–surface area product ($P \cdot s$).

DRUG MODALITY I: DELIVERY ACROSS A PLANAR–TISSUE INTERFACE

General Principles

The formalisms required to describe these time- and spatially dependent concentration profiles, as introduced in Chapter 8, are essentially microscopic mass balances expressed as partial differential equations. As previously noted, the ordinary differential equations used to describe well-mixed compartments are no longer sufficient, since they only account for the time dependence of concentration. To see how these equations are formulated, and to visualize the underlying physiology and metabolism, consider the specific example of drug delivery from a solution across a planar–tissue interface (e.g., as might occur during continuous intraperitoneal infusion of an agent). Figure 9.1A shows a typical concentration profile that might develop across an interface. The region to the left of the y axis corresponds to the region containing the peritoneal infusate at drug concentration C_{inf}, while the region to the right corresponds to the tissue in contact with the infusate. Small circles depict capillaries, and they are assumed to be homogeneously distributed. In this figure, x is the distance from the fluid–tissue interface. The rectangular box represents a typical differential volume element in the tissue. The transport of drug from the infusate into the tissue in this example is taken to be purely diffusional — that is, no convection (pressure-driven flow) is present. The mathematical model leading to an expression for the concentration profile is a differential mass balance over the volume element ΔV:

$$\underset{\substack{\text{rate of conc}\\ \text{change in } \Delta V}}{\frac{\partial C}{\partial t}} = \underset{\substack{\text{net diffusion}\\ \text{in } \Delta V}}{D\frac{\partial^2 C}{\partial x^2}} - \underset{\substack{\text{metabolism}\\ \text{in } \Delta V}}{\frac{k_m}{R}C} - \underset{\substack{\text{net transport}\\ \text{across}\\ \text{microvasculature}}}{p \cdot S - P \cdot s\left(\frac{C}{R} - C_p\right)} \tag{9.1}$$

This equation says that the change in total drug concentration within ΔV over a small increment of time (left-hand term; see Figure 9.1B) is equal to the sum of all the mass fluxes generating this change, namely, the net change in mass due to diffusion into and out of ΔV (first right-hand term) less mass loss due to metabolism within ΔV (second right-hand term) less net mass loss across the microvasculature within ΔV (third right-hand term). In this equation, $C = C(x,t)$ is the tissue concentration of bound plus free drug, R is a constant of proportionality that relates C to the free extracellular concentration of drug C_e, that is,

$$C = RC_e \tag{9.2}$$

k_m/R is the metabolic rate constant,[1] $P \cdot s$ is the product of the permeability coefficient and surface area per volume of tissue accounting for passive movement across the microvasculature, and C_p is the free plasma concentration of drug. The parameter s is analogous to S in Chapter 3 that refers to the surface area of an entire capillary bed. In Equation 9.1, D is the apparent tissue diffusion constant and is equal to $\phi_e\ D_e/\ R$, where ϕ_e is the extracellular volume fraction of the tissue and D_e is the diffusion constant within just the extracellular space. For nonbinding substances distributed solely in the extracellular space of a tissue, $R = \phi_e$ and $D = D_e$. For nonbinding substances that partition equally into the intracellular and extracellular spaces, $R = 1$ and $D = \phi_e D_e$.

Formulation of the model is completed by the specification of initial and boundary conditions. The initial condition, the state of the system just before exposing the interface to drug (the beginning of the intraperitoneal infusion in our example), is that the tissue concentration is everywhere zero, that is, $C(x,0) = 0$. At all times at the fluid–tissue interface, the extracellular concentration equals the infusate concentration; that is,

$$C_e(0,t) = C(0,t)\ /R = C_{inf}$$

where C_{inf} is the constant peritoneal infusate concentration. Far from the interface, the concentration of drug $[C(\infty,t)]$ is determined by the tissue's transport balance with the plasma. If the plasma concentration is zero, then $C(\infty,t) = 0$.

With these initial and boundary conditions, the solution to Equation 9.1 is (3)

$$\frac{C(x,\,t)}{R\,C_{inf}} = \frac{1}{2}\,exp\left[-x\sqrt{k/D}\right]\ erfc\left[\frac{x}{\sqrt{4D\,t}} - \sqrt{k\,t}\right] + \frac{1}{2}\,exp\left[x\sqrt{k/D}\right]\ erfc\left[\frac{x}{\sqrt{4D\,t}} + \sqrt{k\,t}\right] \tag{9.3}$$

where $k = (k_m + P \cdot s)/R$ and *erfc* is the complementary error function (available in standard spreadsheet programs). If no reaction or microvascular loss is present, then this solution simplifies to

$$\frac{C(x,\,t)}{R\ C_{inf}} = erfc\left[\frac{x}{\sqrt{4Dt}}\right] \tag{9.4}$$

When reaction or microvascular loss is present, the steady-state limit of Equation 9.3 is just

$$\frac{C(x)}{R\ C_{inf}} = exp\left[-x\sqrt{k/D}\right] \tag{9.5}$$

In the special steady-state case where the plasma concentration is constant *but not zero* (e.g., as may happen when a large intraperitoneal infusion delivers sufficient mass to increase the plasma concentration to a level consistent with a mass balance between intraperitoneal delivery and whole-body clearance), a generalized form of Equation 9.5 applies — that is,

$$\frac{\dfrac{C(x)}{R} - \dfrac{P \cdot s}{P \cdot s + k_m}\ C_p}{C_{inf} - \dfrac{P \cdot s}{P \cdot s + k_m}\ C_p} = exp\left[-x\sqrt{k/D}\right] \tag{9.5'}$$

where C_p is now the constant plasma concentration.

Equation 9.4 provides a relationship between time and the distance at which a particular concentration is achieved. When clearance rates are small relative to diffusion rates, it states that the distance from the surface (penetration depth) at which a particular concentration C is achieved advances as the square root of time. In other words, to double the penetration of a compound, the exposure time must quadruple. Equation 9.5 states that, given sufficient time and negligible plasma concentration, most compounds will develop a semilogarithmic concentration profile whose slope is determined by the ratio of the clearance rate to the diffusion constant. Note also that the distance over which the concentration decreases to

[1] When drug exchanges rapidly between the intracellular (ICS) and extracellular (ECS) spaces, and also equilibrates rapidly between bound and free forms, it can be shown (2) that $R = \phi_e(1 + K_eB_e) + (1 - \phi_e)(1 + K_iB_i)K_\pi$. Here ϕ_e is the extracellular volume fraction, K_e and K_i are affinity constants for binding, and B_e and B_i are binding capacities in the ECS and ICS, respectively. K_π is the equilibrium ratio of the free intracellular concentration to the free extracellular concentration ($K_\pi = 0$ for substances confined solely to the ECS). Similarly, $k_m = \phi_e k_e + (1 - \phi_e)k_i K_\pi$, where k_e and k_i are fundamental rate constants describing the rates of metabolism in the individual ECS and ICS regions.

one-half its surface value, defined as its penetration distance Γ, is derivable from Equation 9.5 as

$$\Gamma = (\ln 2)/\sqrt{k/D} \tag{9.6}$$

while the approximate time to penetrate this distance by diffusion is

$$t_\Gamma = \Gamma^2/D \tag{9.6'}$$

The results of Equations 9.5 and 9.6 are very useful and we will refer to them repeatedly. One implication of these results is that drug can be delivered to a tissue layer near the exposed surface of an organ, but drug penetration depth depends strongly on the rate of metabolism of the agent. Another is that the delivery of non- or slowly metabolized substances across surfaces for purposes of systemic drug administration is dominated by distributed microvascular uptake in the tissue layer underlying the surface. In the particular case of intraperitoneal administration, the barrier to uptake of drug into the circulation is thus the resistance to transfer across distributed capillary walls and not, as assumed in the early literature, the resistance to transfer across the thin peritoneal membrane, which is relatively permeable.

Distributed pharmacokinetics is characterized not only by spatially dependent concentration profiles but also by dose-response relationships that become spatially dependent. For example, biological responses such as cell kill are often quantified as functions of area under the concentration-vs.-time curve (*AUC*). In compartment models, response is frequently correlated with the area under the plasma-concentration-vs.-time curve, where

$$AUC = \int_0^\infty C_p(t)\, dt \tag{9.7}$$

or, alternatively, with the *AUC* formed by integration over the tissue concentration $C(t)$. With distributed pharmacokinetics, however, the response within each local region of the tissue will vary according to its local exposure to drug. The appropriate correlate of response in this case is thus a spatially dependent *AUC* formed over the local tissue concentration — that is

$$AUC\,(x) = \int_0^\infty C(x, t)\, dt \tag{9.8}$$

In distributed pharmacokinetics, threshold models, in which a biological response is associated with the increase of concentration above a threshold value, are likewise dependent on spatial location.

The use of distributed pharmacokinetic models to estimate expected concentration profiles associated with different modes of drug delivery requires that various input parameters be available. The most commonly required parameters, as seen in Equation 9.1, are diffusion coefficients, reaction rate constants, and capillary permeabilities. As will be encountered later, hydraulic conductivities are also needed when pressure-driven rather than diffusion-driven flows are involved. Diffusion coefficients (i.e., the D_e parameter described previously) can be measured experimentally or can be estimated by extrapolation from known values for reference substances. Diffusion constants in tissue are known to be proportional to their aqueous value, which in turn is approximately proportional to a power of the molecular weight. Hence,

$$D_e = \lambda^2 \alpha D^{37°C}_{aqueous} \propto \lambda^2 \alpha (MW)^{-0.50} \tag{9.9}$$

in which λ accounts for the tortuosity of the diffusion path in tissue, α accounts for any additional diffusional drag of the interstitial matrix over that of pure water, and MW is the molecular weight of the diffusing species. The 0.50 exponent applies to most small molecular weight species. The diffusion constant for a substance of arbitrary molecular weight can be obtained from the ratio of Equation 9.9 for the desired substance to that for a reference substance — that is, from

$$\left(\frac{D_e}{D_{e,ref}}\right) = \left(\frac{MW_{ref}}{MW}\right)^{0.50} \tag{9.10}$$

Reference values are available for many substances, but the one available for a wide variety of tissues is sucrose (4). In the macromolecular range (> 3 kDa), albumin values are available in the literature and the exponent is similar.

Capillary permeability coefficient–surface area product values ($P{\cdot}s$) are also available for hydrophilic agents from molecular weight scaling of reference values (5, 6). In the small molecular weight range shown in Figure 3.4, a relationship very similar to Equation 9.10 is valid:

$$\left(\frac{P \cdot s}{P \cdot s_{ref}}\right) = \left(\frac{MW_{ref}}{MW}\right)^{0.63} \tag{9.11}$$

The similarity of the diffusion and permeability scaling relationships leads to the prediction that, for slowly metabolized substances, the *steady-state* concentration profiles that develop in a tissue following diffusion across an interface (as in Figure 9.1) are nearly independent of molecular weight. This follows

from Equation 9.5, since nearly identical molecular weight scaling factors for k (proportional to $P{\cdot}s$ in this case) and D appear in both the numerator and denominator of the k/D argument. Hence, one would predict that the penetration depths of inulin (MW 5000) and urea (MW 60) would be similar within the interstitial fluid space.

Reaction rate parameters required for the distributed pharmacokinetic model generally come from independent experimental data. One source is the analysis of rates of metabolism of cells grown in culture. However, the parameters from this source are potentially subject to considerable artifact, since cofactors and cellular interactions may be absent *in vitro* that are present *in vivo*. Published enzyme activities are a second source, but these are even more subject to artifact. A third source is previous compartmental analysis of a tissue dosed uniformly by intravenous infusion. If a compartment in such a study can be closely identified with the organ or tissue later considered in distributed pharmacokinetic analysis, then its compartmental clearance constant can often be used to derive the required metabolic rate constant.

Case Study 1: Intraperitoneal Administration of Chemotherapeutic Agents for Treatment of Ovarian Cancer

Some aspects of this mode of delivery have already been introduced as part of our discussion of the general principles for transfer across a planar interface, but now the focus will narrow to two specific chemical agents and the use of one of them in the treatment of ovarian cancer.

The goal of ovarian cancer chemotherapy is to achieve sufficient penetration of the surfaces of tumor nodules to allow effective treatment. These nodules lie on the serosal surfaces of the peritoneum, are not invasive, and are not associated with high probabilities of metastasis. When the cancer is diagnosed early, or when the larger nodules are removed surgically in more advanced disease, the residual nodules in 73% of the cases have maximum diameters of <5 mm (7). Collectively, these characteristics suggest that, if complete irrigation of the serosal surfaces can be achieved, ovarian tumors may be good candidates for treatment by peritoneal infusion.

The present drug of choice for this purpose is cisplatin [*cis*-diamminedichloroplatinum (II)], or its analog carboplatin. As will be discussed in Chapter 30, early compartmental models predicted a substantial pharmacokinetic advantage of intraperitoneal over intravenous delivery (8). A later Phase III trial (7) confirmed that a comparative survival advantage could be achieved with intraperitoneal administration of cisplatin.

The effectiveness of cisplatin depends on its ability to penetrate target tissue. Therefore, we need to estimate its penetration depth from a distributed model such as that represented by Equation 9.1. However, this is difficult to do with ovarian tumors because the permeabilities and reaction rates are not available. Hence, a first estimate is made for penetration of normal peritoneal cavity tissues by ethylenediaminetetraacetic acid (EDTA), a molecule of molecular weight similar to that of cisplatin. The steady-state concentration profiles of EDTA should resemble those of cisplatin in normal peritoneal tissues because both compounds are cleared primarily by permeation through the fenestrated capillaries in these tissues, and the small molecular weight-related differences in $P \cdot s$ and D should cancel out in Equations 9.5 and 9.5′. By first focusing on EDTA, experimental data also become available for assessing the ability of the distributed model to account for the observed spatial dependent of concentration.

EDTA concentration profiles were determined experimentally from data such as those shown in Figure 9.2 (9). In these experiments, a [^{14}C]EDTA solution was infused into the peritoneal cavity of a rat. After 1 hour of exposure (sufficient time to establish steady-state profiles in the tissues), the animal was sacrificed, frozen, and sectioned for autoradiography. The upper panel of Figure 9.2 shows a transverse section across the rat in which a cross section of the large intestine is identified. This cross section is magnified in the lower panel and a grid is shown from which the concentration profile was estimated by quantitative autoradiography. Concentration profiles for most of the peritoneal viscera were obtained in this manner, and the aggregated profiles for the stomach, small intestine, and large intestine are plotted (circles) in Figure 9.3. The concentrations in this figure are all expressed relative to the infusate concentration. Because the mass of EDTA that was infused was sufficiently large to distribute throughout the entire body of the rat, the plasma concentration at the end of the experiment could not be neglected. It is shown as the single data point labeled "Plasma," and is expressed as the ratio of the actual plasma concentration to the infusate concentration. Because EDTA distributes only in the extracellular space, the deep tissue concentration only approaches the "Plasma" concentration reduced by the extracellular volume fraction ϕ_e.

The steady-state formalism of Equation 9.5′, which includes the effects of a constant plasma concentration, should describe these data. Noting from EDTA's distribution into the extracellular space

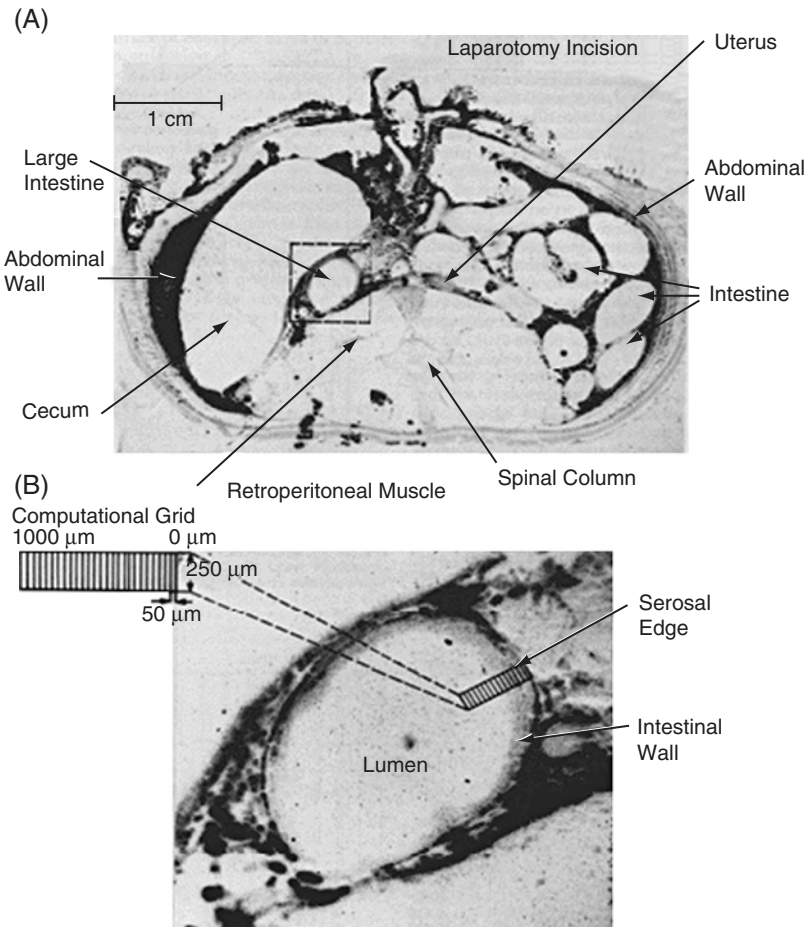

FIGURE 9.2 (A) Autoradiogram of a cross section of peritoneal cavity from a study of transport from the peritoneal cavity to plasma. (B) Close-up of the outlined area (box) in (A). (Reproduced from Flessner MF *et al.* Am J Physiol 1985;248:F425–35.)

that $R = \phi_e$ and from its negligible metabolism that $P \cdot s/(P \cdot s + k_m) \rightarrow 1$, Equation 9.5′ can be simplified to

$$\frac{C(x) - \phi_e C_p}{\phi_e C_{inf} - \phi_e C_p} = exp\Big[-x\sqrt{k/D}\Big] \qquad (9.12)$$

When this equation is fit to the data of Figure 9.3 using ϕ_e and $\sqrt{k/D}$ as fitting parameters, the solid line results. The value of ϕ_e so obtained is reasonable (an extracellular volume fraction of 0.27), and the permeability derived from the $\sqrt{k/D}$ term $\left[= \sqrt{P \cdot s/(\phi_e D_e)}\right]$ agrees with that expected from molecular weight correlations. The theory largely accounts for the data, although it tends to overestimate the concentrations at the deepest penetration, perhaps because vascularity increases as one passes toward the luminal side of the organs. However, the fit is sufficiently good to conclude that the theory has captured most of the relevant physiology and that it can be used to account for or, given availability of parameters, to predict the observed results.

As a predictor of the concentration of cisplatin in normal peritoneal tissues, these data indicate a steady-state penetration depth (distance to half the surface layer concentration) of about 0.1 mm (100 μm). If this distance applied to tumor tissue, penetration even to three or four times this depth would make it difficult to effectively dose tumor nodules of 1- to 2-mm diameter. Fortunately, crude data are available from proton-induced X-ray emission studies of cisplatin transport into intraperitoneal rat tumors, indicating that the penetration into tumor is deeper and is in the range of 1–1.5 mm (10). Such distances are obtained from Equation 9.5 or 9.5′ only if k is much smaller than in normal peritoneal tissues — that is, theory suggests that low permeability coefficient–surface area products in tumor (e.g., due to a developing microvasculature and a lower capillary density) may be responsible for the deeper tumor penetration.

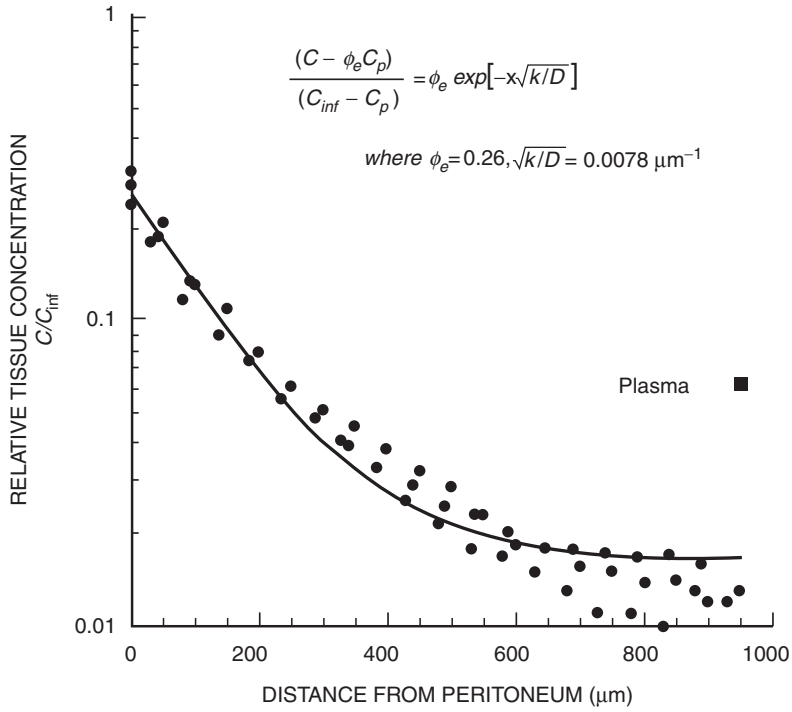

FIGURE 9.3 Profile of [^{14}C]EDTA concentrations (expressed relative to C_{inf}) in gastrointestinal tissues following intraperitoneal infusion. The equation shown in the graph was used to fit the experimental tissue (●) and plasma (■) concentration data, resulting in the solid line curve.

Case Study 2: Intraventricular Administration of Cytosine Arabinoside for the Treatment of JC Virus Infection in Patients with Progressive Multifocal Leukoencephalopathy

Another example of a situation in which distributed pharmacokinetics plays an important role is in the infusion of drug solutions into the lateral ventricles or cisternal space of the brain. Drugs that have been delivered this way include chemotherapeutic agents for the treatment of tumors; antibacterial, antifungal, and antiviral agents for the treatment of infection; and neurotrophic factors for the treatment of neurodegenerative disease.

The principal reason for using this route of administration is to deliver drugs behind the blood–brain barrier (BBB) by taking advantage of the fact that no equivalent barrier exists at the interface between the ventricular fluid space and the interstitial space of the brain parenchyma. That the BBB is often a major problem to be overcome is suggested by the image in Figure 9.4. This autoradiogram shows a longitudinal cross section of a rat that was sacrificed 5 minutes after an intravenous injection of [^{14}C]histamine (11). The compound has distributed throughout most organs of the body, but the brain and spinal cord remain white in this image, indicating no significant delivery of histamine to the central nervous system. With intraventricular delivery of agents, high brain interstitial fluid levels can be achieved, since the BBB now tends to block microvascular efflux of the drug and trap it in the interstitial space, only allowing the drug to be slowly cleared to the plasma and systemic tissues via bulk flow of cerebrospinal fluid through the arachnoid villi.

This approach has been explored in attempts to treat progressive multifocal leukoencephalopathy, a rapidly fatal disease caused by the JC virus and characterized by regions of central nervous system demyelination and markedly altered neuroglia. The virus is known to be sensitive *in vitro* to the action of cytosine arabinoside (ARA-C) concentrations of 40 μ*M* (10 μg/mL) or more (12). Because the agent crosses the blood–brain barrier slowly, Hall *et al.* (13) designed a study to test whether intraventricular/intrathecal administration of ARA-C could successfully treat JC virus in humans. ARA-C was administered as a bolus into the cerebrospinal fluid (CSF) space at the initial rate of 50 mg every 7 days. This ARA-C regimen was found to be

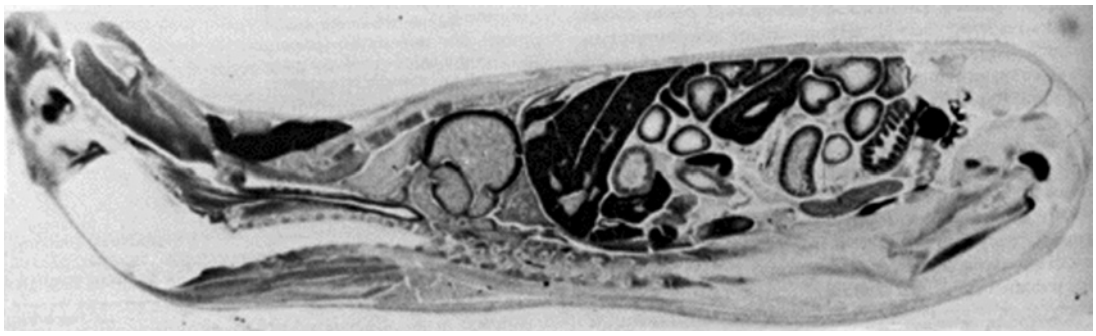

FIGURE 9.4 Autoradiogram showing a sagittal cross section of a rat 5 minutes after an intravenous injection of [^{14}C]histamine. (Reproduced with permission from Pardridge WM *et al.* Ann Intern Med 1986;105:82–95.)

ineffective. However, Zimm *et al.* (14) had previously shown that, after a 30-mg bolus intraventricular injection of ARA-C, CSF concentrations of this drug have a terminal elimination half-life of 3.4 hours and decrease to less than 40 μ*M* in less than 15 hours. Thus, for much of the 7-day dosing period, even the surface concentrations of this drug would not have been expected to exceed the lowest ARA-C concentration found to have antiviral activity *in vitro*. Therefore, choice of the delivery regimen used in the clinical trial probably provided an inadequate test of the potential efficacy of this therapeutic approach.

Groothuis *et al.* (15) used sucrose, an unmetabolized marker compound that has very low capillary permeability, to initially evaluate the therapeutic feasibility of administering chemotherapy by the intraventricular route. Sucrose was infused by osmotic minipump into the lateral ventricle of a rat for 7 days, yielding the concentration profile exhibited in Figure 9.5A, a profile well fit by theoretical Equation 9.5 using published diffusion and permeation constants for sucrose (16). In this experiment, the penetration distances to one-half and one-tenth the surface concentration were 0.9 and 3 mm, respectively. In a subsequent study, Groothuis *et al.* (17) continuously infused ARA-C into the ventricles of rat brain over 7 days. They found that even with continuous administration of ARA-C, tissue concentrations dropped to one-half the surface concentration at a penetration distance of 0.4 mm and to about one-tenth the surface concentration at a penetration distance of 1.0 mm (Figure 9.5B). These distances are of the same order of magnitude but are somewhat less than those achieved with intraventricular delivery of sucrose.

This indicates (see Equation 9.5) that ARA-C is cleared more rapidly than is sucrose, consistent with the known presence of nucleoside transporters in the microvascular walls of the brain as well as with metabolic deamination of ARA-C to uracil arabinoside (14). It is not such a rapid rate of clearance, however, that millimeter penetration depths cannot be achieved in accessible time frames. Indeed, evaluation of Equation 9.6′ (assuming equal partitioning of drug between intracellular and extracellular spaces so that $D = \phi_e D_e$) indicates that 1-mm penetration depths can be achieved in roughly 3 hours. This suggests that a 40-μ*M* effective concentration could have been maintained at this depth throughout the multiple-week exposures of the study conducted by Hall *et al.*, provided the surface concentration was constantly maintained near 400 μ*M* (see Figure 9.5B). In turn, if this concentration were to exist throughout the 140-ml CSF volume (so that total mass in the CSF = 13.6 mg), the 3.4-hour half-time for clearance of the CSF implies that the concentration could only be maintained if the cleared mass were constantly resupplied by infusion at the rate of (13.6/2 mg/3.4 hr) = 2 mg/hr or, equivalently, 336 mg/week. This continuous infusion rate is nearly sevenfold the 50-mg/week bolus rate employed in the Hall *et al.* study. Thus, our example suggests that further trials employing more optimized drug delivery may be indicated before ARA-C can be ruled out definitively as a potential therapeutic agent for patients with multifocal leukoencephalopathy.

Differences between the Delivery of Small Molecules and Macromolecules across a Planar Interface

Previous discussion has indicated that unmetabolized small molecular weight, hydrophilic molecules ($MW < 500$) typically penetrate tissues to (half-surface-concentration) depths that range at steady state from 0.1 to 1 mm. The depth is on the order of 0.1 mm for most tissues of the body, as we have seen in the case

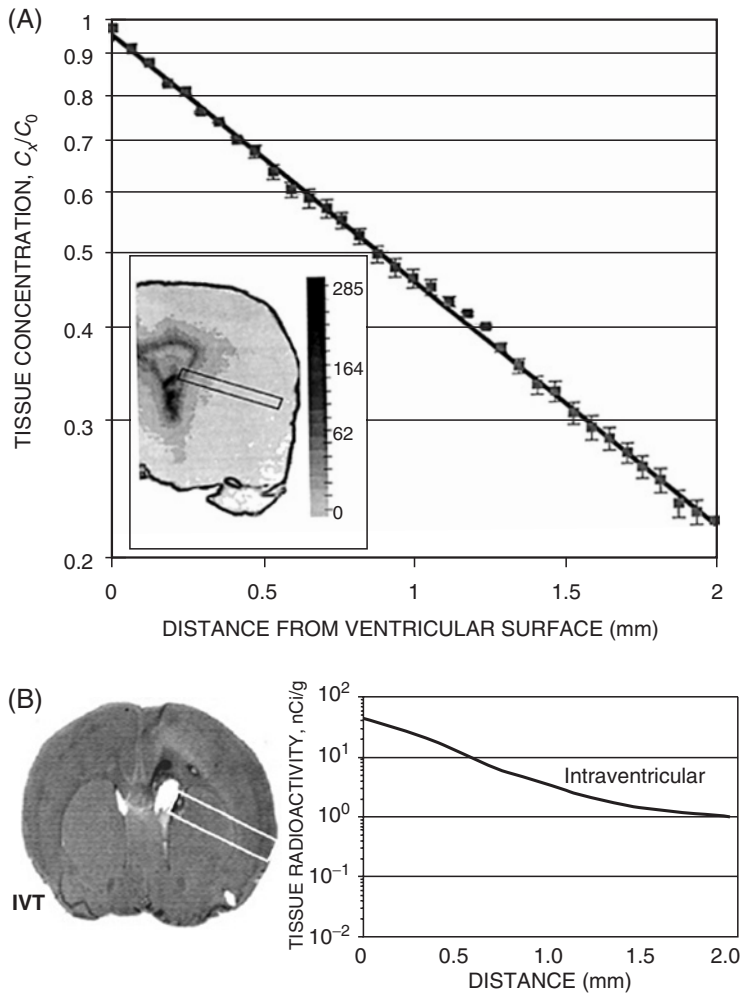

FIGURE 9.5 (A) Concentration profile of [^{14}C]sucrose in rat caudate following intraventricular infusion to steady state (expressed relative to average tissue concentration at tissue surface C_0). Inset shows the autoradiogram of a coronal brain section and the rectangular area used to generate the concentration profile. (B) The concentration profile in brain tissue following 7-day intraventricular (IVT) delivery of labeled cytosine arabinoside to rat brain. The tissue radioactivity data were collected from the rectangular area shown at left. (A) reproduced with permission from Groothuis DR *et al.* J Neurosurg 1999;90:321–31; (B), modified from Groothuis DR *et al.* Brain Res 2000;856:281–90.]

of EDTA's penetration of normal peritoneal tissues. The depth increases 10-fold to 1 mm for tissues characterized by a tight microvascular endothelium, for example, the brain or spinal cord, as a consequence of nearly a 100-fold lower capillary permeability of those barriers. The times for unmetabolized and unbound small molecular weight species to achieve steady-state concentration profiles in tissues are relatively short and tend not to exceed the 4-hour value of sucrose in brain. When metabolism is present, and binding remains negligible, the time to steady state will shorten inversely with an increase in the rate of metabolism and the penetration depth will decrease well below the millimeter value. If linear binding is present, it has no effect on the penetration depth at steady state but proportionally increases the time to attain this steady state. The depth and times can be calculated from Equations 9.6 and 9.6′.

What sort of penetration depth is expected for macromolecules? As with small molecules, the depth is again determined by Equation 9.6, but some differences emerge (6). Were both k and D

for nonmetabolized macromolecules (for which $k = P \cdot s/R$) given as mere extensions of the molecular weight functions for the smaller compounds, the penetration depth would remain relatively independent of molecular weight. However, unmetabolized macromolecules ($MW > 10{,}000$) have been observed to penetrate more deeply at steady state than do their nonmetabolized small molecular weight counterparts such as sucrose (on the order of 2- to 3-fold deeper in visceral or muscle tissues). The primary reason is that capillary $P \cdot s$ values for macromolecules are relatively smaller. $P \cdot s$ for macromolecules is related to molecular weight by a power formula of the form

$$P \cdot s = A(MW)^{-0.6} \tag{9.13}$$

where the exponent is similar to that for small molecules, but A is nearly 10-fold lower (6). Since the penetration depth γ is inversely proportional to the square root of this coefficient, the depth for unmetabolized macromolecules will be about 3-fold larger than for small unmetabolized compounds. As with small molecules, steady-state penetration depths are on the order of a few millimeters at best.

One other important difference exists between small and macromolecular weight molecules: the time required to achieve steady-state concentration profiles across an interface. Maximum penetration is obtained by unmetabolized molecules and the time to steady state is largely controlled by the rate of diffusion through the tissue. For sucrose in brain, this time is approximately 4 hours. However, for a macromolecule of 67 kDa, the diffusion constant decreases 19-fold (4, 18), leading to a corresponding 19-fold increase in the time required to achieve the steady-state profile (cf. Equation 9.4). The 4 hours required for sucrose thus increases to 3 days or more. For both small molecules and macromolecules, these times will greatly decrease as metabolism begins to play a greater role, but only at the cost of a much reduced penetration depth.

Examples of the effects of binding and rapid reaction with macromolecules are demonstrated in Figures 9.6 and 9.7. Figure 9.6 shows the distribution of ^{125}I-labeled brain-derived neurotrophic factor (BDNF; $MW \sim 17{,}000$) following 20 hours of intraventricular infusion into the brain of a rat (19). The penetration depth is very shallow (~ 0.2 mm), far less than the few-millimeter distance theoretically obtainable from an unmetabolized and unbound molecule of this size. Part of the reason for the shallow penetration is that the infusion time is, at most, a third of the time required for unmetabolized and unbound molecules to reach this theoretical distance. An even more important factor is that BDNF receptors, whose

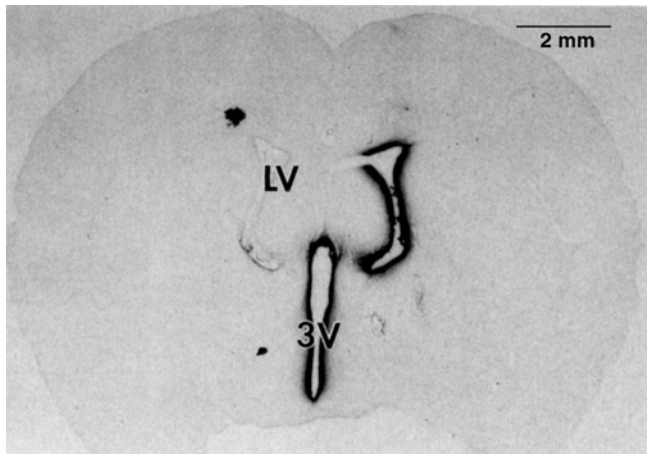

FIGURE 9.6 Autoradiogram showing the distribution of ^{125}I-labeled BDNF in the vicinity of the intraventricular foramen in rat brain following a 20-hour intraventricular infusion. (Reproduced with permission from Yan Q *et al.* Exp Neurol 1994;27:23–36.)

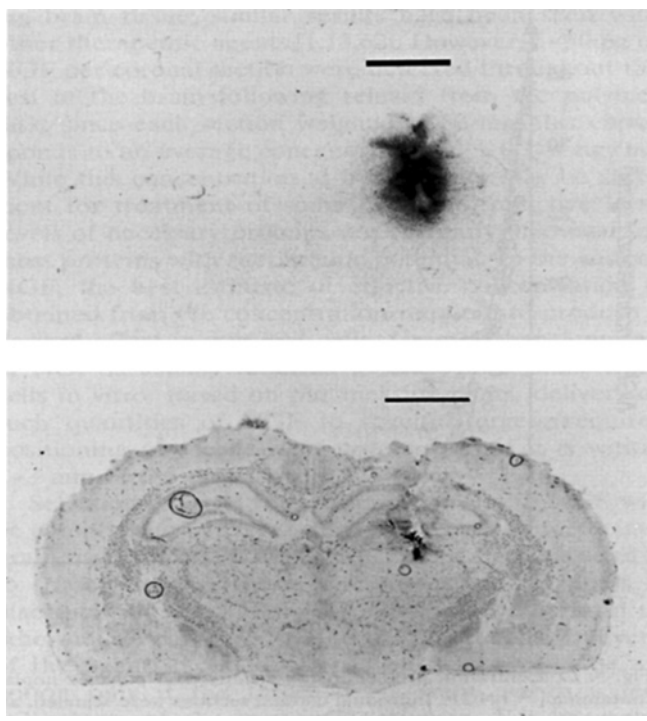

FIGURE 9.7 Autoradiogram (*top*) and unstained photograph (*bottom*) obtained from a coronal section of rat brain 48 hours after implantation of a ^{125}I-labeled NGF-loaded polymer. Bars = 2.5 mm. (Reproduced with permission from Krewson CE *et al.* Brain Res 1995;680:196–206.)

mRNA (trkB) is known from *in situ* hybridization analyses to be present on neurons and glia, bind BDNF and further retard progress to steady state (19). Figure 9.7 shows the distribution of ^{125}I-labeled nerve growth factor (NGF; $MW \sim 14{,}000$) 48 hours after the implantation of a poly(ethylene-covinyl acetate)

disk (2-mm diameter × 0.8-mm thickness) containing this neurotrophic factor (20). The upper panel shows the location of radioactivity in a coronal brain section, including the 0.8-mm-wide contribution from the disk in this view. In this image, the maximum observable extent of diffusion out from the disk is about 0.4 mm on either side of the disk, corresponding to a penetration depth of 0.25 mm (20). This is a steady-state penetration depth since the same distribution shown in Figure 9.7 is also observed after 7 days of infusion. Therefore, the shallow penetration of this protein is due neither to slow diffusion nor to the presence of NGF receptors, since none are present in this region (20), but rather is attributable to degradative metabolic processes that result in an NGF half-life of approximately 30 minutes.

DRUG MODALITY II: DELIVERY FROM A POINT SOURCE — DIRECT INTERSTITIAL INFUSION

General Principles

As has been seen with the examples of intraperitoneal and intraventricular infusion, tissue penetration depths of only a few millimeters are generally achievable by diffusive transport across an interface. If the goal of therapy is to dose entire tissue masses such as glioblastomas or structures of the basal ganglia, millimeter penetrations are insufficient and another mode of drug delivery is required. A mode capable of achieving multicentimeter instead of multimillimeter depths is direct interstitial infusion (21, 22). It is the description of the distributed pharmacokinetics of this modality that is next examined.

In direct interstitial infusion, a narrow-gauge cannula is inserted into tissue and infusate is pumped through it directly into the interstitial space of a target tissue. Figure 9.8, for example, depicts a 32-gauge cannula placed stereotactically into the center of the caudate nucleus of a rat. This type of drug delivery uses volumetric flow rates ranging from 0.01 to 4.0 μL/min. The lower end of this range corresponds to flows provided by osmotic minipumps while the upper end corresponds to flows provided by microinjection (syringe) pumps. For small molecular weight compounds, the lowest flow rates allow all transport to occur by diffusion, even near the tip of the cannula. At higher flow rates, sufficiently high fluid velocities are generated so that pressure-driven bulk flow processes (convection) dominate most transport for both small molecules and macromolecules. Delivery of mass to a homogeneous tissue thus involves the outward radial flow of infused drug solution from the cannula tip, and the concentration of drug changes along that radial path as the drug is progressively exposed to clearance processes. A distributed model is required to quantitatively describe this spatially dependent concentration profile.

Low-Flow Microinfusion Case

The simplest model describing this mode of drug delivery applies to the low volumetric flow range for small molecules — for example, cisplatin delivered at 0.9 μL/hr (23). The model is a differential mass balance for a typical shell volume surrounding the cannula tip. Deriving it in the same fashion as in Equation 9.1, except taking the spherical geometry of the distribution into account, it is

$$\underset{\substack{\text{rate of conc}\\ \text{change in } \Delta V}}{\frac{\partial C}{\partial t}} = \underset{\substack{\text{net diffusion}\\ \text{in } \Delta V}}{D\,\frac{1}{r^2}\,\frac{\partial}{\partial r} r^2 \frac{\partial C}{\partial r}} - \underset{\substack{\text{metabolism}\\ \text{in } \Delta V}}{\frac{k_m}{R}\,C} - \underset{\substack{\text{net transport}\\ \text{across microvasculature}}}{P \cdot s \left(\frac{C}{R} - C_p\right)} \tag{9.14}$$

All parameters have the same definitions as used previously. The initial condition is that drug concentration in the tissue is everywhere zero. The boundary conditions are, first, that the drug concentration remains zero at all times far from the cannula tip and, second, that the mass outflow from the cannula be equal to the diffusive flux through the tissue at the cannula tip, that is, that

$$C(\infty, t) = 0 \quad \text{and} \quad q\,C_{inf} = -4\pi r_o^2 D \left.\frac{\partial C}{\partial r}\right|_{r_o} \tag{9.15}$$

where q is the volumetric flow rate, C_{inf} is the infusate concentration, and r_o is the radius of the cannula. The steady-state solution to this model is

$$C(r) = \frac{q\,C_{inf}}{4\pi D r}\ exp\left(-r\sqrt{k/D}\right) \tag{9.16}$$

where, again, $k = (k_m + P \cdot s)/R$ and $D = \phi_e D_e/R$. For cisplatin, $R = 1$. Equation 9.16 is the radial concentration profile of drug about a cannula tip in homogeneous tissue. It is similar in form to Equation 9.5, including the same parameter dependence of the argument of the exponential, but differs by an extra r factor in the denominator that causes the concentration to drop off faster with distance. For cisplatin, the

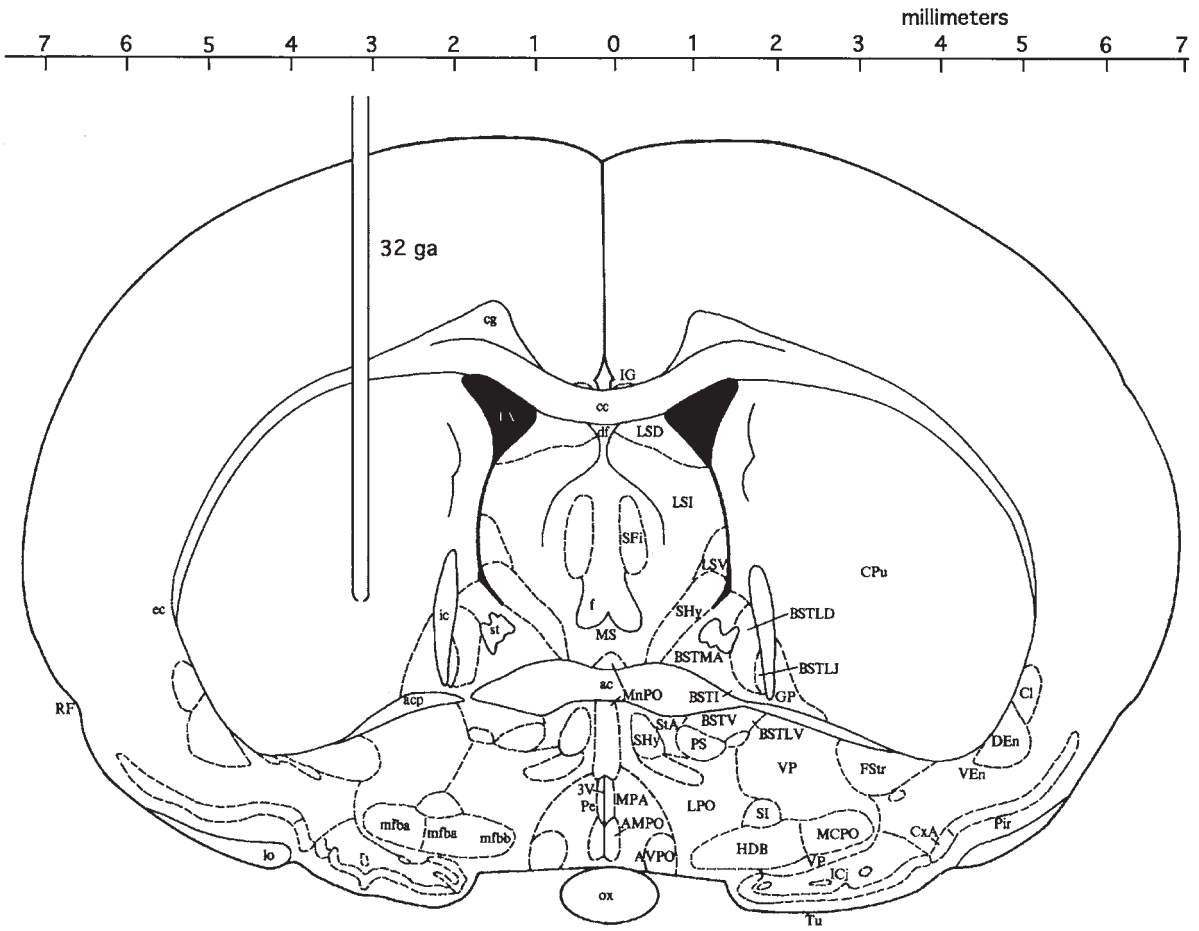

FIGURE 9.8 Schematic drawing of direct interstitial infusion showing a 32-gauge infusion cannula placed in the center of the rat caudate nucleus–putamen.

time to achieve this steady-state profile 4 mm distant from the cannula tip is about 3 hours. Figure 9.9 shows the measured steady-state concentration profile of cisplatin in normal rat brain achieved after 160 hours of infusion at 0.9 μL/hr. The solid line is the theoretical fit to the data showing that the *r*-damped exponential of Equation 9.16 accounts well for the data. The penetration depth is on the order of 0.6 mm, severalfold deeper than observed with EDTA penetration across the peritoneal interface because of the much lower brain capillary permeability, but generally of the same order of magnitude.

High-Flow Microinfusion Case

The submillimeter penetration distances found to hold for transport across tissue interfaces or for low-flow microinfusion are insufficiently large to provide effective dosing for many targets. For example, some brain structures, such as the human putamen or cortex, have centimeter-scale dimensions. Likewise, highly invasive glioblastoma multiforma tumors of the brain are characterized by protrusions of tumor that extend for centimeter distances along vascular and fiber pathways. This mismatch of low-flow microinfusion penetration distance with target dimension provides a rationale for increasing the volumetric infusion rate with the intent of increasing the velocity with which materials move through the interstitium. This retards their exposure to capillary or metabolic clearance mechanisms and increases their penetration depth. In the next few paragraphs, simple estimators of the concentration profiles and distribution volumes that result from high-flow microinfusion are developed for brain from an appropriate distributed drug model (21).

At its core, the distributed model for high-flow microinfusion is once again a differential mass balance for the drug solute in the infusate. However, because the pumps used in this method generate relatively high fluid velocities, transport of molecules

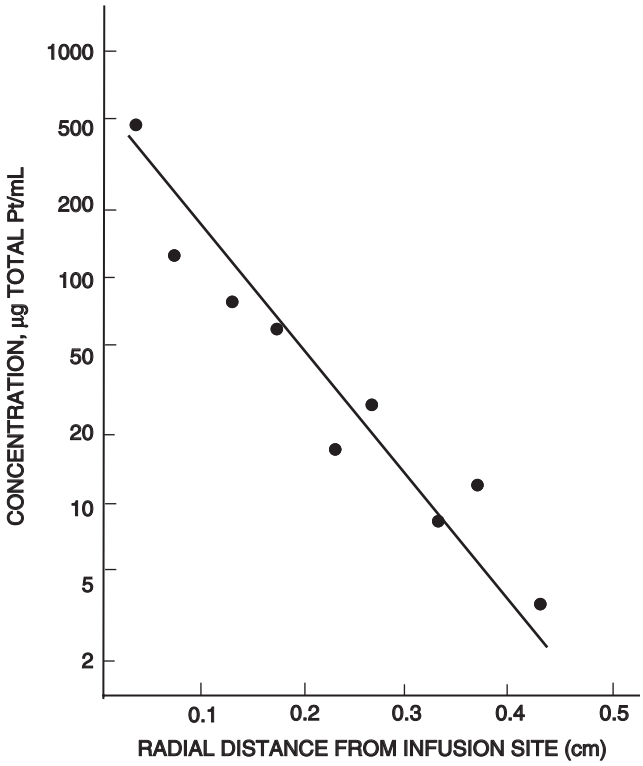

FIGURE 9.9 Concentration profile of cisplatin in rat brain following slow infusion at 0.9 µL/hr for 160 hours. The solid line is the fit of Equation 9.16 to data (●). (Reproduced from Morrison PF, Dedrick RL. J Pharm Sci 1986;75:120–9.)

through tissue is not just diffusive but also convective (i.e., pressure driven). This necessitates additional model equations so that these velocities may be computed. Once again, because of the spatial and time dependence involved, the models take the form of partial differential equations. If the tissue is recognized as a porous medium, then the velocities may be computed from Darcy's Law, which states that the fluid velocity is proportional to the local pressure gradient

$$v = -\kappa \frac{\partial p}{\partial r} \tag{9.17}$$

where κ is defined as the hydraulic conductivity, v is the average fluid velocity in the tissue at position r, and p is the hydrostatic pressure. This equation can be combined with another describing the differential mass balance of water in the brain — that is, the continuity equation,

$$\frac{\partial \rho}{\partial t} = \frac{-1}{r^2} \frac{\partial}{\partial r} r^2 \rho v + \Sigma$$

in which ρ is the density of water (infusate) and Σ is the sum of any source and sink terms. If the brain is considered an incompressible fluid medium and water losses across the microvasculature are negligible (21), then the water density is invariant with time and Σ is negligible, so that the continuity equation reduces to just

$$0 = \frac{1}{r^2} \frac{\partial}{\partial r} r^2 v \tag{9.18}$$

Equations 9.17 and 9.18 can then be combined to generate a single differential equation in pressure; combined with the pressure boundary conditions that (1) pressure is zero at the brain boundary and that (2) the volumetric flow of infusate q equals the flow across the tissue interface at the cannula tip (i.e., $q = 4\pi r^2$; $v = -4\pi r_o^2 [\kappa (\partial p / \partial r)]$ at $r = r_o$), this pressure equation yields the simple result that

$$v = \frac{q}{4\pi r^2} \tag{9.19}$$

The distributed model is completed by forming a differential mass balance for the drug solute in a manner completely analogous to that shown previously in deriving Equation 9.14, except for the inclusion of an additional term describing convective flow:

$$\underset{\substack{\text{rate of conc} \\ \text{change in } \Delta V}}{\frac{\partial C}{\partial t}} = \underset{\substack{\text{net diffusion} \\ \text{in } \Delta V}}{D \frac{1}{r^2} \frac{\partial}{\partial r} r^2 \frac{\partial C}{\partial r}} - \underset{\substack{\text{net convective} \\ \text{flow in } \Delta V}}{\frac{1}{R r^2} \frac{\partial}{\partial r} r^2 v C} - \underset{\substack{\text{metabolism} \\ \text{in } \Delta V}}{\frac{k_m}{R} C} - \underset{\substack{\text{net transport} \\ \text{across microvasculature}}}{P \cdot s \left(\frac{C}{R} - C_p \right)} \tag{9.20}$$

As with low-flow microinfusion, the initial condition is that drug concentration in the tissue is everywhere zero, and the outer boundary condition is that the drug concentration remains zero at all times far from the cannula tip. The boundary condition at the cannula tip (at r_o) differs in that the mass outflow from the cannula is equal to the convective (not diffusive) flux at the cannula tip — that is,

$$q C_{inf} = R 4\pi r_o^2 \, (vC) \big|_{r=r_o} / R \tag{9.21}$$

where q is the volumetric flow rate, C_{inf} is the infusate concentration, and r_o is the radius of the cannula.

In general, the mathematical solution to Equation 9.20 is numerical. However, in the special case of nonendogenous macromolecules ($MW >$ 50,000) and high flow (e.g., 3 µL/min), Equation 9.20

can be greatly simplified because diffusive contributions to transport are negligibly small. Hence it becomes just

$$\frac{\partial C}{\partial t} = -\frac{1}{R\,r^2}\frac{\partial}{\partial r}r^2 vC - kC \qquad (9.22)$$

where, as previously in Equation 9.3, $k = (k_m + P \cdot s)/R$. This equation has a very simple and useful solution for the concentration profile at steady state:

$$\frac{C(r)}{C_{inf}} = Rexp\left[-\frac{4\pi\left(k_m + P \cdot s\right)}{3\,q}\left(r^3 - r_o^3\right)\right] \qquad (9.23)$$

For nonbinding macromolecules confined principally to the extracellular space, $R = \phi_e$ (~ 0.2 in brain) and the interstitial concentration C_e equals C/R (cf. Equation 9.2).

Very simple estimators of the penetration depths that can be achieved by high-flow infusion of macromolecules can be derived from Equation 9.23. The penetration depth at steady state (r_m) and the time required to reach this steady state (t_m) are

$$r_m = \sqrt[3]{2\,q/[4\pi\,(k_m + P \cdot s)]}$$

$$\text{and} \quad t_m = 2R\,/\left[3\left(k_m\ +\ P \cdot s\right)\right] \qquad (9.24)$$

When the characteristic time for degradation of a macromolecule is 33 hours [i.e., $k = \ln 2/(33\ \text{hr})$] and the flow rate q is 3 μL/min, Equation 9.24 predicts that the penetration depth will be 1.8 cm. This is far in excess of the penetration depth that can be achieved by simple diffusive transport, and is the theoretical result that indicates that high-flow microinfusion can provide brain tissue penetrations that intraventricular infusion cannot. Equation 9.24 also predicts that the time required to achieve this depth is 1.2 days, so that long-term infusion into the brain parenchyma is necessary.

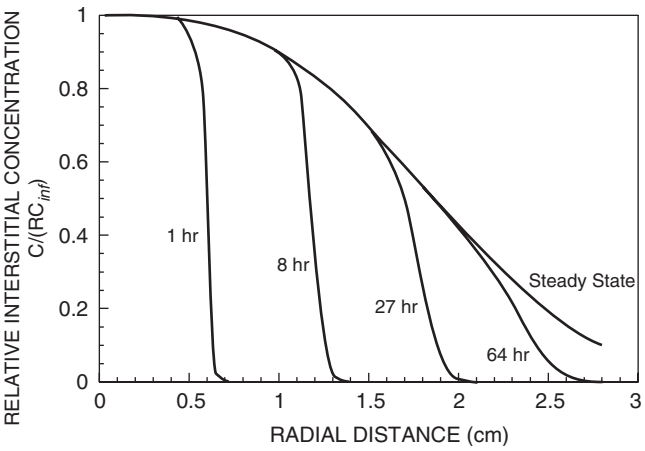

FIGURE 9.10 Simulated interstitial concentration profiles of a 180-kDa macromolecule in nonbinding brain tissue at various times during high-flow microinfusion at 3 μL/min. Model parameters were taken from Table 9.1.

Simulated concentration profiles for nonbinding macromolecules in brain tissue (e.g., albumin or nonbinding antibodies) are presented in Figure 9.10 for $k = \ln 2/(33\ \text{hr})$ and $q = 3$ μL/min. Other parameters representative of 180-kDa proteins are given in Table 9.1. The curve labeled "steady state" (Figure 9.10) and forming an envelope over the other curves from the top left to lower right corner is the relative concentration profile, $C_e/C_{inf} = C/(RC_{inf}) = C/(\phi_e C_{inf})$, given by Equation 9.23. The curves at 1, 8, 27, and 64 hours are numerical results showing the kinetics of

TABLE 9.1 Representative Macromolecular Parameters[a]

Parameter	Symbol	Value	Source
Tissue hydraulic conductivity (cm^4/dyne/sec)	κ	0.34×10^{-8}	Morrison *et al.* (21)
Capillary permeability (cm/sec)	P	1.1×10^{-9}	Blasberg *et al.* (24)
Capillary area/tissue volume (cm^2/cm^3)	s	100	Bradbury (25)
Extracellular fraction	ϕ_e	0.2	Patlak *et al.* (4)
Catheter radius (cm)	r_o	0.0114	32 gauge
Diffusion coefficient (cm^2/sec)	D_e	1.0×10^{-7}	Tao and Nicholson (18)[b]
Volumetric infusion rate (cm^3/sec)	q	5.0×10^{-5}	Typical high-flow infusion rate (3 μL/min)
Metabolic rate constant (sec^{-1})	k_m	1.15×10^{-6}	Arbitrary value[c]

[a] Typical of a 180-kDa protein

[b] The serum albumin value of D_e for gray matter obtained by these authors was scaled to 180 kDa.

[c] Divided by R, this corresponds to a half-life of 33 hours and is roughly five times the average turnover rate of brain protein.

approach to the steady state. Note the characteristic shape of these curves. Up to well beyond 8 hours of infusion, the initial portion of the curve (nearest the cannula tip) follows the steady-state profile and then drops off dramatically, approximating a step function. This concentration front moves radially outward over time, with a small degree of diffusion superimposed on the advancing front, giving rise to the small curvatures observable in Figure 9.10 at the top and bottom of the leading edge. Hence, over much of the infused tissue volume, the interstitial concentration remains relatively close to the infusate concentration and provides for relatively uniform tissue dosing.

The steep concentration profiles and large penetration distances predicted for nonbinding macromolecules have been confirmed by experiment. Figure 9.11 presents an autoradiogram obtained from rat brain following a 4-μL infusion of [^{14}C]albumin at 0.5 μL/min into the gray matter of the caudate through a 32-gauge cannula (26). The image shows a relatively uniform concentration (density) over an approximately spherical infusion volume, the symmetry resulting from the isotropic structure of the gray matter on the spatial scale of these observations. Figure 9.12 is an autoradiogram obtained after infusing 75 μL of ^{111}In-labeled transferrin (*MW* 80,000) at 1.15 μL/min into the white matter tracts of the corona radiata of the cat (22). Two findings are immediately apparent. First, with this much larger volume of infusion, delivery distances of at least a centimeter have been achieved in accordance with theoretical

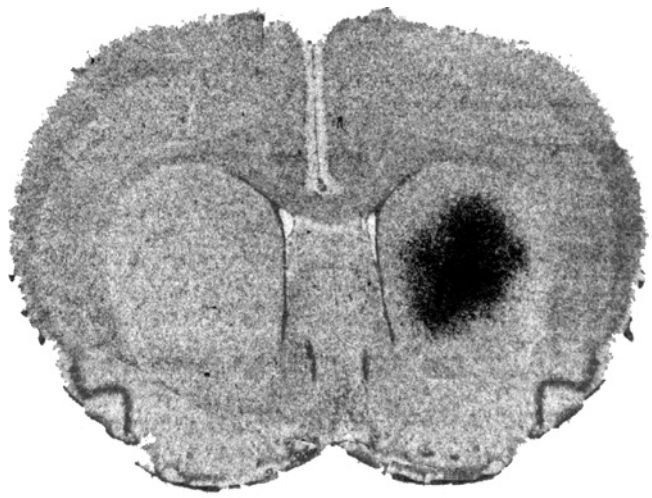

FIGURE 9.11 Autoradiogram of the distribution of [^{14}C]-albumin in rat caudate following a 4-μL infusion at 0.5 μL/min. (Reproduced from Chen MY *et al.* J Neurosurg 1999;90:315–20.)

prediction. Second, the anisotropy of the white matter tracts is evident, indicating that the models of Equations 9.17 and 9.20 must be modified to account for such anisotropy before they are predictive of any details of white matter spread. Figure 9.13 presents both an autoradiogram and a single-photon emission-computed tomographic (SPECT) image of ^{111}In-labeled diethylenetriaminepentaacetic acid (DTPA)–transferrin (*MW* 81,000) following a 10-mL continuous infusion at 1.9 μL/min into the

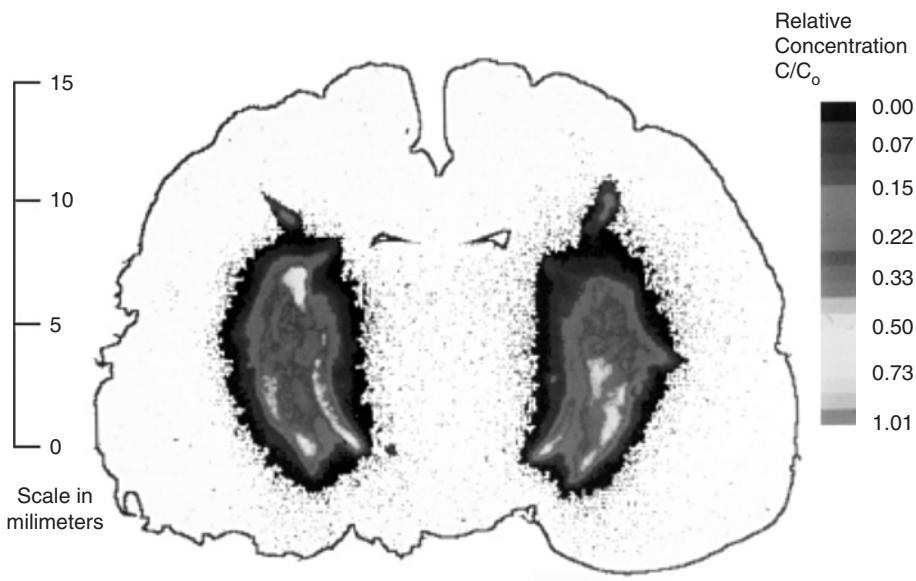

FIGURE 9.12 Autoradiogram of the distribution of ^{111}In-labeled transferrin in cat brain following a 75-μL infusion at 1.15 μL/min into the corona radiata.

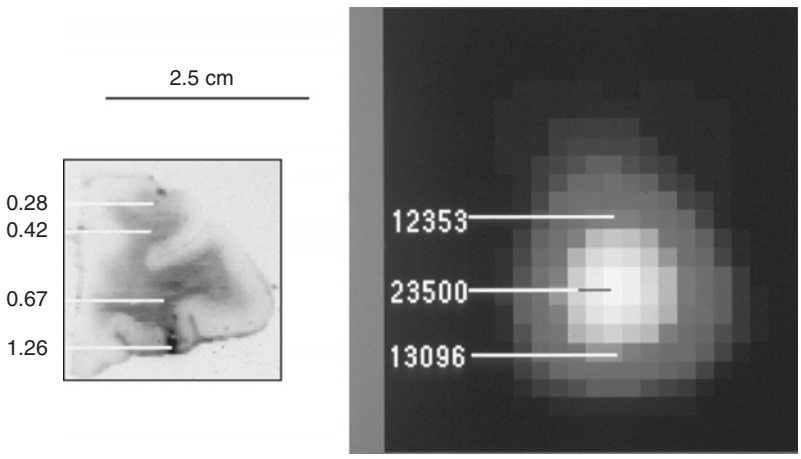

FIGURE 9.13 *Left:* Autoradiogram of a coronal section of the frontal lobe of a rhesus monkey 13 hours after completing a 10-mL infusion of ^{111}In-labeled DTPA–transferrin into the centrum semiovale at 1.9 μL/min. Numerical values represent local tissue concentrations relative to the infusate concentration. *Right:* SPECT image corresponding to the autoradiogram. Numerical values are pixel counts used to assess spread in the dorsal–ventral and medial–lateral directions. (Reproduced from Laske DW *et al.* J Neurosurg 1997;87:586–94.)

centrum semiovale (white matter) of a primate (27). In this case, the infused protein filled over one-third of the infused hemisphere before finding avenues of exit (10 mL exceeds the capacity of the primate hemisphere). The concentration was relatively uniform across the white matter, dropping off to only about 28% of the infusate concentration at a point over a centimeter from the cannula tip. The larger numbers reflect the presence of edema as well as tissue damage and fluid pockets in the vicinity of the cannula tip near the bottom of the section. The spread as determined from SPECT measurements was similar in the anterior–posterior, medial–lateral, and dorsal–ventral directions, ranging from 2 to 3 cm in each direction.

The high-flow distributed model of Equations 9.17, 9.20, and 9.23 describes the concentration profile that is generated in isotropic tissue at the very end of infusion. However, if these profiles are ultimately to be used to predict tissue response to a drug, these are not sufficient, since they do not describe the entire history of tissue exposure to the drug. Once the pumps are turned off, there is a *postinfusion phase* during which further transport through the tissue occurs by diffusion, before clearance mechanisms finally reduce the agent's concentration to a negligible value. This phase is critical in dose-response estimation since it may last a long time relative to the duration of the infusion and may broaden the sharp concentration fronts often present at the termination of infusion. Hence, the distributed model is now extended to include a description of this phase and is used in its entirety to assess likely treatment volumes as a function of degradation rate.

For isotropic tissue, the spherical distribution about the cannula tip at the end of infusion may be imagined as composed of a collection of concentric concentration shells. The postinfusion phase can then be described as the superimposed diffusion of the material from each one of these shells acting independently. Mathematically, at the start of the postinfusion period, the concentration of each shell at distance r from the cannula tip is the value of C (r, t_{inf}) obtained from Equation 9.20 (or 9.23, if applicable). Each of these shell concentrations can be multiplied by a function that accounts for diffusional broadening in the postinfusion phase (28), and integration over all such shells leads to the formula for the postinfusion concentration profile, $C(r, \hat{t})$:

$$C(r, \hat{t}) = \frac{e^{-k\hat{t}}}{2r(\pi D \hat{t})^{1/2}} \int_{\infty}^{0} C(r', t_{inf}) \left[e^{-(r-r')^2/(4D\hat{t})} - e^{-(r+r')^2/(4D\hat{t})} \right] r' dr' \tag{9.25}$$

for $\hat{t} > 0$, where $\hat{t} = t - t_{inf}$ is the time after the end of infusion (21). When this formula is applied to our macromolecule that has a 33-hour degradation time in brain (the example in Figure 9.10), the concentration profiles of Figure 9.14 are generated. The solid line

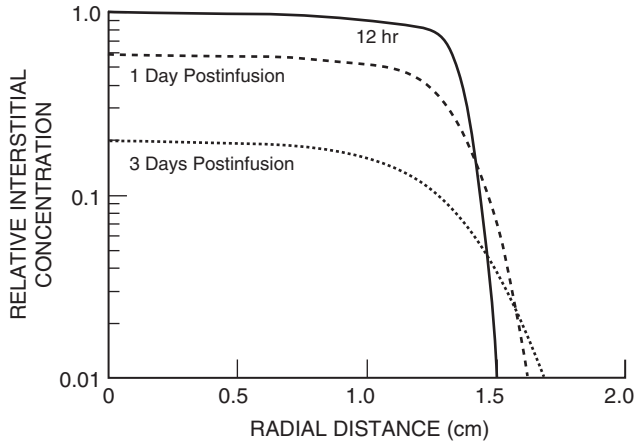

FIGURE 9.14 Simulated interstitial concentration profiles of a 180-kDa macromolecule in nonbinding brain tissue at the end of a 12-hour high-flow infusion at 3 μL/min and at 1 and 3 days postinfusion. Model parameters were taken from Table 9.1. (Reproduced from Morrison PF *et al.* Am J Physiol 1994;266:R292–305.)

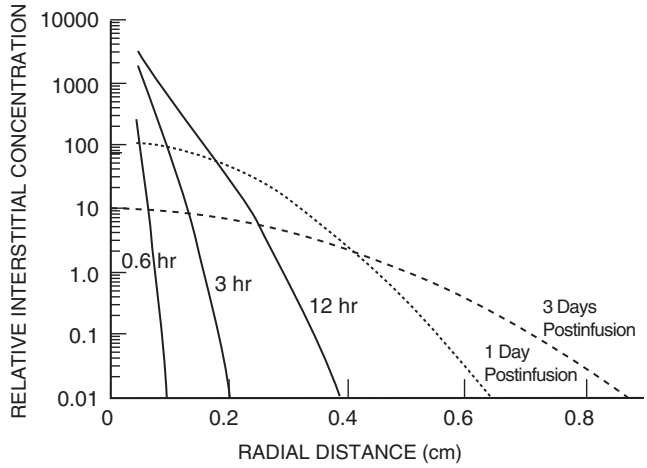

FIGURE 9.15 Simulated interstitial concentration profiles of a 180-kDa macromolecule in nonbinding brain tissue at various times during a 12-hour low-flow infusion at 0.05 μL/hr and at 1 and 3 days postinfusion. Model parameters were taken from Table 9.1. (Reproduced from Morrison PF *et al.* Am J Physiol 1994;266:R292–305.)

represents the concentration profile [the $C(r', t_{inf})$ in Equation 9.25] at 12 hours ($= t_{inf}$) after the initiation of a 3-μL/min infusion. The dotted lines show the profile at 1 and 3 days postinfusion. In the interior of the infused volume, the profile drops in value as the degradative processes exert their effect. However, beyond the initial 12-hour line, concentrations increase to appreciable values (after 1 day, to around 10% of the infusate concentration at 1.5 cm) and then decrease as degradation continues. Although not immediately apparent in this figure, this outward shift could easily account for a 20% increase in dosage volume if the drug remained biologically active at 1% of its infusate concentration.

For comparison with low-flow infusion (pure diffusion) behavior, the same type of plot as Figure 9.14 is shown in Figure 9.15. In this case, computations based on Equation 9.14 were performed in which the same mass of macromolecule is infused over 12 hours but at a much lower flow rate of 0.05 μL/hr (0.00083 μL/min) to assure pure diffusive transport. Because the same infusion time is employed in both the low- and high-flow simulations, the constraint of identical delivered mass at low flow requires that the infusate concentration be increased by several logs. Hence the upper end of the concentration scale in Figure 9.15 is greatly expanded relative to that of Figure 9.14. The more highly sloped lines show the movement of the concentration profile into the tissue by diffusion, with the 12-hour line being the profile at the end of the infusion. At this time, all regions interior to 0.3 cm are exposed to concentrations that are one thousand- to several thousandfold of that seen in the high-flow profile of Figure 9.14, and the penetration depth at 0.01 relative concentration is only 0.4 cm for low infusion versus 1.5 cm for high infusion. However, it is apparent in Figure 9.15 that the steep concentration profiles at the end of 12 hours of low-flow infusion lead to considerable additional penetration in the postinfusion phase, and the penetration depth at 0.01 relative concentration increases to nearly 0.9 cm by 3 days postinfusion. This raises the question of how much dose-response difference actually exists between the two delivery modes when total exposure time is considered.

Figure 9.16 answers this question for one particular dose-response metric. As discussed previously, the response of a tissue to a drug is often correlated with an *AUC* value in which the integrated concentration is the tissue concentration. In our example of nonbinding macromolecular infusion, the tissue concentration is a strong function of the distance from the cannula tip. Hence, the relevant *AUC* is distance dependent and must be computed from an integral of the form presented in Equation 9.8 (with r replacing the x variable). Figure 9.16 shows this $AUC(r)$ function computed for both the low- and high-flow modes of infusion and plotted, not against r, but against the corresponding spherical volume $(4/3)\pi r^3$. All cells contained within this volume will have a response equal to or greater than the response at the surface of the volume corresponding to $AUC(r)$. From independent biological information, a particular response in the target (e.g., a certain percentage of cell kill) is assumed to be identifiable with a particular *AUC* value, AUC_0, shown as the dotted line in Figure 9.16. The infusate concentration would be selected so that

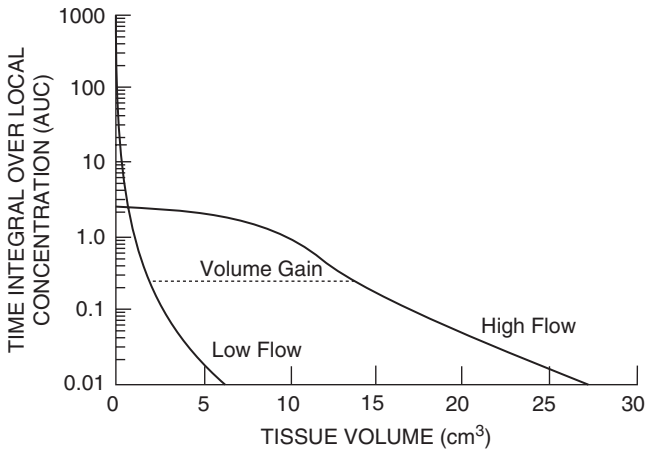

FIGURE 9.16 Simulated area-under-the-curve [$AUC(r)$] as a function of the tissue volume [$(4/3)\pi r^3$] corresponding to radial position (r). Curves correspond to the high- and low-flow infusion rates of Figures 9.14 and 9.15. The dotted line denotes a particular value of AUC corresponding to a particular response level (AUC_0). (Reproduced from Morrison PF *et al.* Am J Physiol 1994;266:R292–305.)

the AUC_0 would lie sufficiently far below the uppermost value of the high-flow line to just assure response at a maximum desired target distance from the tip of the cannula. The difference in spherical volumes between the intersection of the AUC_0 line with the low- and high-flow lines may be interpreted as the gain in treatment volume of high-flow over low-flow infusion. This gain is 12 cm^3 for the AUC_0 shown, and ranges only between 9 and 20 cm^3 for AUC_0 selections over the two logs from 1 to .01. The conclusion from this analysis is that the postinfusional spreading seen with low-flow infusion is not sufficient to compensate for the large delivery volume advantage gained during the infusion phase of high-flow microinfusion.

Tissue treatment volumes of the substance being infused are a strong function of the tissue elimination half-life, which reflects the sum of both metabolic and microvascular tissue clearances. Table 9.2 summarizes how this treatment volume and associated penetration distance varies with the characteristic tissue elimination half-life of the infused species. Various elimination half-lives were used for these simulations and an infusion rate of 3 μL/min into brain for 12 hours was assumed. For the extreme case of a macromolecule undergoing no metabolism, the treatment volume is 27 cm^3, with a penetration distance of 1.9 cm. For a more realistic tissue elimination half-life, as might be encountered with weakly binding monoclonal antibodies or stabilized analogs of somatostatin or enkephalin peptides, this volume and the distance, respectively, decrease only to 14 cm^3 and 1.5 cm.

TABLE 9.2 Tissue Treatment Volume as a Function of Tissue Elimination Half-Life

Tissue elimination half-life[a]	Infinity	33.5 hr	1.0 hr	0.17 hr
Treatment volume (cm^3)	27	14	2.7	0.49
Penetration distance (cm)	1.9	1.5	0.9	0.49

[a] Equal to (ln 2)/k.

When the elimination half-life drops to 1 hour, as is characteristic of the rates encountered with nerve growth factor or stabilized analogs of substance P peptide or glucocerebrosidase enzyme, the treatment volume decreases to 2.7 cm^3, with a penetration distance of 0.9 cm. In a rapid metabolism situation, when the elimination half-life decreases to just 10 minutes, as expected for substances such as native somatostatin, enkephalin, and substance P, the treatment volume diminishes to only 0.5 cm^3. However, the penetration distance is still 0.5 cm and still in excess of the penetration distances encountered with modes of delivery depending on diffusional transport across tissue interfaces. Finally, it should be noted that these penetration distances, computed here for a volumetric infusion rate of 3 μL/min, will decrease with decreases in the flow rate only as the cube root of the reduction factor (cf. Equation 9.24). For example, there will be only a 30% decrease in penetration distance for a 3-fold drop in flow rate to 1 μL/min.

Case Study 3: Chemopallidectomy in Patients with Parkinson's Disease Using Direct Interstitial Infusion

Direct interstitial infusion has been applied to the treatment of patients with advanced Parkinson's disease, and the design of the protocol is instructive (29). Motor control is severely compromised in these patients because degradation of the substantia nigra ultimately results in massive overinhibition of the motor cortex by the globus pallidus interna (Gpi). One therapeutic approach is to thermally ablate a portion of the Gpi to reduce this inhibition and restore freedom of movement. However, thermal ablation also risks destroying the optic nerve that forms the floor of the Gpi structure. Hence, a chemical means of destroying the Gpi has been evaluated as a potentially more selective alternative.

Controlled chemical destruction of the Gpi is possible using direct interstitial infusion of the excitotoxin quinolinic acid (pyridine dicarboxylate; MW 167). The property of quinolinic acid that makes it attractive for this purpose is its ability to selectively

bind to and kill neurons that express the *N*-methyl-D-aspartate (NMDA) receptor but not the myelinated receptor-free fibers forming the optic nerve. Use of this compound does, however, pose a potential toxic risk to other basal ganglia surrounding the Gpi, since these other structures are populated with NMDA-expressing cells. Thus, the goal is to devise a quinolinic acid delivery procedure that targets just the Gpi while sparing its nearest neighbor, the globus pallidus externa (Gpe), and other nearby ganglia.

Development of an administration protocol began with identifying the toxic threshold concentration for quinolinic acid as 1.8 m*M*. This was based on literature data describing neuronal cell kill in the hippocampus (30) and the assumption that an excitotoxin's toxic response is more determined by whether its concentration exceeds a threshold concentration than by an *AUC* measure. The target volume was taken as the largest inscribed sphere that would fit inside the Gpi. A conservative inflow rate of 0.1 μL/min was chosen to avoid any possibility of infusate leak back along the infusion cannula. A 50-minute infusion time was chosen, partly on the basis of its being the longest time easily maintained in surgery and partly because the associated delivery volume of 5 μL would suffice to initially fill the interstitial fluid volume of the inscribed sphere. The infusate concentration was then determined from theory using published transport parameters (29, 31). The complete diffusion–convection model of Equation 9.20 was solved numerically for various infusion times. This theoretical analysis was necessary to account for both convection and the substantial diffusion that results from the small molecular weight of this agent and the relatively low infusion rate. The results are expressed as the solid lines in Figure 9.17, which show tissue concentration relative to the infusate concentration. Postinfusional changes were computed using Equation 9.25, and these results are shown in the figure as the dashed lines. In this example, it is apparent that diffusion occurring after termination of infusion has little effect on extending the volume of distribution, principally because so much diffusive transport is involved even during the infusion. The horizontal line at 0.036 is the relative concentration that is just met at the radius of the inscribed sphere ($r = 1.5$ mm) at the end of infusion (50 minutes), and is equivalent to the relative toxic threshold concentration — that is, $0.036 = C_{threshold}/C_{inf}$. Using the $C_{threshold}$ of 1.8 m*M*, the infusate concentration C_{inf} is found to be 50 m*M*.

Figure 9.18 shows that the 5-μL infusion volume indeed provided localized dosing of the Gpi when biotinylated albumin was infused. The results of a 5-μL infusion of 50 m*M* quinolinic acid on the

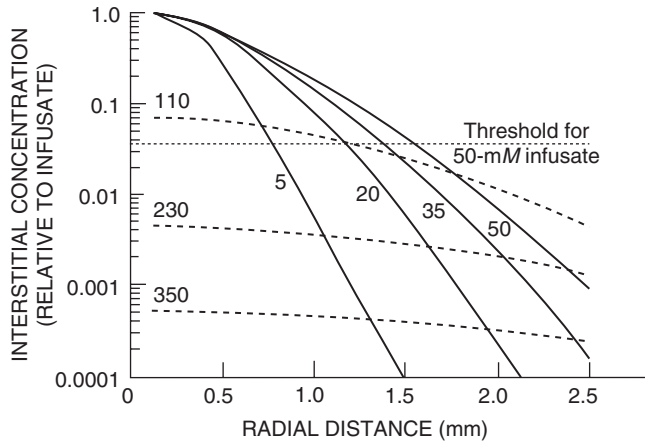

FIGURE 9.17 Relative interstitial concentration of quinolinic acid computed for a 5-μL infusion at 0.1 μL/min of an isotonic 50 m*M* solution into the globus pallidus interna of a primate (50-min infusion time). The horizontal dotted line represents the threshold concentration in relative units. Solid line curves denote profiles generated at the indicated times (minutes) during the infusion; dashed line curves denote the profiles during the postinfusion period, where the numbers are minutes after the initiation of infusion. (Reproduced from Lonser RR *et al.* J Neurosurg 1999;91:294–302.)

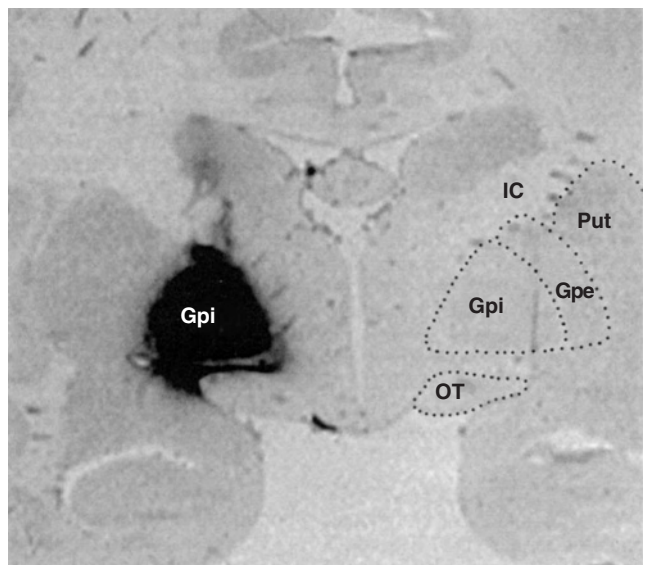

FIGURE 9.18 Coronal section of monkey brain stained for biotinylated albumin immediately after infusion of 5 μL at 0.1 μL/min. Gpi, Globus pallidus interna; Gpe, Globus pallidus externa; OT, optic tract; Put, putamen; IC, internal capsule. (Reproduced from Lonser RR *et al.* J Neurosurg 1999;91:294–302.)

Gpi of hemi-parkinsonized primates are shown in Figure 9.19. The top panel shows the histology of the Gpi tissue on the infused side of the brain, and the bottom panel shows the histology of the noninfused, control side. It is apparent that the large neuronal nuclei seen in the control section are virtually absent in the section from the infused side. The selectivity of Gpi

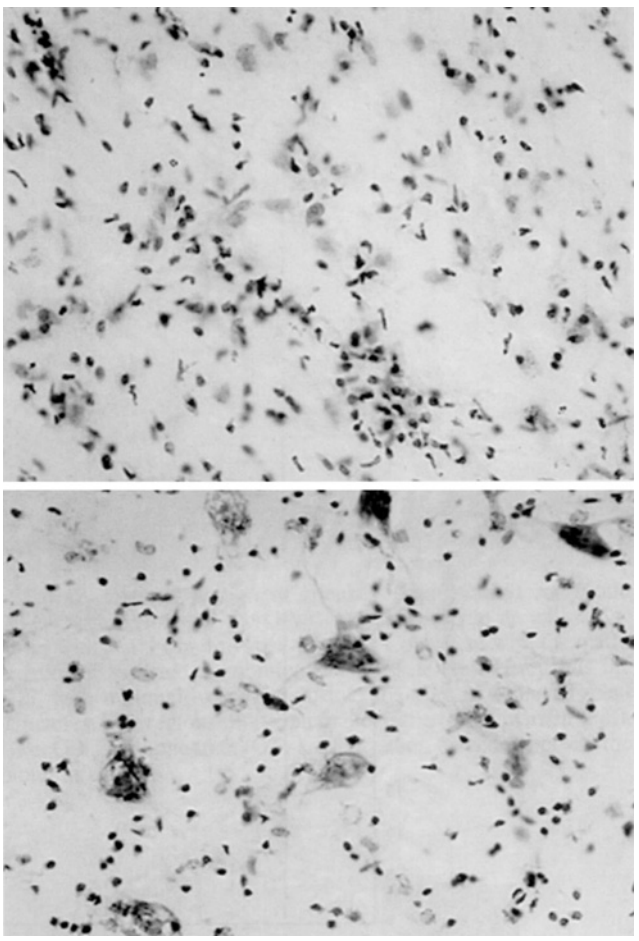

FIGURE 9.19 Photomicrographs of tissue obtained from the globus pallidus interna of a parkinsonian primate. There is complete neuronal ablation and minimal gliosis in the infused Gpi (top) relative to the unlesioned control side (bottom). (Reproduced from Lonser RR *et al.* J Neurosurg 1999;91:294–302.)

targeting was confirmed by quantifying the number of nuclei in nearby gray matter structures. It was found that 87% of the neurons within the Gpi were destroyed, while less than 10% in the Gpe, 4% in the thalamus, 1% in the subthalamus, and 0% in the hippocampus were destroyed. In addition, no toxic changes were observed in the optic tract. Clinically, the treatment resulted in a stable and pronounced improvement in the principal measures of parkinsonism, including rigidity, tremor, bradykinesia, and gross motor skills.

SUMMARY

The general principles underlying distributed kinetic models of drug delivery by transfer across tissue interfaces (intraperitoneal and intraventricular delivery) and by direct interstitial infusion (low- and high-flow microinfusion) have been presented and exemplified for both small and large molecular weight substances. Formulas have been provided to assess the concentration profiles that are likely to be obtained in tissue with these delivery methods, including rough estimators of penetration depth and time to achieve steady-state penetration. Rules for obtaining needed parameters by scaling from reference values also have been provided.

Many other applications of distributed drug kinetics exist, including the spatial and time dependence of drug delivery by microdialysis (2, 31–34), by the two-step delivery of targeting toxic moieties to tumors (35, 36), by the percolation of tightly binding antibodies into intervascular spaces of tissue (1, 37, 38), and by direct interstitial infusion into the spinal cord (39, 40) and peripheral nerves (41). A mathematical model that optimizes the spinal cord delivery of substance P–associated protein toxins for the treatment of chronic neuropathic pain is an example of state-of-the-art formalisms that go beyond simple geometric and homogeneous tissue assumptions; it accounts for anisotropic transport in tissue, anatomically correct boundaries, receptor binding and uptake, metabolism, and dose response in a single integrated finite-element formalism (42, 43). In addition, there are both mechanical and distribution issues involved in models describing potential backflow along the cannula tract during microinfusion (44). The formulations of the biological and physical phenomena involved in these cases are necessarily somewhat different than those presented in our examples. Nonetheless, the general concepts of drug delivery presented in this chapter still apply and serve as a starting point for analysis of these systems as well.

REFERENCES

1. Fujimori K, Covell DG, Fletcher JE, Weinstein JN. A modeling analysis of monoclonal antibody percolation through tumors; a binding site barrier. J Nucl Med 1990;31:1191–8.
2. Morrison PF, Bungay PM, Hsiao JK, Mefford IN, Dykstra KH, Dedrick RL. Quantitative microdialysis. In: Robinson TE, Justice JB Jr, eds. Microdialysis in the neurosciences. Amsterdam: Elsevier; 1991. p. 47–80.
3. Crank J. The mathematics of diffusion. 2nd ed. Oxford: Oxford University Press; 1975. p. 414 (see page 334).
4. Patlak CS, Fenstermacher JD. Measurements of dog blood–brain transfer constants by ventriculocisternal perfusion. Am J Physiol 1975;229:877–84.
5. Rapoport SI, Ohno K, Pettigrew KD. Drug entry into the brain. Brain Res 1979;172:354–9.
6. Dedrick RL, Flessner MF. Pharmacokinetic considerations on monoclonal antibodies. Prog Clin Biol Res 1989;288:429–38.

7. Alberts DS, Liu PY, Hannigan EV, O'Toole R, Williams SD, Young JA, Franklin EW, Clarke-Pearson DL, Malviya VK, DuBeshter B, Adelson MD, Hoskins WJ. Intraperitoneal cisplatin plus intravenous cyclophosphamide versus intravenous cisplatin plus intravenous cyclophosphamide for stage III ovarian cancer. N Engl J Med 1996;335:1950–5.
8. Dedrick RL, Myers CE, Bungay PM, DeVita VT. Pharmacokinetic rationale for peritoneal drug administration in the treatment of ovarian cancer. Cancer Treat Rep 1978;62:1–11.
9. Flessner MF, Fenstermacher JD, Dedrick RL, Blasberg RG. A distributed model of peritoneal–plasma transport: Tissue concentration gradients. Am J Physiol 1985;248:F425–35.
10. Los G, Mutsaers PHA, van der Vijgh WJF, Baldew GS, de Graaf PW, McVie JG. Direct diffusion of *cis*-diamminedichloroplatinum(II) in intraperitoneal rat tumors after intraperitoneal chemotherapy: A comparison with systemic chemotherapy. Cancer Res 1989;49:3380–4.
11. Pardridge WM, Oldendorf WH, Cancilla P, Frank HJ. Blood–brain barrier: Interface between internal medicine and the brain. Ann Intern Med 1986;105:82–95.
12. Hou J, Major EO. The efficacy of nucleoside analogs against JC virus multiplication in a persistently infected human fetal brain cell line. J Neurovirol 1998;4:451–6.
13. Hall CD, Dafni U, Simpson D, Clifford D, Wetherill PE, Cohen B, McArthur J, Hollander H, Yainnoutsos C, Major E, Millar L, Timpone J. Failure of cytarabine in progressive multifocal leukoencephalopathy associated with human immunodeficiency virus infection. N Engl J Med 1998;338:1345–51.
14. Zimm S, Collins JM, Miser J, Chatterji D, Poplack DG. Cytosine arabinoside cereberospinal fluid kinetics. Clin Pharmacol Ther 1984;35:826–30.
15. Groothuis DR, Ward S, Itskovich AC, Dobrescu C, Allen CV, Dills C, Levy RM. Comparison of ^{14}C-sucrose delivery to the brain by intravenous, intraventricular, and convection-enhanced intracerebral infusion. J Neurosurg 1999;90:321–31.
16. Fenstermacher JD. Pharmacology of the blood–brain barrier. In: Neuwelt EA, ed. Implications of the blood–brain barrier and its manipulation, vol 1. New York: Plenum Press; 1989. p. 137–55.
17. Groothuis DR, Benalcazar H, Allen CV, Wise RM, Dills C, Dobrescu C, Rothholtz V, Levy RM. Comparison of cytosine arabinoside delivery to rat brain by intravenous, intrathecal, intraventricular and intraparenchymal routes of administration. Brain Res 2000;856:281–90.
18. Tao L, Nicholson C. Diffusion of albumins in rat cortical slices and relevance to volume transmission. Neuroscience 1996;75:839–47.
19. Yan Q, Matheson C, Sun J, Radeke MJ, Feinstein SC, Miller JA. Distribution of intracerebral ventricularly administered neurotrophins in rat brain and its correlation with trk receptor expression. Exp Neurol 1994;27:23–36.
20. Krewson CE, Klarman ML, Saltzman WM. Distribution of nerve growth factor following direct delivery to brain interstitium. Brain Res 1995;680:196–206.
21. Morrison PF, Laske DW, Bobo RH, Oldfield EH, Dedrick RL. High-flow microinfusion: Tissue penetration and pharmacodynamics. Am J Physiol 1994;266:R292–305.
22. Bobo RH, Laske DW, Akbasak A, Morrison PF, Dedrick RL, Oldfield EH. Convection-enhanced delivery of macromolecules in the brain. Proc Natl Acad Sci U.S.A. 1994;91:2076–80.
23. Morrison PF, Dedrick RL. Transport of cisplatin in rat brain following microinfusion: An analysis. J Pharm Sci 1986;75:120–9.
24. Blasberg, RG, Nakagawa H, Bourdon MA, Groothuis DR, Patlak CS, Bigner DD. Regional localization of a glioma-associated antigen defined by monoclonal antibody 81C6 *in vivo*: Kinetics and implications for diagnosis and therapy. Cancer Res 1987;47:4432–43.
25. Bradbury M. The concept of a blood–brain barrier. New York: John Wiley, 1979. p. 465.
26. Chen MY, Lonser RR, Morrison PF, Governale LS, Oldfield EH. Variables affecting convection-enhanced delivery to the striatum: A systematic examination of rate of infusion, cannula size, infusate concentration, and tissue-cannula sealing time. J Neurosurg 1999;90:315–20.
27. Laske DW, Morrison PF, Lieberman DM, Corthesy ME, Reynolds JC, Stewart-Henney PA, Cummins A, Paik CH, Oldfield EH. Chronic interstitial infusion of protein to primate brain: Determination of drug distribution and clearance with SPECT imaging. J Neurosurg 1997;87:586–94.
28. Carslaw HS, Jaeger JC. Conduction of heat in solids. 2nd ed. Oxford: Oxford University Press; 1959. p. 510.
29. Lonser RR, Corthesy ME, Morrison PF, Gogate N, Oldfield EH. Convective-enhanced selective excitotoxic ablation of the neurons of the globus pallidus interna for treatment of primate parkinsonism. J Neurosurg 1999;91:294–302.
30. Vezzani A, Forloni GL, Serafini R, Rizzi M, Samanin R. Neurodegenerative effects induced by chronic infusion of quinolinic acid in rat striatum and hippocampus. Eur J. Neurosci 1991;3:40–6.
31. Beagles KE, Morrison PF, Heyes MP. Quinolinic acid *in vivo* synthesis rates, extracellular concentrations, and intercompartmental distributions in normal and immune activated brain as determined by multiple isotope microdialysis. J Neurochem 1998;70:281–91.
32. Bungay PM, Morrison PF, Dedrick RL. Steady-state theory for quantitative microdialysis of solutes and water *in vivo* and *in vitro*. Life Sci 1990;46:105–19.
33. Morrison PF, Bungay PM, Hsiao JK, Ball BA, Mefford IN, Dedrick RL. Quantitative microdialysis: Analysis of transients and application to pharmacokinetics in brain. J Neurochem 1991;57:103–19.
34. Morrison PF, Morishige GM, Beagles KE, Heyes MP. Quinolinic acid is extruded from the brain by a probenecid-sensitive carrier system. J Neurochem 1999;72:2135–44.
35. van Osdol WW, Sung CS, Dedrick RL, Weinstein JN. A distributed pharmacokinetic model of two-step imaging and treatment protocols: Application to

streptavidin conjugated monoclonal antibodies and radiolabeled biotin. J Nucl Med 1993;34:1552–64.
36. Sung CS, van Osdol WW, Saga T, Neumann RD, Dedrick RL, Weinstein JN. Streptavidin distribution in metastatic tumors pretargeted with a biotinylated monoclonal antibody: Theoretical and experimental pharmacokinetics. Cancer Res 1994;54:2166–75.
37. Juweid M, Neumann R, Paik C, Perez-Bacete J, Sato J, van Osdol WW, Weinstein JN. Micropharmacology of monoclonal antibodies in solid tumors: Direct experimental evidence for a binding site barrier. Cancer Res 1992;54:5144–53.
38. Baxter LT, Yuan F, Jain RK. Pharmacokinetic analysis of the perivascular distribution of bifunctional antibodies and haptens: Comparison with experimental data. Cancer Res 1992;52:5838–44.
39. Lonser RR, Gogate N, Wood JD, Morrison PF, Oldfield EH. Direct convective delivery of macromolecules to the spinal cord. J Neurosurg 1998; 9:616–22.
40. Wood JD, Lonser RR, Gogate N, Morrison PF, Oldfield EH. Convective delivery of macromolecules in to the naïve and traumatized spinal cords of rats. J Neurosurg 1999;90:115–20.
41. Lonser RR, Weil RJ, Morrison PF, Governale LS, Oldfield EH. Direct convective delivery of macromolecules to peripheral nerves. J Neurosurg 1998;89:610–5.
42. Sarntinoranont M, Banerjee RK, Lonser RR, Morrison PF. A computational model of direct interstitial infusion of macromolecules into the spinal cord. Ann Biomed Eng 2003;31:448–61.
43. Sarntinoranont M, Iadarola MJ, Lonser RR, Morrison PF. Direct interstitial infusion of NK1 targeted neurotoxin into the spinal cord: A computational model. Am. J. Physiol. 2003;285:R243–54.
44. Morrison PF, Chen MY, Chadwick RS, Lonser RR, Oldfield EH. Focal delivery during direct infusion to brain: Role of flow rate, catheter diameter, and tissue mechanics. Am J Physiol 1999;277:R1218–29.

CHAPTER

10

Population Pharmacokinetics

RAYMOND MILLER
Parke-Davis Pharmaceutical Research, Ann Arbor, Michigan

INTRODUCTION

Pharmacokinetic studies in patients have led to the appreciation of the large degree of variability in pharmacokinetic parameter estimates that exists across patients. Many studies have quantified the effects of factors such as age, gender, disease states, and concomitant drug therapy on the pharmacokinetics of drugs, with the purpose of accounting for the interindividual variability. Finding a population model that adequately describes the data may have important clinical benefits in that the dose regimen for a specific patient may need to be individualized based on relevant physiological information. This is particularly important for drugs with a narrow therapeutic range.

The development of a successful pharmacokinetic model allows one to summarize large amounts of data into a few values that describe the whole data set. The general procedure used to develop a pharmacokinetic model is outlined in Table 10.1. Certain aspects of this procedure have been described previously in Chapters 3 and 8. For example, the technique of "curve peeling" frequently is used to indicate the number of compartments that are included in a compartmental model. In any event, the eventual outcome should be a model that can be used to interpolate or extrapolate to other conditions.

Population pharmacokinetic analysis is an extension of the modeling procedure. The purpose of population pharmacokinetic analysis is summarized in Table 10.2.

ANALYSIS OF PHARMACOKINETIC DATA

Structure of Pharmacokinetic Models

As discussed in Chapters 3 and 8, it is often found that the relationship between drug concentrations and time may be described by a sum of exponential terms. This lends itself to compartmental pharmacokinetic analysis in which the pharmacokinetics of a drug are characterized by representing the body as a system of well-stirred compartments, with the rates of transfer between compartments following first-order kinetics. The required number of compartments is equal to the number of exponents in the sum of exponentials equation that best fits the data. In the case of a drug that seems to be distributed homogeneously in the body, a one-compartment model is appropriate, and this relationship can be described in a single individual by the following monoexponential equation:

$$A = \text{Dose} \cdot e^{-kt} \tag{10.1}$$

This equation describes the typical time course of amount of drug in the body (A) as a function of initial dose, time (t), and the first-order elimination rate constant (k). As was described by Equation 2.14, this rate constant equals the ratio of the elimination clearance (CL_E) relative to the distribution volume of the drug (V_d), so that Equation 10.1 can then be expressed in terms of concentration in plasma (C_p).

$$C_p = \frac{\text{Dose}}{V_d} \cdot e^{-(CL_E/V_d)\cdot t} \tag{10.2}$$

TABLE 10.1 Steps in Developing a Pharmacokinetic Model

Step	Activity
1	Design an experiment
2	Collect the data
3	Develop a model based on the observed characteristics of the data
4	Express the model mathematically
5	Analyze the data in terms of the model
6	Evaluate the fit of the data to the model
7	If necessary, revise the model in step 3 to eliminate inconsistencies in the data fit and repeat the process until the model provides a satisfactory description of the data

TABLE 10.2 Purpose of Population Pharmacokinetic Analysis

Estimate the population mean of parameters of interest
Identify and investigate sources of variability that influence drug pharmacokinetics
Estimate the magnitude of intersubject variability
Estimate the random residual variability

Therefore, if one has an estimate of clearance and volume of distribution, the plasma concentration can be predicted at different times after administration of any selected dose. The quantities that are known because they are either measured or controlled, such as dose and time, are called "fixed effects," in contrast to effects that are not known and are regarded as random. The parameters CL_E and V_d are called fixed-effect parameters because they quantify the influence of the fixed effects on the dependent variable, C_p.

Fitting Individual Data

Assuming that we have measured a series of concentrations over time, we can define a model structure and obtain initial estimates of the model parameters. The objective is to determine an estimate of the parameters (CL_E, V_d) such that the differences between the observed and predicted concentrations are comparatively small. Three of the most commonly used criteria for obtaining a best fit of the model to the data are ordinary least squares (OLS), weighted least squares (WLS), and extended least squares (ELS); ELS is a maximum likelihood procedure. These criteria are achieved by minimizing the following quantities, which are often called the objective function (O):

Ordinary least squares (where $\hat{C}_i$ denotes the predicted value of C_i based on the model):

$$O_{OLS} = \sum_{i=1}^{n} (C_i - \hat{C}_i)^2 \tag{10.3}$$

Weighted least squares (where W is typically 1/the observed concentration):

$$O_{WLS} = \sum_{i=1}^{n} W_i (C_i - \hat{C}_i)^2 \tag{10.4}$$

Extended least squares:

$$O_{ELS} = \sum_{i=1}^{n} [W_i (C_i - \hat{C}_i)^2 + \ln \mathrm{var}(\hat{C}_i)] \tag{10.5}$$

The correct criterion for best fit depends upon the assumption underlying the functional form of the variances (var) of the dependent variable C. The model that fits the data from an individual minimizes the differences between the observed and the model-predicted concentrations (Figure 10.1).

What one observes is a measured value that differs from the model-predicted value by some amount called a residual error (also called intrasubject error or within-subject error). There are many reasons why the actual observation may not correspond to the predicted value. The structural model may only be approximate, or the plasma concentrations may have been measured with error. It is too difficult to model all the sources of error separately, so the simplifying assumption is made that each difference between an observation and its prediction is random. When the data are from an individual, and the error model is the additive error model, the error is denoted by ε.

$$C = \frac{\text{Dose}}{V_d} \cdot e^{(-CL_E/V_d)\cdot t} + \varepsilon \tag{10.6}$$

POPULATION PHARMACOKINETICS

Population pharmacokinetic parameters quantify population mean kinetics, between-subject variability (intersubject variability), and residual variability. Residual variability includes within-subject variability, model misspecification, and measurement error. This information is necessary to design a dosage regimen for a drug. If all patients were identical, the same dose would be appropriate for all. However, since

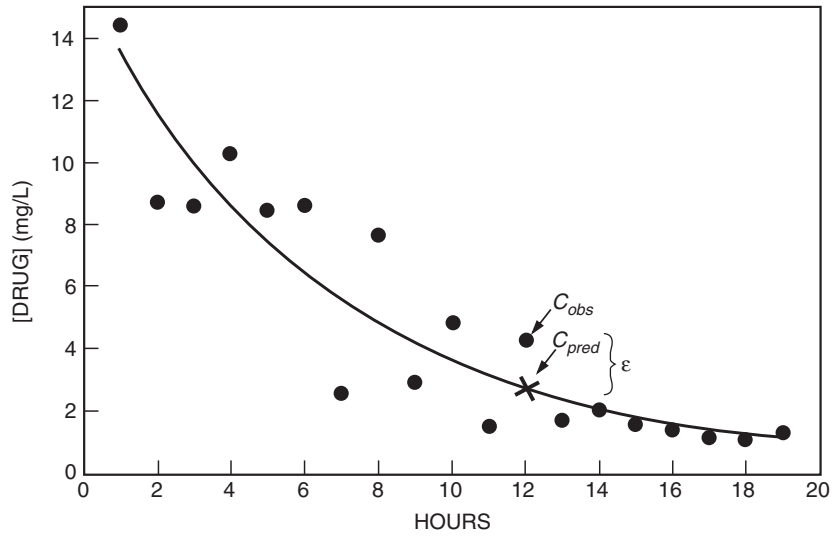

FIGURE 10.1 Fit obtained using a one-compartment model (see Equation 10.6) to fit plasma concentration-vs-time data observed following intravenous bolus administration of a drug; C_{obs} designates the actual measured concentrations and C_{pred} represents the concentrations predicted by the pharmacokinetic model. (Adapted from Grasela TH Jr, Sheiner LB. J Pharmacokinet Biopharm 1991;19(suppl):25S–36S.)

patients vary, it may be necessary to individualize a dose depending on how large the between-subject variation is. For example, to choose an initial dose, one needs to know the relationship between the administered dose and the concentration achieved and thus the pharmacological response anticipated in a patient. This is the same as knowing the typical pharmacokinetics of individuals of similar sex, age, weight, and function of elimination organs. This information is available if one knows the fixed-effect pharmacokinetic parameters governing the relationship of the pharmacokinetics to sex, age, weight, renal function, liver function, and so on. Large, unexplained variability in pharmacokinetics in an apparently homogeneous population can lead to an investigation as to the reason for the discrepancy, which in turn may lead to an understanding of fundamental principles.

Population Analysis Methods

Assume an experiment in which a group of subjects selected to represent a spectrum of severity of some condition (e.g., renal insufficiency) is given a dose of drug, and drug concentrations are measured in blood samples collected at intervals after dosing. The structural kinetic models used when performing a population analysis do not differ at all from those used for analysis of data from an individual patient. One still needs a model for the relationship of concentration to dose and time, and this relationship does not depend on whether the fixed-effect parameter changes from individual to individual or with time within an individual. The population pharmacokinetic parameters can be determined in a number of ways, of which only a few are described in the following sections.

The Naive Pooled Data Method

If interest focuses entirely on the estimation of population parameters, then the simplest approach is to combine all the data as if they came from a single individual (1). The doses may need to be normalized so that the data are comparable. Equation 10.6 would be applicable if an intravenous bolus dose were administered. The minimization procedure is similar to that described in Figure 10.1.

The advantages of this method are its simplicity, familiarity, and the fact that it can be used with sparse data and differing numbers of data points per individual. The disadvantages are that it is not possible to determine the fixed-effect sources of interindividual variability, such as creatinine clearance (CL_{CR}). It also cannot distinguish between variability within and between individuals, and an imbalance between individuals results in biased parameter estimates.

Although pooling has the risk of masking individual behavior, it might still serve as a general guide to the mean pharmacokinetic parameters. If this method is used, it is recommended that a spaghetti plot be made to visually determine if any individual or group of individuals deviates from the central tendency with respect to absorption, distribution, or elimination.

The Two-Stage Method

The two-stage method is so called because it proceeds in two steps (1). The first step is to use OLS to estimate each individual patient's parameters, assuming a model such as that given by Equation 10.6. The minimization procedure described in Figure 10.1 is repeated for each individual independently (Figure 10.2).

The next step is to estimate the population parameters across the subjects by calculating the mean of each parameter, its variance, and its covariance. The relationship between fixed-effect parameters and covariates of interest can be investigated by regression techniques. To investigate the relationship between drug clearance (CL) and creatinine clearance (CL_{CR}), one could try a variety of models, depending on the shape of the relationship. As described in Chapter 5, a linear relationship often is applicable, such as that given by Equation 10.7 (Figure 10.3):

$$CL = \text{INT} + \text{SLOPE} \cdot CL_{CR} \tag{10.7}$$

The intercept in this equation provides an estimate of nonrenal clearance.

The advantages of this method are that it is easy and most investigators are familiar with it. Because parameters are estimated for each individual, these estimates have little or no bias. Pharmacokinetic-pharmacodynamic models can be applied, since individual differences can be considered. Covariates can be included in the model. Disadvantages of the method are that variance–covariance of parameters across subjects are biased and contain elements of interindividual variability, intraindividual variability, assay error, time error, model misspecification, and variability from the individual parameter estimation process. In addition, the same structural model is required for all subjects, and numerous blood samples must be obtained at appropriate times to obtain accurate estimates for step 1.

Nonlinear Mixed-Effects Modeling Method

The nonlinear mixed-effects method is depicted in Figure 10.4 and is described here using the conventions of the NONMEM software (2, 3) and the description by Vozeh *et al.* (3). It is based on the principle that the individual pharmacokinetic parameters of a patient population arise from a distribution that can be described by the population mean and the interindividual variance. Each individual pharmacokinetic parameter can be expressed as a population mean and a deviation, typical for an individual. The deviation is the difference between the population mean and the individual parameter and is assumed to be

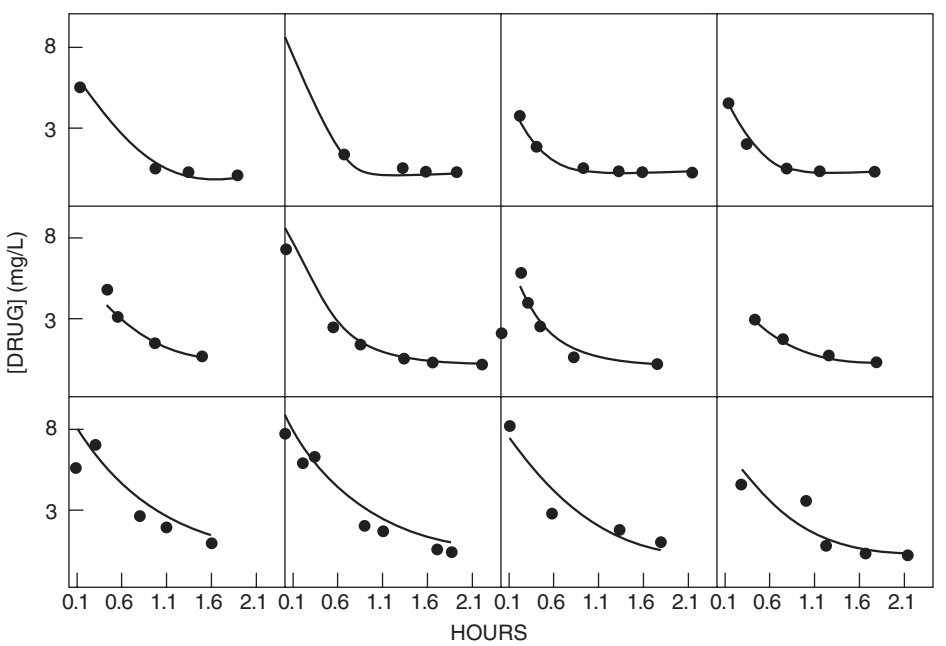

FIGURE 10.2 Fit obtained using a one-compartment model to fit plasma concentration-vs-time data observed following intravenous bolus administration of a drug. Each panel represents an individual patient.

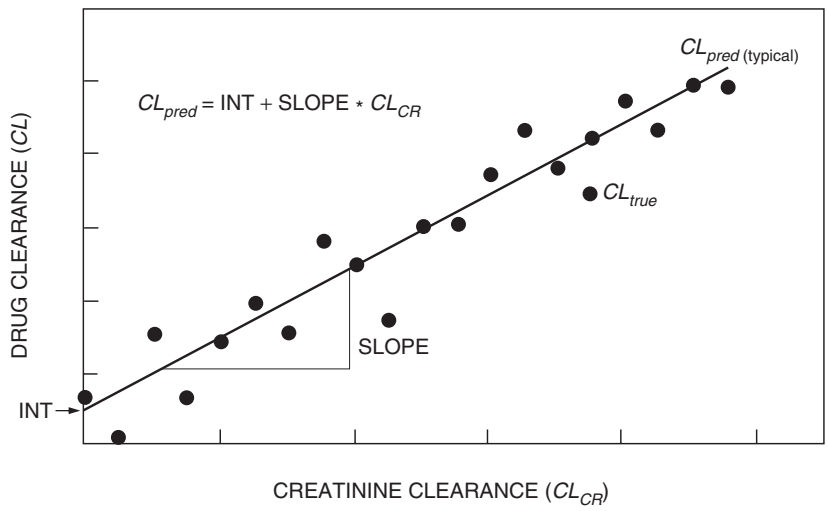

FIGURE 10.3 Linear regression analysis of drug clearance (*CL*) versus creatinine clearance (CL_{CR}). Typical values of drug clearance are generated for an individual or group of individuals with a given creatinine clearance. The discrepancy between the true value for drug clearance (CL_{true}) and the typical value (CL_{pred}) necessitates the use of a statistical model for interindividual variability. INT denotes the intercept of the regression line. (Adapted from Grasela TH Jr, Sheiner LB. J Pharmacokinet Biopharm 1991;19(suppl):25S–36S.)

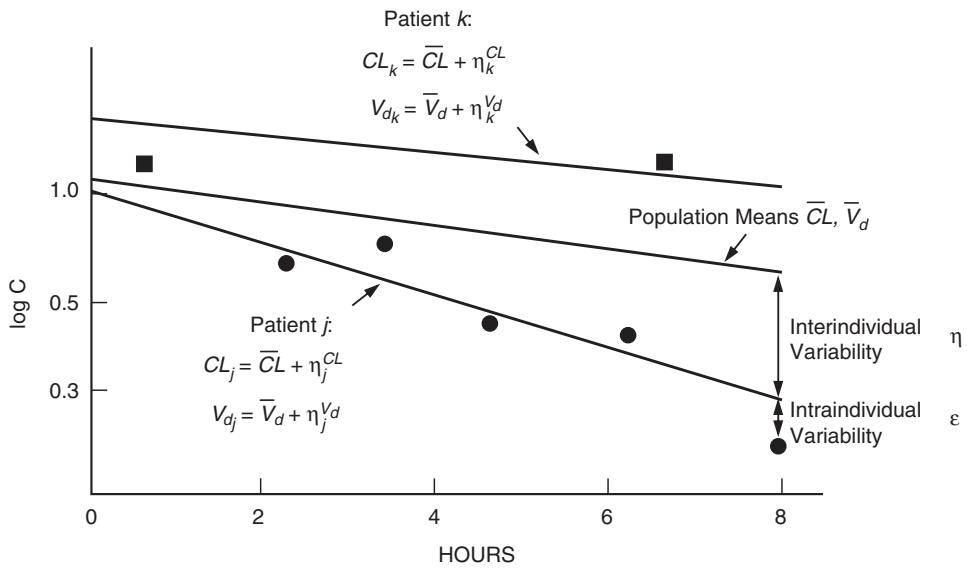

FIGURE 10.4 Graphical illustration of the statistical model used in NONMEM for the special case of a one-compartment model following intravenous bolus administration of a drug. ●, patient *j*; ■, patient *k*. (Adapted from Vozeh S *et al*. Eur J Clin Pharmacol 1982;23:445–51.)

a random variable with an expected mean of zero and variance ω^2. This variance describes the biological variability of the population. The clearance and volume of distribution for patient *j* using the structural pharmacokinetic model described in Equation 10.6 are represented by the following equations:

$$C_{ij} = \frac{\text{Dose}}{V_{d_j}} \cdot e^{(CL_j/V_{d_j}) \cdot t_{ij}} + \varepsilon_{ij}$$

where

$$CL_j = \overline{CL} + \eta_j^{CL}$$

and

$$V_{d_j} = \overline{V_d} + \eta_j^{V_d}$$

where $\overline{CL}$ and $\overline{V_d}$ are the population mean of the elimination clearance and volume of distribution, respectively, and η_j^{CL} and $\eta_j^{V_d}$ are the differences between the population mean and the clearance (CL_j) and volume of distribution V_{d_j}) of patient j. These equations can be applied to patient k by substituting k for j in the equations, and so on for each patient. There are, however, two levels of random effects. The first level, described previously, is needed in the parameter model to help model unexplained interindividual differences in the parameters. The second level represents a random error (ε_{ij}), familiar from classical pharmacokinetic analysis, which expresses the deviation of the expected plasma concentration in patient j from the measured value. Each ε variable is assumed to have a mean zero and a variance denoted by σ^2. Each pair of elements in η has a covariance, which can be estimated. A covariance between two elements of η is a measure of statistical association between these two random variables.

NONMEM is a one-stage analysis that simultaneously estimates mean parameters, fixed-effect parameters, interindividual variability, and residual random effects. The fitting routine makes use of the ELS method. A global measure of goodness of fit is provided by the objective function value based on the final parameter estimates, which, in the case of NONMEM, is minus twice the log likelihood of the data (1). Any improvement in the model would be reflected by a decrease in the objective function. The purpose of adding independent variables to the model, such as CL_{CR} in Equation 10.7, is usually to explain kinetic differences between individuals. This means that such differences were not explained by the model prior to adding the variable and were part of random interindividual variability. Therefore, inclusion of additional variables in the model is warranted only if it is accompanied by a decrease in the estimates of the intersubject variance and, under certain circumstances, the intrasubject variance.

The advantages of the one-stage analysis are that interindividual variability of the parameters can be estimated, random residual error can be estimated, covariates can be included in the model, parameters for individuals can be estimated, and pharmacokinetic–pharmacodynamic models can be used. Since allowance can be made for individual differences, this method can be used with routine data, sparse data, and an unbalanced number of data points per patient (4, 5). The models are also very flexible. For example, a number of studies can be pooled into one analysis while accounting for differences between study sites, and all fixed-effect covariate relationships and any interindividual or residual error structure can be investigated.

Disadvantages arise mainly from the complexity of the statistical algorithms and the fact that fitting models to data is time consuming. The first-order (FO) method used in NONMEM also results in biased estimates of parameters, especially when the distribution of interindividual variability is specified incorrectly. The first-order conditional estimation (FOCE) procedure is more accurate but is even more time consuming. The objective function and adequacy of the model are based in part on the residuals, which for NONMEM are determined based on the predicted concentrations for the mean pharmacokinetic parameters rather than on the predicted concentrations for each individual. Therefore, the residuals are confounded by intraindividual, interindividual, and linearization errors.

MODEL APPLICATIONS

Mixture Models

The first example is a study to evaluate the efficacy of drug treatment or placebo as add-on treatment in patients with partial seizures, and how this information can assist with dosing guidelines. A mixed-effects model was used to characterize the relationship between monthly seizure frequency over 3 months and pregabalin daily dose (0, 50, 150, 300, and 600 mg) as add-on treatment in three double-blind, parallel group studies in patients with refractory partial seizures ($N = 1042$) (6). A subject-specific random-effects model was used to characterize the relationship between seizure frequency and pregabalin dose in individual patients, taking into account placebo effect. Maximum-likelihood estimates were obtained with use of the Laplacian estimation method implemented in the NONMEM program (version V 1.1) (2). The response was modeled as a Poisson process with mean λ. The probability that the number of seizures per 28 days (Y) equals x is given by the following equation:

$$P(Y = x) = e^{-\lambda}\frac{\lambda^x}{x!}$$

The mean number of seizures per 28 days (λ) was modeled as a function of drug effect, placebo effect, and subject-specific random effects, based on the following relationship:

$$\lambda = \text{Base} \cdot (1 + f_d + f_p) \cdot e^{\eta}$$

where Base is the estimated number of seizures per 28 days reported in the baseline period before treatment. The functions f_d and f_p describe the drug effect and placebo effect, and η is the subject-specific random effect.

The structural model that best described the response was an asymptotic decrease in seizure frequency from baseline including a placebo effect (PLAC) in addition to drug effect.

$$\lambda = \text{Base} \cdot \left(1 - \frac{E_{max} \cdot D}{\text{ED}_{50} + D} - \text{PLAC}\right) \cdot e^{\eta_1}$$

E_{max} is the maximal fractional reduction in seizure frequency and ED_{50} is the dose that produces a 50% decrease in seizure frequency from maximum. PLAC is the fractional change in seizure frequency from baseline after placebo treatment. Drug treatment was modeled as an E_{max} model (see Chapter 18) and placebo treatment was modeled as a constant. This model describes a dose-related reduction in seizure frequency with a maximum decrease in seizure frequency of 38%. Half that reduction (ED_{50}) was achieved with a dose of 48.7 mg/day. However, the ED_{50} was not well estimated, since the symmetrical 95% confidence interval included zero. After placebo treatment the average increase in seizure frequency was 10% of baseline.

This analysis suggested that pregabalin reduces seizure frequency in a dose-dependent fashion. However, the results are questionable because of the variability in the prediction of ED_{50}. This may be due to the fact that some patients with partial seizures are refractory to any particular drug and would be nonresponders at any dose. It would be sensible, then, to explore the dose-response relationship for this drug separately in those patients that are not refractory to pregabalin. Actually, it is only this information that is useful in adjusting dose (and setting therapeutic expectations) for those patients who will benefit from treatment. As is often the case, the clinical trials to evaluate this drug were not designed to first identify patients tractable to pregabalin treatment and then to study dose response in only the subset of tractable patients. Thus, to obtain the dose-response relationship for this subset we would need to use the available trial data to first classify each patient (as either refractory or responsive), and then assess the degree of pregabalin anticonvulsant effect as a function of dose in the responders.

In order to justify this approach, it was necessary to evaluate if the patients in these studies represented a random sample from a population composed of at least two subpopulations, one with one set of typical values for response and a second with another set of typical values for response. A mixture model describing such a population can be represented by the following equations:

Subpopulation A (proportion = p):

$$\lambda_1 = \text{Base} \cdot \left(1 - \frac{E_{maxA} \cdot D}{\text{ED}_{50} + D} - \text{PLAC}\right) \cdot e^{\eta_1}$$

Subpopulation B (proportion = $1 - p$):

$$\lambda_2 = \text{Base} \cdot \left(1 - \frac{E_{maxB} \cdot D}{\text{ED}_{50} + D} - \text{PLAC}\right) \cdot e^{\eta_2}$$

where

Base	= Baseline seizure frequency over 28 days
E_{maxA}	= Maximal fractional change in baseline seizures due to drug treatment for subpopulation A
E_{maxB}	= Maximal fractional change in baseline seizures due to drug treatment for subpopulation B
ED_{50}	= Daily dose that produces a 50% reduction in seizure frequency from maximum (mg/day)
PLAC	= Fractional change in seizure frequency from baseline due to placebo treatment
p	= Proportion of subjects in subpopulation A (by default $1-p$ is the proportion in subpopulation B)
η_1	= Intersubject random effect for subpopulation A
η_2	= Intersubject random effect for subpopulation B
$\text{Var}(\eta_1)$	$= \text{Var}(\eta_2) = \omega$

A mixture model implicitly assumes that some fraction (p) of the population has one set of typical values of response, and that the remaining fraction ($1 - p$) has another set of typical values. In this model, the only difference initially allowed in the typical values between the two groups was the maximal fractional reduction in seizure frequency after treatment with pregabalin, that is, E_{maxA} and E_{maxB}. Values for these two parameters and the mixing fraction p were estimated. Random interindividual variability effects η_1 and η_2 were assumed to be normally distributed with zero means and common variance ω. The estimation

method assigns each individual to both subpopulations repeatedly and computes different likelihoods, depending on variables assigned to the subpopulations. This process is carried out for each individual patient record repeatedly as parameter values are varied. The fitting algorithm assigns individuals to the two categories, so that the final fit gives the most probable distribution of patients into the two subpopulations. Introducing the mixture model resulted in a significant improvement in the model fit.

In this case, the maximal response in the one subgroup (subpopulation B) tended toward zero, so the inclusion of an ED_{50} estimate in this population appeared unwarranted. In the final model, the ED_{50} parameter was dropped in this subpopulation so that treatment response in this subgroup defaulted to a constant with random variability that was independent of drug dose. Consequently, the calculated ED_{50} value is representative of only those patients who fall into the subpopulation of pregabalin-responsive patients (subpopulation A), and a dose of approximately 186 mg daily is expected to decrease their seizure frequency by about 50% of baseline. Monte Carlo simulation was used together with the pharmacodynamic parameters and variance for subpopulation A to generate the relationship between expected reduction in seizure frequency and increasing pregabalin dose that is shown in Figure 10.5. Seizure frequency values were simulated for 11,000 individuals (50% female) at doses from 50 to 700 mg pregabalin daily. Exclusion of patients with a baseline value less than six seizures per 28 days to emulate the inclusion criteria for these studies resulted in a total of 8852 individuals, of which 51% were female. The percentage reduction from baseline seizure frequency was calculated for each individual simulated. Percentiles were determined for percentage reduction in seizure frequency at each dose (Figure 10.5). In patients who are likely to respond to pregabalin treatment, doses of 150, 300, and 600 mg pregabalin daily are expected to produce at least a 71, 82, and 90% reduction in seizure frequency, respectively, in 10% of this population. Similarly, with these doses, 50% of this population is expected to show a 43, 57, and 71% reduction in seizure frequency, respectively. These expectations serve as a useful dosing guide for a clinician when treating a patient.

Exposure-Response Models

The second example involves the impact of population modeling of exposure-response data on an

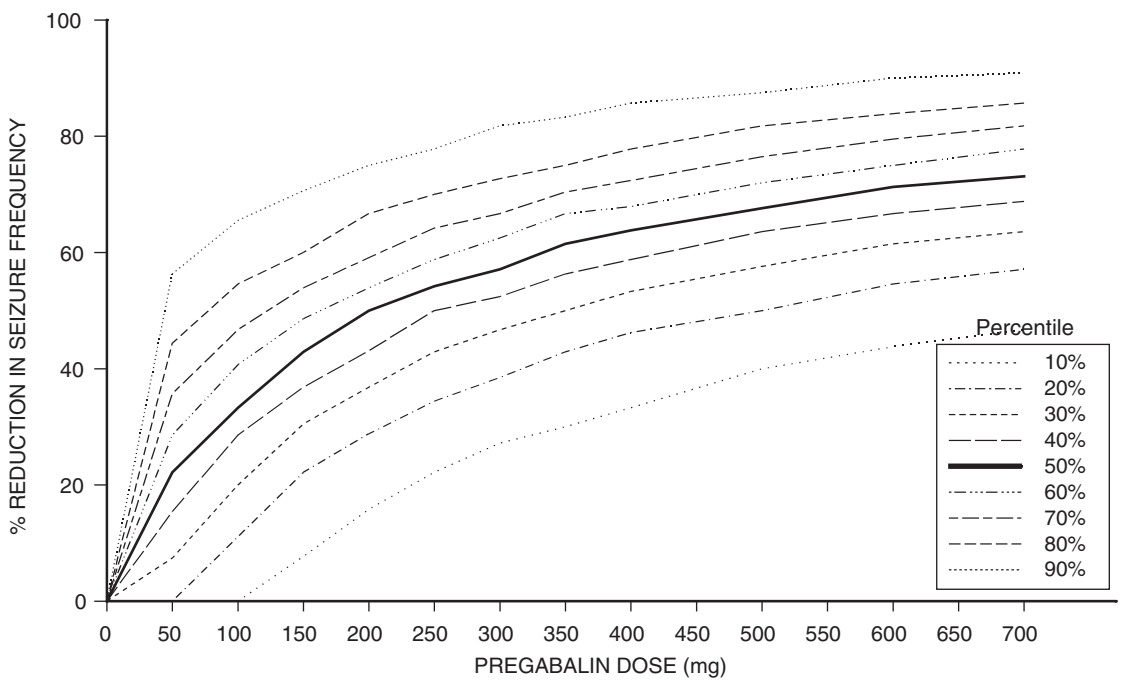

FIGURE 10.5 Expected percentage reduction in seizure frequency with increasing dose in patients who are likely to respond, expressed as percentiles. (Adapted from Miller R, Frame B, Corrigan B, Burger P, Bockbrader H, Garofalo E, Lalonde R. Clin Pharmacol Ther. 2003;73:491–505, with permission from the American Society for Clinical Pharmacology and Therapeutics.)

FDA approval. Usually, evidence of efficacy from two or more adequate and well-controlled clinical trials, along with safety information, is required for the regulatory approval of a new indication for a drug. The idea is that replication of the results of a single trial is needed to rule out the possibility that a finding of efficacy in a single trial is due to chance. This example describes the application of exposure-response analysis to establish an FDA-approvable claim of drug efficacy based on a dose-reponse relationship that was obtained from two pivotal clinical trials that used different final-treatment doses.

Response data for two studies were submitted to the FDA for approval for the treatment of postherpetic neuralgia (PHN). Both studies were randomized, double-blind, placebo-controlled, multicenter studies that evaluated the safety and efficacy of gabapentin administered orally three times a day, compared with placebo. In both studies, the patients were titrated to their final-treatment dose by the end of either week 3 or 4 and then were maintained on these doses for 4 weeks. However, in one study, the final-treatment dose was 3600 mg/day, and in the other study, the patients were randomized to the final-treatment doses of either 1800 or 2400 mg/day. The primary efficacy parameter was the daily pain score, as measured by the patient in a daily diary on an 11-point Likert scale, with zero equaling no pain and 10 equaling the worst possible pain. Each morning the patient self-evaluated pain for the previous day. The dataset consisted of 27,678 observations collected from 554 patients, of which 226 received placebo and 328 received treatment approximately evenly distributed over the three doses. Daily pain scores were collected as integral, ordinal values and the change from baseline pain score was treated as a continuous variable. The mean of the most recent available pain scores observed during the baseline study phase was used for each patient's baseline score. The individual daily pain score was modeled as change from baseline minus effect of drug and placebo:

$$\text{Daily change from baseline pain score} = -(\text{Placebo} + \eta) - (\text{Gabapentin effect} + \eta) + \varepsilon$$

where ε is the residual variability and η is the interindividual variability.

The placebo effect was described using a model made up of two components, an immediate-effect component and an asymptotic time-dependent component, as described in Chapter 20. The gabapentin effect was described by an E_{max} model using the daily dose corrected for estimated bioavailability. Observed and predicted mean population responses are described in Figures 10.6 and 10.7. The advantage of the population approach is that all the data were included in the analysis, allowing valuable information to be captured, such as time of onset of response relative to placebo as well as intraindividual dose response. The model served as a useful tool for integrating information about the characteristics of the drug over the time course of the study. This analysis

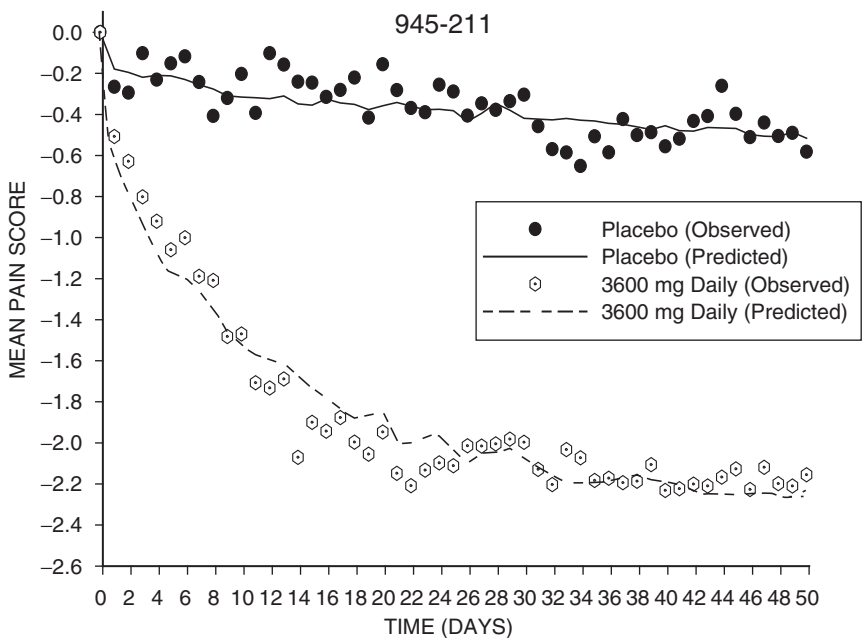

FIGURE 10.6 Change in pain score from baseline over time for study 945-211.

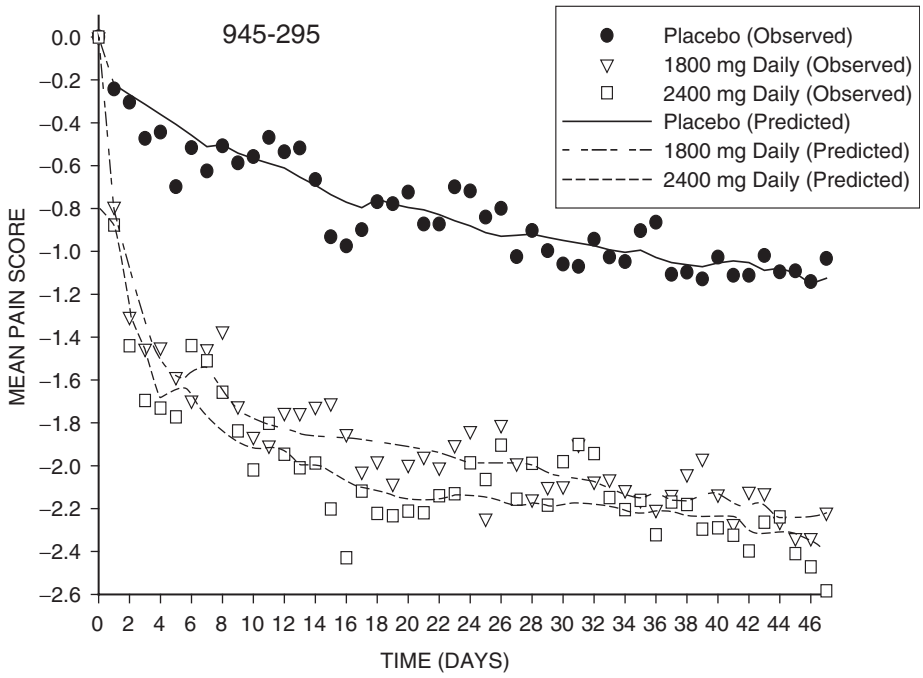

FIGURE 10.7 Change in pain score from baseline over time for study 945-295.

provided the regulators with a clear understanding of the nature of the dose response for gabapentin to help with their decision making.

However, since patients in study 1 were randomized to a final dose of 3600 mg/day and patients in study 2 were randomized to either 1800 or 2400 mg/day, replicate data confirming the efficacy of gabapentin at these doses were not available. This presented a challenging regulatory obstacle to approval of gabapentin for the PHN treatment indication. To further explore the underlying dose-response relationship, the FDA did their own analysis of the data: an initial summary statistical analysis to compare the observed clinical pain score at various levels or days after starting therapy, followed by a modeling and simulation analysis to check the concordance across the different studies. The use of this pharmacokinetic–pharmacodynamic information confirmed evidence of efficacy across the three studied doses to the satisfaction of the FDA review staff. The clinical trials section of the package insert for gabapentin describes studies 1 and 2 and further states "Pharmacokinetic–pharmacodynamic modeling provided confirmatory evidence of efficacy across all doses," to explain the basis for establishing the effectiveness of this drug for the PHN indication (7).

CONCLUSIONS

Population pharmacokinetics describes the typical relationships between physiology and pharmacokinetics, the interindividual variability in these relationships, and their residual intraindividual variability. Knowledge of population kinetics can help one choose initial drug dosage, modify dosage appropriately in response to observed drug levels, make rational decisions regarding certain aspects of drug regulation, and elucidate certain research questions in pharmacokinetics. Patients with a disease for which a drug is intended are probably a better source of pharmacokinetic data than are healthy subjects. However, these types of data are contaminated by varying quality, accuracy, and precision, as well as by the fact that generally only sparse data are collected from each patient.

Although population pharmacokinetic parameters have been estimated either by fitting all individuals' data together as if there were no kinetic differences, or by fitting each individual's data separately and then combining the individual parameter estimates, these methods have certain theoretical problems that can only be aggravated when the deficiencies of typical clinical data are present. The nonlinear mixed-effect analysis avoids many of these deficiencies and

provides a flexible means of estimating population pharmacokinetic parameters.

REFERENCES

1. Sheiner LB. The population approach to pharmacokinetic data analysis: Rationale and standard data analysis methods. Drug Metab Rev 1984; 15:153–71.
2. Beal SL, Sheiner LB. NONMEM user's guides, NONMEM Project Group. San Francisco: University of California; 1989.
3. Vozeh S, Katz G, Steiner V, Follath F. Population pharmacokinetic parameters in patients treated with oral mexiletine. Eur J Clin Pharmacol 1982;23:445–51.
4. Sheiner LB, Rosenberg B, Marathe VV. Estimation of population characteristics of pharmacokinetics parameters from routine clinical data. J Pharmacokinet Biopharm 1997;5:445–79.
5. Grasela TH Jr, Sheiner LB. Pharmacostatistical modeling for observational data. J Pharmacokin Biopharm 1991;19(suppl):25S–36S.
6. Miller R, Frame B, Corrigan B, Burger P, Bockbrader H, Garofalo E, Lalonde R. Exposure-response analysis of pregabalin add-on treatment of patients with refractory partial seizures. Clin Pharmacol Ther 2003;73: 491–505.
7. Physician's Desk Reference. 59th ed. Montvale, NJ: Medical Economics; 2005. p. 2590.

Suggested Additional Reading

Beal SL, Sheiner LB. Estimating population kinetics. CRC Crit Rev Biomed Eng 1982;8:195–222.

Whiting B, Kelman AW, Grevel J. Population pharmacokinetics: Theory and clinical application. Clin Pharmacokinet 1986;11:387–401.

Ludden TM. Population pharmacokinetics. J Clin Pharmacol 1988;28:1059–63.

Sheiner LB, Ludden TM. Population pharmacokinetics/dynamics. Annu Rev Pharmacol Toxicol 1992;32: 185–209.

Yuh L, Beal SL, Davidian M, Harrison F, Hester A, Kowalski K, Vonesh E, Wolfinger R. Population pharmacokinetic/pharmacodynamic methodology and applications. A bibliography. Biometrics 1994; 50:566–75.

Samara E, Grannenman R. Role of population pharmacokinetics in drug development. Clin Pharmacokinet 1997;32:294–312.

This page intentionally left blank

PART

II

DRUG METABOLISM AND TRANSPORT

This page intentionally left blank

CHAPTER

11

Pathways of Drug Metabolism

SANFORD P. MARKEY
National Institute of Mental Health, National Institutes of Health, Bethesda, Maryland

INTRODUCTION

Most drugs are chemically modified or metabolized in the body. The biochemical processes governing drug metabolism largely determine the duration of a drug's action, elimination, and toxicity. The degree to which these processes can be controlled to produce beneficial medical results relies on multiple variables that have been the subject of considerable study, best illustrated by examining several representative drugs. Drug metabolism may render an administered active compound inactive, or activate an inactive precursor, or produce a toxic by-product.

Phenobarbital typifies drugs that are active when administered and then are converted to inactive and more polar metabolites in the liver, as shown in Scheme 11.1. When phenobarbital is hydroxylated, it becomes more water soluble and less lipid-membrane soluble. *p*-Hydroxyphenobarbital is pharmacologically inactive and is either excreted directly or is glucuronidated and then excreted.

Phenobarbital metabolism exemplifies the principles propounded by Richard Tecwyn Williams, a pioneering British pharmacologist active in the mid-twentieth century (1). Williams introduced the concepts of Phase I and Phase II drug metabolism. He described Phase I biotransformations as primary covalent chemical modifications to the administered drug (oxidation, reduction, hydrolysis, etc.), such as the hydroxylation of phenobarbital. Phase II reactions thus involved synthesis or conjugation of an endogenous polar species to either the parent drug or the Phase I modified drug, as exemplified by the glucuronidation of *p*-hydroxyphenobarbital in Scheme 11.1. These concepts have been useful to catalog and categorize newly described chemical biotransformations, especially as the field of drug metabolism developed.

Pyrimidine nucleotides exemplify a class of pharmaceuticals designed to be biotransformed in the body from inactive to active cancer chemotherapeutic agents. In order to effectively interfere with thymidine synthetase, 5-fluorouracil (5 FU) must

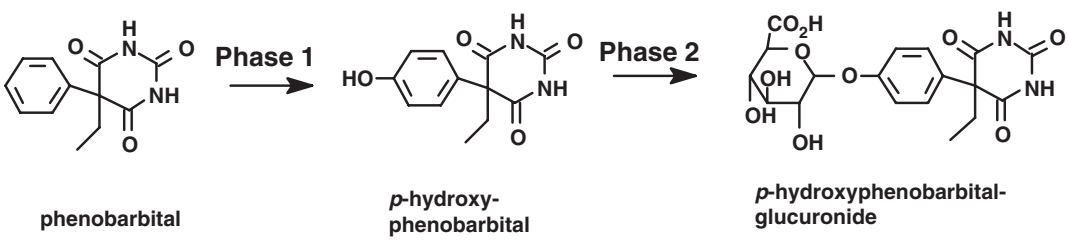

SCHEME 11.1 Metabolism of phenobarbital results in inactive polar metabolites.

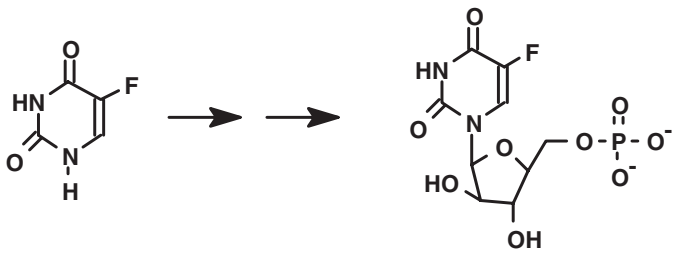

SCHEME 11.2 Metabolism of 5-FU is required to produce the active agent 5-FUMP.

be biotransformed to 5-fluorouracil monophosphate (5-FUMP), as shown in Scheme 11.2. The base 5-FU is not well absorbed as a drug and consequently is administered parenterally. The polar monophosphate is formed within the targeted, more rapidly dividing cancer cells, enhancing the specificity of its action.

Sometimes an active pharmaceutical produces another active agent after biotransformation. An example of a commercially popular drug with an active metabolite is terfenadine (Seldane^{TM}), as shown in Scheme 11.3. As discussed in Chapter 1, the terfenadine oxidative metabolite, fexofenadine (Allegra^{TM}), is now marketed as a safer alternative that avoids potentially fatal cardiac terfenadine side effects.

An example of a popular pharmaceutical with a toxic metabolite is acetaminophen (2, 3). A portion of the acetaminophen metabolized in the liver is converted to a reactive intermediate, *N*-acetyl-*p*-benzoquinoneimine (NAPQI), which is an excellent substrate for nucleophilic attack by free sulfhydryl groups in proteins, as shown in Scheme 11.4. By substituting a high concentration of an alternative thiol for the –SH group in cysteine in liver proteins, and removing the reactive NAPQI from contact with liver proteins, *N*-acetylcysteine (NAcCys) is an effective antidote for acetaminophen overdose (4). The *N*-acetylcysteine adduct is inactive and is excreted in urine.

Knowledge of basic principles of drug metabolism may lead to rational development of more effective pharmaceuticals, as illustrated in Scheme 11.5 by the progression from procaine to procainamide and *N*-acetylprocainamide. Procaine was observed in 1936 to elevate the threshold of ventricular muscle to electrical stimulation, making it a promising antiarrhythmic agent (5). However, it was too rapidly hydrolyzed by esterases to be used *in vivo*, and its amide analog procainamide was evaluated (6). Procainamide has effects similar to those of procaine and is used clinically as an antiarrhythmic drug. It is relatively resistant to hydrolysis; about 60–70% of the dose is excreted as unchanged drug and 20% is acetylated to *N*-acetylprocainamide (NAPA), which also has antiarrhythmic activity. NAPA has been investigated as a

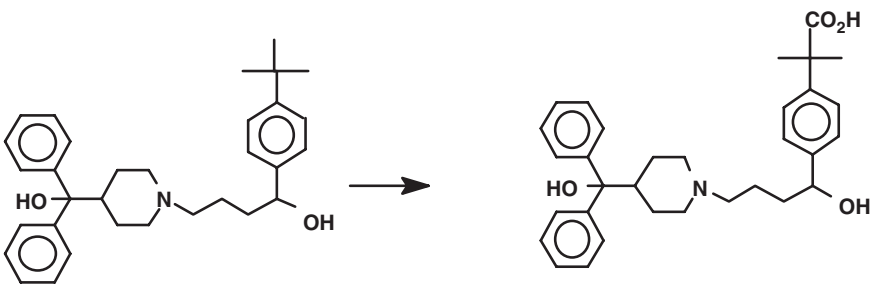

SCHEME 11.3 The active agent terfenadine is converted to another active agent, fexofenadine.

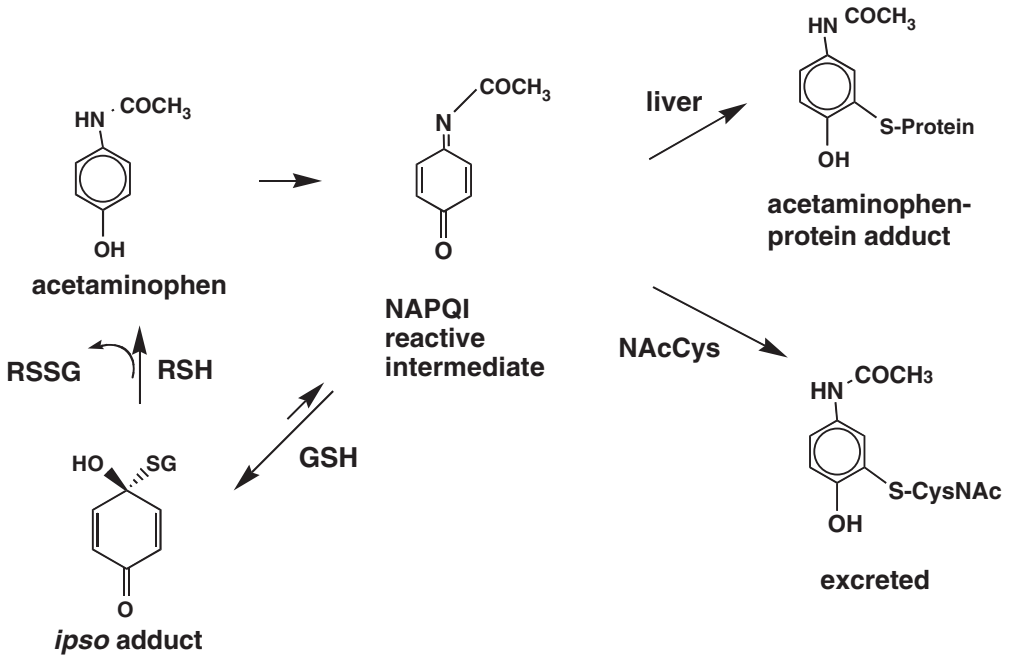

SCHEME 11.4 Acetaminophen is metabolized to a reactive intermediate (NAPQI) that can cause hepatotoxicity by reacting with liver proteins.

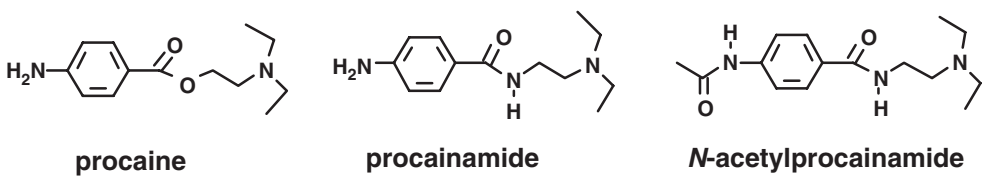

SCHEME 11.5 The structures of procaine, procainamide, and *N*-acetylprocainamide exemplify drug development based upon understanding principles of drug metabolism.

candidate to replace procainamide because it has a longer elimination half-life than does procainamide (2.5 times in patients with normal renal function) and fewer toxic side effects, representing a third generation of procaine development (7).

These examples indicate the relevance of understanding drug metabolism in the context of patient care and drug development. Presenting an overview of drug metabolism in a single chapter is challenging because the field has developed markedly in the past century, with many important scientific contributions being made. Recent books summarize advances in understanding fundamental mechanisms of metabolic processes (8) and the encyclopedic information available regarding the metabolism of specific drugs (9). The broad concepts outlined by R. T. Williams of Phase I and Phase II metabolism are still a convenient framework for introducing the reader to metabolic processes, but these designations do not apply readily to all biotransformations. For example, the metabolic activation of 5-FU and the toxic protein binding of acetaminophen are more usefully described with regard to the specific type of chemical transformation, the enzymes involved, and the tissue site of transformation. Because the liver is a major site of drug metabolism, this chapter introduces first the hepatic Phase I enzymes and the biotransformations that they affect.

PHASE I BIOTRANSFORMATIONS

Liver Microsomal Cytochrome P450 Monooxygenases

Among the major enzyme systems affecting drug metabolism, cytochrome P450 monooxygenases[1] are dominant. In humans, there are 12 gene families of functionally related proteins comprising this group of enzymes. The cytochrome P450 enzymes, abbreviated CYPs (for cytochrome Ps) catalyze drug and endogenous compound oxidations in the liver, and also in the kidneys, gastrointestinal tract, skin, and lungs. Chemically, the processes of oxidation can be written as follows:

$$\text{Drug} + \text{NADPH} + \text{H}^+ + \text{O}_2 \rightarrow$$

$$\text{Oxidized drug} + \text{NADP}^+ + \text{H}_2\text{O}$$

The requirement for NADPH as an energy and electron source necessitates the close association, within the endoplasmic reticulum of the cell, of CYPs with NADPH–cytochrome P reductase, in a 10:1 ratio. To reconstitute the enzyme activity *in vitro*, it is necessary to include the CYP heme protein, the reductase, NADPH, molecular oxygen, and phosphatidylcholine, a lipid surfactant. The electron flow in the CYP microsomal drug oxidizing system is illustrated in Figure 11.1.

[1] In a recent historical review, R. Synder details the history of discovery of cytochrome P450 (Toxicol Sci 2000; 58:3–4). Briefly, David Keilin (1887–1963) of Cambridge University coined the name "cytochromes," for light-absorbing pigments that he isolated from dipterous flies. He named the oxygen-activating enzyme "cytochrome oxidase." Otto Warburg (1833–1970), in Berlin, studied cytochrome oxidase and measured its inhibition by carbon monoxide. He reported that the inhibitory effects of carbon monoxide were reversed by light and that the degree of reversal was wavelength dependent. Otto Rosenthal learned these spectroscopic techniques in Warburg's lab and brought them to the University of Pennsylvania when he fled Germany in the 1930s. There, with David Cooper and Ronald Estabrook, the mechanism of steroid hydroxylation was investigated. Using the Yang–Chance spectrophotometer, they determined the characteristic spectroscopic signature of the cytochrome P450–CO complex and recognized in 1963 that it was the same as that of pig and rat liver microsomal pigments reported in 1958 independently by both M. Klingenberg and D. Garfield. These spectroscopic characteristics were used in 1964 by T. Omura and R. Sato to identify cytochrome P450 as a heme protein. Rosenthal, Cooper, and Estabrook studied the metabolism of codeine and acetanilide, and demonstrated in 1965 that cytochrome P450 is the oxygen-activating enzyme in xenobiotic metabolism as well as in steroid hydroxylation.

The name cytochrome P450 derives from the spectroscopic observation that when drug is bound to the reduced heme enzyme (Fe^{2+}), carbon monoxide can bind to the complex and absorb light at a characteristic and distinctive 450 nm. The CO complex can be dissociated with light and the complex can then absorb oxygen, as shown in Figure 11.2. The spectroscopic properties of the CYP enzyme complex were of significant utility to investigators who characterized this family of enzymes with respect to their substrate specificity, kinetics, induction, and inhibition.

Of the 12 CYP gene families, most of the drug-metabolizing enzymes are in the CYP 1, 2, and 3 families. All have molecular masses of 45–60 kDa. Their naming and classification relate to their degree of amino acid sequence homology. Subfamilies have been assigned to isoenzymes with significant sequence homology to the family (e.g., CYP1A). An additional numerical identifier is added when more than one subfamily has been identified (e.g., CYP1A2). Frequently, two or more enzymes can catalyze the same type of oxidation, indicating redundant and broad substrate specificity. Thus, early efforts to categorize CYPs on the basis of biochemical transformations that they catalyzed led to confusing reports from different investigators; these confusions have now been resolved with gene sequences. Some of the principal drug-metabolizing CYPs are listed in Table 11.1 (10, 11). Three of the CYP families, 1A2, 2C, and 3A4, are shown in boldface in the table because they account for >50% of the metabolism of most drugs. Their levels can vary considerably, requiring further clinical evaluation when patient responses suggest either too much or too little of a prescribed drug is present.

It is instructive to examine which drugs are substrates for various isoforms of CYP enzymes. Table 11.2 lists some of the substrates for different CYP isoforms (10, 11). There are several examples of a single compound that is metabolized by multiple CYP enzymes (acetaminophen, diazepam, caffeine, halothane, warfarin, testosterone, zidovudine), and CYP enzymes that metabolize bioactive endogenous molecules (prostaglandins, steroids) as well as drugs.

The activity (induction or inhibition) of various CYP enzymes is influenced by a variety of factors that have been identified to date. For example, genetic polymorphisms are most significant in CYP families 1A, 2A6, 2C9, 2C19, 2D6, and 2E1. Nutrition effects have been documented in families 1A1, 1A2, 1B1, 2A6, 2B6, 2C8, 2C9, 2C19, 2D6, and 3A4 (10, 11); smoking influences families 1A1, 1A2, and 2E1 (12); alcohol influences family 2E1 (13); drugs influence families 1A1, 1A2, 2A6, 2B6, 2C, 2D6, 3A3, and 3A4, 5; and environmental xenobiotics such as polycyclic aromatic hydrocarbons,

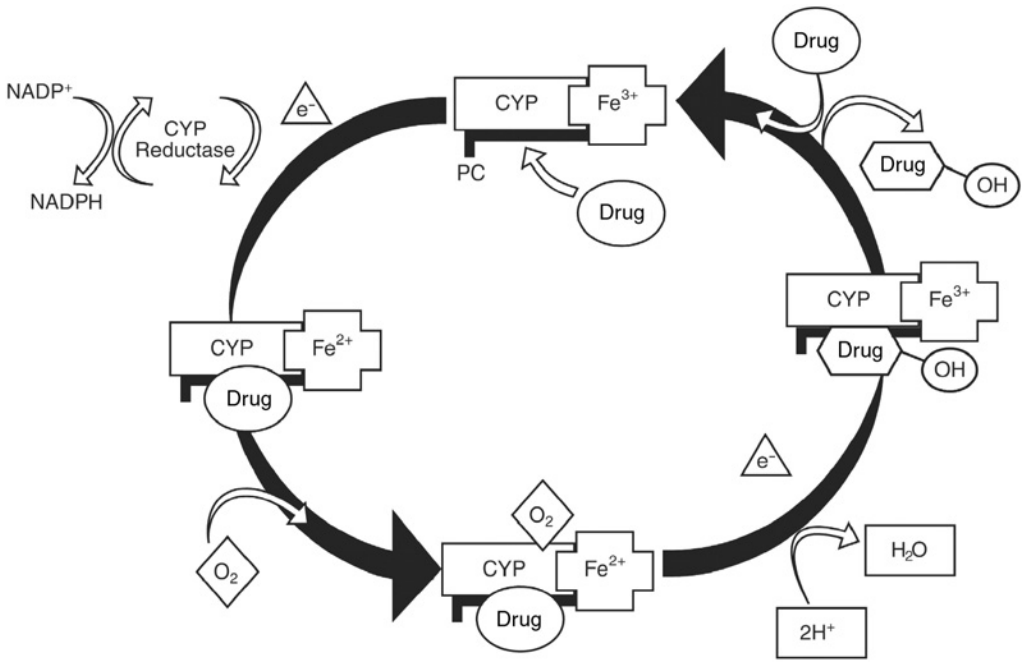

FIGURE 11.1 Free drug enters the cycle (*upper right*) and is complexed to the ferric oxidation state of the heme protein cytochrome P (CYP) in the presence of phosphatidylcholine (PC). The Fe^{3+} is reduced to Fe^{2+} by an electron generated by the conversion of NADPH to $NADP^+$ by the enzyme cytochrome P reductase (*upper left*). The reduced complex absorbs molecular oxygen (*lower middle*). Addition of a second electron from cytochrome P reductase results in the generation of one molecule of water, hydroxylation of one molecule of drug, and the oxidation of iron to Fe^{3+}. When hydroxylated drug is released from the enzyme complex (*upper right*), the cycle repeats.

dioxins, organic solvents, and organophosphate insecticides influence families 1A1, 1A2, 2A6, 1B, 2E1, and 3A4 (10).

The diverse nature of these effects is illustrated by recounting the experience of clinical pharmacologists who studied the pharmacokinetics of felodipine, a dihydropyridine calcium channel antagonist (14). They designed a study to test the effects of ethanol on felodipine metabolism. To mask the flavor of ethanol from the subjects, they tested a variety of fruit juices, selecting double-strength grapefruit juice prepared from frozen concentrate as most effective.

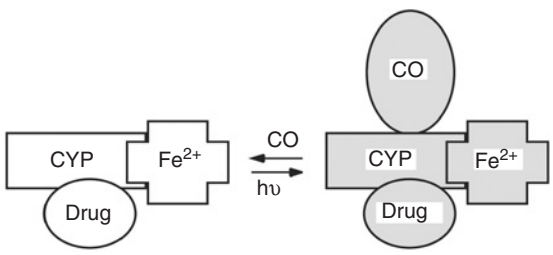

FIGURE 11.2 Cytochrome P450 has a high affinity for carbon monoxide when drugs are bound to the reduced complex, as observed spectroscopically at 450 nm.

TABLE 11.1 Human CYP Enzymes Important in Liver Metabolism of Drugs[a]

CYP enzyme[b]	Level (% of total)	Extent of variability
1A2	**~13**	**~40-fold**
1B1	<1	
2A6	~4	~30- to 100-fold
2B6	<1	~50-fold
2C	**~18**	**25- to 100-fold**
2D6	Up to 2.5	>1000-fold
2E1	Up to 7	~20-fold
2F1	—	—
2J2	—	—
3A4	**Up to 28**	**~20-fold**
4A, 4B	—	—

[a] Data from Rendic S, Di Carlo FJ. Drug Metab Rev 1997;29: 413–580.

[b] Boldface: enzymes that account for >50% of the metabolism of most drugs.

TABLE 11.2 Participation of the CYP Enzymes in Metabolism of Some Clinically Important Drugs[a]

CYP enzyme	Participation in drug metabolism (%)	Examples of substrates
1A1	3	Caffeine, testosterone, (*R*)-warfarin
1A2	10	Acetaminophen, caffeine, phenacetin, (*R*)-warfarin
1B1	1	17β-Estradiol, testosterone
2A6	3	Acetaminophen, halothane, zidovudine
2B6	4	Cyclophosphamide, erythromycin, testosterone
2C family	25	Acetaminophen (2C9), hexobarbital (2C9, 19), phenytoin (2C8, 9, 19), testosterone (2C8, 9, 19), tolbutamide (2C9), (*R*)-warfarin (2C8, 8, 18, 19), (*S*)-warfarin (2C9, 19), zidovudine (2C8, 9, 19)
2E1	4	Acetaminophen, caffeine, chlorzoxazone, halothane
2D6	18.8	Acetaminophen, codeine debrisoquine
3A4	34.1	Acetaminophen, caffeine carbamazepine, codeine, cortisol, erythromycin, cyclophosphamide, (*S*)- and (*R*)-warfarin, phenytoin, testosterone, halothane, zidovudine

[a] Data from Rendic S. Drug Metab Rev 2002;34:83–448.

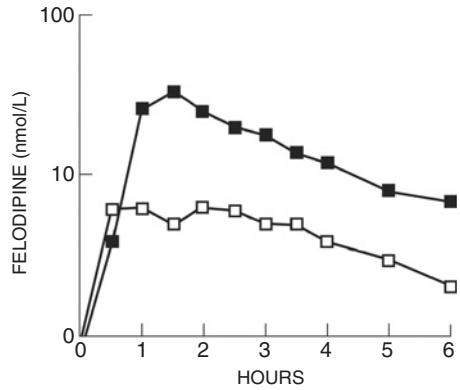

FIGURE 11.3 Plasma felodipine concentrations after oral administration to an individual of a 5-mg dose with (■) and without (□) grapefruit juice. (Reproduced with permission from Bailey DG *et al.* Br J Clin Pharmacol 1998:46;101–10.)

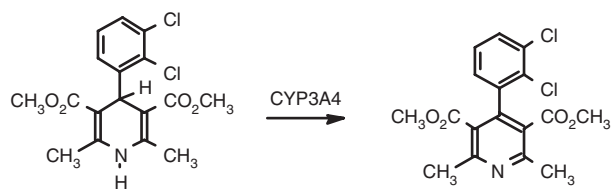

felodipine **oxidized felodipine**

SCHEME 11.6 Oxidation of felodipine by intestinal CYP3A4 limits its bioavailability.

The resulting plasma felodipine concentrations did not differ between the ethanol/felodipine and felodipine groups, but the plasma concentrations in both groups were considerably higher than those seen in any previous study. The effects of repeated grapefruit juice doses are cumulative and, as shown in Figure 11.3, may increase felodipine concentrations as much as fivefold.

Upon further investigation, it was determined that grapefruit juice administration for 6 consecutive days causes a 62% reduction in small bowel enterocyte CYP3A4 protein, thereby inhibiting the first-pass metabolism of felodipine to oxidized felodipine, shown in Scheme 11.6 (15). The effects of grapefruit juice are highly variable among individuals, depending on their basal levels of small bowel CYP3A4, but grapefruit juice does not affect the pharmacokinetics of intravenously administered felodipine because the active constituents of the juice are not absorbed and do not affect liver CYPs. Subsequent studies have shown that the degradation half-life of CYP3A4 normally is 8 hours and that at least 3 days are required to regain normal CYP3A4 function after exposure to grapefruit juice (16).

The effect of grapefruit juice on felodipine kinetics illustrates several of the difficulties and pitfalls that not only confound clinical studies of new drug products, but are a source of concern in clinical medicine. There are likely to be other food and diet supplements with similar constituents and pharmacological activity. For example, Seville orange juice contains some of the same fucocoumarins as found in grapefruit juice and exhibits the same effect with respect to felodipine pharmacokinetics (17). The differing composition of fucocoumarin mixtures in fruit juices produces variability in responses to drugs transported and metabolized by multiple mechanisms. Grapefruit juice constituents also inhibit the multidrug transporter P-glycoprotein, MDR-1, and the multidrug resistance protein 2 (MRP2), resulting in pharmacokinetic effects on cyclosporine metabolism (18). Seville orange juice does not interact with cyclosporine concentrations,

evidence for the fact that the orange juice does not contain those components that interfere with MDR-1 and MRP2 (17). The topic of drug–drug interactions is discussed in greater detail in Chapter 15. However, pharmacologically active CYP inducers or inhibitors may derive from dietary or environmental origin (e.g., insecticides or perfumes) and can only be recognized when appropriate *in vitro* or *in vivo* kinetic studies have been performed. Elderly patients are particularly at risk because they are likely to use multiple drugs as well as dietary and food supplements (19).

The example of felodipine also demonstrates that CYPs outside of the liver may have significant effects on drug concentrations. In addition to the dominant CYP3A family, the GI tract contains CYPs 2D6, 2C, 2B6, and 1A1. Similarly, CYPs are found in lung (CYPs 1A1, 2A6, 2B6, 2C, 2E, 2F, 4B1), kidney (CYPs 1A1, 1B1, 3A, 4A11), skin, placenta, prostate, and other tissues where their inhibition or activation may be of clinical relevance to the efficacy or toxicity of a therapeutic agent.

CYP-Mediated Chemical Transformations

Most drugs are relatively small organic compounds with molecular masses below 500 Da. The action of various CYP isoforms is predictable in that there are several organic structural elements that are principal targets for metabolic transformations. However, the metabolism of any specific drug is not entirely predictable, in that a specific site of metabolism may be favored for one compound and a different site for another, but structurally related, compound. The following examples are chosen to reflect some of the dominant pathways for a specific drug and illustrate the selectivity of the metabolic enzymes.

Aliphatic Hydroxylation

Hydroxylation occurs at aliphatic carbon atoms, frequently at secondary or tertiary sites in preference to primary carbon atoms, as shown in Scheme 11.7.

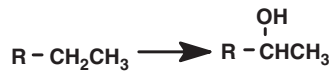

SCHEME 11.7 Hydroxylation occurs at aliphatic carbon atoms, frequently at secondary or tertiary sites in preference to primary carbon atoms.

Ibuprofen, as shown in Scheme 11.8, affords an example of aliphatic hydroxylation. Other drugs similarly metabolized include terfenadine, pentobarbital, and cyclosporine.

Aromatic Hydroxylation

Many aromatic drugs are hydroxylated either directly through asymmetrical oxygen transfer or through an unstable arene oxide intermediate, as shown in Scheme 11.9.

Because the half-life of the epoxide intermediate is short, immediate rearrangement or reaction may lead to a single metabolite or a variety of substituted metabolites. The intermediacy of an epoxide intermediate can be inferred by the identification of para- and meta-hydroxylated and dihydrodiol metabolites, although their relative abundances will vary with substitution and steric considerations. Acetanilide, like phenobarbital discussed previously, exemplifies the aromatic compounds that rearrange rapidly following CYP-mediated arene epoxide formation leading to a single metabolite, as shown in Scheme 11.10.

The major metabolite of phenytoin is *para*-hydroxyphenytoin, formed through an arene epoxide intermediate as shown in Scheme 11.11. Microsomal epoxide hydrolase (HYL1) is widely distributed in tissues and serves a protective role in converting longer lasting arene oxide intermediates to diols. The arene epoxide of phenytoin is detoxified through HYL1 to form the dihydrodiol (20).

Phenytoin administration during pregnancy may produce a constellation of congenital abnormalities, including cleft palate. This has been ascribed to phenytoin–arene oxide reactivity with cellular DNA in tissues lacking the protective effects of HYL1 (21, 22).

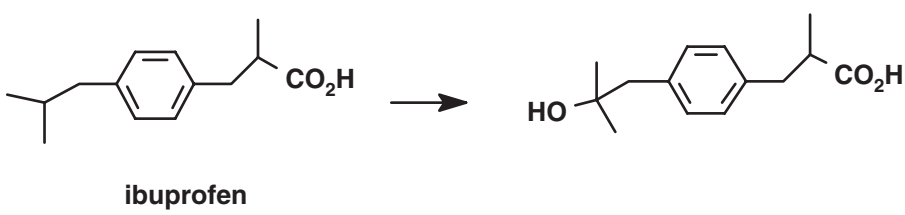

ibuprofen

SCHEME 11.8 Ibuprofen is an example of a drug that undergoes aliphatic hydroxylation. Other drugs similarly metabolized include terfenadine, pentobarbital, and cyclosporine.

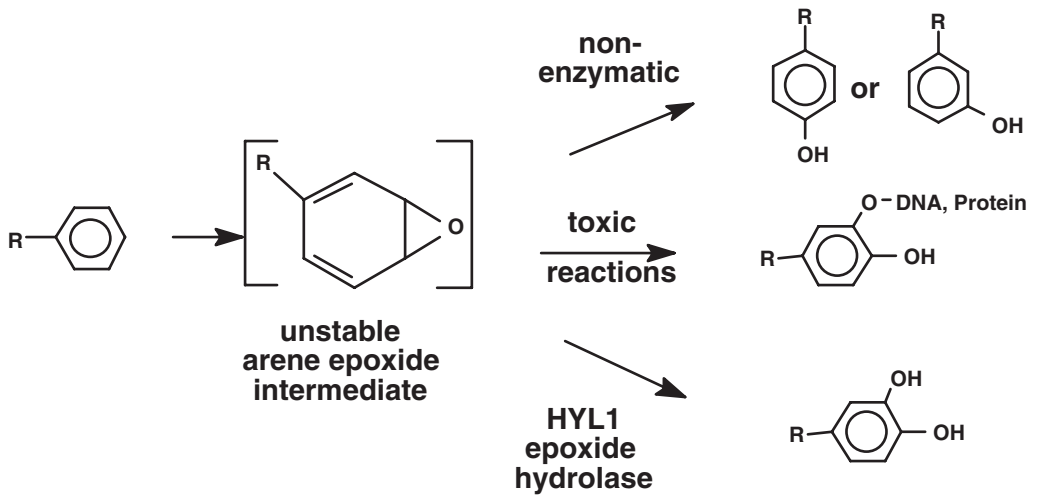

SCHEME 11.9 Hydroxylation of aromatic carbon atoms often proceeds through a reactive and unstable arene epoxide intermediate. HYL1, Microsomal epoxide hydrolase.

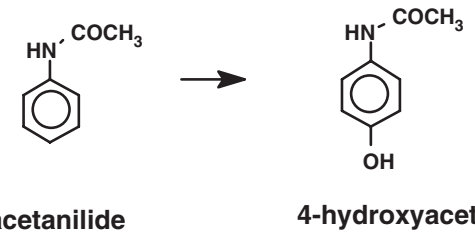

SCHEME 11.10 Acetanilide, like phenobarbital discussed previously, exemplifies the aromatic compounds that rearrange rapidly following CYP-mediated arene epoxide formation.

Gaedigk *et al*. (20) have demonstrated that there is tissue-specific expression of microsomal HYL1 and not a single HYL1 transcript and promoter region. Liang *et al*. (23) identified several potential *cis*-regulatory elements and found that transcription factor GATA-4 is probably the principal factor regulating liver specific expression.

N-Dealkylation (O-Dealkylation, S-Dealkylation)

The mechanism of CYP-catalyzed *N*-dealkylation has received considerable study (24). *N*-Dealkyation

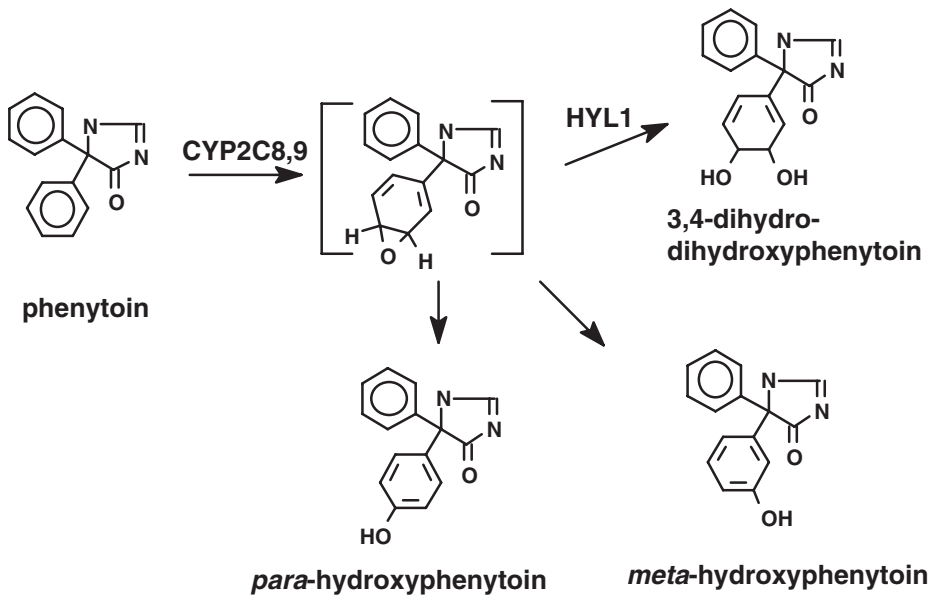

SCHEME 11.11 The metabolism of phenytoin through an unstable arene epoxide results in a triad of oxidized metabolites that is characteristic for this intermediate.

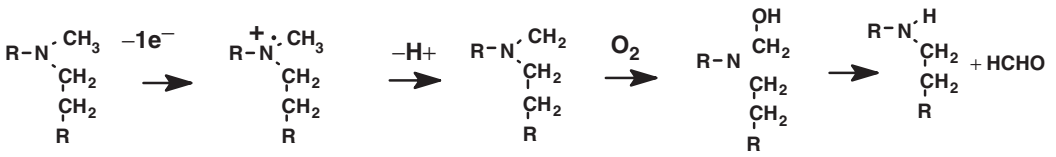

SCHEME 11.12 N-Demethylation generates formaldehyde and is an example of N-dealkylation.

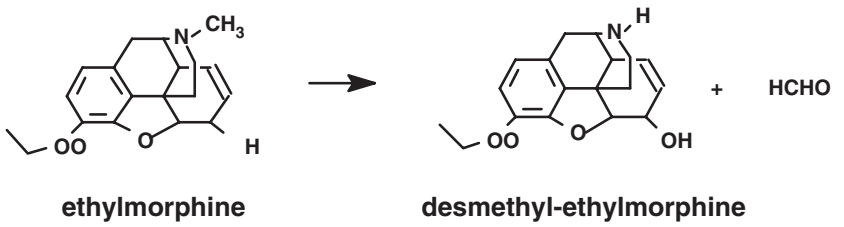

SCHEME 11.13 Ethylmorphine exemplifies drugs metabolized by N-dealkylation; other drugs similarly metabolized include lidocaine, aminopyrine, acetophenetedine, and 6-methylthiopurine.

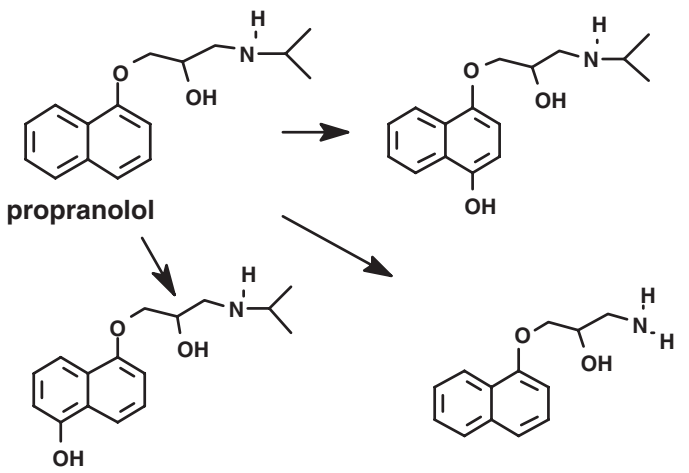

SCHEME 11.14 Propranolol is an example of a compound that forms multiple alternative metabolites. Two different aromatic ring hydroxylated metabolites and the *N*-dealkylated metabolite are excreted in urine.

appears to involve radical cation intermediates and molecular oxygen (not water). Formally, *O*- and *S*-dealkylation are related to *N*-dealkylation, although the mechanisms may differ. N-Demethylation is a frequent route of metabolism of drugs containing methylamine functionalities, as shown in Scheme 11.12.

Drugs containing multiple functional groups are substrates for multiple drug-metabolizing enzymes and pathways. The *N*-demethylation vs *O*-dealkylation of ethylmorphine (Scheme 11.13) demonstrates that one reaction pathway may predominate. Propranolol is an example of a compound that forms multiple alternative metabolites (Scheme 11.14).

Oxidative Deamination

Oxidative deamination proceeds through an unstable carbinolamine intermediate (Scheme 11.15). Amphetamine is an example of a drug metabolized through oxidative deamination (Scheme 11.16).

Dehalogenation

As discussed in Chapter 16, dehalogenation by liver enzymes of a number of inhalation anesthetics (halothane, methoxyflurane) and halogenated solvents yields chemically reactive free radicals that play an important role in the hepatotoxicity of these compounds. Dehalogenation produces a free radical

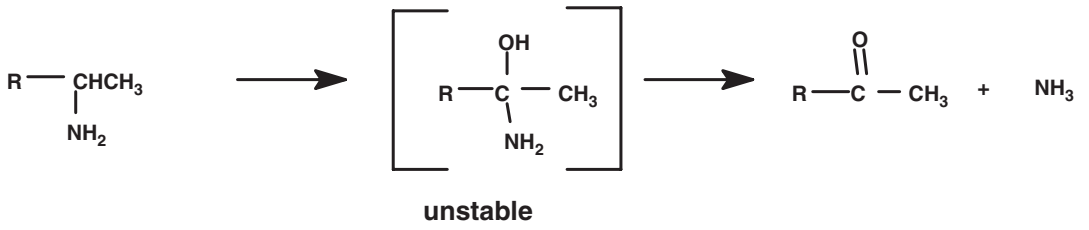

SCHEME 11.15 Oxidative deamination proceeds through an unstable carbinolamine intermediate.

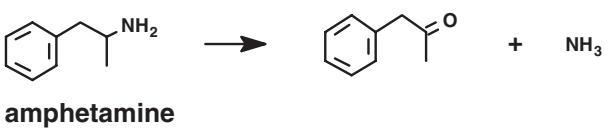

SCHEME 11.16 Amphetamine is metabolized to an inactive ketone.

intermediate that may be detected by its interaction with cellular lipids, as shown in general form in Scheme 11.17. Dehalogenation of carbon tetrachloride is illustrated in Scheme 11.18.

N-Oxidation

Amines are readily oxidized by CYP enzymes. Aliphatic amines are converted to hydroxylamines as shown in Scheme 11.19; compared to the parent amines, hydroxylamines are less basic. Aromatic amines are converted to products that are more toxic than their parent amines are, frequently producing hypersensitivity or carcinogenicity.

Dapsone is oxidized by CYP2E1 with high affinity both *in vitro* and *in vivo*, and also by CYP3A4 (Scheme 11.20). The major side effects of dapsone (methemoglobinemia, agranulocytosis) are linked to its *N*-oxidation (25, 26).

Other *N*-oxidized substrates include mianserin and clozapine, both catalyzed by CYP1A2 and CYP3A4. Because the products are identical to those produced by flavin monooxygenases (FMOs), enzymatic studies are required to identify which enzyme system is active during *in vivo* metabolism.

S-Oxidation

Sulfur is readily oxidized, nonenzymatically as well as enzymatically (Scheme 11.21). Chlorpromazine metabolism provides an example of *S*-oxidation by CYP3A (Scheme 11.22). Chlorpromazine is also metabolized by *N*-oxidation and *N*-dealkylation pathways, resulting in a multiplicity of excreted products.

There are cases of drug substrates metabolized preferentially by CYP3A and not by FMOs. Tazofelone, an experimental agent for treating patients with inflammatory bowel disease, is a sulfur and nitrogen heterocyclic compound that is sulfoxidized by human microsomal CYP3A but not FMO (Scheme 11.23) (28).

Non-CYP Biotransformations

Hydrolysis

Hydrolyses of esters or amides are common reactions catalyzed by ubiquitous esterases, amidases, and

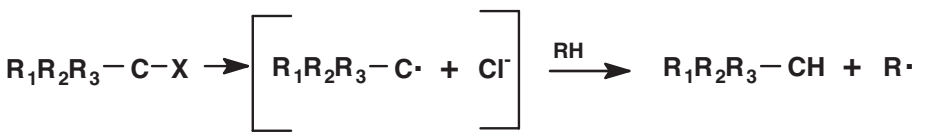

SCHEME 11.17 Dehalogenation produces a free radical intermediate that may be detected by its interaction with cellular lipids.

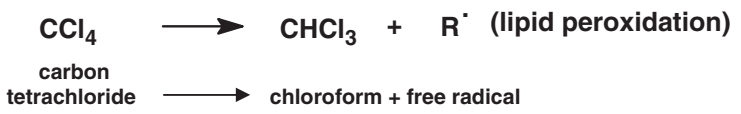

SCHEME 11.18 The metabolism of carbon tetrachloride is characterized by the formation of free radicals. Halothane and methoxyflurane are similarly metabolized.

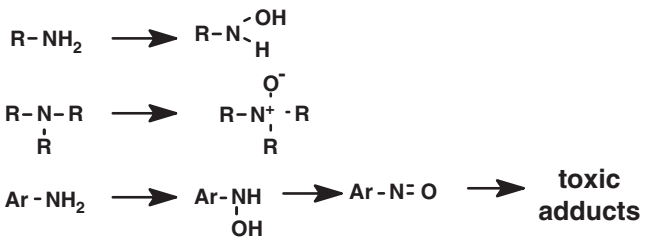

SCHEME 11.19 The nitrogen atom is a site for oxidation, potentially leading to toxic by-products.

proteases found in every tissue and physiological fluid. These enzymes exhibit widely differing substrate specificities. The hydrolytic reactions shown in Scheme 11.24 are the reverse of Phase II conjugation reactions, especially for the acetylation reaction discussed later in this chapter.

Aspirin (acetylsalicylic acid) is an example of a compound that is hydrolyzed readily in plasma (Scheme 11.25). Aspirin has a plasma half-life of 15 minutes in plasma. Salicylic acid, the active metabolite of aspirin (anti-inflammatory activity), has a much longer half-life of 12 hours. However, salicylic acid irritates the gastric mucosa, necessitating the use of acetylsalicylic acid or sodium salicylate in clinical practice.

Reduction

Although most drugs are metabolized by oxidative processes, reduction may be a clinically important pathway of drug metabolism. In most cases these metabolic transformations are carried out by reductase enzymes in intestinal anaerobic bacteria. In the case of

SCHEME 11.20 Dapsone is a substrate for *N*-oxidation.

SCHEME 11.21 Sulfur is readily oxidized, nonenzymatically as well as enzymatically.

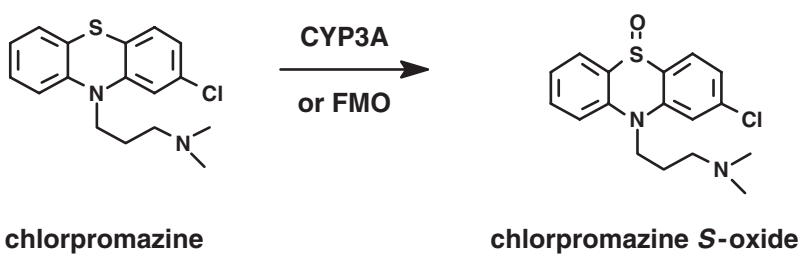

SCHEME 11.22 *S*-Oxidation of chlorpromazine by CYP3A or FMO.

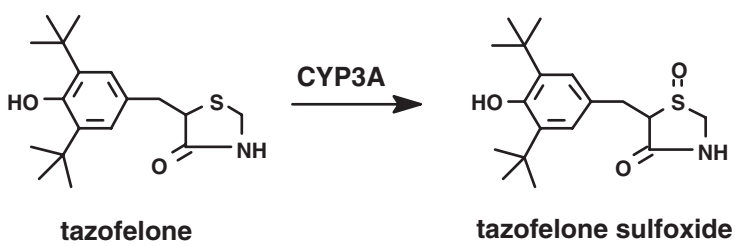

SCHEME 11.23 Although *S*-oxidation is a major route of taxofelone metabolism, this drug also typifies those with multiple alternative sites of metabolism.

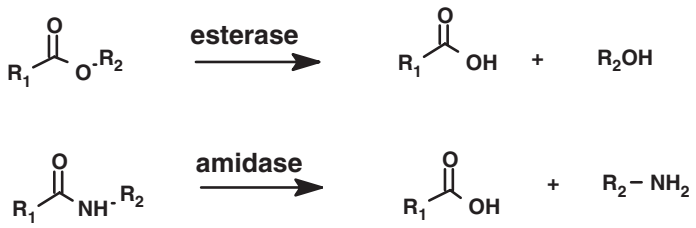

SCHEME 11.24 Hydrolytic enzymes are involved in the metabolism of many endogenous compounds.

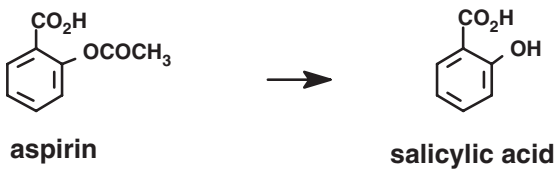

SCHEME 11.25 Structures of aspirin and its active metabolite salicylic acid.

prontosil, an aromatic azo-function (Ar_1–N = N–Ar_2) is reduced, forming two aniline moieties (Ar_1–NH_2, Ar_2–NH_2). One of the reduced metabolites is sulfanilamide, the active antibacterial agent first recognized in 1935 (29). Since biotransformation is required for antibacterial activity, prontosil is referred to as a *prodrug*.

A second example, shown in Scheme 11.26, is the metabolic inactivation of digoxin by *Eubacterium lentum* in the intestine (30). Approximately 10% of patients taking digoxin excrete large quantities of the inactive reduction product dihydrodigoxin (31). As discussed in Chapter 4, the enteric metabolism of digoxin reduces digoxin bioavailability significantly in some patients. Conversely, when such patients require antibiotic therapy, the resulting blood levels of digoxin may reach toxic levels because the antibiotic halts the previously robust inactivation by *E. lentum*, and digoxin bioavailability is thereby increased.

Oxidations

Flavine Monooxygenases

Flavine monooxygenases are microsomal enzymes that catalyze the oxygenation of nucleophilic heteroatom-containing (nitrogen, sulfur, phosphorus, selenium) compounds, producing metabolites structurally similar to those produced by CYPs. Unlike CYPs, the FMOs do not require tight substrate binding to the enzyme, but only a single point contact with the very reactive hydroperoxyflavin monooxygenating agent. FMOs are also unlike CYPs in that FMOs do not contain metal and are very heat labile. The quantitative role of FMOs vs CYPs in the metabolism of any specific drug cannot be predicted from an examination of the drug structure; in fact, many compounds are substrates of both enzymes. Six different mammalian FMO gene subfamilies have been identified and polyclonal antibodies have permitted identification of FMO isoforms from liver and lung from different species (humans, pigs, rabbits) (32). FMOs exhibit a very broad ability to oxidize structurally different substrates, suggesting that they contribute significantly to the metabolism of a number of drugs. FMOs require molecular oxygen, NADPH, and flavin adenosine dinucleotide. Factors affecting FMOs (diet, drugs, sex) have not been as highly studied as they have for CYPs, but it is clear that FMOs are prominent metabolizing enzymes for common drugs such as nicotine and cimetidine (33).

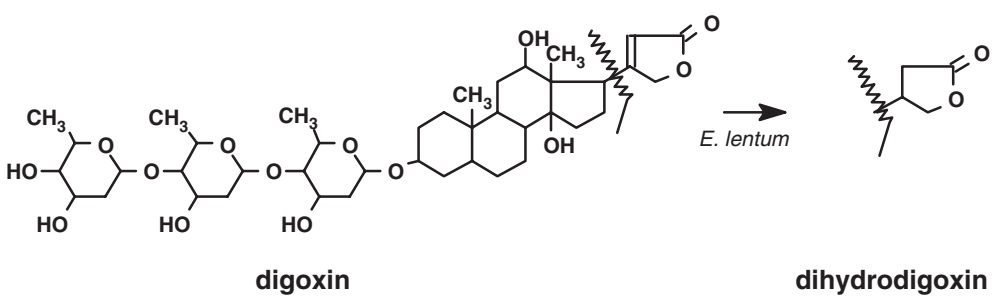

SCHEME 11.26 Reduction of the side chain of digoxin eliminates pharmacologic activity.

SCHEME 11.27 Nicotine is oxidized in a stereospecific manner to an *N*-oxide.

Nicotine is an example of a compound that undergoes FMO3-catalyzed N-oxidation, as shown in Scheme 11.27. About 4% of nicotine is stereoselectively metabolized to trans-(*S*)-(−)-nicotine *N*-1′ oxide in humans by FMO3, whereas 30% of an administered dose appears as cotinine, a CYP2A6 product (34, 35). Other examples of FMO *N*-oxidation include trimethylamine, amphetamine, and the phenothiazines (33). As described previously, FMO3 catalyzes *S*-oxidation of substrates such as cimetidine, shown in Scheme 11.28, and chlorpromazine, also a CYP3A substrate (Scheme 11.22).

Monoamine Oxidases

Monoamine oxidases (MAO-A and MAO-B) are mitochondrial enzymes that oxidatively deaminate endogenous biogenic amine neurotransmitters such as dopamine, serotonin, norepinephrine, and epinephrine. MAOs are like FMOs in that they catalyze the oxidation of drugs to produce drug metabolites that are identical in chemical structures to those formed by CYPs. Because the resulting structures are identical, oxidative deamination by MAO can only be distinguished from CYP oxidative deamination by drug and enzyme characterization, not by metabolite structure. MAOs are found in liver, kidney, intestine, and brain. Some drugs (tranylcypromine, selegiline) have been designed as irreversible "suicide" substrates to inhibit MAO in order to alter the balance of CNS neurotransmitters, and both the response to these inhibitors and the study of *in vitro* enzyme preparations are used to distinguish this enzymatic process. Similarly, diamine oxidase catalyzes oxidative deamination of endogenous amines such as histamine and the polyamines putrescine and cadaverine, and can contribute to the oxidative deamination of drugs. Diamine oxidase is found in high levels in liver, intestine, and placenta, and converts amines to aldehydes in the presence of oxygen, similar to the action of CYPs.

Alcohol and Aldehyde Dehydrogenases

Alcohols and aldehydes are metabolized by liver dehydrogenases that are nonmicrosomal and by nonspecific liver enzymes that are important in the catabolism of endogenous compounds. Ethanol is a special example of a compound whose metabolism is clinically relevant in that ethanol may interact with prescribed pharmaceuticals either metabolically or pharmacodynamically. Ethanol is metabolized first to acetaldehyde by alcohol dehydrogenase and then to acetic acid by aldehyde dehydrogenase, as shown in Scheme 11.29. These enzymes also play an important role in the metabolism of other

SCHEME 11.28 Cimetidine is an example of a drug metabolized by FMO3-catalyzed *S*-oxidation; other FMO3 substrates include chlorpromazine, also a CYP3A substrate.

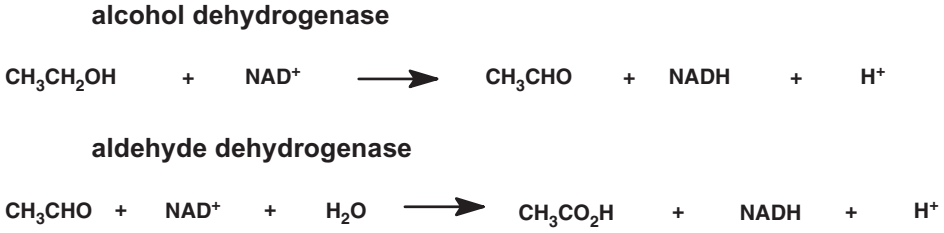

SCHEME 11.29 The metabolic products of alcohol dehydrogenase are substrates for aldehyde dehydrogenase.

drugs containing alcohol functional groups. There are also CYP-dependent microsomal ethanol-oxidizing enzymes that provide metabolic redundancy, but alcohol and aldehyde dehydrogenases are the major enzymes involved in ethanol metabolism under normal physiological conditions.

PHASE II BIOTRANSFORMATIONS (CONJUGATIONS)

Drugs are frequently metabolized by covalent addition of an endogenous species such as a sugar or an amino acid. This addition, or conjugation, usually converts a lipophilic drug into a more polar product, as noted in the example of phenobarbital metabolism to hydroxyphenobarbital-glucuronide (Scheme 11.1). There are multiple conjugation reactions — glucuronidation, sulfation, acetylation, methylation, and amino acid conjugation (glycine, taurine, glutathione). Taken together, these Phase II biotransformations are analogous and comparable. However, their catalytic enzyme systems differ greatly from each other, as do the properties of resulting metabolites. Not all of these metabolites are pharmacologically inactive; some have therapeutic activity whereas others are reactive and toxic intermediates. As a consequence, it is more useful to separately present and discuss each of the three major conjugation reactions. In humans, glucuronidation is a high-capacity pathway, sulfation is a low-capacity pathway, and acetylation exhibits high interindividual variability.

Glucuronidation

The glucuronidation pathway often accounts for a major portion of drug metabolites that are found excreted in urine. Glucuronides are formed by a family of soluble liver microsomal enzymes, the uridine diphosphate (UDP)-glucuronosyltransferases (UGTs). Although glucuronide formation occurs predominantly in the liver, it also takes place in the kidneys and brain. There are two subfamilies comprising multiple (at least 20) isoforms with very different primary amino acid structures (36, 37). The UGT1 subfamily glucuronidates phenols and bilirubin; the substrates for UGT2 include steroids and bile acids. The subfamilies that have been cloned and expressed exhibit limited substrate specificity. The high capacity of human liver for glucuronidation may be due to the broad substrate redundancy in this family. UGTs catalyze the transfer of glucuronic acid from UDP-glucuronic acid to an oxygen or nitrogen atom in a drug substrate, as shown in Scheme 11.30. There is considerable variation allowed in the substrates for glucuronidation, and phenols, alcohols, aromatic or aliphatic amines, and carboxylic acids are suitable functional groups for glucuronidation.

Regarding the glucuronidation of morphine shown in Scheme 11.31, morphine-3-glucuronide is the major metabolite (45–55%); morphine-6-glucuronide is 20–30% of that level. Importantly, morphine-6-glucuronide is a more potent analgesic than is its parent compound in humans. On the other hand, morphine-3-glucuronide lacks analgesic activity, but antagonizes the respiratory depression induced by morphine and morphine-6-glucuronide. Recognition

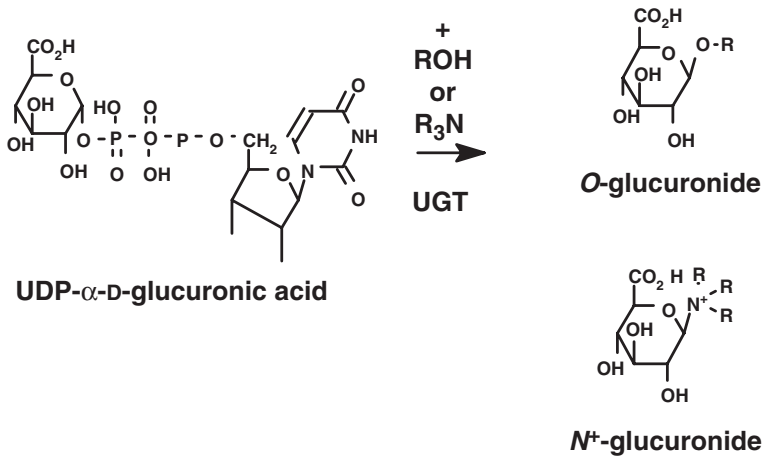

SCHEME 11.30 Nitrogen- and oxygen-linked glucuronide formation markedly enhances the polarity and water solubility of drugs.

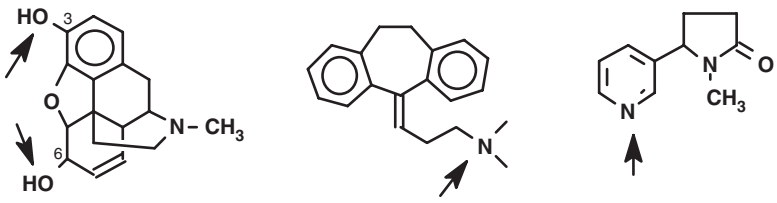

morphine amitriptyline cotinine

SCHEME 11.31 *O*-Glucuronides (ethers) can form from phenols such as morphine (3-phenol), *p*-hydroxyphenobarbital (Scheme 11.1), *p*-hydroxyphenytoin (Figure 2.8), and alcohols such as morphine (6-hydroxyl). *N*-Glucuronides can be formed from aliphatic amines such as amitriptyline, or aromatic amines such as the nicotine metabolite cotinine.

of the potency of morphine-6-glucuronide has led to its testing as a drug for intravenous administration (38, 39).

Drug N^+-glucuronides, the quaternary ammonium products from glucuronidation of tertiary amines, have only recently been identified in urine as major drug metabolites because appropriate analytical methods were not available previously (40). The percentage of the administered dose of amitryptiline excreted in human urine as amitryptiline-N^+-glucuronide is ~8%, and 17% of a nicotine dose is recovered as cotinine-N_1-glucuronide. The pharmacological properties of most drug N^+-glucuronides have not yet been determined, but the *N*-glucuronides of arylamines have carcinogenic properties. In particular, *N*-glucuronides formed in the liver can be hydrolyzed in acidic urine to a reactive electrophilic intermediate that attacks the bladder epithelium.

Sulfation

Sulfation (or sulfonation) is catalyzed by sulfotransferases (STs), which metabolize phenols, hydroxylamines, or alcohols to sulfate esters as shown in Scheme 11.32, converting somewhat polar to very polar functionalities that are fully ionized at neutral pH. Like glucuronidation, there are multiple ST subfamilies (more than 10 in humans). One subfamily is cytosolic and associated with drug metabolism and the other is membrane-bound, localized in the Golgi apparatus, and associated with sulfation of glycoproteins, proteins, and glycosaminoglycans (41). The STs are widely distributed in human tissues. Five cytosolic ST isoforms have been identified and characterized in human tissue; four catalyze sulfation of phenols, one the sulfation of hydroxy steroids.

Also by analogy to glucuronidation, sulfated metabolites may be pharmacologically more active

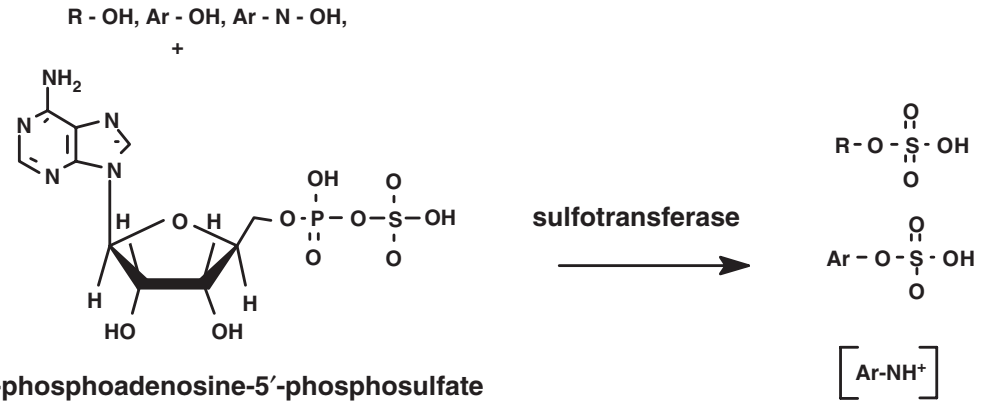

3′-phosphoadenosine-5′-phosphosulfate

SCHEME 11.32 Sulfation (or sulfonation) metabolizes phenols, hydroxylamines, or alcohols to sulfate esters, converting a somewhat polar to a very polar functionality that is ionized at neutral pH.

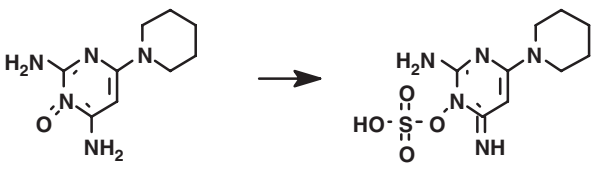

SCHEME 11.33 Topically applied minoxidil requires sulfation for bioactivation.

SCHEME 11.35 Acetylation is the major route of isoniazid metabolism.

than their respective parent drugs. For example, minoxidil (shown in Scheme 11.33), when applied to the scalp for the treatment of baldness, requires bioactivation by STs present in hair follicles (42, 43). Minoxidil sulfate is a potent vasodilator, apparently because it is a potassium channel agonist.

A second example of sulfate bioactivation derives from the observed carcinogenicity of aromatic amines, such as those derived from coal tar (44). The polycyclic aromatic amines are *N*-hydroxylated by CYPs and then sulfated to form unstable *N*-*O*-sulfates that decompose and produce reactive nitrenium ion intermediates, which form DNA and protein adducts. One environmental/genetic hypothesis of colon cancer etiology involves the interaction between dietary aromatic amines and the polymorphic expression of the appropriate STs for their activation to procarcinogenic reactive intermediates (44, 45).

Acetylation

The acetyltransferase enzymes are cytosolic and found in many tissues, including liver, small intestine, blood, and kidney. Acetylation substrates are aromatic or aliphatic amines, or hydroxyl or sulfhydryl groups (Scheme 11.34).

The *N*-acetyltransferase (NAT) enzymes have been most highly characterized in humans for the historical reason that isoniazid, a NAT substrate, has played a pivotal role in treating patients with tuberculosis. The major route of metabolism of isoniazid is shown in Scheme 11.35.

In treating Caucasian and Black patients with isoniazid, it was noted that the half-life of the parent drug was 70 minutes in about one-half of the patients (*rapid acetylators*) and 3 hours in the other half (*slow acetylators*). There are two NAT families of enzymes, NAT1 and NAT2, that are distinguished by their preferential acetylation of *p*-aminosalicylic acid (NAT1) or sulfamethazine (NAT2). As discussed in Chapter 13, isoniazid is a substrate for NAT2, a highly polymorphic enzyme, resulting from at least 20 different NAT2 alleles. Slow acetylators are homozygous for the NAT2 slow acetylator allele(s); rapid acetylators are homozygous or heterozygous for the fast NAT2 acetylator alleles. There are clinical consequences of fast and slow acetylation from the different blood levels of isoniazid that result from patient differences in metabolism. Side effects such as peripheral neuropathy (46) and hepatitis (47) occur more frequently with slow acetylators.

The Phase II acetylation of aromatic hydroxylamines, the products of Phase I metabolism of aromatic amines, constitutes a toxic metabolic pathway that has been implicated in carcinogenesis, as illustrated in Scheme 11.36. Rapid acetylators (with respect to NAT2) have been shown to be associated with an increased risk of colon cancer. The mechanism of this toxicity has implicated the intermediacy of the reactive

SCHEME 11.34 Acetylation targets aromatic or aliphatic amines, hydroxyl or sulfhydryl groups, transferring the acyl group from Coenzyme A to drug substrates.

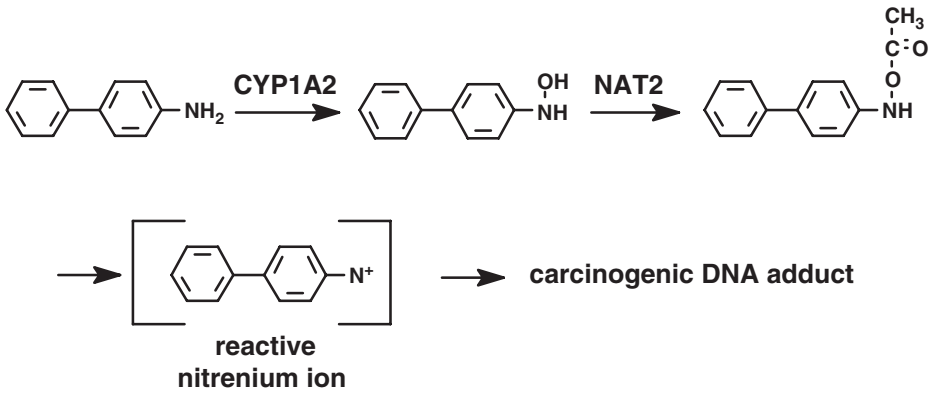

SCHEME 11.36 Reactive nitrenium ions may be produced in the metabolism of aromatic amines through hydroxylation and acetylation.

nitrenium ion, which is formed spontaneously from unstable acetylated aromatic hydroxylamines [48].

ADDITIONAL EFFECTS ON DRUG METABOLISM

Enzyme Induction and Inhibition

The effect of repeated doses of a drug, or of another drug or dietary or environmental constituent on that drug, may be to enhance or inhibit the metabolism of the drug. Both enzyme induction and inhibition are important causes of drug interactions (Chapter 15). Phenobarbital is prototypical of one general type of inducer; polycyclic aromatic hydrocarbons are representative of another class that affects different CYPs. The mechanism for environmental and drug induction of CYPs involves the intermediacy of ligand-regulated transcription factors. The pregnane X receptor (PXR) and the constitutive androstane receptor (CAR) are both heterodimers with the retinoid X receptor and are further described in Chapter 15. PXR and CAR are highly expressed in liver and intestine, and seem to have evolved to exhibit protective and nonspecific responses to a very wide range of exogenous compounds, as shown in Figure 11.4 (49).

Species

Different species metabolize drugs to produce varying and characteristic profiles with regard to percentages of metabolite formed in both Phase I and II reactions. This has long been recognized, but it is now known that there is considerable genetic variability in the primary structures of the CYPs and in their regulatory control through DNA- and ligand-binding domains of the PXR and CAR transcription

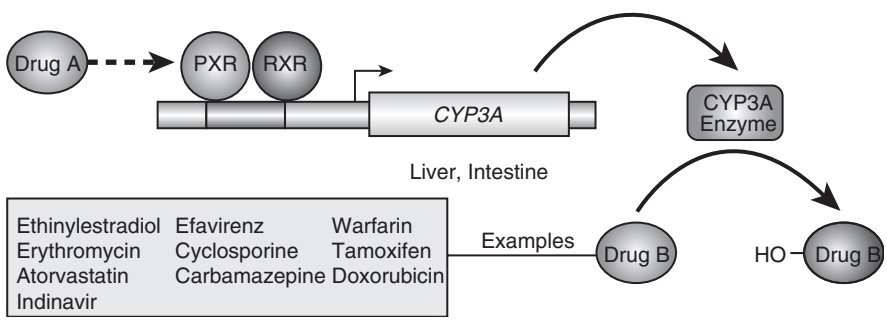

FIGURE 11.4 Mechanistic basis of enzyme induction resulting from drug–drug interactions. The orphan nuclear pregnane X receptor (PXR) is a transcription factor that forms a heterodimer with the nuclear retinoid X receptor (RXR) to regulate expression of the *CYP3A* gene. Drug A binds to PXR and induces expression of the CYP3A enzyme, thereby accelerating metabolism of drug B. (Reproduced with permission from Wilson TM, Kliewer SA. Nat Rev Drug Discov 2002;1:259–66.)

factor receptors. The human and rhesus PXR receptors share 100% homology in their DNA-binding domain, and 95% homology in their ligand-binding domain. In contrast, rats share 96% and 76% homology in their DNA- and ligand-binding domains, respectively. The human CAR receptor DNA-binding domain has 66% homology with the human PXR domain and there is only 45% homology in the ligand-binding domains, allowing for considerable diversity in PXR- and CAR-mediated responses to different compounds. Metabolism studies conducted in rodents, dogs, monkeys, and other species may be useful in establishing guidelines for likely drug effects in humans, but rarely can be used for predictive interspecies scaling, a topic discussed in Chapter 30.

Ruelius (50) has reviewed several examples of species differences in the metabolism of specific drugs. For example, radiolabeled ciramadol, an orally active analgesic, was administered to rats, dogs, rhesus monkeys, and humans. The interspecies comparison of the resulting urinary recovery of parent drug and metabolites in this study (Table 11.3) exemplifies the experience of investigators with other drugs.

Guengerich (51) has reviewed several studies of interspecies activities of CYP isoforms. For example, CYP1A2 has been purified and structurally characterized from rats, rabbits, mice, and humans. The different CYP1A2 isoforms catalyze most of the same biotransformations, but there are cases in which the rat and human isoforms differ in substrate activation. Considering that rat and human CYP1A2 are only 75% homologous in amino acid sequence, it is not surprising that their activities differ. Even a single amino acid mutation in rat CYP1A2 results in significant changes in catalytic activity. Further, the concentrations of CYP1A2 vary by 25-fold in humans (10–245 pmol/mg protein) and differ from those in the rat (4–35 pmol/mg protein in untreated vs 830–1600 pmol/mg protein in polychlorinated biphenyl treated). Monkeys lack CYP1A2, a critical issue in the choice of this animal for cancer bioassays. Interspecies variation in the CYP3A subfamilies provides an especially important example because CYP3A4 is involved in the oxidation of 59% of the drugs used today. Humans express CYPs 3A4, 3A5, and 3A7 (the latter in fetal tissue and placenta); rats express CYPs 3A1, 3A2, 3A9, 3A18, and 3A6; rabbits express only CYP3A6. Such genetically determined enzyme differences are reflected in other drug-metabolizing enzymes and in their responses to inducers and inhibitors, further complicating extrapolation of drug metabolism between species.

Sex

The effects of sex on drug disposition and pharmacokinetics have been incompletely evaluated but may be significant. In addition, the contribution of sex differences is sometimes difficult to separate from the major complicating effects of dietary and environmental inducers and inhibitors on drug-metabolizing enzymes. Sex differences in drug metabolism are considered in detail in Chapter 21.

Age

The effects of age on drug metabolism are discussed in specific chapters dealing with pediatric (Chapter 23) and geriatric (Chapter 24) clinical pharmacology. The most significant age differences are expressed developmentally in that drug-metabolizing enzyme systems frequently are immature in neonates. An important example of this is provided by UDP-glucuronosyltransferase. Particularly in premature infants, hepatic UDP-glucuronosyltransferase activity is markedly decreased and does not reach adult levels until 14 weeks after birth (52). This results in increased serum levels of unconjugated bilirubin and a greater risk of potentially fatal kernicterus, which is likely when the serum bilirubin levels exceed 30 mg/dL. Low conjugation capacity can be exacerbated by

TABLE 11.3 Renal Elimination of Ciramidol and Its Major Metabolites following a Single Oral Dose of [^{14}C]Ciramidol[a]

	Percentage of dose in urine			
Species	**Total radioactivity**	**Unchanged ciramidol**	**Aryl-*O*-glucuronide**	**Alicyclic-*O*-glucuronide**
Rat	64	33	3	5
Dog	—	3	12	—
Rhesus monkey	88	<1	21	32
Human	94	44	38	2

[a] Data from Ruelius HW. Xenobiotica 1987;17:255–65.

concurrent therapy with sulfonamides, which compete with bilirubin for albumin binding, and can be ameliorated either by prenatal therapy of the mother or by postnatal therapy of the infant with phenobarbital to stimulate the gene transcription of CYPs and UDP-glucuronosyltransferase (53). However, phenobarbital therapy is no longer favored as a pharmacological approach to this problem because prenatal therapy with phenobarbital results in a significant decrease in prothrombin levels and because postnatal phototherapy is much more effective (54).

REFERENCES

1. Williams RT. Detoxication mechanisms. London: Chapman and Hall Ltd; 1959. p. 796.
2. Holtzman JL. The role of covalent binding to microsomal proteins in the hepatotoxicity of acetaminophen. Drug Metab Rev 1995;27:277–97.
3. Nelson SD. Mechanisms of the formation and disposition of reactive metabolites that can cause acute liver injury. Drug Metab Rev 1995;27:147–77.
4. Rumack BH. Acetaminophen overdose. Am J Med 1983;75:104–12.
5. Mautz FR. Reduction of cardiac irritability by the epicardial and systemic administration of drugs as a protection in cardiac surgery. J Thorac Surg 1936; 5:612–8.
6. Mark LC, Kayden HJ, Steele JM *et al.* The physiological disposition and cardiac effects of procaine amide. J Pharmacol Exp Ther 1951;102:5–15.
7. Atkinson AJ Jr, Ruo TI, Piergies AA. Comparison of the pharmacokinetic and pharmacodynamic properties of procainamide and *N*-acetylprocainamide. Angiology 1988;39:655–67.
8. Woolf TF, ed. Handbook of drug metabolism. New York: Marcel-Dekker, Inc; 1999. p. 596.
9. Baselt RC. Disposition of toxic drugs and chemicals in man. Foster City, CA: Biomedical Publications; 2002. p. 1146.
10. Rendic S. Summary of information on human CYP enzymes: Human P450 metabolism data. Drug Metab Rev 2002;34:83–448.
11. Rendic S, Di Carlo FJ. Human cytochrome P450 enzymes: A status report summarizing their reactions, substrates, inducers, and inhibitors. Drug Metab Rev 1997;29:413–580.
12. Czekaj P, Wiaderkiewicz A, Florek E, Wiaderkiewicz R. Tobacco smoke-dependent changes in cytochrome P450 1A1, 1A2, and 2E1 protein expressions in fetuses, newborns, pregnant rats, and human placenta. Arch Toxicol 2005;79:13–24.
13. Lieber CS. Cytochrome P-4502E1: Its physiological and pathological role. Physiol Rev 1997;77:517–44.
14. Bailey DG, Malcolm J, Arnold O, Spence JD. Grapefruit juice–drug interactions. Br J Clin Pharmacol 1998;46:101–10.
15. Lown KS, Bailey DG, Fontana RJ *et al.* Grapefruit juice increases felodipine oral availability in humans by decreasing intestinal CYP3A protein expression. J Clin Invest 1997;99:2545–53.
16. Takanaga H, Ohnishi A, Murakami H *et al.* Relationship between time after intake of grapefruit juice and the effect on pharmacokinetics and pharmacodynamics of nisoldipine in healthy subjects. Clin Pharmacol Ther 2000;67:201–14.
17. Malhotra S, Bailey DG, Paine MF, Watkins PB. Seville orange juice–felodipine interaction: Comparison with dilute grapefruit juice and involvement of furocoumarins. Clin Pharmacol Ther 2001;69:14–23.
18. Honda Y, Ushigome F, Koyabu N *et al.* Effects of grapefruit juice and orange juice components on P-glycoprotein- and MRP2-mediated drug efflux. Br J Pharmacol 2004;143:856–64.
19. Bailey DG, Dresser GK. Interactions between grapefruit juice and cardiovascular drugs. Am J Cardiovasc Drugs 2004;4:281–97.
20. Gaedigk A, Leeder JS, Grant DM. Tissue-specific expression and alternative splicing of human microsomal epoxide hydrolase. DNA Cell Biol 1997; 16:1257–66.
21. Buehler BA, Rao V, Finnell RH. Biochemical and molecular teratology of fetal hydantoin syndrome. Neurol Clin 1994;12:741–8.
22. Martz F, Failinger CD, Blake DA. Phenytoin teratogenesis: Correlation between embryopathic effect and covalent binding of putative arene oxide metabolite in gestational tissue. J Pharmacol Exp Ther 1977; 203:231–9.
23. Liang SH, Hassett C, Omiecinski CJ. Alternative promoters determine tissue-specific expression profiles of the human microsomal epoxide hydrolase gene (EPHX1). Mol Pharmacol 2005;67:220–30.
24. Guengerich FP, Yun CH, Macdonald TL. Evidence for a 1-electron oxidation mechanism in N-dealkylation of *N,N*-dialkylanilines by cytochrome P450 2B1. Kinetic hydrogen isotope effects, linear free energy relationships, comparisons with horseradish peroxidase, and studies with oxygen surrogates. J Biol Chem 1996;271:27321–9.
25. Coleman MD. Dapsone toxicity: Some current perspectives. Gen Pharmacol 1995;26:1461–7.
26. Uetrecht J. Drug metabolism by leukocytes and its role in drug-induced lupus and other idiosyncratic drug reactions. Crit Rev Toxicol 1990;20:213–35.
27. Cashman JR. Structural and catalytic properties of the mammalian flavin-containing monooxygenase. Chem Res Toxicol 1995;8:66–81.
28. Surapaneni SS, Clay MP, Spangle LA, Paschal JW, Lindstrom TD. *In vitro* biotransformation and identification of human cytochrome P450 isozyme-dependent metabolism of tazofelone. Drug Metab Dispos 1997;25:1383–8.
29. Tréfouël J, Tréfouël J, Nitti F, Bouvet D. Activité du *p*-aminophénylsulfanilamide sur les infections streptococciques experiméntales de la souris et du lapin. Compt Rend Soc Biol (Paris) 1935;120:227–31.
30. Saha JR, Butler VP Jr, Neu HC, Lindenbaum J. Digoxin-inactivating bacteria: Identification in human gut flora. Science 1983;220:325–27.
31. Bizjak ED, Mauro VF. Digoxin–macrolide drug interaction. Ann Pharmacother 1997;31:1077–9.

32. Krueger SK, Williams DE, Yueh MF *et al.* Genetic polymorphisms of flavin-containing monooxygenase (FMO). Drug Metab Rev 2002;34:523–32.
33. Cashman JR. Human flavin-containing monooxygenase (form 3): Polymorphisms and variations in chemical metabolism. Pharmacogenomics 2002;3:325–39.
34. Cashman JR, Park SB, Berkman CE, Cashman LE. Role of hepatic flavin-containing monooxygenase 3 in drug and chemical metabolism in adult humans. Chem Biol Interact 1995;96:33–46.
35. Park SB, Jacob PD, Benowitz NL, Cashman JR. Stereoselective metabolism of (*S*)-(–)-nicotine in humans: Formation of *trans*-(*S*)-(−)-nicotine *N*-1′-oxide. Chem Res Toxicol 1993;6:880–8.
36. Radominska-Pandya A, Bratton S, Little JM. A historical overview of the heterologous expression of mammalian UDP-glucuronosyltransferase isoforms over the past twenty years. Curr Drug Metab 2005; 6:141–60.
37. Wells PG, Mackenzie PI, Chowdhury JR *et al.* Glucuronidation and the UDP-glucuronosyltransferases in health and disease. Drug Metab Dispos 2004;32:281–90.
38. Christrup LL, Sjogren P, Jensen NH, Banning AM, Elbaek K, Ersboll AK. Steady-state kinetics and dynamics of morphine in cancer patients: Is sedation related to the absorption rate of morphine? J Pain Symptom Manage 1999;18:164–73.
39. Romberg R, Olofsen E, Sarton E, den Hartigh J, Taschner PE, Dahan A. Pharmacokinetic–pharmacodynamic modeling of morphine-6-glucuronide-induced analgesia in healthy volunteers: Absence of sex differences. Anesthesiology 2004;100:120–33.
40. Hawes EM. N^+-Glucuronidation, a common pathway in human metabolism of drugs with a tertiary amine group. Drug Metab Dispos 1998;26:830–7.
41. Kauffman FC. Sulfonation in pharmacology and toxicology. Drug Metab Rev 2004;36:823–43.
42. Baker CA, Uno H, Johnson GA. Minoxidil sulfation in the hair follicle. Skin Pharmacol 1994;7:335–9.
43. Buhl AE, Waldon DJ, Baker CA, Johnson GA. Minoxidil sulfate is the active metabolite that stimulates hair follicles. J Invest Dermatol 1990;95:553–7.
44. Burchell B, Coughtrie MW. Genetic and environmental factors associated with variation of human xenobiotic glucuronidation and sulfation. Environ Health Perspect 1997;105(suppl 4):739–47.
45. Falany CN. Enzymology of human cytosolic sulfotransferases. FASEB J 1997;11:206–16.
46. Holdiness MR. Neurological manifestations and toxicities of the antituberculosis drugs. A review. Med Toxicol 1987;2:33–51.
47. Dickinson DS, Bailey WC, Hirschowitz BI, Soong SJ, Eidus L, Hodgkin MM. Risk factors for isoniazid (NIH)-induced liver dysfunction. J Clin Gastroenterol 1981;3:271–9.
48. Hengstler JG, Arand M, Herrero ME, Oesch F. Polymorphisms of *N*-acetyltransferases, glutathione *S*-transferases, microsomal epoxide hydrolase and sulfotransferases: Influence on cancer susceptibility. Recent Results Cancer Res 1998;154:47–85.
49. Willson TM, Kliewer SA. PXR, CAR and drug metabolism. Nat Rev Drug Discov 2002;1:259–66.
50. Ruelius HW. Extrapolation from animals to man: Predictions, pitfalls and perspectives. Xenobiotica 1987;17:255–65.
51. Guengerich FP. Comparisons of catalytic selectivity of cytochrome P450 subfamily enzymes from different species. Chem Biol Interact 1997;106:161–82.
52. Gourley GR. Bilirubin metabolism and kernicterus. Adv Pediatr 1997;44:173–229.
53. Rubaltelli FF, Griffith PF. Management of neonatal hyperbilirubinaemia and prevention of kernicterus. Drugs 1992;43:64–72.
54. Rubaltelli FF. Current drug treatment options in neonatal hyperbilirubinaemia and the prevention of kernicterus. Drugs 1998;56:23–30.

CHAPTER

12

Methods of Analysis of Drugs and Drug Metabolites

SANFORD P. MARKEY
National Institute of Mental Health, National Institutes of Health, Bethesda, Maryland

INTRODUCTION

Pharmacokinetics requires the determination of a concentration of a drug, its metabolite(s), or an endogenous targeted substance in physiological fluids or tissues with respect to time. These analytical tasks have stimulated the field of analytical chemistry to devise technologies that are appropriately sensitive, precise, accurate, and matched to the demands for speed and automation, important factors in research and clinical chemistry. During the past decade, the principal determinant influencing the choice of competing analytical technologies has been speed — the coupled need to reduce both the time required for assay development and the assay cycle time for large numbers of samples. As a result, instrumentation that can measure drug concentrations in blood, tissue, and urine with minimal chemical treatment has emerged; this is discussed in this chapter using recently published examples.

Several terms used frequently in analytical laboratories have significant and specific definitions, important in the discussion of analytical assays. The *limit of detection* is the minimum mass or concentration that can be detected at a defined signal-to-noise ratio (usually 3:1). The *lower limit of quantification* is the analyte mass or concentration required to give an acceptable level of confidence in the measured analyte quantity, usually 3-fold the limit of detection, or 10-fold background noise. *Sensitivity* of a measurement is the minimum detectable change that can be observed in a specified range. For example, a 1-pg sensitivity may be measured for a pure chemical standard, but in the presence of 1000 pg, the assay sensitivity is the ability to distinguish between 999, 1000, and 1001 pg. *Selectivity* of an assay is the ability of the technique to maintain a limit of detection independent of the sample's matrix. A highly selective assay methodology will not be affected by the presence or type of physiological fluid. *Accuracy* of a method is the ability to measure the true concentration of an analyte; *precision* is the ability to repeat the measurement of the same sample with low variance. *Reproducibility* differs from precision, connoting variability in single measurements of a series of identical samples as compared to repeated measurements of the same sample. The U.S. Food and Drug Administration and the corresponding European agencies have recognized the need to establish standardized definitions and practices for analytical methods. There are several internet sites containing documentation describing terms and practices consistent with regulatory agency guidelines (for example, www.fda.gov/cder/guidance/ and www.vam.org.uk/).

CHOICE OF ANALYTICAL METHODOLOGY

The types of information required largely determine the choices of analytical methodology available. Pharmacokinetic studies for new chemical entities

require determinations of the administered drug and its metabolites. Selective techniques capable of distinguishing between parent drug and metabolites are necessary. For some marketed drugs, good medical practice requires measurements to determine whether patient blood concentrations are within the desired therapeutic index. Instrumentation and immunoassay kits are commercially available for highly prescribed medications with narrow therapeutic indices, as well as for drugs of abuse.

The scale of a planned pharmacokinetic study further determines the assay methodologies to be considered. For a typical pharmacokinetic study of a new chemical entity, the analyst must choose methods suitable for analyzing at least 30 to 50 samples/patient plus 10 to 15 standards and procedural blanks. Quality control measures may require an additional 10 to 15 samples containing pooled and previously analyzed samples, to permit assessment of run-to-run reproducibility. To maximize instrumental efficiency, analysts commonly choose to process more than a single patient's samples at one time, resulting in runs usually containing >100 patient samples plus standards and quality control samples. Standard curves are determinations of instrument response to different known concentrations of analyte, and are required to precede and follow each group of patient samples to assess quality control. Highly automated, rugged, and dependable instrumentation is critical because analyses must continue without interruption until the entire sample set has been analyzed. If the assay cycle time is short (few seconds/sample), the instrumentation requires stability of operation over only 5–10 minutes. However, when assays involve multiple stages, such as derivatization and chromatographic separation, assay cycle time is more typically 5–30 minutes/sample. The resulting requirement for more than 3 days of instrumental operation may introduce conditions and costs that then serve to limit and define the study protocol. When possible, methods that are selective and sensitive and that do not require separation or chemical reactions are chosen, because, clearly, time and cost are critical factors. Early in the drug discovery process, any conceivable and accessible analytical method may be chosen. After demonstration of the potential for commercial development, time and effort can be directed toward simpler and more cost-effective analytical methods that can be marketed as kits for therapeutic drug monitoring.

In the past 10 years, the pharmaceutical industry research laboratories involved in evaluating new agents have shifted their emphasis from predominantly using ultraviolet (UV) to mass spectrometric (MS) detectors with liquid chromatography (LC) separations. The driving force for the utilization of more expensive instrumentation has been the decreasing time allotted for quantitative assay method development. Improvements in mass spectrometric instrumentation have now made LC/MS routine and widely available. The required assay limit of quantification has remained relatively constant for some classes of drugs, typically in range of nanograms to micrograms (per milliliter), but newer drugs are designed to be more selective to minimize side effects, dropping therapeutic concentrations to picograms per milliliter. Once new drugs have passed through the initial stages of development, then the market for therapeutic drug monitoring dictates that more robust and less expensive technologies be utilized, amenable to instrumentation accessible to hospital clinical chemistry laboratories. Consequently, analytical kits sold for drug monitoring are likely to be based upon immunoassay methodologies. The emerging development of chip-based microanalytical methods suggests that instrumentation for therapeutic drug development and monitoring will continue to evolve while using many of the same separation and spectroscopic principles. This chapter is written to provide an introduction to the principles of some of the most commonly used analytical methodologies in clinical pharmacology.

CHROMATOGRAPHIC SEPARATIONS

Chromatography refers to the separation of materials using their relative solubility and absorption differences in two immiscible phases, one stationary and the other mobile. The defining work of Mikhail Tswett in 1903 demonstrated the separation of colored plant pigments on a carbohydrate powder through which hydrocarbon solvents were passed. The same principles apply to the rainbow-like dispersion of colors seen when ink soaks through a shirt pocket.

Modern chromatographic science has refined these basic principles in *high-performance liquid chromatography* (HPLC). A schematic outline of an HPLC instrument is shown in Figure 12.1. Modern HPLC systems are designed to make separations rapid, reproducible, and sensitive. Particulate adsorption material that is packed in a chromatographic column is engineered to have small and uniform particle size (typically, 3 or 5 μm). Columns 1–5 mm in diameter and 5–15 cm long exhibit sufficient resolution to effect useful separations. Columns of such lengths, when packed with small particles, require high pressure (typically, several hundred pounds per square inch) to force solvent flow at 0.1–1.0 mL/min, requiring

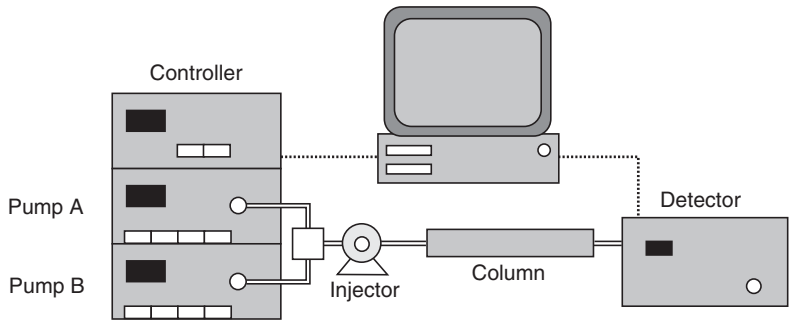

FIGURE 12.1 Schematic of HPLC system, showing component modules.

inert, precision-machined, high-pressure fittings and materials. Pumps are designed to deliver precisely metered, pulseless flow of the mobile phase, composed of either organic and/or aqueous solutions. Pumps are controlled electronically so that a gradient of the mobile-phase solvents from the pumps can be continuously programmed. The polarity, the pH, or the ionic concentration differs in the solutions in solvent reservoirs that are pumped into a mixing chamber and then directed into the column. During an analytical run, this enables the mobile phase to be varied so that materials in a mixture partition with respect to solubility in the mobile phase and adsorption on the stationary phase. When a component is more soluble in the mobile phase than in the film on the particle, it will elute from the column and be detected with respect to a characteristic chemical property, such as UV absorption (Figure 12.1).

The popularity and acceptance of HPLC in clinical assays is due to the versatility and wide applicability of the methodology. Most pharmaceuticals are small molecules (<1000 Da) with some lipid solubility. They commonly share the property that they adsorb to silica particles coated with stable organic hydrocarbon films and can then be eluted when the organic content of the mobile phase is increased. Consequently, a single analytical system can be used for many types of analyses, tailored to each by changing the solvents and gradients. The reproducibility of HPLC separations can be rigorously controlled due to extensive engineering of all of the components in these systems. Reproducibility is especially dependent on consistent gradient elution and establishing equilibrium conditions before each run. The most reproducible HPLC separations are *isocratic*, using a single solvent during the analysis. In practice, the complexity of most biological fluids necessitates mobile-phase gradient programming to accomplish the desired separations and cleanse the column of adsorbed components from each injected sample.

ABSORPTION AND EMISSION SPECTROSCOPY

Spectroscopy is the measurement of electromagnetic radiation absorbed, scattered, or emitted by chemical species. Because different chemical species and electromagnetic radiation interact in characteristic ways, it is possible to tailor instrumentation to detect these interactions specifically and quantitatively. A simple absorption spectrophotometer, depicted schematically in Figure 12.2, contains components that are common to many spectroscopic devices and are representative of many of the basic principles of instrumentation found in analytical biochemistry.

A light source produces radiation over the wavelength region where absorption is to be studied. For the visible spectrum, a source producing radiation between 380 and 780 nm is required; for ultraviolet radiation, radiation between 160 and 400 nm is required. Both wavelength ranges can be supplied by hydrogen or deuterium discharge lamps combined with incandescent lamps. A high-quality light source combines brightness with stability to produce a constant source of radiant energy. The monochromator is a wavelength selector (prism or grating), separating

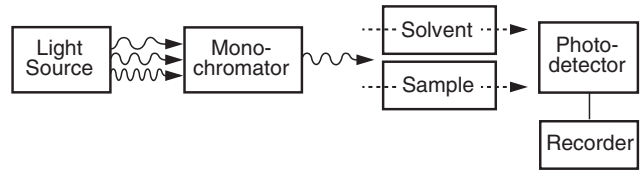

FIGURE 12.2 Schematic layout of components of an absorption spectrophotometer.

the discrete component energies of the light source. The quality of a monochromator is related to its ability to resolve radiation in defined wavelengths without loss of intensity. An inexpensive substitute for a monochromator is a filter, passing a fixed, discrete band of energy. When a discrete wavelength is passed through a solvent or through solvent containing dissolved sample, some of the radiant energy is absorbed, depending upon the chemical structure of the sample. Colored substances, such as hemoglobin, absorb in the visible region. Colorless proteins containing aromatic amino acids absorb UV light at 280 nm; all proteins absorb UV light at 214 nm due to the amide function. Many carbohydrates and lipids do not absorb light in the UV or visible region and are consequently transparent. The absorption characteristics of each chemical structure can be predicted based on the presence or absence of component functional groups, such as aromatic, unsaturated, and conjugated groups.

The quantity of absorbed energy is proportional to the concentration of the sample, the molar absorptivity of the sample and its solvent, and the distance or path length of the sample container or cell. Molar absorptivity is an expression of the intensity of absorbance of a compound at a given wavelength relative to its molar concentration. The light transmitted through the sample or solvent cell is directed onto a photosensitive detector, converted to an electronic signal, and sent through amplifiers to a recorder or computer. Most spectrophotometers contain optics designed so that the signal from light absorbed by the solvent is compared and subtracted from the signal from the light absorbed by the sample in an equal quantity of solvent.

The data resulting from spectrophotometric analyses of a sample in a transparent solvent is termed *optical density*. The measurement of the optical density of a sample at varying wavelengths is the *absorbance spectrum*. The absorbance spectrum of a drug may not be very different from absorbance spectra of many of the common metabolic intermediates in cellular metabolism. Because endogenous cellular intermediates are present typically in 10^3–10^6 greater concentrations than are drugs (typically nanomolar to micromolar), it is usually not possible to use absorbance spectrophotometry alone to detect differences between drug-treated and untreated fluids. However, absorbance spectrophotometers, particularly in the ultraviolet range, are popular detectors for HPLC. For many drugs, the separation power of HPLC can provide sufficient discrimination for quantifying parent drug and metabolites, as illustrated later in this chapter.

Some compounds emit light at characteristic frequencies when radiation of a particular energy is absorbed. The resulting *emission spectrum* is

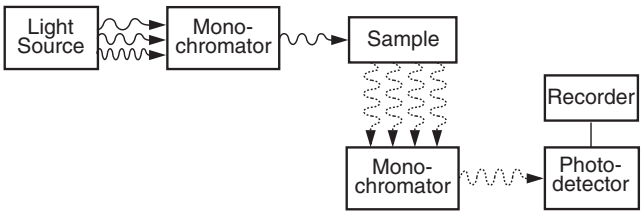

FIGURE 12.3 Schematic layout of components of an emission spectrophotometer.

significantly more unique than is an absorbance spectrum. Consequently, the measurement of emitted (fluorescent or phosphorescent) light can frequently be used for sensitive measurements of trace amounts of naturally luminescent compounds. The instrumentation for emission spectrophotometry is similar to that for absorbance instrumentation in the selection of monochromatic radiation to pass through the sample. Subsequently, a second monochromator or filter is used to collect and separate the radiation emitted prior to detection, as illustrated in Figure 12.3. Drugs that are naturally fluorescent may be candidates for direct fluorescent assay, but frequently a specific separation, such as HPLC, precedes fluorescent detection in order to lower interference from background. A further way to enhance selectivity is to measure the absorption and emission of polarized light. This approach is relevant to large molecules with restricted rotational movements, such as antigen–antibody complexes. An antigen, such as a drug, can be labeled with a fluorescent tag, and the florescent emission of polarized light is measured in a competitive antibody-binding assay, as described for cyclosporine later in this chapter.

IMMUNOAFFINITY ASSAYS

Antibodies created by the immune response system can be powerful analytical reagents exhibiting unique specificity for molecular recognition. Antibodies are proteins that exhibit high affinity toward a specific aspect of an antigen, such as a particular amino acid sequence or chemical structure. The science of generating antibodies to low molecular weight drugs as antigens is highly advanced, beyond the scope of this chapter; in general, however, drugs are covalently bound to multiple sites on a large carrier protein, and antibodies that recognize the drug functionality are harvested. An expanding library of antibodies is commercially available. Additionally, there are commercial services that will generate custom poly- or monoclonal antibodies to any drug or protein.

The analytical use of antibodies is predicated on their specificity and affinity with regard to binding a targeted analyte in the presence of a complex

mixture such as serum. This affinity interaction contrasts with chromatographic media, which bind and release components with respect to general physicochemical parameters, such as acidity, size, and lipid solubility. The antibody–antigen interaction is analogous to the selectivity of a molecular lock-and-key, in contrast to the general nonspecific interactions of chromatography. The epitope (or keylike) region of an antigen that binds to an antibody can be exquisitely specific. Monoclonal antibodies recognize a single epitope; polyclonal antibodies recognize multiple epitopes. Both types of antibodies are likely to recognize, or *cross-react* with, metabolites or congeners of an antigen with unpredictable (but reproducible) affinity. Mass production and purification of mono- and polyclonal antibodies as reagents afford materials that are used routinely to recognize and separate targeted analytes. Antibodies can be bound to films, papers, surfaces, or chromatographic supports. There are inherent variations in the affinities and properties of antibodies. Consequently, cost and availability of antibody materials are directly related to the degree to which they have been pretested and characterized.

Quantification requires measurement of the extent of antibody–antigen interaction, and the assessment of the amount of bound vs free antigen. Immunoaffinity assays must be coupled with colorimetric, spectroscopic, or radiometric detection in order to create an output signal. An assay may incorporate a step to separate the antibody–ligand complex (heterogeneous assay) or may entail direct detection of the extent of antigen–antibody complex formation (homogeneous assay). The latter type of assay is particularly popular in clinical chemistry because of its inherent simplicity. Homogeneous immunoassays may use a marker-labeled antigen (for example, a fluorescent tag on a target analyte drug) to indicate whether binding has decreased or increased, directly reflecting the bound/free ratio of the drug. Examples of immunoaffinity-based assays are discussed later in this chapter using cyclosporine as a target analyte.

Immunoaffinity-based assays are routinely developed for new biologicals and products of the biotechnology industry as part of their characterization as new agents. In contrast, assays used for pharmacokinetic studies of new chemically synthesized entities are less likely to be immunoaffinity based because analysts are required to measure accurately the concentration of the administered parent drug. Metabolism of the parent drug can result in metabolites that are structurally very similar and that cross-react with antibodies to the parent drug, but exhibit different pharmacological activity. For this reason, determination of the structures of these metabolites and, commonly, the measurement of their concentrations are key parts of the analytical requirements associated with drug development. As a general rule, immunoaffinity assays cannot be interpreted without prior knowledge of the metabolic fate of a drug, found by using an assay that is drug and metabolite specific.

MASS SPECTROMETRY

The analysis of the mass of an organic compound provides information on component elements and their arrangement. For example, the mass spectrum of water, H_2O (Figure 12.4A), illustrates several characteristics of such data. The bar graph in Figure 12.4A plots mass-to-charge ratio (m/z) on the x axis, and relative ion intensity on the y axis. All forms of mass spectrometry require the analysis of ions, not neutral molecules. Water, composed only of oxygen (16 Da) and two atoms of hydrogen (1 Da), has a molecular mass of 18 Da. When water is ionized, m/z 18 is not only the *molecular ion* but also the strongest signal, or *base peak*. There are signals seen for unpaired (odd) electron fragment ions containing the components $O^{+\cdot}$ at m/z 16, and OH^{+} at m/z 17, as well as $HOH^{+\cdot}$ There are no signals at other m/z, such as 12, 13, 14, 20, or 21,

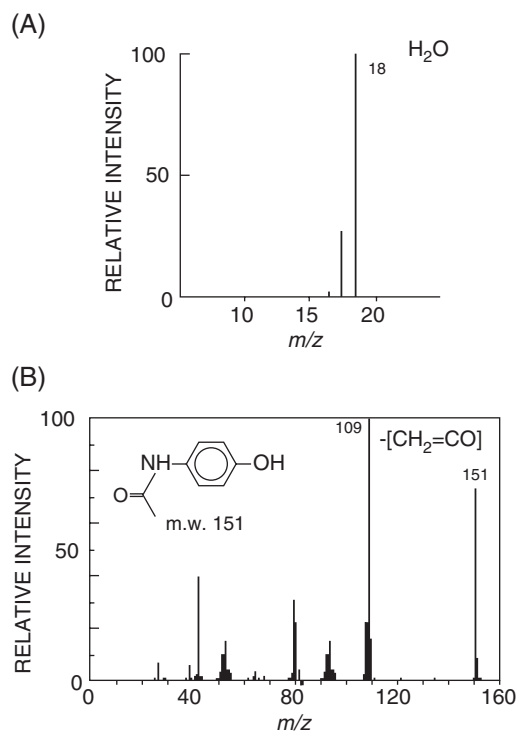

FIGURE 12.4 Electron impact ionization mass spectra of water (A) and acetaminophen (B). The intensities of the fragment ions are normalized against those of the predominant ion (base peak), which, in the case of water, is also the molecular ion with mass/charge ratio (m/z) = 18.

because elements with those masses are not present. To generalize, mass spectra can be interpreted by a simple arithmetic accounting of elemental constituents.

The same principles of analysis can be applied to the mass spectra of more complex organic molecules. For example, the mass spectrum of acetaminophen is shown in Figure 12.4B. A molecular ion is seen for the total assembly of all of the elements $C_8H_9NO_2$ at m/z 151. The strongest signal at m/z 109 derives from the loss of ketene ($CH_2C{=}O$) as a stable neutral fragment from the ionized molecule. The mass spectrum bar graph format presents a fragmentation pattern, revealing characteristics of a molecule's architecture, such as the presence of an acetyl function. The interpretation of electron ionization mass spectra in this way provides a rich resource of substructural information.

How mass spectra are produced largely determines the kind of information in the spectra (1, 2). Mass spectrometry differs from absorbance or emission spectroscopy in that it is a destructive technique, consuming sample used during the measurement process. Mass spectrometry is also a very sensitive technique, consuming as little as a few attomoles (10^{-18} moles, or 10^5 molecules) in the best cases, more typically requiring form 1 to ~10 femtomoles (10^{-15}moles) for the routine quantitative analyses common in the pharmaceutical industry.

From the overview diagram in Figure 12.5, there are several integral components that comprise every mass spectrometer. First, all substances must be ionized in order to be mass analyzed. The physical principles focusing and separating molecules require that the molecules be positively or negatively charged so that electric and magnetic fields affect the motion of the resulting ions. Second, the ions must enter a mass analyzer in a vacuum chamber maintained at a pressure sufficiently low as to permit ions to travel without interacting with other molecules or ions. Third, there must be an ion detector capable of converting the impinging ion beam into an electronic signal. Fourth, there must be controlling electronics, usually integrated with a computer, to regulate the ionization, mass analysis, ion detection, and vacuum systems and to record and process ion signals. There are efficient ionization methods for producing ions *in vacuo* of organic compounds of any size or complexity from gases, liquids, or solids.

Two of the most common mechanisms widely used by investigators in clinical pharmacology are electron (Figure 12.6A) and electrospray ionization (Figure 12.6B). Electron ionization of neutral organic molecules in the vapor phase occurs when electrons emitted from a heated filament remove an electron from the molecule. The resultant odd-electron ions are focused and accelerated into a mass analyzer by electric fields. Electron ionization, and a closely related method, chemical ionization, were the principal methods used in clinical pharmacology until around 1990. Electrospray ionization of neutral organic molecules in liquid solutions occurs when liquids flow through a conductive needle bearing several thousand volts at atmospheric pressure. The emerging liquid forms a sharp cone, with microdroplets of ion clusters bearing multiple charges and attached solvent molecules. A gas stream dries the clusters, and the resulting desolvated singly and multiply charged ions are guided into the vacuum system of the mass analyzer. Because of its compatibility with liquid samples, electrospray is currently the principal method of ionization used in clinical pharmacology assays.

Following ionization, the charged molecular, cluster, or fragment ions are accelerated and focused into a mass analyzer. The type of mass analyzer influences the region and quality of the mass spectrum. Some

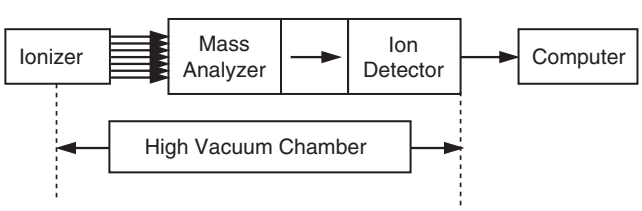

FIGURE 12.5 Schematic overview of components of a mass spectrometer.

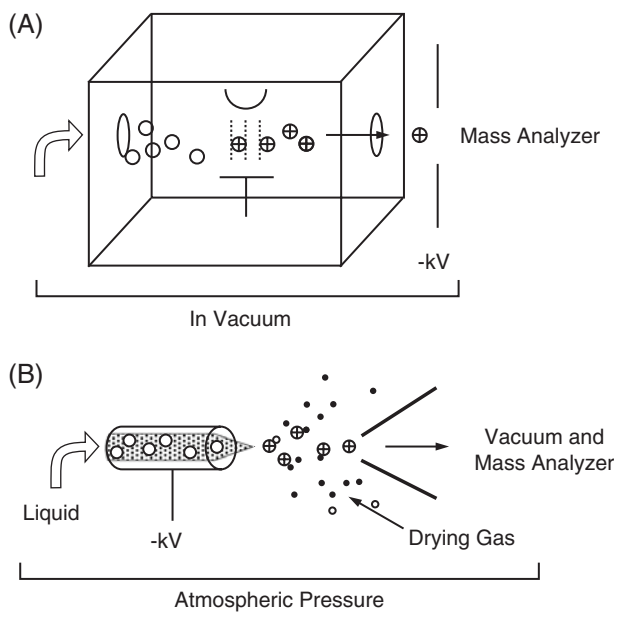

FIGURE 12.6 Schematic representation of electron impact (A) and electrospray (B) mass spectrometer ionization sources.

analyzers have a limited mass range (for example, m/z 0 to 1000, or 0 to 20,000). Others have limited resolution of m/z (for example, the ability to resolve the difference between m/z 1000 and 1001, or 1001.000 and 1001.010). The initial report of mass analysis in pharmacology used magnetic sector mass analyzers in the identification of metabolites of chlorpromazine (3). This work introduced the concept of *selected ion monitoring*, or mass fragmentography, a technique of alternating between preselected ions of interest, thereby enhancing sensitivity and making the mass spectrometer a sophisticated gas chromatographic detector. The principles of online chromatography and selected ion monitoring are integral in all modern mass spectrometric instrumentation. Currently, however, the most commonly used mass analyzers in pharmacology include time-of-flight, quadrupole, and ion traps (illustrated in Figure 12.7).

The time-of-flight (TOF) mass analyzer (Figure 12.7A) separates ions by accelerating a pulse of ions in vacuum and then measuring their time of arrival at a detector. Because all ions are given the same initial kinetic energy, lighter ions arrive at the detector faster than do heavier ions. All ions from a single pulse are analyzed, so there is no upper mass limit on TOF analyzers. Resolution is a function of flight path length and initial position in the beam of pulsed ions. The inherent simplicity, speed, and mass range of TOF analyzers have resulted in low-cost, higher performance instrumentation for routine analyses.

A quadrupole mass analyzer (Figure 12.7B) filters ions using radiofrequency alternating voltages at a constant direct current potential on paired cylindrical rods. A continuous beam of ions enters the alternating field region at low energy. Resonant positive ions of a particular m/z ratio traverse the field region and pass through to the detector, oscillating first to poles of negative charge and then, when the field alternates, being drawn toward the opposite pair of rods. Nonresonant ions collide with the surface of the rods and do not reach the detector. Quadrupole mass filters are designed to filter limited mass ranges, typically m/z 10 to 2000 for organic ion analysis. Quadrupole analyzers are widely used in clinical pharmacology, especially with electrospray ionization.

A quadrupole ion trap (Figure 12.7C) mass analyzer collects ions in stable trajectories using a radiofrequency oscillating voltage on a central ring electrode. A gated electron beam ionizes neutral molecules within the trap, or ions may be injected into the trap from external ion sources. A second radiofrequency field between the end caps causes ions of a particular m/z to go into an unstable trajectory and pass through the holes in one end cap to the ion detector. Several

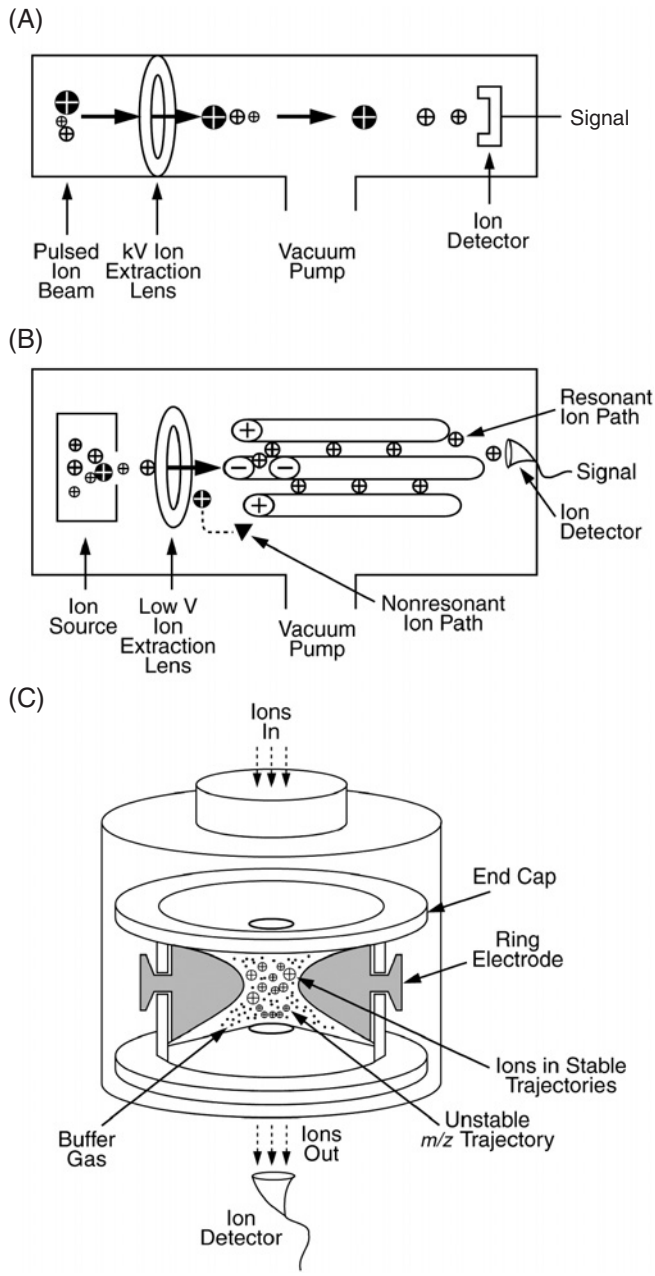

FIGURE 12.7 Schematic representations of three mass analyzers. (A) Time-of-flight; (B) quadrupole; (C) quadrupole ion trap.

millisecond trapping and ejection cycles are performed over defined m/z ranges. The capability of ion traps to store and accumulate selected ions and subsequently to fragment and analyze the fragments has made these a popular low-cost alternative to tandem mass spectrometers.

Permutation of ionization and mass analyzer alternatives presents many instrument configurations to prospective users, and there continues to be significant

instrumentation development leading to new capabilities with different configurations. Consequently, no single ionizer/mass analyzer dominates the clinical pharmacology market. The option of tandem mass analysis may be the deciding factor in instrument selection. Tandem mass analysis, termed MS/MS analysis, entails the separation of a mass-resolved ion beam, and its subsequent fragmentation and further mass analysis. In a two-stage MS/MS analysis, the second mass analyzer provides a mass spectrum of ions from the initial mass spectrum. Some of the most common tandem mass analyzer configurations are quadrupole–quadrupole–quadrupole (qqq), quadrupole–quadrupole–TOF (qqTOF), and linear, or quadrupole, ion trap. MS/MS analysis significantly increases the selectivity of analytical mass spectrometry by requiring not only that a specific mass is characteristic of a compound, but also that specific mass fragments be present in a characteristic pattern to yield a second product ion. In Figure 12.4B, the primary mass spectrum of acetaminophen is characterized by *m*/*z* 151 as a base peak with a significant fragment ion at *m*/*z* 109, which derived from that molecular species. Thus, in a chromatography–MS/MS analysis, an instrument could be set to pass *m*/*z* 151 in a first stage of analysis and *m*/*z* 109 in the second stage. The result would be a time-varying signal representing only ions of *m*/*z* 109 that derived from *m*/*z* 151, a very stringent criterion for mass detection. As a result, this particular signal would be detected only when acetaminophen eluted from the chromatograph.

MS/MS analysis is possible with high sensitivity because the transmission and storage of mass resolved ions are efficient. Because the chemical background is reduced, MS/MS analyses also frequently have enhanced sensitivity and selectivity when compared to MS analyses. Ion traps have a further advantage of allowing serial experiments, by trapping a specific ion, then causing it to fragment, trapping a specific fragment, and then fragmenting and mass analyzing the secondary fragment, and so on (e.g., MS^3 or MS^n).

EXAMPLES OF CURRENT ASSAY METHODS

There are many possible permutations for coupling one of the chromatographic or immunoaffinity separations with one or another of the spectrometric detection technologies. HPLC with UV or fluorescence spectrometry, and HPLC with MS, are among the most widely used quantitative analytical methods in the pharmaceutical development of new chemical entities because of their general applicability and sensitivity relevant to clinical pharmacology. Homogeneous immunoaffinity assays are frequently a first choice for protein or other biotechnology products. Immunoaffinity assays with fluorescence polarization or enzyme reaction monitoring are popular commercialized methods for older chemical entities. A discussion contrasting alternative combined methods of analysis for nucleoside drugs and cyclosporine follows, because these analyses illustrate the variety and respective merits of combined analytical methods widely used in pharmacological research.

HPLC/UV and HPLC/MS Assay of New Chemical Entities — Nucleoside Drugs

Examples of the use of HPLC/UV and HPLC/MS/MS are provided by the analyses of fluoro-dideoxyadenosine (F-ddA; Figure 12.8), a synthetic dideoxynucleoside inhibitor of human immunodeficiency virus (HIV) reverse transcriptase that was evaluated at the Laboratory of Medicinal Chemistry of the National Cancer Institute (NCI). F-ddA is metabolized to fluoro-dideoxyinosine (F-ddI), also a reverse transcriptase inhibitor.

Selection of a suitable assay method for these compounds began with consideration of the chemical characteristics of the drug and the determination of the likely range of blood and tissue concentration required for pharmacological effect (4). F-ddA and F-ddI absorb UV radiation at 260 nm, making them logical candidates for an HPLC/UV assay. The analytical conditions reported for the previously marketed analog, didanosine (ddI), were useful for reference, but, compared to ddI, fluorine substitution makes F-ddA a more lipophilic and acid stable drug.

The analyst facing the challenge of designing an assay begins by characterizing the chromatography of analytes, choosing column materials and eluents either recommended for structurally similar compounds or broadly applicable in pharmacology. Conditions are required that provide retention and elution of F-ddA and F-ddI with symmetrical peak shape and adequate separation. Choice of any specific buffer and

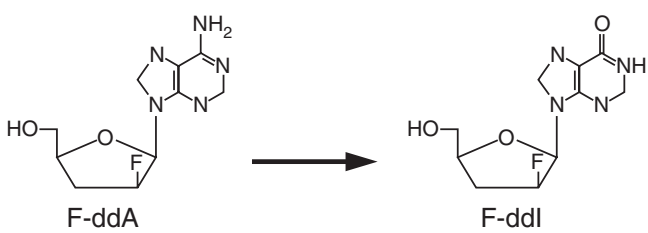

FIGURE 12.8 Chemical structures of F-ddA and F-ddI.

elution program results from incremental trials, with the objective of improving chromatographic separation and peak shape sufficiently to enable quantitative measurement in the biological fluid being sampled. In this case, the investigators used a phenylsilicon reverse-phase column with a mobile-phase linear gradient ranging in composition from 2 to 36% methanol in 0.01 *M* phosphate buffer.

Direct injection of biological fluids into chromatographic columns is possible, but some type of solvent extraction or prefiltration is recommended to preserve the life of the column, by removing cellular debris or particulate material. After obtaining satisfactory chromatograms of pure analyte, the analyst adds the same quantity of analyte to a blank biological fluid to determine the chromatography and background in the presence of the biological matrix. The chromatographic profile of the biological fluid with and without added analyte standards will determine the necessity for alternative chromatographic conditions, column selection, and sample cleanup.

Often filtration can be combined with sample enrichment by flowing the sample through cartridges packed with granular materials or media. Solid-phase extraction cartridges contain any of a wide variety of chromatographic media, such as normal or reverse-phase coated silica or ion exchange polymers. They are like minichromatographic columns, but are optimized for sample cleanup prior to chromatography and not for analytical separations. A cartridge is chosen that will trap target analytes from the biological fluid, permit rinses to remove salts, and allow efficient elution of the analytes in a convenient quantity of organic solvent. In many cases, the process of solid-phase extraction cleanup has been adapted to robotic systems, enabling analysts to scale procedures from single samples to automated 96- or 384-well formats. For the analysis of F-ddA and F-ddI, patient plasma is diluted with water and applied to an octadecylsilyl reverse-phase cartridge, washed with phosphate buffer, and the analytes are eluted with methanol/water. The eluent is concentrated either under a nitrogen stream in a chemical fume hood or in a centrifugal rotary evaporator, and the final sample is redissolved for injection into the analytical column.

Contemporary quantitative assays require the analyst to select appropriate compounds to serve as *internal standards*. A fixed quantity of an internal standard is added to each sample so that the intensity of the signals from the analyte from each sample can be normalized to those from the internal standard and compared to samples analyzed during the same run, or from another analytical set on another date. Internal standards must have chemical properties similar to those of the target analyte, be available in pure form, and be separable on chromatography. Like the target analyte, it is critical that the internal standards are chromatographically well separated from endogenous components. For the NCI F-ddA and F-ddI analyses, the investigators selected the structurally related chloro–analogs as internal standards.

Six to eight different concentrations of each analyte are prepared to construct a set of standard solutions (*standards*) that covers the range of biological sample concentrations to be measured. An aliquot of a solution containing one or more internal standards is precisely added to every tube in the set of standards and biological samples. Data from the analysis of the standards are used to generate a *standard curve* in which relative signal response (i.e., standard response/internal standard response) is plotted against the concentration of the standards. The standard curve then is used to convert the relative signal response from analysis of the biological samples (i.e., biological sample response/internal standard response) to absolute concentration data. Appropriately chosen internal standards and chromatography columns will result in the generation of linear standard curves, with proportional increases in the ratio of analyte to internal standard with increasing mass of analyte.

Biological sample processing may require additional considerations prior to analyses. The expected presence of HIV in the blood samples for F-ddA analyses required the NCI analysts to test methods to inactivate virus without altering the quantification of drug or metabolite. Several procedures were tested and it was determined that the addition of a small quantity of Triton X-100 detergent eliminated virus without affecting sample integrity or chromatography. Many drugs are stable in biological fluids when stored frozen, but chemical stability, reactive intermediary metabolites, and effects of storage may be important considerations in the analyses of other drugs and their metabolites. The addition of chemical preservatives, protein denaturants, or detergents may be required, and these issues are best reviewed at the outset of assay development.

A *chromatogram* is the plot or graph of detector signal (e.g., UV absorbance) vs time that results when a sample is eluted from the chromatographic column and passed through the detector. Typical analytical HPLC chromatographic analysis of many drugs requires 15–35 minutes. Following each chromatographic run, the mobile-phase gradient must be returned to the starting condition, requiring an additional 5–15 minutes for stabilization.

The HPLC/UV chromatograms of pre-dose and F-ddA patient plasma with added 5′-Cl-deoxyadenosine

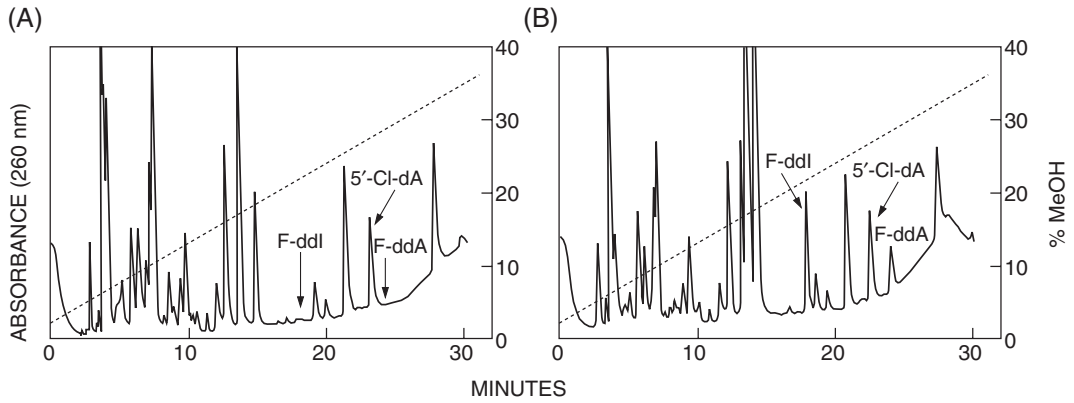

FIGURE 12.9 HPLC/UV analysis of plasma from a patient before (A) and after (B) receiving an F-ddA dose. 5′-Cl-dA was added to the plasma as the internal standard. The plasma analyzed in (B) was obtained 85 minutes after beginning a 100-minute intravenous infusion. Arrows indicate the time of elution for each component. The dotted line indicates the methanol concentration gradient. Data courtesy of Dr. J. Kelly, NCI, NIH.

(5′-Cl-dA) internal standard are shown in Figure 12.9. The dotted line on the chromatogram indicates the composition of the programmed linear elution gradient throughout the run. The pre-dose plasma analysis contains peaks for endogenous plasma components absorbing at 260 nm. The background peaks will vary from individual to individual because dietary substances, other drugs, and intermediary metabolites will contribute to the recorded signal. Therefore, it was important to design the assay so that there were no interfering signals for endogenous components eluting at the expected retention times of F-ddI, or the internal standard (5′-Cl-dA).

The HPLC/UV F-ddA method was used to produce preliminary pharmacokinetic data in monkeys (5). The limit of quantification for both F-ddA and F-ddI was 50 ng/mL using this assay. However, for clinical pharmacokinetic studies, the NCI investigators required a more sensitive assay. Due to the number of clinical samples, an assay faster than 45–50/min/sample was also desirable. Conversion from HPLC/UV to HPLC/MS conditions required the substitution of volatile buffers compatible with electrospray ionization. The analysts defined fast isocratic conditions for the HPLC/MS chromatography, eliminating the need for gradient programming. Because of enhanced detection selectivity, background interference is significantly less with MS than with UV detection, so that chromatography can be faster and gradient programming can be omitted. Therefore, HPLC/MS/MS analysis of the F-ddA samples was completed in 10-minute cycles using a 25% methanol/0.25% acetic acid eluent, about four to five times faster and at 10-fold greater sensitivity than for HPLC/UV gradient analyses.

The electrospray ionization mass spectra of F-ddA and F-ddI are similar to spectra of other nucleosides and typical of many drugs in that they exhibit intense MH^+ protonated molecular ions. Recording the signal from a single characteristic ion produced a *selected ion chromatogram*, a record that is considerably more specific than is a UV absorbance chromatogram. However, MS/MS offers even greater stringency by recording the signal characteristic of a fragment formed from a selected ion, a process known as *selected reaction monitoring* (2). Using MS/MS, the F-ddA-MH^+ ion at m/z 254 is further fragmented in the second mass spectrometer to produce an intense adenine ion (BH_2^+) m/z 136 and a weak F-dideoxy fragment at m/z 119. The unique specificity of this method results from the fact that signals are monitored only from compounds that have the appropriate chromatographic elution time and produce ions at m/z 254 that fragment further to m/z 136 (denoted m/z 254 to 136). Selected reaction monitoring also reduces background without sacrificing signal strength. There is no background signal in pre-dose patient plasma at the retention value for F-ddA. Likewise, there are no interfering signals for F-ddI (m/z 255 to 137).

Like HPLC/UV, quantitative mass spectrometric assays require internal standards to be added to every sample to compensate for fluctuations in sample handling and instrument performance. Commonly, structural analogs of the target analytes are the most readily available internal standards, although for highest precision and accuracy, nonradioactive, stable isotope analogs or isotopomers (^2H, ^{13}C, ^{15}N, ^{18}O) are preferred. For the HPLC/MS/MS analysis of F-ddA, two chloro analog internal standards, 2-Cl-A (m/z 302 to 170) and 2-Cl-I (m/z 303 to 171), were chosen, and the

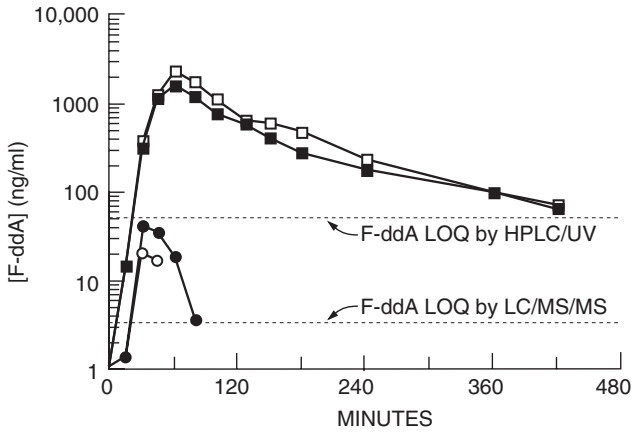

FIGURE 12.10 Plasma concentration vs time profiles for F-ddA and F-ddI after oral administration of 4.5 mg/kg F-ddA to a patient, showing the limit of quantification (LOQ) by different measurements. (●, ○) Levels of F-ddA measured by HPLC/MS/MS and HPLC/UV; (■, □) levels of F-ddI measured by HPLC/MS/MS and HPLC/UV. Data courtesy of Dr. J. Kelley, NCI, NIH.

limit of quantification (LOQ) was 4 ng/ml (16 n*M*) for F-ddA and 8 ng/ml (32 n*M*) for F-ddI.

The pharmacokinetic results obtained with HPLC/UV and HPLC/MS/MS are shown in Figure 12.10. Dotted lines indicate the LOQ for F-ddA by both assay methods. Data for F-ddI obtained by either method show good agreement, being well above the LOQ for both techniques. On the other hand, all of the F-ddA data points are below the LOQ by HPLC/UV. Nonetheless, measurements reported below LOQs can be useful in that they help define what assay sensitivity must be achieved for pharmacokinetic data analysis.

This description of F-ddA quantification provides a specific example from which some general observations about HPLC/UV and LC/MS assays may be drawn. Liquid chromatographic separations are well suited to pharmacokinetic requirements, because the same physicochemical characteristics that determine drug bioavailability (solubility, polarity, chemical stability) can be translated to liquid chromatography. The selectivity of detection (UV absorbance, fluorescence, mass, or mass-to-mass fragment), and not the detector sensitivity, frequently defines assay LOQ. The general applicability of LC/MS/MS recommends its acceptance as a preferred assay method. This preference is reinforced by simpler and more facile assay development using LC/MS/MS, compared to HPLC/UV. Chromatographic separation is critical in HPLC/UV because there is an unavoidable UV background arising from biological matrix components with physicochemical characteristics similar to those of drugs. Consequently, analysts developing HPLC/UV (or fluorescence) methods must test and refine chromatographic columns, solvents, and gradients in order to establish the required selectivity for any target analyte. That process may require days or weeks of research time. Even after chromatographic conditions have been optimized, the analysis of each sample is likely to require 15–30 minutes of chromatography, followed by another 5–30 minutes to accommodate column flushing and re-equilibration to initial conditions. In contrast, LC/MS/MS assays can be developed rapidly by choosing generic chromatographic separation conditions. LC is required mostly to separate analytes from the physiological fluid matrix, with most of the separation selectivity provided by the MS/MS selected reaction monitoring. Analysis cycle times can be reduced to 2 to 5 minutes or less because fast, gradient trap, and elution conditions can be devised with short columns. Finally, LC/MS procedures can be easily modified to include the metabolites in the analyses, simply by adding another target mass and mass fragmentation.

The capability of mass spectrometry to analyze multiple drugs in physiological fluids and the demand of high-throughput screening has led some pharmaceutical companies to test the concept of "cassette dosing," that is, the analysis of pharmacological data generated by simultaneous administration of several drugs to a single animal, cell preparation, or enzyme incubation setup (6, 7). Although LC/MS is compatible with the determination of multiple drugs in a mixture, the drugs are not independent variables when coadministered *in vivo* because of their interactions with metabolic enzymes. Consequently, cassette dosing has not been generally adopted as a means of short-cutting either the *in vitro* or *in vivo* study of drug metabolism.

HPLC/MS/MS Quantitative Assays of Cytochrome P450 Enzyme Activity

Knowledge of potential drug–drug interactions has led to a need to assay specific cytochrome P450 (CYP) enzyme activities to determine whether new drug entities have inhibitory properties. Enzyme activity measurements require kinetic assays that will remain highly specific in the presence of the new drug entities that are being evaluated. That requirement led Walsky and Obach (8) to develop a panel of 12 validated LC/MS/MS assays for 10 of the human CYP enzymes most commonly involved in drug metabolism. The assay of CYP2B6 activity is described in some detail here because it illustrates the principles applied to the separation and analytical steps common to all of the assays. Each CYP enzyme can be distinguished by a

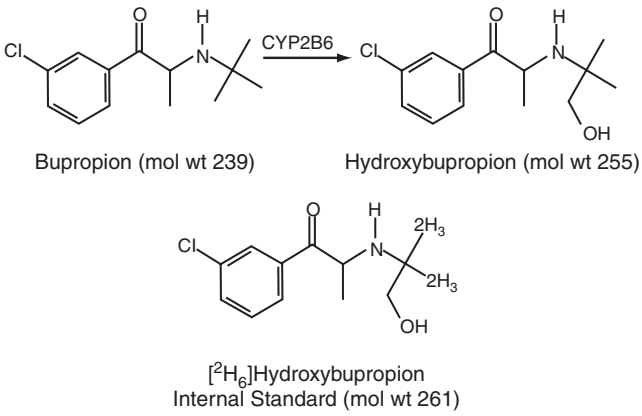

FIGURE 12.11 Metabolism of bupropion by CYP2B6 to hydroxybupropion and the structure of the stable isotope-labeled internal standard [$^2H_6$]hydroxybupropion.

characteristic marker substrate, a compound whose metabolism has been demonstrated to correlate with the concentration of the CYP enzyme protein. Bupropion hydroxylation is a selective *in vitro* indicator of CYP2B6 activity (9, 10) (Figure 12.11).

For the enzyme assay, bupropion is added to pooled liver microsomes and incubated for 20 minutes. Incubations are terminated by the addition of an acidic solution containing a fixed quantity of the deuterium-labeled internal standard [$^2H_6$]hydroxybupropion. The incubation mixture and appropriate standard samples are filtered and stored in 96-well plates for automated LC/MS/MS analyses. Once loaded into the LC/MS injection system, the analyses proceed completely unattended in an automated sequence. HPLC analyses are performed on a short 30-mm reverse-phase column with a 3-minute gradient elution to facilitate rapid analytical cycle times. The eluent from the HPLC column is diverted to waste except during a time-interval bracketing analyte elution. The eluent then is connected to an electrospray needle and the ionized (protonated) analyte and internal standard are transmitted into a tandem mass analyzer, a triple quadrupole in this example (8). At a millisecond frequency, preselected ions are alternatively transmitted from the first quadrupole, into a second quadrupole collision chamber, and the resulting fragment ions are mass separated and detected in the third quadrupole region. In the case of hydroxybupropion and its isotopomer, the protonated molecular species at m/z 256 and 262 (Figure 12.12) are alternatively selected and fragmented (Figure 12.13) many times per second. Both hydroxybupropion and its internal standard fragment due to controlled collisions with inert gas molecules in the second quadrupole chamber. The characteristic chlorophenylacetyl fragments at m/z 139 are produced and are mass separated from other fragments in the third quadrupole. The resulting selected reaction monitoring data can be displayed in a chromatogram format (Figure 12.14). Facile quantification is possible by measuring the ratio of the relative intensity of the signal from unlabeled hydroxybupropion (area = 628) to that from its deuterated isotopomer (area = 96,538). The resulting data are used to construct kinetic profiles. CYP2B6 was determined to exhibit a K_m of 81.7 ± 1.3 and V_{max} of 413 ± 2 pmol/mg/min for microsomes pooled from 54 human livers. Adding varying concentrations of new drug entities permits the measurement of their potential inhibitory properties.

The HPLC/MS/MS assays of other CYP enzymes are very similar in principle and use the identical instrumentation but employ different internal standards. As a consequence of the high degree of specificity of MS/MS selected reaction monitoring, batteries of CYP assays can be robotically programmed for high throughput with little additional manpower.

HPLC/UV and Immunoassays of Cyclosporine: Assays for Therapeutic Drug Monitoring

Cyclosporine (cyclosporine A) is a potent and widely used immunosuppressive agent with a narrow therapeutic index. As a consequence, there is ongoing competition to develop rapid and accurate assays for therapeutic monitoring of cyclosporine blood concentrations in transplant patients treated with this drug. This competition produced refinement and automation of the reference HPLC/UV methods initially developed for cyclosporine as well as the development of faster, automated assays suitable for routine use in hospital clinical laboratories. Consideration of the immunoassay and chromatographic methods developed for cyclosporine offers an opportunity to review the usual process of clinical assay development and maturation. When developing new chemical entities, pharmaceutical researchers pay a premium for the speed of assay development and an assurance of assay selectivity. However, for marketed drugs, clinical laboratories require reliable and accurate assays that are less expensive and less demanding of sophisticated equipment and operator skill.

Cyclosporine is a hydrophobic cyclic peptide of fungal origin and is composed of 11 amino acid residues. The structure of cyclosporine shows that all of the constituent amino acids are aliphatic (Figure 12.15). UV absorbance at 210 nm is due to the amide bonds in the molecule and is consequently not as intense or distinctive as that of many drugs containing aromatic rings. Development of cyclosporine as a pharmaceutical occurred in the 1970s, a period when HPLC/UV, but not LC/MS, methods were

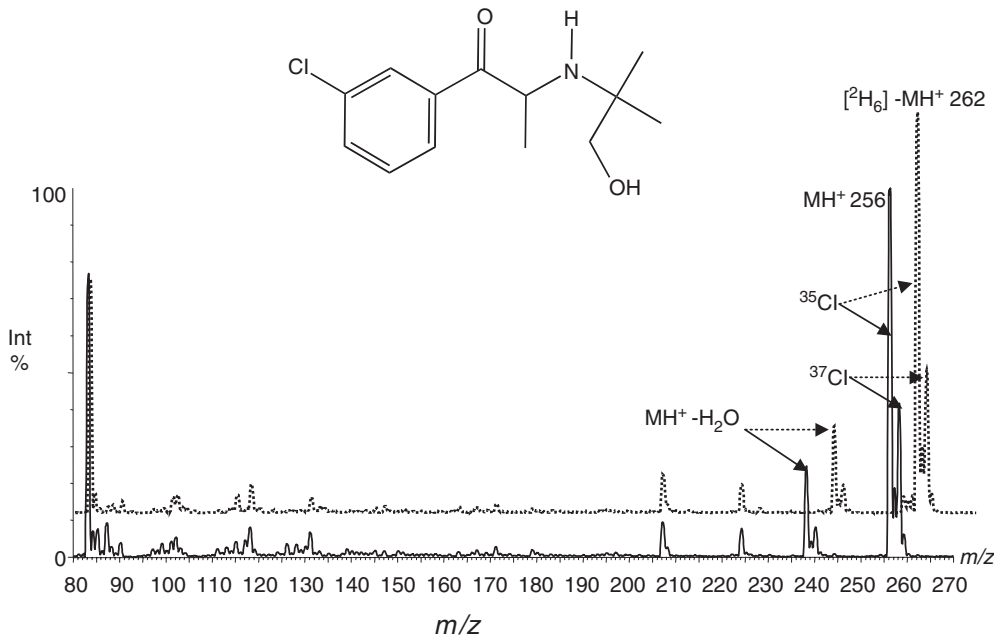

FIGURE 12.12 Electrospray ionization mass spectra of bupropion (*solid line*) and [$^2H_6$]hydroxybupropion (*dotted line*). Note that the protonated molecular ions (MH^+, respectively, at *m/z* 256 and 262) exhibit characteristic chlorine isotope peaks that have 25% of the molecular ion intensity at *m/z* 258 and 264, due to the relative natural abundance of ^{35}Cl and ^{37}Cl. This is reflected also in the MH^+–H_2O ions at *m/z* 238 and 244. Data provided by R.L. Walsky and R.S. Obach, Pfizer, New York, NY.

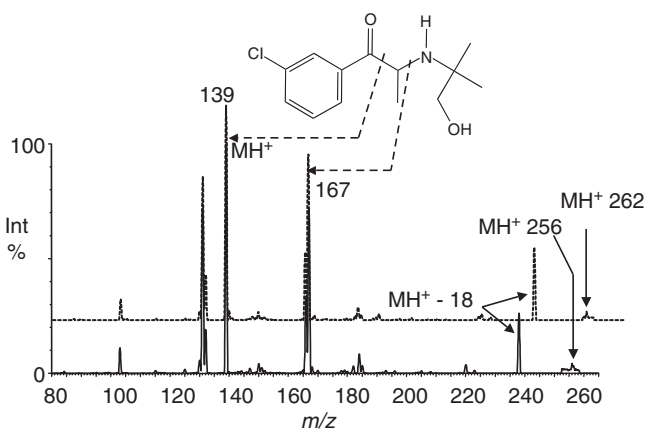

FIGURE 12.13 Collision-induced MS/MS spectra of the MH^+ ions at *m/z* 256 and 262 of hydroxybupropion (*solid line*) and [$^2H_6$]hydroxybupropion (*dotted line*). Note that the fragment ions do not display the characteristic chlorine isotope pattern because only the higher abundance ^{35}Cl species was selected for MS/MS. The origin of fragments at *m/z* 167 and 139 is shown; neither retains deuterium atoms present in the internal standard. Data provided by R.L. Walsky and R.S. Obach, Pfizer, New York, NY.

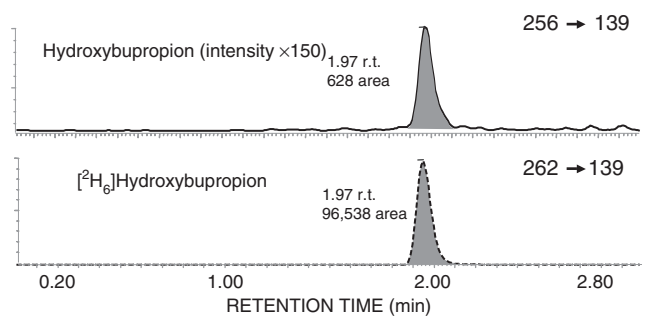

FIGURE 12.14 Selected reaction monitoring reflects the intensity of the transitions *m/z* 256 to 139 and 262 to 139. Note that the peak profiles are free from interference, indicating the specificity and selectivity of the measurement. The internal standard signal is ~153 times the intensity of hydroxybupropion. Data provided by R.L. Walsky and R.S. Obach, Pfizer, New York, NY.

available. Consequently, HPLC/UV was the initial benchmark clinical chemical assay method for cylcosporine, verified subsequently by comparison with newer LC/MS/MS methods (11, 12).

HPLC/UV methods for cyclosporine analyses use whole blood samples with cyclosporine D added as an internal standard (13, 14). Patient blood samples are diluted with a solution of the internal standard in organic solvents to affect cell lysis, dissociation, and solubilization of the cyclosporine. After centrifugation, the analytes in the supernatant are adsorbed on a solid-phase extraction cartridge, washed, and eluted. Interfering lipids are removed from the eluent by extraction with a hydrocarbon solvent, and the sample is separated on a reverse-phase column at 70°C using isocratic conditions, monitoring UV absorbance at 210 nm. Isocratic elution conditions

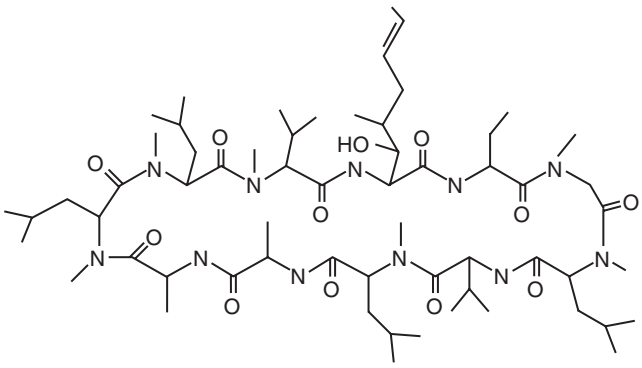

FIGURE 12.15 Chemical structure of cyclosporine.

facilitate faster analytical runs because, as previously noted, there is no time required for resetting gradients and stabilizing the chromatographic conditions. One sample requires 5 to 15 minutes of chromatography time. The LOQ of the HPLC/UV method is ~20–45 μg/L, which is acceptable because the therapeutic range is 80–300 μg/L. Cyclosporine HPLC/UV assay methods have been optimized in a variety of research and commercial laboratories. It is possible for future improvements to be made in sample processing, but this assay represented state-of-the-art HPLC/UV analyses in the mid-1990s (13, 14).

There are several commercial and widely used immunoassays for cyclosporine measurement. Fluorescence polarization immunoassay (FPIA) is one popular technique, typical of a homogeneous immunoassay, and instructive with regard to its principles and limitations. FPIA depends upon the difference in fluorescence characteristics of bound and free fluorescent antigen (15, 16). FPIA instrumentation uses a polarized light source to excite emission by the fluorescein-tagged antigen, in this case fluorescein-tagged cyclosporine. Because cyclosporine is not fluorescent, competition of cyclosporine in patient blood samples with fluorescein-tagged cyclosporine is used as the basis of quantification of cyclosporine concentrations. In the absence of available antibody, the fluorescein-tagged cyclosporine is randomly oriented in solution. Polarized light preferentially excites those molecules with the fluorescein oriented relative to the plane of the incident light. The degree of polarization of the emitted light depends on the percentage of molecules that are fixed or highly oriented. Binding to a macromolecule has the effect of slowing random molecular motion in solutions, and thus bound fluorescein-tagged cyclosporine–antibody complexes emit polarized light more efficiently than does free fluorescein-tagged cyclosporine. By competing with free fluorescein-tagged cyclosporine for antibody complex formation, cyclosporine present in patient blood reduces emission of polarized light and enables the FPIA assay to measure the bound/free ratio of fluorescein-tagged cyclosporine directly and, by reference to a standard curve, the cyclosporine concentration in the blood sample.

FPIA is not affected by background light interference, but is affected by cyclosporine metabolites that cross-react with the antibody. FPIA instrumentation can, in principle, be adapted to quantify any drug for which a fluorescein-tagged analog and specific antibodies can be prepared. The instrumentation is highly automated and designed for routine use in hospital clinical laboratories. Unattended assay of a single sample requires 14 minutes, but most of the time is required for incubation, so analysis of a full carousel of 20 samples requires only 19 minutes. The LOQ for FPIA assays of cyclosporine is 25 μg/L.

Several enzyme immunoassays (EIAs) are also popular commercial clinical assays with cyclosporine measurement capability [e.g., Enzyme Monitored (Multiplied) Immunoassay Technique (EMIT™), Cloned Enzyme Donor Immunoassay (CEDIA™)]. All homogeneous EIAs are competitive immunoassays in which enzyme-labeled antigen competes with sample antigen for a limited quantity of antibody binding sites. The resulting enzyme-labeled antigen–antibody bound complex exhibits a change in its rate of enzymatic action in comparison with free enzyme-labeled antigen. A kinetic measurement of the reaction rate corresponds to determination of the bound/free antigen ratio, and consequently permits the drug concentration in the sample to be measured. The reagents for the cyclosporine EMIT assay use cyclosporine linked to recombinant glucose-6-phosphate dehydrogenase. The active enzyme converts bacterial coenzyme NAD^+ to NADH, resulting in a change of UV absorbance. Enzyme activity is decreased when added monoclonal antibody binds to the cyclosporine-linked enzyme. Highest enzyme activity corresponds to occupation of all antibody sites by high levels of cyclosporine in the blood sample.

The reagents for CEDIA detect the association of two cloned fragments of β-galactosidase, an enzyme that catalyzes the hydrolysis of a chlorophenol-β-galactopyranoside to generate a product detected by UV absorbance at 570 nm. One cloned fragment of the β-galactosidase is linked to cyclosporine. When a monoclonal antibody to cyclosporine is added, competition is established between the cyclosporine in the blood sample and the cyclosporine linked to the β-galactosidase fragment. Higher enzyme activity correlates with higher concentrations of cyclosporine in patient blood. Both EMIT and CEDIA assays are kinetic measurements that are performed in clinical

autoanalyzers, much like the FPIA assay previously described.

In addition to the FPIA, EMIT, and CEDIA methods, several other commercial homogeneous immunoassays have been developed for cyclosporine quantification. Each manufacturer develops and controls the distribution of their antibodies and labeled cyclosporine antigens that define the quantitative response characteristics of their assay kits. Polyclonal antibodies are raised in animals and recognize cyclosporine through a variety of epitope sites; monoclonal antibodies are more specific with regard to structural epitope selection. However, more than 30 cyclosporine metabolites have been characterized and many of them exhibit cross-reactivity (i.e., high affinity) toward poly- and monoclonal antibodies. As a consequence, most of the immunoassays report values that are elevated in comparison to the HPLC/UV or LC/MS/MS reference data. This has led to considerable debate and discussion in the clinical chemistry community with regard to methods for the analysis of cyclosporine and interpretation of the resulting data (11–14, 17–29, 29–32). Several LC/MS/MS methods have been proposed as suitable alternatives in routine clinical chemistry environments (33–35). To some extent, the higher capital cost of the LC/MS/MS equipment is offset by lower reagent expenditures and applicability to multiple clinical drug assays.

Summary of F-ddA, CYP2B6, and Cyclosporine Analyses

The choice of assay technologies illustrated in the discussions of methods for F-ddA, CYP2B6, and cyclosporine demonstrates that there are many chemical, enzymatic, and instrumental options in devising quantitative measurements of drugs and drug metabolites. When new chemical entities are being studied, it is likely that a premium will be paid for the versatility and selectivity of mass spectrometry and the requisite trained scientists required to obtain and interpret data. However, after drugs with narrow therapeutic indices are marketed and widely distributed, commercial considerations will drive the development of techniques that can be applied more widely using general clinical laboratory instrumentation and less highly trained technical staff.

REFERENCES

1. Johnston RAW, Rose ME. Mass spectrometry for chemists and biochemists. Cambridge: Cambridge University Press; 1996.
2. Watson JT. Introduction to mass spectrometry. Philadelphia: Lippincott-Raven; 1997.
3. Hammar CG, Holmstedt B, Ryhage R. Mass fragmentography. Identification of chlorpromazine and its metabolites in human blood by a new method. Anal Biochem 1968;25:532–48.
4. Roth JS, Ford H Jr, Tanaka M, Mitsuya H, Kelley JA. Determination of 2′-beta-fluoro-2′,3′-dideoxyadenosine, an experimental anti-AIDS drug, in human plasma by high-performance liquid chromatography. J Chromatogr B Biomed Sci Appl 1998;712:199–210.
5. Roth JS, McCully CM, Balis FM, Poplack DG, Kelley JA. 2′-Beta-fluoro-2′,3′-dideoxyadenosine, lodenosine, in rhesus monkeys: Plasma and cerebrospinal fluid pharmacokinetics and urinary disposition. Drug Metab Dispos 1999;27:1128–32.
6. Bu HZ, Poglod M, Micetich RG, Khan JK. High-throughput caco-2 cell permeability screening by cassette dosing and sample pooling approaches using direct injection/on-line guard cartridge extraction/tandem mass spectrometry. Rapid Commun Mass Spectrom 2000;14:523–8.
7. Floyd CD, Leblanc C, Whittaker M. Combinatorial chemistry as a tool for drug discovery. Prog Med Chem 1999;36:91–168.
8. Walsky RL, Obach RS. Validated assays for human cytochrome P450 activities. Drug Metab Dispos 2004;32:647–60.
9. Faucette SR, Hawke RL, Lecluyse EL *et al*. Validation of bupropion hydroxylation as a selective marker of human cytochrome P450 2B6 catalytic activity. Drug Metab Dispos 2000;28:1222–30.
10. Hesse LM, Venkatakrishnan K, Court MH *et al*. CYP2B6 mediates the *in vitro* hydroxylation of bupropion: Potential drug interactions with other antidepressants. Drug Metab Dispos 2000;28:1176–83.
11. Oellerich M, Armstrong VW, Schutz E, Shaw LM. Therapeutic drug monitoring of cyclosporine and tacrolimus. Update on Lake Louise Consensus Conference on cyclosporine and tacrolimus. Clin Biochem 1998;31:309-16.
12. Simpson J, Zhang Q, Ozaeta P, Aboleneen H. A specific method for the measurement of cyclosporin A in human whole blood by liquid chromatography–tandem mass spectrometry. Ther Drug Monit 1998;20:294–300.
13. McBride JH, Kim SS, Rodgerson DO, Reyes AF, Ota MK. Measurement of cyclosporine by liquid chromatography and three immunoassays in blood from liver, cardiac, and renal transplant recipients. Clin Chem 1992;38:2300–6.
14. Salm P, Norris RL, Taylor PJ, Davis DE, Ravenscroft PJ. A reliable high-performance liquid chromatography assay for high-throughput routine cyclosporin A monitoring in whole blood. Ther Drug Monit 1993; 15:65–9.
15. Diamandis EP, Christopoulos TK. Immunoassay. San Diego: Academic Press, 1996.
16. Price CP, Newman DJ. Principles and practice of immunoassay. Second Edition, New York Stockton Press, 1997.
17. Aspeslet LJ, LeGatt DF, Murphy G, Yatscoff RW. Effect of assay methodology on pharmacokinetic differences between cyclosporine Neoral and Sandimmune formulations. Clin Chem 1997;43:104–8.

18. Dusci LJ, Hackett LP, Chiswell GM, Ilett KF. Comparison of cyclosporine measurement in whole blood by high-performance liquid chromatography, monoclonal fluorescence polarization immunoassay, and monoclonal enzyme-multiplied immunoassay. Ther Drug Monit 1992;14:327–32.
19. Gulbis B, Van der Heijden J, van As H, Thiry P. Whole blood cyclosporin monitoring in liver and heart transplant patients: Evaluation of the specificity of a fluorescence polarization immunoassay and an enzyme-multiplied immunoassay technique. J Pharm Biomed Anal 1997;15:957–63.
20. Hamwi A, Veitl M, Manner G, Ruzicka K, Schweiger C, Szekeres T. Evaluation of four automated methods for determination of whole blood cyclosporine concentrations. Am J Clin Pathol 1999; 112:358–65.
21. Holt DW, Johnston A, Kahan BD, Morris RG, Oellerich M, Shaw LM. New approaches to cyclosporine monitoring raise further concerns about analytical techniques. Clin Chem 2000;46:872–4.
22. Kivisto KT. A review of assay methods for cyclosporin. Clinical implications. Clin Pharmacokinet 1992;23:173–90.
23. McBride JH, Kim S, Rodgerson DO, Reyes A. Conversion of cardiac and liver transplant recipients from HPLC and FPIA (polyclonal) to an FPIA (monoclonal) technique for measurement of blood cyclosporin A. J Clin Lab Anal 1998;12:337–42.
24. McGuire TR, Yee GC, Emerson S, Gmur DJ, Carlin J. Pharmacodynamic studies of cyclosporine in marrow transplant recipients. A comparison of three assay methods. Transplantation 1992;53:1272–5.
25. Morris RG. Cyclosporin assays, metabolite cross-reactivity, and pharmacokinetic monitoring. Ther Drug Monit 2000;22:160–2.
26. Murthy JN, Yatscoff RW, Soldin SJ. Cyclosporine metabolite cross-reactivity in different cyclosporine assays. Clin Biochem 1998;31:159–63.
27. Oellerich M, Armstrong VW, Kahan B *et al*. Lake Louise Consensus Conference on cyclosporin monitoring in organ transplantation: Report of the consensus panel. Ther Drug Monit 1995;17:642–54.
28. Schutz E, Svinarov D, Shipkova M, *et al*. Cyclosporin whole blood immunoassays (AxSYM, CEDIA, and Emit): A critical overview of performance characteristics and comparison with HPLC. Clin Chem 1998; 44:2158–64.
29. Shaw LM, Holt DW, Keown P, Venkataramanan R, Yatscoff RW. Current opinions on therapeutic drug monitoring of immunosuppressive drugs. Clin Ther 1999;21:1632–52; discussion 1631.
30. Steimer W. Performance and specificity of monoclonal immunoassays for cyclosporine monitoring: How specific is specific? Clin Chem 1999;45:371–81.
31. Takagi H, Uchida K, Takahara S, Takahashi K. 12th quality assessment of cyclosporin blood monitoring by 56 Japanese laboratories. Transplant Proc 1998;30:1706–8.
32. Taylor PJ, Salm P, Norris RL, Ravenscroft PJ, Pond SM. Comparison of high-performance liquid chromatography and monoclonal fluorescence polarization immunoassay for the determination of whole-blood cyclosporin A in liver and heart transplant patients. Ther Drug Monit 1994;16:526–30.
33. Andrews DJ, Cramb R. Cyclosporin: Revisions in monitoring guidelines and review of current analytical methods. Ann Clin Biochem 2002;39:424–35.
34. Ceglarek U, Lembcke J, Fiedler GM *et al*. Rapid simultaneous quantification of immunosuppressants in transplant patients by turbulent flow chromatography combined with tandem mass spectrometry. Clin Chim Acta 2004;346:181–90.
35. Keevil BG, Tierney DP, Cooper DP, Morris MR. Rapid liquid chromatography–tandem mass spectrometry method for routine analysis of cyclosporin A over an extended concentration range. Clin Chem 2002; 48:69–76.

CHAPTER

13

Clinical Pharmacogenetics

DAVID A. FLOCKHART[1] AND LEIF BERTILSSON[2]

[1]*Indiana University School of Medicine, Indianapolis, Indiana*

[2]*Karolinska Institutet at Karolinska University Hospital, Huddinge, Sweden*

INTRODUCTION

The juxtaposition in time of the sequencing of the entire human genome and of the realization that medication errors constitute one of the leading causes of death in the United States (1) has led many to believe that pharmacogenetics may be able to improve pharmacotherapy. As a result, a fairly uncritical series of hopes and predictions have led not only physicians and scientists, but also venture capitalists and Wall Street, to believe that genomics will lead to a new era of "personalized medicine." If this is to occur, it will require a series of accurate and reliable genetic tests that allow physicians to predict clinically relevant outcomes with confidence. This short summary of the state of pharmacogenetics is intended as an introduction to the field, using pertinent examples to emphasize the important concepts of the discipline, which we hope will transcend the moment and serve as a useful group of principles with which to evaluate and follow this rapidly evolving field.

It is particularly important to realize that the huge amount of media, Internet, and marketing hyperbole surrounding pharmacogenetics at this time should be greeted with a healthy dose of scientific skepticism. First, we must note that pharmacogenetics is *not* a new discipline. The coalition of the science of genetics, founded by the work of an Austrian monk, Gregor Mendel, with peas, and the ancient science of pharmacology did not occur until the twentieth century, but it was early in that century. After the rediscovery of the Mendelian laws of genetics at the dawn of the twentieth century, some connection with the ancient science of pharmacology would seem inevitable, and indeed a series of investigators contributed important observations that named and then laid the foundations of the field (Table 13.1) (2). These rested in part in genetics and in part in pharmacology.

In the area of genetics, the separate observations of Hardy and Weinberg that resulted in the Hardy–Weinberg law are particularly pertinent to modern pharmacogenetics. This law states that when an allele with a single change in it is distributed at equilibrium in a population, the incidences p and q of the two resulting alleles will result in a genotype incidence that can be represented by the following equation:

$$p^2 + 2pq + q^2 = 1$$

Two important predictions follow: (1) The incidence of heterozygotes ($2pq$) and of the homozygous q genotype (q^2) can be predicted if the incidence of the homozygous p genotype (p^2) is known. (2) If this equation accurately predicts the incidence of genotypes and alleles, then we are dealing with a single change that results in two alleles and two resultant phenotypes. If genotypes are present in a population in disequilibrium with this law, the influence of population concentrating factors or environment must be invoked, and a pure genetic etiology is inadequate.

In the area of pharmacology, the identification of the series of proteins in the familiar pharmacologic cascade essentially identified not only a series of targets for drugs but also a series of genetic "targets" that might contribute to interindividual variability in

TABLE 13.1 Early History of Pharmacogenetics

Date	Event
1932	First inherited difference in a response to a chemical — inability to taste phenythiourea
World War II	Hemolysis in African-American soldiers treated with primaquine highlights importance of genetic deficiency of glucose-6-phosphate dehydrogenase
1957	Motulsky proposes that "inheritance might explain many individual differences in the efficacy of drugs and in the occurrence of adverse drug reactions"
1959	Vogel publishes "pharmacogenetics: the role of genetics in drug response"
1959	Genetic polymorphism found to influence isoniazid blood concentrations
1964	Genetic differences found in ethanol metabolism
1977	CYP2D6 polymorphism identified by Mahgoub *et al*. and Eichelbaum *et al*.

drug response. The proteins involved turned out to be diverse in structure, function, and location, ranging from those that control and facilitate drug absorption, through the enzymes in the gastrointestinal tract and liver that influence drug elimination, to molecules involved in the complex series of interactions that occur during and after the interaction between drugs and cellular receptor molecules. Along the way, the complexity of human response to exogenous xenobiotics was constantly reemphasized. The complexity was then exploited to the benefit of patients, as demonstrated by the early work on propranolol, the first β-adrenoreceptor blocker, and cimetidine, the first H2-receptor blocker. Subsequent work demonstrated the involvement of multiple intracellular proteins in the second-messenger response proposed by Earl Sutherland, and in the responses to steroids and other exogenous molecules that have intranuclear sites of action. The twentieth century in pharmacology therefore laid the ground for work in the twenty-first century, which will involve the study of genetic changes in this cascade of important proteins, even as genetic information itself leads to the identification of a large number of new protein and genetic drug targets.

HIERARCHY OF PHARMACOGENETIC INFORMATION

An important second principle of modern pharmacogenetics is illustrated in Figure 13.1, in which the hierarchy of useful information from pharmacogenetic studies is illustrated. Although this figure illustrates an information hierarchy for single nucleotide polymorphisms (SNPs), it could equally well be used for deletions, insertions, duplications, splice variants, copy number polymorphisms, or genetic mutations in general. There is a large amount of research activity at the base of this pyramid at the moment, and available information about the presence, incidence, and validity of individual SNPs is large and rapidly expanding as the result of the work of the SNP consortium, the Human Genome Project, and a large number of individual scientists. As we ascend the pyramid toward increasingly functional data, the pyramid becomes dramatically thinner as the databases containing data about nonsynonymous SNPs, nonconservative amino acid changes, and SNPs

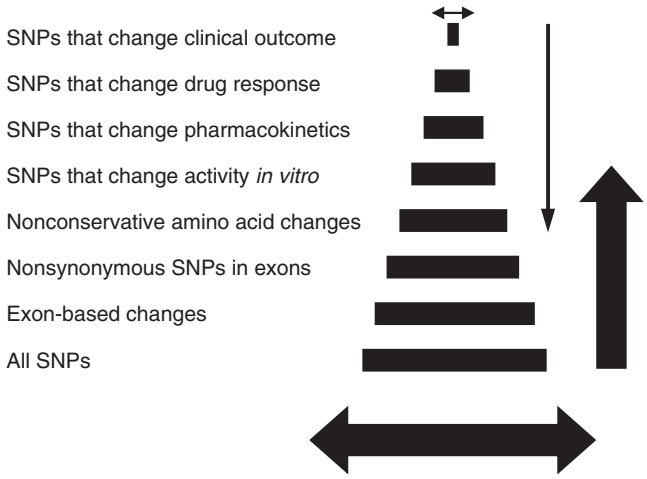

FIGURE 13.1 The hierarchy of pharmacogenetic information from single nucleotide polymorphisms (SNPs). The size of the bar at each level of the pyramid represents an approximation of the number of SNPs in each category. At the base is the total number of SNPs, estimated to be somewhere between 20 million and 80 million. Most of these are not in exons, the expressed sequences that code for proteins, and so the second level is much smaller, in the 300,000 range. Exon-based changes are more likely to result in a clinical effect, but there are good examples of intronic changes and promoter variants that result in important, expressed changes. Nonsynonymous SNPs are those that result in a change in amino acid, and the number of these that are nonconservative and therefore have a greater chance of changing the structure or activity of the protein domain they code for is even smaller. Through a wide range of techniques, laboratory scientists are expressing these variants and testing whether they change activity *in vitro*, and it is clear that most do not, so the number of SNPs at this level of the hierarchy shrinks further. SNPs that result in statistically significant changes in pharmacokinetics due to changes in receptors, transporters, or drug-metabolizing enzymes that are rate limiting are well described, but few and far between. Very few of these result in clinically significant changes and drug response, and even fewer could be measured by the epidemiologists and managers that measure aggregate clinical outcomes.

that change activity *in vitro*, clinical pharmacokinetics, drug response, or finally clinically important outcomes are progressively smaller. The number of SNPs that have been clearly shown to bring about clinically important outcomes is indeed small, and this is reflected in the fact that few pharmacogenetic tests are routinely available to physicians, although a number have become available in the past five years.

This figure also makes clear the long scientific route from the discovery of an individual SNP to the actual demonstration of a clinically important outcome. This is particularly pertinent in view of the simple fact that the vast majority of individual polymorphisms in human DNA likely have no dynamic consequence. A lot of work in the laboratories of molecular biologists and geneticists can therefore be expended to little avail. As a result, a number of clinical pharmacologists and scientists with expertise in pharmacology, genetics, and medicine have elected to start at the other end, the top of the pyramid. By searching for outliers in populations that demonstrate aberrant clinical responses and by focusing on these polymorphisms, they hope to elicit valuable genetic, mechanistic, and clinical lessons. This approach has already borne considerable fruit, as illustrated later in this chapter. It is important to note that these approaches have tended to be most successful when collaborative groups of physicians, pharmacologists, bioinformatics experts, statisticians and epidemiologists, molecular biologists, and geneticists have been able to form translational teams to carry research from the clinic to the laboratory and back.

It is possible for scientists who study specific drug responses to place the phenomena that they study at individual points in time within this hierarchy of information. For example, the cytochrome P450 enzymes present in the human liver and gastrointestinal tract have a long pharmacogenetic history and genetic variants in some are placed at present in the top two rows of the hierarchy. Of course, there are many individual SNPs in the genes corresponding to these enzymes that have no functional consequence, and these remain in the bottom row. In contrast, the majority of the information available at present about drug receptors, transporters, or ketoreductases occupies the lower few rows of the pyramid, although this is starting to change.

For obvious reasons, we have more information about drug responses that are easy to measure. Genetic changes that result in changes in plasma concentrations of drugs that can be measured easily are relatively amenable to study by analytical chemists and clinical pharmacokineticists, whereas genetic polymorphisms in receptors that might influence drug response require careful clinical pharmacologic studies. These simple observations emphasize the need for a qualified cadre of clinical pharmacologists in the field of pharmacogenetics to effectively exploit the huge amount of information made available by the sequencing of the human genome. They perhaps explain also the already apparent concentration of contributions from clinical pharmacologists to the field.

IDENTIFICATION AND SELECTION OF OUTLIERS IN A POPULATION

Figure 13.2 illustrates one useful means of identifying population outliers that allows investigators to focus on these individuals and take information from the top of the hierarchy of information presented in Figure 13.1 and apply it fairly quickly to questions of clinical relevance. Figure 13.2 contains both histograms and Normit plots that illustrate the range of metabolic capacities for CYP2C19 in a population. A Normit plot is essentially a means of describing this range as a cumulative distribution in units of standard deviation from the mean. The cumulative plot of a pure normal distribution will be a straight line, the slope of which is determined by the variance of the distribution. In other words, the steeper the slope, the more tightly the group would be distributed around the mean, whereas a more shallow slope would indicate a more broadly distributed group. The value of this analysis to pharmacogeneticists is that changes in the slope of the line indicate a *new* distribution, and if this different population represents more than 1% of the total, it can reasonably be expected to be genetically stable, and to be termed a *polymorphism*. In the case illustrated, the six subjects on the right were all shown to possess, in both of the alleles coding for CYP2C19, an SNP that was subsequently shown to render the enzyme inactive (3). Figure 13.2 also illustrates the point that a number of probes can be developed to determine the *phenotype* that results from the expression of such a *genotype*. In this case, the study was carried out to demonstrate the utility of a single dose of the proton pump inhibitor omeprazole to serve as a probe for the genetic polymorphism in CYP2C19. As summarized in Table 13.2, ideal characteristics of probes for phenotyping include specificity for the trait in question, sensitivity and ease of available assays, and, most important, the requirement that they be clinically benign. The absence of some of these characteristics in many probes and the difficulty in finding ideal probes are some of the most significant impediments

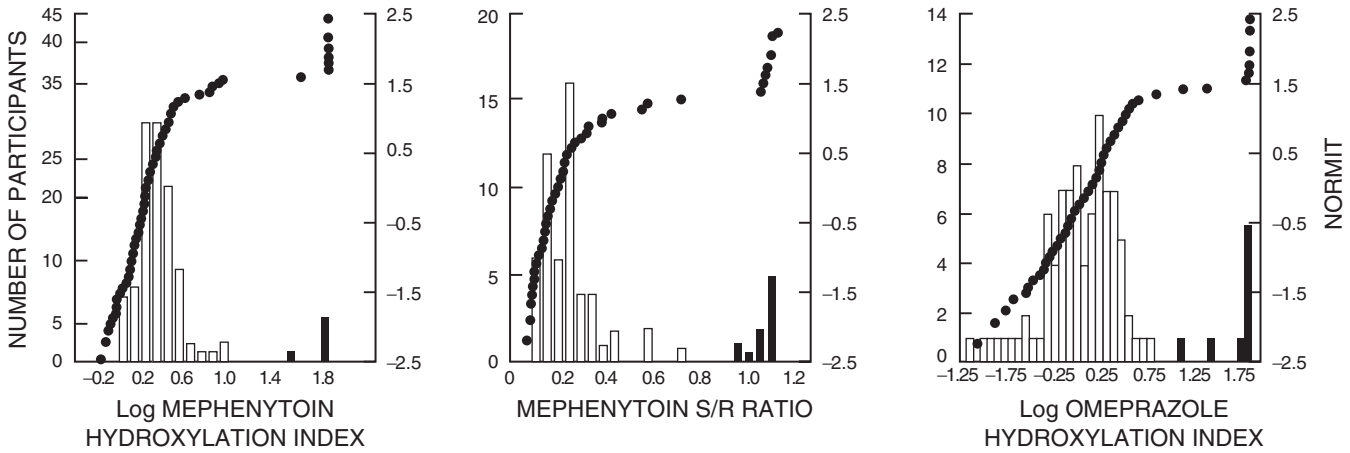

FIGURE 13.2 Normit plots (●) of CYP2C19 activity as indicated by the metabolism of mephenytoin and omeprazole as probe drugs. Comparisons for a population of 142 study partcipants are shown based on log hydroxylation indices for mephenytoin [$\log_{10}$(μmol (*S*)-phenytoin given/μmol 4′-hydroxymephenytoin recovered in urine)] and omeprazole [$\log_{10}$(omeprazole/5′-hydroxyomeprazole)], and ratio of (*S*)-mephenytoin/(*R*)-mephenytoin recovered in urine. In the histograms, rapid metabolizers are represented by lightly shaded bars and slow metabolizers by darkly shaded bars. The same seven individuals were identified by all three methods as poor CYP2C19 metabolizers. (Reproduced with permission from Balian JD *et al.* Clin Pharmacol Ther 1998;57:662–9.)

to progress in developing clinically useful pharmacogenetic tests, and are a key issue that critical scientific evaluators should address.

Upon the identification of an outlier phenotype such as this, the logical next step is a valid demonstration that it can be explained by a genetic change. Family and twin studies are a valuable means of confirming this, and have been the standard in the field since the days of Mendel. These remain an important part of any genetic association study, but they are now being replaced by genetic tests that are able to define changes at specific loci and to test for their presence in broad, unrelated groups of people.

The clinical relevance of the CYP2C19 polymorphism, primarily present in Asian populations (4), has been studied by a number of investigators who have shown that the cure rate for *Helicobacter pylori* infection is greater in patients who are genetic poor metabolizers (5). When given omeprazole doses of 20 mg/day for 4 weeks, these individuals have plasma areas under the curve (AUCs) that are 5- to 10-fold higher than are those of extensive metabolizers (6). The resultant decreases in gastric acid exposure are associated with a clinically important difference in the response of *H. pylori* to treatment (7). As illustrated in Figure 13.3, patients with duodenal ulcers who were poor metabolizers (PMs) had a 100% cure rate, but extensive metabolizers (EMs) with both alleles active had only a 25% cure rate when treated with an omeprazole dose of 20 mg/day. Despite the apparent importance of these data, it might reasonably be argued that selecting a 40- or 60-mg dose of omeprazole for all patients

TABLE 13.2 Properties of an Ideal Probe for Phenotyping

- Specific for the pharmacogenetic trait in question
- Sensitive
- Simple to administer
- Inexpensive
- Easy to assay
- Clinically benign

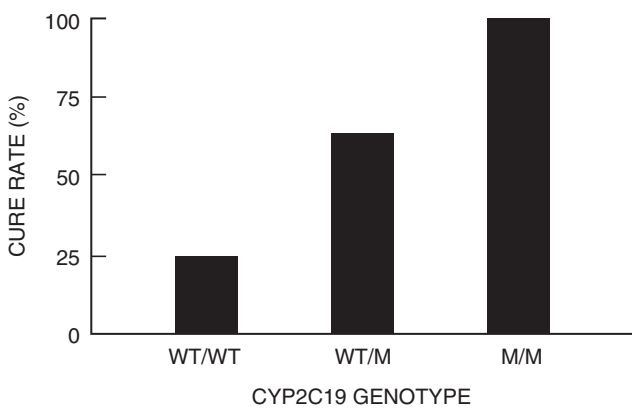

FIGURE 13.3 Effectiveness of omeprazole and amoxacillin in eradicating *Helicobacter pylori* infection in duodenal ulcer patients with CYP2C19 genotypes (WT, wild-type allele; M, mutant allele. (Data from Furuta *et al.* Ann Intern Med 1998;129:1027–30.)

might result in a uniformly beneficial outcome without the need for pharmacogenetic testing.

EXAMPLES OF IMPORTANT GENETIC POLYMORPHISMS

Pharmacologically significant genetic variation has been described at every point of the cascade leading from the pharmacokinetics of drug absorption to the pharmacodynamics of drug effect (Figure 13.1), in many cases reflecting interindividual differences in proteins involved in the absorption, distribution, elimination, and direct cellular action of drugs.

Drug Absorption

One of the most well-known polymorphisms relevant to pharmacodynamic response is in the aldehyde dehydrogenase gene (*ALDH2*) (8). There are 10 human *ALDH* genes and 13 different alleles that result in an autosomal dominant trait that lacks catalytic activity if one subunit of the tetramer is inactive. *ALDH2* deficiency occurs in up to 45% of Chinese, but rarely in Caucasians or Africans, and results in buildup of toxic acetaldehyde and alcohol-related flushing in Asians. Although the genetics of this enzyme and of alcohol metabolism are generally well characterized, a genetic diagnostic test would have little clinical utility because the carriers of the defective alleles are usually acutely aware of it. This illustrates a more widely relevant point: *the availability of genetic testing methodology does not necessarily mean that it is clinically useful, and the incremental value of any pharmacogenetic test is inversely related to our ability to predict drug response with the clinical tools we already have available.*

Drug Distribution

P-Glycoprotein

As discussed in Chapter 14, an elegant series of studies in mice that have the multidrug-resistance (*MDR*) gene for P-glycoprotein (P-gp) knocked out have clearly demonstrated an important role for this multidrug transporter in the absorption and disposition of a large number of clinically important medicines (9–11). The first significant *MDR* mutated allele was shown to change the pharmacokinetics of digoxin in a marked and likely clinically significant manner. Many other transporters have been identified more recently, but the contribution of genetic variation within them to clinical response remains unclear at present. This may in part relate to the ability of most drugs to employ multiple transporters, to the promiscuous ability of many transporters to interact with a large number of drugs, and to the fact that we have yet to identify a human "knockout" of any transporter.

Drug Elimination

The CYP2D6 Polymorphism

No protein involved in drug metabolism or response that has a pharmacogenetic component has been more studied than CYP2D6. In 1977, British investigators described a polymorphism in the hydroxylation of the antihypertensive drug debrisoquine (12, 13). Independently, Eichelbaum *et al.* (14) showed in Germany that the oxidation of sparteine also is polymorphic. The metabolic ratios (MR = ratio of parent drug/metabolite) of the two drugs were closely correlated, indicating that the same enzyme, now termed CYP2D6, is responsible for the two metabolic reactions (15).

The incidence of PMs of debrisoquine/sparteine now has been investigated in many populations, in most of them with a fairly small number of subjects (16). Bertilsson *et al.* (17) found 69 (6.3%) PMs of debrisoquine among 1011 Swedish Caucasians (Figure 13.4). This incidence is very similar to that found in other European (16) and American (18) Caucasian populations. It was shown that the incidence of PMs among 695 Chinese was only 1.0% using the antimode MR = 12.6 established in Caucasian populations (Figure 13.4) (17). A similar low incidence of PMs has been shown in Japanese (18) and Koreans (19).

CYP2D6 Alleles Causing Absent or Decreased Enzyme Activity

The gene encoding the CYP2D6 enzyme is localized on chromosome 22 (20). Using restriction fragment length polymorphism (RFLP) analysis and the allele-specific polymerase chain reaction (PCR), three major mutant alleles were found in Caucasians (21–24). These are now termed *CYP2D6*3*, *CYP2D6*4*, and *CYP2D6*5* (Table 13.3) (25). In Swedish Caucasians, the *CYP2D6*4* allele occurs with a frequency of 22% and accounts for more than 75% of the mutant alleles in this population (26). The *CYP2D6*4* allele is almost absent in Chinese, accounting for the lower incidence of 1% PMs in this population compared to 7% in Caucasians (17). As shown in Table 13.3, the occurrence of the gene deletion (*CYP2D6*5*) is very similar, ranging from 4 to 6% in Sweden, China, and Zimbabwe. This indicates that this is a very old mutation, which occurred before the separation of the three major races 100,000 to 150,000 years ago (27). It is apparent from Figure 13.4

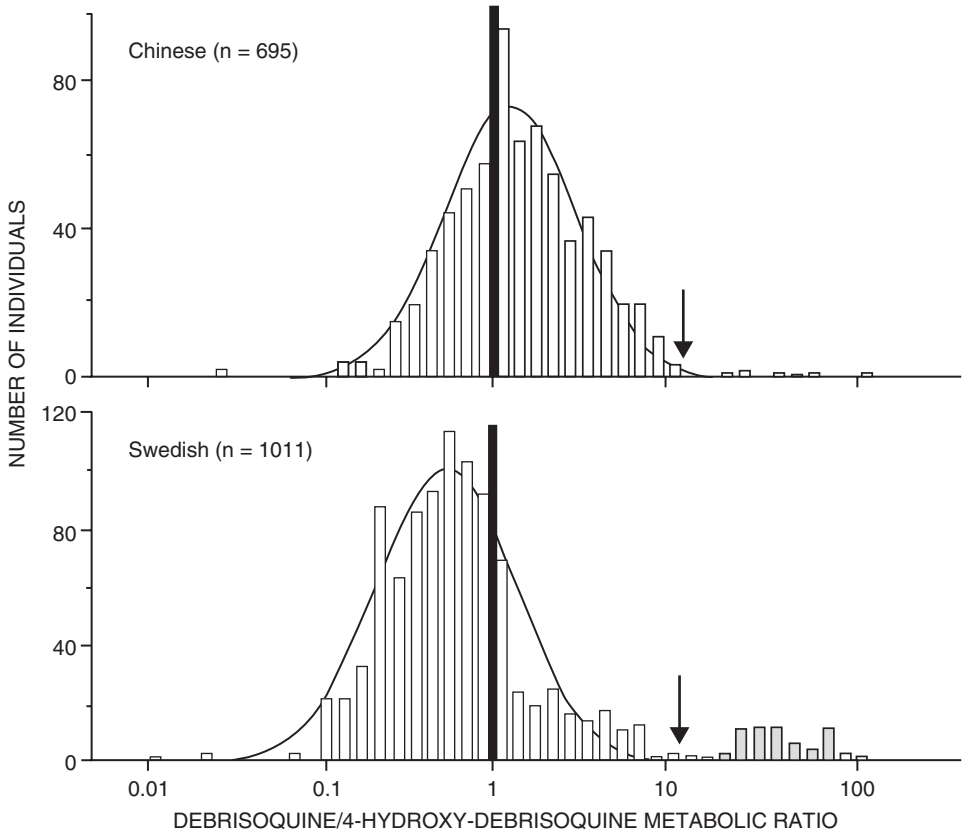

FIGURE 13.4 Distribution of the urinary debrisoquine/4-hydroxydebrisoquine metabolic ratio (MR) in 695 Chinese and 1011 Swedish healthy individuals. The arrows indicate MR = 12.6, the antimode between EMs and PMs established in Caucasians. A line is drawn at MR = 1. Most Chinese EMs have MR > 1, while most Swedish EMs have MR < 1. (Reproduced with permission from Bertilsson L *et al.* Clin Pharmacol Ther 1992;52:388–97.)

that the distribution of the MR of Chinese extensive metabolizers (EMs) is shifted to the right compared to Swedish EMs ($p < 0.01$) (17). Most Swedes have MR < 1, whereas the opposite is true for Chinese study participants. This shows that the mean rate of hydroxylation of debrisoquine is lower in Chinese EMs than in Caucasian EMs (17). This right shift in MR in Asians is due to the presence of a mutant *CYP2D6*10* allele at the high frequency of 51% in Chinese (28, 29) (Table 13.3). The SNP C188T causes a Pro34Ser amino acid substitution that results in an unstable enzyme with decreased catalytic activity (29). As shown in

TABLE 13.3 Frequency of Normal *CYP2D6*1* or *2 Alleles and Some Alleles Causing No or Deficient CYP2D6 Activity in Three Different Populations[a]

CYP2D6 alleles	Functional mutation	Consequence	Allele frequency (%)[b]		
			Swedish	Chinese	Zimbabwean
*1 or *2 (wild type)			69	43	54
*3 (A)	A2637 deletion	Frame shift	21	0	0
*4 (B)	G1934A	Splicing defect	22	0–1	2
*5 (D)	Gene deletion	No enzyme	4	6	4
*10 (Ch)	C188T	Unstable enzyme	n.d.	51	6
*17 (Z)	C1111T	Reduced affinity	n.d.	n.d.	34

[a] Data are from Refs. 8, 26, 27, 29, and 30.
[b] n.d., Not determined.

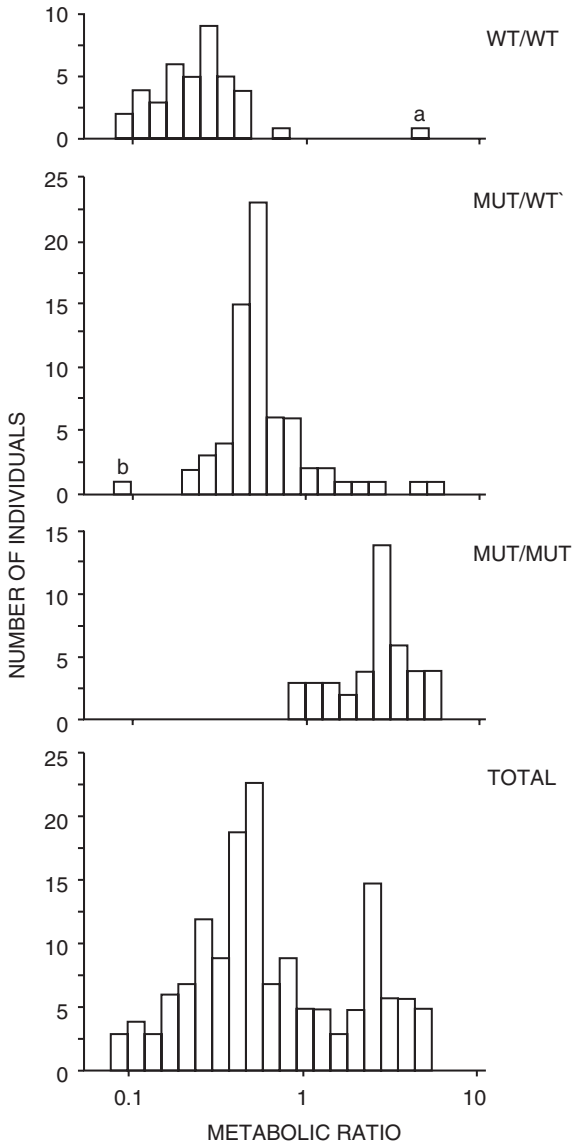

FIGURE 13.5 Distribution of the debrisoquine MR in three genotype groups related to the *CYP2D6*10* allele in 152 Korean individuals. Wild type (WT) = *CYP2D6*1* (or *2) and mutant (MUT) = *CYP2D6*10.* (Reproduced with permission from Roh HK *et al*. Pharmacogenetics 1996;6:441–7.)

Figure 13.5, the presence of this C188T mutation causes a rightward shift in the population of Koreans that was studied (29). The high frequency of this *CYP2D6*10* allele is similar in Chinese, Japanese, and Koreans.

Masimirembwa *et al.* (30) found a right shift of debrisoquine MR in black Zimbabweans similar to that found in Asians. A mutated allele that encodes an enzyme with decreased debrisoquine hydroxylase activity was subsequently identified and named *CYP2D6*17*. Among black Africans, the frequency of this allele was found to be 34% in Zimbabweans (30) (see Table 13.3), 17% in Tanzanians (31), 28% in Ghanaians (32), and 9% in Ethiopians (33). This and many other studies demonstrate the genetic heterogeneity of different populations in Africa. Wennerholm *et al.* (34) administered four different CYP2D6 substrates on separate occasions to Tanzanians with different genotypes. Subjects with the *CYP2D6*17/*17* genotype had a decreased rate of metabolism of debrisoquine and dextromethorphan but normal metabolism of codeine and metoprolol. This demonstrates a changed substrate specificity of the *CYP2D6*17*-encoded enzyme in a population-specific manner (34).

There are population-specific CYP2D6 alleles with the *CYP2D6*4* genotype in Caucasians, with a C1934A mutation giving a splicing defect so that no enzyme is encoded. The *CYP2D6*10* and *CYP2D6*17* alleles in Asians and Africans, respectively, encode two different enzymes with decreased activity. In several studies, a close genotype and phenotype relationship has been demonstrated in Caucasians and Asians (26, 28, 29). However, in studies in Ethiopia (33), Ghana (32), and Tanzania (31) a lower CYP2D6 activity in relation to genotype has been demonstrated, indicating that in addition to genetic factors, environmental factors such as infections or food intake are of phenotypic importance in Africa. Evidence for an environmental influence on CYP2D6-catalyzed debrisoquine hydroxylation also was demonstrated by comparing Ethiopians living in Ethiopia or in Sweden (35).

Gene Duplication, Multiduplication, and Amplification as a Cause of Increased CYP2D6 Activity

The problem of treating debrisoquine PMs with various drugs has been extensively discussed over the years since the discovery of the CYP2D6 polymorphism (16). However, much less attention has been given to patients who are ultrarapid debrisoquine hydroxylators and who lie at the other extreme of the MR distribution. Bertilsson *et al.* (36) described a woman with depression who had an MR of debrisoquine of 0.07; this patient had to be treated with 500 mg of nortriptyline daily to achieve a therapeutic response. This is three to five times higher than the recommended dose. The molecular genetic basis for the ultrarapid metabolism subsequently was identified both in this patient and in another patient, who had to be treated with megadoses of clomipramine (37). These two patients had an *Xba*I 42-kb fragment containing two different functionally active CYP2D6 genes in the CYP2D locus, causing more enzyme to be expressed. That same year, a father and his daughter and son with 12 extra copies of the CYP2D6 gene

were described (38). This was the first demonstration of an inherited amplification of an active gene encoding a drug-metabolizing enzyme. These subjects were ultrarapid hydroxylators of debrisoquine, with MRs ranging from 0.01 to 0.02.

The 12.1-kb fragment obtained by *Eco*RI RFLP analysis represents a duplicated or multiduplicated *CYP2D6*2* gene (38). There are now also a few examples of duplicated *CYP2D6*1* and *CYP2D6*4* genes (39). In Swedish Caucasians, the frequency of subjects having duplicated/multiduplicated genes is about 1% (40). In southern Europe, the frequency increases to 3.6% in Germany (41), 7–10% in Spain (39, 42), and 10% on Sicily (43). The frequency is as high as 29% in black Ethiopians (33) and 20% in Saudi Arabians (44). Thus, there is a European-African north–south gradient in the incidence of CYP2D6 gene duplication. The high incidence among Ethiopians and Saudi Arabians indicates that the high incidence in Spain and Italy may stem from the Arabian conquest of the Mediterranean area (39). The high frequency of duplicated genes among Ethiopians might be the result of a dietary pressure favoring the preservation of duplicated CYP2D6 genes, because this enzyme has the ability to metabolize alkaloids and other plant toxins (44).

Kawanishi *et al.* (45) recently studied 81 depressed patients who failed to respond to antidepressant drugs that are substrates of CYP2D6. CYP2D6 gene duplication was analyzed based on the hypothesis that there is an overrepresentation of ultrarapid metabolizers as a cause of nonresponse. Of the 81 patients, 8 had a gene duplication (9.9% and 95% confidence interval 3.4 to 16.4%) (45), higher than the 1% found in healthy Swedish volunteers (40). These findings suggest that ultrarapid drug metabolism resulting from CYP2D6 gene duplication is a possible factor responsible for the lack of therapeutic response in some depressed patients.

Metabolism of CYP2D6 Drug Substrates in Relation to Genotypes

Although CYP2D6 represents a relatively small proportion of the immunoblottable CYP450 protein in human livers, it is clear that it is responsible for the metabolism of a relatively large number of important medicines (28). Since the discovery of the CYP2D6 polymorphism in the 1970s, almost 100 drugs have been shown to be substrates of this enzyme. Some of these drugs are shown in Table 13.4. The CYP2D6 substrates are all lipophilic bases. Both *in vitro* and *in vivo* techniques may be employed to study whether or not a drug is metabolized by CYP2D6. *In vivo* studies need to be performed to establish the quantitative importance of this enzyme for the total metabolism of the drug. We illustrate here some of the key principles involved in the study of this important enzyme, using the example of the tricyclic antidepressant nortriptyline.

Nortriptyline was one of the first clinically important drugs to be shown to be metabolized by CYP2D6 (46, 47). The early studies, prior to the era of genotyping, were performed in phenotyped panels of healthy study participants and the results subsequently were confirmed in patient studies as well as *in vitro,* using human liver microsomes and expressed enzymes. In a subsequent study, Dalen *et al.* (48) administered nortriptyline as a single oral dose to 21 healthy Swedish Caucasian participants with different genotypes. As seen in the left panel of Figure 13.6, plasma concentrations of nortriptyline were higher in participants with the *CYP2D6*4/*4* genotype (no functional genes) than in those with one to three functional

TABLE 13.4 Some Drugs Whose Metabolism Is Catalyzed by the CYP2D6 Enzyme (Debrisoquine/Sparteine Hydroxylase)

β-Adrenoreceptor blockers	Antidepressants	Neuroleptics	Antiarrhythmic drugs	Miscellaneous
Metoprolol	Amitriptyline	Haloperidol	Encainide	Codeine
Propranolol	Clomipramine	Perphenazine	Flecainide	Debrisoquine
Timolol	Desipramine	Risperidone	Perhexiline	Dextromethorphan
	Fluoxetine	Thioridazine	Propafenone	Phenformin
	Fluvoxamine	Zuclopenthixol	Sparteine	Tramadol
	Imipramine			
	Mianserin			
	Nortriptyline			
	Paroxetine			

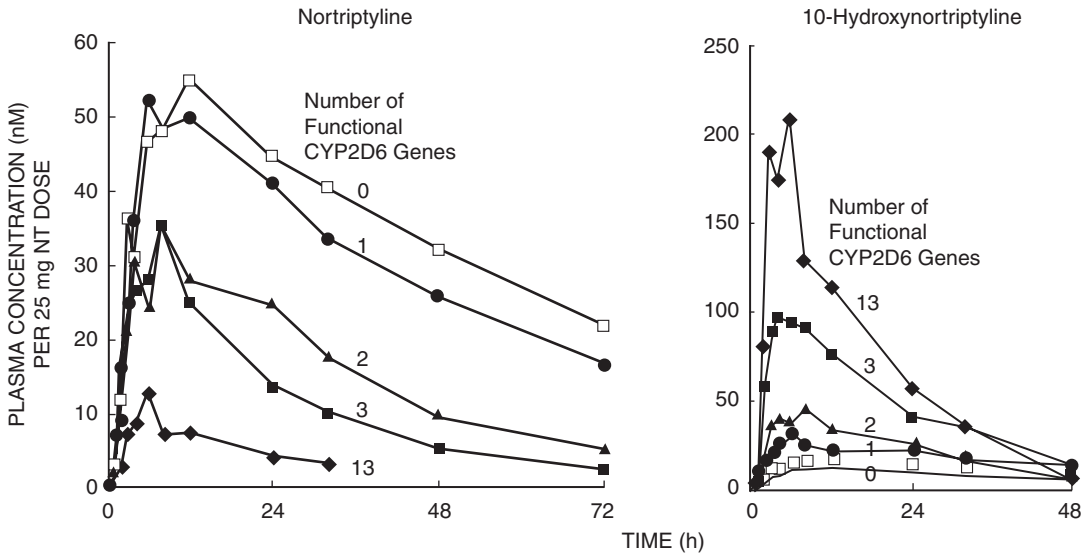

FIGURE 13.6 Mean plasma concentrations of nortriptyline (NT) and 10-hydroxynortriptyline in different genotype groups after a single oral dose of nortriptyline. The numerals close to the curves represent the number of functional CYP2D6 genes in each genotype group. In groups with 0–3 functional genes, there were five individuals in each group. There was only one person with 13 functional genes. (Reproduced with permission from Dalén P *et al.* Clin Pharmacol Ther 1998;63:444–52.)

genes (gene duplication). The plasma concentrations of the parent drug were extremely low in one person with 13 CYP2D6 genes, the son in the family previously mentioned (genotype *CYP2D6*2 × 13/*4*). The plasma concentrations of the nortriptyline metabolite, 10-hydroxynortriptyline, show the opposite pattern, that is, highest concentrations in the person with 13 genes and lowest in the PMs (Figure 13.6, right panel). This study clearly shows the impact of the detrimental *CYP2D6*4* allele as well as the duplication/amplification of the *CYP2D6*2* gene on the metabolism of nortriptyline (48).

A relationship between CYP2D6 genotype and steady-state plasma concentration of nortriptyline and its hydroxy metabolite also has been shown in Swedish depressed patients treated with the drug (49). Using the same protocol as in the study of Dalén *et al.* (48) in Swedish Caucasians, Yue *et al.* (50) investigated the influence of the Asian-specific *CYP2D6*10* allele on the disposition of nortriptyline in Chinese patients living in Sweden. Morita *et al.* (51) correlated the *CYP2D6*10* allele with steady-state plasma levels of nortriptyline and its metabolites in Japanese depressed patients. The conclusion from these two studies is that the Asian *CYP2D6*10* allele encodes an enzyme with decreased nortriptyline-metabolizing activity. However, this effect is less pronounced than is the effect of the Caucasian-specific *CYP2D6*4* allele, which encodes no enzyme at all. Although CYP2D6 genotyping may eventually find clinical use as a tool to predict proper dosing of drugs such as nortriptyline in individual patients, it must, however, be remembered that there are population-specific alleles.

Drugs metabolized by CYP2D6 include all the β-adrenoreceptor blockers that are known to be metabolized, including propranolol (52), metoprolol (53), carvedilol (54), and timolol (55). While few studies of patient response are available, an elegant clinical pharmacologic study has demonstrated lower resting heart rates in PMs who were administered timolol (55). On the other hand, a key principle is illustrated by studies demonstrating that altered pharmacokinetics of propranolol in Chinese patients were *not* accompanied by the expected pharmacodynamic changes (56). In this case, increased concentrations in poor metabolizers apparently were offset by changes in pharmacodynamic responsiveness.

While it is often held that genetic polymorphisms are most important when they affect drugs that have a narrow therapeutic index for which dangerous toxicity may result or perilous lack of effect may ensue, this need not be the case. For example, CYP2D6 converts codeine, likely the most widely prescribed opiate in the world and the mainstay of pain control for a large number of patients, to its active metabolite morphine. Thus, patients who have deficient CYP2D6 are unable to make morphine, and pharmacodynamic studies have shown that this results in decreased pain

control (57) as well as in decreased codeine effects on pupillary size and respiratory function (58).

Last, an important lesson that has been learned from research on CYP2D6 is that many, but not all, genetic polymorphisms can be mimicked by drug interactions. Not only is codeine metabolism by CYP2D6 potently inhibited by quinidine (58), but the inhibition of this enzyme by commonly prescribed drugs such as fluoxetine (59), paroxetine (60, 61), and the majority of antipsychotic drugs (62), including haloperidol (63), is also well described. These interactions are likely clinically relevant and more prevalent in many circumstances than is the PM genotype (64). Of note, the ultrarapid metabolizer phenotype of CYP2D6 has not at present been shown to be mimicked by a drug interaction, and the rare reports of effects of metabolic inducers on CYP2D6 activity are unclear, and appear modest at best (65).

The Thiopurine S-Methyltransferase Polymorphism

One of the most developed examples of clinical pharmacogenomics involves the polymorphism of thiopurine *S*-methyltransferase (TPMT). This is a cytosolic enzyme whose precise physiological role is unknown. It catalyzes the *S*-methylation of the thiopurine agents azathioprine, 6-mercaptopurine, and 6-thioguanine using *S*-adenosylmethionine as a methyl donor (66). Originally found in the kidney and liver of rats and mice, it was subsequently shown to be present in most tissues, including blood cells (67). Due to its good correlation with TPMT activity in other tissues, TPMT activity is measured clinically in easily obtained erythrocytes (67). TPMT activity is polymorphic and a trimodal distribution has been demonstrated in Caucasians (67). About one person in 300 is homozygous for a defective TPMT allele, with very low or absent enzyme activity. Eleven percent are heterozygous with an intermediate activity (67). The frequency with which TPMT activity is lost varies in different populations and has been reported to be as low as 0.006–0.04% in Asian populations, in contrast to the frequency of 0.3% in Caucasians (68).

The TPMT gene is located on chromosome 6 and includes 10 exons (68). *TPMT*3A*, the most common mutated allele, contains two point mutations in exons 7 (G460A and Ala154Thr) and 10 (A719G and Tyr240Lys). Two other alleles contain a single mutation, the first SNP (*TPMT*3B*) and the second SNP (*TPMT*3C*) (69). Aarbakke *et al.* (70) have reviewed the variant alleles of the TPMT gene and the relationship to TPMT deficiency. In Caucasians, *TPMT*3A* accounts for about 85% of mutated alleles, and in such populations the analysis of the known alleles may predict the TPMT activity phenotype. In a Korean population, *TPMT*3A* was absent and the most common allele was *TPMT*3C* (71, 72). However, early investigations focused on allele-specific screening for only four alleles, namely, *TPMT*2*, *TPMT*3A*, *TPMT*3B*, and *TPMT*3C* (72). Due to the limited scope of the screening used in the majority of studies investigating ethnic-specific TPMT allele frequencies, continued studies in different populations involving full-gene sequencing or similar techniques seem necessary (73). Otherwise, selecting only those alleles that are more frequent in a single population may result in important alleles being overlooked in other populations.

Azathioprine and 6-mercaptopurine are immunosuppressants that are used to treat patients with several conditions, including immunological disorders, and to prevent acute rejection in transplant recipients. In Europe, azathioprine, the precursor of 6-mercaptopurine, has been the thiopurine of choice in inflammatory bowel disease, whereas in parts of North America, 6-mercaptopurine is more commonly used. 6-Mercaptopurine also is commonly used in acute lymphoblastic leukemia of childhood (74). Azathioprine is an imidazole derivative of 6-mercaptopurine and is metabolized nonenzymatically to 6-mercaptopurine as shown in Figure 13.7. 6-Mercaptopurine is metabolized by several pathways, one of which is catalyzed by TPMT and leads to inactive methylthiopurine metabolites. Other pathways catalyzed by several other enzymes lead to the active thioguanine nucleotides (6-TGNs). The resulting 6-TGNs act as purine antagonists through their incorporation into DNA and subsequent prevention of DNA replication. The reduction in DNA replication suppresses various immunological functions in lymphocytes, T-cells, and plasma cells (74). Numerous studies have shown that TPMT-deficient patients are at very high risk of developing severe hematopoietic toxicity if treated with conventional doses of thiopurines (75). High concentrations of 6-TGNs in patients with low TPMT activity may cause toxicity and bone marrow suppression. On the other hand, low concentrations in patients with high TPMT activity may increase the risk of therapeutic failure and also of liver toxicity, due to the accumulation of other metabolites such as 6-methylmercaptopurine nucleotides (Figure 13.7). Other less serious side effects of azathioprine are gastrointestinal symptoms such as nausea and vomiting. These side effects represent azathioprine intolerance that is not clearly associated with TPMT activity or metabolite levels.

Another important issue apart from avoiding adverse effects is, of course, the treatment effect. Several studies have shown a relationship between

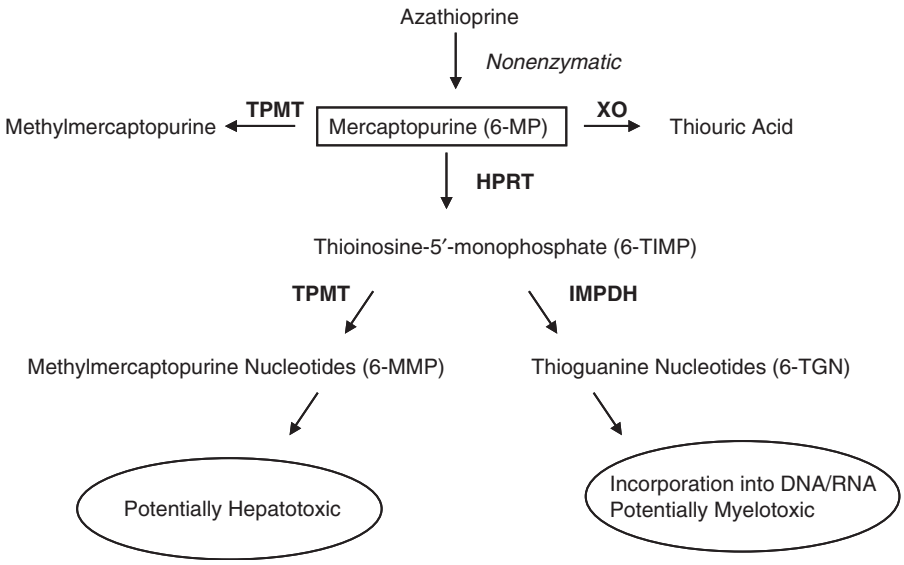

FIGURE 13.7 Thiopurine metabolic pathways. TPMT, Thiopurine methyltransferase; XO, xanthine oxidase; HPRT, hypoxanthine guanine phosphoribosyltransferase; IMPDH, inosine monophosphate dehydrogenase.

therapeutic effects and TPMT activity or 6-TGN concentrations in red blood cells. However, more clinical studies are needed to establish therapeutic concentration ranges for the various conditions in which these drugs are used. So far, most drug effect studies are focused on 6-TGN concentrations. However, other enzymes and metabolites are also involved in the complex metabolism of thiopurines. Thus, there might be other as yet unknown factors involved in the metabolism and action of thiopurine drugs that are better correlated with treatment outcome and that should be focused on. These, notably, CYP2C9, CYP2C19, and CYP2D6 could reasonably be found in further studies.

In conclusion, low TPMT activity due to TPMT polymorphism can lead to severe myelosuppression in patients treated with thiopurines such as 6-mercaptopurine. A number of studies have shown pretreatment TPMT status testing to be cost-effective and a reliable way of predicting life-threatening bone marrow toxicity. Many authors, including the present authors, are of the opinion that TPMT phenotype status testing should be incorporated in routine clinical practice to avoid severe adverse drug reactions and to adjust dosing in patients identified with *intermediate* as well as low to absent TPMT activity. Although the pretreatment TPMT status of patients can be measured by phenotype or genotype, the clinical utility of measuring TPMT genotype is uncertain in view of the difficulties involved in interpreting the consequences of novel polymorphism detection and the chance of missing clinically relevant allelic variation in different racial groups. There clearly is a need for further genotype–phenotype correlation studies as well as for further drug effect studies in which relevant metabolites are monitored. Furthermore, standard genotyping techniques cannot, as yet, predict those individuals with very high TPMT activities who may not respond to standard doses of azathioprine or 6-mercaptopurine. Thus, despite its clinical importance, pharmacogenetic testing for this polymorphism remains problematic, since a large number of alleles must be tested, genetic haplotype identification is difficult, and phenotypic measurements that quantify the enzyme in erythrocytes remain more useful than do genetic tests.

N-Acetyltransferase 2

In marked contrast to the data on genetic changes in thiopurine methyltransferase, mutations in *N*-acetyltransferase 2 (NAT-2) are very common, but have little clinical significance (8). NAT-2 can therefore be placed on the pyramid of genetic information at a point where clear pharmacokinetic changes have been noted, but important pharmacodynamic consequences have not yet been demonstrated. In addition, as with CYP2D6, it is clear that a large number of mutations and at least 17 different alleles contribute to this change in activity (76). The slow acetylator phenotype is present in roughly 50% of Caucasian and African populations studied, but in as few as 10% of Japanese and in as many as 80% of Egyptians (77, 78).

Woosley *et al.* (79) demonstrated that slow acetylators develop positive antinuclear antibody (ANA) titers and procainamide-induced lupus more quickly than do rapid acetylators. However, this finding did not lead to widespread phenotypic or genetic testing because all patients will develop positive ANA titers after one year of procainamide therapy and almost a third will have developed arthralgias and/or a skin rash (80). Although a number of researchers have attempted to associate this polymorphism with the risk for xenobiotic-induced bladder, colorectal (81), or breast cancer (82), there are at present no compelling data that warrant phenotypic testing for this polymorphism in order to improve treatment with any medicine, much less a genetic test that would have to accurately identify such a large number of alleles.

Mutations That Influence Drug Receptors

β2-*Adrenoreceptor Mutations in Asthma*

Since the first descriptions of genetic polymorphisms in the β2 receptor that may play a pathogenic role in the development of asthma (83, 84), a number of investigators have shown an association between these mutations and patient response to treatment for this disease. A number of missense mutations within the coding region of the type 2 β-receptor gene on chromosome 5q31 have been identified in humans. In studies utilizing site-directed mutagenesis and recombinant expression, three loci at amino acid positions 16, 27, and 164 have been found to significantly alter *in vitro* receptor function. The Thr164Ile mutation displays altered coupling to adenylyl cyclase, the Arg16Gly mutation displays enhanced agonist-promoted down-regulation, and the Gln27Glu form is resistant to down-regulation (84). The frequencies of these various β2-adrenoreceptor (β2AR) mutations are no different in asthmatic than in normal populations, but Lima *et al.* (85) have shown that the albuterol-evoked increase in forced expiratory volume in 1 second (FEV_1) was higher and bronchodilatory response was more rapid in Arg16 homozygotes than in a cohort of carriers of the Gly16 variant. In addition, an association has been demonstrated between the same β2AR polymorphism and susceptibility to bronchodilator desensitization in moderately severe stable asthmatics. Although these data are compelling, careful studies have concluded that the β2AR genotype is not a major determinant of fatal or near-fatal asthma (86), and widespread testing of asthmatic patients for the presence of genetic polymorphisms in the β2AR is not yet routinely carried out. Nevertheless, a number of other potential target proteins may alter the susceptibility and response of asthmatic patients, including histamine *N*-methyltransferase (87) and the lipoxygenase system, and further developments in the genetics of asthma pharmacotherapy seem likely.

Mutations in Endothelial Nitric Oxide Synthase

An association has been made between cardiovascular disease and specific mutations in endothelial nitric oxide synthase (eNOS), the enzyme that creates nitric oxide via the conversion of citrulline to arginine in endothelial cells and in platelets (88). A firmer understanding of the mechanism of this effect has been provided by a series of careful studies of forearm vascular vasodilation conducted by Babaoglu and Abernethy (89), who showed that acetylcholine, but not nitroprusside-mediated vasodilation, was compromised by the Glu298Asp mutation in this enzyme. These results demonstrate the value of careful clinical pharmacologic studies in confirming a pharmacological consequence of a polymorphism that otherwise would only have had an association with cardiovascular disease. The implications of these findings for patients with hypertension, congestive heart failure, and a variety of other disorders are clear issues for future investigation.

Somatic Mutations in the EGF Receptor in Tumors

From the perspective of general practitioners and most patients, the treatment of non-small-cell lung cancer has not significantly advanced over the past 20 years. The advent of treatment with the tyrosine kinase inhibitor gefitinib brought a new approach, but it was clear from the start that only a few patients appeared to benefit. Recently, mutations in the epidermal growth factor receptor (EGFR) have been identified that appear to identify a subpopulation of patients who do respond well (90). This work has identified "gain of function" somatic mutations within the tumors of these patients that appear to *enhance* their responsiveness to gefitinib, an important conceptual advance from the assumption that all mutations are inevitably deleterious. While the study was conducted on only a small number of patients and their tumors, it is not difficult to recognize the potential importance of this finding for those patients whose tumors do carry the relevant mutations that correlate with a positive response to gefitinib treatment. Further studies are ongoing that have been designed to replicate these data in larger populations, and to refine the genetic signature of "responder" tumors. These data also directly

challenge the prevailing paradigm that a drug should be effective in all patients in order to be useful.

Combined Variants in Drug Metabolism and Receptor Genes: Value of Drug Pathway Analysis

Each drug has a pharmacokinetic pathway of absorption, metabolism, and disposition that is ultimately linked to an effect pathway involving receptor targets and downstream signaling systems. It is clearly possible that many of the proteins in these pathways may be genetically polymorphic. It is instructive to examine one pathway in which consideration of the effect on patient response of variants in a gene involved in drug metabolism combined with variants in a receptor provides greater predictive power than when either is considered alone.

Warfarin is a commonly used anticoagulant that requires careful clinical management to balance the risks of overanticoagulation and bleeding with those of underanticoagulation and clotting. In a series of well-designed studies, Rettie *et al.* (91) first showed that CYP2C9 is the principal enzyme involved in the metabolism of (*S*)-warfarin, the active stereoisomer of warfarin. Two relatively common variant forms with reduced metabolic activity have been identified, CYP2C9*2 and CYP2C9*3 (92). Patients with these genetic variants have been shown to require lower maintenance doses of warfarin, and these investigators subsequently showed a direct association between CYP2C9 genotype and anticoagulation status or bleeding risk (93). Finally, employing knowledge of the pathway of warfarin's action via vitamin K carboxylase (VKOR), these authors showed, first in a test population and then in a validation population of 400 patients at a different medical center, that predictions of patient response based on identification of variants in the carboxylase combined with those in CYP2C9 were more powerful than when only a single variant was used (94).

A final key pharmacogenetic principle made clear by these studies is the crucial importance of replicating pharmacogenetic findings in relatively large datasets consisting of patients in real clinical practice. This is related to the very first pharmacogenetic principle described in this chapter, namely, that the excessive initial hyperbole surrounding many pharmacogenetics studies before they are replicated has resulted in an inappropriately high level of expectation of clinically meaningful results in the near term, and may have impeded researchers who wish to replicate the data in other populations.

CONCLUSIONS AND FUTURE DIRECTIONS

There are many potential pitfalls that lie in the way of researchers on the route from the discovery of a mutation in human DNA that codes for a pharmacologically important protein to the development of a clinically useful pharmacogenetic test. Very few such tests have been developed as yet, but a considerable number seem likely to be found useful over the next decade in guiding the treatment of patients with cancer, asthma, depression, hypertension, and pain.

In the development of new pharmacogenetic tests, as for any other clinically applied test, assay sensitivity, specificity, and positive predictive value will have to be scrutinized rigorously. In addition, the reliability of DNA testing in terms of intra- and interday variability and the rigor of assays when applied to multiple DNA samples will have to be demonstrated almost more carefully than it would be for routine assays for serum chemistries or hematology. This is because there are significant societal pressures that insist upon the accuracy of a diagnostic test that informs a physician and a patient about an individual's genetic makeup. The requirement for robust tests has not prevented any other technology from entering clinical practice though, and already a number of array-based genetic tests are available that are able to diagnose genotypes simultaneously at a relatively large number of loci.

When the technical barrier of developing tests with adequate sensitivity, specificity, and reproducibility is overcome, it seems very likely that the practice of medicine will evolve so that individual patients can be treated for their diseases with appropriately individualized doses of medicines, or indeed different medicines directed at specific therapeutic targets, based on their genotype or phenotype.

REFERENCES

1. Kohn LT, Corrigan JM, Donaldson MS, editors; Committee on Quality of Health Care in America. To err is human: Building a safer health system. Washington, DC: National Academy Press; 1999.
2. Nebert DW. Pharmacogenetics: 65 candles on the cake. Pharmacogenetics 1997;7:435–40.
3. Balian JD, Sukhova N, Harris JW, Hewett J, Pickle L, Goldstein JA, Woosley RL, Flockhart DA. The hydroxylation of omeprazole correlates with *S*-mephenytoin metabolism: A population study. Clin Pharmacol Ther 1995;57:662–9.
4. Desta Z, Zhao X, Shin JG, Flockhart DA. Clinical significance of the cytochrome P450 2C19 polymorphism. Clin Pharmacokinet 2002;41:913–58.

5. Furuta T, Ohashi K, Kamata T, Takashiima M, Kosuge K, Kawasaki T *et al.* Effect of genetic differences in omeprazole metabolism on cure rates for *Helicobacter pylori* infection and peptic ulcer. Ann Intern Med 1998;129:1027–30.
6. Andersson T, Regardh CG, Lou YC, Zhang Y, Dahl M-L, Bertilsson L. Polymorphic hydroxylation of *S*-mephenytoin and omeprazole metabolism in Caucasian and Chinese subjects. Pharmacogenetics 1992;2:25–31.
7. Furuta T, Ohashi K, Kosuge K, Zhao XJ, Takashima M, Kimura M *et al. CYP2C19* genotype status and effect of omeprazole on intragastric pH in humans. Clin Pharmacol Ther 1999;65:552–61.
8. Kalow W, Bertilsson L. Interethnic factors affecting drug metabolism. Adv Drug Res 1994;25:1–53.
9. Schinkel AH, Smit JJ, van Tellingen O, Beijnen JH, Wagenaar E, van Deemter L *et al.* Disruption of the mouse mdr1a P-glycoprotein gene leads to a deficiency in the blood–brain barrier and to increased sensitivity to drugs. Cell 1994;77:491–502.
10. Schinkel AH, Wagenaar E, Mol CAM, van Deemter L. P-Glycoprotein in the blood–brain barrier of mice influences the brain penetration and pharmacological activity of many drugs. J Clin Invest 1996;97:2517–24.
11. van Asperen J, Schinkel AH, Beijnen JH, Nooijen WJ, Borst P, van Telligen O. Altered pharmacokinetics of vinblastine in Mdr1a P-glycoprotein-deficient mice. J Natl Cancer Inst 1996;88:994–9.
12. Mahgoub A, Idle JR, Dring LG, Lancaster R, Smith RL. Polymorphic hydroxylation of debrisoquine in man. Lancet 1977;2:584–6.
13. Tucker GT, Silas JH, Iyun AO, Lennard MS, Smith AJ. Polymorphic hydroxylation of debrisoquine in man. Lancet 1977;2:718.
14. Eichelbaum M, Spannbrucker N, Steincke B, Dengler HJ. Defective N-oxidation of sparteine in man: A new pharmacogenetic defect. Eur J Clin Pharmacol 1979;16:183–7.
15. Eichelbaum M, Bertilsson L, Säwe J, Zekorn C. Polymorphic oxidation of sparteine and debrisoquine: Related pharmacogenetic entities. Clin Pharmacol Ther 1982;31:184–6.
16. Eichelbaum M, Gross AS. The genetic polymorphism of debrisoquine/sparteine metabolism: Clinical aspects. In: Kalow W, ed. Pharmacogenetics of drug metabolism. New York: Pergamon Press; 1992. p. 625–48.
17. Bertilsson L, Lou Y-Q, Du Y-L, Liu Y, Kuang T-Y, Liao X-M *et al.* Pronounced differences between native Chinese and Swedish populations in the polymorphic hydroxylations of debrisoquin and *S*-mephenytoin [erratum in Clin Pharmacol Ther 1994;55:648]. Clin Pharmacol Ther 1992;51:388–97.
18. Nakamura K, Goto F, Ray WA, McAllister CB, Jacqz E, Wilkinson GR *et al.* Interethnic differences in genetic polymorphism of debrisoquin and mephenytoin hydroxylation between Japanese and Caucasian populations. Clin Pharmacol Ther 1985;38:402–8.
19. Sohn DR, Shin SG, Park CW, Kusaka M, Chiba K, Ishizaki T. Metoprolol oxidation polymorphism in a Korean population: Comparison with native Japanese and Chinese populations. Br J Clin Pharmacol 1991;32:504–7.
20. Eichelbaum M, Baur MP, Dengler HJ, Osikowska-Evers BO, Tieves G, Zekorn C, Rittner C. Chromosoaml assignment of human cytochrome P450 (debrisoquine/sparteine type) to chromosome 22. Br J Clin Pharmacol 1987;23:455–8.
21. Gonzalez FJ, Skoda RC, Kimura S, Umeno M, Zanger UM, Nebert DW *et al.* Characterization of the common genetic defect in humans deficient in debrisoquine metabolism. Nature 1988;331:442–6.
22. Gaedigk A, Blum M, Gaedigk R, Eichelbaum M, Meyer UA. Deletion of the entire cytochrome P450 CYP2D6 gene as a cause of impaired drug metabolism in poor metabolizers of the debrisoquine/sparteine polymorphism. Am J Hum Genet 1991;48:943–50.
23. Heim M, Meyer UA. Genotyping of poor metabolisers of debrisoquine by allele-specific PCR amplification [see comments]. Lancet 1990;336:529–32.
24. Heim M, Meyer UA. Evolution of a highly polymorphic human cytochrome P450 gene cluster: *CYP2D6*. Genomics 1992;14:49–58.
25. Daly AK, Brockmoller J, Broly F, Eichelbaum M, Evans WE, Gonzalez FJ *et al.* Nomenclature for human *CYP2D6* alleles. Pharmacogenetics 1996;6:193–201.
26. Dahl M-L, Johansson I, Palmertz MP, Ingelman-Sundberg M, Sjöqvist F. Analysis of the *CYP2D6* gene in relation to debrisoquin and desipramine hydroxylation in a Swedish population. Clin Pharmacol Ther. 1992;51:12–7.
27. Bertilsson L, Dahl M-L, Dalén P, Al-Sjurbaji A. Molecular genetics of CYP2D6: Clinical relevance with focus on psychotropic drugs. Br J Clin Pharmacol 2002;54:111–22.
28. Wang S-L, Huang J-D, Lai M-D, Liu B-H, Lai M-L. Molecular basis of genetic variation in debrisoquine hydroxylation in Chinese subjects: Polymorphism in RFLP and DNA sequence of *CYP2D6*. Clin Pharmacol Ther 1993;53:410–8.
29. Johansson I, Oscarson M, Yue QY, Bertilsson L, Sjöqvist F, Ingelman-Sundberg M. Genetic analysis of the Chinese chromosome P4502D locus: Characterization of variant CYP2D6 genes present in subjects with diminished capacity for debrisoquine hydroxylation. Mol Pharmacol 1994;46:452–9.
30. Masimirembwa C, Hasler JA, Bertilsson L, Johansson I, Ekberg O, Ingelman-Sundberg M. Phenotype and genotype analysis of debrisoquine hydroxylase (CYP2D6) in a black Zimbabwean population. Reduced enzyme activity and evaluation of metabolic correlation of CYP2D6 probe drugs. Eur J Clin Pharmacol 1996;51:117–22.
31. Wennerholm A, Johansson I, Massele AY, Jande M, Alm C, Aden-Abdi Y, Dahl M-L, Ingelman-Sundberg M, Bertilsson L, Gustafsson LL. Decreased capacity for debrisoquine metabolism among black Tanzanians: Analyses of the CYP2D6 genotype and phenotype. Pharmacogenetics 1999;9:707–14.
32. Griese EU, Asante-Poku S, Ofori-Adjei D, Mikus G, Eichelbaum M. Analysis of the *CYP2D6* mutations and their consequences for enzyme function in a West African population. Pharmacogenetics 1999;9:715–23.
33. Aklillu E, Persson I, Bertilsson L, Johansson I, Rodrigues F, Ingelman-Sundberg M. Frequent distribution of ultrarapid metabolizers of debrisoquine in

an Ethiopian population carrying duplicated and multiduplicated functional *CYP2D6* alleles. J Pharmacol Exp Ther 1996;278:441–6.
34. Wennerholm A, Dandara C, Sayi J, Svennson J-O, Aden Abdi Y, Ingeman-Sundberg M *et al*. The African-specific *CYP2D6*17* allele encodes an enzyme with changed substrate specificity. Clin Pharmacol Ther 2002;71:77–88.
35. Aklillu E, Herrlin K, Gustafsson LL, Bertilsson L, Ingelman-Sundberg M. Evidence for environmental influence on CYP2D6-catalysed debrisoquine hydroxylation as demonstrated by phenotyping and genotyping of Ethiopians living in Ethiopia or in Sweden. Pharmacogenetics 2002;12:375–83.
36. Bertilsson L, Åberg-Wistedt A, Gustafsson LL, Nordin C. Extremely rapid hydroxylation of debrisoquine: A case report with implication for treatment with nortryptyline and other tricyclic antidepressants. Ther Drug Monitor 1985;7:478–80.
37. Bertilsson L, Dahl M-L, Sjoqvist F, Åberg-Wistedt A, Humble M, Johansson I *et al*. Molecular basis for rational megaprescribing in ultrarapid hydroxylators of debrisoquine. Lancet 1993;341:63.
38. Johansson I, Lundqvist E, Bertilsson L, Dahl M-L, Sjöqvist F, Ingelman-Sundberg M. Inherited amplification of an active gene in the cytochrome P450 CYP2D6 locus as a cause of ultrarapid metabolism of debrisoquine. Proc Natl Acad Sci USA 1993;90:11825–9.
39. Bernal ML, Sinues B, Johansson I, McLellan RA, Wennerholm A, Dahl M-L *et al*. Ten percent of North Spanish individuals carry duplicated or triplicated *CYP2D6* genes associated with ultrarapid metabolism of debrisoquine. Pharmacogenetics 1999;9:657–60.
40. Dahl M-L, Johansson I, Bertilsson L, Ingelman-Sundberg M, Sjöqvist F. Ultrarapid hydroxylation of debrisoquine in a Swedish population: Analysis of the molecular genetic basis. J Pharmacol Exp Ther 1995;274:516–20.
41. Sachse C, Brockmoller J, Bauer S, Roots I. Cytochrome P450 2D6 variants in a Caucasian population: Allele frequencies and phenotypic consequences. Am J Hum Genet 1997;60:284–95.
42. Agúndez JAG, Ledesma MC, Ladero JM, Benitez J. Prevalence of *CYP2D6* gene duplication and its repercussion on the oxidative phenotype in a white population. Clin Pharmacol Ther 1995;57:265–9.
43. Scordo MG, Spina E, Facciola G, Avenoso A, Johansson I, Dahl M-L. Cytochrome P450 2D6 genotype and steady state plasma levels of risperidone and 9-hydroxyrisperidone. Psychopharmacology 1999;147:300–5.
44. McLellan RA, Oscarson M, Seidegard J, Evans DA, Ingelman-Sundberg M. Frequent occurrence of CYP2D6 gene duplication in Saudi Arabians. Pharmacogenetics 1997;7:187–91.
45. Kawanishi C, Lundgren S, Ågren H, Bertilsson L. Increased incidence of *CYP2D6* gene duplication in patients with persistent mood disorders: Ultrarapid metabolism of antidepressants as a cause of non response. A pilot study. Eur J Clin Pharmacol 2004;59:803–7.
46. Bertilsson L, Eichelbaum M, Mellström B, Säwe J, Schulz H-U, Sjöqvist F. Nortryptyline and antipyrine clearance in relation to debrisoquine hydroxylation in man. Life Sci 1980;27:1673–7.
47. Mellström B, Bertilsson L, Säwe J, Schulz H-U, Sjöqvist F. E- and Z-10-hydroxylation of nortryptyline: Relationship to polymorphic debrisoquine hydroxylation. Clin Pharmacol Ther 1991;30:189–93.
48. Dalén P, Dahl M-L, Ruiz MLB, Nordin J, Eng R, Bertilsson L. 10-Hydroxylation of nortriptyline in white persons with 0, 1, 2, 3, and 13 functional *CYPD6* genes. Clin Pharmacol Ther 1998;63:444–52.
49. Dahl M-L, Bertilsson L, Nordin C. Steady state plasma levels of nortryptyline and its 10-hydroxy metabolite: Relationship to the *CYP2D6* genotype. Psychopharmacology 1996;123:315–9.
50. Yue Q-Y, Zhong Z-H, Tybring G, Dalén P, Dahl M-L, Bertilsson L, Sjöqvist F. Pharmacokinetics of nortriptyline and its 10-hydroxy metabolite in Chinese subjects of different *CYP2D6* genotypes. Clin Pharmacol Ther 1998;64:384–90.
51. Morita S, Shimoda K, Someya T, Yoshimura Y, Kamijima K, Kato N. Steady state plasma levels of nortriptyline and its hydroxylated metabolites in Japanese patients: Impact of *CYP2D6* genotype on the hydroxylation of nortriptyline. J Clin Psychopharmacol 2000;20:141–9.
52. Ward SA, Walle T, Walle UK, Wilkinson GR, Branch RA. Propanolol's metabolism is determined by both mephenytoin and debrisoquin hydroxylase activities. Clin Pharmacol Ther 1989;45:72–9.
53. Johnson JA, Burlew BS. Metoprolol metabolism *via* cytochrome P4502D6 in ethnic populations. Drug Metab Dispos 1996;24:350–5.
54. Zhou HH, Wood AJ. Stereoselective disposition of carvedilol is determined by CYP2D6. Clin Pharmacol Ther 1995;57:518–24.
55. McGourty JC, Silas JH, Fleming JJ, McBurney A, Ward JW. Pharmacokinetics and beta-blocking effects of timolol in poor and extensive metabolizers of debrisoquin. Clin Pharmacol Ther 1985; 38:409–13.
56. Zhou HH, Koshakji RP, Silberstein DJ, Wilkinson GR, Wood AJ. Racial differences in drug response: Altered sensitivity to and clearance of propanolol in men of Chinese descent as compared with American whites. N Engl J Med 1989;320:565–70.
57. Poulsen L, Brøsen K, Arendt-Nielsen L, Gram LF, Elbaek K, Sindrup SH. Codeine and morphine in extensive and poor metabolizers of sparteine: Pharmacokinetics, analgesic effect and side effects. Eur J Clin Pharmacol 1996;51:289–95.
58. Caraco Y, Sheller J, Wood AJ. Impact of ethnic origin and quinidine coadministration on codeine's disposition and pharmacodynamic effects. J Pharmacol ExpTher 1999;290:413–22.
59. Otton SV, Wu D, Joffe RT, Cheung SW, Sellers EM. Inhibition by fluoxetine of cytochrome P450 2D6 activity. Clin Pharmacol Ther 1993;53:401–9.
60. Sindrup SH, Brøsen K, Gram LF, Hallas J, Skjelbo E, Allen A *et al*. The relationship between paroxetine and the sparteine oxidation polymorphism. Clin Pharmacol Ther 1992;51:278–87.

61. Alderman J, Preskorn SH, Greenblatt DJ, Harrison W, Penenberg D, Allison J *et al.* Desipramine pharmacokinetics when coadministered with paroxetine or sertraline in extensive metabolizers. J Clin Psychopharmacol 1997;17:284–91.
62. Shin JG, Soukhova N, Flockhart DA. Effect of antipsychotic drugs on human liver cytochrome P-450 (CYP) isoforms *in vitro*: Preferential inhibition of CYP2D6. Drug Metab Dispos 1999;27:1078–84.
63. Ereshefsky L. Pharmacokinetics and drug interactions: Update for new antipsychotics [see comments]. J Clin Psychiatry 1996;57(suppl 11):12–25.
64. Goff DC, Midha KK, Brotman AW, Waites M, Baldessarini RJ. Elevation of plasma concentrations of haloperidol after the addition of fluoxetine. Am J Psychiatry 1991;148:790–2.
65. Dilger K, Greiner B, Fromm MF, Hofmann U, Kroemer HK, Eichelbaum M. Consequences of rifampicin treatment on propafenone disposition in extensive and poor metabolizers of CYP2D6. Pharmacogenetics 1999;9:551–9.
66. Krynetski EY, Tai HL, Yates CR, Fessing MY, Loennechen T, Schuetz JD *et al.* Genetic polymorphism of thiopurine *S*-methyltransferase: Clinical importance and molecular mechanisms. Pharmacogenetics 1996;6:279–90.
67. Weinshilboum RM, Sladek SL. Mercaptopurine pharamacogenetics: Monogenic inheritance of erythrocyte thiopurine methyltranferease activity. Am J Hum Genet 1980;32:651–62.
68. Yates CR, Krynetski EY, Loennechen T, Fessing MY, Tai HL, Pui CH *et al.* Molecular diagnosis of thiopurine *S*-methyltransferase deficiency: Genetic basis for azathioprine and mercaptopurine intolerance. Ann Intern Med 1997;126:608–14.
69. Szumlanski C, Otterness D, Her C, Lee D, Brandriff B, Kelsell D *et al.* Thiopurine methyltransferase pharmacogenetics: Human gene cloning and characterization of a common polymorphism. DNA Cell Biol 1996;15:17–30.
70. Aarbakke J, Janka-Schaub G, Elion GB. Thiopurine biology and pharmacology. Trends Pharmacol Sci 1997;18:3–7.
71. Lennard L. Clinical implications of thiopurine methyltransferase — optimization of drug dosage and potential drug interactions. Ther Drug Monitor 1998;20:527–31.
72. Otterness D, Szumlanski C, Lennard L, Klemetsdal B, Aarbakke J, Park-Hah JO *et al.* Human thiopurine methyltransferase pharmacogenetics: Gene sequence polymorphisms. Clin Pharmacol Ther 1997;62:60–73.
73. van Aken J, Schmedders M, Feuerstein G, Kollek R. Prospects and limits of pharmacogenetics: The thiopurine methyltransferase (TPMT) experience. Am J Pharmacogenomics 2003;3:149–55.
74. Baker DE. Pharmacogenomics of azathioprine and 6-mercaptopurine in gastroenterologic therapy. Rev Gastroenterol Disord 2003;3:150–7.
75. McLeod HL, Yu J. Cancer pharmacogenomics: SNPs, chips and the individual patient. Cancer Invest 2003;21:630–40.
76. Agúndez JAG, Olivera M, Martinez C, Ladero JM, Benitez J. Identification and prevalence study of 17 allelic variants of the human NAT2 gene in a white population. Pharmacogenetics 1996;6:423–8.
77. Lin HJ, Han CY, Lin BK, Hardy S. Ethnic distribution of slow acetylator mutations in the polymorphic *N*-acetyltransferase(nat2) gene. Pharmacogenetics 1994;4:125–34.
78. Lin HJ, Han CY, Lin BK, Hardy S. Slow acetylator mutations in the human polymorphic *N*-acetyltransferase gene in 786 Asians, blacks, Hispanics, and whites: Application to metabolic epidemiology. Am J Hum Genet 1993;52:827–34.
79. Woosley RL, Drayer DE, Reidenberg MM, Nies AS, Carr K, Oates JA. Effect of acetylator phenotype on the rate at which procainamide induces antinuclear antibodies and the lupus syndrome. N Engl J Med 1978;298:1157–9.
80. Kosowsky BD, Taylor J, Lown B, Ritchie RF. Long-term use of procaine amide following acute myocardial infarction. Circulation 1973;47:1204–10.
81. Lee EJ, Zhao B, Seow-Choen F. Relationship between polymorphism of *N*-acetyltransferase gene and susceptibility to colorectal carcinoma in a Chinese population. Pharmacogenetics 1998; 8:513–7.
82. Ambrosone CB, Freudenheim JL, Graham S, Marshall JR, Vena JE, Brasure JR *et al.* Cigarette smoking, *N* acetyltransferase 2 genetic polymorphisms, and breast cancer risk. JAMA 1996;276:1494–501.
83. Reihsaus E, Innis M, MacIntyre N, Liggett SB. Mutations in the gene encoding for the β_2-adrenergic receptor in normal and asthmatic subjects. Am J Respir Cell Mol Bio 1993;8:334–9.
84. Liggett SB. Polymorphisms of the β_2-adrenergic receptor and asthma. Am J Respir Crit Care Med 1997;156:S156–62.
85. Lima JJ, Thomason DB, Mohamed MHN, Eberle LV, Self TH, Johnson JA. Impact of genetic polymorphisms of the β_2-adrenergic receptor on albuterol bronchodilator pharmacodynamics. Clin Pharmacol Ther 1999;65:519–25.
86. Weir TD, Mallek N, Sandford AJ, Bai TR, Awadh N, Fitzgerald JM *et al.* β_2-Adrenergic receptor haplotypes in mild, moderate and fatal/near fatal asthma. Am J Respir Crit Care Med 1998;158:787–91.
87. Preuss CV, Wood TC, Szumlanski CL, Raftogianis RB, Otterness DM, Girard B *et al.* Human histamine *N*-methyltransferase pharmacogenetics: Common genetic polymorphisms that alter activity. Mol Pharmacol 1998;53:708–17.
88. Hibi K, Ishigami T, Tamura K, Mizushima S, Nyui N, Fujita T *et al.* Endothelial nitric oxide synthase gene polymorphism and acute myocardial infarction. Hypertension 1998;32:521–6.
89. Abernethy DR, Babaoglu MO. Polymorphic variant of endothelial nitric oxide synthase (eNOS) markedly impairs endothelium-dependent vascular relaxation [abstract]. Clin Pharmacol Ther 2000;67:141.
90. Lynch TJ, Bell DW, Sordella R, Gurubhagavatula S, Okimoto RA, Brannigan BW *et al.* Activating mutations in the epidermal growth factor receptor underlying responsiveness of non-small-cell lung cancer to gefitinib. N Engl J Med 2004;350: 2129–39.
91. Rettie AE, Eddy AC, Heimark LD, Gibaldi M, Trager WF. Characteristics of warfarin hydroxylation catalyzed by human liver microsomes. Drug Metab Dispos 1989;17:265–70.

92. Rettie AE, Wienkers LC, Gonzalez FJ, Trager WF, Korzekwa KR. Impaired (*S*)-warfarin metabolism catalysed by the R144C allelic variant of CYP2C9. Pharmacogenetics 1994;4:39–42.
93. Higashi MK, Veenstra DL, Kondo LM, Wittkowsky AK, Srinouanprachanh SL, Farin FM *et al.* Association between CYP2C9 genetic variants and anticoagulation-related outcomes during warfarin therapy. JAMA 2002;287:1690–8.
94. Rieder MJ, Reiner AP, Gage BF, Nickerson DA, Eby CS, McLeod HL *et al.* Effect of *VKORC1* haplotypes on transcriptional regulation and warfarin dose. N Engl J Med 2005;352:2285–93.

This page intentionally left blank

CHAPTER

14

Equilibrative and Concentrative Transport Mechanisms

PETER C. PREUSCH
National Institute of General Medical Sciences, National Institutes of Health, Bethesda, Maryland

INTRODUCTION

The processes of drug absorption, distribution, metabolism, and elimination include membrane transport steps that traditionally have been thought of as being mediated by passive diffusion. For example, a small molecule of moderate polarity such as ethanol, which serves as a marker for total body water, diffuses freely through all membranes, whereas a large, highly polar molecule such as inulin, which serves as a marker of extracellular fluid space, is unable to cross cell wall membranes. Passive diffusion also appears to mediate the distribution of anesthetic gases and many lipophilic drugs. However, in recent years, there has been increased appreciation of the role that specific membrane transport proteins play in the processes of drug absorption, distribution, and elimination by both renal and nonrenal pathways. The potential to exploit such transporters to enhance drug bioavailability and to improve tissue-specific delivery has been recognized. The role of membrane transport proteins as principal agents in the resistance of some tumors to chemotherapy and in the development of microbial antibiotic resistance has become well established. The potential benefit of intentional cotherapy to enhance drug absorption and efficacy has been explored.

Recent advances include systemization of the nomenclature for transporters (as a result of the completion of the human genome), solution of the molecular structure of several transporters, and increased evidence that individual variations in transporter genes contribute to variations in drug responses and adverse drug reactions. Interest in membrane transporters in drug therapy has led to a series of meetings and books addressing this area of research (1–4).

MECHANISMS OF TRANSPORT ACROSS BIOLOGICAL MEMBRANES

Research *in vitro* and *in vivo* (particularly in microorganisms) has defined four basic mechanisms of transport across biological membranes (5–7):

1. Passive diffusion (i.e., self-diffusion across the lipid bilayer).
2. Facilitated diffusion (i.e., via antibiotic carriers or membrane channels).
3. Carrier-mediated transport (i.e., via membrane transporter proteins).
4. Carrier-mediated active transport (i.e., via energy-linked transporters).

Active transport may be subdivided into primary transport, which is directly coupled to substrate oxidation or high-energy phosphate hydrolysis, or secondary transport, which is coupled to cotransport of another molecule or ion down its thermodynamic gradient. We will first consider the thermodynamics of membrane transport and then review the four basic mechanisms.

Thermodynamics of Membrane Transport

The basic principles of transport across a semipermeable membrane and the relevant thermodynamic and flux equations governing transport are well established. Books on transport appear quite regularly and often include this material in an introductory chapter (8). Friedman (5), Fournier (9), and Lakshminarayanaiah (10) give quite exhaustive treatments of the problem from the bioengineering, biophysical, and biological points of view. The following discussion, with reference to Figure 14.1 and Table 14.1, is limited to the most basic thermodynamic equations and a qualitative discussion of the principles.

For a neutral solute, the thermodynamic driving force for transport across the membrane (ΔG_{transp}) is determined by the ratio of solute concentrations inside [S_i] and outside [S_o] the membrane and is given by the first term of Equation 14.1.

$$\Delta G_{transp} = 2.303RT \log [S_i]/[S_o] + nF\,\psi + \Delta G_{pump} \quad (14.1)$$

where R = 1.987 cal/mol°K = 8.314 Joules/mol°K, T = absolute temperature in °K, n = Avogadro's number, F = 23.06 cal/mol-mV = 96.5 Joules/mol-mV, and $\Delta\psi$ = transmembrane electrical potential (mV). This movement is entropically driven, since there are more ways to arrange molecules in the larger volume represented by the sum of the compartment volumes than there are in the donor volume alone. An order of magnitude difference in concentration corresponds to an energy of 1.35 kcal/mol (5.67 kJ/mol) at 23°C, or 1.41 kcal/mol (5.94 kJ/mol) at 37°C. At equilibrium, the concentration on both sides of the membrane will be equal.

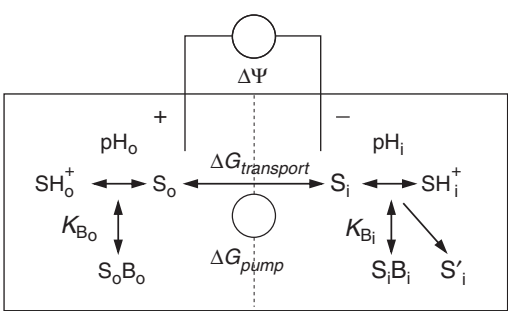

FIGURE 14.1 Model for equilibrative transport across a permeable membrane separating two compartments, arbitrarily designated outside (o) or inside (i), containing a diffusible solute S. The solute is shown as occurring in equilibrium with a non-membrane permeant protonated state SH^+ and with non-membrane-permeant macromolecular bound species SB. The pH and dissociation constants (K_B) of the binding sites for S may differ in the two compartments. S is shown as undergoing irreversible chemical conversion to another species, S′, in the inside compartment only. (See text for additional details.)

TABLE 14.1 Thermodynamic Factors in Drug Transport

Driving force	Example	Relevant compartments
Diffusion	Caffeine	All body compartments
Membrane potential	^{99m}Tc-Labeled sestamibi	Cardiac mitochondria
pH trapping	Phenobarbital	Renal tubule
Protein binding	Warfarin	Plasma/liver distribution
Active transport	Captopril	Small intestine
Chemical modification	Cytarabine	Leukocyte

For a charged solute, the driving force must also include a term reflecting any transmembrane potential difference ($\Delta\psi$). This term may add to or oppose the driving force of the initial concentration gradient. At equilibrium (ΔG = zero) the concentration gradient must be in balance with the electrostatic potential difference. Thus, charged species may be concentrated (electrophoresed) into a compartment against a concentration gradient. An order of magnitude difference in concentration of a charged solute across a membrane corresponds to 58.5 mV at 23°C and 61.5 mV at 37°C for a singly charged species, and about 30 mV for a doubly charged species, and so on. Alternately, one can consider the process of transporting a charged molecule across a membrane as a process that will contribute to establishing a transmembrane potential. Such transport is called electrogenic. The combined effect of the concentration gradient of an ion across the membrane and the influence of the membrane potential defines the electrochemical potential gradient for that species across the membrane. This total electrochemical potential may be expressed in kilocalories, Joules, or, commonly, millivolts. Most cells, whether microorganisms in growth medium or mammalian cells in communication with body fluids, have a negative potential inside versus their surroundings. Therefore, the uptake of cations into cells is a thermodynamically favorable process.

In the case of active transport, the movement of the substrate is coupled to some other energetic process (ΔG_{pump}), such as cotransport of another substrate or ion according to its electrochemical potential gradient or the hydrolysis of ATP. Active transport is generally considered to involve specifically coupled

reactions catalyzed by a single transmembrane protein assembly. For example, members of the ATP-binding cassette family of transport proteins specifically couple the energy of ATP hydrolysis to the pumping of substrate molecules across a transmembrane concentration gradient. Members of the major facilitator superfamily couple the transport of protons, sodium, potassium, or other ions (including organic ions such as α-ketoglutarate) down their electrochemical concentration gradients to transport of a host of other ions and molecules.

In real cells, multiple transmembrane pumps and channels maintain and regulate the transmembrane potential. Furthermore, those processes are at best only in a quasi-steady state, not truly at equilibrium. Thus, electrophoresis of an ionic solute across a membrane may be a passive equilibrative diffusion process in itself, but is effectively an active and concentrative process when the cell is considered as a whole. Other factors that influence transport across membranes include pH gradients, differences in binding, and coupled reactions that convert the transported substrate into another chemical form. In each case, transport is governed by the concentration of free and permeable substrate available in each compartment. The effect of pH on transport will depend on whether the permeant species is the protonated form (e.g., acids) or the unprotonated form (e.g., bases), on the pK_a of the compound, and on the pH in each compartment. The effects can be predicted with reference to the Henderson–Hasselbach equation (Equation 14.2), which states that the ratio of acid and base forms changes by a factor of 10 for each unit change in either pH or pK_a:

$$\text{pH} = \text{p}K_a + \log \frac{[\text{base}]}{[\text{acid}]} \tag{14.2}$$

Thus, if the unprotonated form of a base with pK_a of 9.0 is permeant (e.g., amines) and the pH outside increases from 7 to 8, the concentration of the free base increases from 1% to about 10% of the total (a large effect). If the protonated form were the permeant species of similar pK_a (e.g., phenols), the same unit pH change would yield a change in the permeant species from about 99% to 90% of the total (not a very important change). Transmembrane gradients of metal ions or other titrants that interact with drug molecules will similarly affect drug transport, depending on the concentration ranges, dissociation constants, and identity of the free drug or complex as the permeant species.

Plasma protein binding is important in pharmacokinetics because it influences the concentration of free drug available for transport. As discussed in Chapter 15, this leads to interactions between compounds that compete for the same binding sites on serum albumin. However, coadministered compounds also may compete for tissue binding sites, as demonstrated by the interaction between quinidine and digoxin (11). The extent of drug distribution across a membrane will depend on the relative affinity of competing compounds for both plasma and tissue binding sites.

Finally, transport can also be driven by the conversion of intracellular substrate to another chemical form. For example, in the case of nucleoside drugs, conversion to the corresponding nucleotides by appropriate kinases may be the limiting factor in cellular uptake and activation. The same principle applies to sulfation, glucuronidation, prodrug activations, or other metabolic processes that provide a removal of the transported species from the transportable (free) internal pool. In some cases, transport is directly coupled to substrate modification, as in the uptake of sugars into bacterial cells by phosphoenolpyruvate (PEP)-coupled phosphorylation systems.

Passive Diffusion

Passive diffusion is the transport of a molecule across a lipid bilayer membrane according to its electrochemical potential gradient without the assistance of additional transporter molecules. This process can be studied in pure lipid membranes, although it is acknowledged that the properties of even relatively pure lipid patches in native membranes are altered by the high density of neighboring protein molecules. The physical and functional properties of membranes can be modeled with varying levels of detail and mathematical complexity. The simplest model represents the membrane as a single semipermeable barrier separating two uniform aqueous compartments. Transport is characterized by a single reversible rate constant. A more complex model represents the membrane as an intervening third compartment of 25–30 Å thickness with properties equivalent to a bulk organic solvent. Transport is modeled as a reversible partition of molecules from the donor aqueous phase into the membrane compartment and rate-limiting release of the solute from the organic membrane phase into the receiving compartment. This model yields a rate equation of the same form as the Michaelis–Menten equation in enzyme kinetics. Although such kinetics are observed for mediated membrane transport, they are not typically observed for simple diffusive transport. A more sophisticated model adds barriers of high charge density and high dielectric constant on either side of the organic compartment to represent

the phospholipid head groups. Still other models may incorporate unstirred diffusion layers extending into the aqueous compartments. These models reveal different points of view about what constitutes the most important rate-determining barrier to bulk transport.

Molecular dynamics simulations (12, 13) have provided a provocative image of passive diffusion of solute molecules within the membrane bilayer (Figure 14.2). These simulations illustrate the rapid but restricted mobility of the lipid side chains, and demonstrate that the membrane hydrophobic region is not particularly well modeled by bulk solvent properties. They suggest the spontaneous formation of voids and transient channels within the membrane and the ability of small molecules and ions to diffuse within the membrane by hopping among these voids (~8-Å jumps on a 5-psec time scale).

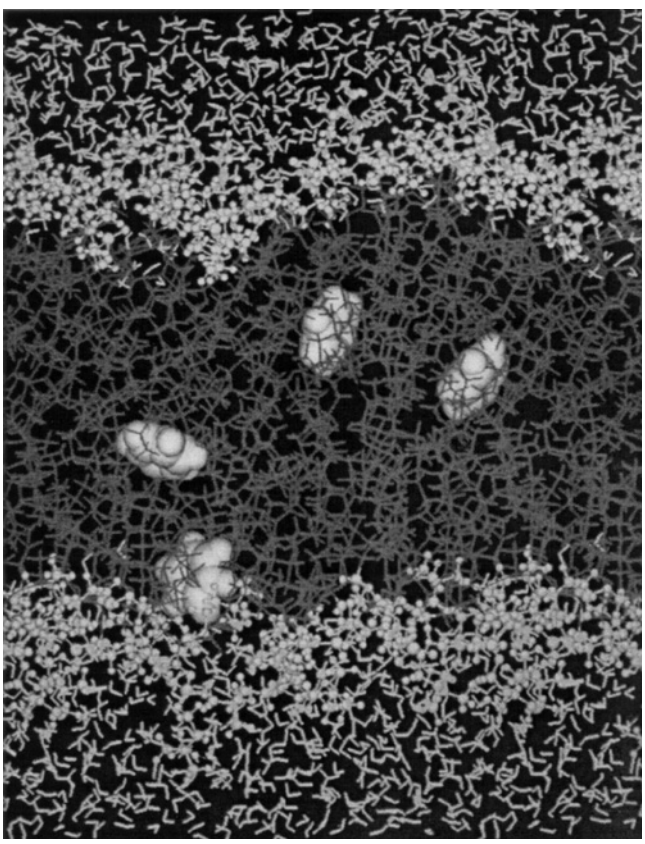

FIGURE 14.2 Molecular dynamics simulation of the diffusion of benzene within a hydrated lipid bilayer membrane. Benzene molecules are shown as Corey–Pauling–Koltun (CPK) models; atoms in the phospholipid head groups are shown as ball and stick models; and hydrocarbon chains and water molecules as dark and light stick models, respectively. (Reproduced with permission from Bassolino-Klimas D, Alper HE, Stouch TR. Biochemistry 1993;32:12624–37.)

They highlight the importance of concerted large conformational motions, occurring with relatively low frequency compared to the continual small motions (~1.5 Å occurring on the 100-fsec time scale). Thus far, these methods have been used to successfully model the diffusion of water, hydrogen ions, small organic molecules, and various drugs within the bilayer. They have provided reasonably good agreement with experimental data on intramembrane diffusion. The types of motion available to small molecules such as benzene differ qualitatively from those available to a fairly large organic drug such as nifedipine.

Thus far, no one has successfully modeled the full process of transport of druglike molecules from one aqueous compartment into the membrane and into the other aqueous compartment. The problem has been that the feasible time scale for molecular dynamics simulations is presently in the nanosecond range, whereas the rates of drug transport are typically in the millisecond range. The process has been approximated for several small compounds by constraining solute molecules to different specific depths in a simulated membrane. Both the free energy of partitioning from an aqueous to a lipid environment and the local diffusion coefficients at each depth can be calculated. These can be used to calculate an overall permeability coefficient. The relative values (but not the absolute values) agree with experimental data (14, 15).

Extensive efforts have been made to develop quantitative structure/activity relationships (QSARs) that predict membrane transport (16, 17). Particularly extensive use has been made of log P (log solvent/water partition coefficient values) and the Hansch equation (Equation 14.3):

$$\log(1/C) = -k(\log P)^2 + k'(\log P) + \rho\sigma + k'' \quad (14.3)$$

where C = substrate concentration or dose producing a given effect (ED_{50}, IC_{50}, rate of reaction or transport), $\log P$ = partition coefficient or lipophilicity factor π, σ = Hammett electronic substituent effect constants, and k, k', k'', ρ = regression coefficients. Derivation of this correlation originally was based on the expectation that passive diffusion across a lipid bilayer would be the limiting factor in drug action, but many other factors, such as enzyme inhibition and receptor binding data, often also correlate well. The octanol/water partition coefficient ($\log P_{octanol/water}$) is most commonly used and is generally assumed unless otherwise noted. Reverse-phase HPLC and immobilized artificial membrane methods for estimating log P have largely replaced actual liquid/liquid extraction methods for determining these values (18, 19). The ability to correlate log P values with structure has become quite

TABLE 14.2 Sample of QSAR Studies on Transport[a]

Drug class	System	Physical parameters correlated with activity[b]
Absorption as log (% absorbed), log permeability, or log *k*		
Barbiturates	Gastric	$\log P_{CHCl_3/water}$, R_m
Sulfonamides	Gastric	$\log P_{isoamyl/alcohol/water}$
Anilines	Gastric	pK_a
Xanthines	Intestinal	$D_{pH\ 5.3}$
Cardiac glycosides	Intestinal	$\log P_{octanol/water}$, R_m
Excretion as log (% excreted), log *CL*, or log *k*		
Penicillins	Biliary	$\log P$
Sulfathiazoles	Biliary	$\log P_{octanol/water}$, pK_a
Sulfapyridines	Renal	R_m, pK_a
Sulfonamides	Renal	π, pK_a
Amphetamines	Renal	$\log P_{heptane/buffer}$

[a] Adapted from Table VI in Austel B, Kutter R. Absorption, distribution and metabolism of drugs. In: Toplis JG, ed. Quantitative structure activity relationships. Medicinal chemistry monographs, vol 19. New York: Academic Press; 1983. p. 437–96.

[b] Parameters: k = rate constant, CL = clearance, P = partition coefficient for indicated solvents, R_m = relative mobility under specific chromatographic conditions, $D_{pH\ 5.3}$ = distribution coeffficient (a partition coefficient corrected for fractional ionization at pH 5.3), π = substitutent lipophilicity values.

good, and calculated log P values (CLOGP) are now often used.

Table 14.2 presents a selection of drugs, transport sites, and parameters that have been studied in QSAR studies relevant to drug absorption and excretion measurements excerpted from a much larger table (17). Overall conclusions from this work are that transportability correlates with (1) lipophilicity (log P), (2) water solubility, (3) pK_a, and (4) molecular weight. Correlations with lipophilicity are almost always good. Although different log P ranges are optimal for oral ($\log P = 0.5-2.0$), buccal ($\log P =$ 4–4.5), and topical ($\log P > 2.0$) delivery, there is much overlap. Unfortunately, increasing drug lipophilicity may increase delivery generally throughout the body and do little to improve selective delivery to target tissues. Water solubility bears on the total concentration available for transport (e.g., in GI absorption). Solubility is more difficult to predict from structure than is log P, although calculated estimates can be made from melting point data and calculated solvation energies. Molecular weight is related to diffusivity $\left(D \propto 1/1\sqrt{\text{MW}}\right)$, in both the membrane and the aqueous phases. It has been found empirically that there is a cutoff molecular weight (< 500–650) above which passive diffusion across most biological membranes is excluded. An analysis of 2245 compounds from the World Drug Index database for which human clinical data are available led to the so-called Lipinsky's Rules of 5 (20). Poor absorption is predicted if two or more of the following occur: (1) H-bonding donor groups > 5, (2) H-bonding acceptor groups > 5, (3) (N + O atoms) > 10, (4) MW > 500, and (5) CLOGP > 5.0 (or measured log $P > 4.15$).

Apart from these basic rules of thumb, the ability to predict the relationship between molecular structure and transport across biological membranes is limited beyond narrow ranges of known compounds. Confounding factors include inaccurate, incomplete, and/or noncomparable data, and the potential existence of multiple drug transport mechanisms in real biological membranes. In particular, limited QSAR data are available for the specific drug transporters that are considered in the following sections.

Carrier-Mediated Transport: Facilitated Diffusion and Active Transport

Several characteristics distinguish carrier-mediated transport from passive diffusion. Rates are generally faster than for passive diffusion, and transport is solute specific and shows a greater temperature variation (Q_{10}). Transport is saturable, resembling Michaelis–Menten enzyme kinetics. Transport rates may not be the same in both directions across the membrane at a given substrate concentration. Transport may be inhibitable by competitive transport substrates or by noncompetitive inhibitors acting at other sites. Transport may be regulated by cell state (e.g., by phosphorylation, induction, or repression of transporter molecules) or by gene copy number. Transport is tissue specific because it depends on the expression of particular transporters that do not occur in all membranes. Active transport is a special form of carrier-mediated transport in which solute concentration is mechanistically linked to energetically favorable reactions (Equation 14.1). Distinction between primary pumps and secondary transporters may be made on the basis of cosubstrate dependence (e.g., oxidative substrate, adenosine triphosphate, or phosphenolpyruvate requirement) or of the effects of various ionophores, uncouplers, and inhibitors of primary pumps.

Mechanisms of drug transport *in vivo* have been better established in bacterial systems than in mammalian systems, owing to greater experimental control and ability to genetically manipulate properties of the bacterial systems. Table 14.3 lists examples of drugs for which the transport in bacteria is dominated by the indicated mechanisms (7).

TABLE 14.3 Transport Mechanisms in Bacteria[a]

Transport mechanism	Example
Passive diffusion across lipid bilayer	Fluoroquinolones
	Tetracyclines (hydrophobic)
Facilitated diffusion (nonselective)l	β-Lactams
	Tetracyclines (hydrophilic)
Mediated transport (selective)	Imipenem
	Catechols
Active transport	Aminoglycosides
	Cycloserine

[a] Adapted from Table 1 in Hancock REW. Bacterial transport as an import mechanism and target for antimicrobials. In: Georgopapadakou NH, ed. Drug transport in antimicrobial and anticancer chemotherapy. New York: Marcel Dekker, Inc.; 1995. p. 289–306.

The distinction between facilitated diffusion through channels and carrier-mediated transport is somewhat artificial, but may be justified on the basis of specificity. For example, β-lactams in general can pass through nonselective bacterial outer membrane porin (e.g., OmpF) channels via passive diffusion, whereas imipenem (and related zwitterionic carbapenems) can also utilize OprD channels, which preferentially recognize basic amino acids and dipeptides. The identification of mutants that selectively confer imipenem resistance suggests that more intimate protein–drug associations are involved in carrier-mediated transport than in facilitated diffusion, which may be limited only by pore diameter.

The tetracyclines provide an interesting example in that bacterial uptake is passive (by both nonmediated and carrier-mediated pathways), efflux is active, and their transport is subject to pH, membrane potential, and metal ion gradient effects (21). Tetracycline is both a weak base ($pK_{a1} = 3.3$) and a weak acid ($pK_{a2} = 7.7$, $pK_{a3} = 9.7$) and is subject to pH trapping. Furthermore, the anions can chelate divalent cations such as magnesium, forming metal chelates that have altered solubility. Uptake across the outer membrane of gram-negative bacteria is nonmediated for hydrophobic tetracyclines and carrier mediated via porins (e.g., OmpF) for hydrophilic homologs. Nonmediated diffusion via the lipopolysaccharide depends on the uncharged species, whereas carrier-mediated diffusion via the porins favors the magnesium-bound anion (net positive charge) and is enhanced by the Donnan membrane potential. In contrast to most mammalian membranes, passive diffusion across the lipopolysaccharide outer membrane of *Escherichia coli* is slower for more hydrophobic analogs and may account for their lower antimicrobial activity. Uptake across the cytoplasmic membrane is by nonmediated passive diffusion of the neutral species, and is thermodynamically driven by the pH gradient across the inner membrane (pH 7.8 inside, pH 6.1 outside, for cells grown at a nominal pH 7.0). On the other hand, efflux of tetracycline is due to active transport via TetA, which catalyzes antiport of the $[Mg–anion\ chelate]^{1+}$ (out) in exchange for a proton (in).

Uptake Mechanisms Dependent on Membrane Trafficking

Pinocytosis (cell sipping) has been thought to be a nonspecific, nonsaturable, non-carrier-mediated form of membrane transport via vesicular uptake of bulk fluid into cells from the surrounding medium (22, 23). This mechanism is most relevant to large particles and polymer conjugates. The term "pinocytosis" has fallen from favor and one suspects that many events previously ascribed to nonspecific pinocytosis are now recognized as being due to specific *receptor-mediated endocytosis*. Endocytosis is specific and intrinsic to the mechanism of action of many macromolecular drugs. This process is also used to deliver small molecules as prodrugs, and mediates the distribution and clearance of many contemporary pharmacological agents, including many biotechnology products, most peptide hormones, and cytokines (e.g., insulin, growth hormone, erythropoetin, granulocyte colony-stimulating factor, and interleukins) (24).

Receptor-mediated endocytosis plays an important role in the pharmacokinetics and nephro- and ototoxicity of aminoglycoside antibiotics. As was shown in Chapter 3 (Figure 3.6), gentamicin exhibits flip-flop kinetics, wherein elimination appears as the initial phase, followed by a very slow distribution phase (25). The first phase corresponds to clearance from plasma by glomerular filtration, the second phase to redistribution of drug from the tissues, particularly kidney, back into the central compartment. After glomerular filtration, aminoglycosides are taken up via endocytosis at the brush border by renal proximal tubule epithelial cells (26). The accumulation of antibiotic (as much as 10% of the dose) in these cells results in lysosomal disruption and cell necrosis, producing dose-limiting nephrotoxicity. However, the uptake is saturable, so that, for a given total intravenous dose, accumulation in the kidney is lower when multiple intermittent doses are given rather than when a continuous dose is infused over the same time period (27). This allows far greater peak therapeutic

concentrations than could be tolerated otherwise, a clinically important consideration because aminoglycosides exhibit peak concentration-dependent bactericidal effects (28). The optimum dose and interval for various aminoglycosides remain areas of ongoing research (29, 30).

The endocytosis of aminoglycosides via clathrin-coated pits is thought to involve initial binding of the polybasic cationic drugs to anionic lipids. Recently, megalin (also known as gp330 and as low-density lipoprotein receptor-related protein-2), a receptor protein on the brush border, has been implicated (31). Megalin knockout mice accumulate only about 5% as much of an intraperitoneal gentamicin dose in their kidneys as do wild-type mice. This protein is involved in the uptake of many low molecular weight proteins containing positively charged regions, including vitamin-binding proteins, lipoproteins, hormones, and also calcium. Competition for megalin binding between calcium and aminoglycosides may be the basis for the ability of oral calcium loading to attenuate aminoglycoside nephrotoxicity. The megalin receptor is most highly expressed in proximal renal tubule cells. It is also expressed in an eclectic assortment of other cells, including the epithelium of the inner ear, which may explain ototoxicity associated with long-term aminoglycoside treatment (32, 33).

Transcytosis is the receptor-mediated uptake of a ligand on one side of the cell, vesicular transport across the cell, and exocytosis of the vesicle contents on the opposite side. This process is responsible for the uptake of the iron-binding protein transferrin (Tf) across the blood–brain barrier (BBB) by the transferrin receptor (TfR). Monoclonal antibodies that recognize the transferrin receptor (mABTfR) are also carried across the cell and have been used to deliver various cargos. An early demonstration used mABTfR conjugated to avidin to deliver vasoactive intestinal peptide (VIPa) disulfide-linked to biotin. Reductases in the brain cleaved the disulfide linkage, releasing VIPa to express its pharmacological effect (Figure 14.3) (34, 35).

Applications of transcytosis have been extended to additional receptors, cargos, and delivery sites (36). The TfR has been used to deliver ^{111}In-labeled DTPA–EGF–PEG–biotin–streptavidin–mABTfR (DTPA = the metal chelator diethylenetriaminepentaacetic acid; EGF = endothelial cell-derived growth factor; PEG = polyetheylene glycol) across the BBB, where binding to cells expressing EGF receptor (EGFR) was useful

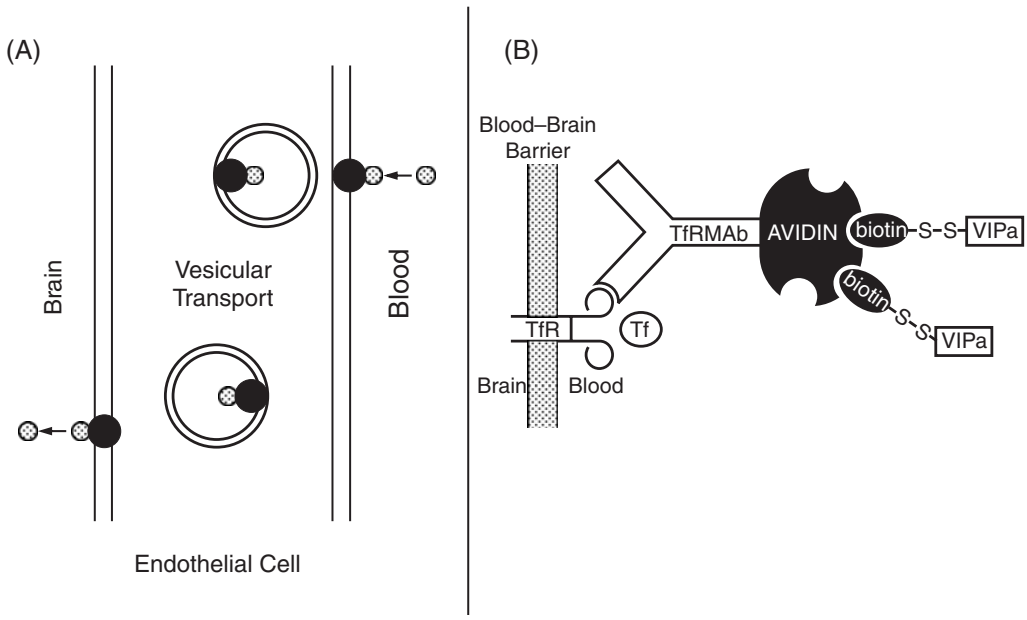

FIGURE 14.3 Mechanism of transcellular drug delivery across the blood–brain barrier. (A) Schematic representation of vesicle trafficking and topology. (B) An example of this drug transport mechanism in the delivery of a biotin–vasoactive intestinal peptide (VIPa) disulfide-linked prodrug across the blood–brain barrier via the transferrin receptor. See text for details. (Adapted from Bickel U, Pardridge WM. Vector-mediated delivery of opiod peptides to the brain. In: Rapaka RS, ed. Membranes and barriers: Targeted drug delivery. NIDA Res Monograph 154. Washington, D.C.: NIH Pub. #95-3889; p. 28–46.)

for radioisotopic imaging of brain tumors. Delivery of brain-derived neurotrophic factor (BDNF) as a BDNF–biotin–streptavidin–mABTfR conjugate was shown to be neuroprotective in a rat stroke model. Delivery of antisense oligonucleotides against human EGFR (hEGFR) to human glioma cell brain tumors in a severe combined immunodeficient (SCID) mouse model was accomplished by encapsulating the oligos in liposomes that were modified by attachment of both PEG–mABTfR (which facilitated transport across the BBB) and PEG–mABInsulinR (which facilitated uptake into the glioma cells). A similar approach has been used to deliver the vectors for tyrosine hydroxylase gene therapy in a Parkinson's disease model.

The vitamin B12 receptor, which facilitates uptake of the vitamin–intrinsic factor vitamin-binding protein complex, has been used to enhance oral delivery and gastrointestinal uptake of peptides and proteins as their vitamin B12 conjugates (37). Commercial efforts are under way to exploit this receptor as well as the fetal Fc receptor, which facilitates intestinal uptake of antibodies from colostrum/milk (38), and the polymeric immunoglobulin receptor, which facilitates the serosal to mucosal transport of IgA and IgM (39).

Protein transduction is a property of certain protein sequences (e.g., *Drosophila antennapedia* homeobox domain, human immunodeficiency virus TAT protein transduction domain, transportan, and penetratin) that are capable of penetrating cell membranes and delivering conjugated cargos (e.g., peptides, proteins, nucleic acids) into the cell and even the nucleus (40–43). Simple highly basic peptides (e.g., multimers of lysine or arginine) function similarly (44). The mechanism and cellular apparatus required for uptake are unclear, but initially appeared to be self-directed, energy independent, and not receptor mediated. Recent work suggests uptake may be via endocytosis and depend on the presence of negatively charged glycosaminoglycans on the surface of target cells (45, 46). In any case, these fusion proteins have been used to deliver pharmacologically active substances in both *in vitro* and *in vivo* animal models (47, 48). For example, the Arg_7-peptide was used to deliver a cardioprotective peptide agonist of protein kinase Cε to intact rat heart in an isolated organ ischemia–reperfusion model (49). The third helix of the Antennapedia homeobox domain was used to enhance gene therapy using adenovirus to deliver green fluorescent protein (GFP) or β-galactosidase reporters and endothelial nitric oxide synthase (NOS) in a $NOS3^{-/-}$ mouse model or vascular endothelial growth factor in a mouse ischemic hind limb model (50).

Paracellular Transport and Permeation Enhancers

The majority of this chapter focuses on transport across cell membranes. However, *paracellular transport*, or movement between cells, is also important in drug action. Paracellular transport is of interest for the delivery of hydrophilic and macromolecular drugs and for molecules that would otherwise be degraded during transcellular passage. Paracellular transport is less selective with respect to size, charge, and hydrophobicity of the solute than is either passive diffusion or transporter-mediated processes. Selected tissue barriers, such as gastrointestinal epithelium, epithelial (ductal) surfaces of hepatic and renal cells, and capillaries forming the blood–brain barrier, are rendered highly impermeable to many molecules by the formation of tight junctions between cells. Considerable work has gone into characterizing the macromolecular components and overall structure of tight junctions (51, 52). Permeation enhancers are molecules that disrupt the function of tight junctions and increase paracellular transport (53–58). Substances such as calcium chelators, bile salts, anionic surfactants, medium-chain fatty acids, alkyl glycerols, cationic polymers, cytochalsin D, tumor necrosis factor-α (TNF-α), and enterotoxins have been tested in various *in vitro* assays and *in vivo* animal models. Permeation enhancers have been used in animal models to increase the bioavailability of orally delivered medications and to improve transport into brain tissues. Mannitol, ceftoxin, dextrans, proteins, radiocontrast dyes, and various ions have been used as markers of enhanced permeability.

DESCRIPTION OF SELECTED MEMBRANE PROTEIN TRANSPORTERS

A large number of transport functions in various tissues have been defined physiologically and/or pharmacologically. A substantial number can now be associated with specific gene, mRNA, and deduced protein sequences. Relatively few have been isolated and fully characterized biochemically. Lists of transport functions, transporters, and substrates can be found in various reviews (59–67). It is not always clear when the nomenclature refers to a transport activity or to specific, genetically defined transport protein. A nice compilation of transporter sequence data is given in Griffith and Sansom (68). Table 14.4 provides a partial listing of membrane transporter families.

The ATP-binding cassette (ABC) superfamily and the major facilitator (MF) superfamily account for the majority of membrane transporters.

TABLE 14.4 Partial Listing of Membrane Transporters

Transporter family	HUGO[a] designation	Common names of representative substrates
ABC superfamily		
MDR-1,2	ABCB1,4	P-Glycoprotein, organic cations, neutrals, lipids
cBAT/BSEP	ABCB11	Canalicular bile acid transporter, bile salts
MRP1,2,3, . . . , *n*	ABCC1, . . . , *n*	Organic anions, GSX conjugates, GSH cotransport
cMOAT	ABCC2	Canalicular multispecific anion transporter (= MRP2)
BCRP/MXR	ABCG2	Mitoxantrone, doxorubicin, daunorubicin
Major facilitator superfamily		
PEPT1,2	SLC15A1,2	Proton-coupled oligopeptide transporter
CNT1,2	SLC28A1,2	Na^+-coupled nucleotide transporter
NTCP	SLC10A1,2	Na^+-coupled taurocholate protein
OATP	SLC21A3	Polyspecific organic anion transport protein
OAT-K1	SLC21A4	Renal methotrexate transporter
OCT	SLC22A1,2	Organic cation transporters electrogenic
RFC	SLC19A1	Reduced folate carrier

[a] Human Genome Organization.

Peptide transporters of both types have been reported. Both anion and cation pumps of both types are known. Although most ABC family members catalyze active transport coupled to ATP hydrolysis, members of the MF superfamily may catalyze either mediated diffusion or active transport (coupled most often to H^+ or Na^+ cotransport). A few examples suffice to illustrate the general points.

ATP-Binding Cassette Superfamily

P-Glycoprotein

The most extensively studied drug transporter, and the paradigm for the ABC transport superfamily, is P-glycoprotein (P-gp), the product of the *mdr1* (multidrug resistance) gene (69–71). This transporter was discovered during the 1970s through studies of chemotherapy-resistant tumors in cancer patients. Multidrug resistance can be acquired both by patients receiving chemotherapy and by cultured cells exposed to chemotherapeutic agents *in vitro*. Cells, which become resistant to one chemotherapeutic agent, are often found to also be resistant to a wide range of other drugs to which they have never been exposed. Although other mechanisms can occur, the most common mechanism entails increased expression of a membrane phospho-glycoprotein of approximately 170 kDa, which is an active efflux transporter. This protein was dubbed P-glycoprotein (P for altered permeability). Human MDR-1 and MDR-2 are 76% identical in sequence, but only MDR-1 plays a role in drug resistance. MDR-2 is most likely involved in transport of phosphatidylcholine. Similar proteins occur in rodents, and knockout mice have been valuable in defining the *in vivo* roles of these proteins.

The *mdr1* gene encodes a 1280-amino acid protein, and is thought to contain 12 hydrophobic transmembrane (TM) helices (two groups of six) with globular cytosolic domains inserted between TM6 and TM7 and at the end of TM12 (Figure 14.4). This motif is characteristic of the ABC superfamily of membrane transport proteins. Each of the globular domains contains one ATP hydrolysis site that includes the canonical Walker A (nucleotide binding) and Walker B (magnesium binding) sequences, which also occur in other ATPases. In addition, both include the Walker C (linker peptide or dodecapeptide) region that is a signature of the ABC superfamily. Another notable member of the class is the cystic fibrosis transmembrane conductance regulator (CFTR), which has an identical topology, but seems to function as an ATP-regulated chloride channel.

The multidrug resistance-related protein (MRP) family and the mitoxantrone-resistance (MXR) family discussed in the following section are also ABC transporters. All members of the class include two TM domains and two cytoplasmic ATPase domains. The order of these domains within a polypeptide and their arrangements into single or multiple polypeptides include all possible variations. In some cases, the proteins are expressed as half-transporters containing only one TM domain and one ATPase domain. However, these appear to be functional as either homo- or heterodimers with another TM and ATPase domain. Three glycosylation sites occur within the first extracellular loop of P-gp. These are not required for transport function, but do affect the half-life of the protein, its folding within the endoplasmic reticulum, and its delivery to the cell surface. A series of phosphorylation sites occurs in the linker domain between the first half-molecule and the second half. Again, these are not required for transport activity, but may play a regulatory role.

The mechanism of ATP hydrolysis by MDR-1 has been examined and is not fundamentally different

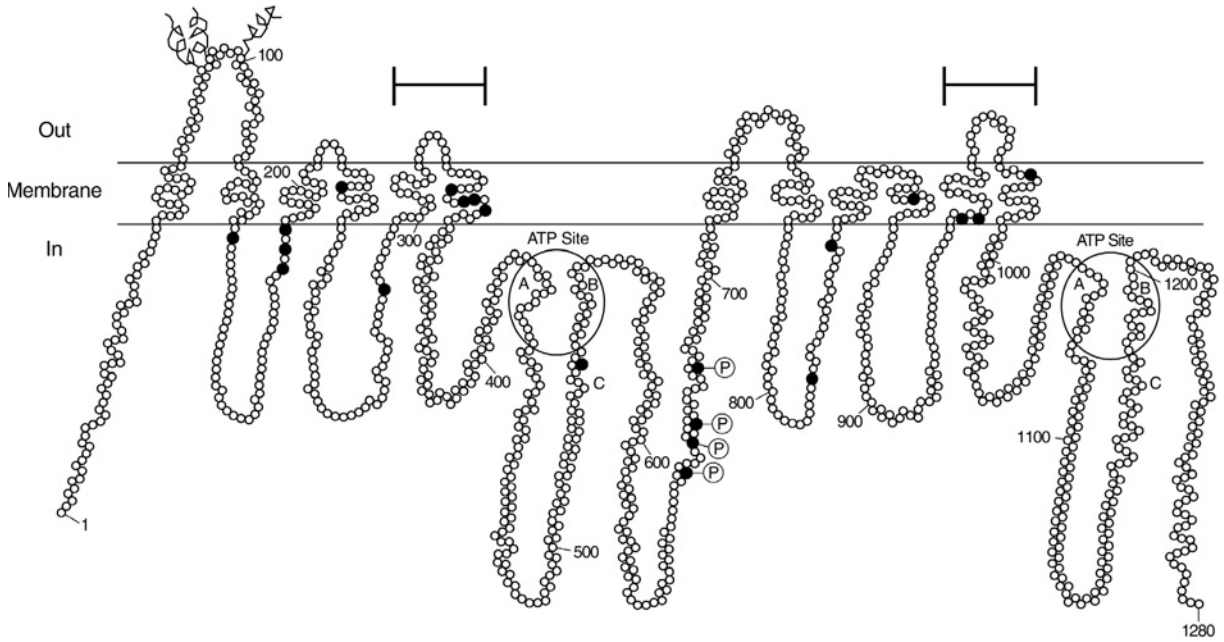

FIGURE 14.4 A hypothetical two-dimensional model of human P-glycoprotein based on hydropathy analysis of the amino acid sequence and its functional domains, depicting amino acid residues (○), the positions of selected mutations that alter the substrate specificity of P-gp (●), ATP sites (*large circles*), N-linked glycosylation sites (*squiggly lines*), phosphorylation sites (*circled P*), and Walker A, B, and C regions. Numbers refer to specific amino acid positions, and bars above the model indicate regions labeled with photoaffinity analogs. (Reproduced with permission from Ambudkar SV, Dey S, Hrycyna CA, Ramachandra M, Pastan I, Gottesman MM. Annu Rev Pharmacol Toxicol 1999;39:361–98.)

from that of the more familiar F1 ATPase, but the mechanism of coupling ATP hydrolysis to transmembrane transport of substrates is clearly quite different. Turnover of the enzyme probably involves a two-stroke sequence: (1) binding of substrate and hydrolysis at one of the ATP sites in order to load the transported molecule on one side of the membrane and (2) hydrolysis at the second ATP site in order to expel the substrate from the other side of the membrane. An alternate two-stroke model involves (1) substrate binding followed by ATP hydrolysis to expel the substrate from the cell and (2) ATP hydrolysis at the second site in order to re-cock the enzyme into a conformation that can bind substrate. These mechanisms are not distinguishable at this time. Evidence suggests that substrate binds by absorption from within the inner leaflet of the membrane bilayer, rather than from bulk solvent in the cytosol. In this sense, the action of MDR-1 is like that of MDR-2, which is thought to flip phosphatidylcholine from the inner leaflet to the outer leaflet of the membrane. MDR-1 has been called a hydrophobic vacuum cleaner, whose evolutionary job was to clean membranes of foreign natural toxins. Expulsion of substrate into the aqueous phase outside the cell is facilitated by trapping agents (such as serum albumin) that prevent re-entry of the hydrophobic substrate into the membrane. Intracellular auxillary proteins may also play a role in delivering hydrophobic substrates to the transporter binding site.

The structure of P-glycoprotein has not been determined. However, X-ray crystallographic structures have been determined for bacterial members of the ABC transporter family: the MsbA lipid A "flippases" from *E. coli* (72) and *Vibrio cholera* (73) and the cobalamin uptake transporter BtuCD protein of *E. coli* (74). These structures are consistent with the overall picture of P-glycoprotein function described here.

The most challenging mechanistic question about P-gp is the basis of its ability to transport such a wide range of molecular structures (see Chapter 15, Table 15.2). Correlations with lipophilicity (e.g., log *P*) essentially reflect the concentration of the substrate in the membrane with K_m values in the 1–10 mmol of drug per mole lipid range, despite solution concentrations ranging over the 1–10 n*M* range (75). For comparable membrane concentrations, H-bond acceptors are most important. Pharmacophore search algorithms suggest two important patterns: Type I, having two acceptors spaced 2.5 Å apart, and Type II, having three acceptors spaced 2.5 Å apart in

a V-shape, with the outer two 4.6 Å apart (76). Binding requires at least one of these units. Transport requires at least two Type I units. These requirements can be related to the position of H-bond donor groups in the proposed transport pathway (see later). Additional factors affecting binding and transport include molecular weight, size or surface area, and presence of amine groups and unsaturated rings. Size, surface area, or cross-sectional areas may be related to ability to fit through the proposed transport channel. In the low dielectric medium of the membrane (or interior of a protein shielded from water), the strengths of electrostatic bonds (aromatic-ring cation, H-bonds, and dipole–dipole interactions) are much stronger than they are in water. Substrates with low electrostatic bonding energy may bind but are not transported (e.g., inhibitors, such as progesterone, dexamethasone, hydrocortisone, quinidine, terfenadine, GF120918, S9788). Substrates with intermediate bonding energy are transported but may be competitive inhibitors of other substrates (e.g., aldosterone, *cis*-flupenthixol, diltiazem, nicardipine, trifluoperazine, verapamil). Those with high bonding energy are transported slowly and thus are also inhibitors (e.g., cyclosporine, SDZ PSC-833).

Extensive substrate structure–activity studies and transporter mutagenesis, chemical, and photolabeling studies have been used to test structure–function hypotheses for P-gp. The model that emerges is one of multiple partially overlapping binding sites with few absolutely required determinants. Most of the substrate-contacting residues are located in two clusters in TM5,6 and TM11,12. It is hypothesized that these form two binding sites: one for high-affinity substrate recognition inside the cell, and one for low-affinity binding effectively outside the cell. There may also be an allosteric binding site, but the kinetics of membrane-bound enzymes and their substrates are difficult to interpret.

Multidrug Resistance-Related Protein

The MRP family of transporters is closely related and structurally similar to the MDR family (64, 65). MRP1 was initially identified in lung cells, which were known not to express P-gp. It has been shown to pump anionic compounds (as opposed to the cations pumped by P-gp). Substrates for MRP1 include anionic natural products; glutathione, glucuronyl, and sulfate conjugates; and, in some cases, neutral molecules coupled to glutathione transport without conjugation. In liver cells, MRP1 is present on the sinusoidal surface of the hepatocyte. MRP2 is similar to MRP1, except in its tissue distribution and localization. In liver cells, it is expressed on the canalicular membrane, and is also known as the canalicular multispecific organic anion transporter (cMOAT). Homology searching has revealed seven MRP family members. MRP3 is similar to MRP1, but with narrower substrate specificity. MRP4 and MRP5 act as nucleotide transporters. MRP6 and MRP7 can be recognized by their sequences, but their functions are unknown at this time.

Multifacilitator Superfamily Transporters

The Nucleotide Transporters

The nucleotide transporter (NT) family is illustrative of the multifacilitator superfamily (60, 61). Both naturally occurring nucleosides and most nucleoside drugs are very hydrophilic and do not readily cross bilayer membranes except by mediated or active transport. The relevant transport activities have been defined functionally by their substrates, cosubstrates, and inhibitor sensitivities. Currently known nucleoside transport activities are either equilibrative or concentrative. The equilibrative transporters allow the free exchange of nucleosides across membranes according to their concentration gradients. Concentrative transporters translocate nucleosides into a cell against a thermodynamic gradient by coupling transport to the electrogenic cotransport of sodium ions into the cell. Equilibrative (e) transporters are ubiquitous. Two classes can be distinguished: nitrobenzylthioinosine sensitive (es) or insensitive (ei). Five classes of concentrative transporters (N1–N5) can be distinguished by their substrate specificities. These transporters are selectively expressed in epithelial tissues (intestine, kidney, and choroid plexus) and in lymphoid cells and tissues.

The es transporter of erythrocytes has been identified by photoaffinity labeling, purified, and characterized as a relative of the equilibrative GLUT1 glucose transporter (a member of the 12-transmembrane-spanning helices major facilitator superfamily). Variations in molecular weight and glycosylation state occur in various species and tissues. The N3 concentrative transporter of rabbit kidney SNST1 was cloned by hybridization to a probe for the rabbit intestine Na^+-coupled glucose transporter SGLT1 (a member of the Na^+-coupled organic cotransporter family). As in the case of the GLUT1 family, the sequence suggests a protein with 12 transmembrane spans; however, in this instance several amino acid residues are clearly implicated in the Na^+ cotransport function. An N2 transporter gene (*cnt1*) has been cloned from rat intestine by expression in *Xenopus* oocytes.

In this case, the sequence suggests a 14-TM-helix protein with multiple glycosylation and phosphorylation sites. Although differing in molecular detail, it is likely that all members of the equilibrative and Na^+-linked families will be similar in overall three-dimensional structure and transport mechanism. However, there is a wealth of detailed variation upon which selectivity in drug transport or transporter inhibition may eventually be based.

Cells differ in their reliance on nucleoside uptake and salvage versus *de novo* biosynthetic pathways for normal growth, and, hence, they differ in their sensitivity to nucleoside drugs. Table 14.5 [adapted from Tables 1–4 in Cass (61)] lists some nucleoside drugs, diseases for which they have been used, and the transporters that recognize them. In addition to the es, ei, and N1–N5 nucleoside transporters, some nucleoside drugs also utilize nucleobase (NB) transporters.

The greatest successes with nucleoside drugs have been in the treatment of leukemias, lymphomas, HIV, and herpes virus infections. These drugs act intracellularly after conversion to nucleotide phosphates, generally by blocking DNA synthesis. Although nucleoside transport is important, the limiting step that defines the activity of nucleoside drugs is often the nucleotide kinase-mediated conversion of the nucleoside to the nucleotide. However, resistance to nucleoside therapy has been observed for cells with reduced transport activity as well as for cells with altered kinase activity or altered target sensitivity.

TABLE 14.5 Nucleoside Drugs, Indications, and Transporters[a]

Nucleoside drug	Clinical indication	Transporter specificity[b]
Cladribine (Cl-dAdo)	Leukemia	es, ei, N1, N5
Cytarabine (araC)	Leukemia	es, ei
2-Fludarabine (F-araA)	Leukemia	es, N1, N5
Pentostatin (dCF)	Leukemia	es
Floxidine (F-dURd)	Colon cancer	es, ei
Didanosine (ddI)	HIV	es, NB
Zalcitabine (ddC)	HIV	es, N2
Zidovudine (AZT)	HIV	N2
Acyclovir (ACV)	HSV	NB
Gancyclovir (GCV)	HSV	es, NB
Vidarabine (araA)	HSV	es, ei, N1
Idoxuridine (IdUrd)	HSV	es
Trifluridine (F3-dThd)	HSV	Not determined
Ribavirin (RBV)	RNA/DNA viruses	Not determined

[a] Adapted from Tables 1–4 in Cass CE. Nucleoside transport. In: Georgopapadakou NH, ed. Drug transport in antimicrobial and anticancer chemotherapy. New York: Marcel Dekker, Inc.; 1995. p. 408–51.

[b] es, Equilibrative transporter sensitive to nitrobenzylthioinosine (NBT); ei, equilibrative transporter insensitive to NBT; N1–N5, concentrative transporters; NB, nucleobase.

Bacterial Nutrient Transporter Models for the Multifacilitator Superfamily

The *E. coli* lactose permease (product of the *lacY* gene) is the best-described member of the multifacilitator superfamily (MFS). The permease LacY couples the thermodynamically unfavorable concentration of lactose into the cell to the favorable uptake of protons. Extensive sequence insertion–deletion, site-directed mutagenesis, chemical labeling, cross-linking, spin label, and fluorescent label techniques have been used to determine the topology and to study structure–function relationships in this protein (Figure 14.5) (77). These approaches showed that the protein contains 12 TM helices, provided a basic model for their organization in the membrane, and revealed substrate-induced changes in organization suggestive of the transport pathways and mechanism. Remarkably, only six of the amino acids in the side chains are irreplaceable.

Attempts to obtain three-dimensional structures of MFS proteins have long been frustrated by their inherent conformational flexibility. A low-resolution (6.5 Å) structure was obtained for the oxalate transporter (OxlT) from *Oxalobacter formigenes* by single-particle cryoelectron microscopy (78). This model shows a twofold-symmetrical arrangement of 12 TM helices, forming a central pore with oxalic acid bound. A high-resolution (3.5 Å) structure of a conformationally restricted mutant of *E. coli* Lac permease with a lactose analog bound was determined (79) and published simultaneously with that of the glycerol-3-phosphate transporter (GlpT) from *E. coli* in the absence of substrate (80). These structures showed the same helical arrangement as the OxlT structure but allowed sequentially specific identification of the protein components. The helices are organized into two distinct domains composed of six N-terminal helices and six C-terminal helices with equivalent packing, related to each other by intramolecular twofold rotation. In the LacY structure, an internal hydrophilic cavity (~25 Å wide by 15 Å deep) is formed by helices I, II, IV, V and helices VII, VIII, X, XI, in which the lactose analog was observed bound to the predicted Glu126 (helix IV) and Arg144 (helix V) residues. Additional details of the substrate binding site and proton pathway are evident and these enhance interpretation of the earlier biochemical studies.

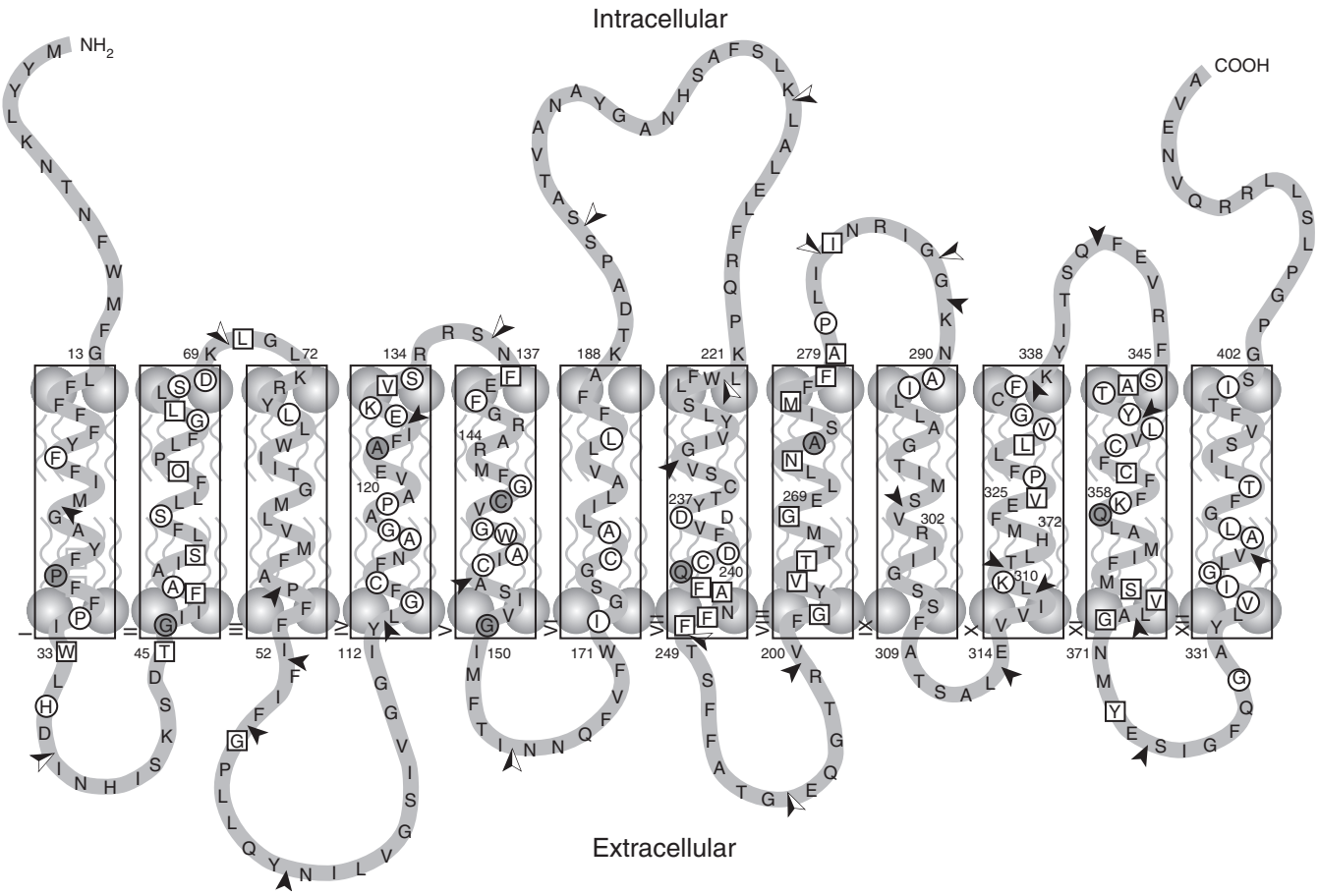

FIGURE 14.5 Secondary structure model of Lac permease. Residues crucial for active transport are E126, R144, E269, R302, H322, and E325; charge pairs are D237–K358 and D240–K319. Solid rectangle outlines represent helical regions defined by single-amino-acid deletion analysis. Ionizable residues D68, K73, R74, E131, K131, E139, R142, and K336 are predicted to be within the cytoplasmic ends of transmembrane helices II, III, IV, and V by deletion analysis. Residues in squares represent positions where transport activity of single Cys replacement mutants are inhibited by *N*-ethylmaleimide treatment. Residues in circles represent positions where missense mutations have been shown to inhibit lactose accumulation. Residues in P28, G46, A127, C148, G159, Q242, A273, and Q359 represent positions where both results have been observed. Two-tone arrowheads indicate locations where discontinuities in the primary sequence ("split" Lac permeases) have been introduced, and solid arrowheads indicate regions where polypeptides have been inserted into the permease. In general, most splits/insertions in the loop regions are tolerated (except in the VIII–IX loop) and most splits/insertions in the putative transmembrane domain result in little or no transport activity. (Reproduced with permission from Kaback HR, Sabin-Toth M, Weinglass AB. The kamikaze approach to membrane transport. Nat Rev Mol Cell Biol 2001;2:610–20.)

The GlpT transporter is proposed to function via a single-binding-site, alternating-access mechanism. The translocation pathway is proposed to occur between the N- and C-terminal halves of the protein. Binding of glycerol-3-phosphate (G3P) is proposed to occur at the site formed between Arg45(helix I) and Arg269(helix VII) and is proposed to lower the barrier for conformational exchange. A rocking motion is proposed to expose the binding site to alternate membrane faces. Exchange of G3P for inorganic phosphate (Pi) allows the protein to return to its starting conformation and allows the higher cytoplasmic Pi concentration to drive uptake of G3P.

ROLE OF TRANSPORTERS IN PHARMACOKINETICS AND DRUG ACTION

There is increasing recognition of the important role played by protein transporter molecules in the processes of drug absorption, distribution, and elimination. This is particularly true with respect to the barrier and drug-eliminating functions of gastrointestinal epithelial cells, hepatocytes, and renal tubule cells (62). Figure 14.6 depicts a schematic of drug transport in the body and some of the known transport proteins. Transporters also are important

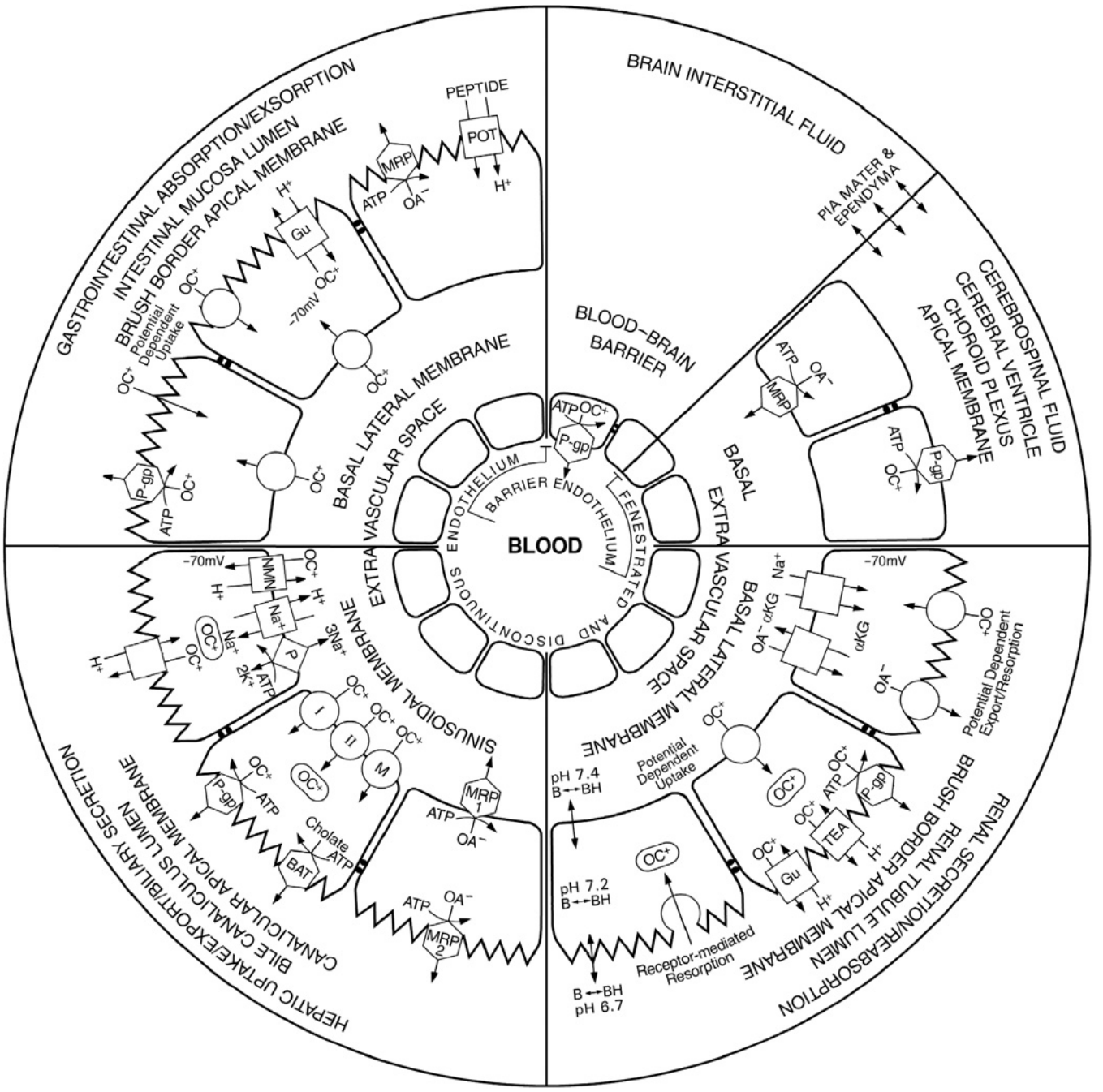

FIGURE 14.6 Schematic of drug transport in the body, indicating cellular topology for selected transporters. Capillaries and epithelial cells with tight junctions are represented by ••, organic cations by OC^+, and organic anions by OA^-. Members of the ABC superfamily of transport proteins (⬡) include P-glycoprotein (P-gp); multidrug resistance proteins MRP1, MRP2, or cMOAT; and the bile acid transporter (BAT). Active transporters (□) include the guanidium transporter (Gu), triethylammonium transporter (TEA), *N*-methylnicotinamide transporter (NMN), and proton-coupled oligopeptide transporter (POT). Carrier-mediated transport or facilitated diffusion (◯) includes the Type I (I) and Type II (II) cation carriers and the multispecific non-charge-selective carrier (M). Also represented are Na^+/K^+ P-type ATPase (Ⓟ) and intracellular sequestration (▭).

determinants of the response of cancers and bacteria to chemotherapy.

Role of Transporters in Drug Absorption

As described in Chapter 4, oligopeptide and monocarboxylic acid transporters facilitate the absorption of certain drugs. There have been a number of demonstrations that these natural transport pathways can be exploited to enhance drug action. An example demonstrating this concept is the discovery that valacyclovir is a substrate for the PEPT-1 transporter (81). Valacyclovir is an amino acid ester prodrug of the antiviral drug acyclovir. The usefulness of acyclovir is somewhat limited by its poor bioavailability. However, the oral bioavailability of valacyclovir is increased three- to fivefold in humans. Experiments using a rat intestinal perfusion model demonstrated a 3- to 10-fold increased intestinal permeability of valacyclovir over acyclovir. The effect was specific (i.e., exhibited structure–activity preferences among a family of amino acid ester prodrugs), and was stereospecific for L-valine, saturable, inhibitable by known PEPT-1 substrates (cephalexin, dipeptides), and competitive with other amino acid ester prodrugs (e.g., Glyacyclovir, Val-AZT). Studies using Chinese hamster ovary (CHO) cells expressing hPEPT-1 demonstrated competition between valacyclovir and the classic PEPT-1 substrate [^{3}H]glycylsarcosine. Experiments in Caco-2 cells showed enhanced, saturable, and inhibitable mucosal to serosal transport, consistent with active transport via the PEPT-1 transporter. In contrast, serosal to mucosal transport was shown to be by passive diffusion. Furthermore, transport was accompanied by hydrolysis of the prodrug, such that although drug was taken up as valacyclovir, it appeared on the serosal side as acyclovir. Following up the valacyclovir–PEPT-1 discoveries, valganciclovir was developed to exploit the same delivery strategy (82). In a clinical trial for cytomegalovirus prophylaxis, a daily oral dose of 900 mg valganciclovir was as effective as a daily 1-hour intravenous infusion of 5 mg/kg ganciclovir at (83, 84).

These examples are unusual in that valacyclovir is an amino acid ester of a nucleoside that does not closely resemble the normal dipeptide substrates of the PEPT-1 transporter. A number of other drugs (such as methotrexate) are probably transported by proteins that normally transport the metabolites that they resemble and antagonize (e.g., folates). However, these cases represent fortuitous examples of drug transportability "natural selection" during the drug discovery and development process. With increased understanding of the specificity determinants of nutrient transport, a rational basis for designing or redesigning drugs to exploit specific transporters may emerge. For example, XP13512 is a prodrug of gabapentin, which is beginning Phase II clinical trials. Absorption of gabapentin is limited by saturation of relevant small intestinal amino acid transporters. XP12512, which is metabolized to gabapentin in the intestine and liver, has a sustained action due to its ability to use several uptake transporters located in the large as well as the small intestine (85, 86).

As discussed in Chapters 4 and 15, both P-gp and CYP3A4 are colocalized in intestinal epithelial cells and may limit bioavailability either by intestinal first-pass metabolism by CYP3A4 or by P-gp-mediated exsorption. Many of the substrates for CYP3A4 are also substrates for P-gp (see Table 4.2), so that many CYP3A4 substrates may also be competing for transport by P-gp or may modify its level of expression (87). There is no sequence homology between these proteins and likely no tertiary structural homology. However, both likely have similar broadly accessible hydrophobic pockets.

Competition between substrates for limiting transporter molecules and other effects lead to drug–drug, drug–food, and drug–dietary supplement interactions very similar to those seen with CYP450s. In an explicit test of GI absorption/exsorption interactions, small intestinal secretion of intravenously infused talinolol, a β1-adrenergic receptor antagonist, has been studied in healthy volunteers using a steady-state perfusion technique (88). Perfusion of dexverapamil [(*R*)-verapamil] into the intestinal lumen lowered the intestinal secretion of talinolol 29–56%. The conclusion is that bioavailability of talinolol is in part limited by exsorption and may be subject to drug interactions during absorption. In this study (*R*)-verapamil was used because it is known to affect P-gp-mediated drug transport, but is devoid of the pharmacological effects of (*S*)-verapamil. Hence, it can be used safely as a probe in clinical studies of P-gp inhibition. P-gp can be activated as well as inhibited, as evidenced by the ability of grapefruit juice to increase P-gp activity, partially counteracting its inhibition of CYP3A4-mediated first-pass metabolism (89, 90).

Role of Transporters in Drug Distribution

Transporters are critical in the function of capillary endothelium, where they contribute to the blood–brain, blood–germinal epithelium (blood–testis and blood–ovary), and blood–placental barriers. Endothelial cells in each of these tissues express high levels of MDR-1. The existence of a blood–brain barrier is well established and is thought to arise

from the formation of tight junctions between brain endothelial cells as well as the action of drug efflux pumps (91, 92).

The importance of MDR-1 in the blood–brain barrier was dramatically revealed by an incident involving ivermectin toxicity in knockout mice. In mice, there are two MDR-1 isoforms, encoded by *mdr1a*/*mdr1b*. These differ in their tissue distribution and specificity, and *mdr1a*, *mdr1b*, and combined knockout mice have been created. Ivermectin is routinely used in rodent facilities as an antihelmenthic to control parasitic worms. The day after one mouse colony was given standard ivermectin treatment, all of the homozygous *mdr1* knockout mice were found dead. The level of ivermectin was found to be 100-fold higher in their brains than in the brains of normal mice (93). Normal homozygotes and *mdr1* heterozygotes appeared to have normal drug responses. Homozygous knockouts were viable, but very sensitive to xenobiotics, with the combined *mdr1a*/*mdr1b* knockouts being the most sensitive (94). Other MDR-1 substrates include digoxin and loperamide. Loperamide is related to the opiate narcotics, but is widely used as an antidiarrheal agent, because it does not normally get into the brain. In the MDR knockout mice, loperamide was found to be addictive because it could not be excluded from the brain (95). The clinical significance of P-glycoprotein in preventing CNS effects of loperamide was demonstrated in a study of quinidine potentiation of the opiate-induced depression of the respiratory response to carbon dioxide rebreathing (96). Quinidine inhibits P-glycoprotein, and its coadministration with loperamide exerts independent effects, increasing both loperamide's CNS activity and plasma concentrations.

Other tissues with high MDR-1 concentrations include the apical surface of pancreatic duct cells, the adrenal cortex, and the choroid plexus. In the case of secretory glands, MDR-1 may be necessary to protect the gland from its own products and perhaps to assist with their export (e.g., hydrophobic steroids synthesized by the adrenal glands). The choroid plexus is responsible for the secretion of cerebrospinal fluid. It consists of epithelial cells with a basal surface in contact with the blood and an apical surface facing the ventricular space. MDR-1 is located on the apical surface of choroid plexus cells, analogous to its location in other tissues. This location does not put MDR-1 in a position to protect the brain, since transport across the arachnoid membrane separating the CSF and brain cells is thought to be unimpeded. However, choroid plexus cells have been shown to express MRP on their basolateral surface, consistent with a brain-protective role for this transport protein (97).

In addition to MDR-1 and MRP1, several other blood–brain barrier and choroid plexus transporters have been recognized (98). These include the organic anion-transporting polypeptides (OATP1 and OATP2), organic cation transporters (OCTs), and several additional MRP isoforms. These transporters play roles in uptake and efflux of physiologically important brain chemicals as well as drugs. For example, sodium-independent OATP2 transports some steroids and their conjugates, the amino acids glutamate and aspartate, and the peptide Leu-enkephalin, as well as pravastatin, fexofenadine, and digoxin. The potential dependent OCTs on the apical surface of the choroids plexus appear to serve as efflux transporters, taking organic cations from the CSF into the epithelial cell. OCT-3 is expressed at high levels in brain cells and has been shown to transport cimetidine, amphetamine, and methamphetamine, as well as serotonin and dopamine.

Transporters are also critical to target tissue uptake of drugs from the extravascular space. As discussed in Chapter 3, transport of drugs between the vascular and extravascular spaces, except in capillaries with tight junctions, is probably by nonmediated diffusion and bulk flow. However, specific transporters are necessary for many drugs to enter target cells and also for transport to their subcellular sites of action. Specific examples include the nucleotide transporter family responsible for antiviral and anticancer drug uptake (61) and the reduced folate carrier that is essential for methotrexate uptake (99). Studies initially looking for yeast mutants resistant to cisplatin toxicity and confirmed in mammalian knockout mice cells have identified the copper uptake protein Ctr1 as essential to cellular uptake of this important anticancer drug (100). On the other hand, a copper export transporter, the Menkes disease-related protein of the trans-golgi and plasma membrane (ATP7A), has been shown to mediate cisplatin export and is elevated in ovarian cancer patients who did not respond to cisplatin therapy (101). Ectopic or elevated expressions of the related Wilson's disease trans-golgi and bile canalicular copper export protein (ATP7B) are associated with cisplatin resistance in cancers of prostate, esophagus, stomach, breast, ovary, and oral mucosa (102, 103).

Many tissues also express the same drug export pumps that occur in the barrier epithelial tissues (e.g., MDR, MRP, MXR), and these may be important in normal tissues, as well as in drug-resistant cancers. For example, P-gp may contribute to resistance to peptidomimetic HIV protease inhibitors (e.g., indinavir, saquinavir, and nelfinavir) in AIDS patients. These drugs are substrates for P-gp, and this transporter

prevents their passage across the blood–brain barrier. This has the effect of limiting the access of these drugs to HIV within the central nervous system. Furthermore, lymphocytes and macrophages are among the cell types that normally express P-gp at low levels, including the $CD4^+$-expressing T-lymphocytes, targets of HIV infection. In some cases, protease inhibitor resistance of HIV-infected cells may be due to increased expression of MDR-1, rather than mutation of the HIV protease (104).

Role of Transporters in Drug Elimination

Each epithelial barrier tissue displays a similar cellular topology, with basal surfaces in communication with the extravascular space and apical surfaces featuring high-surface-area brush border membranes that face into extravascular compartments. The topology of transporter expression is similar for at least certain transporters in these cells. Thus, MDR-1 is expressed on the apical surface of each of these cells, consistent with a role in drug excretion from mucosal cells back into the intestinal lumen, from hepatocytes into the bile canaliculus, and from the kidney into the renal tubule duct (62). Other important apical cation transporters in these tissues include the TEA/H^+ and guanidinium/H^+ proton-coupled antiporters. Protection from hydrophobic cations is a particularly important problem for cell survival. Most cells are negatively polarized inside (~ -70 mV). Hydrophobic cations will accumulate spontaneously within these cells by simple diffusion. Active transport pumps are necessary to expel undesirable materials back out of the cell and out of the body. The overall pH gradient across the renal tubule cell (blood pH = 7.4, intracellular pH = 7.2, and tubule fluid pH = 6.7) also facilitates the net export of weak bases. In some tissues, such as liver, uptake through the basolateral (sinusoidal) membrane may be facilitated. Two organic cation transporters (Type I and Type II) and a non-charge-selective multispecific carrier have been identified in this organ.

Organic anion transport is also important. MRP is located on both the apical (canalicular) and basal (sinusoidal) surfaces of hepatocytes. Anionic drugs and conjugated drugs are excreted both into blood, where they are cleared by the kidney, and into the bile. Renal clearance of anions presents the converse problem to organic cation accumulation. That is, an active transport system is necessary to accumulate anions into the renal tubule cell from the blood (110). This is facilitated by a two-stage secondary pump. In the first stage, the primary sodium gradient is used to drive coupled uptake of sodium and α-ketoglutarate. The α-ketoglutarate gradient is then used to drive organic anion uptake by a coupled antiport mechanism. Export of organic anions on the brush border membrane into the tubule fluid is facilitated and potential dependent.

The number of organic cation and organic anion transporters recognized has increased over the years. Differences in their patterns of expression and their overlapping substrate specificities are being slowly worked out (111). Nucleoside transporters are important in the disposition and targeting of nucleoside analogs to kidney. All five known nucleoside transporters are present. Concentrative transporters (CNTs) localize primarily to the apical membrane while equilibrative transporters (ENTs) localize primarily to the basolateral membrane. These localizations favor the reabsoption of naturally occurring nucelosides and their therapeutic analogs, therefore targeting nucleoside therapies to renal tumors (112).

The Wilson's disease transporter (ATP7B) of the hepatic golgi–bile canaliculus mediates elimination of excess copper from the body and may play an important clinical role in eliminating cisplatin, carboplatin, and other congeners in patients with hepatocellular carcinoma (103). However, elimination also occurs via hepatocellular conversion to glutathione conjugates that are secreted via MRP2 (102).

Role of Transporters in Drug Interactions

Interactions involving drugs that have a low therapeutic index are the most clinically significant. These are discussed in Chapter 15 (Tables 15.1 and 15.2 list cytochrome P450 and P-gp and other transporter substrates, inhibitors, and inducers that may be involved in drug–drug interactions). As discussed there, it is noteworthy that many of the inducers of cytochrome P450 also induce drug transporters, and this induction may be mediated by the same regulatory systems [e.g., pregnane X receptors (PXR) and the constitutive androstane receptor (CAR)].

Digoxin is a substrate for P-gp, and clinically significant digoxin toxicity has been reported in patients who have been treated simultaneously with quinidine, verapamil, or amiodarone. In one study, coadministration of quinidine reduced both the renal and the nonrenal clearance of digoxin to the extent that total clearance was reduced by 35% (11). Digoxin is not metabolized extensively, and studies in cell culture and in knockout mice demonstrate that both of these clearance mechanisms appear to be mediated primarily by P-gp (113). CNS levels of digoxin in wild-type but not *mdr1a* knockout mice also were increased by this interaction with quinidine, suggesting effects on P-gp transport in the blood–brain barrier as well. In a controlled study, wherein maintenance-dose digoxin

therapy was initially established, addition of verapamil was shown to increase plasma digoxin levels 60–90% (114). In addition to increasing bioavailability, verapamil was shown to decrease renal clearance of digoxin, apparently through inhibition of renal tubular P-gp. The conclusion from this study is that the dose of digoxin should be reduced and retitrated when verapamil cotherapy is instituted. Studies of hospital records suggest the need for adjustment of digoxin dose in over half of patients who are treated simultaneously with quinidine or amiodarone (115).

Another drug–drug transport interaction of potential clinical significance involves the immunosuppressant drug tacrolimus (FK-506), which is a substrate for both cytochrome P450 (CYP3A) and P-gp (116). These enzymes act together to limit drug bioavailability through repeated efflux and re-exposure of drug to the metabolic action of P450 in the small intestine. P-Glycoprotein controls FK-506 distribution through the blood–brain barrier as well as into targeted lymphocytes. A large number of interactions, involving either inhibition or induction, have been predicted by *in vitro* methods, and many have been confirmed in animal models and clinical studies.

Drug–drug transport interactions are important in combination therapy with HIV protease inhibitors (117). Many protease inhibitors are substrates for and inhibitors of CYP3A4 and P-gp. Different combination effects (e.g., intrinsic clearance of amprenavir is reduced by nelfinavir and indinavir, but not saquinavir) depend on the extent to which one or both of these enzymes are affected.

The growing use of herbal and other dietary supplements by the lay population suggests that an increase in dietary supplement–drug interactions may occur. For example, St. John's wort (*Hypericum perforatum*) was shown to decrease the digoxin AUC by 25% after 10 days of treatment (118). The effect appears to reflect induction of P-gp expression. Whether the active component leading to induction is the same or different from hypericin (one of the putative active antidepressant components of St. John's wort) is not known. A significant number of other herbal supplement–drug interactions are known, including interactions with HIV protease inhibitors and with anticoagulants (119). It is not clear whether the effects are on metabolism or transport.

P-gp Inhibition as an Adjunct to Treating Chemotherapy-Resistant Cancers

Recognition of the importance of drug resistance efflux pumps has motivated a number of attempts to improve drug therapy by specific coadministration of P-gp inhibitors. Inhibition of P-gp or of its enhanced transcription in tumors may be a component in the anticancer activities of some agents such as ecteinascide 743 (ET-743) (120). Since the therapeutic index of verapamil, cyclosporine, and other marketed P-gp inhibitors is too narrow, dexverapamil and valspodar are among a number of new compounds that are being synthesized and evaluated for this specific purpose. So far, the coadministration of P-gp inhibitors and anticancer drugs has yielded mixed results. This reflects in part the natural history of the cancers being treated and the existence of multiple resistance mechanisms.

An extensive survey of MDR-1 mRNA expression levels in cancer patient tissue samples and normal controls suggested that three types of MDR-1 behavior may be distinguished in different cancer cells (121, 122): (1) MDR-1 is normally expressed in transporting epithelium, liver, colon, kidney, pancreas, and adrenal gland. Expression of MDR-1 remains high in cancers derived from these tissues. (2) Cancer cells derived from other tissues that normally do not express MDR-1 may be induced to express it when selected by drug treatment, and promoter analysis has shown that P-gp expression is induced by a variety of xenobiotics. This appears to result from clonal selection for resistant cells during the initial phase of drug treatment and leads to patient relapse following an initially successful response to therapy. Such relapses are commonly seen in leukemias, lymphomas, breast, and ovarian cancers. (3) Cancer cells that normally do not express MDR-1 may acquire expression in the absence of drug selection by undergoing significant DNA changes that completely alter the normal regulatory mechanisms of the cell. Examples include chronic myelogenous leukemia (CML), sarcomas, and neuroblastomas. Expression of MDR-1 may coincide with transformation of the cancer to a more malignant form, such as occurs during the blast crisis phase in CML. In the chronic phase of CML the cancer is susceptible to chemotherapy, but in the blast phase it becomes resistant.

The responses of these three cancer types were found to differ during clinical trials of MDR-1 inhibitors (123). For the first class, MDR-1 inhibition has had little effect on the efficacy of the cancer therapy. It appears that too many other transporters and drug resistance mechanisms are present in front-line defense organs such as kidney, liver, and intestine. For the second class, at least transiently improved responses to anticancer drugs have been seen with MDR-1 inhibitor cotherapy. However, a second relapse is seen as other transport

and resistance mechanisms become active. In the Southwest Oncology Group (SWOG) trial for acute nonlymphocytic leukemia, results were most promising when MDR-1 inhibitor cotherapy was begun with the initial course of chemotherapy (124). Although a contributing factor to the failure of P-gp inhibitor cotherapy is the existence of other transporters with overlapping specificity, discovery of additional inhibitors, such as fumitremorgin C, an inhibitor of the breast cancer resistance protein (BCRP) multidrug resistance transporter, may improve efficacy of this approach (125).

In a novel twist on the idea of altering P-gp function in cancer patients, experiments have examined the potential of using *mdr1* gene therapy to selectively protect hematopoietic cells from the side effects of cancer therapy (126, 127). Using a retroviral vector, a mutant *mdr1* gene (F983A), which is resistant to the P-gp inhibitor *trans*-(*E*)-flupentixol, was transfected into bone marrow cells. This allowed the cells to survive increased doses of daunomycin and vinblastine. Treatment of target cells under the same conditions with the P-gp inhibitor increased their sensitivity to the drugs without compromising the protection of the mutant *mdr1* transfected cells.

Role of Transporters in Microbial Drug Resistance

Bacterial cells are similar to mammalian cells in that they bear an internal negative charge and naturally accumulate organic cations. Transport systems apparently evolved long ago to eliminate natural cationic toxins. Mechanisms of drug uptake in bacteria utilize outer membrane (OM) porins, periplasmic binding proteins, and inner membrane (IM) pumps (7, 21). Relatively selective channels may be used by some antibiotics (e.g., imipenem), and nutrient transporters may be used by others (e.g., aminoglycosides). The discovery of resistance due to reduced uptake has been a key to understanding the role of specific transporters in antibiotic transport. Antibiotics that mimic siderophores (e.g., by including catechol groups) utilize uptake mechanisms used by bacteria for uptake of iron. Such agents and modes of drug delivery have been "naturally selected" by antibiotic drug screening programs. Only recently has structure-based drug design been explored in an attempt to take explicit advantage of these systems. Notably, the FepA and Fhu siderophore transporters were until recently the only active transport systems for which high-resolution structures had been determined.

In addition to mutations that alter drug uptake, several systems are known to confer bacterial drug resistance by enhancing drug efflux (e.g., resistance to tetracyclines, quinolones, and macrolides). These include transporters in the MF family (e.g., TetA), the resistance–nodulation division (RND) family (AcrAB, EmrAB, TolC), the small multidrug resistance (SMR) pumps, and the ABC family (128). These systems have highly varied membrane topologies, subunit structures, and bioenergetics. Of particular interest is the LmrA gene product, which appears to be an ABC-type half-transporter similar to MXR and a potentially ideal candidate for biophysical and mechanistic studies.

PHARMACOGENETICS AND PHARMACOGENOMICS OF TRANSPORTERS

Pharmacogenomics of Drug Transport

Pharmacogenomic approaches are being applied to reveal the rich diversity of transporters present in the rapidly growing database of sequences (129–132). Classifications of transporter genes may be constructed based on translocation mechanism (transporter or channel), origin, topology, domain structures, energetics (passive or active), energy source (ATPase, H^+- or Na^+-coupled secondary pump), substrate specificity, sequences, and three-dimensional structure. BLAST (Basic Local Alignment Search Tool), INCA (Integrative Neighborhood Cluster Analysis), and other sequence analysis tools have been used to describe the relationships between transporters. Sadée *et al*. (129) have applied these methods to examine the relationships between the H^+/dipeptide, facilitative glucose, sodium/glucose, sodium/nucleoside, amino acid transporter, sodium neurotransmitter symporter, and ABC transporter families in species ranging from bacteria to mammals. This approach has led to the identification of additional putative human proton/oligopeptide transporter genes (133).

Saier *et al*. (134–137) have developed a system of transporter classification (T.C. number) analogous to the Enzyme Commission (E.C. number) system for uniquely identifying enzymes. Transporters are organized as follows:

W = Type and energy source.
X = Transporter family or superfamily.
Y = Transporter subfamily.
Z = Substrate(s) transported.

Each transporter is assigned a unique identifier, for example, T.C. #W.X.Y.Z. In the system, two proteins

were designated as being in the same family if at least one 60-residue segment showed a percentage amino acid sequence identity greater than 9 standard deviations above the result expected for randomly shuffled sequences. Two proteins were designated as being in the same superfamily if they could each be related to another protein by this definition, but could not be directly related to each other. Additional members of the superfamilies are identified as "missing" links are found. This system was adopted by the Nomenclature Committee of the International Union of Biochemistry and Molecular Biology (138). An alternative nomenclature has been established by the Human Genome Organization Gene Nomenclature Committee (139). This system is gaining in popularity. A good introduction to this system as applied to the multifacilitator superfamily [or solute carrier (SLC) families] is provided by Hediger *et al*. (140).

Saier and coworkers have constructed a database that organizes data derived from the microbial organisms for which completely sequenced genomes are available and have conducted extensive cross-species analyses (141). A total of 81 distinct families were identified. Two superfamilies, the ABC and the multifacilitator superfamilies, account for 50% of all microbial transporters. Probable transported solutes could be ascribed to 80–90% of the putative transport proteins. The number of transporters is roughly proportional to genome size, and the patterns of transporter usage are correlated with microbial physiology and ecological niche. These data also yield insight into the evolutionary origins of membrane transporters and into the origins of bacterial multidrug resistance. Certainly, evolution of the four major drug resistance transporter types occurred in four major stages, well before human development of antibiotic therapy. However, proliferation of substrate-specific pumps has occurred frequently and is ongoing.

The Institute for Genome Research (TIGR) has also completed analyses of several completed genomes (142, 143). They have allowed an estimate of the number of transporters in the genomes and defined the minimal set of transporter functions necessary for different metabolic lifestyles. The TIGR web site (144) provides access to annotated sequences of human transporter genes and transcripts, and cDNAs, through the Expressed Gene Anatomy Database (EGAD). Sadée and coworkers (145) have begun the Human Membrane Transporter Database. This database includes information on transporter families, sequences, tissue distributions, and substrates/drugs transported. For example, all transporters expressed in human kidney can be easily retrieved. Thus far, approximately 250 human membrane transporters are known, including 100 putative ABC family transporters. Estimates of the total number of transporters in the human genome range from 500 to 2500 (e.g., perhaps 4 to 5% of the proteome). It is expected that many of these transporters can recognize drugs and therefore might affect the drug response in the body.

The availability of the complete human genome sequence and the ability to compare sequence data with the completed genomic sequences of other organisms have enabled the systematic identification of many new transporter genes (i.e., the transportome). For example, an approach using 28 members of the multifacilitator superfamily to search the National Center for Biotechnology Information (NCBI) database of expressed sequence tags revealed not only the 73 previously characterized MFS genes, but also 43 new MFS gene candidates (146). The challenge has shifted from cloning the genes responsible for functionally characterized transport activities (e.g., by expression cloning) to identifying the transported substrates of genomically characterized transporters (e.g., chemogenomics).

Matrix array chips based on short or longer oligonucleotides or cDNAs and other methods have been used to analyze transporter gene expression in various cells and tissues (147). For example, arrays of synthetic 70-mer oligonucleotides have been used to analyze the expression of 461 transporter genes in the 60 human cancer cell lines that have been used by the National Cancer Institute to screen for potential new anticancer drugs (148). Expression levels were then correlated with the known pattern of sensitivity of the cells to 119 standard anticancer drugs with putatively known mechanisms of action. The approach identified expected known interactions, such as correlation of level of expression of SLC29A1 (nucleoside transporter ENT1) with sensitivity to nucleoside analogs and the level of expression of ABCB1 (P-gp) and resistance to 19 known P-gp substrates. The approach identified compounds not previously recognized as MDR-1 substrates. It also identified ABCB5 (previously unknown function) as a novel chemoresistance factor. These findings were confirmed by siRNA silencing of the relevant genes, leading to increased sensitivity.

In another example, real-time polymerase chain reaction (RT-PCR) was used to determine expression levels of the 48 known human ABC-type transporters in the NCI-60 cell lines, and these levels were correlated with sensitivity to 1429 candidate anticancer drugs (149, 150). Patterns of expression correlated moderately well with tissue of origin and were independent of sequence homology among

family members. As expected, expression of ABCB1 (MDR-1-P-gp) was negatively correlated with sensitivity to known substrates and not correlated or positively correlated for known nonsubstrates. Interestingly, several compounds were strongly positively correlated with ABCB1 expression, meaning that their actions are somehow potentiated. This approach identified 18 compounds that were not previously well known as P-gp substrates. This conclusion was corroborated by reversal of resistance to these compounds in cells that overexpress MDR-1-P-gp upon cotreatment with the MDR-1 antagonist PSC 833. This study also identified 131 other highly inverse-correlated gene–drug pairs. These included several members of the ABCC (MRP), including 14 compounds linked to ABCC2 (MRP2-cMOAT) expression and one compound linked to ABCC11 (cyclic nucleotide transporter). Surprisingly, several transporters generally thought to be important in drug resistance showed only weak correlations and some of their known substrates were not identified [e.g., ABCC1 (MRP1), ABCG2 (MXR-BCRP)]. The authors stressed the value of these highly parallelized studies and statistical analyses as an unbiased method for discovering substrate specificities. The power of these approaches is increasing with the inclusion of additional genes, better hybridization controls, inclusion of proteomic data, and correlation with additional data from the >100,000 compounds that have been tested in the NCI-60 cells.

In a particularly impressive example of functional genomics, the expression profiles for 12,599 gene sequence tags in shed human duodenum cells and in Caco-2 cells were correlated with the *in vitro* and *in vivo* human duodenal permeability of 26 drugs (151). Of these genes, 37–47% [26–44% of expected genes relevant to absorption, distribution, metabolism, and excretion (ADME)] were expressed both in human duodenum cells and in Caco-2 cells. However, the level for over 1000 genes showed a greater than fivefold variation between cell types. Variations of over threefold were found for more than 70 of the transporters that were assayed. Reasonably good correlations ($R = 85\%$) were found between *in vivo* and *in vitro* permeability measurements for passively absorbed drugs. However, variations of 3- to 35-fold above the expected passive permeability values were observed for drugs absorbed by transporter-mediated processes. These variations correlated with differences in gene expression. Interhuman variability in transporter expression in this study ranged from 3 to 294% of the mean for 31% of the genes studied. This work is helping to define which transporters are relevant to the transport of specific drugs.

Pharmacogenetics of Drug Transport

Individual genetically determined variations in transporter function may contribute to interindividual differences in therapeutic and/or adverse effects of drugs. Several studies have shown that variations in transporter gene sequences do occur. However, the clinical significance of these variations generally is not yet well documented. For example, as discussed in Chapter 4, the intestinal hPEPT-1 transporter plays a role in absorption of peptide-like cephalosporin antibiotics and other drugs. Interindividual variations in hPEPT-1 may account for the large interindividual variations in bioavailability that have been observed (129).

The first polymorphism in the MDR-1 gene was identified by comparing cDNAs cloned from normal human adrenal gland and a cochicine-selected multidrug-resistant cell line derived from an epidermoid carcinoma (152, 153). Nine nucleotide sequence differences were noted, but only two altered the coding sequence. A variation, TT → GA at NT544–555 (Gly185Val), was shown to be associated with an enhanced resistance to colchicine relative to other MDR substrates, and was thought to arise during selection of the cells. A second variation, G → T at NT2677 (Ser893Ala), was thought to reflect a naturally occurring, nonselected genetic polymorphism. The NT2677 polymorphism was used by Mickley *et al*. (154) to examine the allelic expression of MDR-1 in normal tissues, in unselected and drug-selected cell lines, and in malignant lymphomas. In normal tissue samples 43% were heterozygous, 42% were homozygous for G, and 15% were homozygous for T ($n = 83$), and expression from each allele was similar. In drug-selected cells and relapsed lymphomas, expression of only one allele at an elevated level was frequently found. In work with experimental animals, comparisons between *mdr1a* genes of mouse strains that are inherently resistant or sensitive to ivermectin neurotoxicity revealed a specific restriction fragment length polymorphism (RFLP) that is predictive of the observed phenotype (155).

Hoffmeyer *et al*. (156) used overlapping PCR primers to examine much of the MDR-1 sequence in genomic DNA isolated from healthy normal volunteers. MDR-1 expression was assayed in duodenal biopsy samples by immunohistochemistry and Western blotting, and *in vivo* intestinal P-gp activity was estimated using digoxin as a marker. Fifteen polymorphisms were identified among 24 individuals. Seven were located within introns, three were at wobble positions that did not alter the coded amino acid, one was in the 5′-noncoding region, and one

occurred just prior to the initiator methionine site. Three resulted in amino acid substitutions (Asn21Asp, Phe103Leu, Ser450Asn). Oddly, the NT2677 polymorphism was not detected in this sample. Only the polymorphism C/T at wobble position NT3435 was correlated with altered MDR-1 function. Levels of expression were twofold lower and plasma digoxin levels were significantly higher in homozygous T-allele subjects. Heterozygotes were intermediate. It is most likely that this effect reflects changes in mRNA processing, rather than other effects on expression. In a sample of 188 individuals, 48.9% were heterozygous and 22.4% were homozygous for the T allele. Because this variation is widely occurring, it may contribute to the need to individualize digoxin dosage in patients treated with this drug.

A total of 29 MDR-1 single-nucleotide polymorphism (SNP) variants have been characterized as of 2004 (Table 14.6) (157), but the significance of any given SNP is difficult to assess. Consistent comparisons and consistent data have not been obtained on the influence of these SNPs on mRNA or protein levels or on MDR-1 function with probe drugs. It is increasingly recognized that functionally important differences reflect haplotype differences (i.e., multiple linked SNPs in the same allele), rather than any single SNP. For example, the 16-hour AUC of fexofenadine for homozygous individuals designated MDR-1*1 (1236C, 2677G, 3435C) was 40% greater than for homozygous individuals designated MDR-1*2 (1236T, 2677T, 3435T) (158). Altered penetration of protease inhibitors into lymphocytes due to lower P-gp expression may be responsible for the greater efficacy of antiretroviral therapy (higher CD4 cell counts) reported in patients who were homozygous for the 3435T allele than in those homozygous for the 3435T allele (159). Significant differences in haplotype frequencies are found among various racial and ethnic groups, based on mathematical models of population data (160). Sorting out important differences in individual haplotype influences on drug response will require further improvements in technology for direct molecular haplotype analysis.

Polymorphisms of the MXR/BRCP gene (ABCG2 or ABCP) may also be clinically important and may account for the sixfold variation in bioavailability of topotecan and its congeners. Variations in the coding sequence have been observed for drug-selected cellular variants (MXR and BRCP) and for cDNAs produced from human intestine and liver samples (161). Allele frequencies vary from a few percent to 100% for some ethnic, racial, and geographic/cultural groups. Exon 5 NT421 C $\rightarrow$ A (Q141K), the most common variant allele, results in lower expression of ABACG2 protein, due to differences in protein synthesis, rather than mRNA or protein stability. Patients treated with intravenous diflomotecan with one 141K allele ($n = 5$) achieved plasma levels three times higher than those

TABLE 14.6 Example P-Glycoprotein Polymorphisms[a]

Nucleotide position	Location	Effect	Allelic frequency	Expression mRNA/protein	Probe drug phenotype
A61G	Exon 2	Asn21Asp	11.2%	—	Digoxin AA = AG
G1199A	Exon 11	Ser400Asn	5.5%	—	Digoxin GG = AA
G2677T	Exon 21	Ala893Ser	41.6%	GG ≤ Gm* = m*m*	Digoxin GG ≤ Gm* ≤ Tm*
G2677A	Exon 21	Ala893Thr	1.9%	GG ≤ Gm* = m*m*	Digoxin GG ≤ Gm* ≤ Tm*
C3435T	Exon 26	Wobble	53.9%	CC ≤ CT ≤ TT	Digoxin CC ≤ CT ≤ TT Nelfinavir CC > CT > CC Cyclosporine, talinolol, loperamide CC = CT = TT

[a] Excerpted and adapted from Tables 1–3 in Woodahl and Ho (157). Expression in this table refers to intestine. The probe drug phenotype column reflects the most frequent outcome observed for various trials and measures (e.g., AUC, C_{max}, C_{min}); m* = T or A.

of patients homozygous for 141Q allele ($n = 15$), but did not show any difference on oral administration (162). In another study, no effect was seen in irinotecan pharmacokinetics (163). Thus, genetic variation in the ABCG2 sequence does not by itself account for this variability. A search for quantitative trait loci (QTL) has been conducted using data already collected on genetic expression markers in strains of inbred mice using microchip arrays (see www.webqtl.org). Loci having major effects on ABCG2 expression include ABCG2 itself (chromosome 6), *cyp2d*, and *mdr1a/b* (ABCG2 enhanceed in *mdr1a/b* knockout mice), but the effects vary by tissue. GF120918 (an ABCG2 inhibitor) increases the AUC of substrates and is even more effective in *mdr1a/b* knockout mice (164). Other sources of variability include genes relevant to cholestasis and bilirubin excretion (GXR).

Differences in organic cation transporters and organic anion transporters contribute to differences in drug disposition. Functionally important polymorphisms (Cys88Arg and Gly401Ser at 0.6 and 3.2%, respectively, within Caucasians) have been demonstrated in the human organic cation transporter 1 (OCT-1 = SLC22A1) (165). Four functionally important nonsynonymous polymorphisms in the OCT-2 (SLC22A2) gene were found at >1% frequency in an ethnically diverse population sample (166). OCT-1 is expressed primarily on the basolateral side of hepatocytes and intestinal epithelial cells. OCT-2 is primarily expressed on the basolateral side of renal tubule cells. The clinical consequences of variations in these two genes are expected to vary with the dominant clearance mechanism (i.e., renal vs nonrenal) and site of pharmacodynamic action of drugs (167).

Fourteen nonsynonymous polymorphisms have been detected in the liver-specific hepatic uptake organic anion transport polypeptide C (OATP-C). Their frequency of distribution differs by race, corresponding to 16 different OATP-C alleles. Altered uptake OATP-C substrates estrone sulfate and estradiol 17-β-glucuride were demonstrated *in vitro* for several SNPs, including T521C (Val174Ala) and G1763C (Gly488Ala), which occur in 14% of the European-American and 9% of the African-American populations, respectively (168). In a study of 120 healthy Japanese volunteers, five nonsynonymous variants in OATP-C and one nonsynonymous variant were found in the organic anion transport 3 (OAT-3). The later polymorphism did not affect the pharmacokinetics of the probe drug pravastatin. However, subjects with the OATP-C variant designated as the *15 allele (Asp130Ala174) had reduced total and nonrenal clearance of pravastatin in comparison to those with the *1b allele (Asp130Val174). Nonrenal clearance values were 2.0 ± 0.4 L-kg^{-1} hr^{-1} for *1b/*1b ($n = 4$) and 1.1 ± 0.3 L-kg^{-1} hr^{-1}for *1b/*15 ($n = 9$) volunteers, and 0.29 L-kg^{-1} hr^{-1} for the lone *15/*15 volunteer (169). Additional variations in the OATP and OAT families are reviewed in Tirona and Kim (170) and Marzolini *et al*. (171).

The Pharmacogenetics of Membrane Transporters project supported by the National Institute of General Medical Sciences (NIGMS; http://pharmacogenetics.ucsf.edu) reports natural variations in transporter gene sequences after systematically exploring and functionally characterizing these genetic variations by expression in cell cultures, and then relating these variations to clinical observations in the Studies of Pharmacokinetics in Ethnically Diverse Populations (SOPHIE) study. Datasets are available through the Pharmacogenetics Knowledge Base (http://www.pharmgkb.org). As of January 2005, variations had been documented in the coding regions of 24 membrane transporter genes. Functional screening had been completed for >80 variants in the SLC family in cell cultures. Over 600 individuals had been enrolled into SOPHIE.

Analysis of exons and flanking intronic regions for 24 transporters in 247 ethnically diverse DNA samples from the NIGMS Human Cell Repository at the Coriell Institute revealed 680 SNPs. Of these, 175 were synonymous, 155 caused amino acid changes, and 29 caused small insertions and deletions. Variations occurred more frequently in predicted extramembrane loops than in predicted transmembrane transporter domains. Differences were observed in the frequency of occurrence of particular SNPs among ethnic/racial populations (172). For example, CNT1 (SLC28A1) is a nucleoside salvage pathway uptake transporter found on the apical membrane of epithelial tissues as well as on the surface of cells targeted by anticancer therapy. Thus, it may contribute to both the plasma and the intracellular concentrations of nucleoside analog drugs. It was found to be one of the most variable transporters among the 24 SLCs studied to date. This is in contrast to the ubiquitously expressed equilibrative nucleoside transporter ENT1 (SLC29A1), which showed little variation and no loss-of-function variants. For CNT1, 58 coding-region SNPs and 58 haplotypes were identified, 44 of which contained at least one amino acid variant. More than half of these haplotypes were population specific. For example, a single base pair deletion (bp1153) occurred at a frequency of 3% in the African-American population. The functional consequences of the 15 single amino acid variants were studied by expression of vectors with site-directed mutations in *Xenopus laevis* oocytes. Most were active in thymidine uptake, except Ser546Pro and

the bp1153 deletion. One of the four common variants occurring in more than 20% of the total population sample (i.e., Val189Ile) showed an approximately twofold lower affinity for the anticancer nucleoside analog gemcitabine (23.5 ± 1.5 μ*M*) compared to the reference sequence (13.8 ± 0.6 μ*M*) (173).

FUTURE DIRECTIONS

Structural Biology of Membrane Transport Proteins

Relatively few membrane transport proteins have been structurally characterized. Some of the best understood examples to date are the lactose permease and glycerol-3-phosphate transporter and the Ca^{2+} P-type ATPase (which is a primary ion pump). Other structurally well-characterized transport proteins include the bacterial porins and siderophore receptor proteins. In addition, structures have been determined for several ion channels and additional bacterial transporters that are either directly relevant to or models for proteins important in drug transport. The following web sites, maintained by Hartmut Michel and Stephen White, respectively, contain exceptionally useful listings of these and other solved membrane protein structures and are frequently updated:

http://www.mpibp-frankfurt.mpg.de/michel/public/memprotstruct.html.
http://blanco.biomol.uci.edu/MemPro_resources.html.

In Silico Prediction of Drug Absorption, Distribution, Metabolism, and Elimination

The long-term goal of drug transport research is to improve the predictability of the process and hence of ADME processes as a function of molecular structure in various experimental models, in the human population, and in the individual patient. As noted in Chapters 3 and 4, various computational approaches have been taken to predict drug distribution and absorption and its components for a given molecular structure (174). Molecular properties such as polar surface area, electrostatic potential, polarizability, H-bonding strengths, and Lewis acid/base strength have been calculated with or without consideration of conformational dynamics [see Table 16.6 in van de Waterbeemb *et al.* (174) for an exhaustive listing]. Statistical approaches for relating calculations to experimental data include multiple linear regression, partial least-squares projections, comparative molecular field analysis (COMFA), and neural network methods. These approaches have been applied to predictions of human *in vivo* intestinal permeability or absorption data (175, 176) and blood–brain barrier permeability data (177).

Several commercial products are available. One example is GastroPlus and ADMET software from Simulations Plus, Inc. (see http://www.simulations-plus.com/index.html). Another example is KnowItAll ADME/Tox from BioRad/Sadtler Informatics. These programs use neural net algorithms to develop mathematical models relating measured or calculated molecular properties to a database of measured experimental results (e.g., MDCK cell, human jejunum, blood–brain barrier permeabilities). They can be used for *in silico* screening of large libraries of compounds or proposed compounds before they are synthesized. Using these methods, predictions of effective permeability coefficients (P_{eff}) based on calculated chemical properties have been approximately as good as predictions based on measured Caco-2 data (178). Reasonably good *in silico* predictions of blood–brain barrier permeablility can also be achieved (179). In general, the closer the structures of the training dataset to the test compounds, the better the predictions will be.

These approaches go a step beyond the therapeutic classification scheme of Amidon and Lennernäs (180), described in Chapter 4, or the Lipinsky Rule of 5 (20), described for predicting the suitability of a molecule as a drug candidate. Some of the models incorporate saturable drug transport. However, most of the models do not yet explicitly take into account the growing data on specific drug transporter molecules.

Work has been done to computationally model transporter structure, and this work will gain in value as additional high-resolution three-dimensional membrane protein structures are solved. Similar to the QSAR studies for P-gp described in this chapter, protein structural and substrate affinity modeling approaches have also been applied to various other transporters (181). The resulting three-dimensional structure–function relationships should be useful to understanding how individual genetic differences in transporter function will affect drug transport.

REFERENCES

1. Pang DC, Amidon GL, Preusch PC, Sadée W. Second AAPS–NIH frontier symposium: Membrane transporters and drug therapy. American Association of Pharmaceutical Sciences. AAPS PharmSci 1999;1:E7. (Internet at http://www.aapsj.org/view.asp?art=ps010205.)

2. AAPS workshop on drug transporters in ADME: From bench to bedside, March 7–9, 2005. (Internet at http://www.aapspharmaceutica.com/meetings/meeting.asp?id=43.)
3. A biennial meeting on membrane transporters in drug delivery and drug targeting has been organized by Matthias Hediger in 1999, 2001, 2003, 2005. Programs available. (Internet at http://www.bioparadigms.org/conference/index.htm.)
4. Amidon GL, Sadée W, eds. Membrane transporters as drug targets. New York: Kluwer Academic/Plenum Publishers; 1999.
5. Friedman MH. Principles and models of biological transport. New York: Springer-Verlag; 1986.
6. Stein WD. Channels, carriers, and pumps: An introduction to membrane transport. New York: Academic Press; 1990.
7. Hancock REW. Bacterial transport as an import mechanism and target for antimicrobials. In: Georgopapadakou NH, ed. Drug transport in antimicrobial and anticancer chemotherapy. New York: Marcel Dekker, Inc.; 1995. p. 289–306.
8. Van Winkle LJ. Biomembrane transport. San Diego: Academic Press; 1999.
9. Fournier RL. Basic transport phenomena in biomedical engineering. Philadelphia: Taylor & Frances Publishers; 1999.
10. Lakshminarayanaiah N. Equations of membrane biophysics. New York: Academic Press; 1984.
11. Hager WD, Fenster P, Mayersohn M, Perrier D, Graves P, Marcus FI *et al*. Digoxin–quinidine interaction. N Engl J Med 1979;300:1238–41.
12. Bassolino-Klimas D, Alper HE, Stouch TR. Solute diffusion in lipid bilayer membranes: An atomic level study by molecular dynamics simulation. Biochemistry 1993;32:12624–37.
13. Bassolino D, Alper H, Stouch TR. Drug–membrane interactions studied by molecular dynamics simulation: Size dependence of diffusion. Drug Des Discov 1996;13:135–41.
14. Bemporad D, Essex JW, Luttmann C. Permeation of small molecules through a lipid bilayer: A computer simulation study. J Phys Chem B 2004;108:4875–84.
15. Bemporad D, Luttmann C, Essex JW. Computer simulation of small molecule permeation across a lipid bilayer: Dependence on bilayer properties and solute volume, size, and cross-sectional area. Biophys J 2004;87:1–13.
16. Hansch C, Leo A. Exploring QSAR fundamentals and applications in chemistry and biology. Washington, DC: American Chemical Society; 1995.
17. Austel B, Kutter R. Absorption, distribution, and metabolism of drugs. In: Toplis JG, ed. Quantitative structure/activity relationships. Medicinal chemistry monographs, vol 19. New York: Academic Press; 1983. p. 437–96.
18. Yang CY, Cai SJ, Liu H, Pidgeon C. Immobilized artificial membranes — screens for drug membrane interactions. Adv Drug Del. Rev 1997;23:229–56.
19. Ong S, Liu H, Pidgeon C. Immobilized artificial membrane chromatography: Measurements of membrane partition coefficient and predicting drug membrane permeability. J Chromatogr A 1996;728:113–28.
20. Lipinski CA, Lombardo F, Dominy BW, Feeney PJ. Experimental and computational approaches to estimates solubility and permeability in drug discovery and development settings. Adv Drug Deliv Rev 1997;23:3–25.
21. Chopra I. Tetracycline uptake and efflux in bacteria. In: Georgopapadakou NH, ed. Drug transport in antimicrobial and anticancer chemotherapy. New York: Marcel Dekker, Inc.; 1995. p. 221–44.
22. Vasey PA, Kaye SB, Morrison R, Twelves C, Wilson P, Duncan R *et al*. Phase I clinical and pharmacokinetic study of PK1 [*N*-(2-hydroxypropyl)-methacylamide copolymer doxorubicin]: First member of a new class of chemotherapeutic agents–drug polymer conjugates. Clin Cancer Res 1999;5:83–94.
23. Abdellaoui K, Boustta M, Morjani H, Vert M. Uptake and intracellular distribution of 4-amino-fluorescein-labelled poly(L-lysine citramide imide) in K562 cells. J Drug Target 1998;5:193–206.
24. Swaan PW. Recent advances in intestinal macromolecular drug delivery via receptor-mediated transport pathways. Pharm Res 1998;15:826–34.
25. Schentag JJ, Jusko WJ, Vance JW, Cumbo TJ, Abrutyn E, DeLattre M, Gerbracht LM. Gentamicin disposition and tissue accumulation on multiple dosing. J Pharmacokinet Biopharm 1977;5:559–77.
26. Whelton A, Solez K. Aminoglycoside nephrotoxicity — a tale of two transports. J Lab Clin Med 1982;99:148–55.
27. Bennett WM, Plamp CE, Elliott WC, Parker RA, Porter GA. Effect of basic amino acids and aminoglycosides on 3H-gentamicin uptake in cortical slices of rat and human kidney. J Lab Clin Med 1982;99:156–62.
28. Atkinson AJ Jr. Gentamicin kinetics: A simulation case study. In: Foster DM, Atkinson AJ Jr. Principles of pharmacokinetic data analysis: Modeling and simulation (workshop manual). Seattle: SAAM Institute, Inc.; 2004.
29. Freeman CD, Nicolau DP, Belliveau PP, Nightingale CH. Once-daily dosing of aminoglycosides: Review and recommendations for clinical practice. J Antimicrob Chemother 1997;39:677–86.
30. Peloquin CA, Berning SE, Nitta AT, Simone PM, Goble M, Huitt GA, Iseman MD, Cook JL, Curran-Everett D. Aminoglycoside toxicity: Daily versus thrice-weekly dosing for treatment of mycobacterial diseases. Clin Infect Dis 2004;38:1538–44.
31. Nagai J, Takano M. Molecular aspects of renal handling of aminoglycosides and strategies for preventing the nephrotoxicity. Drug Metab Pharmacokinet 2004;19:159–70.
32. Tran Ba Huy P, Bernard P, Schacht J. Kinetics of gentamicin uptake and release in the rat. Comparison of inner ear tissues and fluids with other organs. J Clin Invest 1986;77:1492–500.
33. de Jager P, van Altena R. Hearing loss and nephrotoxicity in long-term aminoglycoside treatment of patients with tuberculosis. Int J Tuberc Lung Dis 2002;6:622–7.
34. Bickel U, Pardridge WM. Vector-mediated delivery of opiod peptides to the brain. NIDA Res Monogr 1995;154:28–46.

35. Pardridge WM, Wu D, Sakane T. Combined use of carboxyl-directed protein pegylation and vector-mediated blood–brain barrier drug delivery system optimizes brain uptake of brain-derived neurotrophic factor following intravenous administration. Pharm Res 1998;15:576–82.
36. Pardridge WM. Blood–brain barrier drug targeting: The future of brain drug development. Mol Interv 2003;3:90–105, 51.
37. Russell-Jones GJ. The potential use of receptor-mediated endocytosis for oral drug delivery. Adv Drug Deliv Rev 2001;46:59–73.
38. McCarthy KM, Yoong Y, Simister NE. Bidirectional transcytosis of IgG by the rat neonatal Fc receptor expressed in a rat kidney cell line: A system to study protein transport across epithelia. J Cell Sci 2000;113:1277–85.
39. Apodaca G, Mostov KE. Transcytosis of placental alkaline phosphatase–polymeric immunoglobulin receptor fusion proteins is regulated by mutations of Ser664. J Biol Chem 1993;268:23712–9.
40. Perez F, Joliot A, Bloch-Gallego E, Zahraoui A, Triller A, Prochiantz A. Antennapedia homeobox as a signal for the cellular internalization and nuclear addressing of a small exogenous peptide. J Cell Sci 1992; 102:717–22.
41. Han K, Jeon MJ, Kim KA, Park J, Choi SY. Efficient intracellular delivery of GFP by homeodomains of *Drosophila* Fushi-tarazu and Engrailed proteins. Mol Cells 2000;10:728–32.
42. Morris MC, Depollier J, Mery J, Heitz F, Divita G. A peptide carrier for the delivery of biologically active proteins into mammalian cells. Nat Biotechnol 2001;19:1173–6.
43. Ford KG, Souberbielle BE, Darling D, Farzaneh F. Protein transduction: An alternative to genetic intervention? Gene Ther 2001;8:1–4.
44. Mi Z, Mai J, Lu X, Robbins PD. Characterization of a class of cationic peptides able to facilitate efficient protein transduction *in vitro* and *in vivo*. Mol Ther 2000;2:339–47.
45. Vives E. Cellular uptake of the Tat peptide: An endocytosis mechanism following ionic interactions. J Mol Recognit 2003;16:265–71.
46. Console S, Marty C, Garcia-Echeverria C, Schwendener R, Ballmer-Hofer K. Antennapedia and HIV transactivator of transcription (TAT) "protein transduction domains" promote endocytosis of high molecular weight cargo upon binding to cell surface glycosaminoglycans. J Biol Chem 2003;278:35109–14.
47. Green I, Christison R, Voyce CJ, Bundell KR, Lindsay MA. Protein transduction domains: Are they delivering? Trends Pharmacol Sci 2003;24:213–5.
48. Dietz GP, Bahr M. Delivery of bioactive molecules into the cell: The Trojan horse approach. Mol Cell Neurosci 2004;27:85–131.
49. Chen L, Wright LR, Chen CH, Oliver SF, Wender PA, Mochly-Rosen D. Molecular transporters for peptides: Delivery of a cardioprotective ϵ-PKC agonist peptide into cells and intact ischemic heart using a transport system, R(7). Chem Biol 2001;8:1123–9.
50. Gratton JP, Yu J, Griffith JW, Babbitt RW, Scotland RS, Hickey R, Giordano FJ, Sessa WC. Cell-permeable peptides improve cellular uptake and therapeutic gene delivery of replication-deficient viruses in cells and *in vivo*. Nat Med 2003;9:357–62.
51. Stevenson BR, Keon BH. The tight junction: Morphology to molecules. Annu Rev Cell Dev Biol 1998;14:89–109.
52. Gonzalez-Mariscal L, Betanzos A, Nava P, Jaramillo BE. Tight junction proteins. Prog Biophys Mol Biol 2003;81:1–44.
53. Ward PD, Tippin TK, Thakker DR. Enhancing paracellular permeability by modulating epithelial tight junctions. Pharm Sci Technol Today 2000;3:346–58.
54. Thanou M, Florea BI, Langemeyer MW, Verhoef JC, Juninger HE. N-Trimethylated chitosan chloride (TMC) improves the intestinal permeation of the peptide drug buserelin *in vitro* (Caco-2 cells) and *in vivo* (rats). Pharm Res 2000;17:27–31.
55. Lee HJ, Zhang Y, Pardridge WM. Blood–brain barrier disruption following the internal carotid arterial perfusion of alkyl glycerols. J Drug Target 2002;10:463–7.
56. Cox DS, Raje S, Gao HL, Salama NN, Eddington ND. Enhanced permeability of molecular weight markers and poorly bioavailable compounds across Caco-2 cell monolayers using the absorption enhancer, zonula occludens toxin. Pharm Res 2002;19:1680–8.
57. Salama NN, Fasano A, Thakar M, Eddington ND. The effect of ΔG on the transport and oral absorption of macromolecules. J Pharm Sci 2004;93:1310–19.
58. Salama NN, Fasano A, Thakar M, Eddington ND. The impact of ΔG on the oral bioavailability of low bioavailable therapeutic agents. J Pharmacol Exp Ther 2005;312:199–205.
59. Fei Y-J, Ganapathy V, Leibach F. Molecular and structural features of the proton-coupled oligopeptide transporter superfamily. Prog Nucleic Acid Res Mol Biol 1998:58:239–61.
60. Wang J, Schaner ME, Thomassen S, Su S-F, Piquette-Miller M, Giacomini KM. Functional and molecular characteristics of Na^+-dependent nucleoside transporters. Pharm Res 1997;14:1524–31.
61. Cass CE. Nucleoside transport. In: Georgopapadakou NH, ed. Drug transport in antimicrobial and anticancer chemotherapy. New York: Marcel Dekker, Inc.; 1995. p. 408–51.
62. Zhang L, Brett CM, Giacomini KM. Role of organic cation transporters in drug absorption and elimination. Annu Rev Pharmacol Toxicol 1998;38:431–60.
63. Silverman JA, Schrenk D. Hepatic canalicular membrane 4: Expression of the multidrug resistance genes in the liver. FASEB J 1997;11:308–13.
64. Muller M, de Vries EGE, Jansen PLM. Role of multidrug resistance protein (MRP) in glutathione S-conjugate transport in mammalian cells. J Hepatol 1996;24(suppl 1):100–8.
65. Madon J, Eckhardt U, Gerloff T, Stieger B, Meier PJ. Functional expression of the rat liver canalicular isoform of the multidrug resistance-associated protein. FEBS Lett 1997;406:75–8.
66. Meier PJ, Eckhardt U, Schroeder A, Hagenbuch B, Stieger B. Substrate specificity of sinusoidal bile acid and organic anion uptake systems in rat and human liver. Hepatology 1997;26:1667–77.

67. Surendran N, Covitz KM, Han H, Sadée W, Oh GM, Amidon GL *et al*. Evidence for overlapping substrate specificity between large neutral amino acid (LNAA) and dipeptide (hPEPT1) transporters for PD 158473, an NMDA antagonist. Pharm Res 1999;16:391–5.
68. Griffith J, Sansom C. The transporter factsbook. San Diego: Academic Press; 1998.
69. Ambudkar SV, Pastan I, Gottesman MM. Cellular and biochemical aspects of multidrug resistance. In: Georgopapadakou NH, ed. Drug transport in antimicrobial and anticancer chemotherapy. New York: Marcel Dekker, Inc.; 1995. p. 525–47.
70. Ambudkar SV, Dey S, Hrycyna CA, Ramachandra M, Pastan I, Gottesman MM. Biochemical, cellular, and pharmacological aspects of the multidrug transporter. Annu Rev Pharmacol Toxicol 1999;39:361–98.
71. Ambudkar SV, Kimchi-Sarfaty C, Sauna ZE, Gottesman MM. P-Glycoprotein: From genomics to mechanism. Oncogene 2003;22:7468–85.
72. Chang G and Roth CB. Structure of MsbA from *E. coli*: A homolog of the multidrug resistance ATP binding cassette (ABC) transporters. Science 2001;293: 1793–800.
73. Chang G. Structure of MsbA from *Vibrio cholera*: A multidrug resistance ABC transporter homolog in a closed conformation. J Mol Biol 2003;330:419–30.
74. Locher KP, Lee AT, Rees DC. The *E. coli* BtuCD structure: A framework for ABC transporter architecture and mechanism Science 2002;296:1091–8.
75. Seelig A, Landwojtowicz E, Fischer H, Blatter XL. Towards P-glycoprotein structure–activity relationships. In: van de Waterbeemd H, Lennernäs H, and Artursson P. Drug bioavailability — Estimation of solubility, permeability, absorption and bioavailability. Methods and Principles of Medicinal Chemistry, vol 18. Weinheim: Wiley-VCH Verlag GmbH & Co; 2003. Chap 20, p. 461–92.
76. Seelig, A. A general pattern for substrate recognition by P-glycoprotein. Eur J Biochem 1998;251:252–61.
77. Kaback HR, Sabin-Toth M, Weinglass AB. The kamikaze approach to membrane transport. Nat Rev Mol Cell Biol 2001:2:610–20.
78. Hirai T, Heymann JAW, Shi D, Sarker R, Maloney PC, Subramaniam S. Three dimensional structure of a bacterial oxalate transporter. Nat Struct Biol 2002;9:597–600.
79. Abramson J, Smirnova I, Kasho V, Verner G, Kaback HR, Iwata S. Structure and mechanism of the lactose permease of *Escherichia coli*. Science 2003;301:610–5.
80. Huang Y, Lemieux MJ, Song J, Auer M, Wang DN. Structure and mechanism of the glycerol-3-phosphate transporter from *Escherichia coli*. Science 2003;301:616–20.
81. Han H, de Vrueh RL, Rhie JK, Covitz KM, Smith PL, Lee CP *et al*. 5′-Amino acid esters of antiviral nucleosides, acyclovir, and AZT are absorbed by the intestinal PEPT1 peptide transporter. Pharm Res 1998;15:1154–9.
82. Sugawara M, Huang W, Fei YJ, Leibach FH, Ganapathy V, Ganapathy ME. Transport of valganciclovir, a ganciclovir prodrug, via peptide transporters PEPT1 and PEPT2. J Pharm Sci 2000;89:781–9.
83. Curran M, Noble S. Valganciclovir. Drugs 2001;61: 1145–50.
84. Pescovitz MD, Rabkin J, Merion RM, Paya CV, Pirsch J, Freeman RB *et al*. Valganciclovir results in improved oral absorption of ganciclovir in liver transplant patients. Antimicrob Agents Chemother 2000;44:2811–5.
85. Cundy KC, Branch R, Chernov-Rogan T, Dias T, Estrada T, Hold K *et al*. XP13512 [(+/−)-1-([(α-isobutanoyloxyethoxy)carbonyl] aminomethyl)-1-cyclohexane acetic acid], a novel gabapentin prodrug: I. Design, synthesis, enzymatic conversion to gabapentin, and transport by intestinal solute transporters. J Pharmacol Exp Ther 2004;311:315–23.
86. Cundy KC, Annamalai T, Bu L, De Vera J, Estrela J, Luo W *et al*. XP13512 [(+/−)-1-([(α-isobutanoyloxyethoxy) carbonyl] aminomethyl)-1-cyclohexane acetic acid], a novel gabapentin prodrug: II. Improved oral bioavailability, dose proportionality, and colonic absorption compared with gabapentin in rats and monkeys. J Pharmacol Exp Ther 2004;311:324–33.
87. Yu DK. The contribution of P-glycoprotein to pharmacokinetic drug–drug interactions. J Clin Pharmacol 1999;39:1203–11.
88. Gramatte T, Oertel R. Intestinal secretion of intravenous talinolol is inhibited by luminal *R*-verapamil. Clin Pharmacol Ther 1999;66:239–45.
89. Eagling VA, Profit L, Black DJ. Inhibition of the CYP3A4-mediated metabolism and P-glycoprotein-mediated transport of the HIV-1 protease inhibitor saquinavir by grapefruit juice components. Br J Clin Pharmacol 1999;48:543–52.
90. Soldner A, Christians U, Susanto M, Wacher VJ, Silverman JA, Benet LZ. Grapefruit juice activates P-glycoprotein-mediated drug transport. Pharm Res 1999;16:478–85.
91. Bradbury MWB, ed. Physiology and pharmacology of the blood–brain barrier. Handbook of experimental pharmacology, vol 103. New York: Springer-Verlag; 1992.
92. Davson H, Segal M. Physiology of the cerebrospinal fluid and blood–brain barrier. Boca Raton, FL: CRC Press; 1996. p. 8.
93. Schinkel AH, Smit JJ, van Tellingen O, Beijnen JH, Wagenaar E, van Deemter L *et al*. Disruption of the mouse *mdr1a* P-glycoprotein gene leads to deficiency in the blood–brain barrier and to increased sensitivity to drugs. Cell 1994;77:491–502.
94. Schinkel AH, Mayer U, Wagenaar E, Mol CA, van Deemter L, Smit JJ *et al*. Normal viability and altered pharmacokinetics in mice lacking mdr1-type (drug-transporting) P-glycoproteins. Proc Natl Acad Sci USA 1997;94:4028–33.
95. Schinkel AH, Wagenaar E, Mol CA, van Deemter L. P-glycoprotein in the blood–brain barrier of mice influences the brain penetration and pharmacological activity of many drugs. J Clin Invest 1996;97:2517–24.
96. Sadeque AJM, Wandel C, He H, Shah S, Wood AJJ. Increased drug delivery to the brain

by P-glycoprotein inhibition. Clin Pharmacol Ther 2000;68:231–7.
97. Rao VV, Dahlheimer JL, Bardgett ME, Snyder AZ, Finch RA, Sartorelli AC *et al*. Choroid plexus epithelial expression of MDR1 P-glycoprotein and multidrug resistance-associated protein contribute to the blood–cerebrospinal fluid drug-permeability barrier. Proc Natl Acad Sci USA 1999;96:3900–5.
98. Golden PL, Pollack GM. Blood–brain barrier efflux transport. J Pharm Sci. 2003;92:1739–53.
99. Rothem L, Ifergan I, Kaufman Y, Priest DG, Jansen G, Assaraf YG. Resistance to multiple novel antifolates is mediated via defective drug transport resulting from clustered mutations in the reduced folate carrier gene in human leukaemia cell lines. Biochem J 2002;367:741–50.
100. Ishida S, Lee J, Thiele DJ, Herskowitz I. Uptake of the anticancer drug cisplatin mediated by the copper transporter Ctr1 in yeast and mammals. Proc Natl Acad Sci USA 2002;99:14298–302.
101. Samimi G, Safaei R, Katano K, Holzer AK, Rochdi M, Tomioka M, Goodman M, Howell SB. Increased expression of the copper efflux transporter ATP7A mediates resistance to cisplatin, carboplatin, and oxaliplatin in ovarian cancer cells. Clin Cancer Res 2004;10:4661–9.
102. Gary Kruh. Lustrous insights into cisplatin accumulation: Copper transporters. Clin Cancer Res 2003;9: 5087–9.
103. Sugeno H, Takebayashi Y, Higashimoto M, Ogura Y, Shibukawa G, Kanzaki A *et al*. Expression of copper-transporting P-type adenosine triphosphatase (ATP7B) in human hepatocellular carcinoma. Anticancer Res 2004;24:1045–8.
104. Lee CGL, Gottesman MM. HIV-1 protease inhibitors and the MDR1 multidrug transporter. J Clin Invest 1998;101:287–8.
105. Subramanian A, Ranganathan P, Diamond SL. Nuclear targeting peptide scaffolds for lipofection of nondividing mammalian cells. Nat Biotechnol 1999;17:873–7.
106. Gerschenson M, Erhart SW, Paik CY, St Claire MC, Nagashima K, Skopets B *et al*. Fetal mitochondrial heart and skeletal muscle damage in *Erythrocebus patas* monkeys exposed *in utero* to 3′-azido-3′-deoxythymidine. AIDS Res Hum Retroviruses 2000;16:635–44.
107. McKenzie R, Fried MW, Sallie R, Conjeevaram H, Di Bisceglie AM, Park Y *et al*. Hepatic failure and lactic acidosis due to fialuridine (FIAU), an investigational nucleoside analogue for chronic hepatitis B. N Engl J Med 1995;333:1099–105.
108. Birkus G, Hitchcock MJ, Cihlar T. Assessment of mitochondrial toxicity in human cells treated with tenofovir: Comparison with other nucleoside reverse transcriptase inhibitors. Antimicrob Agents Chemother 2002;46:716–23.
109. Cabrita MA, Hobman TC, Hogue DL, King KM, Cass CE. Mouse transporter protein, a membrane protein that regulates cellular multidrug resistance, is localized to lysosomes. Cancer Res 1999;59:4890–7.
110. Pritchard JB, Miller DS. Renal secretion of organic anions and cations. Kidney Int 1996;49:1649–54.
111. Dresser MJ, Leabman MK, Giacomini KM. Transporters involved in the elimination of drugs in the kidney: Organic anion transporters and organic cation transporters. J Pharm Sci 2001;90:397–421.
112. Mangravite LM, Badagnani I, Giacomini KM. Nucleoside tranporters in disposition and targeting of nucleoside analogs in the kidney. Eur J Pharmacol 2003;479:269–81.
113. Fromm MF, Kim RB, Stein CM, Wilkinson GR, Roden DM. Inhibition of P-glycoprotein-mediated drug transport: A unifying mechanism to explain the interaction between digoxin and quinidine. Circulation 1999;99:552–7.
114. Verschraagen M, Koks CH, Schellens JH, Beijnen JH. P-glycoprotein system as a determinant of drug interactions: The case of digoxin–verapamil. Pharmacol Res 1999;40:301–6.
115. Freitag D, Bebee R, Sunderland B. Digoxin–quinidine and digoxin–amiodarone interactions: Frequency of occurrence and monitoring in Australian repatriation hospitals. J Clin Pharm Ther 1995;20:179–83.
116. Christians U, Jacobsen W, Benet LZ, Lampen A. Mechanisms of clinically relevant drug interactions associated with tacrolimus. Clin Pharmacokinet 2002;41:813–51.
117. Pfister M, Labbe L, Lu JF, Hammer SM, Mellors J, Bennett KK, Rosenkranz S, Sheiner LB, AIDS Clinical Trial Group Protocol 398 investigators. Effect of coadministration of nelfinavir, indinavir, and saquinavir on the pharmacokinetics of amprenavir. Clin Pharmacol Ther 2002;72:133–41.
118. Johne A, Brockmoller J, Bauer S, Maurer A, Langheinrich M, Roots I. Pharmacokinetic interaction of digoxin with an herbal extract from St. John's wort *(Hypericum perforatum)*. Clin Pharmacol Ther 1999;66:338–45.
119. Fugh-Berman A. Herb–drug interactions. Lancet 2000;355:134–8. (See also erratum and comment: Lancet 2000;355:1019–20.)
120. Scotto KW, Johnson RA. Transcription of the multidrug resistance gene MDR1: A therapeutic target. Mol Interv 2001;1:117–25.
121. Goldstein LJ, Gottesman MM, Pastan I. Expression of MDR1 gene in human cancer. Cancer Treat Res 1991;57:101–19.
122. Goldstein LJ, Pastan I, Gottesman MM. Multidrug resistance in human cancers. Crit Rev Oncol Hematol 1992;12:243–53.
123. Wilson WH, Bates SE, Fojo A, Bryant G, Zhan Z, Regis J *et al*. Controlled trial of dexverapamil, a modulator of multidrug resistance, in lymphomas refractory to EPOCH chemotherapy. J Clin Oncol 1995;12:1995–2004.
124. Leith CP, Kopecky KJ, Chen IM, Eijdems L, Slovak ML, McConnell TS *et al*. Frequency and clinical significance of the expression of multidrug resistance proteins MDR1/P-glycoprotein, MRP1, and LRP in acute myeloid leukemia: A Southwest Oncology Group study. Blood 1999;94:1086–99.
125. Allen JD, van Loevezijn A, Lakhai JM, van der Valk M, van Tellingen O, Reid G *et al*. Potent and specific inhibition of the breast cancer resistance protein multidrug transporter *in vitro*

and in mouse intestine by a novel analogue of fumitremorgin C. Mol Cancer Ther 2002;1:417–25.
126. Licht T, Pastan I, Gottesman MM, Herrmann F. The multidrug-resistance gene in gene therapy of cancer and hematopoietic disorders. Ann Hematol 1996;72:184–93.
127. Hafkemeyer P, Licht T, Pastan I, Gottesman MM. Chemoprotection of hematopoietic cells by a mutant P-glycoprotein resistant to a potent chemosensitizer of multidrug-resistant cancers. Hum Gene Ther 2000;11:555–65.
128. Lewis K. Multidrug resistance efflux. In: Broome-Smith JK, Baumberg S, Stirling CJ, Ward FB, eds. Transport of molecules across microbial membranes. 58th Symposium of the Society for General Microbiology, University of Leeds, September 1999. London: Cambridge University Press; 1999. p. 15–40.
129. Sadée W, Graul RC, Lee AY. Classification of membrane transporters. In: Amidon GL, Sadée W, eds. Membrane transporters as drug targets. New York: Kluwer Academic/Plenum Publishers; 1999. p. 29–58.
130. Sadée W. Genomics and drugs: Finding the optimal drug for the right patient. Pharm Res 1998;15:959–63.
131. Evans WE, Relling MV. Pharmacogenomics: Translating functional genomics into rational therapeutics. Science 1999;286:487–91.
132. Lee VH, Sporty JL, Fandy TE. Pharmacogenomics of drug transporters: The next drug delivery challenge. Adv Drug Deliv Rev 2001;50(suppl 1):S33–40.
133. Botka CW, Wittig TW, Graul RC, Nielsen CU, Higaka K, Amidon GL, Sadée W. Human proton/oligopeptide transporter (POT) genes: Identification of putative human genes using bioinformatics. AAPS PharmSci 2000;2:E16.
134. Saier MH Jr, Paulsen IT, Sliwinski MK, Pao SS, Skurray RA, Nikaido H. Evolutionary origins of multidrug and drug-specific efflux pumps in bacteria. FASEB J 1998;12:265–74.
135. Saier MH Jr, Tseng T-T. Evolutionary origins of transmembrane transport systems. In: Transport of molecules across microbial membranes. 58th Symposium of the Society for General Microbiology, University of Leeds, September 1999. London: Cambridge University Press; 1999. p. 252–74.
136. Paulsen IT, Sliwinski MK, Saier MH Jr. Microbial genome analyses: Global comparisons of transport capabilities based on phylogenies, bioenergetics and substrate specificities. J Mol Biol 1998;277:573–92.
137. Paulsen IT, Sliwinski MK, Nelissen B, Goffeau A, Saier MH Jr. Unified inventory of established and putative transporters encoded within the complete genome of *Saccharomyces cerevisiae*. FEBS Lett 1998;430:116–25.
138. Internet at http://www.chem.qmul.ac.uk/iubmb/mtp.
139. Internet at http://www.gene.ucl.ac.uk/nomenclature.
140. Hediger MA, Romero MF, Peng JB, Rolfs A, Takanaga H, Bruford EA. The ABCs of solute carriers: Physiological, pathological and therapeutic implications of human membrane transport proteins. Introduction. Pflugers Arch 2004;447:465–8.
141. Internet at http://www.tcdb.org.
142. Clayton RA, White O, Ketchum KA, Venter JC. The first genome from the third domain of life. Nature 1997;387:459–62.
143. Fraser CM, Norris SJ, Weinstock GM, White O, Sutton GG, Dodson R *et al*. Complete genome sequence of *Treponema pallidum*, the syphilis spirochete. Science 1998;281:375–88.
144. Internet at www.tigr.org. A list of known human transporters is given under the heading EGAD Cellular Roles/Metabolism/Transport.
145. Yan Q, Sadée W. Human membrane transporter database: A Web-accessible relational database for drug transport studies and pharmacogenomics. AAPS PharmSci 2000;2:E20. (See also http://www.aapspharmsci.org/view.asp?art=ps020320&pdf=yes; http://lab.digibench.net/transporter.)
146. Brown S, Chang JL, Sadée W, Babbitt PC. A semiautomated approach to gene discovery through expressed sequence tag data mining: Discovery of new human transporter genes. AAPS PharmSci 2003;5:E1.
147. Huang Y, Sadée W. Drug sensitivity and resistance genes in cancer chemotherapy: A chemogenomics approach. Drug Discov Today 2003;8:356–63.
148. Huang Y, Anderle P, Bussey KJ, Barbacioru C, Shankavaram U, Dai Z, Reinhold WC, Papp A, Weinstein JN, Sadée W. Membrane transporters and channels: Role of the transportome in cancer chemosensitivity and chemoresistance. Cancer Res 2004;64:4294–301.
149. Ross DD, Doyle LA. Mining our ABCs: Pharmacogenomic approach for evaluating transporter function in cancer drug resistance. Cancer Cell 2004;6:129–37.
150. Szakacs G, Annereau JP, Lababidi S, Shankavaram U, Arciello A, Bussey KJ, Reinhold W, Guo Y, Kruh GD, Reimers M, Weinstein JN, Gottesman MM. Predicting drug sensitivity and resistance: Profiling ABC transporter genes in cancer cells. Cancer Cell 2004;6:105–7. (Comment in Cancer Cell 2004;6:129–37.)
151. Sun D, Lennernäs H, Welage LS, Barnett JL, Landowski CP, Foster D, Fleisher D, Lee KD, Amidon GL. Comparison of human duodenum and Caco-2 gene expression profiles for 12,000 gene sequences tags and correlation with permeability of 26 drugs. Pharm Res 2002;19:1400–16.
152. Choi KH, Chen CJ, Kriegler M, Roninson IB. An altered pattern of cross-resistance in multidrug-resistant human cells results from spontaneous mutations in the mdr1 (P-glycoprotein) gene. Cell 1988;53:519–29.
153. Kioka N, Tsubota J, Kakehi Y, Komano T, Gottesman MM, Pastan I *et al*. P-glycoprotein gene (MDR1) cDNA from human adrenal: Normal P-glycoprotein carries Gly185 with an altered pattern of multidrug resistance. Biochem Biophys Res Commun 1989;162:224–31.
154. Mickley LA, Lee JS, Weng Z, Zhan Z, Alvarez M, Wilson W *et al*. Genetic polymorphism in MDR-1: A tool for examining allelic expression in normal cells, unselected and drug-selected cells, and human tumors. Blood 1998;91:1749–56.
155. Umbenhauer DR, Lankas GR, Pippert TR, Wise LD, Cartwright ME, Hall SJ *et al*. Identification of a P-glycoprotein-deficient subpopulation in the CF-1

mouse strain using a restriction fragment length polymorphism. Toxicol Appl Pharmacol 1997;146:88–94.
156. Hoffmeyer S, Burk O, von Richter O, Arnold HP, Brockmoller J, Johne A *et al*. Functional polymorphisms of the human multidrug-resistance gene: Multiple sequence variations and correlation of one allele with P-glycoprotein expression and activity *in vivo*. Proc Natl Acad Sci USA 2000;97:3473–78.
157. Woodahl EL, Ho RJ. The role of MDR1 genetic polymorphisms in interindividual variability in P-glycoprotein expression and function. Curr Drug Metab 2004;5:11–9.
158. Kim RB, Leake BF, Choo EF, Dresser GK, Kubba SV, Schwarz UI *et al*. Identification of functionally variant MDR1 alleles among European Americans and African Americans. Clin Pharmacol Ther 2001;70:189–99.
159. Fellay J, Marzolini C, Meaden ER, Back DJ, Buclin T, Chave JP *et al*. Swiss HIV Cohort Study. Lancet 2002;359:30–6. (Comment in Lancet 2002;359:2114; author reply: Lancet 2002;359:2214–5.)
160. Kroetz DL, Pauli-Magnus C, Hodges LM, Huang CC, Kawamoto M, Johns SJ *et al*. Pharmacogenetics of membrane transporters investigators. Pharmacogenetics 2003;13:481–94. (Erratum in Pharmacogenetics 2003;13:701.)
161. Zamber CP, Lamba JK, Yasuda K, Farnum J, Thummel K, Schuetz JD, Schuetz EG. Natural allelic variants of breast cancer resistance protein (BCRP) and their relationship to BCRP expression in human intestine. Pharmacogenetics 2003;13:19–28.
162. Sparreboom A, Gelderblom H, Marsh S, Ahluwalia R, Obach R, Principe P, Twelves C, Verweij J, McLeod HL. Diflomotecan pharmacokinetics in relation to ABCG2 421C>A genotype. Clin Pharmacol Ther 2004;76:38–44.
163. de Jong FA, Marsh S, Mathijssen RH, King C, Verweij J, Sparreboom A, McLeod HL. ABCG2 pharmacogenetics: Ethnic differences in allele frequency and assessment of influence on irinotecan disposition. Clin Cancer Res 2004;10:5889–94.
164. Cisternino S, Mercier C, Bourasset F, Roux F, Scherrmann JM. Expression, up-regulation, and transport activity of the multidrug-resistance protein Abcg2 at the mouse blood–brain barrier. Cancer Res 2004;64:3296–301.
165. Kerb R, Brinkmann U, Chatskaia N, Gorbunov D, Gorboulev V, Mornhinweg E *et al*. Identification of genetic variations of the human organic cation transporter hOCT1 and their functional consequences. Pharmacogenetics 2002;12:591–5.
166. Leabman MK, Huang CC, Kawamoto M, Johns SJ, Stryke D, Ferrin TE *et al*. Polymorphisms in a human kidney xenobiotic transporter, OCT2, exhibit altered function. Pharmacogenetics 2002;12:395–405.
167. Schinkel AH, Jonker JW. Polymorphisms affecting function of the human organic cation transporter hOCT1 (SLC22A1): What are the consequences? Pharmacogenetics 2002;12:589–90.
168. Tirona RG, Leake BF, Merino G, Kim RB. Polymorphisms in OATP-C: Identification of multiple allelic variants associated with altered transport activity among European- and African-Americans. J Biol Chem 2001;276:35669–75.
169. Nishizato Y, Ieiri I, Suzuki H, Kimura M, Kawabata K, Hirota T *et al*. Polymorphisms of OATP-C (SLC21A6) and OAT3 (SLC22A8) genes: Consequences for pravastatin pharmacokinetics. Clin Pharmacol Ther 2003;73:554–65.
170. Tirona RG, Kim RB. Pharmacogenomics of organic anion-transporting polypeptides (OATP). Adv Drug Deliv Rev 2002;54:1343–52.
171. Marzolini C, Tirona RG, Kim RB. Pharmacogenomics of the OATP and OAT families. Pharmacogenomics 2004;5:273–82.
172. Leabman MK, Huang CC, DeYoung J, Carlson EJ, Taylor TR, de la Cruz M *et al*. Natural variation in human membrane transporter genes reveals evolutionary and functional constraints. Proc Natl Acad Sci USA 2003;100:5896–901.
173. Gray JH, Mangravite LM, Owen RP, Urban TJ, Chan W, Carlson EJ *et al*. Functional and genetic diversity in the concentrative nucleoside transporter, CNT1, in human populations. Mol Pharmacol 2004;65:512–9.
174. van de Waterbeemd H, Lennernäs H, and Artursson P. Drug bioavailability — estimation of solubility, permeability, absorption and bioavailability. Methods and principles of medicinal chemistry, vol 18. Weinheim: Wiley-VCH Verlag GmbH & Co.; 2003.
175. Winiwarter S, Ax F, Lennernäs H, Hallberg A, Pettersson C, Karlen A. Hydrogen bonding descriptors in the prediction of human *in vivo* intestinal permeability. J Mol Graph Model 2003;21:273–87.
176. Krarup LH, Christensen IT, Hovgaard L, Frokjaer S. Predicting drug absorption from molecular surface properties based on molecular dynamics simulations. Pharm Res 1998;15:972–8.
177. Iyer M, Mishru R, Han Y, Hopfinger AJ. Predicting blood–brain barrier partitioning of organic molecules using membrane-interaction QSAR analysis. Pharm Res 2002;19:1611–21.
178. Bolger MB. Computational methods to predict biopharmaceutical properties. AAPS meeting, Indianapolis, Oct 29–Nov 2, 2000. (Internet at http://www.simulations-plus.com/pdf_files/aaps_2000_report.pdf.)
179. KnowItAll ADME/Tox Blood–Brain Barrier Permeability Predictor. (Internet at http://biorad.com/pages/SAD/collateral/predictors_blood_brain_barrier.pdf.)
180. Amidon GL, Lennernäs H, Shah VP, Crison JR. A theoretical basis for a biopharmaceutic drug classification the correlation of *in vitro* drug product dissolution and *in vivo* bioavailability. Pharm Res 1995;12:413–20.
181. Chang C, Ray A, Swaan P. *In silico* strategies for modeling membrane transporter function. Drug Discov Today 2005;10:663–71.

Additional Sources of Information

Pharma SNP Consortium of the Japan Pharmaceutical Manufacturers Association. (Internet at http://www.jpma.or.jp/12english/publications/pub019b_genome; http://www.jpma.or.jp/12english/topics/topics030820_5.html.)

Ishikawa T, Tsuji A, Inui K, Sai Y, Anzai N, Wada M *et al*. The genetic polymorphism of drug transporters: Functional analysis approaches. Pharmacogenomics 2004;5:67–99.
SNP Consortium Ltd. (Internet at http://snp.cshl.org.)
National Center for Biotechnology Information Entrez SNP interface. (Internet at http://www.ncbi.nlm.nih.gov/entrez/query.fcgi?CMD=Limits&DB=snp.)
International HapMap Project. (Internet at http://www.hapmap.org/index.html.en.) The International HapMap Consortium. The International HapMap Project. Nature 2003;426:789–96.

This page intentionally left blank

CHAPTER

15

Drug Interactions

SARAH ROBERTSON AND SCOTT PENZAK
Clinical Center, National Institutes of Health, Bethesda, Maryland

INTRODUCTION

A drug interaction results when the effects of a drug are altered in some way by the presence of another drug, by food, or by environmental exposure. Until recently, little emphasis had been placed on predicting potential drug interactions during the process of drug development. Now, however, more time and energy are devoted to identifying drug interactions in the preclinical setting; this is largely due to the discovery of life-threatening interactions among marketed medications (e.g., potentially fatal arrhythmia due to terfenadine and ketoconazole interaction) (1, 2). Both the U.S. Food and Drug Administration and the European Agency for the Evaluation of Medicinal Products require that *in vivo* studies be conducted early in drug development in order to provide information about metabolic routes of elimination and potential contributions to metabolic drug–drug interactions.

Epidemiology

It is widely recognized that the risk of developing an adverse drug reaction (ADR) secondary to a drug–drug interaction increases significantly with the number of medications a patient is receiving. Adverse drug reactions are estimated to be responsible for 4.2–6% of all hospital admissions in the United States (3). Reports on the incidence of drug interactions vary widely, with estimates as high as 50% (4). Data from older studies tend to overestimate the frequency by including clinically insignificant and theoretical interactions. The true incidence of clinically significant ADRs that occur as a result of drug–drug interactions is largely unknown. Further, the frequency and significance of drug interactions vary considerably among different patient populations. HIV patients, for instance, are at greater risk for developing adverse reactions due to drug interactions because of the nature and quantity of medications they are on, as well as the pathophysiology of their disease state (5, 6). The elderly are also at an increased risk for adverse medication events due to changes in their metabolic and renal function, and increased polypharmacy (7).

It is not difficult to identify at least one interaction among a complex medication regimen; the key for clinicians, however, is to target those interactions that are potentially clinically significant. Drug interactions are regarded as clinically meaningful when they have the potential to produce excessive toxicity or reduce therapeutic activity. Most clinically significant drug interactions are unintentional and can result in negative outcomes. However, some interactions can be exploited for their potential clinical benefit. The protease inhibitor ritonavir, for instance, is widely administered at low doses to HIV-infected patients in order to increase, or "boost," plasma concentrations of coadministered protease inhibitors by inhibiting their metabolism. Benefits of ritonavir-boosting include reduced pill burden, elimination of food restrictions, and improved virologic response in treatment-experienced patients (8).

Classifications

An interaction is typically described by the medications or class of medications it involves,

the mechanism by which it occurs, the resulting effect (toxicity or loss of efficacy), the clinical severity of the effect (minor, moderate, or severe), and the likelihood that the adverse outcome is due to the interaction in question (unlikely, possible, suspected, probable, or established). *Minor drug interactions* usually have limited clinical consequences and require no change in therapy. An example of a minor interaction is that which occurs between hydralazine and furosemide. The pharmacologic effects of furosemide may be enhanced by concomitant administration of hydralazine, but generally not to a clinically significant degree (9). While minor drug interactions can generally be disregarded when assessing a medication regimen, *moderate interactions* often require an alteration in dosage or increased monitoring. Combining rifampin and isoniazid, for instance, leads to an increase in the incidence of hepatotoxicity. Despite this interaction, the two drugs are still used in combination along with frequent monitoring of liver enzymes. *Severe interactions*, on the other hand, should generally be avoided whenever possible, as they result in potentially serious toxicity. For example, ketoconazole causes marked increases in cisapride exposure, which may lead to the development of QT prolongation and life-threatening ventricular arrhythmia (10, 11). It is recommended that these drugs not be used in combination.

Mechanisms of drug interactions can be characterized as either pharmacodynamic or pharmacokinetic. A pharmacodynamic interaction results when a drug interferes with a second drug at its target site, or changes in some way its anticipated pharmacologic response. The consequence of this interaction results in additivity, synergy, or antagonism of the intended effect. An example of a pharmacodynamic interaction is the synergism that results from combining two or more anti-infectives in the treatment of a resistant pathogen. Alternatively, increased neutropenia resulting from the coadministration of zidovudine and ganciclovir and increased central nervous system depression from combining sedatives or hypnotics are examples of additive toxicity (12). Pharmacodynamic interactions do not involve changes in the concentration of drug in plasma or at the targeted site of action. Pharmacokinetic interactions, on the other hand, occur when one drug alters the absorption, distribution, metabolism, or elimination of another drug, thereby changing its concentration in plasma and, consequently, at the targeted site of action. Clinically significant drug interactions are most often due to alterations in pharmacokinetics, secondary to modulation of drug metabolism. In some cases a significant interaction may result from a combination of both pharmacokinetic and pharmacodynamic mechanisms. For instance, the interaction between cerivastatin and gemfibrozil, which has resulted in cases of severe rhabdomyolysis, is likely due to the inhibition of cerivastatin metabolism by gemfibrozil (i.e., pharmacokinetic interaction), in addition to the propensity of both drugs to cause skeletal muscle toxicity (i.e., pharmacodynamic interaction) (13–15).

MECHANISMS OF DRUG INTERACTIONS

Interactions Affecting Drug Absorption

Interactions affecting drug absorption may result in changes in the *rate* of absorption, the *extent* of absorption, or a combination of both. Interactions resulting in a reduced rate of absorption are not typically clinically important for maintenance medications, as long as the total amount of drug absorbed is not affected. On the other hand, for acutely administered medications, such as sedative-hypnotics or analgesics, a reduction in the rate of absorption may cause an unacceptable delay in the onset of the drug's pharmacologic effect. The extent to which a drug is absorbed can be affected by changes in drug transport time or gastrointestinal motility, gastrointestinal pH, intestinal cytochrome P450 (CYP) enzyme and transport protein activity, and drug chelation in the gut. In general, a change in the extent of drug absorption that exceeds 20% is generally considered to be clinically significant (16).

As described in Chapter 4, medications that alter GI motility can affect drug absorption by changing the rate at which drugs are transported into and through the small intestine, the primary site of absorption for most drugs. The prokinetic agent metoclopramide, for instance, increases the rate of drug transport through the gut, thereby increasing the rate of absorption for certain drugs and also altering the extent of absorption in some cases. For instance, despite no change in cyclosporine elimination clearance, the mean area under the plasma concentration-vs-time curve (AUC) and maximum serum concentration (C_{max}) of cyclosporine increased by 22 and 46%, respectively, when it was given with metoclopramide to 14 kidney transplant patients. Further, the time to reach C_{max} (T_{max}) was significantly shorter following administration of this combination (17).

For some drugs, absorption is limited by a compound's solubility, with dissolution being highly dependent on gastric pH. The antiretroviral agent didanosine, for example, is an acid-labile compound, originally formulated as a buffered preparation to improve its bioavailability. Other medications, such as atazanavir and certain azole antifungals (particularly

itraconazole and ketoconazole), require an acidic environment for adequate absorption (18–20). As such, these medications should be administered 2 hours before or 1 hour after antacids or buffered drugs. Likewise, proton-pump inhibitors and H2-receptor antagonists markedly reduce the absorption and plasma concentration of these agents (19–21). The bioavailability of itraconazole has been shown to improve when it is administered with a cola beverage in patients being treated with an H2-receptor antagonist (22).

Drug absorption may also be limited by the formation of insoluble complexes that result when certain drugs are exposed to di- and trivalent cations in the gastrointestinal tract. Quinolone antibiotics chelate with coadministered magnesium, aluminum, calcium, and iron-containing products, significantly limiting quinolone absorption (23). Ciprofloxacin absorption was shown to decrease by 50–75% when administered within 2 hours of aluminum hydroxide or calcium carbonate tablets (24). Additionally, tetracycline antibiotics have long been known to complex with antacids and iron in the gut (25, 26). Antacids, cation-containing supplements, and dairy products should be separated from quinolone and tetracycline administration by at least 2 hours to ensure adequate absorption of antibiotic. Adsorbents, such as the cholesterol-lowering anionic exchange resin cholestyramine, bind multiple medications when coadministered (27). Although dosing separation improves the bioavailability of coadministered medications, ion-exchange resins require frequent dosing, making dose scheduling difficult for patients on complex medication regimens.

Administration with food may also significantly impact the bioavailability and pharmacokinetics of medications. Most protease inhibitors, for instance, have significantly improved absorption in the presence of food, with bioavailability increased by as much as 500% (28). Other drugs that exhibit improved bioavailability with food include valganciclovir and cyclosporine. Cyclosporine exposure more than doubled when it was given with a meal to healthy volunteers (29). Conversely, agents such as isoniazid, rifampin, and the protease inhibitor indinavir are better absorbed on an empty stomach (30–32). A study in healthy volunteers demonstrated a 57% reduction in the AUC of isoniazid when it was administered with a meal versus on an empty stomach (33). Although food does not significantly affect the AUC of rifampin, it does decrease the C_{max} by 36%, potentially compromising its antimycobacterial activity (34).

Alteration of normal gut flora has been proposed as a mechanism to explain alterations in the concentrations of several drugs, including digoxin, oral contraceptives, and warfarin, during antibiotic coadministration. It has been speculated that the well-established digoxin/macrolide interaction that has resulted in cases of digoxin toxicity is due to modification of gut flora, leading to decreases in bacterial digoxin metabolism by *Eubacterium lentum* (35–37). However, most antibiotics do not appear to interact with digoxin, despite their apparent elimination of digoxin-metabolizing *E. lentum*. Given that *E. lentum* colonization of the small intestine is relatively rare, a more plausible explanation for this interaction in most people is inhibition of P-glycoprotein transport in the intestines and kidney, resulting in increased digoxin absorption and a reduction in renal elimination (38–40).

Combined oral contraceptive (COC) failure has been attributed to the coadministration of certain antibiotics. The proposed mechanism for loss of COC efficacy is a reduction in the drug's enterohepatic recirculation secondary to loss of hydrolysis of steroid conjugates by gut flora (41). Despite multiple case reports of COC failure during treatment with penicillins and trimethoprim/sulfamethoxazole, *in vivo* studies have failed to observe a reduction in plasma concentrations of estrogen or progesterone with antibiotic use (42–45). Most of the evidence supporting the COC–penicillin interaction is anecdotal, with an actual incidence indistinguishable from that of the general COC failure rate (46).

Interactions Affecting Drug Distribution

Theoretically, drugs that are highly protein bound (>90%) may displace other highly protein-bound drugs from binding sites, thereby increasing drug distribution. In actuality, there are very few clinically relevant interactions that result from disruption of protein binding (4). For restrictively metabolized drugs, as the fraction of unbound drug increases due to displacement of drug from protein binding sites, elimination of unbound drug increases, to return unbound concentrations to their previous levels, (see Chapter 7, Figure 7.2). The transient increase in unbound concentration may be clinically important for drugs with a limited distribution, a narrow therapeutic index, or a long elimination half-life (47). As nonrestrictively metabolized drugs rely on hepatic blood flow for their elimination, increases in the fraction of unbound drug in plasma do not result in immediate compensatory elimination of unbound drug (see Chapters 5 and 7). However, no examples of clinically significant plasma protein displacement interactions involving nonrestrictively metabolized drugs have been identified (48).

Interactions Affecting Drug Metabolism

As described in Chapter 11, drug metabolism is composed of two distinct pathways of biochemical processing, Phase I and Phase II. Phase I is a chemical modification (typically oxidation, hydrolysis, or reduction reactions) performed primarily by members of the CYP enzyme family (49). Phase II metabolism consists of the biotransformation of endogenous compounds by reactions such as glucuronidation, sulfation, methylation, acetylation, and glycine conjugation. Modulation of CYP-mediated metabolism is the primary mechanism by which one drug interacts with another. As such, this chapter focuses primarily on interactions resulting from inhibition and/or induction of Phase I enzymes. Table 15.1 provides a list of some of the

TABLE 15.1 Selected Cytochrome P450 Substrates, Inhibitors, and Inducers

Enzyme	Substrates	Inhibitors	Inducers
CYP3A4	Alprazolam	Amprenavir	Amprenavir
	Amiodarone	Atazanavir	Barbiturates
	Atorvastatin	Cimetidine	Carbamazepine
	Buspirone	Clarithromycin	Dexamethasone
	Carbamazepine	Delavirdine	Efavirenz
	Cisapride	Diltiazem	Nevirapine
	Clarithromycin	Efavirenz	Phenytoin
	Cyclosporine	Erythromycin	Pioglitazone
	Dapsone	Fluconazole	Rifampin
	Dihydropyridine calcium channel blockers	Fluvoxamine	Rifabutin
		Grapefruit juice (intestinal 3A4)	Ritonavir
	Diltiazem		St. John's wort
	Efavirenz	Indinavir	Troglitazone
	Erythromycin	Itraconazole	
	Ergot alkaloids	Ketoconazole	
	Estrogens	Lopinavir	
	Fentanyl	Nefazodone	
	Lovastatin	Nelfinavir	
	Midazolam	Norfloxacin	
	Nefazodone	Norfluoxetine	
	Phosphodiesterase inhibitors	Ritonavir	
		Saquinavir	
	Pioglitazone	Verapamil	
	Prednisolone	Voriconazole	
	Progesterone		
	Protease Inhibitors		
	Quinidine		
	(*R*)-Warfarin		
	Rifampin		
	Sertraline		
	Sirolimus		
	Simvastatin		
	Tacrolimus		
	Testosterone		
	Trazadone		
	Triazolam		

TABLE 15.1 Continued

Enzyme	Substrates	Inhibitors	Inducers
CYP1A2	Caffeine	Cimetidine	Broccoli
	Clozapine	Ciprofloxacin	Brussel sprouts
	Haloperidol	Clarithromycin	Carbamazepine
	Olanzapine	Erythromycin	Char-grilled meat
	(*R*)-Warfarin	Fluvoxamine	Modafinil
	Propranolol	Norfloxacin	Rifampin
	Theophylline		Ritonavir
	Tricyclic antidepressants		Smoking
	Zileuton		
CYP2C9	Amytriptyline	Fluconazole	Rifampin
	Diclofenac	Fluvastatin	Secobarbital
	Fluvastatin	Fluvoxamine	
	Ibuprofen	Omeprazole	
	Irbesartan	Sulfamethoxazole	
	Losartan	Trimethoprim	
	Naproxen		
	Piroxicam		
	Phenytoin		
	(*S*)-Warfarin		
	Sulfonylureas		
	Valproic Acid		
CYP2C19	Carisoprodol	Cimetidine	Carbamazepine
	Citalopram	Fluoxetine	Norethindrone
	Diazepam	Fluvoxamine	Prednisone
	Indomethacin	Ketoconazole	Rifampin
	Lansoprazole	Lansoprazole	
	Nelfinavir	Omeprazole	
	Omeprazole	Ticlopidine	
	Pantoprazole	Topiramate	
	Phenytoin		
	Propranolol		
CYP2D6	Amphetamine	Cimetidine	Dexamethasone
	Codeine	Fluoxetine	Rifampin
	Desipramine	Fluvoxamine	
	Dextromethorphan	Haloperidol	
	Fluoxetine	Ketoconazole	
	Haloperidol	Lansoprazole	
	Lansoprazole	Paroxetine	
	Methadone	Quinidine	
	Metoprolol	Probenecid	
	Paroxetine	Ritonavir	
	Propranolol	Sertraline (weak)	
	Risperidone	Terbinafine	
	Tamoxifen	Ticlopidine	
	Tramadol		

(continued)

TABLE 15.1 Continued

Enzyme	Substrates	Inhibitors	Inducers
CYP2B6	Bupropion	Efavirenz[a]	Phenobarbital
	Efavirenz	Nelfinavir[a]	Rifampin
	Methadone	Ritonavir[a]	
	Cyclophosphamide	Thiotepa	
	Ifosfamide	Ticlopidine	

[a] Possible inhibitors, based on *in vitro* data.

most commonly encountered substrates, inducers, and inhibitors of selected CYP isoenzymes.

Enzyme Inhibition

Inhibition of enzyme activity is a common mechanism of clinically significant metabolic drug interactions. Enzyme inhibition decreases the rate of drug metabolism, thereby increasing the amount of drug in the body, leading to accumulation and potential toxicity (Figure 15.1). Enzyme inhibition may be described by its reversibility, ranging from rapidly reversible to irreversible. Interactions due to reversible metabolic inhibition can be further categorized into competitive, noncompetitive, or uncompetitive mechanisms.

In *reversible inhibition*, enzymatic activity is regained by the systemic elimination of inhibitor, such that the time to enzyme recovery is dependent on the elimination half-life of the inhibitor. *Competitive inhibition* is characterized by competition between substrate and inhibitor for the enzyme's active site. Competition for enzyme binding can be overcome by increasing the concentration of substrate, thereby sustaining the velocity of the enzymatic reaction despite the presence of an inhibitor (50, 51). The degree to which the substrate K_m for the reaction is increased by inhibition depends upon the concentration of inhibitor present. In contrast, *noncompetitive enzyme inhibition* cannot be overcome by increased substrate concentration. In noncompetitive inhibition the inhibitor binds to a separate site on the enzyme, rendering the enzyme–substrate complex nonfunctional (50, 51). *Uncompetitive inhibition* results when the inhibitor binds only to the substrate–enzyme complex. From a clinical standpoint, uncompetitive inhibition is rare, since saturation of enzyme with substrate is not common *in vivo*. Further, uncompetitive inhibition is clinically insignificant when the substrate concentration is well below the reaction's K_m (50). The following equations describe these reversible inhibition mechanisms:

Competitive inhibition:

$$\%\ \text{inhibition} = \frac{[I]/K_i}{1 + [I]/K_i + [S]/K_m}$$

Noncompetitive inhibition:

$$\%\ \text{inhibition} = \frac{[I]/K_i}{1 + [I]/K_i}$$

Uncompetitive inhibition:

$$\%\ \text{inhibition} = \frac{[I]/K_i}{1 + [I]/K_i + K_m/[S]}$$

$[I]$ and $[S]$ are the respective concentrations of inhibitor and substrate, K_i is the inhibitory constant, and K_m is the Michaelis–Menten constant for substrate metabolism by the enzyme.

Irreversible or quasi-irreversible metabolic inhibition occurs when either the parent compound or a metabolic intermediate binds to the reduced ferrous heme portion of the P450 enzyme, thereby inactivating it (51). In *irreversible inhibition*, or "suicide inhibition," the intermediate forms a covalent bond with the CYP protein or its heme component, causing permanent

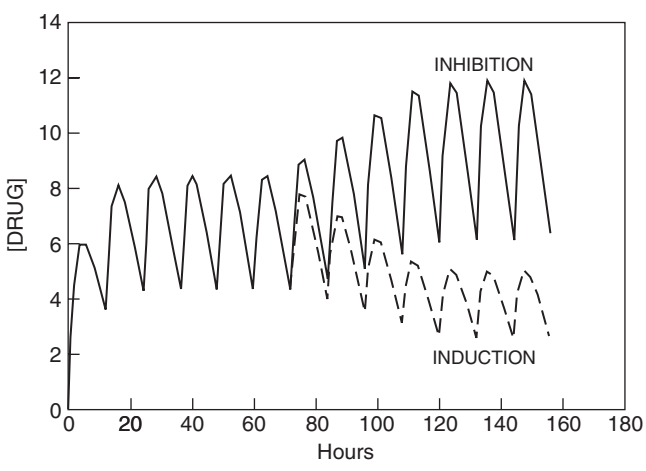

FIGURE 15.1 Theoretical plasma concentration–time profiles of a drug in the presence of a CYP enzyme inducer (*dashed line*) and inhibitor (*solid line*).

inactivation. In *quasi-irreversible* inhibition the intermediate is so tightly bound to the heme portion of the enzyme that it is practically irreversibly bound. As such, quasi-irreversible and irreversible mechanisms of inhibition are indistinguishable *in vivo* (51). In irreversible inhibition, also referred to as "mechanism-based inhibition," the time to metabolic recovery is dependent upon the synthesis of new enzyme, rather than upon the dissociation and elimination of the inhibitor, as in the case of reversible inhibition. Examples of irreversible inhibitors include the macrolide antibiotics erythromycin and troleandomycin, which inhibit CYP3A4 by forming stable metabolite–inhibitor complexes following their metabolic activation (52). Potent inhibitors of CYPs are typically lipophilic compounds, and often include an N-containing heterocycle, such as a pyridine, imidazole, or triazole functional group (51). The azole antifungal ketoconazole is a classic example of a potent CYP3A4 inhibitor with a sterically available nitrogen group.

Investigation into the ketoconazole–terfenadine interaction following reports of cardiac toxicity secondary to terfenadine accumulation led the FDA to begin requiring characterization of metabolic pathways of new drugs and their enzyme modulation potential (53). By identifying the metabolic pathways of a drug in the early stage of its development, it is possible to predict which drugs may have the potential to interact *in vivo* prior to conducting clinical investigations. Utilization of high-throughput fluorometric screening allows pharmaceutical companies to screen compounds early in preclinical drug development in an attempt to avoid developing potent CYP inhibitors. *In vitro* findings of enzyme inhibition may be extrapolated to predict clinical interactions from *in vitro* measurements of the enzyme–inhibitor dissociation constant (K_i) and the maximum concentration of inhibitor achieved *in vivo* (I). When the I/K_i ratio exceeds 1, the compound in question is considered to have a high inhibitory risk, while those with ratios between 0.1 and 1 are considered to be at medium risk, and those with ratios <0.1 are at low risk (51). In some cases, the potential benefit of a drug must be weighed against the relative risk associated with its potential for CYP inhibition. Many protease inhibitors, for instance, are potent inhibitors of CYP3A4, though their use is widespread as a result of their vital clinical utility in treating patients with HIV infection.

Despite having 10–50% less CYP3A content than is found in the liver, the gut remains an important site for many drug interactions (54). Furanocoumarins in grapefruit juice, for instance, both reversibly and irreversibly inhibit CYP3A4 in the small intestine (55). As a result, grapefruit juice significantly increases the bioavailability of a number of CYP3A4 substrates, including cyclosporine, saquinavir, midazolam, calcium channel blockers, terfenadine, and certain hydroxymethyl glutaryl coenzyme A (HMG CoA) reductase inhibitors (55–61). Other drugs that significantly alter intestinal CYP3A4 metabolism include ketoconazole, itraconazole, erythromycin, cyclosporine, and verapamil (54). CYP3A4 inhibition often occurs in conjunction with P-glycoprotein (P-gp) inhibition in the gut, complicating estimates of the relative contribution of gut wall metabolism to drug interactions (see Chapter 4, Table 4.2).

Enzyme Induction

A series of events lead to increased synthesis of CYP isoenzymes, with a resultant augmentation of their catalytic activity. This *enzyme induction* may increase the intestinal and hepatic clearance of drugs, subsequently altering serum concentrations (Figure 15.1). Though the mechanism responsible for CYP1A induction has been known for over 30 years, the mechanisms underlying CYP2 and CYP3 induction remained largely unknown until recently, when the pregnane X receptor (PXR) and the constitutive androstane receptor (CAR) were identified as inducers of CYP3A and CYP2B, respectively (62–65). In most cases of enzyme induction, increases in enzyme synthesis result from increased genetic transcription through activation of nuclear receptors. One exception is the induction of CYP2E1 by ethanol, in which ethanol stabilizes the enzyme following transcription, with no effect on receptor-mediated activation (66).

The nuclear hormone receptor superfamily is composed of three subclasses of structurally related transcription-regulating proteins that are activated by endogenous and exogenous ligand binding. Class III nuclear receptors include the orphan nuclear receptors PXR and CAR, both of which are prominently expressed in the liver and intestines (67). The orphan nuclear receptor PXR mediates the induction of CYP3A4, CYP2B6, CYP2C9, as well as *MDR1*, the gene responsible for P-gp expression (67, 68). The nuclear receptor contains two binding domains, for DNA binding and ligand binding. PXR binds as a heterodimer with the retinoid X receptor (RXR) to the DNA response elements of the regulatory region of CYP3A genes (Figure 15.2). For full activation of CYP3A4, a coordinated effort between two distinct PXR-response elements on the 5′ end of CYP3A4 is required (68). Unlike other nuclear receptors, PXR has evolved to be highly nonspecific, with the ability to bind a large and diverse group of ligands. In many

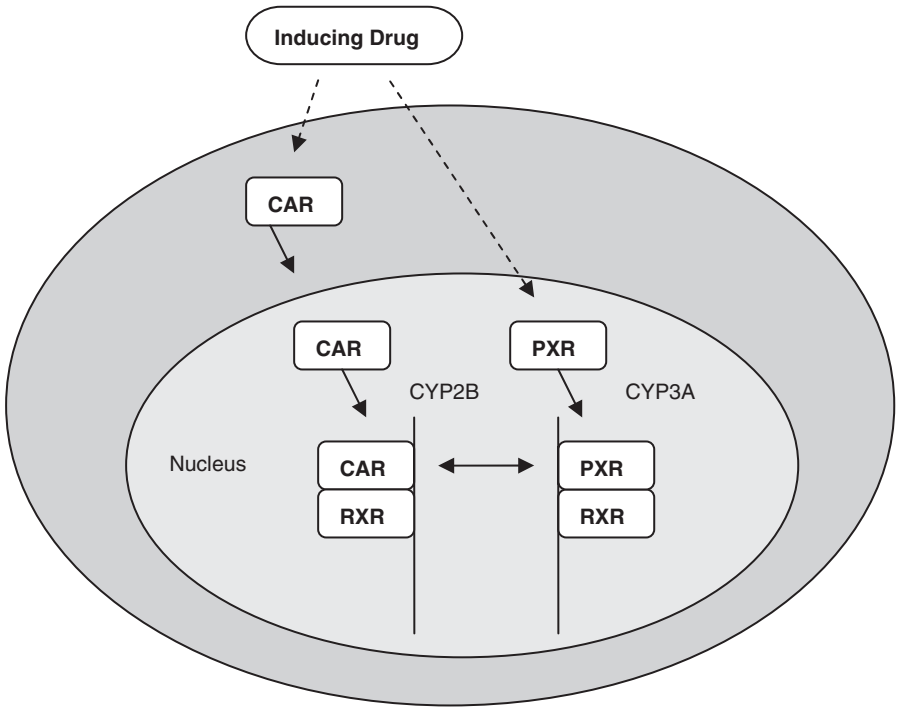

FIGURE 15.2 Drug activation of nuclear receptors PXR and CAR.

cases a drug may act as a ligand for PXR, though its specificity for the receptor is demonstrated only at concentrations that far exceed *in vivo* concentrations associated with its clinical use. Exogenous and endogenous compounds that bind with varying degrees of affinity to PXR include rifampin, mifepristone, phenobarbital, calcium channel blockers, clotrimazole, steroid hormones, St. John's wort, HMG CoA reductase inhibitors, protease inhibitors, and hyperforin (65, 67).

Unlike PXR, CAR is normally located in the cytosol, translocating to the nucleus in response to activation by ligand binding. Once in the nucleus, CAR forms a heterodimer with RXRα, binding to the appropriate response element and activating the transcription of targeted genes (Figure 15.2). CAR has been identified as a mediator of phenobarbital-type induction of CYP2B6, CYP3A4, CYP2C9, and *MDR1* (67, 68). CAR and PXR appear to be interrelated, in that many compounds, such as phenobarbital, interact with both receptors. In addition, certain gene response elements are recognized and activated by both CAR and PXR. In addition to their role in CYP induction, CAR and PXR also appear to have a role in the expression of Phase II conjugative enzymes and transport proteins, including multidrug-resistant (MDR) proteins, intestinal P-gp, and organic anion transport proteins (OATPs) (67, 68).

The rifamycins are well known for their potent and relatively nonspecific induction of CYP enzyme activity. Rifampin is frequently utilized as a prototype inducer in drug interaction studies that seek to evaluate the effects of induction on drugs that are known CYP3A4 substrates. Other important inducers of CYP3A4 include the anticonvulsants phenytoin, carbamazepine, and phenobarbital, and the HIV nonnucleoside reverse transcriptase inhibitors (NNRTIs) nevirapine and efavirenz. Since metabolic induction results in a reduced pharmacologic effect of these drugs, patients administered any of these agents may be at risk for loss of efficacy of coadministered CYP3A4 substrates.

Examples of clinically significant induction interactions include the risk of treatment failure and the development of drug-resistant virus in HIV patients treated with a protease inhibitor (CYP3A4 substrate) and efavirenz (CYP3A4 inducer) without appropriate increases in dose or the addition of a pharmacokinetic "booster" such as ritonavir. Likewise, transplant patients maintained on cyclosporine or tacrolimus risk acute allograft rejection when therapy with CYP3A4 inducers is initiated without close monitoring of cyclosporine and tacrolimus blood levels. St. Johns wort has emerged as an important inducer of

CYP3A4 activity, significantly decreasing plasma concentrations and the pharmacologic effect of a number of agents, including alprazolam, amitriptyline, cyclosporine, indinavir, methadone, nevirapine, simvastatin, tacrolimus, and oral contraceptives (69–77).

Though induction of CYP is generally associated with potential treatment failure, administration of a CYP inducer may also produce toxicity by increasing the accumulation of a toxic metabolite, such as in the case of acetaminophen, as described in Chapter 16.

Interactions Involving Drug Transport Proteins

Considerable progress has been made in recent years in the identification and characterization of drug transport proteins in humans. As described in Chapter 13, a variety of transport proteins may be involved to different extents in drug interactions that alter the absorption, distribution, metabolism, and elimination of medications. Transporters such as the MDR proteins, P-glycoprotein, multidrug resistance-related proteins (MRPs), organic anion transport polypeptides (OATPs), organic cation transporters (OCTs), and organic anion transporters (OATs) may be altered by xenobiotics, thereby affecting the disposition of coadministered drugs that are transported by these proteins. Table 15.2 contains a list of substrates, inhibitors, and inducers of P-gp and other transport proteins.

P-Glycoprotein

The most well known of the drug transporters, P-glycoprotein, has been identified at multiple anatomic locations, including the apical surface of renal tubules, intestinal and placental epithelial cells, the canalicular surface of hepatocytes, the luminal surface of blood–brain capillaries, and the surface of lymphocyte subsets (78, 79). P-Glycoprotein (P-gp) has broad substrate specificity, transporting a large number of chemically unique endogenous and exogenous substances. In general, P-gp functions to limit drug exposure in the body, excreting drug into bile at the liver, into the intestinal lumen in the gut, and into renal tubules in the kidney. In addition, extrusion by P-gp limits drug access to the brain and lymphocytes (78).

Induction of P-Glycoprotein

P-Glycoprotein functions in the gut primarily to affect the rate rather than the extent of drug absorption (68) (see Chapter 4, Figure 4.2). However, P-gp increases substrate exposure to luminal CYP3A4 metabolism during the process of drug efflux. Consequently, coadministration of a CYP3A4–P-gp

TABLE 15.2 Drugs reported to interact with P-gp, OATP, and OAT transport proteins[a]

Protein	Substrates	Inhibitors	Inducers
P-gp	Amitriptyline	Amiodarone	Amiodarone
	Amiodarone	Amitriptyline	Anticancer agents[c]
	Amprenavir	Amprenavir	Bromocriptine
	Anticancer agents[b]	Astemizole	Clotrimazole
	Atorvastatin	Bepredil	Colchicine
	Cefoperazone	Carvedilol	Cyclosporine
	Chorambucil	Chlorpromazine	Dexamethasone
	Chlorpromazine	Clarithromycin	Diltiazem
	Cimetidine	Cortisol	Erythromycin
	Ciprofloxacin	Cyclosporine	Grapefruit juice
	Cisplatin	Desipramine	Indinavir
	Clarithromycin	Diltiazem	Morphine
	Colchicine	Dipyridamole	Nicardipine
	Cyclosporine	Disulfiram	Nifedipine
	Dexamethasone	Doxepin	Probenecid
	Digoxin	Erythromycin	Rifampin
	Diltiazem	Felodipine	Ritonavir

(continued)

TABLE 15.2 Continued

Protein	Substrates	Inhibitors	Inducers
	Domperidone	Fluphenazine	Saquinavir
	Erythromycin	GF 120918	Sirolimus
	Estradiol	Grapefruit juice	St. John's Wort
	Fentanyl	Haloperidol	Tacrolimus
	Fexofenadine	Imatinab	Verapamil
	Grepafloxacin	mesylate	Yohimbine
	Hydrocortisone	Imipramine	
	Imatinab mesylate	Indinavir	
	Indinavir	Itraconazole	
	Itraconazole	Ketoconazole	
	Lansoprazole	Lovastatin	
	Levofloxacin	LY 335979	
	Lidocaine	Mefloquine	
	Loperamide	Nelfinavir	
	Losartan	Nicardipine	
	Lovastatin	Nifedipine	
	Methadone	OC 144-093	
	Methotrexate	Ofloxocin	
	Methylprednisolone	Progesterone	
	Morphine	Propafenone	
	Nadolol	Propranolol	
	Nelfinavir	Quinidine	
	Norfloxacin	Rifampin	
	Nortriptyline	Ritonavir	
	Ondansetron	Saquinavir	
	Omeprazole	Simvastatin	
	Pantoprazole	Sirolimus	
	Phenytoin	Tacrolimus	
	Pravastatin	Tamoxifen	
	Propranolol	Testosterone	
	Quinidine	Terfenadine	
	Ranitidine	Troleandomycin	
	Ritonavir	Valspodar (PSC 833)	
	Rhodamine 123	Vinblastine	
	Saquinavir	Verapamil	
	Tacrolimus	XR 9576	
	Timolol		
	Trimethoprim		
	Verapamil		
OATPs	Dexamethasone	Grapefruit juice	
OATP-A	Fexofenadine	Orange juice	
	Indinavir	Rifampin	
	Nelfinavir		
	Rifampin		
	Ritonavir		

TABLE 15.2 Continued

Protein	Substrates	Inhibitors	Inducers
	Saquinavir		
	Verapamil		
OATP-B	Penicillin G		
OATP-C	Cyclosporine	Cyclosporine	
	HMG-CoA reductase inhibitors	Rifampin	
	Methotrexate		
	Penicillin G		
	Rifampin		
	17-β-Estradiol glucoronide		
OATP8	Digoxin	Rifampin	
	Methotrexate		
	Rifampin		
OATs			
OAT1	Acyclovir	Betamipron	
	Adefovir	Cephalosporins	
	Angiotensin-converting enzyme inhibitors	Probenecid	
	Bumetanide		
	β-Lactam antibiotics		
	Cephalosporins		
	Cidofovir		
	Cimetidine		
	Furosemide		
	Ganciclovir		
	Losartan		
	Minocycline		
	NSAIDs		
	Probenecid		
	Ranitidine		
	Tetracycline		
	Various anticancer agents		
	Valproate		
	Zidovudine		
OAT2	Minocycline	Probenecid	
	Probenecid		
	Salicylate		
	Tetracycline		
	Zidovudine		
OAT3	Angiotensin-converting enzyme inhibitors	Cephalosporins	
	Bumetanide	Probenecid	
	β-Lactam antibiotics	NSAIDs	

(continued)

TABLE 15.2 Continued

Protein	Substrates	Inhibitors	Inducers
	Cephalosporins		
	Cimetidine		
	Furosemide		
	NSAIDs		
	Probenecid		
	Ranitidine		
	Tetracycline		
	Various anticancer agents		
	Zidovudine		
OAT4	Acyclovir	Betamipron	
	Adefovir	Cephalosporins	
	Bumetanide	Probenecid	
	β-Lactam antibiotics	KW-3902	
	Cephalosporins		
	Cidofovir		
	Furosemide		
	Ganciclovir		
	Methotrexate		
	NSAIDs		
	Probenecid		
	Tetracycline		
	Zidovudine		

[a] Data from Lieber (66), Schinkel and Jonker (78), Ieiri *et al*. (79), Mikkaichi *et al*. (93), and Miyazaki *et al*. (96).
[b] Actinomycin D, bisantrene, chlorambucil, cisplatin, cytarabine, daunorubicin, docetaxel, doxorubicin, epirubicin, etoposide, fluorouracil, hydroxyurea, mitomycin C, mitoxantrone, paclitaxel, tamoxifen, topotecan, taxol, vinblastine, vincristine.
[c] Chlorambucil, cisplatin, daunorubicin, doxorubicin, etoposide, fluorouracil, hydroxyurea, methotrexate, mitoxantrone, tamoxifen, vinblastine, vincristine.

substrate along with a P-gp inducer may result in decreased systemic exposure secondary to increased contact with intestinal CYP3A4. As discussed in Chapter 4, there is considerable overlap in drug specificity for P-gp and CYP3A (see Tables 15.1 and 15.2). Further, comodulation of CYP3A is a common feature of P-gp inhibitors and inducers.

Coadministration of a P-gp modulator also does not reduce the bioavailability of P-gp substrates when the passive influx of drug greatly exceeds the rate of efflux by P-gp. For instance, when therapeutic doses of indinavir are administered, intestinal lumen concentrations of this protease inhibitor far exceed its K_m for P-gp-mediated efflux (80, 81). Therefore, it is likely that indinavir saturates intestinal P-gp at these concentrations, and passive diffusion of drug through enterocytes exceeds P-gp-mediated efflux. Thus, indinavir is one of several examples of P-gp substrates with reasonably good oral bioavailability (see Table 4.2) (81). In contrast, saquinavir is a P-gp substrate that is large, poorly water soluble, and slowly absorbed (28). Presumably its K_m value for P-gp transport exceeds concentrations normally achieved in the gut, leading to its poor oral bioavailability. In comparing these two protease inhibitors, one would expect a coadministered P-gp inhibitor to have a greater effect on saquinavir exposure, compared to indinavir. Cyclosporine and paclitaxel are also examples of drugs for which P-gp plays a significant role in limiting absorption, despite their relatively high oral doses. As such, the absorption of these agents is susceptible to P-gp modulation in the intestine (82, 83).

As P-gp is localized on the canalicular surface of hepatocytes, only P-gp substrates that are excreted

in bile without significant hepatic metabolism will be susceptible to drug interactions that result from modulation of hepatic P-gp. Digoxin and fexofenadine are such examples, and both have been used as probes of P-gp activity.

The nuclear receptor PXR appears to be responsible for induction of *MDR1*, causing activation of P-gp in a dose- and site-dependent manner (83). Coinducers of P-gp and CYP3A include phenobarbital, phenytoin, dexamethasone, rifampin, and St. John's wort (84–86). Following reports of substantial decreases in digoxin concentrations in patients concurrently treated with rifampin, the interaction was studied in healthy volunteers. Concurrent rifampin administration reduced digoxin plasma concentrations significantly after oral administration, but to a lesser extent after intravenous administration, suggesting that the rifampin–digoxin interaction is mediated primarily by alterations in intestinal P-gp (87).

Inhibition of P-Glycoprotein

The mechanism of P-gp inhibition appears to be complex, involving competition for its drug-binding sites as well as blockade of the ATP hydrolysis that is necessary for its transport function (83). Examples of clinically significant drug interactions involving P-gp inhibition include increased digoxin exposure following administration of P-gp inhibitors verapamil and quinidine (88–90). Administration of quinidine with the P-gp substrate loperamide was found to produce respiratory depression in a group of healthy volunteers, despite no change in plasma loperamide concentrations (91). The basis for this interaction is that quinidine inhibits P-gp at the blood–brain barrier, resulting in greater CNS penetration of loperamide and potentially serious neurotoxicity.

CYP3A4 inhibitors that have demonstrated P-gp inhibition include erythromycin, itraconazole, cyclosporine, diltiazem, and several protease inhibitors. As a result of considerable overlap with CYP3A4, the true effect of P-gp modulation on drug interactions involving P-gp substrates is unclear. Further, poor differentiation between P gp modulation in the intestine and liver makes it difficult to determine the relative contribution of P-gp to a specific drug interaction.

As in the liver, drugs that undergo renal P-gp transport are susceptible to interactions resulting from modulation of P-gp. Inhibition of renal P-gp may lead to the development of unexpected toxicities or improved clinical efficacy secondary to increased drug exposure. Clarithromycin was found to increase the bioavailability of and reduce the renal clearance of digoxin in a group of healthy volunteers, resulting in a 1.7-fold increase in digoxin AUC (92). Thus, the previously reported clarithromycin–digoxin interaction that results in increased digoxin exposure is likely the result of P-gp inhibition in both the intestine and kidney.

There has been considerable interest in the potential use of P-gp inhibition to optimize pharmacotherapy of anticancer and antiretroviral agents. Significant efforts have been made to exploit P-gp blockade in an effort to enhance chemotherapy uptake in tumors expressing P-gp-mediated drug resistance, to improve chemotherapy bioavailability, and to increase exposure to tumors protected by the blood–brain barrier. Research is also being directed at using P-gp inhibitors in HIV patients to improve protease inhibitor uptake into T-lymphocytes and virologic sanctuaries such as the brain and testes.

Organic Anion Transport Polypeptides

As discussed in Chapter 13, the OATP family is expressed in multiple organ systems, and its substrates consist of a broad spectrum of endogenous compounds, including bile acids, thyroid hormones, and conjugated steroids, as well as exogenous drugs such as digoxin, pravastatin, methotrexate, and certain nonsteroidal anti-inflammatory drugs (NSAIDs) (93). In contrast to P-gp and MRP-mediated drug transport, the OATPs generally mediate drug *influx*, thereby increasing the intestinal absorption and hepatic uptake of drugs. Thus, inhibition of intestinal OATP would be expected to result in decreased plasma concentrations of substrates, while inhibition of hepatic OATP would result in increased plasma concentrations.

Fexofenadine and digoxin are both well-known substrates for OATP transport, though the relative contribution of OATP modulation on drug interactions involving these two agents is unclear, since both are also P-gp substrates. The 60–80% reduction in fexofenadine bioavailability that results from orange, apple, and grapefruit juice consumption, however, is likely the result of OATP inhibition, rather than of P-gp induction (94).

Inhibitors of OATP transport are typically sterically bulky compounds, including anions, cations, and neutral compounds (95). Various medications have been shown to interact with OATPs, including HMG CoA reductase inhibitors, cyclosporine, quinidine, rifampin, ketoconazole, verapamil, and certain protease inhibitors. Cyclosporine and rifampin have relatively high ratios of plasma concentration to K_i, suggesting the potential for clinically significant drug–drug interactions via modulation of OATP. On the other hand, plasma concentrations of pravastatin are

thought to be too low to cause significant OATP-mediated interactions (95). More studies on human OATP transporters are needed to quantify the potential for OATP inhibitors to cause transport-mediated drug interactions.

Organic Anion Transporters

To date, six organic anion transport members have been identified and found to play important roles in the distribution and elimination of both endogenous and exogenous substances in the kidneys, liver, and brain (96). The OAT transporters are inhibited by several therapeutic agents, including probenecid, pravastatin, cimetidine, cephalosporin antibiotics, thiazide and loop diuretics, acetazolamide, and certain NSAIDs (96–99). The relatively low plasma concentrations of most OAT inhibitors, in relation to their K_i values, suggest that many inhibitors identified *in vitro* are not capable of causing clinically significant drug–drug interactions (95). Exceptions include probenecid and the cephalosporins, which have relatively lower K_i values. Probenecid administration has been found protect against cidofovir-mediated nephrotoxicity by limiting its OAT-1-mediated renal transport (100). Probenecid has also been shown to decrease the CSF clearance of the OAT substrate zidovudine, prolonging its half-life in the brain (101). Further investigation into human OAT transporters is necessary to identify OAT-mediated drug interactions that should be avoided or possibly exploited to improve pharmacotherapy.

Interactions Affecting Renal Excretion

The pharmacokinetic properties of drugs that are primarily renally excreted may be altered by changes to active transport systems, urinary pH, and renal blood flow. Passive diffusion of molecules into and out of the tubule lumen is dependent upon their extent of ionization, with only the nonionized form able to diffuse through the lipid membrane. Changes in pH alter the ionization of weakly acidic and basic drugs, thereby affecting their degree of passive diffusion. Since most weakly acidic and basic drugs are metabolized to inactive compounds prior to renal excretion, changes in urinary pH do not affect the elimination of most drugs. Exceptions include the acidic compounds phenobarbital, aspirin, and other salicylates, whose serum levels have been demonstrated to decrease with concurrent antacid or sodium bicarbonate administration (102, 103). Changes in urinary pH have been exploited to increase drug excretion in situations of phenobarbital and salicylate overdose.

As described previously, drugs that inhibit or compete for the same active transport system in the renal tubules can decrease excretion, thereby increasing the amount of drug retained. A classic example of this mechanism is that of probenecid use with penicillin or cephalosporins — an interaction that has been utilized to increase antibiotic exposure for difficult-to-treat pathogens (104). Another example is the development of methotrexate toxicity in patients concurrently treated with NSAIDs. Studies and case reports have identified various NSAIDS, including aspirin, ibuprofen, indomethacin, and naproxen, as having the potential to cause life-threatening methotrexate toxicity via inhibition of the drug's tubular secretion (105, 106). NSAIDS may also contribute to an increase in serum methotrexate concentrations by decreasing renal tissue perfusion through the inhibition of prostaglandin synthesis. Inhibition of renal blood flow has also been hypothesized as the potential mechanism behind elevated serum lithium levels that result during concurrent NSAID use (107).

PREDICTION AND CLINICAL MANAGEMENT OF DRUG INTERACTIONS

In Vitro Screening Methods

In vitro systems are commonly employed to assess the potential for CYP and transport protein-mediated drug interactions. Microsomes, liver and kidney slices, isolated and cultured hepatocytes, membrane vesicles, and recombinant human DNA-transfected cells are all methods of determining the roles of metabolism and drug transport in drug interactions. Unfortunately, most *in vitro* methods are able to assess the potential for inhibition, but not induction. For inhibitors that also cause enzyme induction or influence multiple metabolic pathways, *in vitro* predictions may be markedly different from *in vivo* findings. Further, inhibitors that are identified by *in vitro* screening methods may be found to inhibit CYP enzymes or transport proteins only at exceedingly high concentrations. Since it is not always possible to predict the concentration of a drug or its metabolites at specific sites *in vivo*, it is often difficult to define the clinical significance of such findings. Predicting clinically relevant interactions is also confounded by individual patient characteristics, including underlying disease states, organ dysfunction, obesity, environmental factors (e.g., cigarette smoke), and genetics (47). As described in Chapter 21, sex-related differences in receptor density and sensitivity and in enzyme and

transport protein activity may also contribute to pharmacokinetic and pharmacodynamic variation between males and females.

Genetic Variation

As discussed in Chapter 14, genetic polymorphisms occur in many human CYP enzymes, with most appearing in enzymes CYP2A6, CYP2C9, CYP2C19, and CYP2D6 (51). Genotypic variation in CYP enzyme activity affects not only the extent of drug metabolism, but also the degree to which various drug interactions impact drug metabolism. Quinidine, a potent CYP2D6 inhibitor, significantly alters codeine's conversion to morphine via CYP2D6 O-demethylation in CYP2D6 extensive metabolizers (EMs). In genetically poor metabolizers (PMs) of CYP2D6 substrates, however, codeine's metabolism is already substantially diminished, and the addition of quinidine does not significantly affect the rate of codeine's conversion to morphine (108). Drug interaction predictions based on pharmacogenetics is less straightforward when the enzyme modulator or substrate interacts with more than one enzyme. For instance, when rifampin was administered with codeine to CYP2D6 EMs and PMs, codeine's conversion to morphine was enhanced in EMs, but not in PMs. However, despite the enhanced rate of O-demethylation in EMs, morphine plasma concentrations were reduced overall due to rifampin's relatively greater induction of codeine's N-demethylation pathway, as well as its induction of morphine's metabolism to inactive metabolites (108).

Phenotyping enzyme activity is a practical approach to studying metabolic drug interactions in humans, allowing for diverse patient characteristics such as genotypic variation to be considered. As described for the assessment of liver disease and drug metabolism in Chapter 7, drugs that are exclusively, or at least principally, metabolized by a specific enzymatic pathway may be administered to individuals as "probe drugs" for that particular enzyme. *In vivo* enzyme activity is assessed by measuring the plasma concentration or urine excretion of parent drug and metabolite(s). A probe drug is often administered in the presence of a potential inhibitor or inducer to evaluate the extent of the modulator's effect on enzyme activity.

Clinical Management of Drug Interactions

A basic understanding of mechanisms that contribute to drug interactions is essential to their identification and clinical management. Potentially significant drug interactions can be often be identified and circumvented by obtaining a thorough medication history that includes use of over-the-counter and alternative therapies, by making patient-appropriate drug selections, and by providing counseling in cases of time- or food-related interactions. The use of plasma concentration monitoring may be appropriate to guide therapy in cases in which established dosing recommendations for a particular drug interaction cannot be found. Table 15.3 contains a list of literature and web sites that offer up-to-date information regarding drug interactions and drug metabolism pathways that may be helpful when assessing the risk of a potential interaction. In addition, the U.S. Food and Drug Administration has issued guidelines on conducting *in vivo* and *in vitro* drug interaction studies to facilitate research in this area (109, 110). These documents are available online and review current state-of-the-art study design and analysis.

TABLE 15.3 Drug Interaction Resources

Bachmann, KA. Drug interactions handbook. Hudson, OH: Lexi-Comp; 2003

Flockhart D. CYP450 Online interaction table. Available at http://medicine.iupui.edu/flockhart/table.htm

U.S. Food and Drug Administration. Guidance for industry. Drug interaction/drug metabolism studies in the drug development process: Studies *in vitro*. Rockville, MD, 1997. Available at http://www.fda.gov/cder/guidance/clin3.pdf

U.S. Food and Drug Administration. *In vivo* drug metabolism/drug interaction studies — study design, data analysis, and recommendations for dosing and labeling. Rockville, MD: 1999. Available at http://www.fda.gov/cder/guidance/index.htm

Hansten PD, Horn JR. Managing clinically important drug interactions. St. Louis, MO: Facts and Comparisons; 2003

Levy RH, Thummel KE, Trager WF, Hansten PD, Eichelbaum M. Metabolic drug interactions. Philadelphia, PA: Lippincott Williams & Williams; 2000

Liverpool HIV Pharmacology Group. HIV drug interaction charts. Available at http://www.hiv-druginteractions.org

Piscitelli SC, Rodvold KA. Drug interactions in infectious diseases. Totowa, NJ: Humana Press; 2000

Stockley IH. Stockley's drug interactions. London, England: Pharmaceutical Press; 2002

Tatro DS. Drug interaction facts. St. Louis, MO: Facts and Comparisons; 2004

REFERENCES

1. Monahan BP, Ferguson CL, Killeavy ES *et al*. Torsades de pointes occurring in association with terfenadine use. JAMA 1990;264:2788–90.
2. Zimmermann M, Duruz H, Guinand O *et al*. Torsades de pointes after treatment with terfenadine and ketoconazole. Eur Heart J 1992;13:1002–03.
3. Stephens M. Introduction. In: Talbot J, Waller P, eds. Stephens' detection of new adverse drug reactions. West Sussex, England: John Wiley & Sons, Ltd; 2004. p.1–88.
4. Stockley IH. General considerations and an outline survey of some basic interaction mechanisms. In: Stockley IH, ed. Stockley's drug interactions. London, England: Pharmaceutical Press; 2002. p. 1–14.
5. Dasgupta A, Okhuysen PC. Pharmacokinetic and other drug interactions in patients with AIDS. Ther Drug Monit 2001;23:591–605.
6. Van Cleef GF, Fisher EJ, Polk RE. Drug interaction potential with inhibitors of HIV protease. Pharmacotherapy 1997;42:1553–56.
7. Routledge PA, O'Mahony MS, Woodhouse KW. Adverse drug reactions in elderly patients. Br J Clin Pharmacol 2004;57:121–6.
8. Panel on clinical practices for treatment of HIV infection. Guidelines for the use of antiretroviral agents in HIV-infected adults and adolescents. October 29, 2004. (Internet at http://AIDSinfo.nih.gov.)
9. Nomura A, Yasuda H, Katoh K *et al*. Hydralazine and furosemide kinetics. Clin Pharmacol Ther 1982;32:303–6.
10. Bohets H, Lavrijsen K, Hendrickx J *et al*. Identification of the cytochrome P450 enzymes involved in the metabolism of cisapride: *In vitro* studies of potential co-medication interactions. Br J Pharmacol 2000;129:1655–67.
11. Propulsid®, cisapride [package insert]. Titusville, NJ: Janssen Pharmaceutica (package insert revised 01/2000).
12. Hochster H, Dieterich D, Bozzette S *et al*. Toxicity of combined ganciclovir and zidovudine for cytomegalovirus disease associated with AIDS: An AIDS clinical trials group study. Ann Intern Med 1990;113:111–17.
13. Backman JT, Kyrklund C, Neuvonen M, Neuvonen PJ. Gemfibrozil greatly increases plasma concentrations of cerivastatin. Clin Pharmacol Ther 2002;72:685–91.
14. Shek A, Ferrill MJ. Statin-fibrate combination therapy. Ann Pharmacother 2001;35:908–17.
15. Murdock DK, Murdock AK, Murdock RW *et al*. Long-term safety and efficacy of combination gemfibrozil and HMG-CoA reductase inhibitors for the treatment of mixed lipid disorders. Am Heart J 1999;138:151–5.
16. Gugler R, Allgayer H. Effects of antacids on the clinical pharmacokinetics of drugs: An update. Clin Pharmacokinet 1990;18:210–9.
17. Wadhwa NK, Schroeder TJ, O'Flaherty E, Pesce AJ, Myre SA, First MR. The effect of oral metoclopramide on the absorption of cyclosporine. Transplant Proc 1987;19:1730–3.
18. Reyataz™, atazanavir [package insert]. Princeton, NJ: Bristol-Myers Squibb Company (package insert issued 7/2004).
19. Van der Meer JWM, Keuning JJ, Scheijgrond HW *et al*. The influence of gastric acidity on the bioavailability of ketoconazole. J Antimicrob Chemother 1980;6:552–554.
20. Sporanox®, itraconazole [package insert]. Titusville, NJ: Janssen Pharmaceutical Products, L.P. (package insert revised 1/2004).
21. Dear Health Care Provider letter. Bristol-Myers Squibb Co., December, 2004.
22. Lange D, Pavao JH, Wu J, Klausner M. Effect of a cola beverage on the bioavailability of itraconazole in the presence of H2 blockers. J Clin Pharmacol 1997;37:535–40.
23. Polk RE. Drug–drug interactions with ciprofloxacin and other fluoroquinolones. Am J Med 1989;87(suppl 5A):76S–81S.
24. Schentag JJ, Watson WA, Nix D *et al*. Time dependent interactions between antacids and quinolone antibiotics. Clin Pharmacol 1988;43:135.
25. D'Arcy PF and McElnay JC. Drug–antacid interactions: Assessment of clinical importance. Drug Intell Clin Pharm 1987;21:607–17.
26. Neuvonen PJ. Interactions with the absorption of tetracyclines. Drugs 1976;11:45–54.
27. Farmer JA, Gotto AM Jr. Antihyperlipidaemic agents. Drug interactions of clinical significance. Drug Safety 1994;11:201–9.
28. Invirase®, saquinavir mesylate [package insert]. Nutley, NJ: Roche Laboratories, Inc. (package insert revised 12/2003).
29. Gupta SK, Benet LZ. Food increases the bioavailability of cyclosporine in healthy volunteers. Biopharm Drug Dispos 1989;10:591–6.
30. Peloquin CA, Namdar R, Singleton MD, Nix DE. Pharmacokinetics of rifampin under fasting conditions, with food, and with antacids. Chest 1999;155:12–8.
31. Peloquin CA, Namdar S, Dodge AA, Nix DE. Pharmacokinetics of isoniazid under fasting conditions, with food, and with antacids. Int J Tuberc Lung Dis 1999;3:703–10.
32. Crixivan®, indinavir sulfate [package insert]. Whitehouse Station, NJ: Merck & Co., Inc. (package insert revised 5/2004).
33. Melander A, Danielson K, Hanson A, et al. Reduction of isoniazid bioavailability in normal men by concomitant intake of food. Acta Med Scand 1976;200:93–7.
34. Burman WJ, Gallicano K, Peloquin C. Comparative pharmacokinetics and pharmacodynamics of the rifamycin antibacterials. Clin Pharmacokinet 2001;40:327–41.
35. Trivedi S, Hyman J, Lichstein E. Clarithromycin and digoxin toxicity [letter]. Ann Intern Med 1998;128:604.
36. Bizjak ED, Mauro VF. Digoxin–macrolide drug interaction. Ann Pharmacother 1997;31:1077–9.
37. Lindenbaum J, Rund DG, Butler VP, Tse-Eng D, Saha JR. Inactivation of digoxin by the gut flora: Reversal by antibiotic therapy. N Engl J Med 1981;305:789–94.

38. Berndt A, Gramatté T, Kirch W. Digoxin–erythromycin interaction: *In vitro* evidence for competition for intestinal P-glycoprotein. Eur J Pharmacol 1996;50:538.
39. Wagasugi H, Yano I, Ito T et al. Effect of clarithromycin on renal excretion of digoxin: Interaction with P-glycoprotein. Clin Pharmacol Ther 1998;64:123–8.
40. Rengelshausen J, Göggelmann C, Burhenn J *et al*. Contribution of increased oral bioavailability and reduced renal clearance of digoxin to the digoxin–clarithromycin interaction. Br J Clin Pharmacol 2003;56:32–8.
41. Back DJ, Breckenridge AM, Crawford FE, MacIver M, Orme ML, Rowe PH. Interindividual variation and drug interactions with hormonal steroid contraceptives. Drugs 1981;21:46–61.
42. Grimmer SFM, Allen WL, Back DJ, Breckenridge AM, Orme M, Tjia T. The effect of cotrimazole on oral contraceptive steroids in women. Contraception 1983;28:53–9.
43. Friedman CI, Huneke AL, Kim MH, Powell J. The effect of ampicillin on oral contraceptive effectiveness. Obstet Gynecol 1980;55:33–7.
44. Back DJ, Breckenridge AM, MacIver M *et al*. The effect of ampicillin on oral contraceptive steroids in women. Br J Clin Pharmacol 1982;14:43–8.
45. Shenfield GM. Oral contraceptives. Are drug interactions of clinical significance? Drug Saf 1993;9:21–37.
46. Dickinson BD, Altman RD, Neilsen NH, Sterling MI. Drug interactions between oral contraceptives and antibiotics. Obstet Gynecol 2001;98:853–60.
47. Shapiro LE, Shear NH. Drug interactions: Proteins, pumps, and P-450s. J Am Acad Dermatol 2002;47:467–84.
48. Sansom LN, Evans AM. What is the true clinical significance of plasma protein binding displacement interactions? Drug Saf 1995;12:227–33.
49. Lewis DF. 57 varieties: The human cytochromes P450. Pharmacogenomics 2004;5:305–18.
50. Thummel KE, Kunze KL, Shen DD. Metabolically-based drug–drug interactions: Principles and mechanisms. In: Metabolic drug interactions. Levy RH, Thummel KE, Trager WF, Hansten PD, Eichelbaum M, eds. Philadelphia: Lippincott Williams & Williams; 2000. p. 3–47.
51. Bachmann KA, Ring BJ, Wrighton SA. Drug-drug interactions and the cytochromes P450. In: Drug metabolizing enzymes: CYP450 and other enzymes in drug discovery and development. Lee JS, Obach S, and Fisher MB, eds. New York: Marcel Dekker, Inc.; 2003. p. 311–36.
52. Dansette PM, Delaforge M, Sartori E, Beaune P, Jaouen M, Mansuy D. Drug interactions with macrolide antibiotics: Specificity of pseudo-suicide inhibition and induction of cytochrome P-450. Adv Exp Med Biol 1986;197:155–62.
53. Collins JM. Regulatory viewpoint: Prediction of drug interactions from *in vitro* studies. In: Levy RH, Thummel KE, Trager WF, Hansten PD, Eichelbaum M, eds. Metabolic drug interactions. Philadelphia: Lippincott Williams & Wilkins; 2000. p. 41–7.
54. Doherty MM, Charman WN. The mucosa of the small intestine. Clin Pharmacokinet 2002;41:235–53.
55. Kupferschmidt HR, Ha WH, Ziegler PL *et al*. Interaction between grapefruit juice and midazolam in humans. Clin Pharmacol Ther 1995;58:20–8.
56. Lilja JJ, Kivisto KT, Neuvonen PJ. Grapefruit juice–simvastatin interaction: Effect on serum concentrations of simvastatin, simvastatin acid, and HMG-CoA reductase inhibitors. Clin Pharmacol Ther 1998;64:477–83.
57. Benton RE, Honig PK, Zamani K *et al*. Grapefruit juice alters terfenadine pharmacokinetics, resulting in prolongation of repolarization on the electrocardiogram. Clin Pharmacol Ther 1996;59:383–8.
58. Bailey DG, Spence JD, Munoz C *et al*. Interaction of citrus juices with felodipine and nifedipine. Lancet 1991;337:268–9.
59. Ducharme MP, Warbasse LH, Edwards DJ. Disposition of intravenous and oral cyclosporine after administration with grapefruit juice. Clin Pharmacol Ther 1995;57:485–91.
60. Kufperschmidt HH, Fattinger KE, Ha HR *et al*. Grapefruit juice enhances the bioavailability of the HIV protease inhibitor saquinavir in man. Br J Clin Pharmacol 1998;45:355–9.
61. Bailey DG, Bend JR, Arnold MO *et al*. Erythromycin–felodipine interaction: Magnitude, mechanism and comparison with grapefruit juice. Clin Pharmacol Ther 1996;60:25–33.
62. Kliewer SA, Moore JT, Wade L *et al*. An orphan nuclear receptor activated by pregnane defines novel steroid signaling pathway. Cell 1998;92:73–82.
63. Sueyoshi T, Kawamoto T, Zelko I, Honkakoshi P, Negishi M. The repressed nuclear receptor CAR responds to phenobarbital in activating the human CYP2B6 gene. J Biol Chem 1999;274:6043–6.
64. Lehmann JM, McKee DD, Watson MA, Willson TM, Moore JT, Kliewer SA. The human orphan nuclear receptor PXR is activated by compounds that regulate CYP3A4 gene expression and cause drug interactions. J Clin Invest 1998;102:1016–23.
65. Honkakoski P, Sueyoshi T, Negishi M. Drug-activated nuclear receptors CAR and PXR. Ann Med 2003;35:172–82.
66. Lieber CS. Cytochrome P-4502E1: Its physiological and pathological role. Physiol Rev 1997;77:517–44.
67. Handschin C, Meyer UA. Induction of drug metabolism: The role of nuclear receptors. Pharmacol Rev 2003;55:649–73.
68. Christians U. Transport proteins and intestinal metabolism: P-glycoprotein and cytochrome P4503A. Ther Drug Monit 2004;26:104–6.
69. Piscitelli SC, Burstein AH, Chaitt D *et al*. Indinavir concentrations and St. John's wort. Lancet 2000;355:547–8.
70. Ruschitzka F, Meier PJ, Turina M, Luscher TF, Noll G. Acute heart transplant rejection due to Saint John's wort. Lancet 2000;355:548–9.
71. Johne A, Schmider J, Brockmoller J *et al*. Decreased plasma levels of amitriptyline and its metabolites on comedication with an extract from St. John's wort (*Hypericum perforatum*). J Clin Psychopharmacol 2002;22:46–54.

72. Markowitz JS, Donovan JL, DeVane CL *et al*. Effect of St John's wort on drug metabolism by induction of cytochrome P450 3A4 enzyme. JAMA 2003;290:1500–4.
73. Eich-Hochli D, Oppliger R, Golay KP, Baumann P, Eap CB. Methadone maintenance treatment and St. John's wort — a case report. Pharmacopsychiatry 2003;36:35–7.
74. de Maat MM, Hoetelmans RM, Mathot RA *et al*. Drug interaction between St John's wort and nevirapine. AIDS 2001;15:420–1.
75. Sugimoto K, Ohmori M, Tsuruoka S *et al*. Different effects of St John's wort on the pharmacokinetics of simvastatin and pravastatin. Clin Pharmacol Ther 2001;70:518–24.
76. Hebert MF, Park JM, Chen YL, Akhtar S, Larson AM. Effects of St. John's wort (*Hypericum perforatum*) on tacrolimus pharmacokinetics in healthy volunteers. J Clin Pharmacol 2004;44:89–94.
77. Hall SD, Wang Z, Huang SM *et al*. The interaction between St John's wort and an oral contraceptive. Clin Pharmacol Ther 2003;74:525–35.
78. Schinkel AH, Jonker JW. Mammalian drug efflux transporters of the ATP binding cassette (ABC) family: An overview. Adv Drug Deliv Rev 2003;55:3–29.
79. Ieiri I, Takane H, Otsubo K. The MDR1 (ABCB1) gene polymorphism and its clinical implications. Clin Pharmacokinet 2004;43:553–76.
80. Hochman JH, Chiba M, Nishime J, Yamazaki M, Lin JH. Influence of P-glycoprotein on the transport and metabolism of indinavir in Caco-2 cells expressing cytochrome P-450 3A4**.** J Pharmacol Exp Ther 2000;292:310–8.
81. Lin JH. Drug–drug interaction mediated by inhibition and induction of P-glycoprotein. Adv Drug Deliv Rev 2003;55:53–81.
82. Benet LZ, Cummins CL, Wu CY. Transporter-enzyme interactions: Implications for predicting drug–drug interactions from *in vitro* data. Curr Drug Metab 2003;4:393–8.
83. Lin JH, Yamazaki M. Role of P-glycoprotein in pharmacokinetics: Clinical implications. Clin Pharmacokinet 2003;42:59–98.
84. Durr D, Stieger B, Kullak-Ublick GA *et al*. St. John's Wort induces intestinal P-glycoprotein/MDR1 and intestinal and hepatic CYP3A4. Clin Pharmacol Ther 2000;68:598–604.
85. Zhao JY, Ikeguchi M, Eckersberg T *et al*. Modulation of multi-drug resistance gene expression by dexamethasone in cultured hepatoma cells. Endocrinology 1993;133:521–8.
86. Schuetz EG, Beck WT, Schuetz JD. Modulators and substrates of P-glycoprotein and cytochrome P450 3A coordinately upregulated these proteins in human colon carcinoma cells. Mol Pharmacol 1996;49:311–18.
87. Greiner B, Eichelbaum M, Fritz, P *et al*. The role of intestinal P-glycoprotein in the interaction of digoxin and rifampin. J Clin Invest 1999;104:147–53.
88. Mordel A, Halkin H, Zulty L *et al*. Quinidine enhances digitalis toxicity at therapeutic serum digoxin levels. Clin Pharmacol Ther 1993;53:457–62.
89. Su FG, Huang JD. Inhibition of the intestinal digoxin absorption and exsorption by quinidine. Drug Metab Dispos 1996;24:142–7.
90. Verschraagen M, Koks CHW, Schellens JHM *et al*. P-glycoprotein system as a determinant of drug interactions: The case of digoxin–verapamil. Pharmacol Res 1999;40:301–6.
91. Sadeque AJ, Wandel C, He H, Shah S, Wood AJ. Increased drug delivery to the brain by P-glycoprotein inhibition. Clin Pharmacol Ther. 2000;68:231–7.
92. Rengelshausen J, Göggelmann C, Burhenne J *et al*. Contribution of increased oral bioavailability and reduced nonglomerular renal clearance of digoxin to the digoxin–clarithromycin interaction. J Clin Pharmacol 2003;56:32–8.
93. Mikkaichi T, Suzuki T, Tanemoto M, Ito S, Abe T. The organic anion transporter (OATP) family. Drug Metab Pharmacokin 2004;19:171–9.
94. Dresser GK, Bailey DG, Leake BF *et al*. Fruit juices inhibit organic anion transporting polypeptide-mediated drug uptake to decrease the oral availability of fexofenadine. Clin Pharmacol Ther 2002;71:11–20.
95. Shitara Y, Sato H, Sugiyama Y. Evaluation of drug–drug interaction in the hepatobiliary and renal transport of drugs. Annu Rev Pharmacol Toxicol 2005;45:689–723.
96. Miyazaki H, Sekine T, Endou H. The multispecific organic anion transporter family: Properties and pharmacological significance. Trends Pharmacol Sci 2004;25:654–62.
97. Khamdang S, Takeda M, Shimoda M *et al*. Interactions of human- and rat-organic anion transporters with pravastatin and cimetidine. J Pharmacol Sci 2004;94:197–202.
98. Uwai Y, Saito H, Hashimoto Y, Inui KI. Interaction and transport of thiazide diuretics, loop diuretics, and acetazolamide via rat renal organic anion transporter rOAT1. J Pharmacol Exper Ther 2000;295:261–5.
99. Mulato AS, Ho ES, Cihlar T. Nonsteroidal anti-inflammatory drugs efficiently reduce the transport and cytotoxicity of adefovir mediated by the human renal organic anion transporter 1. J Pharmacol Exper Ther 2000;295:10–15.
100. Lacy SA, Hitchcock MJM, Lee WA, Tellier P, Cundy KC. Effect of oral probenecid coadministration on the chronic toxicity and pharmacokinetics of intravenous cidofovir in cynomolgus monkeys. Toxicol Sci 1998;44:97–106.
101. Wang Y, Wei Y, Sawchuk RJ. Zidovudine transport within the rabbit brain during intracerebroventricular administration and the effect of probenecid. J Pharm Sci 1997;86:1484–90.
102. Proudfoot AT, Krenzelok EP, Vale JA. Position paper on urine alkalinization. J Toxicol Clin Toxicol. 2004;42:1–26.
103. Hansten PD, Hayton WL. Effect of antacid and ascorbic acid on serum salicylate concentrations. J Clin Pharmacol 1980;20:236–31.
104. Stockley IH. Antibacterial and anti-infective agent drug interactions. In: Stockley IH, ed. Stockley's drug interactions. 6th ed. London: Pharmaceutical Press; 2002. p. 128–232.
105. Tracy TS, Krohn K, Jones DR, Bradley JD, Hall SD, Brater DC. The effects of salicylate, ibuprofen, and

naproxen on the disposition of methotrexate in patients with rheumatoid arthritis. Eur J Clin Pharmacol 1992;42:121–5.
106. Dupuis LL, Koren G, Shore A, Silverman ED, Laxter RM. Methotrexate–nonsteroidal anti-inflammatory drug interaction in children with arthritis. J Rheumatol 1990;17:1469–73.
107. Stockley IH. Lithium drug interactions. In: Stockley IH, ed. Stockley's drug interactions. 6th ed. London: Pharmaceutical Press; 2002. p. 651–66.
108. Caraco Y, Sheller J, Wood AJJ. Pharmacogenetic determinants of codeine induction by rifampin: The impact on codeine's respiratory, psychomotor and miotic effects. J Pharmacol Exper Ther 1997;281:330–6.
109. CDER. Guidance for Industry. Drug interaction/drug metabolism studies in the drug development process: Studies *in vitro*. Rockville, MD: Food and Drug Administration; 1997. (Internet at: http://www.fda.gov/cder/guidance/index.htm.)
110. CDER. Guidance for Industry. *In vivo* drug metabolism/drug interaction studies — study design, data analysis, and recommendations for dosing and labeling. Rockville, MD: Food and Drug Administration; 1999. (Internet at: http://www.fda.gov/cder/guidance/index.htm.)

This page intentionally left blank

CHAPTER

16

Biochemical Mechanisms of Drug Toxicity

ARTHUR J. ATKINSON, JR.* AND SANFORD P. MARKEY†

**Clinical Center, National Institutes of Health, †National Institute of Mental Health, National Institutes of Health, Bethesda, Maryland*

INTRODUCTION

Several attempts have been made to classify different types of adverse drug reactions, and different classifications actually may be appropriate for different purposes. One approach is that proposed by Rawlins and Thomas (1) (see Chapter 25). According to this classification, Type A reactions consist of augmented but qualitatively normal pharmacological responses, whereas Type B reactions are those that are qualitatively bizarre. Some Type B reactions represent drug allergy or hypersensitivity, and others represent what was initially labeled idiosyncratic. However, progressively fewer adverse drug reactions are still regarded as simply idiosyncratic as more is learned about their mechanistic basis.

Approximately 70–80% of the adverse drug reactions that occur in clinical practice can be classified as Type A (2). This category consists of reactions that generally are mediated through pharmacologic receptors and have a pharmacokinetic basis with an obvious dose-response relationship. Hepatotoxic reactions to acetaminophen also have been assigned to this category. However, this and a number of other adverse reactions are mediated by chemically reactive cytotoxic metabolites and deserve separate consideration from a mechanistic standpoint. Allergic or hypersensitivity reactions comprise an additional 6–10% of the adverse drug reactions that are encountered clinically (3), and most of them also entail initial covalent binding of a chemically reactive drug metabolite to an endogenous macromolecule.

This chapter focuses on some representative adverse drug reactions that reflect the chemical reactivity of drugs and metabolites rather than their binding to specific pharmacologic receptors. Although these reactions are commonly thought of as not being dose related, they occur in many cases only after the dose-dependent formation of chemically reactive compounds exceeds a critical threshold that overcomes host detoxification and repair mechanisms. Therefore, it may be possible to minimize the severity or even occurrence of these reactions by prescribing the lowest therapeutically effective drug dose or by coadministering an agent that blocks reactive metabolite formation or bolsters endogenous detoxification mechanisms.

Drug-Induced Methemoglobinemia

Drug-induced methemoglobinemia is an adverse reaction that has been studied for over 50 years and serves as a paradigm for our understanding of the biochemical mechanism underlying a number of toxic reactions to drugs. Pioneering investigations by Brodie and Axelrod (4) on the metabolism of acetanilide demonstrated that methemoglobin levels following administration of this drug paralleled plasma levels of aniline, suggesting that phenylhydroxylamine was involved in methemoglobin formation (Figure 16.1). These investigators also found that when another metabolite of acetanilide, 4-hydroxyacetanilide, was administered to humans it had analgesic activity that was equal to that of acetanilide, yet did not cause an increase in methemoglobin levels. These findings

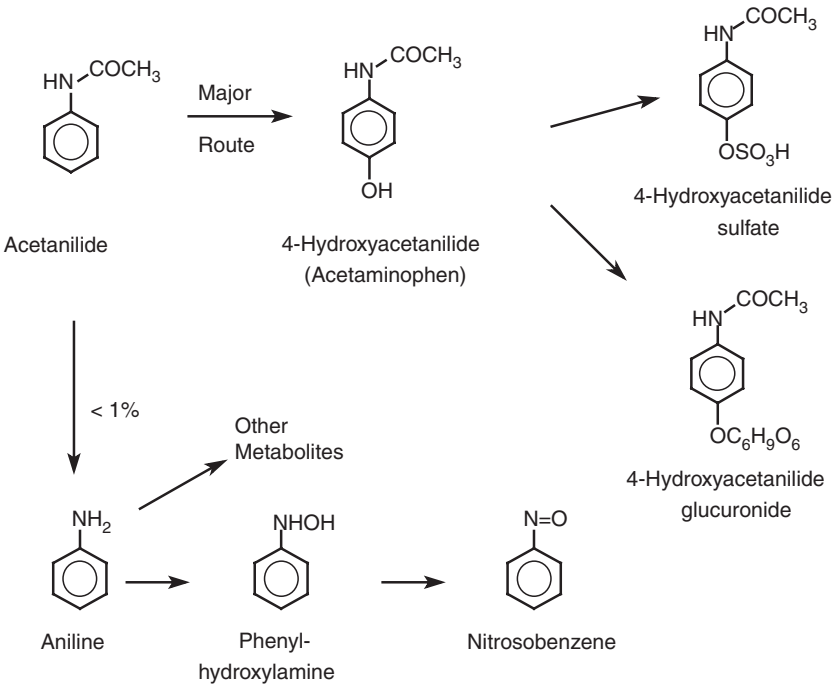

FIGURE 16.1 Metabolism of acetanilide. The major route of metabolism is via hydroxylation to form 4-hydroxyacetanilide (acetaminophen). Less than 1% is deacetylated to form aniline.

provided the impetus for the subsequent introduction of this metabolite as the analgesic drug acetaminophen.

In fact, methemoglobin is being formed constantly in normal erythrocytes. In the process of binding oxygen, oxyhemoglobin is converted to a superoxoferriheme ($Fe^{3+}O_2^{\bullet-}$) complex (5, 6). Although tissue release of oxygen restores heme iron to its ferrous state, some oxygen is dissociated from hemoglobin as superoxide ($O_2^{\bullet-}$), resulting in oxidation of hemoglobin to ferric methemoglobin. The spontaneous formation of methemoglobin is counteracted by the enzymatic reduction of heme iron to the ferrous form, so that less than 1% of total hemoglobin normally is present as methemoglobin. However, higher levels of methemoglobinemia are present in individuals with hemoglobin M or other genetically rare hemoglobins that are highly vulnerable to low levels of oxidizing agents. Another rare cause of methemoglobinemia results from a deficiency in NADH-dependent cytochrome b_5 methemoglobin reductase (NADH-diaphorase) that normally reduces ferric to ferrous heme.

Drugs and other xenobiotics that cause methemoglobinemia react either stoichiometrically or in a cyclic fashion to convert heme iron from the ferrous to the ferric state. A partial list of these compounds is provided in Table 16.1. Nitrites are representative of stoichiometrically acting compounds. An account of an outbreak of methemoglobinemia that occurred in a cafeteria, whose staff had inadvertently placed sodium nitrite in a batch of oatmeal and in a salt shaker, was popularized several years ago in a story

TABLE 16.1 Partial List of Compounds Producing Methemoglobinemia[a]

Stoichimetrically acting	Presumed cyclical mechanism
Sodium nitrite	Aniline
Amyl nitrite	Nitrobenzene
Butyl nitrite	Acetanilinde
Isobutyl nitrite	Phenacetin
Nitric oxide	Sulfanilamide
Silver nitrate	Sulfamethoxazole
	Dapsone
	Primaquine
	Benzocaine
	Prilocaine
	Metoclopramide

[a] Data from Coleman MD, Coleman NA. Drug Saf 1996;14: 394–405.

entitled "Eleven Blue Men" (7). Abuse of amyl, butyl, and isobutyl nitrates continues to result in a number of fatal episodes of methemoglobinemia (5). On the other hand, most drugs that cause methemoglobinemia form metabolites that interact in a cyclic fashion to convert hemoglobin to methemoglobin, as shown for acetanilide in Figure 16.2. Because less than 1% of an administered acetanilide dose is metabolized to aniline, relatively little methemoglobin would be formed were it not for the fact that phenylhydroxylamine is regenerated from nitrosobenzene by the reducing action of cellular glutathione (6). The drugs listed in the right-hand column of Table 16.1 also are presumably converted to hydroxylamine metabolites by N-oxidation, as described in Chapter 11. It is not clear why some people are more prone to develop methemoglobinemia than are others. However, it is known that neonates express low levels of functional NADH–diaphorase and are particularly prone to this adverse reaction when treated with methemoglobin-forming drugs (5).

The fact that many of the drugs listed in Table 16.1 incorporate aniline or aniline analogs in their structure is a legacy that, for many drugs, stems from the origin of early pharmaceutical development in the German dye industry. Chloramphenicol, which actually is a natural compound that incorporates a nitrosobenzene moiety (Figure 16.3), causes aplastic anemia in 1 in 20,000–40,000 of individuals who are treated with this antibiotic (8). The exact mechanism by which chloramphenicol causes aplastic anemia is unknown, but also appears to involve the nitroso group, since similar toxicity has not been associated with thiamphenicol, a chloramphenicol analog in which the nitroso group is replaced with a methylsulfone group (Figure 16.3).

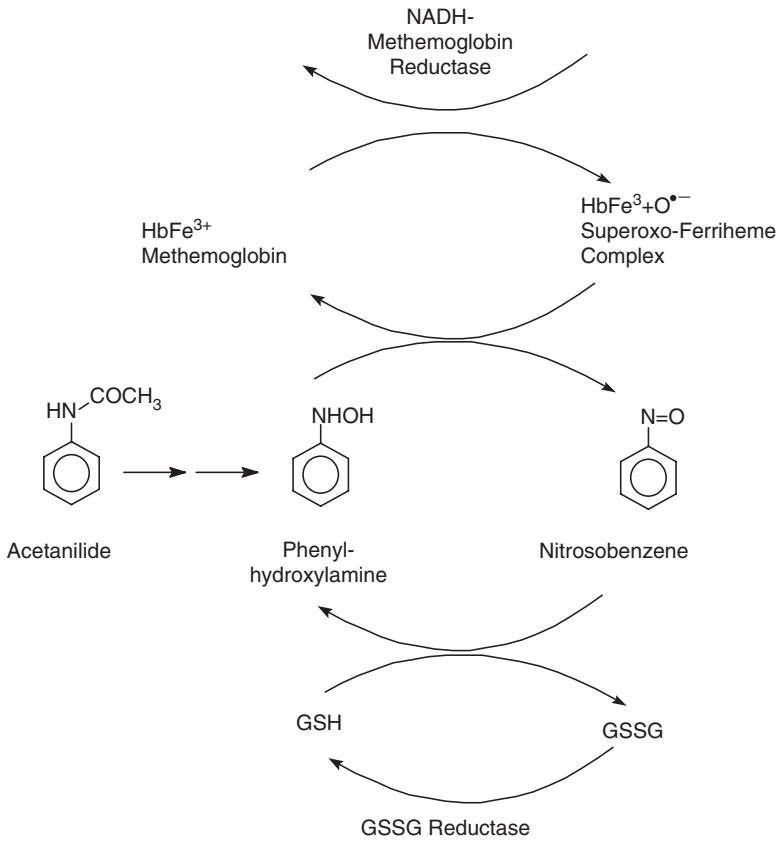

FIGURE 16.2 Cyclic mechanism by which a single molecule of phenylhdroxylamine is able to oxidize several hemoglobin molecules to methemoglobin, thereby overcoming the reductive capacity of NADH-methemoglobin reductase (NADH-diaphorase). Glutathione (GSH) maintains the cycle by reducing nitrosobenzene back to phenylhydroxylamine, and is itself regenerated from the GSSG dimer by the action of GSSG reductase (also called glutathione reductase).

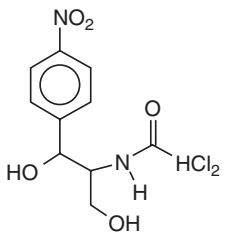

Chloramphenicol

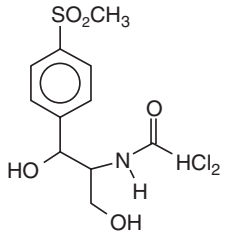

Thiamphenicol

FIGURE 16.3 Chemical structures of chloramphenicol and thiamphenicol. Thiamphenicol, in which the nitroso group of chloramphenicol is replaced by a methylsulfone group, retains antibiotic activity, but does not cause the aplastic anemia that is a major concern with chloramphenicol therapy.

Role of Covalent Binding in Drug Toxicity

With the exception of some anticancer drugs, chemicals directly toxic to tissues are eliminated in the drug development process, so drug toxicity involving covalent binding usually is mediated by chemically reactive metabolites. Current mechanistic understanding of these toxic reactions usually extends to identification of the reactive metabolite and metabolic pathway involved. In some cases, protective mechanisms for scavenging reactive metabolites and metabolite–target protein adducts also have been identified. However, mechanistic information about events linking adduct formation to observed clinical toxicity is lacking in most cases.

A general scheme for adverse reaction mechanisms of this type is shown in Figure 16.4. As was emphasized in Chapter 11, drug-metabolizing enzymes can convert drugs into either inactive, nontoxic compounds or chemically reactive metabolites. Although these reactive metabolites can cause toxic reactions by forming covalent linkages with a variety of macromolecules, in many cases they also can be inactivated by further metabolism and excretion, or by binding to endogenous scavenger molecules such as glutathione. In these cases, there is a metabolic balance between reactive metabolite formation and elimination that may be altered by genetic factors, or perturbed by disease, environmental factors, or concomitant therapy with other drugs.

These reactions are not generally thought of as dose related. However, mass action law considerations dictate that the extent of reactive metabolite formation, and hence adverse reaction risk, will also be a function of drug dosage. It also can be inferred from Figure 16.4 that part of the interindividual

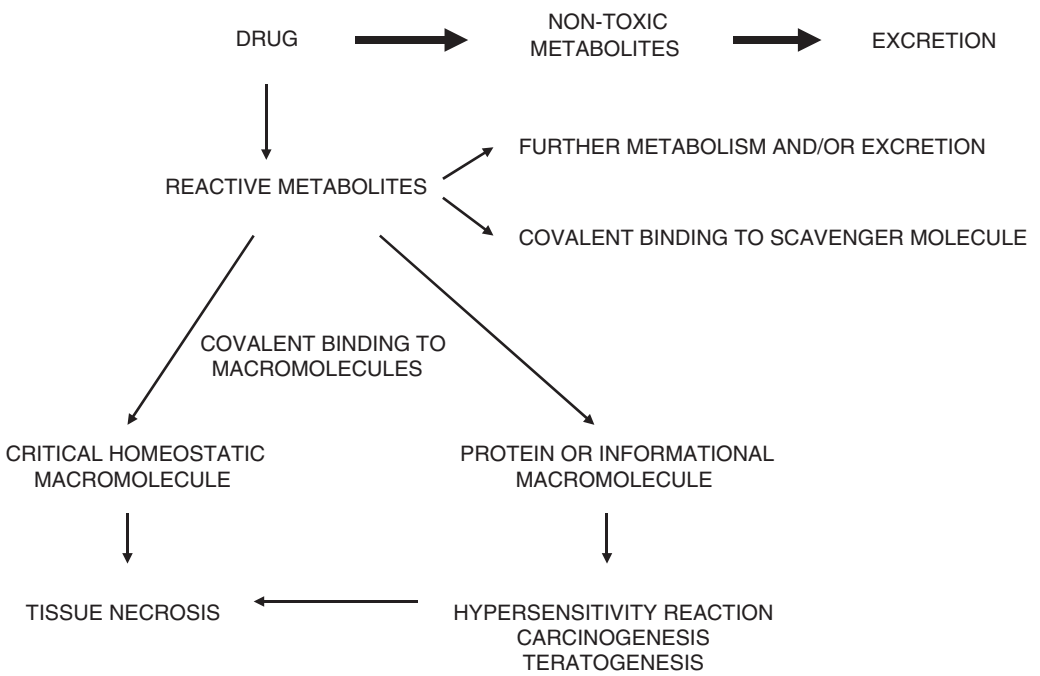

FIGURE 16.4 General scheme for the role played by reactive drug metabolites in causing a variety of adverse reactions. The reactive metabolites usually account for only a small fraction of total drug metabolism and are too unstable to be chemically isolated and analyzed. In many cases, covalent binding of these metabolites to tissue macromolecules only occurs after their formation exceeds a critical threshold that overcomes host detoxification and repair mechanisms.

variability in incidence of these reactions reflects varying activity in the parallel pathways involved in metabolizing drugs to either nontoxic or reactive metabolites. In some cases, it has been possible to actually relate the risk of an adverse drug reaction to polymorphic drug-metabolizing phenotype.

DRUG-INDUCED LIVER TOXICITY

Few areas have been as confusing to clinicians as is the perplexing array of adverse drug reactions affecting the liver. Given the central role that the liver plays in drug metabolism, it is not surprising that many drugs are converted to compounds that cause liver damage. In fact, liver injury has been estimated to be the principal safety reason for terminating clinical trials during drug development and for withdrawing marketed drugs (9). Traditional classifications of drug hepatotoxicity, such as that shown in Table 16.2, have been based on descriptions of observed histopathology rather than on an understanding of the basic mechanism involved (10). We focus the discussion here on representative adverse reactions that damage the liver either through covalent binding of a reactive metabolite or through an idiosyncratic mechanism.

TABLE 16.2 Classification of Drug-Induced Liver Toxicity

I. Hepatocellular necrosis
A. Zonal necrosis (CCl_4 type)
CCl_4
Halogenated benzenes
Acetaminophen
B. Viral hepatitis-like (cincophen type)
Isoniazid
Iproniazid
Halothane
II. Uncomplicated cholestasis (steroid type)
Anabolic steroids
Estrogens
III. Nonspecific hepatitis with cholestasis (chlorpromazine type)
Phenothiazines
Isoniazid
Erythromycin estolate
IV. Drug-induced steatosis
Tetracycline

Hepatotoxic Reactions Resulting from Covalent Binding of Reactive Metabolites

A major advance in our understanding of the role of covalent binding of reactive metabolites in causing hepatotoxic drug reactions was provided by Brodie and his co-workers in 1971 (11). These investigators administered ^{14}C-labeled bromobenzene to rats and showed that the radioactivity was localized to centrilobular hepatocytes in the region of greatest liver damage and could not be removed from this area by washing the tissue with solvents. Binding did not occur when the bromobenzene was added directly to liver slices *in vitro*, but binding after *in vivo* administration was enhanced when rats were pretreated with phenobarbital, and was reduced when they were pretreated with SKF-525A, an inhibitor of drug metabolism. The conclusion was drawn that bromobenzene was being converted to an active arene oxide metabolite that was the proximate hepatotoxin (Figure 16.5). It was subsequently shown that detoxifying enzymes and glutathione played an important protective role in removing this arene oxide before it could react covalently with liver macromolecules (12).

Acetaminophen

A pattern of liver necrosis similar to that caused by bromobenzene is observed in patients who ingest massive doses of acetaminophen (Table 16.2). This toxic reaction also has been produced experimentally in mice and rats and is thought to occur in two phases. An initial metabolic phase in which acetaminophen is converted to a reactive iminoquinone metabolite is followed by an oxidation phase in which an abrupt increase in mitochondrial permeability, termed *mitochondrial permeability transition* (MPT), leads to the release of superoxide and the generation of oxidizing nitrogen and peroxide species that result in hepatocellular necrosis (13, 14).

After therapeutic doses, acetaminophen is primarily converted to inactive glucuronide and sulfate conjugates. However, as was shown in Scheme 11.4 (Chapter 11), a small amount of acetaminophen is oxidized by CYP2E1, CYP1A2, and CYP3A4 to *N*-acetyl-*p*-benzoquinoneimine (NAPQI) (15), which is chemically reactive and is scavenged by conjugation with glutathione (16). In the setting of an acetaminophen overdose, when NAPQI formation is sufficient to deplete more than 70% of hepatic glutathione, excess NAPQI now binds covalently to cysteine residues on proteins (16). The *in vitro* demonstration that exogenous sulfhydryl donors can

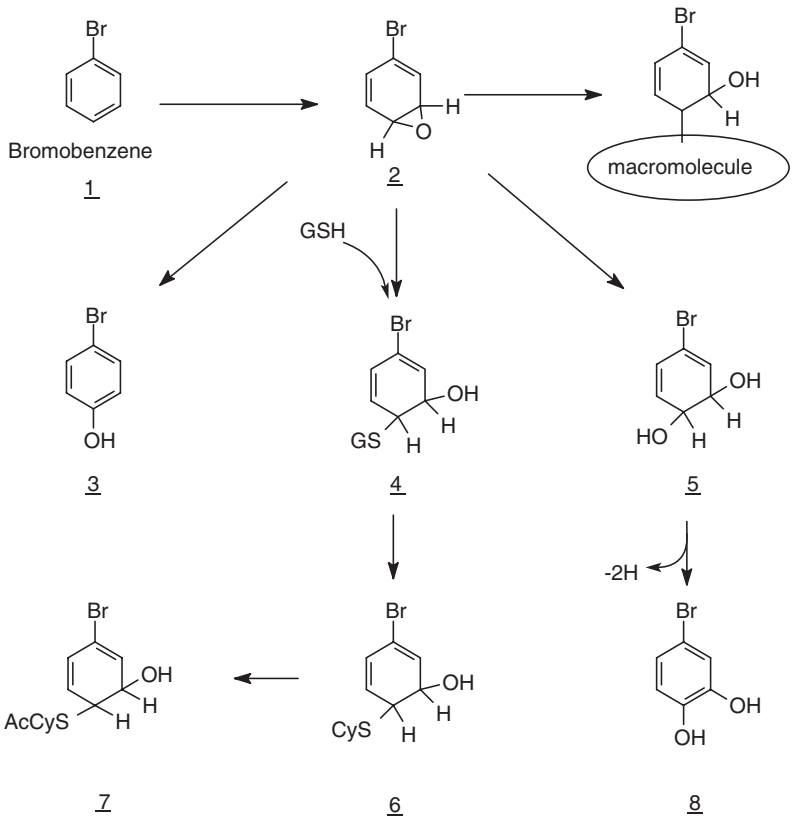

FIGURE 16.5 Metabolism of bromobenzene (**1**) to a chemically reactive epoxide (arene oxide) metabolite (**2**) that can then either bind covalently to nearby macromolecules, be scavenged by glutathione (GSH) (**4**) and be further metabolized (**6**, **7**), or be converted nonenzymatically or by epoxide hydrolase to stable hydroxylated metabolites (**3**, **5**, **8**).

minimize NAPQI adduct formation and hepatotoxicity (17) has provided the rationale for the clinical use of *N*-acetylcysteine to treat patients after acetaminophen overdose (18).

On the other hand, when transgenic mice with the humanized constitutive androstane receptor (hCAR) were treated with phenobarbital or even acetaminophen, CYP1A2 and CYP3A11 (the murine equivalent of CYP3A4) expression increased and the animals were more sensitive to acetaminophen hepatotoxicity (15). Activation of the pregnane X receptor (PXR) also induced CYP3A11 activity in mice and augmented NAPQI formation and acetaminophen toxicity (19). Presumably, induction of CYP2E1-mediated NAPQI formation by ethanol explains the increased susceptibility of alcoholic patients to acetaminophen hepatotoxicity. An unexplained paradox is that mice lacking glutathione *S*-transferase Pi (GSTπ) have increased resistance to acetaminophen hepatotoxicity (20). Because the extent of NAPQI–protein adduct formation and glutathione depletion is similar in wild-type and *GSTπ* null mice, this gene must exert its effect at a subsequent phase of the hepatotoxic process. In that regard, GSH regeneration was found to be more rapid in *GSTπ* null than in wild-type mice.

Although a number of NAPQI–hepatic protein adducts have been identified, it has been difficult to identify the hepatic macromolecules that are the critical targets (21, 22). However, there is recent experimental evidence that NAPQI leads to MPT by binding to a thiol moiety in the multiple conductance channel, or pore, of mitochondria (13, 14). Addition of the reducing agent dithothreitol in a mouse hepatocyte model of the second phase of acetaminophen toxicity completely prevents MPT and the subsequent oxidative events leading to hepatotoxicity (14). Cyclosporine A, which associates with cyclophilin D in the MPT pore, also has been shown to be protective. Although the reaction of NAPQI with GSH and protein sulfhydryl groups is very rapid, there is a delay of several hours before MPT occurs. In part, this delay appears to represent events involved in the migration of NAPQI from its site of microsomal formation to the

mitochondrial compartment. A novel *ipso* adduct of NAPQI, formed by nucleophilic addition of GSH to the NAPQI double bond (see Chapter 11, Scheme 11.4), has been identified that could serve as a quasi-stable intermediate, enabling this migration to occur without adduct formation with intervening cytosolic proteins (23). Base-catalyzed elimination of GSH in the vicinity of the mitochondrial pore would reform NAPQI, resulting in adduct formation with pore protein sulfhydryl groups.

Finally, there is evidence that Kupffer cells are a source of the anti-inflammatory cytokine interleukin-10 (IL-10) that may play an important protective role by minimizing formation of reactive nitrogen species when superoxide is released following MPT (24). Pro-inflammatory cytokines (e.g., macrophage migration inhibitory factor) may exacerbate hepatocellular necrosis, whereas chemokines (e.g., monocyte chemoattractant protein-1) appear to reduce the extent of hepatotoxicity and facilitate eventual hepatocyte regeneration in surviving patients (13).

Isoniazid

The widespread use of isoniazid prophylaxis for tuberculosis has focused attention on the liver injury caused by this drug. About 20% of patients treated with isoniazid will show elevated blood concentrations of liver enzymes and bilirubin that subside as treatment is continued (25). However, clinical hepatitis develops in some patients, and these reactions can prove fatal. Current understanding of the mechanism of isoniazid-induced hepatotoxicity is based on the metabolic pathways shown in Figure 16.6 (26, 27). It has been demonstrated in an animal model that hepatotoxicity is correlated with plasma concentrations of hydrazine but not of acetylhydrazine or isoniazid (28), and that pretreatment with an amidase inhibitor can prevent toxicity (27). However, it is postulated that hydrazine is further metabolized to a chemically reactive hepatotoxin by the cytochrome P450 system, and *in vitro* studies with hepatocytes have implicated CYP2E1 as the cytochrome P450 isoform responsible for cytotoxic metabolite formation (29).

A number of features of isoniazid hepatotoxicity can be interpreted by reference to the metabolic scheme shown in Figure 16.6. First, phenotypic slow acetylators are more prone to liver damage than are rapid acetylators (Table 16.3) (30). Not only were hydrazine plasma concentrations higher in slow acetylators than in rapid acetylators treated with isoniazid for 14 days (31), but, in another study, urine excretion of hydrazine was higher in slow than in rapid acetylators, whereas urine excretion of acetylhydrazine and diacetylhydrazine was lower (32). A study utilizing *NAT2* genotyping confirmed that individuals with slow acetylator genotypes have a significantly higher risk of developing antituberculosis drug-induced hepatitis than do those with rapid acetylator genotypes (OR: 2.87 vs. 0.35), and further demonstrated that slow acetylators are more likely to develop severe hepatic injury, compared to rapid acetylators (33). Second, it has been shown that patients with wild-type CYP2E1 (CYP2E1 c1/c1) have a higher rate of antituberculosis drug-induced hepatitis than do those whose enzyme incorporates the variant c2 allele (34). Although there was no difference in the basal activity of the CYP2E1 genotypes, isoniazid inhibited CYP2E1 c1/c1 to a lesser extent than it did enzymes containing the variant allele. Thus, individuals with wild-type CYP2E1 would be expected to have an increased formation rate of the postulated reactive hepatotoxic metabolite. Induction of CYP2E1 by ethyl alcohol also appears to account for the increased incidence of liver damage in alcoholic patients who are treated with isoniazid. In fact, the protective benefit of the rapid acetylator phenotype is no longer apparent in this group of patients (30).

TABLE 16.3 Age and Aetylator Phenotype Affect % Risk of Isoniazid-Induced Hepatitis[a]

	Acetylator phenotype	
Age (years)	**Fast**	**Slow**
<35	3.7%	13.0%
≥35	13.2%	37.0%

[a] Data from Dickinson DS *et al*. J Clin Gastroenterol 1981;3:271–9.

Despite these advances in our understanding of the risk factors that predispose to isoniazid-induced hepatotoxicity, it remains unclear whether age, the predominant risk factor (Table 16.3), exerts its effects either on isoniazid metabolism or on protective mechanisms that as yet remain undefined. Clearly, more work is needed in this area, especially because understanding the biochemical basis of these risk factors plays a central role in developing guidelines for using isoniazid for chemoprophylaxis of tuberculosis (35).

Immunologically Mediated Hepatotoxic Reactions

Immune mechanisms also play a prominent role in some hepatotoxic adverse drug reactions (36). Because a minimum molecular weight of 1000 Da generally is

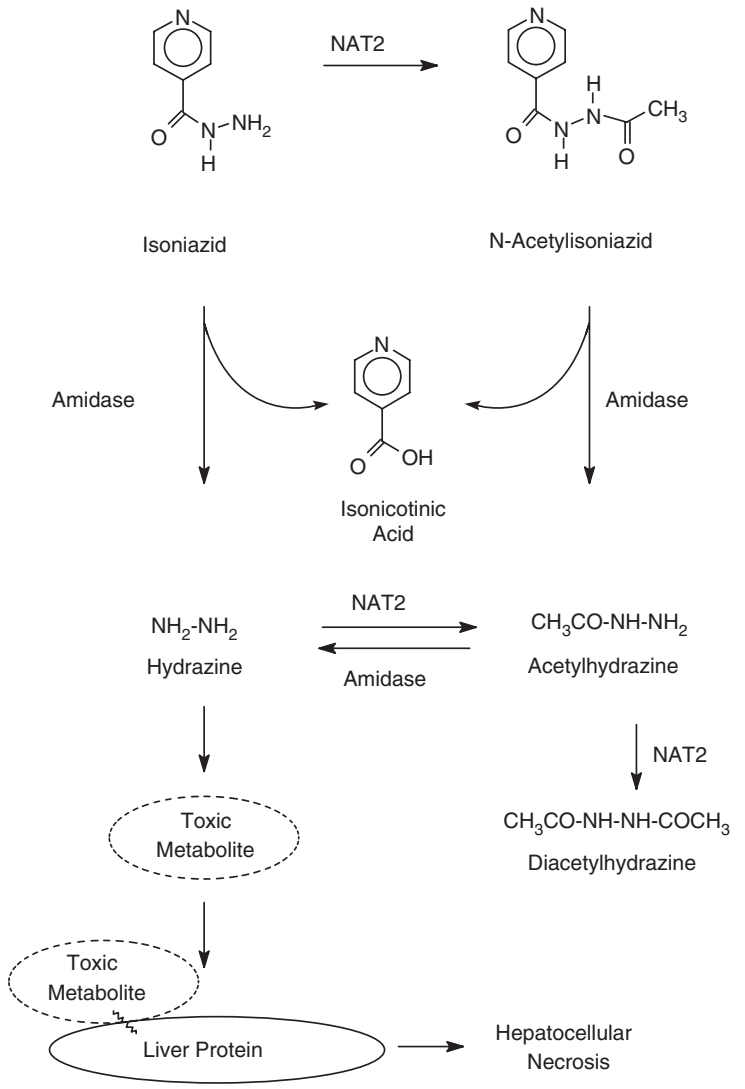

FIGURE 16.6 Metabolism of isoniazid to hydrazine, which is then activated by cytochrome P450 enzymes to a chemically reactive metabolite. *N*-Acetyltransferase (NAT2) acts at several points in this scheme to reduce hydrazine concentrations. This accounts for the fact that rapid acetylators are less likely than slow acetylators to develop isoniazid-induced hepatitis. On the other hand, chronic alcohol consumption induces cytochrome P450 enzymes, thereby increasing the extent of toxic metabolite formation from hydrazine and the risk of hepatitis.

needed for a molecule to elicit an immune response, most drugs elicit immune responses by functioning as haptens. In most cases this entails initial formation of a chemically reactive metabolite that then binds covalently to a macromolecule to form a neoantigen. The reactive metabolite may in some cases function as a direct hepatotoxin as well as an immunogen (37) (see Figure 16.4). The enzyme that metabolizes the drug may be among the macromolecular targets and may subsequently be inactivated by the reactive metabolite, a phenomenon referred to as *suicide inhibition*. After transport of the neoantigen to the cell membrane, humoral or cellular immune responses are triggered and result in hepatocellular damage.

Traditionally, immune mediated toxicity has been suspected on clinical grounds, such as the presence of fever, rash, an eosinophil response, a delay between exposure to the toxin and the onset of clinical symptoms, and the accelerated recurrence of symptoms and signs of toxicity after readministration

of the drug (38). However, recent investigations have began to provide a framework for understanding the mechanism of these reactions.

Halothane

Halothane is a volatile general anesthetic that was introduced into the practice of clinical anesthesia in 1956. Shortly after its introduction, two forms of hepatic injury were noted to occur in patients who received halothane anesthesia. A subclinical increase in blood concentration of transaminase enzymes is observed in 20% of patients and has been attributed to lipid peroxidation caused by the free radical formed by reductive metabolism of halothane, as shown in Figure 16.7 (39, 40). The second form of toxicity is a potentially fatal hepatitis-like reaction that is characterized by severe hepatocellular necrosis and is thought to be initiated by the oxidative formation of trifluoroacetyl chloride (Figure 16.7). Fatal hepatic necrosis occurs in only 1 of 35,000 patients exposed to halothane, but the risk of this adverse event is greater in females and is increased with repeat exposure, obesity, and advancing age (40). Because the onset of halothane hepatitis is delayed but is more frequent and occurs more rapidly following multiple exposures, and because these patients usually are febrile and demonstrate eosinophilia, this reaction is suspected of having an immunologic basis. This hypothesis is strengthened by the finding that serum from patients with halothane hepatitis contains antibodies that react specifically with the cell membrane of hepatocytes harvested from halothane-anesthetized rabbits, rendering them susceptible to the cytotoxic effects of normal lymphocytes (38).

Satoh *et al*. (41) have further elucidated the mechanism of halothane hepatitis by demonstrating that the reactive acyl chloride metabolite shown in Figure 16.7 binds covalently to the surface membranes of hepatocytes of rats injected with halothane. Among the macromolecular targets of this metabolite is CYP2E1. This is the cytochrome P450 isoform that predominates in forming trifluoroacetyl chloride from halothane, and 45% of patients with halothane hepatitis form autoantibodies against CYP2E1 as well as antibodies against neoantigens formed by this reaction (42). A number of other macromolecular targets are located in the endoplasmic reticulum, where they appear to act as chaperones involved in protein folding (43). At present, it is not certain that these antibodies play a pathogenetic role in halothane hepatitis, and it is possible that cell-mediated immune mechanisms might be of greater importance. In that regard, Furst *et al*. (44) have demonstrated that Kupffer cells are involved as antigen-presenting cells in a guinea pig model of halothane hepatitis.

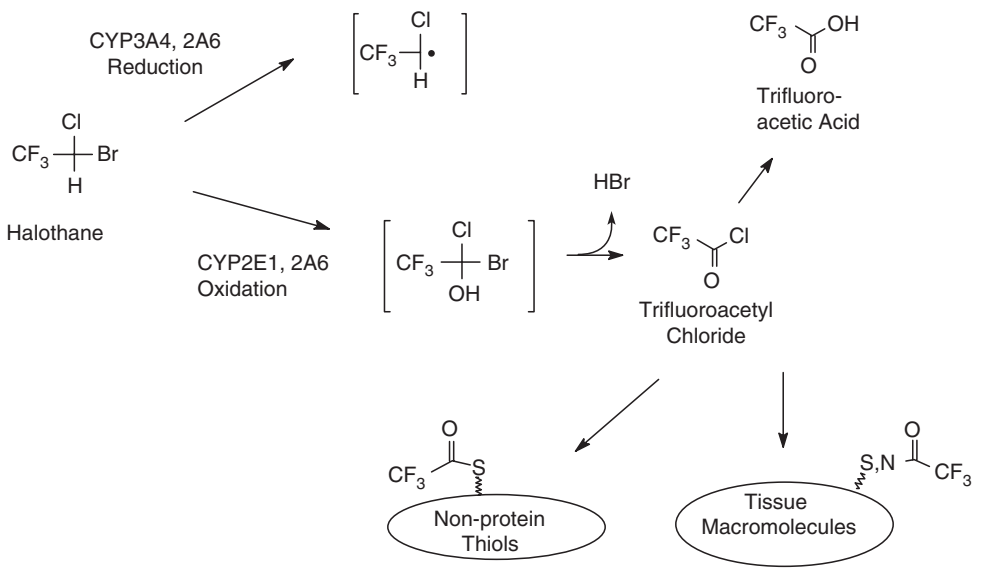

FIGURE 16.7 Oxidation of halothane by CYP2E1 leads to formation of trifluoroacetyl chloride, which can be nonenzymatically converted to trifluoroacetic acid, can be scavenged by glutathione, or can bind covalently to tissue macromolecules, thereby causing liver damage. A reductive metabolic pathway generates free radicals that cause lipid peroxidation, but this pathway does not appear to be involved in the pathogenesis of halothane hepatitis.

It is not clear why so few patients who receive halothane anesthesia are prone to develop hepatitis. Eliasson *et al*. (45) propose that patient risk reflects alterations in the balance between the activity of CYP2E1, which they found to vary by 30-fold in human liver samples, and the protective ability of glutathione and other nonprotein thiols to scavenge trifluoroacetyl chloride (Figure 16.7). This would explain the increased risk of halothane hepatitis in obese subjects, who have elevated activities of CYP2E1, and older individuals, in whom hepatic glutathione levels may be decreased. In this regard, Kharasch *et al*. (46) have found that patients treated before halothane anesthesia with disulfiram, a specific CYP2E1 inhibitor, formed less trifluoroacetic acid than did those who received no pretreatment. These investigators demonstrated in subsequent animal studies that disulfiram pretreatment also reduced formation of trifluoroacetylated protein adducts, lending support to their hypothesis that a single pre-anesthetic dose of disulfiram might block formation of the neoantigens responsible for immune sensitization and thereby provide effective prophylaxis against halothane hepatitis (47).

Tienilic Acid

Tienilic acid (ticrynafen) is a uricosuric diuretic that was initially marketed in the United States in 1979. It was withdrawn a few months later because of hepatitis-like adverse reactions that developed in approximately 1 of 1000 patients treated with the drug but were fatal in 10% of the patients who developed overt jaundice (48). The onset of overt toxicity generally occurred 1 to 6 months after starting therapy with tienilic acid, and fever, rash, and eosinophilia were reported in some of the patients. These findings led investigators to suspect an immunologic basis for this adverse reaction.

Beaune *et al*. (49) found that the serum of patients with tienilic acid-induced hepatitis contained antimicrosomal antibodies that inhibited formation of the 5-hydroxy metabolite of tienilic acid (Figure 16.8). These antibodies are specifically directed to the CYP2C9 isoenzyme that metabolizes tienilic acid and to the neoantigen formed by covalent binding of this isoenzyme with the presumed thiophene sulfoxide reactive intermediate shown in Figure 16.8 (50, 51), and a three-site conformational epitope that reacts with autoantibodies in sera from patients with tienilic acid-induced hepatitis has been identified near the active site of CYP2C9 (52). This specificity of antibody formation is in contrast with the spectrum of antibodies that are formed after halothane exposure, suggesting that the reactive metabolite formed from tienilic acid is so unstable that it reacts primarily with the enzyme that forms it. In that regard, site-directed mutagenesis has been used to replace serine in the 365 position of CYP2C9 with alanine (53). The resultant Ser395Ala mutant retained the enzymatic ability to hydroxylate tienilic acid without being inactivated, strongly suggesting that the serine hydroxyl group is the nucleophilic target for the postulated electrophilic intermediate shown in Figure 16.8.

Robin *et al*. (50) have shown in a rat model that both unaltered CYP2C11, the analog of CYP2C9 in humans, and the CYP2C11 adduct formed after tienilic acid exposure migrate from the endoplasmic reticulum to the plasma membrane by a microtubule-dependent vesicular route. However, plasma

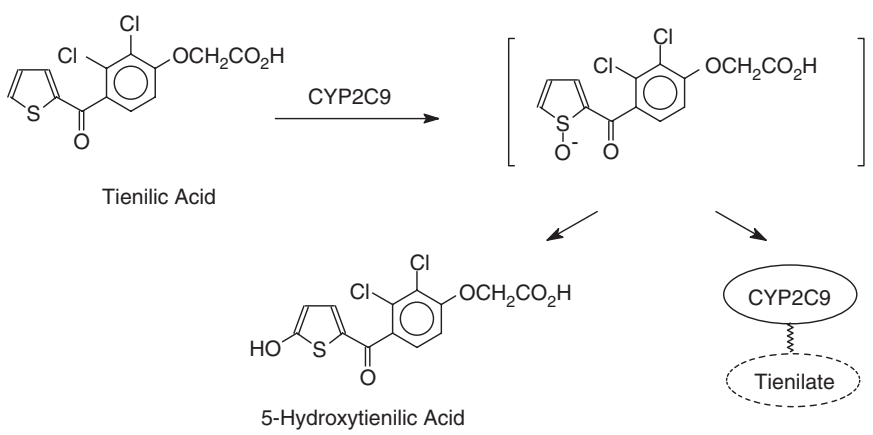

FIGURE 16.8 Oxidation of tienilic acid by CYP2C9 to an unstable electrophilic thiophene sulfoxide, which binds specifically with CYP2C9 to form a haptenic conjugate or reacts with water to form 5-hydroxytienilic acid.

membrane expression of the adduct is more prolonged than is that of CYP2C11. These authors hypothesize that the immune reaction in tienilic acid hepatitis is directed against both CYP2C9 and alkylated CYP2C9 that are expressed on the plasma membrane of hepatocytes. As yet unknown are the relative roles played by antibody and cell-mediated mechanisms in mediating the hepatotoxicity that occurs subsequent to immune recognition (52).

MECHANISMS OF OTHER DRUG TOXICITIES

Although little is known about the mechanism of many drug toxic reactions, it is likely that covalent binding mediates many of them. Small alterations in chemical structure also may result in quite different patterns of organ involvement in drug toxic reactions. Mitchell *et al*. (54) have shown that mice treated with large doses of furosemide develop hepatocellular necrosis, presumably due to epoxidation of the furan ring (Figure 16.9). However, these investigators found that furan and several closely related furan congeners also may cause toxic reactions in the kidney and lung, as shown in Table 16.4 (55). In some cases, the site of toxicity could be shifted from one organ to another by pretreatment with agents (such as phenobarbital) that alter the activity of drug-metabolizing enzymes. In each case, the presumed reactive metabolite was a furan epoxide analogous to that shown for furosemide in Figure 16.9. Similarly, *in situ* metabolism of acetaminophen by kidney microsomal enzymes occurs by the same pathways shown in Chapter 11, Scheme 11.4, and is responsible for causing acute renal tubular necrosis (56).

These observations underscore the importance of extrahepatic drug metabolism, because toxic reactions targeting organs other than the liver probably reflect the formation of reactive metabolites in these tissues, rather than the peripheral effects of toxic metabolites formed in the liver. Tissue-specific differences in protective mechanisms may also underlie the organ specificity of some adverse drug reactions. Chemically reactive metabolites not only are involved in the pathogenesis of localized tissue or organ cytotoxic reactions but also play an important role in mediating adverse drug reactions that are characterized by systemic manifestations of hypersensitivity, as well as carcinogenic and teratogenic adverse reactions.

TABLE 16.4 Predominant Sites of Toxicity Caused by Furan Analogs[a]

Liver	Kidney	Lung
Furan	Furan	Ipomeanol
Furosemide	2-Ethylfuran	
2-Furamide	2,3-Benzofuran	
2-Acetylfuran	2-Furoic acid	
2-Furfurol	3-Furoic acid	
2-Ethyl furoate		
2-Methoxyfuran		
Dibenzofuran		

[a] Data in mice and rats from Mitchell JR *et al*. Nature 1974;251:508–10.

Systemic Reactions Resulting from Drug Allergy

Only recently has there been appreciation of the important role of immune mechanisms in mediating hepatotoxicity and other organ-specific damage. However, anaphylaxis and other systemic reactions traditionally associated with drug allergy also usually entail covalent binding of a drug or reactive drug metabolite to form multivalent hapten–carrier complexes. Exceptions to this general rule are insulin,

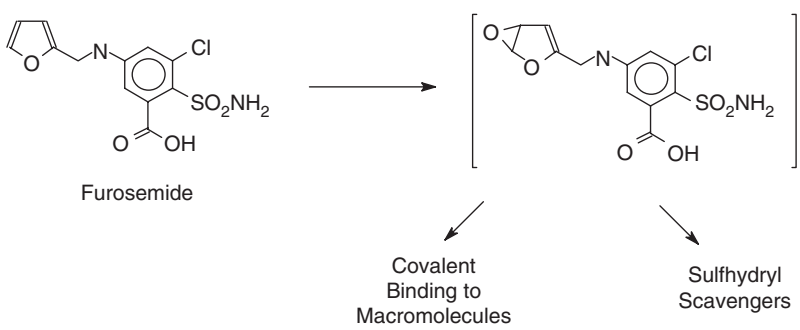

FIGURE 16.9 Proposed metabolism of furosemide to a chemically reactive furanic epoxide.

dextran, and other macromolecules, and quaternary ammonium compounds that have multiple copies of a single epitope (57).

Allergic Reactions to Penicillin

Allergic reactions to penicillin are a common cause of allergic drug reactions and have been reported in various studies to occur in 0.7–8% of patients treated with this drug (58). As shown in Table 16.5, the spectrum of allergic reactions to penicillin spans all four categories of the Gell and Coombs classification that is described in Chapter 25. Anaphylaxis is the most serious of these reactions. It occurs in about 0.01% of patients who receive penicillin and has a fatality rate of 9% (59). Penicillin-induced cytopenias, interstitial nephritis, and serum sickness reactions occur more frequently with prolonged high-dose therapy (60). Contact dermatitis occurs primarily after cutaneous exposure to penicillin, but is infrequent in patients, since topical penicillin formulations have been discontinued. Consequently, it occurs primarily in nurses, pharmacists, and others whose skin comes in repeated contact with the drug.

Penicillin is unusual in that it forms immunogenic hapten–carrier complexes by binding directly to macromolecules in plasma and on cell surfaces (Figure 16.10). But even though prior metabolic activation is not required, it has been found that hapten formation is facilitated by one or more low molecular weight serum factors (58). Conversely, the haptenation of penicillin–protein conjugates has been shown to be reversible, although the specific enzymes mediating this have not been identified (61). The penicilloyl–protein conjugate constitutes more than 90% of the haptenic products and is the major antigenic determinant for the formation of penicillin-specific immunoglobulins and T-cells (62). This antigenic determinant is involved in 75% of IgE-mediated allergic reactions and most of the other reactions shown in Table 16.5. Although the minor antigenic determinants are present only in low abundance, they play an important role in some IgE-mediated reactions. The extent of hapten formation and the probability of eliciting a penicillin-specific immune response appear to increase as a function of the cumulative penicillin dose (63). In one study, 50% of patients who received at least 2 g of penicillin for 10 days had an IgG and/or an IgE antibody response (60).

TABLE 16.5 Representative Immune-Mediated Reactions to Penicillin

Gell and Coombs type[a]	Mechanism	Clinical presentation
I	IgE-mediated	Anaphylaxis, uticaria
II	IgG or IgM mediated, complement-dependent cytolysis	Hemolytic anemia, thrombocytopenia, interstitial nephritis
III	Immune complex mediated, complement dependent	Serum sickness, drug fever, vasculitis
IV	T-cell lymphocyte mediated	Contact dermatitis, morbilliform skin rash

[a] Gell PGH, Coombs RRA. Clinical aspects of immunology. Oxford: Blackwell; 1963.

The likelihood that haptenic products are formed in everyone who receives penicillin, and the frequency with which penicillin-specific antibody responses occur, stand in marked contrast to the infrequent occurrence of allergic reactions to this drug. The cumulative risk of penicillin allergy appears to be related to the persistence of penicillin-specific antibodies, with the half-life of pencilloyl IgE antibodies reported to range from 10 to more than 1000 days (60). In this regard, dehaptenation was noted to be slower than normal in penicillin-allergic patients (61). Although it has been found that penicillin allergic reactions are less common in the young, it is not clear whether youth is an independent protective factor or simply reflects the fact that the young are likely to have had less cumulative exposure to penicillin. Other constitutional or genetic factors are also likely to be important determinants of individual proclivity to develop allergic reactions to penicillin and other drugs.

In clinical practice, both a history of prior penicillin allergy and skin testing can be used to identify individuals at risk for penicillin allergic reactions. These approaches were compared in a National Institute of Allergy and Infectious Diseases-sponsored study of 1539 hospitalized patients in whom penicillin therapy was indicated (64). Patients received skin tests both with benzylpenicilloyl-octalysine, to determine major determinant reactivity, and with a minor determinant mixture of benzylpenicillin, benzylpenicilloate, and benzylpenicilloyl-*N*-propylamine. Of the positive skin test reactors, 84% had major determinant reactivity and the remaining 16% had positive tests with only the minor determinant mixture. As shown in Table 16.6, most patients with a negative history also had negative skin tests, and none of these patients had an allergic reaction to penicillin. A substantial percentage of patients with a history of penicillin allergy were found to have negative skin tests. Penicillin

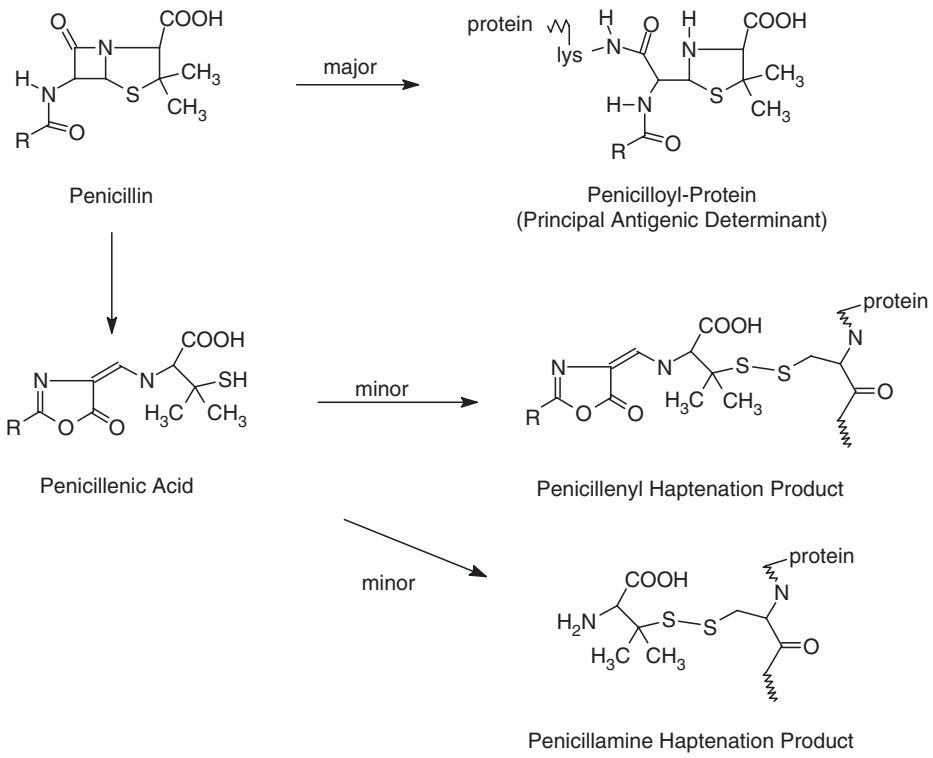

FIGURE 16.10 Hapten determinants formed by penicillins that contain a β-lactam ring linked to various side chains (R). The primary route of haptenation involves acylation of the ε-amino group of lysine residues of serum or cell surface proteins to form a penicilloyl or major antigenic determinant. Isomerization of penicillin leads to the generation of compounds that form disulfide bonds with the cysteine sulfhydryl groups of proteins. These epitopes are termed minor determinants.

therapy of patients with a positive or unknown history of penicillin allergy but negative skin tests resulted in a 1.3% incidence of immediate or accelerated IgE-mediated allergic reactions. Most patients with positive skin tests were treated with other antibiotics, but two of the nine individuals who received penicillin had immediate or accelerated allergic reactions and two others developed rashes on days 3 and 9 of penicillin-therapy, respectively. Because primary reliance is placed on history to identify penicillin-allergic individuals, it would appear that the patients at greatest risk are the 4% of history-negative patients who nonetheless react to skin testing.

TABLE 16.6 Comparison of Allergy History with Penicillin Skin Test Results[a]

	Allergy history	
Skin test	**Positive**	**Negative**
Positive	18%	4%
Negative	80%	95%
Uninterpretable	3%	1%

[a] Data from Sogn DD *et al*. Arch Intern Med 1992;152:1025–32.

Procainamide-Induced Lupus

Although a number of drugs are capable of inducing a systemic lupus erythematosus-like reaction, procainamide is the most common cause of drug-related lupus. Kosowski *et al*. (65) found that all patients treated with procainamide for more than a year developed antinuclear antibodies, but that procainamide-induced lupus occurred in slightly less than one-third of those who began therapy. The fact that procainamide contains an aniline moiety, similar to many drugs that cause methemoglobinemia, led to initial speculation that its N-acetylated metabolite (NAPA) might have antiarrhythmic efficacy but would be less likely to cause this adverse effect (Figure 16.11) (66). This was first demonstrated by switching a patient with procainamide-induced lupus to NAPA, whereupon both the arthralgic symptoms of drug-induced lupus and antinuclear antibody

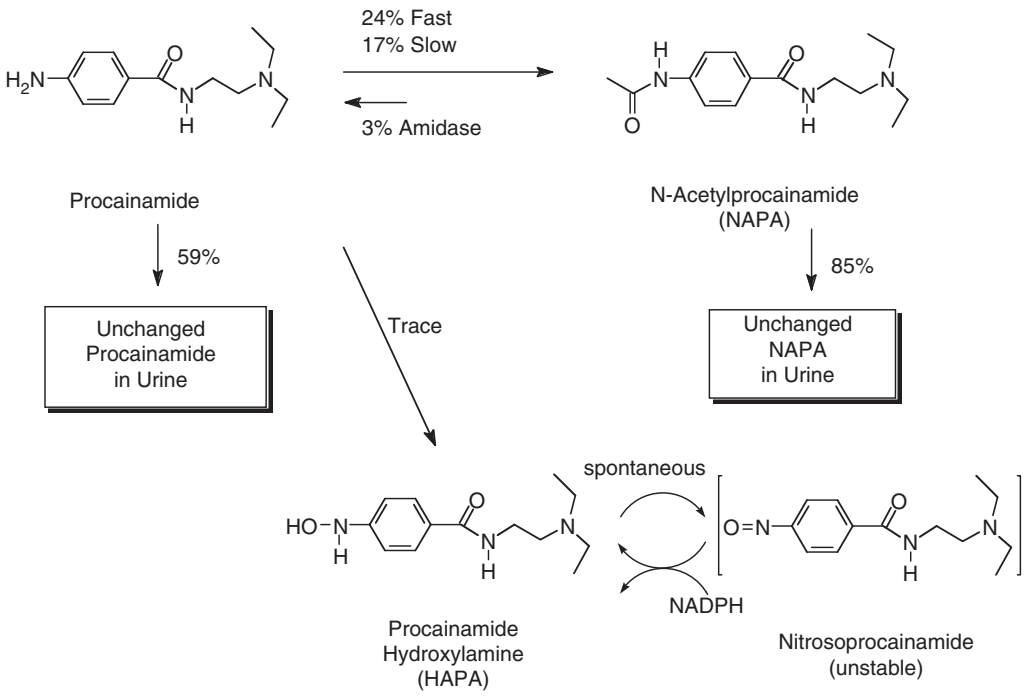

FIGURE 16.11 Simplified scheme of procainamide metabolism. In individuals with normal kidney function, renal excretion of unchanged drug accounts for more than half the elimination of a procainamide dose, whereas acetylation by NAT2 accounts for only 24% and 17% of elimination in rapid and slow acetylators, respectively. A small amount is of procainamide is metabolized to a hydroxylamine, which is in equilibrium with a postulated chemically unstable and reactive nitroso compound that is capable of haptenic binding to histone proteins.

titers returned to normal (67). Subsequent confirmation was provided by long-term studies in which patients received effective antiarrhythmic therapy with NAPA without developing this reaction (68, 69). However, the immunologic safety of NAPA is relative rather than absolute, because approximately 3% of an administered NAPA dose is converted to procainamide by deacetylation (Figure 16.11) (70). In this regard, Kluger *et al*. (68) described a patient who developed drug-induced lupus when treated with NAPA doses sufficient to produce plasma procainamide concentrations of 1.6 μg/mL. The fact that these symptoms subsided when the NAPA dose was reduced, so that procainamide levels fell to 0.7 μg/mL, suggests that there is a threshold procainamide level that must be exceeded before this toxic reaction occurs.

Uetrecht (71) provided further evidence that the arylamine group of procainamide is implicated in the development of drug-induced lupus by demonstrating that procainamide is metabolized to a hydroxylamine (HAPA) (Figure 16.11). HAPA is in equilibrium with a chemically unstable nitroso compound that is capable of covalent binding to histones and other proteins and, by rendering them antigenic, may initiate the immune reaction leading to procainamide-induced lupus (72). Although hepatic CYP2D6 is capable of forming HAPA from procainamide (73), it is likely that the relevant reactive metabolites are generated by myeloperoxidase within activated neutrophils or monocytes (72, 74). Based on studies in which HAPA but not procainamide prevented the induction of anergy in murine T-cells, Kretz-Rommel and Rubin (75) concluded that covalent binding of HAPA to histones does not occur. However, their results supported the alternative possibility that the redox cycling of nitrosoprocainamide and HAPA (Figure 16.11) interferes with the redox-linked pathway involved in T-cell activation. Their further investigations with murine thymocytes demonstrated that exposure to HAPA interferes with the positive selection process by which these cells acquire unresponsiveness to self-antigens during their maturation to T-cells (76). Subsequent export of these autoreactive T-cells from the thymus would then have the potential to break B-cell tolerance and result in systemic autoimmunity.

In a prospective study of procainamide-treated patients, Rubin *et al*. (77) had previously found that serum IgG, IgM, and IgA autoantibodies against

histone, single-stranded DNA, and the [(H2A-H2B)-DNA] complex appeared after an average of 7 months of procainamide therapy. The (H2A-H2B) dimer is a component of the histone octamer (78), and it is of particular interest that 16 of the 19 patients in this study who were destined to develop procainamide-induced lupus developed high titers of IgG autoantibodies to the [(H2A-H2B)-DNA] complex. By contrast, only two of the nine asymptomatic patients were found to have IgG anti-[(H2A-H2B)-DNA] activity that was, at most, only 3% of that measured in the symptomatic patients. Although the effect of PAHA exposure on T-cell maturation is not antigen specific, the predominance of autoantibodies to histones is presumed to reflect the fact that chromatin contains the most abundant self-peptides that T-cells encounter during positive selection (76).

Similar antibodies are found in patients with systemic lupus erythematosus and it has been proposed that lupus nephritis results from IgG binding to [(H2A-H2B)-DNA] in nucleosomal material that is deposited in the glomerulus by the circulation (78). Because renal involvement is not a feature of drug-induced lupus, it appears that factors other than antibody binding to [(H2A-H2B)-DNA] are responsible for nephritis. However, the systemic symptoms of drug-induced lupus may result from inflammatory mechanisms involved in the clearance of immune complexes.

Carcinogenic Reactions to Drugs

It has been realized that chemicals can cause cancer since 1775, when Percival Potts observed a high incidence of scrotal cancer in chimney sweeps (79). Despite intensive study, much remains to be learned about the mechanistic details of chemical carcinogenesis, of which drug-induced carcinogenesis is a subcategory. Since 1969, the International Agency for Research on Cancer (IARC) has conducted an evaluation of the carcinogenic risk of pharmaceuticals, assigning them to five groups based on the strength of evidence linking compounds to carcinogenesis (80). Table 16.7 lists pharmaceuticals that are regarded as being either carcinogenic or probably carcinogenic to humans. In addition to these single compounds, combinations of the following compounds are also regarded as carcinogenic: analgesic formulations containing phenacetin, MOPP chemotherapy (nitrogen mustard, vincristine, procarbazine, and prednisone), 8-methyoxypsoralen combined with UVA radiation, and combined or sequential oral contraceptive regimens containing estrogens and progestins.

TABLE 16.7 IARC List of Carcinogenic and Probably Carcinogenic Pharmaceuticals[a]

Pharamaceutical	Carcinogenic	Probably carcinogenic
Cytotoxic drugs		
	Chlornaphazine	Adriamycin
	Myleran	Azacitidine
	Chlorambucil	BCNU[b]
	Methyl-CCNU[c]	CCNU
	Cyclophosphamide	Chlorozotocin
	Melphalan	Cisplatin
	Thiotepa	Nitrogen mustard
	Treosulfan	*N*-nitroso-*N*-methylurea
		Procarbazine
Immuno-suppressants		
	Azathioprine	
	Cyclosporine	
Hormone agonists and antagonists		
	Diethylstilbestrol	Oxymetholone
	Tamoxiphen	Testosterone
Other		
	Arsenic trioxide	Phenacetin
		Chloramphenicol
		5-Methoxypsoralen

[a] Data from Marselos M and Vainio H. Carcinogenesis 1991;12:1751–66, and White INH. Carcinogenesis 1999;20:1153–60.
[b] BCNU, Bis(chloroethyl)nitrosourea.
[c] CCNU, Choroethyl-cyclohexyl-nitrosourea.

Chemical carcinogens are generally regarded as being either genotoxic or nongenotoxic, although some carcinogens, such as estrogens, may exert a combination of these effects. Some toxic drugs, such as alkylating agents used in cancer chemotherapy, are directly genotoxic but others require prior conversion to reactive metabolites. Dioxin and some other nongenotoxic carcinogens appear to activate intracellular receptors, leading to changes in gene expression that result in cancer (81). Regardless of mechanism, chemical carcinogenesis is a complex process requiring sequential stages of initiation, promotion, and progression (79). As a result, there is usually a delay of several years between exposure to carcinogens and the appearance of drug-induced cancers.

Secondary Leukemia following Cancer Chemotherapy

The success of chemotherapeutic regimens for cancer has resulted in an increasing number of patients who develop a secondary myeloid leukemia.

Data collected from patients who were treated with alkylating agents for Hodgkin's disease, ovarian cancer, and other malignancies provided the initial demonstration that chemotherapy is associated with an excess risk of subsequent treatment-related myelodysplastic syndrome (t-MDS) that progresses to acute myeloid leukemia (t-AML) (82, 83). This risk is greatest in patients more than 40 years old, is greater in males than in females, and is proportionate to the dose and duration of chemotherapy. The risk reaches a peak approximately 5 years after initiating chemotherapy and persists for up to 10 years. Estimates range from less than 0.3% to 10% for the cumulative 10-year incidence of secondary acute myeloid leukemia in patients who have received chemotherapy for Hodkgin's disease (83). The World Health Organization (WHO) classification includes two types of t-MDS and t-AML: an alkylating agent/radiation-related type and a topoisomerase II inhibitor-related type (84).

Approximately two-thirds of cases that follow exposure to alkylating agents present as t-MDS, and those presenting as t-AML have myelodysplastic features (84). Alkylation of hematopoietic progenitor cell DNA during chemotherapy with these agents appears to be the genotoxic event that initiates a multistep carcinogenic process by causing genetic mutations that alter cell growth (Figure 16.12). In animal studies, this has been shown to result in a permanent loss of stem cell reserve and the maintenance of hematopoiesis by a succession of individual stem cell clones (82). Following this preliminary clonal restriction, it appears that a chromosomal abnormality develops in a clone that results in some selective growth advantage. All together, eight different genetic pathways have been identified in patients who develop t-MDS and t-AML (86). However, deletion or loss of chromosome 7 or monosomy 7 is the abnormality most frequently observed following therapy with alkylating agents (85, 86). In these individuals, leukemic transformation is thought to accompany subsequent mutations of the *RAS* gene and methylation of the *p15* putative tumor suppressor gene (86, 87).

The next most common genetic pathway encountered in patients previously treated with alkylating agents is characterized by defects in the long arm of chromosome 5, deletions or loss of 5q, or monosomy 5 (85, 86). Mutations of the *p53* tumor suppressor gene occur frequently in these patients and are associated with a very poor prognosis (88). Wild-type *p53* exerts tumor suppressor effects by blocking activation of cyclin–Cdk complexes, thus impeding cell cycle

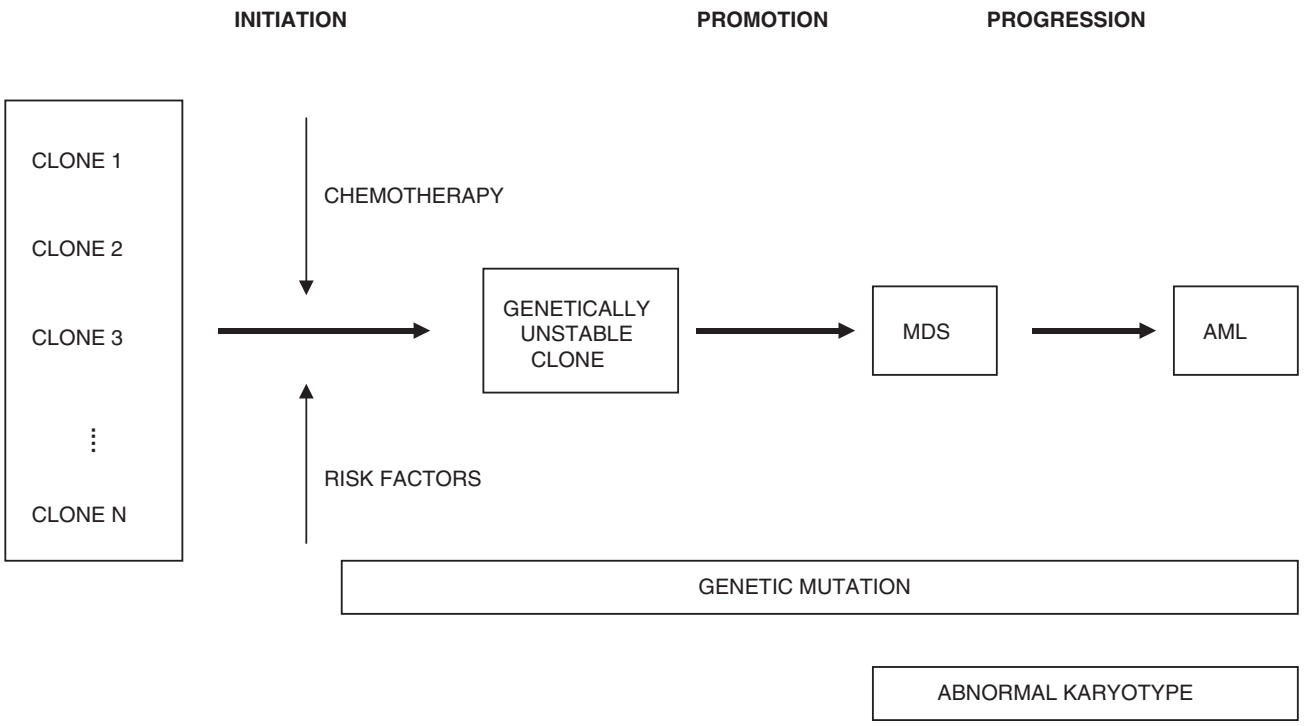

FIGURE 16.12 Hypothetical scheme for the pathogenesis of secondary myelodysplastic syndrome (MDS) and acute myeloid leukemia (AML) following cancer chemotherapy with alkylating agents.

progression through G_1 by modulating the balance between DNA replication and repair and by binding both to damaged DNA and to transcription repair factors (89). Loss of these functions presumably mediates progression from t-MDS to t-AML. In addition, it has been proposed by analogy with Fanconi anemia that abnormalities affecting the long arm of chromosome 5 may lead to a structural or functional loss of the interferon response factor-1 (*IRF-1*) gene, which functions as a tumor suppressor gene (90). The product of this gene (IRF-1) is expressed constitutively in normal progenitor cells and has the biological effect of inhibiting growth and stimulating inhibition. In normal cells, interferon γ (IFNγ) induces IRF-1 and inhibits cell growth. But IFNγ actually stimulates cell growth in cells incapable of an IRF-1 response and may provide the selection pressure that is needed for the outgrowth of a leukemogenic mutant stem cell clone.

The second WHO category of treatment-related myeloid neoplasms consists of t-AML following chemotherapy with topoisomerase II-directed epipodophyllotoxins and DNA-intercalating anthracyclines (84). The onset of leukemia in these patients generally occurs only 2 to 3 years after chemotherapy and is rarely preceded by MDS (83, 89). The genetic pathway following therapy with epipodophyllotoxins is characterized by balanced translocations to chromosome band 11q23 such that the myeloid–lymphoid leukemia gene (*MLL*) at this locus combines with one of a number of partner genes (86). This chimeric rearrangement results in production of fusion proteins that cause growth dysregulation and leukemic transformation (89).

The genetic pathway following therapy with topoisomerase II inhibitors is characterized by chimeric rearrangements of the core-binding factor genes Runt-related transcription factor 1, *RUNX1* (initially called acute myeloid leukemia 1, *AML1*), at 21q22, and *CBFP*, at 16q22 (84). These genes are key regulators of hematopoiesis (84). Loss of *RUNX1* function contributes to hematopoietic abnormalities and malignancy in patients with a familial platelet disorder who develop AML, and presumably plays a similar role in this t-AML pathway (91). The CBFβ subunit of the core-binding factor heterodimer binds to RUNX-1, thereby enhancing its DNA binding and activity.

Only a small fraction of chemotherapy-treated patients subsequently develop t-MDS/t-AML, and the risk-determining genetic factors are largely unexplored. These factors presumably range from individual differences in the molecular genetic and biochemical processes relating to carcinogenic susceptibility and DNA repair to differences in the genes regulating drug transport and metabolism (89, 92). For example, it has been proposed that the hypoxanthine–guanine phosphoribosyl transferase gene (*HPRT*) mutation assay can be used to measure the susceptibility of somatic cells to genetic damage following cancer therapy and thus serve as a biomarker of risk for the subsequent development of t-AML (89).

Diethylstilbestrol-Induced Vaginal Cancer

In 1971, Herbst *et al*. (93) reported the unusual occurrence of vaginal clear cell adenocarcinoma in eight young women. The precipitating factor appeared to be the fact that their mothers had been treated with diethylstilbestrol (DES) in order to prevent spontaneous abortion and premature delivery in what were deemed to be high-risk pregnancies. Estimates place the incidence of clear cell adenocarcinoma of the vagina at 1.5 per 1000 women who were exposed *in utero* to DES (94).

DES is a nonsteroidal estrogen that crosses the placenta and targets intranuclear estrogen receptors that develop in the fetal genital tract early in intrauterine life. During fetal development, Müllerian-derived columnar epithelium is replaced by a hollow core of squamous epithelium that arises from the vaginal plate (95). But neonatal DES exposure leads in mice to persistence of Müllerian-type columnar epithelium in the upper vagina and cervix and subsequent adenosis. DES exerts proliferative effects by binding to the classic estrogen receptor (ER-α), and it has been thought that increased cell proliferation might be carcinogenic by causing an increase in spontaneous errors associated with DNA replication and increasing the replication of clones of cells carrying these errors (78). Consistent with a role for ER-α in mediating DES carcinogenesis are observations following neonatal exposure to DES that the incidence of atypical uterine hyperplasia and cancer was increased in mutant mice that overexpress ER-α, and that squamous metaplasia of the vaginal epithelium was absent in ER-α knockout mice (96).

However, estrogen receptor-mediated events cannot fully explain the carcinogenic properties of estrogens, and there is mounting evidence that DES has direct genotoxic effects that result from its metabolism in target tissues (97, 98). The pathways of DES metabolism are partly depicted in Figure 16.13 (97, 99). It can be seen that redox cycling between the semiquinone and quinone metabolites generates superoxide anion radicals that may cause oxidative damage to DNA and other cellular macromolecules (97). In addition, chemically reactive

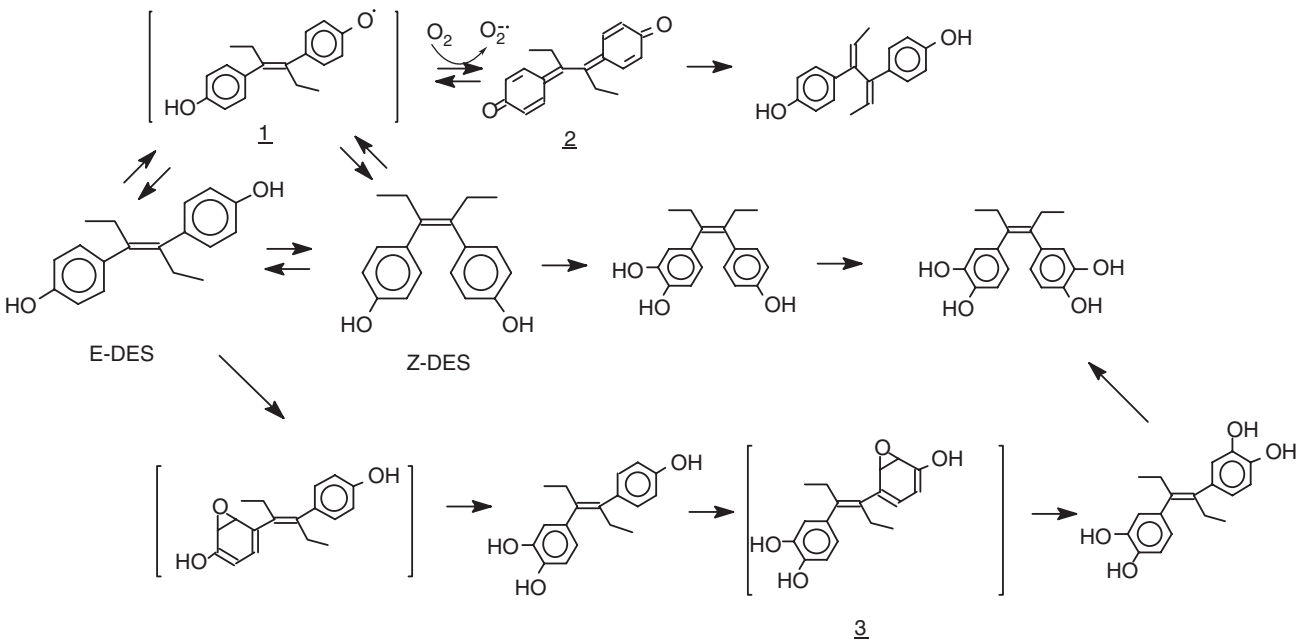

FIGURE 16.13 Partial scheme for the metabolism of diethylstilbestrol (DES). DES is administered as the trans isomer (E-DES), which, in solution, is in equilibrium with the cis isomer (Z-DES). Cytochrome P450 enzymes oxidize E-DES and Z-DES to a postulated chemically reactive semiquinone (**1**), which is further oxidized to a quinone (**2**), thereby generating reactive oxygen species (ROS) that oxidize cellular macromolecules. Redox cycling is perpetuated and ROS formation is amplified by two enzymes, cytochrome P450 or cytochrome b_5 reductase, which reduce the quinone back to the semiquinone. The unstable semiquinone and diol epoxide (**3**) metabolites are presumably those that bind to DNA to form adducts and initiate carcinogenesis.

semiquinone and diol epoxide metabolites are formed that are capable of forming either stable or depurinating DNA adducts (98). Stable DNA adducts are formed when reactive metabolites react with exocyclic amino groups on adenine or guanine. Depurinating adducts result when these metabolites bind to the N-3 or N-7 position of adenine or the N-7 or C-8 position of guanine. The depurinating adducts destabilize the glycosidic bond to deoxyribose, spontaneously releasing the purine base and the metabolite that is bound to it. It is believed that depurinating adducts are the primary culprits in the process of tumor initiation, and that mutations result from misrepair or misreplication of the apurinic sites (98). Stable DNA adducts could also play a role in carcinogenesis by interfering with error-free repair of the apurinic sites.

Consistent with the pathogenetic role of impaired DNA repair is the finding of mutations in DNA polymerase β that have been observed in a hamster kidney model of DES carcinogenesis (97). Although specific gene defects have not been identified in DES-induced clear cell adenomas in humans, up-regulation of the normal *p53* tumor suppressor gene has been described, and has been attributed to a normal cellular response to persistent DNA damage or genetic instability (100). Molecular genetic analysis has provided evidence of microsatellite instability in all the DES-induced and in 50% of the spontaneous clear cell adenoma tissue samples that were analyzed, again suggesting that defective DNA repair represents a critical molecular feature of this tumor type (101). Even though the genotoxic effects of DES may initiate carcinogenesis, estrogen receptor-mediated proliferative stimuli from endogenous estrogens would appear to play an important role in tumor promotion and progression, insofar as the adenocarcinomas primarily occur after the onset of menstruation (95).

Teratogenic Reactions to Drugs

Although the principles of teratogenesis are described more fully in Chapter 22, certain general concepts are central to an understanding of the way in which drugs cause teratogenic adverse reactions. First, teratogens cause a specific abnormality, or pattern of abnormalities, in the fetus, such as phocomelia resulting from maternal therapy with thalidomide (102). However, even known teratogens will not exert a teratogenic effect unless they are given during the relevant period of fetal organogenesis, generally

during the first trimester of pregnancy. In addition, fetal exposure must also exceed a critical threshold for teratogenesis to occur. The level of exposure is not only determined by the rate of drug transfer across the placenta but also by fetal clearance mechanisms (103). Unfortunately, the ability of the fetal liver to provide teratogenic protection is limited by the facts that the liver does not begin to form until the fourth week of pregnancy and that smooth endoplasmic reticulum is not detectable in fetal hepatocytes until the twelfth week of pregnancy (104). Finally, it is likely that genetic factors also determine the outcome of exposure to teratogens.

Fetal Hydantoin Syndrome

Hanson *et al*. (105) coined the term "fetal hydantoin syndrome" to describe a pattern of malformations that occurs in epileptic women who are treated with phenytoin during pregnancy. The clinical features of the syndrome include craniofacial anomalies, such as cleft lip or palate, a broad, depressed nasal bridge and inner epicanthic folds, nail and digital hypoplasia, prenatal and postnatal growth retardation, and mental retardation. These authors estimated that about 11% of exposed fetuses have the syndrome with serious sequelae, but that almost three times as many have lesser degrees of impairment. The magnitude and difficulty of this problem are underscored by the estimate that hydantoin therapy is prescribed during 2 per 1000 pregnancies, and by the fact that the risks of untreated epilepsy exceed the teratogenic risk of anticonvulsant therapy.

Phenytoin, phenobarbital, and carbamazepine are teratogenic anticonvulsant drugs that also cause hypersensitivity reactions that include skin rash, fever, and hepatitis (106). The cytochrome P450-mediated hydroxylation of all three drugs proceeds via the formation of chemically reactive epoxide intermediates (as shown for phenytoin in Chapter 11, Scheme 11.11). A pathogenetic role for phenytoin epoxide is suggested by the finding that the activity of epoxide hydrolase, the enzyme that converts the epoxide to a nontoxic dihydrodiol metabolite, is deficient in lymphocytes from patients with phenytoin-induced hepatotoxic reactions (107). Covalent binding of phenytoin to rat gingival proteins also suggests that metabolic activation plays a pathogenetic role in the gingival hyperplasia that occurs in 30–70% of patients receiving long-term phenytoin therapy (108).

Martz *et al*. (109) used a mouse model to provide the first evidence that the epoxide metabolite of phenytoin might be similarly implicated in mediating teratogenic reactions to this drug. Pregnant mice were treated with a single dose of phenytoin on gestational day 11. Their fetuses were subsequently found to have a 4% incidence of cleft palate and other anomalies, and inhibition of epoxide hydrolase with trichloropropene oxide resulted in at least a doubling of this incidence. Furthermore, administration of radioactive phenytoin resulted in covalent binding of the radioactivity to gestational tissue macromolecules. By assaying lymphocytes for epoxide hydrolase activity, as had been done for patients with phenytoin hepatotoxicity, Strickler *et al*. (110) demonstrated that the occurrence of major birth defects, including cleft lip or palate, congenital heart anomalies, and microcephaly, was correlated with subnormal epoxide hydrolase activity. Subsequently, Buehler *et al*. (111) obtained samples of amniocytes at amniocentesis and were able to correlate low amniocyte levels of epoxide hydrolase activity with an increased risk of developing the fetal hydantoin syndrome.

However, Tiboni *et al*. (112) have shown that embryos from pregnant mice pretreated with fluconizole, an inhibitor of phenytoin hydroxylation, had an increased rather than a decreased frequency of cleft palate. This argues against a teratogenic role for the epoxide metabolite of phenytoin and supports the alternative explanation proposed by Winn and Wells (113), that phenytoin is bioactivated by embryonic peroxidases to free radical intermediates, which in turn form hydroxyl radicals, superoxide anion, and hydrogen peroxide. The teratogenic effects of phenytoin are then thought to result from functional alterations caused by the action of these reactive oxygen species on embryonic DNA, protein, and lipid.

This hypothesis is supported by the finding that incubation of phenytoin-exposed mouse embryos in the presence of superoxide dismutase or catalase blocked formation of 8-hydroxy-2′-deoxyguanosine, a marker of DNA oxidation, and reduced or eliminated all dysmorphic abnormalities. The pathogenic role of superoxide in phenytoin teratogenesis is further supported by the finding that inducible nitric oxide synthase knockout murine embryos ($-/-$ *iNOS*) have a reduced frequency of embryopathy when exposed to phenytoin (114). These mice lack iNOS, which converts arginine to nitric oxide; the nitric oxide then can react with superoxide to form perioxynitrite, which in turn decomposes to release hydroxyl radicals and nitrite radicals. Whereas the hydroxyl radicals thus formed contribute to DNA, protein, and lipid oxidation, the nitrite radicals lead to protein and DNA nitration and protein cross-linking. Additional evidence that oxidative DNA damage may play an important role in phenytoin teratogenesis is provided by the finding that *p53* knockout mice, in whom

DNA repair is deficient, are more susceptible to these reactions (115). Therefore, although the exact changes in macromolecular structure and function responsible for phenytoin teratogenesis remain to be identified, it is likely that DNA damage plays a critical role in much the same way as has been described for carcinogenic reactions.

REFERENCES

1. Rawlins MD, Thomas SHL. Mechanisms of adverse drug reactions. In: Davies DM, Ferner RE, de Glanville H, eds. Davies's textbook of adverse drug reactions. 5th ed. London: Chapman & Hall Medical; 1998. p. 40–64.
2. Melmon KL. Preventable drug reactions — causes and cures. New Engl J Med 1971;284:1361–8.
3. Goldstein RA, Patterson R. Drug allergy: Prevention, diagnosis, and treatment. Ann Intern Med 1984;100:302–3.
4. Brodie BB, Axelrod J. The fate of acetanilide in man. J Pharmacol Exp Ther 1948;94:29–38.
5. Coleman MD, Coleman NA. Drug-induced methaemoglobinaemia — treatment issues. Drug Saf 1996;14:394–405.
6. Coleman MD. Use of *in vitro* methaemoglobin generation to study antioxidant status in diabetic erythrocyte. Biochem Pharmacol 2000;60:1409–16.
7. Roueché B. The medical detectives. New York: Penguin Books; 1988. p. 3–13.
8. Yunis AA. Chloramphenicol: Relation of structure to activity and toxicity. Annu Rev Pharmacol Toxicol 1988;28:83–100.
9. Ballet F. Hepatotoxicity in drug development: Detection, significance and solutions. J Hepatol 1997;26 (suppl 2):26–36.
10. Popper H, Rubin E, Gardiol D, Schaffer F, Paronetto F. Drug-induced liver disease: A penalty for progress. Arch Intern Med 1965;115:128–36.
11. Brodie BB, Reid WD, Cho AK, Sipes G, Krishna G, Gillette JR. Possible mechanism of liver necrosis caused by aromatic organic compounds. Proc Natl Acad Sci USA 1971;68:160–4.
12. Zampaglione N, Jollow DJ, Mitchell JR, Stripp B, Hamrick M, Gillette JR. Role of detoxifying enzymes in bromobenzene-induced liver necrosis. J Pharmacol Exp Ther 1973;187:218–27.
13. James LP, Mayeux PR, Hinson JA. Acetaminophen-induced hepatotoxicity. Drug Metab Dispos 2003;31:1499–506.
14. Reid AB, Kurten RC, McCullough SS, Brock RW, Hinson JA. Mechanisms of acetaminophen-induced hepatotoxicity: Role of oxidative stress and mitochondrial permeability transition in freshly isolated mouse hepatocytes. J Pharmacol Exp Ther 2005;312:509–16.
15. Zhang J, Huang W, Chua SS, Wei P, Moore DD. Modulation of acetaminophen-induced hepatotoxicity by the xenobiotic receptor CAR. Science 2002;298:422–4.
16. Mitchell JR, Jollow DJ, Potter WZ, Gillette JR, Brodie BB. Acetaminophen-induced hepatic necrosis. IV. Protective role of glutathione. J Pharmacol Exp Ther 1973;187:211–7.
17. Mitchell JR, Thorgeirsson SS, Potter WZ, Jollow DJ, Keiser H. Acetaminophen-induced hepatic injury: Protective role of glutathione in man and rationale for therapy. Clin Pharmacol Ther 1974;16:676–84.
18. Rumack BH. Acetaminophen overdose. Am J Med 1983;75:104–12.
19. Guo GL, Moffit JS, Nicol CJ, Ward JM, Aleksunes LA, Slitt AL, Kliewer SA, Manautou JE, Gonzalez FJ. Enhanced acetaminophen toxicity by activation of the pregnane X receptor. Toxicol Sci 2004;82:374–80.
20. Henderson CJ, Wolf CR, Kitteringham N, Powell H, Otto D, Park BK. Increased resistance to acetaminophen hepatotoxicity in mice lacking glutathione *S*-transferase Pi. Proc Natl Acad Sci USA 2000;97:12741–5.
21. Pumford NR, Halmes NC. Protein targets of xenobiotic reactive intermediates. Annu Rev Pharmacol Toxicol 1997;37:91–117.
22. Qui Y, Benet LZ, Burlingame AL. Identification of the hepatic protein targets of reactive metabolites of acetaminophen *in vivo* in mice using two-dimensional gel electrophoresis and mass spectrometry. J Biol Chem 1998;273:17940–53.
23. Chen W, Shockcor JP, Tonge R, Hunter A, Gartner C, Nelson SD. Protein and nonprotein cysteinyl thiol modification by *N*-acetyl-*p*-benzoquinone imine via a novel ipso adduct. Biochemistry 1999;38:8159–66.
24. Ju C, Reilly TP, Bourdi M, Radonovich MF, Brady JN, George JW, Pohl LR. Protective role of Kupffer cells in acetaminophen-induced hepatic injury in mice. Chem Res Toxicol 2002;15:1504–13.
25. Mitchell JR, Long MW, Thorgeirsson UP, Jollow DJ. Acetylation rates and monthly liver function tests during one year of isoniazid preventive therapy. Chest 1975;68:181–90.
26. Lauterberg BH, Smith CV, Todd EL, Mitchell JR. Oxidation of hydrazine metabolites formed from isoniazid. Clin Pharmacol Ther 1985;38:566–71.
27. Sarich TC, Adams SP, Petricca G, Wright JM. Inhibition of isoniazid-induced hepatotoxicity in rabbits by pretreatment with an amidase inhibitor. J Pharmacol Exp Ther 1999;289:695–702.
28. Sarich TC, Youssefi M, Zhou T, Adams SP, Wall RA, Wright JM. Role of hydrazine in the mechanism of isoniazid hepatotoxicity in rabbits. Arch Toxicol 1996;70:835–40.
29. Delaney J, Timbrell JA. Role of cytochrome P450 in hydrazine toxicity in isolated hepatocytes *in vitro*. Xenobiotica 1995;25:1399–410.
30. Dickinson DS, Bailey WC, Hirschowitz BI, Soong S-J, Eidus L, Hodgkin MM. Risk factors for isoniazid (INH)-induced liver dysfunction. J Clin Gastroenterol 1981;3:271–9.
31. Blair IA, Tinoco RM, Brodie MJ, Care RA, Dollery CT, Timbrell JA *et al*. Plasma hydrazine concentrations in man after isoniazid and hydralazine administration. Human Toxicol 1985;4:105–202.
32. Peretti E, Karlaganis G, Lauterburg BH. Increased urinary excretion of toxic hydrazino metabolites of isoniazid by slow acetylators. Effect of a slow-release preparation of isoniazid. Eur J Clin Pharmacol 1987;33:283–6.

33. Huang Y-S, Chern H-D, Su W-J, Wu J-C, Lai S-L, Yang S-Y, Chang F-Y, Lee S-D. Polymorphism of the *N*-acetyltransferase 2 gene as a susceptibility risk factor for antituberculosis drug-induced hepatitis. Hepatology 2002;35:883–9.
34. Huang Y-S, Chern H-D, Su W-J, Wu J-C, Chang S-C, Chang C-H, Chang F-Y, Lee S-D. Cytochrome P450 2E1 genotype and susceptibility to antituberculosis drug-induced hepatitis. Hepatology 2003;37:924–30.
35. American Thoracic Society. Treatment of tuberculosis and tuberculosis infection in adults and children. Am Rev Respir Dis 1986;134:355-63.
36. Boelsterli UA, Zimmerman HJ, Kretz-Rommel A. Idiosyncratic liver toxicity of nonsteroidal antiinflammatory drugs: Molecular mechanisms and pathology. Crit Rev Toxicol 1995;25:207–35.
37. Chen M, Gandolfi AJ. Characterization of the humoral immune response and hepatotoxicity after multiple halothane exposures in guinea pigs. Drug Metab Rev 1997;29:103–22.
38. Vergani D, Mieli-Vergani G, Alberti A, Neuberger J, Eddleston ALWF, Davis M *et al*. Antibodies to the surface of halothane-altered rabbit hepatocytes in patients with severe halothane-associated hepatitis. N Engl J Med 1980;303:66–71.
39. Beaune P, Pessayre D, Dansette P, Mansuy D, Manns M. Autoantibodies against cytochromes P450: Role in human diseases. Adv Pharmacol 1994;30: 199–245.
40. Ray DC, Drummond GB. Halothane hepatitis. Br J Anaesth 1991;67:84–99.
41. Satoh H, Fukuda Y, Anderson DK, Ferrans VJ, Gillette JR, Pohl LR. Immunological studies on the mechanism of halothane-induced hepatotoxicity: Immunohistochemical evidence of trifluoroacetylated hepatocytes. J Pharmacol Exp Ther 1985;233:857–62.
42. Bourdi M, Chen W, Peter RM, Martin JL, Buters JTM, Nelson SD *et al*. Human cytochrome P450 2E1 is a major autoantigen associated with halothane hepatitis. Chem Res Toxicol 1996;9:1159–66.
43. Amouzadeh HR, Bourdi M, Martin JL, Martin BM, Pohl LR. UDP-glucose:glycoprotein glucosyltransferease associates with endoplasmic reticulum chaperones and its activity is decreased *in vivo* by the inhalation anesthetic halothane. Chem Res Toxicol 1997;10:59–63.
44. Furst SM, Luedke D, Gaw H-H, Reich R, Gandolfi AJ. Demonstration of a cellular immune response in halothane-exposed guinea pigs. Toxicol Appl Pharmacol 1997;143:245–55.
45. Eliason E, Gardner I, Hume-Smith H, de Waziers I, Beaune P, Kenna JG. Interindividual variability in P450-dependent generation of neoantigens in halothane hepatitis. Chem Biol Interact 1998; 116:123–41.
46. Karasch ED, Hankins D, Mautz D, Thummel KE. Identification of the enzyme responsible for oxidative halothane metabolism: Implications for prevention of halothane hepatitis. Lancet 1996;347:1367–71.
47. Spracklin DK, Emery ME, Thummel KE, Kharasch ED. Concordance between trifluoroacetic acid and hepatic protein trifluoroacetylation after disulfiram inhibition of halothane metabolism in rats. Acta Anaesthesiol Scand 2003;47:765–70.
48. Zimmerman HJ, Lewis JH, Ishak KG, Maddrey WC. Ticrynafen-associated hepatic injury: Analysis of 340 cases. Hepatology 1984;4:315–23.
49. Beaune P, Dansette PM, Mansuy D, Kiffel L, Finck M, Amar C *et al*. Human anti-endoplasmic reticulum autoantibodies appearing in a drug-induced hepatitis are directed against a human liver cytochrome P-450 that hydroxylates the drug. Proc Natl Acad Sci USA 1987;84:551–5.
50. Robin M-A, Maratrat M, Le Roy M, Le Breton F-P, Bonierbale E, Dansette P *et al*. Antigenic targets in tienilic acid hepatitis. Both cytochrome P450 2C11 and 2C11-tienilic acid adducts are transported to the plasma membrane of rat hepatocytes and recognized by human sera. J Clin Invest 1996;98:1471–80.
51. Lopez-Garcia MP, Dansette PM, Mansuy D. Thiophene fderivatives as new mechanism-based inhibitors of cytochromes P-450: Inactivation of yeast-expressed human liver cytochrome P-450 2C9 by tienilic acid. Biochemistry 1994;33:166–75.
52. Lecoeur S, André C, Beaune PH. Tienilic acid-induced hepatitis: Anti-liver and -kidney microsomal type 2 autoantibodies recognize a three-site conformational epitope on cytochrome P4502C9. Mol Pharmacol 1996;50:326–3.
53. Melet A, Assrir N, Jean P, Lopez-Garcia MP, Marques-Soares C, Jaouen M, Dansette PM, Sari M-A, Mansuy D. Substrate selectivity of human cytochrome P450 2C9: Importance of residues 476, 365, and 114 in recognition of diclofenac and sulfaphenazole and in mechanism-based inactivation by tienilic acid. Arch Biochem Biophys 2003;409:80–91.
54. Mitchell JR, Nelson WL, Potter WZ, Sasame HA, Jollow DJ. Metabolic activation of furosemide to a chemically reactive, hepatotoxic metabolite. J Pharmacol Exp Ther 1976;199:41–52.
55. Mitchell JR, Potter WZ, Hinson JA, Jollow DJ. Hepatic necrosis caused by furosemide. Nature 1974; 251:508–10.
56. McMurtry RJ, Snodgrass WR, Mitchell JR. Renal necrosis, glutathione depletion, and covalent binding after acetaminophen. Toxicol Appl Pharmacol 1978;46:87–100.
57. Adkinson NF Jr. Drug allergy. In: Middleton E Jr, Ellis EF, Yunginger JW, Reed CE, Adkinson NF Jr, Busse WW. Allergy: Principles and practice. St. Louis: Mosby; 1998. p. 1212–24.
58. DiPiro JT, Adkinson NF Jr, Hamilton RG. Facilitation of penicillin haptenation to serum proteins. Antimicrob Agents Chemother 1993;37:1463–7.
59. Saxon A, Beall GN, Rohr AS, Adelman DC. Immediate hypersensitivity reactions to beta-lactam antibiotics. Ann Intern Med 1987;107:204–15
60. Adkinson NF. Risk factors for drug allergy. J Allergy Clin Immunol 1984;74:567–72.
61. Sullivan TJ. Dehaptenation of albumin substituted with benzylpenicillin G determinants [abstract]. J Allergy Clin Immunol 1988;81:222.
62. Weltzien HU, Padovan E. Molecular features of penicillin allergy. J Invest Dermatol 1998;110:203–6.

63. Lafaye P, Lapresie C. Fixation of penicilloyl groups to albumin and appearance of anti-penicilloyl antibodies in penicillin-treated patients. J Clin Invest 1988; 82:7–12.
64. Sogn DD, Evans R III, Shepherd GM, Casale TB, Condemi J, Greenberger PA *et al*. Results of the National Institute of Allergy and Infections Diseases Collaborative Clinical Trial to test the predictive value of skin testing with major and minor penicillin derivatives in hospitalized adults. Arch Intern Med 1992;152:1025–32.
65. Kosowsky BD, Taylor I, Lown B, Ritchie RF. Long-term use of procainamide following acute myocardial infarction. Circulation 1973;47:1204–10.
66. Drayer DE, Reidenberg MM, Sevy RW. *N*-Acetylprocainamide: An active metabolite of procainamide. Proc Soc Exp Biol Med 1974;146: 358–63.
67. Stec GP, Lertora JJL, Atkinson AJ Jr, Nevin MJ, Kushner W, Jones C *et al*. Remission of procainamide-induce lupus erythematosus with *N*-acetylprocainamide therapy. Ann Intern Med 1979;90:799–801.
68. Kluger J, Drayer DE, Reidenberg MM, Lahita R. Acetylprocainamide therapy in patients with previous procainamide-induced lupus syndrome. Ann Intern Med 1981;95:18–23.
69. Atkinson AJ Jr, Lertora JJL, Kushner W, Chao GC, Nevin MJ. Efficacy and safety of *N*-acetylprocainamide in the long-term treatment of patients with ventricular arrhythmias. Clin Pharmacol Ther 1983;33:565–76.
70. Stec GP, Ruo TI, Thenot J-P, Atkinson AJ Jr, Morita Y, Lertora JJL. Kinetics of *N*-acetylprocainamide deacetylation. Clin Pharmacol Ther 1980;28:659–66.
71. Uetrecht JP. Reactivity and possible significance of hydroxylamine and nitroso metabolites of procainamide. J Pharmacol Exp Ther 1985;232:420–5.
72. Kubicka-Muranyi M, Goebels R, Goebel C, Uetrecht J, Gleichmann E. T lymphocytes ignore procainamide, but respond to its reactive metabolites in peritoneal cells: Demonstration by the adoptive transfer popliteal lymph node assay. Toxicol Appl Pharmacol 1993;122:88–94.
73. Lessard É, Hamelin BA, Labbé L, O'Hara G, Bélanger PM, Turgeon J. Involvement of CYP2D6 activity in the N-oxidation of procainamide in man. Pharmacogenetics 1999;9:683–96.
74. Jiang X, Khursigara G, Rubin RL. Transformation of lupus-inducing drugs to cytotoxic products by activated neutrophils. Science 1994;266:810–3.
75. Kretz-Rommel A, Rubin RL. A metabolite of the lupus-inducing drug procainamide prevents anergy induction in T cell clones. J Immunol 1997;158: 4465–70.
76. Kretz-Rommel A, Rubin RL. Disruption of positive selection of thymocytes causes autoimmunity. Nat Med 2000;6:298–305.
77. Rubin RL, Burlingame RW, Arnott JE, Totoritis MC, McNally EM, Johnson AD. IgG but not other classes of anti-[(H2A-H2B)-DNA] is an early sign of procainamide-induced lupus. J Immunol 1995;154:2483–93.
78. Burlingame RW, Rubin RL. Autoantibody to the nucleosome subunit (H2A-H2B)-DNA is an early and ubiquitous feature of lupus-like conditions. Mol Biol Rep 1996;23:159–66.
79. Graham MA, Riley RJ, Kerr DJ. Drug metabolism in carcinogenesis and cancer chemotherapy. Pharmacol Ther 1991;51:275–89.
80. Marselos M, Vainio H. Carcinogenic properties of pharmaceutical agents evaluated in the IARC Monographs programme. 1991;12:1751–66.
81. Green S. Nuclear receptors and chemical carcinogenesis. Trends Pharmacol Sci 1992;13:251–5.
82. List AF, Jacobs A. Biology and pathogenesis of the myelodysplastic syndromes. Semin Oncol 1992; 19:14–24.
83. Leone G, Mele L, Pulsoni A, Equitani F, Pagano L. The incidence of the secondary leukemias. Haematologica 1999;84:937–45.
84. Vardiman JW, Harris NL, Brunning RD. The World Health Organization (WHO) classification of the myeloid neoplasms. Blood 2002;100:2292–302.
85. Levine EG, Bloomfield CD. Leukemias and myelodysplastic syndromes secondary to drug, radiation, and environmental exposure. Semin Oncol 1992;19:47–84.
86. Pedersen-Bjergaard J, Andersen MK, Christiansen DH, Nerlov C. Genetic pathways in therapy-related myelodysplasia and acute myeloid leukemia. Blood 2002;99:1909–12.
87. Christiansen DH, Pedersen-Bjergaard J. Methylation of $p15^{INK4B}$ is common, is associated with deletion of genes on chromosome arm 7q and predicts a poor prognosis in therapy-related myelodysplasia and acute myeloid leukemia. Leukemia 2003;17: 1813–9.
88. Christiansen DH, Andersen MK, Pedersen-Bjergaard J. Mutations with loss of heterozygosity of *p53* are common in therapy-related myelodysplasia and acute myeloid leukemia after exposure to alkylating agents and significantly associated with deletion or loss of 5q, a complex karyotype, and a poor prognosis. J Clin Oncol 2001;19:1405–13.
89. Smith MA, McCaffrey RP, Karp JE. The secondary leukemias: Challenges and research directions. J Natl Cancer Inst 1996;88:407–18.
90. Lensch MW, Rathbun RK, Olson SB, Jones GR, Bagby GC Jr. Selective pressure as an essential force in molecular evolution of myeloid leukemic clones: A view from the window of Fanconi anemia. Leukemia 1999;13:1784–9.
91. Speck NA, Gilliland DG. Core-binding factors in haematopoiesis and leukemia. Nat Rev Cancer 202;2:502–13.
92. Rund D, Ben-Yehuda D. Therapy-related leukemia and myelodisplasia: Evolving concepts of pathogenesis and treatment. Hematology 2004;9:179–87.
93. Herbst AL, Ulfelder H, Poskanzer DC. Adenocarcinoma of the vagina: Association of maternal stilbestrol therapy with tumor appearance in young women. N Engl J fMed 1971;284:878–81.
94. Hatch EE, Palmer JR, Titus-Ernstoff L, Noller KL, Kaufman RH, Mittendorf R *et al*. Cancer risk in

women exposed to diethylstilbestrol *in utero*. JAMA 1998;280:630–4.
95. Herbst AL. Behavior of estrogen-associated female genital tract cancer and its relation to neoplasia following intrauterine exposure to diethylstilbestrol (DES). Gynecol Oncol 2000;76:147–56.
96. Dickson RB, Stancel GM. Chapter 8: Estrogen receptor-mediated processes in normal and cancer cells. J Natl Cancer Inst Monogr 2000;27:135–45.
97. Roy D, Palangat M, Chen C-W, Thomas RD, Colerangle J, Atkinson A, Yan Z-J. Biochemical and molecular changes at the cellular level in response to exposure to environmental estrogen-like chemicals. J Toxicol Environ Health 1997;50:1–29.
98. Cavalieri E, Frenkel K, Liehr JG, Rogan E, Roy D. Chapter 4: Estrogens as endogenous genotoxic agents — DNA adducts and mutations. J Natl Cancer Inst Monogr 2000;27:75–93.
99. Haaf H, Metzler M. *In vitro* metabolism of diethylstibestrol by hepatic, renal and uterine microsomes of rats and hamsters. Effects of different inducers. Biochem Pharmacol 1985;34:3107–15.
100. Waggoner SE, Anderson SM, Luce MC, Takahashi H, Boyd J. p53 protein expression and gene analysis in clear cell adenocarcinoma of the vagina and cervix. Gynecol Oncol 1996;60:339–44.
101. Boyd J, Takahashi H, Waggoner SE, Jones LA, Hajek RA, Wharton JT *et al*. Molecular genetic analysis of clear cell adenocarcinomas of the vagina and cervix associated and unassociated with diethylstilbestrol exposure *in utero*. Cancer 1996;77:507–13.
102. Taussig HB. A study of the German outbreak of phocomelia: The thalidomide syndrome. JAMA 1962;180:1106–14.
103. Szeto HH. Maternal–fetal pharmacokinetics: Summary and future directions. NIDA Res Monogr 1995;154:203–7.
104. Ring JA, Ghabrial H, Ching MS, Smallwood RA, Morgan DJ. Fetal hepatic drug elimination. Pharmacol Ther 1999;84:429–45.
105. Hanson JW, Myrianthopoulos NC, Harvey MAS, Smith DW. Risks to the offspring of women treated with hydantoin anticonvulsants, with emphasis on the fetal hydantoin syndrome. Pediatr 1976;89:662–8.
106. Shear NH, Spielberg SP. Anticonvulsant hypersensitivity syndrome. *In vitro* assessment of risk. J Clin Invest 1988;82:1826–32.
107. Spielberg SP, Gordan GB, Blake DA, Goldstein DA, Herlong HF. Predispostion to phenytoin hepatotoxicity assessed *in vitro*. N Engl J Med 1981;305:722–7.
108. Wortel JP, Hefferren JJ. Rao GS. Metabolic activation and covalent binding of phenytoin in the rat gingiva. J Periodontal Res 1979;14:178–81.
109. Martz F, Failinger C 3rd, Blake DA. Phenytoin teratogenesis: Correlation between embryopathic effect and covalent binding of putative arene oxide metabolite in gestational tissue. J Pharmacol Exp Ther 1977; 203:231–9.
110. Strickler SM, Dansky LV, Miller MA, Seni M-H, Andermann E, Spielberg SP. Genetic predisposition to phenytoin-induced birth defects. Lancet 1985;2:746–9.
111. Buehler BA, Delimont D, van Waes M, Finnell RH. Prenatal prediction of risk of the fetal hydantoin syndrome. N Engl J Med 1990;322:1567–72.
112. Tiboni GM, Giampietro F, Angelucci S, Moio P, Bellati U, Di Illio C. Additional investigation on the potentiation of phenytoin teratogenicity by fluconazole. Toxicol Lett 2003;145:219–29.
113. Winn LM, Wells PG. Phenytoin-initiated DNA oxidation in murine embryo culture, and embryo protection by the antioxidative enzymes superoxide dismutase and catalase: Evidence for reactive oxygen species-mediated DNA oxidation in the molecular mechanism of phenytoin teratogenicity. Mol Pharmacol 1995;48:112–20.
114. Kasapinovic S, McCallum GP, Wiley MJ, Wells PG. The peroxynitrite pathway in development: Phenytoin and benzo[*a*]pyrene embryopathies in inducible nitric oxide synthase knockout mice. Free Radic Biol Med 2004;37:1703–11.
115. Wells PG, Kim PM, Laposa RR, Nicol CJ, Parman T, Winn LM. Oxidative damage in chemical teratogenesis. Mutat Res 1997;396:65–78.

This page intentionally left blank

PART

III

ASSESSMENT OF DRUG EFFECTS

This page intentionally left blank

CHAPTER

17

Physiological and Laboratory Markers of Drug Effect

ARTHUR J. ATKINSON, JR.* **AND PAUL ROLAN†**
*Clinical Center, National Institutes of Health, Bethesda, Maryland,
†ICON — Medeval Clinical Pharmacology, Manchester Science Park, Manchester, United Kingdom

BIOLOGICAL MARKERS OF DRUG EFFECT

The selection and measurement of relevant drug effects is an increasingly important part of clinical pharmacology. Traditionally, the efficacy and safety of drug therapy have been assessed using *clinical endpoints*, such as survival, onset of serious morbidity, or symptomatic response. Nonetheless, these endpoints have obvious disadvantages as useful measures in monitoring the response of individual patients to existing drug therapy, and increase the duration and cost of the clinical trials that are needed to evaluate potential new drugs. These constraints have provided the impetus for identifying more accessible response markers, or *biomarkers*, that can be assessed more easily and rapidly than can more definitive clinical endpoints. In some cases, these biomarkers have served as *surrogate endpoints* and have provided the basis for regulatory approval of new drugs under the conditions stipulated in the following excerpt from the Code of Federal Regulations (1):

> FDA may grant marketing approval for a new drug product on the basis of adequate and well-controlled trials establishing that the drug product has an effect on a surrogate endpoint that is reasonably likely, based on epidemiologic, therapeutic, pathophysiologic, or other evidence, to predict clinical benefit or on the basis of an effect on a clinical endpoint other than survival or irreversible morbidity. (*Title 21, Section 314.50, Subpart H of the Code of Federal Regulations*) (1)

Examples of some commonly used biomarkers and surrogate endpoints are listed along with clinical endpoints for several therapeutic classes in Table 17.1.

In a number of clinical trials, initial conclusions based on the response of candidate surrogate endpoints were not borne out by the subsequent clinical response. These unexpected results have fueled concerns that many proposed surrogate endpoints may not accurately predict meaningful clinical outcomes (2–4). One of the most notable examples is provided by the Cardiac Arrhythmia Suppression Trial (CAST) in which a dichotomy was found between suppression of ventricular ectopy and increased mortality in patients who received long-term therapy with antiarrhythmic drugs (5). The impetus for the trial was provided by the fact that patients who have sustained a myocardial infarction, and subsequently have ventricular ectopy with more than 10 premature ventricular depolarizations per hour, have a fourfold increase in mortality rate. A total of 1498 patients were entered in the trial and were randomized to receive encainide, flecainide, or placebo. However, after a mean treatment period of 10 months, the safety monitoring board stopped the trial because 63 patients died while receiving these antiarrhythmic drugs, whereas only 26 placebo-treated patients died ($P = 0.0001$). Although complete understanding of the mechanisms underlying the excess mortality is lacking, it is presumed that the adverse proarrhythmic effects of drug therapy outweighed the

TABLE 17.1 Examples of Biomarkers and Surrogate Endpoints

Therapeutic class	Biomarker/ surrogate	Clinical endpoint
Physiologic markers		
Antihypertensive drugs	↓ Blood pressure	↓ Stroke
Drugs for glaucoma	↓ Intraocular pressure	Preservation of vision
Drugs for osteoporosis	↑ Bone density	↓ Fracture rate
Antiarrhythmic drugs	↓ Arrhythmias	↑ Survival
Laboratory markers		
Antibiotics	Negative culture	Clinical cure
Antiretroviral drugs	↑ CD4 count, ↓ viral RNA	↑ Survival
Antidiabetic drugs	↓ Blood glucose	↓ Morbidity
Lipid-lowering drugs	↓ Cholesterol	↓ Coronary artery disease
Drugs for prostate cancer	↓ Prostate-specific antigen	Tumor response

TABLE 17.2 Biomarker and Endpoint Terms

Term	Definition
Biological marker (biomarker)	A physical sign or laboratory measurement that occurs in association with a pathological process and has putative diagnostic and/or prognostic utility
Surrogate endpoint	A biomarker that is intended to serve as a substitute for a clinically meaningful endpoint and is expected to predict the effect of a therapeutic intervention
Clinical endpoint	A clinically meaningful measure of how a patient feels, functions, or survives
Intermediate endpoint	A clinical endpoint that is not the ultimate outcome but is nonetheless of real clinical benefit
Ultimate outcome	A clinical endpoint such as survival, onset of serious morbidity, or symptomatic response that captures the benefits and risks of an intervention

benefit provided by suppression of arrhythmias resulting from underlying cardiac disease (Figure 17.1). Supporting this interpretation is the finding that patients receiving antiarrhythmic drugs had an increased incidence of fatal arrhythmias and of shock after recurrent myocardial infarction.

Further controversy surrounding biomarkers and surrogate endpoints stems from ambiguity in the terminology that has been used by members of the different disciplines that are engaged in the design, conduct, analysis, and regulatory evaluation of clinical trials. For this reason, a number of proposals have been made to clarify this terminology (4, 6). A synthesis of these proposals is presented in Table 17.2. A hierarchy is implicit in this sequence of definitions in that relatively few biomarkers are robust enough to serve as surrogate endpoints. For example, blood pressure and serum cholesterol concentrations are the only surrogate endpoints that are currently used in the United States as the basis for approval of cardiovascular drugs (4).

Although an intermediate endpoint is associated with clinical benefit, this benefit may be more than offset by the adverse effects of drug therapy when the ultimate outcome is considered. For example, ventricular fibrillation is associated with increased mortality in the setting of acute myocardial infarction. The demonstration that lidocaine effectively prevents ventricular fibrillation in myocardial infarction patients at first provided a rationale for treating these patients prophylactically with this drug (7). However, subsequent meta-analyses of several studies by MacMahon (8) and Hine (9) indicated that this use of lidocaine therapy actually worsens patient

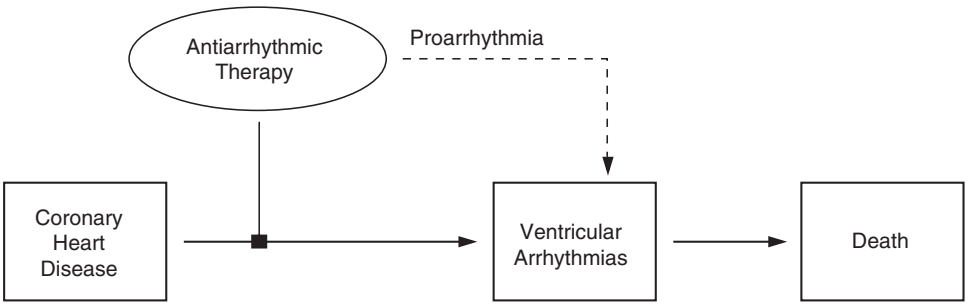

FIGURE 17.1 Path diagram illustrating the potential of adverse proarrhythmic effects of antiarrhythmic drug therapy (*dashed line*) to outweigh the potential benefit of suppressing ventricular arrhythmias in patients with coronary heart disease.

survival, so prophylactic lidocaine therapy is no longer regarded as the standard of care for patients with acute myocardial infarction (10). Although a subsequent observational study indicated that primary ventricular fibrillation is associated with a 2.5-fold increase in mortality and confirmed that prophylactic lidocaine reduces the incidence of this arrhythmia (11), it is likely that a large prospective randomized clinical trial, in which mortality is the primary endpoint, will be needed before current therapeutic recommendations will be changed (12).

One frequent point of confusion is whether a clinical rating scale, such as the Hamilton Depression scale, is a biomarker or a clinical endpoint. As these scales attempt to capture the multifaceted dimensions of a complex clinical condition, they are in fact clinical endpoints. However, they are like intermediate endpoints because they do not encompass all dimensions of the disease being evaluated or the therapeutic response in all patients.

IDENTIFICATION AND EVALUATION OF BIOMARKERS

Most of the biomarkers listed in Table 17.1 were identified in studies of pathophysiology and epidemiology that demonstrated an association between the marker and the presence or prognosis of the underlying clinical condition. Once a putative biomarker is identified, its subsequent evaluation consists of an analysis of its *validity*, in the traditional sense of precision, bias, and reproducibility, and of its *predictive utility*.

For example, laboratory biomarkers are used to establish prognosis and to predict or monitor response to therapy or disease progression in patients with cancer. A few of these biomarkers, such as prostate-specific antigen, also have had diagnostic utility. Because tumor biomarkers play a critical role in patient management, rigorous assessment of their validity is required and their marketing in the United States is regulated by the Food and Drug Administration under the Medical Device Law (13). Currently, candidate tumor markers are evaluated with respect to their analytical sensitivity and specificity and the robustness of the cutoff value that is chosen to distinguish positive from negative test results. Different antibody assays for the same tumor biomarkers can give different results, in part because tumor antigen proteins have several distinct epitopes protruding from their surface (14). Therefore, studies are required to compare new and old versions of a given tumor biomarker assay (13). The AIDS Clinical Trials Group has implemented similarly rigorous programs for standardization and quality control of biomarker measurements in patients with HIV-1 infection (15).

Statistical criteria have played an important role in assessing the predictive utility of biomarkers (*criterion validity*), but it is always hazardous to equate causation with statistical association. For that reason, increasing emphasis has been placed on establishing the *biological plausibility*, or *construct validity*, of biomarkers. Thus, clinical and epidemiological observations led to the conclusion that elevated blood pressure was associated with an increased risk of atherosclerotic cardiovascular disease, heart failure, stroke, and kidney failure (16). Subsequent pathophysiologic studies in humans and in animal models then were particularly helpful in establishing a firm linkage between hypertension and cerebral hemorrhage and infarction (17). A later epidemiologic study demonstrated that the risk of stroke and coronary heart disease is correlated with the extent of diastolic blood pressure elevation (18). In the aggregate, this considerable evidence supports the biological plausibility of using blood pressure as a surrogate endpoint. In clinical practice, the measurement of blood pressure is used to diagnose hypertension, to estimate its severity, and to monitor response to antihypertensive therapy.

Further support for using blood pressure as a surrogate endpoint is provided by the concordance of evidence from a number of clinical trials in which blood pressure lowering with low-dose diuretics and β-blockers was shown to reduce the incidence of stroke, coronary artery disease, and congestive heart failure in hypertensive patients (19). Of particular interest is a meta-analysis that was conducted to compare the extent of blood pressure reduction achieved in different clinical trials with the maximum benefit that was anticipated on epidemiolgic grounds (Table 17.3) (20). The decrease in stroke incidence anticipated for a 5- to 6-mm Hg average reduction in diastolic blood pressure was fully realized with only 2 to 3 years of antihypertensive therapy.

TABLE 17.3 Incidence Change Resulting from a 5–6-mm Hg Change in Diastolic Blood Pressure[a]

Event	Clinical trial result		Epidemiologic expectation (95% CI)
	Observed result	95% CI	
Stroke	42%	33–50%	35–40%
Coronary heart disease	14%	4–22%	20–25%

[a] Data from Collins R, Peto R, Mac Mahon S *et al*. Lancet 1990;335:827–38.

However, the reduction in coronary heart disease risk was substantially less than the maximum anticipated benefit, perhaps reflecting the fact that atherosclerosis is a chronic and largely irreversible process with a multifactorial etiology.

More recently, it has been shown that hypokalemia and other dose-related adverse metabolic effects of thiazide diuretics increase the risk of sudden death and negate the cardiovascular benefit of blood pressure lowering when high doses these drugs are prescribed (21). Hence, another explanation for the apparent inability of antihypertensive therapy to lower mortality in patients with coronary heart disease is that high thiazide doses were used in many of the trials that were analyzed. As pointed out by Temple (2), this explanation is supported by the results of a trial of antihypertensive therapy in elderly patients with isolated systolic hypertension (22). In this study, only low doses of a thiazide diuretic were prescribed and a 4-mm Hg average decrease in diastolic blood pressure was associated with a 36% reduction in the 5-year incidence of stroke and a 25% reduction in the incidence of coronary heart disease. Similar concerns have been raised about the clinical efficacy of antihypertensive therapy with short-acting calcium-channel-blocking drugs, which lower blood pressure but have been found to increase the risk of myocardial infarction in hypertensive patients (23). These observations emphasize the point, diagrammed in Figure 17.2, that sole reliance on even a well-established surrogate endpoint can lead to erroneous conclusions when beneficial effects on the surrogate are outweighed by unexpected adverse effects.

Figure 17.2 also emphasizes that it is inherently more difficult to demonstrate the benefit of antihypertensive therapy in preventing coronary heart disease than in preventing stroke because, in the former case, therapy is directed against only one of the less dominant predisposing risk factors. To deal with the complexity of this problem, Shatzkin and colleagues (24) have proposed a means for calculating the extent to which response measured by the clinical

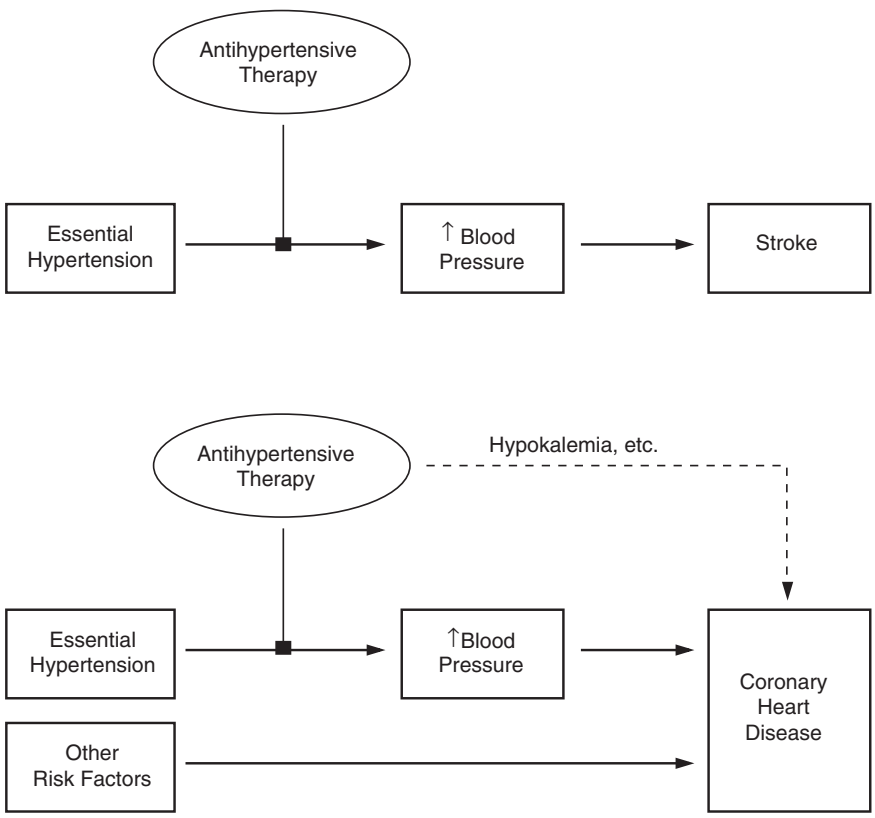

FIGURE 17.2 Path diagrams illustrating the difference in complexity involved in demonstrating the efficacy of antihypertensive therapy in reducing the incidence of stroke and coronary heart disease. The anticipated benefit in reducing the incidence of coronary heart disease is offset by the deleterious effects of some antihypertensive drug regimens. In addition, hypertension is just one of many factors that contribute to the risk of developing coronary heart disease.

endpoint can be attributed to a biomarker. The formula for calculating this *attributable proportion (AP)* is

$$AP = S\left(1 - \frac{1}{R}\right)$$

where S is the sensitivity (the proportion of patients with the clinical endpoint who are biomarker positive) and R is the relative risk (the incidence of the clinical endpoint in patients who are biomarker positive divided by the incidence in those who are biomarker negative). More elaborate analyses also have been proposed for estimating the proportion of treatment effect explained by a biomarker (25, 26).

Ideally a biomarker would capture the full relationship between a given therapy and a clinical endpoint before being relied upon to serve as a surrogate endpoint (27). However, this expectation seems unrealistic, as illustrated by the complexity of the relationship between hypertension, antihypertensive therapy, and the incidence of coronary heart disease (Figure 17.2). In view of this uncertainty, regulatory acceptance of a biomarker as a surrogate for a clinical endpoint is to some extent dependent on a risk/benefit assessment that includes the availability of alternative effective therapy, the difficulty of obtaining clinical endpoint data, and the safety data base of the drug in question (4). Risk/benefit assessment is complicated by the fact that multiple drug actions are usual, but their extent is seldom fully anticipated. Frequently, the dose-response or concentration-response relationship for the desired effect is quite different from that of an undesired effect, so that dosing based solely on a therapeutic biomarker or surrogate endpoint may not lead to an optimal clinical response. In addition, the onset of some adverse effects is delayed or infrequent enough so that they do not become apparent in clinical trials that for practical reasons are of limited duration and size.

USES OF BIOMARKERS AND SURROGATE ENDPOINTS

A high level of stringency is required when the response of a biomarker to drug therapy is proposed as a surrogate for a clinical endpoint and is intended to be used as the basis for regulatory approval of an application to market a new drug. On the other hand, biomarkers need not achieve surrogate endpoint status in order to play an important role in facilitating our understanding of disease mechanisms and natural history, in expediting the development of new drugs, and in improving the quality of patient care (28). In addition, the emphasis placed on using biomarkers to evaluate therapeutic efficacy has obscured the equally important role that they can play in evaluating the toxic potential of drug therapy. Indeed, biomarkers have the potential to be most valuable in detecting a predisposition to or risk of drug toxicity, thus increasing the frequency with which these signals can be captured in premarketing clinical trials. There is an urgent need for further development in this area. One current example is prolongation of the electrocardiographic QT interval that is used as a biomarker to identify drugs that could cause the potentially fatal *torsades de pointes* arrhythmia (29). Blood level measurements also can serve as a biomarker for toxicity as well as efficacy, both in the initial stages of drug development and in subsequent clinical use.

Some applications of biomarkers are outlined in Table 17.4. Many, but not all, biomarker applications are part of the drug development process that was diagrammed in Chapter 1 (Figure 1.1). Studies to provide an epidemiologic and pathophysiologic basis for biomarkers have been alluded to already, and these generally precede their use in

TABLE 17.4 Some Applications of Biomarkers and Surrogate Endpoints

Predevelopment studies of target illness
• Used to correlate with diagnosis and prognosis • Used to help elucidate pathophysiology of disease
Preclinical drug development
• Used to confirm proposed pharmacologic activity *in vivo* • Used to explore plasma level-response relationships in animal studies
Phase I–II clinical studies
• Used to demonstrate pharmacologic activity in humans • Used to define dose or plasma level-response relationships
Phase III clinical studies
• Used as a basis for stratifying patient groups • Used for compliance and safety monitoring • Used as basis for interim analysis of patient response • Used as basis for conditional regulatory approval
Phase IV clinical studies
• Used in studies designed to establish new indications for marketed drugs • Used as a basis for regulatory approval of formulation changes and of generic drugs
Application in clinical practice
• Used to establish diagnosis and prognosis • Used as an aid in selecting therapy • Used to monitor response to treatment

drug development. In preclinical and early clinicaldevelopment, biomarkers can provide evidence of *in vivo* pharmacologic activity and can define the dose or range of plasma concentrations that is likely to be effective in subsequent studies.

In large-scale clinical trials, biomarkers such as CD4 count may be useful for patient stratification (30). Blood levels and toxicity biomarkers also could be used for safety monitoring. Biomarkers used as efficacy measures in exploratory Phase II clinical trials may be helpful in reaching a go/no-go decision regarding further development of a particular drug. Here, as in earlier phases of drug development, the extent of validation of a biomarker is of concern primarily to the sponsor. However, a more stringent standard of validity is required in a pivotal Phase III trial of a new drug if a biomarker is proposed as a surrogate endpoint to be used as the basis for regulatory approval. In fact, even when regulatory approval is based on results obtained with a surrogate endpoint, that approval is contingent on subsequent verification of clinical benefit (1). Similar considerations apply to Phase IV studies that are designed to establish additional clinical indications for a marketed drug. As was described in Chapter 4, blood level measurements of new product formulations and of generic drug products are relied upon as a surrogate for formal efficacy studies in establishing bioequivalence. In addition, as was discussed in Chapter 2, drug levels are used to guide dose adjustment and monitor therapy with drugs that have a narrow therapeutic index and no readily observable clinical endpoint. Measurements of blood pressure, intraocular pressure, serum total cholesterol, and prostate-specific antigen are among the many biomarkers that are used in routine clinical practice for establishing diagnosis and prognosis, for selecting therapy, and for subsequent patient monitoring.

Use of Serum Cholesterol as a Biomarker and Surrogate Endpoint

Although serum cholesterol measurements are an accepted surrogate endpoint for lipid-lowering therapy, there is a long history of controversy regarding the value of this therapy in preventing coronary heart disease (31). Epidemiologic studies provided initial evidence that increasing serum cholesterol concentrations were associated with an increased risk of death from coronary heart disease (Figure 17.3) (32). This relationship was confirmed by studies conducted in a number of animal models (33). Taken together, this evidence provided strong support for the hypothesis

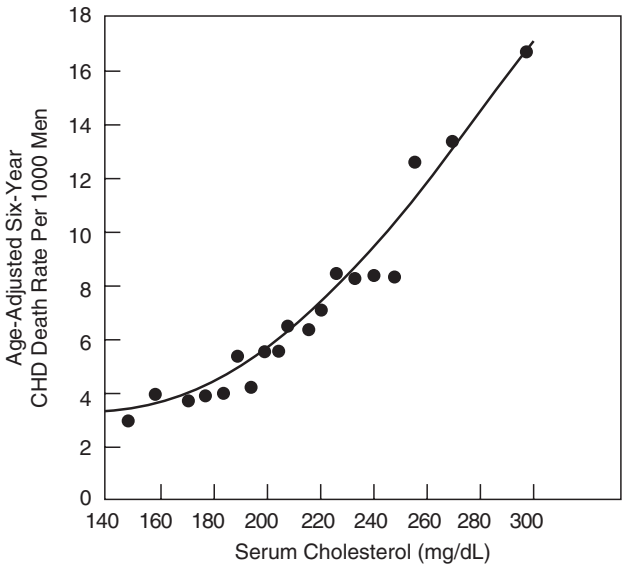

FIGURE 17.3 Relation of serum cholesterol to coronary heart disease death in a population of 361,662 men aged 35–57 years. The average duration of follow-up was 6 years. (Reproduced with permission from Gotto AM Jr, LaRosa JC, Hunninghake D, Grundy SM, Wilson PW, Clarkson TB, Hay JW, Goodman DS. Circulation 1990;81:1721–33.)

that reducing cholesterol levels would lower morbidity and mortality from coronary heart disease. Accordingly, serum cholesterol has played an important role as a biomarker in the clinical development of inhibitors of 3-hydroxy-3-methylglutaryl coenzyme A (HMG CoA) reductase and other lipid-lowering agents. This experience illustrates both some important uses of biomarkers and some of the continuing pitfalls surrounding their use as surrogate endpoints.

Role of Serum Cholesterol in the Simvastatin Development Program

Measurements of serum cholesterol were used in a Phase II dose-ranging study in which simvastatin doses, ranging from 2.5–40 mg once daily to 1.25–40 mg twice daily, were administered to 43 patients with heterozygous familial hypercholesterolemia (34). The study duration was only 6 weeks and only four study centers were needed for patient recruitment. Based on the results shown in Figure 17.4, it was concluded that simvastatin had suitable efficacy whether given once or twice daily, and that 20 mg/day represented an appropriate starting point for dosing in subsequent studies. These results were then incorporated in a definitive randomized, placebo-controlled Phase III trial in which 4444 patients with coronary heart disease were followed in 94 centers for a median of 5.4 years (35). Patients receiving simvastatin initially were treated with a daily dose of

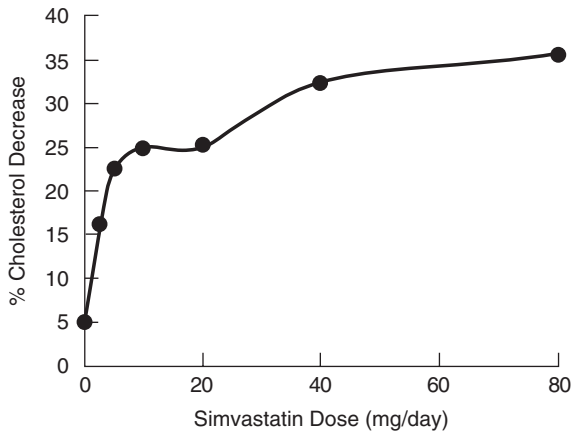

FIGURE 17.4 Results of a study that established the dose-response relationship between simvastatin dose and percent reduction in serum cholesterol levels in patients with heterozygous familial hypercholesterolemia.

20 mg that subsequently was adjusted as needed to lower serum cholesterol concentrations to the range of 117–200 mg/dL. The study demonstrated that simvastatin therapy reduced total cholesterol by a mean of 25% during the study (average low-density lipoprotein cholesterol reduction was 34%), and was associated with a 34% reduction in the incidence of major coronary events. Total mortality was 30% less for patients who were treated with simvastatin than for those who received placebo.

The inclusion of clinical endpoints in this larger Phase III study provided the first definite evidence that lipid-lowering therapy could reduce total mortality in patients with coronary heart disease. Subgroup analysis subsequently indicated that the relationship between lowering low-density lipoprotein (LDL) cholesterol and reducing major clinical events was curvilinear, in that decreases in cholesterol level resulted in continuing but progressively smaller reductions in major coronary events (36). This is consistent with the epidemiologic findings shown in Figure 17.3, and supports clinical practice guidelines that recommend lowering LDL cholesterol levels to or below 100 mg/dL for patients who have established coronary heart disease or a greater than 20% 10-year risk of myocardial infarction or coronary heart disease death, and to less than 130 mg/dL for high-risk patents with a 10–20% risk of these events (37). An even more aggressive LDL cholesterol goal of less than 70 mg/dL that may be of additional benefit for high-risk patients is currently optional and is under further evaluation (37).

Unanticipated Consequences of Cholesterol-Lowering Therapy

Of particular interest are the results of the West of Scotland Coronary Prevention Study in which the relationship between the observed incidence of coronary heart disease events was compared with that predicted from an equation that incorporates cholesterol levels, smoking history, diabetes, blood pressure, and other risk factors that were known at the time (38). These results, shown in Figure 17.5, indicate that the predicted and observed event rates in patients who received placebo were similar. On the other hand, coronary event rates in pravastatin-treated patients were consistently lower than were

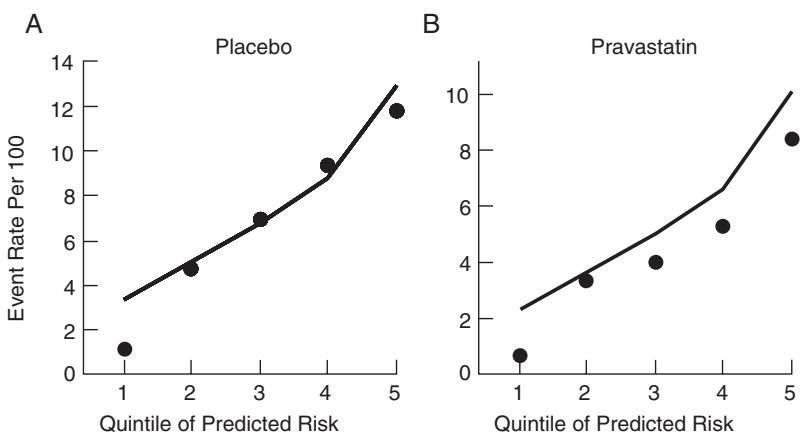

FIGURE 17.5 Comparison of observed risk of a coronary heart disease event (•) and predicted risk (lines) for patients receiving either placebo or pravastatin over the 4.4-year duration of the West of Scotland Coronary Prevention Study. (Reproduced with permission from West of Scotland Coronary Prevention Group. Circulation 1998;97:1440–5.)

those that were predicted. This finding suggests that pravastatin has therapeutic effects that extend beyond lipid lowering. In addition, most studies with HMG CoA-reductase inhibitors have demonstrated a more rapid onset of therapeutic benefit than would be expected just from their lipid-lowering properties (39). After pravastatin therapy was shown to reduce plasma concentrations of C-reactive protein (CRP), it was proposed that this class of drugs has anti-inflammatory effects that augment the clinical benefit of lowering serum cholesterol levels (40).

CRP now is known to be a marker of coronary heart disease risk that is independent of serum cholesterol. Studies have shown not only that the combination of CRP and lipid measurements predicts relative risk of myocardial infarction better than when either biomarker is used alone (41), but also that CRP is a stronger predictor of risk than is serum cholesterol level (42). Despite the aggregation of statistical evidence that CRP has criterion validity as a biomarker of cardiovascular risk, its construct validity was initially questioned because CRP traditionally has been regarded as a nonspecific acute-phase reactant. In fact, patients with bacterial infection, autoimmune disease, and cancer typically have CRP serum levels more than 20 times higher than the concentration range of 1–5 μg/mL used to predict cardiovascular risk in individuals without an acute inflammatory process (43). However, support for a mechanistic role of CRP in the atherosclerotic process has been provided by *in vitro* studies demonstrating that CRP acts on endothelial cells to produce a range of atherogenic effects. For example, it was shown that CRP induces endothelial cell production of monocyte chemoattractant protein-1, a chemokine involved in recruiting monocytes into blood vessel walls, where they are transformed into macrophages and ingest cholesterol to form foam cells, and that this effect of CRP was blocked by simvastatin (44). Additional studies have shown that CRP also activates human endothelial cells to express adhesion molecules, selectins, interleukin-6, and endothelin-1, and decreases expression of endothelial nitric oxide synthase (43). However, a crucial step in the evaluation of this biomarker is lacking in that there is no evidence yet that therapy aimed at lowering CRP concentrations actually reduces coronary heart disease risk. Nonetheless, CRP and serum cholesterol are likely to be used increasingly as conjoint biomarkers of cardiovascular risk (43).

It is relatively uncommon for the clinical benefit of therapeutic interventions to exceed predictions based on biomarker response. Far more often, unanticipated adverse effects diminish or nullify the clinical benefits expected from drug effects on a biomarker. For example, probucol, a drug structurally unrelated to HMG CoA inhibitors, exerted pronounced lipid-lowering effects and received marketing approval in the 1970s, even though long-term survival studies were not conducted. Probucol also was known to prolong the electrocardiographic QT interval. In a scenario reminiscent of that encountered with antiarrhythmic drugs (Figure 17.1), subsequent investigations indicated that this drug was proarrhythmic in that it caused *torsades de pointes* ventricular tachycardia (45). Therefore, it is hazardous to assume *a priori* that any drug that lowers cholesterol will also improve patient survival.

Application of Serial Biomarker Measurements

In some cases, it has been useful to monitor the rate of change of serial laboratory biomarker measurements. More than thirty years ago, weekly measurements of the steady-state ratio of cerebrospinal fluid (CSF) to blood glucose concentrations (R_{CSF}) were used to monitor the response to therapy of patients with cryptococcal meningitis (46). Meningeal infection with *Cryptococcus neoformans* disrupts carrier-mediated facilitated diffusion of glucose between blood and CSF and results in initially low R_{CSF} values in these patients (46, 47). With effective therapy, R_{CSF} was found to rise at a rate of 0.013 ± 0.002 ($\pm$ SD) per day until it reached the normal range of 0.45–0.65. In one patient, a decline in R_{CSF} during therapy preceded clinical evidence of deterioration. More recently, measurements of tumor biomarker half-life have been shown to be useful in assessing the efficacy of therapeutic interventions, and tumor biomarker doubling time has been used to evaluate the probability of metastasis or tumor recurrence (14).

Measurement of both CD4 lymphocytes and viral load are currently regarded as somewhat independent biomarkers of disease progression rate in patients infected with HIV-1 (48, 49). It has been found that serial measurements are more informative than is a single measurement of viral load, in that failure to account for the evolution of viral load can lead to underestimates of progression risk (50). In addition, analysis of the kinetics of HIV-1 viral load and turnover of peripheral blood mononuclear cells has provided fundamental insight into viral replication rates and the need for long-term therapy with even highly active antiretroviral drug regimens (51, 52). Finally, both increases in CD4 lymphocyte count and reductions in viral load have attained surrogate endpoint status and have been used as the basis for accelerated approval of several antiretroviral drugs.

However, no single marker has been shown to explain fully the spectrum of clinical response to therapeutic intervention (15).

FUTURE DEVELOPMENT OF BIOMARKERS

So far we have considered biomarkers whose validity has been either somewhat established or discredited by their use in clinical practice or in clinical trials. However, the utility of biomarkers in aiding both drug development and the diagnosis and management of patients has resulted in the introduction of many new biomarkers, many of which are less well characterized. Innovative but incompletely evaluated biomarkers are particularly likely to play an important role in exploratory studies of a new drug candidate. Unfortunately, the degree of innovation represented by a biomarker is likely to vary inversely with the extent of its validation (53). This is a consequence of the fact that prior use in clinical trials is an important component of biomarker evaluation.

One scheme of categorizing the multitude of established and candidate biomarkers is presented in Figure 17.6. Type 1 biomarkers reflect a drug's initial pharmacologic action. As such, they confirm primary pharmacology but may not be correlated with downstream mechanistic events or clinical effects. These biomarkers generally consist of *in vitro* studies to confirm that a drug binds to a certain receptor or ion channel, or elicits an *in vivo* response that is easily measured but separate from an effect on disease mechanism. Positron emission tomography has made it possible to assess receptor binding even in humans, and was used in an innovative dose-ranging study to demonstrate that a 0.48 mg/kg dose of a reversible monamine oxidase type B (MAO-B) inhibitor was needed to achieve more than 90% blockade of irreversible L-[^{11}C]deprenyl binding to central nervous system MAO-B (54). Here blockade of irreversible L-[^{11}C]deprenyl binding was used as the biomarker, and it was estimated that a 1-year Phase II study in patients with Parkinson's disease would have been required had conventional clinical endpoints been used for dose-ranging studies.

Type 2 biomarkers reflect drug effects on the targeted disease mechanism and, like serum cholesterol and CRP, are more likely to be predictive of beneficial clinical response to a therapeutic intervention. Because toxic effects may offset the benefits of drug therapy, there has been increasing interest in developing Type 3 biomarkers that could provide an early warning of possible drug toxicity. Because there is a quantitative relationship between QT interval prolongation and the risk of *torsades de pointes*, this interval is widely used as a biomarker to assess the proarrhythmic risk of drugs, even though it is an imperfect predictor of this risk. For example, some drugs, such as pentobarbital, prolong the QT interval but actually reduce the risk of torsades by also decreasing the trans-myocardial dispersion of repolarization that is a predisposing factor in initiating re-entrant arrhythmias (55). Nonetheless, the potential lethality of drug-induced ventricular arrhythmias and noninvasive accessibility of QT interval measurements has prompted development of a concept paper that will result in established guidelines for evaluating drug-induced QT interval prolongation (56). Since QT interval prolongation is integral

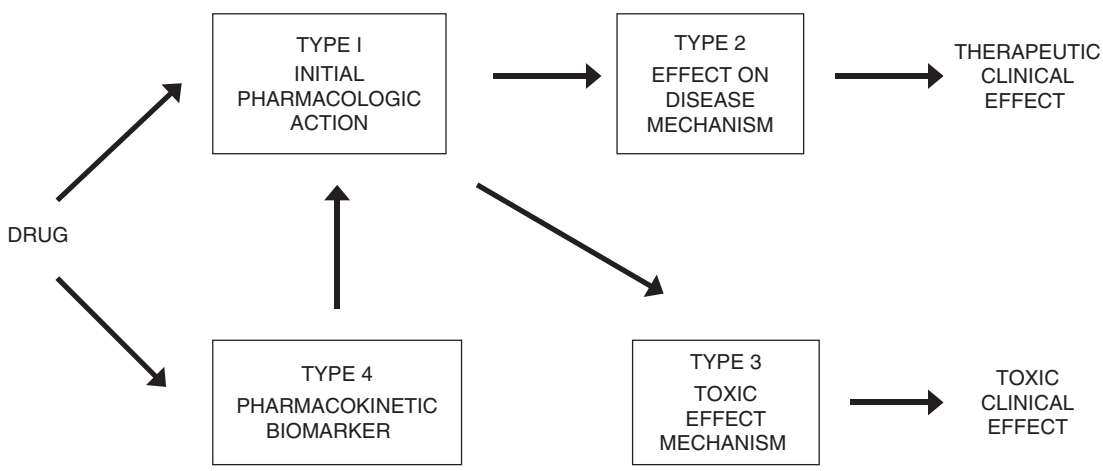

FIGURE 17.6 Mechanistic classification of biomarkers interposed between drug administration and observed therapeutic or toxic clinical effects. (Further explanation is provided in the text.)

to the mechanism of action of many antiarrhythmic drugs, particular emphasis is being placed on drugs that are intended for uses other than arrhythmia control.

Recent advances in pharmacogenetics have led to the development of Type 4 biomarkers that reflect interindividual differences in genes that encode transporters, enzymes, receptors, and other proteins involved in drug action or in the processes of drug absorption and disposition (57). Thiopurine methyltransferase (TPMT) is an example of an enzyme that exhibits important genetic polymorphism, in that patients with one or two nonfunctional TPMT alleles have a high risk of hematopoietic toxicity when treated with standard doses of 6-mercaptopurine and other thiopurine drugs (58). Although measurement of TPMT activity has become an accepted biomarker for identifying patients at high risk of thiopurine drug toxicity, regulatory authorities have stopped short of mandating testing for TPMPT status before prescribing therapy with 6-mercaptopurine (57).

In the near future, it is likely that genomics and proteomics will expand the current repertoire of biomarkers. Pharmacogenomics already has played an important role in the mechanism-driven development of trastuzumab and several other oncology drugs (59). The observation that the *HER2* gene, which encodes the HER2 epidermal growth factor receptor, is overexpressed in 25–30% of breast cancer patients and is correlated with increased tumor aggressiveness, led to the successful development of traztuzumab, a humanized monoclonal antibody directed against the extracellular domain of this receptor (60). HER2 overexpression not only served as a useful biomarker during many phases of traztuzumab development (59), but now provides the labeled indication for prescribing the drug (61).

Although it is expected that most disease states will be characterized by a typical gene expression pattern in one or more tissues of relevance, the pathophysiology of most common diseases is multifactorial. For this reason, the expression pattern of multiple genes frequently will be needed to develop a "signature" that could be used to confirm diagnosis, to establish prognosis, to choose the most appropriate therapy for an individual patient, and to monitor patient response (62). Accordingly, future developments in pharmacogenomics are likely to incorporate the use of microarrays that can analyze the differential expression of as many as 10,000 genes in a single experiment (63, 64). Expression proteomics also has considerable potential in characterizing multifactorial diseases, and is based on the use of two-dimensional gel electrophoresis, matrix-assisted laser desorption and ionization time-of-flight mass spectrometry (MALDI–TOF MS), protein biochips, and other techniques to identify a disease-specific protein signature that can serve as a biomarker (65). Petricoin *et al*. (66) have successfully demonstrated that differential expression of low molecular weight serum proteins can identify patients with diagnosed ovarian cancer, but this approach has not yet been used to diagnose patients with early-stage disease in whom therapeutic response is most favorable, or as an aid to monitoring patient response to therapy. On the other hand, proteomics has provided insight into the molecular mechanism involved in the nephrotoxicity of cyclosporine (67), and has considerable potential in providing biomarkers for the early detection and mechanistic elucidation of drug-induced liver and cardiac toxicity (65).

The use of gene expression array and differential protein expression technology poses a substantial bioinformatic challenge, but progress already is being made in developing relational database management systems that can store, process, and analyze the data that will be generated by high-throughput methods (66, 68, 69). Despite the technical challenges that remain, advances in developing bioinformatics packages and heuristic cluster algorithms have the potential to provide panels of relevant biomarkers that can transform drug development and patient therapy, and supercede reliance on single biomarkers, at least in patients with cancer and other multifactorial diseases (70, 71).

REFERENCES

1. Code of Federal Regulations, Title 21, Vol. 5, Parts 300 to 499. Washington, DC: U.S. Government Printing Office; April 1, 1997.
2. Temple RJ. A regulatory authority's opinion about surrogate endpoints. In: Nimmo WS, Tucker GT, eds. Clinical measurement in drug evaluation. New York: J Wiley; 1995.
3. Fleming TR, DeMets DL. Surrogate end points in clinical trials: Are we being misled? Ann Intern Med 1996;125:605–13.
4. Temple R. Are surrogate markers adequate to assess cardiovascular disease drugs? JAMA 1999;282:790–5.
5. Echt DS, Liebson PR, Mitchell B, Peters RW, Obias-Manno D, Barker AH, Arensberg D, Baker A, Friedman L, Greene L, Huther ML, Richardson DW, CAST Investigators. Mortality and morbidity of patients receiving encainide, flecainide or placebo: The cardiac arrhythmia suppression trial. N Engl J Med 1991;324:781–8.
6. NIH Definitions Working Group. Biomarkers and surrogate endpoints in clinical research: Definitions and conceptual model. In: Downing GL, ed. Biomarkers and surrogate endpoints: Clinical research and applications. Amsterdam: Elsevier; 2000. p. 1–9.

7. Lie KI, Wellens HJ, van Capelle FJ, Durrer D. Lidocaine in the prevention of primary ventricular fibrillation: A double-blind, randomized study of 212 consecutive patients. N Engl J Med 1974;291:1324–6.
8. MacMahon S, Collins R, Peto R, Koster RW, Yusuf S. Effects of prophylactic lidocaine in suspected acute myocardial infarction: An overview of results from the randomized controlled trials. JAMA 1988;260:1910–6.
9. Hine LK, Laird N, Hewitt P, Chalmers TC. Meta-analytic evidence against prophylactic use of lidocaine in acute myocardial infarction. Arch Intern Med 1989;149:2694–8.
10. Campbell RWF. Arrhythmia prevention in the hospital phase of acute myocardial infarction. In: Califf RM, Mark DB, Wagner GS, eds. Acute coronary care. 2nd ed. St. Louis: Mosby-Year Book; 1995. p. 371–6.
11. Wyman MG, Wyman RM, Cannom DS, Criley JM. Prevention of primary ventricular fibrillation in acute myocardial infarction with prophylactic lidocaine. Am J Cardiol 2004;94:545–51.
12. Yadav AV, Zipes DP. Prophylactic lidocaine in acute myocardial infarction: Resurface or reburial? Am J Cardiol 2004;94:606–8.
13. Aziz KJ. Tumor markers: Reclassification and new approaches to evaluation. Adv Clin Chem 1999;33:169–99.
14. Bidart J-M, Thuillier F, Augereau C, Chalas J, Daver A, Jacob N, Labrousse F, Voitot H. Kinetics of serum tumor marker concentrations and usefulness in clinical monitoring. Clin Chem 1999;45:1695–707.
15. Mildvan D, Landay A, De Gruttola V, Machado SG, Kagan J. An approach to the validation of markers for use in AIDS clinical trials. Clin Infect Dis 1997; 24:764–74.
16. Chobanian AV. The influence of hypertension and other hemodynamic factors in atherogenesis. Prog Cardiovasc Dis 1983;26:177–96.
17. Russell RWR. How does blood-pressure cause stroke? Lancet 1975;ii:1283–5.
18. MacMahon S, Peto R, Cutler J, Collins R, Sorlie P, Neaton J, Abbott R, Godwin J, Dyer A, Stamler J. Blood pressure, stroke, and coronary heart disease: Part I, prolonged differences in blood pressure: Prospective observational studies corrected for the regression dilution bias. Lancet 1990;335:765–74.
19. Psaty BM, Smith NL, Siscovick DS, Koepsell TD, Weiss NS, Heckbert SR, Lemaitre RN, Wagner EH, Furberg CD. Health outcomes associated with antihypertensive therapies used as first-line agents: A systematic review and meta-analysis. JAMA 1997;277:739–45.
20. Collins R, Peto R, MacMahon S, Hebert P, Fiebach NH, Eberlein KA, Godwin J, Qizilbash N, Taylor JO, Hennekens CH. Blood pressure, stroke, and coronary heart disease: Part 2, short-term reductions in blood pressure: Overview of randomized drug trials in their epidemiological context. Lancet 1990;335:827–38.
21. Siscovick DS, Raghunathan TE, Psaty BM, Koepsell TD, Wicklund KG, Lin X, Cobb L, Rautaharju PM, Copass MK, Wagner EH. Diuretic therapy for hypertension and the risk of primary cardiac arrest. N Engl J Med 1994;330;1852–7.
22. SHEP Cooperative Research Group. Prevention of stroke by antihypertensive drug treatment in older persons with isolated systolic hypertension: Final results of the systolic hypertension in the elderly program (SHEP). JAMA 1991;265:3255–64.
23. Furberg CD, Psaty BM, Meyer JV. Dose-related increase in mortality in patients with coronary heart disease. Circulation 1995;92:1326–31.
24. Shatzkin A, Freedman LS, Schiffman MH, Dawsey SM. Validation of intermediate end points in cancer research. J Natl Cancer Inst 1990;82:1746–52.
25. Freedman LS, Graubard BI. Statistical validation of intermediate endpoints for chronic diseases. Stat Med 1992;11:167–78.
26. Lin DY, Fleming TR, De Gruttola V. Estimating the proportion of treatment effect explained by a surrogate marker. Stat Med 1997;16:1515–27.
27. Prentice RL. Surrogate endpoints in clinical trials: definition and operational criteria. Stat Med 1989;8:431–40.
28. Lesko LJ, Atkinson AJ Jr. Use of biomarkers and surrogate endpoints in drug development and regulatory decision making. Ann Rev Pharmacol 2001;41:347–66.
29. Woosley RL, Chen Y, Freiman JP, Gillis RA. Mechanism of the cardiotoxic actions of terfenadine. JAMA 1993;269:1532–6.
30. Miller V, Mocroft A, Reiss P, Katlama C, Papadopoulos AI, Katzenstein T, van Lunzen J, Antunes F, Phillips AN, Lundgren JD, for the EuroSIDA Study Group. Relations among CD4 lymphocyte nadir, antiretroviral therapy, and HIV-1 disease progression: Results from the EuroSIDA study. Ann Intern Med 1999;130:570–7.
31. Davey Smith G, Pekkanen J. Should there be a moratorium on the use of cholesterol lowering drugs? BMJ 1992;304:431–4.
32. Gotto AM Jr, LaRosa JC, Hunninghake D, Grundy SM, Wilson PW, Clarkson TB, Hay JW, Goodman DS. The cholesterol facts: A summary of the evidence relating dietary fats, serum cholesterol, and coronary heart disease: A joint statement by the American Heart Association and the National Heart, Lung, and Blood Institute. Circulation 1990;81:1721–33.
33. Wissler RW, Vesselinovitch D. Can atherosclerotic plaques regress? Anatomic and biochemical evidence from nonhuman animal models. Am J Cardiol 1990;65:33F–40F.
34. Mol MJTM, Erkelens DW, Gevers Leuven JA, Schouten JA, Stalenhoef AFH. Effects of synvinolin (MK-733) on plasma lipids in familial hypercholesterolaemia. Lancet 1986;ii:936–9.
35. Scandinavian Simvastatin Survival Study Group. Randomised trial of cholesterol lowering in 4444 patients with coronary heart disease: The Scandinavian Simvastatin Survival Study (4S). Lancet 1994;344:1383–9.
36. Pedersen TR, Olsson AG, Færgeman O, Kjekshus J, Wedel H, Berg K, Wilhelmsen L, Haghfelt T, Thorgeirson G, Pyörälä K, Miettinen T, Christophersen B, Tobert JA, Musliner TA, Cook TJ, for the Scandinavian Simvastatin Survival Study Group. Lipoprotein changes and reduction in the incidence of major coronary heart disease events in the Scandinavian Simvastatin Survival Study. Circulation 97:1998;1453–60.
37. Grundy SM, Cleeman JI, Merz CN, Brewer HB Jr, Clark LT, Hunninghake DB, Pasternak RC, Smith SC Jr, Stone NJ; Coordinating Committee of the National Cholesterol Education Program. Implications of recent

clinical trials for the National Cholesterol Education Program Adult Treatment Panel III Guidelines. J Am Coll Cardiol 2004;44:720–32.
38. West of Scotland Coronary Prevention Study Group. Influence of pravastatin and plasma lipids on clinical events in the West of Scotland Coronary Prevention Study (WOSCOPS). Circulation 1998;97:1440–5.
39. Vaughan CJ, Murphy MB, Buckley BM. Statins do more than just lower cholesterol. Lancet 1996;348:1079–82.
40. Ridker PM, Rifai N, Pfeffer MA, Sacks F, Braunwald E, for the Cholesterol and Recurrent Events (CARE) Investigators. Long-term effects of pravastatin on plasma concentration of C-reactive protein. Circulation 1999;100:230–5.
41. Ridker PM. Evaluating novel cardiovascular risk factors: Can we better predict heart attacks? Ann Intern Med 1999;130:933–7.
42. Ridker PM, Rifai N, Rose L, Buring JE, Cook NR. Comparison of C-reactive protein and low density lipoprotein cholesterol levels on the prediction of first cardiovascular events. N Engl Med 2002;347:1557–65.
43. Yeh ETH, Willerson JT. Coming of age of C-reactive protein: Using inflammation markers in cardiology. Circulation 2003;107:370–2.
44. Pasceri V, Chang J, Willerson JT, Yeh ETH. Modulation of C-reactive protein-mediated monocyte chemoattractant protein-1 induction in human endothelial cells by anti-atherosclerosis drugs. Circulation 2001;103:2531–34.
45. Reinoehl J, Frankovich D, Machado C, Kawasaki R, Baga JJ, Pires LA, Steinman RT, Fromm BS, Lehmann MH. Probucol-associated tachyarrhythmic events and QT prolongation: Importance of gender. Am Heart J 1996;131:1184–91.
46. Atkinson AJ Jr. The cerebrospinal fluid glucose concentration. Steady state and kinetic studies in patients with cryptococcal meningitis. Am Rev Resp Dis 1969;99:59–66.
47. Atkinson AJ Jr, Weiss MF. Kinetics of blood-cerebrospinal fluid glucose transfer in the normal dog. Am J Physiol 1969;216:1120–6.
48. O'Brien WA, Hartigan PM, Martin D, Esinhart J, Hill A, Benoit S, Rubin M, Simberkoff MS, Hamilton JD, the Veterans Affairs Cooperative Study Group on AIDS. Changes in plasma HIV-1 RNA and CD4+ lymphocyte counts and the risk of progression to AIDS. N Engl J Med 1996;334:426–31.
49. Engels EA, Rosenberg PS, O'Brien TR, Goedert JJ, for the Multicenter Hemophilia Cohort Study. Plasma HIV viral load in patients with hemophilia and late-stage HIV disease: A measure of current immune suppression. Ann Intern Med 1999;131:256–64.
50. O'Brien TR, Rosenberg PS, Yellin F, Goedert JJ. Longitudinal HIV-1 RNA levels in a cohort of homosexual men. J Acquir Immune Defic Syndr Hum Retrovirol 1998;18:155–61.
51. Ho DD, Neumann AU, Perelson AS, Chen W, Leonard JM, Markowitz M. Rapid turnover of plasma virions and CD4 lymphocytes in HIV-1 infection. Nature 1995;373:123–6.
52. Perelson AS, Essunger P, Cao Y, Vesanen M, Hurley A, Saksela K, Markowitz M, Ho DD. Decay characteristics of HIV-1 infected compartments during combination therapy. Nature 1997;387:188–91.
53. Rolan P. The contribution of clinical pharmacology surrogates and models to drug development — a critical appraisal. Br J Clin Pharmacol 1997;44: 219–25.
54. Bench CJ, Price GW, Lammertsma AA, Cremer JC, Luthra SK, Turton D, Dolan RJ, Kettler R, Dingemanse J, Da Prada M, Biziere K, McClelland GR, Jamieson VL, Wood ND, Frackowiak RSJ. Measurement of human cerebral monamine oxidase type B (MAO-B) activity with positron emission tomography (PET): A dose ranging study with the reversible inhibitor Ro 19-6327. Br J Clin Pharmacol 1991; 40:169–73.
55. Fenichel RR, Malik M, Antzelevitch C, Sanguinetti M, Roden DM, Prior SG, Ruskin JN, Lipicky RJ, Cantilena LR, Independent Academic Task Force. Drug-induced torsades de pointes and implications for drug development. J Cardiovasc Electrophysiol 2004;15:475–95.
56. CDER, CBER. The clinical evaluation of QT/QT_C interval prolongation and proarrhythmic potential for non-antiarrhythmic drugs. Preliminary Concept Paper, Rockville: FDA; 2004. (Internet at http://www.fda.gov/cder/guidance/index.htm.)
57. Lesko LJ, Woodcock J. Translation of pharmacogenomics and pharmacogenetics: A regulatory perspective. Nat Rev Drug Discov 2004;3:763–9.
58. Krynetski E, Evans WE. Drug methylation in cancer therapy: Lessons from the TPMT polymorphism. Oncogene 2003;22:7403–13.
59. Park JW, Kerbel RS, Kelloff GJ, Barrett JC, Chabner BA, Parkinson DR, Peck J, Ruddon RW, Sigman CC, Slamon DJ. Rationale for biomarkers and surrogate end points in mechanism-driven oncology drug development. Clin Cancer Res 2004;10:3885–96.
60. Slamon DJ, Leyland-Jones B, Shak S, Fuchs H, Paton V, Bajamonde A, Fleming T, Eiermann W, Wolter J, Pegram M, Baselga J, Norton L. Use of chemotherapy plus a monoclonal antibody against HER2 for metastatic breast cancer that overexpresses HER2. N Engl J Med 2001;344:783–92.
61. Physician's Desk Reference. 58th ed. Montvale, NJ: Medical Economics; 2004. p. 1356.
62. Van Ommen GJB, Bakker E, den Dunnen JT. The human genome project and the future of diagnostics, treatment, and prevention. Lancet 1999;354 (suppl 1):5–10.
63. Debouck C, Goodfellow PN. DNA microarrays in drug discovery and development. Nat Genet 1999;21:48–50.
64. Hiltunen MO, Niemi M, Ylä-Herttuala S. Functional genomics and DNA array techniques in atherosclerosis research. Curr Opin Lipidol 1999;10:515–9.
65. He Q-Y, Chiu J-F. Proteomics in biomarker discovery and drug development. J Cell Biochem 2003;89:868–86.
66. Petricoin EF 3rd, Ardekani AM, Hitt BA, Leviine PJ, Fusaro VA, Steinberg SM, Mills GB, Simone C, Fishman DA, Kohn EC, Liotta LA. Use of proteomic patterns in serum to identify ovarian cancer. Lancet 2002;359:572–7.
67. Aicher L, Wahl D, Arce A, Grenet O, Steiner S. New insights into cyclosporine A nephrotoxicity by proteome analysis. Electrophoresis 1998;19:1998–2003.

68. Braxton S, Bedilion T. The integration of microarray information in the drug development process. Curr Opin Biotechnol 1998;9:643–9.
69. Carlisle AJ, Prabhu VV, Elkahloun A, Hudson J, Trent JM, Linehan WM *et al*. Development of a prostate cDNA microarray and statistical gene expression analysis package. Mol Carcinogen 2000;28:12–22.
70. Scherf U, Ross DT, Waltham M, Smith LH, Lee JK, Tanabe L *et al*. A gene expression database for the molecular pharmacology of cancer. Nat Genet 2000;24:236–44.
71. Bichsel VE, Liotta LA, Petricoin EF 3rd. Cancer proteomics: From biomarker discovery to signal pathway profiling. Cancer J 2001;7:69–78.

This page intentionally left blank

CHAPTER

18

Dose-Effect and Concentration-Effect Analysis

ELIZABETH S. LOWE* **AND FRANK M. BALIS†**

**AstraZeneca Pharmaceuticals, Wilmington, Delaware,* †*Pediatric Oncology Branch, National Cancer Institute, National Institutes of Health, Bethesda, Maryland*

BACKGROUND

The intensity and duration of a drug's pharmacological effect are proportional to the dose of the drug administered and the concentration of the drug at its site of action. This simple fundamental principle of pharmacology has a pervasive influence on our approach to the study and use of drugs, from the basic research laboratory to the management of patients receiving drug therapy in the clinic. *Pharmacodynamics* is the discipline that quantifies the relationship between drug concentration at the site of drug action and the drug's pharmacological effect. A drug's pharmacological effect can be monitored and quantified at several levels, including at a molecular or cellular level *in vitro*, in a tissue or organ *in vitro* or *in vivo*, or in the whole organism (Table 18.1). The endpoint that is used to measure effect may differ at each level even for the same drug, and at the organism level the overall pharmacological effect may be the sum of multiple drug effects and the physiologic response of the organism to these drug effects.

Figure 18.1 is an example of a dose-effect study with a molecular endpoint. Patients who were scheduled for resection of their brain tumor received a dose of O^6-benzylguanine (O^6-BG) intravenously 10 to 27 hours prior to surgery (1). O^6-BG irreversibly inactivates the DNA repair protein O^6-alkylguanine-DNA alkyltransferase (AGT), which mediates resistance to some alkylating agent therapy in brain tumors. To determine the dose of O^6-BG that most effectively inhibits AGT activity, a sample of tumor tissue was snap frozen and tumor AGT levels were measured and related to the dose. The dose-effect curve shows an inverse relationship between the O^6-BG dose and the amount of remaining tumor AGT activity (fmol/mg protein), with higher doses resulting in lower tumor AGT activity. The optimal biological dose was defined as the dose achieving AGT levels <10 fmol/mg protein in at least 11 of 13 patients treated at that dose level. As shown in Figure 18.1, all 11 patients at the 100 mg/m^2 dose level had tumor AGT levels <10 fmol/mg protein. There was no O^6-BG-related toxicity from this dose (1).

When the drug-effect endpoint, such as change in blood pressure, is measured on a continuous scale, the dose-effect relationship is termed *graded*, whereas an all-or-none endpoint, such as alive or dead, results in a dose-effect relationship that is *quantal*. Graded dose-effect relationships can be measured in a single biological unit that is exposed to a range of doses, and dose or drug concentration is related to the *intensity* of the effect. Quantal dose-effect relationships are measured in a population of subjects that are treated with a range of doses, and the dose is related to the *frequency* of the all-or-none effect at each dose level.

Figure 18.2 illustrates a graded dose-effect relationship for recombinant human erythropoietin (rhEPO) in patients with end-stage renal disease (2). Erythropoietin, which is produced by the kidney in response to hypoxia, is a naturally occurring hematopoietic growth factor that stimulates bone marrow production

TABLE 18.1 Endpoints for Measuring Drug Effect at Different Levels for the New Class of Molecularly Targeted Anticancer Drugs That Inhibit Farnesyl Protein Transferase

Level	Endpoint
Molecular	Inhibition of farnesyl protein transferase, farnesylation of target substrate proteins such as HDJ2
Cellular	Inhibition of cellular proliferation *in vitro*, induction of apoptosis
Tissue	Change in the size of measurable tumors
Organism	Prolonged survival, reduction in tumor-related symptoms, enhanced quality of life

of red blood cells. Patients with end-stage renal disease are deficient in erythropoietin, and, as a result, they are usually severely anemic and transfusion dependent. In this dose-finding study, 18 patients with end-stage renal disease and baseline hematocrit <20% were treated with rhEPO at doses ranging from 1.5 to 500 units/kg in cohorts of 3 to 5 patients per dose level. The effect of the rhEPO is measured as the peak absolute increment in the hematocrit. At the lowest dose levels (1.5 and 5 units/kg), there was no effect on hematocrit, but starting at a dose of 15 units/kg, the hematocrit increased by 4–22% as the rhEPO dose

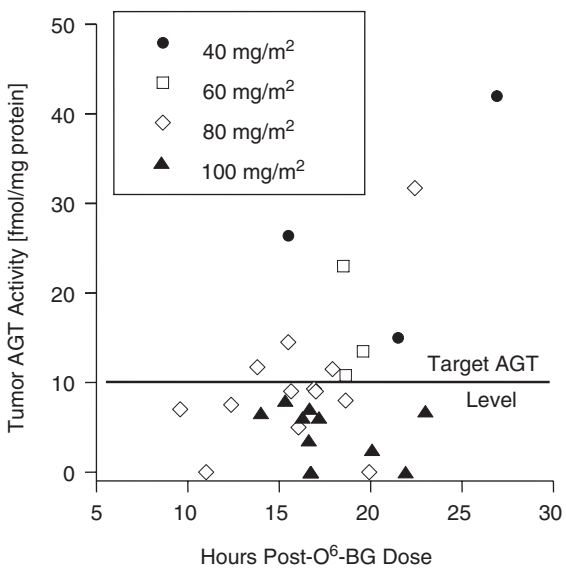

FIGURE 18.1 Activity level of the DNA repair protein, O^6-alkylguanine-DNA alkyltransferase (AGT) in brain tumor surgical specimens from patients treated with escalating doses of the irreversible AGT inhibitor, O^6-benzylguanine (O^6-BG), prior to surgery. All 11 patients treated at the 100 mg/m^2 dose level had undetectable levels of the target enzyme in tumor specimens. (Adapted from data published by Friedman HS, Kokkinakis DM, Pluda J et al. J Clin Oncol 1998;16:3570–5.)

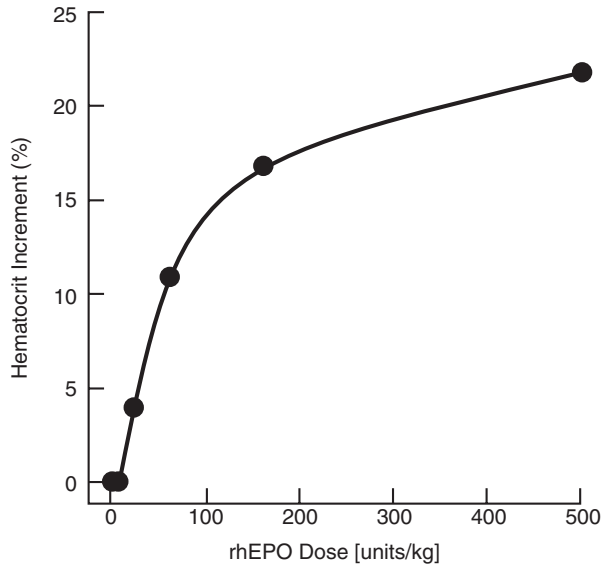

FIGURE 18.2 Dose effect curve for recombinant human erythropoietin (rhEPO) in patients with end-stage renal disease. Each point represents the mean absolute increase in hematocrit in a cohort of three to five patients. (Adapted from data published by Eschbach JW, Egrie JC, Downing MR *et al.* N Eng J Med 1987;316:73–8.)

increased. The shape of the dose-effect curve is a rectangular hyperbola, which asymptotically approaches a maximum effect. This means that there is a "diminishing return" at higher doses because the incremental increase in hematocrit is smaller with each incremental increase in rhEPO dose.

DRUG–RECEPTOR INTERACTIONS

The pharmacological effects of rhEPO and most drugs result from their noncovalent interaction with *receptors* (Figure 18.3). A receptor can be any cellular macromolecule to which a drug selectively binds to initiate its pharmacological effect. Cellular proteins are the most important class of drug receptors, especially cellular proteins that are receptors for endogenous regulatory ligands, such as hormones, growth factors, and neurotransmitters. The drug's chemical structure is the primary determinant of the class of receptors with which the drug will interact. Receptors on the cell surface have two functional domains — a *ligand-binding domain* that is the drug binding site and an *effector domain* that propagates a signal and results in an effect (Figure 18.3). The interaction of a drug and its receptor is reversible and conforms to the *law of mass action*:

$$C + R \underset{k_2}{\overset{k_1}{\rightleftharpoons}} C - R$$

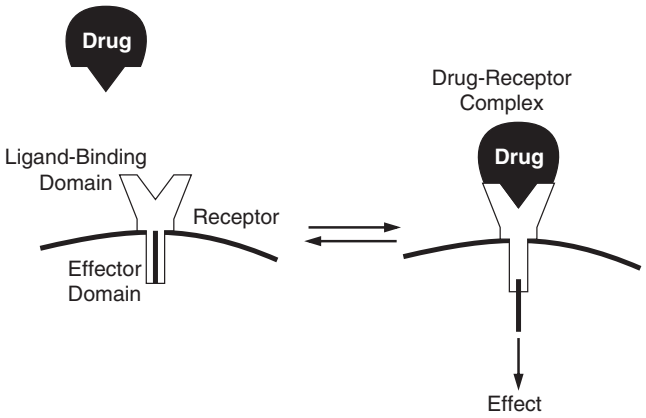

FIGURE 18.3 Drug–receptor interaction. A drug molecule binds reversibly to the ligand-binding domain of a receptor on the cell surface and the receptor propagates the signal into the cell via its effector domain, resulting in a pharmacological effect.

where C is the free drug concentration at the site of action, R is the concentration of unoccupied receptor in tissue, $C - R$ is the concentration of receptors occupied by drug, and k_1 and k_2 are the proportionality constants for the formation and dissociation of the drug receptor complex.

Receptor Occupation Theory

The receptor *occupation theory* of drug action equates drug effect to receptor occupancy. The intensity of drug effect is proportional to the number of receptors that are occupied by drug and the maximum effect occurs when all receptors are occupied by drug. The relationship between drug effect and the concentration of free drug at the site of action (C) can be described at equilibrium by the following equation:

$$\text{Effect} = \frac{\text{Maximum effect} \cdot C}{K_D + C}$$

where the maximum effect is the intensity of the pharmacological effect that occurs when all of the receptors are occupied, and K_D, which equals k_2/k_1, is the equilibrium dissociation constant of the drug–receptor complex. The dissociation constant (K_D) is also a measure of the affinity of a drug for its receptor, analogous to the Michaelis–Menten constant (K_m), which is a measure of the affinity of a substrate for its enzyme. The expression $C/(K_D + C)$ in this equation represents the fraction of receptors that are occupied with drug. When $C \gg K_D$, the expression equals 1 (i.e., all of the receptors are occupied with drug), and Effect = Maximum effect.

The equation relating a drug's pharmacological effect to its concentration describes a hyperbolic function that is shown graphically in Figure 18.4A. As free drug concentration increases, the drug effect asymptotically approaches the maximum effect. When the free drug concentration on the x-axis is transformed to a logarithmic scale, the dose-effect curve becomes sigmoidal, with a central segment that is nearly log-linear (Figure 18.4B). Semilogarithmic dose-effect curves allow for a better assessment of the dose-effect relationship at low doses and of a wide range of doses on the same plot. The EC_{50} is the dose at which 50% of the maximum effect is produced or

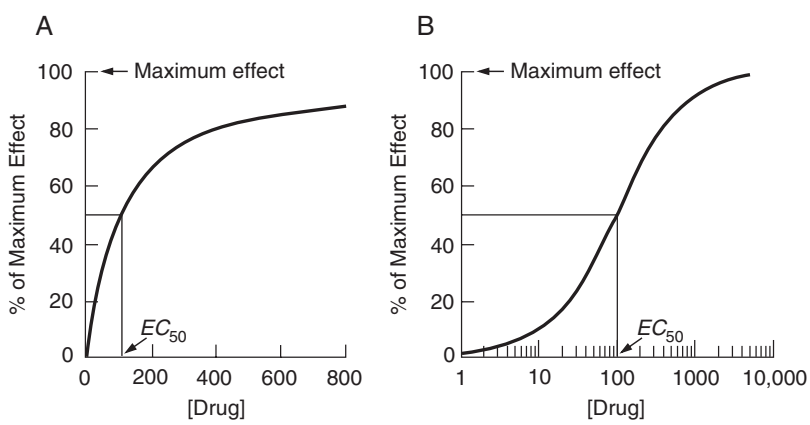

FIGURE 18.4 Dose-effect curves plotted using a (A) linear or (B) logarithmic scale for drug dose/concentration on the x-axis. The function relating effect to dose/concentration is based on the receptor occupation theory, described in the text. The relationship is nonlinear and with each increment in dose/concentration there is a diminishing increment in effect. EC_50 is the dose/concentration producing half of the maximum effect.

the concentration of drug at which the drug is half-maximally effective. On a semilogarithmic plot, the EC_{50} is located at the midpoint, or inflection point, of the curve. When the relationship between receptor occupancy and effect is linear, the $K_D = EC_{50}$. If there is amplification between receptor occupancy and effect, such as if the receptor has catalytic activity when the receptor ligand is bound, then the EC_{50} lies to the left of the K_D.

Receptor-Mediated Effects

Figure 18.5A shows dose-effect curves for the types of pharmacological effects that can be elicited when a drug interacts with its receptor. Drugs that interact with a receptor and elicit the same stimulatory effect as does the receptor's endogenous ligand are called *agonists*. An agonist that produces less than the maximum effect at doses or concentrations that saturate the receptor is a *partial agonist*. An *antagonist* binds to a receptor but produces no effect. Antagonists produce their pharmacological effects by inhibiting the action of an agonist that binds to the same receptor.

Dose-effect curves are also useful for studying pharmacodynamic drug interactions (Figure 18.5B). A *competitive antagonist* binds to the same binding site as does the agonist, and the competitive antagonist can be displaced from the binding site by an excess of the agonist. Therefore, the maximum effect of an agonist can still be achieved in the presence of a competitive antagonist, if a sufficient dose or concentration of the agonist is used. The competitive antagonist lowers the potency of the agonist, but does not alter its efficacy. A *noncompetitive antagonist* binds irreversibly to the same binding site as does the agonist, or it interacts with other components of the receptor to diminish or eliminate the effect of the drug binding to the receptor. A noncompetitive antagonist prevents the agonist, at any concentration, from producing its maximum effect. Typically, a dose-effect curve with this type of interaction will reveal a reduced apparent efficacy, but the potency of the drug is unchanged.

GRADED DOSE-EFFECT RELATIONSHIP

The drug–receptor concept of drug action and the receptor occupation theory describe a graded dose-effect relationship, in which the responding system is capable of showing a progressively increasing effect with increasing dose or drug concentration. Graded dose-effect relationships are measured by exposing an individual or a specific organ or tissue to increasing amounts of drug and quantifying the resulting effect on a continuous scale. Although the dose-effect curve can take on a variety of shapes, the classical graded dose-effect curve is the rectangular hyperbola described previously (Figure 18.4).

Figure 18.6 demonstrates a graded concentration-effect study of an intravenous infusion of lidocaine at a rate of 8.35 mg/min in patients with

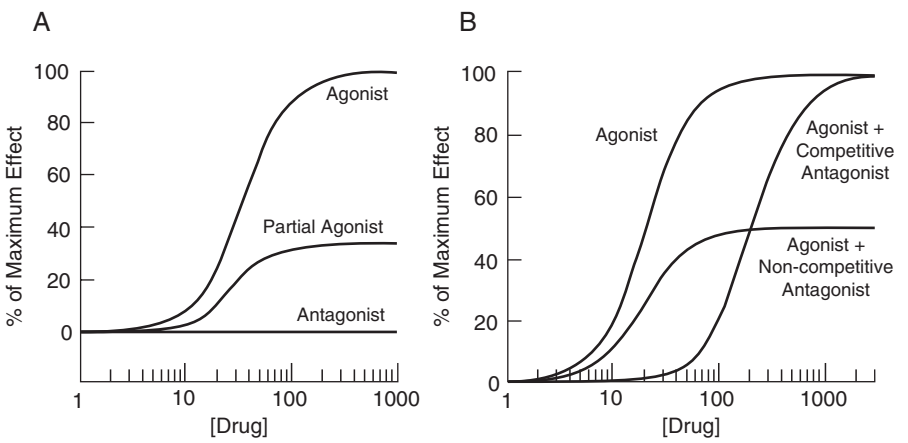

FIGURE 18.5 (A) Dose-effect curves describing the types of pharmacological effects produced when a drug interacts with its receptor. An *agonist* produces the maximum stimulatory effect, a *partial agonist* produces less than the maximum stimulatory effect, and an *antagonist* elicits no effect, but inhibits the effect of an agonist. (B) Dose-effect curves for the combination of an agonist and antagonist. A competitive antagonist reduces the potency of the agonist, but not the maximum effect. A noncompetitive antagonist reduces the efficacy (maximum effect), but does not alter the potency of the agonist.

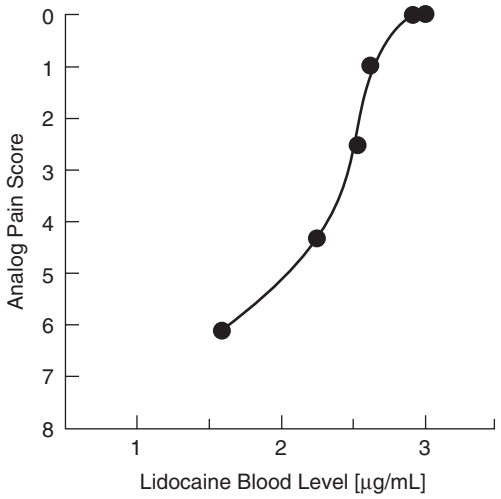

FIGURE 18.6 Graded concentration-effect curve for intravenous lidocaine in patients with neuropathic pain. Pain was scored from 0 to 10 with an analog pain scale. The median pretreatment pain score was 7 and a score of 0 meant no pain. Blood levels of lidocaine were measured every 10 minutes and pain was scored at the same time points. The graph relates the blood level of lidocaine to the severity of pain. (Adapted from data published by Ferrante FM, Paggioli J, Cherukuri S, Arthur GR. Anesth Analg 1996;82:91–7.)

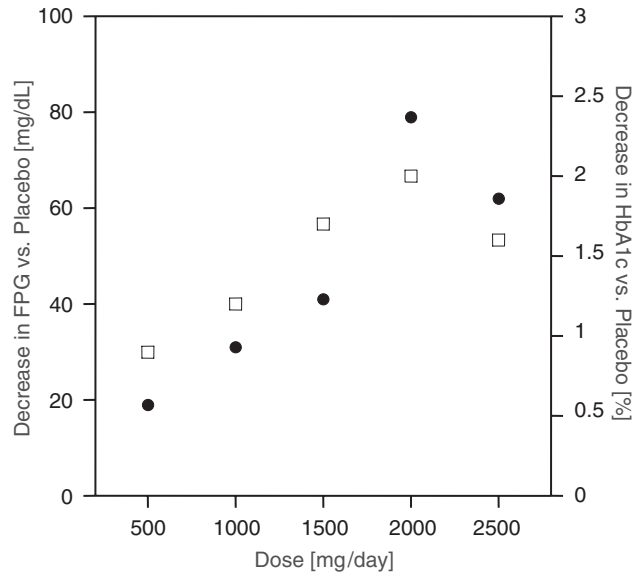

FIGURE 18.7 Graded dose-effect curves for the oral antihyperglycemic agent, metformin, relative to a placebo in patients with a fasting plasma glucose (FPG) exceeding 180 mg/dL. Reductions in FPG (●) and HbA1c (□) occurred in a dose-dependent manner. (Adapted from data published by Garber AJ, Duncan TG, Goodman AM. Am J Med 1997;102;491–7.)

neuropathic pain (3). The severity of pain was measured using a visual analog pain scale (0 to 10) at 10-minute intervals, and blood levels of lidocaine were also measured at 10-minute intervals. Patients had a median pain score of 7 prior to the initiation of therapy, and the maximal effect, no pain, had a score of 0. The concentration-effect curve for lidocaine is very steep. The pain decreased over a concentration range of 0.62 µg/mL. This steep concentration-effect curve indicates that the response to intravenous lidocaine is characterized by a precipitous break in pain over a narrow range in lidocaine concentrations.

Figure 18.7 demonstrates a typical example of a graded dose-effect curve from a study that evaluated the dose-effect relationship for the antihyperglycemic agent metformin. Metformin lowers glucose variables by increasing insulin sensitivity in peripheral tissues and inhibiting hepatic glucose production. Patients with a fasting plasma glucose (FPG) exceeding 180 mg/dL were randomized to receive either a placebo or metformin at one of five escalating doses ranging from 500 to 2500 mg/day (4). The monitored endpoints of the study included FPG and levels of glycosylated hemoglobin (HbA_{1c}), a surrogate for chronic hyperglycemia. At the end of the study, FPG had declined by 19–84 mg/dL and HbA_{1c} had declined by 0.6–2.0% in patients receiving metformin compared to placebo. Predictably, the decreases in FPG and HbA_{1c} were disproportionate due to the slow turnover of hemoglobin. Metformin reduced both FPG and HbA_{1c} in a dose-related fashion, with the maximum effect on both endpoints occurring at the upper limits of the dose range (2000 mg). The minimum effective dose was found to be 500 mg/day rather than 1500 mg/day, as was previously thought, allowing in subsequent clinical practice an upward titration of metformin doses above this minimum if needed to achieve the target effect.

Dose-Effect Parameters

Potency and *efficacy* are parameters that are derived from graded dose-effect curves and that can be used to compare drugs that elicit the same pharmacological effect. Potency, which is a measure of the sensitivity of a target organ or tissue to a drug, is a relative term that relates the amount of one drug required to produce a desired level of effect to the amount of a different drug required to produce the same effect. On the semilogarithmic graded dose-effect plot, the curve of the more potent agent is to the left, and the EC_{50} is lower. A drug's potency is influenced by its affinity for its receptor. In Figure 18.8, Drug A is more potent than is Drug B.

Figure 18.9 shows the *in vitro* dose-effect curves for two thiopurine analogs, thioguanine (TG) and mercaptopurine (MP). The thiopurines are antimetabolites that are used in the treatment of acute leukemia.

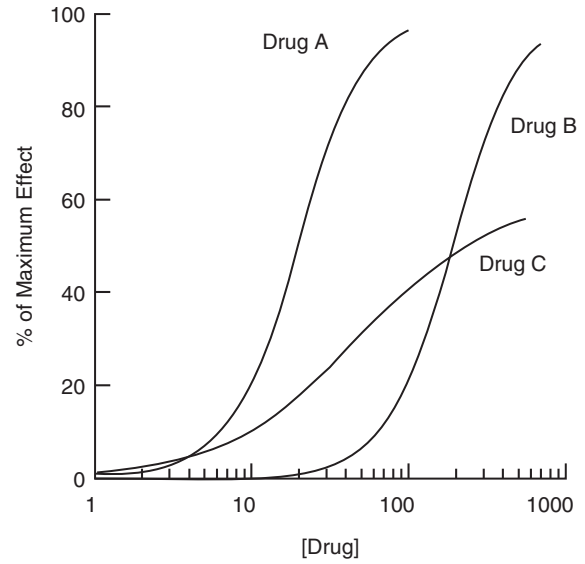

FIGURE 18.8 Evaluation of the relative potency and efficacy of drugs that produce the same pharmacological effect. Drug A is more potent than is Drug B, and Drugs A and B are more efficacious than is Drug C.

Both drugs have multiple sites of action, but their primary mechanism of action is felt to be the result of their incorporation into DNA strands. Effect is measured *in vitro* as the percentage of leukemic cells killed in the presence of drug compared to untreated controls for three different leukemic cell lines (5). The dose-effect curves show that thioguanine is approximately 10-fold more potent than is mercaptopurine, despite the fact that both analogs have very similar chemical structures and are converted to the same active intracellular metabolite (deoxythioguanosine triphosphate) prior to their incorporation into DNA. The two drugs appear to have similar efficacy in this *in vitro* study. Considerable weight is placed on these *in vitro* concentration-effect studies for anticancer drugs because it has not been possible to define therapeutic concentrations *in vivo* in animal models or patients.

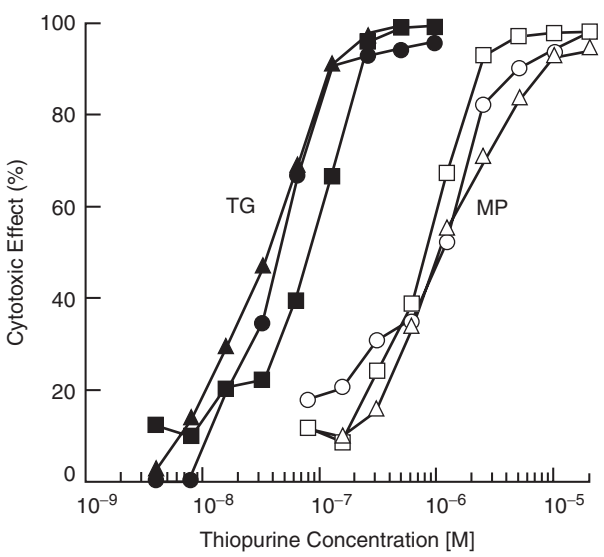

FIGURE 18.9 Concentration-effect curves for the thiopurine analogs, mercaptopurine (MP, *open symbols*) and thioguanine (TG, *closed symbols*). Effect is the percentage of cells killed *in vitro* relative to an untreated control in MOLT 4 (squares), CCRF-CEM (*triangles*), and Wilson (*circles*) leukemia cell lines. TG is 10-fold more potent than is MP. (Reproduced with permission from Adamson PC, Poplack DG, Balis FM. Leukemia Res 1994;18:805–10.)

Efficacy is the drug property that allows the receptor-bound drug to produce its pharmacological effect. The relative efficacy of two drugs that elicit the same effect can be measured by comparing the maximum effects of the drugs. In Figure 18.8, Drugs A and B are more efficacious than is Drug C. *Intrinsic activity* (α), which is a proportionality factor that relates drug effect in a specific tissue to receptor occupancy, has become a standard parameter for quantifying the ability of a drug to produce a response:

$$\text{Effect} = \alpha \cdot \left(\frac{\text{Maximum effect} \cdot \text{Dose}}{K_D + \text{Dose}} \right)$$

The value for intrinsic activity ranges from 1 for a full agonist to 0 for an antagonist, and the fractional values between these extremes represent partial agonists. Intrinsic activity is a property of both the drug and the tissue in which drug effect is measured.

Comparing the dose-effect curves of drugs that produce the same pharmacological effect can also provide information about the site of action of the drugs. Drugs A and B in Figure 18.8 have parallel dose-effect curves with identical shapes and the same level of maximal response. This suggests, but does not prove, that these two drugs act through the same receptor. Conversely, Drugs A and C have nonparallel dose-response curves, suggesting that they have different sites of action.

Dose Effect and Site of Drug Action

Graded concentration-effect studies may be useful for establishing the mechanism of action of a drug at a molecular or biochemical level by assessing the drug–receptor interaction. The xanthine analog, theophylline, which is a potent relaxant of bronchial smooth muscle, is used for the treatment of asthma. However, theophylline has a narrow therapeutic range, and at concentrations above this therapeutic range patients can experience vomiting, tremor, seizures, and cardiac arrhythmias. Theophylline interacts with multiple receptors that could account for its

antiasthmatic effect and its toxicity. Theophylline is an adenosine receptor antagonist and it inhibits phosphodiesterase (PDE). These two mechanisms have been proposed as the basis for the antiasthmatic effects of theophylline and other xanthines.

In Figure 18.10, the drug concentration required to elicit *in vitro* relaxation of tracheal smooth muscle in isolated guinea pig tracheal segments for a series of xanthine analogs, including theophylline, is related to the drug concentration required to antagonize the A_1-adenosine receptor (Figure 18.10A) or to inhibit brain soluble PDE (Figure 18.10B) (6). The relative potencies of these xanthine analogs as adenosine receptor antagonists do not correlate with their potencies as tracheal relaxants. However, there is an association between PDE inhibition and tracheal relaxant activity, suggesting that PDE inhibition is the primary site of drug action. This type of graded concentration-effect analysis can lead to the development of more selective agents. In this case, xanthine analogs that are more potent PDE inhibitors and weaker adenosine receptor antagonists may be more effective and less toxic antiasthmatics.

QUANTAL DOSE-EFFECT RELATIONSHIP

Whereas a graded dose-effect relationship relates drug dose and concentration to the intensity of a drug's effect measured on a continuous scale in a single biological unit, the *quantal* dose-effect relationship relates dose to the frequency of the all-or-none effect in a population of individuals. The minimally effective dose, or *threshold dose*, of the drug that evokes the all-or-none effect is identified by gradually increasing the dose in each subject. When displayed graphically as a frequency distribution histogram, with threshold dose levels as the independent variable (x-axis) and the number of subjects who respond at each threshold dose level on the y-axis, the quantal dose-effect curve assumes a normal frequency distribution, or bell-shaped curve (Figure 18.11A). The threshold dose level at which the effect occurs with maximum frequency is in the middle portion of the dose range. For most drugs a wide range of threshold doses is required to produce the all-or-none effect in a population of individuals. This variability results from differences in pharmacokinetics and in end-organ or tissue sensitivity to the drug (pharmacodynamics) within the population.

A quantal dose-effect relationship can also be graphically displayed as a cumulative dose-effect curve, in which the cumulative percentage of individuals experiencing an effect is plotted as a function of the threshold dose. The normal frequency distribution in Figure 18.11A takes on a sigmoidal shape when the same data are plotted as a cumulative dose-effect curve (Figure 18.11B). The median effective dose (ED_{50}) for the quantal dose-effect relationship is the dose at

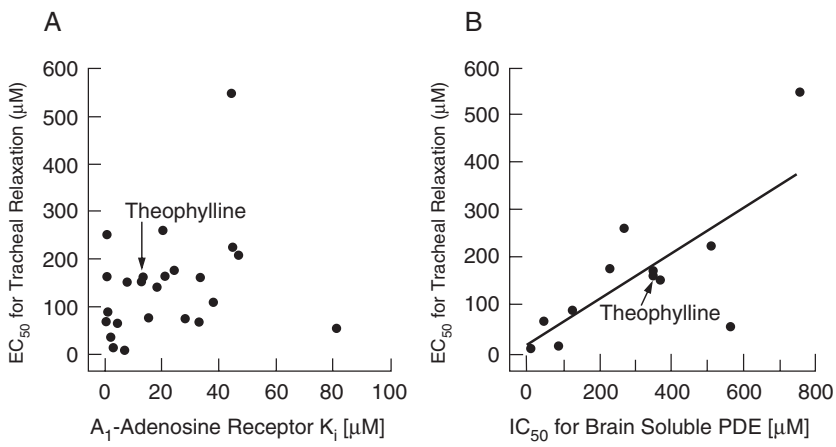

FIGURE 18.10 Correlation between concentration effect at the tissue level measured by EC_{50} for relaxation of guinea pig trachea and concentration effect at the receptor level for (A) antagonism of the A_1-adenosine receptor and (B) inhibition of phosphodiesterase for a series of xanthine analogs, including theophylline. The correlation between EC_{50} for tracheal relaxation and IC_{50} for phosphodiesterase inhibition suggests that phosphodiesterase inhibition is the primary site of action for the antiasthmatic effects of these drugs. (Reproduced with permission from Brackett LE, Shamim MT, Daly JW. Biochem Pharmacol 1990;39:1897–904.)

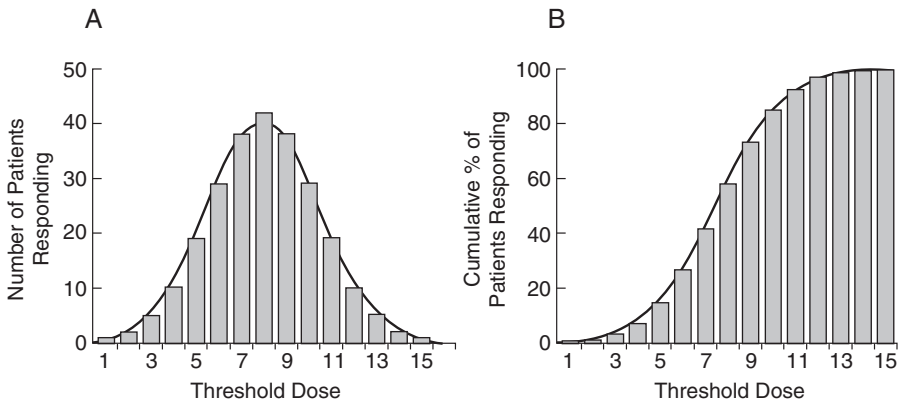

FIGURE 18.11 Population-based, quantal dose-effect curves plotted in (A) as a frequency distribution histogram relating the threshold dose required to produce an all-or–none effect to the number of patients responding at each threshold dose, and (B) as a cumulative distribution, in which the cumulative fraction of patients responding at each dose is plotted as a function of the dose.

which 50% of the population on the cumulative dose-effect curve responds to the drug. The cumulative dose-effect curve reflects the manner in which most quantal dose-effect studies are performed in a population of individuals. It is usually not practical in human or animal trials to define the threshold dose for each individual by gradually increasing the dose in each study participant. Therefore, in most studies, groups of individuals are treated at each different dose level, and the fraction of those who respond at each dose level represents the cumulative proportion of individuals whose threshold dose is at or below the administered dose. This is equivalent to the cumulative distribution.

When administered to an organism, a drug produces a desired therapeutic effect but is also likely to produce at least one toxic effect. As a result, a single dose-effect curve does not adequately characterize the full spectrum of effects from the drug. The toxic effects of a drug can also be described by separate quantal dose-effect curves, and the safety of a drug depends on the degree of separation between the dose that produces the therapeutic effect and the dose that produces unacceptable toxic effects.

Cardiotoxicity, which can lead to congestive heart failure and death, is a toxic effect of the anticancer drug, doxorubicin. A cumulative dose-effect analysis demonstrated that doxorubicin cardiotoxicity is related to the lifetime dose of the drug (Figure 18.12) and provided the basis for the definition of safe lifetime dose levels (7). The lifetime dose of doxorubicin is now limited to less than 400–450 mg/m^2, which is associated with a <5% risk of developing congestive heart failure.

Therapeutic Indices

Therapeutic indices quantify the relative safety of a drug and can be estimated from the cumulative quantal dose-effect curves of a drug's therapeutic and toxic effects. Figure 18.13 shows the doses that are used in the calculation of these indices.

The *therapeutic ratio* is a ratio [TD_{50}/ED_{50}] of the dose at which 50% of patients experience the toxic effect to the dose at which 50% of patients experience the therapeutic effect. A therapeutic ratio of 2.5 means that approximately 2.5 times as much drug

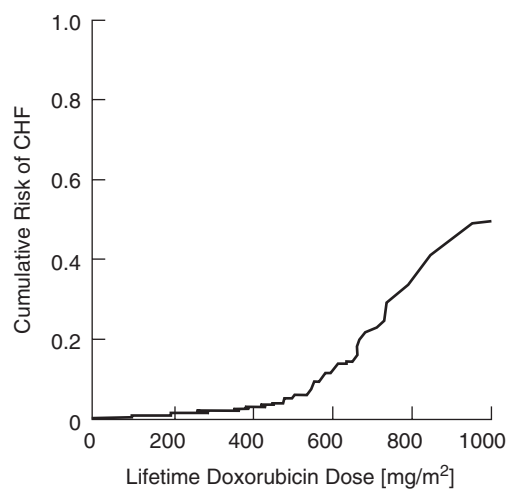

FIGURE 18.12 Cumulative risk of developing congestive heart failure (*chf*) as a function of the lifetime dose of doxorubicin. (Reproduced with permission from Van Hoff DD, Layard MW, Basa P *et al.* Ann Intern Med 1979;91:710–7.)

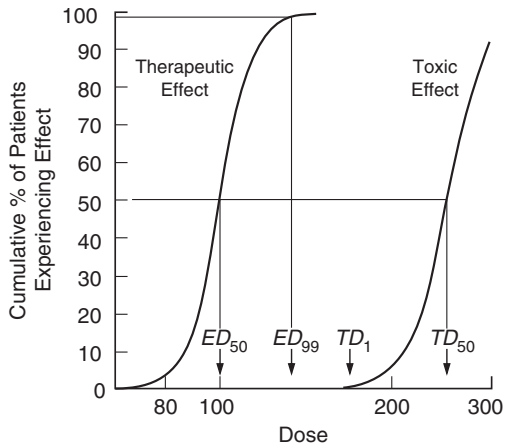

FIGURE 18.13 Cumulative quantal dose-effect curves for a drug's therapeutic and toxic effects. The ED_{50} and ED_{99} are the doses required to produce the drug's therapeutic effect in 50% and 99% of the population, respectively. The TD_1 and TD_{50} are the doses that cause the toxic effect in 1% and 50% of the population, respectively.

is required to cause toxicity in half of the patients than is needed to produce a therapeutic effect in the same proportion of patients. However, this ratio of toxic to therapeutic dose may not be consistent across the entire dose range if the dose-effect curves for the therapeutic and toxic effects are not parallel.

The goal of drug therapy is to achieve the desired therapeutic effect in all patients without producing toxic effects in any patients. Therefore, an index that uses the lowest toxic and highest therapeutic doses is more consistent with this goal than is the therapeutic ratio. The *certainty safety factor* (*CSF*) is the ratio of TD_1/ED_{99}. A CSF >1 indicates that the dose effective in 99% of the population is less than the dose that would be toxic in 1% of the population. If the CSF <1, there is overlap between the maximally effective (ED_{99}) and minimally toxic (TD_1) doses. Unlike the therapeutic ratio, this measure is independent of the shapes of the cumulative quantal dose-effect curves for the therapeutic and toxic effects. The *standard safety margin* $\{[(TD_1 - ED_{99})/ED_{99}] \times 100\}$ also uses TD_1 and ED_{99} but is expressed as the percentage by which the ED_{99} must be increased before the TD_1 is reached.

Dose Effect and Defining Optimal Dose

Characterization of the dose-effect relationship is an important component of clinical trials performed during the initial stages of clinical drug development. These early trials frequently follow a dose-escalation design in which increasing dose levels of drug are administered to cohorts of patients until the maximal effect is achieved or the dose-limiting toxicity is encountered. The optimal dose is identified from these dose-effect relationships for the therapeutic and toxic effects.

Johnston (8) reviewed the dose-finding studies of a variety of antihypertensive agents and compared the initial recommended dosage range from these dose-finding studies with the lowest effective dose identified in subsequent randomized clinical trials and the currently recommended dose (Table 18.2). Based on this dose-effect meta-analysis, he concluded that many antihypertensive agents were introduced into clinical practice at excessively high doses. He attributed this to reliance on a dose-escalation trial design in which the dose was escalated too rapidly, resulting in a failure to define the lower part of the dose-effect relationship. In many of the cases, the initial dose produced the maximum therapeutic effect, but the dose continued to be escalated without any clear evidence of increased efficacy. The initial recommended doses often appeared to be on the plateau of the dose-effect curve rather than in the desired range; at these higher doses, there is very little added benefit but a significantly greater risk for toxicity. A current trend is to avoid this pitfall by identifying the minimum dose required for satisfactory effect (MDSE) (9).

For anticancer drugs, tumor response is often related to *dose intensity*, and this dose-effect relationship is the basis for treating cancer patients with the maximum tolerated dose of these drugs, administered at the shortest possible dosing interval. Dose intensity, or dose rate, is the amount of drug administered within a defined period of time (e.g., mg/week). The strong relationship between doxorubicin dose intensity and the percentage of patients with osteogenic sarcoma who achieved greater than 90% tumor necrosis is shown in Figure 18.14 (10).

TABLE 18.2 Comparison of Recommended Doses for Antihypertensive Agents Based on Initial Dose-Finding Clinical Trials and Subsequent Experience in Randomized Clinical Trials and Clinical Practice[a]

Drug	Dose range (mg)		Lowest effective dose (mg)
	Early studies	Present dose	
Propranolol	160–5000	160–320	80
Atenolol	100–2000	50–100	25
Hydrochlorothiazide	50–400	25–50	12.5
Captopril	75–1000	50–150	37.5
Methyldopa	500–6000	500–3000	750

[a] Data from Johnson GD. Pharmacol Ther 1992;55:53–93.

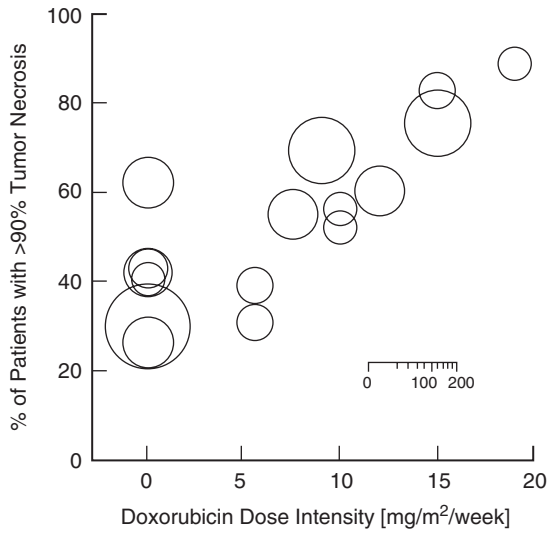

FIGURE 18.14 Dose intensity meta-analysis for doxorubicin in patients with osteosarcoma. Each bubble represents a separate clinical trial and the size of the bubble is proportional to the number of patients treated during the trial. Doxorubicin was administered prior to definitive surgical resection and effect is >90% necrosis of tumor in the resected specimen. Dose intensity or dose rate is measured in mg/m^2/week. (Reproduced with permission from Smith MA, Ungerleider RS, Horowitz ME, Simon R. J Natl Cancer Inst 1991;83:1460–70.)

A dose intensity analysis such as this one is useful in defining the optimal dose of an anticancer drug if a relationship between dose and therapeutic effect is observed.

PHARMACODYNAMIC MODELS

Pharmacodynamic models mathematically relate a drug's pharmacological effect to its concentration at the effect site. Examples of the types of pharmacodynamic models that have been employed include the fixed-effect model, maximum-effect models (E_{max} and sigmoid E_{max}), and linear and log-linear models (11). Unlike pharmacokinetic models, pharmacodynamic models are time independent. However, these models can be linked to pharmacokinetic models, as discussed in Chapter 19.

Fixed-Effect Model

The fixed-effect pharmacodynamic model is a simple model that relates drug concentration to a pharmacological effect that is either present or is absent, such as sleep, or is a defined cutoff for a continuous effect, such as diastolic blood pressure <90 mm Hg in a patient with hypertension. The specific pharmacological effect is present when the drug concentration is greater than a threshold level required to produce the effect, and the effect is absent when the drug concentration is below the threshold. This threshold concentration varies among individuals and the fixed-effect model quantifies the likelihood or probability that a given concentration will produce an all-or-none effect based on the population distribution of threshold concentrations. This model is used primarily in the clinical setting. For example, based on a study correlating digoxin levels with toxicity, the probability of toxicity is 50% at a digoxin level of 3 ng/mL (12).

Maximum-Effect (E_{max} and Sigmoid E_{max}) Models

Although the maximum-effect pharmacodynamic models are empirically based, they do incorporate the concept of a maximum effect predicted by the drug–receptor interactions described earlier. The Hill equation, which takes the same form as the equation describing drug effect as a function of receptor occupancy, relates a continuous drug effect to the drug concentration at the effect site as shown:

$$\text{Effect} = \frac{E_{max} \cdot C^n}{EC_{50}^n + C^n}$$

where E_{max} is the maximum effect, EC_{50} is the drug concentation producing 50% of E_{max}, C is the drug concentration, and the exponential constant, n (the *Hill constant*), controls the slope of the resulting sigmoid-shaped curve, as shown in Figure 18.15 (13). If there is a baseline effect in the absence of drug, the effect term on the left-hand side of the equation can be expressed

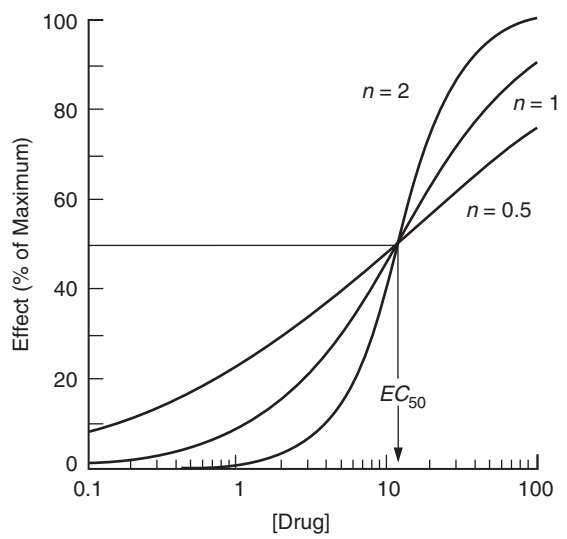

FIGURE 18.15 Sigmoid E_{max} pharmacodynamic model relating drug effect to the drug concentration at the effect site. The three curves show the effect of the exponential Hill (H) constant n on the slope of the sigmoid curves.

as the absolute or percentage change from baseline. Maximum-effect models describe a hyperbolic relationship between drug concentration and effect such that there is no effect in the absence of drug, there is a maximum effect (E_{max}) when concentrations approach infinity, and there is a diminishing increment in effect as the concentration rises above the EC_{50}.

The E_{max} model is a simpler form of the sigmoid E_{max} model, with a slope factor $n = 1$, so that

$$\text{Effect} = \frac{E_{max} \cdot C}{EC_{50} + C}$$

In Figure 18.16, the E_{max} model is used to quantify the relationship between theophylline serum level and improvement in pulmonary function as measured by the increase in forced expiratory volume in 1 second (FEV_1) in six patients who were treated with placebo and three incremental doses of theophylline (14).

Linear and Log-Linear Model

In the linear model, concentration-effect relationships are described by the following equation:

$$\text{Effect} = E_0 + \beta \cdot C$$

where E_0 is the baseline effect prior to treatment, β is the slope of the line, and C is the drug concentration. Although the linear model will predict no effect when drug concentrations are zero, it cannot predict a maximum effect. Therefore, for many effects, this model is only applicable over a narrow concentration range. At low drugs concentrations ($\ll EC_{50}$), the slope will approach the value of E_{max}/EC_{50}.

When the maximum-effect models are plotted on a semilogarithmic scale, the sigmoidal curves are log-linear within the range of 20–80% of the maximum effect, and can be described by the *log-linear model* (Effect $= \beta \cdot \log C + I$, where I is the intercept). The disadvantages of this approach are that the pharmacologic effect cannot be predicted when the drug concentration is zero because of the logarithmic function, and the maximum effect cannot be predicted at very high concentrations. For example, the data shown in Figure 18.16 were linearized in the original report by plotting them with a logarithmic abscissa (14). This linearized version of the plot unfortunately obscured the fact that theophylline levels above 15 µg/mL result in relatively little gain in therapeutic efficacy. Thus maximum-effect models, which do not have these limitations, may be preferable to the linear models over a broad drug concentration range. Although simpler linear models are necessary when effects are linear over narrow concentration ranges, semilogarithmic plots should not be used to linearize curvilinear dose-effect relationships.

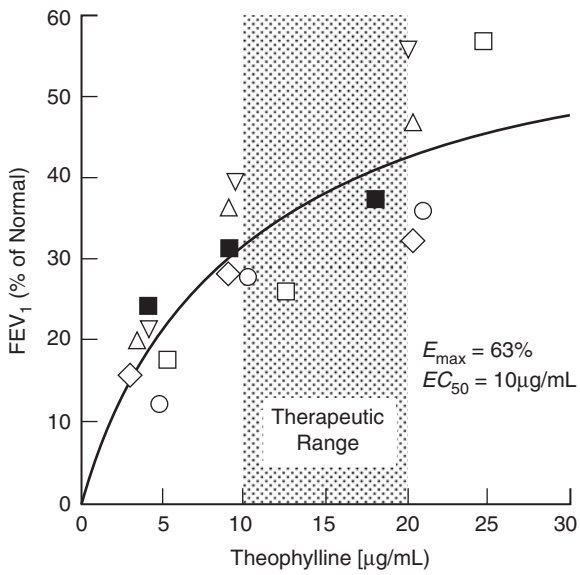

FIGURE 18.16 Theophylline pharmacodynamics in patients with asthma. Effect, which was measured as improvement in forced expiratory volume in 1 second (FEV1), is related to the serum drug level in six patients, who were studied after placebo and three incremental doses of theophylline. An E_{max} model is fit to the concentration-effect data. Based on this analysis, a therapeutic range of 10–20 µg/mL was proposed (*shaded area*). (Adapted from data published by Mitenko PA, Ogilvie RI. N Engl J Med 1973; 289:600–3.)

CONCLUSION

The dose- or concentration-effect relationship is a central tenet of pharmacology. Dose-effect studies contribute to our understanding of the site of action of a drug, the selection of a dose and dosing schedule, the determination of an agent's potency and efficacy, and the elucidation of drug interactions. An essential aspect of the preclinical and clinical evaluations of any new drug is the careful delineation of the dose-effect relationship over the anticipated dosing range for the drug's therapeutic and toxic effects. More rational individualized dosing regimens that incorporate adaptive dosing, therapeutic drug monitoring, and the determination of risk/benefit from therapeutic indices have evolved from the integration of our knowledge of pharmacokinetics and pharmacodynamics.

REFERENCES

1. Friedman HS, Kokkinakis DM, Pluda J, Friedman AH, Cokgor I, Haglund MM *et al*. Phase I trial of O^6-benzylguanine for patients undergoing surgery for malignant glioma. J Clin Oncol 1998;16:3570–5.

2. Eschbach JW, Egrie JC, Downing MR, Browne JK, Adamson JW. Correction of the anemia of end-stage renal disease with recombinant human erythropoietin: Results of a combined phase I and II clinical trial. N Engl J Med 1987;316:73–8.
3. Ferrante FM, Paggioli J, Cherukuri S, Arthur GR. The analgesic response to intravenous lidocaine in the treatment of neuropathic pain. Anesthes Analges 1996;82:91–7.
4. Garber AJ, Duncan TG, Goodman AM, Mills DJ, Rohlf JL. Efficacy of metformin in type II diabetes: Results of a double-blind, placebo-controlled, dose-response trial. Am J Med. 1997;102:491–7.
5. Adamson PC, Poplack DG, Balis FM. The cytotoxicity of thioguanine vs mercaptopurine in acute lymphoblastic leukemia. Leukemia Res 1994;18:805–10.
6. Brackett LE, Shamim MT, Daley JW. Activities of caffeine, theophylline, and enprofylline analogs as tracheal relaxants. Biochem Pharmacol 1990; 39:1897–904.
7. Von Hoff DD, Layard MW, Basa P, Davis HL, Von Hoff AL, Rozencweig M *et al*. Risk factors for doxorubicin-induced congestive heart failure. Ann Intern Med 1979;91:710–7.
8. Johnston GD. Dose-response relationships with antihypertensive drugs. Pharmacol Ther 1992;55:53–93.
9. Rolan P. The contribution of clinical pharmacology surrogates and models to drug development — A critical appraisal. Br J Clin Pharmacol 1997;44:219–25.
10. Smith MA, Ungerleider RS, Horowitz ME, Simon R. Influence of doxorubicin dose intensity on response and outcome for patients with osteogenic sarcoma and Ewing's sarcoma. J Natl Cancer Inst 1991;83:1460–70.
11. Holford NHG, Scheiner LB. Understanding the dose-effect relationship: Clinical applications of pharmacokinetic–pharmacodynamic models. Clin Pharmacokinet 1981;6:429–53.
12. Piergies AA, Worwag EM, Atkinson AJ Jr. A concurrent audit of high digoxin plasma levels. Clin Pharmacol Ther 1994;55:353–8.
13. Wagner JG. Kinetics of pharmacologic response. J Theor Biol 1968;20:173–201.
14. Mitenko PA, Ogilvie RI. Rational intravenous doses of theophylline. N Engl J Med 1973;289:600–3.

CHAPTER

19

Time Course of Drug Response

NICHOLAS H. G. HOLFORD* **AND ARTHUR J. ATKINSON, JR.†**

**University of Auckland, Auckland, New Zealand,*

†Clinical Center, National Institutes of Health, Bethesda, Maryland

Therapeutic drug responses are a consequence of drug exposure. Exposure describes the intensity and time course of drug treatment. Most clinicians and patients behave as if they believe drug exposure is defined by the drug dose. However, the central dogma of clinical pharmacology is that drug actions are determined by drug concentration. Events leading up to such concentrations include the therapeutic consultation between patient and prescriber, the patient's decision to obtain and take the medication, and the time course of delivery and loss of drug from the site of action. Taking a dose of drug is only part of this chain and provides incomplete predictive information regarding the time course of response.

Pharmacokinetics provides a rational framework for understanding how the time course of observable drug concentration (usually in plasma) is related to the dose. The principles of pharmacodynamics described in Chapter 18 provide a companion framework for understanding the relationship between concentration and response. However, these scientific disciplines are not enough to describe the time course of drug response, for two main reasons:

1. Plasma is not the site of action of most drugs, so responses will be delayed in relation to pharmacokinetic predictions of plasma concentrations. The only exception is a limited number of drugs (e.g., heparin) whose action directly affects physical components of plasma.
2. The action of a drug is not the same as the drug response. A cascade of events links receptor activation to physiological changes, and these in turn are linked via complex pathophysiological mechanisms to the desired therapeutic benefit.

Recognizing these processes, it is useful to distinguish between the pharmacologic *action* (e.g., stimulation of a receptor, inhibition of an enzyme), the physiologic *effect* (e.g., bronchodilatation, lowering of cholesterol), and the therapeutic *response* (e.g., relief of an asthma attack, reduction of risk of a cardiovascular event).

The two reasons given for elaborating the time course of drug response give rise to two basic conceptual approaches for describing the delay between plasma concentrations and changes in physiological effect (1). In the first approach, the effect is considered to be a direct consequence of drug action and the delay is thought to reflect the time required for the drug to reach its site of pharmacologic action, or *biophase*. In the second approach, the drug is thought to alter the synthesis or degradation of some factor, usually an endogenous compound that mediates the physiological effect. With each approach, the basic relationships between drug concentration and intensity of effect that were described in Chapter 18 can be applied to the pharmacodynamic analysis. The relationship between drug-induced effects on pathophysiology and therapeutic response is often too complex to describe in detailed mechanistic terms and usually involves the pragmatic application of pharmacodynamic models linking observable biomarkers of drug effect to response as if the biomarkers were themselves drug concentrations.

PHARMACOKINETICS AND DELAYED PHARMACOLOGIC EFFECTS

In some cases it is biologically plausible to identify as the site of drug action one of the compartments used to characterize the kinetics of drug distribution. As was described in Chapter 3, Sherwin *et al*. (2) noted that the time course of insulin-stimulated glucose utilization parallels expected insulin concentrations in the slowly equilibrating compartment of a three-compartment model of insulin distribution (see Chapter 3, Figure 3.3). Since the kinetics of drug in this compartment may correspond to insulin concentrations in skeletal muscle interstitial fluid (3), it is reasonable to use this pharmacokinetic compartment to predict this particular insulin effect. In a study of digoxin pharmacokinetics and inotropic effects, Kramer *et al*. (4) observed that there is a close relationship between the time course of these effects and estimated digoxin concentrations in the slowly equilibrating peripheral compartment of a three-compartment pharmacokinetic model (Figure 19.1). Although the heart comprises only a small fraction of total body muscle mass, there is some physiological justification for identifying myocardium as a component of this compartment. The authors noted that the time course of inotropic response could also reflect a delay due to the time required for the cascade of digoxin-initiated intracellular events to result in increased myocardial contractile force. However,

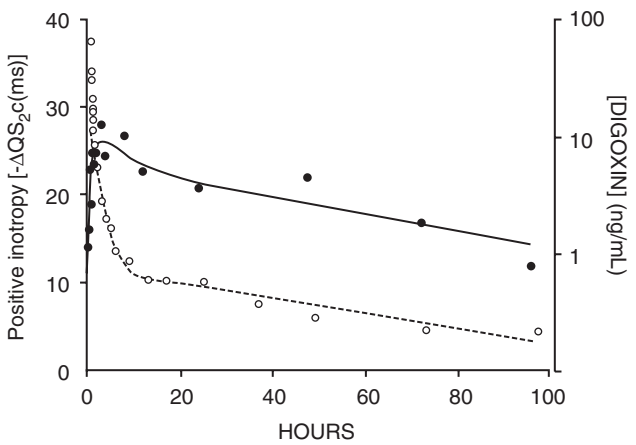

FIGURE 19.1 A mechanistic model describing the slow binding of digoxin to its receptor was used to fit the solid and dotted lines to average measurements of plasma digoxin concentration, made after a bolus dose of this drug (○) and inotropic effect assessed from the heart-rate-corrected change in the QS_2 interval (●). (Reproduced with permission from Weiss M and Kang W. Pharm Res 2004;21: 231–6, who based this analysis on plasma concentration and effect data taken from Kramer WG, Kolibash AJ, Lewis RP, Bathala MS, Visconti JA, Reuning RH. J Pharmacokinet Biopharm 1979;7:47–61.)

it has been shown that neither the distribution of digoxin from plasma to the myocardium nor the intracellular consequences of Na^+/K^+-ATPase inhibition are the key determinants of the slow onset of digoxin action. It is the slow dissociation of digoxin from Na^+/K^+-ATPase that best explains the slow equilibration between plasma digoxin and intensity of enzyme inhibition (5). In this regard, models in which the effects of lysergic acid diethylamide on arithmetic performance are related to concentrations in a peripheral compartment of a pharmacokinetic model appear to result from coincidence and do not have such an obvious physiological rationale (6).

The Biophase Compartment

Because only a small fraction of an administered drug dose actually binds to receptors or in other ways produces an observed response, it is reasonable to suppose that the biophase may have kinetic properties that are distinct from those of the splanchnic and somatic tissues that, as discussed in Chapter 3, primarily govern the overall drug distribution process. This was first appreciated by Segre (7), who introduced the concept of a separate biophase compartment to explain the fact that the pressor effects of norepinephrine lagged appreciably behind its concentration profile in blood. Hull *et al*. (8) and Sheiner *et al*. (9) independently incorporated a biophase compartment in their pharmacokinetic–pharmacodynamic models linking plasma concentrations of neuromuscular blocking drugs to their skeletal muscle paralyzing effects.

Figure 19.2 is a schematic diagram of a pharmacokinetic–pharmacodynamic model in which a biophase compartment links drug concentrations in plasma to observed effects. The mathematical characteristics of this biophase compartment have been described in detail by Sheiner *et al*. (9) and by Holford and Sheiner (10). In Figure 19.2, the pharmacokinetics of drug distribution and elimination are characterized by a single compartment (V_1). Since no drug actually passes from V_1 to V_B, the amount of drug X in compartment V_1 merely serves as a forcing function with respect to the biophase, and the differential equation for drug in V_1 can be written as follows:

$$dX/dt = -k_{01}X$$

The differential equation for drug in the biophase compartment is

$$dX/dt = k_{B1}X - k_{0B}B \qquad (19.1)$$

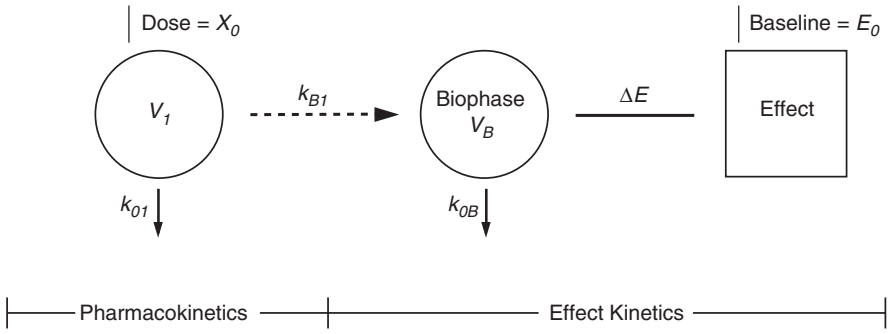

FIGURE 19.2 A delayed pharmacodynamic model in which the kinetics of drug distribution and elimination are modeled with a single compartment (V_1), which receives a bolus input dose (X_0) and has an elimination rate constant k_{01}. Plasma concentrations are linked to a biophase compartment (V_B), and ΔE transduces drug concentrations in the biophase compartment into changes in the observed effect (E). The baseline value for the effect is given by E_0 so that $E = E_0 + \Delta E$. The time course of the observed effects is governed by the rate constant k_{0B}. The arrow linking V_1 and V_B is dashed to indicate that no mass transfer occurs between these compartments and that k_{B1} is not an independent parameter of the system (see text).

Expressing these in Laplace notation (see Appendix I) gives two simultaneous equations (Equations 19.2 and 19.3),

$$sX(s) - X_0 = -k_{01}X(s) \tag{19.2}$$

or

$$X(s) = \frac{X_0}{s + k_{01}} \tag{19.3}$$

and

$$sB(s) = k_{B1}X(s) - k_{0B}B(s) \tag{19.4}$$

or

$$B(s) = \frac{k_{B1}X(s)}{s + k_{0B}} \tag{19.5}$$

Substituting $X(s)$ as defined by Equation 19.3 into Equation 19.5 yields

$$B(s) = \frac{X_0 k_{B1}}{(s + k_{01})(s + k_{0B})}$$

Taking the inverse Laplace transform of this expression for the general case when $k_{01} \neq k_{0B}$:

$$B = \frac{X_0 k_{B1}}{(k_{0B} - k_{01})}\left(e^{-k_{01}t} - e^{-k_{0B}t}\right) \tag{19.6}$$

From Equation 19.1, we see that at steady state

$$k_{B1}X_{SS} = k_{0B}B_{SS}$$

where X_{SS} and B_{SS} are the respective steady-state values for X and B. To interpret biophase concentration-related effects in terms of their equivalent steady-state plasma concentrations, we equate their steady-state concentrations by letting $B_{SS} = X_{SS}$ and $V_B = V_1$. Therefore, $k_{B1} = k_{0B}$, and Equation 19.6 can be rewritten to describe biophase concentrations as

$$[B] = \frac{X_0 k_{0B}}{V_1(k_{0B} - k_{01})}\left(e^{-k_{01}t} - e^{-k_{0B}t}\right) \tag{19.7}$$

k_{0B} is the only additional parameter required to characterize the biophase compartment that is not obtained from the conventional kinetic analysis of drug distribution and elimination.

If we make the assumptions that drug distribution to and from the site of action is first order (i.e., no active transport is involved) and that drug actions are directly determined by the unbound, unionized drug concentration in water at the site of action, then at steady state the drug concentration in plasma water will be directly proportional to its concentration at the site of action. We can therefore use parameters estimated from biophase concentrations (such as the EC_{50}) to predict the drug effects from unbound, unionized plasma concentrations.

A characteristic feature of delayed response is the existence of a hysteresis loop when plasma concentrations are plotted against effects occurring at the

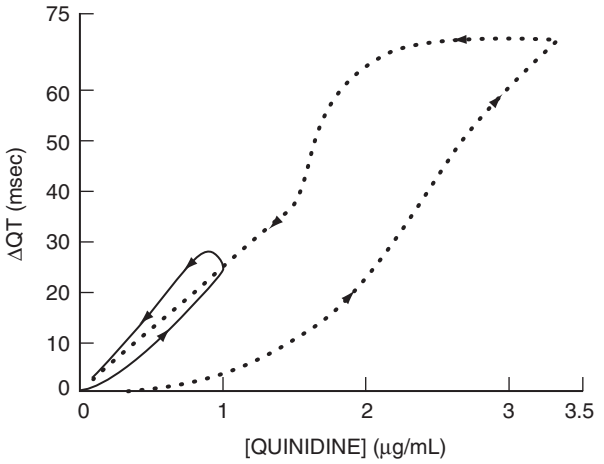

FIGURE 19.3 Predicted changes in QT interval after administration of intravenous *(dotted line)* and oral *(solid line)* single doses of quinidine to healthy subjects (12). The delay in effect with respect to plasma concentration causes hysteresis loops. The slope of the biophase concentration effect relationship is greater after oral doses due to active metabolites formed during quinidine absorption. (Reproduced with permission from Holford NHG, Coates PE, Guentert TW, Riegelman S, Sheiner LB. Br J Clin Pharmacol 1981;11:187-95.)

same time. This is shown in Figure 19.3, in which plasma concentrations of quinidine have been related to changes in electocardiographic QT intervals. When the effect of the drug increases with concentration, then the loop has a counterclockwise direction, but if the effect decreases with concentration, then the loop goes clockwise (e.g., if potassium channel conductance had been used to observe the effect of quinidine). In both cases the loop is described as showing hysteresis.

Incorporation of Pharmacodynamic Models

The models described in Chapter 18 that are used to relate steady-state plasma concentrations of drug to observed effects can also be applied to the time course of drug effects.

Linear Response Models

If the relationship between change in effect (ΔE) and biophase concentration is linear, biophase concentrations can be related to ΔE by a constant (β) such that

$$\Delta E = \beta [B] \tag{19.8}$$

Biophase concentrations then are related to observations made on the effect variable (E) as follows:

$$E = E_0 + \beta [B] \tag{19.9}$$

where E_0 is the baseline observed effect . The arithmetic sign of β determines if the change in effect either added to or subtracted from the baseline value.

A linear model was used to show that the blood-pressure-lowering effects and blockade of transmission across sympathetic ganglia caused by *N*-acetylprocainamide drug followed a similar time course in dogs (11). This pharmacokinetic–pharmacodynamic analysis was used to provide supporting evidence for the conclusion that the observed hypotensive effect of the drug was mediated by its ganglionic blocking action. This detailed analysis in dogs then was extended to demonstrate that the hypotensive effects of *N*-acetylprocainamide in a human subject were similar in intensity and time course.

A linear model also was used to relate biophase quinidine concentrations to the time course of electrocardiographic QT interval changes after intravenous and oral dosing of this drug (12). As shown in Figure 19.3, the slope was greater after oral doses and that was attributed to the formation of active metabolites of quinidine during first-pass metabolism of the oral dose (13).

E_{max} Models

The apparently linear relationship between biophase concentration and pharmacologic response usually reflects the fact that effects have been analyzed over only a limited concentration range (14). In many cases, an E_{max} model is required to analyze more pronounced effects, such as the blood pressure response of cats to norepinephrine. This was the concentration-effect relationship initially analyzed by Segre (7) when he proposed a model for the time course of biophase concentrations. For the E_{max} model, ΔE in Equation 19.8 is described by

$$\Delta E = \frac{E_{max}}{EC_{50} + [B]} \tag{19.10}$$

The linear-effect model defines this relationship adequately as long as biophase drug concentrations, $[B]$, are substantially less than is the EC_{50}. However, the decision to use an E_{max} rather than a linear model is usually determined by the available data rather than by theoretical considerations. For example, in one study of QT interval prolongation by an antiarrhythmic drug, a linear-effect model was satisfactory for analyzing the response of four patients but an E_{max} model was required to analyze the exaggerated response of a fifth patient (15).

Although the mathematical form of the E_{max} model is physiologically realistic (7), no physiological

significance has been assigned to E_{max} and EC_{50} estimates in most applications of this model. Nonetheless, E_{max} values in some cases may provide an indication of the maximal degree to which a particular intervention can affect enzyme or receptor activity. It also may be possible to find similarities between EC_{50} values and drug binding affinity. For example, ε-aminocaproic acid is a lysine analog that has clot-stabilizing antifibrinolytic effects because it binds to lysine binding sites on plasminogen, preventing its attachment to fibrin. A study of ε-aminocaproic acid kinetics and antifibrinolytic effects in humans provided an IC_{50} estimate, analogous to EC_{50} in Equation 19.10, of 63.0 ± 19.7 μg/mL, which was similar to the *in vitro* estimate of 0.55 mM, or 72 μg/mL, for the ε-aminocaproic acid–plasminogen dissociation constant (16). In fact, these results represent an oversimplification of physiological reality, since plasminogen has one high-affinity and four low-affinity sites that bind ε-aminocaproic acid (17).

Sigmoid E_{max} Models

In some cases, Equation 19.10 will need to be modified to account for the fact that the biophase concentration-effect relationship is sigmoid rather than hyperbolic. This modification was necessary in analyzing the pharmacokinetics and effects of *d*-tubocurarine (9). In this case, the following equation was used to relate estimated biophase concentrations of *d*-tubocurarine to the degree of skeletal muscle paralysis (ΔE), ranging from normal function to complete paralysis ($E_{max} = 1$) caused by this drug:

$$\Delta E = \frac{E_{max}}{EC_{50}^{n} + [B]^{n}} [B]^{n} \qquad (19.11)$$

Equation 19.11 was developed initially by Hill (18) to analyze the oxygen-binding affinity of hemoglobin. For normal human hemoglobins and those of most other mammalian species, n has values ranging from 2.8 to 3.0 (19). This reflects cooperative subunit interactions between the four heme elements of the hemoglobin tetramer. Proteins such as myoglobin that have a single heme subunit, and tetrameric hemoglobins such as hemoglobin H that lack subunit cooperativity, have n values of 1.0. On the other hand, if oxygenation of one hemoglobin subunit caused an infinite increase in the oxygen binding affinity of the other subunits, n would equal 4. Therefore, the n values for normal hemoglobins indicate that there is strong but not infinite cooperativity in oxygen binding by the four heme subunits.

Wagner (20) first proposed using the Hill equation to analyze the relationship between drug concentration and pharmacologic response. However, the physiologic significance of n values estimated in pharmacokinetic–pharmacodynamic studies is far less well understood than it is in the case of oxygen binding to hemoglobin. Accordingly, n is currently regarded in these studies as simply an empirical parameter that confers sigmoidicity and steepness to the relationship between biophase concentrations and pharmacologic effect. This is illustrated by Figure 19.4 in which Equation 19.11 was used to analyze the relationship between tocainide plasma concentration and antiarrhythmic response (21). It can be seen from this figure that the shape of the concentration-response curves approximates that of a step function as n values increase. In fact, pharmacokinetic–pharmacodynamic models can be developed for *quantal responses* simply by fixing n at an arbitrary large value, such as 20 (14). In that case, the EC_{50} parameter estimate will indicate the threshold concentration of drug needed to provide the quantal response.

Sigmoid E_{max} models have been particularly useful in the pharmacokinetic–pharmacodynamic analysis of anesthetic drugs (22). Waveform analyses of electroencephalographic (EEG) morphology have served as biomarkers for anesthetic effects, and show characteristic changes that are different for barbiturates, benzodiazepines, and opiates. Since it often is impossible to conduct clinical studies of these agents at steady state, pharmacokinetic–pharmacodynamic investigations have been performed under conditions in which drug concentrations in plasma and effects are constantly changing. The time delay between changes in drug concentration and effect has been analyzed using a biophase compartment, such as that shown in Figure 19.2.

Of practical clinical importance is the role that pharmacokinetic–pharmacodynamic analysis played in optimizing dosing guidelines for using midazolam as an intravenous anesthetic agent (22). Drug approval was based on results of traditional studies, from which it was estimated that midazolam was no more than twice as potent as diazepam, the benzodiazepine with which clinicians had the greatest familiarity (23). However, after considerable patient morbidity and mortality was encountered in routine clinical practice, pharmacokinetic–pharmacodynamic studies provided a significantly greater estimate of midazolam relative potency (24). The EEG effect chosen in comparing midazolam with diazepam was total voltage from 0 to 30 Hz, as obtained from aperiodic waveform analysis. The results summarized in Table 19.1 show that the two agents have similar E_{max} values, indicating similar

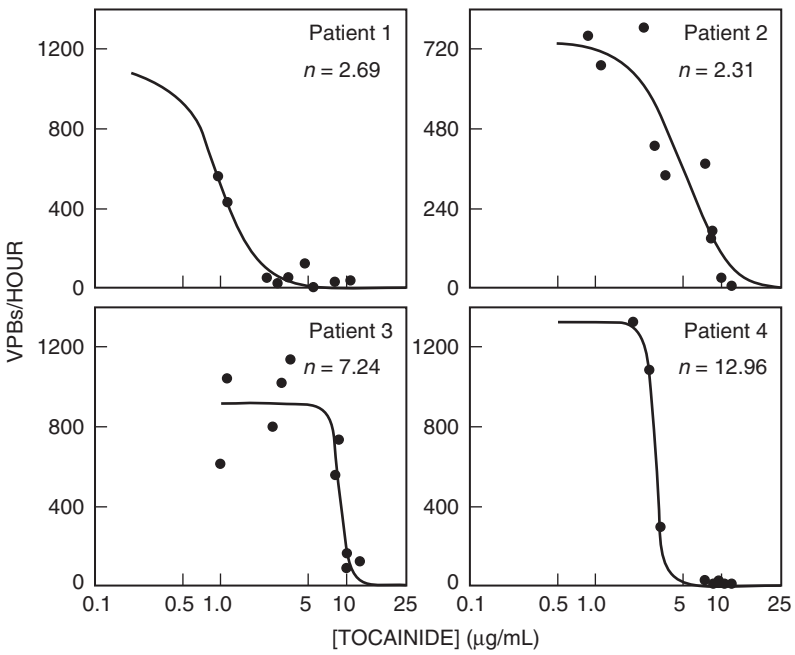

FIGURE 19.4 Relationship between plasma concentrations of tocainide and suppression of ventricular premature beats (VPBs) for four representative patients. The relationship between VPB frequency and tocainide concentrations shown by the solid curves was obtained from a nonlinear least-squares regression analysis of the data using Equation 19.10. The estimate of n for each patient can be compared with the shape of the tocainide concentration–antiarrhythmic response curve. (Reproduced with permission from Meffin PJ, Winkle RA, Blaschke TF, Fitzgerald J, Harrison DC. Clin Pharmacol Ther 1977;22:42–57.)

efficacy, but that the EC_{50} of midazolam is 5.5 times less than that of diazepam, demonstrating that midazolam is that much more potent than diazepam. In addition, the equilibration half-life between plasma and the biophase compartment, calculated as

$$t_{1/2(k_{0B})} = \frac{0.693}{k_{0B}}$$

is three times longer for midazolam than for diazepam. This suggests that repeat doses of midazolam should be spaced at a longer interval, compared to diazepam (22). No physiological significance has been attached to the values of the Hill coefficient, n, that were obtained in these studies. However, investigations in rats have demonstrated a correlation between the EC_{50} of EEG effects and estimates of K_i obtained from *in vitro* studies of the ability of a series of benzodiazepines to displace [^{3}H]flumazenil from benzodiazepine receptors (Figure 19.5) (25).

TABLE 19.1 Comparison of Parameters Describing Midazolam and Diazepam Effect Kinetics[a]

Drug	$t_{1/2(k_{0B})}$(min)	E_{max} (μV)	EC_{50} (ng/mL)	n ↓
Midazolam	5.6	141	171	1.8
Diazepam	1.9	137	946	1.7

[a] Parametric analysis results from Bührer *et al*. Clin Pharmacol Ther 1990;48:555–67.

Changes in the Relationship Between Biophase Concentration and Drug Effect

So far we have considered examples in which the relationship between drug concentration in the biophase compartment and the effect is time invariant. This is not the case for drugs that exhibit *pharmacologic tolerance*, in which the intensity of an effect after initial drug exposure subsequently declines despite maintenance of similar biophase drug concentrations. Pharmacologic tolerance is characteristically revealed by plotting plasma concentration against effect and observing a *proteresis* loop. If the drug causes an increase in effect, the loop will have a clockwise direction, while an inhibitory drug effect will have a counterclockwise direction.

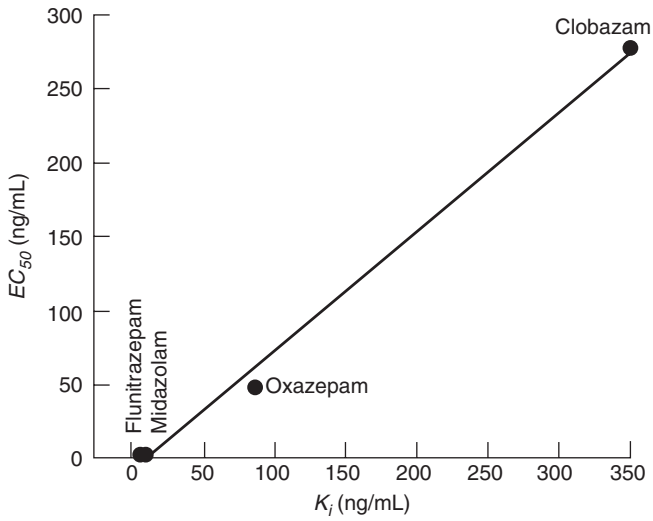

FIGURE 19.5 Relationship in rats between the EC_{50} of EEG effects (averaged amplitude in the 11.5–30 Hz frequency band) and estimates of K_i obtained from *in vitro* studies of the ability of four benzodiazepines to displace [3H]flumazenil from benzodiazepine receptors on brain tissue homogenates. Estimates of EC_{50} were based on free benzodiazepine concentrations not bound to plasma proteins. (Data from Mandema JW, Sansom LN, Dios-Vièitez MC, Hollander-Jansen M, Danhof M. J Pharmacol Exp Ther 1991;257:472–8.)

There is now general agreement that tolerance develops rapidly to the cardiovascular and euphoric effects of cocaine (26, 27). This phenomenon has been characterized by studies in which a bolus injection of cocaine was followed by an exponentially tapering infusion, so that relatively constant plasma concentrations were maintained while pharmacologic effects were observed (28). Both the cardiovascular and euphoric effects of cocaine were analyzed with a biophase compartment and linear response model. Function generators were used to characterize the acute development of tolerance by reducing effect intensity, β in Equation 19.8. The increase in heart rate that followed cocaine administration decreased with a 31-minute average half-life from its peak to a plateau that averaged 33% of peak values. Changes in blood pressure paralleled the increase and subsequent decline in heart rate (26). However, subjective evaluation of cocaine-induced euphoria declined to baseline with an average half-life of 66 minutes. The slower development of tolerance to the euphoric response might reflect other phenomena, such as a placebo response based on subjective expectations or a different physiological feedback system. Alternative models for tolerance have been evaluated by Gardmark *et al*. (29). Among the mechanisms proposed are the formation of a drug metabolite that acts as an antagonist and the depletion of a precursor substance when conversion to an active mediator is stimulated by the drug.

Sensitization refers to an increase in pharmacologic response despite maintenance of constant biophase concentrations of drug. Adverse clinical consequences of sensitization are observed perhaps most commonly following abrupt withdrawal of β-adrenergic blocking drug therapy in patients with coronary heart disease and include ventricular arrhythmias, worsening of angina, and myocardial infarction (30). Although several mechanisms have been proposed, these adverse events primarily reflect the fact that chronic therapy with β-adrenergic receptor-blocking drugs causes an increase in the number of available β-adrenergic receptors, a phenomenon termed *up-regulation* (30, 31). When therapy with β-adrenergic receptor-blocking drugs is stopped abruptly, the decline in up-regulated receptors lags behind the elimination of the receptor-blocking drug, resulting in a period of exaggerated responses to normal circulating catecholamine levels.

Using data describing the time course of receptor up-regulation in lymphocytes, Lima *et al*. (32) have developed a kinetic model of the fractional increase in β-adrenergic receptors that occurs with the institution of β-adrenergic receptor-blocking drug therapy, and of its subsequent decline when this therapy is stopped. A modification of Equation 19.10 was used to characterize the initial intensity of β-adrenergic receptor agonist-induced chronotropic response in the presence of a β-adrenergic receptor antagonist. Supersensitivity was then modeled by simply multiplying this estimate of initial intensity by the expected increase in β-adrenergic receptor density.

PHYSIOKINETICS — TIME COURSE OF EFFECTS DUE TO PHYSIOLOGICAL TURNOVER PROCESSES

In almost all cases, effects are mediated by an endogenous substance, and drugs modulate these effects indirectly by affecting either the production or elimination of this effect mediator (Figure 19.6). In addition to delays in drug effect due to pharmacokinetic distribution to the site of action, there are delays determined by the turnover of these effect mediators. The time course of the physiological mediator can be thought of as an example of *physiokinetics*. Delays of a few minutes, or perhaps an hour or so, might plausibly be explained by distribution of a drug to its site of action, but the rate-limiting step for longer delays is likely to be physiokinetic rather than pharmacokinetic.

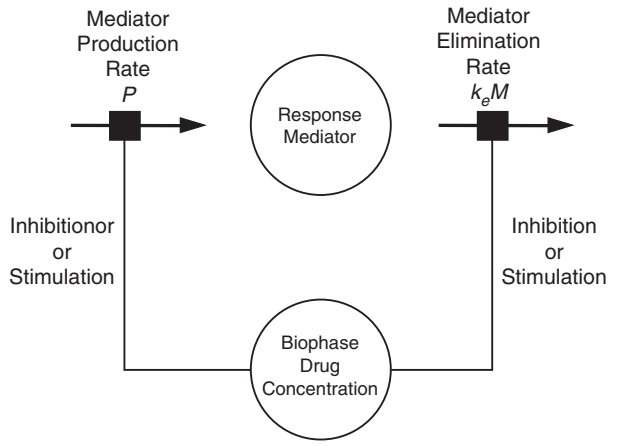

FIGURE 19.6 Basic concept of physiological turnover models. Observed effects are mediated by an endogenous substance (effect mediator). Drugs modulate these effects by either inhibiting or stimulating the production or elimination of this mediator. This accounts for the fact that the development of these drug effects is delayed beyond the time required for the drug to reach its pharmacologic site of action (biophase).

If the formation rate (P) of the mediator (M) is regarded as a zero-order process and the elimination rate of the mediator is regarded as first order, the following equation describes the mass balance of the mediator:

$$dM/dt = P - k_eM \tag{19.12}$$

where k_e is the first-order elimination rate constant. Drugs then can be modeled as exerting their effects by altering initial values of either P or k_e. Implicit in Equation 19.12 is the fact that the rate of onset of effect is governed by the elimination rate of the mediator.

Warfarin is a classic example of a delayed action drug that exerts its anticoagulant effects by blocking synthesis of vitamin K-dependent clotting factors (Factors II, VII, IX, and X). This effect can be analyzed by adding to Equation 19.12 a forcing function (f_c) to relate the degree of inhibition of clotting factor synthesis (P) to the plasma concentration of warfarin:

$$dM/dt = P \cdot f_c - k_eM \tag{19.13}$$

Nagashima *et al*. (33) developed a model in which the forcing function was modeled as proportional to the logarithm of the warfarin concentration in plasma. However, Pitsiu *et al*. (34) subsequently found that a sigmoid E_{max} model (Equation 19.11) is more suitable for modeling the relationship between plasma concentrations of *S*-warfarin, the active isomer of warfarin, and inhibition of coagulation factor formation.

Any of the pharmacodynamic models that we have described for pharmacologic effects can serve as forcing functions in Equation 19.13, and model choice is guided best by an understanding of the mechanism of drug action and by the information content of the available data. For example, Sharma and Jusko (1) have selected the following modification of the E_{max} model to illustrate the general use of a forcing function to model inhibition of either mediator synthesis or elimination:

$$f_c = 1 - \frac{I_{max}[B]}{IC_{50} + [B]}$$

where I_{max} is the maximal fractional degree of inhibition provided by any drug concentration [B] and IC_{50} is the concentration required for half-maximal inhibitory effect. The corresponding forcing function for stimulatory drug effects would be given by

$$f_c = 1 + \frac{E_{max}[B]}{EC_{50} + [B]}$$

In addition to warfarin, Sharma and Jusko (1) have listed a large number of other drugs with delays attributable to changes in mediator turnover. These range from H_2-receptor antagonists, diuretics, and bronchodilators to corticosteroids, nonsteroidal anti-inflammatory drugs, and interferon.

THERAPEUTIC RESPONSE, CUMULATIVE DRUG EFFECTS, AND SCHEDULE DEPENDENCE

So far we have focused our attention on the time course of drug effect. While the study of these effects can be helpful in understanding the mechanism of drug action and factors affecting efficacy and potency, it usually does not provide information on how drug exposure influences therapeutic response.

Clinical response can be defined as the effect of drug treatment on the clinical endpoint of how the patient feels, functions, or survives. Some clinical responses can be described by composite scales that are commonly used in drug development for regulatory approval [e.g., the Unified Parkinson's Disease Rating Scale (UPDRS) and the Alzheimer's Disease Assessment Scale (ADAS)]. These scales can be treated as if they were continuous measures of drug response and, as discussed in Chapter 20, are amenable to pharmacokinetic–pharmacodynamic modeling involving delayed effects even if no concentrations are available (35). This seemingly broad

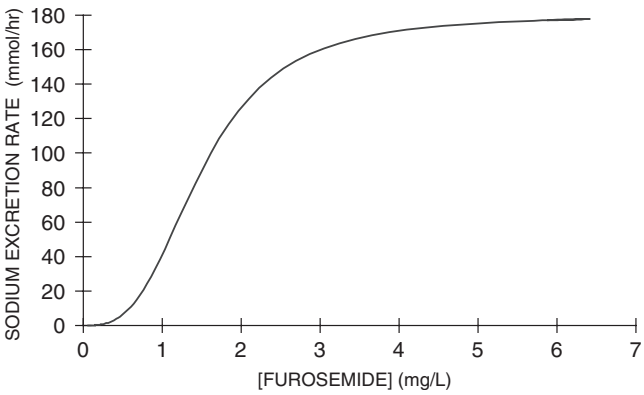

FIGURE 19.7 The diuretic effect of furosemide is to increase the excretion rate of sodium. The pharmacodynamics of furosemide show a steep concentration effect relationship, with a clear maximum effect (180 mmol/hr of Na^+). The EC_{50} is 1.5 mg/L and the Hill coefficient (n) is 3.

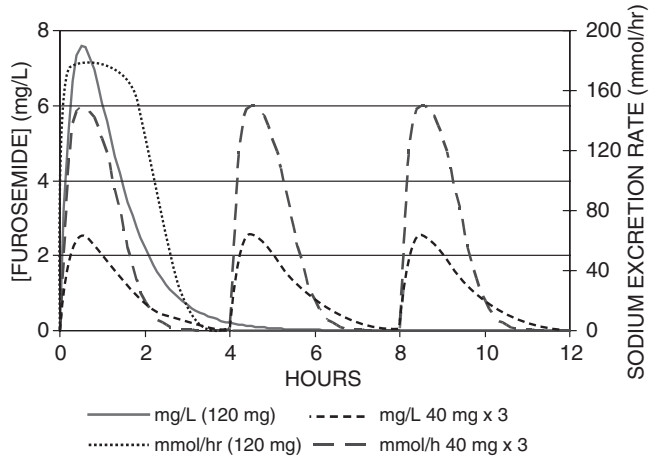

FIGURE 19.8 The time course of furosemide concentration and natriuretic effect after 3 doses of 40 mg compared with those parameters after a single dose of 120 mg. Notice that the concentrations after 120 mg are exactly three times higher than after 40 mg, but the peak effect after 40 mg is quite close to the peak after 120 mg because the 120-mg dose is limited by effects approaching E_{max}. The cumulative sodium loss after 120 mg is 400 mmol, while the three 40-mg doses produce a 600-mmol loss.

definition of clinical response nevertheless excludes almost all of the drug effects we have discussed so far. For example, some responses are related to the cumulative effects of previous drug doses.

The acute treatment of congestive heart failure commonly involves the use of a diuretic to get rid of excess fluid that has accumulated as edema of the lungs and lower extremities. As shown in Figure 19.7, a high-efficacy diuretic such as furosemide has a steep concentration effect relationship, with a clearly defined maximum effect on sodium excretion. After an oral furosemide dose of 120 mg that causes almost maximal sodium excretion, the time course of drug concentrations reaches a peak about 6 mg/L, which is well above the EC_{50} of 1.5 mg/L (Figure 19.8). A lower dose of 40 mg produces concentrations that are one-third of the 120-mg dose, but the natriuretic effects are not decreased in proportion to the dose. When three 40-mg doses are given over 12 hours, the cumulative effect measured by total sodium excretion is 50% greater than that seen after a single 120-mg dose. Despite the same total dose and the same cumulative area under the concentration time curve from the two patterns of dosing, the clinical response would be less with the single 120-mg dose. This is an example of the phenomenon of *schedule dependence*.

Schedule dependence occurs when the drug effect is reversible, the concentrations exceed the EC_{50} so that effects approach E_{max} with proportionately less drug effect at high concentrations, and the clinical response is related to the cumulative drug effect. The phenomenon is expected to be quite common but is not often recognized clinically because of wide variability in response and other confounding factors such as disease progression.

The reduction of pain and other symptoms due to peptic ulceration may be quite closely linked to the current effect of a drug on acid secretion, but the rate of healing and eventual disappearance of an ulcer is a slow process, determined in part by the extent and duration of gastric acid secretion suppression over several weeks. The clinical response of ulcer healing is therefore a consequence of the cumulative degree of acid inhibition. Proton pump inhibitors such as omeprazole bind irreversibly to the proton pump to suppress gastric acid secretion. The extent of inhibition is close to 100% and responses are related to cumulative effects, but the irreversible nature of the drug action means that schedule dependence is not observed.

Many clinical responses are described in terms of *events*. An event might be death, a stroke, a myocardial infarction, an epileptic seizure, admission to hospital, need for supplementary treatment, and so on. The occurrence of an event or the time to an event can be modeled using a survival function. The word *survival* relates most obviously to a death event, but the term is commonly used in a much broader context to describe the probability that the event under study will not occur.

The hazard/survival approach allows complex pharmacokinetic–pharmacodynamic influences to affect the hazard and thus occurrence of an event. At the jth observation time, $t[j]$, which follows a previous observation at time $t[j-1]$, a patient is observed either to have survived or to have had an event. The exact

time of the event may not be known, but is between $t[j-1]$ and $t[j]$. The hazard [*h(t)*, sometimes called instantaneous risk] of an event a time t is shown as

$$h(t) = f(\mathbf{B},\ X) \tag{19.14}$$

where **B** is a set of parameters describing the hazard as a function of X (time, dose, etc). Potential time-varying covariates for the hazard are cholesterol concentrations (heart attack event), blood pressure (stroke event), or concentration of an anticonvulsant drug (seizure event). The chances of an event are related both to the size of the hazard and the time that the patient is exposed to the hazard. The cumulative hazard from 0 to t [*H(t)*] can be related to the probability of an event, as illustrated by Equation 19.15 for the case of a constant hazard:

$$\begin{aligned} H(t) &= \int_0^t h(t) \\ &= \int_0^t \beta_0 \\ &= \beta_0 \cdot t \end{aligned} \tag{19.15}$$

In this equation, β_0 is the instantaneous risk of an event when the hazard is constant. The probability of surviving ($P_{survival}$) from time 0 to time $t[j-1]$ is shown in Equation 19.16:

$$P_{survival}(t[j-1]) = \exp(-H(t[j-1])) \tag{19.16}$$

The probability of an event (P_{drop}) in the interval $t[j-1]$ to $t[j]$ is given by

$$P_{drop}(t[j] - t[j-1]) = 1 - \exp(-(H(t[j] - H(t[j-1])))) \tag{19.17}$$

The event occurs sometime in this interval but the exact time is not known (internal censored event). According to Hu and Sale (36), the probability that an event has occurred before time $t[j]$ is estimated by

$$P_{drop}(t[j])_{EST} = P_{survival}(t[j-1]) \cdot P_{drop}(t[j] - t[j-1]) \tag{19.18}$$

In other words, it is the probability of survival up to the previous observation multiplied by the probability of the event since the last observation.

Cox *et al*. (37, 38) use a somewhat similar model for modeling the time to an event whose time is known:

$$P_{event}(t[j]) = P_{survival}(t[j]) \cdot h(t) \tag{19.19}$$

The use of a hazard function to describe time-varying risk of an event is a flexible method for bringing together pharmacokinetics, changes in drug effects on biomarkers, and other risk factors such as concomitant changes in disease severity. It has been applied to understand the need for additional pain medication in clinical trials of analgesics (39) and to the suppression of vomiting events caused by chemotherapy (38). Study of long-term drug effects requires incorporation of a disease progression model into the analysis, and this will be the subject of the next chapter.

REFERENCES

1. Sharma A, Jusko WJ. Characteristics of indirect pharmacodynamic models and applications to clinical drug responses. Br J Clin Pharmacol 1998;45:229–39.
2. Sherwin RS, Kramer KJ, Tobin JD, Insel PA, Liljenquist JE, Berman M, Andres R. A model of the kinetics of insulin in man. J Clin Invest 1974; 53:1481–92.
3. Steil GM, Meador MA, Bergman RN. Thoracic duct lymph. Relative contribution from splanchnic and muscle tissue. Diabetes 1993;42:720–31.
4. Kramer WG, Kolibash AJ, Lewis RP, Bathala MS, Visconti JA, Reuning RH. Pharmacokinetics of digoxin: Relationship between response intensity and predicted compartmental drug levels in man. J Pharmacokinet Biopharm 1979;7:47–61.
5. Weiss M, Kang W. Inotropic effect of digoxin in humans: Mechanistic pharmacokinetic/pharmacodynamic model based on slow receptor binding. Pharm Res 2004;21:231–6.
6. Wagner JG, Aghajanian GK, Bing OHL. Correlation of performance test scores with "tissue concentration" of lysergic acid diethylamide in human subjects. Clin Pharmacol Ther 1968;9:635–8.
7. Segre G. Kinetics of interaction between drugs and biological systems. Farmaco Ed Sci 1968;23:907–18.
8. Hull CJ, Van Beem HBH, McLeod K, Sibbald A, Watson MJ. A pharmacodynamic model for pancuronium. Br J Anaesth 1978;50:1113–23.
9. Sheiner LB, Stanski DR, Vozeh S, Miller RD, Ham J. Simultaneous modeling of pharmacokinetics and pharmacodynamics: Application to *d*-tubocurarine. Clin Pharmacol Ther 1979;25:358–71.
10. Holford NHG, Sheiner LB. Understanding the dose-effect relationship: Clinical application of pharmacokinetic–pharmacodynamic models. Clin Pharmacokinet 1981;6:429–53.
11. Eudeikis JR, Henthorn TK, Lertora JJL, Atkinson AJ Jr, Chao GC, Kushner W. Kinetic analysis of the vasodilator and ganglionic blocking actions of *N*-acetylprocainamide. J Cardiovasc Pharmacol 1982;4:303–9.

12. Holford NHG, Coates PE, Guentert TW, Riegelman S, Sheiner LB. The effect of quinidine and its metabolites on the electrocardiogram and systolic time intervals: Concentration-effect relationships. Br J Clin Pharmacol 1981;11:187–95.
13. Vozeh S, Bindschedler M, Ha HR, Kaufmann G, Guentert TW, Follath F. Pharmacodynamics of 3-hydroxyquinidine alone and in combination with quinidine in healthy persons. Am J Cardiol 1987;59:681–4.
14. Holford NHG, Sheiner LB. Pharmacokinetic and pharmacodynamic modeling *in vivo*. CRC Crit Rev Bioengineer 1981;5:273-322.
15. Piergies AA, Ruo TI, Jansyn EM, Belknap SM, Atkinson AJ Jr. Effect kinetics of *N*-acetylprocainamide-induced QT interval prolongation. Clin Pharmacol Ther 1987;42:107–12.
16. Frederiksen MC, Bowsher DJ, Ruo TI, Henthorn TK, Ts'ao C-H, Green D, Atkinson AJ Jr. Kinetics of epsilon-aminocaproic acid distribution, elimination, and antifibrinolytic effects in normal subjects. Clin Pharmacol Ther 1984;35:387–93.
17. Markus G, DePasquale JL, Wissler FC. Quantitative determination of the binding of ε-aminocaproic acid to native plasminogen. J Biol Chem 1978; 253:727–32.
18. Hill AV. The possible effects of the aggregation of the molecules of hemoglobin on its dissociation curves. J Physiol 1910;40:iv–vii.
19. Bunn HF, Forget BG, Ranney HM. Human hemoglobins. Philadelphia: W.B. Saunders; 1977. p. 35–41.
20. Wagner JG. Kinetics of pharmacologic response: I. Proposed relationships between response and drug concentration in the intact animal and man. J Theor Biol 1968;20:173–201.
21. Meffin PJ, Winkle RA, Blaschke TF, Fitzgerald J, Harrison DC. Response optimization of drug dosage: Antiarrhythmic studies with tocainide. Clin Pharmacol Ther 1977;22:42–57.
22. Stanski DR. Pharmacodynamic modeling of anesthetic EEG drug effects. Annu Rev Pharmacol Toxicol 1992;32:423–47.
23. Magni VC, Frost RA, Leung JWC, Cotton PB. A randomized comparison of midazolam and diazepam for sedation in upper gastrointestinal endoscopy. Br J Anaesth 1983;55:1095–101.
24. Bührer M, Maitre PO, Crevoisier C, Stanski DR. Electroencephalographic effects of benzodiazepines. II. Pharmacodynamic modeling of the electroencephalographic effects of midazolam and diazepam. Clin Pharmacol Ther 1990;48:555–67.
25. Mandema JW, Sansom LN, Dios-Vièitez MC, Hollander-Jansen M, Danhof M. Pharmacokinetic–pharmacodynamic modeling of the electroencephalographic effects of benzodiazepines. Correlation with receptor binding and anticonvulsant activity. J Pharmacol Exp Ther 1991;257:472–8.
26. Ambre JJ. Acute tolerance to pressor effects of cocaine in humans. Ther Drug Monit 1993;15:537–40.
27. Foltin RW, Fischman MW, Levin FR. Cardiovascular effects of cocaine in humans: Laboratory studies. Drug Alcohol Depend 1995;37:193–210.
28. Ambre JJ, Belknap SM, Nelson J, Ruo TI, Shin S-G, Atkinson AJ Jr. Acute tolerance to cocaine in humans. Clin Pharmacol Ther 1988;44:1–8.
29. Gårdmark M, Brynne L, Hammarlund-Udenaes M, Karlsson MO. Interchangeability and predictive performance of empirical tolerance models. Clin Pharmacokinet 1999;36:145–67.
30. Nattel S, Rangno RE, Van Loon G. Mechanism of propranolol withdrawal phenomenon. Circulation 1979;59:1158–64.
31. Houston MC, Hodge R. Beta-adrenergic blocker withdrawal syndromes in hypertension and other cardiovascular diseases. Am Heart J 1988; 116:515–23.
32. Lima JJ, Krukenmyer JJ, Boudoulas H. Drug- or hormone-induced adaptation: Model of adrenergic hypersensitivity. J Pharamacokinet Biopharm 1989;17:347–64.
33. Nagashima R, O'Reilly RA, Levy G. Kinetics of pharmacologic effects in man: The anticoagulant action of warfarin. Clin Pharmacol Ther 1969;10:22–35.
34. Pitsiu M, Parker EM, Aarons L, Rowland M. Population pharmacokinetics and pharmacodynamics of warfarin in healthy young adults. Eur J Pharm Sci 1993;1:151–7.
35. Holford NHG, Peace KE. Results and validation of a population pharmacodynamic model for cognitive effects in Alzheimer patient treated with tacrine. Proc Natl Acad Sci USA 1992;89:11471–5.
36. Hu C, Sale ME. A joint model for nonlinear longitudinal data with informative dropout. J Pharmacokinet Pharmacodyn 2003;30:83–103.
37. Cox EH, Sheiner LB. Model for repeated measures time-to-event data with time-varying concentration and hazard. 2001. (Internet at ftp://ftp.globomaxnm.com/Public/nonmem/non_continuous.)
38. Cox EH, Veyrat-Follet C, Beal SL, Fuseau E, Kenkare S, Sheiner LB. A population pharmacokinetic–pharmacodynamic analysis of repeated measures time-to-event pharmacodynamic responses: The antiemetic effect of ondansetron. J Pharmacokinet Biopharm 1999;27:625–44.
39. Sheiner LB. A new approach to the analysis of analgesic drug trials, illustrated with bromfenac data. Clin Pharmacol Ther 1994;56:309–22.

This page intentionally left blank

CHAPTER

20

Disease Progress Models

NICHOLAS H. G. HOLFORD*, DIANE R. MOULD†, AND CARL C. PECK‡

*University of Auckland, Auckland, New Zealand,

†Projections Research Inc., Phoenixville, Pennsylvania,

‡Center for Drug Development Science, University of California Center, Washington, D.C.

CLINICAL PHARMACOLOGY AND DISEASE PROGRESS

Clinical pharmacology, like many disciplines, can be viewed from several perspectives. In the context of a clinical trial of a therapeutic agent, clinical pharmacology provides a conceptual framework for relating drug treatment to responses observed in a clinical trial. In the context of simulation and modeling, it is useful to think of clinical pharmacology as a model itself — that is, the combination of disease progress and drug action:

$$\text{Clinical pharmacology} = \text{Disease progress} + \text{Drug action} \qquad (20.1)$$

Disease progress refers to the evolution of a disease over time. Specifically, it can be used to describe the time course of a biomarker or clinical outcome, reflecting the status of a disease. The status is a reflection of the state of the disease at a point in time. The disease status may improve or worsen over time, or may be a cyclical phenomenon (e.g., malarial quartan fever or seasonal affective disorder). Therefore, a model of disease progress is a mathematical expression that describes the expected changes in status over time.

Drug action refers to all the pharmacokinetic and pharmacodynamic processes involved in producing a drug effect on the disease. The effect of the drug is assumed to influence the disease status. Pharmacokinetic and pharmacodynamic drug properties are the major attributes determining drug action and its effect on the time course of progression of the disease. Disease progress models can be extended to include terms that account for the changes in disease progress that are the result of drug treatment. We call such a combined model the "clinical pharmacology model" for the drug (Equation 20.1).

DISEASE PROGRESS MODELS

In this chapter, we describe the basic elements of clinical pharmacology models for use in describing the time course of disease progress and the changes in progress in response to treatment. These models have two basic components: the first describes the disease progress without therapeutic intervention and the second defines the change in progress as a result of treatment.

"No Progress" Model

The simplest model of disease progress assumes there is no change in disease status during the period of observation. Previously, this has been reflected in simple pharmacodynamic models, such as those described in Chapter 19, by the constant "baseline effect" parameter, often symbolized by E_0 (1). A constant baseline is a common assumption made in the design and analysis of clinical trials. Such an analysis ignores the progression of disease during the course of the trial by comparing the effect of drug treatment groups at similar points in time. This is a reflection of a "minimalist" approach to clinical trial design and

analysis that seeks only to falsify the null hypothesis and not to learn by an informative description of the observed phenomena (2, 3). The assumption that there is no change in disease status over time does not allow the analyst to infer anything about the effect of the drug on the rate of disease progress.

Linear Progress Model

The linear disease progress model (Equation 20.2) assumes a constant rate of change of a biomarker or clinical outcome that reflects the disease status (S) at any time, t, from the initial observation of the patient — for example, at the time of entry into a clinical trial. The rate of change can be defined in terms of a baseline disease status (S_0) and a slope (α), which reflects the change from baseline status with time:

$$S(t) = S_0 + \alpha \cdot t \tag{20.2}$$

Using this model as a basis to describe the effect of drug on the time course of disease progress, there are three drug effect patterns possible. Treatment can change the patient status without affecting the rate of progress (offset pattern), it can alter the rate of progress of the disease (slope pattern), or it can do both of these things (combined slope and offset pattern).

Offset Pattern

We define a drug-induced shift upward or downward without a change in slope of the disease status line as the offset pattern. The effect of the drug, E_{OFF}, can be thought of as modifying the baseline parameter S_0 as shown in Equation 20.3:

$$S(t) = S_0 + E_{OFF}(C_{e,A}) + \alpha \cdot t \tag{20.3}$$

This model can be used to describe a nonpersistent drug effect (sometimes termed "symptomatic") — for example, lowering of blood pressure by an antihypertensive agent that persists during periods of exposure to the drug, but with a return to pretreatment status on cessation of therapy. The onset of drug effect may be delayed by adding an effect compartment to the drug action part of the model, which is more realistic, by making active drug concentrations at the effect site ($C_{e,A}$) delayed in relation to plasma drug concentrations (4).

Slope Pattern

We define a drug-induced increase or decrease in the rate of progression of disease status as the slope pattern. The effect of the drug, E_{SLOPE}, can be thought of as modifying the slope parameter α as shown in Equation 20.4:

$$S(t) = S_0 + [E_{SLOPE}(C_{e,A}) + \alpha] \cdot t \tag{20.4}$$

Compared to the offset pattern, this model can be used to describe a more permanent (disease-modifying), protective drug effect — for example, slowing the progression of a disease such as rheumatoid arthritis. In this case, the cessation of therapy would not be expected to result in a return to pretreatment status. In general, we might expect some delay in the onset of effect (predicted by $C_{e,A}$), but an instantaneous effect model to describe the drug effect on the slope parameter may be sufficient because changes in status tend to develop slowly when the slope changes.

Combined Offset and Slope Pattern

Both an offset effect and a slope effect may be combined to describe the changes in disease status (Equation 20.5):

$$S(t) = S_0 + E_{OFF}(C_{e,A}) + [E_{SLOPE}(C_{e,A}) + \alpha] \cdot t \tag{20.5}$$

Figure 20.1 illustrates the offset and slope models and the combination of both types of effect. The offset pattern of drug effect provides an explicit definition of a temporary or symptomatic effect of a drug. In contrast, the slope pattern of drug effect defines a drug with a disease-modifying, protective effect.

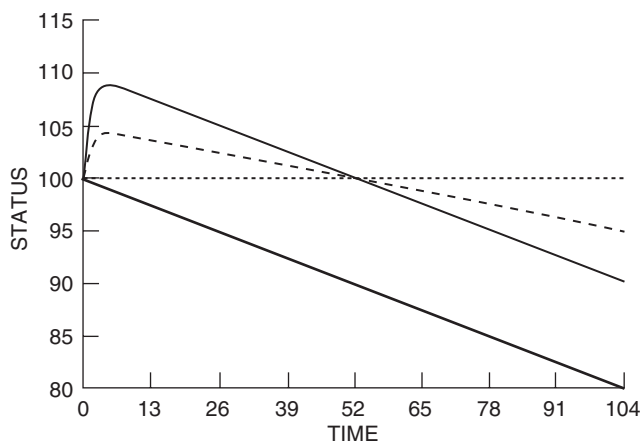

FIGURE 20.1 The thick line depicts the natural course ("natural history") of disease progress without therapeutic intervention (Equation 20.2). The thin line describes an offset pattern ("symptomatic") as a consequence of treatment (Equation 20.3). The dotted line reflects a slope pattern with a change in the rate of progress of the disease ("protective") (Equation 20.4). The *dashed line* shows the combination of both offset and slope patterns (Equation 20.5).

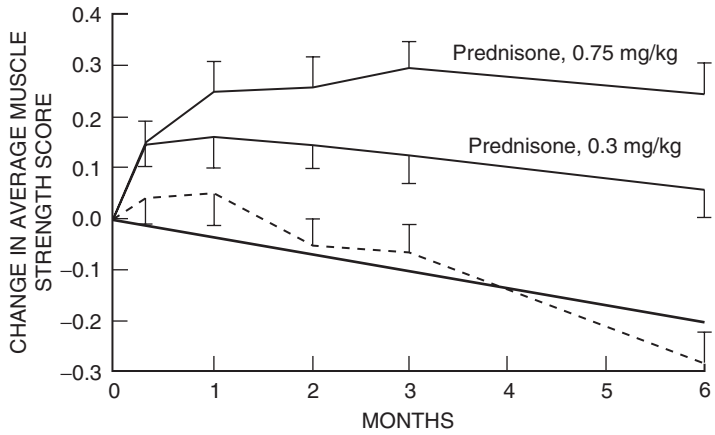

FIGURE 20.2 Example of linear disease progress and offset drug effect pattern when prednisone is used to treat muscular dystrophy. The heavy solid line is the expected natural history of progressive loss of muscle strength. The dashed line shows the transient improvement due to the placebo response. The two upper lines demonstrate the delayed offset pattern of drug effect at two doses of prednisone. (Reproduced with permission from Griggs RC , Moxley RT 3rd, Mendell JR, Fenichel GM, Brooke MH, Pestronik A *et al.* Arch Neurol 1991;48:383–8.)

The pattern of disease progress in the absence of drug is usually referred to as the natural history of the disease (Figure 20.1). A study by Griggs *et al.* (5) reporting temporary increases in muscle strength of muscular dystrophy patients treated with prednisone illustrates an application of the offset drug effect pattern (Figure 20.2).

Figure 20.3 shows a similar offset pattern of the effect of zidovudine in CD4 cell measurements in HIV patients (6). However, in this case, the model of disease progress uses functions that are not simply straight lines under placebo (polynomial; Equation 20.6) and zidovudine treatment (combined polynomial and exponential; Equation 20.7):

$$\text{Placebo}\,(t) = \text{CD4}_0 - k_1 \cdot t - k_2 \cdot t^2 \tag{20.6}$$

$$\text{Treatment}\,(t) = [B + (k_5 \cdot \text{CD4}_0) + (k_6 \cdot \text{CD4}_0^2)] \cdot \left(e^{-k_3 \cdot t} - e^{-k_4 \cdot t}\right) \tag{20.7}$$

The parameters B and k_1 through k_6 are used to describe how CD4 can be predicted from baseline CD4_0 and time. Models for multiple periods of treatment with placebo and active drug (with different

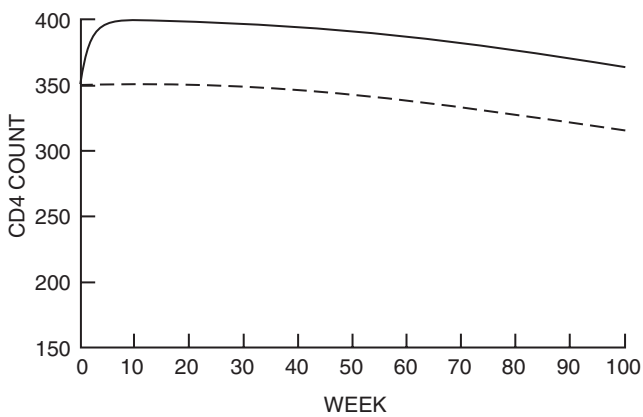

FIGURE 20.3 Time course of CD4 cell count in patients given placebo (*dashed line*) and zidovudine (*solid line*) treatment. (Reproduced with permission from Sale M, Sheiner LB, Volberding P, Blaschke TF. Clin Pharmacol Ther 1993;54:556–66.)

doses) have been used with a disease progress model to describe the response to tacrine in Alzheimer's disease. Figure 20.4 shows the placebo and active treatment components as well as the disease progress model (7). The predicted time course of response in patients with Alzheimer's disease in a complex clinical trial design combining disease progress, placebo, and tacrine effects is shown in Figure 20.5 (8). In this figure, the upper curve reflects the expected patient status, which would reflect a combination of disease progress and the effect of placebo on the time course of disease progress. In the lower curve, the sequential effects of varying treatments, including doses of placebo (P) and 40 and 80 mg/day of tacrine, were simulated. The difference between the control and active groups increases notably over the duration of the trial. This underscores the point that it is essential to incorporate appropriate models of disease progress as well as to account for placebo effect during any clinical trial simulation.

Finally, a disease progress model can reflect more complex drug action. Phenomena such as a drug concentration-effect delay, tolerance, and rebound to both placebo and active treatments can be made using a linear offset model. These effects can be accounted for by including the appropriate terms. For instance, a delay in onset can be accounted for by the addition of an effect compartment, and tolerance and rebound

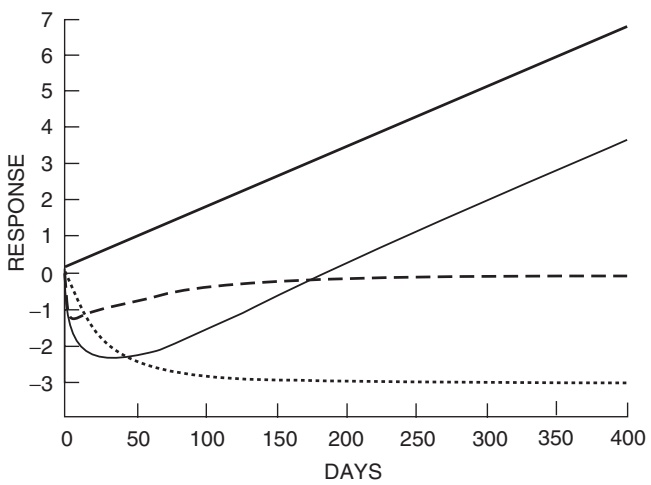

FIGURE 20.4 Models of Alzheimer's disease progress (*thick line*), placebo effect (*dotted line*), and drug effect (*dashed line*) in absence of disease progress, and combined (drug plus placebo) response to active drug in the presence of disease progress (*thin line*). Drug effect is assessed by subtracting placebo response and disease progress from the combined response that is observed with drug therapy. (Reproduced with permission from Holford NHG. Population models for Alzheimer's and Parkinson's disease. In: Aarons L, Balant LP, editors. The population approach: Measuring and managing variability in response, concentration and dose. Brussels: COST B1 European Commission; 1997. p. 97–104.)

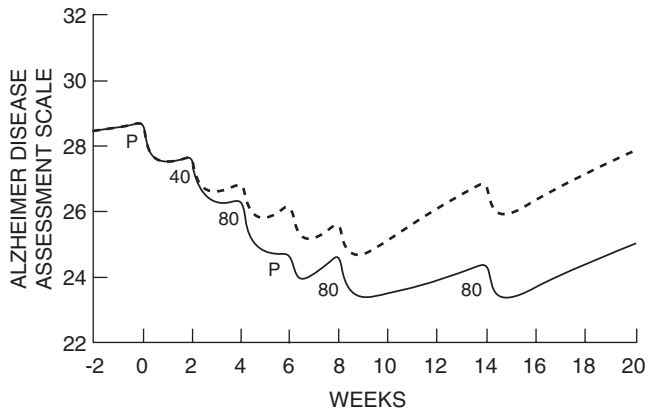

FIGURE 20.5 The upper curve shows the time course of predicted responses in a patient receiving placebo treatments as part of the three-part trial design used to evaluate tacrine in Alzheimer's disease. The lower curve shows the simulated response in a patient receiving a particular sequence of placebo (P) followed by tacrine (40 or 80 mg/day). (Reproduced with permission from Holford NH, Peace KE. Proc Natl Acad Sci USA 1992;89:11466–70.)

effects can be described by the addition of a precursor pool compartment, which would limit the effect of drug activity.

Asymptotic Progress Model

Zero Asymptote

A common pattern of disease progress provides for the patient's return to health or recovery without treatment intervention. For example, the time course of postoperative pain can be expected to start at a baseline state, which would be expected to involve intense levels of pain. However, over a few days the level of pain experienced by the patient would be expected to decrease until eventually pain is no longer perceived. This recovery can be approximated by an exponential model with an asymptote of zero, indicating the absence of pain. As shown in Equation 20.8, the parameters of this model are the baseline pain status S_0 and the half-life of progression, T_{prog}:

$$S(t) = S_0 \cdot e^{-\ln 2/T_{\text{prog}} \cdot t} \tag{20.8}$$

The asymptote model is particularly useful for illustrating one of the primary potential drawbacks of not accounting for disease progress. Because patients are expected to improve over time, a simple minimalist approach to the comparison of different drug effects would be expected to be dependent on the time of comparative assessment. If the comparison were made at a point in time where recovery has largely occurred, the difference between treatments would probably be undetectable.

As with the linear model of disease progress, the consequences of therapeutic intervention on the asymptotic model of disease progress can be described by including terms to account for the expected action of a drug. Drugs may exert an immediate and transient symptomatic effect, they may act to alter the progress of the disease, such as shortening the time to recovery, or they may do both.

Zero-Asymptote Offset Model Pattern

As shown in Equation 20.9, drug action models based on the zero-asymptote model can be extended to include an offset term [E_{OFF} ($C_{e,A}$)] in the model of progress describing symptomatic benefit such as the relief of pain from a simple analgesic:

$$S(t) = E_{OFF}(C_{e,A}) + S_0 \cdot e^{-\ln 2/T_{Prog} \cdot t} \tag{20.9}$$

As with the offset model for the linear disease progress model, the effect of drug would be expected to disappear on cessation of therapy in this offset model. Again, a delay to the onset of drug effect can be incorporated with the use of an effect compartment component.

Zero-Asymptote Slope Pattern

In addition, an exponentially progressing pattern of disease progress (parameterized by a half-life of progression) can reflect a protective benefit of drug treatment if the therapeutic intervention enhances the return to the normal state or shortens the half-life of the recovery process. Equation 20.10 describes the protective benefit:

$$S(t) = S_0 \cdot e^{-\ln 2/[E_{TP}(C_{e,A}) + T_{Prog}] \cdot t} \tag{20.10}$$

Combined Offset and Slope Pattern

The effects of a therapeutic agent (E_{TP}) on the progress of a disease may include both an immediate palliative effect and a reduction in the overall recovery time. Equation 20.11 describes the combination of these actions on the zero-asymptote disease progress model:

$$S(t) = E_{OFF}(C_{e,A}) + S_0 \cdot e^{-\ln 2/[E_{TP}(C_{e,A}) + T_{Prog}] \cdot t} \tag{20.11}$$

Figure 20.6 illustrates the expected changes in the progress of a disease, which can be described using the zero-asymptote model.

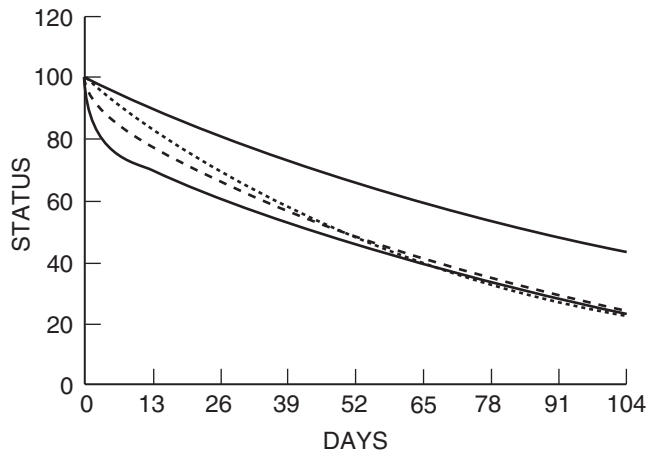

FIGURE 20.6 Patterns of drug effect with the zero-asymptote progress model. The thick line describes the normal expected time course of recovery without therapeutic intervention. The thin line shows the change when a drug that affects symptoms is administered. The dotted line illustrates the expected time course of disease when an agent is given which hastens recovery (protective) and the dashed line describes the expected results from administering an agent that exhibits both an immediate symptomatic effect and a protective effect on the time course of disease progress.

Nonzero Asymptote

Another pattern of disease progress encompasses reaching a "burned out" state (S_{SS}). This state is thought to happen when diseases such as rheumatoid arthritis reach a point when disease processes damage tissue beyond repair by any therapeutic means. This irreversibly damaged state can be described by another exponential model. Since the onset of the disease process is usually not known, the model can be expressed according to Equation 20.12, where t is time after the start of observing the disease from a baseline state (S_0) and the half-life of progression is T_{prog}:

$$S(t) = S_0 \cdot e^{-\ln 2/T_{Prog} \cdot t} + S_{SS} \cdot \left(1 - e^{-\ln 2/T_{Prog} \cdot t}\right) \tag{20.12}$$

Offset Pattern

Therapeutic treatment can affect disease status without altering the time to reach a burned out steady-state status, S_{SS}. This improvement in patient status would be expected to be transient and dependent on continual drug exposure. Equation 20.13 describes the effect of adding a drug that has a symptomatic effect [$E_{OFF}(C_{e,A})$] on patient status:

$$S(t) = E_{OFF}(C_{e,A}) + S_0 \cdot e^{-\ln 2/T_{Prog} \cdot t} + S_{SS} \cdot \left(1 - e^{-\ln 2/T_{Prog} \cdot t}\right) \tag{20.13}$$

Slope Pattern

Additional models for drug effects on the non-zero-asymptote model include two patterns of protective drug effects. These assume a drug effect changing either the burned out state, S_{SS};

$$S(t) = S_0 \cdot e^{-\ln 2/T_{Prog} \cdot t} + [E_{OFF}(C_{e,A}) + S_{SS}] \cdot \left(1 - e^{-\ln 2/T_{Prog} \cdot t}\right) \quad (20.14)$$

or affecting the half-life of progression, T_{prog},

$$S(t) = S_0 \cdot e^{-\ln 2/[E(C_{e,A}) + T_{Prog}] \cdot t} + S_{SS} \cdot \left(1 - e^{-\ln 2/[E(C_{e,A}) + T_{Prog}] \cdot t}\right) \quad (20.15)$$

Offset and Slope Patterns

Figure 20.7 illustrates the non-zero-asymptote model with all three patterns of disease progress influenced by drug effect. Patterns similar to this have been described in patients with Parkinson's disease treated with levodopa (11A). Drug exposure starts at 1.0 time units and is stopped at 8.0 time units. In Equation 20.16 the effects of symptomatic improvement and the two functions describing the action of drug both on the burned out state and on the time to reach this state have been included:

$$S(t) = E_{OFF}(C_{e,A}) + S_0 \cdot e^{-\ln 2/[E_{TP}(C_{e,A}) + T_{Prog}] \cdot t} + [E_{SS}(C_{e,A}) + S_{SS}] \cdot \left(1 - e^{-\ln 2[E_{TP}(C_{e,A}) + T_{Prog}] \cdot t}\right) \quad (20.16)$$

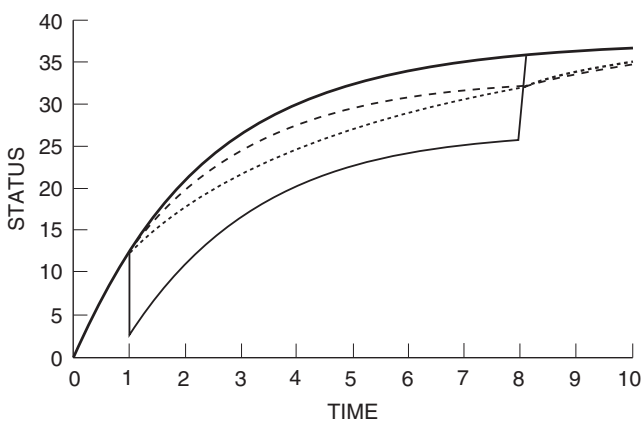

FIGURE 20.7 Non-zero-asymptote model with natural history (*thick line*) offset pattern (thin line), and two types of protective pattern drug effects: SSS, effect on steady-state burned out state (*dashed line*), and Tprog, effect on half-life of disease progress (*dotted line*).

Physiological Turnover Models

The time course of drug effect can often be understood in terms of drug-induced changes in physiological turnover processes controlling synthesis rate (R_{syn}) or elimination of a physiological mediator (9, 10). These models can be readily extended to describe disease progress by incorporating a time-varying change (Pharmaco-Dynamic Inhibition, PDI) in either synthesis or elimination. For example, if the rate constant (k_{loss}) describing loss of a physiological mediator starts from a baseline state, k_{loss0}, and decreases with a half-life of $T50_{loss}$, then the time course of the disease state can be described by solving the differential equation given in Equation 20.17:

$$dS/dt = R_{syn} - k_{loss} \cdot PDI \cdot S \quad (20.17)$$

where

$$k_{loss} = k_{loss0} \cdot \left[1 + (MaxProg - 1) \cdot \left(1 - e^{\ln 2/T50_{loss} \cdot t}\right)\right] \quad (20.18)$$

MaxProg is a parameter that determines the fractional change in k_{loss0} at infinite time. The effect of a drug (PDI) might be to inhibit loss, in which case PDI would be modeled by Equation 20.19, where $C_{e,A}$ is the effect site concentration and C50 is the value of $C_{e,A}$ causing a 50% inhibition of loss:

$$PDI = 1 - \frac{C_{e,A}}{C50 + C_{e,A}} \quad (20.19)$$

Figure 20.8 illustrates the four basic drug effect patterns when the input or output parameter changes with an exponential time course. As an example of this type of disease progress model, consider postmenopausal osteoporosis reflected by the net loss of bone mass after the menopause. Bone loss may be due to decreased formation or increased resorption of bone. Figure 20.9 illustrates the time course of bone mass change due to increased bone loss and the effect of administering a drug to reduce that loss. For example, raloxifene has been shown to be beneficial in women with postmenopausal osteoporosis (11). The pattern of increase in bone mineral density observed after treatment with raloxifene or placebo resembles the curves shown in Figure 20.10. However, the treatment duration in this dataset was too short to identify the actual mechanism of raloxifene effect on disease progress.

Growth Models

Another approach to modeling the course of disease progress is to use a growth function. The growth

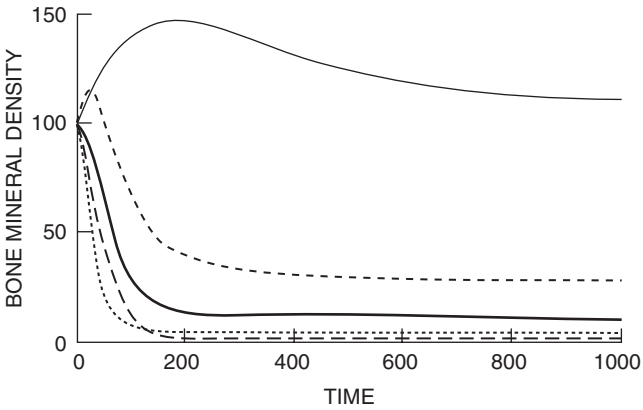

FIGURE 20.8 Disease progress due to a time-varying increase in the rate of loss of a physiological mediator of the response. The thick line shows the time course of response in the untreated state with an increase in the loss of physiological mediator. If the response was change in bone mass from a baseline of 100 at time zero, then the rate of bone loss would be increased by a factor of 10, reaching a new steady state after 200 time units. The time to steady state is determined both by the time course of change in rate of bone loss and by the turnover time of bone. The other four lines show the patterns expected from four different kinds of drug effect. Potentially therapeutic effects are inhibition of bone loss (*thin line*) and stimulation of bone synthesis (*upper dashed line*). Deleterious drug effects are inhibition of synthesis (*lower dashed line*) and stimulation of bone loss (dotted line).

function might be used to describe something such as tumor growth or bacterial cell increase, where growth is dependent on the number of cells dividing actively. A simple function that can be used to describe the growth of a response R is given in Equation 20.20 (12, 13):

$$dR/dt = k_{\text{growth}} \cdot R - k_{\text{death}} \cdot R \qquad (20.20)$$

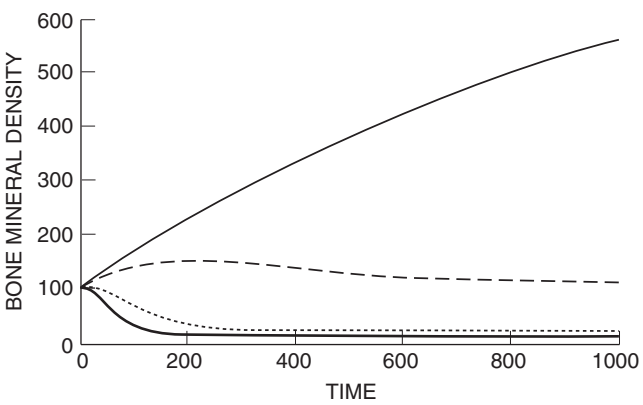

FIGURE 20.9 The pattern and time course of response to treatment is crucially dependent on the dose. This shows the same model as that illustrated in Figure 20.8, without treatment (*thick line*) and with three different dose rates of a drug that reduces the rate of loss of physiological substance (*dotted line*, dose rate of 10; *dashed line*, dose rate of 100; *thin line*, dose rate of 1000).

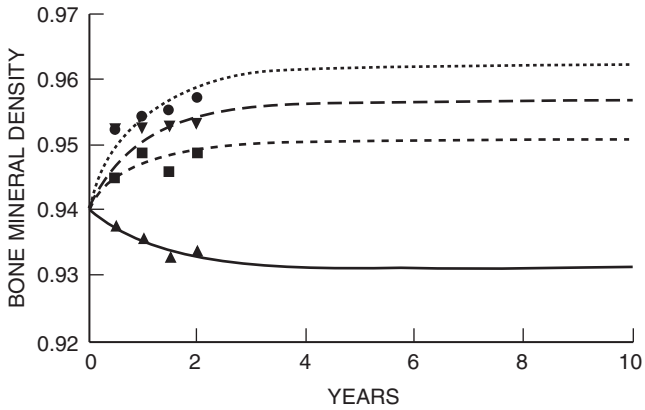

FIGURE 20.10 20.10 Bone mineral density change with placebo and three doses of raloxifene. Symbols indicate observed responses to placebo (▲) and daily doses of 30 mg (■), 60 mg (▼), and 150 mg (●). Curves show predictions assuming disease progress is due to increased loss, and raloxifene reduces loss. The model is the same as that shown in Figures 20.8 and 20.9. (Curves fit to lumbar spine data from Delmas PD, Bjarnason NH, Mitlak BH, Ravoux A-C, Shah AS, Huster WJ *et al*. N Engl J Med 1997;337:1641–7.)

The solution to this equation describes an exponential increase in cell count with time.

As with the other physiological models, the effect of drug treatment may be realized by slowing the growth rate (k_{growth}) or increasing the cell death rate (k_{death}). In the latter case, this effect can be incorporated by including a term for the effect of drug concentration ($C_{\text{e,A}}$) on the rate constant for cell decrease, as shown in Equation 20.21:

$$dR/dt = k_{\text{growth}} \cdot R - k_{\text{death}} \cdot R \cdot C_{\text{e,A}} \qquad (20.21)$$

A further refinement of the simple cell growth model would describe cells that, through mutation or other processes, may become resistant to drug treatment. The change of cell characteristic from a responsive to an unresponsive state can be either reversible or irreversible. Equations 20.22 and 20.23 describe the reversible case, which may be reflective of cells moving between sensitive phases (R_{S}) and phases that are not sensitive to therapeutic intervention (R_{R}) (14):

$$dR_{\text{s}}/dt = k_{\text{growth}} \cdot R_{\text{S}} - k_{\text{SR}} \cdot R_{\text{S}} + k_{\text{RS}} \cdot R_{\text{R}} - k_{\text{death}} \cdot R_{\text{S}} \qquad (20.22)$$

and

$$dR_{\text{R}}/dt = k_{\text{SR}} \cdot R_{\text{S}} - k_{\text{RS}} \cdot R_{\text{R}} \qquad (20.23)$$

where the rates of transformation to and from the resistant state are indicated by k_{SR} and k_{RS}, respectively.

Another series of functions frequently used to describe growth kinetics are the Gompertz functions (15). These functions are unique in that they describe a rapid initial rapid rate of growth (β), followed by a slower phase of growth until a finite limit (β_{max}) is reached. This behavior makes the Gompertz functions particularly useful for describing disease progress where there is a maximum level of impairment associated with the disease (e.g., a burned out state). Consequently, Gompertz functions have been used to describe the pharmacodynamics of antibacterial agents (16), as well as other systems in which growth kinetics are important. Equations 20.24 and 20.25 describe a Gompertz function of cell growth in which the cells oscillate between a therapeutically sensitive state (R_S) and a resistant state (R_R). The effect of drug concentration ($C_{e,A}$) is described using an E_{max} equation that acts to reduce the number of responsive cells in the system by increasing loss (k_{SO}) independently of transformation to or from the resistant state:

$$\frac{dR_S}{dt} = k_{RS} \cdot R_R + \beta \cdot R_S \cdot (\beta_{max} - R_S) - \left[k_{SR} + \left(1 + \frac{E_{max} \cdot C_{e,A}}{EC50 + C_{e,A}} \right) \cdot k_{SO} \right] \cdot R_S \quad (20.24)$$

$$dR_{SR}/dt = k_{SR} \cdot R_S - k_{RS} \cdot R_R \quad (20.25)$$

Figure 20.11 shows the expected pattern of growth of cells in three different treatment groups. In the low-dose treatment group, cell regrowth is expected to be rapid, and there is some evidence of regrowth near the 20-day time point even in the high-dose group.

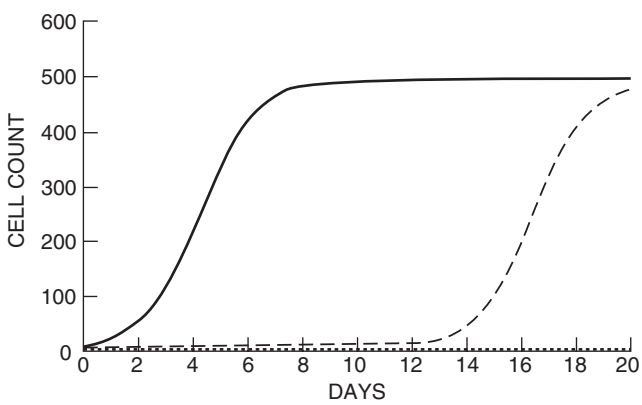

FIGURE 20.11 Growth curves for responsive cells exposed to three different treatment regimens: untreated (*solid line*), inadequately treated with a low drug dose (*broken line*), and adequately treated with a higher drug dose (*dashed line*). The curves show that cell regrowth following inadequate treatment is rapid.

CONCLUSION

The use of models to describe disease progress is an important tool that allows the analyst to appropriately evaluate the effects of drug treatment on the time course of disease. In the "learning versus confirming" paradigm (3), inclusion of models for disease progress can focus attention more clearly on the objectives of a clinical trial. In early, "learning-phase" studies, the model of disease progress can be developed and the mechanism of drug action is elucidated. Subsequently, clinical trials can be designed to account for variability in the natural history of disease, which increases the statistical power to distinguish between the effects of different treatments and thus "confirm" the effectiveness of the drug. Once the disease progress model has been defined and an effect of the drug on progress has been accepted, study designs can be defined that optimize clinical activity. In some cases, the mechanism of action of the drug may suggest innovative combination therapies or novel treatment approaches that would not have been considered without knowledge of the disease and the effect of drug on disease progress.

In this chapter, we have described some examples of models that can be used to describe the natural history of disease. We have also suggested modifications to these models that can be used to account for the effect of drug treatment. The development of an appropriate model for disease progress is ideally a team-based approach. It requires the input of clinical experts as to the validity of the status measure used to describe the progress of the disease, statisticians to advise on the inferences that can be drawn from clinical trial observations, and pharmacometricians to determine the appropriateness and utility of the clinical pharmacology model for predicting the response to treatment and to provide guidance to the patient and prescriber on how to use the drug safely and effectively.

REFERENCES

1. Holford NHG, Sheiner LB. Understanding the dose-effect relationship: Clinical application of pharmacokinetic-pharmacodynamic models. Clin Pharmacokinet 1981;6:429–53.
2. Sheiner LB. Clinical pharmacology and the choice between theory and empiricism. Clin Pharmacol Ther 1989;46:605–15.
3. Sheiner LB. Learning versus confirming in clinical drug development. Clin Pharmacol Ther 1997; 61:275–91.
4. Holford NHG, Sheiner LB. Kinetics of pharmacologic response. Pharmacol Ther 1982;16:143–66.

5. Griggs RC, Moxley RT, Mendell JR, Fenichel GM, Brooke MH, Pestronk A *et al.* Prednisone in Duchenne Dystrophy: A randomized, controlled trial defining the time course and dose response. Arch Neurol 1991;48:383–8.
6. Sale M, Sheiner LB, Volberding P, Blaschke TF. Zidovudine response relationships in early human immunodeficiency virus infection. Clin Pharmacol Ther 1993;54:556–66.
7. Holford NHG. Population models for Alzheimer's and Parkinson's disease. In: Aarons L, Balant LP, editors. The population approach: Measuring and managing variability in response, concentration and dose. Brussels: COST B1 European Commission; 1997. p. 97–104.
8. Holford NHG, Peace KE. Methodologic aspects of a population pharmacodynamic model for cognitive effects in Alzheimer patients treated with tacrine. Proc Natl Acad Sci USA 1992;89:11466–70.
9. Holford NHG. Physiological alternatives to the effect compartment model. In: D'Argenio DZ, editor. Advanced methods of pharmacokinetic and pharmacodynamic systems analysis. New York: Plenum Press; 1991. p. 55–68.
10. Dayneka NL, Garg V, Jusko WJ. Comparison of four basic models of indirect pharmacodynamic responses. J Pharmacokinet Biopharm 1993;21:457–78.
11. Delmas PD, Bjarnason NH, Mitlak BH, Ravoux A-C, Shah AS, Huster WJ *et al.* Effects of raloxifene on bone mineral density, serum cholesterol concentrations, and uterine endometrium in postmenopausal women. N Engl J Med 1997;337:1641–7.

11A. Holford NHG, Chan PL, Nutt JG, Kieburtz K, Shoulson I. Disease progression and pharmacodynamics in Parkinson disease – evidence for functional protection with levodopa and other treatments. J Pharmacokinet Pharmacodyn. 2006 Jun;33(3): 281–311.

12. Jusko W. Pharmacodynamics of chemotherapeutic effects: dose–time–response relationships for phase-nonspecific agents. J Pharm Sci 1971;60:892–5.
13. Zhi J, Nightingale C, Quintiliani R. A pharmacodynamic model for the activity of antibiotics against microorganisms under non saturable conditions. J Pharm Sci 1986;25:1063–7.
14. Jusko W. A pharmacodynamic model for cell cycle-specific chemotherapeutic agents. J Pharmacokinet Biopharm 1973;1:175–200.
15. Prior JC, Vigna YM, Schulzer M, Hall JE, Bonen A. Determination of luteal phase length by quantitative basal temperature methods: Validation against the midcycle LH peak. Clin Invest Med 1990;13:123–31.
16. Yano Y, Oguma T, Nagata H, Sasaki S. Application of a logistic growth model to pharmacodynamic analysis of *in vitro* bactericidal kinetics. J Pharm Sci 1998;87:1177–83.

This page intentionally left blank

PART

IV

OPTIMIZING AND EVALUATING PATIENT THERAPHY

This page intentionally left blank

CHAPTER

21

Pharmacological Differences between Men and Women

MAYLEE CHEN*, JOSEPH S. BERTINO, JR.†, MARY J. BERG‡, AND ANNE N. NAFZIGER†

*The Research Institute, Bassett Healthcare, Cooperstown, New York, †Ordway Research Institute, Inc., Albany, New York, ‡University of Iowa College of Pharmacy, Iowa City, Iowa (deceased)

> If most drugs had been developed in mixed gender populations, then the extent to which these issues contribute to gender-related variability in drug response would be clearer. However, women were systematically excluded from many clinical trials until relatively recently, and gender-related differences in drug response have only been sporadically reported. [Berg *et al.* NIH Publication No. 99-4386; 1999. p. 151 (1)]

The introduction of women's health as an issue in the l980s not only began the examination of disease and conditions specific to women, but also started to ask the question of whether women and men responded the same or differently to medications. This also raised questions regarding proper dosing of medicines for different sexes and members of different ethnic groups. Therefore, the whole issue of women's health extends beyond its origins just 25 years ago. In accordance with currently accepted usage, those differences that reflect biological differences between men and women that are physiologic, hormonal, or reproductive in nature will be referred to as *sex differences*, whereas cultural differences, such as differences in smoking behavior, will be referred to as *gender differences* (2).

The study of a pharmacological agent, such as a prescription medicine, an over-the-counter drug, an alternative medicine such as St. John's wort, or even a nutritional supplement, requires an interdisciplinary approach. Knowledge of pharmacokinetics, pharmacodynamics, pharmacogenetics, chronopharmacology, modulators, and biologic/molecular markers must all be incorporated to ensure the development of safe and efficacious medications (1). Adverse drug events are known to be more prevalent in women than in men (3). Reasons for this may include not only sex differences in hormonal levels, pharmacokinetics, and pharmacodynamics, but also gender differences. There is a higher rate of medication use among women and different adverse event reporting rates for men and women. Drug–drug, drug–nutrient, drug–herbal, and drug–smoking interactions may also alter pharmacokinetics or pharmacodynamics and may lead to possible differences in adverse drug events.

PHARMACOKINETICS

The first medication to be sex-analyzed for pharmacokinetic differences was antipyrine in 1971 (4). Antipyrine is entirely eliminated by hepatic metabolism; the initial study found that the half-life of antipyrine was shorter in women than in men. A subsequent study concluded that the clearance of antipyrine was the same for women and men only on day 5 of the menstrual cycle (5). In the 1980s, benzodiazepines were the first group of drugs examined for sex-specific differences in pharmacokinetics. At that time, the reporting of sex-analyzed pharmacokinetic studies began to approach the levels seen in the 1990s (Figure 21.1). Conduct of studies analyzed by sex has been facilitated by the passage of the National Institutes of Health (NIH) Revitalization Act of 1993 and the issuance of U.S Food and Drug

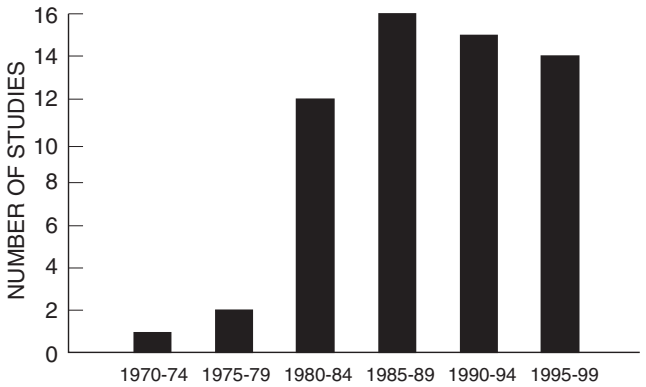

FIGURE 21.1 Reporting of sex-analyzed pharmacokinetic studies of drugs in various therapeutic classes from 1970 through 1999. (Data from Berg MJ. J Gender-Specif Med 1999;2:18–20.)

Administration (FDA) guidelines in the same year (4). In 2001, the General Accounting Office (GAO) report stated that while the number of women in clinical trials improved, the FDA needs to do better in terms of effectively overseeing that studies actually compile and present data according to sex (6). For instance, out of 300 new drug applications submitted to the FDA between the years of 1995 and 2000, only 163 had sex analysis as part of the submission. Sex-based pharmacodynamic assessment was done for just 39 of 122 new medical entities (7).

Absorption

Absorption encompasses not only the absorption of drugs from the gastrointestinal tract, but also absorption from muscle, subcutaneous fat, and lung. Of these various routes of absorption, most data pertain to oral bioavailability. As discussed in Chapter 4, the rate and extent of gastrointestinal absorption are influenced by multiple factors, such as gastric acid secretion, presence of pepsin, gastric emptying time, gastrointestinal blood flow, and surface area. Molecular size, drug ionization, and gut metabolism and transport are also important (8). Unfortunately, there are only a few published studies that adequately evaluate the potential for differences in drug absorption between men and women.

Some studies show that gastric emptying is slower in women than in men, thus slowing drug absorption from distal gastrointestinal sites (9, 10). Women have also been found to have higher gastric pH. The exact mechanisms behind these observations are unknown. Steroid hormones have been implicated, but data are inconsistent. It is unclear whether differences in factors such as increased gastric pH or decreased gastric emptying are clinically relevant. In one study of the bioavailability of aspirin, this drug was absorbed more rapidly in women than in men, but there was no sex difference in the extent of its absorption (11). Women may also have different levels of gastrointestinal enzyme activity. For example, women have less aspirin esterase activity in the gut. As a result, there is less first-pass metabolism of aspirin in women, and this may account for the increase in aspirin bioavailability (12).

Sex differences in other gastrointestinal enzymes have been postulated to account for differences observed in first-pass metabolism and bioavailability. For example, one study noted higher blood alcohol concentrations in women after oral intake but failed to find a difference when alcohol was administered intravenously (13). The suggestion was made that perhaps women have less alcohol dehydrogenase (ADH) in the gut and this partly explains why women have higher blood alcohol levels than men do after consuming the same amount of alcohol (14). This hypothesis should be considered cautiously, since ADH is an enzyme that displays polymorphism and ADH genotype was not reported. In addition, it would be important to know alcohol consumption history, since CYP2E1, another enzyme that metabolizes alcohol, is induced by chronic alcohol intake. Other studies evaluating sex differences in bioavailability have failed to adjust for weight (15).

Distribution

Drug distribution is affected by many factors, including plasma or tissue protein binding, body weight, body composition, and body fluid spaces (8). Of these, total body weight, muscle mass, and fat composition are the major determinants of drug distribution, and women may differ from men in both of these factors.

Women on average have lower body weight, less muscle mass, and a higher percentage of body fat accompanied by smaller organs and smaller intravascular volumes (16). For these reasons, the volumes of distribution of lipophilic drugs are expected to be greater in women after normalization for body weight. For example, a higher percentage of fat has been implicated in the higher volume of distribution observed in women taking lipophilic medications such as diazepam, nitrazepam, and chlordiazepoxide (17–21). Furthermore, the increased proportion of adipose tissue in women may explain the faster onset to effect and prolonged duration of action of lipophilic drugs such as vecuronium (22). In a similar manner, the smaller volumes of distribution observed in women, regarding hydrophilic drugs such as metronidazole, may be due to the smaller volume

of total body water seen in people with lower body weights (23).

While many reported sex differences are due solely to differences in body size, recent studies suggest that a true sex difference in drug distribution may occur with fluoroquinolones. Following intravenous administration of levofloxacin, a study found a significant decrease in volume of distribution in women even after adjusting for total body weight or lean body mass (24). Another study with radiolabeled fleroxacin found greater drug accumulation in the liver, blood, and myocardium of women, whereas men had greater accumulation in muscle (25).

As was emphasized in Chapter 3, protein binding may influence drug distribution. There are three major drug-binding proteins in plasma: albumin, α_1-acid glycoprotein, and α-globulins. Of these, albumin is the major protein and no sex difference has been found in its concentrations (26). Estrogen decreases α_1-acid glycoprotein concentrations, and this may account for the fact that drugs bind less extensively to this protein in women than in men (21). Despite this, no significant differences in unbound disopyramide concentrations (a substrate of α_1-acid glycoprotein) have been identified (27). Sex-independent factors such as disease states or inflammatory conditions can also alter plasma concentrations of α_1-acid glycoprotein (28). Although there may be sex differences in both α_1-acid glycoprotein concentrations and binding, there is no solid evidence that these differences have clinical importance. Other drug-binding proteins include corticosteroid-binding globulin, sex-hormone-binding globulin, and various lipoproteins, and sex may influence the plasma concentrations of these proteins (29).

Renal Excretion

Renal excretion is a major route of elimination for many drugs. Most of the available data evaluating sex differences in renal excretion have examined glomerular filtration. Since glomerular filtration rate is directly proportional to lean body weight, and since men in general tend to be larger than women are, differences in renal excretion rates most likely reflect differences in weight. Thus, men have significantly higher creatinine clearance compared to women but differences diminish once results are adjusted for weight. Following single-dose administration of fleroxacin, lomefloxacin, or temafloxacin, the renal clearance of these fluoroquinolones was significantly higher in men than in women but no significant difference was noted when clearance was corrected for total body weight (30).

Less is known of the impact of sex on tubular secretion or tubular reabsorption. Renal tubular secretion or reabsorption has not been well studied in humans and the few available studies contain serious design flaws. At present there does not appear to be a sex difference in the renal elimination of drugs.

Sex Differences in Metabolic Pathways

The assumption that structurally related compounds exhibiting a similar mechanism of action are also pharmacokinetically similar should not be made. Perhaps the best example of this complexity is provided by the benzodiazepines. Among the members of this group, a wide variety of findings has been reported. Oxidation is reported to be greater in women than in men for alprazolam, diazepam, and dimethyldiazepam. Reduction is reported to be the same for men and women for bromazepam, lorazepam, nitrazepam, and triazolam. Conjugation is reported to be greater in men than in women for chlordiazepoxide, oxazepam, and temazepam. Some clarification can be provided by focusing on whether sex differences occur in the specific Phase I and Phase II metabolic pathways that were described in Chapter 11.

Phase I Metabolic Pathways

Pharmacogenetic studies play an integral role in our understanding of drug metabolism. To date, primary emphasis has been placed on Phase I reactions mediated by cytochrome P450 (CYP) enzymes. Accumulated data show that the activities of most drug-metabolizing enzymes are affected by genetics but probably not by sex, although there are conflicting *in vivo* data. In many published studies, subjects were not genotyped. Therefore, it is not possible to rule out a gene-dose effect as a potential confounding factor when assessing sex differences in metabolism. Gene-dose effects are seen when there are variant genes present that explain differences in rates of drug metabolism. Many of the studies that suggest a sex difference have had other methodological problems. For example, the biomarkers used were not specific for the enzyme under study, or inappropriate phenotype sampling, sample handling, or metabolic ratios were used. From a genetic standpoint, since the alleles that code for the common CYP isozymes are not carried on the sex chromosomes, there should not be sex differences in activity. Variability may therefore be explained by genetic and environmental differences. If sex differences exist, these might be hormonally mediated and would manifest as phenotypic differences.

The six members of the cytochrome P450 enzyme superfamily that are primarily responsible for Phase I

drug metabolism are CYP1A2, CYP2C9, CYP2C19, CYP2D6, CYP2E1, and CYP3A isoenzymes. In the following section, *in vivo* human data on sex differences will be emphasized. Some *in vitro* and animal data suggest sex differences in drug metabolism that are not found with *in vivo* human data.

CYP1A2 is an isoenzyme that is responsible for oxidation of drugs such as caffeine (31). An early study using caffeine as a CYP1A2-specific probe drug found lower activity in women compared to men (32). Although this study used a validated probe drug (caffeine), the reported measurements used a urinary metabolic ratio that has been found to be poorly correlated with CYP1A2 activity (33, 34). More recent studies show no sex difference in enzyme activity (35, 36). Studies of the CYP2C9 isoenzyme using a variety of probes have not found a sex difference in enzyme activity (37–39), and based on available literature, CYP2C9 activity does not appear to be sex dependent (26). CYP2C19 is another enzyme that demonstrates genetic polymorphism. There is large interethnic variation in the frequency of poor metabolizers, with 12–25% of Asians and 2–5% of African-Americans and Caucasians, respectively, being poor metabolizers (1, 40). Studies using mephenytoin or piroxicam appear to demonstrate sex differences in metabolic activity (41, 42). When the data are controlled for the use of oral contraceptives and weight, the sex difference in enzyme activity disappears. In subjects genotyped and categorized into homozygous or heterozygous extensive metabolizers, no sex difference was found (43). Thus there is no clear evidence of a sex difference in CYP2C19 activity.

The CYP2D6 isoenzyme is polymorphic and metabolizes more than 40 drugs commonly in use, including antidepressants, antiarrhythmics, analgesics, and beta-blockers. Poor metabolizers comprise 5–10% of the Caucasian population but only about 2% of African-American or Asian populations. Heterozygous extensive metabolizers (or intermediate metabolizers) are common in African-American and Asian populations but many studies do not report genotypes or ethnicity. Although rat studies suggest a sex difference in metabolic activity of CYP2D6 (male greater than female), this finding has not been replicated in primates (44, 45). The limited *in vivo* human data exhibit conflicting results. Studies using clomipramine and ondansetron as CYP2D6 substrates showed small but significant differences in enzyme activity, with men having greater activity than women (46, 47), but neither omeprazole nor clomipramine are validated probe drugs for CYP2D6. Other studies using the validated probe dextromethorphan have shown greater CYP2D6 activity in women compared to men (48, 49). Although Hägg *et al.* (48) evaluated 611 adults, they were not genotyped and thus a gene-dose effect cannot be ruled out. Although available data are conflicting, there is not clear support of sex difference in CYP2D6 activity.

The CYP3A isoenzymes account for 30% of the total amount of expressed CYPs in the human liver and metabolize greater than 50% of commonly prescribed drugs (50). The majority of the studies do not show a sex difference in CYP3A activity (51). Among the studies that do show a difference, most found women to have higher metabolic activity. Studies investigating sex differences in triazolam clearance showed a trend of increased clearance in women that did not reach statistical significance (52–54). Another study evaluated the contribution of intestinal and hepatic CYP3A to an interaction between midazolam and clarithromycin and found significantly higher oral midazolam clearance in women (55). One explanation for this finding is that women have higher hepatic CYP3A content due to higher CYP3A4 messenger RNA (mRNA) expression (56). However, a recent trial investigating genotype–phenotype associations found no sex-related difference in midazolam clearance by CYP3A4 and CYP3A5 (57).

Some evidence suggests that CYP3A activity may be influenced by endogenous sex hormones (58). Endogenous hormones and their fluctuations in premenopausal women may be one explanation for reported differences in metabolism between premenopausal and postmenopausal women. For example, studies of tirilazad pharmacokinetics suggest higher clearance in premenopausal women than in postmenopausal women or in men (59), and the relationship between menopausal status and clearance was consistent when examined in different ways (60, 61). Other investigators have failed to find an influence of menstrual cycle phases (as surrogates for endogenous hormone changes) on CYP3A activity (62). One study showed no effect of exogenous sex hormones (oral contraceptives) on CYP3A activity (63). CYP3A 4/5 genotyping may be important in differentiating CYP3A isozyme activity, although this is a controversial area. Recently, the apparent sex difference in CYP3A has been postulated to be due to a higher hepatic content of P-glycoprotein (P-gp) in men (64). The premise is that since many drugs are substrates for both P-gp and CYP3A, and since women have been observed to have lower hepatic content of P-gp, more drug will be available intracellularly to be metabolized by CYP3A. However, a recent study of human liver samples showed no difference in hepatic P-gp content between males and females (65).

There is little information available about sex differences in the activity of CYP2E1 and even less

about the other Phase I enzymes, called non-P450 monoxygenases (27, 28).

Thus, there does not appear to be a clear sex difference in the activity of the Phase I P450 isoenzymes discussed here. Most of the studies show wide intersubject variability in enzyme activity that is independent of sex. Furthermore, once data are controlled for age, weight, smoking status, and hormone use, there is little evidence for sex-dependent variability. In the future, large studies with genotype information and appropriate probe drugs will shed more light on this area.

Phase II Metabolic Pathways

Although genetic polymorphisms are observed with Phase II enzymes, the effect of sex on the expression of Phase II enzymes is even less well documented than is the case with Phase I enzymes. The majority of studies analyzed for sex differences have failed to genotype subjects and most studies have small numbers of subjects and therefore may not have adequate power for finding sex differences, if they exist. Paracetamol glucuronidation is the pathway most frequently studied. One study showed a 22% higher clearance in men compared to women (66), and similar results were obtained by others (67, 68). None of these studies controlled for weight, and when the results are normalized for weight, no sex differences are found (69). No sex differences have been observed for sulfation, xanthine oxidation, or *N*-acetyltransferase activity (26, 36, 70).

Multiple Metabolic Pathways

Although we have associated a number of drugs with a specific metabolic pathway, metabolism of many drugs actually involves multiple pathways operating either in series or in parallel. Hence, many drugs are first oxidized in a Phase I reaction, which is often the rate-limiting step in metabolism (71), followed by Phase II conjugation (16). The role that sex may have in Phase II metabolism may therefore be difficult to discern. Several isoenzymes are also commonly involved in the Phase I metabolism of a drug. For example, ring oxidation of propranolol is mediated by CYP2D6 and side-chain cleavage is via CYP2C and CYP1A. In addition, propranolol is glucuronidated (16, 72, 73). Therefore, there are multiple Phase I and II metabolic pathways that can be affected by genetics and the environment. These separate processes must be explored before concluding, for example, that sex differences exist for the finding of higher propranolol concentrations in women compared to men.

Drug Transporters

Most information evaluating for sex differences in drug transporters is from rodent studies. Results in animal models suggest a sex difference in multidrug-resistant (MDR) drug transporter expression (74) and in kidney organic cation transporter proteins (OCT-2) (75). Data obtained from animal studies should be applied to humans with caution, and human data are lacking. P-gp is the only drug transporter that has been evaluated to any extent for sex dependence in humans. A study of human liver samples found a twofold higher P-gp expression in men compared to women (76), but a larger study found no sex difference (56). Human sex differences in kidney P-gp have not been examined (75). There is limited information regarding sex variability in expression of human OCT-2.

Drug Metabolism Interactions of Particular Importance to Women

While numerous studies have evaluated the effect of oral contraceptives and postmenopausal hormone replacement on drug clearance, many were flawed by poor study design. Table 21.1 lists studies that were of crossover or sequential design such that each subject was evaluated in the contraceptive phase and placebo phase. These study designs minimize the effect of interindividual variability. In most studies there was no effect of hormonal therapy on drug metabolism, but in some there were interactions that inhibited or increased the metabolism of concurrently administered drugs.

Higher clearance rates primarily reflect the ability of oral contraceptives to increase the activity of glucuronyltransferases. The mechanisms by which oral contraceptives decrease drug metabolism are unknown. We also do not know to what extent the estrogen or the progesterone components of oral contraceptives participate in these interactions (58). Although postmenopausal hormone replacement is becoming less prevalent, drug metabolism interactions resulting from hormone replacement therapy also warrant consideration, but few data are available (77–82).

Women use herbal and dietary supplements at higher rates than men do. This rise in use of alternative therapies places women at increased risk of significant drug interactions, specifically drug–herb and drug–nutrient interactions (83–89). For instance, St. John's wort, a popular antidepressant, contains at least seven groups of chemical compounds. These include naphthodianthrons (hypericin and pseudohypericin), flavonoids (quercetin, hyperoside, and rutin),

TABLE 21.1 Effects of Exogenous Sex Hormones on Drug Metabolism

Metabolic pathway Probe	Estrogen	Progestin	PK change parameter[a]
CYP1A2			
Antipyrine[b] [1]	none	norethisterone enanthate	Cl ↑ 11%
Caffeine [2]	ethinylestradiol	norgestimate	AUC ↓ 29%*
CYP2C9			
S-warfarin [2]	ethinylestradiol	norgestimate	AUC ↑ 9%
CYP2C19			
Omeprazole [3]	ethinylestradiol	levonorgestrel	AUC ↑ 48%**
	none	levonorgestrel	AUC ↓ 2%
Omeprazole [2]	ethinylestradiol	norgestimate	AUC ↑ 219%**
CYP2D6			
Dextromethorphan [2]	ethinylestradiol	norgestimate	AUC ↓ 20%*
CYP3A			
ERBT [4]	none	medroxyprogesterone oral	Cl "no change"
	none	medroxyprogesterone IM	Cl ↑ 23%
Midazolam, oral [5]	ethinylestradiol	gestogene	AUC ↑ 21%*
Midazolam, IV [6]	ethinylestradiol	norgestrel	AUC ↓ 12.4%
Midazolam, IV [2]	ethinylestradiol	norgestimate	AUC ↑ 7%
Nifedipine [7]	ethinylestradiol	dienogest	AUC ↓ 3.5%
	ethinylestradiol	levonorgestrel	AUC ↓ 8.2%
Prednisolone [4]	none	medroxyprogesterone oral	Cl "no change"
	none	medroxyprogesterone IM[b]	Cl ↑ 26%

PK = pharmacokinetic; Cl = clearance; AUC = area under the plasma concentration vs. time curve; ERBT = erythromycin breath test; IM = intramuscular; IV = intravenous

[a] Those that are significantly different after endogenous sex hormones are indicated as follows: * P value < .001, ** P value < .05.

[b] Antipyrine is metabolized by several metabolic pathways.

biflavones, tannic acid, phenylpropanes, and hyperforin. Several of these chemical entities have been implicated in affecting the activity of metabolic enzymes or drug transporters. Hypericin induces CYP1A2 and thus may affect theophylline metabolism. Quercetin induces P-gp. St. John's wort interacts with indinavir, a protease inhibitor, via induction of CYP3A isoenzymes. St. John's wort also has been reported to decrease the concentration of cyclosporine, a CYP3A and P-gp substrate, in heart transplant patients (87). St. John's wort also decreases the concentration of digoxin, presumably because it induces P-gp, thus decreasing absorption and increasing excretion of this drug.

Chronopharmacology, Menstrual Cycle, and Menopause

Chronopharmacology concerns itself with the effects of biological rhythms on drugs. Although little work has been done in this area, it is known that disease states and therapeutic responses are not time invariant (90, 91). Chronopharmacokinetics also includes the impact of circadian rhythms on hepatic drug metabolism (92). The highest activity for the P450 system, oxidative reactions, and glucuronide conjugation is during the waking hours while the highest activity for sulfate and glutathione conjugation is during the resting period. It has been assumed that the need for medications is the same over 24 hours. In the future, drug dosing schedules may be optimized based on an understanding of chronopharmacology. To date, cefodizime is the only drug for which there has been a sex-based analysis of chronopharmacology, and the authors of the analysis interpreted the findings as evidence for a sex difference (93). When cefodizime was administered intravenously four times per day, the area under the plasma concentration-vs-time curve (AUC) was lower in women at 1200 and 1800, compared to men ($p < 0.001$). However, there was large between-subject variability in the AUCs and the reported differences may therefore not be clinically relevant. These findings of sex differences in chronopharmacology have not been replicated.

Chronopharmacology also includes the impact of the menstrual cycle on drug pharmacokinetics and

pharmacodynamics (93). The menstrual cycle includes the follicular, ovulatory, and luteal phases that are accompanied by substantial hormonal changes. Therefore, it cannot be assumed that a premenopausal woman has the same kinetic profile as a man in the same age range. Although there are increasing numbers of studies that control for menstrual cycle phase, few studies have encompassed all the different phases of the menstrual cycle. A compounding confounder is that investigators do not use consistent definitions of the menstrual cycle phases. As a result, published data are conflicting about whether menstrual cycle phases significantly influence pharmacokinetics, although the weight of evidence suggests that the phases of the menstrual cycle do not have a clinically significant impact (94).

TABLE 21.2 Drugs with Known Risk of *Torsades de Pointes* That Is Greater in Women Than in Men[a]

Drug category	Examples
Antiarrhythmics	Amiodarone, disopyramide, ibutilide procainamide[b], quinidine, sotalol
Anti-infectives	Chloroquine, clarithromycin, erythromycin, pentamidine
Antihistamines	Astemizole,[c] terfenadine[c]
Antipsychotics	Chlorpromazine, haloperidol, pimozide, thioridazine
Other	Cisapride,[c] domperidone,[c] dropeidol, methadone, probucol[c]

[a] Data from The University of Arizona Center for Education and Research on Therapeutics, Arizona Health Sciences Center, Tucson, AZ. (Internet at http://www.torsades.org.)

[b] No data showing greater risk in women compared to men.

[c] These drugs have been removed from the U.S. market.

PHARMACODYNAMICS

There are few studies of pharmacodynamics that are analyzed by sex and even fewer that combine pharmacokinetics and pharmacodynamics. The most information to date has been provided on the cardiovascular effects of drugs, followed by pharmacodynamic studies of analgesics, immunosuppressants, and antidepressants.

Cardiovascular Effects

Perhaps the most dramatic example of sex differences in pharmacologic response is given by the greater risk that women have of developing the life-threatening ventricular arrhythmia called *torsades de pointes* after taking certain medications (95). Women have a risk of developing *torsades de pointes* from these medications that is at least twice as great as that of men (95–98). The demonstration that *torsades de pointes* is an important side effect of terfenadine first attracted widespread attention to the severity of this problem and led to the withdrawal of this antihistamine from the market in 1998. Other drugs that increase the risk of *torsades de pointes* include those listed in Table 21.2, and a frequently updated list can be found online at www.torsades.org.

Terfenadine and presumably other drugs that cause *torsades de pointes* block the delayed rectifier potassium current and this initially lengthens the electrocardographic QT interval (99). More than 49 drugs currently in use have been shown to lengthen the QT interval and have the presumed potential to cause *torsades de pointes*. In some cases, QT prolongation may be explained by higher concentration of drugs experienced by women because of their smaller size (100). However, *torsades de pointes* does not occur in every patient who is treated with these drugs. Large intra-individual variations in QT prolongation are common. Other factors that may predispose to this arrhythmia include hypokalemia, hypomagnesmia, hypothyroidism, renal failure, and congestive heart failure (95, 97, 101, 102).

Women appear to be at an increased risk of *torsades de pointes* because the baseline heart rate-corrected QT interval in women is, on average, longer than it is in men (103). The length of the QT interval is similar in males and females at birth, but shortens in males at puberty. The risk of this arrhythmia shows no sex difference before adolescence, and women have an increased incidence of *torsades de pointes* only after puberty. These observations are consistent with the fact that sex hormones affect potassium channel activity. Thus, estrogens have a down-regulating effect on potassium channel activity and androgens may be responsible for the QT interval shortening that is seen in postpubertal males (95, 96, 104).

Quinidine also causes *torsades de pointes* and, in a retrospective review of cases dating back to 1962, the observed prevalence of this arrhythmia in women was 60% as compared with an expected rate of 43% (95). It has been shown that the pharmacokinetics of quinidine are similar in men and women, but there is a pharmacodynamic difference in that the QT interval is longer in women than in men who are treated with this drug (105), with greater QTc prolongation occurring in women at equivalent serum quinidine concentrations (106). Similarly, women have three times the risk of developing *torsades de pointes* while receiving sotalol (97, 107, 108). It is particularly instructive that *torsades*

de pointes was not noted in the initial clinical safety studies of the lipid-lowering drug probucol, even though QT prolongation was described. However, these safety studies were confined to male patients and *torsades de pointes* was first reported to be a serious side effect of this drug only when studies that included both men and women were reviewed (109).

Propranolol provides another important example of a cardiovascular drug that combines sex differences in pharmacokinetics and in pharmacodynamics. In the Beta-Blocker Heart Attack Trial, equal doses of propranolol were given to men and women, but women were found to have higher plasma concentrations compared to men (1, 73, 110). However, when an isoproterenol challenge infusion was used to assess the actual degree of β-adrenoreceptor blockade, it was found that women had a lower sensitivity to propranolol that compensated for their higher plasma concentrations (111, 112). These offsetting pharmacokinetic and pharmacodynamic effects negate the need to reduce propranolol doses in women, an action that could reduce the overall effectiveness of this drug in this sex.

Sex differences in patient response also were noted in a trial that was designed to assess the efficacy of aspirin and dipyridamole in preventing recurrent stroke (113). There were fewer strokes and a marked reduction in mortality in men but much less of an effect in women. A large cardiovascular primary prevention trial provides further support for sex differences in the pharmacodynamics of aspirin (114). Women who took aspirin (100 mg) every other day had a reduced total risk of stroke but no decrease in the risk of myocardial infarction. This observation is in direct contrast to findings from the Physician's Health Study that found a 44% reduced risk of myocardial infarction among men over 50 years of age (115, 116). Differences in hormonal milieu are believed to provide at least a partial explanation for this difference (115). There is a biochemical basis for the finding that aspirin acts differently in women than in men (117). *In vitro* studies have shown that when the same amount of aspirin was added to the blood of males and females, platelet aggregation decreased more in men than in women (118). Further investigation indicated that when aspirin was added to blood from orchiectomized men, there was only a modest change in platelet aggregation. However, when testosterone was added to these blood samples, platelet aggregation was similar to that seen with blood from nonorchiectomized men. Therefore, testosterone appears to play in important role in aspirin-mediated inhibition of platelet aggregation and may be the basis for the observed *in vivo* sex difference.

Other sex-related differences in cardiovascular effect include the finding that antihypertensive drugs such as amlodipine exhibit greater antihypertensive effects in women than in men (119). Whether this greater response is due to differences in pharmacokinetics or pharmacodynamics is difficult to determine. Better blood pressure control could be explained by higher plasma drug concentrations in women, but pharmacokinetic differences do not necessarily correlate with the pharmacodynamic effects of antihypertensive drugs.

Analgesic Effects

There are three main types of opioid receptors at which opiates are thought to act: μ, κ, and δ receptors. In a study focusing on κ receptors, the analgesic effects of nalbuphine and butorphanol were greater in women than in men (120, 121). A randomized study found a nonsignificant trend toward greater morphine efficacy in men, but another found greater morphine potency, and slower onset of action but no pharmacokinetic differences in women (122). Many human studies did not control for confounding variables such as comorbidities, renal function, or concurrent medications, and often were conducted in the laboratory rather than in the clinical setting (123). Meperidine, morphine, and fentanyl have been reported to cause higher rates of nausea and vomiting in women, but it is not known whether the differences were pharmacodynamic or pharmacokinetic (124). The proposed mechanisms behind these apparent sex differences have been differences in body size, sex hormone concentrations, differences in opioid receptor density, and/or differences in binding affinity in the area of the brain involved in pain control (125). Unfortunately, none of the hypotheses proposed to explain these differences have been well studied.

Sex Differences in Immunology and Immunosuppression

There is indirect evidence of sex differences in immunology. Women have a higher incidence of autoimmune diseases such as multiple sclerosis, rheumatoid arthritis, and systemic lupus erythematosus. The influence of sex hormones on the immune system may provide insight into these immunological disorders. For example, estrogen stimulates both humoral and cell-mediated immunity, whereas testosterone has the opposite effect (126). Therefore, it is not surprising that there is sex-dependent variability in response to immunosuppressive agents.

Two groups of agents have been investigated for sex differences: corticosteroids and cytotoxic T-cell-suppressing agents. Women have been shown to have greater total body clearance of methylprednisolone than men have and also are more sensitive to suppression of endogenous cortisol production (127). The IC_{50} value for cortisol suppression was 17 times lower in women than in men. However, these pharmacokinetic and pharmacodynamic sex differences were offsetting, such that the net response to a given dose of methylprednisolone was similar in both men and women. In another study, men were found to have a higher oral clearance and larger volume of distribution of prednisolone compared to women, but these pharmacokinetic changes did not result in overall response differences (128).

In vivo information on cytotoxic T-cell-suppressing agents is very limited, but men and women have not been found to have sex-dependent differences in inhibition of lymphocyte proliferation, (129). Although numerous studies have postulated the presence of sex differences based on a higher incidence of organ rejection and increased mortality in women, it is not clear that these observations are due to sex differences (130). In an *in vitro* study, it was found that cyclosporine was metabolized faster by small intestinal microsomes from females, but this finding was based on only four female samples (131).

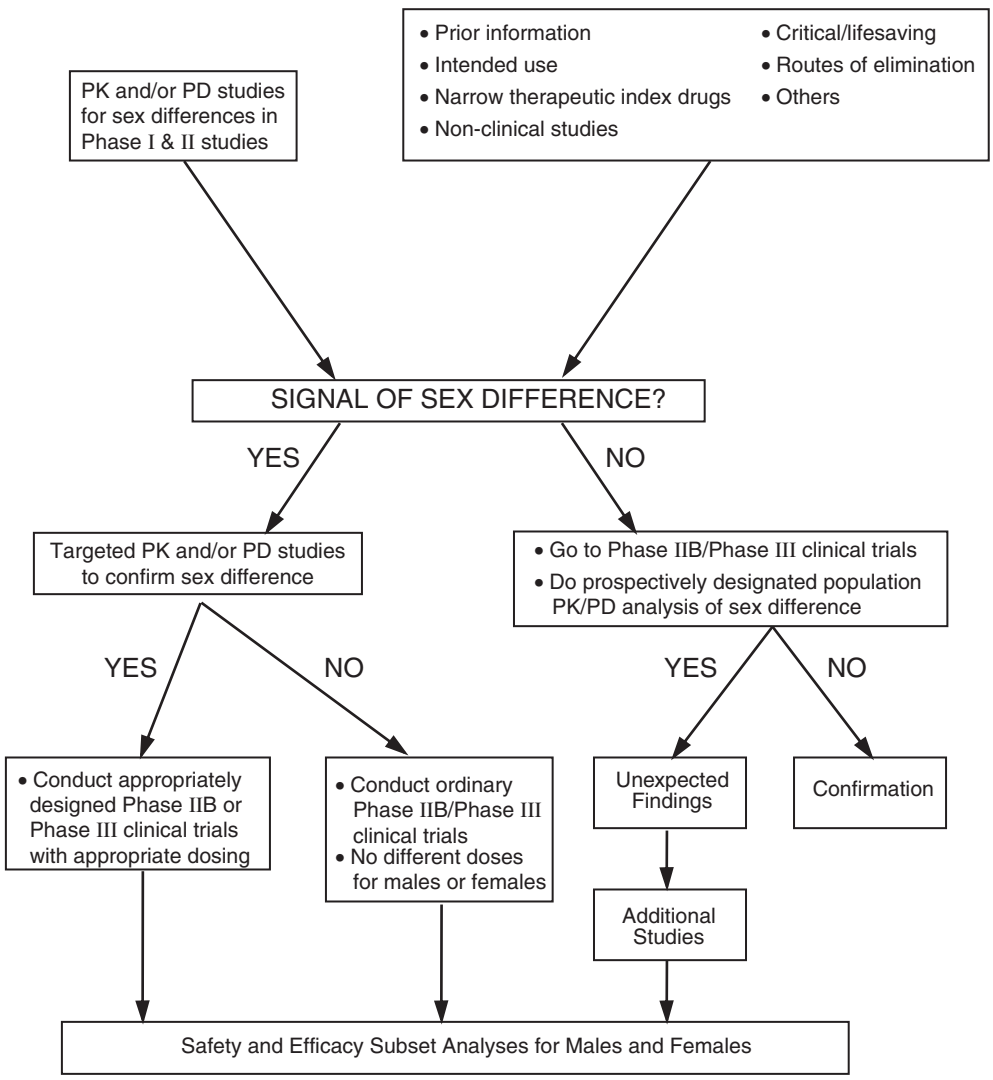

FIGURE 21.2 Decision tree for thinking about ways to assess sex differences during the development of medical products. [Modified from Gender studies in product development: Scientific issues and approaches. Executive summary. U.S. FDA, 1999. (Internet at http://www.fda.gov/womens/Executive.html).]

SUMMARY

There are few quality data on pharmacokinetic differences between men and women. Often, study findings are inconsistent, inconclusive, and of questionable clinical significance. To date, the evidence suggests that there may be sex differences in the area of pharmacodynamics. Unfortunately, there have been few investigations of sex differences in pharmacodynamics. This lack of research is most likely due to the challenge of investigating pharmacodynamic effect.

Since mandated by law in 1993, the National Institutes of Health has made progress in sponsoring sex-analyzed studies. As a result of an interdisciplinary meeting held in 1995, the Food and Drug Administration also has developed the algorithm shown in Figure 21.2 for sex-based analysis of pharmaceutical development studies. This excellent algorithm incorporates both basic and applied data to detect sex differences and should be used by the pharmaceutical industry as a guide to foster further well-designed studies.

REFERENCES

1. Berg MJ, Ketley JN, Merkatz R, Meittelman A. A report of the task force on the NIH Women's Health Research Agenda for the 21st Century, vol 2. Bethesda, MD: NIH Publication No. 99-4386; 1999. p. 151.
2. Kim JS, Nafziger AN. Is it sex or is it gender? Clin Pharmacol Ther 2000;68:1–3.
3. Kando JC, Yonkers KA, Cole JO. Gender as a risk factor for adverse events to medications. Drugs 1995;50:1–6.
4. Berg MJ. Drugs, vitamins, and gender. J Gend Specif Med 1999;2:18–20.
5. Nayak VK, Kshirsagar NA, Desai NK, Satoskar RS. Influence of menstrual cycle on antipyrine pharmacokinetics in healthy Indian female volunteers. Br J Clin Pharmacol 1988;26:604–6.
6. United States General Accounting Office. GAO Report to Congressional Requesters. Women's Health. Women sufficiently represented in new drug testing, but FDA oversight needs improvement. Washington, D.C.: Publication No. GAO-01-754; July 2001.
7. Wood S. Sex differences between men and women enrolled in clinical trials. In: American Society for Clinical Pharmacology and Therapeutics educational symposium; June 6–7, 2004. Washington, D.C.: ASCPT; 2004.
8. Gandhi M, Aweeka F, Greenblatt RM, Blaschke TF. Sex differences in pharmacokinetics and pharmacodynamics. Annu Rev Pharmacol Toxicol 2004; 44:499–523.
9. Datz FL, Christian PE, Moore J. Gender-related differences in gastric emptying. J Nucl Med 1987;28:1204–7.
10. Degen LP, Phillips SF. Variability of gastrointestinal transit in healthy women and men. Gut 1996; 39:299–305.
11. Aarons L, Hopkins K, Rowland M, Brossel S, Thiercelin JF. Route of administration and sex differences in the pharmacokinetics of aspirin, administered as its lysine salt. Pharm Res 1989;6:660–6.
12. Ho PC, Triggs EJ, Bourne DW, Heazlewood VJ. The effects of age and sex on the disposition of acetylsalicylic acid and its metabolites. Br J Clin Pharmacol 1985;19:675–84.
13. Baraona E, Abittan CS, Dohmen K, Moretti M, Pozzato G, Chayes ZW *et al.* Gender differences in pharmacokinetics of alcohol. Alcohol Clin Exp Res 2001;25:502–7.
14. Seitz HK, Egerer G, Simanowski UA, Waldherr R, Eckey R, Agarwal DP *et al.* Human gastric alcohol dehydrogenase activity: Effect of age, sex, and alcoholism. Gut 1993;34:1433–7.
15. Vree TB, Dammers E, Valducci R. Sex-related differences in the pharmacokinetics of isosorbide-5-mononitrate (60 mg) after repeated oral administration of two different original prolonged release formulations. Int J Clin Pharmacol Ther 2004; 42:463–72.
16. Harris RZ, Benet LZ, Schwartz JB. Gender effects in pharmacokinetics and pharmacodynamics. Drugs 1995;50:222–39.
17. Abel JG, Sellers EM, Naranjo CA, Shaw J, Kadar D, Romach MK. Inter- and intrasubject variation in diazepam free fraction. Clin Pharmacol Ther 1979;26:247–55.
18. Greenblatt DJ, Abernethy DR, Locniskar A, Ochs HR, Harmatz JS, Shader RI. Age, sex, and nitrazepam kinetics: Relation to antipyrine disposition. Clin Pharmacol Ther 1985;38:697–703.
19. Ochs HR, Greenblatt DJ, Divoll M, Abernethy DR, Feyerabend H, Dengler HJ. Diazepam kinetics in relation to age and sex. Pharmacology 1981;23:24–30.
20. Roberts RK, Desmond PV, Wilkinson GR, Schenker S. Disposition of chlordiazepoxide: Sex differences and effects of oral contraceptives. Clin Pharmacol Ther 1979;25:826–31.
21. Routledge PA, Stargel WW, Kitchell BB, Barchowsky A, Shand DG. Sex-related differences in the plasma protein binding of lignocaine and diazepam. Br J Clin Pharmacol 1981;11:245–50.
22. Houghton IT, Aun CS, Oh TE. Vecuronium: An anthropometric comparison. Anaesthesia 1992; 47:741–6.
23. Carcas AJ, Guerra P, Frias J, Soto A, Fernandez-Aijon A, Montuenga C *et al.* Gender differences in the disposition of metronidazole. Int J Clin Pharmacol Ther 2001;39:213–8.
24. Overholser BO, Kays MB, Lagvankar S, Goldman M, Mueller BA, Sowinski KM. Pharmacokinetics of intravenously administered levofloxacin in men and women. Pharmacotherapy 2005; in press.
25. Fischman AJ, Livni E, Babich J, Alpert NM, Liu YY, Thom E *et al.* Pharmacokinetics of [^{18}F]fleroxacin in healthy human subjects studied by using positron emission tomography. Antimicrob Agents Chemother 1993;37:2144–52.

26. Meibohm B, Beierle I, Derendorf H. How important are gender differences in pharmacokinetics? Clin Pharmacokinet 2002;41:329–42.
27. Kishino S, Nomura A, Di ZS, Sugawara M, Iseki K, Kakinoki S *et al.* Alpha-1-acid glycoprotein concentration and the protein binding of disopyramide in healthy subjects. J Clin Pharmacol 1995;35:510–4.
28. MacKichan JJ. Influence of protein binding and use of unbound (free) drug concentrations. In: Evans WE, Schentag JJ, Jusko WJ, editors. Applied pharmacokinetics: Principles of therapeutic drug monitoring. 3rd ed. Vancouver, WA: Applied Therapeutics Inc.; 1992. p. 5-1–5-48.
29. Wilson K. Sex-related differences in drug disposition in man. Clin Pharmacokinet 1984;9:189–202.
30. Sörgel F, Naber KG, Mahr G, Gottschalk B, Stephan U, Seelmann R *et al.* Gender related distribution of quinolones. Eur J Clin Microbiol Infect Dis 1991;10(special):189–190.
31. Wrighton SA, Stevens JC. The human hepatic cytochromes P450 involved in drug metabolism. Crit Rev Toxicol 1992;22:1–21.
32. Relling MV, Lin JS, Ayers GD, Evans WE. Racial and gender differences in *N*-acetyltransferase, xanthine oxidase, and CYP1A2 activities. Clin Pharmacol Ther 1992;52:643-58.
33. Denaro CP, Wilson M, Jacob P 3rd, Benowitz NL. Validation of urine caffeine metabolite ratios with use of stable isotope-labeled caffeine clearance. Clin Pharmacol Ther 1996;59:284–96.
34. Streetman DS, Bertino JS Jr, Nafziger AN. Phenotyping of drug-metabolizing enzymes in adults: A review of *in-vivo* cytochrome P450 phenotyping probes. Pharmacogenetics 2000;10:187–216.
35. Bebia Z, Buch SC, Wilson JW, Frye RF, Romkes M, Cecchetti A *et al*. Bioequivalence revisited: Influence of age and sex on CYP enzymes. Clin Pharmacol Ther 2004;76:618–27.
36. Kashuba AD, Bertino JS Jr, Kearns GL, Leeder JS, James AW, Gotschall R *et al*. Quantitation of three-month intraindividual variability and influence of sex and menstrual cycle phase on CYP1A2, *N*-acetyltransferase-2, and xanthine oxidase activity determined with caffeine phenotyping. Clin Pharmacol Ther 1998;63:540–51.
37. Brunner HR. The new angiotensin II receptor antagonist, irbesartan: Pharmacokinetic and pharmacodynamic considerations. Am J Hypertens 1997; 10:311S–17S.
38. Scripture CD, Pieper JA. Clinical pharmacokinetics of fluvastatin. Clin Pharmacokinet 2001;40:263–81.
39. Vachharajani NN, Shyu WC, Smith RA, Greene DS. The effects of age and gender on the pharmacokinetics of irbesartan. Br J Clin Pharmacol 1998;46:611–3.
40. Lamba JK, Dhiman RK, Kohli KK. CYP2C19 genetic mutations in North Indians. Clin Pharmacol Ther 2000;68:328–35.
41. Karim A, Noveck R, McMahon FG, Smith M, Crosby S, Adams M *et al*. Oxaprozin and piroxicam, nonsteroidal antiinflammatory drugs with long half-lives: Effect of protein-binding differences on steady-state pharmacokinetics. J Clin Pharmacol 1997;37:267–78.
42. Tamminga WJ, Wemer J, Oosterhuis B, Weiling J, Wilffert B, de Leij LF *et al*. CYP2D6 and CYP2C19 activity in a large population of Dutch healthy volunteers: Indications for oral contraceptive-related gender differences. Eur J Clin Pharmacol 1999;55:177–84.
43. Kim MJ, Bertino JS, Jr., Gaedigk A, Zhang Y, Sellers EM, Nafziger AN. Effect of sex and menstrual cycle phase on cytochrome P450 2C19 activity with omeprazole used as a biomarker. Clin Pharmacol Ther 2002;72:192–9.
44. Maloney AG, Schmucker DL, Vessey DS, Wang RK. The effects of aging on the hepatic microsomal mixed-function oxidase system of male and female monkeys. Hepatology 1986;6:282–7.
45. Schmucker DL, Wang RK. Effects of aging on the properties of rhesus monkey liver microsomal NADPH-cytochrome c (P-450) reductase. Drug Metab Dispos 1987;15:225–32.
46. Gex-Fabry M, Balant-Gorgia AE, Balant LP, Garrone G. Clomipramine metabolism. Model-based analysis of variability factors from drug monitoring data. Clin Pharmacokinet 1990;19:241–55.
47. Pritchard JF, Bryson JC, Kernodle AE, Benedetti TL, Powell JR. Age and gender effects on ondansetron pharmacokinetics: Evaluation of healthy aged volunteers. Clin Pharmacol Ther 1992;51:51–5.
48. Hägg S, Spigset O, Dahlqvist R. Influence of gender and oral contraceptives on CYP2D6 and CYP2C19 activity in healthy volunteers. Br J Clin Pharmacol 2001;51:169–73.
49. Labbé L, Sirois C, Pilote S, Arseneault M, Robitaille NM, Turgeon J *et al*. Effect of gender, sex hormones, time variables and physiological urinary pH on apparent CYP2D6 activity as assessed by metabolic ratios of marker substrates. Pharmacogenetics 2000;10:425–38.
50. Sakuma T, Endo Y, Mashino M, Kuroiwa M, Ohara A, Jarukamjorn K *et al*. Regulation of the expression of two female-predominant CYP3A mRNAs (CYP3A41 and CYP3A44) in mouse liver by sex and growth hormones. Arch Biochem Biophys 2002;404:234–42.
51. Cotreau MM, von Moltke LL, Greenblatt DJ. The influence of age and sex on the clearance of cytochrome P450 3A substrates. Clin Pharmacokinet 2005;44:33–60.
52. Greenblatt DJ, Harmatz JS, Shapiro L, Engelhardt N, Gouthro TA, Shader RI. Sensitivity to triazolam in the elderly. N Engl J Med 1991;324:1691–8.
53. Greenblatt DJ, Harmatz JS, von Moltke LL, Wright CE, Shader RI. Age and gender effects on the pharmacokinetics and pharmacodynamics of triazolam, a cytochrome P450 3A substrate. Clin Pharmacol Ther 2004;76:467–79.
54. Smith RB, Divoll M, Gillespie WR, Greenblatt DJ. Effect of subject age and gender on the pharmacokinetics of oral triazolam and temazepam. J Clin Psychopharmacol 1983;3:172–6.
55. Gorski JC, Jones DR, Haehner-Daniels BD, Hamman MA, O'Mara EM Jr, Hall SD. The contribution of intestinal and hepatic CYP3A to the interaction between midazolam and clarithromycin. Clin Pharmacol Ther 1998;64:133–43.
56. Wolbold R, Klein K, Burk O, Nussler AK, Neuhaus P, Eichelbaum M *et al*. Sex is a major determinant

of CYP3A4 expression in human liver. Hepatology 2003;38:978–88.
57. Floyd MD, Gervasini G, Masica AL, Mayo G, George AL Jr, Bhat K *et al*. Genotype-phenotype associations for common CYP3A4 and CYP3A5 variants in the basal and induced metabolism of midazolam in European- and African-American men and women. Pharmacogenetics 2003;13:595–606.
58. Laine K, Tybring G, Bertilsson L. No sex-related differences but significant inhibition by oral contraceptives of CYP2C19 activity as measured by the probe drugs mephenytoin and omeprazole in healthy Swedish white subjects. Clin Pharmacol Ther 2000;68:151–9.
59. Hulst LK, Fleishaker JC, Peters GR, Harry JD, Wright DM, Ward P. Effect of age and gender on tirilazad pharmacokinetics in humans. Clin Pharmacol Ther 1994;55:378–84.
60. Fleishaker JC, Hulst-Pearson LK, Peters GR. Effect of gender and menopausal status on the pharmacokinetics of tirilazad mesylate in healthy subjects. Am J Ther 1995;2:553–560.
61. Fleishaker JC, Pearson LK, Pearson PG, Wienkers LC, Hopkins NK, Peters GR. Hormonal effects on tirilazad clearance in women: Assessment of the role of CYP3A. J Clin Pharmacol 1999;39:260–7.
62. Kashuba AD, Bertino JS, Jr., Rocci ML, Jr., Kulawy RW, Beck DJ, Nafziger AN. Quantification of 3-month intraindividual variability and the influence of sex and menstrual cycle phase on CYP3A activity as measured by phenotyping with intravenous midazolam. Clin Pharmacol Ther 1998;64: 269–77.
63. Shelepova T, Nafziger AN, Victory J, Kashuba AD, Rowland E, Zhang Y, Sellers E, Kearns GL, Leeder S, Gaedigk A, Bertino JS, Jr. Effect of oral contraceptives (OCS) on drug metabolizing enzymes (DMES) as measured by the validated cooperstown 5+1 cocktail (5 + 1). ABSTRACT. Clinical Pharmacology and Therapeutics 2003;73(2):PI–49.
64. Cummins CL, Wu CY, Benet LZ. Sex-related differences in the clearance of cytochrome P450 3A4 substrates may be caused by P-glycoprotein. Clin Pharmacol Ther 2002;72:474–89.
65. Paine MF, Ludington SS, Chen ML, Stewart PW, Huang SM. Does sex influence proximal small intestinal CYP3A or P-gp expression? Clin Pharmacol Ther 2005;77:P2.
66. Miners JO, Attwood J, Birkett DJ. Influence of sex and oral contraceptive steroids on paracetamol metabolism. Br J Clin Pharmacol 1983;16:503–9.
67. Abernethy DR, Divoll M, Greenblatt DJ, Ameer B. Obesity, sex, and acetaminophen disposition. Clin Pharmacol Ther 1982;31:783–90.
68. Divoll M, Abernethy DR, Ameer B, Greenblatt DJ. Acetaminophen kinetics in the elderly. Clin Pharmacol Ther 1982;31:151–6.
69. Tanaka E. Gender-related differences in pharmacokinetics and their clinical significance. J Clin Pharm Ther 1999;24:339–46.
70. Gleiter CH, Gundert-Remy U. Gender differences in pharmacokinetics. Eur J Drug Metab Pharmacokinet 1996;21:123–8.
71. Beierle I, Meibohm B, Derendorf H. Gender differences in pharmacokinetics and pharmacodynamics. Int J Clin Pharmacol Ther 1999;37:529–47.
72. Berg MJ. Status of research on gender differences. Gender-related health issues: An international perspective. In: Berg MJ, Francke GN, Rollings MR, editors. Gender-related health issues. An international perspective. Washington, D.C.: American Pharmaceutical Association; 1996. p. 37–68.
73. Walle T, Walle UK, Cowart TD, Conradi EC. Pathway-selective sex differences in the metabolic clearance of propranolol in human subjects. Clin Pharmacol Ther 1989;46:257–63.
74. Piquette-Miller M, Pak A, Kim H, Anari R, Shahzamani A. Decreased expression and activity of P-glycoprotein in rat liver during acute inflammation. Pharm Res 1998;15:706–11.
75. Morris ME, Lee HJ, Predko LM. Gender differences in the membrane transport of endogenous and exogenous compounds. Pharmacol Rev 2003;55:229–40.
76. Schuetz EG, Furuya KN, Schuetz JD. Interindividual variation in expression of P-glycoprotein in normal human liver and secondary hepatic neoplasms. J Pharmacol Exp Ther 1995;275:1011–8.
77. Greenblatt DJ, Abernethy DR, Locniskar A, Harmatz JS, Limjuco RA, Shader RI. Effect of age, gender, and obesity on midazolam kinetics. Anesthesiology 1984;61:27–35.
78. Gustavson LE, Benet LZ. Menopause: Pharmacodynamics and pharmacokinetics. Exp Gerontol 1994;29:437–44.
79. Gustavson LE, Legler UF, Benet LZ. Impairment of prednisolone disposition in women taking oral contraceptives or conjugated estrogens. J Clin Endocrinol Metab 1986;62:234–7.
80. Harris RZ, Tsunoda SM, Mroczkowski P, Wong H, Benet LZ. The effects of menopause and hormone replacement therapies on prednisolone and erythromycin pharmacokinetics. Clin Pharmacol Ther 1996;59:429–35.
81. Holazo AA, Winkler MB, Patel IH. Effects of age, gender and oral contraceptives on intramuscular midazolam pharmacokinetics. J Clin Pharmacol 1988; 28:1040–5.
82. Schwartz JB, Capili H, Daugherty J. Aging of women alters *S*-verapamil pharmacokinetics and pharmacodynamics. Clin Pharmacol Ther 1994;55:509–17.
83. Ernst E. Second thoughts about safety of St John's wort. Lancet 1999;354:2014–6.
84. Fugh-Berman A. Herb–drug interactions. Lancet 2000;355:134–8.
85. Piscitelli SC, Burstein AH, Chaitt D, Alfaro RM, Falloon J. Indinavir concentrations and St John's wort. Lancet 2000;355:547–8.
86. Risk of drug interactions with St. John's wort and indinavir and other drugs. 2000. (Internet at http://www.fda/gov/cder/drug/advisory/stjwort.htm.)
87. Johne A, Brockmoller J, Bauer S, Maurer A, Langheinrich M, Roots I. Pharmacokinetic interaction of digoxin with an herbal extract from St John's wort (*Hypericum perforatum*). Clin Pharmacol Ther 1999;66:338–45.

88. Roby CA, Anderson GD, Kantor E, Dryer DA, Burstein AH. St John's wort: Effect on CYP3A4 activity. Clin Pharmacol Ther 2000;67:451–7.
89. Ruschitzka F, Meier PJ, Turina M, Luscher TF, Noll G. Acute heart transplant rejection due to Saint John's wort. Lancet 2000;355:548–9.
90. Lemmer B. Circadian rhythm in blood pressure: Signal transduction regulatory mechanisms and cardiovascular medication. Stuttgart: Medpharm Scientific Publishers; 1996. p. 91–117.
91. Reinberg AE, Ashkenazi IE. Chronopharmacology: Should we individualize drug treatments. Stuttgart: Medpharm Scientific Publishers; 1996. p. 71–89.
92. Labrecque G, Belanger PM. Biological rhythms in the absorption, distribution, metabolism and excretion of drugs. Pharmacol Ther 1991;52:95–107.
93. Jonkman JH, Reinberg A, Oosterhuis B, fde Noord OE, Kerkhof FA, Motohashi Y *et al*. Dosing time and sex-related differences in the pharmacokinetics of cefodizime and in the circadian cortisol rhythm. Chronobiologia 1988;15:89–102.
94. Kashuba AD, Nafziger AN. Physiological changes during the menstrual cycle and their effects on the pharmacokinetics and pharmacodynamics of drugs. Clin Pharmacokinet 1998;34:203–18.
95. Ebert SN, Liu XK, Woosley RL. Female gender as a risk factor for drug-induced cardiac arrhythmias: Evaluation of clinical and experimental evidence. J Women's Health 1998;7:547–57.
96. Drici MD, Knollmann BC, Wang WX, Woosley RL. Cardiac actions of erythromycin: Influence of female sex. JAMA 1998;280:1774–6.
97. Makkar RR, Fromm BS, Steinman RT, Meissner MD, Lehmann MH. Female gender as a risk factor for torsades de pointes associated with cardiovascular drugs. JAMA 1993;270:2590–7.
98. Woosley RL. Drugs that prolong the QT interval and/or induce Torsades de Pointes ventricular arrhythmia. 2005. (Internet at http://www.torsades.org.)
99. Woosley RL, Chen Y, Freiman JP, Gillis RA. Mechanism of the cardiotoxic actions of terfenadine. JAMA 1993;269:1532–6.
100. Wolbrette DL. Risk of proarrhythmia with class III antiarrhythmic agents: Sex-based differences and other issues. Am J Cardiol 2003;91:39D–44D.
101. Bagchi N, Brown TR, Parish RF. Thyroid dysfunction in adults over age 55 years. A study in an urban US community. Arch Intern Med 1990;150:785–7.
102. Kumar A, Bhandari AK, Rahimtoola SH. Torsade de pointes and marked QT prolongation in association with hypothyroidism. Ann Intern Med 1987; 106:712–3.
103. Bazett HC. An analysis of the time relations of electrocardiograms. Heart 1920;7:353–70.
104. Drici MD, Burklow TR, Haridasse V, Glazer RI, Woosley RL. Sex hormones prolong the QT interval and downregulate potassium channel expression in the rabbit heart. Circulation 1996;94:1471–4.
105. Roden DM, Woosley RL, Primm RK. Incidence and clinical features of the quinidine-associated long QT syndrome: Implications for patient care. Am Heart J 1986;111:1088–93.
106. Benton RE, Sale M, Flockhart DA, Woosley RL. Greater quinidine-induced QTc interval prolongation in women. Clin Pharmacol Ther 2000;67:413–8.
107. Lehmann MH, Hardy S, Archibald D, Quart B, MacNeil DJ. Sex difference in risk of torsade de pointes with *d,l*-sotalol. Circulation 1996;94:2535–41.
108. Pratt CM, Camm AJ, Cooper W, Friedman PL, MacNeil DJ, Moulton KM *et al*. Mortality in the Survival With ORal D-sotalol (SWORD) trial: Why did patients die? Am J Cardiol 1998;81:869–76.
109. Reinoehl J, Frankovich D, Machado C, Kawasaki R, Baga JJ, Pires LA *et al*. Probucol-associated tachyarrhythmic events and QT prolongation: Importance of gender. Am Heart J 1996;131:1184–91.
110. Walle T, Byington RP, Furberg CD, McIntyre KM, Vokonas PS. Biologic determinants of propranolol disposition: Results from 1308 patients in the Beta-Blocker Heart Attack Trial. Clin Pharmacol Ther 1985; 38:509–18.
111. Berg MJ. Pharmacokinetics and pharmacodynamics of cardiovascular agents. J Gender Specif Med 1999;2:22–4.
112. Flockhart DA, Drici MD, Samuel C, Abernethy DR, Woosley RL. Effects of gender on propranolol pharmacokinetics and pharmacodynamics [abstract]. FASEB J 1996;10:A429.
113. Sivenius J, Laakso M, Penttila IM, Smets P, Lowenthal A, Riekkinen PJ. The European Stroke Prevention Study: Results according to sex. Neurology 1991;41:1189–92.
114. Ridker PM, Cook NR, Lee IM, Gordon D, Gaziano JM, Manson JE *et al*. A randomized trial of low-dose aspirin in the primary prevention of cardiovascular disease in women. N Engl J Med 2005; 352:1293–304.
115. Levin RI. The puzzle of aspirin and sex. N Engl J Med 2005;352:1366–8.
116. Steering Committee of the Physicians' Health Study Research Group. Final report on the aspirin component of the ongoing Physicians' Health Study. N Engl J Med 1989;321:129–35.
117. Levin RI, Harpel PC, Weil D, Chang TS, Rifkin DB. Aspirin inhibits vascular plasminogen activator activity *in vivo*. Studies utilizing a new assay to quantify plasminogen activator activity. J Clin Invest 1984;74:571–80.
118. Spranger M, Aspey BS, Harrison MJ. Sex difference in antithrombotic effect of aspirin. Stroke 1989; 20:34–7.
119. Kloner RA, Sowers JR, DiBona GF, Gaffney M, Wein M. Sex- and age-related antihypertensive effects of amlodipine. The Amlodipine Cardiovascular Community Trial Study Group. Am J Cardiol 1996; 77:713–22.
120. al'Absi M, Wittmers LE, Ellestad D, Nordehn G, Kim SW, Kirschbaum C *et al*. Sex differences in pain and hypothalamic–pituitary–adrenocortical responses to opioid blockade. Psychosom Med 2004; 66:198–206.
121. Gear RW, Miaskowski C, Gordon NC, Paul SM, Heller PH, Levine JD. Kappa-opioids produce significantly greater analgesia in women than in men. Nat Med 1996;2:1248–50.

122. Sarton E, Teppema L, Dahan A. Sex differences in morphine-induced ventilatory depression reside within the peripheral chemoreflex loop. Anesthesiology 1999;90:1329–38.
123. Craft RM, Bernal SA. Sex differences in opioid antinociception: Kappa and 'mixed action' agonists. Drug Alcohol Depend 2001;63:215–28.
124. Cepeda MS, Farrar JT, Baumgarten M, Boston R, Carr DB, Strom BL. Side effects of opioids during short-term administration: Effect of age, gender, and race. Clin Pharmacol Ther 2003; 74:102–12.
125. Craft RM. Sex differences in opioid analgesia: "From mouse to man." Clin J Pain 2003;19:175–86.
126. Salem ML. Estrogen, a double-edged sword: Modulation of TH1- and TH2-mediated inflammations by differential regulation of TH1/TH2 cytokine production. Curr Drug Targets Inflamm Allergy 2004; 3:97–104.
127. Lew KH, Ludwig EA, Milad MA, Donovan K, Middleton E Jr, Ferry JJ *et al*. Gender-based effects on methylprednisolone pharmacokinetics and pharmacodynamics. Clin Pharmacol Ther 1993;54:402–14.
128. Magee MH, Blum RA, Lates CD, Jusko WJ. Prednisolone pharmacokinetics and pharmacodynamics in relation to sex and race. J Clin Pharmacol 2001;41:1180–94.
129. Ferron GM, Jusko WJ. Species- and gender-related differences in cyclosporine/prednisolone/sirolimus interactions in whole blood lymphocyte proliferation assays. J Pharmacol Exp Ther 1998;286:191–200.
130. Esmore D, Keogh A, Spratt P, Jones B, Chang V. Heart transplantation in females. J Heart Lung Transplant 1991;10:335–41.
131. Lampen A, Christians U, Bader A, Hackbarth I, Sewing KF. Drug interactions and interindividual variability of cyclosporin metabolism in the small intestine. Pharmacology 1996;52:159–68.
132. Joshi JV, Gupta KC, Hazari KT, Gokral J, Pohujani S, Satoskar R. Salivary antipyrine half-life during injectable progestagen contraception. Clin Pharmacokinet 1986;11(2):171–5.
133. Palovaara S, Tybring G, Laine K. The effect of ethinyloestradiol and levonorgestrel on the CYP2C19-mediated metabolism of omeprazole in healthy female subjects. Br J Clin Pharmacol 2003; 56(2):232–7.
134. Tsunoda SM, Harris RZ, Mroczkowski PJ, Benet LZ. Preliminary evaluation of progestins as inducers of cytochrome P450 3A4 activity in postmenopausal women. J Clin Pharmacol 1998;38(12):1137–43.
135. Palovaara S, Kivisto KT, Tapanainen P, Manninen P, Neuvonen PJ, Laine K. Effect of an oral contraceptive preparation containing ethinylestradiol and gestodene on CYP3A4 activity as measured by midazolam 1'-hydroxylation. Br J Clin Pharmacol 2000; 50(4):333–7.
136. Belle DJ, Callaghan JT, Gorski JC, Maya JF, Mousa O, Wrighton SA, Hall SD. The effects of an oral contraceptive containing ethinyloestradiol and norgestrel on CYP3A activity. Br J Clin Pharmacol 2002; 53(1):67–74.
137. Balogh A, Gessinger S, Svarovsky U, Hippius M, Mellinger U, Klinger G, Hoffmann A, Oettel M. Can oral contraceptive steroids influence the elimination of nifedipine and its primary pryidine metabolite in humans? Eur J Clin Pharmacol 1998;54:729–34.

CHAPTER

22

Drug Therapy in Pregnant and Nursing Women

CATHERINE S. STIKA AND MARILYNN C. FREDERIKSEN
Department of Obstetrics and Gynecology, Northwestern University Medical School, Chicago, Illinois

The pregnant woman is perhaps the last true therapeutic orphan. Because of the ethical, medicolegal, and fetal safety concerns regarding pregnant women, few pharmacokinetic, pharmacodynamic, or clinical trials are conducted during pregnancy. The majority of drugs that are marketed in the United States, therefore, carry the following statement (1) in their labeling:

> There are, however, no adequate and well-controlled studies in pregnant women. Because animal reproductive studies are not always predictive of human response, this drug should be used during pregnancy only if clearly needed. [Zinacef (cefuroxime) labeling; PDR; 2005. p. 1678]

This places the burden squarely on the practitioner to assess the risks and benefits of a particular agent in a given clinical situation. The risk most often considered is the fetal risk of teratogenesis, or drug-induced malformation, irrespective of the gestational age during the pregnancy when therapy is initiated. Pregnant women are more often than not left untreated in an attempt to avoid any perceived fetal risk related to use of a pharmacologic agent, and the effect of untreated maternal disease on either the pregnancy outcome or the offspring is not always considered. Issues of appropriate dosage and frequency of administration are often not evaluated, so that the usual adult dose is prescribed without thought to any changes dictated by physiologic differences between nonpregnant and pregnant women.

There are two compelling reasons for studying drugs and drug therapy during pregnancy. The first relates to the changing age of reproduction. Pregnancy once was mainly undertaken by healthy, younger women, but the age of reproduction now includes women ranging in age from 10 to approximately 50 years, and with *in vitro* fertilization and egg donation, even older women undertake pregnancy. Moreover, the age of a woman's first pregnancy has been steadily rising in the United States, with an increasing number of first pregnancies occurring after age 30 (2). The expansion of the reproductive age range, coupled with the occurrence of pregnancy later in life, increases the number of women who may require drug therapy for diseases present prior to pregnancy and who may need to continue therapy during pregnancy. Knowledge of drug therapy during pregnancy is needed if these women with underlying diseases are to be optimally treated.

The second reason supporting the need to study drugs during pregnancy relates to the physiologic changes that occur with gestation. To accommodate fetal growth and development, and perhaps provide a measure of safety for the woman, pregnancy alters a woman's underlying physiology. This altered physiology can affect the pharmacokinetics of drugs. The changes may alter peak drug concentration and time to peak drug concentration by affecting drug absorption, may decrease drug binding to plasma proteins and increase drug distribution volume, and may cause variations in either renal and/or hepatic drug clearance. Extrapolation of pharmacokinetic data from drug studies largely conducted in nonpregnant

subjects to pregnant women fails to account for the impact of physiologic changes that occur during pregnancy. This disregard for the changes in maternal physiology may affect drug efficacy and ultimately may impact the overall pregnancy outcome.

These issues have begun to be addressed by the Food and Drug Administration, which has established a Pharmacokinetics in Pregnancy Working Group of the Pregnancy Labeling Task Force, associated with the Center for Drug Evaluation and Research.

PREGNANCY PHYSIOLOGY AND ITS EFFECTS ON PHARMACOKINETICS

Rather than present a list of the many changes in maternal physiology that occur during pregnancy, the focus here is to select those changes that have the greatest potential to alter the absorption, distribution, and elimination of drugs in pregnant women.

Gastrointestinal Changes

The effect of progesterone on smooth muscle activity has long been thought to prolong gastric emptying and gastrointestinal transit time during all of pregnancy. However, most of the early studies were done in women during labor (3, 4). Studies of acetaminophen absorption using real-time ultrasonographic assessment of gastric emptying in nonlaboring women have shown no differences in gastric emptying during the first and third trimesters and in the postpartum period (5, 6). Only in the third trimester of pregnancy are orocecal transit times prolonged. This effect is due to the lower level of pancreatic polypeptide that occurs in the third trimester of pregnancy and results in reduced gastrointestinal motility (5). Pregnant women, however, have a decrease in gastric acid secretion that results in a correspondingly higher gastric pH (7).

The effects of gastrointestinal changes that occur during pregnancy were studied with ampicillin, a drug that is only 40% absorbed orally (8). Women were studied while they were pregnant as well as after pregnancy, thus serving as their own controls. The absolute bioavailability of ampicillin was evaluated by administering ampicillin both orally and intravenously to each woman during pregnancy and again postpartum. Pregnancy did not appear to change the extent of ampicillin absorption or the time to peak drug concentration (t_{max}). However, peak drug levels were found to be lower during pregnancy.

Cardiovascular Effects

The cardiovascular effects that occur during pregnancy include plasma volume expansion, an increase in cardiac output, and changes in regional blood flow. By the sixth to eighth week of pregnancy, plasma volume has expanded and continues to increase until approximately 32 to 34 weeks of pregnancy (9). For a singleton gestation, this increase in plasma volume is 1200–1300 mL, or approximately 40% higher than the plasma volume of nonpregnant women. Plasma volume expansion is even greater for multiple gestations (10). There are also significant increases in extracellular fluid space and total body water that vary somewhat with patient weight. These changes in body fluid spaces are summarized in Table 22.1 (11, 12).

The increase in plasma volume is accompanied by a gradual increase in cardiac output that begins in the first trimester of pregnancy. By 8 weeks' gestation, cardiac output can be as much as 50% greater, and by the third trimester is at least 30–50% greater than in the nonpregnant state (13). Early in pregnancy, an increase in stroke volume accounts for the increased cardiac output. In later pregnancy, the increase in cardiac output is the result of both elevated maternal heart rate and a continued increase in stroke volume (14).

Regional blood flow changes also occur in pregnant women and can affect drug distribution and elimination. Blood flow increases to the uterus, kidneys, skin, and mammary glands, with a compensatory decrease in skeletal muscle blood flow. At full term, blood flow to the uterus represents about 20–25% of cardiac output and renal blood flow is 20% of cardiac output (15). There is increased blood flow to the skin to dissipate the additional heat produced by the fetus (16). Blood

TABLE 22.1 Body Fluid Spaces in Pregnant and Nonpregnant Women[a,b]

Patient	Weight (kg)	Plasma volume (mL/kg)	ECF space (L/kg)	TBW (L/kg)	Ref.
Nonpregnant		49			9
	<70		0.189	0.516	11
	70–80		0.156	0.415	11
	>80		0.151	0.389	11
Pregnant		67			9
	<70		0.257	0.572	12
	70–80		0.255	0.514	12
	>80		0.240	0.454	12

[a] Modified from Frederiksen *et al*. Clin Pharmacol Ther 1986;40:321–8.

[b] Abbreviations: ECF, extracellular fluid; TBW, total body water.

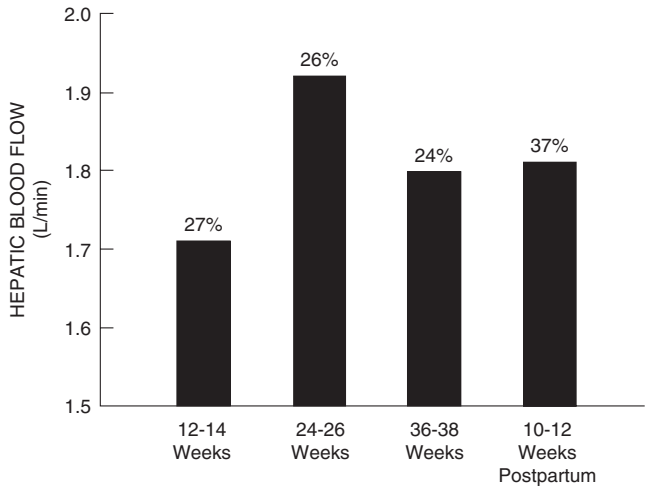

FIGURE 22.1 Hepatic blood flow expressed in L/min (*bars*) and as percentage of cardiac output (*numbers above bars*) during pregnancy and in the postpartum period. Although the absolute value of hepatic blood flow is unchanged, it comprises a significantly lower percentage of cardiac output during pregnancy, compared to postpartum. (Data from Robson SC *et al.* Br J Obstet Gynaecol 1990;97:720–4.)

flow to the mammary glands is increased during pregnancy in preparation for lactation postpartum (17). As shown in Figure 22.1, hepatic blood flow is maintained unchanged during pregnancy but constitutes a lower percentage of cardiac output than in the nonpregnant condition because of the increased proportion of blood flow to the uterus and kidneys (18). As a result of these hemodynamic changes, there is a decreased proportion of cardiac output available to skeletal muscle and other vascular beds.

These multiple physiological changes in pregnant women may affect drug distribution. In some cases, it is possible to correlate pregnancy-associated changes in distribution volume (V_d) with changes in extracellular fluid space (ECF), total body water (TBW), and drug binding to plasma proteins using the following equation, which was developed in Chapter 3:

$$V_d = \text{ECF} + f_u(\text{TBW} - \text{ECF}) \qquad (22.1)$$

where f_u is the fraction of unbound drug.

Blood Composition Changes

Plasma albumin concentration decreases during pregnancy (19, 20). The decrease in albumin concentration from 4.2 g/dL in the nonpregnant woman to 3.6 g/dL in the midtrimester of pregnancy (Figure 22.2) has long been attributed to a "dilutional effect'' caused by plasma volume expansion. However, a more likely explanation is that this decrease in plasma albumin concentration represents either a reduction in the rate of albumin synthesis or an increase in the rate of albumin clearance (see Chapter 1, Equation 1.1). Additional support for this explanation is provided by the fact that the plasma concentrations of total protein (19) and α_1-acid glycoprotein (21), which binds many basic drugs, are relatively unchanged during pregnancy.

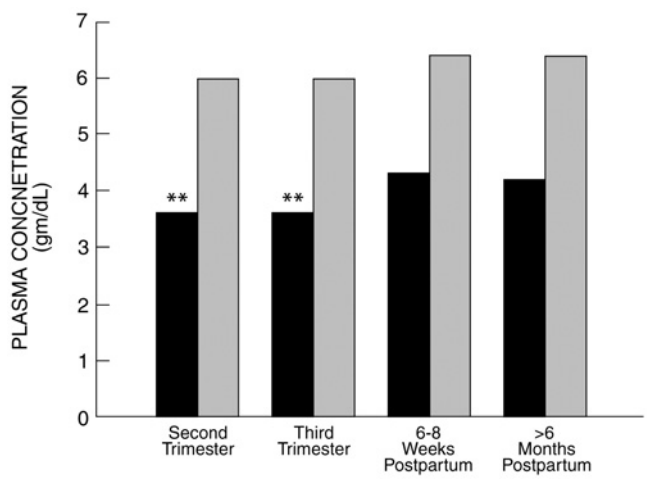

FIGURE 22.2 Albumin (*black bars*) and total protein (*gray bars*) concentrations during the second and third trimesters of pregnancy and in the postpartum period. Albumin concentrations are reduced significantly during pregnancy when compared to postpartum values at >6 months (** = $P < 0.01$). (Data from Frederiksen MC *et al.* Clin Pharmacol Ther 1986;40:321–8.)

The reduction in albumin concentration potentially can alter the binding of drugs commonly bound to serum albumin. In a study of theophylline pharmacokinetics during the second and third trimesters of pregnancy, theophylline protein binding to plasma proteins was reduced to only 11 and 13% of total plasma concentrations, respectively, compared with 28% at 6 months postpartum (20). Although the decrease in the serum concentration of albumin may be thought to account for these differences, a subsequent study showed that the albumin binding sites for theophylline were actually increased during pregnancy, but the binding affinity constant was significantly lower during pregnancy than in the nonpregnant state (22).

Pregnancy is also associated with a partially compensated respiratory alkalosis that may affect the protein binding of some drugs. Respiratory changes in pregnancy include a decrease in arterial partial pressure of carbon dioxide to 30.9 mm Hg, most likely due to the effect of progesterone (23, 24). In compensation, serum bicarbonate decreases, and maternal serum pH increases slightly to 7.44 (23).

Renal Changes

Accompanying the increased blood flow to the kidneys is an increase in glomerular filtration rate (GFR). This increase begins by the sixth week of gestation, gradually rises into the early portion of the third trimester (25), and plateaus or falls slightly until delivery. This increase in GFR is reflected in an increase in inulin and creatinine clearance during pregnancy. Tubular reabsorption processes, however, do not appear to be changed during pregnancy. (26)

For drugs predominantly cleared by the kidney, the increase in GFR will increase drug clearance during pregnancy. Cefuroxime, a cephalosporin predominantly eliminated by the kidneys, has a significantly greater clearance in the midtrimester of pregnancy than during either delivery or the postpartum period (27). Tobramycin clearance mirrors the GFR changes in pregnancy, with the highest clearance and shortest half-life found in the midtrimester, with a decrease in clearance and corresponding longer half-life in the third trimester (28).

Even for a drug primarily eliminated by hepatic metabolism in nonpregnant women, the increase in GFR can significantly affect total drug clearance during pregnancy. For example, the renal clearance of theophylline, a drug largely eliminated by CYP1A2 metabolism, was found to increase during pregnancy so that its total elimination clearance was not significantly reduced but was maintained at 86% of its value 6 months postpartum (20).

Hepatic Drug-Metabolizing Changes

The activity of hepatic drug-metabolizing enzymes also changes during pregnancy and can affect drug elimination clearance. Pregnancy is an estrogenic state with 100-fold increases in estradiol levels over a woman's nonpregnant baseline (29, 30). Progesterone, the hormone responsible for sustaining gestation, also dramatically rises during pregnancy from luteal levels of 30–40 ng/mL to levels of 100–200 ng/mL (31–33). These changes in estrogen and progesterone, as well as in other placental hormones, can alter hepatic enzymatic activity.

CYP3A4 Substrates

The clearances of drugs metabolized by CYP3A4 have been shown to be consistently increased in multiple studies of pregnant women. Because midazolam is exclusively eliminated by CYP3A4 metabolism (34, 35), midazolam clearance and the serum concentration ratio of 1′-hydroxymidazolam to midazolam are recognized markers of CYP3A4 activity. (36, 37) In pregnant women at term, the clearance of midazolam has been shown to be 2.9-fold greater than in nonpregnant women (38). The metabolic ratio of cortisol, a nonspecific probe of CYP3A4 activity, was increased in pregnant women near term when compared to the same women 1 week and 3 months postpartum (39). The clearance of nifedipine was increased 4-fold in women during the third trimester of pregnancy in comparison to historical controls (40). Methadone, a drug used to treat heroin addiction during pregnancy, also is a CYP3A4 substrate. In a study of methadone pharmacokinetics during pregnancy, methadone clearance doubled in the midtrimester but fell somewhat in the third trimester (41). This change was both statistically and clinically significant because the lower methadone plasma levels will result in symptoms of methadone withdrawal unless methadone dosage is increased during pregnancy. In a study of the extended release formulation of metronidazole, which is primarily metabolized by CYP3A4, the total oral clearance in pregnant women during the second and early third trimester was 27% greater than in nonpregnant women (42). The mean maximum concentration of metronidazole was approximately 25% lower in pregnancy and the difference in areas under the concentration curves (AUCs) in pregnant versus nonpregnant women approached significance.

The critical stimulus for CYP3A4 induction in pregnancy has not been identified. However, both estradiol and estrone, as well as the natural progestins, including progesterone, pregnenolone, 17-hydroxyprogesterone, and 5β-pregnane-3,20-dione, have been shown to activate the human orphan nuclear pregnane X receptor (PXR). As described in Chapters 11 and 15, PXR forms a heterodimer complex with the 9-*cis*-retinoic acid receptor (RXR). This hPXR/RXR complex then binds to the promotor region of the *CYP3A4* gene, also called the rifampicn/dexamethasone response element, and serves as a key transcriptional regulator (43, 44).

CYP1A2 Substrates

The elimination clearance of caffeine, a CYP1A2 substrate, was shown to decrease by a factor of two by midgestation and by a factor of three by the third trimester compared to the postpartum period (45). Although the intrinsic hepatic clearance of theophylline was reduced during pregnancy (Figure 22.3), there was substantially less change in its hepatic clearance because of the pregnancy-associated decrease in theophylline binding to plasma proteins (20). As a result of the offsetting changes in renal and hepatic clearance referred to previously, the total elimination clearance of theophylline was unchanged in the third trimester of pregnancy

CYP2D6 Substrates

Wadelius *et al*. (46) found that CYP2D6 activity, known to be genetically determined, was actually increased during pregnancy in individuals who were homozygous and heterozygous extensive metabolizers. The activity of this enzyme, however, was decreased in homozygous poor metabolizers.

CYP2C9 Substrates

The hepatic clearance of phenytoin, a restrictively eliminated drug that is predominantly a CYP2C9 substrate, increases during pregnancy, resulting in correspondingly lower total plasma concentrations (47). This is in large part a reflection of the decrease in protein binding that is well documented for phenytoin, as free plasma concentrations of this drug have been shown to remain relatively constant until late in pregnancy when the intrinsic clearance of this drug does increase (48, 49).

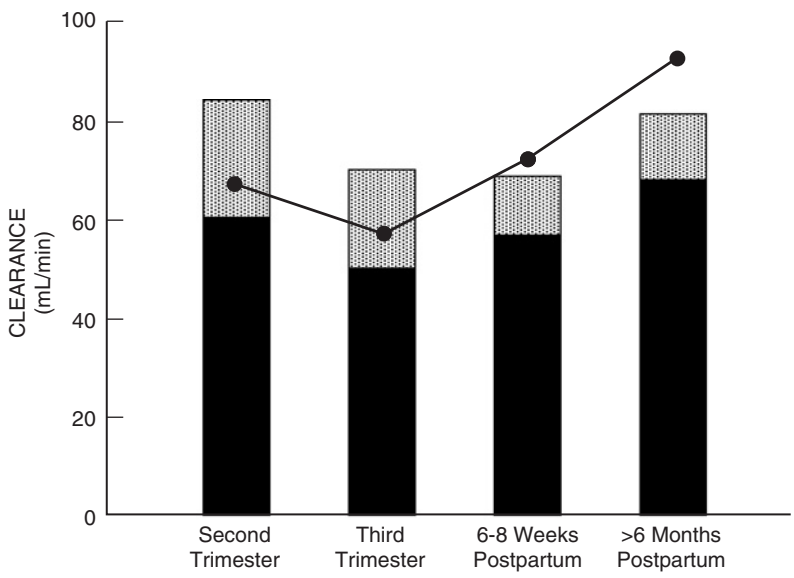

FIGURE 22.3 Theophylline clearance measured during the second and third trimesters of pregnancy and in the postpartum period. During pregnancy, the substantial drop in the intrinsic hepatic clearance (●) of this CYP1A2 substrate is attenuated by decreased theophylline binding to plasma proteins and increased glomerular filtration rate, so that overall elimination clearance, consisting of the sum of hepatic clearance (*solid bars*) and renal clearance (*stippled bars*), is relatively unaffected. (Data from Frederiksen MC *et al*. Clin Pharmacol Ther 1986; 40:321–8.)

CYP2C19 Substrates

The metabolism of proguanil, an antimalarial drug, to its active metabolite, cycloguanil, is dependent on CYP2C19 activity. The metabolic ratio of proguanil to cycloguanil has been shown to increase by approximately 60% during pregnancy (50). In a population-based study, CYP2C19 dependent clearance decreased by 50% (51).

NAT2 Substrates

Using caffeine to examine the changes in hepatic enzymatic activity during pregnancy, Bologna *et al*. (52) studied both pregnant and nonpregnant epileptic women and showed that the activity of *N*-acetyltransferase (NAT) was decreased during pregnancy. Tsutsumi *et al*. (53) also used caffeine to show that the activity of *N*-acetyltransferase-2 was decreased in normal healthy women during pregnancy.

Glucuronidation

Lamotrigine, an anticonvulsant and mood-stabilizing drug, is metabolized by glucuronidation. Lamotrigine clearance has been studied by Tran *et al*. (54) during pregnancy and shown to increase by greater than 50%, necessitating dose adjustment. The clearance of lamotrigine returns rapidly to stable nonpregnant levels after delivery so that dose reductions are required in the first 2 weeks postpartum (54, 55).

Betamethasone is glucuronidated by the liver and its clearance has been shown to be higher in pregnant than in nonpregnant women (56). In twin gestations, betamethasone has been shown to have a higher clearance and correspondingly shorter half-life than in singleton gestations (56). This is thought to be caused by increased metabolism of betamethasone by the additional fetoplacental unit present in twin pregnancies. The shorter half-life and higher clearance may explain the decreased efficacy of betamethasone in reducing the incidence of respiratory distress syndrome in twin gestations.

Peripartum Changes

The physiologic changes which begin early in gestation are most pronounced in the third trimester of pregnancy. Further physiologic changes occur during labor and delivery. There is an even further increase in cardiac output, blood flow to muscle mass decreases, and there is a cessation of gastrointestinal activity (57). The onset of uterine contractions decreases placental blood flow and drug distribution to the fetus. During the intrapartum period there also may be a change in the pharmacodynamics of drugs, but this is largely unstudied.

Drugs are very commonly studied during the intrapartum period, probably for no other reason than the amount of drug distributed to the fetus can be estimated from cord blood obtained at delivery. However, the pharmacokinetics of drugs given during this period have been shown to be different from their pharmacokinetics during the antepartum period. An intrapartum study of cefuroxime showed that clearance was lower than during pregnancy but higher than in the remote postpartum period (58). Morphine clearance has been shown to be markedly increased during labor, resulting in a shortening of its elimination half-life that reduces the dosing interval required for adequate pain relief during labor (59).

Postpartum Changes

In the early postpartum period, maternal pregnancy physiologic changes are sustained, with an elevated cardiac output, decreased plasma albumin concentration, and increased GFR (60, 61). The cardiovascular changes of pregnancy are sustained as long as 12 weeks after delivery (62). However, maternal hepatic enzymatic activity may either rapidly reverse within 24 hours of delivery or return to normal gradually during the first months after delivery (55, 63).

The physiology of the postpartum period seems to have great interindividual variability, since pharmacokinetic studies during this period show greater variability among postpartum women compared to studies conducted in either nonpregnant women or normal volunteers. As shown in Figure 22.4, a study of clindamycin pharmacokinetics in five postpartum women demonstrated that there was a 15-fold variation in peak drug concentrations and that t_{max} varied from 1 to 6 hours after oral administration (64). Similarly, a study of gentamicin in the postpartum period showed distribution volume estimates that varied from 0.1 to 0.5 L/kg, as compared with distribution volume estimates from studies in nonpregnant volunteers that ranged from only 0.2 to 0.3 L/kg (65).

PHARMACOKINETIC STUDIES DURING PREGNANCY

Results of Selected Pharmacokinetic Studies in Pregnant Women

Although an exhaustive survey of pharmacokinetic studies is not possible, the purpose here is to present illustrative studies that best demonstrate the effects of

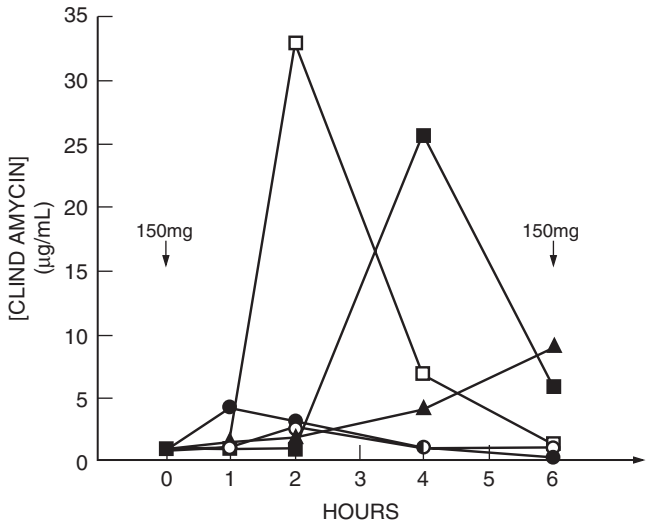

FIGURE 22.4 Plasma concentrations of clindamycin measured in five postpartum women over a 6-hour period after oral administration of a 150-mg dose. (Reproduced with permission from Steen B, Rane A. Br J Clin Pharmacol 1982;13:661–4.)

maternal physiologic changes on the pharmacokinetics of drugs and potentially dosing and drug efficacy.

Ampicillin

The pharmacokinetics of both intravenously and orally administered ampicillin were studied serially in 26 women who served as their own controls (8). The study combined data from women whose pregnancies ranged from 13 to 33 weeks' gestation, which blurred assessment of the effects of the progression of changes in maternal physiology that occurs during the second and third trimester of pregnancy. Perhaps because both intravenous and oral doses need to be administered, ampicillin is the only medication for which absolute bioavailability has been examined during pregnancy. No difference in the extent of ampicillin absorption or in time to peak drug concentrations was seen between pregnant and nonpregnant women, but peak levels in pregnant women were lower than those in nonpregnant women. Although this study demonstrated an absolute increase in the distribution volume of ampicillin, it did not include an analysis of the effect of the change in maternal weight on the volume of distribution. Both renal and total elimination clearance (CL) of ampicillin increased by approximately 50% during pregnancy and resulted in correspondingly lower plasma concentrations. Another study of ampicillin pharmacokinetics in the third trimester of pregnancy showed an increase in the steady-state volume of distribution on a liter/kilogram basis (66). Unfortunately, for this study, the authors used male controls as an historic reference population.

Caffeine

The pharmacokinetics of caffeine also were studied serially during and after pregnancy (45). Although only oral doses were administered, V_d/F showed no change when calculated on a liter/kilogram basis to take into account the change in weight during and after pregnancy. On the other hand, CL/F was decreased by a factor of two by midgestation and by a factor of three in the third trimester compared to the postpartum period (45).

Theophylline

The pharmacokinetics of intravenously administered theophylline pharmacokinetics have been studied serially in women during and after pregnancy (20). As described previously, theophylline binding to plasma proteins was reduced during the second and third trimesters of pregnancy to 11 and 13% of total plasma concentrations, respectively, compared with 28% at 6 months postpartum. This appears to reflect the fact that the albumin binding affinity constant for theophylline is significantly lower during pregnancy than in the nonpregnant state, even though there is an increased number of albumin binding sites (22). The steady-state distribution volume of theophylline was increased during the second and third trimesters of pregnancy. As shown in Table 22.2, the increases were similar to what was predicted from Equation 22.1 using measured values for protein binding and the estimates of extracellular fluid volume and total body water shown in Table 22.1.

TABLE 22.2 Comparison of Expected with Measured Values of Theophylline Distribution Volume[a]

	$V_{(dss)}$[b]	
Patient	**Expected (L)**	**Measured (L)**
Pregnant		
24–26 weeks	32.0 ± 2.0	30.3 ± 6.6
36–38 weeks	37.9 ± 1.9	36.8 ± 4.2
Postpartum		
6–8 weeks	28.0 ± 1.1	28.4 ± 3.0
>6 months	26.9 ± 2.3	30.7 ± 4.4

[a] Data from Frederiksen *et al*. Clin Pharmacol Ther 1986;40:321–8.
[b] Mean values for five women ± SD.

Renal clearance of theophylline paralleled the pregnancy-associated increase in creatinine clearance and accounted for 30 and 28% of total theophylline elimination in the second and third trimesters, respectively, compared to only 16% at 6 months postpartum. As was shown in Figure 22.3, the intrinsic clearance of theophylline was reduced substantially during pregnancy. Hepatic clearance showed substantially less change because of the pregnancy-associated decrease in theophylline binding to plasma proteins. As a result of the offsetting changes in renal and hepatic clearance, total elimination clearance of theophylline in the third trimester of pregnancy averaged 86% of its value at 6 months postpartum. Although this reduction in elimination clearance was not statistically significant, it combined with the increase in theophylline distribution volume to significantly increase theophylline elimination half-life from an average of 4.4 hours in the nonpregnant state (assessed 6 months postpartum) to 6.5 hours in the third trimester of pregnancy.

Cefuroxime

The pharmacokinetics of intravenously administered cefuroxime were studied serially in seven women during pregnancy, at delivery, and in the remote postpartum period (27). Distribution volume ($V_{d(extrap)}$) during pregnancy and at delivery approximated the expected ECF volumes shown in Table 22.1. However, the difference in these volumes and the postpartum value was not statistically significant and there was no change in the weight-normalized distribution volumes. On the other hand, cefuroxime is largely eliminated by renal excretion, and renal clearance was significantly greater during pregnancy than that measured either at delivery or in nonpregnant women. As a result, plasma cefuroxime concentrations resulting from a 750-mg dose were significantly lower during pregnancy.

Methadone

The pharmacokinetics of orally administered methadone were studied serially in nine women at 20–24 weeks and 35–40 weeks of pregnancy and at 1–4 weeks and 8–9 weeks postpartum (41). There was no significant change in methadone binding to plasma proteins during pregnancy. Renal methadone clearance during pregnancy was approximately twice its value in the postpartum periods. However, renal clearance contributed only minimally to total methadone clearance and this change did not reach statistical significance. On the other hand, estimates of *CL/F* during pregnancy were also doubled and this change was both statistically and clinically significant, resulting in a corresponding lowering of methadone plasma levels and symptoms of methadone withdrawal in some women near the end of gestation. Because the clearance of other CYP3A4 substrates is increased during pregnancy, it was concluded in this study that increased metabolic clearance rather than decreased bioavailability was responsible for the decrease in *CL/F*.

Anticonvulsants

The total plasma concentrations of most anticonvulsant drugs have been shown to decrease during pregnancy. This is in large part a reflection of the decrease in protein binding that is well documented for phenytoin (47, 48), carbamazepine (48), and phenobarbital (49). However, these drugs are restrictively eliminated and unbound concentrations of carbamazepine (38, 67) and phenobarbital (49) remain unchanged during pregnancy, reflecting the fact that their intrinsic clearance is unchanged. As is the case for patients with impaired renal function (see Chapter 5), dosage of phenytoin and these other anticonvulsants should not be increased in pregnant women based solely on decreases in total plasma concentration. On the other hand, Tomson *et al*. (48) monitored phenytoin plasma levels serially in 36 women during pregnancy and in the nonpregnant state. Intrinsic clearance was increased only during the third trimester of pregnancy, resulting in unbound plasma concentrations that averaged 16% lower than in the nonpregnant state (Figure 22.5), and this may warrant increasing phenytoin doses for some women late in pregnancy.

Other Drugs

The clearance of a number of other drugs that are eliminated primarily by renal excretion has also been shown to increase during pregnancy. For example, the pharmacokinetics of subcutaneously administered enoxaprin, a low molecular weight heparin, were studied serially in 13 women at 12–15 weeks and 30–33 weeks of gestation and 6–8 weeks postpartum (68). Compared to postpartum values, elimination clearance was increased by approximately 50% in the first gestational study period but was not significantly increased in the later period. In another study, the clearance of tobramycin was shown to peak in the midtrimester and decrease during the third trimester (28).

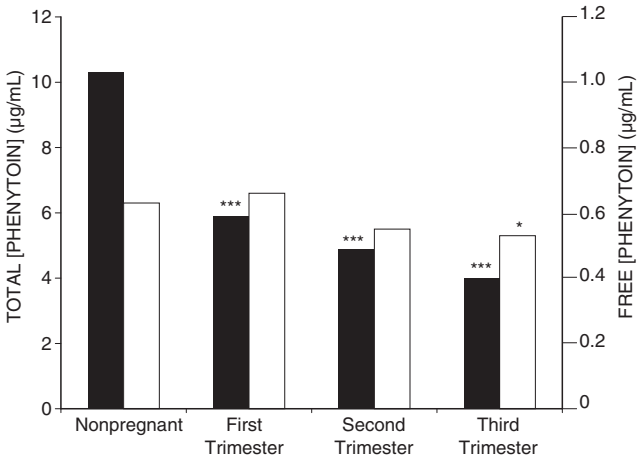

FIGURE 22.5 Total (*black bars*) and free (*white bars*) plasma concentrations of phenytoin in nonpregnant and pregnant women (* = P <0.05, *** = P < 0.001) (Data from Tomson T *et al.* Epilepsia 1994;35:122–30.)

Plasma concentrations of orally administered nifedipine, another CYP3A4 substrate, have been reported to be decreased in 15 women with pregnancy-induced hypertension who were studied during the third trimester of pregnancy but not subsequently postpartum (69). Estimates of *CL/F* averaged 2.0 L/hr/kg, compared to a value of 0.49 L/hr/kg that was reported in a study of nonpregnant volunteers. Another study of nifedipine pharmacokinetics in eight patients with preeclampsia indicated that *CL/F* remains elevated in the immediate postpartum period, averaging 3.3 L/hr/kg in this clinical setting (70).

First-pass conversion of a prodrug to an active drug has been studied in pregnancy with the drug valacyclovir (71). Orally administered valacyclovir produced three times higher plasma levels of acyclovir than when acyclovir was administered orally. However, the levels achieved with valacyclovir were somewhat lower than the reported levels in normal volunteers. On the other hand, acyclovir pharmacokinetics were, overall, similar to what has been reported in nonpregnant women.

Guidelines for the Conduct of Drug Studies in Pregnant Women

Studying drugs in pregnancy requires special considerations, and guiding principles for these studies were formally published by the Pharmacokinetics in Pregnancy Working Group of the Pregnancy Labeling Task Force in the *Guidance for Industry — Pharmacokinetics in Pregnancy — Study Design, Data Analysis, and Impact on Dosing and Labeling,* in October, 2004 (72).

Although abstinence from the use of pharmacologic agents is held forth as the ideal during pregnancy, studies have shown that most pregnant women use either prescribed or over-the-counter drugs during pregnancy (73, 74). Ethically, drug studies in pregnancy cannot be done in normal pregnant "volunteers," but only in women who require a drug for a clinical reason. For this reason, study design for these trials must include the ethical argument that the woman would be using the particular agent during pregnancy to treat a medical condition. For FDA approval of drugs specific to pregnancy, such as a tocolytic agents, oxytocic agents, and a drug to treat preeclampsia, studies must be done during pregnancy. However, drugs commonly used by women of childbearing potential, such as antidepressants, asthma medications, antihypertensive agents, and antihistamines, also can be justifiably studied during pregnancy. Drugs can be studied not only when given for maternal indications (e.g., hypertension or asthma), but also when given for fetal indications (e.g., fetal supraventricular tachycardia).

Some subpopulations of pregnant women, however, often have altered physiology that may affect pharmacokinetics. Therefore, to separate the effects of the specific pathophysiology of the subpopulation on the pharmacokinetics of the drug from those resulting from pregnancy-related changes in general, studies in these women should be designed so that maximal information is obtained. As a first step, population pharmacokinetic techniques can serve as a screening tool to establish the need for further intensive pharmacokinetic studies. For drugs that are chronically administered, these intensive studies should be conducted serially during the second and third trimesters of pregnancy and in the postpartum period, so that each woman serves as her own control. Ideally, both an early and a remote postpartum evaluation should be included. However, drugs used only during the peripartum period need only be studied at that time. Studies should incorporate *in vitro* measurements of drug binding to plasma proteins, and use established tracer substances or concurrent noninvasive measures of physiology as reference markers. For bioavailability evaluations, the stable isotope method described in Chapter 4 would decrease the number of studies necessary and decrease the biologic variation between studies. Caffeine has been used as a probe to assess the effects of pregnancy on drug metabolism and has the advantage over the "cocktail" approaches described in Chapter 7 in that only a single drug is needed to simultaneously assess a number of metabolic pathways (Figure 22.6).

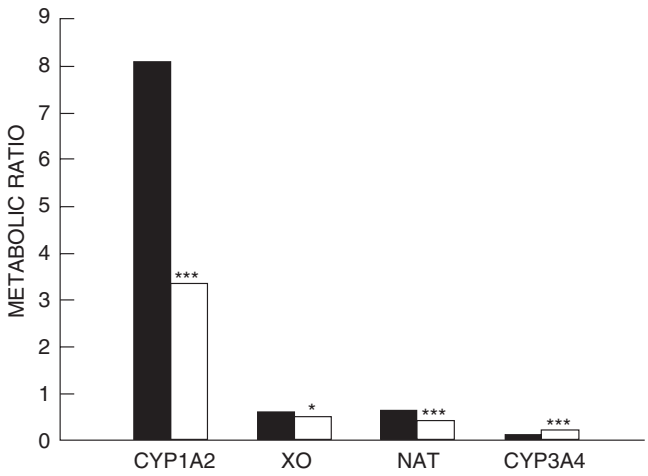

FIGURE 22.6 Paired comparisons of measured ratios of caffeine metabolites to parent drug in nonpregnant (*solid bars*) and pregnant (*open bars*) women. Comparisons were made of the metabolic activities of CYP1A2, xanthine oxidase (XO), *N*-acetyltransferase (NAT), and CYP3A4 (* = P <0.05, *** = P <0.005). (Data from Bologa M *et al.* J Pharmacol Exp Ther 1991;257:735–40.

PLACENTAL TRANSFER OF DRUGS

The placenta was long thought to be a barrier to drugs and chemicals administered to the mother. However, the thalidomide tragedy, reported independently by McBride (75) and Lenz (76), showed that the placenta was capable of transferring drugs ingested by the mother to the fetus, with the potential for great harm. On the other hand, placental transfer of drugs administered to the mother has been used to treat fetal arrhythmias, congestive heart failure, and other conditions (77).

The placenta develops from a portion of the zygote and thus has the same genetic endowment as the developing fetus (78). The embryonic/fetal component consists of trophoblastic-derived chorionic villi, which invade the maternal endometrium and are exposed directly to maternal blood in lake-like structures called lacunae. These villi create the large surface area necessary for maternal–fetal transfer in what becomes the intervillous space of the placenta. Here the maternal blood pressure supplies pulsatile blood flow in jetlike streams from the spiral arteries of the endometrium, to bathe the chorionic villi and allow for transfer of gases, nutrients, and metabolic products. Biologically, the human placenta is classified as a hemochorial placenta because maternal blood is in direct contact with the fetal chorionic membrane. It is this membrane that determines what is transferred to the fetus.

For the most part, drugs and other substances given to the mother will be transferred to the fetus. Drugs cross the placenta largely by simple diffusion. Factors affecting drug transfer are similar to those affecting transfer across other biological membranes and include the molecular mass, lipid solubility, and degree of ionization of the compound. Generally, drugs and chemicals with a molecular mass of less than 600 Da traverse the placenta readily, while drugs with a molecular mass larger than 1000 Da transfer less readily, if at all. Compounds that are uncharged and more lipid soluble are also more readily transferred.

Recently, P-glycoprotein (P-gp) has been shown to play a critical role in the active transport of a large number of maternally administered drugs back into maternal circulation and away from the fetus. As described in Chapter 14, P-gp is a large, 140-170-kDa transmembrane phospho-glycoprotein whose role as an energy-dependent efflux transporter was first elucidated in the investigation of cellular multidrug resistance. Coded for by the *MDR1* gene, P-gp belongs to a superfamily of ATP-binding cassette transporters that are present in all organisms, from bacteria to humans (79–81). Actively excreting absorbed molecules from the cytoplasm, the evolutionary job of P-gp has been to reduce exposure to xenobiotics, or foreign, natural toxins (82, 83). Numerous seemingly structurally unrelated drugs are substrates for this transporter. In general, these compounds can be categorized as hydrophobic, often planar aromatic molecules that are neutral or positively charged at physiological pH.

In humans, P-gp is expressed on trophoblastic cells throughout pregnancy (82, 84–86). It has been located on apical surfaces of endodermal cells of the mouse yolk sac (87), in the vesicles of the brush border membrane of the human syncytiotrophoblast that directly faces maternal blood, but not within maternal vascular endothelium (83, 84, 86–95). Actively transporting molecules in a basolateral-to-apical direction, the role of P-gp within the placenta is similar to its function at other sites: it extrudes drugs from the placenta back into maternal circulation, thereby protecting the developing fetus from potential toxic factors within the maternal circulation (95).

In genetically altered *mdr1a/b (−/−)* knockout mice without P-gp, both transplacental transport of P-gp substrates and the incidence of fetal malformations increase (93). Transplacental transport of the P-gp substrates, digoxin, saquinavir and paclitaxel, was increased 2.4-, 7-, and 16-fold, respectively, in the knockout mice compared to transport in the wild-type animals. In another murine study, *mdr1a/b (−/−)* fetuses were susceptible to cleft palate malformation induced by prenatal exposure to a photoisomer of avermectin B1a, whereas their wild-type littermates were protected from the teratogen (87).

An active transport mechanism has long been suspected to account for the placental barrier that causes maternal and fetal concentrations for many drugs to differ (96, 97). Studies of maternal–fetal transport of medications used during pregnancy in HIV-positive women have shown variable penetration into the fetus (98, 99). Whereas the maternal–fetal drug ratios for zidovudine, lamivudine, and nevirapine (approximately 0.85, 1.0, and 0.9, respectively) demonstrate good fetal penetration, most protease inhibitors, nelfinavir, ritonavir, saquinivir, and lopinavir, are known P-gp substrates and do not cross the placenta in detectable levels (98).

Several studies have examined the interaction between selective serotonin reuptake inhibitors (SSRIs) and P-gp and have shown that not all members of this class of drugs are P-gp substrates. Concentrations of paroxetine and venlafaxine, but not fluoxetine, were significantly increased in the brains of *mdr1a/b (−/−)* knockout mice compared to concentrations in the wild-type mice.(100) In cell culture studies, sertraline, its metabolite desmethylsertraline, and paroxetine were shown to be potent inhibitors of P-gp; however, citalopram and venlafaxine were only weak inhibitors (101, 102).

There are factors that affect the transfer of drugs and chemicals that are unique to the placenta. The placenta has a pore system that allows for bulk water flow across the placenta and can be responsible for small drugs and chemicals crossing the membrane by solvent drag. Within the placenta, there is also a process of endocytosis that is capable of transferring large immunoglobulins to the fetus. Placental tissue has a full complement of cytochrome enzymes capable of metabolizing drugs and chemicals, and some of these metabolites may then transfer more readily to the fetus than the parent drugs do. The permeability and diffusion properties of the placenta may increase as the placenta matures due to a decrease in thickness of the trophoblastic epithelium forming the chorionic membrane.

One of the factors affecting drug transfer to the fetus is the amount of drug delivered to the intervillous space by utero-placental blood flow. Blood flow to the uterus and placenta increases during pregnancy, from 50 mL/min at 10 weeks' gestation to 500–600 mL/min at term (78). Maternal blood flow to the uterus is also influenced by posture, diseases affecting maternal vasculature (such as hypertension and diabetes), placental size, and uterine contractions. For example, maternal cardiac output and utero-placental blood flow are reduced in the supine position and placental perfusion virtually ceases during a contraction. Placentas that are small for gestational age, or those with diffuse calcifications, are less efficient at transferring any maternal compounds to the fetus. Diseases (such as diabetes, which can thicken the chorionic membrane), may also potentially affect diffusion of drugs into the fetal circulation.

TERATOGENESIS

During the 38 weeks that comprise human gestation, the human conceptus develops from a one-cell zygote to the fully developed newborn infant. This complicated process has a high degree of wastage, with approximately 70% of conceptions lost prior to implantation, 20% lost from spontaneous abortion, and 15% born prematurely. Major congenital abnormalities that are recognized at birth occur in approximately 2 to 3 infants per 100. Minor anomalies occur in another 7 to 14 infants per 100. Major birth defects cause 20% of infant mortality and are responsible for the majority of childhood hospitalizations.

From the patient's perspective, a birth defect may be any abnormality of the infant found at birth. This may include birth injuries, such as a cephalohematoma or a brachial plexus injury. However, birth defects are usually considered to be structural defects of the newborn. Structural defects have been broken down into four major categories: a *malformation*, which is a structural defect caused by an intrinsic problem in embryologic differentiation and/or development; a *disruption*, which is an alteration in shape or structure of a normally differentiated part, such as a limb amputation from an amniotic band or a vascular event; a *deformation*, which is an alteration in the shape or structure of a normally differentiated part, such as a Potter's facies or metatarsus adductus, that is often due to a mechanical constraint; and a *dysplasia*, which is a primary defect in cellular organization into tissues (103). A *teratogen* is a chemical substance that can induce a malformation during development. An expansion of the definition includes an adverse effect on the developing fetus either in causing a structural abnormality or in altering organ function. This should be distinguished from a *mutagen*, which causes a genetic mutation whose effects cannot be seen for at least a generation.

Underlying causes of birth defects are shown in Table 22.3. It should be appreciated that approximately 90% of birth defects have a genetic component. Birth defects caused by drugs represent the one group of anomalies that can potentially be prevented. However, it is a small list of drugs that have been proved to cause human anomalies (Table 22.4). Potential effects of drugs on the developing fetus

TABLE 22.3 Human Reproductive Risk

Cause of anomalies	Percentage of total anomalies
Chromosomal	5
Single gene	20
Polygenic/multifactorial	65
Environmental	10
Irradiation	<1
Maternal disease	1–2
Infection	2–3
Drugs and chemicals	4–5

include altered structural development during the first trimester, producing a dysmorphic infant; altered fetal growth during the second and third trimester of pregnancy; and altered function of organ systems.

TABLE 22.4 Known Human Teratogens

Agent	Teratogenic effect
Carbamazepine	Facial dysmorphogenesis, neural tube defect
Phenytoin	Facial dysmorphogenesis, mental retardation, growth retardation, distal digital hypoplasia
Valproate	Lumbosacral spina bifida, facial dysmorphogenesis
Trimethadione	Facial dysmorphogenesis, intrauterine growth retardation, intrauterine fetal demise, neonatal demise
Coumadin	Nasal hypoplasia, epiphyseal stippling, optic atrophy
Alcohol	Facial dysmorphogenesis, growth retardation, mental retardation
Diethylstilbestrol	Vaginal adenosis, uterine anomalies, vaginal carcinogenesis
Androgens	Masculinization of the female genitalia
Methyl mercury	Growth retardation, severe mental retardation
ACE inhibitors[a]	Oligohydramnios, potential lung hypoplasia, postnatal renal failure
Folic acid antagonists (aminopterin, methotrexate)	Abortion, intrauterine growth retardation, microcephaly, hypoplasia of frontal bones
Thalidomide	Phocomelia
Isotretinoin	CNS anomalies, including optic nerve abnormalities, anomalies, cardiovascular malformations, thymic abnormalies
Inorganic iodides	Fetal goiter
Tetracycline	Bone deposits, teeth discoloration
Lithium	Ebstein's anomaly

[a] ACE, Angiotensin-converting enzyme.

Principles of Teratology

The principles of teratology have been articulated by Wilson (104). The first principle is that teratogens act with specificity. A teratogen produces a specific abnormality or constellation of abnormalities. For example, thalidomide produces phocomelia, and valproic acid produces neural tube defects. This specificity also applies to species, because drug effects may be seen in one species and not in another. The best example is cortisol, which produces cleft palate in mice but not in humans.

The next principle is that teratogens demonstrate a dose-effect relationship. Given to the mother at a specific time during gestation, low doses can produce no effect, intermediate doses can produce the characteristic pattern of malformation, and higher doses will be lethal to the embryo. Dose-effect curves for most teratogens are steep, changing from minimal to maximal effect by dose doubling. Increasing the dose beyond that found to be lethal to the embryo will eventually lead to maternal death. This is used as an endpoint in animal teratogenicity studies.

The third principle is that teratogens must reach the developing conceptus in sufficient amounts to cause their effects. The extent of fetal exposure to drugs and other xenobiotics is determined not only by maternal dose, route of elimination, and placental transfer, but also by fetal elimination mechanisms. Because the fetal liver is interposed between the umbilical vein and systemic circulation, drugs transferred across the placenta are subject to fetal first-pass metabolism (77). This protective mechanism is compromised by ductus venosus shunting, which enables 30–70% of umbilical venous blood flow to bypass the liver. After drugs reach the fetal system circulation, hepatic metabolism constitutes the primary elimination mechanism and renal excretion is relatively ineffective because the fetal kidney is immature and fetal urine passing into the amniotic fluid is swallowed by the fetus. CYP3A7 is a fetal-specific enzyme that accounts for about one-third of fetal hepatic cytochrome P450. CYP1A1, CYP2C8, CYP2D6, and CYP3A3/4 have also been identified in fetal liver. These enzymes are not only protective, but their presence in fetal tissues other than liver is also capable of converting drugs into chemically reactive teratogenic intermediates such as phenytoin epoxide (see Scheme 11.11) (105).

The fourth principle is that the effect that a teratogenic agent has on a developing fetus depends upon the stage during development when the fetus is exposed. From conception to implantation there is an all-or-nothing effect, in that the embryo, if exposed to a teratogen, either survives unharmed or dies.

This concept developed from Brent's studies of the effects of radiation on the developing embryo and may or may not apply to fetal exposure to chemicals (106). After implantation, during the process of differentiation and embryogenesis, the embryo is very susceptible to teratogens. However, since teratogens are capable of affecting many organ systems, the pattern of anomalies produced depends on which organ systems are differentiating at the time of teratogenic exposure. A difference of one or two days can result in a slightly different pattern of anomalies. After organogenesis, a teratogen can affect the growth of the embryo by producing growth retardation, or by changing the size or function of a specific organ. Of particular interest is the effect of psychoactive agents, such as cocaine, crack, or antidepressants, on the developing central nervous system during the second and third trimesters of pregnancy, as these drugs can potentially affect the function and behavior of the infant after delivery. Giving a teratogen after the fetus has developed normally has no effect on the development of organs already formed. For example, beginning lithium after cardiac development, or valproic acid after the closure of the neural tube, will not produce either drug's characteristic anomalies.

The fifth principle is that susceptibility to teratogens is influenced by the genotype of the mother and fetus. Animal studies have shown that certain animal strains are more susceptible to the production of malformations when exposed to a teratogen, compared to other animal strains. In humans, the fetus homozygous for the recessive allele associated with decreased epoxide hydrolase activity has an increased risk of developing the full fetal hydantoin syndrome (105). Maternal smoking increases the risk for the development of cleft lip and palate in a fetus carrying the atypical allele for transforming growth factor (107). Single mutant genes or polygenic inheritance may explain why certain fetuses are unusually susceptible to teratogens.

Mechanisms of teratogenesis include genetic interference, gene mutation, chromosomal breakage, interference with cellular function, enzyme inhibition, and altered membrane characteristics. The response of the developing embryo to these insults is failure of cell–cell interaction crucial for development, interference with cell migration, or mechanical cellular disruption. The common endpoint is cell death — teratogenesis causing fewer cells. Most mechanisms of teratogenesis are theoretical, not well understood, and imply a genetic component. One exception is the mechanism of thalidomide teratogenesis. In susceptible species, thalidomide causes oxidative DNA damage. Pretreatment with phenyl-*N*-*tert*-butylnitrone (PBN), a free radical trapping agent, reduces the occurrence of thalidomide embryopathy, suggesting that the mechanism is free radical-mediated oxidative DNA damage (108).

Measures to Minimize Teratogenic Risk

All new drug applications filed with the Food and Drug Administration include data from developmental and reproductive toxicology (DART) studies. These studies, most of which are conducted in mice, rats, and rabbits, examine the effects of the particular agent on all aspects of reproduction, including oogenesis, spermatogenesis, fertility, and fecundity, as well as effects on litter size, spontaneous resorption, fetal malformation, fetal size, and newborn pup function. All studies are designed with dose escalations and with maternal death as the endpoint. Information from these teratologic experiments with the drug is included in the drug labeling. Most human teratogenic reactions to new drugs have been predicted from animal studies. However, animal data are not always applicable to humans, since most animals have a shorter gestational clock than humans have. Species vary in their susceptibility to teratogens, with some animal models being either more or less susceptible to teratogenesis than humans are. If an agent does not produce an anomaly in animal studies, it does not prove that the agent is innocuous in humans.

Safety of a drug for use in human pregnancy is demonstrated by observational studies after the drug is marketed. Proof of teratogenicity in humans is supported by the following events: a recognizable pattern of anomalies; a higher prevalence of the particular anomaly or anomalies in patients exposed to an agent than in a control population; presence of the agent during the stage of organogenesis of the organ system affected; increased incidence of the anomaly after introduction of the agent; and production of the anomaly in experimental animals by administration of the agent during the appropriate stage of organogenesis. Epidemiologic clues to teratogenesis are often found in case reports of abnormal infants, but these are biased in that an abnormal infant is more likely reported than is a normal infant, and the background rate of malformations is high. Better studies are conducted prospectively with an exposed and unexposed control population found before pregnancy outcome is known. Although population-based large-cohort studies begun prior to pregnancy are considered the best type, they are expensive to conduct and limited to those agents used at the time of the study.

A general approach to reduce the risk of human teratogenesis includes planning for pregnancy. Prior

to conception, women with medical problems should be counseled about medications they chronically use, which ones can safely be continued throughout pregnancy, and which ones should be discontinued. Medications should be evaluated and changed if necessary to decrease teratogenic risk. Plasma level monitoring of unbound concentrations of antiepileptic drugs may be helpful in optimizing seizure control, decreasing the need for multiple-drug therapy, and minimizing dosage and fetal risk. Since more than 50% of pregnancies in the United States are unplanned, all women should be treated as potential antenatal patients and counseled regarding use of any new drug in a potential pregnancy. Therefore, when a woman of childbearing potential develops a new medical problem, counseling for pregnancy should be included in management. In general, the use of agents widely used during pregnancy is preferred to use of newer agents. Just stopping pharmacologic therapy or leaving the issue up to the woman does not help her and may place both the mother and the fetus at risk for adverse pregnancy outcome.

When using a known human teratogen, particular attention should be given to prevention of pregnancy. This includes counseling the patient on the fetal effects of the drug being used and on the use of one or more effective forms of contraception. Therapy should be begun with a normal menstrual period or no more than 2 weeks from a negative pregnancy test. When renewing prescriptions for these drugs, it is necessary to verify again that the patient is not pregnant.

DRUG THERAPY IN NURSING MOTHERS

Transfer of drugs into breast milk is bidirectional, reflecting passive diffusion of unbound drug between plasma and blood, rather than active secretion. Factors that affect the milk concentration include binding to maternal plasma proteins, protein binding in milk, lipid content of milk, and physiochemical factors of the drug (109). As shown in Figure 22.7, drug concentrations in breast milk are usually less than plasma concentrations are and there usually is a fixed ratio between milk and plasma concentrations (110). Concentration-dependent saturation of the plasma protein binding precludes calculation of a fixed milk:plasma ratio for a few drugs (Figure 22.8) (111). However, in the usual case, drug concentrations measured in plasma and breast milk are used to calculate a milk:plasma ratio (M/P), from which the daily drug dose to the infant is estimated as follows:

$$\text{Infant dose/day} = C_{\text{maternal}} \times M/P \times V_{\text{milk}} \quad (22.2)$$

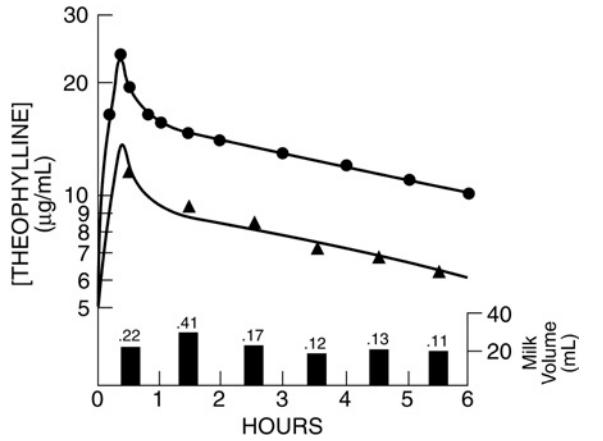

FIGURE 22.7 Kinetic analysis of theophylline plasma (●) and milk (▲) concentrations after intravenous administration of a 3.2- to 5.3-mg/kg aminophylline dose. The lines represent the least-squares fit of the measured concentrations. The interval and volume of each milk collection are shown by the solid bars. The milligram recovery of theophylline in each breast-milk collection is shown by the numbers above the bars. (Reproduced with permission from Stec GP *et al.* Clin Pharmacol Ther 1980;28:404–8.)

where C_{maternal} is the average maternal plasma concentration of drug during nursing and V_{milk} is the volume of maternal milk ingested each day, usually estimated as 150 mL/kg (109). This estimate of infant dose is often reported as a percentage of administered maternal dose.

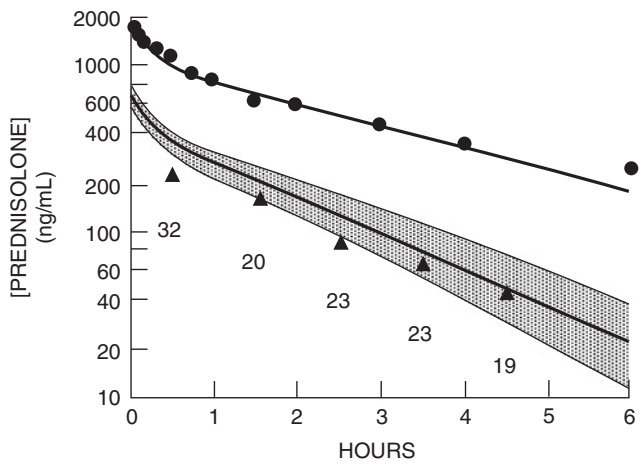

FIGURE 22.8 Kinetic analysis of prednisolone plasma (●) concentrations after intravenous administration of a 50-mg prednisolone dose. The lines represent the least-squares fit of the measured plasma concentrations. Measured milk concentrations (▲) are plotted along with the range (*shaded area*) of unbound prednisolone plasma concentrations expected if serum transcortin binding capacity is allowed to vary ±1 SD from its reported mean The volume (in milliliters) of each breast milk sample is shown by the numbers below the milk concentrations. (Reproduced with permission from Greenberger PA *et al.* Clin Pharmacol Ther 1993;53:324–8.)

TABLE 22.5 Antidepressant Drugs and Breast Feeding

Drug (and metabolite)	Protein binding (%)	M/P[a]	Infant dose[b] (%)	Detectable in infant plasma	Reported infant toxicity	Ref.
NE reuptake inhibitors[a]						
Amitriptyline	95	0.5–1.6	1.0	No	No	113, 114
(Nortriptyline)	92	0.7–1.1		No[c]		
(*E*-10-OH-Nortriptyline)		0.7		Yes[c]		
Doxepin	15–32	1.1–1.7	2.2	Yes	Respiratory	115, 116
(*N*-Desmethyldoxepin)		1.0–1.5		Yes	depression	
Serotonin reuptake inhibitors						
Fluoxetine	>95	0.5–1.5	11	Yes	Colic	117, 118
(Norfluoxetine)	>95	0.6–1.2		Yes		
Sertraline	99	1.9	0.5	Yes	No	119
(*N*-Desmethylsertraline)		1.6		Yes		
Combined reuptake inhibitors						
Venlafaxine	27	4.1	8	No	No	120
(*O*-Desmethylvenlafaxine)	3	3.1		Yes		
Atypical antidepressants						
Bupropion	84	5.8	<1	No	No	121
(Hydroxybupropion)		0.1		No		
(Theohydrobupropion)		1.5		No		
Trazodone	93	0.1	<1	Not measured	No	122

[a] Abbreviations: M/P = ratio of concentrations in maternal milk and plasma, NE = norepinephrine.
[b] Expressed as percentage of maternal dose for combined parent drug and measured metabolites.
[c] Both nortriptyline and 10-hydroxynortriptyline concentrations have been measured in the serum of nursing infants whose mothers were treated with nortriptyline (123).

Infant blood levels also can be monitored and levels are usually less than those required for pharmacologic effects. Table 22.5 summarizes representative data for some of the antidepressant drugs that have been used to treat women with postpartum depression. Based on information similar to that in this table, amitryptyline, nortryptyline, and sertraline have been among the antidepressant drugs of choice during breast feeding (112). Regardless of drug choice, an important clinical point, a consequence of the bidirectional transfer of drug between plasma and breast milk, is that infant dosage can be minimized by breast feeding just prior to drug administration, when maternal serum concentration is lowest (110).

Drugs considered safe for pregnancy are usually safe during the lactation period. Drugs contraindicated during lactation include antineoplastics, immune suppressants, ergot alkaloids, gold, iodine, lithium carbonate, radiopharmaceuticals, social drugs of abuse, and certain antibiotics.

REFERENCES

1. Zinacef (cefuroxime) labeling, in Physicians' Desk Reference, 54th ed. Montvale, NJ: Medical Economics; 2005. p. 1678.
2. Births: Preliminary data for 1999. National Vital Statistics Reports. vol 48, number 14. Atlanta, GA: Centers for Disease Control; 2000.
3. Hunt JN, Murray FA. Gastric function in pregnancy. J Obstet Gynaecol Br Emp 1958;65:78–83.
4. Parry E, Shields R, Turnbull AC. Transit time in the small intestine in pregnancy. J Obstet Gynaecol Br Commonw 1970;77:900–1.
5. Chiloiro M, Darconza G, Piccioli E, De Carne M, Clemente C, Riezzo G. Gastric emptying and orocecal transit time in pregnancy. J Gastroenterol 2001;36:538–43.
6. Wong CA, Loffredi M, Ganchiff JN, Zhao J, Wang Z, Avram MJ. Gastric emptying of water in term pregnancy. Anesthesiology 2002;96:1395–400.
7. Gryboski WA, Spiro HM. The effect of pregnancy on gastric secretion. N Engl J Med 1976;255:1131–7.
8. Philipson A. Pharmacokinetics of ampicillin during pregnancy. J Infect Dis 1977;136:370–6.
9. Lund CV, Donovan JC. Blood volume during pregnancy: Significance of plasma and red cell volumes. Am J Obstet Gynecol 1967;98:394–403.
10. Hytten F. Blood volume changes in normal pregnancy. Clin Haematol 1985;14:601–12.
11. Petersen VP. Body composition and fluid compartments in normal, obese and underweight human subjects. Acta Med Scand 1957;108:103–11.
12. Plentl AA, Gray MJ. Total body water, sodium space and total exchangeable sodium in normal and

toxemic pregnant women. Am J Obstet Gynecol 1959;78:472–8.
13. Lees MM, Taylor SH, Scott DM, Kerr MR. A study of cardiac output at rest throughout pregnancy. J Obstet Gynaecol Br Commonw 1967;74:319–28.
14. Robson SC, Hunter S, Boys RJ, Dunlop W. Serial study of factors influencing changes in cardiac output during human pregnancy. Am J Physiol 1989;256:H1060–5.
15. Metcalfe J, Romney SL, Ramsey LH, Burwell CS. Estimation of uterine blood flow in women at term. J Clin Invest 1955;34:1632–8.
16. Ginsburg J, Duncan SL. Peripheral blood flow in normal pregnancy. Cardiovasc Res 1967;1:132–7.
17. Thoresen M, Wesch J. Doppler measurements of changes in human mammary and uterine blood flow during pregnancy and lactation. Acta Obstet Gynecol Scand 1988;67:741–5.
18. Robson SC, Mutch E, Boy RJ, Woodhouse KH. Apparent liver blood flow during pregnancy: A serial study using indocyanine green clearance. Br J Obstet Gynaecol 1990;97:720–4.
19. Mendenhall HW. Serum protein concentrations in pregnancy: I. Concentrations in maternal serum. Am J Obstet Gynecol 1970;106:388–99.
20. Frederiksen MC, Ruo TI, Chow MJ, Atkinson AJ Jr. Theophylline pharmacokinetics in pregnancy. Clin Pharmacol Ther 1986;40:321–8.
21. Wood M, Wood AJJ. Changes in plasma drug binding and α_1-acid glycoprotein in mother and newborn infant. Clin Pharmacol Ther 1981;29:522–6.
22. Connelly RJ, Ruo TI, Frederiksen MC, Atkinson AJ Jr. Characterization of theophylline binding to serum proteins in nonpregnant and pregnant women. Clin Pharmacol Ther 1990;47:68–72.
23. Lucius H, Gahlenbeck H, Kleine HO, Fabel H, Bartels H. Respiratory functions, buffer system and electrolyte concentrations of blood during human pregnancy. Respir Physiol 1970;9:311–7.
24. Lyons HA, Antonio R. The sensitivity of the respiratory center in pregnancy and after the administration of progesterone. Trans Assoc Am Physicians 1959;72:173–80.
25. Davison JM, Hytten FE. Glomerular filtration during and after pregnancy. J Obstet Gynaecol Br Commonw 1974;81:588–95.
26. Davison JM, Hytten FE. The effect of pregnancy on the renal handling of glucose. J Obstet Gynaecol Br Commonw 1975;82:374–81.
27. Philipson A, Stiernstedt G. Pharmacokinetics of cefuroxime in pregnancy. Am J Obstet Gynecol 1982;142:823–8.
28. Bourget P, Fernandez H, Delouis C, Taburet AM. Pharmacokinetics of tobramycin in pregnant women, safety and efficacy of a once-daily dose regimen. J Clin Pharm Ther 1991;16:167–76.
29. Buster JE, Abraham GE. The applications of steroid hormone radioimmunoassys to clinical obstetrics. Obstet Gynecol 1975;46:489–99.
30. Devroey P, Camus M, Palermo G, Smitz J, Van Waesberghe L, Wsanto A *et al*. Placental production of estradiol and progesterone after oocyte donation in patients with primary ovarian failure. Am J Obstet Gynecol 1990;162:66–70.
31. Schneider MA, Davies MC, Honour JW. The timing of placental competence in pregnancy after oocyte donation. Fertil Steril 1993;59:1059–64.
32. Mishell DR, Thorneycroft IH, Nagata Y, Murata T, Nakamura RM. Serum gonadotropin and steroid patterns in early human gestation. Am J Obstet Gynecol 1971;117:631–42.
33. Tulchinsky D, Hobel CJ. Plasma human and chorionic gonadotropin, estrone, estradiol, estriol, progesterone and 17α-hydroxyprogesterone in human pregnancy. 3. Early normal pregnancy. Am J Obstet Gynecol 1973;117:884–93.
34. Kronbach T, Mathys D, Umeno M, Gonzalez FJ, Meyer UA. Oxidation of midazolam and triazolam by human liver cytochrome P450IIIA4. Mol Pharmacol 1989;36:89–96.
35. Gorski JC, Hall SD, Jones DR, VandenBranden M, Wrighten SA. Regioselective biotransformation of midazolam by members of the human cytochrome P450 3A (CYP 3A) subfamily. Biochem Pharmacol 1994;47:1643–53.
36. Thummel KE, Shen DD, Podoll TD, Kunze KL, Trager WF, Hartwell PS *et al*. Use of midazolam as a human cytochrome P450 3A probe: I. *In vitro–in vivo* correlations in liver transplant patients. J Pharmacol Exper Ther 1994;271:549–56.
37. Thummel KE, Shen DD, Podoll TD, Kunze KL, Trager WF, Bacchi CE *et al*. Use of midazolam as a human cytochrome P450 3A probe: II. Characterization of inter- and intra-individual hepatic CYP3A variability after liver transplantation. J Pharmacol Exp Ther 1994;271:557–66.
38. Kanto J, Sjövall S, Erkkola R, Himberg J-J, Kangas L. Placental transfer and maternal midazolam kinetics. Clin Pharmacol Ther 1983;33:786–91.
39. Ohkita C, Goto M. Increased 6-hydroxycortisol excretion in pregnant women: Implication of drug-metabolizing enzyme induction. DICP 1990; 24:814–6.
40. Prevost RR, Aki SA, Whybrew WD, Sibai BM. Oral nifedipine pharmacokinetics in pregnancy-induced hypertension. Pharmacother 1992;12:174–7.
41. Pond SM, Kreek MJ, Tong TG, Raghunath J, Benowitz NL. Altered methadone pharmacokinetics in methadone-maintained pregnancy women. J Pharmacol Exp Ther 1985;233:1–6.
42. Stika CS, Andrews W, Frederiksen MC, Mercer B, Sabai B, Antal E. Steady state pharmacokinetic study of Flagyl® ER in pregnant patients during the second to third trimester of pregnancy [abstract]. Clin Pharmacol Ther 2004;75:P24.
43. Lehmann JM, McKee DD, Watson MA, Willson TM, Moore JT, Kliewer SA. The human orphan nuclear receptor PXR is activated by compounds that regulate CYP3A4 gene expression and cause drug interactions. J Clin Invest 1998;102:1016–23.
44. Goodwin B, Hodgson E, Liddle C. The orphan human pregnane X receptor mediates the transcription activation of CYP3A4 by rifampicin through a distal enhancer module. Mol Pharmacol 1999; 56:1329–39.
45. Aldridge A, Bailey J, Neims AH. The disposition of caffeine during and after pregnancy. Semin Perinatol 1981;5:310–4.

46. Wadelius M, Darj E, Freene G, Rane A. Induction of CYP2D6 in pregnancy. Clin Pharmacol Ther 1997;62:400–7.
47. Tomson T, Lindbom U, Ekqvist B, Sundqvist A. Epilepsy in pregnancy: A prospective study of seizure control in relation to free and total plasma concentrations of cabamazepine and phenytoin. Epilepsia 1994:35:122–30.
48. Tomson T, Lindbom U, Ekqvist B, Sundqvist A. Disposition of cabamazepine and phenytoin in pregnancy. Epilepsia 1994:35:131–5.
49. Chen SS, Perucca E. Lee JN, Richens A. Serum protein binding and free concentration of phenytoin and phenobarbitone in pregnancy. Br J Clin Pharmacol 1982;3:547–52.
50. McGready R, Stepniewska K, Seaton E, Cho T, Cho D, Ginsberg A *et al*. Pregnancy and use of oral contraceptives reduces the biotransformation of proguanil to cycloguanil. Eur J Clin Pharmacol 2003;59:553–7.
51. McGready R, Stepniewska K, Edstein MD, Cho T, Gilveray CT, Looareesuwan S *et al*. The pharmacokinetics of atovaquone and proguanil in pregnant women with acute falciparum malaria. Eur J Clin Pharmacol 2003;59:545–52.
52. Bologa M, Tang B, Klein J, Tesoro A, Koren G. Pregnancy-induced changes in drug metabolism in epileptic women. J Pharmacol Exp Ther 1991; 257:735–40.
53. Tsutsumi K, Kotegawa T, Matsuki S, Tanaka Y, Ishii Y, Kodama Y, Kuranari M, Miyakawa I, Nakano S. The effect of pregnancy on cytochrome P4501A2, xanthine oxidase, and *N*-acetyltransferase activities in humans. Clin Pharmacol Ther 2001;70:121–5.
54. Tran TA, Leppik IE, Blesi K, Sathanandan ST, Remmel R. Lamotrigine clearance during pregnancy. Neurology 2002;59:251–5.
55. Ohman I, Vitois S, Tomson T. Lamotrigine in pregnancy: Pharmacokinetics during delivery, in the neonate, and during lactation. Epilepsia 2000; 41:709–13.
56. Ballabh P, Lo ES, Kumari J, Cooper TB, Zervoudakis I, Auld PAM, Krauss AN. Pharmaokinetics of betamethasone in twin and singleton pregnancy. Clin Pharmacol Ther 2002;71:39–45.
57. Lees MM, Scott DH, Kerr MG. Haemodynamic changes associated with labour. J Obstet Gynaecol Br Commonw 1970;77:29–36.
58. Philipson A, Stiernstedt G. Pharmacokinetics of cefuroxime in pregnancy. Am J Obstet Gynecol 1982;142:823–8.
59. Gerdin E, Salmonson T, Lindberg B, Rane A. Maternal kinetics of morphine during labour. J Perinat Med 1990;18:479–87.
60. Ueland K, Metcalfe J. Circulatory changes in pregnancy. Clin Obstet Gynecol 1975;18:41–50.
61. Sims EAH, Krantz KE. Serial studies of renal function during pregnancy and the puerperium in normal women. J Clin Invest 1958;37:1764–74.
62. Capeless EL, Clapp JF. When do cardiovascular parameters return to their preconception values? Am J Obstet Gynecol 1991;165:883–6.
63. Dam M, Christiansen J, Munck O, Mygind KI. Antiepileptic drugs: Metabolism in pregnancy. Clin Pharmacokin 1979;4:53–62.
64. Steen B, Rane A. Clindamycin passage into human milk. Br J Clin Pharmacol 1982;13:661–4.
65. Del Priore G, Jackson-Stone M, Shim EK, Garfinkel J, Eichmann MA, Frederiksen MC. A comparison of once-daily and eight hour gentamicin dosing in the treatment of postpartum endometritis. Obstet Gynecol 1996;87:994–1000.
66. Kubacka RT, Johnstone HE, Tan HSI, Reeme PD, Myre SA. Intravenous ampicillin pharmacokinetics in the third trimester of pregnancy. Ther Drug Monit 1983;5:55–60.
67. Yerby MS, Friel PN, Miller DQ. Carbamazepine protein binding and disposition in pregnancy. Ther Drug Monit 1985;7:269–73.
68. Casele HL, Laifer SA, Woelders DA, Venkataramanan R. Changes in the pharmacokinetics of the low-molecular-weight heparin enoxaparin sodium during pregnancy. Am J Obstet Gynecol 1999;181:1113–7.
69. Prevost RR, Aki SA, Whybrew WD, Sibai BM. Oral nifedipine pharmacokinetics in pregnancy-induced hypertension. Pharmacotherapy 1992;12:174–7.
70. Barton JR, Prevost RR, Wilson DA, Whybrew WD, Sibai BM. Nifedipine pharmacokinetics and pharmacodynamics during the immediate postpartum period in patients with preeclampsia. Am J Obstet Gynecol 1991;165:951–4.
71. Kimberlin DF, Weller S, Whitley RJ, Andrews WW, Hauth JC, Lakeman F *et al*. Pharmacokinetics of oral valacyclovir and acyclovir in late pregnancy. Am J Obstet Gynecol 1998;179:846–51.
72. CDER. pharmacokinetics in pregnancy — study design, data analysis, and impact on dosing and labeling. Draft guidance for industry. Rockville: FDA; 2004. (Internet at http://www.fda.gov/cder/guidance/index.htm.)
73. Nelson MM, Forfar JO. Association between drugs administered during pregnancy and congenital abnormalities of the fetus. Br Med J 1971;1:523–7.
74. Bonati M, Bortolus R, Marchetti F, Romero M, Tognoni G. Drug use in pregnancy: An overview of epidemiological (drug utilization) studies. Eur J Clin Pharmacol 1990;38:325–8.
75. McBride WG. Thalidomide and congenital abnormalities [letter]. Lancet 1961:ii1358.
76. Lenz W. Kindliche missbildungen nach medikament während der gravidität. Deutsch Med Wschr 1961;86:2555–6.
77. Morgan DJ. Drug disposition in mother and foetus. Clin Exp Pharmacol Physiol 1997;24:869–73.
78. Martin CB. The anatomy and circulation of the placenta. In: Barnes AC, editor. Intra-uterine development. Philadelphia: Lea & Febiger; 1968. p. 35–67.
79. Higgins CF. ABC transporters: From microorganisms to man. Annu Rev Cell Biol 1992;8:67–113.
80. Gottesman MM Pastan I, Ambudkar SV. P-Glycoprotein and multidrug resistance. Curr Opin Immunol 1996;6:610–7.
81. Schinkel AH, Wagenaar E, Mol CAAM, van Deemter L. P-Glycoprotein in the blood–brain barrier

of mice influences the brain penetration and pharmacological activity of many drugs. J Clin Invest 1996;97: 2517–24.
82. Mylona P, Glazier JD, Greenwood SL, Slides MK, Sibley CP. Expression of the cystic fibrosis (CF) and multidrug resistance (MDR1) genes during development and differentiation in the human placenta. Mol Hum Reprod 1996;2:693–8.
83. Nakamura Y, Ikeda S, Furukawa T, Sumizawa T, Tani A, Akiyama S, Nagata Y. Function of P-glycoprotein expressed in placenta and mole. Biochem Biophys Res Commun 1997;235:849–53.
84. MacFarland A, Abramovich DR, Ewen SW, and Pearson CK. Stage-specific distribution of P-glycoprotein in first-trimester and full-term human placenta. Histochem J 1994;26:417–23.
85. Allikmets R, Schriml LM, Hutchinson A, Romano-Spica V, Dean M. A human placenta-specific ATP-binding cassette gene (ABCP) on chromosome 4q22 that is involved in multidrug resistance. Cancer Res 1998;58:5337–9.
86. St.-Pierre MV, Serrano MA, Macias RIR, Dubs U, Hoechli M, Lauper U, Meier PJ, Marin JJG. Expression of members of the multidrug resistance protein family in human term placenta. Am J Physiol 2000;279:R1495–503.
87. Lankas GR, Wise LD, Cartwright ME, Pippert T, Umbenhauer DR. Placental P-glycoprotein deficiency enhances susceptibility to chemically induced birth defects in mice. Reprod Toxicol 1998;12:457–63.
88. Sugawara I, Kataoka I, Moroshima Y, Hamada H, Tsuruo T, Itoyama S, Mori S. Tissue distribution of P-gylcoprotein encoded by a multidrug-resistant gene as revealed by a monoclonal antibody, MRK 16. Cancer Res 1988;48:1926–9.
89. Sugawara I. Expression and function of P-glycoprotein (mdr1 gene product) in normal and malignant tissues. Acta Pathol Jap 1990;40:545–53.
90. Tanabe M, Ieiri I, Nagata N, Inoue K, Ito S, Kanamori Y *et al*. Expression of P-glycoprotein in human placenta: Relation to genetic polymorphism of the multidrug resistance (MDR)-1 gene. J Pharmacol Exp Ther 2001;297:1137–43.
91. Cordon-Cardo C, O'Brien JP, Boccia J, Casals D, Bertino JR, Melamed MR. Expression of the multidrug resistance gene product (P-glycoprotein) in human normal and tumor tissues. J Histochem Cytochem 1990;38:1277–87.
92. Mylona P, Hoyland JA, Sibley CP. Sites of mRNA expression of cystic fibrosis (CF) and multidrug resistance (MDR-1) genes in the human placenta of early pregnancy: No evidence for complementary expression. Placenta 1999;20:493–6.
93. Smit JW, Huisman MT, van Tellingen O, Wilshire HR, Schinkel AH. Absence or pharmacological blocking of placental P-glycoprotein profoundly increased fetal drug exposure. J Clin Invest 1999;104:1441–7.
94. Trezise AE, Romano PR, Gill DR, Hyde SC, Sepulveda FV, Buchwald M, Higgins CF. The multidrug resistance and cystic fibrosis genes have complementary patterns of epithelial expression. EMBO J 1992;11:4291–303.
95. Ushigome F, Takanaga H, Matsua H, Yanai S, Tsukimori K, Nakano H *et al*. Human placental transport of vinblastine, vincristine, digoxin and progesterone: Contribution of P-glycoprotein. Eur J Pharmacol 2000;408:1–10.
96. Pacifici GM, Nottoli R. Placental transfer of drugs administered to the mother. Clin Pharmacokinet 1995;28:235–69.
97. van der Aa EM, Peereboom-Stegeman JHJC, Noordhoek J, Gribnau FWJ, Russel FGM. Mechanisms of drug transfer across the human placenta. Pharm World Sci 1998;20:139–48.
98. Marzolini C, Rudin C, Decosterd LA, Telenti A, Schreyer A, Biollaz J, Buclin T. Swiss mother–child HIV cohort study. Transplacental passage of protease inhibitors at delivery. AIDS 2002;16:889–93.
99. Casey BM, Bawdon RE. Placental transfer of ritonavir with zidovudine in the *ex vivo* placental perfusion model. Am J Obstet Gynecol 1998;179:758–61.
100. Uhr M, Steckler T, Yassouridis A, Holsboer F. Penetration of amitriptyline, but not fluoxetine, into brain is enhanced in mice with blood–brain barrier deficiency due to mdr1a P-glycoprotein gene disruption. Neuropsychopharmacol 2000;22:380–7.
101. Weiss J, Dormann S-MG, Martin-Facklam M, Kerpen CJ, Ketabi-Kiyanvash N, Haefeli WE. Inhibition of P-glycoprotein by newer antidepressants. J Pharmacol Exp Ther 2003;305:197–204.
102. Weiss J, Kerpen CJ, Lindenmaier H, Dormann S-MG, Haefeli WE. Interaction of antiepileptic drugs with human P-glycoprotein *in vitro*. J Pharmacol Exp Ther 2003;307:262–7.
103. Jones KL. Smith's recognizable patterns of human malformation. 5th ed. Philadelphia: WB Saunders; 1997. p. 1–3.
104. Wilson JG. Current status of teratology — general principles and mechanisms derived from animal studies. In: Wilson JG, Fraser FC, editors. Handbook of teratology. vol I. General principles and etiology. New York: Plenum Press; 1977. p 47–74.
105. Buehler BA, Delimont D, van Waes M, Finnell RH. Prenatal prediction of risk of the fetal hydantoin syndrome. N Engl J Med 1990;31:322:1567–72.
106. Brent RL. Radiation teratogenesis. Teratology 1980; 21:281–98.
107. Shaw GM, Wasserman CR, Lammer EJ, O'Malley CD. Murray JC, Basart AM *et al*. Orofacial clefts, parental cigarette smoking, and transforming growth factor-alpha gene variants. Am J Hum Genet 1996;58:551–61.
108. Parman T, Wiley MJ, Wells PG. Free radical mediated oxidative DNA damage in the mechanism of thalidomide teratogenicity. Nat Med 1999;5:582–5.
109. Begg EJ, Atkinson HC, Duffull SB. Prospective evaluation of a model for the prediction of milk:plasma drug concentrations from physicochemical characteristics. Br J Clin Pharmacol 1992;33:501–5.
110. Stec GP, Greenberger P, Ruo TI, Henthorn T, Morita Y, Atkinson AJ Jr, Patterson R. Kinetics of theophylline transfer to breast milk. Clin Pharmacol Ther 1980; 28:404–8.
111. Greenberger PA, Odeh YK, Frederiksen MC, Atkinson AJ Jr. Pharmacokinetics of prednisolone transfer to breast milk. Clin Pharmacol Ther 1993;53:324–8.

112. Wisner KL, Perel JM, Findling RL. Antidepressant treatment during breast-feeding. Am J Psychiatry 1996;153:1132–7.
113. Brixen-Rasmussen L, Halgrener J, Jørgensen A. Amitriptyline and nortriptyline excretion in human breast milk. Psychopharmacology 1982;76:94–5.
114. Breyer-Pfaff U, Entenmann A, Gaertner HJ. Secretion of amitriptyline and metabolites into breast milk [letter]. Am J Psychiatry 1995;152:812–3.
115. Kemp J, Ilett KF, Booth J, Hackett LP. Excretion of doxepin and *N*-desmethyldoxepin in human milk. Br J Clin Pharmacol 1985;20:497–9.
116. Matheson I, Pande H, Alertsen AR. Respiratory depression caused by *N*-desmethyldoxepin in breast milk [letter]. Lancet 1985;2:1124.
117. Taddio A, Ito S, Koren G. Excretion of fluoxetine and its metabolite, norfluoxetine, in human breast milk. J Clin Pharmacol 1996;36:42–7.
118. Lester BM, Cucca J, Andreaozzi L, Flanagan P, Oh W. Possible association between fluoxetine hydrochloride and colic in an infant. J Am Acad Child Adolesc Psychiatry 1993,32:1253–5.
119. Kristensen JH, Ilett KF, Dusci LJ, Hackett LP, Yapp P, Wojnar-Horton RE *et al*. Distribution and excretion of sertraline and *N*-desmethylsertraline in human milk. Br J Clin Pharmacol 1998; 45:453–7.
120. Ilett KF, Hackett LP, Dusci LJ, Roberts MJ, Kristensen JH, Paech M *et al*. Distribution and excretion of venlafaxine and *O*-desmethylvenlafaxine in human milk. Br J Clin Pharmacol 1998;45:459–62.
121. Briggs GG, Samson JH, Ambrose PJ, Schroeder DH. Excretion of bupropion in breast milk. Ann Pharmacother 1993,27:431–3.
122. Verbeeck RK, Ross SG, McKenna EA. Excretion of trazodone in breast milk. Br J Clin Pharmacol 1986;22:367–70.
123. Wisner KL, Perel JM. Serum nortriptyline levels in nursing mothers and their infants. Am J Psychiatry 1991;148:1234–6.

This page intentionally left blank

CHAPTER

23

Drug Therapy in Neonates and Pediatric Patients

ELIZABETH FOX AND FRANK M. BALIS
National Cancer Institute, National Institutes of Health, Bethesda, Maryland

BACKGROUND

The use of drugs in newborns, infants, and children is often based on safety, efficacy, and pharmacological data generated in adults, but the practice of scaling adult drug doses to infants and children based on body weight or body surface area (BSA) does not account for the developmental changes that affect drug pharmacokinetics or target tissue and organ sensitivity to the drug. In fact, this dosing practice has resulted in therapeutic tragedies that illustrate the importance of understanding the effects of ontogeny on drug pharmacokinetics and drug effect and the need for separate clinical trials and pharmacological studies of drugs in pediatric patient populations.

Chloramphenicol Therapy in Newborns

The chloramphenicol-induced gray baby syndrome is an example of the potential dangers inherent in treating newborns based on dosing recommendations in adults. Chloramphenicol is detoxified in the liver primarily through conjugation with glucuronide. Because of its broad spectrum of activity, it was widely used to treat a variety of infections in the 1950s, including nursery infections in neonates. Hospital-acquired bacterial infections in the newborn nursery were often due to less sensitive bacterial strains, compared to strains found outside the newborn nursery; consequently, premature and full-term infants were treated with adult doses scaled to the infant body weight or with doses exceeding those recommended in adults (1). In the late 1950s case reports of unexplained deaths in newborns who were receiving chloramphenicol appeared; these deaths and led to a controlled clinical trial of chloramphenicol therapy in premature newborns who were at high risk of infection because they were born more than 24 hours after spontaneous rupture of membranes. The standard of care for these newborns was empirical treatment with antibiotics, but newborns studied in this trial were assigned to one of four groups: (1) no antibiotics, (2) procaine penicillin and streptomycin, (3) chloramphenicol, and (4) all three antibiotics (Table 23.1) Mortality was substantially higher in the newborns receiving chloramphenicol, and nearly two-thirds of the newborns receiving chloramphenicol died, compared to the <20% mortality rate in newborns who did not receive chloramphenicol. In infants weighing more than 2000 grams at birth, 45% receiving chloramphenicol died compared with 25% in the non-chloramphenicol-treated groups. This high mortality rate was ascribed to chloramphenicol toxicity (2).

The *gray baby syndrome* refers to a characteristic constellation of physical signs — consisting of vomiting, refusal to feed, respiratory distress (irregular rapid respiration), abdominal distention, periods of cyanosis, passage of loose, green stools, flaccidity, ashen color, hypothermia, vascular collapse, and death (usually by the fifth day of life) — that was recognized in the chloramphenicol-treated patients. Fifty-eight percent of the infants who received chloramphenicol and

TABLE 23.1 Mortality in Premature Neonates at Increased Risk of Bacterial Infection Who Were Randomized to One of Four Empiric Antibiotic Treatment Groups[a]

	All premature newborns		Good-prognosis premature newborns (birthweight 2001–2500 g)	
Treatment	Number	Deaths	Number	Deaths
No empiric antibiotics	32	6	17	1
Penicillin + streptomycin[b]	33	6	24	0
Chloramphenicol[b]	30	19	16	8
Penicillin + streptomycin + chloramphenicol[b]	31	21	15	6

[a] Reproduced with permission from Burns LE *et al*. N Engl J Med 1959;261:1318–21.

[b] Intramuscular doses of antibiotics: procaine penicillin, 150,000–600,000 units/day; streptomycin, 50 mg/kg/day; chloramphenicol, 100–165 mg/kg/day.

survived had similar signs that completely resolved 24–36 hours after discontinuing the drug.

Studies of chloramphenicol pharmacokinetics were subsequently performed in newborns and children. High concentrations of chloramphenicol and its metabolites accumulated in newborns who developed toxicity (Figure 23.1A), and presumably accounted for the severe toxicity. This accumulation of drug on a dosing regimen that is tolerable in adults resulted from the reduced capacity of newborns to metabolize chloramphenicol by glucuronide conjugation. When studied at lower doses in a group of children over a wider age range, the rate of chloramphenicol metabolism was found to be highly age dependent. The half-life was 26 hours in the newborns, 10 hours in the infants, and 4 hours in the older children (Figure 23.1B) (3).

As demonstrated by chloramphenicol, the pharmacological impact of developmental changes that affect drug disposition are often discovered only after unexpected or severe toxicity in infants and children leads to detailed pharmacological studies. Therapeutic tragedies such as this could be avoided by performing pediatric pharmacological studies during the drug development process, as exemplified by the clinical development of zidovudine for use in newborns, infants, and children.

Zidovudine Therapy in Newborns, Infants, and Children

Zidovudine is a synthetic nucleoside analog that blocks replication of the human immunodeficiency virus (HIV) by inhibiting reverse transcriptase. The primary indication for zidovudine administration in newborns is the prevention of vertical transmission of HIV. Like chloramphenicol, zidovudine is eliminated in adults primarily by glucuronide conjugation, suggesting that newborns may have a reduced capacity to eliminate zidovudine. However, unlike

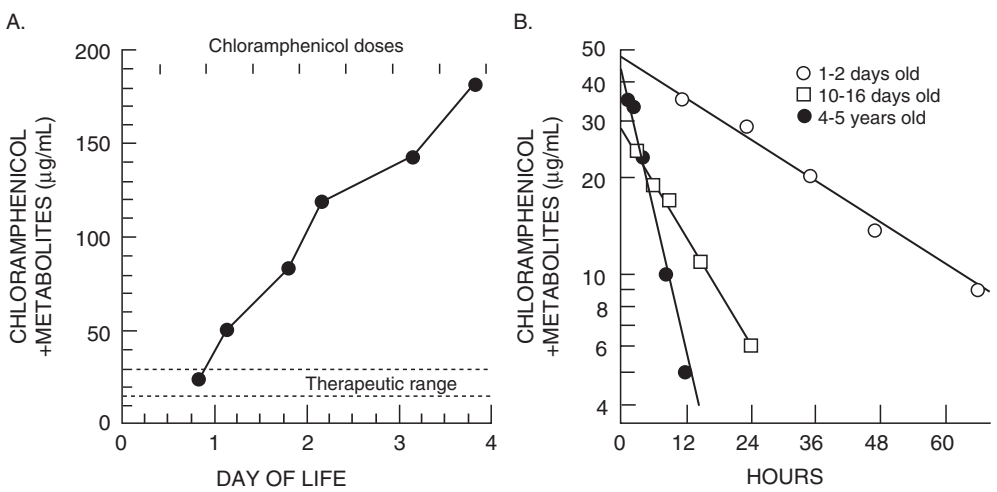

FIGURE 23.1 (A) Plasma concentration of chloramphenicol and its metabolites in a newborn who received intravenous chloramphenicol every 12 hours at doses equivalent to those recommended for adults. (Reproduced with permission from Burns LE *et al*. N Engl J Med 1959;261:1318–21.) (B) The concentration-vs-time profile for chloramphenicol in newborns and children, demonstrating the age-dependent elimination of chloramphenicol and its metabolites. (Reproduced with permission from Weiss CF *et al*. N Engl J Med 1960;262:787–94.)

TABLE 23.2 Zidovudine Pharmacokinetic Parameters for Various Age Groups[a]

Population	Age	CL_E (mL/min/kg)	$T_{1/2}$ (hr)	F (%)
Preterm infants	5.5 days	2.5	7.2	—
	17.7 days	4.4	4.4	—
Term infants	14 days	10.9	3.1	89
	14 days	19.0	1.9	61
Children	1–13 years	24	1.5	68
Adults	—	21	1.1	63

[a] Data from Klecker RW Jr *et al*. Clin Pharmacol Ther 1987;41:407–12; Balis F *et al*. J Pediatr 1989;114:880–4; Mirochnick M *et al*. Antimicrob Agents Chemother 1998;42:808–12; and Boucher FD *et al*. J Pediatr 1993;122:137–44.

chloramphenicol, prior to widespread administration of zidovudine to newborns and infants born to HIV-infected mothers, the pharmacology and safety of the drug were carefully studied in this population and age-specific dosing guidelines were developed.

The pharmacokinetic parameters for zidovudine in various age groups are presented in Table 23.2 (4–7). Newborns cleared zidovudine more slowly than did children and adults, and the clearance in preterm newborns is slower than in the full-term infants. Zidovudine clearance rapidly increases over the first few weeks of life, consistent with the up-regulation of glucuronidation pathways in newborns after birth, and by 2 weeks of age approaches values in older children and adults. In addition, the extent of zidovudine absorption (F) in newborns at 14 days of age is higher than in older children, presumably because of reduced first-pass metabolism. Based on these studies, a safe and potentially effective dose of zidovudine was defined for term and preterm newborns (6–8).

The pharmacology and safety of zidovudine were also studied in the prenatal and perinatal setting in pregnant women. Based on these studies, a placebo-controlled, double-blind, randomized trial of zidovudine was conducted in HIV-infected pregnant women to determine if zidovudine could block maternal–fetal transmission of HIV. Mothers received 100 mg of zidovudine orally, five times daily; then, at the onset of labor and through delivery, mothers received a continuous intravenous infusion of zidovudine (1 mg/kg/hr). Beginning 8–12 hours after birth, full-term newborns were treated with 2 mg/kg of zidovudine orally every 6 hours for 6 weeks. The HIV transmission rate from mother to child was significantly reduced by administering zidovudine before, during, and after delivery. Equally important, newborn infants experienced no substantial adverse events from this regimen (9).

Development of Federal Regulations

Many Food and Drug Administration (FDA) regulations that impact on pediatric drug development and dosing are the result of therapeutic tragedies that occurred in children. The 1938 Food, Drug and Cosmetic Act (FDCA), which is described in Chapter 34, was legislated in part due to the deaths of 107 children from sulfanilamide elixir, which contained diethylene glycol as the vehicle. In 1962, the Harris–Kefauver Amendment to the FDCA mandated that drugs had to be safe and effective in the population for which they were marketed. This amendment states that safety and efficacy in one population cannot be assumed for another population — specifically, results from studies done in adults cannot be transferred to infants or children. The impetus for this amendment was the recognition of fetal malformations from maternal ingestion of thalidomide.

FDA regulations enacted in 1979 were intended to increase the number of drugs available to infants and children through voluntary measures. However, over the next two decades, only 25% of newly marketed drugs had sufficient clinical safety and efficacy data in infants and children (10). In 1994, the FDA requested drug companies to survey existing data that could support labeling for pediatric use of marketed drugs. Only 430 supplements were submitted in response to the 1994 rule, and a majority of the supplements simply added the disclaimer, "Safety and effectiveness in pediatric patients have not been established." Only 65 supplements provided enough data to justify new pediatric labeling for all pediatric age groups.

With these voluntary measures, the proportion of new drugs with adequate pediatric labeling has not increased since 1991. Overall, 40% of new drugs were not felt to be of potential use in childhood diseases, but less than half of the remaining 60% had pediatric studies performed or pediatric labeling at the time of approval (11). Failed efforts to gain voluntary compliance led to legislative measures that empower the FDA to require pediatric studies for selected marketed drugs and new drugs that are likely to be used in a substantial number of pediatric patients, or could be an improvement over current treatment of childhood diseases. This regulation, the 1997 Food and Drug Administration Modernization Act (FDAMA), also provided incentives (extension of exclusivity) to drug companies for performing clinical trials in the pediatric population.

The 1998 Pediatric Final Rule allowed the FDA to require pharmaceutical companies to perform studies in children as part of new drug development if the agent had potential uses in children, thereby pushing pharmaceutical companies to complete pediatric studies earlier in the drug development process. From 1999 through 2002, 12 drugs were newly approved for children or were labeled for use in a pediatric population under the Pediatric Rule. After a court challenge of the Pediatric Rule was upheld, Congress passed the Best Pharmaceuticals for Children Act (BPCA), which has provisions for on-patent and off-patent medications. The on-patent program is voluntary, privately funded, and offers the incentive of a 6-month extension of marketing exclusivity for companies that provide pediatric information. By the end of 2004, 85 products were studied under this program and relabeled to include information for the pediatric population, and 200 additional products were being studied. BPCA also authorized federal funding for pediatric studies of drugs that no longer have exclusivity or patent protection, established the Office of Pediatric Therapeutics within the FDA, and instituted monitoring of adverse events for drugs granted pediatric exclusivity (12–14). In 2003, the Pediatric Research Equity Act was signed into law, requiring all applicants for new active ingredients, new indications, or new dosage forms, regimens, or routes of administration to contain a pediatric assessment (15).

These regulations aim to ensure proper and useful pediatric dosing information on all pharmaceutical products that are used in pediatric populations. The consequences of inadequate pediatric dosing information include a greater risk of toxicity, as occurred with chloramphenicol; ineffective treatment due to underdosing; and an unwillingness of physicians to prescribe newer, potentially more efficacious drugs for children because pediatric dosing recommendations are not available. Appropriate pediatric labeling would help ensure the availability of a pediatric formulation that is palatable and acceptable for the intended ages of children and would prevent denial of third-party reimbursement on the basis of a lack of labeling (16).

ONTOGENY AND PHARMACOLOGY

Because clinical investigation of new agents is not uniformly performed in newborns, infants, and children, we have a poor understanding of the effect of ontogeny on the pharmacokinetics and pharmacodynamics of most drugs. However, we can often anticipate age-related differences in pharmacokinetics and the intensity of drug effects based on our knowledge of the maturation process. During childhood, changes in body mass and composition and the maturation of excretory organs have a substantial effect on pharmacokinetics. As with chloramphenicol and zidovudine, the most dramatic changes occur during the first days to months of life. Predicting the effect of growth and development on pharmacodynamics is more difficult because there is less information regarding age-related changes in drug–receptor expression.

The FDA subdivides the pediatric population into five age groups: (1) preterm newborn infants, (2) term newborn infants (0–27 days of age), (3) infants and toddlers (28 days to 23 months), (4) children (2–11 years of age), and (5) adolescents (12 to 16 or 18 years of age, depending on region). The category of "preterm infant" is heterogeneous due to the impact of gestational age, unique neonatal diseases, and organ susceptibility to toxicity. Term infants undergo rapid physiologic changes in total body water and in renal and hepatic function during the first few days of life. CNS maturation with completion of myelination occurs in the infant and toddler age group. Children experience accelerated skeletal growth, weight gain, psychomotor development, and the onset of puberty, and sexual maturation is achieved during the adolescent period (17). These five pediatric stages are arbitrary groupings and do not necessarily coincide with the periods of greatest physiologic change that affect the clinical pharmacology of drugs.

Drug Absorption

As discussed in Chapter 4, the bioavailability of orally administered drugs is influenced by gastric acid secretion, gastrointestinal motility, intestinal absorptive surface area, bacterial colonization of the gut, and the intestinal and liver activity of drug-metabolizing enzymes that are responsible for presystemic metabolism of drugs (18). Gastric pH is neutral at birth, but drops to pH 1–3 within hours of birth. Gastric acid secretion then declines on days 10–30, and does not approach adult values until approximately 3 months of age. This lower level of gastric acid secretion contributes to the increased bioavailability in newborns of acid-labile drugs, such as the penicillins (19).

Gastric emptying is delayed and irregular in the newborn, but approaches adult values by 6–8 months of age. Intestinal motility is also irregular and highly dependent on feeding patterns in newborn. In newborns, decreased gastrointestinal motility can delay drug absorption and result in lower peak plasma drug concentrations, but does not alter the fraction of drug

TABLE 23.3 Relative Gastrointestinal Absorption of Selected Drugs in Infants and Adults[a]

Gastrointestinal drug absorption		
Increased in newborns	**Infants = adults**	**Decreased in newborns**
Penicillin	Theophylline	Phenytoin
Ampicillin	Sulfonamides	Acetaminophen
Erythromycin		Phenobarbital
Digoxin		
Zidovudine		

[a] Data from Loebstein R, Koren G. Pediatr Rev 1998;19:423–8.

TABLE 23.4 Plasma Protein Binding of Selected Drugs in Cord Blood and Adult Blood[a]

	Plasma protein binding (%)	
Drug	**Cord blood**	**Adult**
Acetaminophen	36.8	47.5
Chloramphenicol	31	42
Morphine	46	66
Phenobarbital	32.4	50.7
Phenytoin	74.4	85.8
Promethazine	69.8	82.7

[a] Data from Kurz H *et al*. Eur J Clin Pharmacol 1977;11:469–72.

absorbed for most drugs. In children, gastrointestinal transit time may be increased (10).

The ratio of absorptive surface area to BSA is greater in infants and children than in adults. Although pancreatic enzyme excretion is low in newborns, malabsorption does not occur and no effect on drug absorption has been observed. The newborn intestine is colonized with bacteria within days of birth, but the spectrum of bacterial flora may change over the first few years of life. The patterns and extent of colonization depend on age, type of delivery, type of feeding, and concurrent drug therapy (20). Compared to adults, the capacity of intestinal bacterial flora to inactivate orally administered digoxin is decreased and digoxin bioavailability is thereby increased in infants less than 2 years old (21). The relative gastrointestinal drug absorption of selected drugs in infants and adults is presented in Table 23.3.

Drug Distribution

Factors that affect drug distribution include the physicochemical properties of the drug, cardiac output, regional blood flow, body composition (e.g., extracellular water and adipose tissue), and the degree of protein and tissue binding. Serum albumin, α_1-acid glycoprotein, and total protein concentrations are lower at birth and during early infancy, but approach adult levels by 1 year of age. Lower plasma protein levels result in lower levels of drug binding to plasma proteins (Table 23.4). Although the absolute differences in the fraction of drug bound may be only 10–20%, for highly protein-bound drugs this could make a substantial difference in the free drug concentration in plasma. For example, promethazine is nearly 70% protein bound in cord blood and 83% protein bound in adult blood. This translates into a nearly twofold higher concentration of free promethazine in cord blood (22). Higher free drug concentrations can enhance drug delivery to tissues. Because drug assays used in clinical therapeutic drug monitoring usually measure total (protein bound plus free) drug concentrations, the higher free fraction in children also influences the interpretation of plasma drug concentrations relative to therapeutic ranges defined in adults, in whom a smaller fraction of the measured total drug concentration is unbound (23).

Body composition, especially water and fat content, are also highly age dependent (Figure 23.2) (24). Total body water accounts for a larger fraction of body weight in newborns than in older children and adults. There is also a larger fraction of extracellular water at birth. As a result of this change and

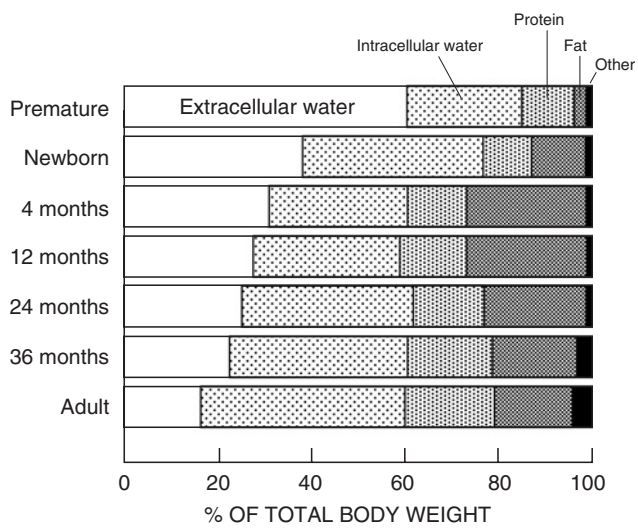

FIGURE 23.2 Age-related changes in body composition. (Reproduced with permission from Kaufman RE, Pediatric pharmacology. In: Aranda JV, Yaffe SJ, editors. Pediatric pharmacology, therapeutic principles in practice. Philadelphia: WB Saunders; 1992. p. 212–9.)

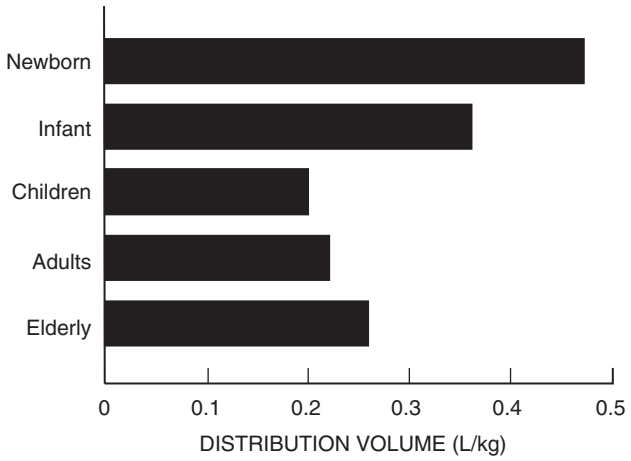

FIGURE 23.3 The distribution volume of sulfisoxazole in newborns, infants, children, and adults. (Data from Routledge P. J Antimicrob Chemother 1994;34(suppl A):19–24.)

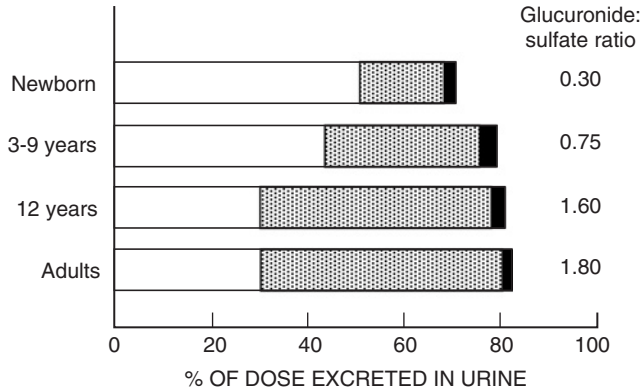

FIGURE 23.4 Percentage of the dose of acetominophen excreted in the urine as unchanged drug (*solid bars*), glucuronide conjugate (*stippled bars*), or sulfate conjugate (*open bars*) in selected age groups. The ratio of glucuronide:sulfate excreted in the urine increases with age. (Reproduced with permission from Miller RP *et al*. Clin Pharmacol Ther 1976;19:284–94.)

the decrease in binding to plasma proteins previously described, the apparent distribution volume of the water-soluble drug, sulfisoxazole, is greater in newborns and infants than in adults when normalized to body weight or surface area (Figure 23.3) (19). Because they have a higher proportion of body fat than adults have, lipid-soluble drugs also have a larger weight- or BSA-normalized distribution volume in infants than in older individuals (25).

Drug Metabolism

The capacity of the liver to metabolize drugs is lower at birth, and the rate of development of the various metabolic pathways is highly variable and may be influenced by exposure to drugs *in utero* and postnatally. Generalizations about the rate of maturation of drug-metabolizing enzyme systems during infancy and childhood are difficult because of the lack of data, the degree of variability, and the inducibility of some enzyme systems. Oxidative capacity is reduced at birth but appears to develop over days, as evidenced by the decline in the half-life of ibuprofen, which has a half-life greater than 30 hours in premature infants in the first day of life compared with less than 2 hours in children and adults (26). During childhood, oxidative capacity for drugs exceeds that in adults, especially when expressed per kilogram of body weight (19). In contrast, the activity of alcohol dehydrogenase does not approach adult levels until 5 years of age (27). The development of other Phase I reactions (e.g., hydrolysis, demethylation) has not been well characterized (20).

Because of variation in the rate of maturation of drug-metabolizing enzymes, the primary metabolic pathway for some drugs may be different in newborns and infants than in adults. For example, the activity of glucuronide conjugation is low at birth and does not approach adult levels until 3 years of age, but sulfate conjugation is active *in utero* and at birth and declines in relative importance with age. Therefore, drugs that are eliminated in adults by glucuronide conjugation may be cleared primarily as sulfate conjugates in newborns and infants (20, 28). This is demonstrated by age-related differences in acetaminophen metabolism. In adults, the glucuronide conjugate is the primary urinary metabolite of acetaminophen, whereas in newborns, a higher proportion of the dose is excreted as the sulfate conjugate. In young children, both the sulfate conjugate and glucuronide are present in urine (Figure 23.4). Despite these quantitative differences in the metabolic pathways used to inactivate the drug, the overall elimination rate constant for the parent drug was not age dependent. Therefore, in the case of acetaminophen metabolism, sulfate conjugation compensated for the developmental deficiency in glucuronidation (29).

The cytochrome P450 hepatic drug-metabolizing enzymes catalyze the biotransformation of a wide variety of compounds. These enzymes are regulated by genetic, environmental, and hormonal factors, and recent evidence suggests that there may also be a developmental component to the regulation of their expression and level of activity (Figure 23.5) (30–33). For example, CYP3A, which is the primary drug-metabolizing cytochrome P450 subfamily in adults, undergoes functional maturation over the first month

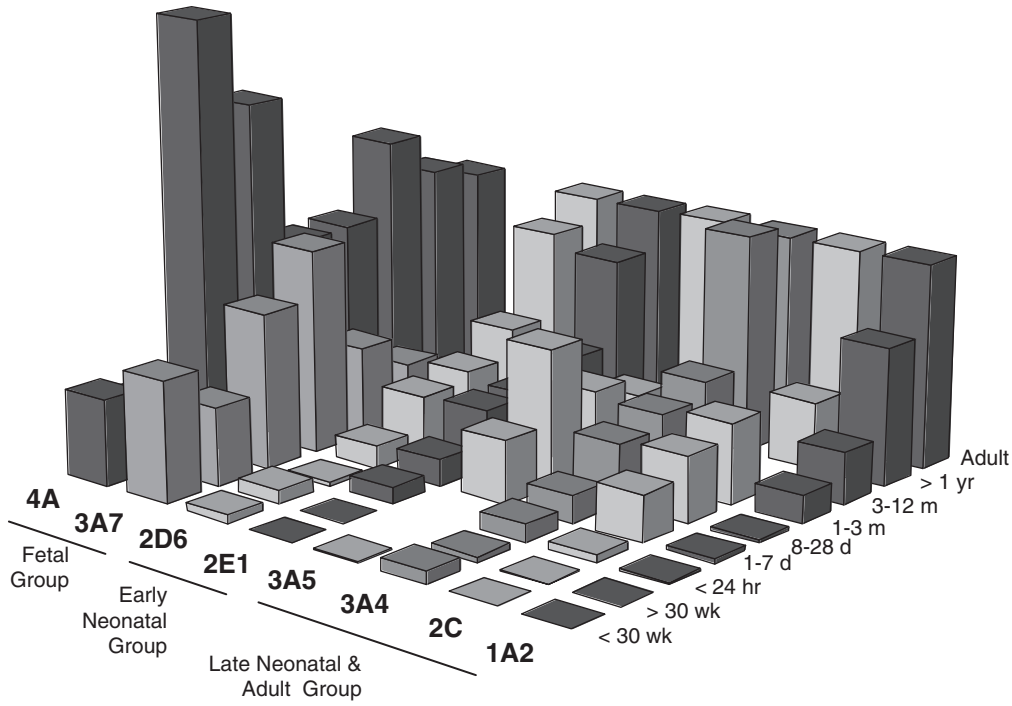

FIGURE 23.5 Development of cytochrome P450 isoforms in the human liver. The P450 protein content of human liver microsomes was examined using immunoblots at various gestational and postnatal ages. Values are presented as percentage of adult P450 content for each isoform. (Reproduced with permission from Cresteil T. Food Addit Contam 1998;15:45–51.)

of life in full-term newborns (16, 34). CYP3A7, the major fetal hepatic cytochrome P450 enzyme, can be detected early in fetal development, peaks at approximately 2 weeks postnatal age, then declines to low levels in adults as CYP3A4 activity increases (35). CYP3A4 and to a lesser extent CYP3A5 are responsible for a majority of the drug metabolism by the cytochrome P450 system in adults (34).

The administration of cisapride to premature infants for the treatment of gastroesophageal reflux illustrates the clinical relevance of the ontogeny of CYP3A4. Cisapride is a substituted piperidinyl benzamide that is metabolized by oxidation via hepatic and intestinal CYP3A4. Serious cardiac dysrhythmias, including ventricular tachycardia, ventricular fibrillation, *torsades de pointes*, and sudden death, have been reported in patients with reduced hepatic metabolism of cisapride. Because the rate of cisapride biotransformation is greater by CYP3A4 compared to CYP3A7, the low content of CYP3A4 in neonates appears to be responsible for the plasma accumulation of cisapride, with resulting QTc interval prolongation and serious ventricular arrhythmias that have been reported in premature infants receiving cisapride (36, 37).

CYP1A1 and CYP2E1 are also present early in fetal development and metabolize exogenous toxins and alcohol, respectively. Hepatic CYP2D6, CYP2C8/9, and CYP2C18/19 become active at birth (38). CYP1A2, which is responsible for caffeine metabolism, is not functional in embryonic or fetal liver; however, it becomes active at 4 to 5 months of age. In adults, CYP1A2 is highly inducible and therefore highly variable among individuals. In neonates, caffeine elimination half-life is longer in breast-fed infants than in formula-fed infants, suggesting CYP1A2 activity may be influenced by diet in the infant (39).

Renal Excretion

Renal function is limited at birth because the kidneys are anatomically and functionally immature. In full-term newborns, glomerular filtration rate (GFR) is 10–15 mL/min/m^2, and in premature infants the GFR is only 5–10 mL/min/m^2. GFR doubles by 1 week of age, because of a postnatal drop in renal vascular resistance and increase in renal blood flow, and reaches adult values by 1 year of age (Figure 23.6) (40, 41). A glomerular/tubular imbalance is present in newborns, because glomerular function matures more

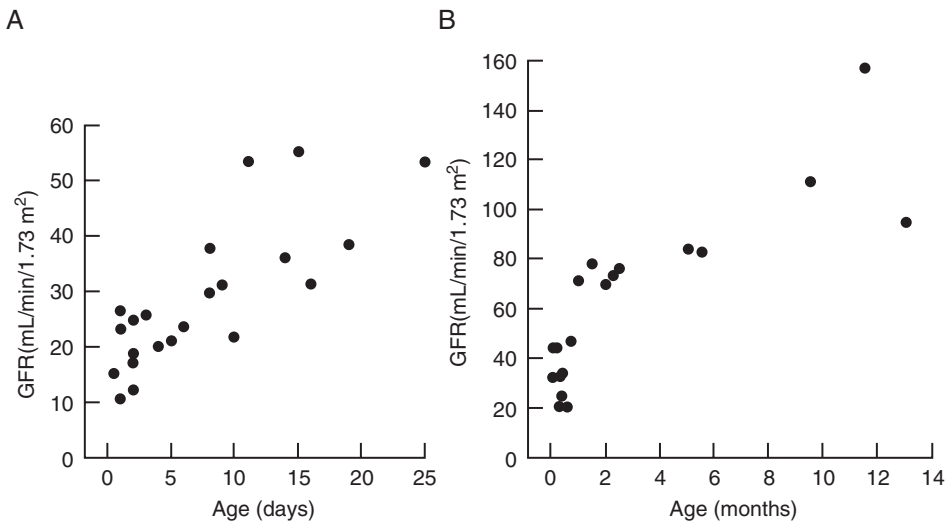

FIGURE 23.6 Glomerular filtration rate (GFR) in newborns (A) and through the first year of life (B). When normalized for body surface area, GFR reaches adult values by 1 year of age. (Data from Aperia A *et al*. Acta Paediatr Scand 1975;64:393–8 and Guignard J *et al*. J Pediatr 1975;87:268–72.)

rapidly than does renal tubular secretion. Although renal tubular secretory function is impaired at birth, it also approaches adult values by 1 year of age (18).

Renal clearance of drugs is delayed in newborns and young infants, necessitating dose reductions (Figure 23.7), but after 8 to 12 months of age, renal excretion of drugs is comparable with that of older children and may even exceed that of adults. In young children, the ratio of renal size relative to BSA is larger than in adults, and drug clearance normalized to BSA can exceed that in adults. Because renal clearance is more efficient in children, the dose of aminoglycosides required to achieve effective antibiotic plasma concentrations in children is usually 1.5- to 2-fold higher than in adults. The dosing interval in children also may need to be shorter than in adults (39).

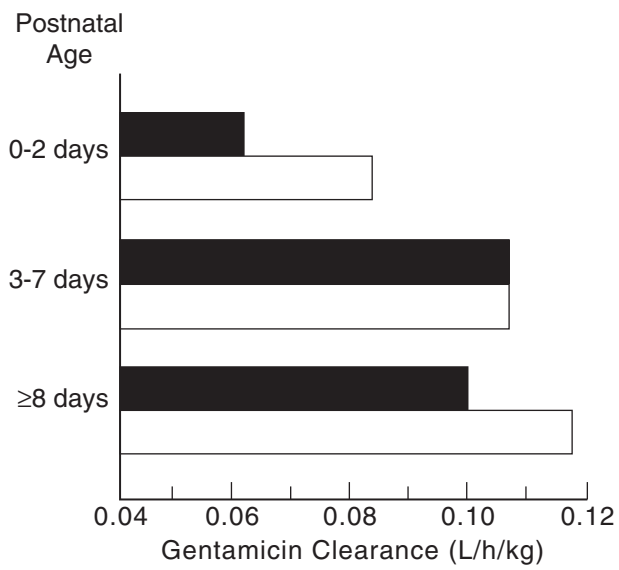

FIGURE 23.7 Plasma clearance of gentamicin in premature (<37-week gestation, *solid bars*) and full-term (*open bars*) newborns at various postnatal ages. (Data from Pons G *et al*. Ther Drug Monit 1988;10:42–7.)

THERAPEUTIC IMPLICATIONS OF GROWTH AND DEVELOPMENT

Drug effect is related to the free drug concentration at the target site and the presence and density of drug receptors at the target site. The free drug concentration at the target site is determined by the dose and pharmacokinetics of the drug. Developmental changes in body composition, level of protein binding, and excretory organ function have a significant impact on plasma drug concentration and, therefore, the amount of drug that reaches the target site. These developmental changes must be taken into account when devising a dose and dosing schedule for infants and children of different ages. The rapid changes that occur postnatally may require frequent dose adjustments during the first few days to weeks of life. Antibiotic doses, for example, are frequently increased after the first 7 days of life, to account for the initial rapid increase in renal function. Drug receptor expression over the course of normal growth and development has not been well

studied, but could also modulate a drug's effect during infancy and childhood.

Effect on Pharmacokinetics

Developmental changes in liver and kidney excretory function during infancy and childhood may necessitate dose adjustments to achieve a therapeutic drug concentration. For example, theophylline dose recommendations are age specific during childhood to compensate for changes in drug clearance. The overall elimination clearance of theophylline (renal excretion + hepatic metabolism) is markedly delayed in newborns (20 mL/min/kg in preterm newborns), and the recommended dose in this population is 4 mg/kg/day. However, theophylline clearance in children (100 mL/min/kg) is 40% higher than in adults (70 mL/min/kg), and children will require higher body-weight-normalized doses than do adults [42–44]. The effect of the age-dependent clearance rate of theophylline on the dose required to maintain a therapeutic drug level is shown in Figure 23.8. In this study, more than 3500 serum theophylline concentrations were measured in 1073 patients who ranged in age from 1 to 73 years (median, 9 years) (45). The dose of sustained-release theophylline was adjusted to achieve a serum level between 10 and 20 μg/mL. The higher dose required to achieve this therapeutic serum concentration in younger patients is a reflection of lower bioavailablity and more rapid clearance of theophylline than in adults. Females require a lower weight-adjusted dose at an earlier age than do males, presumably because females tend to enter puberty at an earlier age (46).

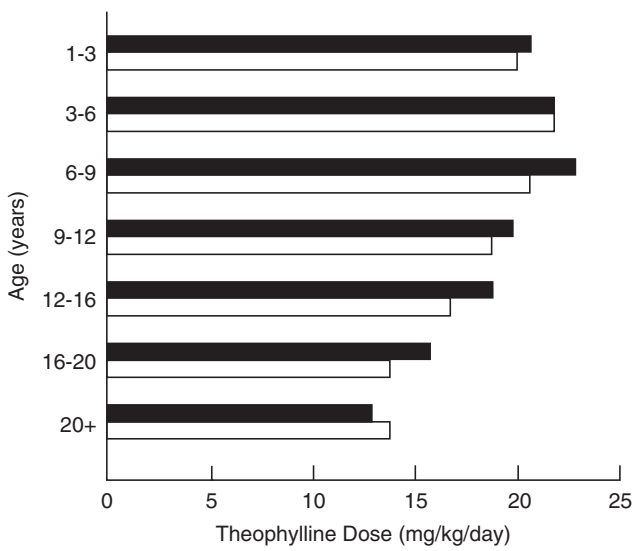

FIGURE 23.8 Effect of age-related clearance of theophylline on the dose of sustained-release theophylline required to maintain a therapeutic drug level (range: 10–20 μg/mL) in males (*solid bars*) and females (*open bars*) across a broad age range. (Reproduced with permission from Milavetz G *et al*. J Pediatr 1986;109:351–4.)

There may also be age-dependent changes in the route of elimination of drugs, as illustrated by theophylline. In premature newborns, over 50% of the drug is excreted unchanged in the urine, compared with 10% in adults. Although theophylline is N-methylated to caffeine in all age groups, the elimination of caffeine is slower in newborns than in adults. Therefore, caffeine is measurable in the serum of the newborn, but by 6 to 12 months of age is metabolized more rapidly and is no longer detectable. Additionally, the metabolism of theophylline by liver cytochrome P450 enzymes, including CYP1A2, increases during infancy. By 2 to 3 years of age, the fraction of theophylline excreted unchanged in the urine has dropped to 15%, and theophylline is eliminated primarily by hepatic metabolism throughout adulthood.

Age-dependent clearance of busulfan also has a direct impact on the clinical outcome of patients treated with this anticancer drug. Busulfan is a bifunctional alkylating agent that is an important component of preparative regimens for bone marrow transplantation. In children <5 years of age, the apparent clearance of busulfan is two- to threefold higher than it is in adults, due to enhanced glutathione conjugation (primary route of elimination) in children (47). As a result, steady-state plasma concentrations of busulfan resulting from a standard dose were lower in young children (Figure 23.9). Although the incidence and severity of busulfan-related toxicity was also lower in young children, the graft rejection rate was significantly higher (48).

Differences in the relative size of body organs or tissues between children and adults can also impact the pharmacokinetics of drugs. The liver and kidney are relatively larger in newborns compared to adults. Liver size as a percentage of total body weight peaks during early childhood, and this coincides with the enhanced clearance of hepatically metabolized drugs, such as theophylline. A correlation of drug clearance with liver mass is less apparent for drugs metabolized by enzymes with substantial extrahepatic expression, such as CYP3A4, CYP3A5, and isoforms of glucuronyltransferase (18).

The size of the central nervous system (CNS), which is disproportionately larger in infants as compared to adults, has a quantifiable effect on drug concentrations achieved in the cerebrospinal fluid (CSF) after intrathecal administration of drugs, and influences the dosing of intrathecal therapy in infants and young children. For example, CSF methotrexate concentrations after

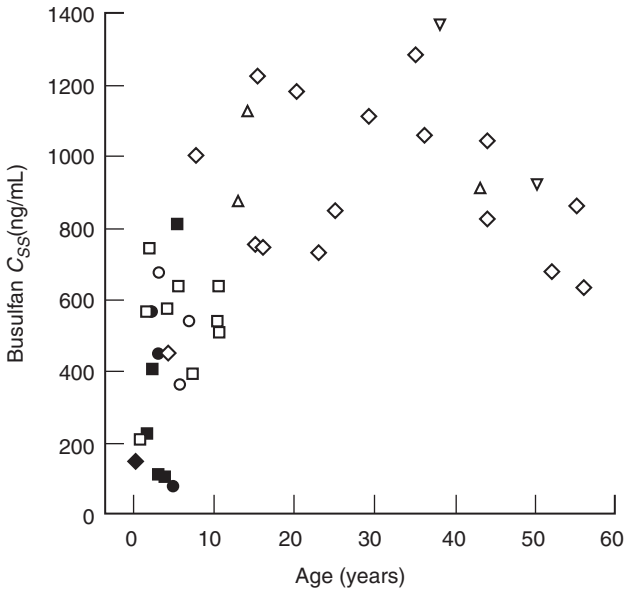

FIGURE 23.9 Plasma busulfan steady-state concentrations (C_{SS}) as a function of age. Patients were treated with 16–30 mg/kg of busulfan in combination with cyclophosphamide prior to bone marrow transplant. Closed symbols represent patients who rejected their graft or had a mixed chimera. Patients who experienced grade 0 treatment-related toxicity are designated by circles; grade 1 toxicity by squares; grade 2 toxicity, by diamonds; grade 3 toxicity, by upright triangles; and grade 4 toxicity, by inverted triangles. Young children had substantially lower C_{SS}, less toxicity, and were at greater risk for graft rejection. (Data from Slattery JT *et al*. Bone Marrow Transplant 1995;16:31–42.)

an intrathecal dose of 12 mg/m^2 are age dependent (Figure 23.10A) (49). Higher CSF concentrations were observed in adults, intermediate concentrations in adolescents, and low concentrations in children. The low concentrations in children also were associated with an increased risk of treatment failure. The physiologic reason for this age discrepancy relates to the difference in the rate of growth of the CNS relative to the rest of the body (Figure 23.10B). By 3 years of age, CNS volume is 80% of the adult volume, while BSA, on which the methotrexate dose is based, increases at a slower rate toward the eventual adult value. If the dose of an intrathecally administered drug is calculated based on BSA, young children receive a lower dose relative to their CNS volume than do adults. Based on this observation, a pharmacokinetically guided, age-based intrathecal dosing schedule was devised for methotrexate. Patients less than 1 year of age receive 6 mg, patients who are 1 year old receive 8 mg, patients who are 2 years old receive 10 mg, and patients 3 years of age and older receive a 12-mg dose. With this age-adjusted dosing schedule, CSF methotrexate concentrations were less variable than with the standard 12-mg/m^2 dose, even though this adaptive dosing schedule results in a >50% absolute dose increase in young children and a lower dose in patients older than 10 years (Figure 23.11) (49). The age-adjusted dosing regimen for intrathecal methotrexate has had a

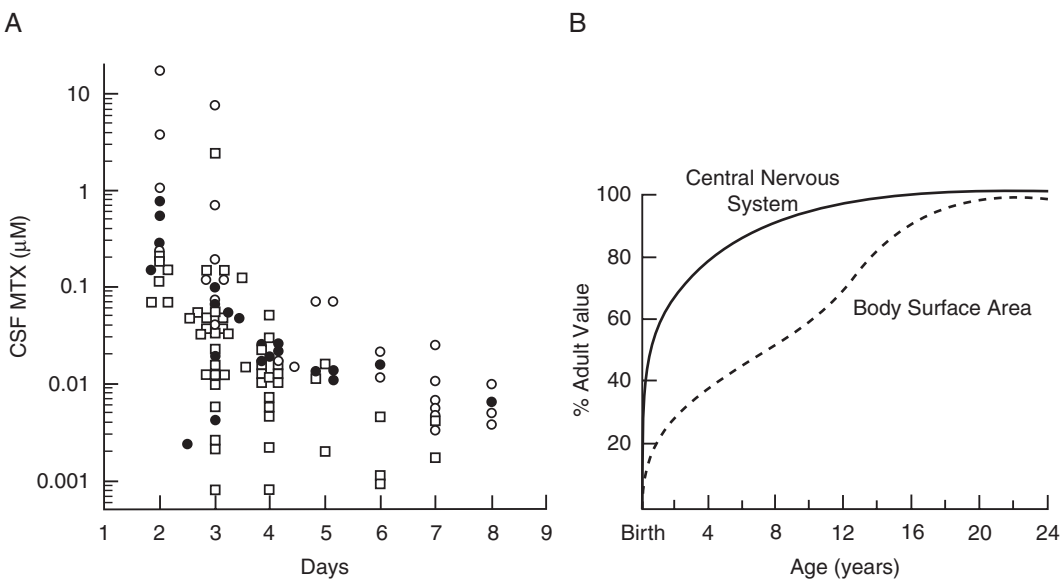

FIGURE 23.10 (A) Cerebrospinal fluid (CSF) methotrexate N(MTX) concentrations after an intrathecal dose of 12 mg/m^2. Children designated as open squares and adolescents designated as closed circles had lower concentrations than did adults represented as open circles, and lower concentrations were associated with a higher risk of treatment failure. (B): Growth rate of central nervous system volume relative to whole body growth represented by body surface area. (Reproduced with permission from Bleyer WA. Cancer Treat Rep 1977;61:1419–25.)

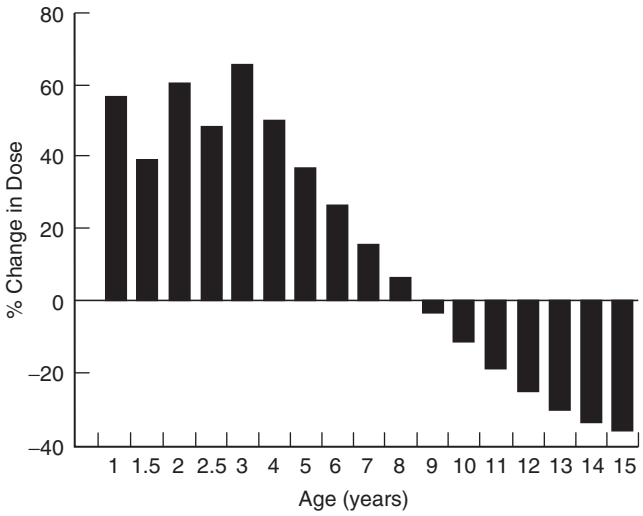

FIGURE 23.11 Percentage change in the dose of intrathecal methotrexate using the age-adjusted dosing schedule (<1 yr, 6 mg; 1 yr, 8 mg; 2 yr, 10 mg; ≥ 3 yr, 12 mg) relative to administering a 12-mg/m^2 dose adjusted to body surface area (horizontal line at 0%).

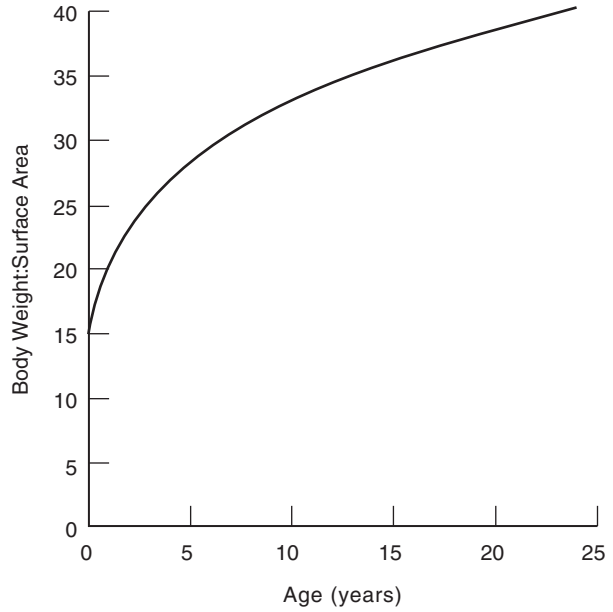

FIGURE 23.12 Relationship between body weight and body surface area during childhood and adolescence.

significant impact on the efficacy of preventative therapy in children with acute lymphoblastic leukemia. The overall CNS relapse rate was significantly lower with the new regimen and the greatest improvement occurred in children <3 years of age (50).

For most systemically administered drugs, specific adaptive dosing methods, such as those developed for intrathecal methotrexate, do not exist, and the dose is usually scaled to body weight or surface area. Figure 23.12 depicts the relationship between weight and BSA at various ages. BSA is greater relative to weight in newborns, but weight increases more rapidly than does BSA during childhood and adolescence. Many physiologic parameters, such as cardiac output, blood volume, extracellular fluid volume, GFR, renal blood flow, and metabolic rate, are better correlated with BSA than with weight. As a general rule, drug doses developed in adults or older children that are normalized to weight will result in a lower dose in infants than when scaling doses are normalized to BSA from adults to infants. For example, when normalized to body weight, the clearance of zidovudine is higher in younger than in older children (Figure 23.13), indicating that scaling the dose to body weight will result in lower serum concentrations at a given dose in the younger age group (5). Clinical experience has shown that dosing according to BSA usually results in more uniform plasma drug concentrations across a broad age range.

On the other hand, scaling the dose to BSA may not always be the best method for dosing infants. Vincristine is an anticancer drug that causes peripheral neuropathy, and, in clinical trials, younger patients appeared to be more susceptible to this toxicity. Vincristine clearance based on BSA was lower in infants compared to older children and adolescents (Figure 23.14), thus a dose scaled to BSA would result in higher plasma concentrations in younger patients

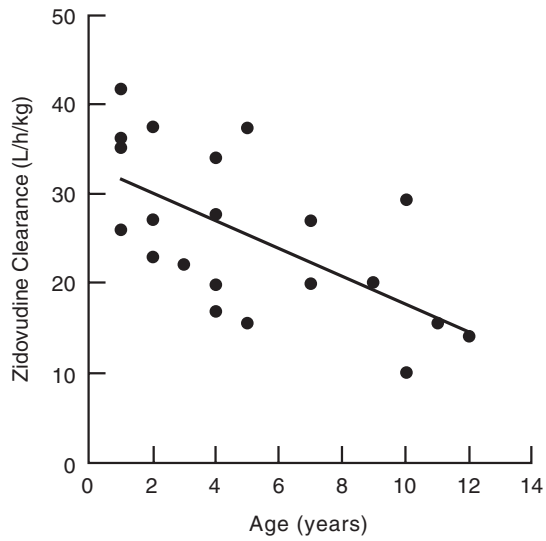

FIGURE 23.13 Relationship between age and zidovudine clearance normalized to body weight. (Data from Balis F *et al*. J Pediatr 1989;114:880–4.)

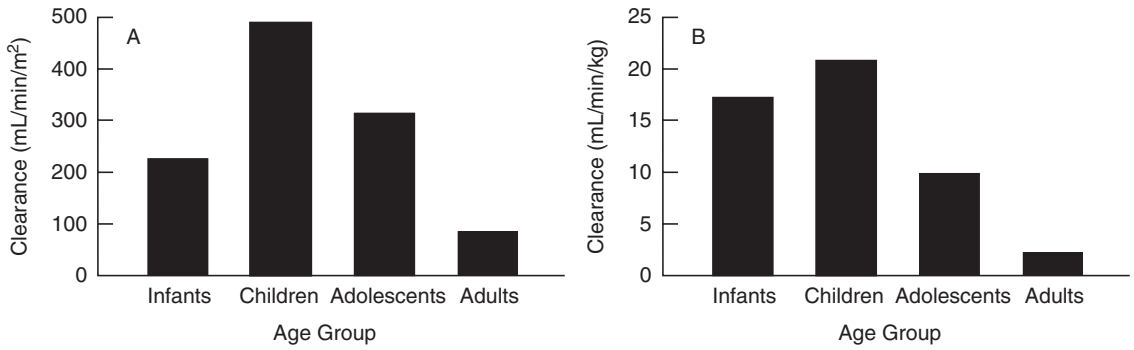

FIGURE 23.14 Comparison of vincristine clearance normalized to body surface area (A) with clearance normalized to body weight (B) in infants, children, adolescents, and adults. This drug is unusual in that the risk of developing neurotoxicity is greater for infants dosed on the basis of body surface area than when doses are based on body weight. (Reproduced with permission from Crom WR, *et al*. J Pediatr 1994;125:642–9.)

and would account for the greater toxicity. For this reason, the vincristine dose for infants is now routinely scaled to body weight, resulting in a lower vincristine dose and less toxicity in this age group (51).

Effect on Pharmacodynamics

The effect of normal growth and development on the pharmacodynamics of drugs has been less well studied. Age-dependent variation in receptor number, receptor affinity for drugs, or the responsiveness of the target organ or tissue to receptor occupancy could influence drug effect. Drugs may also alter the growth and development process or express effects that are dependent on the stage of development, such as the enamel dysplasia caused by tetracycline in young children or the depression of linear growth by corticosteroids.

Age-dependent, receptor-mediated drug effects have been observed with dopamine. The effect of dopamine on blood flow (estimated by measuring the pulsatility index by ultrasonography) was assessed in the right renal, superior mesenteric, and middle cerebral arteries in sick premature infants (52). Renal blood flow increased during the dopamine infusion, but mesenteric and cerebral blood flow were not altered. In adults, dopamine does increase blood flow to the intestine, indicating that the lack of response in preterm neonates is related to the immaturity of the mesenteric vascular bed.

Effect of Childhood Diseases

The spectrum of diseases that occur in the pediatric population is also quite different than diseases that afflict adults, and the effect of pediatric diseases on the pharmacokinetics and pharmacodynamics of the drugs used to treat these diseases requires more study. For example, in cystic fibrosis, the major organs associated with drug disposition, including the gastrointestinal tract, pancreas, heart, liver, and kidney, can be affected. The underlying defect in chloride transport can cause inspissated secretions, leading to tissue damage of these organs and tissues. Surprisingly, the clearance of a wide variety of drugs, including drugs that are metabolized by the liver and drugs that are excreted by the kidney, is enhanced in patients with cystic fibrosis (Figure 23.15). The exact mechanism of the increased clearance is not clear, but these patients require larger doses of antibiotics to

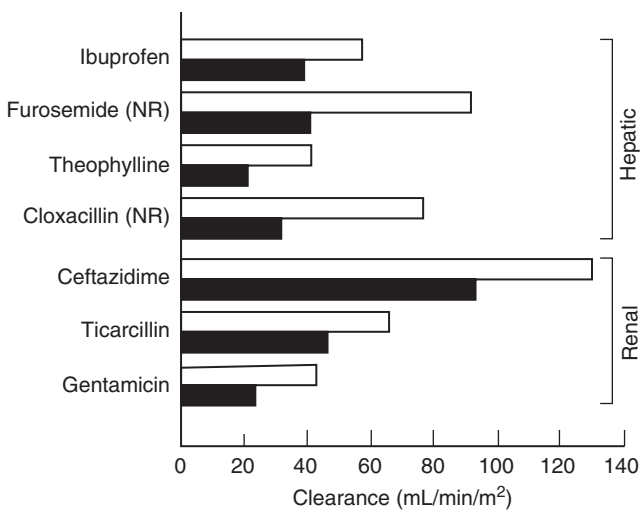

FIGURE 23.15 Comparison of hepatic and renal clearance of selected drugs in children with cystic fibrosis (*open bars*) and in controls (*solid bars*). Clearance is enhanced in patients with cystic fibrosis. (Data from Rey E *et al*. Clin Pharmacokinet 1998;35:313–29.)

achieve therapeutic plasma drug concentrations than do children who do not have cystic fibrosis (53).

CONCLUSIONS

Consideration of the impact of developmental changes occurring throughout the newborn period, infancy, childhood, and adolescence will lead to more rational, safer, and more effective use of drugs in the pediatric population. The examples in this chapter highlight the substantial impact of normal growth and development on the pharmacokinetics and pharmacodynamics of drugs, and emphasize the need for separate detailed clinical studies in newborns and children. To date, pediatric clinical trials have not been systematically performed for either marketed or new drugs, because of economic, ethical, and technical factors.

Pediatric diseases are rare relative to adult diseases. Thus, for most drugs, the pediatric market share is small and there has been little financial incentive for pharmaceutical companies to perform studies in children for the purpose of developing specific labeling for childhood disease, either during initial development or after marketing approval has been obtained. New FDA regulations are designed to rectify this situation by requiring testing in pediatric populations and by providing incentives to pharmaceutical companies for completing those studies.[1]

Ethical constraints have also contributed to the hesitancy to perform studies in the pediatric population. Under current federal regulations governing biomedical research, children are afforded special protection. These federal regulations limit research studies that do not provide direct benefit to the pediatric subjects that participate. This means that drug studies can only be performed in children who have the disease that the drug is intended to treat. Thus, unlike initial drug testing in normal adult volunteers, the initial pharmacokinetic and safety testing usually cannot be done in normal pediatric volunteers (54). Compounding this is the fact that it is technically more challenging to perform research in children, especially in newborns, in whom the most dramatic developmental changes occur.

The Pediatric Pharmacology Research Unit (PPRU) is a network of experienced clinical investigators committed to facilitating pharmacological research in the pediatric medical community (55). Acting as a consortium, the PPRU has the potential to provide access to a very large population of infants and children with varied diagnoses. The PPRU offers expertise in pediatric pharmacology and in the conduct of biomedical research involving children.[2]

REFERENCES

1. Lietman PS. Chloramphenicol and the neonate-1979 view. Clin Perinatol 1979;6:151–62.
2. Burns LE, Hodgman JE, Cass AB. Fatal circulatory collapse in premature infants receiving chloramphenicol. N Engl J Med 1959;261:1318–21.
3. Weiss CF, Glazko AJ, Weston JK. Chloramphenicol in the newborn infant. N Engl J Med 1960;262:787–94.
4. Klecker RW Jr, Collins JM, Yarchoan R, Thomas R, Jenkins JF, Broder S, Myers CE. Plasma and cerebrospinal fluid pharmacokinetics of 3′-azido-3′-deoxythymide: A novel pyrimidine analog with potential application for the treatment of patients with AIDS and related diseases. Clin Pharmacol Ther 1987;41:407–12.
5. Balis F, Pizzo P, Eddy J, Wilfert C, McKinney R, Scott G, Murphy RF, Jaronsinski PF, Falloon J, Poplack DG. Pharmacokinetics of zidovudine administered intravenously and orally in children with human immunodeficiency virus infection. J Pediatr 1989;114:880–4.
6. Mirochnick M, Capparelli E, Dankner W, Sperling RS, vanDyke R, Spector SA. Zidovudine pharmacokinetics in premature infants exposed to human immunodeficiency virus. Antimicrob Agents Chemother 1998;42:808–12.
7. Boucher FD, Modlin JF, Weller S, Ruff AA, Mirochnick M, Pelton SP, Wilfert C, McKinney R Jr, Crain MJ, Elkins MM, Blum MR, Prober CG. Phase 1 evaluation of zidovudine administered to infants exposed at birth to the human immunodeficiency virus. J Pediatr 1993;122:137–44.
8. O'Sullivan MJ, Boyer PJ, Scott GB, Parks PW, Weller S, Blum R, Balsley J, Bryson YJ. The pharmacokinetics and safety of zidovudine in the third trimester of pregnancy for women infected with human immunodeficiency virus and their infants: Phase I Acquired Immunodeficiency Syndrome Clinical Trial Group Study (protocol 082) Zidovudine Collaborative Working Group. Am J Obstet Gynecol 1993;168: 1510–6.
9. Connor EM, Sperling RS, Gelber R, Kiselev P, Scott G, O'Sullivan MJ, vanDyke R, Bey M, Shearer W, Jacobson RL, Jimenez E, O'Neill E, Bazin B, Delfraissy J-F, Culnane M, Coombs R, Elkins M, Moye J, Stratton P, Balsley J. Reduction of maternal–infant transmission of human immunodeficiency virus type I with zidovudine treatment. N Engl J Med 1994;331:1173–80.

[1] Additional information on pediatric initiatives by FDA's Center for Drug Evaluation and Research can be found at http://FDA.gov/CDER/pediatric/index.htm.

[2] Information about the Pediatric Pharmacology Research Unit (PPRU) can be found by visiting their link through the National Institute of Child Health and Human Development Center for Research for Mothers and Children; Endocrine, Nutrition, and Growth Branch, at http://www.nichd.nih.gov/crmc/eng/eng.htm.

10. Loebstein R, Koren G. Clinical pharmacology and therapeutic drug monitoring in neonates and children. Pediatr Rev 1998;19:423–8.
11. Friedman M, Shalala DE. Regulations requiring manufacturers to assess the safety and effectiveness of new drugs and biological products in peditric patients (21 CRF Parts 201, 312, 314, and 601). Federal Register 1998;63:66632–72.
12. Cooper KJ. Pediatric marketing exclusivity — as altered by the Best Pharmaceuticals for Children Act of 2002. Food Drug Law J 2002;57:519–44.
13. Steinbrook R. Testing medications in children. N Engl J Med 2002;347:1462–70.
14. McKinney RE Jr. Congress, the FDA, and the fair development of new medications for children. Pediatrics 2003;112:669–70.
15. Hirschfeld S. Pediatric Patients and Drug Safety. J Pediatr Hematol Oncol 2005;27:122–4.
16. Leeder JS, Adciock K, Gaedigk A, Gotschall R, Wilson JT, Kearns GL. Delayed maturation of cytochrome P450 3A (CYP3A) activity *in vivo* in the first year of life [abstract]. Pediatr Res 2000;**47**:472A.
17. Hubbard W. International conference on harmonisation; E11: Clinical investigation of medicinal products in the pediatric population. Federal Register 2000;65:19777–81.
18. Kearns G, Abdel-Rahman SM, Alander SW, Blowey DL, Leeder, JS, Kauffman RE. Developmental pharmacology — Drug disposition, action, and therapy in infants and children. N Engl J Med 2003;349:1157–67.
19. Routledge P. Pharmacokinetics in children. J Antimicrob Chemother 1994;34(suppl A):19–24.
20. Reed MD, Besunder JB. Developmental pharmacology: Ontogenic basis of drug disposition. Pediatr Clin North America, 1989;36:1053–74.
21. Linday L, Dobkin JF, Wang TC, Butler VP Jr, Saha JR, Lindenbaum R. Digoxin inactivation by the gut flora in infancy and childhood. Pediatrics 1987;79:544–8.
22. Kurtz H, Michels H, Stickel HH. Differences in the binding of drugs to plasma proteins from newborns and adult man. Eur J Clin Pharmacol 1977;11:469–72.
23. Morselli PL. Clinical pharmacology of the perinatal period and early infancy. Clin Pharmacokinet 1989;**17**(suppl 1):13–28.
24. Kaufman RE. Pediatric pharmacology. In: Aranda JV, Yaffe SJ, editors. Pediatric pharmacology, therapeutic principles in practice. Philadelphia: WB Saunders; 1992. p. 212–19.
25. Kearns GL, Reed MD. Clinical pharmacokinetics in infancy and children, a reappraisal. Clin Pharmacokinet 1989;17(suppl 1):29–67.
26. Aranda J, Varvarigou A, Beharry K, Bansal R, Bardin C, Modanlou H *et al*. Pharmacokinetics and protein binding of intravenous ibuprofen in premature newborn infant. Acta Paediatr 1997;86:289–93.
27. Pikkarainen PH, Raiha NC. Development of aldohol dehydrogenase activity in human liver. Pediatr Res 1967;1:165–8.
28. de Wildt S, Kearns GL, Leeder S, van den Anker JN. Glucuronidation in humans. Clin Pharmacokinet 1999;36:439–52.
29. Miller RP, Roberts JR, Fischer LJ. Acetaminophen elimination kinetics in neonates, children, and adults. Clin Pharmacol Ther 1976;19:284–94.
30. Kearns GL. Pharmacogenetics and development: Are infants and children at increased risk for adverse outcomes? Curr Opin Pediatr 1995;**7**:220–33.
31. Blake MJ, Castro L, Leeder JS, Kearns GL. Ontogeny of drug metabolizing enzymes in the neonate. Semin Fetal Neonatal Med 2005;10:123–38.
32. de Wildt S, Kearns GL, Leeder S, van den Anker JN. Cytochrome P450 3A ontogeny and drug distribution. Clin Pharmacokinet 1999;37:485–505.
33. Cresteil T. Onset of xenobiotic metabolism in children: Toxicological implications. Food Addit Contam 1998;15:45–51.
34. Oesterheld JR. A review of developmental aspects of cytochrome P450. J Child Adolesc Psychopharmacol 1998;8:161–74.
35. Lacroix D, Sonnier M, Moncion A, Cheron G, Cresteil T. Expression of CYP3A in the human liver — evidence that the shift between CTP3A7 and CYP3A4 occurs immediately after birth. Eur J Biochem 1997;247:625–34.
36. Treluyer J-M, Rey E, Sonnier M, Pons G, Cresteil T. Evidence of impaired cisapride metabolism in neonates. Br J Clin Pharmacol 2001;52:419–25.
37. Kearns GL, Robinson PK, Wilson JT, Wilson-Costelo D, Knight GR, Ward RM, van den Anker JN; Pedatric Pharmacology Research Unit Network. Cisapride disposition in neonates and infants: In vivo reflection of cytochrome P450 3A4 ontogeny. Clin Pharmacol Ther 2003;74:312–25.
38. Treluyer J, Jacqz-Aigrain E, Alvarez F, Cresteil T. Expression of CYP2D6 in developing human liver. Eur J Biochem 1991;202:583–8.
39. Pons G, d'Athis P, Rey E, deLauture D, Richard MO, Badoul J, Olive G. Gentamicin monitoring in neonates. Ther Drug Monit 1988;10:42–7.
40. Aperia A, Broberger O, Thodenius K, Zetterstrom R. Development of renal control of salt and fluid homeostasis during the first year of life. Acta Pediatr Scand 1975;64:393–8.
41. Guignard J, Torrado A, Da Cunha O, Gautier E. Glomerular filtration in the first three weeks of life. J Pediatr 1975;87:268–72.
42. Kraus DM, Fischer JH, Reitz SJ, Kecskes SA, Yeh TF, McCulloch KM, Tung EC, Cwik MJ. Alterations in theophylline metabolism during the first year of life. Clin Pharmacol Ther 1993;54:351–9.
43. Grygiel JJ, Birkett DJ, Phill D. Effect of age on patterns of theophylline metabolism. Clin Pharmacol Ther 1980;28:456–62.
44. Ueno K, Kasuhiko T, Shokawa M, HoriuchiY. Age-dependent changes of renal clearance of theophylline in asthmatic children [letter]. Ann Pharmacother 1994;28:281–2.
45. Tserng K-Y, Takieddine FN, King KC. Developmental aspects of theophylline metabolism in premature infants. Clin Pharmacol Ther 1983;33:522–8.
46. Milavetz G, Vaughan LM, Weinberger MM, Hendeles L. Evaluation of a scheme for establishing and maintaining dosage of theophylline in ambulatory patients with chronic asthma. J Pediatr 1986;109:351–4.
47. Gibbs JP, Murray G, Risler L, Chien JY, Dev R, Slattery JT. Age-dependent tetrahydrothiophenium

ion formation in young children and adults receiving high-dose busulfan. Cancer Res 1997;57:5509–16.
48. Slattery JT, Sanders JE, Buckner RL, Schaffer RL, Lambert KW, Langer FP, Anasetti C, Bensinger WI, Fisher LD, Appelbaum FR, Hansen JA. Graft-rejection and toxicity following bone marrow transplantation in relation to busulfan pharmacokinetics. Bone Marrow Transplant 1995;16:31–42.
49. Bleyer WA. Clinical pharmacology of intrathecal methotrexate. II. An improved dosage regimen derived from age-related pharmacokinetics. Cancer Treat Rep 1977;61:1419–25.
50. Bleyer WA, Coccia PF, Sather HN, Level C, Lukens J, Niebrugge DJ *et al*. Reduction in central nervous system leukemia with a pharmacokinetically dervived intrathecal methotrexate dosage regimen. J Clin Oncol 1983;1:317–25.
51. Crom WR, deGraaf SS, Synold T, Uges DR, Bloemhoef H, Rivera G, Christensen M, Mahmoud H, Evans WE. Pharmacokinetics of vincristine in children and adolescents with acute lymphocytic leukemia. J Pediatr 1994;125:642–9.
52. Seri I, Abbasi S, Wood DC, Gerdes JS. Regional hemodynamic effects of dopamine in the sick preterm neonate. J Pediatr 1998;133:728–34.
53. Rey E, Treluyer T-M, Pons G. Drug disposition in cystic fibrosis. Clin Pharmacokinet 1998;35:313–29.
54. American Academy of Pediatrics Committee on Drugs. Guidelines for the ethical conduct of studies to evaluate drugs in pediatric populations. Pediatrics 1995;95:286–94.
55. Cohen S. The Pediatric Pharmacology Research Unit (PPRU) Network and its role in meeting pediatric labeling needs. Pediatrics 1999;105:664–5.

This page intentionally left blank

CHAPTER

24

Drug Therapy in the Elderly

DARRELL R. ABERNETHY
Gerontology Research Center, National Institute on Aging, Baltimore, Maryland

INTRODUCTION

A hallmark of aging in humans is the development of multiple, coexisting physiological and pathophysiological changes that may benefit from drug therapy. It is not uncommon for the older individual to have 5 to 10 diagnoses, each of which has one or more proved beneficial therapies (Table 24.1). Examples abound: hypertension, coronary artery disease, osteoarthritis, osteoporosis, type 2 diabetes mellitus, and treated prostate or breast cancer often coexist in an individual patient. In addition, treatable insomnia, depression, and anxiety may be present, either independently or associated with primary medical illnesses. As the number of individuals who are greater than 85 years old dramatically increases, the incidence of Alzheimer's disease and other forms of cognitive impairment for which somewhat effective treatment is available will increase as well (Figure 24.1). This will increase medication exposure and the potential for drug interactions (see Chapter 15) even more. With the availability of medications that are in many instances dramatically effective, it is imperative to understand the impact of multiple current medications (high drug burden) on the older individual.

A number of studies over the past three decades have demonstrated that the likelihood of adverse drug effect increases with the number of drugs prescribed (1, 2). There is a disproportionate increase in both total and severe adverse drug reactions when more than five drugs are coadministered (3). Adverse drug effects also are more likely in older patients when certain drugs, such as warfarin, theophylline, or digoxin, are among the drugs prescribed. However, the absolute number of drugs the patient concurrently receives is probably the best predictor of an adverse drug event (Figure 24.2) (2).

Further complicating this issue is the fact that the relative therapeutic benefit of treatments such as thrombolytic therapy, hypocholesterolemic therapy, postmyocardial infarction β-locker treatment, and angiotensin-converting enzyme inhibitor treatment in congestive heart failure in patients over the age of 75 is similar to that seen in younger patients. Unfortunately, these data create a dilemma in that dramatic therapeutic advances have been made for many illnesses that afflict the elderly, yet administration of multiple medications increases the likelihood of adverse drug events.

PATHOPHYSIOLOGY OF AGING

It is useful to think of the aging process in physiological, not chronological terms. That being said, a chronological definition is often used to stratify the aging population into three groups: *young old*, age 65–75 years; *old*, age 75–85 years; and *old old*, age ≥85 years. Nearly all of the research that describes pharmacokinetics and pharmacodynamics in older individuals has been obtained from study of the young old, that is, individuals ≤75 years old. Therefore, the validity of extrapolating these findings to the older age groups may be questioned. In contrast, the data describing adverse drug events in older as compared to younger patients are obtained from patient

TABLE 24.1 Age-Related Chronic Medical Conditions[a]

Condition	Frequency per 1000 Persons in the United States		
	Age < 45 years	Age 46–64 years	Age > 65 years
Arthritis	30	241	481
Hypertension	129	244	372
Hearing impairment	37	141	321
Heart disease	31	134	295
Diabetes	9	57	99
Visual impairment	19	48	79
Cerebrovascular disease	1	16	63
Constipation	11	19	60

[a] From Zisook S, Downs NS. J Clin Psych 1998;59(suppl 4):80–91; data from Dorgan CA, editor. Statistical record of health and medicine. New York: International Thompson Publishing Co; 1995.

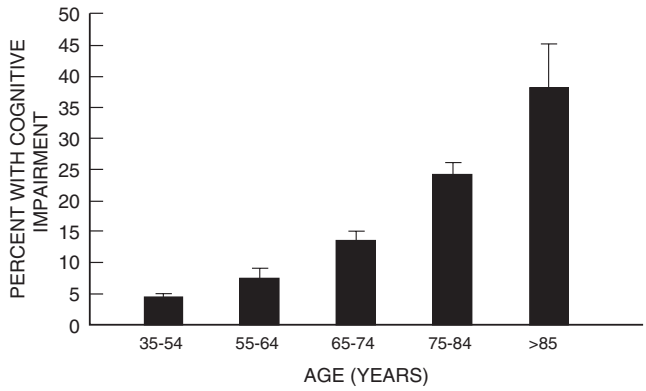

FIGURE 24.1 Age-related impairment in cognitive function as defined by six or more errors in the Mini-Mental Status Exam. (Data from Robins LN, Regier DA, editors. Psychiatric disorders in America: the Epidemiolgic Catchment Area Study. New York: The Free Press; 1991.)

populations and databases the include the full age spectrum of the elderly. The general physiological changes that occur with aging can be characterized as a decrease in maximum performance capacity and loss of homeostatic reserve (4). Although these changes occur to different degrees for each organ system or function, they are present in individuals who are in good health and are accentuated in individuals during illness.

Placed in the context of response to drugs, it is most useful to discuss age-related physiological changes that occur in integrated functions. Systemic drug responses are the result of the complex interaction of specific and nonspecific drug effects, and the direct and indirect physiological or pathological responses to these drug effects. The sum of these effects is the pharmacodynamic response that is observed, whether therapeutic or toxic. Therefore, the age-related changes that occur in physiological or psychological function prior to drug exposure are helpful in predicting and describing a particular drug response.

The observed pharmacodynamic response is the result of extent of drug exposure, determined by drug pharmacokinetics (Table 24.2), and sensitivity

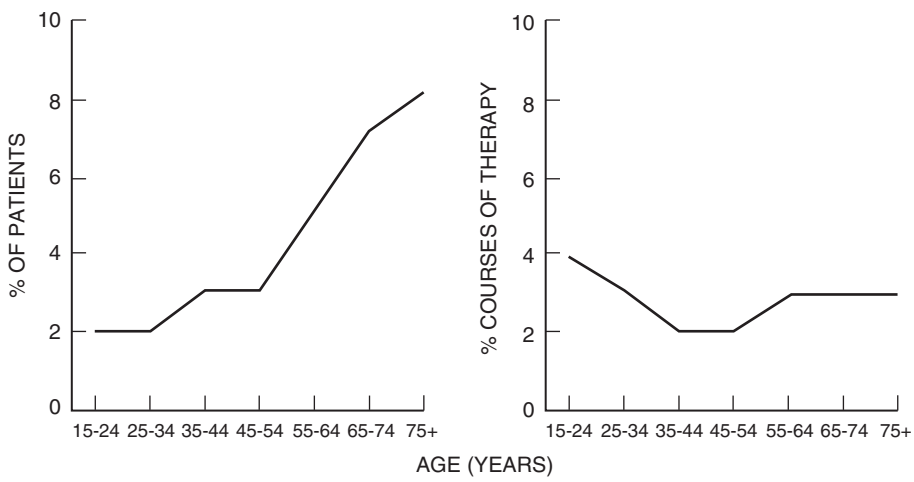

FIGURE 24.2 The relationship of increasing age and likelihood of adverse drug events (*left panel*), and the relationship of increasing age and adverse drug reactions when corrected for number of drugs per patient (*right panel*). (Reproduced with permission from Gurwitz JH, Avorn J. Ann Intern Med 1991;114:956–66.)

TABLE 24.2 Pharmacokinetic Changes in the Elderly

Process	Change with age
Gastrointestinal absorption	—
Drug distribution	
Central compartment volume	— or ↓
Peripheral compartment volume	
Lipophilic drugs	↑↑
Hydrophilic drugs	↓↓
Plasma protein binding	
Binding to albumin	↓
Binding to α_1-acid glycoprotein	— or ↑
Drug elimination	
Renal elimination	↓↓
Hepatic metabolism	
Phase I reactions	
CYP3A	↓
CYP1A2	— or ↓
CYP2D6	— or ↓
CYP2C9	— or ↓
CYP2C19	— or ↓
CYP2E1	— or ↓
Phase II reactions	
Glucuronidation	—
Sulfation	—
Acetylation	—

to a given drug exposure, determined by the state of function of the effectors of drug response such as receptor–cellular transduction processes (Figure 24.3). We will discuss the age-related changes that have been described for renal drug elimination and hepatic and extrahepatic drug biotransformations. We will then briefly review the age-related changes that have been described for central nervous system function, autonomic nervous system function, cardiovascular function, and renal function. These functions are selected, as each has been rather comprehensively evaluated in the healthy elderly and a great diversity of drugs can have adverse as well as beneficial effects on these functions. We will describe and/or predict the effect of these changes on drug pharmacodynamics at a given drug exposure for drug groups commonly used in older patients. Due to incidence and prevalence of cancer in older patients, we will review the information available to guide cancer chemotherapy in this patient group. Finally, we will discuss drug groups for which increased age confers greater risk for drug toxicity, along with the mechanism when known.

AGE-RELATED CHANGES IN PHARMACOKINETICS

Age-Related Changes in Renal Clearance

The most consistent and predictable age-related change in drug pharmacokinetics is that of renal clearance of drugs. Renal function, including renal blood flow, glomerular filtration rate, and active renal tubular secretory processes, all decline with increasing age (5). Although there is considerable variability in this decline, an approximation of the decline in glomerular filtration rate has been usefully characterized by the Cockroft–Gault equation described in Chapter 1 and discussed as a guide to drug dosing

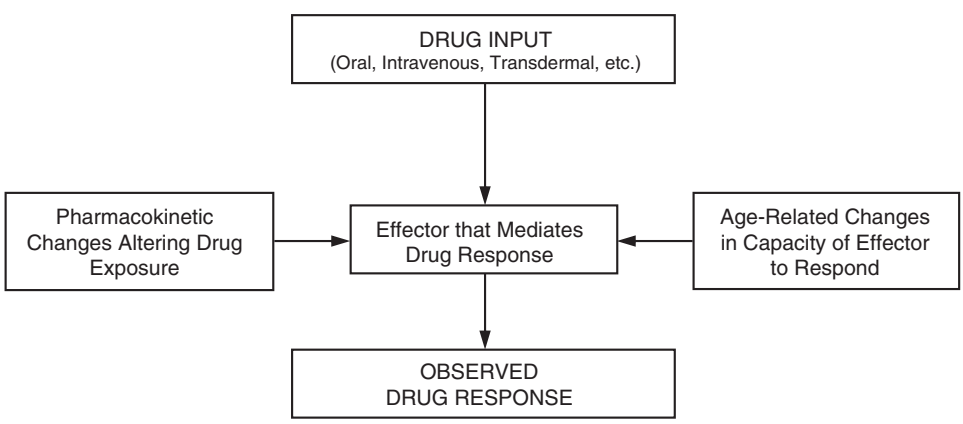

FIGURE 24.3 Observed drug responses in elderly patients represent the combined effects of drug input and age-related pharmacokinetic and pharmacodynamic changes.

TABLE 24.3 Some Drugs with Decreased Clearance in the Elderly

Route of clearance	Representative drugs
Renal	All aminoglycosides, vancomycinm, digoxin, procainamide, lithium, sotalol, atenolol, dofetilide, cimetidine
Single Phase I metabolic pathway CYP3A	Alprazolam, midazolam, triazolam, verapamil, diltiazem, dihydropyridine calcium channel blockers, lidocaine
CYP2C	Diazepam, phenytoin, celecoxib
CYP1A2	Theophylline
Multiple Phase I metabolic pathways	Imipramine, desipramine, trazodone, hexobarbital, flurazepam

in Chapter 5 (6). For men, creatinine clearance can be estimated from this equation as follows:

$$CL_{CR}\,(\text{mL/min}) = \frac{(140 - \text{age})(\text{weight in kg})}{72(\text{serum creatinine in mg/dL})}$$

For women, this estimate should be reduced by 15%.

Drugs that are eliminated primarily by glomerular filtration, including aminoglycoside antibiotics, lithium, and digoxin, have an elimination clearance that decreases with age in parallel with the decline in measured or calculated creatinine clearance (7–9). The renal clearance of drugs undergoing active renal tubular secretion also decreases with aging (Table 24.3). For example, the decrease in renal tubular secretion of cimetidine has been shown to parallel the decrease in creatinine clearance in older patients (10). On the other hand, the renal clearance/creatinine clearance *ratio* of both procainamide and *N*-acetylprocainamide decreases in the elderly, indicating that with aging the renal tubular secretion of these drugs declines more rapidly than creatinine clearance does (11).

Age-Related Changes in Hepatic and Extrahepatic Drug Biotransformations

Drug biotransformations occur in quantitatively important amounts in the liver, gastrointestinal tract, kidneys, lung, and skin. However, nearly all organs have some metabolic activity. As described in Chapter 11, *in vivo* drug biotransformations are commonly separated into Phase I and Phase II biotransformations. Phase I biotransformations are catalyzed by membrane-bound enzymes found in the endoplasmic reticulum and Phase II biotransformations occur predominantly in the cytosol, with the exception of the UDP-glucuronosyltransferases that are membrane bound to the endoplasmic reticulum membranes. Phase I biotransformations are primarily catalyzed by enzymes of the cytochrome P450 monoxygenase system (CYP450), with the important members of this enzyme family for drug biotransformations being CYP3A, CYP2D6, CYP2C, CYP1A2, and CYP2E1.

Phase I biotransformations catalyzed by CYP3A have most consistently been shown to be decreased in aging, with the decrease on the order of 10–40%. The drugs studied that are prototype CYP3A substrates and exemplify this are midazolam and triazolam (12, 13). The result of this decrease in drug biotransformation is decreased metabolic clearance and increased exposure to drug of the individual at a given dose. The clinical consequence of this is that older patients treated with a given dose of triazolam experience increased sedation and impaired task performance (14). Quantitatively significant CYP3A activity in the gastrointestinal wall, which catalyzes biotransformation of drugs prior to and during absorption, has been demonstrated. However, it is unknown if this is altered in aging as well (16).

There is some suggestion that Phase I biotransformations catalyzed by CYP2C are decreased with age, with modest decreases in clearance of warfarin (CYP2C9) and phenytoin (CYP2C19) reported in older individuals. However, this is much less well established (17, 18). Similarly, Phase I biotransformation by CYP1A2 may be somewhat decreased in older individuals, and decreased theophylline and caffeine clearances have been reported (19). However, this too is not well established.

Phase II biotransformations are little changed with aging, based on studies of glucuronidation, sulfation, and acetylation. Prototype substrates studied for glucuronidation have been lorazepam and oxazepam; for sulfation, acetaminophen; and for acetylation, isoniazid and procainamide.

As discussed in Chapter 14, genetic polymorphisms for the Phase I enzymes (CYP2D6 and CYP2C19) and the Phase II enzymes (*N*-acetyltransferase and the methyltransferases thiopurine methyltransferase, catechol *O*-methyl transferase, and thiol methyltransferase) may significantly alter exposure to relevant drug substrates. Evaluation of the frequency

of polymorphic variants with increasing age has consistently shown that the same frequencies occur in older individuals as in younger individuals.

AGE-RELATED CHANGES IN EFFECTOR SYSTEM FUNCTION

Central Nervous System

It is important to separate age-related and disease-related changes in central nervous system (CNS) function. A number of changes have been noted in the absence of dementing illness, Parkinson's disease, and primary psychiatric disease. Brain aging proceeds in a relatively selective fashion, with the prefrontal cortex and the subcortical monoaminergic nuclei most affected. In the case of the prefrontal cortex, progressive loss of volume with aging is consistently shown. Age-related slowing in mental-processing function is a consistent finding, but the mechanism is uncertain. Aging has been associated with changes in brain activation during encoding and retrieval processes of memory function. Older individuals have more widespread task-related brain activation to conduct the same tasks as compared to younger individuals. One postulate has been that older individuals need to recruit greater brain resources to conduct the same memory function (20). Even in the absence of parkinsonism, the dopaminergic systems are diminished as a function of age. The dopaminergic impairment has been most clearly defined for processes related to dopamine D2 receptors (21).

An important pharmacodynamic principle is that older individuals have increased sensitivity to a given exposure of some CNS depressant drugs. After accounting for age-related pharmacokinetic changes that may cause greater drug exposure at a given dose, the aged individual is more sensitive to the opiate anesthetic induction agents propofol, fentanyl, and alfentanil (22–24). In the case of propofol, the concentration needed to induce anesthesia in a 75-year-old healthy individual was approximately one-half that required for a 25-year-old individual (22, 23). A similar increase in pharmacodynamic sensitivity to fentanyl and alfentanil has been described, with, again, a 50% decease in the dose required to induce the same degree of drug effect in older individuals (up to 89 years) as compared to younger individuals (24). The mechanism for the increased pharmacodynamic sensitivity to these opiates is unknown.

These findings for opiates are in contrast to findings with the barbiturate thiopental and the benzodiazepines midazolam and triazolam (14, 25, 26). Although a substantially lower dose of these drugs is needed to induce anesthesia or the same degree of sedation in older than in younger individuals, this is the result of the pharmacokinetic changes of aging. When drug effect is normalized to arterial drug concentration, the concentration-effect relationship is similar in the young and the elderly. For ambulatory elderly patients, the clinical consequences of increased exposure to benzodiazepines due to decreased Phase I metabolic clearance can be devastating, with an increased incidence of hip fracture noted in older patients taking long half-life benzodiazepines (27). These drugs (e.g., flurazepam and diazepam) undergo Phase I biotransformation, and the decreased clearance seen in the elderly results in markedly greater drug accumulation, even when taken once daily as a sedative-hypnotic (28, 29).

There are fewer data on adverse drug effects caused by neuroleptic and antidepressant drugs in older patients. However, as shown in Figure 24.4, it is now clear that older patients have three- to five-fold higher incidence of tardive dyskinesia than younger patients do when "typical" neuroleptics (e.g., phenothiazines and haloperidol) are administered (30–32). Across studies, 10–20% of younger patients develop tardive dyskinesia after 3 years or more of neuroleptic treatment, while 40–60% of older patients are affected within the same treatment period (32). It is unknown if this is related to age-dependent pharmacokinetic or pharmacodynamic changes. The newer neuroleptics, such as risperidol and olanzapine, have a much lower incidence of tardive dyskinesia in all patient groups studied and may be of considerable clinical utility for this reason (33). However, it will require some time to definitively establish the spectrum of adverse as well as therapeutic effects of these drugs.

There has been less comprehensive analysis of other classes of CNS active drugs, but the general clinical

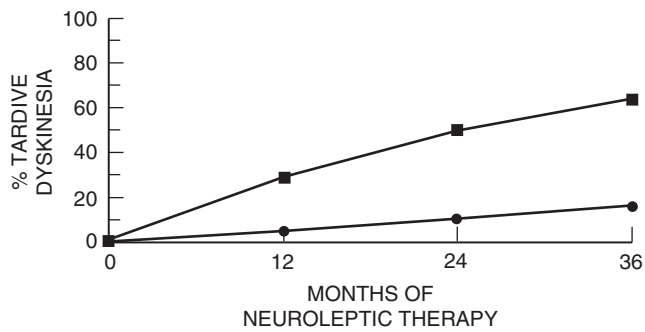

FIGURE 24.4 Cumulative incidence of neuroleptic-induced tardive dyskinesia in old (■) and young (●) adults. (Reproduced with permission from Jeste DV. J Clin Psychiatry 2000;61(suppl 4):27–32.)

impression is that older patients are more sensitive to side effects and require a lower dose of drug to achieve similar therapeutic benefit. Pharmacokinetic studies for lithium, which undergoes renal elimination, and tricyclic antidepressants, which undergo Phase I biotransformation, show decreased clearance on the basis of age-related decrease in renal function and age-related decrease in Phase I drug-metabolizing capacity, respectively (8, 34).

Autonomic Nervous System

The age-related changes in autonomic nervous system (ANS) function are very diverse, and are likely to be associated with many of the age-related changes observed in drug response and toxicity across many therapeutic classes of drugs. Cardiovagal function is diminished, as indicated by age-related decreases in resting heart rate and beat-to-beat heart rate variability. Older individuals have lower vagal tone, as indicated by less increase in heart rate with atropine administration. Other findings consistent with this conclusion are that older individuals have decreased heart rate variation, with deep breathing and reduced increases in heart rate in response to standing. Baroreflex function is also impaired in the healthy elderly, and this is accentuated in the presence of illness common in older patients, such as hypertension and diabetes mellitus (35). Cardiac sympathetic function is also altered, as demonstrated by decreased tachycardic response to isoproterenol and increased circulating plasma norepinephrine (36, 37). An integrated response that reflects many of these age-related changes is that of orthostatic hypotension, which is substantially increased in older individuals (38). The degree of orthostatic decrease in blood pressure in older patients may be particularly evident in the postprandial state and may be exacerbated in older patients who are treated with diuretics (39, 40). Thermoregulatory homeostasis is also impaired in the elderly who have a higher thermoreceptor threshold and decreased sweating when perspiration is initiated (35).

Data are sparse that conclusively establish that altered drug effects result from impaired ANS function, perhaps due to the difficulty in ascribing a particular drug effect to a particular ANS function. However, increased orthostatic hypotension seen at baseline, in addition to drugs that cause sympathetic blockade, such as typical neuroleptics and tricyclic antidepressants, is likely to be a contributing factor to the increased incidence of hip fracture noted in patients receiving these drugs (41). Similarly the anticholinergic effects of many drugs, including antihistamines and neuroleptics, may not only accentuate orthostatic blood pressure changes, but may also be associated with greater cognitive impairment in older individuals. Impaired thermoregulation at baseline may also be accentuated by administration of these drugs because they have potent anticholinergic effects that further disable thermoregulatory responses. It is unclear at this time how age-related ANS changes may relate to the cardiac proarrhythmic effects of drugs that prolong the electrocardiographic QT interval. However, there is a clear association of increasing age with the proarrhythmic effects of neuroleptic drugs (42). It is clear that these ANS changes markedly alter systemic cardiovascular responses to a drug such as the α- and β-adrenergic blocking drug labetalol, which, as shown in Figure 24.5, lowers blood pressure to a greater extent in older than in younger hypertensive

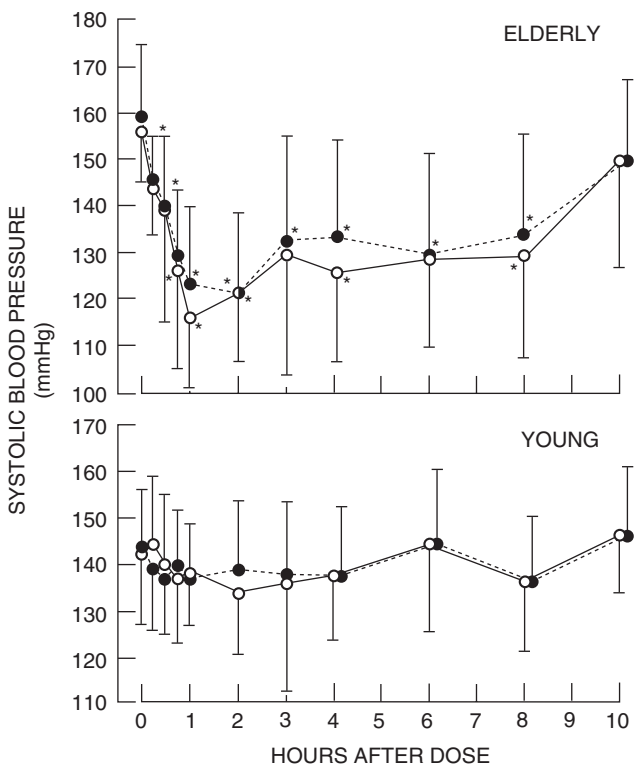

FIGURE 24.5 Comparison of changes in erect (○) and sitting (●) systolic blood pressures between elderly (*upper panel*) and young (*lower panel*) hypertensive patients treated with a daily oral labetalol dose of 200 mg. Bars represent the standard deviation from the mean and asterisks indicate values that are significantly different ($P < 0.05$) from the baseline in that posture for the respective group. No differences were noted between sitting and standing blood pressure for either group. (Reproduced with permission from Abernethy DR, Schwartz JB, Plachetka JR, Todd EL, Egan JM. Am J Cardiol 1987;60:697–702.)

patients while decreasing heart rate to a much lesser extent (43).

Cardiovascular Function

The age-related changes in cardiovascular function that relate to drug responses are usefully separated into changes in cardiac and changes in peripheral vascular function. But this separation must be made with the understanding that the pharmacodynamic responses seen are generally an integrated function of ANS, cardiac, and peripheral vascular function.

Cardiac output at rest is not substantially changed with age in the absence of superimposed cardiac disease. However, components of the cardiac cycle are indeed changed. Heart rate is decreased, reflecting the decrease in parasympathetic withdrawal noted previously, and perhaps impaired β-adrenergic and sinoatrial function. Left ventricular mass and left ventricular stroke volume are increased, which allows cardiac output to be maintained in the face of decreased heart rate. However, diastolic relaxation is slowed, making the late left ventricular filling that is associated with atrial contraction a more important determinant of stroke volume in the elderly. Chronotropic response to β-adrenergic stimulation is impaired, but it is uncertain if this is the cause or the result of increased circulating norepinephrine levels (44). Cellular and molecular mechanisms for these changes have been studied in some detail in animal models and may offer some insight into drug responses. The prolonged left ventricular contraction period and slowed diastolic relaxation may be associated with decreased uptake of calcium by the sarcoplasmic reticulum (45). Many potential mechanisms for the impairment in β-adrenoceptor function have been suggested, but this remains controversial.

The pharmacodynamic consequences of these age-related changes can be substantial. Impaired β_1-adrenergic responsiveness results in a decreased tachycardic response to both direct pharmacologic stimulation by drugs, such as isoproterenol (36), and indirect reflex sympathetic stimulation induced by vasodilating drugs, such as the calcium antagonist drug nisoldipine (46). Conversely, the decrease in heart rate caused by β_1-adrenoceptor blockade is reduced in elderly patients (43). Although diastolic relaxation is slowed as a usual consequence of aging, this slowing progresses in many older patients to the extent that symptoms of congestive heart failure occur. As many as 40% of elderly patients with clinical congestive heart failure have normal left ventricular function when it is defined as left ventricular ejection fraction $\geq$ 40% (47, 48). When these patients with diastolic dysfunction are treated with loop diuretics, they are particularly susceptible to intravascular volume depletion that is manifest clinically as increased orthostatic hypotension (49). If the volume depletion is sufficient to decrease vital organ perfusion, other symptoms may occur, such as central nervous system depression and decreased renal function (50).

Vascular stiffness increases with age, even in the absence of disease. This may be due to both structural and functional changes, with increased deposition of collagen and other ground substance evident on microscopic or molecular examination (51). In addition, advanced age by itself decreases endothelial-mediated relaxation, even in the absence of concurrent diseases, such as hypertension and hypercholesterolemia, and environmental exposures, such as cigarette smoking, that are associated with impaired vascular endothelial relaxation (52). Not only is β_1-adrenergic function impaired, but β_2-adrenergic-mediated peripheral vasodilatation is impaired as well, due to decreased β-adrenergic vascular relaxation (53). The clinical result of these changes is an increase in pulse pressure, with systolic blood pressure disproportionately increased relative to diastolic blood pressure.

The pharmacodynamic consequences of these age-related cardiovascular changes are quite diverse. With initial administration of a nonselective β-adrenoceptor blocking drug, the decrease in heart rate is diminished. However, one would predict as well that the β_2-adrenoceptor blockade-mediated increase in peripheral vascular resistance would be diminished simultaneously. Clinical data indicate that β-blocker therapy for hypertension may indeed be somewhat less effective in older hypertensive patients. However, the limited data available indicate that β-blocker therapy is as efficacious in older as in younger patients after myocardial infarction and for the treatment of congestive heart failure. Administration of an α-adrenergic blocking drug (e.g., terazosin for the treatment of urinary retention due to prostate hypertrophy) results in greater hypotensive response in the older individual due to lack of reflex β-adrenergic stimulation (54).

The response of older individuals to calcium channel antagonists is a combination of changes in direct drug effects and age-related alterations in reflex responses to drug effect. Hypotensive responses are maintained because direct arterial vasodilatation remains intact, even though there is the age-related impairment in reflex sympathetic stimulation, as previously noted (55). For verapamil and diltiazem, atrioventricular nodal conduction delay is less in older than

in younger individuals, while sinoatrial suppression is greater in the elderly (56, 57). Mechanisms for these changes are unclear but are thought to entail a complex summation of changes in direct drug effects and age-related ANS and cardiac function changes.

Angiotensin-converting enzyme inhibitors may be less effective in treating hypertension in older than in younger patients (58). The mechanism for this is probably related to the low-renin state and resulting decreased role of the circulating renin–angiotensin–aldosterone axis in maintaining blood pressure in older hypertensive patients (59, 60). Conversely, available data indicate that angiotensin-converting enzyme inhibitors are extremely effective treatment for congestive heart failure in older as well as in younger patients (61).

Renal Function

Kidney morphology and renal function change markedly with aging. These changes have been associated with pharmacokinetic changes (decreased renal drug clearance) and also changes in pharmacodynamics for three drug classes important for the elderly — nonsteroidal anti-inflammatory drugs, angiotensin-converting enzyme inhibitors, and diuretics — and each may have responses altered by renal aging.

The anatomic changes associated with aging include a decrease in kidney weight that, from the fourth to the ninth decade of life, may fall by as much as one-third. This loss of renal mass occurs primarily from the renal cortex and results in decreased numbers and size of glomeruli. The remaining blood vessels may then produce shunts between afferent and efferent arterioles. The functional result is a decline in glomerular filtration rate that averages 0.75 mL/min/year, but is quite variable. Perhaps as many as one-third of individuals have no decrease in glomerular filtration rate while others have more rapid decreases. Renal plasma flow, measured by *p*-aminohippurate clearance, decreases more with age than does glomerular filtration rate as measured by inulin clearance, and may be decreased as much as 50% in individuals in the ninth decade as compared to the fourth decade of life. The result is that filtration fraction (glomerular filtration rate/renal plasma flow) increases in the elderly (5, 62). These findings also may be related to intrarenal impairment in vascular endothelial vasodilating function, as demonstrated by an attenuated vasodilatory response to acetylcholine. Consistent with findings in other vascular beds, intrarenal vasoconstrictive responses to angiotensin II are maintained in the elderly. Circulating atrial natriuretic hormone is increased in older individuals, and this may be responsible for suppressing renal renin secretion. This suppression leads to decreased basal activation of the renin–angiotensin–aldosterone axis (63). As mentioned previously, the age-associated decrease in renal tubular secretion parallels the decrease in glomerular filtration rate for some drugs (10), but occurs more rapidly for others (11). The decrease in renal tubular reabsorption, at least as measured by glucose reabsorption, appears to parallel the decline in glomerular filtration rate. A final impairment in renal tubular function that occurs with aging is manifest as a decreased capacity to concentrate or dilute urine, resulting in an impaired ability to excrete a free-water load and to retain sodium during states of volume depletion (64).

Altered or accentuated responses to nonsteroidal anti-inflammatory drugs in elderly patients include azotemia, decreased glomerular filtration rate, sodium retention, and hyperkalemia (65, 66). A common basis for these effects is likely to rest in part on the increased dependence of the aging kidney on vasodilating prostaglandins that results from the age-related decrease in plasma flow. Furthermore, selective inhibition of cyclooxygenase-2 in older patients may decrease glomerular filtration rate to the same extent as occurs with nonselective cyclooxygenase inhibitors (67, 68). The increased likelihood of sodium retention in older patients may also be associated with the loss of action of vasodilating prostaglandins, decreased glomerular filtration, and decreased renal tubular capacity to concentrate sodium in the decreased urine volume. The increased likelihood of hyperkalemia may reflect a preexisting state of relative hyporeninemic hypoaldosteronism in older individuals, exacerbated either by loss of prostaglandin effect on renin secretion or by increased effective intravascular volume due to drug-induced sodium retention (63–68).

Treatment with angiotensin-converting enzyme inhibitors is also more likely to be associated with hyperkalemia in older individuals (69). Impaired angiotensin II formation limits this potent stimulus for aldosterone secretion, and this is superimposed on the already age-related decrease in activity of the renin–angiotensin–aldosterone axis. The same drug-induced hyporeninemic hypoaldosteronism is predicted for the angiotensin receptor blockers. However, to date this has not been documented clincally.

Thiazide diuretic-induced hyponatremia is much more common in older than in younger patients, probably due to thiazide-mediated impairment in renal diluting capacity superimposed on the already present age-related decrease in capacity to dilute urine. Older studies indicated this was an extremely common cause

of moderate to severe hyponatremia. However, this may occur less frequently now that lower doses of thiazide diuretics are used to treat hypertension (70–72).

Hematopoietic System and the Treatment of Cancer

Available data suggest that the antitumor therapeutic response of older patients is optimal when exposure to appropriate chemotherapy is the same as for younger patients. For example, the treatment of non-Hodgkin's lymphoma with cyclophosphamide, doxorubicin, vincristine, and prednisone (CHOP) or etoposide, mitoxantrone, and prednimustine (VMP) is less effective in older patients when dose reductions are made (73, 74). Similarly, treatment of metastatic breast cancer in younger and older patients with the same dose intensity of doxorubicin-based chemotherapy resulted in similar outcomes as measured by time to progression of disease and overall survival (75).

However, these findings must be coupled with the known increased risk of hematopoietic toxicity in older patients undergoing cancer chemotherapy. The risk of myelosuppression is increased in patients over the age of 70 (76), leading to the recommendation that these patients receive hematopoietic growth factor treatment during cancer chemotherapy (76, 77). Such treatment has been associated with a decrease in febrile neutropenia and sepsis-related mortality (76, 78, 79). Anemia, defined as a hemoglobin concentration of less than 13 g/dL in men and 12 g/dL in women, is common in older adults (80), and its presence is an independent risk factor for myelotoxicity associated with anthracycline, epipodophyllotoxin, and camptothecin chemotherapy (81). This is at least in part due to changes in the tissue distribution of these drugs, which are highly bound to red blood cells. These findings have led to a recommendation that hemoglobin level should be maintained at 12 g/dL in older patients undergoing chemotherapy (82). Irrespective of the age of cancer patients, comorbid conditions (e.g., heart disease, renal dysfunction, and hepatobiliary disease) and functional status are the most important predictors of survival (83, 84). Identification of comorbid conditions by clinical and laboratory assessment and of functional status using comprehensive geriatric assessment has been proposed as the most effective way to target therapeutic interventions in older cancer patients (85).

With respect to the pharmacokinetics and pharmacodynamics of specific cancer chemotherapy drugs in older patients, the goal is to achieve a desired tissue exposure to the drug(s) in the context of the age-related changes in drug disposition described in other sections of this chapter. Specific for anticancer agents is the role of erythrocyte and platelet binding of these drugs. Chemotherapy itself may cause anemia and/or thrombocytopenia in older patients. In the case of anemia, a diminished response to chemotherapy has been described that perhaps is due to decreased tissue delivery of drugs (86). A summary of reported age-associated pharmacokinetic and pharmacodynamic changes for specific drugs is shown in Table 24.4 (87–94). However, for many anticancer drugs and tumors, similar information is not available to guide therapy despite the demonstration that such information can be used to treat older patients more effectively.

DRUG GROUPS FOR WHICH AGE CONFERS INCREASED RISK FOR TOXICITY

In addition to the adverse pharmacodynamic consequences described, for which there is at least a potential mechanistic understanding, it is more difficult to formulate a mechanistic explanation for a number of drug toxicities that are more frequent in older than in younger patients.

Theophylline neurotoxicity and cardiotoxicity are increased in older patients. Although it is unclear whether decreased theophylline clearance and increased exposure in older patients fully explain this apparent sensitivity, clinical reports are uniform in identifying age as a major contributing risk factor for theophylline toxicity (95, 96). This has resulted in much less use of theophylline in older patients.

Isoniazid-induced hepatotoxicity is more likely to occur in individuals who are more than 35 years old (97). Attempts to establish a pharmacokinetic or pharmacogenetic explanation have been unsatisfactory. Nevertheless, this clinical finding led to the subsequent recommendation that isoniazid be withheld from individuals with a positive tuberculin skin test ($\geq$15 mm) but no other risk factors (98). Because approximately 5–10 % of patients with a positive tuberculin test will develop active tuberculosis and elderly individuals are at highest risk, there currently is concern that appropriate chemoprophylaxis is not being made available to individuals who are $\geq$50 years of age (99). In view of the fact that routine clinical monitoring has reduced the risk of severe heptatotoxicity in recent years, current guidelines do not put an age limit on the use of isoniazid to treat latent tuberculosis, but simply discourage tuberculin testing in low-risk individuals (100).

Neuroleptic-induced tardive dyskinesia has been discussed. However, the mechanism for tardive dyskinesia is not well established. It is clear that increased

TABLE 24.4 Summary of Age-Related Changes in Disposition and Effect of Chemotherapeutic Agents

Drug	Pharmacokinetic change in older patients[a]	Pharmacodynamic change in older patients	Ref.
Cyclophosphamide	—	↑ Myelosuppression	87
Ifosfamide	↑ V_d, ↓ clearance, ↑ $t_{1/2}$ (dose reduction for decreased renal function)[b]	?	88
Melphalan	Dose reduction for decreased renal function[b]	?	88
Chlorambucil	—	—?	87
Dacarbazine	Dose reduction for decreased renal function[b]	—?	88
Temozolomide	—	↑ Hematotoxicity	87
Busulfan	—	?	87
Carmustine	? ↑ V_d, dose reduction for decreased renal function[b]	?	88
Cisplatin	Dose reduction for decreased renal function[b]	↑ Hematotoxicity, ↑ nausea	87, 88
Carboplatin	Dose reduction for decreased renal function[b]	?	87
Oxaliplatin	?	?	87, 88
Vincristine	?	?	87
Vinblastine	?	?	87
Vinorelbine	—	—	87
Paclitaxel	—	—	89
Docetaxel	↓ Clearance (CYP3A4)	?	87
Etoposide	↓ Clearance, dose reduction for decreased renal function[b]	?	87
Teniposide	?	?	87
Irinotecan	↑ AUC	?	90
Topotecan	↓ Clearance, dose reduction for decreased renal function[b]	—?	87, 91
Methotrexate	↓ Clearance, ? $t_{1/2}$, dose reduction for decreased renal function[b]	—	87, 92
5-Fluorouracil	—	? —	87
Capecitabine	? —	—	87
Cytarabine	↓ Clearance , dose adjustment for decreased renal function[b]	—	87
Gemicitabine	↓ Clearance, ↑ $t_{1/2}$	—	93
Fludarabine	Dose adjustment for decreased renal function[b]	—	87
Hydroxyurea	Dose adjustment for decreased renal function[b]	—	87
Doxorubicin	—	↑ Cardiotoxicity	87
Daunorubicin	—	?	87
Idarubicin	Dose adjustment for decreased renal function[b]	?	87
Epirubicin	—	?	87
Mitoxantrone	—	? ↑ Hematotoxicity	87
Bleomycin	—	—	87, 88
Mitomycin C	? ↑ AUC	? ↑ Myelosuppression	94

—, [a] No change, often based on steady-state plasma concentration rather than full pharmacokinetic analysis.

[b] Dose adjustment for renal function is in some cases recommended based on clinical experience rather than on documented pharmacokinetic changes.

patient age contributes significantly to the risk of developing tardive dyskinesia with the "typical" neuroleptics (32–34).

Nonsteroidal anti-inflammatory drugs are probably more likely to induce gastric ulceration in older than in younger patients (10). This may be the result of decreases in gastric mucosal prostaglandins in the elderly (102), with drug-induced inhibition of gastric prostaglandins being superimposed on this age-related decrease.

CONCLUSIONS

Older patients frequently have multiple coexisting diseases that are often very effectively treated with medications. There is little doubt that the risk of a specific drug therapy, such as angiotensin-converting enzyme inhibitor treatment of patients with congestive heart failure, is in most instances far outweighed by the benefit of therapy. However, the concurrent presence of multiple diseases in older patients results in their being treated with multiple medications, which itself is a risk factor for adverse drug events. Therefore, it is an appropriate generalization to assume that the risk/benefit ratio, or the therapeutic index, of any given therapy is narrowed for older patients. Understanding age-related pathophysiology can in some instances allow for prediction of age-related changes in drug disposition and effect. However, drug therapy continues to be a significant contributor to morbidity and mortality in the elderly (3).

REFERENCES

1. Smith JW, Seidl LG, Cluff LE. Studies on the epidemiology of adverse drug reactions. V. Clinical factors influencing susceptibility. Ann Intern Med 1966;65:629–40.
2. Hutchinson TA, Flegel KM, Kramer MS, Leduc DG, Kong HH. Frequency, severity and risk factors for adverse drug reactions in adult outpatients. J Chronic Dis 1986;39:533–42.
3. Gurwitz JH, Field TS, Avorn J, McCormick D, Jain S, Eckler M, Benser M, Edmondson AC, Bates DW. Incidence and preventability of adverse drug events in the nursing home setting. Am J Med 2000;109:87–94.
4. Hall DA. The biomedical basis of gerontology. Littleton, MA: John Wright PSG, Inc.; 1984.
5. Davies DF, Shock NW. Age changes in glomerular filtration rate, effective renal plasma flow, and tubular excretory capacity in adult males. J Clin Invest 1950;29:496–507.
6. Cockcroft DW, Gault MH. Prediction of creatinine clearance from serum creatinine. Nephron 1976;16:31–41.
7. Morike K, Schwab M, Klotz U. Use of aminoglycosides in elderly patients: Pharmacokinetic and clinical considerations. Drugs Aging 1997;10:259–77.
8. Sproule BA, Hardy BG, Shulman KI. Differential pharmacokinetics of lithium in elderly patients. Drugs Aging 2000;16:165–77.
9. Cusack B, Kelly J, O'Malley K, Noel J, Lavan J, Horgan J. Digoxin in the elderly: Pharmacokinetic consequences of old age. Clin Pharmacol Ther 1979;25:772–6.
10. Drayer DE, Romankiewicz J, Lorenzo B, Reidenberg MM. Age and renal clearance of cimetidine. Clin Pharmacol Ther 1982;31:45–60.
11. Reidenberg MM, Camacho M, Kluger J, Drayer DE. Aging and renal clearance of procainamide and acetylprocainamide. Clin Pharmacol Ther 1980; 28:732–5.
12. Greenblatt DJ, Abernethy DR, Locniskar A, Harmatz JS, Limjuco RA, Shader RI. Effect of age, gender, and obesity on midazolam kinetics. Anesthesiology 1984;61:27–35.
13. Greenblatt DJ, Divoll M, Abernethy DR, Moschitto LJ, Smith RB, Shader R. Reduced clearance of triazolam in old age: Relation to antipyrine oxidizing capacity. Br J Clin Pharmacol 1983;15:303–9.
14. Greenblatt DJ, Harmatz JS, Shapiro L, Engelhardt N, Gouthro TA, Shader RI. Sensitivity to triazolam in the elderly. N Engl J Med 1991;324:1691–8.
15. Watkins PB, Wrighton SA, Schuetz EG, Molowa DT, Guzelian PS. Identification of glucocorticoid-inducible cytochromes P-450 in the intestinal mucosa of rats and man. J Clin Invest 1987;80:1029–36.
16. Gatmaitan ZC, Arias IM. Structure and function of P-glycoprotein in normal liver and small intestine. Adv Pharmacol 1993;24:77–97.
17. Shepherd AMM, Hewick DS, Moreland TA, Stevenson IH *et al*. Age as a determinant of sensitivity to warfarin. Br J Clin Pharmacol 1977;4:315–20.
18. Bauer LA, Blouin RA. Age and phenytoin kinetics in adult epileptics. Clin Pharmacol Ther 1982;31:301–4.
19. Jusko WJ, Gardner MJ, Mangione A, Schentag JJ, Koup JR, Vance JW. Factors affecting theophylline clearances: Age, tobacco, marijuana, cirrhosis, congestive heart failure, obesity, oral contraceptives, benzodiazepines, barbiturates, and ethanol. J Pharm Sci 1979;68:1358–66.
20. Raz N. Aging of the brain and its impact on cognitive performance: Integration of structural and functional findings. In: Craik FIM, Salthouse TA, editors. The handbook of aging and cognition. 2nd ed. Mahwah, NJ: Lawrence Erlbaum Associates; 2000. p. 1–90.
21. Volkow ND, Gur RC, Wang G-J, Fowler JS, Moberg PJ, Ding Y-S, Hitzemann R, Smith G, Logan J. Association between decline in brain dopamine activity with age and cognitive and motor impairment in healthy individuals. Am J Psychiatry 1998;155:344–9.
22. Schnider TW, Minto CF, Shafer SL, Gambus PL, Andresen C, Goodale DB, Youngs EJ. The influence of age on propofol pharmacodynamics. Anesthesiology 1999;90:1502–16.
23. Olmos M, Ballester JA, Vidarte A, Elizalde JL, Escobar A. The combined effect of age and premedication on the propofol requirements for induction by target controlled infusion. Anesth Analg 2000;90:1157–61.
24. Scott JC, Stanski DR. Decreased fentanyl and alfentanil dose requirements with age. A simultaneous pharmacokinetic and pharmacodynamic evaluation. J Pharmacol Exp Ther 1987;240:159–66.
25. Stanski DR, Maitre PO. Population pharmacokinetics and pharmacodynamics of thiopental: The effect of age revisited. Anesthesiology 1990;72:412–22.
26. Jacobs JR, Reves JG, Marty J, White WD, Bai SA, Smith LR. Aging increases pharmacodynamic sensitivity to the hypnotic effects of midazolam. Anesth Analg 1995;80:143–8.

27. Ray WA, Griffin MR, Downey W. Benzodiazepines of long and short elimination half-life and the risk of hip fracture. JAMA 1989;262:3303–7.
28. Greenblatt DJ, Shader RI, Abernethy DR. Drug therapy: Current status of benzodiazepines. N Engl J Med 1983;309–354–358, 410–16.
29. Greenblatt DJ, Allen MD, Shader RI. Toxicity of high-dose flurazepam in the elderly. Clin Pharmacol Ther 1977;21:355–61.
30. Saltz BL, Woerner MG, Kane JM, Lieberman JA, Alvir JMJ, Bergmann KJ, Blank K, Koblenzer J, Kahaner K. Prospective study of tardive dyskinesia incidence in the elderly. JAMA 1991;266:2402–6.
31. Jeste DV, Caligiuri MP, Paulsen JS, Heaton RK, Lacro JP, Harris J, Bailey A, Fell RL, McAdams LA. Risk of tardive dyskinesia in older patients: A prospective longitudinal study of 266 outpatients. Arch Gen Psychiatry 1995;52:756–65.
32. Woerner MG, Alvir JMJ, Saltz BL, Lieberman JA, Kane JM. Prospective study of tardive dyskinesia in the elderly: Rates and risk factors. Am J Psychiatry 1998;155:1521–8.
33. Jeste DV, Lacro JP, Bailey A, Rockwell E, Harris MJ, Caligiuri MP. Lower incidence of tardive dyskinesia with risperidone compared with haloperidol in older patients. J Am Geriatr Soc 1999;47:716–9.
34. Abernethy DR, Greenblatt DJ, Shader RI. Imipramine and desipramine disposition in the elderly. J Pharmacol Exp Ther 1985;232:183–8.
35. Low PA. The effect of aging on the autonomic nervous system. In: Low PA, editor. Clinical autonomic disorders. 2nd ed, Philadelphia: Lippincott-Raven; 1977. p. 161–75.
36. Vestal RE, Wood AJJ, Shand DG. Reduced beta-adrenoceptor sensitivity in the elderly. Clin Pharmacol Ther 1979;26:181–6.
37. Ziegler MG, Lake CR, Kopin IJ. Plasma noradrenaline increases with age. Nature 1976;261:333–5.
38. Rodstein M, Zeman FD. Postural blood pressure changes in the elderly. J Chronic Dis 1957;6:581–8.
39. Lipsitz LA, Nyquist RP, Wei JY, Rowe JW. Postprandial reduction in blood pressure in the elderly. N Engl J Med 1983;309:81–3.
40. van Kraaij DJW, Jansen RWMM, Gribnau FWJ, Hoefnagels WHL. Diuretic therapy in elderly heart failure patients with and without left ventricular systolic dysfunction. Drugs Aging 2000;16:289–300.
41. Ray WA, Griffin MR, Schaffner W, Baugh DK, Melton LJ. Psychotropic drug use and the risk of hip fracture. N Engl J Med 1987;316:363–9.
42. Reilly JG, Ayis SA, Ferrier IN, Jones SJ, Thomas SHL. QT_c-interval abnormalities and psychotropic drug therapy in psychiatric patients. Lancet 2000;355:1048–52.
43. Abernethy DR, Schwartz JB, Plachetka JR, Todd EL, Egan JM. Comparison in young and elderly patients of pharmacodynamics and disposition of labetalol in systemic hypertension. Am J Cardiol 1987;60: 697–702.
44. Lakatta EG. Cardiovascular aging research: The next horizons. J Am Geriatr Soc 1999;47:613–25.
45. Maciel LMZ, Polikar R, Rohrer D, Popovich BK, Dillmann WH. Age-induced decreases in the messenger RNA coding for the sarcoplasmic reticulum Ca^{2+}-ATPase of the rat heart. Circ Res 1990;67:230–4.
46. van Harten J, Burggraaf J, Ligthart GJ, van Brummelen P, Breimer DD. Single- and multiple-dose nisoldipine kinetics and effects in the young, the middle-aged, and the elderly. Clin Pharmacol Ther 1989;45:600–7.
47. ACC/AHA Task Force Report. Guidelines for the evaluation and management of chronic heart failure in the adult. Circulation 2001;104:2996–3007.
48. Tresch DD. The clinical diagnosis of heart failure in older patients. J Am Geriatr Soc 1997;45:1128–33.
49. Bonow RO, Udelson JE. Left ventricular diastolic dysfunction as a cause of congestive heart failure: Mechanisms and management. Ann Int Med 1992;117:502–10.
50. van Kraaij DJW, Jansen RWMM, Bouwels LHR, Hoefnagels WHL. Furosemide withdrawal improves postprandial hypotension in elderly patients with heart failure and preserved left ventricular systolic function. Arch Int Med 1999;159:1599–1605.
51. Cangiano JL, Martinez-Maldonado M. Isolated systolic hypertension in the elderly. In: M. Martinez-Maldonado, editor. Hypertension and renal disease in the elderly. Oxford: Blackwell Scientific Publications; 1992. p. 79–94.
52. Andrawis NS, Jones DS, Abernethy DR. Aging is associated with endothelial dysfunction in the human forearm vasculature. J Am Geriatr Soc 2000;48:193–8.
53. Pan HYM, Hoffman BB, Porshe RA, Blaschke TF. Decline in beta-adrenergic receptor-mediated vascular relaxation with aging in man. J Pharmacol Exp Ther 1986;239:802–7.
54. Hosmane BS, Maurath CJ, Jordan DC, Laddu A. Effect of age and dose on the incidence of adverse events in the treatment of hypertension in patients receiving terazosin. J Clin Pharmacol 1992;32:434–43.
55. Abernethy DR, Gutkowska J, Winterbottom LM. Effects of amlodipine, a long-acting dihydropyridine calcium antagonist in aging hypertension: Pharmacodynamics in relation to disposition. Clin Pharmacol Ther 1990;48:76–86.
56. Abernethy DR, Schwartz JB, Todd EL, Luchi R, Snow E. Verapamil pharmacodynamics and disposition in young versus elderly hypertensive patients. Ann Int Med 1986;105:329–36.
57. Schwartz JB, Abernethy DR. Responses to intravenous and oral diltiazem in elderly versus younger patients with systemic hypertension. Am J Cardiol 1987;59:1111–7.
58. Verza M, Cacciapuoti F, Spiezia R, D'Avino M, Arpino G, D'Errico S, Sepe J, Varricchio M. Effects of the angiotensin converting enzyme inhibitor enalapril compared with diuretic therapy in elderly hypertensive patients. J Hypertens 1988;6(suppl 1):S97–S99.
59. Crane MG, Harris JJ. Effect of aging on renin activity and aldosterone excretion. J Lab Clin Med 1976;87:947–59.
60. Hall JE, Coleman TG, Guyton AC. The renin-angiotensin system: Normal physiology and changes in older hypertensives. J Am Geriatr Soc 1989;37:801–13.

61. Agency for Health Care Policy and Research (AHCPR). Heart failure: Evaluation and treatment of patients with left ventricular systolic dysfunction. J Am Geriatr Soc 1998;46:525–9.
62. Lindeman RD. Overview: Renal physiology and pathophysiology of aging. Am J Kidney Dis 1990;26:275–82.
63. Miller M. Hyponatremia: Age-related risk factors and therapy decisions. Geriatrics 1998;53:32–48.
64. Rowe JW, Minaker KL, Levi M. Pathophysiology and management of electrolyte disturbances in the elderly. In: Martinez-Maldonado M., editor. Hypertension and renal disease in the elderly. Boston: Blackwell Scientific Publications; 1992. p. 170–84.
65. Gurwitz JH, Avorn J, Ross-Degnan D, Lipsitz LA. Nonsteroidal anti-inflammatory drug associated azotemia in the very old. JAMA 1990;264:471–5.
66. Field TS, Gurwitz JH, Glynn RJ, Salive ME, Gaziano JM, Taylor JO, Hennekens CH. The renal effects of nonsteroidal anti-inflammatory drugs in older people: Findings from the Established Populations for Epidemiologic Studies of the Elderly. J Am Geriatr Soc 1999;47:507–11.
67. Whelton A, Schulman G, Wallemark C, Drower EJ, Isakson PC, Verburg KM, Geis S. Effects of celecoxib and naproxen on renal function in the elderly. Arch Int Med 2000;160:1465–70.
68. Swan SK, Rudy DW, Lasseter KC, Ryan CF, Buechel KL, Lambrecht LJ, Pinto MB, Dilzer SC, Obrda O, Sundblad KJ, Gumbs CP, Ebel DL, Quan H, Larson PJ, Schwartz JI, Musliner TA, Gertz BJ, Brater DC, Yao S-L. Effect of cyclooxygenase-2 inhibition on renal function in elderly persons receiving a low salt diet. Ann Intern Med 2000;133:1–9.
69. Reardon LC, Macpherson DS. Hyperkalemia in outpatients using angiotensin-converting enzyme inhibitors. Arch Intern Med 1998;158:26–32.
70. Sunderam SG, Mankikar GD. Hyponatremia in the elderly. Age Ageing 1983;12:77–80.
71. Fichman M, Vorherr H, Kleeman G. Diuretic-induced hyponatremia. Ann Intern Med 1971;75:853–63.
72. Ashraf N, Locksley R, Arieff A. Thiazide-induced hyponatremia associated with death or neurologic damage in outpatients. Am J Med 1981;70:1163–8.
73. Dixon DO, Neilan B, Jones SE, Lipschitz DA, Miller TP, Grozea PN, Wilson, HE. Effect of age on the therapeutic outcome in advanced diffuse histiocytic lymphoma: The Southwest Oncology Group experience. J Clin Oncol 1986;4:295–305.
74. Tirelli U, Errante D, Van Glabbeke M, Teodorovic I, Kluin-Nelemans JC, Thomas J, Bron D, Rosti G, Zagonel V, Noordijk EM. CHOP is the standard regimen in patients ≥70 years of age with intermediate-grade and high-grade non-Hodgkin's lymphoma: Results of a randomized study of the European Organization for Research and Treatment of Cancer Lymphoma Cooperative Study Group. J Clin Oncol 1998;16:27–34.
75. Ibrahim NK, Frye DK, Buzdar AU, Walters RS, Hortobagyi GN. Doxorubicin-based chemotherapy in elderly patients with metastatic breast cancer. Tolerance and outcome. Arch Int Med 1996;156:882–8.
76. Balducci L, Lyman GH. Patients aged ≥70 are at high risk for neutropenic infection and should receive hemopoietic growth factors when treated with moderately toxic chemotherapy. J Clin Oncol 2001;19:1583–5.
77. Balducci L, Yates J. General guidelines for the management of older patients with cancer. Oncology (Huntingt) 2000;14:221–7.
78. Lyman GH, Kuderer NM, Djulbegovic B. Prophylatic granulocyte colony-stimulating factor in patients receiving dose-intensive cancer chemotherapy: A meta-analysis. Am J Med 2002;112:406–11.
79. Lyman GH, Kuderer N, Agboola O, Balducci L. Evidence-based use of colony-stimulating factors in elderly cancer patients. Cancer Control 2003;10:487–99.
80. Ania BJ, Suman VJ, Fairbanks VF, Rademacher DM, Melton LJ 3rd. Incidence of anemia in older people: An epidemiologic study in a well defined population. J Am Geriatr Soc 1997;45:825–31.
81. Schrijvers D, Highley M, De Bruyn E, Van Oosterom AT, Vermorken JB. Role of red blood cells in pharmacokinetics of chemotherapeutic agents. Anticancer Drugs 1999;10:147–53.
82. Winn RJ, McClure J. The NCCN clinical practice guidelines in oncology: A primer for users. J Natl Compr Cancer Network 2003;1:5–13.
83. Satariano WA, Ragland DR. The effect of comorbidity on 3-year survival of woman with primary breast cancer. Ann Intern Med 1994;120:104–10.
84. Extermann M, Overcash J, Lyman GH, Parr J, Balducci L. Comorbidity and functional status are independent in older cancer patients. J Clin Oncl 1998;16:1582–7.
85. Ferrucci L, Guralnik JM, Cavazzini C, Bandinelli S, Lauretani F, Bartali B, Reppetto L, Longo DL. The frailty syndrome: A critical issue in geriatric oncology. Crit Rev Oncol Hematol 2003; 46:127–37.
86. Eisenhauer EA, Vermorken JB, van Glabbeke M. Predictors of response to subsequent chemotherapy in platinum pretreated ovarian cancer: A multivariate analysis of 704 patients. Ann Oncol 1997;8:963–8.
87. Wildiers H, Highley MS, de Bruijn EA, van Oosterom AT. Pharmacology of anticancer drugs in elderly population. Clin Pharmacokinet 2003;42:1213–42.
88. Kintzel PE, Dorr RT. Anticancer drug renal toxicity and elimination: Dosing guidelines for altered renal function. Cancer Treat Rev 1995;21:33–64.
89. Nakamura Y, Sekine I, Furuse K, Saijo N. Retrospective comparison of toxicity and efficacy in phase II trails of 3-h infusions of paclitaxel for patients 70 years of age or older and patients under 70 years of age. Cancer Chemother Pharmacol 2000;46:114–8.
90. Miya T, Goya T, Fujii H, Ohtsu T, Itoh K, Igarashi T, Minami H, Sasaki Y. Factors affecting the pharmacokinetics of CPT-11: The body mass index, age and sex are independent predictors of pharmacokinetic parameters of CPT-11. Invest New Drugs 2001; 19:61–7.
91. O'Reilly S, Rowinsky EK, Slichenmyer W, Donehower RC, Forastiere AA, Ettinger DS, Chen TL, Sartorius S, Grochow LB. Phase I and pharmacologic

study of topotecan in patients with impaired renal function. J Clin Oncol 1996;14:3062–73.
92. Gelman RS, Taylor SG. Cyclophosphamide, methotrexate, and 5-fluorouracil chemotherapy in women more than 65 years old with advanced breast cancer: The elimination of age trends in toxicity by using doses based on creatinine clearance. J Clin Oncol 1984;2:1404–13.
93. Lichtman SM, Skirvin JA. Pharmacology of antineoplastic agents in older cancer patients. Oncology (Huntingt) 2000;14:1743–55.
94. Miya T, Sasaki Y, Karato A, Saijo N. Pharmacokinetic study of mitomycin C with emphasis on the influence of aging. Jpn J Cancer Res 1992;83:1382–5.
95. Shannon M, Lovejoy FH. The influence of age vs peak serum concentration on life-threatening events after chronic theophylline intoxication. Arch Intern Med 1990;150:2045–8.
96. Schiff GD, Hegde HK, LaCloche L, Hryhoczuk DO. Inpatient theophylline toxicity: Preventable factors. Ann Intern Med 1991;114:748–53.
97. Kopanoff DE, Snider DE Jr, Caras GJ. Isoniazed-related hepatitis: A U.S. Public Health Service cooperative surveillance study. Am Rev Resp Dis 1979;117:992–1001.
98. American Thoracic Society. Treatment of tuberculosis and tuberculosis infection in adults and children. Am J Respir Crit Care Med 1994; 149:1359–74.
99. Sorresso DJ, Mehta JB, Harvil LM, Bently S. Underutilization of isoniazid chemoprophylaxis in tuberculosis contacts 50 year of age and older. A prospective analysis. Chest 1995;108: 706–11.
100. American Thoracic Society. Targeted tuberculin testing and treatment of latent tuberculosis infection. MMWR Morb Mortal Wkly Rep 2000;49(No RR-6):1–51.
101. Gabriel SE, Jaakkimainen L, Bombardier C. Risk for serious gastrointestinal acomplications related to use of nonsteroidal anti-inflammatory drugs. Ann Intern Med 1991;115:787–96.
102. Cryer B, Lee E, Feldman M. Factors influencing gastroduodenal mucosal prostaglandin concentrations: Roles of smoking and aging. Ann Intern Med 1992; 116:636–640.

CHAPTER

25

Clinical Analysis of Adverse Drug Reactions

KARIM ANTON CALIS*, EMIL N. SIDAWY†, AND LINDA R. YOUNG‡

*University of Maryland School of Pharmacy, Baltimore, Maryland, and Mark O. Hatfield Clinical Research Center, National Institutes of Health, Bethesda, Maryland,

†Shady Grove Adventist Hospital, Rockville, Maryland,

‡Carilion Medical Center, Roanoke, Virginia

INTRODUCTION

Adverse drug reactions (ADRs) represent an important public health problem. Despite efforts to reduce the incidence of medication-related adverse events, morbidity and mortality from drug-induced disease continue to be unacceptably high. Furthermore, methods for ADR detection, evaluation, and monitoring remain inadequate. Although some ADRs are idiosyncratic and unpredictable, others can be anticipated based on knowledge of a medication's clinical pharmacology. In fact, an estimated 30–60% of ADRs may be preventable (1–5).

Regrettably, adverse reactions to medications are generally not well studied, and the mechanisms of some remain poorly described. The problem is further exacerbated by the inadequate training that clinicians receive in the basic principles of applied pharmacology and therapeutics. This chapter focuses on the clinical detection of ADRs and on factors that may increase ADR risk.

Epidemiology

Although some adverse drug reactions are minor and resolve without sequelae, others can cause permanent disability or death. ADRs occur commonly, but estimates of incidence vary considerably. This is due to substantial underreporting of ADRs and differences in study methodology, populations studied, and ADR definitions. Adverse drug reactions account for 2.9–15.4% of all hospital admissions in the United States (6, 7). The incidence may be highest in the elderly and other compromised populations. Nearly 16% of nursing home residents are hospitalized because of an ADR (8). A significant risk factor for hospitalization is the concomitant use of seven or more medications.

ADRs are believed to be the fourth to sixth leading cause of death among hospitalized patients (1). A recent study suggests that an estimated 6.7% of hospitalized patients experience serious adverse drug reactions (defined as those that require or prolonged hospitalization, are permanently disabling, or result in death) (1). Of 1133 drug-related adverse events reported in a study of more than 30,000 medical records, 19.4% were attributable to an adverse drug reaction (4). The incidence of ADRs in hospitalized HIV-infected patients was reported to be 20% (9). Up to 30% of patients may experience an ADR while hospitalized, of which 3% may be life-threatening, and most receive an average of nine drugs per hospitalization (10). Adverse drug reactions have been reported to increase the length of hospital stay by 2.2 to 4.6 days and to increase hospital costs by more than $2500 per event (11). The economic burden of ADRs has been estimated to be in the billions of dollars annually (12).

Definitions

The terminology for describing adverse drug events can be confusing (13). An adverse drug event can be defined as any undesirable experience associated

with the use of a medical product in a patient. This broad definition includes adverse drug reactions and other events (including medication errors) related to the prescribing, preparation, dispensing, or administration of medications. Karch and Lasagna (14) defined an ADR as any response to a drug that is noxious and unintended and that occurs at doses used in humans for prophylaxis, diagnosis, or therapy, excluding failure to accomplish the intended purpose. The World Health Organization (WHO) adopted a slightly modified version of this definition. According to WHO, an ADR is any response to a drug that is noxious and unintended and that occurs at doses normally used in humans for prophylaxis, diagnosis, or therapy of disease, or for the modification of physiological function (15). Both definitions are limited to reactions caused by medications and purposely exclude therapeutic failures, overdose, drug abuse, noncompliance, and medication errors. The U.S. Food and Drug Administration (FDA) defines an ADR as any undesirable experience associated with the use of a medical product in a patient (16). The FDA defines serious reactions as those that are life-threatening; require intervention to prevent permanent injury; or result in death, initial or prolonged hospitalization, disability, or congenital anomaly.

CLASSIFICATION

Adverse drug reactions can be classified simply according to their onset or severity. ADRs are occasionally classified as acute, subacute, or latent. Acute events are those observed within 60 minutes after the administration of a medication and include anaphylactic shock, severe bronchoconstriction, and nausea or vomiting (17). Subacute reactions occur within 1 to 24 hours and include maculopapular rash, serum sickness, allergic vasculitis, and antibiotic-associated diarrhea or colitis. Latent reactions require 2 or more days to become apparent and include eczematous eruptions, organ toxicity, and tardive dyskinesia.

ADRs can also be classified as mild, moderate, or severe. Mild reactions, such as dysgeusia associated with clarithromycin, are bothersome but may not require a change in therapy. Moderate reactions, such as amphotericin B-induced hypokalemia, often require a change in therapy, additional treatment, or continued hospitalization. Reactions that are disabling or life-threatening, or those that considerably prolong hospitalization, are classified as severe (18).

The classification of Rawlins and Thompson is perhaps the most widely used to describe adverse drug reactions (19). Although this classification system continues to evolve, it serves a useful purpose. Adverse reactions are categorized as Type A or B. Type A reactions are those that extend directly from a drug's pharmacological effects. They are often predictable and dose dependent and may account for up to two-thirds of all ADRs. Type A reactions also include adverse effects resulting from drug overdose and drug–drug interactions. Sedation caused by an antihistamine and hypotension caused by a β-adrenergic antagonist are considered Type A reactions. Type B reactions are idiosyncratic or immunologic reactions that are often rare and unpredictable. Examples of Type B reactions include aplastic anemia caused by chloramphenicol or rash induced by β-lactam antibiotics. Albeit not universally accepted, other authors have extended this classification system to include Types C, D, and E reactions to describe "chemical," delayed, and end-of-treatment reactions, respectively.

Gell and Coombs (20) developed a classification system (Types I through IV) to describe immune-mediated hypersensitivity reactions to medications (Figure 25.1). Immune system components such as intact skin, phagocytes, and complement act as constant barriers to foreign invasion. Lymphocytic and antibody activities are increased after repeated exposure to antigens. Drug molecules or metabolites act as antigens and induce the production of antibodies. Antibodies are produced if lymphocytes are able to recognize the antigenic determinants of foreign particles. Drugs may cause more than one of the four types of hypersensitivity reactions in this classification scheme. For example, as described in Chapter 16, reactions to penicillins can be classified under more than one type based on clinical presentation and associated laboratory findings.

Type I reactions are IgE mediated and cause manifestations of allergic symptoms due to the release of immune mediators such as histamine or leukotrienes. These reactions typically occur within minutes of drug exposure and may manifest as generalized pruritus, urticaria, angioedema, anaphylaxis, rhinitis, or conjunctivitis (21). Anaphylaxis can result from exposure to any antigen (e.g., penicillin) and may be fatal in the absence of prompt medical intervention.

Type II reactions involve cytotoxic antibodies (IgG or IgM mediated), which react with antigens on the cell surface; the antigen–antibody combination then causes cell damage due to the presence of neutrophils and monocytes or complement-induced cell lysis. Examples of Type II reactions are the hemolytic anemias

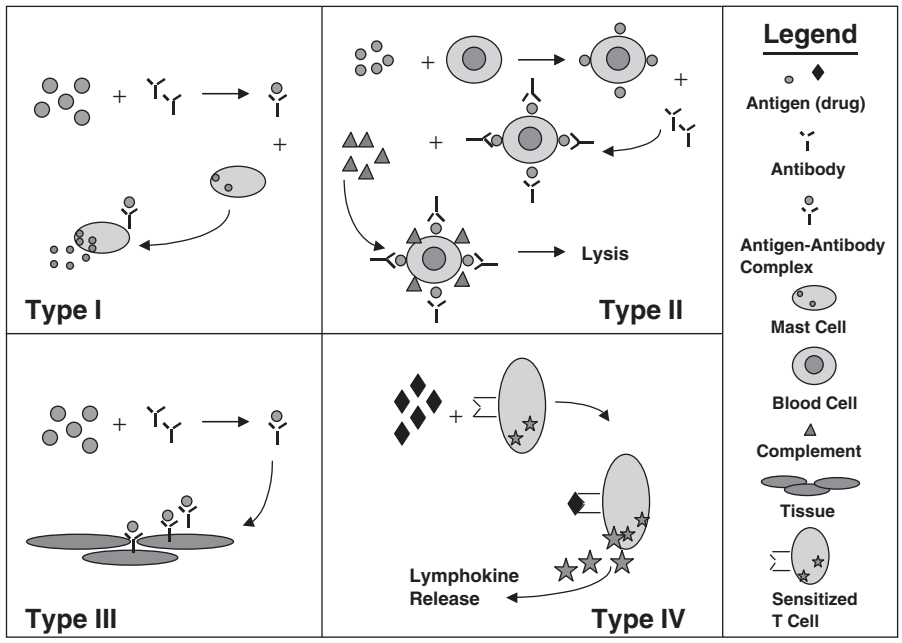

FIGURE 25.1 Mechanisms of hypersensitivity reactions. Type I: Antigens bind to antibodies on mast cells, causing degranulation and release of histamine and other mediators. Type II: Antibodies attach to cell-surface antigens, causing activation of complement or other effector cells (neutrophils, K-lymphocytes, etc.), resulting in cell damage and cell death. Type III: Antigen–antibody complexes are deposited in tissue. Type IV: T-cells are sensitized to a specific antigen, thereby causing lymphokine release. (Reproduced with permission from Young LR, Wurtzbacher JD, Blankenship CS. Am J Manag Care 1997;3:1884–906.)

caused by methyldopa or quinine. Acute graft rejection is another Type II hypersensitivity reaction.

Type III reactions are caused by tissue injury due to immune complexes. The antigen–antibody complexes are usually cleared by the immune system; however, repeated contact with antigens can cause the complex to deposit in tissue and result in tissue injury. Serum sickness is the classic example of a Type III reaction. Medications associated with serum sickness include many antibiotics, phenytoin, salicylates, barbiturates, nonsteroidal anti-inflammatory drugs, isoniazid, antisera, hydralazine, captopril, and sulfonamides. Procainamide-induced lupus, described in Chapter 16, is also considered a Type III reaction.

Type IV reactions occur when T-cells bind to a specific antigen, thereby causing the release of cytokines. The onset of these reactions may be delayed by more than 12 hours. Topical application of drugs may result in allergic contact dermatitis and photosensitivity. These reactions typically manifest initially as a skin rash but may become systemic upon subsequent exposure to the antigen.

CLINICAL DETECTION

Adverse reactions can result from the use of drugs, diagnostic agents, biologicals (including vaccines), nutrients, fluids, electrolytes, and complementary or alternative products. Adverse effects may be attributable to the parent compound, a metabolite, a pharmaceutical excipient, or even a component of the drug delivery system. Occasionally, more than one agent may be involved. Adverse drug reactions, whether expected or not, occur with nearly all medications and have been observed regardless of route or mode of administration. The drug classes most commonly associated with ADRs are listed in Table 25.1.

Some ADRs are caused by most or all medications in a class, while others are agent specific. Nausea, vomiting, and diarrhea have been observed with most antibiotics, yet only chloramphenicol and certain sulfonamide antibiotics have been consistently implicated as causes of aplastic anemia. Some pharmacological effects, such as sedation from an antihistamine, may be considered adverse effects when they are

TABLE 25.1 Drug Classes Commonly Reported as Causes of Adverse Reactions

Drug class	Examples of reported adverse reactions
Antimicrobial agents	Diarrhea, rash, pruritus
Antineoplastics	Bone marrow suppression, alopecia, nausea and vomiting
Anticoagulants	Hemorrhage, bruising
Cardiovascular drugs	Heart block, arrhythmias, edema
Antihyperglycemics	Hypoglycemia, diarrhea, gastrointestinal discomfort
Nonsteroidal anti-inflammatory drugs	Gastrointestinal ulceration and bleeding, renal insufficiency
Opiate analgesics	Sedation, dizziness, constipation
Diuretics	Hypokalemia, hyperuricemia, hyperglycemia
Diagnostic agents	Hypotension, nephrotoxicity, allergic reactions
Central nervous system agents	Dizziness, drowsiness, headache, hallucination, neuroleptic malignant syndrome, serotonin syndrome

not intended, but desired effects when they are prescribed specifically for an indication for which they may be beneficial (e.g., sleeping aid). Several body systems are commonly affected by ADRs and few are spared (Table 25.2). Adverse effects range from nonspecific symptoms to organ-specific toxicity that can be confirmed objectively. Certain medications are widely recognized for selectively targeting specific organs or body systems. For example, the aminoglycoside antibiotics are known to cause nephrotoxicity and ototoxicity; most antineoplastics produce predictable bone marrow suppression, and bleomycin and busulfan cause pulmonary fibrosis.

Drug metabolites have been implicated in the pathogenesis of some adverse drug reactions. (This is diagrammed in Figure 16.4, Chapter 16. The specific chemical mechanisms of adverse reactions involving drug metabolites are described in Chapters 11 and 16.) Herbal products have been identified as a source of serious adverse reactions and interactions (22). Since the passage of the Dietary Supplements Health and Education Act of 1994 (DSHEA), the use of herbal and dietary supplements has increased dramatically in the United States.

Pharmaceutical excipients and drug delivery systems have also been associated with severe allergic

TABLE 25.2 Body Systems Commonly Affected by Adverse Drug Reactions

Body system	Examples of reported adverse reactions
Central nervous system	Anxiety, depression, extrapyramidal reactions, ataxia, hyperactivity, insomnia, malaise, pain, vertigo, dystonia, asthenia, seizures
Cardiovascular	Angina, arrhythmias, palpitations, congestive heart failure, syncope, hemorrhage, thrombosis, embolism
Endocrine	Gynecomastia, hypothyroidism, adrenal suppression
Gastrointestinal and hepatic	Gastritis, dyspepsia, dysphagia, colitis, anorexia, hematemesis, pancreatitis, ascites, jaundice, hepatitis
Renal and genitourinary	Vaginitis, hematuria, dysmenorrhea, proteinuria, urinary retention, interstitial nephritis
Hematologic	Blood dyscrasias, anemias, thrombocytopenia
Dermatologic	Pruritus, urticaria, alopecia, bruising, purpura, rash, petechiae
Metabolic	Osteoporosis, fluid, electrolyte, and acid–base disorders
Musculoskeletal	Myalgia, arthralgia, neuropathy, rhabdomyolysis
Respiratory	Bronchospasm, allergic rhinitis, dyspnea, respiratory depression, pulmonary fibrosis, epistaxis, hemoptysis
Sensory	Dysgeusia, impaired vision, ototoxicity, tinnitus, diplopia

and nonallergic adverse reactions (23–25). Excipients are pharmacologically inert substances that include binders, fillers, coloring agents, buffers, lubricants, detergents, emulsifiers, flavoring agents, solvents, adsorbants, aerosol propellants, stabilizers, and sweeteners. Some of the adverse effects are mild and self-limiting. Lactose in some products may be associated with gastrointestinal complaints and diarrhea in lactose-intolerant patients. Sorbitol-containing liquid preparations can also cause diarrhea. Examples of excipients found to cause morbidity or mortality include the sulfite preservatives, the coloring agent tartrazine, and the polyoxyethylated castor oils (Cremophor®) used as emulsifiers in parenteral products. *p*-Aminobenzoic acid (PABA) and PABA derivatives have been associated with severe allergic reactions. The first major drug-related tragedy in U.S. history was caused by the solvent diethylene glycol found in a formulation of the oral antibiotic sulfanilamide. Exposure to this substance resulted in more than 100 deaths and led to passage of the Food and Drug Act of 1937. Occasionally, even drug formulations have been reported to cause adverse effects. Gastrointestinal irritation, bezoars, and intestinal obstruction have been reported as a result of drug formulations that do not disintegrate or dissolve properly.

Components of drug delivery systems have also been associated with severe reactions. Reports of latex allergy continue to increase as more healthcare workers are exposed to medical devices that contain this substance, including protective gloves. Incidence of latex sensitization ranges from 1 to 6% of the general population and about 8 to 12% of continuously exposed healthcare workers (26, 27). Leaching of the plasticizer di-2-ethylhexylphthalate (DEHP) from intravenous drug delivery systems has also been associated with toxicity, particularly in susceptible individuals exposed for long periods.

Risk Factors

Factors believed to contribute to the high incidence of adverse reactions were outlined in Chapter 1. Since many adverse reactions are predictable, recognition and understanding of potential risk factors may be the most critical steps in ADR prevention. Table 25.3 lists the primary ADR risk factors.

Concurrent use of multiple medications is another major ADR risk factor. The potential for clinically significant drug interactions and additive adverse effects increases as the number of medications in a regimen increases (28, 29). In a study of over 9000 hospital admissions, the strongest predictor of ADRs was the large number of concurrent prescription medications (OR = 2.94) (30). Irrational prescribing, inappropriate use, or insufficient monitoring of medications can predispose to adverse outcomes. To minimize the incidence of adverse reactions, each medication must have a clear indication, and specific therapeutic and toxic endpoints should be established prior to the start of treatment. Factors that contribute to polypharmacy include increasing age, multiple medical conditions, overprescribing, multiple medical providers, absence of a primary care provider, use of multiple pharmacies, frequent drug regimen changes, hoarding of medications, and self-treatment (31). Polypharmacy is of particular concern in the elderly because they are already susceptible to ADRs. Elderly patients often suffer disproportionately from various acute and chronic illnesses and are likely to require more medications (31). They are also more likely than are their younger counterparts to have impaired CNS function and to not adhere to the prescribed regimen. Elderly patients in the community use an average of three prescription and nonprescription medications, while those in nursing homes receive an average of five to eight prescription drugs at the same time (32). Patient education and ongoing medication regimen review can minimize the problem of polypharmacy.

TABLE 25.3 ADR Risk Factors

- Concurrent use of multiple medications
- Multiple comorbid conditions
- Drug dose and duration of exposure
- Extremes of age (neonates, children, and elderly)
- Female sex
- Genetic predisposition
- Prior history of drug reactions and hypersensitivity
- End-organ dysfunction
- Altered physiology
- Inappropriate medication prescribing, use, or monitoring
- Lack of patient education and other system failures

The presence of multiple comorbid conditions (e.g., diabetes, asthma, congestive heart failure, obesity) further increases the risk of ADRs. Such patients may have altered physiology and some degree of end-organ dysfunction (e.g., renal, hepatic, cardiovascular, pulmonary). Conditions such as renal dysfunction may not be readily apparent in the elderly or in those with muscle wasting or malnutrition.

The extent and duration of drug exposure can also predispose to toxicity. This is particularly true for patients with end-organ dysfunction. An estimated

70–80% of adverse drug reactions may be dose related (33). Not surprisingly, the medications most commonly associated with adverse reactions are those with narrow therapeutic indices, such as digoxin, warfarin, heparin, theophylline, aminoglycosides, and anticonvulsants (34).

Age may be an important risk factor for the development of ADRs, and young children and the elderly may be particularly vulnerable. Despite this risk, documentation of ADRs in these groups is poor, and adverse reactions are often attributed to nondrug causes. Moreover, there is often inadequate experience with medications in these populations because they are often excluded from clinical trials (35).

The incidence of ADRs increases with increasing age (30). In addition to the increased risk posed by polypharmacy and comorbid conditions, there are important age-related changes in the pharmacokinetic disposition of a number of medications in the elderly (see Chapter 24). Although drug absorption is least likely to be affected, drug distribution, metabolism, and elimination are often altered (36). Age-related decreases in renal function are probably most important. However, changes in body composition, particularly the relative increase in adipose tissue that occurs with aging, may increase the distribution volume of lipid-soluble medications, thereby prolonging their half-life and altering peak and trough plasma concentrations. For example, the increased distribution volume of benzodiazepines in elderly patients results in lowered peak and raised trough plasma concentrations after a dose of these drugs. The net effect in the elderly is that these drugs have a reduced efficacy in inducing sleep and an exacerbated posthypnotic hangover effect. Pharmacodynamic changes may also be affected by age but are not consistently predictable. In general, elderly patients may be more sensitive to the effects of many medications and often require lower initial dosages (32).

Children of all ages also may be particularly susceptible to adverse drug reactions. In a surveillance study of over 10,000 pediatric admissions to several hospitals, 0.2% of admissions to the neonatal intensive care unit were caused by ADRs (37). Twenty-two percent of children with cancer were hospitalized as a result of ADRs. Among all other pediatric admissions studied, 2% were possibly or probably due to ADRs. The drugs most frequently implicated were phenobarbital, aspirin, phenytoin, ampicillin or amoxicillin, theophylline or aminophylline, trimethoprim-sulfamethoxazole, and diphtheria–pertussis–tetanus vaccine. Dosages of some medications begun in childhood (e.g., antiasthmatics, antiepileptics, stimulants, and insulin) may require careful adjustment during adolescence to minimize the risk of ADRs (40). Changes in body weight, drug distribution, and drug clearance can influence drug disposition and affect dosing.

As emphasized in Chapter 23, neonates are especially vulnerable to ADRs because they are sometimes exposed to drugs before birth and have immature renal and hepatic drug clearance capacities. Additionally, there is insufficient information on the clinical pharmacology of various drugs in this age group to guide rational pharmacotherapy (38, 39).

Women appear to be at greater risk for ADRs than do men (41–43). Data from the Glaxo Wellcome–Sunnybrook Drug Safety Clinic gathered over a 10-year period suggest that women over 18 years of age experience more ADRs than do their age-matched male counterparts (44). More than 77% of all ADRs, including those classified as severe, were reported in women. A recent cohort study evaluating the adverse-event experience with 48 newly marketed drugs in the United Kingdom revealed an incidence per 10,000 patients of 12.9 ADRs in males and 20.6 in females (42). Females over the age of 19 years were 43–69% more likely to experience a suspected ADR. Sex differences in pharmacokinetics and pharmacodynamics, differences in circulating hormone concentrations, and more frequent use of medications that inhibit hepatic metabolism are all cited as possible explanations for the observed differences (43). Women may also use more medications and are more likely to report adverse effects (43). Historically, women have been underrepresented in clinical trials, but this imbalance is reversing as regulations on their participation have changed (41).

Race and ethnicity may also be risk factors for ADRs. Prior personal or family history of ADRs may be predictive of future adverse reactions. Genetic polymorphisms for many metabolic reactions are described in Chapter 13 and have been well documented (45). Prescribing some medications without regard to genetic differences in metabolism can result in therapeutic failures or drug toxicity (45, 46). For example, differences in acetylator phenotype can alter the metabolism of some drugs and influence the risk of certain adverse reactions. Slow acetylators, for example, may be more likely than rapid acetylators to develop hepatotoxicity from isoniazid treatment. The biochemical basis for this difference is described in Chapter 16.

Genetic differences can also influence the likelihood of some drug interactions. For example, coadministration of the antiarrhythmic propafenone to patients being treated with metoprolol substantially reduces metoprolol metabolic clearance in extensive

CYP2D6 metabolizers, thereby resulting in exaggerated β-adrenoreceptor blockade and possibly precipitating congestive heart failure, nightmares, and blurred vision. This interaction essentially converts extensive CYP2D6 metabolizers to poor metabolizers, a phenomenon termed phenocopying, but does not impair metoprolol metabolism in poor metabolizers (45, 47).

Detection Methods

ADRs are sometimes not recognized and often go unreported. In fact, the principal limitation of ADR detection methods is the lack of awareness of what constitutes an ADR. Most ADRs are brought to medical attention by subjective reports and patient complaints. Linkage of a drug with an ADR is most often suspected on the basis of temporal association, but more objective confirmatory evidence often is lacking. Additionally, there are perceived barriers to reporting ADRs, and some clinicians fear that reporting suspected ADRs may expose them to liability. Moreover, many clinicians often fail to attribute new signs or symptoms, or changes in laboratory tests or diagnostic studies, to drug therapy. Medications should be carefully screened and systematically ruled out as possible causes of any abnormal finding on physical examination or from laboratory tests or diagnostic procedures.

Given the perceived failure of spontaneous reporting systems and the paucity of ADR reports, some institutions have instituted more active methods of ADR detection to supplement spontaneous reports. Medication order screening has become a common practice in U.S. hospitals. Manual chart reviews and audits and computer programs are used for retrospective, concurrent, and prospective medication utilization evaluation. Certain events often prompt an evaluation of a suspected adverse reaction. These include abrupt discontinuation of a medication, abrupt dosage reduction, orders for antidotes and emergency medications, orders for special tests or serum drug concentration measurements, and abnormal results from laboratory tests and medical procedures.

Spontaneous reports to the FDA and drug manufacturers, postmarketing surveillance, and data from ongoing observational studies and clinical trials provide other means for detecting important ADRs that may have not been detected during drug development.

Clinical Evaluation

Clinical evaluation of adverse drug reactions requires careful assessment of the patient and evaluation of pertinent factors. The patient's clinical status and severity of the reaction should be determined promptly in order to fully characterize the event and plan the optimal initial course of action. After obtaining a detailed description of the event, a differential diagnosis can be formulated that considers alternative etiologies. Alternative explanations for the adverse findings (e.g., nondrug causes, exacerbation of preexisting condition, laboratory error) should be carefully evaluated, based on the characteristics of all clinical signs and symptoms. These include severity, extent, temporal factors (onset, duration, frequency), presence of palliative or provoking factors, quality (character or intensity), response to treatment, and other associated findings.

A medical history (including a systematic review of body systems) and a physical examination should be obtained, along with relevant laboratory tests and diagnostic procedures. Relevant patient factors should be noted, including age, race, ethnicity, sex, height, weight, and body composition. Concurrent medical conditions or other factors should be considered that may cause, aggravate, or even mask or confound the manifestations of the reaction. These include conditions such as dehydration, autoimmune disorders, end-organ dysfunction, malnutrition, HIV infection, or pregnancy. Recent invasive medical procedures, treatments (e.g., dialysis), or surgery and any resultant complications (e.g., hypotension, shock, infection) should also be noted. Exposure to contrast material, radiation, or environmental or occupational hazards, and use of tobacco, caffeine, alcohol, and illicit substances should be investigated.

Because of the importance of drug interactions (see Chapter 15), a detailed medication history should be recorded that identifies all prescription, nonprescription, and alternative or complementary medications used by the patient. In addition to medication dosage, other factors that may contribute to the development of adverse reactions include medication administration route, method, site, schedule, rate, and duration. A history of allergies, intolerances, and other medication reactions should be fully investigated. The potential for cross-allergenicity or cross-reactivity should not be overlooked. The possibility of drug-induced laboratory test interference (analytical or physiological) and drug–drug or drug–nutrient interactions should also be explored.

Management of specific adverse reactions is beyond the scope of this chapter. However, it is intuitive that the offending agent should be discontinued if the event is life-threatening or intolerable to the patient, especially when a reasonable alternative exists (48). Palliative and supportive care

(e.g., hydration, glucocorticoids, or compresses) may be necessary for management of some adverse reactions. In some cases, specific reversal agents or antidotes are also needed (e.g., flumazenil for benzodiazepines, naloxone for opioids, and protamine for heparin). Some medications should not be stopped abruptly, and gradual dosage reduction may obviate rebound effects or other complications. In some circumstances, rechallenge with the suspected medication or desensitization may be warranted. Because some adverse reactions are delayed or may have an unpredictable course, careful monitoring and reevaluation are essential.

Causality Assessment

It is often challenging to establish a cause-and-effect relationship between a drug and a specific adverse reaction. This is especially true when appropriate ADR information is incomplete, inconsistent, or altogether lacking. Additional confounding factors include coadministration of other medications, nondrug variables, and concurrent illnesses.

Several methods used to determine causality have been described and compared (49–52). The Naranjo algorithm, perhaps the most commonly accepted causality assessment instrument, is presented in Table 25.4 (53). Most methods of causality evaluation emphasize reproducibility and validity of the data. *Reproducibility* depends on the precision of the instrument and thereby affects its reliability. Lack of reproducibility results from random error. Reproducibility is achieved when inter- and intraobserver variability are small, or when agreement between observations is high (54, 55). *Validity* is the extent to which a test accurately measures what it was designed to measure. Lack of validity most often results from experimental error. Validity of a test can be evaluated by measuring its sensitivity and specificity. This is difficult to establish when a gold standard is absent — as is often the case in ADR assessment (54, 55). Causality assessment instruments attempt to quantify information about adverse drug reactions and determine the

TABLE 25.4 Naranjo ADR Probability Scale[a]

To assess the adverse drug reaction, please answer the following questionnaire and give the pertinent score.

	Yes	No	Do Not Know	Score
1. Are there previous *conclusive* reports on this reaction?	+1	0	0	__
2. Did the adverse event appear after the suspected drug was administered?	+2	−1	0	__
3. Did the adverse reaction improve when the drug was discontinued or a *specific* antagonist was administered?	+1	0	0	__
4. Did the adverse reactions appear when the drug was readministered?	+2	−1	0	__
5. Are there alternative causes (other than the drug) that could on their own have caused the reaction?	−1	+2	0	__
6. Did the reaction reappear when a placebo was given?	−1	+1	0	__
7. Was the drug detected in the blood (or other fluids) in concentrations known to be toxic?	+1	0	0	__
8. Was the reaction more severe when the dose was increased, or less severe when the dose was decreased?	+1	0	0	__
9. Did the patient have a similar reaction to the same or similar drugs in *any* previous exposure?	+1	0	0	__
10. Was the adverse event confirmed by any objective evidence?	+1	0	0	__
			Total Score	__

ADR probability classification based on total score

9	Highly probable
5–8	Probable
1–4	Possible
0	Doubtful

[a] Reproduced with permission from Naranjo CA, Busto U, Sellers EM, Sandor P, Ruiz I, Roberts EA *et al*. Clin Pharmacol Ther 1981;30:239–45.

TABLE 25.5 Clinical Evidence Suggestive of Causality

- Temporal relationship
- Positive dechallenge
- Positive rechallenge
- Dose-response relationship
- Biological plausibility
- Absence of alternative etiologies
- Objective confirmation
- Prior reports of reaction
- Past history of reaction to same or related medication

probability that an ADR was caused by a specific medication. The presence of some or all of the elements listed in Table 25.5 increases the probability of drug culpability in association with an ADR.

A chronological or temporal relationship between the administration of a drug and the development of an adverse reaction is essential for establishing causality. The time to onset of reaction must be plausibly related to the administration of the drug. However, because some reactions may not appear for weeks or months after the start of therapy with a medication, they may be erroneously implicated as the cause of the reaction. The presence or absence of alternative etiologies and confounding variables also must be investigated (49, 56). A history of the reaction in a patient receiving the same drug or a similar compound increases the possibility that the association may be causal, and prior reports of similar reactions lend credibility to a cause-and-effect relationship. The absence of prior reports decreases the likelihood but does not eliminate the possibility that the reaction is due to the medication in question. If a precedent cannot be found, the plausibility of the reaction should be based on a consideration of the known clinical pharmacology of the drug (56). Further evidence to support an assertion of drug culpability requires objective data, such as abnormally high serum drug concentrations, specific physical examination findings, or other laboratory or diagnostic data characteristic of a drug reaction.

A positive dechallenge (i.e., when a reaction resolves after a drug is discontinued or a specific antagonist is administered) suggests that the medication may be culpable. A positive rechallenge (i.e., when signs or symptoms of the reaction recur after the drug is readministered) provides even more convincing evidence linking the drug to the reaction, but may not be ethically permissible and clinically justifiable. In any case, rechallenge should be done only after dechallenge is complete and signs and symptoms of the reaction have completely abated (57). The probability of a cause-and-effect relationship is further strengthened if the reaction worsens when a higher dose of the medication is administered. To further evaluate the probability of a drug-induced effect, Naranjo (58) suggests that a placebo challenge be considered.

Reporting Requirements

Documentation and reporting of adverse events are critical steps in the effort to prevent ADRs. Adverse reactions should be clearly described and documented in the medical record. This is mandated by the Joint Commission on Accreditation of Healthcare Organizations (JCAHO) as a method for preventing serious adverse reactions from re-exposure to a medication to which a patient may be allergic or intolerant. Most adverse reactions, however, are not properly documented or reported. Despite the importance of spontaneous adverse drug reaction reporting, it is estimated that only 1 in 10 serious adverse drug reactions is reported to the FDA. Given the large number of drug prescriptions written each year in the United States, this figure most likely overestimates the number of reports.

The reason most often cited for the lack of adverse event reporting is uncertainty about the causality of an adverse reaction. Although confirmation of an ADR is ideal, it is often not feasible. The FDA readily acknowledges this limitation and continues to encourage the reporting of all *suspected* adverse drug reactions through its MedWatch program. Detailed instructions for reporting adverse events associated with drugs, medical devices, vaccines, and veterinary products is provided online by the FDA (http://www.fda.gov/medwatch/report/hcp.htm). The essential components of an ADR report are listed in Table 25.6. The FDA is particularly interested in receiving reports of adverse reactions involving new chemical entities and serious reactions involving any medical product.

Adverse drug reaction data are largely drawn from spontaneous reports to the FDA or pharmaceutical manufacturers, postmarketing surveillance studies, and published case reports or case series. These sources are critical for identifying ADRs that are not detected or clearly characterized during preregistration clinical trials. ADRs are least likely to be detected when they have a low incidence, when drug exposure is minimal or infrequent, when the ADR manifestation or effect has a high background frequency (e.g., common symptom due to causes other than the medication), and when a time or dose relationship is weak or absent (59).

TABLE 25.6 Essential Components of an ADR Report

- Patient demographics
- Suspected product's name and manufacturer
- Relevant history and preexisting medical conditions
- Other medications or treatments
- Detailed description of the adverse event and its management
  - Date of onset
  - Dates and times that suspected drug was started and stopped
  - Dose, frequency, and route/method of drug administration
- Outcome of event (e.g., death, disability, prolonged hospitalization)
- Relevant laboratory tests or diagnostic findings
- Information regarding dechallenge and rechallenge
- Presence of confounding variables

Pharmaceutical manufacturers are required to report serious adverse drug events to the FDA within 15 days of receiving a report. All other reports are submitted on a quarterly basis for the first 3 years after marketing, and annually thereafter. Reports of serious adverse reactions, either during clinical trials or after drug marketing, occasionally result in FDA-mandated inclusion of "black box" warnings in the product label. These warnings usually are drug specific, but occasionally pertain to an entire pharmacological class of medications. New data relating to drug safety and efficacy also sometimes prompt the FDA to require pharmaceutical manufacturers to disseminate "dear doctor" letters to alert healthcare providers of findings that have the potential for substantial impact on public health. These and other safety notifications can be accessed at the FDA web site (http://www.fda.gov/medwatch/safety.htm).

ADR DETECTION IN CLINICAL TRIALS

Methodology

Detection of adverse reactions during clinical trials requires careful and systematic evaluation of study participants before, during, and after drug exposure. Objective data must be gathered to determine that study subjects meet all inclusion criteria and do not have any conditions that preclude their participation. Standard laboratory and diagnostic tests are used to establish patients' baseline health and functional status. Such tests should be appropriate for the drug and condition under investigation and should be conducted at predetermined intervals. Typically, serum chemistries and renal, hepatic, hematologic, electrolyte, and mineral panels are included. A complete medical history (including a review of all body systems) and physical examination and a complete medication history (including allergies and intolerances) should be included. Use of prescription, nonprescription, and alternative and complementary medications by study participants should be specifically documented.

Study protocols should clearly outline how adverse events will be detected, managed, and reported. Study data should be entered on case report forms designed for the study, and a quality control mechanism for ensuring the accuracy and integrity of the data should be established prior to the start of data collection. Computerized record keeping (i.e., electronic case report forms) can facilitate audits, data management, and data analysis. Adverse drug event questionnaires using extensive checklists of symptoms organized by body system have been developed for use in clinical trials (60). These are typically administered at baseline and at predetermined intervals during and after a study. To increase their utility and allow for comparisons between treatment groups, the questionnaires should be administered by a blinded investigator. Since healthy individuals who are free of illness and not taking medications can occasionally experience symptoms similar to those reported as drug side effects, adequate controls must be used in studies examining adverse drug reactions (61). Comprehensive questionnaires increase the likelihood that patient interviews are conducted in a consistent and nonsuperficial manner. Moreover, they minimize the risk of bias (particularly from focusing on known adverse effects) and can be useful for inter- and intrasubject comparisons. Of course, study participants should be encouraged to report all serious, unexpected, or bothersome symptoms, especially those that persist or require some treatment or intervention.

Toxicity criteria developed by the WHO and the National Cancer Institute (NCI) provide guidelines for objectively and systematically categorizing adverse effects according to type and severity grade. NCI's Common Toxicity Criteria (CTC) are particularly useful for studies involving antineoplastic drugs but are equally applicable to other drug categories. The CTC organizes related adverse events alphabetically according to body system or disease. For example, the "endocrine" category includes specific adverse effects such as gynecomastia and hypothyroidism. Specific criteria are detailed for grading the severity of each adverse effect. The CTC can be accessed at the NCI's Cancer Theraphy Evaluation Program web site (http://ctep.info.nih.gov/CTC3/default.htm).

Limitations

Despite attempts to screen candidate drugs during the early stages of preclinical development and to identify all serious adverse effects during the course of preregistration clinical trials, some drugs are approved for marketing that later are found to pose unacceptable public health risks. This is not altogether surprising given the limitations of study participant enrollment and duration of therapy during the clinical development of new drugs. Given these and other constraints, rare and unusual ADRs often cannot be detected before marketing approval is granted. Uncommon adverse reactions (e.g., those affecting 0.2% of patients or fewer) frequently will not be detected during clinical development (51). For example, it has been estimated that 3000 patients at risk must be studied in order to have 95% certainty in detecting an ADR with an incidence of 1/1000 (62). Given that most drugs are approved despite limited experience in humans, a drug such as chloramphenicol, which causes aplastic anemia with an incidence of 1 in 20,000 or less, would likely be approved today without realizing its potential to induce blood dyscrasias.

Even under optimal conditions, some ADRs will not be detected because drug exposure may be limited (i.e., short-term studies). Also, some latent ADRs may go undetected because of superficial monitoring or insufficient follow-up. Occasionally, ADRs may not be detected readily because they manifest slowly and exhibit symptoms that closely resemble those of the underlying condition for which the drug was being used. An example of this is the severe mitochondrial damage and subsequent hepatic injury induced by the synthetic nucleoside analog fialuridine (FIAU), which was being investigated for the treatment of hepatitis B infection (63).

Not only are study participants too few in number to detect uncommon ADRs, but typically they are not representative of the population at large that is likely be exposed to the medication in routine clinical use. Many studies have traditionally excluded children, the elderly, women of childbearing age, and patients with severe forms of the target disease. Moreover, patients with multiple comorbidities and those taking potentially interacting medications are often not included. It is, therefore, not surprising that even well-designed and impeccably conducted studies yield results that often are not generalizable.

Reporting Requirements

All experimental studies involving human participants require the approval of an institutional review board (IRB) and ongoing review of study progress. The IRB is specifically charged with the responsibility of safeguarding the rights and welfare of human research participants. In many cases, the study is monitored by a data and safety monitoring board (DSMB) in cooperation with the IRB. The DSMB reviews all reports of adverse reactions and conducts interim analyses of the data to ensure that study participants are not subjected to excessive risks or denied treatment with an effective medication if one arm of a study is found to be superior to another. Drugs being studied under an investigational new drug application (IND) must conform to criteria set forth by the FDA. Under these criteria, all adverse events must be promptly reported to the FDA, the IRB, and the drug sponsor. Serious adverse events (as defined earlier in this chapter) must be reported within 15 calendar days — 7 days if they are life-threatening or result in death. This reporting requirement cannot be waived even if causality (relationship of the event to the agent being investigated) has not been clearly established. Serious unexpected adverse events (those not described in the approved product label or the investigators' brochure for investigational new drugs) require particular attention.

INFORMATION SOURCES

Information regarding adverse effects of medications is available from many sources and in multiple formats (i.e., print, CD-ROM, online). Table 25.7 lists selected sources of ADR information. To assist in ADR detection, evaluation, and management, critical data regarding adverse reactions are needed (Table 25.8).

This information may be gleaned from specialized ADR resources, texts, and other tertiary sources, including the FDA-approved product label. However, this information must often be augmented using additional data from secondary sources. At minimum, this should include searches of the bibliographic databases from the National Library of Medicine (Medline and Toxnet) and Excerpta Medica (Embase).

Primary reports describing adverse reactions and drug-induced diseases include spontaneous reports and other unpublished data available from the manufacturer or the FDA. All reports of adverse reactions reported to the FDA can be retrieved (without identifiers) under the legal authority of the Freedom of Information Act. Anecdotal and descriptive reports of ADRs (including case reports and case series) are occasionally reported in the literature but are often incomplete and inconclusive. Guidelines for evaluating adverse drug reaction reports have been described (56).

TABLE 25.7 Selected Sources of ADR Information

Tertiary sources	Secondary sources	Primary sources
• General drug reference books (e.g., AHFS Drug Information,[a] Mosby's GenRx,[b] and the Physicians' Desk Reference) • Medical and pharmacotherapy textbooks • Specialized resources pertaining to ADRs and drug-induced diseases (e.g., Drug-Induced Diseases: Prevention, Detection, and Management; Meyler's Side Effects of Drugs; Davies's Textbook of Adverse Drug Reactions) • Drug interactions resources (e.g., Drug Interaction Facts, Drug Interactions Analysis and Management, Evaluation of Drug Interactions) • Micromedex databases (e.g., TOMES DRUGDEX, POISINDEX) • Review articles pertaining to individual ADRs or drug-induced diseases	• MEDLARS databases (e.g., Medline, Toxnet)[c] • Excerpta Medica (Embase) • International Pharmaceutical Abstracts • Current Contents • Biological Abstracts (Biosis) • Science Citation Index • Clin-Alert • Reactions • Cochrane Library	• Spontaneous reports or unpublished experience Individual clinicians FDA Manufacturer • Anecdotal and descriptive reports Case reports Case series • Observational studies Case-control Cross-sectional Cohort • Experimental and other study designs Clinical trials Meta-analyses

[a] AHFS, American Hospital Formulary Service.
[b] GenRx, The Complete Reference to generic and Brand Drugs.
[c] MEDLARS, Medical literature Analysis and Retrieval System.

Observational studies, including case-control, cross-sectional, and cohort studies, do not establish causality but can reveal associations of risk, the strength of which is measured by relative risk (cohort studies) or odds ratio. Design flaws and bias, however, occasionally render these studies altogether unreliable. Record-linkage studies using large prescription and medical databases are increasingly being used to gather data regarding ADRs (56, 59). Because they often include information from hundreds of thousands of patient records, well-designed linkage studies have the potential to generate robust epidemiological data. Prospective, randomized, controlled experimental studies (i.e., clinical trials) also can establish causality. These, along with well-designed meta-analyses, are useful for identifying and quantifying certain types of adverse effects. Nonetheless, even these study designs have their limitations.

TABLE 25.8 Essential Elements for Characterizing ADRs

- Incidence and prevalence
- Mechanism and pathogenesis
- Clinical presentation and diagnosis
- Time course
- Dose relationship
- Reversibility
- Cross-reactivity/cross-allergenicity
- Treatment and prognosis

REFERENCES

1. Lazarou J, Pomeranz BH, Corey PN. Incidence of adverse drug reactions in hospitalized patients. JAMA 1998;279:1200–5.
2. Dartnell JG, Anderson RP, Chohan V, Galbraith KJ, Lyon ME, Nestor PJ *et al*. Hospitalisation for adverse events related to drug therapy: Incidence, avoidability and costs. Med J Aust 1996;164:659–62.
3. Bates DW, Cullen DJ, Laird N, Petersen LA, Small SD, Servi D *et al*. Incidence of adverse drug events and potential adverse drug events. Implications for prevention. ADE Prevention Study Group. JAMA 1995;274:29–34.
4. Leape LL, Brennan TA, Laird N, Lawthers AG, Localio AR, Barnes BA, *et al*. The nature of adverse events in hospitalized patients. Results of the Harvard Medical Practice Study II. N Engl J Med 1991;324:377–84.
5. Shumock GT, Thornton JP, Witte WK. Comparison of pharmacy-based concurrent surveillance and medical record retrospective reporting of adverse drug reactions. Am J Hosp Pharm 1991;48:1974–6.
6. Beard K. Adverse reactions as a cause of hospital admission in the aged. Drugs Aging 1992;2:356–67.
7. Prince BS, Goetz CM, Rihn TL, Olsky M. Drug-related emergency department visits and hospital admissions. Am J Hosp Pharm 1992;49:1696–700.

8. Cooper JW. Adverse drug reaction-related hospitalizations of nursing facility patients: A 4-year study. South Med J 1999;92:485–90.
9. Harb G, Alldredge B, Coleman R, Jacobson M. Pharmacoepidemiology of adverse drug reactions in hospitalized patients with human immunodeficiency virus disease. J Acquir Immune Defic Syndr 1993;6:919–26.
10. Jick H. Adverse drug reactions: The magnitude of the problem. J Allergy Clin Immunol 1984;74:555–7.
11. Bates DW, Spell N, Cullen DJ, Burdick E, Laird N, Petersen LA *et al*. The costs of adverse drug events in hospitalized patients. Adverse Drug Events Prevention Study Group. JAMA 1997;277:307–11.
12. Johnson JA, Bootman JL. Drug-related morbidity and mortality: A cost-of-illness model. Arch Intern Med 1995;155:1949–56.
13. Leape LL. Preventing adverse drug events. Am J Health-Syst Pharm 1995;52:379–82.
14. Karch FE, Lasagna L. Adverse drug reactions. A critical review. JAMA 1975;234:1236–41.
15. Anon. ASHP guidelines on adverse drug reaction monitoring and reporting. Am J Hosp Pharm 1989;46:336–7.
16. Kennedy DL, McGinnis T. Monitoring adverse drug reactions: The FDA's new Medwatch program. P and T 1993;18:833-4, 839–42.
17. Hoigné R, Lawson DH, Weber E. Risk factors for adverse drug reactions — epidemiological approaches. Eur J Clin Pharmacol 1990;39:321–5.
18. Classen DC, Pestotnik SL, Evans RS, Lloyd JF, Burke JP. Adverse drug events in hospitalized patients. Excess length of stay, extra costs, and attributable mortality. JAMA 1997;277:301–6.
19. Rawlins MD, Thomas SHL. Mechanisms of adverse drug reactions. In: Davies DM, Ferner RE, de Glanville H, editors. Davies's textbook of adverse drug reactions. 5th ed. London: Chapman & Hall Medical; 1998. p. 40–64.
20. Coombs RRA, Gell PGH. Classification of allergic reactions responsible for clinical hypersensitivity and disease. In: Gell PGH, editor. Clinical aspects of immunology. Oxford: Oxford University Press; 1968. p. 575–96.
21. Mathews KP. Clinical spectrum of allergic and pseudoallergic drug reactions. J Allergy Clin Immunol 1984;74:558–66.
22. D'Arcy PF. Adverse reactions and interactions with herbal medicines. Part 2. drug interactions. Adverse Drug React Toxicol Rev 1993;12:147–62.
23. Uchegbu IF, Florence AT. Adverse drug events related to dosage forms and delivery systems. Drug Saf 1996;14:39–67.
24. Wong YL. Adverse effects of pharmaceutical excipients in drug therapy. Ann Acad Med Singapore 1993;22:99–102.
25. Napke E. Excipients, adverse drug reactions and patients' rights. Can Med Assoc J 1994;151:529–33.
26. Liss GM, Sussman GL, Deal K, Brown S, Cividino M, Siu S, *et al*. Latex allergy: Epidemiological study of 1351 hospital workers. Occup Environ Med 1997;54:335–42.
27. Liss GM, Sussman GL. Latex sensitization: Occupational versus general population prevalence rates. Am J Ind Med 1999;35:196–200.
28. Clyne KE, German MR. Adverse drug reaction reporting. Focus on cost and prevention. Pharm and Ther 1992;17:1145–56.
29. French DG. Avoiding adverse drug reactions in the elderly patient: Issues and strategies. Nurse Practitioner 1996;21:90, 96–7, 101–7.
30. Carbonin P, Pahor M, Bernabei R, Sgadari A. Is age an independent risk factor of adverse drug reactions in hospitalized medical patients? J Am Geriatr Soc 1991;39:1093–9.
31. Colley CA, Lucas LM. Polypharmacy: The cure becomes the disease. J Gen Intern Med 1993;8:278–83.
32. Cohen JS. Avoiding adverse reactions. Effective lower-dose drug therapies for older patients. Geriatrics 2000;55:54–6, 59–60, 63–4.
33. Melmon KL. Preventable drug reactions — causes and cures. N Engl J Med 1971;284:1361–8.
34. Gentry CA, Rodvold KA. How important is therapeutic drug monitoring in the prediction and avoidance of adverse reactions? Drug Saf 1995;12:359–63.
35. Gurwitz JH, Avorn J. The ambiguous relation between aging and adverse drug reactions. Ann Intern Med 1991;114:956–66.
36. Chutka DS, Evans JM, Fleming KC, Mikkelson KG. Drug prescribing for elderly patients. Mayo Clin Proc 1995;70:685–93.
37. Mitchell AA, Lacouture PG, Sheehan JE, Kauffman RE, Shapiro S. Adverse drug reactions in children leading to hospital admission. Pediatrics 1988;82:24–9.
38. Knight M. Adverse drug reactions in neonates. J Clin Pharmacol 1994;34:128–35.
39. Gupta A, Waldhauser LK. Adverse drug reactions from birth to early childhood. Pediatr Clin North Am 1997;44:79–92.
40. Nightingale SL, Hoffman FA. Medwatch and adolescence. J Adolesc Health 1994;15:279–80.
41. Merkatz RB, Temple R, Sobel S, Feiden K, Kessler DA. Women in clinical trials of new drugs. A change in Food and Drug Administration policy. The Working Group on Women in Clinical Trials. N Engl J Med 1993;329:292–6.
42. Martin RM, Biswas PN, Freemantle SN, Pearce GL, Mann RD. Age and sex distribution of suspected adverse drug reactions to newly marketed drugs in general practice in England: Analysis of 48 cohort studies. Br J Clin Pharmacol 1998;46:505–11.
43. Kando JC, Yonkers KA, Cole JO. Gender as a risk factor for adverse events to medications. Drugs 1995;50:1–6.
44. Tran C, Knowles SR, Liu BA, Shear NH. Gender differences in adverse drug reactions. J Clin Pharmacol 1998;38:1003–9.
45. Eichelbaum M, Kroemer H, Mikus G. Genetically determined differences in drug metabolism as a risk factor in drug toxicity. Toxicol Lett 1992;64/65:115–22.
46. Lennard MS. Genetically determined adverse drug reactions involving metabolism. Drug Saf 1993;9:60–77.
47. Eichelbaum M. Pharmacokinetic and pharmacodynamic consequences of stereoselective drug metabolism in man. Biochem Pharmacol 1988;37:93–6.
48. Sheffer AL, Pennoyer DS. Management of adverse drug reactions. J Allergy Clin Immunol 1984;74:580–8.

49. Danan G, Benichou C. Causality assessment of adverse reactions to drugs — I. A novel method based on the conclusions of international consensus meetings: Application to drug-induced liver injuries. J Clin Epidemiol 1993;46:1323–30.
50. Miremont G, Haramburu F, Begaud B, Pere JC, Dangoumau. Adverse drug reactions: Physicians' opinions versus a causality assessment method. Eur J Clin Pharmacol 1994;46:285–9.
51. Michel DJ, Knodel LC. Comparison of three algorithms used to evaluate adverse drug reactions. Am J Hosp Pharm 1986;43:1709–14.
52. Pere JC, Begaud B, Haramburu F, Albin H. Computerized comparison of six adverse drug reaction assessment procedures. Clin Pharmacol Ther 1986;40:451–61.
53. Naranjo CA, Busto U, Sellers EM, Sandor P, Ruiz I, Roberts EA *et al*. A method for estimating the probability of adverse drug reactions. Clin Pharmacol Ther 1981;30:239–45.
54. Hutchinson TA, Flegel KM, HoPingKong H, Bloom WS, Kramer MS, Trummer EG. Reasons for disagreement in the standardized assessment of suspected adverse drug reactions. Clin Pharmacol Ther 1983;34:421–6.
55. Hutchinson TA, Lane DA. Assessing methods for causality assessment of suspected adverse drug reactions. J Clin Epidemiol 1989;42:5–16.
56. Lortie FM. Postmarketing surveillance of adverse drug reactions: Problems and solutions. Can Med Assoc J 1986;135:27–32.
57. Girard M. Conclusiveness of rechallenge in the interpretation of adverse drug reactions. Br J Clin Pharmacol 1987;23:73–9.
58. Naranjo CA, Shear NH, Lanctot KL. Advances in the diagnosis of adverse drug reactions. J Clin Pharmacol 1992;32:897–904.
59. Meyboom RHB, Egberts ACG, Edwards IR, Hekster YA, de Koning FHP, Gribnau FWJ. Principles of signal detection in pharmacovigilance. Drug Saf 1997;16:355–65.
60. Corso DM, Pucino F, DeLeo JM, Calis KA, Gallelli JF. Development of a questionnaire for detecting potential adverse drug reactions. Ann Pharmacother 1992;26:890–6.
61. Reidenberg MM, Lowenthal DT. Adverse nondrug reactions. N Engl J Med 1968;279:678–9.
62. Lewis JA. Post-marketing surveillance: How many patients? Trends Pharmacol Sci 1981;2:93–4.
63. McKenzie R, Fried MW, Sallie R, Conjeevaram H, Di Bisceglie AM, Park Y *et al*. Hepatic failure and lactic acidosis due to fialuridine (FIAU), an investigational nucleoside analogue for chronic hepatitis B. N Engl J Med 1995;333:1099–105.

CHAPTER

26

Quality Assessment of Drug Therapy

CHARLES E. DANIELS
Skaggs School of Pharmacy and Pharmaceutical Sciences, University of California, San Diego, California

INTRODUCTION

In 2004, 36 new molecular entities or biological products were approved for clinical use by the U.S. Food and Drug Administration (1). Dozens of new drugs, new combinations, and new dosage forms are approved each year. The availability of valuable new agents creates opportunities for improved therapeutic outcomes, but also creates increased opportunities for inappropriate medication use. The clinical pharmacologist is expected to hold generalized medication use expertise that can be applied across the organization in the clinical practice and in independent and collaborative research activities. Quality assessment and improvement of medication use constitute an important skill set.

The objective of this chapter is to review medication use quality issues in an institutional context and highlight their impact on patient care and clinical research. The focus is on three themes: understanding the medication use system and organizational interests in medication use, understanding the application of drug use monitoring as a tool to improve medication use; and understanding processes to identify and improve medication errors.

Adverse Drug Events

Ernst (2) projected that costs of $177 billion a year are attributable to medication misuse. Adverse drug events (ADEs) are instances when patient harm results from the use of medication. This includes both adverse drug reactions, which were discussed in Chapter 25, and medication errors, all of which are inherently preventable. A 1999 Institute of Medicine report estimated that 98,000 Americans die each year due to medical error (3). This includes diagnostic mistakes, wrong-site surgery, and other categories of error, including medication errors. Approximately 20% of all medical errors are medication related (4, 5).

A medication error is any preventable event that may cause or lead to inappropriate medication use or patient harm while medication is in the control of a healthcare professional, patient, or consumer (6). Not all medication errors reach the patient. These are often referred to as "near misses." They are not usually considered to be ADEs only because no harm was done. Preventable ADEs are a subset of medication errors that cause harm to a patient (7). Figure 26.1 depicts the relationship between ADEs, medication errors, and adverse drug reactions (8). Because adverse drug reactions are generally unexpected, they are not presently considered to be a reflection of medication use quality in a classic sense. However, as genetic variances become a more prominent consideration in drug selection and monitoring, it may be possible to predict and avoid some of the reactions that have been previously unexpected. This offers an opportunity to improve the quality of medication use.

Medication errors are costly and are a diversion from the intended therapeutic objective. Morbidity or mortality are possible outcomes of medication errors. A 1997 study by Bates *et al.* (9) found that 6.5 ADEs occur for every 100 nonobstetric hospital admissions, and that 28% of them were preventable. It also was determined that 42% of life-threatening and

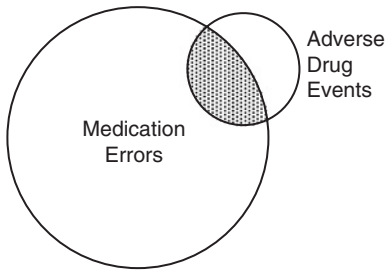

FIGURE 26.1 Diagram showing the relationship between medication errors and adverse drug events. Because some adverse drug events are preventable, they are also considered to be medication errors (*shaded area*). (Adapted from Bates DW *et al*. J Gen Intern Med 1995;10:199–205.)

serious ADEs were preventable. Preventable ADEs were responsible for an increased length of hospital stay of 4.6 days and $5857 per event. The cost for all ADEs was projected to be $5.6 million per year just for the institution in which the study was conducted. Anderson *et al*. (10) conducted a simulation of the impact of integrated medication use system and projected $1.4 million in excess costs that might have been saved had the components of the system been effectively integrated. These findings imply that safer medication use, with fewer adverse medication events, is a cost-effective target.

Medication Use Process

Medications are prescribed, distributed, and consumed under the assumption that the therapeutic plan will work as intended to provide the expected outcome. It is clear from previous chapters that there are many biological system issues that will influence success of the plan. Other organizational and societal system issues also influence success of the therapeutic plan as profoundly as do the biological systems issues. A prescriber writes an order for a medication based on the best available information, the likely diagnosis, and the expected outcome. A pharmacist reviews the requested medication order (prescription), clarifies it based upon additional information about the patient or medication (allergies, drug interactions, etc.), prepares the medication for use, counsels the patient about the drug, and gives it to the patient. The patient is responsible for understanding the therapeutic objective, knowing about the drug, creating a daily compliance plan (deciding when to take the drug), watching for good or bad results, and providing feedback to the prescriber or pharmacist regarding planned or unplanned outcomes. This process occurs over a variable period of time, in a system where the key participants of the process seldom speak with each other. Each action creates an opportunity for success or failure. Is there any wonder that the quality and integrity of the system are compromised on a regular basis?

The medication use system in an institutional setting offers even more complexity, with more chances for error. The five subsystems of the medication system in a hospital are selection and procurement of drugs, drug prescribing, preparation and dispensing, drug administration, and monitoring for medication or related effects (11). Evaluation and improvement of medication use quality require consideration of all of these subsystems.

Figure 26.2 is a flowchart of appropriate, safe, effective, and efficient use of medications in the hospital setting (12). It incorporates the role of the prescriber, nurse, pharmacist, and patient in a typical inpatient environment. It also depicts the role of the organization's pharmacy and therapeutics committee and quality improvement functions, which will be discussed later in this chapter. The decision to treat a patient in a hospital or extended-care facility typically adds a nurse or other healthcare provider (respiratory therapist, etc.) to the trio described in the ambulatory care setting. Every time that individual has to read, interpret, decide, or act is yet another opportunity for a mistake to occur. Each of the steps in the medication use process provides an opportunity for correct or incorrect interpretation and implementation of the tactics that support the therapeutic plan. With this many opportunities for medication misadventures to occur, it is easy to understand why tracking and improving quality are important aspects of medication use.

Phillips and colleagues (13) found a 236% increase in medication error-related deaths for hospitalized patients between 1983 and 1993. The same study showed an increase of over 800% for outpatient medication error deaths. The reported growth in medication error deaths may be partially attributed to more accurate reporting, but clearly represents a growth in the problem of medication errors from potent drugs. A 2002 poll commissioned by the American Society of Health-System Pharmacists concluded that the top two concerns of patients regarding hospitalization were related to drug–drug interactions and medication errors (14). A study by Bates *et al*. (15) determined that the 56% of medication errors in a hospital setting were associated with the ordering process, 6% with transcription of written orders, 4% with pharmacy dispensing, and 34% with administration of medications. Another study by Barker *et al*. (16) of medication administration in 36 healthcare settings identified a 19% total error rate during medication administration. Based on these findings it is easily concluded that there

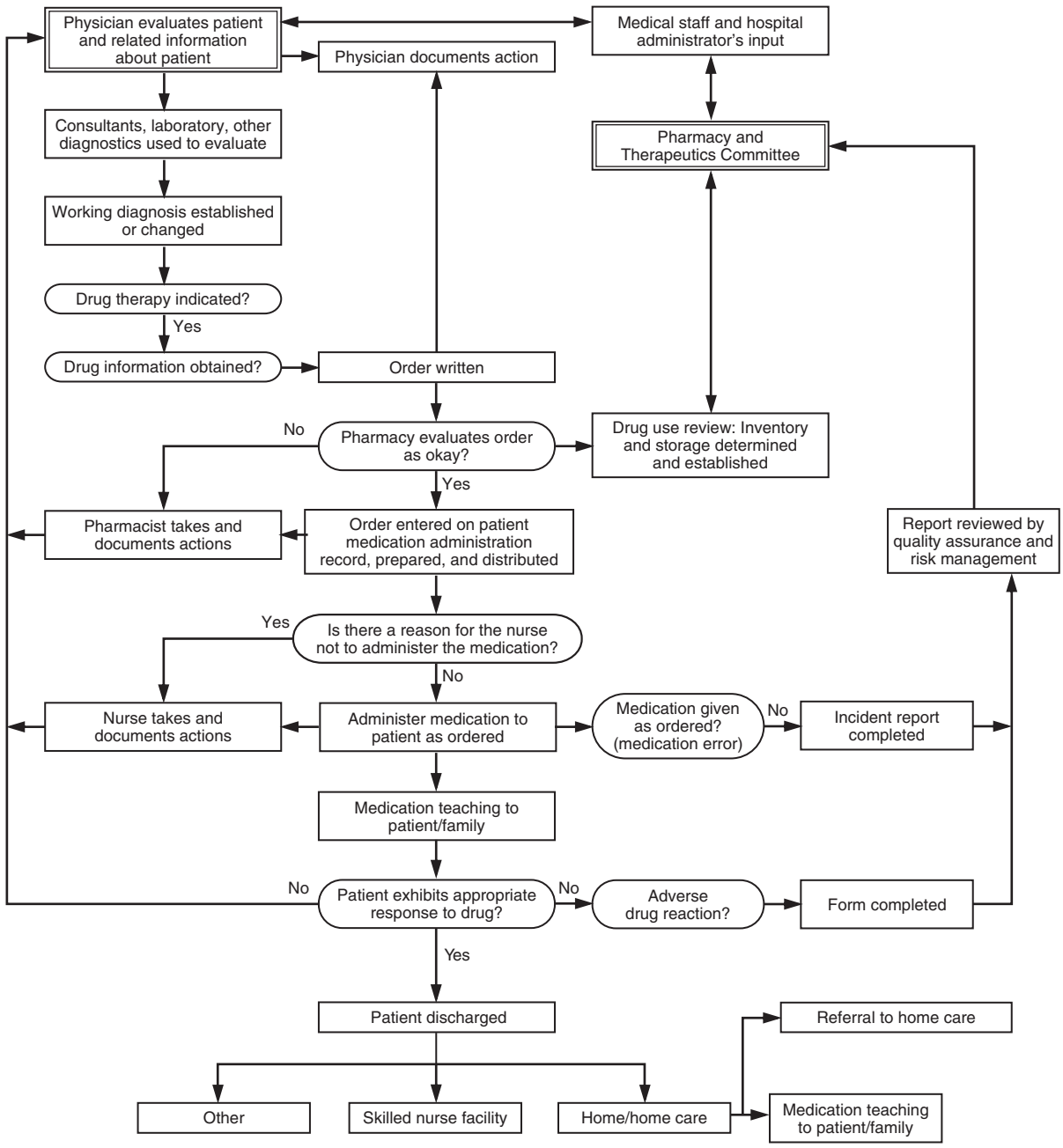

FIGURE 26.2 Flowchart of the inpatient medication use process, showing the start and end points (*double-boxed rectangles*), intervening actions (*rectangles*), and decision-making steps (*ovals*) required for appropriate, safe, effective, and efficient medication use. (Reproduced with permission from Atkinson AJ Jr, Nadzam DM, Schaff RL. Clin Pharmacol Ther 1991;50:125–8.)

is room for improvement in how medications are used in the inpatient and outpatient setting.

Improving the Quality of Medication Use

There are multiple facets to the quality assessment of medication use. Among them are monitoring of adverse medication events and medication use evaluation programs. To improve medication use, Berwick (17) has applied the industrial principles of continuous quality improvement to the healthcare setting. The critical elements of this approach are collection and use of data with a system focus. Deming (18) has championed the use of the Shewhart Cycle in continuous quality improvement. As shown in Figure 26.3,

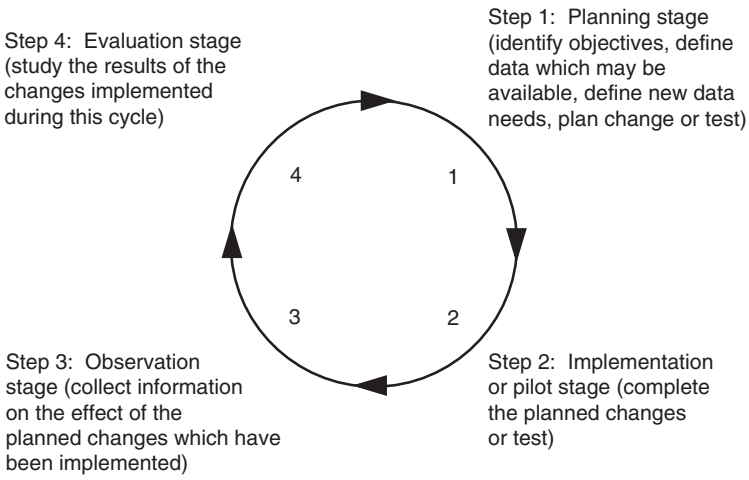

FIGURE 26.3 The Shewhart cycle. The cycle is repeated with desired improvements implemented with each iteration and the measured results used to guide the design of the next cycle. (Reproduced with permission from Deming WE. Out of the crisis. Cambridge, MA: MIT Press; 2000. p. 87–9.)

the Shewhart cycle is an approach for implementing systematic change based on data collection and evaluation with each iteration of the cycle. Each time the work cycle is completed, the result is compared to the expected outcome or ideal target. Modifications that improve the result are permanently incorporated into the process. Changes with no impact or a negative result will be deleted in the next iteration. Deming's message is that ongoing process and system change, along with measurement of the result, provide the feedback loop to support continuous improvement of the product or service.

ORGANIZATIONAL INFLUENCES ON MEDICATION USE QUALITY

Several external organizations and internal elements of the healthcare system have an interest in optimizing medication use. These include the hospital or health system, the medical staff, the group purchasing organization with which the hospital participates for the contractual purchase of drugs, and external regulatory or accreditation organizations (e.g., Joint Commission on Accreditation of Healthcare Organizations, HealthCare Financing Agency, National Council on Quality Assurance, state and local public health agencies). There is interest in what drugs are used, when and how they are used, the economic impact of drug selection, and outcomes that result in safe and effective use of medications.

The Joint Commission on Accreditation of Healthcare Organizations (JCAHO) is the organization that accredits most hospitals, health systems, and home care agencies. A significant element of the overall JCAHO review of patient care involves medication use quality and medication system safety. Accreditation standards for medication-related activities are applied across the organization. Hospitals are expected to present evidence that ordering, dispensing, administering, and monitoring of medications are overseen by the medical staff. The organization must be able to demonstrate that policies for safe medication use practices are in place. Quality-directed medication use is a key performance element for accreditation. Ongoing medication use evaluation, adverse medication event investigation, medication use performance improvement, and compliance with National Patient Safety Goals are required to meet the standards. The National Council on Quality Assurance accredits many managed care organizations. State professional boards (medicine, nursing, or pharmacy) provide oversight of specialized domains such as prescribing, dispensing, and administering medications. Most healthcare facilities are also regulated by local or state health departments, which often have local regulations on medication-related issues.

It is the responsibility of the medical staff in a healthcare organization to oversee medication use activities, ranging from product selection to long-term monitoring. This includes development of medication use policies, selection of drug products that are appropriate to the needs of the patient population being

served, and oversight of the quality of medication use. The pharmacy and therapeutics committee is frequently the focal point for medication-related activities within the organization. The pharmacy and therapeutics committee develops policies for managing drug use and administration, manages the formulary system, and evaluates the clinical use of drugs (19).

The exact structure of the pharmacy and therapeutics committee may vary to meet the unique needs and structure of the organization. It routinely reports to the medical staff executive committee or other leadership group within the medical staff organization. The committee is made up of representatives from the principal medication-using services (internal medicine, surgery, pediatrics, etc.) within the organization, plus representatives from the nursing services, pharmacy services, quality improvement program, and hospital administration. The chair of the committee is most frequently a clinician with experience in systemwide activities and, most important, an interest in quality use of medications. It is customary for the director of the pharmacy department to serve as the executive secretary for the committee to assure a working link between pharmacy department and committee activities.

Pharmacy and therapeutics committees usually meet 6–12 times per year. The schedule is dependent on the traditions of the organization and the amount of work included during the full committee meeting. The agenda should be prepared under the supervision of the committee chair and distributed well in advance of the meeting to allow all participants to read formulary drug monographs and drug use reports before the meeting. Ongoing elements of many committees are special standing subcommittees or focused task force workgroups. Typical standing subcommittees focus on antimicrobial agents and medication use evaluation. Standing subcommittees are appropriate for providing ongoing special expertise on matters that can be referred back to the full committee for action. The task force workgroup is used to address special limited-scope issues, such as *ad hoc* evaluations of agents within a given therapeutic drug class.

Medication Policy Issues

The pharmacy and therapeutics committee is expected to oversee important policies and procedures associated with the use of medications. Medication policy includes a wide range of issues, from who may prescribe or administer drugs, to what prescribing direction and guidance are appropriate to assure safe and appropriate use of high-risk, high-volume, high-cost, or problem-prone drugs. Policies are often needed to identify who may prescribe or administer medications, to assure consistent supply or quality of drug products, or to allocate drugs in times of shortage. Responsibility for developing policies to address special circumstances or issues is often delegated to the pharmacy and therapeutics committee by the organization. Examples of this type of policy are special drug class restriction, (e.g., antimicrobial agents) and use of agents for sedation during medical procedures.

Formulary Management

The objective of an active formulary program is to direct medication use to preferred agents, which offer a therapeutic or safety benefit or an economic advantage. This serves as a quality/benefit-driven opportunity when optimally implemented. A statement of principles of a Sound Drug Formulary System was developed in 2000 by a consortium composed of the U.S. Pharmacopoeia, the Department of Veterans Affairs, the American Society of Health-System Pharmacists, the Academy of Managed Care Pharmacists, and the National Business Coalition on Health (20). In this statement, a formulary is defined as "a continually updated list of medications and related information, representing the clinical judgment of physicians, pharmacists, and other experts in the diagnosis and or treatment of disease and promotion of health." A specific formulary is intended for use in a defined population. The defined population may consist of patients in a single hospital, patients seen within a group practice, a managed care patient population (local, regional, or national), or even an entire community.

Historically, formulary drug inclusion or exclusion has been used as an administrative hurdle to discourage prescribers from using less desirable drugs. The historical approach to formulary decision making was based on a simple "on formulary" or "not-on formulary" approach. Formulary drugs were available immediately with no special requirements. Often a formulary drug was selected by the prescriber to avoid a prolonged waiting period for the nonformulary item to be ordered and made available for the patient. This approach was more effective when the array of effective drug choices was somewhat limited, and the principal cost and quality management need was to reduce the number of "me-too" products.

With the advent of many of the newest generation of products, including monoclonal antibodies and cytokine agents, it is not logical to simply limit the formulary availability of these novel agents. Accordingly, the standard for most institutions has been to include these novel drugs with committee approved restrictions and guidelines for use. In the future, genomics and genetic diversity, which can influence

toxicity and effectiveness, will play an important role in formulary drug management. The ability to better customize patient-specific drug response will require a more sophisticated approach in selecting the most appropriate drug.

Drug Selection Process

Effective formulary development is based upon the scientific evaluation of drug safety, clinical effectiveness, and cost–impact (20). That information is used by the committee to determine the specific value and risk of the drug for the patient population to whom the drug will be administered. The committee evaluates a given drug relative to the disease states typically treated in this population. For instance, the presence or absence of certain tropical diseases may impact on the need to include some antimicrobial agents on the formulary. The evaluation of a drug should include discussion of what doses and duration of therapy might be most appropriate in order to establish guidelines for measuring prescribing quality. In some cases, it may be necessary to determine which healthcare professionals are appropriately trained or qualified to prescribe a particular drug. The committee may elect to restrict the use of a drug to certain specialists (e.g., board-trained cardiologists for high-risk antiarrhythmic agents) or the drug may be restricted by the manufacturer or FDA to those prescribers who have received some drug-specific training and have been approved by the supplier (e.g., thalidomide).

Economic evaluation of medications is a routine element of formulary development. The development of many effective but expensive drugs, which are likely to cost thousands of dollars for a single short course of therapy or tens of thousands for long-term therapy, has placed financial impact at center stage in product selection. The availability of these high-cost agents has created a new specialty discipline called pharmacoeconomics. A growing list of academic medical centers have established units that focus research and practice efforts on outcomes measurement of drug therapy. These programs often provide sophisticated evaluations of the economic or quality-of-life elements of drug use.

It is noteworthy that drug costs, and their impact, are perceived differently from different perspectives in the healthcare system. Each component of the healthcare system (hospital, home care, ambulatory provider) may have a different perspective on the cost of therapy. Hospitals are usually responsible for all drug-related costs (drug purchase, medication administration, laboratory monitoring, etc.) for the finite period of time that a patient is hospitalized. A stand-alone outpatient drug benefit manager might only worry about the drug cost for the nonhospitalized portion of the therapy. The overall health system may be at financial risk for all elements of outpatient and inpatient care. Because each element of the system may be responsible for a different component of the total cost of care, the cost–impact of a given drug product selection may be different for each element. The "societal perspective" often represents yet another view of drug costs in that it incorporates nonhealthcare costs and the value of lost days of work and disability. Formulary inclusion is not routinely based on that level of evaluation, but public policy may be influenced by that information.

The cost–impact analysis of two hypothetical drug choices shown in Figure 26.4 demonstrates the role of cost perspective in the formulary selection process. Both regimens offer the same long-term clinical result and adverse reaction profile. This analysis shows that the decision as to which drug is the lower cost option will vary with the perspective of the organization that is responsible for the different inpatient and outpatient components of care. This dilemma is a regular element of the formulary selection process in many institutions. The puzzle becomes more complex when one is trying to decide what elements of cost (e.g., laboratory tests or other monitoring activities) should be included. Despite this lack of clarity, the cost–impact of drug therapy on different stakeholders require that this issue be considered in the decision process.

Most hospitals and healthcare organizations participate in a purchasing group to leverage volume-driven price advantages. The makeup and operations of these groups vary widely, but the price agreements and changing landscape of drug pricing add an additional dimension to the drug price factor. A specific drug may be the lowest price option for a given contract period, after which the choice may change. In another variation, a package of prices for bundled items may cause the price for a given item to change, depending on the use of yet another item. How this influences formulary decisions is a function of the drug and many other factors.

Formulary Tactics

In addition to drug selection, the pharmacy and therapeutics committee is responsible for considering formulary tactics to support the overall goal of optimal medication use. Several of these tactics have been used successfully to direct drug use toward preferred agents. The most obvious tactic to direct use away from a given agent is to exclude it from the formulary. The use of nonformulary agents usually triggers

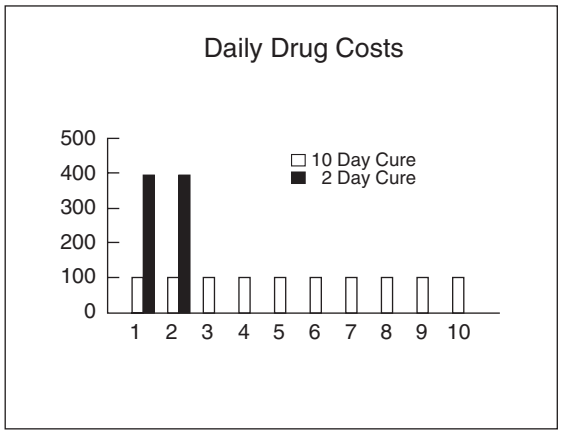

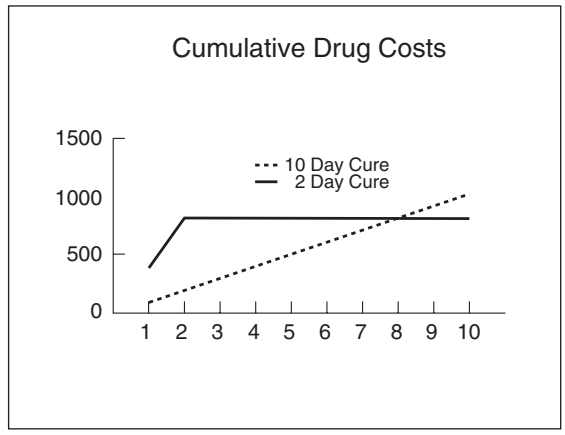

Financial Responsibility at Discharge

	Daily Cost	10 Day Total	Total at Hospital Discharge
2 Day Cure	$400	$800	$800
10 Day Cure	$100	$1000	$300

Perspective Based Financial Responsibility

	2 Day Cure	10 Day Cure
Hospital	$800	$300
Outpatient Payer	$0	$700
Total	$800	$1000

FIGURE 26.4 Financial perspective in formulary decision-making. Comparison of two treatment options: 2-day cure at $400 per day versus 10-day cure at $100 per day, with an anticipated hospital stay of 3 days.

some required override, or *post hoc* review of use by the committee or designated individual. A second tactic involves a global management of medication use by therapeutic class. This tactic can be employed to minimize the use of drugs with a less clear profile of therapeutic efficacy or safety. A decision to limit the number of agents from a given drug class can also provide some advantages in price contracting, if formulary inclusion is effective in directing medication use to lower cost agents.

Limiting prescribing rights for some specific drugs to a subset of prescribers who possess special expertise that qualifies them to use these drugs can improve the quality of drug use. In many cases, drug restriction is managed by one or more gatekeepers whose approval is required prior to beginning therapy with the drug (e.g., infectious disease approval prior to start of a specified antibiotic). In some cases, direct financial incentives have been used to encourage use of a given drug or group of drugs. These formulary tactics have been used to influence decision-making by prescribers, pharmacists, and patients.

Analysis and Prevention of Medication Errors

Reason (21) has described a model for looking at human error that portrays a battle between the sources of error and the system-based defenses against them. This model is often referred to as the "Swiss cheese model" because the defenses against error are displayed as thin layers with holes that are described as latent error in the system. Figure 26.5 demonstrates the model as applied to medication error. Each opportunity for error is defended by the prescriber, pharmacist, nurse, and patient. When a potential error is identified and corrected (e.g., dose error, route of administration error) the event becomes a "near miss" rather than an ADE. In those cases in which the holes in the Swiss cheese line up, a preventable medication error occurs. The Swiss cheese model provides an interesting framework for research in this field.

The latent errors in the medication use system have been described in several studies. Major contributors to errors in medication use were found to be knowledge gap related to drug therapy (30%);

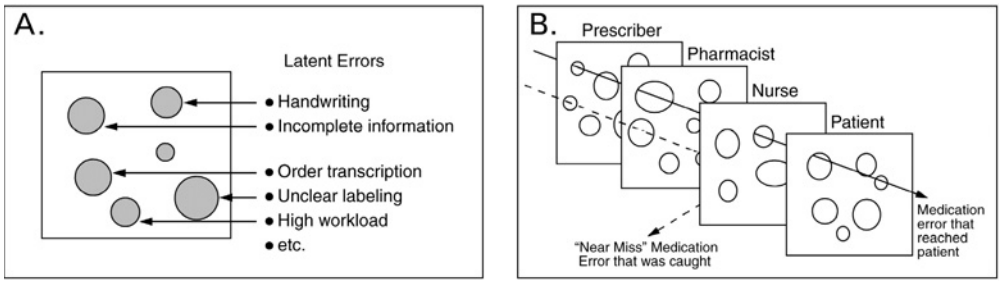

FIGURE 26.5 Latent medication system errors (A) and defensive layers against error (B) in the medication system.

knowledge gap related to patient factors (30%); errors in dose calculations, placement of decimal points, and dosage units (18%); and nomenclature failures, such as wrong drug name or misinterpreted abbreviation (13%) (22). Cohen (23) describes six common causes of medication error based on his review of events reported to public reporting databases. These causes of errors include failed communication, poor drug distribution practices (including verbal orders), dose miscalculations, drug- and device-related problems (such as name confusion, labeling, or poor design), and lack of patient education on the drugs that are prescribed for their use. Leape *et al.* (24) identified 13 proximal causes of medication errors in an academic medical center. They are detailed in Table 26.1.

Medication Error Data

The rate and nature of medication errors has been studied by several authors. Nightingale *et al.* found a medication error rate of 0.7% in a British National Health Service general hospital (25). Rothschild *et al.* (26) found 36.2% preventable adverse events plus an additional 149.7 serious errors per 1000 patient days.

TABLE 26.1 Proximal Causes of Medication Errors[a]

Lack of knowledge of the drug	Faulty dose checking
Lack of information about the patient	Infusion pump and parenteral delivery problems
Violation of rules	Inadequate monitoring
Slips and memory lapses	Drug stocking and delivery problems
Transcription errors	Preparation errors
Faulty checking of identification	Lack of standardization
Faulty interaction with other services	

[a] Adapted from Leape LL *et al.* Systems analysis of adverse drug events. JAMA 1995;274:35–43.

Medication ordering or execution represented 61% of the serious errors. Slips and lapses rather than rule-based or knowledge errors were most common. Lesar *et al.* (22) describe the results of a review of 2103 clinically significant medication errors in an academic medical center. It was determined that 0.4 % of medication orders were in error: 42% of the errors were overdosage, and 13% were the result of drug allergies that were not accounted for prior to prescribing. This work showed that medication errors result most frequently from failure to alter dose or drug after changes in renal or hepatic status, missed allergies, wrong drug name, wrong dosage form (e.g., IV for IM), use of abbreviations, or incorrect calculation of a drug dose. They concluded that an improved organizational focus on technological risk management and training should reduce errors and patient risk of ADEs.

Given the latent errors associated with some elements of human performance, it seems likely that automation may reduce error. Several studies have demonstrated the value of computer assistance in the medication order entry process. Rules-based physician order systems have been shown to identify and reduce the chances of adverse medication events due to drug duplication, calculation errors, and drug–drug interactions (25, 27–30). Despite these demonstrated advantages to computer-assisted medication ordering, the process is still far from error free. MedMARx data from 2003 showed that nearly 20% of the medication errors reported to that national database were associated with problems in computerization and automation (31). A large number of these were order entry errors associated with interruptions during order entry. Another study showed that an early-generation computerized prescriber order entry system facilitated some error types due to formatting and display limitations (32). In still another study, Nebeker *et al.* (33) found that ADEs continued to occur following the implementation of a computer prescriber order entry system. They concluded that effective decision support functions are required to prevent

order entry-related medication errors associated with computerized prescribing systems.

Some therapeutic categories of medications might be predicted to be prone to error due to narrow therapeutic index, complexity of therapy, or other factors. Phillips *et al.* (13) found that analgesics, central nervous system agents, and nontranquilizer psychotropic drugs were most frequently associated with deaths due to medication errors. Lesar *et al.* (22) found antimicrobials and cardiovascular drugs to be the most error-prone therapeutic categories in an academic medical center. Calabrese *et al.* (34) found vasoactive drugs and sedative/analgesics to be most problematic in the ICU setting. Based on these nonconverging findings, it might be concluded that the specific drugs of concern are unique to the institution or practice setting, a conclusion that is partially true. The JCAHO (35) has identified a list of drugs and drug practices that are associated with high risk for significant error based upon high report rates, and the Institute for Safe Medication Practices (36) also has identified drugs that should generate a high alert due to risk for medication errors. Lambert and colleagues (37, 38) have described a series of experiments that test the likelihood of drug name confusion based on fixed similarity patterns. This theoretical concept is providing the basis for selecting drug names that minimize the chance of sound-alike errors (39).

Research methods on medication error data are not standardized. Therefore, they are subject to some limitations in generalizability. Because widespread interest in developing scientific approaches for reducing medication error is relatively recent, there are few well-established methods for conducting research in this field. However, funding for research in safe medication use and error reduction is available from several public and private sources, including the Agency for Healthcare Research and Quality.

Medication error data collection and analysis for clinical use and quality improvement are also complex activities. Observational data, *post hoc* review of medical records, and self-reporting have all have been used with varying degrees of success for research and functional applications. Each offers strengths and weaknesses, and the appropriate method for data collection is in large part a function of its intended use and the resources available to collect it.

Most hospitals collect internal medication error data through a voluntary reporting mechanism. This system is used as the backbone of error reporting because it requires minimal resources for data collection and is supported by organizational risk management programs. Voluntary reporting is presumed to underreport total errors. It is widely believed that most significant errors are reported when they are identified, but many mistakes are never recognized. Many other errors are determined to be insignificant and, therefore, not formally reported. For these reasons, it is difficult to determine in the hospital setting if changes in a given series of numbers represent a real change or simply a different level of reporting.

Figure 26.6 illustrates a typical presentation of aggregated or high-level medication error data in an institutional setting. This presentation allows for general trends in total numbers to be plotted and tracked over time. Review of high-level data shows trends and provides a framework for the first level of error analysis. Major changes can be seen, which may trigger more intense analysis. However, this high-level data approach does not provide any detail to the analyst regarding the subcomponents of the composition of the reported errors. As a result, the pitfalls in drawing conclusions from aggregated high-level data can make these conclusions problematic. For instance, one might presume that administration of medication to the wrong patient is generally more serious than is administration of a medication at the wrong time. However, an increase of five "wrong patient" errors and a decrease of five "wrong time" errors for a

A.

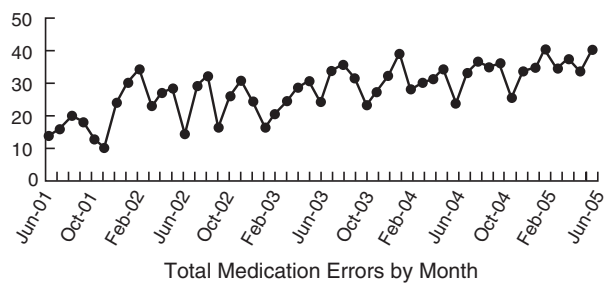

Total Medication Errors by Month

B.

	Jun-02	Sep-02	Dec-02	Mar-03	Jun-03	Sep-03	Dec-03	Mar-04	Jun-04	Sep-04	Dec-04	Mar-05	Mean
Wrong Drug	5	3	6	2	10	2	4	5	4	8	2	2	4.4
Wrong Dose	11	17	8	13	6	12	18	17	21	15	22	14	14.5
Duplicate Dose	10	4	3	8	2	16	4	11	9	11	6	17	8.4
Wrong Route	3	2	4	0	2	1	1	5	3	0	3	1	2.1
Wrong Time	15	25	12	33	15	19	27	31	17	26	10	29	21.6
Wrong Fluid	6	7	4	10	3	8	7	5	8	2	3	2	5.4
Wrong Rate	16	20	12	17	21	8	24	8	11	19	23	14	16.1
Wrong Device	2	0	0	1	3	1	4	2	0	1	2	2	1.5
IV Infiltration	0	2	1	0	3	2	0	0	4	0	2	0	1.2
Total	**68**	**80**	**50**	**84**	**65**	**69**	**89**	**84**	**77**	**82**	**73**	**81**	**75.2**

Medication Errors by Quarter

FIGURE 26.6 Typical presentation of medication error data in aggregate form by month (A) or categorized by error type on a quarterly basis (B).

specific time period will register as a zero change for that period if only aggregated data are used. If fact, it may represent a serious degradation in some element of the medication system that will not be seen through this level of error analysis.

Classification and analysis of medication error data by error type are recommended as a method to spot potentially important changes in system performance. The National Coordinating Council for Medication Error Reporting and Prevention system for classifying medication errors may be used (6). Commercial systems for cataloging and analyzing medication errors are available. A potentially valuable element of some programs is the ability to share anonymous data with other hospitals for comparison with similar institutions (40). Regardless of the system used to classify and analyze medication error data, clear and consistent classification must be made to avoid confounding conclusions regarding underlying problems.

Reducing Medication Errors

Collection and use of medication error data at the hospital level are challenging but important functions. A key organizational principle in quality improvement is to make reporting errors a nonpunitive process. This usually increases the number of errors that will be reported, but not the number occurring. Making errors visible is an important step in the process of finding and fixing system-related problems (41). The ongoing monitoring of ADE data (both medication errors and adverse drug reactions) is an important responsibility of the pharmacy and therapeutics committee. The committee is the organization's only convergence point for all medication-related issues. This convergence allows for a full review of the medication use process for system adjustments.

To identify opportunities for reducing medication errors, it is important that each error be carefully reviewed by a limited number of individuals to gain intimate knowledge of each reported incident. Collection and classification of error data must be followed by use of a careful epidemiological approach to problem solving at the system level. Narrative data, which may not be seen by looking at the categorical data alone, can be used to provide important details about proximal causes and latent error that may have contributed to the event. Success in this type of error reduction requires the reviewers to read between the lines, look for common threads between reports, and link multiple errors that are the result of system weaknesses.

There is still work to be done in understanding errors in the medication use process. However, available information provides suggestions on how to reduce medication errors. Bates's (42) ongoing studies of medication errors led to eight specific error prevention strategies: (1) unit-dose medication dispensing, (2) targeted physician education on optimal medication use, (3) inclusion of the clinical pharmacist in decision-making patient activities, (4) computerized medication checking, (5) computerized order entry by the prescriber, (6) standardized processes and equipment, (7) automated medication dispensing systems, and (8) bar-coded medications for dispensing and administration. Other authors have reached similar conclusions.

The more complex the patient's drug therapy regimen, the greater the likelihood that adverse medication events will occur. Cullen *et al.* (43) determined that the rate of preventable and potential adverse drug events was twice as high in intensive care units, compared to nonintensive care units. This was attributed to the higher number of drugs used in the ICU. Lesar *et al.* (44) reviewed medication prescribing errors over a 9-year period and concluded that the incidence of prescribing error increased as intensity of care increased and new drugs became available. Koechler *et al.* (45) reported that greater than five current medications, 12 or more doses per day, or medication regimen changes four or more times in a year were all predictors for drug therapy problems in ambulatory patients. Transition between levels of care or components of the healthcare system put patients at risk for medication errors. Cornish (46) found that 53% of patients they studied had at least one medication unintentionally not ordered during the transition from home status to inpatient admission, but that dose errors were also a significant problem. Gray *et al.* (47) determined that the occurrence of an ADE was positively related to the number of new medications received at hospital discharge. The knowledge that some patients are at higher risk for ADEs suggests possible high-return intervention targets. When selecting improvement opportunities, it is wise to look for those areas most likely to yield results.

Examples of system improvements to reduce medication errors have been reported in several projects. Leape *et al.* (48) reduced medication errors in an intensive care unit by inclusion of a pharmacist on the clinical rounding team. Flynn *et al.* (49) identified interruptions (telephone calls, conversations, etc.) during critical phases of pharmacist drug preparation activities as significant contributors to errors in medication preparation. Comprehensive efforts to prevent medication errors include the four-pronged medication error analysis program from the Institute for Safe Medication Practices (50). This four-pronged

approach includes evaluation of specific medication errors, evaluation of aggregated error data and near-miss data for the hospital, as well as evaluation of error reports from other hospitals. In addition, effective medication error prevention includes ongoing monitoring of drug therapy trends, changes in medication use patterns, information from the hospital quality improvement or risk management program, and general hospital programmatic information.

Monitoring institutional trends in medication use can provide clues to possible high-risk or error-prone therapies. Increased use of drugs with a history of medication errors, such as patient-controlled analgesia, should alert organizations to develop safeguards to protect against errors before, rather than after, they become problems. Cohen and Kilo (36) describe a framework for improving the use of high-alert drugs, which is based on reducing or eliminating the possibility of error, making errors visible, and minimizing the consequences of errors. Table 26.2 presents change concepts for safeguarding against errors when using high-risk drugs.

Medication error prevention opportunities also may present themselves in unusual hospital programmatic information from sources not routinely applied to medication safety. For instance, reports of laboratory-related incidents or hospital information system problems may be indicators that medication-related problems can be expected. Thoughtful use of this information may prevent medication-related errors attributed to supplemental systems that are critical to safe and appropriate medication use. Reports of staff shortages within an institution (e.g., critical care nurses, nurse anesthetists) can be used to identify potential problem areas prior to medication error reports. Likewise, reports of planned construction or information system conversions may be an indicator that routines will be interrupted. Thus, use of hospital program information in a prospective way can be used to provide safe alternatives that avoid medication errors before they occur.

System improvements may improve the quality of prescribing by standardizing to an expert level. Morris (51) described the development, testing, and use of computerized protocols for management of intravenous fluid and hemodynamic factors in patients with acute respiratory distress syndrome. Evans *et al.* (52) used a computerized anti-infectives management

TABLE 26.2 Safeguarding against Errors in High-Risk Drugs[a]

Concept	Example
Build in system redundancies	Independent calculation of pediatric doses by more than one person (e.g., prescriber and pharmacist)
Use fail-safes	IV pumps with clamps that automatically shut off flow during power outage
Reduce options	Use of a single concentration of heparin for infusion (e.g., 25,000 units in 250 ml of saline)
Use forcing functions	Preprinted order forms for chemotherapy drugs that require patient height and weight information before preparation and dispensing
Externalize or centralize error-prone processes	Prepare IV admixtures in the pharmacy instead of on nursing units
Use differentialization	Supplemental labels for dosage forms that are not appropriate for intravenous use without dilution
Store medications appropriately	Store dopamine and dobutamine in separate locations
Screen new products	Review new formulary requests for labeling, packaging, and medication use issues that may be error prone
Standardize and simplify order communication	Avoid use of verbal orders
Limit access	Restrict access to the pharmacy during "nonstaffed" hours and follow up on all medications removed from the pharmacy during this time
Use constraints	Require approval before beginning therapy (e.g., attending signature on chemotherapy orders)
Use reminders	Place special labels on products when they are dispensed by the pharmacy to remind of special procedures for use (e.g., double-check rate calculation of insulin infusions)
Standardize dosing procedures	Develop standardized dose and rate charts for products such as vasoactive drugs (e.g., infusion rate expressed as micrograms per kilogram per minute)

[a] Adapted from Cohen MR, Kilo CM. High-alert medications: Safeguarding against errors. In: Cohen MR, editor. Medication errors. Washington, D.C.: American Pharmaceutical Association; 1999. p. 5.3–5.11.

program to improve the quality of medication use and reduce costs. In consideration of all that is currently known, Leape (53) provided a simple set of recommendations to reduce medical error: reduce reliance on memory, improve access to information, error-proof critical tasks, standardize processes, and instruct healthcare providers on possible errors in processes. These simple but thoughtful recommendations are an important concept that can help to reduce medication errors.

Medication Use Evaluation

Medication use evaluation (also referred to as drug use evaluation, or MUE) is a required component of the medication use quality improvement process. It is a performance improvement method with the goal of optimizing patient outcomes (54). The first element of drug use tracking is global monitoring of organizational drug use. This can be completed by routine evaluation of totals and changes in drug use within a therapeutic drug category. The American Hospital Formulary Service has created a comprehensive therapeutic classification system that is often used for drug use monitoring, but other commercial medication databases are also available (55).

Figure 26.7 is an example of a global drug use report that may be used to look for trends and variations in medication use. This report should be examined for changes that represent increases or decreases in comparison to previous reporting periods. A change in any specific category or group of drugs may be important and worthy of specific follow up. Smaller changes that support a trend over time can demonstrate ongoing changes in drug use patterns. Changes seen in global-level monitoring may trigger a focused evaluation to further assess the appropriateness with which certain medications are used.

Medication use evaluation has historically been categorized with regard to how and when data collection or intervention occurs (Table 26.3). Most medication use evaluations are retrospective, as exemplified by an analysis of 8 years of emergency department prescribing data by Catarino *et al.* (56). These authors found that, despite the availability of published lists of medications that are not generally appropriate for geriatric patients, one or more of those inappropriate medications were prescribed for 12.6% of elderly patients during their emergency department visits. Table 26.3 also describes concurrent and prospective reviews classified based on the use and timing of intervention as part of the process that is used for screening and incorporation of data.

Focused Medication Use Evaluation

Focused or targeted medication use evaluation follows a reasonably well-established cycle: identification of a potential problem in the use of a specific drug or therapy, collection and comparison of data, determination of compliance with a pre-established guideline/expectation, and action as needed to improve discrepancies between expected and measured results. This type of medication use evaluation provides an excellent opportunity to apply the Shewhart cycle for continuous quality improvement (Figure 26.3). Focused medication use projects are typically selected for a specific reason. Table 26.4 lists reasons to consider drugs for focused evaluation projects.

Concurrent or Prospective Focused Medication Use Review

Concurrent or prospective focused medication use review activities can be used to prevent medication-related adverse events and improve the quality of medication use. Information system support has been demonstrated to enhance response to changes in predefined laboratory values. Notice of abnormalities in coagulation, renal function, blood glucose, and electrolytes are all potential indicators of medication use problems in individual patients. When laboratory test results are reported along with specific drugs, it is possible to respond to potential medication-related problems before serious negative outcomes occur. Kuperman *et al.* (59) concluded that incorporation of an automatic alerting system in the laboratory data system resulted in a 38% shorter response to appropriate treatment following alert to a critical value.

Strategies for Improving Medication Use

One approach to improving the quality of drug use is the development and implementation of medication use guidelines. This evidential approach to the use of medications is designed to rely on the best available clinical evidence to develop a treatment plan for a specific illness or use of a specific drug or drugs. Simple medication use guidelines can be developed based on literature and the best judgment of in-house experts. Development of more formal clinical practice guidelines is a complex process that relies on well-defined methods to combine the results of multiple studies to draw statistical conclusions. These sophisticated products are often addressed by professional or governmental organizations.

The use of "counterdetailing" by designated hospital staff to offset the impact of pharmaceutical sales

			SPENT FY 99	SPENT FY 00	SPENT FY 01	SPENT FY 02	SPENT FY 03	SPENT FY 04
4:00:00	**ANTIHISTAMINE**		$17,564	$21,175	$28,185	$41,918	$54,237	$64,221
8:00:00	**ANTI-INFECTIVE AGENTS**							
	80400	AMEBICIDES	$0	$1,522	$332	$884	$1,321	$746
	80800	ANTHELMINTICS	$2,510	$996	$2,623	$1,231	$1,834	$2,702
	81202	AMINOGLYCOSIDES	$9,457	$13,457	$10,351	$35,468	$47,014	$35,272
	81204	ANTIFUNGAL ANTIBIOTICS	$256,806	$320,884	$357,206	$946,657	$1,082,165	$1,056,544
	81206	CEPHALOSPORINS	$221,196	$197,231	$162,850	$180,186	$188,435	$146,069
	81207	β-LACTAMS	$59,322	$77,722	$77,703	$90,073	$112,235	$81,442
	81208	CHLORAMPHENICOLS	$626	$204	$172	$771	$1,331	$34
	81212	ERYTHROMYCINS	$52,106	$69,377	$89,793	$112,984	$109,499	$92,816
	81216	PENICILLINS	$50,569	$41,427	$65,243	$46,314	$61,153	$89,200
	81224	TETRACYCLINES	$16,872	$4,427	$4,788	$4,569	$8,820	$5,962
	81228	MISCELLANEOUS ANTIBIOTICS	$38,577	$35,347	$35,261	$37,811	$41,473	$80,727
	81600	ANTITUBERCULOSIS AGENTS	$33,141	$27,937	$42,335	$53,318	$46,223	$39,438
	81800	ANTIVIRALS	$658,157	$1,399.246	$2,472,982	$3,251,543	$3,417,004	$3,775,675
	82000	ANTIMALARIAL AGENTS	$82,141	$60,942	$20,848	$19,051	$20,577	$17,524
	82200	QUINOLONES	$82,319	$113,064	$94,705	$117,380	$116,301	$119,356
	82400	SULFONAMIDES	$7,053	$6,730	$3,425	$3,660	$2,770	$4,579
	82600	SULFONES	$5,207	$4,839	$4,651	$4,972	$5,366	$3,735
	83200	ANTITRICHOMONAL AGENTS	$1,493	$3,923	$677	$924	$1,454	$1,627
	83600	URINARY ANTI-INFECTIVES	$5,974	$2,009	$2,142	$1,632	$2,836	$763
	84000	MISCELLANEOUS ANTI-INFECTIVES	$28,489	$34,661	$30,211	$27,401	$19,394	$23,766
	TOTAL ANTI-INFECTIVE AGENTS		$1,612,016	$2,415,944	$3,478.297	$4,936,828	$5,287,206	$5,577,978
16:00:00	**BLOOD DERIVATIVES TOTAL**		$212,109	$188,350	$204,843	$236,087	$348,825	$11,095
20:00:00	**BLOOD FORMATION AND COAGULATION**							
	200404	IRON PREPARATIONS	$2,867	$2,687	$2,402	$2,240	$2,012	$6,150
	201204	ANTICOAGULANTS	$41,207	$66,851	$75,294	$114,764	$179,357	$146,496
	201208	ANTIHEPARIN AGENTS	$141	$237	$83	$182	$156	$52,186
	201216	HEMOSTATICS	$56,030	$21,246	$27,266	$48,408	$75,817	$65,886
	201600	HEMATOPOIETIC AGENTS	$1,228,251	$1,526,711	$1,471,910	$1,515,326	$2,027,767	$1,406,002
	202400	HEMORRHEOLOGIC AGENTS	$3,179	$2,717	$2,046	$3,014	$6,683	$1,109
	204000	THROMBOLYTIC AGENTS	$47,054	$72,684	$58,657	$87,678	$72,382	$51,789
	TOTAL BLOOD FORMATION AND COAG		$1,378,728	$1,693,133	$1,637,657	$1,771,613	$2,142,912	$1,729,616
24:00:00	**CARDIOVASCULAR DRUGS**							
	240400	CARDIAC DRUGS	$168,786	$185,225	$179,912	$197,914	$258,000	$264,424
	240600	ANTILIPEMIC AGENTS	$237,143	$237,827	$298,091	$269,520	$298,957	$333,476
	240800	HYPOTENSIVE AGENTS	$97,583	$89,871	$106,383	$112,858	$122,181	$117,703
	241200	VASODILATING AGENTS	$20,063	$21,023	$28,385	$39,040	$26,947	$25,841
	241600	SCLEROSING AGENTS	$0	$0	$0	$0	$0	$220
	TOTAL CARDIOVASCULAR DRUGS		$523,575	$533,946	$612,771	$619,332	$706,085	$741,664

FIGURE 26.7 Sample therapeutic category drug monitoring report based upon therapeutic classifications used by the American Hospital Formulary Service (55).

TABLE 26.3 Drug Use Review Categories

Review category	Data collection model	Typical application	Comments
Retrospective	Data are collected for a fixed period; data may be archival or represent accumulation of new patients for a fixed period of time	Data archive review of emergency department prescribing for geriatric patients (56)	Supports large-scale epidemiologic approach; no active intervention to change medication use patterns occurs due to the *post-hoc* data collection process
Concurrent	Each new order generates an automatic review of previously approved criteria for use within a specified period of the initiation of therapy	Review of naloxone to investigate possible nosocomial adverse medication event	
	Laboratory or other monitoring criteria are reported for all patients on the drug; abnormal laboratory or other monitoring criteria are reported for all patients on the drug on a regular basis	Digoxin monitoring based upon daily review of digoxin serum levels (57); regular review of serum creatinine for patients on aminoglycosides	
Prospective	Each new order for the drug is evaluated for compliance with previously approved criteria for use; variances to the criteria require intervention prior to initiation of therapy	Medication use guidelines (ketorolac) (58); restricted antibiotics	

forces has been an effective strategy for improving medication use (60). The objective of this category of quality improvement program is to educate prescribers regarding the organization's approved and preferred medication use guidelines. This has been implemented by providing literature and prescriber contact from a pharmacist or other staff member to support the desired medication use objective.

Several approaches have been described for improving medication use through the use of dosing service teams. Demonstrated enhancements in the quality of medication use have been reported for anticoagulants, antimicrobials, anticonvulsants, and other drugs. The common method of these programs is the use of expert oversight (physicians or pharmacists) to manage therapy with the targeted drug. Therapeutic management may rely on algorithms, pharmacokinetic models, or preapproved collaborative plans (61–71).

Adoption of standardized medication order forms has been demonstrated to increase the quality of medication use and the effectiveness of medications that are prone to error (72, 73). Chemotherapy, patient-controlled analgesia, and antimicrobial drug therapy are likely candidates for order standardization. Yet another approach to improved medication use is implementation of alert systems for sudden, unexpected actions, such as medication stop orders, or use of antidote-type drugs, such as diphenhydramine,

TABLE 26.4 Selection of Targets for Focused Medication Use Review[a]

- Medication is known or suspected to cause adverse reactions or drug interactions
- Medication use process affects large number of patients or medication is frequently prescribed
- Medication is potentially toxic or causes discomfort at normal doses
- Medication is under consideration for formulary retention, addition, or deletion
- Medication is expensive
- Medication is used in patients at high risk for adverse reactions
- Medication or process is a critical component of care for a specific disease, condition, or procedure
- Medication is most effective when used in a specific way
- Medication or process is one for which suboptimal use would have a negative effect on patient outcomes or system costs

[a] Adapted from American Society of Health-System Pharmacists. ASHP guidelines on medication-use evaluation.

hydrocortisone, or naloxone. A computerized application of this method was described by Classen *et al.* (74). Another computerized system described by Paltiel *et al.* (75) improved outcomes by using a flashing alert on a computer monitor to highlight low potassium levels, thereby increasing the rate of therapeutic interventions and decreasing hypokalemia in patients at discharge.

SUMMARY

The medication use process is a complex system intended to optimize patient outcomes within organizational constraints. Quality medication use involves selection of the optimal drug, avoidance of adverse medication events, and completion of the therapeutic objective. Safe medication practices focus on the avoidance of medication errors. Medication use review and ongoing medication monitoring activities focus on optimizing medication selection and use. These two approaches are important means of assessing and optimizing the quality of medication use.

REFERENCES

1. CDER. 2004 Report to the nation —- Improving public health through drugs. Rockville, MD: FDA; 2005. p. 13. (Internet at http://www.fda.gov/cder/reports/rtn/2004/Rtn2004.pdf.)
2. Ernst FR, Grizzle AJ. Drug-related morbidity and mortality: Updating the cost-of-illness mo. J AM Pharm Assoc 2001;41:192–9.
3. Committee on Quality of HealthCare in America. To err is human: Building a safer health system. In: Kohn LT, Corrigan JM, Donaldson MS, editors. Washington, DC: National Academy Press; 1999. p. 223.
4. Leape LL, Brennan TA, Laird N, Lawthers AG, Localio AR, Barnes BA *et al.* The nature of adverse events in hospitalized patients. Results of the Harvard Medical Practice Study II. N Engl J Med 1991;324:377–84.
5. Thomas EJ, Brennan TA. Incidence and types of preventable adverse events in elderly patients: Population based review of medical records. BMJ 2000;320:741–4.
6. National Coordinating Council for Medication Error Reporting and Prevention. Rockville, MD: U.S. Pharmacopoeia; 1999. (Internet at http://www.nccmerp.org.)
7. American Society of Health-System Pharmacists. Suggested definitions and relationships among medication misadventures, medication errors, adverse drug events, and adverse drug reactions. Am J Health-Syst Pharm 1998;55:165–6.
8. Bates DW, Boyle DL, Vander Vliet MB, Schneider J, Leape L. Relationship between medication errors and adverse drug events. J Gen Intern Med 1995; 10:199–205.
9. Bates DW, Spell N, Cullen DJ, Burdick E, Laird N, Petersen LA *et al.* The costs of adverse drug events in hospitalized patients. JAMA 1997;277:307–11.
10. Anderson JG, Jay SJ, Anderson M, Hunt TJ. Evaluating the capabilities of information technology to prevent adverse drug events: A computer simulation approach J Am Med Inform Assoc. 2002;9:479–90.
11. Nadzam DM. A systems approach to medication use. In: Cousins DD, editor. Medication use: A systems approach to reducing errors. Oakbrook Terrace, IL: Joint Commission on Accreditation of Healthcare Organizations; 1998. p. 5–17.
12. Atkinson AJ Jr, Nadzam DM, Schaff RL. An indicator-based program for improving medication use in acute care hospitals. Clin Pharmacol Ther 1991;50:125–8.
13. Phillips DP, Christenfeld N, Glynn LM. Increase in US medication-error deaths between 1983 and 1993. Lancet 1998;351:643–4.
14. Anon. Survey reveals patient concerns about medication-related issues. ASHP calls for increased patient access to pharmacists in hospitals and health systems. Bethesda, MD: American Society of Health System Pharmacists; 2002. (Internet at http://www.ashp.org/news/ShowArticle.cfm?id=2996.)
15. Bates DW, Cullen DJ, Laird N, Petersen LA, Small SD, Servi D *et al.* Incidence of adverse drug events and potential adverse drug events. Implications for prevention. JAMA 1995;274:29–34.
16. Barker KN, Flynn EA, Pepper GA, Bates DW, Mikeal RL. Medication errors observed in 36 healthcare facilities. Arch Intern Med 2002;162:1897–1903.
17. Berwick DM. Continuous improvement as an ideal in healthcare. N Engl J Med 1989;320:53–6.
18. Deming WE. Out of the crisis. Cambridge, MA: MIT Press; 2000. p. 87–9.
19. American Society of Health-System Pharmacists. ASHP statement on the pharmacy and therapeutics committee. Am J Hosp Pharm 1992;49:2008–9.
20. Coalition Working Group. Principles of a sound formulary system. Rockville, MD: US Pharmacopoeia; 2000. p 5. (Internet at http://www.usp.org/pdf/EN/patientSafety/pSafetySndFormPrinc.pdf.)
21. Reason J. Human error. Cambridge, UK: Cambridge University Press; 1990.
22. Lesar TS, Briceland L, Stein DS. Factors related to errors in medication prescribing. JAMA 1997; 77:312–7.
23. Cohen MR. Causes of medication errors. In: Cohen MR, editor. Medication errors. Washington, DC: American Pharmaceutical Association; 1999. p. 198–212.
24. Leape LL, Bates DW, Cullen DJ, Cooper J, Demonaco HJ, Gallivan T *et al.* Systems analysis of adverse drug events. JAMA 1995;274:35–43..
25. Nightingale PG, Adu D, Richards NT, Peters M. Implementation of rules based computerised bedside prescribing and administration: Intervention study. BMJ 2000;320:750–3.
26. Rothschild JM, Landrigan CP, Cronin JW. The Critical Care Safety Study: The incidence and nature of adverse events and serious medical errors in intensive care. Crit Care Med 2005;33:1694–1700.

27. Bates DW, Leape LL, Cullen DJ, Laird N, Petersen NA, Teich JM *et al.* Effect of computerized physician order entry and a team intervention on prevention of serious medication errors. JAMA 1998;280:1311–6.
28. Bates DW, Teich JM, Lee J, Seger D, Kuperman GJ, Ma'Luf N *et al.* The impact of computerized physician order entry on medication error prevention. J Am Med Inform Assoc 1999;6:313–21.
29. Pestotnik SL, Classen DC, Evan RS, Burke JP. Implementing antibiotic practice guidelines through computer-assisted decision support: Clinical and financial outcomes. Ann Intern Med 1996;124:884–90.
30. Raschke RA, Gollihare B, Wunderlich TA, Guidry JR, Leibowitz AI, Peirce JC *et al.* A computer alert system to prevent injury from adverse drug events: Development and evaluation in a community teaching hospital. JAMA 1998;280:1317–20.
31. MEDMARX 5thAnniversary Data Report: A chartbook of 2003 findings and trends 1999–2003. Rockville, MD: U.S. Pharmacopoeia; 2005. (Internet at http://www.usp.org/products/medMarx/.)
32. Koppel R, Metlay JP, Cohen A, Abaluck B, Localio AR, Kimmel SE, Strom BL. Role of computerized physician order entry systems in facilitating medication errors. JAMA 2005;293:1197–203.
33. Nebeker JR, Hoffman JM, Weir R, Bennett CL, Hurdle JF. High rates of adverse drug events in a highly computerized hospital. Arch Intern Med 2005; 165:1111–6.
34. Calabrese AD, Erstad BL, Brandl K, Barletta JF, Kane SL, Sherman DS. Medication administration errors in adult patients in the ICU. Intensive Care Med 2001;27:1592–8.
35. High-alert medications and patient safety. Sentinel Event Alert 11(Nov 19) 1999.
36. Cohen MR, Kilo CM. High-alert medications: Safeguarding against errors. In: Cohen MR, editor. Medication errors. Washington, DC: American Pharmaceutical Association, 1999. p. 5.3–5.11.
37. Lambert BL. Predicting look-alike and sound-alike medication errors. Am J Health-Syst Pharm 1997;54:1161–71.
38. Lambert BL, Lin SJ, Chang KY, Gandhi SK. Similarity as a risk factor in drug-name confusion errors: The look-alike (orthographic) and sound-alike (phonetic) model. Med Care 1999;37:1214–25.
39. Lambert BL, Lin SJ, Tan H. Designing safe drug names. Drug Saf 2005;28:495–512.
40. MedMARx™. Rockville, MD: U.S. Pharmacopoeia; 2005. (Internet at http://www.usp.org/patientSafety/medmarx/.)
41. Nolan TW. System changes to improve patient safety. BMJ 2000;320:771–3.
42. Bates DW. Medication errors. How common are they and what can be done to prevent them? Drug Saf 1996;15:303–10
43. Cullen DJ, Sweitzer BJ, Bates DW, Burdick E, Edmonson A, Leape LL. Preventable adverse drug events in hospitalized patients: A comparative study of intensive care and general care units. Crit Care Med 1997;25:1289–97.
44. Lesar TS, Lomaestro BM, Pohl H. Medication-prescribing errors in a teaching hospital. A 9-year experience. Arch Intern Med 1997;157:1569–76.
45. Koecheler JA, Abramowitz PW, Swim SE, Daniels CE. Indicators for the selection of ambulatory patients who warrant pharmacist monitoring. Am J Hosp Pharm 1989;46:729–32.
46. Cornish PL, Knowles SR, Marchesano R, Tam V, Shadowitz S, Juurlink DN, Etchells EE. Unintended medication discrepancies at the time of hospital admission. Arch Intern Med 2005;165:424–9.
47. Gray SL, Mahoney JE, Blough DK. Adverse drug events in elderly patients receiving home health services following hospital discharge. Ann Pharmacother 1999;33:1147–53.
48. Leape LL, Cullen DJ, Clapp MD, Burdick E, Demonaco HJ, Erickson JI *et al.* Pharmacist participation on physician rounds and adverse drug events in the intensive care unit. JAMA 1999;282:267–70.
49. Flynn EA, Barker KN, Gibson JT, Pearson RE, Berger BA, Smith LA. Impact of interruptions and distractions on dispensing errors in an ambulatory care pharmacy. Am J Health Syst Pharm 1999;56:1319–25.
50. Four-pronged medication error evaluation. ISMP Medication Safety Alert. 1999;4(19):2.
51. Morris AH. Developing and implementing computerized protocols for standardization of clinical decisions. Ann Intern Med 2000;132:373–83.
52. Evans RS, Pestotnik SL, Classen DC, Clemmer TP, Weaver LK, Orme JF *et al.* A computer-assisted management program for antibiotics and other antiinfective agents. N Engl J Med 1998;338:232–8.
53. Leape LL. Error in medicine. JAMA 1994;272:1851–7.
54. American Society of Health-System Pharmacists. ASHP guidelines on medication-use evaluation. Am J Health Syst Pharm 1996;53:1953–5.
55. American Hospital Formulary Service. Drug information 2000. Bethesda (MD): American Society of Hospital Pharmacists; 2000. p. ix–xi.
56. Caterino JM, Emond JA, Camargo CA Jr. Inappropriate medication administration to the acutely ill elderly: A nationwide emergency department study, 1992–2000. J Am Geriatr Soc 2004;52:1847–55.
57. Piergies AA, Worwag EM, Atkinson AJ Jr. A concurrent audit of high digoxin plasma levels. Clin Pharmacol Ther 1994;55:353–8.
58. Krstenansky PM. Ketorolac injection use in a university hospital. Am J Hosp Pharm 1993;50:99–102.
59. Kuperman GJ, Teich JM, Tanasijevic MJ, Ma'Luf N, Rittenberg E, Jha A *et al.* Improving response to critical laboratory results with automation: Results of a randomized controlled trial. J Am Med Inform Assoc 1999;6:512–22.
60. Soumerai SB, Avorn J. Predictors of physician prescribing change in an educational experiment to improve medication use. Med Care 1987;25:210–21.
61. Ellis RF, Stephens MA, Sharp GB. Evaluation of a pharmacy-managed warfarin-monitoring service to coordinate inpatient and outpatient therapy. Am J Hosp Pharm 1992;49:387–94.
62. Dager WE, Branch JM, King JH, White RH, Quan RS, Musallam NA *et al.* Optimization of inpatient warfarin therapy: Impact of daily consultation by a pharmacist-managed anticoagulation service. Ann Pharmacother 2000;34:567–72.
63. Destache CJ, Meyer SK, Bittner MJ, Hermann KG. Impact of a clinical pharmacokinetic service on

patients treated with aminoglycosides: A cost-benefit analysis. Ther Drug Monit 1990;12:419–26.
64. Cimino MA, Rotstein CM, Moser JE. Assessment of cost-effective antibiotic therapy in the management of infections in cancer patients. Ann Pharmacother 1994;28:105–11.
65. Okpara AU, Van Duyn OM, Cate TR, Cheung LK, Galley MA. Concurrent ceftazidime DUE with clinical pharmacy intervention. Hosp Formul 1994;29:392–4, 399, 402–4.
66. Kershaw B, White RH, Mungall D, Van Houten J, Brettfeld S. Computer-assisted dosing of heparin. Management with a pharmacy-based anticoagulation service. Arch Intern Med. 1994;154:1005–11.
67. De Santis G, Harvey KJ, Howard D, Mashford ML, Moulds RF. Improving the quality of antibiotic prescription patterns in general practice. The role of educational intervention. Med J Aust 1994;160:502–5.
68. Donahue T, Dotter J, Alexander G, Sadaj JM. Pharmacist-based i.v. theophylline therapy. Hosp Pharm 1989;24:440, 442–8, 460.
69. Ambrose PJ, Smith WE, Palarea ER. A decade of experience with a clinical pharmacokinetics service. Am J Hosp Pharm 1988;45:1879–86.
70. Li SC, Ioannides-Demos LL, Spicer WJ, Spelman DW, Tong N, McLean AJ. Prospective audit of an aminoglycoside consultative service in a general hospital. Med J Aust 1992;157:308–11.
71. McCall LJ, Dierks DR. Pharmacy-managed patient-controlled analgesia service. Am J Hosp Pharm 1990;47:2706–10.
72. Lipsy RJ, Smith GH, Maloney ME. Design, implementation, and use of a new antimicrobial order form: A descriptive report. Ann Pharmacother 1993; 27:856–61.
73. Frighetto L, Marra CA, Stiver HG, Bryce EA, Jewesson PJ. Economic impact of standardized orders for antimicrobial prophylaxis program. Ann Pharmacother 2000;34:154–60.
74. Classen DC, Pestotnik SL, Evans RS, Burke JP. Description of a computerized adverse drug event monitor using a hospital information system. Hosp Pharm 1992;27:774, 776–9, 783.
75. Paltiel O, Gordon L, Berg D, Israeli A. Effect of a computerized alert on the management of hypokalemia in hospitalized patients. Arch Intern Med 2003;163:200–4.

This page intentionally left blank

PART

V

DRUG DISCOVERY AND DEVELOPMENT

This page intentionally left blank

CHAPTER

27

Portfolio and Project Planning and Management in the Drug Discovery, Development, and Review Process

CHARLES GRUDZINSKAS
NDA Partners LLC, Annapolis, Maryland, and University of California, San Francisco, Center for Drug Development Science, Washington, D.C.

INTRODUCTION

Drug discovery, development, and regulatory review are complex, lengthy, and costly processes that involve in excess of 10,000 activities. To manage and optimize the returns of this complex, lengthy, and costly process, the biopharmaceutical industry has embraced the two disciplines of (1) portfolio design, planning, and management (PDPM) and (2) contemporary project planning and management (PPM). The obvious benefits of good portfolio and project planning and management are shown in Table 27.1.

The beneficial use of these two tools by both the industry and the Food and Drug Administration (FDA) is evidenced by prioritized resource allocations and significant decreases in both drug development times and FDA review times. We are now entering an era where the time from the first-in-human (FIH) trial to submission of a New Drug Application (NDA) is, dependent on the therapeutic claim(s), expected to range from 3 to 4 years, rather than the 5 to 7 years that traditionally have been required. Likewise, as a result of the introduction of project management techniques into the FDA review process, FDA review times for regular NDAs were reduced from the 1988 average of 34.1 months, to a median of 14.6 months in 1999 (1).

The median review times for both NDA and Biologic License Application (BLA) reviews for new molecular entities (NMEs) reported by the FDA are shown in Table 27.2 (2). For NMEs, the median standard review time reported for the cohort of NDAs and BLAs that were approved in 2004 is 24.7 months. However, review times for priority review NMEs have been reduced to a current plateau of approximately 6 months, with the exception of the 16.3-month review time reported for 2002. One NDA was reviewed within 18 days of NDA submission as the first pilot for what was then termed the *Rolling NDA* (3). This remarkably short duration was accomplished by the FDA and the sponsor (National Institute on Drug Abuse/National Institutes of Health) using the same project management database. The project database integrated the sponsor's drug development/NDA preparation network and the FDA's NDA review networks. In 2004, 21 priority NDAs were reviewed with a median review time of 6.0 months, and the antiviral division has recently reviewed several HIV treatment NDAs in under 3 months (4).

What Is a Portfolio?

A *well-planned and managed* pharmaceutical research and development (R&D) portfolio can be defined as "The combination of a*ll* R&D projects, that based on past company and industry performance,

TABLE 27.1 Benefits of Good Portfolio and Project Planning and Management

The organization is able to do more with less
The organization is able to optimize the value of a portfolio of projects
Provides for common expectations when projects are being jointly developed
Better planning
Better decision-making
Projects finish on time
Projects finish within budget

will predictably yield valuable new products at the *rate needed* to support the planned growth of the organization." Portfolio design, planning, and management are the processes that the industry uses to ensure a well-balanced and value-optimized portfolio. Likewise, the FDA and other regulatory agencies have a portfolio of projects that include review of Investigational New Drug Applications (INDs), review of IND annual reports, meetings with sponsors, NDA reviews and advisory committee meetings, as well as legislated initiatives and reporting obligations.

TABLE 27.2 CDER Approval Times for Priority and Standard NMEs and New BLAs

	Priority review		Standard review	
Calendar year	Number approved	Median total approval time (months)	Number approved	Median total approval time (months)
1995	10	7.9	19	17.8
1996	9	9.6	35	15.1
1997	18	6.7	30	15.0
1998	16	6.2	14	13.4
1999	19	6.9	16	16.3
2000	9	6.0	18	19.9
2001	7	6.0	17	9.0
2002	7	26.3	10	15.9
2003	9	6.7	12	23.1
2004[a]	21	6.0	13	14.7

[a] Beginning in 2004, these figures include new BLAs for therapeutic biologic products transferred from the Center for Biologics Evaluation and Research (CBER) to the Center for Drug Evaluation and Research (CDER) effective 10/1/2003.

What Is Project Planning and Management?

Project planning is an integral part of project management, which is defined in the Project Management Institute's *Guide to the Project Management Body of Knowledge* (5) as "the application of knowledge, skills, tools, and techniques to project activities in order to meet or exceed stakeholder needs and expectations from a project." For an excellent text on the application of project management principles, the reader is referred to *Practical Project Management* by Dobson (6). An excellent resource for those who would like to become actively involved in biopharmaceutical project management is the Drug Information Association's (DIA) Project Management Special Interest Advisory Committee (PM SIAC). Information on how to join the DIA PM SIAC can be found on the DIA web site (7).

PORTFOLIO DESIGN, PLANNING, AND MANAGEMENT

Portfolio management is the term that is used to describe the overall process of program and franchise management. This process actually includes the three dimensions of portfolio design, portfolio planning, and portfolio management. Each of these three dimensions is described in this section. The five components needed for the successful use of portfolio design, planning, and management are identified in Table 27.3. If any one (or more) of the five components are missing or not fully operational, then the likelihood of successful PDPM will be limited.

Most large organizations have now adopted the portfolio management team (PMT) concept. PMT membership consists of the senior management of the organization, and the mission of the PMT is to oversee the successful design, planning, and management of the organization's portfolio. The PMT usually has several working groups that focus on specific therapeutic areas. The ultimate responsibility of the PMT is to ensure that the portfolio has been optimized to maximize its potential expected value.

TABLE 27.3 The Five Components of Successful Portfolio Design, Planning, and Management

Portfolio design
Portfolio planning
Portfolio management
Portfolio management teams
Portfolio optimization using sensitivity analysis

Maximizing Portfolio Value

Portfolio value is maximized by appropriately prioritizing the projects within the portfolio based on the future potential financial value of each project multiplied by its probability of success. The future value of each development project is based on a calculation of its net present value (NPV). In this calculation, the anticipated financial return from the project is compared with that of an alternative investment of an equivalent amount of capital (8). The general equation for calculating NPV is

$$NPV = I_0 + \frac{I_1}{1+r} + \frac{I_2}{(1+r)^2} + \cdots + \frac{I_n}{(1+r)^n} \quad (27.1)$$

where the I values are given a negative sign for annual net cash outflow and a positive sign for projected net annual income. The subscripts and exponents correspond to the number of years of projected development and marketing time, and r, termed the *discount rate*, is the rate of return of an alternate investment, such as U.S. Treasury Bills.

An NPV analysis using a 5% discount rate is summarized for a hypothetical drug in Table 27.4. It is assumed that the drug will be developed within 4 years at a total cost of $500 million. Because this investment is spread over 4 years, development funds budgeted for this project that are unexpended after year 0 are assumed to be earning 5% interest until spent, and are discounted accordingly. Marketing begins in year 4 but income is similarly discounted as shown in Equation 27.1 and is assumed to be negligible when patent protection expires after year 7. The NPV for the project is the sum of the discounted cash inflows and outflows over the life of the product, and in this case is $31.3 million. The NPV is far less than the $150 million difference between total income and expenditures for the project, because this latter difference makes no allowance for potential alternative use of the money. The *internal rate of return* is another metric that may be helpful in evaluating different projects in a portfolio (8). The internal rate of return is defined simply as the discount rate needed to yield an NPV of zero, and would be 6.78% for the hypothetical project shown in Table 27.4.

TABLE 27.4 Discounted Cash Flows for a Hypothetical Drug Development Project[a]

	Development		Marketing	
Year	Expense	Discounted expense	Income	Discounted income
0	($25)	($25)	—	—
1	($75)	($71.4)	—	—
2	($200)	($181.4)	—	—
3	($200)	($172.8)	—	—
4	—	—	$50	$41.1
5	—	—	$100	$78.4
6	—	—	$200	$149.2
7	—	—	$300	$213.2

[a] Dollar amounts are in millions. In this case, NPV (sum of discounted cash flows) equals $31.3 million.

The probability of success is the product of the probability of technical success, the probability of regulatory success, and the probability of commercial success. The criteria for these probabilities of success need to be clearly defined and characterized so that future PMTs can translate the impact of project progress and decisions on the value of the projects in the portfolio (see section on portfolio optimization using sensitivity analysis).

It is easy to see that projects that are at the FDA (or other worldwide regulatory review bodies) for review will most commonly have the highest probability of success. Therefore, they are likely to have the highest overall financial value in the portfolio (overall value equals possible future value times the probability of success), whereas projects that are in the discovery stage will have the lowest overall value in the portfolio (but are the life-blood of the organization 4 to 5 years in the future). It is the role of the PMT to develop a "balanced portfolio" that supports both the near-term, mid-term, and long-term needs of the organization. The R&D senior management team needs to ensure that organizational resources are properly allocated according to the agreed-upon prioritization.

Portfolio Design

It is not an overstatement to say that the near-term and long-term future of a biopharmaceutical company depends on the size and likelihood of success of its pipeline. The pipeline is the totality of a company's portfolio, consisting of projects ranging from very early discovery, to marketed products that are ending their current life cycle and will need a line extension (new formulation or expanded indications) to remain competitive. A pharmaceutical R&D portfolio begins with a vision of the intended growth rate of the organization. Based on the envisioned growth rate, a portfolio can be developed that is based on what the future pipeline will need to look like at each stage of the drug development process. The size of the pipeline needed at each stage of drug development is estimated from both past industry

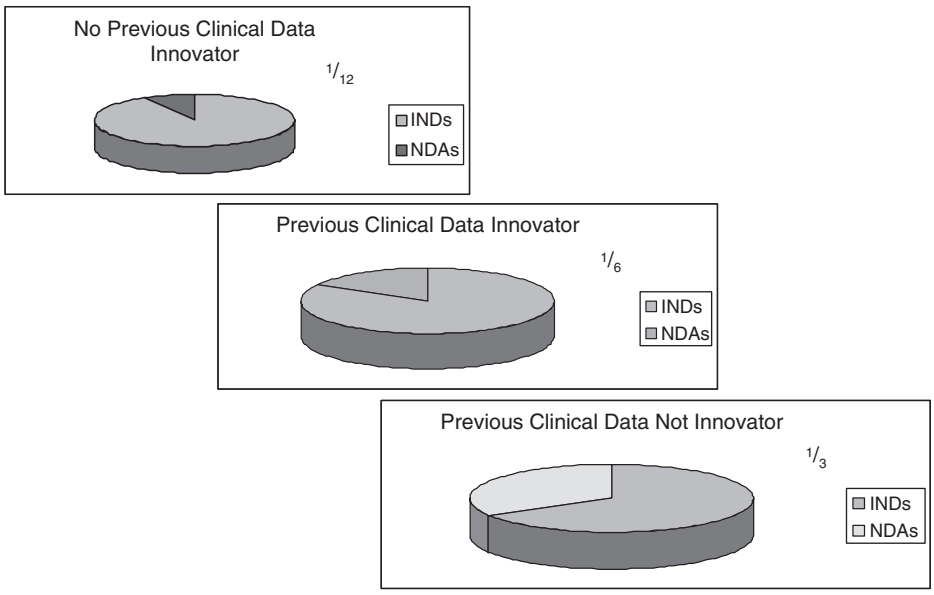

FIGURE 27.1 The success rates for U.S. Investigational New Drug Applications (INDs) based on whether previous clinical experience was involved in the decision to prepare and file an IND (NDA, New Drug Application). "Innovator" refers to the IND sponsor as discovering the drug candidate. "Not innovator" refers to the IND sponsor as in-licensing the drug candidate. (Adapted from DiMasi J. Clin Pharmacol Ther 2002;69:297–307.)

and regulatory experiences. The probability of a drug candidate maturing to an approved drug has been extensively studied by the Center for the Study of Drug Development (CSDD) at Tufts. The CSDD reports that only one compound reaches the market for every 12 (8% success rate) that enter the clinical development process (9). In the CDDS study of U.S. Investigational New Drug Applications, the odds of success for any one clinical candidate appeared to depend on whether the drug candidate had been studied clinically elsewhere before IND filing to initiate clinical trials in the United States. These various probabilities are shown in Figure 27.1.

In Figure 27.1 we see that INDs that are filed in the United States for drug candidates for which there is prior clinical experience before initiating U.S. clinical trials have enhanced probabilities of achieving market approval ranging from 1 out of 6 (16%) to 1 out of 3 (33%). This increase in approval success rate forms the basis for a strategy that organizations use to optimize the probability of achieving U.S. market approval for an individual clinical candidate. Indeed, if one assumes that drug candidates for which INDs are filed with previous non-U.S. clinical experience have already achieved proof of concept with regard to clinical safety and activity, then one can assume that drug candidates in Phase II might have a probability of market approval of 16–33 %, in contrast to the 8% probability observed for drug candidates lacking clinical experience prior to IND submission. Therefore, as shown in the portfolio pyramid in Figure 27.2, a company that wants to have one new product (NDA or BLA) approved each year would have to submit 12 new INDs each year for drug candidates with no previous clinical experience, or as few as three, if the three clinical candidates had already achieved a proof of concept with regard to safety and activity. Naturally, if a company wanted to develop two or three new NDAs/BLAs each year, it would have to have a pipeline that is, respectively, two or three times as large as is illustrated in Figure 27.2.

Portfolio Planning

Once the portfolio vision and design have been defined, the organization can focus on how to build that portfolio. As projects mature from one stage to the next, or are terminated for lack of success, additional projects will need to be added to the various stages of the portfolio to ensure a portfolio of adequate size at each stage. To maintain an aggressive portfolio, companies have acknowledged that it is nearly impossible to fill the pipeline by being dependent only on homegrown research. There are many sources for new products in addition to the organization's own discovery program. For example,

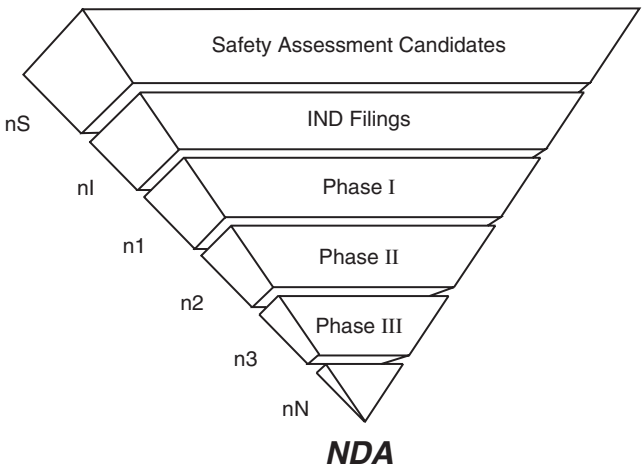

FIGURE 27.2 Size of the drug development portfolio needed to support a New Drug Application (NDA) pipeline. nS, Number of compounds that will need to be screened each year; nI, number of Investigational New Drug Applications (INDs) that will need to be submitted each year; n1, number of Phase I projects that will need to be initiated each year; n2, number of Phase II projects that will need to be initiated each year; n3, number of Phase III projects that will need to be initiated each year; nN, number of NDAs that will need to be submitted each year, based on the portfolio of compounds screened, INDs filed, and Phase I–Phase III projects initiated each year.

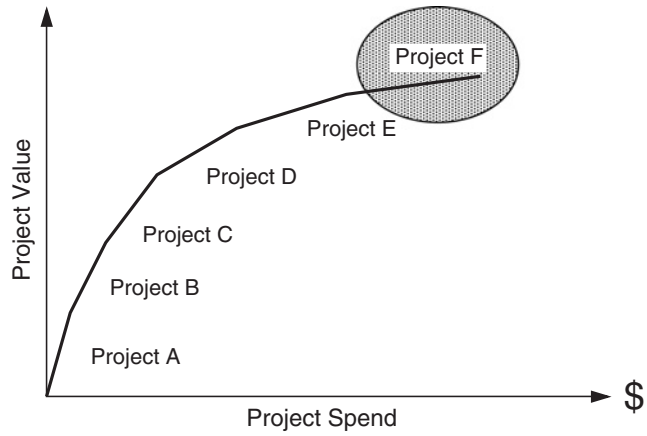

FIGURE 27.3 Relationship between project value and R&D funds invested in their clinical development (project spend). The value of this hypothetical portfolio would be the cumulative value of its constituent projects. Project F clearly has the lowest expected value per "project spend." These low-value projects are usually considered as candidates for termination. In addition to termination as a possibility, effective companies evaluate the low-expected-value projects to identify the drivers that would lead to a significant increase in the project's expected value (see text, "Portfolio Optimization Using Sensitivity Analysis," and Figure 27.5).

companies can fill out their portfolios by entering into joint ventures and alliances with both established and start-up organizations. Additional sources of new products include licensing early-stage research from the National Institutes of Health (NIH), universities, and foundations (e.g., the Red Cross). Thus, the planning process includes both the identification and the successful in-licensing of the products needed to populate the stages of the drug development process that we saw in Figure 27.2.

Portfolio Management

Portfolio management is primarily focused on the prioritization of projects within the portfolio. Several consulting groups and software programs are available to aid in the management of an existing portfolio. These same tools can be used to explore "what-if" scenarios to determine how the addition or deletion of projects to the portfolio either increases or decreases the portfolio's overall value. As with most processes of this nature, the most important consideration is the quality of the information regarding the potential value and probability of success of each project. Precise evaluations of the commercial, regulatory, and technical probabilities need to come from those in the organization who have sufficient experience to be able to make educated and reliable estimates of both expected values and probabilities.

As illustrated in Figure 27.3, organizations can graph the value that is expected to be gained vs the cost of the R&D needed to achieve the overall value that is calculated for each project. Organizations can then make decisions as to how to allocate resources based on the "steepness" of the slope of each project, keeping in mind that projects closest to the market, which have the highest probability of success, will likely have the steepest slope. In the next section we examine how to avoid the pitfall of assuming that projects (such as the one identified in the oval in Figure 27.3) necessarily need to be terminated because they have less than acceptable expected value vs cost slopes. Indeed, we will see how to determine how to increase the expected value of low-value projects.

Obviously, organizations will want to populate their portfolio with projects that balance potential value and probability of success, as illustrated in Figure 27.4. Clearly the most desirable projects are in Quadrant I (high value with a high probability of success). Projects in Quadrant IV, with low value and low probability of success, should be examined for ways to increase the expected project value or probability of success, or should be recommended for termination. Unfortunately, few projects fall into Quadrant I, so a typical portfolio is composed of projects mostly from Quadrants II and III (most organizations try to

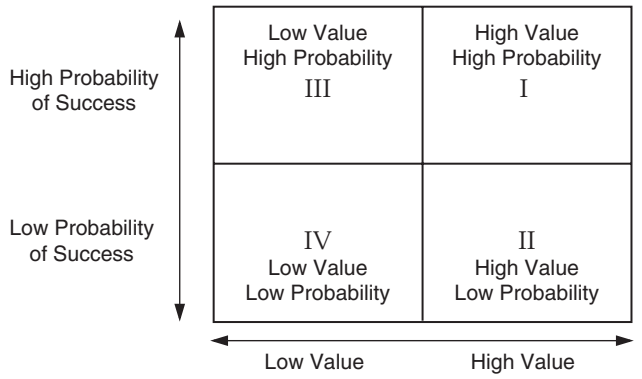

FIGURE 27.4 Four-quadrant table used for portfolio analysis in which projects are evaluated on the basis of their potential financial return (value) and probability of development success.

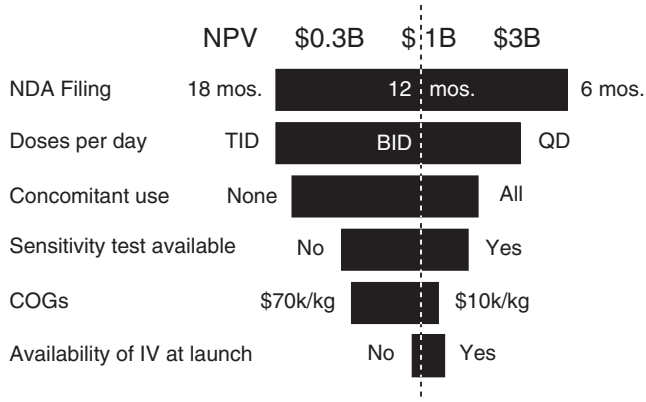

FIGURE 27.5 "Tornado" chart illustrating a sensitivity analysis for the development of a hypothetical antibiotic. NPV, Net present value; COGs, cost of goods.

avoid Quadrant IV-type projects). Several analogies are often used to describe the four quadrants comprising Figure 27.4, of which the author's favorites are shown in Table 27.5.

Portfolio Optimization Using Sensitivity Analysis

Sensitivity analysis is used to identify and quantify project characteristics that are major factors in the expected value of a project, and is one of the most powerful tools of modern portfolio management. Sensitivity analyses serve two goals. The first goal is to identify the project characteristics that were used to determine the project value, the so-called value drivers, and ensure that the project plan developed by the project team solidly supports these value drivers. For example, a value driver for a potential sedative hypnotic might be that it has no potentiation or interaction with alcohol. Because much of the value of this project depends on this product characteristic, the project team will plan to assess this expected value driver as early as possible in the development cycle.

The second goal is to identify characteristics that, *if added* to the project characteristics, would significantly increase the expected value of the project. This type of sensitivity analysis is important for all projects in the portfolio, but is critically important for those that are in danger of being terminated from the portfolio for lack of adequate value. The results of a sensitivity analysis are plotted with ranges of value for each criterion and are called tornado charts because their shape resembles that of the meteorological phenomenon. Using as an example the project plan shown in Figure 27.5 for a hypothetical oral antibiotic, we see that the portfolio analysis has determined that the "as planned" NPV for the project is $1 billion (represented by the dotted axis on the tornado chart). The stipulation of "as planned" underscores an important caveat, for the value determined was based on the project goals shown in Table 27.6.

What one can learn from this sensitivity analysis is that the scenario with the highest probability of occurring ("most likely") is the one that incorporates the following realities:

- The NDA will be filed in 12-months.
- Twice-a-day dosing will be established.

TABLE 27.5 The Four Portfolio Quadrants

Quadrant	Analogy
I	A diamond mine
II	Betting the ranch
III	A sure bet
IV	A turkey ranch

TABLE 27.6 Example of "As Planned" Goals for a Hypothetical Oral Antibiotic

Goal	Comment
NDA filing	In 12 months
Dose regimen	Twice a day
Concomitant use	With some (but not all) drugs likely to be used by this population
Laboratory kit	Available at launch
Cost of goods	~$25,000/kg
IV formulation	Not available at launch

- The product can be administered concomitantly with many, but not all, of the drugs that might be expected to be used by this patient population.
- A diagnostic kit for antibiotic sensitivity will not be widely available at the time that product marketing is launched.
- The cost of goods will be in the range of $25,000/kg.
- It is unlikely that an intravenous form of the drug will be available at launch.

This "most likely" scenario values the oral antibiotic at $1 billion. The bars for each of the critical goals indicate that product value would be increased by $2 billion if the NDA could be filed in 6 months. Likewise, the value would be reduced to $300,000 if the time required for NDA filing slips to 18 months. The sensitivity analysis also indicates that the product could have an increased value of $2.5 billion if a once-a-day formulation could be developed. Although other changes would also increase the NPV of the product, the first two (a NDA within 6 months and a once-a-day formulation) provide the greatest increase in value. Clearly the PMT and the senior management board would focus the project resources on these two high-value areas. If there were limited resources, then the project team would be asked which of the two increased value goals (NDA or once-a-day formulation) would be the most likely to be achieved.

Once the portfolio has been designed, planned, and managed for optimization, it is the project team's job to make it happen.

PROJECT PLANNING AND MANAGEMENT

Project planning and management for the biopharmaceutical industry began in the early 1980s and became an integral part of the R&D organization by the mid-1980s. The paper entitled *Change + Communication = Challenge — Management of New Drug Development* provides a review of the tools that are still used in biopharmaceutical project management (10). Project planning and management have progressed to the point that there are now six dimensions of project planning and management that are routinely used to plan and manage biopharmaceutical projects (Table 27.7). An overview of each of these dimensions will be provided.

TABLE 27.7 Project Management Dimensions in the Biopharmaceutical Industry

Project planning
Project scheduling
Team management
Resource allocation
Decision-making
Process leadership and benchmarking

Project Planning

Defining a Project

Biopharmaceutical projects, like all projects, consist of three components, which must be planned and managed in an integrated manner. These three components are *project specifications*, *project resources*, and *project timing*. These components can be thought of as "the what?," "the how/where?," and "the when?" of a project, respectively. Once these three components have been defined and agreed upon, the resulting project components are known as the *baseline specifications*, the *baseline resources*, and the *baseline timing*.

Project specifications (the what?) include (1) the projected effectiveness, safety, and especially the differentiation criteria of a project, (2) formulations (e.g., oral, parenteral, transdermal, modified release), and (3) package styles (e.g., bottles, ampoules, and blister packs). Drug development organizations have recently adopted the use of *Target Product Profiles* (*TPP*) to define the expectations of a particular project. In some cases, TPPs are used as early as drug discovery to define the selection criteria for identifying "leads" (e.g., orally active, does not inhibit cytochrome P450 3A4, can be used in combination with drug X). The TPP frequently will include both the "optimal" and the "threshold" metric for acceptability. The threshold metric is identified as the metric that, if not achieved, will prompt serious review of the project for possible termination. A companion planning and decision-making tool is the *Target Package Insert* (*TPI*). The TPI reflects the target labeling that the organization hopes to achieve. The TPP is used as a tool both for planning the clinical and nonclinical activities to generate evidence that will hopefully be convincing to regulatory authorities and for inventorying the new knowledge that has been generated along with the organization's level of confidence that it will support the desired labeling. The TPI is the baseline for desired labeling. A *Draft Package Insert* (*DPI*) begins to evolve as the new knowledge is generated and is constantly compared to the baseline TPI to evaluate whether the drug candidate is likely to achieve the value level of the TPI that was used to justify the selection of the drug candidate and the continued allocation of the organization's resources to the project.

In 2001, the Office of Drug Evaluation IV (ODE IV) of the FDA's Center for Drug Evaluation and Review introduced a pilot program, "Targeted Product Information" to encourage the use of the TPI (11). The ODE IV and Pharmaceutical Research Manufacturers Association (PhRMA) collaborated to develop this TPI template that may be used by sponsors in their drug development programs. In June 2004, the FDA and PhRMA distributed "A White Paper on the Role and Utility of a Target Product Profile in the Clinical Drug Development Process" (12). As stated in the abstract from the white paper, "The purpose of this White Paper is to summarize the intent, utility, and case studies from use of a TPP. This White Paper is intended to be an educational resource to sponsors and FDA personnel who use this tool to help attain a shared understanding about a drug development program and the desired outcomes."

Project resources (the how/where?) includes funding, staff (both internal and external), study participants, beds, clinical supplies, bulk drug, animals, cages, and in-house and outsourced facilities.

Project timing (the when?) consists of the timing for both the overall project and for the subproject goals.

Time can also be thought of as a resource. However, time is the one resource that cannot be replaced. An organization can provide additional staff, funds, animals, study participants, and so on, but the organization cannot recapture time once it has been consumed. Project timing can be established by three processes. The first process of establishing project timing is by the forward planning process based on project specifications and available (sometimes limited) resources. The second process for establishing project timing is by an impending deadline, which the organization uses to define the balance between (1) project specifications that can be accomplished within the specified project time frame and (2) the available project resources. The third process for establishing project timing is to set the deadline, define what must be accomplished, and then resource accordingly to ensure the defined project can be completed by the deadline.

It needs to be noted that project planning and project scheduling are two separate but interdependent dimensions. The ideal way to develop a drug development program is to first define the goals of the project (see label-drivenquestion-based development planning in Chapter 33). Once the goals are defined, a core project team is established. It is the role of this team to (1) develop a strategic and tactical plan that defines and supports the major project objectives, (2) define the project Go/No-Go decisions with prespecified decision criteria, as far as possible, (3) identify the individual activities, the supporting tasks, and resources (funding, people, and facilities) that will be needed to accomplish the project objectives, and (4) identify both the order in which these tasks need to be carried out and any interdependencies between activities.

There are at least two approaches for defining the order of the activities. The first is the "plan for success" approach in which as many activities as possible are conducted in parallel to provide the shortest time path to the Go/No-Go decisions (proof of mechanism, proof of concept, etc.) and to the project completion. The second approach is used when there are very scarce resources or when there is a low probability of project success. This second approach defers expensive activities until a proof of concept (POC) has been achieved for the project. Once the POC has been achieved, then a plan-for-success-style development plan for the project will be developed and implemented. One can also stage the development of lower prioritized projects in a portfolio, if resources are limited, or if the risk is still high and the project needs to be managed more conservatively by the organization.

An Example of a Project Definition

An example of a project definition in the biopharmaceutical industry would be the development of a new chemical entity for the indication of treating mild to severe congestive heart failure (CHF), with both an oral and an intravenous formulation being developed, and with a projected development time of 3 years to NDA submission and a budget of $75,000,000. A subproject would be to complete a clinical POC for the severe CHF indication for the intravenous formulation in 1 year with a budget of $9,000,000.

The Project Management Triangle

Project components can be represented as the three sides of a triangle, as illustrated in Figure 27.6. This representation is quite useful, since once the project components have been established, the length of each side (component) of the project management triangle can be locked in. As usually happens with any project, changes constantly occur. If a project is changed by expanding the number of indications or formulations, then we realize from our geometric analogy that one or both of the other two components need to change. Either the project resource component must be increased to adhere to the original schedule, or the project timing component must be lengthened to maintain the project resource component as originally defined, or a balance needs to occur, involving a

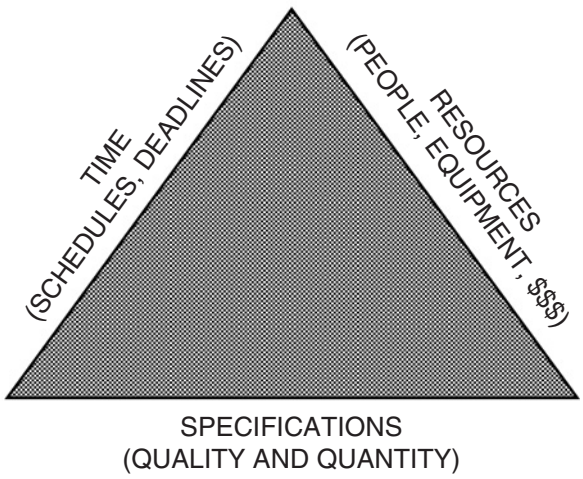

FIGURE 27.6 The project management triangle. A change in one side of the triangle necessitates changes in one or more of the other sides.

change in both the project timing and project resource components.

The Project Cycle

As illustrated in Figure 27.7, the project cycle consists of six stages (13). The first stage of a project, the *initiation stage*, encompasses the planning stage, which includes the definition of the three project components (specifications, resources and timing), even in a preliminary fashion. The project initiation stage includes creation of a project team composed of individuals representing the many disciplines needed to complete the project. This stage usually begins with a kickoff meeting in which the project goals and the project components are presented, team members are introduced to each other, and agreement is reached regarding operating procedures for the project team. The second stage of a project is called the *implementation stage*. During this stage, project planning, project scheduling, and resource allocation actually start. For a drug development project these first efforts will probably focus on the preparation of bulk active compound for formulation screening and animal safety studies, and the start of these animal studies (e.g., see Chapter 29). The third stage of a project is called the *monitoring and tracking stage*. The critically important point to be made regarding monitoring and tracking is to focus and limit attention on "what is tracked" so that linkage is established to the major milestones which will determine whether or not forward motion on the project is being made. The fourth stage is the *reporting stage*. The decision on what needs to be reported and to whom the information needs to be reported should be based on what decisions will be made and by whom. Clearly, the level of detail reported to a project team member is more than the level needed by senior management to make major decisions. The next stage is the *decision-making stage*. A key point to remember regarding the decision-making stage is that a useful definition of a decision is "an allocation of resources." When a decision is made, resources must be either added to a project, taken away from it, or maintained. The next project stage is the *completion/termination stage*. This stage is reached for each project cycle and is determined by either achieving or not achieving the project goals and objectives of that cycle.

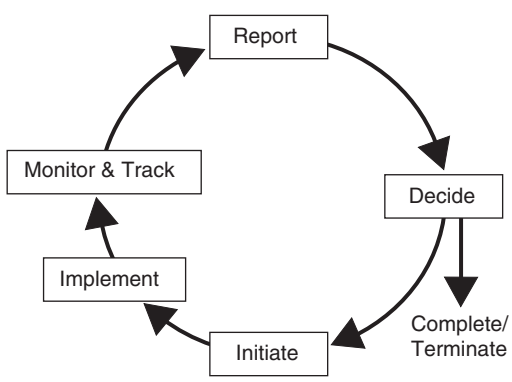

FIGURE 27.7 The project cycle. (Adapted from Szakonyi R. How to successfully keep R&D projects on track. Mt. Airy, MD: Lomond Publications, Inc.; 1988.)

PROJECT PLANNING AND MANAGEMENT TOOLS

Several tools that are useful in the planning and management of biopharmaceutical projects are identified in Table 27.8. Definitions can be found in the Project Management Institute's (PMI) *A Guide to the Project Management Body of Knowledge* (5) and within the tutorial and help sections of Microsoft Project®.

TABLE 27.8 Project Planning and Management Tools

Decision trees
Milestone charts
PERT charts
Gantt charts
Work breakdown structures
Financial tracking

It is important to point out that these tools are useful only after the project objectives, goals, Go/No-Go decisions, decision criteria, and operating assumptions have been established. The project planning management tools are presented in Table 27.8 in the order in which they would be introduced in a project planning process.

Decision Trees

The use of decision trees became more frequent in biopharmaceutical organizations during the mid-1990s as companies realized that drug development programs could indeed be completed in under 48 months. An example of the decision tree that was developed by CDER for the IND review process is shown in Figure 27.8. This example was obtained from the CDER Handbook web site (14). For each of the boxes shown in this figure, the web site includes a narrative that can be accessed by clicking on the respective box. The web site contains a similarly informative decision tree for the NDA review process. The industry uses similar decision trees with prespecified criteria for success at each decision point. Decision points for a specific biopharmaceutical project should focus on technical hurdles such as those shown in Table 27.9.

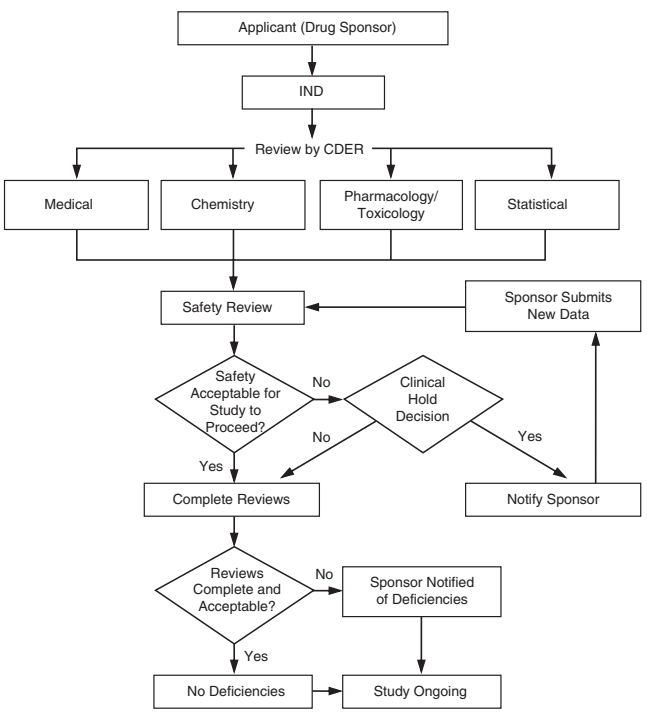

FIGURE 27.8 The decision tree used for the IND review process by the Center for Drug Evaluation and Research (CDER). (Reproduced from the CDER web site at http://www.cder.fda.gov/cder/handbook.)

TABLE 27.9 Specific Project Go/No-Go Decisions

The serious toxicity observed in dogs is not observed in primates
A stable IV formulation has now been identified
An effective dose and a dosing regimen have been characterized
A process to reduce the high cost of goods has been achieved
The human safety observed is as predicted
Clinical activity is observed at 1/20th the highest no-adverse-effect human dose
Synergy is demonstrated with the new combination product
Highest survival ever observed is reported with this test medication

Milestone Charts

Milestone charts consist of a tabulation of major drug development milestones. Whereas the Go/No-Go decisions discussed previously are very project specific, development milestones are much more generic and can usually be applied to a wide variety of projects. Typical milestones for pharmaceutical development are shown in Table 27.10.

PERT/CPM Charts

PERT (Performance Evaluation Review, and Tracking) and CPM (Critical Path Method) charts (flowcharts) show the flow, connectivity, and interdependency of project tasks, activities, and goals. A PERT chart (Figure 27.9) depicts the activities in the order that they will need to be carried out, either in series or in parallel. These charts also identify which activities need to be completed (or initiated) before the next activity, which is dependent on it, can be initiated.

CPM is the methodology used to identify the longest, or *critical path* from project initiation to project completion. In Figure 27.9, the critical path is Path 3 (A + B + E + G + H), since this path is the

TABLE 27.10 Typical Project Milestones

Chemical lead identified
Clinical candidate selected
First-in-human trial initiated
Effective dose and dose regimen characterized
Phase III trials initiated
Phase III trials completed
NDA/BLA submitted
NDA/BLA approved
Product launched

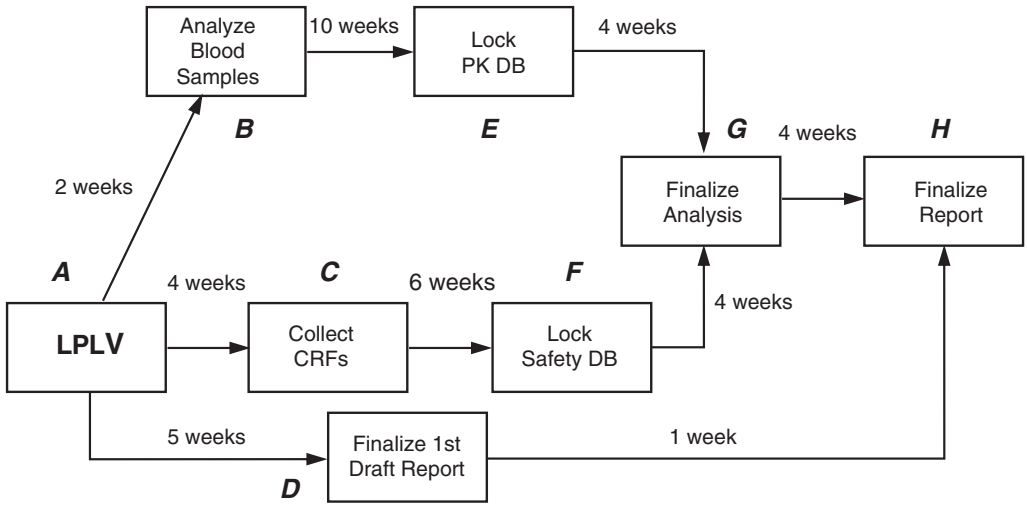

FIGURE 27.9 A PERT chart showing three paths. Path 1 (A + D + H) will require 6 weeks. Path 2 (A + C + F + G + H) will require 18 weeks. Path 3 (A + B + E + G + H) is the longest, requiring 20 weeks, and is the critical path. LPLV, Last patient, last visit; CRFs, case report forms; PK, pharmacokinetic; DB, database.

longest path from "A" to "H." The significance of the critical path is twofold. The first point is that if any activity on the critical path is delayed by 1 day, the whole project will be delayed by 1 day. The second point is that once the critical path activities have been identified, the project team has three jobs to focus on. The first job is to find a way to shorten the critical path. The second job is to track critical path activities very closely to ensure that there is no slippage. The third job is to track all of the activities that could possibly negatively impact the critical path to ensure that these "subcritical path activities" are initiated and completed as scheduled.

Gantt Charts

Horizontal bar charts (Figure 27.10) are used to view (1) the length (duration) of each task, activity, and objective, (2) the temporal relationship between various activities, and (3) the actual progress vs the original plan that has been made on each task, activity, and objective. A number of project-tracking software systems are available and provide the ability to view the whole project as well as just the high-level objectives (milestones and decisions).

Project progress is shown in a number of ways — for example, by shading part of the activity bar to indicate the proportion of the activity that has been completed (e.g., 75% shaded to represent that 75% of the participants needed for a clinical trial have been enrolled). A particularly effective way to track both project progress and to identify key activities that are lagging behind the agreed-on schedule is to set up a comparison bar chart that includes the current bar chart schedule, the previous bar chart schedule, and the bar chart schedule that was originally planned. Project teams have found it very beneficial to view the project Gantt chart in a variety of presentations, such as a Gantt chart of all project activities that are scheduled to start within the next 90 days and a Gantt chart of all project activities that are scheduled to end within the next 90 days. To make the best use of project team meeting time, it is advisable to have the project Gantt chart updated before each team meeting so that the project team is fully informed of the current project timelines and any exceptions to the agreed-on schedule. With a fully updated and informed project schedule, the project team can make the decisions and recommendations required to maintain the desired progress of their project.

Work Breakdown Structures

A work breakdown structure (WBS) can be thought of as an organizational chart of tasks and activities needed to achieve the project objectives. The project WBS can be arranged either by deliverables (e.g., formulations, clinical trials) or by resource (e.g., formulation chemist, clinical trial monitor). A common way of illustrating these different approaches is by analogy with the construction of a new house. One part of the construction WBS would include plumbing and might be sorted by either house level or by room. A second option would be to sort the construction

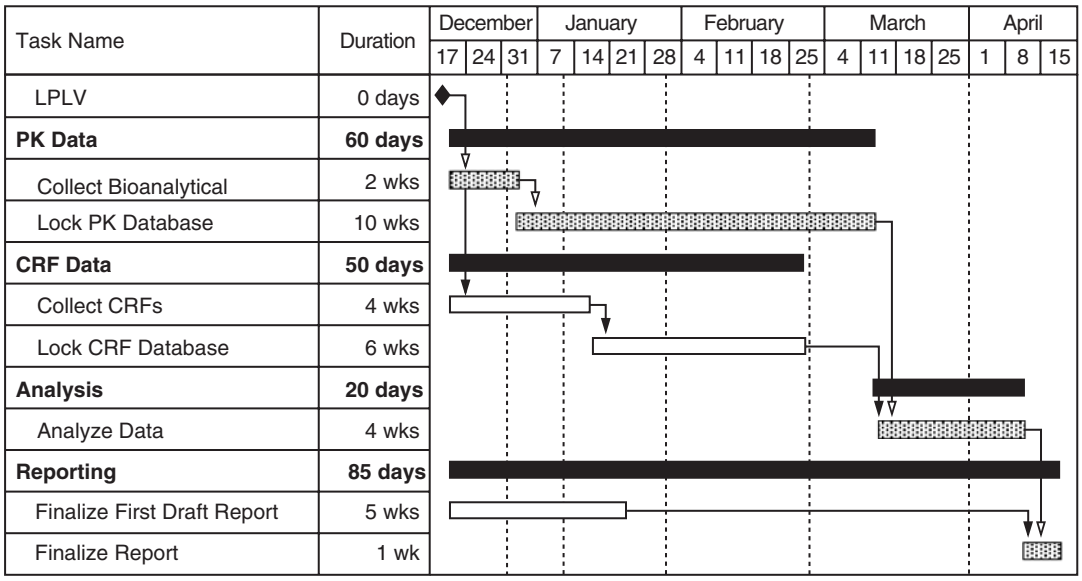

FIGURE 27.10 A Gantt chart (bar chart) with the critical path indicated by the stippled bars and arrows. LPLV, Last patient, last visit; PK, pharmacokinetic; CRF, case report form.

WBS by rooms, with each room having as part of its WBS items such as framing, pluming, wiring, flooring, drywall, painting, and so on.

Financial Tracking

The financial tracking of individual projects has become an increasingly important role for biopharmaceutical project teams. In some organizations, a member of the R&D comptroller's office is a member of the project team. In other cases, individuals from this office are available to support the project team. The project team is asked on an annual basis to project the funds needed for the project over the next 36 months for the project to meet the goals that have been approved by the organization. The team is also asked to help track the project costs on a real-time basis and to make quarterly projections as to the spend rate over the next 12 months. Although some organizations have developed financial tracking tools internally, a number of project-driven financial tracking tools are now commercially available (e.g., Microsoft Project®, SAP).

Project Scheduling

As mentioned earlier, the project schedule is a product of the scope of the project objectives, project resources, and time requirements. Projects can either be scheduled to complete no later than a specified date, in which case an appropriate balance of objectives and resources has to be determined. In other cases, the project objects are established, the resources that are available for the project are allocated, and the project team uses project management software to predict when the project is likely to be completed given the limitations of the allocated resources. Clearly, allocation of more resources to a resource-limited project could accelerate the project significantly.

PROJECT TEAM MANAGEMENT AND DECISION-MAKING

Core Project Teams

In the pharmaceutical industry the formal use of core project teams to accelerate drug development began in the early 1980s. Rather than review the attributes and value of the team concept here, the reader is referred to an excellent text on the subject by Katzenbach and Smith (15). The current standard for biopharmaceutical project team structure is the matrix team, which is made up of core team members from relevant functional organizations that are needed for the development of a new drug (i.e., toxicology, discovery, analytical, formulations, clinical, and regulatory), a project team leader, and a project manager. It is the project manager's role to ensure that current project information has been incorporated into the various project planning and management tools that the organization is using. Using project management tools, the project manager develops various project

scenarios for use at project decision-making meetings. Each core team member represents the combined functions of his or her department and is supported by his or her own set of team members back in that department. Each core team member is also the team leader of his or her respective functions for the project, which maybe called subteams (e.g., clinical subteam, regulatory subteam).

The term *matrix* refers to the fact that project team members have a dual reporting relationship and therefore are known as multiply supervised employees (MSEs). The traditional matrix team concept has performed adequately. But, as initially conceived, the performance evaluation of team members was conducted only by their departmental management, so that the focus of team members was usually centered on their functional department. However, this evaluation structure was modified in the early 1990s by having each team member's performance evaluated, at least in part, by his or her project team leader. This change has greatly increased the effectiveness of the matrix team approach.

In the mid-1980s, Abbott Pharmaceuticals introduced the concept of the "project venture team" in which those who worked on a particular project reported to a project department head. In the mid-1990s, Lilly introduced the concept of "heavyweight teams." Heavyweight teams are formed at the end of Phase II and members of these teams devote their entire time to the advancement of a single project to NDA submission, approval, and launch. Most recently, both matrix and heavyweight teams are adopting the concept of colocation or a project "village." Although the core team team members are formally part of a functional department, their "project offices" are all within a few feet of each other. This project village concept has been particularly successful because it fosters rapid and frequent communication among the core team members. Several large biopharmaceutical companies are now building new facilities just to create space for the "villages" for the colocation of project teams.

Project Team Leadership and Project Support

Project teams can be led and supported in a number of different ways, as identified in Table 27.11.

FDA Project Teams

With the advent of the Prescription Drug User Fee Act (PDUFA), which legislated new timelines for NDA reviews, the FDA introduced the project team concept for both IND and NDA reviews. For INDs, an FDA project team is established upon IND submission. When an NDA is received, an important responsibility of the NDA review team is to determine whether the submission is adequate for review by the FDA. Within 45 days of the NDA submission, the NDA review team will either accept the NDA for review or return the submission to the sponsor along with the reasons why it was not acceptable for review (Refuse to File). The role of project manager has been created in both CDER and CBER. An FDA medical officer generally leads the technical review and a project manager, sometimes called a regulatory manager, oversees the process.

TABLE 27.11 Team Leadership and Project Support Alternatives

Team approach	Advantages	Disadvantages
Team leadership		
Dual Leadership Technical Process	Provides both strong technical *and* process leadership	Two bosses, mixed signals
Technical (usually clinical)	Strong technical leadership	Limited management of process; usually a part-time role in a full-time job
Full-time team leader	Team leader is dedicated to project	Might not have strong technical knowledge of the project; might be leading multiple projects
Team support		
Dedicated project manager	Provides both strong process and project planning *and* management support	None
None	None	Places excess burden on the project team leader to both lead and provide process and project planning and management support

Effective Project Meetings

The ability to manage a meeting effectively is a skill that is most highly regarded in all types of organizations. Effective meetings rarely occur without good preparation and effective meeting management. A well-developed agenda is the most effective tool for holding a successful meeting. Indeed, in some organizations the mantra is becoming "no agenda, no attenda." Having the right people attend the meeting is as important as having an effective agenda. This means that the team leader, the project manager, and all of the team members have a special responsibility to ensure that those who are needed at the meeting do indeed attend. With modern-day video capabilities and conference calling, many meetings can be very effective and productive even when not all the participants can be at the same physical site. It is important for one person to be responsible for ensuring that all of the remote-site participants receive meeting materials in advance of the meeting, either electronically or by fax or mail. It is not acceptable to delay a meeting for 15 to 30 minutes while everyone is waiting for a fax to be sent to participants at a remote site. Most organizations have multimedia tools in their libraries to help their staff develop effective meeting management skills.

Resource Allocation

Resource allocation has become more important with the advent of prioritized portfolios. Once a portfolio is prioritized by the PMT, and the core project team has been informed of their project's priority, the core project team will allocate the available resources for their project in a manner that will provide for the most progress to be made over a given budget period, usually 12 months. For those who manage a department, resource allocation takes on an added dimension, for although a department head may have adequate resources for all of the approved projects, the need for the resources might not be evenly spaced over the next 12 months. For example, the portfolio of projects might need 75% of the department's annual resources in the first 6 months and the remaining 25% in the second 6 months. Ideally, project team leaders, project managers, and department staff will help to resolve this mismatch by meeting and developing several alternative scenarios for senior management review and approval. For the decisions to be soundly based, management will ask each team to identify the impact of each alternative scenario on the project objectives and milestones.

Effective Project Decision-Making

Decision Trees

An excellent example of a decision trees is shown in Figure 27.8. This example outlines the IND regulatory review and approval process. Similar decision trees are developed by project teams within the biopharmaceutical industry. Project teams are now being asked not only to construct decision trees, but to develop contingency plans based on "what-if" scenarios far in advance of the next decision points. The goal is to ensure that the project will not lose forward motion in the event of a "no" decision that requires rework or another loop through the project cycle, or a decision by the PMT that resources for a particular project are more urgently needed for another project.

Prespecified Decision Criteria

To facilitate the decision-making process, project teams should develop prespecified criteria for each decision point or contingency. These criteria provide the critical targets for the project and speed up the decision-making process. An example of clinical go/no-go decision criteria for a potential antihypertensive drug might be "lowers diastolic blood pressure by at least 10 mmHg for at least 6 months in at least 80% of the subjects treated with the middle of three doses, with a side-effect profile no worse than that observed for the active control." One can only imagine the debate that will occur if the blood pressure lowering observed at 6 months is 8 mmHg. Finally, effective decision-making must include an assessment of resource allocation because, as previously emphasized, decision-making is in reality the allocation of resources.

Process Leadership and Benchmarking

It is appropriate to conclude this chapter with some comments about process leadership and benchmarking. The ability to understand how all the complex pieces of drug development come together can only be learned through hands-on experience as a team leader or project manager. Corporate management in the biopharmaceutical industry is now counting on individuals with this experience to identify ways in which the drug development process can be shortened even further than we have seen in the recent past.

Benchmarking has become an important tool that is being used to identify ways in which an organization can quantify, and then exceed, industry standards for the time, cost, and quality of the R&D activities that are needed to discover and bring a new drug to market. Benchmarks can be as broad as "How long should it

take from the FIH trial to NDA submission?" to "How long should it take to design an approvable clinical protocol and case report form for a one-site clinical study?" The Centre for Medicines Research (CMR) has been formally conducting benchmarking studies for the industry and additional information can be found on their web site (16).

The emphasis on both process leadership and benchmarking in the project planing and management domain of biopharmaceutical R&D truly illustrates the level of maturity and sophistication that the discipline of PPM has achieved.

REFERENCES

1. FDA/CDER. Approval times (in months) for NDAs and NMEs approved fiscal years 1988–2000 (updated 11/21/2000). (Internet at http://www.fda.gov/cder/rdmt/fy00ndaap.htm).
2. FDA Talk Paper (T05-09), 2004 FDA Accomplishments, March 22, 2004. (Internet at http://www.fda.gov/bbs/topics/ANSWERS/2005/ANS01346.html.)
3. Grudzinskas CV, Wright C. Reshaping the drug development and review process — a case study of an 18-day approval. Pharmaceutical Executive, October 1994;14:74–80.
4. FDA/CDER. 1999 Report to the Nation. (Internet at http://www.fda.gov/cder/reports/rtn99.pdf.)
5. PMI Standards Committee. Guide to the project management body of knowledge (a PMBOK® Guide). Newtown Square, PA: Project Management Institute; 2000.
6. Dobson M. Practical Project management. Mission, KS: SkillPath Publications; 1996. p. 288.
7. Drug Information Association. (Internet at www.diahome.org.)
8. Baker SL. Perils of the internal rate of return. (Internet at http://hadm.sph.sc.edu/Courses/Econ/invest/invest.html.)
9. DiMasi J. Risks in new drug development: Approval success rates for investigational drugs. Clin Pharmacol Ther 2002;69:297–307.
10. Grudzinskas C. Change + communication = challenge — management of new drug development. Clin. Res. Pract. Drug Regul. Affairs 1988;6:87–111.
11. FDA/CDER. ODE IV Pilot targeted product information. (Internet at http://www.fda.gov/cder/tpi/default.htm.)
12. FDA/PhRMA. Target product profile (TPP): A white paper on the role and utility of a target product profile in the clinical drug development process. June 15, 2004. Internet at http://www.diahome.org/content/community/TPP_White_Paper.doc.)
13. Szakonyi R. How to successfully keep R&D projects on track. Mt Airy, MD: Lomond Publications Inc.; 1988. p. 103.
14. FDA/CDER. The CDER handbook. (Internet at http://www.fda.gov/cder/handbook.)
15. Katzenbach C, Smith D. The wisdom of teams: Creating the high-performance organization. New York: Harperbusiness; 1994. p. 336.
16. CMR International. Global clinical performance metrics programme. (Internet at www.cmr.org; see "CMR Programs.")

This page intentionally left blank

CHAPTER

28

Drug Discovery

SHANNON DECKER AND EDWARD A. SAUSVILLE
Marlene and Stewart Greenebaum Cancer Center, University of Maryland, Baltimore, Maryland

INTRODUCTION

Drug discovery can be described as the process of identifying chemical entities that have the potential to become therapeutic agents. A continuing need for drug discovery exists because there are still many diseases inadequately served by existing therapies. Marketed drugs at this point in time represent a relatively small number of drug target types. Drugs targeted against G-protein-coupled receptors, nuclear (hormone) receptors, and ion channels represent slightly less than 50% of the market. By far, drugs directed against enzymes represent the largest portion of marketed drugs (1). Expansion into new types of drug targets may be necessary to fill certain therapeutic voids, but one of the issues is how to choose a target likely to succeed, especially when venturing into less well-explored types of drug targets such as protein–protein interactions.

The traditional pharmaceutical research and development process suffers from a high attrition rate. For every new drug brought to the market, most estimates suggest that researchers will typically have employed over 100 screens looking for drug leads, winnowing down from tens of thousands of compounds (Figure 28.1). Lead discovery research is also costly and time-consuming, taking by some estimates over 5 years and $200 million, not including the even more substantial time and costs associated with drug development (2). Even having a lead compound in hand, compounds then fail in the development phase for a number of reasons that are unpredictable in the lead discovery phase: unacceptable toxicity, lack of *in vivo* efficacy, market reasons, and poor biopharmaceutical properties. Development can also slow down appreciably in the face of synthetic complexity, low potency, an ambiguous toxicity finding, inherently time-intensive target indication, and, again, because of poor biopharmaceutical properties (3). Carefully thought out and employed strategies for drug discovery are therefore needed, particularly when entering new drug target arenas.

This chapter discusses four important considerations in drug discovery: definition of drug targets, generating diversity, definition of lead structures, and qualifying leads for transition to early trials. Many of the examples will be drawn from the realm of cancer chemotherapy, but the principles should be broadly applicable to a wide variety of disease types.

DEFINITION OF DRUG TARGETS

Early drug discovery up through the 1960s was largely characterized by testing mixtures of natural products in bioassays, yielding drugs such as digitalis, rauwolfia, penicillins, anthracyclines, vincas, paclitaxel, and camptothecins. Although natural-product extracts are still screened for potential drug candidates, due to the complexities associated with identifying the active agent in the extract, screening efforts in most industrial sectors have gradually moved in the direction of testing pure compounds, resulting in the discovery of drugs such as the sulfas, diuretics, hypoglycemics, and antihypertensives.

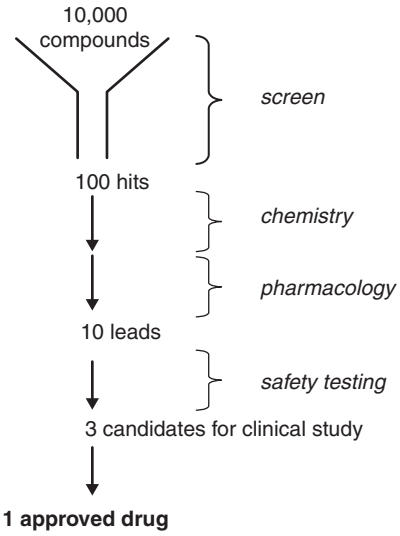

FIGURE 28.1 The screening funnel. Loss of compounds is to be expected as candidates proceed through the preclinical process.

As the technology became available, the use of bioassays evolved into the use of more focused enzymatic assays, from which derived angiotensin-converting enzyme inhibitors, cholesterol-lowering statins, and reverse transcriptase and protease inhibitors. In a more recent evolution, investigators are also employing combinatorial methods to bring mixtures of compounds to bear against many targets, in some cases expressed in engineered organisms such as yeast or invertebrates.

There are two contrasting philosophies behind drug discovery. The first and more traditional is an "empirical" philosophy, where the initial drug lead is recognized by a functionally useful effect. For example, penicillin was recognized by its antibacterial effect, rauwolfia by its antihypertensive effect. Having found a compound that produces a desired biological effect *in vitro*, one then goes on to optimize the molecule, its pharmacology, and the dosing schedule before proceeding to later stage drug development activities.

Empirical Drug Discovery

Empirical drug discovery, despite its successes, is not without intrinsic problems: the identification of a lead compound is divorced from an understanding of its mechanism of action, making lead optimization difficult since there is no easily quantifiable way to ascertain whether an analog will have greater effect. Additionally, the value of an empirical screen depends on its predictive ability. In some cases, such as acid hyposecretion or H_2-receptor binding assays,

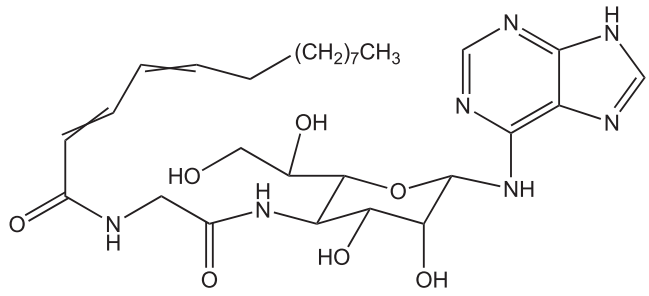

FIGURE 28.2 Structure of KRN5500.

a positive result in such an assay is now recognized to correlate highly with a prediction for a useful antiulcer therapy. On the other hand, an agent demonstrating activity in more than one-third of tested mouse models of anticancer activity still has at best a 50% chance of showing efficacy in a Phase II clinical trial (4).

As an example of the difficulties facing "empirical" discovery and development strategies, the spicamycin analog KRN5500 from Kirin Brewery (Figure 28.2) was discovered through an empirical approach and had a broad spectrum of antitumor activity in *in vivo* anticancer models (Figure 28.3A). While efficacious concentrations of 2–5 μ*M* were achievable in the mouse when administered daily for 5 consecutive days (Figure 28.3B), when the same schedule was used in the initial clinical trial, the maximum tolerated dose produced concentrations of no more than 1 μ*M* and a number of patients experienced unacceptable grade 4 toxicity, including interstitial pneumonitis not predicted in the animal models. In this case then, the lack of a correspondence between tolerated rodent and human pharmacology allowed a compound to proceed all the way to human clinical trials, only to produce unacceptable toxicity (5).

Rational Drug Discovery

Rational drug discovery, by contrast, produces drug leads either by designing compounds to act against a particular biochemical target or by screening compounds until identifying candidates that act against the target's function (Figure 28.4). In a rational approach, one returns at every step of development to the question of whether the drug candidate continues to act on the target. This hopefully allows one to identify failures at an earlier stage and to continually adjust "organism"-related effects such as distribution and pharmaceutic properties while retaining core mechanistic features that allow activity. This approach was used very effectively in the identification of the initial

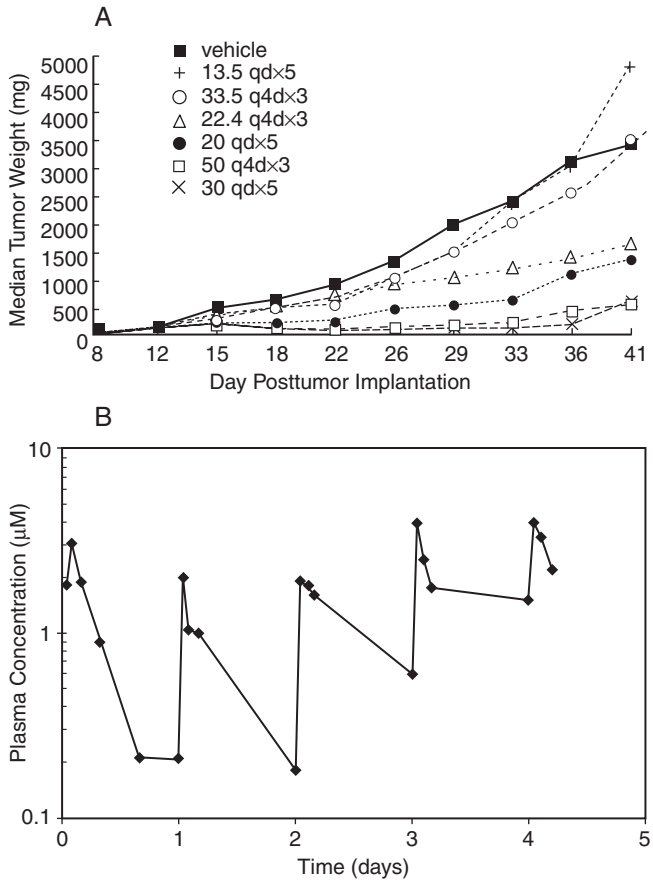

FIGURE 28.3 Enthusiasm for an empirically active anticancer agent KRN5500. (A) Effect of drug on the rate of growth of COLO205 xenograft models in athymic mice (doses from 13.5 mg/kg to 50 mg/kg). (B) Mouse plasma concentrations at 20 mg/kg/day of KRN5500. (Panel A reproduced with permission from Burger AM *et al*. Clin Cancer Res 1997;3:455–63; Panel B, unpublished National Cancer Institute data provided by S. Stinson).

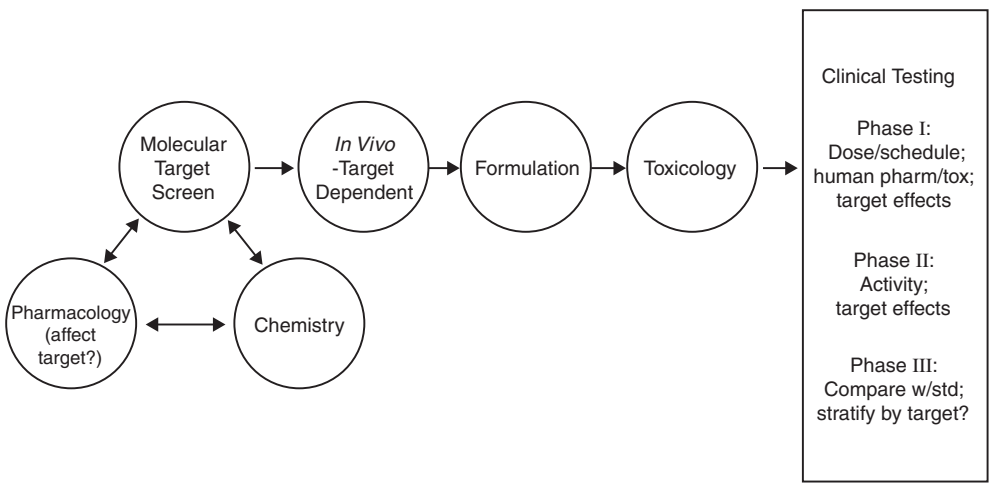

FIGURE 28.4 The rational drug discovery paradigm directed at a molecular target.

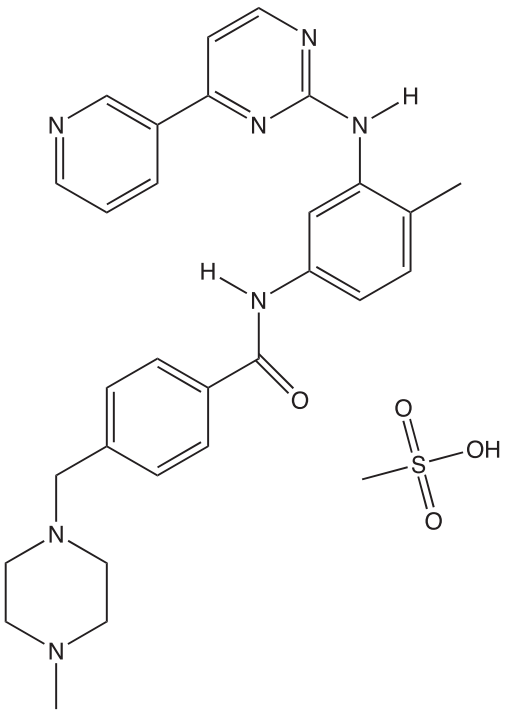

FIGURE 28.5 Structure of imatinib (Gleevec®).

HIV protease inhibitors, of metoprolol as an antihypertensive, and of methotrexate as an antifolate antitumor therapy.

The development of imatinib (Gleevec®) (Figure 28.5), which has been extensively described in a host of publications (6–8) also serves as an excellent example of a rational approach to drug discovery. Briefly, the bcr–abl oncoprotein, with increased tyrosine kinase activity, was identified as a potential target in certain leukemias due to its apparent pathogenicity in cells bearing translocations between chromosomes 9 and 22, which produces the "Philadelphia" chromosome present in chronic myelogenous leukemia (CML). It also occurs in certain cases of acute lymphocytic leukemia (ALL). Although the bcr–abl oncoprotein is able to modulate signal transduction events downstream, it is absent in normal tissues. Natural products such as erbstatin, lavendustin, and piceatannol were initially identified as bcr–abl-directed agents. Alternative strategies to lead optimization that considered protein kinase structure led in part to the compound now called imatinib. Subsequent *in vivo* testing confirmed antitumor efficacy, but only on a schedule of administration that assured the continuous block of bcr–abl phosphorylating activity (7). Clinical trials produced dramatic results in patients with chronic phase CML. Responses that were less impressive in duration occurred in patients with blast crisis and in patients with ALL who had the Philadelphia chromosome.

To proceed with a rational approach, however, begs the question of how to identify a molecular target. The imatinib example could be said to represent a biological approach, proceeding from a cytogenetic observation through to identification of the target bcr–abl oncoprotein. Initiatives such as the Cancer Genome Anatomy Project (http://cgap.nci.nih.gov) allow other biological approaches to target definition, such as finding genes that are expressed in cancer cells but not in normal cells. Such gene expression profiling allowed for the identification of distinct types of diffuse large B-cell lymphoma and the stratification of patients into high- and low-risk groups (9). The high-risk profiles can then indicate which expressed protein sets might be valuable as targets for new agents directed against aggressive lymphoma.

Occasionally, a retroactive approach is possible, where one can start with a drug that was initially identified through more empirical means, and then identify the drug's binding partners. Once identified, these targets can be screened to allow definition of additional candidates, particularly when the original candidate has failed at later stages of drug development for reasons such as unacceptable toxicity or formulation problems. The geldanamycins, members of the benzoquinoid ansamycin antibiotics, represent an example of such an approach. In the late 1980s, researchers saw that these compounds "reversed" the oncogene *src*-transformed phenotype of rat kidney cell lines and decreased steady-state phosphorylation levels without appearing to have any direct effect on src kinases (10, 11). In an attempt to further explicate the mechanism of this class of compounds, a geldanamycin derivative was immobilized to a bead and affinity precipitated the molecular targets with which the drug interacted, thus teasing out heat shock protein 90 (HSP90) as the binding partner (12). Consistent with these binding data, certain geldanamycins inhibited specifically the formation of a previously described src–HSP90 heteroprotein complex. Two compounds in the geldanamycin class (Figure 28.6) are currently undergoing clinical testing, and HSP90 is considered an active target for exploration for geldanamycin-like molecules as well as other classes.

In addition to biological and retroactive approaches to molecular target definition, one can also return to classical approaches of cell metabolism and biochemistry. Since these suggest single targets, they can be inefficient. Chemical genetics approaches have recently been explored with libraries of molecules and precisely defined organisms.

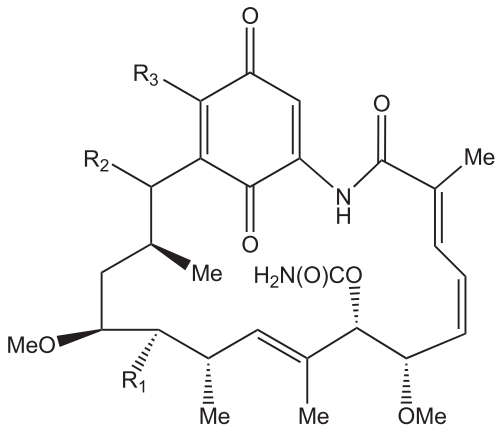

	NSC	R_1	R_2	R_3
Geldanamycin	122750	OH	H	OMe
17AAG	330507	OH	H	$NHCH_2CH{=}CH_2$

FIGURE 28.6 Structure of two compounds in the geldanamycin class. Cancer Chemotherapy National Service Center (NSC) numbers are shown with structural details.

GENERATING DIVERSITY

Not every drug lead will become a successful drug. Geldanamycin, for example, produced unacceptable hepatotoxicity. The next-generation derivative, 17-allylaminogeldanamycin, required the development of a novel egg phospholipid formulation, which is unpopular with patients and clinicians. Having accepted HSP90 or any other molecular target as a viable lead for drug discovery, how does one find sufficient molecules to test against this target, particularly if an initial lead looks like it may not pan out?

Natural Products

Historically, natural products have been considered an excellent source of drug leads due to the amazing diversity found in plant and marine life. A single molecule can contain lipophilic, hydrophilic, acidic, and basic elements, all of which can contribute to a molecule's value as a drug. Further, the diversity of natural products available from plants, marine life, and microbes has barely been scratched. Finally, traditional medicinal use of certain plants for the treatment of certain ailments can provide tantalizing leads. The discovery of the anesthetic lidocaine stemmed from the observation that certain Asian camels refused to eat a certain type of reed. Characterization of the compound gramine isolated from the reed as responsible for producing a numbing sensation when tasted led to lead optimization around the structure of gramine that ultimately culminated in the drug lidocaine.

By some accountings, natural products and their derivatives comprise over a quarter of known drugs (13). Natural products are not, however, without some issues to take into consideration. The collection of source materials can be problematic from several standpoints. Physical availability of the plant or organism can be a significant issue — for instance, in the case of a plant that can only be collected during its 2-week flowering interval in spring. Increasing attention has also been paid to the need to respect the rights of the source countries of the material. Further, on finding a "hit" in a natural product extract, the isolation and structural definition of the compound in the extract responsible for producing the activity is no trivial matter (Figure 28.7), even assuming that it is a single compound in the extract that is responsible.

Chemical Compound Libraries

In addition to natural product sources, chemical compound libraries are used frequently in the drug discovery process. These libraries can range from small, focused libraries specifically synthesized with a particular target in mind to massive, randomly generated libraries. While there is still the problem of deconvolution of an active library, synthetically generated libraries do have a few advantages over natural product extract mixtures. There are typically equal

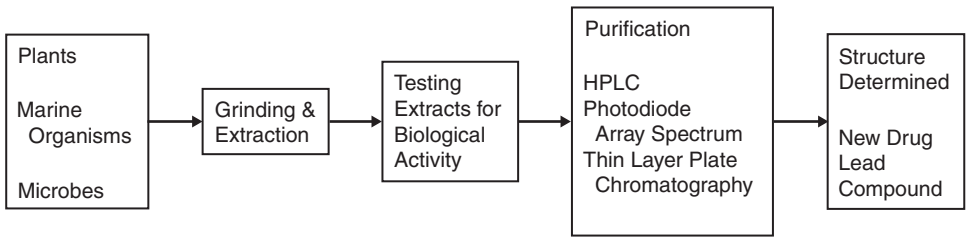

FIGURE 28.7 Steps in natural-product-derived drug discovery.

TABLE 28.1 Lipinski Rule of Five

Compounds with two or more of the following characteristics are flagged as likely to have poor oral absorption

- More than five hydrogen-bond donors
- Molecular weight >500
- *c* log *P* (a measure of partitioning of compound between octanol and water) >5
- Sum of Ns and Os (a rough measure of hydrogen-bond acceptors) >10

concentrations of the compounds. The chemical structures and synthetic pathway are known. Finally, some structure–activity relationships can be deduced by comparing active to inactive members of a library.

Many of the earliest combinatorial libraries were primarily composed of peptides, often without regard to the potential for success of these peptides as drugs. Lipinski's now commonly accepted "Rule of Five" provides guidelines for molecular characteristics likely to be associated with poor oral drug absorption (Table 28.1) (3). Since the larger the peptide, the easier to create diversity, the initial peptide libraries were often composed of compounds with all of Lipinski's undesirable characteristics, such that even if a hit was identified in a screen it was unlikely to be viable for drug development activities. Further, libraries with hundreds to thousands of inactive compounds in a single well, along with one or two active components, could dilute the potency to the point where active compounds were undetectable. Later generations of libraries have attempted to incorporate these Lipinski rules into their initial design by the inclusion of more chemical functional groups in the scaffold and/or natural product backbones. Many libraries now have fewer compounds per well. Newer libraries therefore are more readily amenable to a wide range of bioassays against soluble acceptors, membrane-bound receptors, microorganisms, differentiation (stem cells), etc.

DEFINITION OF LEAD STRUCTURES

The next issue in the drug discovery process following definition of target and sources of diversity is the definition of a lead structure. Lead structures can arise from biochemical or cell-based screens or through structure-based design. Broach and Thorner provide a more exhaustive description of screening strategies than is possible here (14).

Biochemical Screens

Biochemical screens directed against enzymes or transcription factors in 96-well, 384-well, and even 1526-well formats are used quite commonly to identify drug leads. For example, phosphatases Cdc25A and B are overexpressed in many cultured cancer cell lines, and Cdc25A additionally suppresses apoptosis. Overexpression of Cdc25A or B has been detected in human breast, head and neck, cervical, skin, lymph, lung, and gastric cancers. These phosphatases are therefore considered reasonable targets for eventual anticancer therapies. To quickly detect potential Cdc25 phosphatase inhibitors, a high-throughput screen was developed in which fluorescein diphosphate is added to glutathione *S*-transferase (GST)-Cdc25 in assay buffer and the fluorescent output is read as a measure of enzyme inhibition (15). Both targeted array libraries and diverse chemical libraries were used and a hit was identified. Validation of the potential hit from this assay was then done at the cellular, biochemical, and genetic levels, confirming that the hit from the initial screen binds tightly to the catalytic domain of Cdc25A and causes G_2/M arrest.

In a further example from the cancer arena, the transcription factor hypoxia-inducible factor 1 (HIF-1) plays key roles in the regulation of cell response to hypoxia. HIF-1 governs vascular endothelial growth factor (VEGF) and other angiogenic response genes. Overexpression of HIF-1 has been associated with tumor progression, treatment failure, and poor survival, leading to efforts to find pharmacologic modulators of HIF-1. A reporter construct incorporating luciferase was developed and used in a high-throughput assay to look for inhibitors of HIF-1. One of the "hits" to emerge from this screening effort was topotecan, an S-phase-specific agent that causes cytotoxicity by a mechanism dependent on DNA replication-mediated DNA damage. In follow-up testing it was determined that topotecan inhibits HIF-1 accumulation independently of its effects on DNA. Further, topotecan produced sustained inhibition of tumor growth in U251-hypoxia-responsive element (HRE) xenografts in a schedule-dependent fashion that was associated with a marked decrease of HIF-1α protein levels, angiogenesis, and the expression of HIF-1 target genes in tumor tissue (16).

Cell-Based Screens

While cell-based screens have been used in purely empirical screening efforts, they can also be used as the basis of target identification or verification. The

National Cancer Institute's 60-cell-line screen, which is described in Chapter 29 and elsewhere (17–20), consists of nine histologically based panels of human tumor cell lines. In the typical screen, drugs are added to the cell lines at five different concentrations with a 48-hour drug exposure. The dose response of each individual cell line to the drug is then plotted, and the 50% growth inhibition (GI_{50}), total growth inhibition (TGI), and 50% lethal concentration (LC_{50}) indices are calculated. In an alternative method of viewing the data, the mean log GI_{50}, TGI, or LC_{50} is placed as the center point of the so-called mean graph, and the individual values for a particular cell line are plotted as deflections from the mean. By means of a pattern recognition algorithm known as "COMPARE" that generates a Pearson correlation coefficient, it is then possible to compare the pattern of the tested drug with that of any other tested drug. The impetus to compare the patterns of activity of different drugs arose from the observation that drugs with similar mechanisms of action have similar patterns of antitumor activity. For instance, if a compound has a high correlation coefficient with the known tubulin binder paclitaxel, it is likely that the tested compound interacts with tubulin in some fashion. Confirmatory testing of the mechanism of action is of course necessary.

In addition to testing drugs in the 60-cell-line panel, numerous researchers have measured the levels of various molecular targets in each of the 60 cell lines. It is then possible to correlate the activity of a drug with the levels of a particular target. One of the first molecular targets measured in the 60 cell lines was the mRNA expression of the epidermal growth factor receptor (EGFR). A COMPARE analysis of this target profile with agents tested in the 60-cell-line screen produced positive correlations with agents known to inhibit EGFR or otherwise interact with this pathway. This type of COMPARE analysis can provide confirmation that the effect of a drug against a target seen in a biochemical assay translates to a cell culture setting, thus helping to confirm the choice of a drug lead (21).

COMPARE analysis can also be used to identify *de novo* new classes of compounds directed against known targets. For many years, the camptothecin class of compounds was the only explored class of inhibitors of topoisomerase I, an enzyme responsible for DNA single-strand breaks and religation. COMPARE analysis, however, showed a high correlation between camptothecins and a previously unexplored class of compounds known as indenoisoquinolines. Confirmatory testing revealed that the indenoisoquinolines did in fact inhibit topoisomerase I (22).

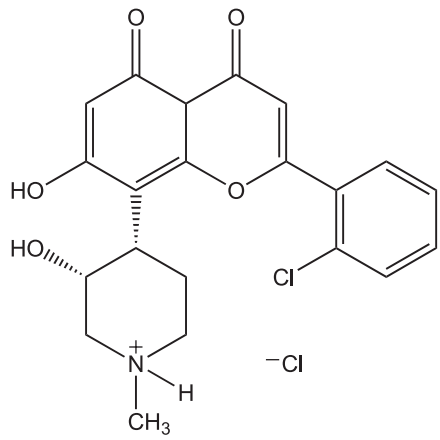

FIGURE 28.8 Structure of flavopiridol.

Structure-Based Drug Design

In addition to various screens, structure-based drug design can also be used in the definition of a lead structure and can further be used in the optimization of the lead compound (23). The cyclin-dependent kinase (Cdk) family is considered a target for cancer therapy due to the role of these kinases in cell cycle regulation and progression. Flavopiridol, a drug currently in clinical testing, is a pan-Cdk inhibitor, acting on the ATP-binding site of Cdks 1, 2, 4, 6, 7, and 9 (Figure 28.8). While nonspecific for Cdks, there is a 10- to >100-fold difference in sensitivity of Cdks to flavopiridol as compared to other kinases such as EGFR, protein kinase A (PKA), and PKC. It is not yet clear however whether a pan-Cdk inhibitor is optimal or whether a compound specifically inhibiting one particular Cdk would be better. To explore this issue, investigators utilized the known structures of ATP and a flavopiridol derivative bound to Cdk2 and synthesized a series of thio- and oxoflavopiridols, attempting to find a lead compound with Cdk specificity different than that of the parent flavopiridol (24, 25). Molecular modeling shows that the thio ether addition places the chlorophenyl ring in closer proximity to amino acids M85 and K89 of Cdk1, thus resulting in greater selectivity for Cdk1 than for Cdk2 (26).

QUALIFYING LEADS FOR TRANSITION TO EARLY TRIALS

The goal of the drug discovery process is obviously to find molecules that could be suitable for eventual clinical testing. Following definition of an optimized lead structure, however, a substantial amount of drug

development work remains to be done before the agent is ready to enter clinical testing. Once a drug lead is available the dose, route, and schedule of administration of the drug should be optimized if possible in appropriate *in vivo* efficacy models (the drug development process will be explored in greater detail in subsequent chapters). For molecules designed under the "rational" philosophy, the optimization process should capitalize on target-directed effects. Initial pharmacokinetic determinations should provide verification that the concentration required to cause an effect *in vitro* is achievable *in vivo*. Development of an acceptable formulation is also important at this stage. It may even be necessary to consider additional analogs of the lead structure if any of the testing indicates that the original lead is in any way untenable.

Following, or in conjunction with, these activities, preclinical pharmacology studies are typically conducted, with the goals of developing sensitive analytical methods for drugs in biological fluids and tissues; determining *in vitro* stability and protein binding; determining pharmacokinetics in rodents and dogs; identifying and analyzing metabolites; defining optimal dose schedule and blood sampling times; correlating peak plasma concentrations and/or AUC with efficacy, safety and toxicity; and evaluating analogs if necessary to determine an optimal development candidate.

Safety testing is required by the FDA before the drug lead is eligible for human testing. For an oncology therapeutic, the FDA currently requires that a drug be tested in two species, a rodent and nonrodent. The studies should follow the proposed clinical route and schedule. As discussed in Chapter 29, the objectives of these studies are to determine in appropriate animal models the maximum tolerated dose (MTD), dose-limiting toxicities (DLTs), schedule-dependent toxicity, reversibility of adverse effects, and a safe clinical starting dose. Only after all of these preclinical studies is it possible to proceed to clinical testing.

Among the drugs that have recently navigated all of the preclinical and clinical development hurdles successfully is bortezomib (Velcade®, PS-341) (Figure 28.9), a dipeptide boronic acid that inhibits the 20S proteasome. This molecule represents a paradigmatic illustration of the optimal function of a cancer drug discovery and development program, as it proceeded from initial entry into preclinical studies to FDA approval in 7 to 8 years. The ubiquitin–proteasome pathway plays a critical role in the regulated degradation of proteins involved in cell cycle control and tumor growth. The originating company selected PS-341 from a group of analogs because of its potent proteasome inhibitory activity, although there were other analogs that had slightly better efficacy in some *in vivo* models (27). The company nevertheless demonstrated not only the ability of PS-341 to reduce the growth of a PC-3 prostate tumor in mice, but also that it did so concordant with its effect on the biochemical target. PS-341 did cause some toxicity in animals, so the question became whether the "safe" dose in animals was in the efficacy range for humans. During the course of the clinical trials, proteasome activity was measured *ex vivo* and dose escalation proceeded to the point of required proteasome inhibition, in contrast to standard clinical trials where dose escalation proceeds to a maximum tolerated dose. Clinical activity was observed in patients with multiple myeloma, and bortezomib was approved by the FDA in 2003.

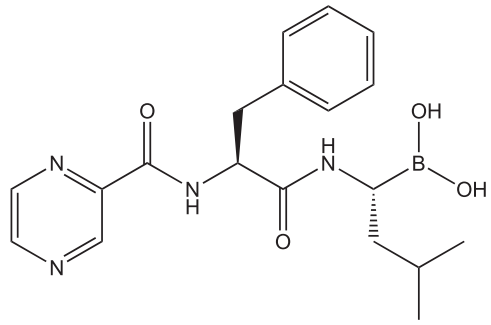

FIGURE 28.9 Structure of bortezomib (Velcade®).

REFERENCES

1. Verdine GL. The combinatorial chemistry of nature. Nature 1996;384(suppl):11–3.
2. Petsko GA. For medicinal purposes. Nature 1996;384(suppl):7–9.
3. Lipper RA. *E pluribus* product. Mod Drug Discov 1999;2:55–60.
4. Johnson JI, Decker S, Zaharevitz D, Rubinstein LV, Venditti JM, Schepartz S, Kalyandrug S, Christian M, Arbuck S, Hollingshead M, Sausville EA. Relationships between drug activity in NCI preclinical *in vitro* and *in vivo* models and early clinical trials. Br J Cancer 2001;84:1424–31.
5. Supko JG, Eder JP Jr, Ryan DP, Seiden MV, Lynch TJ, Amrein PC, Kufe DW, Clark JW. Phase I clinical trial and pharmacokinetic study of the spicamycin analog KRN5500 administered as a 1-hour intravenous infusion for five consecutive days to patients with refractory solid tumors. Clin Cancer Res 2003;9:5178–86.
6. McWhirter JR, Galasso DL, Wang JY. A coiled-coil oligomerization domain of Bcr is essential for the transforming function of Bcr–Abl oncoproteins. Mol Cell Biol 1993;13:7587–95.

7. le Coutre P, Mologni L, Cleris L, Marchesi E, Buchdunger E, Giardini R, Formelli F, Gambacorti-Passerini C. *In vivo* eradication of human Bcr–Abl-positive leukemia cells with an Abl kinase inhibitor. J Natl Cancer Inst 1999;91:163–8.
8. Druker BJ, Sawyers CL, Kantarjian H, Resta DJ, Reese SF, Ford JM, Capdeville R, Talpaz M. Activity of a specific inhibitor of the Bcr–Abl tyrosine kinase in the blast crisis of chronic myeloid leukemia and acute lymphoblastic leukemia with the Philadelphia chromosome. N Engl J Med. 2001;344:1038–42.
9. Alizadeh AA, Eisen MB, Davis RE, Ma C, Lossos IS, Rosenwald A, Boldrick JC, Sabet H, Tran T, Yu X, Powell JI, Yang L, Marti GE, Moore T, Hudson J Jr, Lu L, Lewis DB, Tibshirani R, Sherlock G, Chan WC, Greiner TC, Weisenburger DD, Armitage JO, Warnke R, Levy R, Wilson W, Grever MR, Byrd JC, Botstein D, Brown PO, Staudt LM. Distinct types of diffuse large B-cell lymphoma identified by gene expression profiling. Nature 2000;403:503–11.
10. Uehara Y, Hori M, Takeuchi T, Umezawa H. Phenotypic change from transformed to normal induced by benzoquinonoid ansamycins accompanies inactivation of p60src in rat kidney cells infected with Rous sarcoma virus. Mol Cell Biol 1986;6:2198–206.
11. Uehara Y, Murakami Y, Sugimoto Y, Mizuno S. Mechanism of reversion of Rous sarcoma virus transformation by herbimycin A: Reduction of total phosphotyrosine levels due to reduced kinase activity and increased turnover of p60v-src1. Cancer Res 1989;49:780–5.
12. Whitesell L, Mimnaugh EG, Costa BD, Myers CE, Neckers LM. Inhibition of heat shock protein HSP90–pp60^{v-src} heteroprotein complex formation by benzoquinone ansamycins: Essential role for stress proteins in oncogenic transformation Proc Natl Acad Sci USA 1994;91:8324–8.
13. Newman DJ, Cragg GM, Snader KM. Natural products as sources of new drugs over the period 1981–2002. J Nat Prod 2003;66:1022–37.
14. Broach JR, Thorner J. High-throughput screening for drug discovery. Nature 1996;384(suppl):14–6.
15. Brisson M, Nguyen T, Vogt A, Yalowich J, Giorgianni A, Tobi D, Bahar I, Stephenson CR, Wipf P, Lazo JS. Discovery and characterization of novel small molecule inhibitors of human Cdc25B dual specificity phosphatase. Mol Pharmacol 200;66:824–33.
16. Rapisarda A, Zalek J, Hollingshead M, Braunschweig T, Uranchimeg B, Bonomi CA, Borgel SD, Carter JP, Hewitt SM, Shoemaker RH, Melillo G. Schedule-dependent inhibition of hypoxia-inducible factor-1alpha protein accumulation, angiogenesis, and tumor growth by topotecan in U251-HRE glioblastoma xenografts. Cancer Res 2004;64:6845–8.
17. Alley MC, Scudiero DA, Monks PA, Hursey ML, Czerwinski MJ, Fine DL, Abbott BJ, Mayo JG, Shoemaker RH, Boyd MR. Feasibility of drug screening with panels of human tumor cell lines using a microculture tetrazolium assay. Cancer Res 1988;48:589-601.
18. Boyd MR, Paull KD. Some practical considerations and applications of the national cancer institute *in vitro* anticancer drug discovery screen. Drug Dev Res 1995;34:91–109.
19. Scherf U, Ross DT, Waltham M, Smith LH, Lee JK, Tanabe L, Kohn KW, Reinhold WC, Myers TG, Andrews DT, Scudiero DA, Eisen MB, Sausville EA, Pommier Y, Botstein D, Brown PO, Weinstein JN. A gene expression database for the molecular pharmacology of cancer. Nat Genet 2000; 24:236–44.
20. Weinstein JN, Myers TG, O'Connor PM, Friend SH, Fornace AJ Jr, Kohn KW, Fojo T, Bates SE, Rubinstein LV, Anderson NL, Buolamwini JK, van Osdol WW, Monks AP, Scudiero DA, Sausville EA, Zaharevitz DW, Bunow B, Viswanadhan VN, Johnson GS, Wittes RE, Paull KD. An information-intensive approach to the molecular pharmacology of cancer. Science 1997;275:343–9.
21. Wosikowski K, Schuurhuis D, Johnson K, Paull KD, Myers TG, Weinstein JN, Bates SE. Identification of epidermal growth factor receptor and c-erbB2 pathway inhibitors by correlation with gene expression patterns. J Natl Cancer Inst 1997;89: 1505–15.
22. Kohlhagen G, Paull KD, Cushman M, Nagafuji P, Pommier Y. Protein-linked DNA strand breaks induced by NSC 314622, a novel noncamptothecin topoisomerase I poison. Mol Pharmacol 1998;54:50–8.
23. Blundell TL. Structure-based drug design. Nature 1996;384(suppl):23–6.
24. Arris CE, Boyle FT, Calvert AH, Curtin NJ, Endicott JA, Garman EF, Gibson AE, Golding BT, Grant S, Griffin RJ, Jewsbury P, Johnson LN, Lawrie AM, Newell DR, Noble ME, Sausville EA, Schultz R, Yu W. Identification of novel purine and pyrimidine cyclin-dependent kinase inhibitors with distinct molecular interactions and tumor cell growth inhibition profiles. J Med Chem 2000; 43:2797–804.
25. De Azevedo WF Jr, Mueller-Dieckmann HJ, Schulze-Gahmen U, Worland PJ, Sausville E, Kim SH. Structural basis for specificity and potency of a flavonoid inhibitor of human CDK2, a cell cycle kinase. Proc Natl Acad Sci USA 1996;93:2735–40.
26. Kim KS, Sack JS, Tokarski JS, Qian L, Chao ST, Leith L, Kelly YF, Misra RN, Hunt JT, Kimball SD, Humphreys WG, Wautlet BS, Mulheron JG, Webster KR. Thio- and oxoflavopiridols, cyclin-dependent kinase 1-selective inhibitors: Synthesis and biological effects. J Med Chem 2000;43:4126–34.
27. Adams J, Palombella VJ, Sausville EA, Johnson J, Destree A, Lazarus DD, Maas J, Pien CS, Prakash S, Elliott PJ. Proteasome inhibitors: A novel class of potent and effective antitumor agents. Cancer Res 1999;59:2615–22.

This page intentionally left blank

CHAPTER

29

Preclinical Drug Development

CHRIS H. TAKIMOTO AND MICHAEL WICK
Institute for Drug Development, Cancer Therapy and Research Center, San Antonio, Texas

INTRODUCTION

From the first time a promising molecule is identified in a drug discovery and screening program to the time it enters a first-in-human Phase I clinical trial, an enormous amount of scientific work and evaluation must be performed. Preclinical development, as defined in this chapter, encompasses all of the activities that must take place before a new chemical entity can be administered to humans. As such, it spans the gap between drug discovery and clinical testing.

This chapter describes the general processes and concepts involved in the preclinical development of agents, with specific examples taken from the field of oncology. In the present era, there is an increasing public expectation that scientific advances in biological research will be applied to clinical medicine as rapidly as possible. Our growing understanding of the molecular basis of human disease is driving the development of new, rationally designed, targeted medical therapies. As a consequence, the level and quality of science currently supporting the drug development process are unprecedented, and nowhere is this more evident than in the field of oncology.

In the past several decades, promising anticancer agents were primarily screened for their cytotoxic effects against rapidly growing cells. Not surprisingly, agents developed under this guiding principle often lacked selectivity of action, resulting in high degrees of toxicity in normal tissues. Historically, excessive systemic toxicity was the hallmark of conventional cancer chemotherapy. However, our understanding of cancer biology has fundamentally changed. Tumors are now recognized as composite systems containing both abnormal malignant cells and a variety of normal cells. This complex interaction between tumor and normal tissues is responsible for important properties such as tumor blood vessel growth, invasion, and metastases. This new comprehensive understanding of cancer biology has led to the characterization of a large number of unique molecular targets for therapeutic intervention (1).

The recognition and characterization of many novel and new cancer-related molecular targets, coupled with high-throughput screening and sophisticated, genetically engineered testing systems, have fundamentally altered developmental therapeutics programs in oncology. No longer is cytotoxicity the primary screening criterion for promising anticancer agents. Instead, the discovery of modern anticancer therapies now starts with identification of novel molecular targets uniquely present within cancer cells. The characterization of these molecular targets is followed by extensive screening efforts, often employing massive libraries of chemical compounds to discover agents that interact with these targets. After a promising lead compound is identified, additional testing of modified derivatives is implemented in further screening tests in laboratory cell lines and animal models. Ultimately, an optimal drug candidate suitable for clinical testing is identified. This shift in approach emphasizes the importance of developing new strategies for preclinical drug development.

COMPONENTS OF PRECLINICAL DRUG DEVELOPMENT

The components of preclinical drug development can be divided into four general areas that include (1) *in vitro* studies to define a new agent's pharmacologic properties, (2) drug supply and manufacturing, (3) drug formulation, and, finally, (4) *in vivo* studies in animal models to provide an initial proof of therapeutic principle and demonstrate the potential for clinical efficacy.

In Vitro Studies

Preliminary *in vitro* studies of a new pharmacologic agent are closely related to drug discovery and screening efforts. Historically, past screening strategies for anticancer agents used *in vitro* assays to identify agents with growth inhibitory or cytotoxic potency in cultured murine or human tumor cell lines. However, more recent approaches now utilize well-characterized assays for specific pharmacologic properties of interest as a principal screening tool. Examples of such *in vitro* screening assays include the ability to bind to receptors, inhibit specific enzymes, or stabilize or destabilize multiprotein complexes. Follow-up laboratory studies can help to characterize further the specificity of a drug's molecular mechanism of action and to explore potential off-target drug effects. Understanding the molecular pharmacology of a drug at this early stage is important for characterizing the full range of a drug's potential pharmacodynamic actions. These studies can also provide insight into possible mechanisms of drug resistance. With the recent advent of molecular target-based drug screening programs, as discussed in Chapter 28, the molecular pharmacology of promising compounds is well defined at relatively early stages of preclinical development.

In vitro assessment of new drugs can be performed in intact cell lines or cell-free systems. Examples of cell-free systems include assays that measure enzyme inhibition, receptor binding, protein–small molecule interactions, or interference with components of important signal transduction pathways. These types of tests may form the basis for high-throughput screening assays employed in large-scale drug discovery or combinatorial chemistry efforts designed to identify new agents with specific molecular properties. For example, the ability to decrease downstream enzyme activation and protein phosphorylation by direct inhibition of specific kinase activities was assessed in a screening program designed to identify potential small-molecule inhibitors of phosphoinositide-dependent protein kinase-1 (PDK-1) (2). Recombinant PDK-1 and a peptide substrate were incubated with Mg and [γ-^{32}P]ATP in the presence of test agents using a range of concentrations. Inhibition of kinase activity was assessed by comparison of phosphorylated versus total substrate in the presence and absence of the test molecules. Results from these screens identified three inhibitors with IC_{50} values in the low nanomolar range.

Cell-free systems utilizing nuclear magnetic resonance (NMR) and X-ray crystallography techniques also can be vital in gathering important information for the design of specifically targeted drug therapies (3–6). Changes in tertiary structure of an important protein following its interaction with a small molecule or the three-dimensional characterization of a target enzyme's active binding site may greatly assist in the rational design of novel inhibitors or it can accelerate the subsequent development of related analogs. These types of tests may help form the basis for high-throughput screening assays employed in large-scale drug discovery or combinatorial chemistry efforts designed to identify new agents with unique molecular properties.

Another approach to preclinical *in vitro* drug testing is to use genetically characterized cell lines to assess drug effects against cells containing known specific DNA mutations. For example, the National Cancer Institute (NCI) has been studying the use of genetically defined yeast strains as a screening tool for the *in vitro* testing of potential anticancer agents (7). The identification of drugs that selectively kill yeast cells containing the same molecular mutations that are commonly found in human cancers, such as *p53* or *ras* gene mutations, could lead to the discovery of entirely new classes of drugs with selective activity against cancer cells. Obviously, this approach depends on a detailed understanding of the specific molecular abnormalities that exist in human cancers and on the ability to characterize and grow yeast strains containing defined mutations analogous to those found in human tumors.

Although the demonstration of anticancer effects *in vitro* is quite far removed from anticancer activity in clinical studies, it does provide some predictive information about a compound's potential for clinical utility. Cell line studies performed *in vitro* also provide the opportunity to study the biochemical and molecular effects of a new agent on various cell processes, such as macromolecule synthesis of RNA, DNA, or proteins. Effects on tumor cell growth, cell cycle distribution, cell differentiation, or the induction of apoptosis can also be readily measured at this stage of drug development. Growth inhibitory activity against human tumor cell lines growing in culture forms the basis for the screen utilizing 60 human tumor

cell lines, which is the principle anticancer screening instrument used by the NCI (8). Finally, the relative cytotoxic potency against cell lines derived for specific human tumors can also provide a preliminary assessment of the likely spectrum of antitumor activity of a new agent.

In vitro cell line studies are also useful for analyzing specific mechanisms of drug resistance. Modified lines have been developed that differ from parental wild-type cells in their expression of specific drug-resistance mechanisms. Common examples include cell lines that express the P-glycoprotein-mediated, multidrug-resistance (MDR) phenotype, or the multidrug-resistance protein (MRP), both of which confer drug resistance to a wide variety of natural product anticancer agents. Assessment of the relative antitumor activity in an MDR-expressing cell line compared to the nonresistant, parental wild-type cells can provide information regarding the potential importance of this particular mechanism of drug resistance for a new anticancer agent (9).

In vitro methods may also have utility for predicting important pharmacokinetic parameters, such as oral absorption and hepatic metabolism. For example, oral bioavailability can be predicted by measuring drug transport across a monolayer of Caco-2 human colon carcinoma cells, as discussed in Chapter 4 (9, 10). Specific pathways of potential importance for drug metabolism and elimination can be explored using well-defined drug-metabolizing enzyme systems (11, 12). When coupled with sensitive qualitative analytical methods, such studies can identify metabolites that may be searched for *in vivo*. Furthermore, these studies can also identify potentially relevant drug interactions arising from competition for common drug-metabolizing enzymes, such as CYP3A4 (12). Finally, *in vitro* protein binding studies prior to *in vivo* testing can provide early information as the extent of distribution of a novel agent and can help interpret the free and bound concentrations observed in pharmacokinetic studies performed *in vivo* (see Guidance for industry: Drug metabolism/drug interaction studies in the drug development process: Studies *in vitro*, available on the Internet at http://www.fda.gov/cder).

Drug Supply and Formulation

Prior to entering clinical trials, adequate drug supplies of pharmaceutical-grade material must be available. This may require the development of bulk chemical synthesis protocols or, in the case of natural product isolation, adequate amounts of raw materials for the extraction of either a drug or its synthetic precursors. Manufacturing of pharmaceutical products for clinical testing in the United States must be conducted under current Good Manufacturing Practice (cGMP) guidelines that have been specifically defined by the U.S. Food and Drug Administration (FDA). An extensive discussion of these regulations is beyond the scope of this text, but the current regulations have been published in the U.S. Code of Federal Regulations and are available over the Internet at the U.S. FDA web site (http://www.fda.gov/cder).

Drug supply problems initially delayed the development of paclitaxel, a natural product antitumor agent with activity against ovarian, breast, and lung cancer (13). Paclitaxel is found in the bark of the Pacific yew tree, *Taxus brevifolia* (14). Poor yields (0.01%) of paclitaxel from harvested tree bark meant that very large amounts of the plant product were necessary to sustain the clinical development of this agent (15). As a consequence, its availability during the early clinical testing program was limited. However, pharmaceutical scientists have now found that more favorable yields of paclitaxel precursors can be isolated from the yew tree needles, which represent a renewable source material (16). Semisynthetic production of paclitaxel from these precursors has helped to improve the supply of this active anticancer agent.

Formulation of drugs for clinical use may also present major difficulties in developing new agents. This is particularly true for drugs that require special routes or methods of administration, such as transdermal, inhalational, or tropical therapies, or for agents that are given as timed-released formulations. However, even routine intravenous administration can sometimes be challenging for drug formulation scientists. For example, paclitaxel is poorly soluble in standard aqueous intravenous solutions. Clinical development of this agent could not proceed until a suitable intravenous formulation in Cremophor EL (polyoxyethylated castor oil) was developed (13). However, use of complex vehicles such as Cremophor EL can have substantial clinical consequences. The high incidence of potentially life-threatening anaphylactoid hypersensitivity reactions seen during short infusions of paclitaxel has been attributed to the intravenous administration of Cremophor EL (17–19). Another example of a formulation problem that delayed clinical development of a drug involved 9-aminocamptothecin (9-AC), an insoluble camptothecin derivative. Clinical development of 9-AC was given a high priority by the NCI in 1989; however, clinical trials of this natural product derivative did not begin until 1993. This delay represented the time required

to develop a suitable formulation of 9-AC in dimethylacetamide, polyethylene glycol, and phosphoric acid (20, 21).

In Vivo Studies — Efficacy Testing in Animal Models

Research in cancer biology has identified many properties that distinguish a malignant from a normal cell, including uncontrolled growth, metastasis, dedifferentiation, genetic plasticity, and drug resistance. However, only uncontrolled growth has been extensively studied as a target for cancer chemotherapy. Newer therapeutic strategies now in clinical testing include interfering with the metastatic cascade, inducing differentiation, interrupting autocrine or paracrine growth loops, blocking tumor angiogenesis pathways, inhibiting cell cycle and growth signaling cascades, enhancing tumor immunogenicity, and reversing drug resistance. However, despite substantial advances in developing *in vitro* laboratory models, many of these approaches can only be adequately assessed *in vivo* in animal model systems.

Mouse and rat model systems have several advantages over the use of higher mammals for investigating mammalian biology and disease states. The release of a draft sequence of the mouse genome in 2002 and the ongoing efforts to complete the sequencing of the rat genetic code have enabled the molecular identification of important mutations involved in the pathogenesis of human diseases, such as cancer, diabetes, arterial atherosclerosis, and hypertension. In addition, numerous genetically well-defined animal lines with distinct phenotypic characteristics are readily available in both rat and mouse species. Furthermore, the short generation times and the relatively modest maintenance costs of these models makes them extremely attractive for examining the targeted activity of various therapeutic reagents in preclinical development.

A number of animal model systems have been developed to provide tumor microenvironments that mimic the clinical situation. However, there are no perfect animal models for drug development. The adequacy of any specific animal model depends on its validity, selectivity, predictability, and reproducibility (22). In cancer chemotherapy, animal models are selected to simultaneously demonstrate antitumor efficacy and evaluate systemic toxicities in an intact organism. Ideally, the tumor system under study in the animal model should be genetically stable over time, with homogeneous characteristics that mimic human tumor biology. In oncology, a variety of diverse animal models for human tumors have been developed. These models can be broadly categorized in to three groups: (1) spontaneous models, including those originating from natural or induced mutations; (2) engineered models, including transgenic and knockout animals, and (3) transplanted tumor models, with a focus on implanted and orthotopic tumors in cancer drug development.

Spontaneous Models

Models resembling human disease states may arise spontaneously in animals at a certain age or period of development, or they may be induced by invasive interventions such as treatments with drugs, chemical toxins, or radiation. Cardiovascular drug development routinely utilizes a number of these models for research in hypertension, hypertrophic cardiomyopathies, and heart failure. One well-defined cardiovascular animal model is the spontaneously hypertensive rat (SHR), originating from a colony of hypertensive Wistar rats developed in Kyoto, Japan (23, 24). Another example is the obese Zucker rat, an animal model of non-insulin-dependent type 2 diabetes (25, 26). In the Zucker rat, a single defect in the gene coding the leptin receptor (*ob*) results in insulin resistance, hyperglycemia, and hypoinsulinemia. In oncology, inbred or outbred animals with one or more naturally occurring genetic mutations comprise a majority of spontaneous animal tumor models. Several models have also been identified and characterized in cancer research, including the Min mouse that has a mutation in the adenomatous polyposis coli (*APC*) gene and spontaneously develops adenomatous polyps that are considered precursors for colon cancer (27). Another is the 7,12-diemethylbenz[*a*]anthracene (DMBA) or 1-methyl-1-nitrosourea (MNU) induced mammary carcinoma model for the study of breast cancer (1).

Although spontaneous tumors closely resemble the human clinical situation, a number of factors make these models poorly reproducible in controlled settings. These include difficulties in adequately staging the tumors, variations in their natural history, and the low yields of animals that actually develop tumors. Consequently, spontaneous tumors have greater utility in the study of carcinogenesis and chemoprevention, and are somewhat less useful as routine therapeutic models for studying the treatment of established tumors.

Engineered Models

An exciting area of ongoing research is the increasing use of genetically engineered animals for preclinical drug testing. Transgenic and knockout

mice are genetically altered to develop spontaneous endogenous tumors in a predictable fashion. Because of this, they can provide a versatile environment for testing novel experimental therapies. Advantages of these newer systems include organ- or site-specific targeting, more natural growth rates and patterns of growth, and, most significantly, the use of immunocompetent animals (28, 29). Disadvantages are that the cost of these specialized animals can be high and, in some cases, their use may require a commercial license. Furthermore, the development of endogenous tumors often occurs late in the animals' life span, which can delay experiment times, and the diversity of different histological tumor types available is low. Finally, the correlation between activity in transgenic animal tumors and clinical anticancer activity has not been completely validated.

Transgenic mice arise from the introduction of a foreign gene into the pronucleus of a fertilized egg. This can be accomplished by microinjection (28, 29), retroviral infection (30), or embryonal stem cell transfer (31). This latter technique involves the transfer of genetic material into embryonal stem cells that can then be transplanted into blastocysts to create a chimeric mouse. If the germ cells in the chimeric animal are derived from the embryonal stem cells, then the offspring of the animal will be transgenic and will express the inserted gene of interest. The capability of introducing and expressing a specific gene of interest in an intact organism provides a powerful means for manipulating the genetic milieu of an experimental animal.

Several transgenic models have been identified and characterized in recent years. One important example is the transgenic hypertensive TG(mREN2)27 rat model, the genome of which contains the mouse renin transgene that results in increased local angiotensin II concentrations, leading to hypertension and insulin resistance. Insertion of known oncogenes, such as *ras* (32) or *N-myc* (33), can generate transgenic animals that develop spontaneous tumors in a predictable fashion. For example, transgenic mice expressing a mutated *ras* gene frequently develop mammary tumors and can be used to screen for agents active in breast cancer (32). This model is also useful for testing novel agents that specifically target abnormalities in the *ras* signaling pathway, such as farnesyl transferase inhibitors (34). Use of organ-specific promoters can further enhance the power of these systems. For example, the association of the human *c-myc* oncogene with an immunoglobulin promoter can lead to the development of pre-B-cell lymphomas (35), while its association with a mouse mammary tumor virus promoter can result in mammary gland tumors (36). Tumor resistance genes, such as the multiple-drug-resistance gene (*mdr*), have also been inserted and expressed in transgenic animals (37). These animals are highly resistant to a variety of different natural product antitumor agents and are able to tolerate otherwise lethal doses of drugs in this class. Such animals may be useful as screens for agents that can reverse the multidrug-resistant phenotype.

Knockout mice are animals that have been genetically altered to remove both alleles of a specific gene (38). This is accomplished by homologous recombination techniques that insert the defective gene into embryonic stem cells that are then isolated and injected into a blastocyst to generate heterozygous mice. Further inbreeding will generate homozygous "knockout" animals (38). Knockout animals can be developed that are similar to transgenic animals in that they lack the function of a specific tumor suppressor gene, such as *p53*, and have a very high incidence of spontaneous tumor development (39). If the tumor suppressor gene is required for viability of the animal during embryonic development, conditional knockout animals have been developed that selectively inactivate the gene of interest in specific tissues at defined periods in the animal's lifetime. Currently, these models are being extensively used in the study of carcinogenesis and chemoprevention; however, their application in testing therapeutic agents is growing.

Transplanted Tumors

Transplanted animal or human tumor xenograft models are some of the most widely used tools for studying experimental therapeutics in cancer. Established transplantable murine tumors have been extensively characterized and demonstrate excellent homogeneity and reproducibility (40). Examples of murine tumors commonly used in preclinical screening of antitumor agents include Lewis lung carcinoma, melanoma B16, sarcoma 180, L1210 leukemia, and P388 leukemia. A major advantage of these transplantable syngeneic murine tumors is that the animals under study have intact immune systems. However, disadvantages include the rapid growth of these tumors, which is substantially greater than is seen in human tumors, and the fact that most of these models are rodent based.

An important advance in preclinical models for anticancer agents was the development of immunosuppressed mouse strains that allowed for the reproducible implantation and growth of human tumor cells *in vivo*. The first xenograft of a human colon cancer cell line into immunocompromised "nude" mice was reported in 1969 by Rygaard and Povlsen (41).

These mouse strains contained an autosomal recessive mutation in the *nu* (for nude) gene on chromosome 11. Homozygous mutations in the *nu* gene resulted in the absence of hair, poor growth, decreased fertility, an absent thymus gland, and a shortened life span (41, 42). These animals exhibited a severe T-cell immunologic defect that impaired their ability to reject tissue transplants. Consequently, these animals could tolerate the implantation and growth of human tumor cell xenografts. This discovery led to a revolution in experimental therapeutics in cancer research (43–45). Currently, xenograft tumors have been established for virtually all common human solid tumors. A high degree of correlation has been observed between the sensitivity of disease-specific human xenografts and complete clinical response rates in the same tumor type (46, 47).

Severe combined immune deficiency (SCID) mice are another commonly employed immunosuppressed host for human tumor xenografts. These mice lack functional T- and B-cells and are more immunodeficient than nude mice are. This may explain in part the higher ease of growth of some human tumor xenograft models in these animals (48). The ability of SCID mice to support the growth of primary leukemia cell lines derived from patients with acute and chronic leukemia has led to the use of these animals as primary models for testing agents with antileukemic activity (49). However, the greater sensitivity of these animals to toxic drug effects and greater expense have made SCID mice less popular than their nude counterparts as a routine platform for screening for agents with activity against solid tumors.

In NCI screening studies, simplicity and ease of access make subcutaneous implantation the most common approach for growing human tumor xenografts in mice. Injection of human tumor cell suspensions into the animal's flank leads to implantation and growth over a period of days to weeks. Human tumor xenografts can also be implanted in other sites. Implantation in the renal subcapsule has the advantage of requiring a relatively short inoculation time prior to drug treatment, making it particularly useful for short-term *in vivo* assays. Tumors are implanted as a small tissue fragment under the kidney capsule of the nude mouse (50). Because the renal subcapsule is a relatively immunopriviliged site, human tumor xenograft implantation has also been employed successfully in immunocompetent mice (51, 52). Renal subcapsule-implanted tumors maintain much of the same morphology and growth characteristics as the original tumor from which they were derived (51, 52). In most cases, cell–cell contact is preserved and cells maintain the spatial relationships found in the original tumor. Thus, renal subcapsule implants may be a much more representative model for metastatic human tumors than are subcutaneous xenografts. Renal subcapsular tumor responses can be assessed in a variety of ways, including the measurement of subcapsular renal site, clonogenic assay of surgically removed tumors following *in vivo* treatment, or overall animal survival (53).

Orthotopic xenograft models involve implanting tumors into defined sites within the animal to mimic metastases to specific organs. This concept is based on the premise that tumor metastases are not random, but occur because of a specific tropism or affinity of various tumors to grow in specific sites (54). This is based on the familiar "seed and soil" hypothesis originally proposed in 1889 by Paget (55). Orthotopic xenograft models have been developed for a number of different tumors, including renal cell carcinoma (56), central nervous system tumors (57), and pancreatic, prostate, colon, and lung cancers (54). However, because of their expense and technical difficulties, orthotopic xenograft models have not been routinely used by the NCI.

Despite their popularity, xenograft models still have limitations (58). For example, subcutaneous xenograft implants metastasize infrequently and are rarely invasive. Therefore, animal survival is not an ideal endpoint for subcutaneous xenograft studies because death usually results from gross tumor bulk. In addition, xenograft growth in the subcutaneous space obviously differs from most clinical human tumors, with shorter tumor doubling times, better organized tumor vasculature, and less overall necrosis (59). Finally, because they are immunocompromised, nude mouse models are poor systems for studying therapies that depend upon the host's immune system or that require species-specific host tissue effects. Rigorous attention to maintaining a sterile laboratory environment is essential because infections in these animals are common.

The NCI has implemented the hollow fiber *in vivo* screening assay as part of their anticancer agent screening program (60, 61). This technique involves the insertion of human tumor cells into polyvinylidene fluoride biocompatible hollow fibers that can be implanted intraperitoneally or subcutaneously into immunocompetent mice. The hollow fibers prevent lymphocytes from infiltrating the human tumor cells, but systemically administered drug can still penetrate into the growing tumor mass. An additional advantage of this system is that more than one xenograft cell line can be implanted into a single animal. Recent data also suggest that neovascularization can arise from extended incubation of subcutaneously implanted tumor cell lines growing in hollow fibers (62).

Thus, this model may also prove useful in screening for antiangiogenic agents.

In Vivo Studies — Preclinical Pharmacokinetic and Pharmacodynamic Testing

A well-designed drug development program should fully integrate pharmacokinetic and pharmacodynamic studies early in the preclinical testing process. Preclinical animal studies provide the first opportunity to perform detailed single-dose and multiple-dose toxicology and toxicokinetic studies. Although the development plan has to be flexible and tailored for each individual agent, some broad general guidelines can be formulated for preclinical pharmacokinetic studies. The first step requires the development of a sensitive and reliable analytical assay for the test compound and any associated metabolites. The assay must be able to detect drug concentrations in the relatively small blood volumes obtained from animals such as rodents. Currently, the most commonly employed analytical methods utilize the liquid chromatography and mass spectrometry (LC/MS)-based techniques described in Chapter 12. These LC/MS technologies have largely supplanted standard high-performance liquid chromatography (HPLC) methods because of their greater specificity and sensitivity.

After an appropriate assay is developed, formal pharmacokinetic studies can be designed in the animal species of interest. In oncology, species selection should be based on the types of preclinical models employed for efficacy and toxicity testing. As previously discussed, antitumor efficacy and proof-of-principle studies are typically conducted in rodents, while toxicity studies are generally tested in two different animal species, such as rodents and dogs. Ideally, the same formulation of drug planned for clinical use should be tested in these preclinical models. Defining the pharmacokinetics of a new agent in the same animal species used for efficacy and toxicity testing allows for the collection of pharmacodynamic data relating drug exposure to drug effects. Assessment of pharmacodynamic drug effects in animal target tissues is often of great importance because similar measurements in specific target organs or in actual tumors are difficult to perform in humans. This information can be extremely valuable for the design of first-in-human studies of these agents.

In Vivo Studies — Preclinical Toxicology

Before any agent can enter into first-in-human studies, a battery of preclinical toxicological studies are required. The major goals of these preclinical toxicology assessments are to determine a safe starting dose for Phase I studies and to assess the drug's toxicity profile after both acute and chronic administration. Historically, anticancer chemotherapeutic agents have included some of the most toxic pharmacologic agents used in clinical medicine. In the 1970s, the NCI performed its preclinical toxicology studies in dogs and monkeys. Starting doses for clinical studies were calculated as one-third the lowest toxic dose for the most sensitive animal species, either monkey or dog (63). In 1979, FDA guidelines recommended that one-tenth the dose that causes lethality in 10% of the treated mice (LD_{10}) could be selected as the starting dose for clinical trials. The NCI adopted this policy, but also added additional toxicology studies in dogs to its routine preclinical testing guidelines (63). Currently, most agents in clinical development undergo single-dose and multidose toxicity testing in at least two mammalian species, one of which must be a nonrodent. At the NCI, these studies are typically conducted in mice and beagle dogs (64).

In 1980, the NCI Division of Cancer Treatment adopted the following general guidelines for preclinical toxicology studies of anticancer agents (64): murine single-dose and multidose (daily $\times$ 5) studies are performed to determine the doses that result in 10, 50, and 90% lethality (LD_{10}, LD_{50}, and LD_{90}, respectively). The mouse equivalent LD_{10} ($MELD_{10}$), in mg/m^2, is converted to the $MELD_{10}$ dose for dogs using the following formula for scaling from species to species:

$$\text{MELD}_{10}\ (\text{mg/m}^2) \text{ in dogs} = (\text{Km dog/Km mouse}) \times \text{MELD}_{10}\ (\text{mg/m}^2) \text{ in mice}$$

where Km (species) is the surface-to-weight ratio for each species (65). The Km values are 3 for mice, 6 for rats, and 20 for dogs, whereas corresponding values for humans are 25 for children and 37 for adults (65). One-tenth of the calculated $MELD_{10}$ in dogs is then administered to beagle dogs and, if no toxicity is seen, the dose is escalated until minimal reversible toxicity is observed. This dose, defined as the toxic dose low (TDL), is the lowest dose that produces drug-induced pathologic changes in either hematological, chemical, clinical, or morphological parameters in the test animals. In addition, double the TDL must not produce any lethality in the test species. The human equivalent of one-third the TDL in dogs is then recommended as the starting Phase I dose in humans (64). Further details regarding allometry and animal scale-up issues are discussed in Chapter 30.

In 1980, the European Organization for Research and Treatment of Cancer (EORTC) adopted more

streamlined guidelines for assessing preclinical toxicology in animals (66). Use of rodent-only toxicology was instituted with full histopathological studies conducted only in mice and more limited studies performed in rats. One-tenth the mouse LD_{10} was used as the clinical Phase I starting dose. A review of the EORTC use of these guidelines in the testing of over 50 different new agents in human clinical studies found no ethical or safety problems, leading to the conclusion that preclinical rodent-only toxicology allowed for a considerable savings in cost and time (66).

In the United States, the FDA has issued guidelines that make specific recommendations for the nonclinical pharmacology and toxicology sections of an Investigational New Drug application (IND). These guidelines are available on the FDA web site (http://www.fda.gov/cder/PharmTox/guidances.htm).

DRUG DEVELOPMENT PROGRAMS AT THE NCI

History

Systematic drug screening began at the NCI in 1955 with the establishment of the Cancer Chemotherapy National Service Center (NSC) screening program (67). Even today, all screened compounds are given an NSC number to aid in their identification. However, until the 1980s, most screening was performed *in vivo* using murine P388 or L1210 leukemia cell lines (68). These hematological murine tumors were employed because they were generally inexpensive, stable, reproducible, and easily handled. However, these *in vivo* screening efforts also had substantial limitations. Screening with rapidly growing leukemic cells was biased toward identifying compounds with activity against rapidly growing tumors with high growth fractions. The relative lack of success during this period in identifying agents with activity against common human solid tumors was thought to be due, at least in part, to the lack of more appropriate screening models.

Because of these limitations, the NCI in 1989 changed to a rationally designed "disease-oriented" screening panel incorporating 60 cell lines derived from a variety of different human solid tumors (69). Currently, this cell line screen is a key component of the NCI's comprehensive *in vitro* and *in vivo* preclinical screening and drug development program.

The 3-Cell-Line Prescreen and 60-Cell-Line Screen

Because over 85% of the compounds submitted for screening are found to have no antiproliferative activity, the NCI adopted a 3-cell-line prescreen in 1999. All compounds submitted to the NCI are now prescreened *in vitro* against a panel of three highly sensitive human tumor lines that include the MCF-7 breast, NCI-H640 lung, and the SF-268 glioma cell lines. Demonstration of growth inhibitory activity is required in this prescreen panel before a compound can proceed to advanced testing in the full 60-cell-line screen.

Originally, the NCI 60-cell-line screening panel was composed of lines derived from seven different human histological tumor types, including brain, colon, leukemia, lung, melanoma, ovarian, and renal cancers (69). Later, breast and prostate cancer cell lines were also added (70). An automated sulforhodamine blue cytotoxicity assay is used to assess the relative potency of a compound against all 60 cell lines using five different drug concentrations incubated for a standard 48 hours. Endpoint parameters that are calculated for each individual cell line include the GI_{50}, which is defined as the drug concentration that inhibits growth by 50%; the TGI, which is the lowest drug concentration that totally inhibits cell growth; and the LC_{50}, which is the lowest concentration that kills 50% of cells.

These data are then analyzed by the COMPARE algorithm, which is a software program that categorizes and compares different groups of agents based on their patterns of cytotoxic activity in the 60-cell-line screen (Figure 29.1) (71). This powerful program can identify similar classes of anticancer agents, such as platinum analogs, microtubule agents, or topoisomerase I inhibitors, based purely on their cytotoxicity patterns (72). Thus, hypotheses can be generated about the potential mechanisms of action of completely new anticancer agents using data generated in the 60-cell-line screening panel. New and exciting agents with a novel mechanism of action may he identified by the screen if they demonstrate a unique pattern of antitumor activity. Thus, the COMPARE program has converted a relatively simple test of growth inhibition into a sensitive probe for studying drug pharmacology.

Recent efforts have made the 60-cell-line screen an even more powerful tool for analyzing drug effects at the molecular level. This new approach involves the characterization of the relative expression of specific molecular targets important for drug sensitivity in each of the cell lines contained in the 60-cell-line screen (Figure 29.2). For example, this diverse group of targets can include oncogenic proteins such as RAS, N-myc, p53, RB protein, or key metabolic enzymes, such as thymidylate synthase, dihydrofolate reductase, or topoisomerases I and II. Relative expression of drug-resistance proteins, such as P-glycoprotein or MRP, is another example. Characterization of these

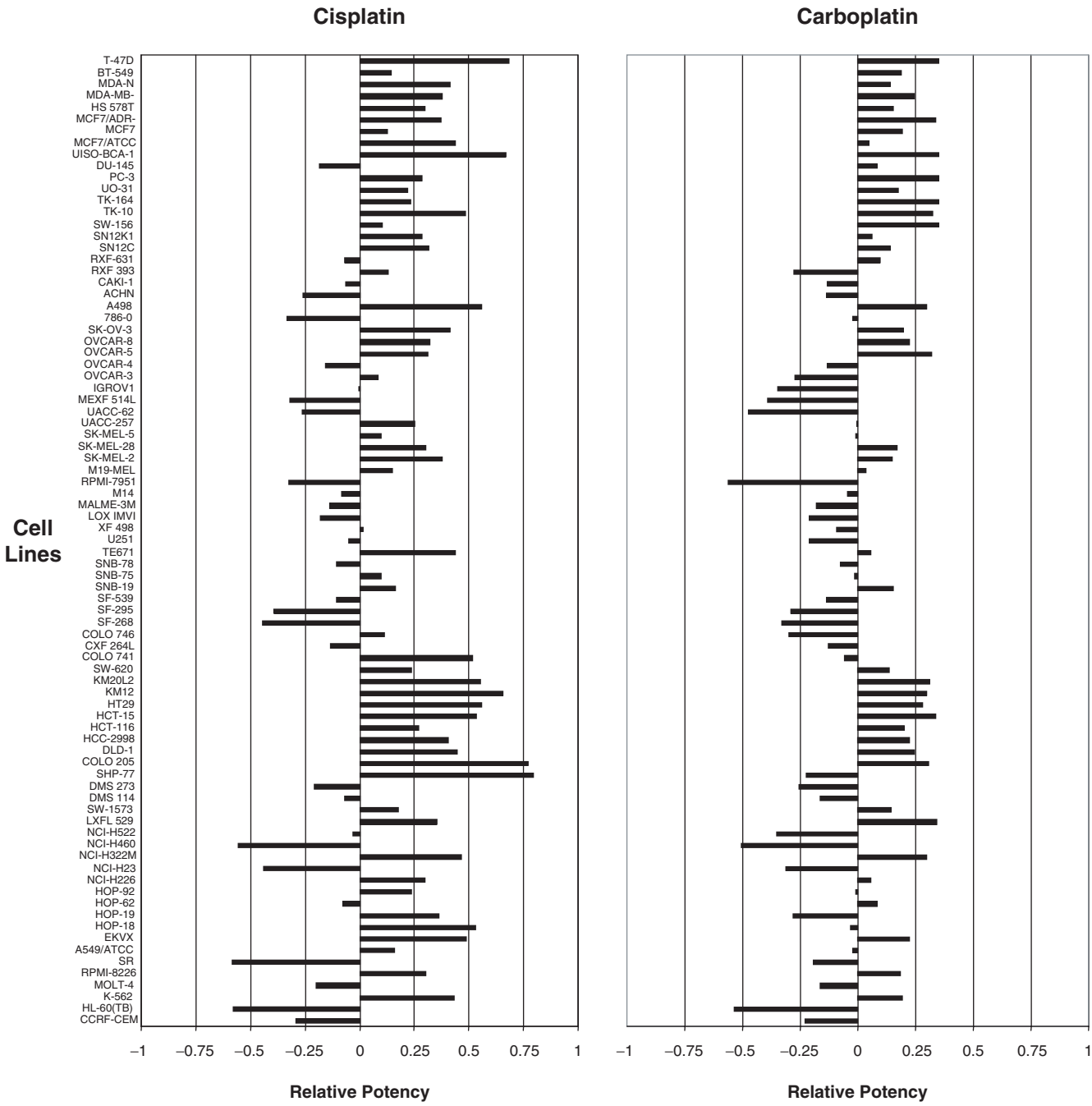

FIGURE 29.1 COMPARE program algorithm output. Plots of the growth inhibitory potency (mean relative sensitivity of various cell lines used in the NCI drug screening panel) for cisplatin and carboplatin. The zero value represents the mean concentration required to inhibit 50% growth for all of the cell lines (GI_{50}). The horizontal bars represent the relative difference in the GI_{50} value for a particular cell line from the mean value, using a logarithmic scale. Cell lines with a bar extending to the right of zero have a GI50 greater than the mean and are more resistant, while those that extend to the left have a GI_{50} lower than the mean and are more sensitive. The patterns of growth inhibitory potency are very similar for these two platinum analogs. (Data obtained from the NCI web site at http://dtp.nci.nih.gov.)

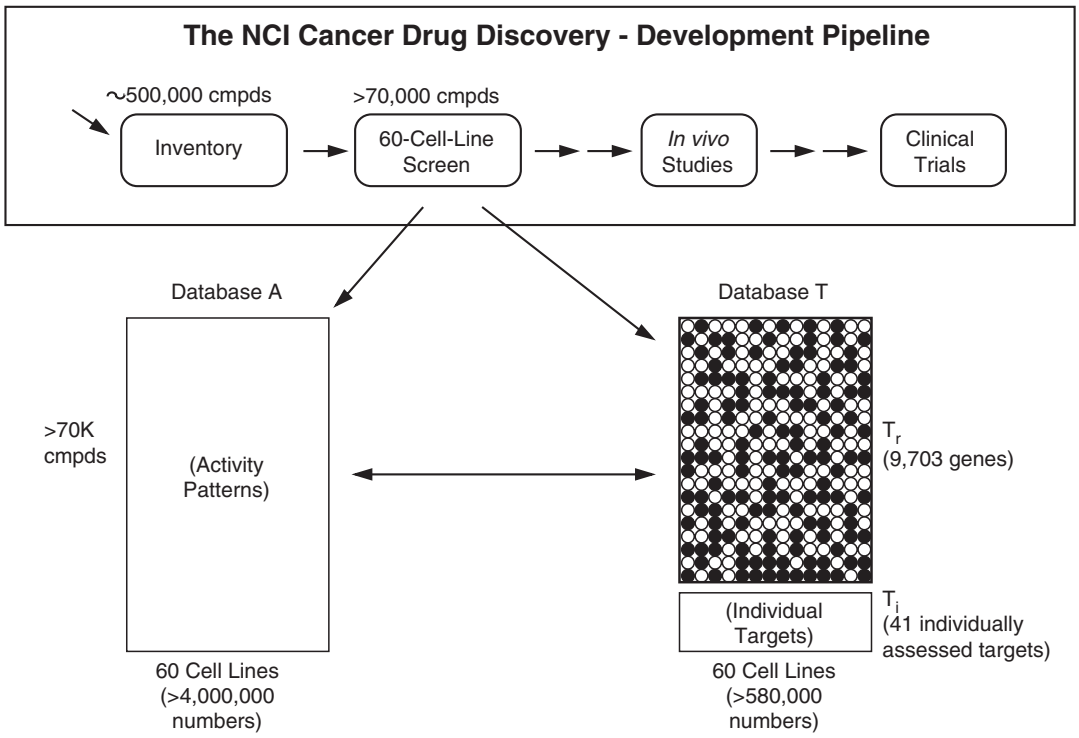

FIGURE 29.2 Molecular target expression in the NCI screening program. A schematic representation of the database generation or molecular target gene expression in the NCI drug discovery–development program. Each row of the activity database (Database A) represents the pattern of cytotoxic activity of a specific compound across the 60 cell lines, and each column represents the pattern of sensitivities of a particular cell line to the compounds tested. The gene expression database (T_r) contains fluorescence hybridization ratio values from two-color cDNA microarray measurements on the 60 cell lines. Microarray experimental data provide information on the relative expression of literally thousands of different potentially important molecular targets that may be related to drug efficacy. Also added to the target database is the relative expression of 40 additional individually measured molecular targets (T_i) that is the product of many experiments in different laboratories, as compiled at the NCI's DTP Internet site located at http://dtp.nci.nih.gov. The sum of T_r and T_i constitute an overall database (Database T) of molecular targets. Analysis of the relationships between Database A (cytotoxic activity) and Database T (relative molecular target expression) can potentially identify novel and new agents being screened that have cytotoxic activity against defined patterns of gene expression common to various types of human tumors. (Reproduced with permission from Scherf U *et al*. Nat Genet 2000;24:236–44. Additional information may be found on the Internet at http://discover.nci.nih.gov.)

molecular targets in each of the 60 cell lines allows for the screening data to be analyzed from an entirely new perspective. The relative pattern of drug sensitivity in each cell line can now be correlated with the relative expression of hundreds or more of different specific molecular targets (Figure 29.2). This generates a much more data-rich screening tool for analyzing new compounds. Because of the complexity and wealth of information generated, it also creates a major bioinformatics challenge. However, pioneering work by Weinstein *et al*. (73) in analyzing this type of data-rich information has enabled correlations to be made between patterns of drug sensitivity in the cell lines and the relative expression of these molecular targets.

This is an extremely powerful approach for identifying novel new anticancer agents based on their activity in cell lines expressing different molecular targets relevant to drug action. In addition, it is rapidly becoming possible to characterize the relative expression of thousands of different specific molecular targets at the mRNA level in the 60 cell lines using cDNA microarray chip technology (74). This flood of additional information will further increase the power of this approach.

Although the utility of this method of anticancer drug screening and discovery must still be proved, its potential is great. Conceptually, it is important because it extends the "disease-oriented" approach, originally envisioned when the 60-cell-line screen was created, to

a more comprehensive drug discovery approach that is based on molecular targets. Thus, the 60 cell lines no longer represent a simple collection of cell lines arising from nine different human histological tumor types; instead, they have been transformed into a panel of thousands of different molecular targets, each of which is expressed at 60 different levels. Each individual target can then be individually correlated with drug sensitivity for any new or novel anticancer agent that is screened (75). This correlation has enormous potential for identifying new molecular target-based agents for further clinical development.

NCI Drug Development Process

The NCI's drug discovery and development efforts are overseen by the Developmental Therapeutics Program (http://dtp.nci.nih.gov) (76). This program is designed to facilitate and guide the development of novel therapeutic agents for the treatment of cancer and AIDS. Through its various programs and branches, an impressive range of resources is made available to the pharmaceutical, biotechnology, and academic communities. More than 70,000 compounds have been screened since the system was established in 1990. The process begins when a compound or agent submitted to the NCI undergoes preliminary *in vitro* screening. Based on results of the 3-cell-line screen and 60-cell-line screen for particular compounds some are then selected for further *in vivo* testing in animals based upon a variety of factors, including overall potency, novel patterns of antitumor activity, unique chemical structure, or novel potential mechanism of action. Animal studies are initially conducted at the NCI with 12 different human cell lines using the previously described hollow fiber assay. The initial *in vivo* data are used to select promising compounds for more extensive human xenograft studies. At the NCI, human xenografts are implanted subcutaneously and the drugs are administered intraperitoneally. A relative difference in the tumor weight ratio of treated to control animals of less than 0.5 is considered promising for further development.

Highly promising agents emerging from the *in vivo* screen can be selected for further preclinical studies. These include studies designed to determine an acceptable clinical formulation and select the optimal dose, route, and schedule of administration. Procurement of sufficient drug for further preclinical and clinical studies is planned, and drug assay development for pharmacokinetic studies is also initiated. If no additional problems arise and the compound remains promising, then the agent may be selected for continued preclinical development. This requires a major commitment of research resources, including cGMP drug manufacturing contracts, current Good Laboratory Practice (cGLP) preclinical toxicology studies in two different species with histopathological correlation, and animal pharmacokinetic and toxicokinetic studies. In fact, toxicology, manufacturing, and formulation frequently represent the most costly steps in preclinical drug development. Only if a compound successfully navigates these final stages of preclinical development is a commitment made to initiate Phase I clinical trials, and an NCI-sponsored IND application is filed with the FDA. A substantial commitment is also made by the NCI to conduct an appropriate Phase I and Phase II clinical research program. Guidelines have been established for structuring partnership agreements between the NCI and drug sponsors in industry or academia in such a way that the sponsor's intellectual property rights are protected (77). Further information about this program is available at http://dtp.nci.nih.gov.

Clearly, the NCI efforts in anticancer drug development are extensive and will continue to grow and change as the science of drug discovery and development evolves. The tremendous advances now occurring in our understanding of the molecular basis of human cancer and the identification of new molecular targets for developmental therapeutics ensure that this will continue to be an active and exciting program in the future.

THE CHALLENGE — MOLECULARLY TARGETED THERAPIES AND NEW PARADIGMS FOR CLINICAL TRIALS

Clinical pharmacologists involved in preclinical and early clinical drug development face a number of new challenges in the current era. The greatest of these is to develop new molecularly targeted therapies as expeditiously as possible. In cancer therapeutics, all new compounds in the developmental pipeline have well-defined molecular mechanisms of action that are extensively studied in preclinical models. In the ideal clinical program, these molecular mechanisms would be analyzed further in Phase I and Phase II clinical trials. However, these trials are technically difficult to perform because they require sampling of tumor or normal tissues in patients undergoing experimental therapy. Nonetheless, this approach is particularly relevant for anticancer agents because only a small percentage of experimental compounds entering into clinical testing are successfully approved as clinically useful therapies (78).

As scientists devoted to the study of developmental therapeutics in humans, clinical pharmacologists are in an ideal position to span the interface between preclinical and clinical drug development studies. The preclinical experiments described in this chapter provide a wealth of information regarding a new agent's toxicology, determinants of response, and mechanisms of drug action. Furthermore, developing new technologies and model systems will allow us to better charactreize drug absorption, metabolism, and drug safety and efficacy before initiating Phase I trials. Although optimally using this preclinical information to rationally design early clinical trials remains a daunting challenge, successfully meeting this challenge offers the best opportunity for improving our therapeutic options for treating human disease.

REFERENCES

1. Teicher BA. Molecular cancer therapeutics: Will the promise be fulfilled? In: Prendergast GC, editor. Molecular cancer therapeutics: Strategies for drug discovery and development. Hoboken, NJ: John Wiley & Sons, Inc.; 2004. p. 8–40.
2. Feldman RI, Wu JM, Polokoff MA *et al*. Novel small molecule inhibitors of 3-phosphoinositide-dependent kinase-1. J Biol Chem 2005;280:19867–74.
3. Geney R, Sun L, Pera P *et al*. Use of the tubulin bound paclitaxel conformation for structure-based rational drug design. Chem Biol 2005;12:339–48.
4. Glen RC, Allen SC. Ligand-protein docking: Cancer research at the interface between biology and chemistry. Curr Med Chem 2003;10:763–7.
5. Gottschalk KE, Kessler H. The structures of integrins and integrin–ligand complexes: Implications for drug design and signal transduction. Angew Chem Int Ed Engl 2002;41:3767–74.
6. Seddon BM, Workman P. The role of functional and molecular imaging in cancer drug discovery and development. Br J Radiol 2003;76 Spec No 2:S128–38.
7. Hartwell LH, Szankasi P, Roberts CJ, Murray AW, Friend SH. Integrating genetic approaches into the discovery of anticancer drugs. Science 1997;278:1064–8.
8. Monks A, Scudiero D, Skehan P *et al*. Feasibility of a high-flux anticancer drug screen using a diverse panel of cultured human tumor cell lines. J Natl Cancer Inst 1991;83:757–66.
9. Jansen WJ, Hulscher TM, van Ark-Otte J, Giaccone G, Pinedo HM, Boven E. CPT-11 sensitivity in relation to the expression of P170-glycoprotein and multidrug resistance-associated protein. Br J Cancer 1998; 77:359–65.
10. Wilson G. Cell culture techniques for the study of drug transport. Eur J Drug Metab Pharmacokinet 1990;15:159–63.
11. Iwatsubo T, Hirota N, Ooie T *et al*. Prediction of *in vivo* drug metabolism in the human liver from *in vitro* metabolism data. Pharmacol Ther 1997;73:147–71.
12. Thummel KE, Wilkinson GR. *In vitro* and *in vivo* drug interactions involving human CYP3A. Annu Rev Pharmacol Toxicol 1998;38:389–430.
13. Rowinsky EK, Donehower RC. Paclitaxel (taxol). N Engl J Med 1995;332:1004–14.
14. Wani MC, Taylor HL, Wall ME, Coggon P, McPhail AT. Plant antitumor agents. VI. The isolation and structure of taxol, a novel antileukemic and antitumor agent from *Taxus brevifolia*. J Am Chem Soc 1971;93:2325–7.
15. Rao KV, Hanuman JB, Alvarez C *et a.l.* A new large-scale process for taxol and related taxanes from *Taxus brevifolia*. Pharm Res 1995;12:1003–10.
16. Witherup KM, Look SA, Stasko MW, Ghiorzi TJ, Muschik GM, Cragg GM. *Taxus* spp. needles contain amounts of taxol comparable to the bark of *Taxus brevifolia*: Analysis and isolation. J Nat Prod 1990;53:1249–55.
17. Liebmann J, Cook JA, Mitchell JB. Cremophor EL, solvent for paclitaxel, and toxicity. Lancet 1993;342:1428.
18. Lorenz W, Schmal A, Schult H *et al*. Histamine release and hypotensive reactions in dogs by solubilizing agents and fatty acids: Analysis of various components in Cremophor EL and development of a compound with reduced toxicity. Agents Actions 1982;12:64–80.
19. Theis JG, Liau-Chu M, Chan HS, Doyle J, Greenberg ML, Koren G. Anaphylactoid reactions in children receiving high-dose intravenous cyclosporine for reversal of tumor resistance: The causative role of improper dissolution of Cremophor EL. J Clin Oncol 1995;13:2508–16.
20. Dahut W, Harold N, Takimoto C *et al*. Phase I and pharmacologic study of 9-aminocamptothecin given by 72-hour infusion in adult cancer patients. J Clin Oncol 1996;14:1236–44.
21. Rubin E, Wood V, Bharti A *et al*. A Phase I and pharmacokinetic study of a new camptothecin derivative, 9-aminocamptothecin. Clin Cancer Res 1995;1:269–76.
22. Khleif SN, Curt GA. Animal models in drug development. In: Holland JF, Bast BR, Morton DL, Frei E III, Kufe DW, Weischelbaum RR, editors. Cancer medicine. Baltimore, MD: Williams & Wilkins; p. 855–68.
23. Tsotetsi OJ, Woodiwiss AJ, Netjhardt M, Qubu D, Brooksbank R, Norton GR. Attenuation of cardiac failure, dilatation, damage, and detrimental interstitial remodeling without regression of hypertrophy in hypertensive rats. Hypertension 2001;38:846–51.
24. Bing OH, Conrad CH, Boluyt MO, Robinson KG, Brooks WW. Studies of prevention, treatment and mechanisms of heart failure in the aging spontaneously hypertensive rat. Heart Fail Rev 2002;7:71–88.
25. Kasiske BL, O'Donnell MP, Keane WF. The Zucker rat model of obesity, insulin resistance, hyperlipidemia, and renal injury. Hypertension 1992;19(1 suppl): I110–5.
26. Van Zwieten PA, Kam KL, Pijl AJ, Hendriks MG, Beenen OH, Pfaffendorf M. Hypertensive diabetic rats in pharmacological studies. Pharmacol Res 1996; 33:95–105.
27. Thompson MB. The Min mouse: A genetic model for intestinal carcinogenesis. Toxicol Pathol 1997; 25:329–32.

28. Rosenberg MP, Bortner D. Why transgenic and knockout animal models should be used (for drug efficacy studies in cancer). Cancer Metastasis Rev 1998; 17:295–9.
29. Thomas H, Balkwill F. Assessing new anti-tumour agents and strategies in oncogene transgenic mice. Cancer Metastasis Rev 1995;14:91–5.
30. Jaenisch R. Retroviruses and embryogenesis: Microinjection of Moloney leukemia virus into midgestation mouse embryos. Cell 1980;19:181–8.
31. Hooper M, Hardy K, Handyside A, Hunter S, Monk M. HPRT-deficient (Lesch–Nyhan) mouse embryos derived from germline colonization by cultured cells. Nature 1987;326:292–5.
32. Dexter DL, Diamond M, Creveling J, Chen SF. Chemotherapy of mammary carcinomas arising in ras transgenic mice. Invest New Drugs 1993;11:161–8.
33. Sheppard RD, Samant SA, Rosenberg M, Silver LM, Cole MD. Transgenic N-*myc* mouse model for indolent B cell lymphoma: Tumor characterization and analysis of genetic alterations in spontaneous and retrovirally accelerated tumors. Oncogene 1998;17:2073–85.
34. Mangues R, Corral T, Kohl NE *et al*. Antitumor effect of a farnesyl protein transferase inhibitor in mammary and lymphoid tumors overexpressing N-*ras* in transgenic mice. Cancer Res 1998;58:1253–9.
35. Schmidt EV, Pattengale PK, Weir L, Leder P. Transgenic mice bearing the human *c-myc* gene activated by an immunoglobulin enhancer: A pre-B-cell lymphoma model. Proc Natl Acad Sci USA 1988;85:6047–51.
36. Weaver ZA, McCormack SJ, Liyanage M *et al*. A recurring pattern of chromosomal aberrations in mammary gland tumors of MMTV–*c-myc* transgenic mice. Genes Chromosomes Cancer 1999;25:251–60.
37. Dell'Acqua G, Polishchuck R, Fallon JT, Gordon JW. Cardiac resistance to adriamycin in transgenic mice expressing a rat alpha-cardiac myosin heavy chain/human multiple drug resistance 1 fusion gene. Hum Gene Ther 1999;10:1269–79.
38. Majzoub JA, Muglia LJ. Knockout mice. N Engl J Med 1996;334:904–7.
39. Donehower LA. The *p53*-deficient mouse: A model for basic and applied cancer studies. Semin Cancer Biol 1996;7:269–78.
40. Rockwell S. *In vivo–in vitro* tumour cell lines: Characteristics and limitations as models for human cancer. Br J Cancer 1980;41(suppl 4):118–22.
41. Rygaard J, Povlsen CO. Heterotransplantation of a human malignant tumour to "Nude" mice. Acta Pathol Microbiol Scand 1969;77:758–60.
42. Flanagan SP. 'Nude,' a new hairless gene with pleiotropic effects in the mouse. Genet Res 1966; 8:295–309.
43. Gazdar AF, Carney DN, Sims HL, Simmons A. Heterotransplantation of small-cell carcinoma of the lung into nude mice: Comparison of intracranial and subcutaneous routes. Int J Cancer 1981;28:777–83.
44. Houghton JA, Taylor DM. Maintenance of biological and biochemical characteristics of human colorectal tumours during serial passage in immune-deprived mice. Br J Cancer 1978;37:199–212.
45. Neely JE, Ballard ET, Britt AL, Workman L. Characteristics of 85 pediatric tumors heterotransplanted into nude mice. Exp Cell Biol 1983;51:217–27.
46. Giovanella BC, Stehlin JS Jr., Shepard RC, Williams LJ Jr. Correlation between response to chemotherapy of human tumors in patients and in nude mice. Cancer 1983;52:1146–52.
47. Nowak K, Peckham MJ, Steel GG. Variation in response of xenografts of colo-rectal carcinoma to chemotherapy. Br J Cancer 1978;37:576–84.
48. Liu M, Bishop WR, Wang Y, Kirschmeier P. Transgeneic versus xenograft mouse models of cancer: Utility and issues. In: Prendergast GC, editor. Molecular cancer therapeutics: Strategies for drug discovery and development. Hoboken, NJ: John Wiley & Sons, Inc.; 2004. p. 204–26.
49. Uckun FM. Severe combined immunodeficient mouse models of human leukemia. Blood 1996;88:1135–46.
50. Bogden AE, Cobb WR, Lepage DJ *et al*. Chemotherapy responsiveness of human tumors as first transplant generation xenografts in the normal mouse: Six-day subrenal capsule assay. Cancer 1981;48:10–20.
51. Aamdal S, Fodstad O, Nesland JM, Pihl A. Characteristics of human tumour xenografts transplanted under the renal capsule of immunocompetent mice. Br J Cancer 1985;51:347–56.
52. Aamdal S, Fodstad O, Pihl A. Human tumor xenografts transplanted under the renal capsule of conventional mice. Growth rates and host immune response. Int J Cancer 1984;34:725–30.
53. Edelstein MB, Smink T, Ruiter DJ, Visser W, van Putten LM. Improvements and limitations of the subrenal capsule assay for determining tumour sensitivity to cytostatic drugs. Eur J Cancer Clin Oncol 1984;20:1549–56.
54. Hoffman RM. Fertile seed and rich soil: The development of clinically relevant models of human cancer by surgical orthotopic implantation of intact tissue. In: Teicher BA, editor. Anticancer drug development guide: Preclinical screening, clinical trials and approval. Totowa, NJ: Humana Press; 1997. p. 127–44.
55. Paget S. The distribution of secondary growth in cancer of the breast. Lancet 1889;1:571.
56. Fidler IJ. Rationale and methods for the use of nude mice to study the biology and therapy of human cancer metastasis. Cancer Metastasis Rev 1986;5:29–49.
57. Shapiro WR, Basler GA, Chernik NL, Posner JB. Human brain tumor transplantation into nude mice. J Natl Cancer Inst 1979;62:447–53.
58. Gura T. Systems for identifying new drugs are often faulty. Science 1997;278:1041–2.
59. Steel GG, Courtenay VD, Peckham MJ. The response to chemotherapy of a variety of human tumour xenografts. Br J Cancer 1983;47:1–13.
60. Hollingshead MG, Alley MC, Camalier RF *et al*. *In vivo* cultivation of tumor cells in hollow fibers. Life Sci 1995;57:131–41.
61. Plowman J, Dykes JJ, Hollingshead MG, Simpson-Herren L, Alley MC. Human tumor xenograft models in NCI drug development. In: Teicher BA, editor. Anticancer drug development guide: Preclinical screening, clinical trials and approval. Totowa, NJ: Humana Press; 1997. p. 101–25.
62. Phillips RM, Pearce J, Loadman PM *et al*. Angiogenesis in the hollow fiber tumor model influences drug delivery to tumor cells: Implications for anticancer drug screening programs. Cancer Res 1998;58:5263–6.

63. Grieshaber CK, Marsoni S. Relation of preclinical toxicology to findings in early clinical trials. Cancer Treat Rep 1986;70:65–72.
64. Toppmeyer DL. Phase I trial design and methodology. In: Teicher BA, editor. Anticancer drug development guide: Preclinical screening, clinical trials and approval. Totowa, NJ: Humana Press; 1997. p. 227–47.
65. Freireich EJ, Gehan EA, Rall DP, Schmidt LH, Skipper HE. Quantitative comparison of toxicity of anticancer agents in mouse, rat, hamster, dog, monkey, and man. Cancer Chemother Rep 1966;50:219–44.
66. Connors TA, Pinedo HM. Drug development in Europe. In: Teicher BA, editor. Anticancer drug development guide: Preclinical screening, clinical trials and approval. Totowa, NJ: Humana Press; 1997. p. 271–88.
67. Zubrod CG. The national program for cancer chemotherapy. JAMA 1972;222:1161–2.
68. Waud WR. Murine L1210 and P388 leukemia. In: Teicher BA, editor. Anticancer drug development guide: Preclinical screening, clinical trials and approval. Totowa, NJ: Humana Press; 1997. p. 59–74.
69. Boyd MR. The NCI *in vitro* anticancer drug discovery screen: Concept, implementation, and operation, 1985–1995. In: Teicher BA, editor. Anticancer drug development guide: Preclinical screening, clinical trials and approval. Totowa, NJ: Humana Press; 1997. p. 23–42.
70. Holbeck SL. Update on NCI *in vitro* drug screen utilities. Eur J Cancer 2004;40:785–93.
71. Paull KD, Shoemaker RH, Hodes L *et al*. Display and analysis of patterns of differential activity of drugs against human tumor cell lines: Development of mean graph and COMPARE algorithm. J Natl Cancer Inst 1989;81:1088–92.
72. Rixe O, Ortuzar W, Alvarez M *et al*. Oxaliplatin, tetraplatin, cisplatin, and carboplatin: Spectrum of activity in drug-resistant cell lines and in the cell lines of the National Cancer Institute's Anticancer Drug Screen panel. Biochem Pharmacol 1996;52:1855–65.
73. Weinstein JN, Myers TG, O'Connor PM *et al*. An information-intensive approach to the molecular pharmacology of cancer. Science 1997;275:343–9.
74. Scherf U, Ross DT, Waltham M *et al*. A gene expression database for the molecular pharmacology of cancer. Nat Genet 2000;24:236–44.
75. Shi LM, Myers TG, Fan Y *et al.* Mining the National Cancer Institute Anticancer Drug Discovery Database: Cluster analysis of ellipticine analogs with p53-inverse and central nervous system-selective patterns of activity. Mol Pharmacol 1998;53: 241–51.
76. Takimoto CH. Anticancer drug development at the US National Cancer Institute. Cancer Chemother Pharmacol 2003;52(suppl 1):S29–33.
77. Sausville EA. Working with the National Cancer Institute. In: Teicher BA, editor. Anticancer drug development guide: Preclinical screening, clinical trials and approval. Totowa, NJ: Humana Press; 1997. p. 217–26.
78. Kelloff GJ, Sigman CC. New science-based endpoints to accelerate oncology drug development. Eur J Cancer 2005;41:491–501.

CHAPTER

30

Animal Scale-Up

ROBERT L. DEDRICK* **AND ARTHUR J. ATKINSON, JR.†**

*Office of Research Services, National Institutes of Health, Bethesda, Maryland,

†Clinical Center, National Institutes of Health, Bethesda, Maryland

INTRODUCTION

The title of this chapter, derived from a talk presented to a chemical engineering audience, was meant as a play on words by analogy to the design and scale-up of chemical plants. The title of the field has stuck, but the play has been lost. To most of those interested in clinical pharmacology, "plant scale-up" probably conveys quite a different idea. The science and technology of chemical engineering have proved to be a powerful methodology for addressing a variety of problems in pharmacokinetics, such as extrapolation from one biological system to another. The experimental systems include *in vitro* cultures and isolated organ perfusions as well as animals.

Despite the influence of allometry on the development of biology and an underlying belief that experimental systems provide useful information about humans, disproportionate emphasis has been placed on species differences. This would appear to derive from the culture of biology, because differences among species have often been more interesting than similarities and because these differences can provide important information on the development of species. We recognize that no other animal is the same as a human in any general biological sense and that insistence on "sameness" in a model system is illusory. It is proposed here that we adopt more of an engineering-design view when we develop experimental systems in pharmacokinetics and attempt to use data from these systems for predictive purposes. If we do this, it is axiomatic in biology, as in engineering, that the model system is *never* the same as the prototype. Interpretation is always required. In some simple systems, concepts of similitude place design on a sound theoretical basis. But in more complex situations, rigorous similitude may not be attainable. In these cases, it is often possible to model parts of a complex system and use model-dependent information in a design process that incorporates sound theoretical principles but often contains judgment and experience as well. The approach is illustrated by a discussion of the extrapolation of data from one biological system to another.

This chapter contains a brief discussion of allometry, physiological pharmacokinetics, and the use of *in vitro* systems to predict drug metabolism in experimental animals and human study participants.

ALLOMETRY

Adolph (1) observed that many physiological processes and organ sizes show a relatively simple power-law relationship with body weight when these are compared among mammals. The allometric equation proposed by Adolph is

$$P = a(BW)^m \tag{30.1}$$

where P = physiological property or anatomic size, a = empirical coefficient, BW = body weight, m = allometric exponent.

Note that a is not dimensionless; its value depends on the units in which P and BW are measured, while the exponent, m, is independent of the system of units.

TABLE 30.1 Representative Allometric Coefficients and Exponents[a]

Process/organ	Coefficient	Exponent
Metabolic functions (mL/hr)		
Inulin clearance	1.74	0.77
Creatinine clearance	4.2	0.69
Hippurate clearance	5.4	0.80
Liver slice O_2 consumption[b]	3.3	0.77
Organ weights (g)		
Kidney	0.0212	0.85
Liver	0.082	0.87
Heart	0.0066	0.98
Blood	0.055	0.99
Brain	0.081	0.70

[a] Insert body weight in Equation 30.1 in grams. (Data from Adolph EF. Science 1949;109:579–85.)
[b] Measured at standard temperature and pressure.

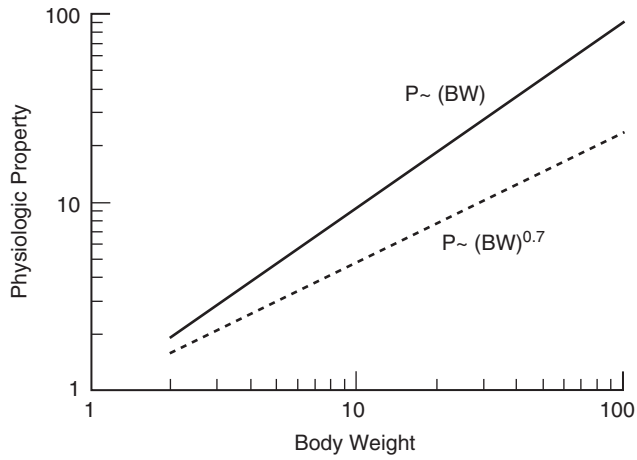

FIGURE 30.1 Illustrative allometric chart. The physiologic property and body weight are in arbitrary dimensionless units.

Note further that if $m = 1$, then P is proportional to BW. If $m < 1, P$ increases less rapidly than does BW. If $m > 1$, P increases more rapidly than does BW. Adolph listed empirical coefficients and exponents for several physiological parameters and some of these are summarized in Table 30.1.

General allometric correlations such as these can obscure some interesting and important interspecies differences. Brain size in humans and nonhuman primates, for example, is considerably larger than would be expected from other mammals. Some implications of this have been discussed with reference to regional drug delivery to the brain (2).

Dividing both sides of Equation 30.1 by BW shows that

$$P/BW = a(BW)^{m-1} \qquad (30.2)$$

Thus, if the allometric exponent is less than unity, as observed for many measures of physiologic function, the function per unit of body weight *decreases* as body weight increases.

These concepts are illustrated in Figure 30.1, which shows a plot of an illustrative physiologic property versus body weight, both in arbitrary dimensionless terms, on a log–log plot. Equation 30.1 is linearized in this form, with a slope equal to the allometric exponent, a. If the property were proportional to body weight, as is often the case for the distribution volume of a drug, increasing the body weight from 1 to 100 would result in a concomitant increase in the property. If the allometric exponent were 0.7, which is more typical of renal excretion and hepatic metabolism (Table 30.1), then increasing the body weight from 1 to 100 would result in an increase in the property from 1 to 25 and a value of the property per unit body weight only one-fourth as large.

In more concrete terms, if $m = 0.7$ for the renal clearance of a particular drug, the clearance per unit body weight in a 20-gram mouse would expected to be $[(70{,}000)/(20)]^{0.3} = 12$ times that in 70-kg human. If the volume of distribution is similar on a liter per kilogram basis between the two species (such as body water) and the drug is cleared only by the kidney, then, as a rough approximation, the elimination half-life would be 12 times longer in the human. Thus, 1 hour in a mouse would be pharmacokinetically equivalent to 12 hours in a human.

This observation led Dedrick *et al*. (3) to demonstrate that methotrexate plasma concentration vs. time data for several species were superimposable when plasma concentrations were normalized for dose/(body weight) and chronological time was converted to an "equivalent time" by dividing it by body weight raised to the 0.25 power. This was an empirically determined parameter for methotrexate. The form of the correlation should be useful for interspecies plasma concentration data for other drugs — particularly those that are not metabolized. The exponent on body weight could be determined empirically but would be expected to be similar to that for methotrexate.

If the volume of distribution of a drug is proportional to body weight and its elimination clearance is proportional to body weight to the 0.75 power, then it

follows directly that its half-time would be

$$t_{1/2} = \frac{0.693 V_d}{CL} = \frac{0.693 a BW^{1.0}}{a' BW^{0.75}} \propto BW^{0.25} \qquad (30.3)$$

This equation can easily be generalized for other exponents.

Allometric principles may be used to answer a variety of questions relevant to the application of preclinical pharmacokinetic data to the design of dose regimens for humans. Two examples are the use of data from animals to estimate the human pharmacokinetic parameters needed for selecting a starting dose for Phase I studies, and the design of intraperitoneal dose regimens for antineoplastic drugs.

Use of Allometry to Predict Human Pharmacokinetic Parameters

Allometric scaling to predict distribution volume from studies in three animal species, rat, dog, and monkey, has been found to be reasonably satisfactory, although monkey data alone provided the least biased estimates (5). As might be expected from the interspecies scalability of physiological factors related to renal function (Table 30.1), it has also been found that human clearance estimates for renally eliminated drugs were reasonably accurate, especially when a correction factor was introduced to account for species differences in renal blood flow (6). On the other hand, interspecies scaling has been problematic for drugs that are eliminated primarily by hepatic metabolism. To circumvent this difficulty, Mahmood and Balian (6) proposed three different approaches for predicting elimination clearance in humans based on the allometric exponent m that is obtained when Equation 30.1 is applied to animal data:

Method I: If the exponent lies between 0.55 and 0.7, then Equation 30.1 can be applied without correction.

Method II: If the exponent lies between 0.7 and 1.0, the allometric equation for predicting clearance is normalized according to the maximum life span potential for each animal species, as initially proposed by Boxenbaum (7).

Method III: If the exponent exceeds 1.0, the allometric equation for predicting clearance is normalized according to the brain weight of each animal species, as initially proposed by Mahmood and Balian (8).

Recently, a more comprehensive analysis of allometric scaling results for 103 drugs in three species (rats, dogs, and monkeys) indicated that Equation 30.1 yielded a predicted/observed ratio of human elimination clearances between 0.5 and 2.0 for only 55 of the compounds (9). In addition, this poor predictive performance was not improved by incorporating empirical correction factors based on maximum life span potential or brain weight. This objective analysis of a large compound dataset is particularly welcome, inasmuch as Bonate and Howard (10) have pointed out that the literature on allometric scaling has generally been biased by the preferential inclusion of studies in which application of this technique has been successful. As a result, considerable caution is warranted if only allometric scaling is relied on to guide initial dose selection in Phase I clinical trials.

Use of Allometry in Designing Intraperitoneal Dose Regimens

Intraperitoneal administration of antineoplastic drugs has been shown to increase the survival of patients with ovarian cancer that has spread to the serosal surface of the peritoneum (11), and is under active investigation in patients with peritoneal mesothelioma or gastrointestinal cancers that have metastasized to the peritoneum (12). Although first attempted 50 years ago, the resurgence of interest in intraperitoneal chemotherapy was prompted by the development of a simple compartmental model for intraperitoneal pharmacokinetics (Figure 30.2), and the rationale that this route of administration should achieve higher regional levels of peritoneal exposure to antineoplastic drugs than could be safely achieved with intravenous chemotherapy (13). As described in Chapter 9, key issues include both the kinetics of absorption of the drug from the peritoneal cavity and the depth of penetration of the drug into tumor nodules. The rate of absorption of the drug from the peritoneal cavity is equal to $PA([C_{PC} - C_{PL})$, where PA is the peritoneal permeability–surface area product, C is drug concentration, and the subscripts PC and PL refer, respectively, to peritoneal cavity and plasma.

Allometric scaling may be used to answer a variety of questions relevant to the design of preclinical studies of intraperitoneal pharmacokinetics. Figure 30.3 shows the variation of PA, which is approximately equivalent to peritoneal clearance if $C_{PC} >> C_{PL}$, for urea and inulin in rats, rabbits, dogs, and humans (14). The slope of the urea line is 0.74 while the slope of the inulin line is 0.62. The average of these is 0.68, or approximately two-thirds as might be expected for peritoneal surface area. This would imply that the intrinsic membrane permeability, P, is similar among

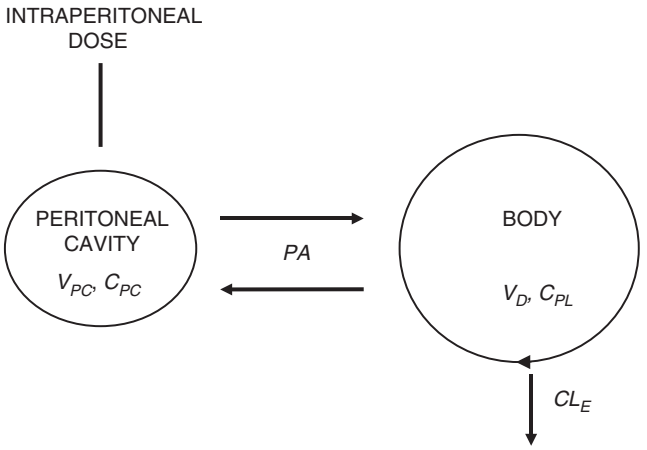

FIGURE 30.2 Two-compartment model for peritoneal pharmacokinetics. Drug administered via a catheter is placed in the peritoneal cavity with a distribution volume of V_{PC}, yielding concentrations within the peritoneum of C_{PC}. Subsequent transfer between the peritoneum and the body compartment is mediated by diffusion with a permeability coefficient–surface area product of *PA*. CL_E is the elimination clearance from the body. Plasma drug concentrations (C_{PL}) and systemic toxicity are minimized because the distribution volume of the body compartment (V_D) is much greater than V_{PC} and because CL_E prevents complete equilibration of concentrations in the two compartments. (Adapted from Dedrick RL *et al.* Cancer Treat Rep 1978;62:1–11.)

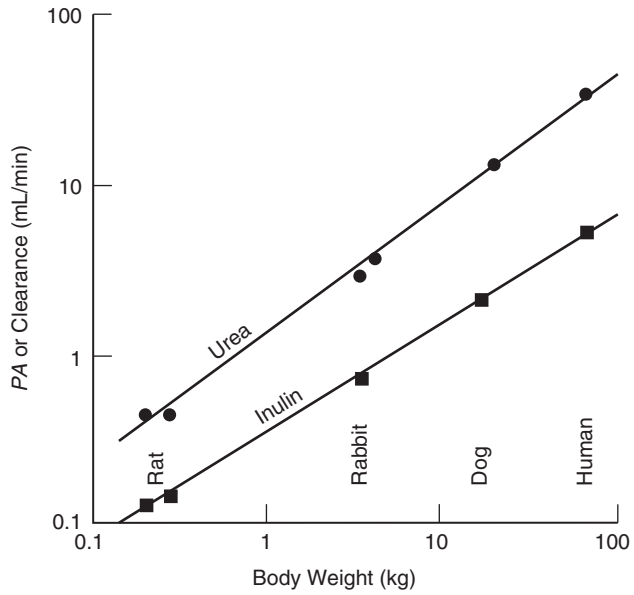

FIGURE 30.3 Peritoneal permeability–surface area product or clearance versus body weight across four species for urea (•) and inulin (■). (Reproduced from Dedrick RL *et al.* ASAIO J 1982;5:1–8.)

the species. That this is plausible is supported by a spatially distributed model devised to examine the penetration of drug into tissue (14). If the drug does not react with the tissue, then the peritoneal permeability may be shown to be $P = [D(ps)]^{1/2}$, where D is the diffusivity of the drug in the tissue, p is the capillary permeability, and s is the capillary surface area per unit volume of tissue. Perhaps surprisingly, the permeability of continuous capillaries appears to be very similar among mammals, as shown for a number of solutes in cat leg, human forearm, and dog heart (Figure 30.4). As discussed in Chapter 3, the diffusivity of uncharged low molecular weight hydrophilic compounds across capillaries approximates their diffusivity in water. These observations support the similarity of P among mammalian species.

During the design of preclinical studies of intraperitoneal drug administration, consideration must be given to the fact that *PA* is relatively larger in small laboratory animals than it is in humans. The time constant for drug absorption from the peritoneal cavity is V_{PC}/PA, where V_{PC} is the intraperitoneal volume. Since *PA* varies approximately as the 0.7 power of body weight, the pharmacokinetic time scales in the peritoneal cavity can be duplicated among species if the volume that is given to the laboratory animals also varies as the 0.7 power of body weight. Then, to simulate the time course of peritoneal drug concentration in a 70-kg human patient receiving 2 liters (29 mL/kg) of drug-containing solution, a 200-gram rat would have to be given $(200/70{,}000)^{0.7}$ (2000) = 33 mL.

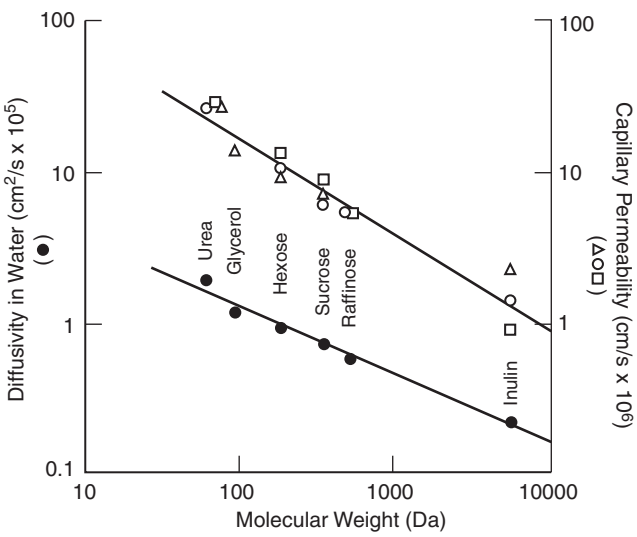

FIGURE 30.4 Aqueous diffusivity (•) and capillary permeability in cat leg (○), human forearm (□), and dog heart (△) of hydrophilic solutes vs. molecular weight. (Reproduced from Dedrick RL *et al.* ASAIO J 1982;5:1–8.)

PHYSIOLOGICAL PHARMACOKINETICS

The distribution and disposition of a drug in the body result from a complex set of physiological processes and biochemical interactions. In principle, it is possible to describe these processes and interactions in mathematical terms and, if sufficient data are available, to predict the time course of drug and metabolite(s) in different species and at specific anatomic sites (15). A physiological pharmacokinetic model was developed to predict the deamination of cytosine arabinoside (ARA-C) in humans from enzyme parameters determined from homogenates of human tissue (16). ARA-C is converted to its inactive metabolite, uracil arabinoside (ARA-U) by cytidine deaminase, the activity of which varies substantially among tissues.

The basis of a physiological pharmacokinetic model is a flow diagram showing the anatomic relationships among various organs and tissues. Figure 30.5

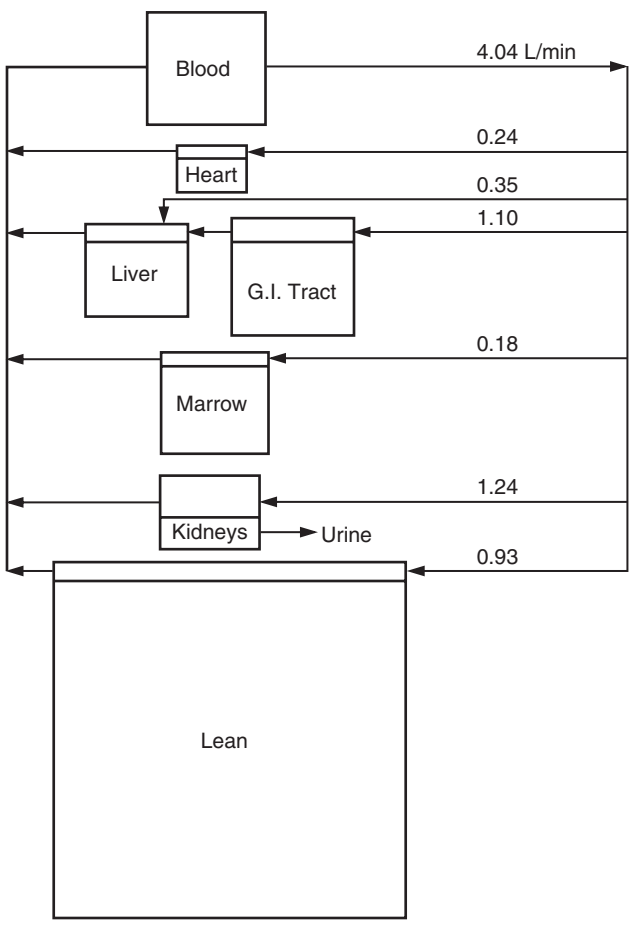

FIGURE 30.5 Physiological model for ARA-C pharmacokinetics. (Reproduced from Dedrick RL *et al.* Biochem Pharmacol 1972; 21:1–16.)

was employed to incorporate both principles of drug distribution within the body and saturable enzyme kinetics. The accumulation of a drug within a compartment is described by an appropriate mass-balance equation. As an illustration, we consider the accumulation of a drug in the kidney, which is assumed both to metabolize the drug by a saturable process and to clear it by filtration and possibly secretion. It is further assumed that the concentration within the compartment is uniform and equal to that of venous blood.

$$V_K \frac{dC_K}{dt} = Q_K C_B - Q_K C_K - CL_K C_B - \left[\frac{V_{max,K}\, C_K}{K_{m,K} + C_K}\right] V_K \tag{30.4}$$

where V = compartment volume (mL), C = drug concentration (μg/mL), t = time (min), Q = blood flow rate (mL/min), V_{max} = maximum rate of metabolism [μg/(min · mL)], K_m = Michaelis constant (μg/mL), CL = nonmetabolic clearance (mL/min) and the subscripts K and B refer to kidney and arterial blood, respectively.

Similar equations can be written for all relevant compartments. If parameters are chosen, the resulting set of nonlinear ordinary differential equations can be solved numerically to yield predictions of the concentration of the drug and metabolite(s) in each of the compartments as a function of time. Of course, the simplifying assumptions here can be relaxed to include much more detail concerning plasma and tissue binding, transport at the level of the blood capillary and cell membrane, and spatial nonuniformity — but at the cost of increasing complexity and the requirement for more parameters.

Figure 30.6 shows a prediction of the plasma concentration of ARA-C and total radioactivity (ARA-C plus ARA-U) following administration of two separate bolus intravenous injections of 1.2 mg/kg to a 70-kg woman. All compartment sizes and blood flow rates were estimated *a priori*, and all enzyme kinetic parameters were determined from published *in vitro* studies. None of the parameters was selected specifically for this patient; only the dose per body weight was used in the simulation. The prediction has the correct general shape and magnitude. It can be made quantitative by relatively minor changes in model parameters with no requirement to adjust the parameters describing metabolism.

Examination of Equation 30.4 or its counterpart for any drug-metabolizing organ shows that blood flow and organ metabolism interact (see Chapter 7). The chemical reaction occurs at a concentration equal to the concentration in the organ, which has been

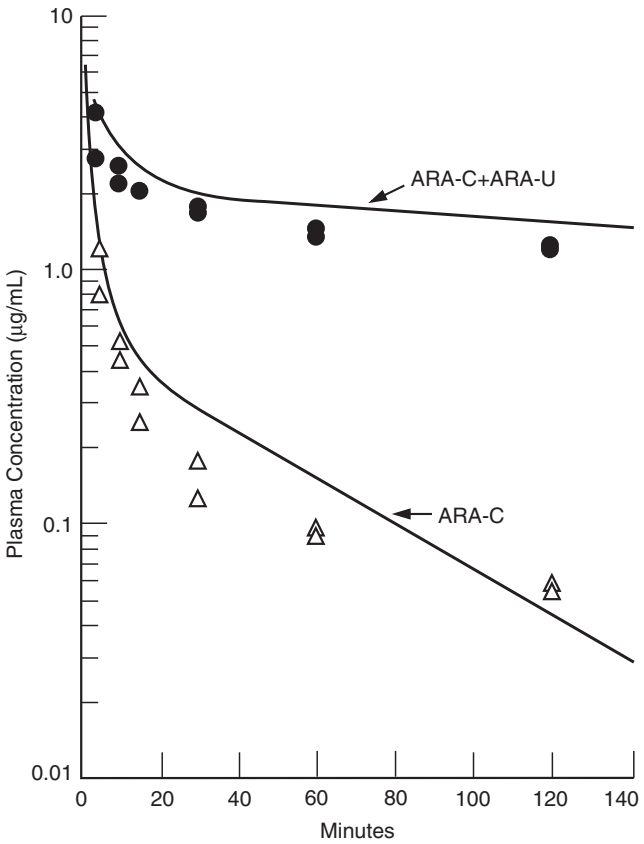

FIGURE 30.6 Predicted (*solid lines*) and observed (*symbols*) concentrations of ARA-C and total radioactivity (ARA-C + ARA-U) in the plasma of a 70-kg female patient following two separate intravenous injections of 1.2 mg/kg. (Reproduced from Dedrick RL *et al.* Biochem Pharmacol 1972;21:1–16.)

assumed in this example to equal the concentration in the venous blood draining that organ. Because the organ cannot metabolize more drug than reaches it by flow, the absolute upper limit on the organ's contribution to metabolism is QC_B. This is known as *flow limitation*. Whenever the intrinsic clearance is large compared with the blood flow, attenuation of the effects of enzyme induction or inhibition should be expected. In fact, analysis of pharmacokinetics *in vivo* may require knowledge of the size and blood flow of all compartments, including those that do not directly play a major role in drug metabolism.

Cytidine deaminase had been reported to vary greatly among mammalian species, both in its kinetic characteristics and in its dominant location (17). In humans, the highest levels (μg ARA-C/min · g) were found in the liver with smaller amounts in the kidney and heart. By comparison, the highest levels in the mouse were found in the kidney, while the dog had very low enzyme activities and the monkey had high levels in liver, heart, kidney, and lean tissue. The Michaelis constant was found to vary by a factor of seven from the human to the mouse. We simulated plasma and tissue concentrations in these several species to verify the participation of the tissues in the distribution process and to further validate the pharmacokinetic model. The model is quite general and can be applied to any mammalian species with the proper choice of blood flows, organ sizes, kidney clearance, and enzyme kinetic parameters. The model was quite successful in simulating ARA-C distribution and deamination in the several species, with the expected result that the drug is eliminated very rapidly by the monkey, less rapidly by the human and mouse, and very slowly by the dog.

While the interspecies variability in metabolism precludes the possibility of a simple allometric relationship for the plasma kinetics of ARA-C, the nonmetabolic clearance by the kidney does exhibit a power-law relationship with body weight. Figure 30.7 shows the kidney clearance of ARA-C and its deaminated product ARA-U on a log–log plot as a function of body weight for mice, monkeys, dogs, and humans. The slope is 0.80, which is essentially the same as the value of 0.77 for inulin (1).

Like ARA-C, 5-fluorouracil (5-FU) is extensively and variably metabolized among species. The principal catabolic enzyme is dihydropyrimidine dehydrogenase (DPD). Khor *et al*. (18) examined 5-FU plasma kinetics of mice, rats, and dogs that had been rendered functionally deficient in the enzyme by administration of an inhibitor. They compared these data with plasma

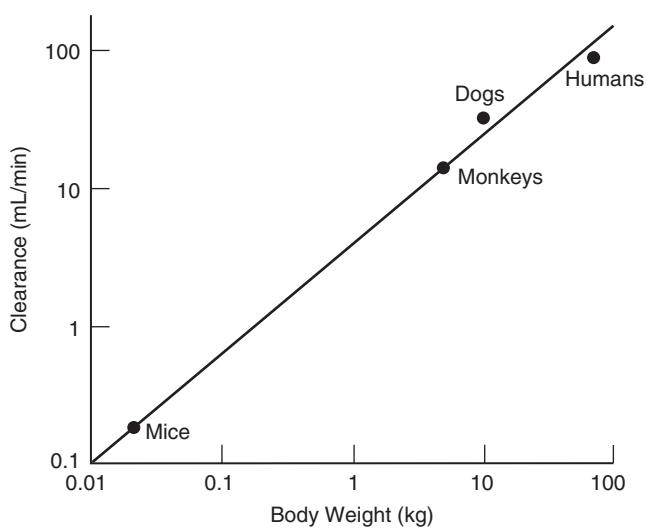

FIGURE 30.7 Kidney clearance of ARA-C and ARA-U vs body weight for mice, monkeys, dogs, and humans. (Reproduced from Dedrick RL *et al.* Biochem Pharmacol 1973;22:2405–17.)

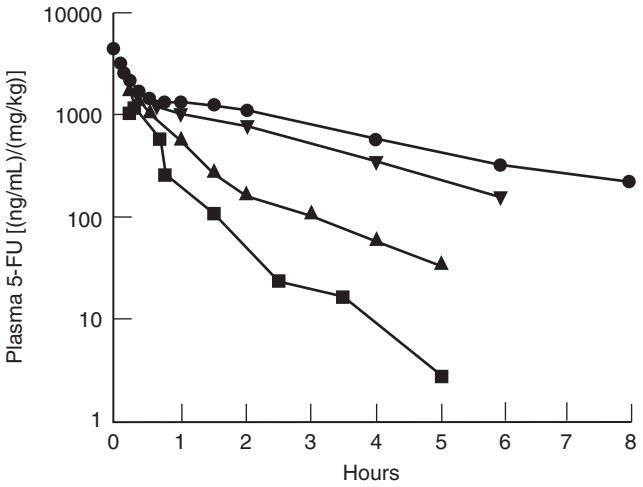

FIGURE 30.8 Dose-normalized 5-FU concentrations in plasma of experimental animals [mouse (■), rat (▲), dog (▼)] and in a human (●), all lacking dihydropyrimidine dehydrogenase activity. (Reproduced with permission from Khor SP *et al.* Cancer Chemother Pharmacol 1997;39:233–8.)

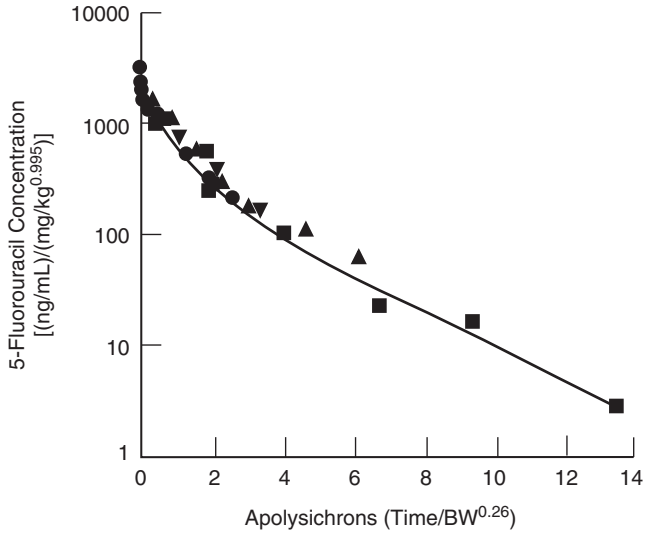

FIGURE 30.9 Complex Dedrick plot of data from Figure 30.8. (symbols are the same as in Figure 30.8). (Reproduced with permission from Khor SP *et al.* Cancer Chemother Pharmacol 1997; 39:233–8.)

levels in a human who was genetically deficient in DPD. The data are shown in Figure 30.8. The ordinate has been made comparable among the studies by division of the plasma concentration (ng/mL) by the dose (mg/kg). Examination of the curves shows that the mouse clears 5-FU most rapidly, followed by the rat, dog, and human. As discussed in the section on allometry, the natural pharmacokinetic time scale is the volume of distribution divided by the clearance. If the volume of distribution is proportional to BW and the kidney clearance is proportional to $(BW)^m$, then the times can be normalized by dividing the clock time by the pharmacokinetic time scale, which would be proportional to $(BW)^{1-m}$. This normalization is shown in Figure 30.9. In the figure, the exponent on body weight was fitted on both the concentration and time scales. It was found empirically to be 0.995 and 0.26, respectively. These exponents agree with the values of one and one-quarter that we had observed for methotrexate (3).

IN VITRO–IN VIVO CORRELATION OF HEPATIC METABOLISM

The liver has been the focus of most drug metabolism studies. While there is extrahepatic metabolism of some drugs, which may be extensive in some cases, the liver is generally considered the dominant organ in drug metabolism. Since liver tissue can be obtained from most species, including humans, *in vitro* study of hepatic metabolism has been an active and productive field of investigation. Studies have been conducted on microsomal preparations, hepatocytes, and liver slices. Interpretation is required for extrapolating *in vitro* results to the pharmacokinetically relevant rate of metabolism by the liver in the body. Issues such as drug binding in the culture medium and in plasma, distribution between plasma and red blood cells, and penetration into liver slices must be considered. Further, stability and intraspecies variability of liver specimens are important considerations.

Houston (19) has reviewed the prediction of *in vivo* intrinsic clearance of cytochrome P450 substrates in the rat from studies using microsomal preparations and isolated hepatocytes. The results are reproduced in Figures 30.10 and 30.11. In the calculation, Houston normalized to a standard rat weight (SRW) of 250 grams with an 11-gram liver containing 1.9×10^9 hepatocytes and yielding 500 mg of microsomal protein. Liver blood flow of 20 mL/min was assumed. Nineteen drugs were summarized for the microsomal predictions; 17 drugs are included in the hepatocyte calculations. In Figures 30.10 and 30.11 the solid symbols represent metabolite formation during *in vitro* studies while the open symbols represent substrate loss. By reference to the liver blood flow of 20 mL/min, it is apparent that drugs exhibiting both relatively low and high extraction ratios were included. The diagonal line is the line of identity on which the observations would fall if the prediction were exact. It is clear that the predictions from hepatocytes are generally better than those from microsomes, and only one of the

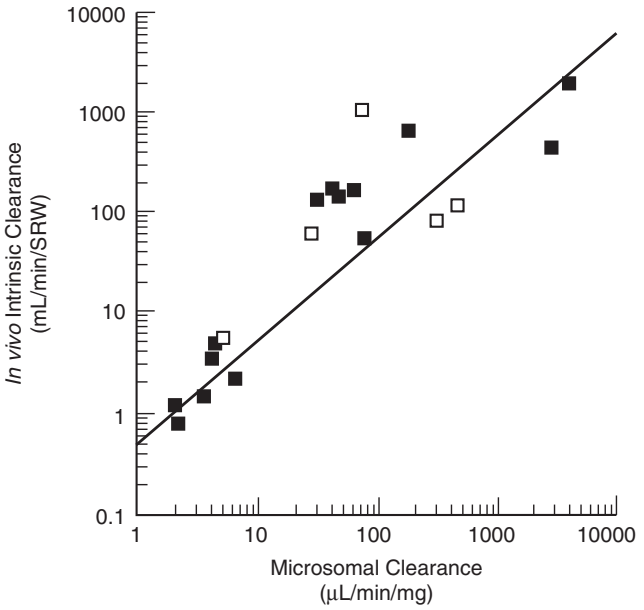

FIGURE 30.10 Intrinsic clearance *in vivo* versus hepatic microsomal clearance of 19 drugs metabolized by cytochromes P450 in the rat. The line represents the predicted correlation. *In vitro* clearance was measured either by substrate loss (□) or metabolite formation (■). Intrinsic clearance was normalized to a standard rat weight (SRW) of 250 grams. (Reproduced with permission from Houston JB. Biochem Pharmacol 1994;47:1469–79.)

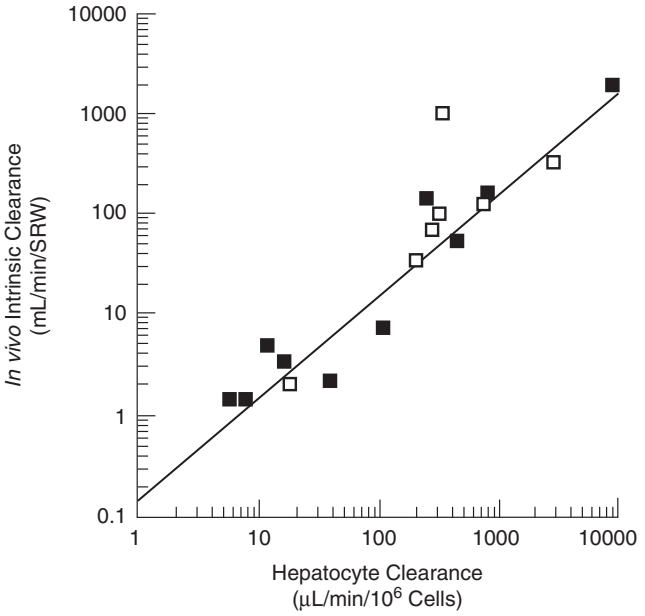

FIGURE 30.11 Intrinsic clearance *in vivo* versus hepatocyte clearance of 17 drugs metabolized by cytochromes P450 in the rat. The line represents the predicted correlation. Hepatocyte clearance was measured either by substrate loss (□) or metabolite formation (■). Intrinsic clearance was normalized to a standard rat weight (SRW) of 250 grams. (Reproduced with permission from Houston JB. Biochem Pharmacol 1994;47:1469–79.)

17 data points predicted from hepatocytes is very far from the expected value. The microsomal predictions are fairly good at low clearances but there is frequently an underprediction at higher values. The observation may reflect the fact that local environment and probably the configuration of the cytochrome P450 isoform in microsomal preparations differ significantly from those in hepatocytes.

Similar predictions of *in vivo* intrinsic clearance in the human from *in vitro* data have been produced by Ito *et al.* (20). The results are shown in Figure 30.12. The liver blood flow of about 1 mL/min · g places the intrinsic clearances in perspective. These correlations show considerably more variability than do those for the rat. This reflects both methodologic difficulties and probably a large variability of enzyme activities within the human population. Also, there seems to be a systematic underprediction for low-clearance drugs. This may reflect difficulties in measuring these low rates *in vitro* and/or extrahepatic metabolism.

Thummel *et al.* (21) avoided the intrinsic variability of enzyme acctivity in the human population by predicting *in vivo* clearances from *in vitro* kinetic data in liver transplant patients. They were interested in using midazolam (MDZ) as a probe of CYP3A isoforms in the liver. Because biopsies were performed for the medical management of the transplant patients, the authors had the ethical opportunity to study enzyme activity in biopsies from human livers following transplantation. In addition, MDZ pharmacokinetics were studied in the recipients of the same transplanted livers. Five of the liver recipients provided sufficient tissue for the determination of

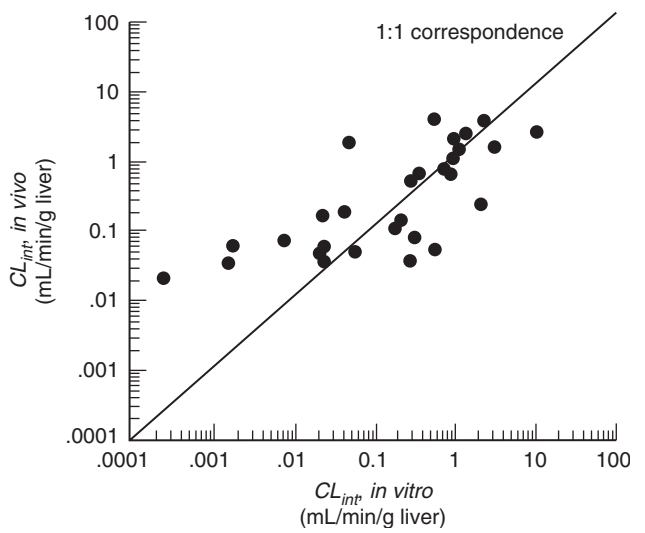

FIGURE 30.12 Observed versus predicted intrinsic metabolic clearance of 29 drugs in humans. (Reproduced with permission from Ito K *et al.* Annu Rev Pharmacol Toxicol 1988;38:461–99.)

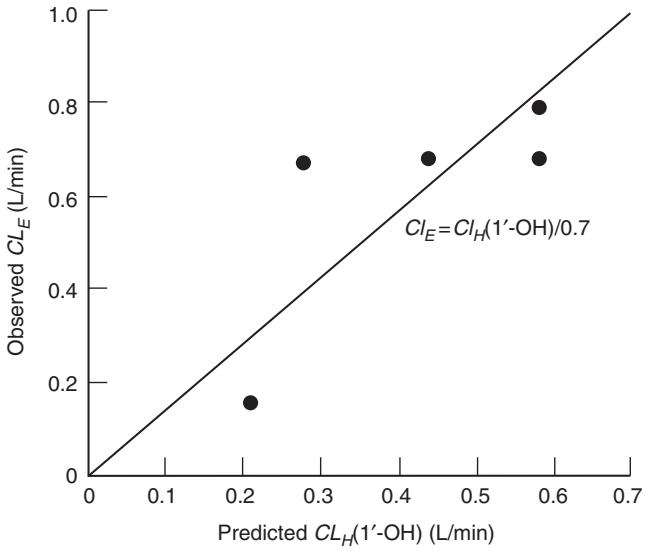

FIGURE 30.13 Observed total elimination clearance (CL_E) of midazolam (MDZ) in liver transplant patients versus hepatic clearance (CL_H) of 1′-OH MDZ predicted from biopsy specimens. The line is the predicted hepatic clearance of MDZ if the 1′-hydroxylation pathway accounts for 70% of the substrate loss. (Data from Thummel KE *et al*. J Pharmacol Exp Ther 1994;271:549–56.)

V_{max} and K_m for MDZ 1′-hydroxylation. V_{max} determined for each biopsy sample was then scaled to the estimated total liver mass and intrinsic clearance estimated as total liver V_{max}/K_m. Hepatic clearance then was predicted from Equation 7.6 in Chapter 7. Figure 30.13 compares the observed total elimination clearance with predicted hepatic clearance based on the assumption that the 1′-hydroxylation pathway accounts for 70% of the substrate loss. The prediction is quite good. The average absolute deviation between the five observed data points and their predicted values is only 28%, and the differences are uniformly distributed.

REFERENCES

1. Adolph EF. Quantitative relations in the physiological constitutions of mammals. Science 1949;109:579–85.
2. Dedrick RL, Oldfield EH, Collins JM. Arterial drug infusion with extracorporeal removal. I. Theoretic basis with particular reference to the brain. Cancer Treat Rep 1984;68:373–80.
3. Dedrick RL, Bischof KB, Zaharko DS. Interspecies correlation of plasma concentration history of methotrexate (NSC-740). Cancer Chemother Rep 1970;54:95–101.
4. Ward KW, Smith BR. A comprehensive quantitative and qualitative evaluation of extrapolation of intravenous pharmacokinetic parameters from rat, dog, and monkey to humans. II. Volume of distribution and mean residence time. Drug Metab Dispos 2004; 32:612–19.
5. Mahmood I. Interspecies scaling of renally secreted drugs. Life Sci 1998;63:2365–71.
6. Mahmood I, Balian JD. Interspecies scaling: Predicting clearance of drugs in humans. Three different approaches. Xenobiotica 1996;26:887–95.
7. Boxenbaum H. Interspecies scaling, allometry, physiological time, and the ground plan of pharmacokinetics. J Pharmacokinet Biopharm 1982;10:201–27.
8. Mahmood I, Balian JD. Interspecies scaling: Predicting pharmacokinetic parameters of antiepileptic drugs in humans form animals with special emphasis on clearance. J Pharm Sci 1996;85:411–4.
9. Nagilla R, Ward KW. A comprehensive analysis of the role of correction factors in the allometric predictivity of clearance from rat, dog, and monkey to humans. J Pharm Sci 2004;93:2522–34.
10. Bonate PL, Howard D. Critique of prospective allometric scaling: Does the emperor have clothes? J Clin Pharmacol 2000;40:335–40.
11. Alberts DS, Liu PY, Hannigan EV, O'Toole R, Williams SD, Young JA, Franklin EW, Clarke-Pearson DL, Malviya VK, DuBeshter B, Adelson MD, Hoskins WJ. Intraperitoneal cisplatin plus intravenous cyclophosphamide versus intravenous cisplatin plus intravenous cyclophosphamide for stage III ovarian cancer. N Engl J Med 1996;335:1950–5.
12. Markman M. Intraperitoneal antineoplastic drug delivery: Rationale and results. Lancet Oncol 2003;4:277–83.
13. Dedrick RL, Myers CE, Bungay PM, DeVita VT Jr. Pharmacokinetic rationale for peritoneal drug administration in the treatment of ovarian cancer. Cancer Treat Rep 1978;62:1–11.
14. Dedrick RL, Flessner MF, Collins JM, Schultz JS. Is the peritoneum a membrane? ASAIO J 1982;5:1–8.
15. Ings RMJ. Interspecies scaling and comparisons in drug development and toxicokinetics. Xenobiotica 1990;20:1201–31.
16. Dedrick RL, Forrester DD, Ho DHW. *In vitro–in vivo* correlation of drug metabolism — deamination of 1-β-D-arabinofuranosylcytosine. Biochem Pharmacol 1972;21:1–16.
17. Dedrick RL, Forrester DD, Cannon JN, El Dareer SM, Mellett LB. (1973). Pharmacokinetics of 1-β-D-arabinofuranosylcytosine (Ara-C) deamination in several species. Biochem Pharmacol 1973;22:2405–17.
18. Khor SP, Amyx H, Davis ST, Nelson D, Baccanari DP, Spector T. Dihydropyrimidine dehydrogenase inactivation and 5-fluorouracil pharmacokinetics: Allometric scaling of animal data, pharmacokinetics and toxicodynamics of 5-fluorouracil in humans. Cancer Chemother Pharmacol 1997;39:233–8.
19. Houston JB. Utility of *in vitro* metabolism data in predicting *in vivo* metabolic clearance. Biochem Pharmacol 1994;47:1469–79.
20. Ito K, Iwatsubo T, Kanamitsu S, Nakajima Y, Sugiyama Y. Quantitative prediction of *in vivo* drug clearance and drug interactions from *in vitro* data on metabolism, together with binding and transport. Annu Rev Pharmacol Toxicol 1998;38:461–99.
21. Thummel KE, Shen DD, Podoll TD, Kunze KL, Trager WF, Hartwell PS *et al*. Use of midazolam as a human cytochrome P-450 3A probe: I. *In vitro–in vivo* correlations in liver transplant patients. J Pharmacol Exp Ther 1994;271:549–56.

This page intentionally left blank

CHAPTER

31

Phase I Clinical Studies

JERRY M. COLLINS
Division of Cancer Treatment and Diagnosis, National Cancer Institute, Rockville, Maryland

INTRODUCTION

In the drug development pipeline, Phase I clinical studies sit at the interface between the end of preclinical testing and the start of human exploration (see Chapter 1, Figure 1.1). Somewhat surprisingly, this stage of drug development does not generally attract much attention. For clinical pharmacologists as well as other practitioners of drug development, the entry of a novel molecular entity into human beings for the first time is unquestionably a very exciting event.

Some features of a Phase I study are invariant; others have changed considerably over time. On a periodic basis, a set of new investigators enters the field, and almost everyone is inclined to reinvent the design features of Phase I studies. First-in-human studies are an extraordinary opportunity to integrate pharmacokinetic (PK), pharmacodynamic (PD), and toxicology information while launching the new molecule on a path for rational clinical development (1). Above all, this is a major domain for application of the principles of clinical pharmacology.

The ongoing re-engineering of the entire drug development process places additional scrutiny on Phase I. Drug discovery and high-throughput screening have created a bulge in the pipeline as it heads toward the clinic. It is essential that truly useful medicines are not lost in the sheer numbers of compounds under evaluation, and it is just as essential that marginal candidates be eliminated as expeditiously as possible. Although the science generated via the discovery and development process can be dazzling, the "art" of Phase I trials requires continual focus on safety and the probability of therapeutic effect (2).

The nomenclature for early clinical studies is not fully standardized. In addition to first-in-human evaluations, Phase I trials are appropriate throughout the drug development process as specific issues arise that require clinical pharmacologic investigation. Further, some exploratory first-in-human studies are currently being described as "Phase Zero," in which the goals are somewhat different from classic Phase I trials.

DISEASE-SPECIFIC CONSIDERATIONS

There is a large amount of conceptual similarity in the approach to Phase I trial design, regardless of the therapeutic area; however, there are some important differences. One major consideration is the selection of the population of humans for the Phase I study. For most therapeutic indications, healthy volunteers are the participants. They are compensated for the inconveniences of participating in the study, but they are not in a position to receive medical benefit. The use of healthy volunteers substantially limits the ability to observe the desired therapeutic goal. For example, if an agent is intended to correct metabolic deficiencies, or lower elevated blood pressure, there may be no detectable changes in healthy participants.

In several therapeutic areas, patients with the disease, rather than healthy volunteers, participate in Phase I studies. This tradition is strongest in oncology, because many cytotoxic agents cause damage to DNA. For similar reasons, many anti-AIDS drugs are not tested initially in healthy persons. In neuropharmacology, some categories of drugs have an acclimatization or tolerance aspect, which makes them difficult

to study in healthy persons (3). On the other hand, as oncology drugs have shifted toward different targets and with milder side effect profiles, more first-in-human trials of these agents are being conducted in healthy populations.

The primary goal of Phase I studies is always to evaluate safety in humans. When patients participate in a study, there is an additional element of therapeutic intent. In determining human safety, there has been an emphasis on defining the maximum tolerated dose (MTD) as an endpoint of the study. Whereas determination of the MTD is important from the standpoint of clinical toxicology, the MTD has been selected in many cases as the dose for subsequent clinical trials, resulting in the registration and initial marketing of drug doses that are inappropriately high for some clinical conditions (4). However, because the therapeutic index for anticancer drugs is so narrow, and because the disease is life-threatening, the concept of MTD has played a central role in Phase I studies of these drugs. A large portion of this author's experience with Phase I trials has been in the area of anticancer drugs; thus, the examples here will be taken from oncology.

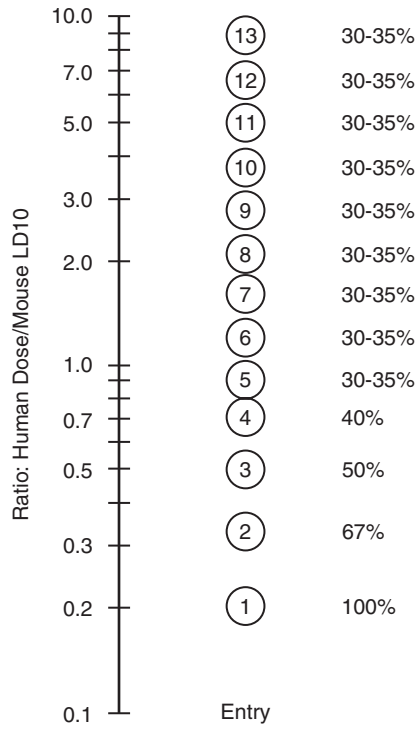

FIGURE 31.1 Modified Fibonacci dose escalation procedure, expressed as a ratio of the human dose to a reference dose in mice [e.g., the 10% lethal dose (LD_{10})]. Human studies typically start at one-tenth the murine dose, expressed on the basis of body surface area. If tolerated, the next dose is initially doubled, then the percentage change at each escalation step decreases. (Reproduced from Collins JM, Zaharko DS, Dedrick RL, Chabner BA. Cancer Treat Rep 1986;70:73–80.)

STARTING DOSE AND DOSE ESCALATION

Regardless of the details for Phase I trial design, the two essential elements are the starting dose and the dose escalation scheme. For a first-in-human study, selection of the starting dose is caught in a conflict between a desire for safety (leading to a cautious choice) versus an interest in efficiency. When patients take part in a Phase I trial, efficiency is also tied to a desire to provide therapeutic benefit, and can stimulate a more aggressive choice of starting dose.

The same conflicts exist for the escalation scheme. Once the current dose level has been demonstrated to be safe, the move to next higher level is clouded by uncertainty about the steepness of the dose–toxic response curve. Recently, there has been an appreciation of the linkage between choices for starting dose and escalation rate. In particular, the combination of a cautious starting dose with a very conservative escalation rate can lead to trials that are so lengthy that they serve the interests of no one.

Modified Fibonacci Escalation Scheme

Some version of the modified Fibonacci escalation scheme is probably the most frequently used escalation scheme, particularly in oncologic Phase I studies. However, its pre-eminence is fading. The sequence of escalation steps for a typical scheme is shown in Figure 31.1. Implicit in the design of this scheme is an attempt to balance caution and aggressiveness. Rapid increases in dose are prescribed at early stages of the trial (i.e., starting with a doubling of the dose), when the chance of using a nontoxic dose is highest. The incremental changes in dose become more conservative at later stages (e.g., 30%) when the probability of side effects has increased. When a modified Fibonacci design is submitted to the local review board and regulatory authorities for approval, the escalation rate is completely determined in advance, at least until toxicity intervenes.

Many variations of the Fibonacci scheme have arisen, driven by statistical and/or pharmacologic principles. In particular, the accelerated titration designs have been replacing standard Fibonacci schemes in many oncologic studies (5). From the perspective of clinical pharmacology, a particularly attractive goal is to integrate whatever is known about the properties of the drug into an adaptive design. One type of adaptive design modulates the rate of

dose escalation based upon plasma concentrations of the drug, as described in the next section. The formal application of adaptive design has declined as empirical schemes have become more efficient, but the inclusion of specific PK, PD, and pharmacogenetic tasks has risen steeply.

Pharmacologically Guided Dose Escalation

The pharmacologically guided dose escalation (PGDE) design is based upon a straightforward PK–PD hypothesis: When comparing animal and human doses, expect equal toxicity for equal drug exposure (6, 7). A fundamental principle of clinical pharmacology is that drug effects are caused by circulating concentrations of the unbound ("free") drug molecule, and are less tightly linked to the administered dose (see Chapter 2, Figure 2.1). The advantage of PGDE is that it minimizes the numbers of patients at risk, and pays more attention to the individual patient's risk of receiving too low a dose. A series of Phase I studies were found to be excessively lengthy because a starting dose was chosen that was too low, thus pushing the major portion of the trial into the conservative portion of the modified Fibonacci design.

As illustrated in Figure 31.2, for PGDE, there is a continual evaluation of plasma concentrations as the trial is under way. Thus, unlike a modified Fibonacci design, the escalation rate is adapted throughout the procedure. Although the decisions are expressed in terms of pharmacokinetics (plasma concentrations of the drug), the design is named "pharmacologic" because it is intended to permit adjustments in the target plasma concentration, based upon pharmacodynamic information, such as species differences in

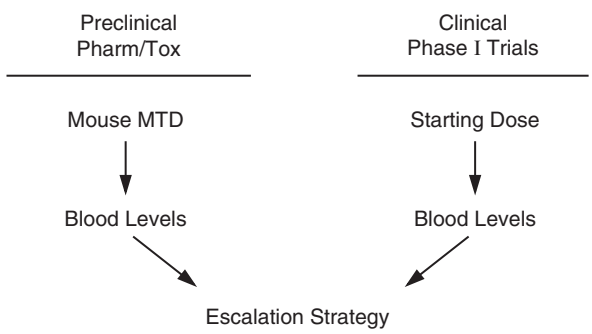

FIGURE 31.2 Bridges between preclinical and clinical development: pharmacologically guided dose escalation. As an alternative to the fixed procedure for increasing doses (e.g., Figure 31.1), the size of each dose escalation step is based on current concentrations of drug in human blood, along with target concentrations defined in preclinical studies. MTD, Maximum tolerated dose.

90% inhibitory concentration (IC_{90}) for bone marrow or tumor cells.

A retrospective survey was conducted prior to embarking on "real-time" use of PGDE. The results shown in Figure 31.3 permit a comparison of limiting doses in humans versus mice. The doses used for this comparison were normalized for body surface area (e.g., 100 mg/m^2), which is very exceptional for any other therapeutic class. The use of body surface area in clinical dosing for oncology has faded substantially, but it remains an excellent metric for cross-species comparisons.

There are two major conclusions from an evaluation of the data in Figure 31.3:

1. There is enormous scatter in the ratio of human:murine tolerable doses. Thus, while murine doses may seem to give reasonable predictions for acceptable human doses on the average, there is no predictive consistency that could be relied upon for any specific drug about to enter Phase I study.
2. The drug exposure (area under the curve; AUC) ratio at approximately equitoxic doses has much less variability, indicating that pharmacokinetic differences account for almost all of the differences observed for toxic doses of this set of drugs between humans and mice.

What is the underlying cause for these interspecies differences? For equal doses, differences in plasma AUC values simply indicate differences in total body clearance. Renal and metabolic elimination processes are the major contributors to total body clearance. When allometric scaling is used as described in Chapter 30, renal clearance tends to exhibit only small differences across species, whereas there are many examples of interspecies differences in metabolism. Further, across many drug categories, metabolism is quantitatively more important than is renal elimination. Therefore, more emphasis on interspecies differences in drug metabolism could improve Phase I studies. The next two sections provide specific examples of the impact of monitoring metabolism during early human studies.

Interspecies Differences in Drug Metabolism

The data in Table 31.1 for iododeoxydoxorubicin (I-Dox) were obtained during first-in-human studies conducted by Gianni *et al.* (8). There was greater exposure to the parent drug in mice, and to the hydroxylated metabolite (I-Dox-ol) in humans. Overall, there was a 50-fold difference in the relative AUC exposure ratios (metabolite:parent drug) for humans and

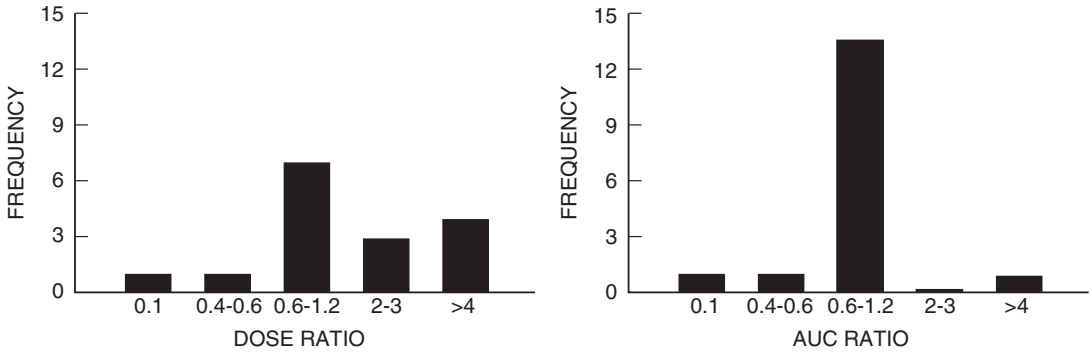

FIGURE 31.3 Survey of acute toxicity of anticancer drugs in humans versus mice. Comparisons based upon dose (*left panel*) exhibit more scatter than do those based on drug exposure (AUC) (*right panel*).

TABLE 31.1 AUC Values in Plasma for Iododeoxydoxorubicin (I-Dox) and Its Metabolite (I-Dox-ol) in Mouse and Human Equitoxic Doses[a]

Compound	Mouse (μ*M*·hr)	Human (μ*M*·hr)
I-Dox	5.0	0.3
I-Dox-ol	1.2	4.0

[a] Data from Gianni L *et al.* J Natl Cancer Inst 1990;82:469–77.

mice. Because I-Dox and I-Dox-ol are approximately equieffective and equitoxic, these exposure comparisons are also indicative of pharmacologic response. This extreme example of an interspecies difference in drug metabolism was comparable to studying one molecule (the parent) in mice, and then (unintentionally) studying a different molecule (the metabolite) in humans. The similarity in potency of the parent molecule and metabolite was fortuitous and not expected ordinarily, especially for both desirable and adverse effects.

Figure 31.4 illustrates an interspecies difference in paclitaxel metabolism (9). The principal metabolite formed in humans was not produced by rat microsomes. This example illustrates the potential of *in vitro* studies to discover interspecies differences in metabolism. In most cases, it is no longer necessary to wait for *in vivo* Phase I studies to discover such differences, and certainly not advisable. Regulatory authorities around the world have encouraged early consideration of interspecies metabolic comparisons.

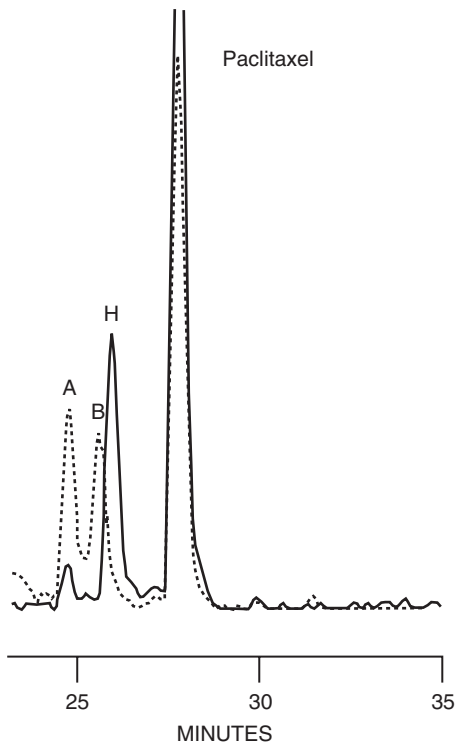

FIGURE 31.4 High-performance liquid chromatograms comparing *in vitro* paclitaxel metabolism by hepatic microsomes from rats (*dotted line*) and humans (*solid line*). The major human metabolite, designated peak H, was not formed by rats. (Adapted from Jamis-Dow CA, Klecker RW, Katki AG, Collins JM. Cancer Chemother Pharmacol 1995;6:107–14.)

Active Metabolites

During first-in-human studies with the investigational anticancer drug penclomedine, it was discovered that exposure to parent drug concentrations was less than 1% of the exposure to its metabolite, demethylpenclomedine (10). As shown in Figure 31.5, exposure to the parent drug was very brief, while the metabolite accumulated during the course of a 5-day treatment cycle. Because the toxicity of the parent molecule limits the amount of tolerable exposure to the metabolite, which provides the antitumor effect, the penclomedine case

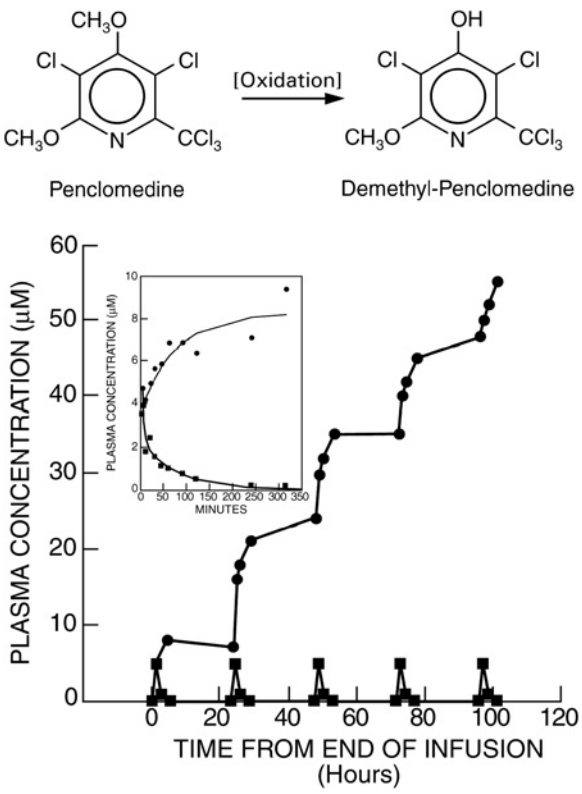

FIGURE 31.5 The investigational anticancer drug, penclomedine, was administered to patients once a day for 5 consecutive days. The parent drug disappeared rapidly from plasma, whereas the demethyl metabolite accumulated over the course of therapy. (Adapted from Hartman NR, O'Reilly S, Rowinsky EK, Collins JM, Strong JM. Clin Cancer Res 1996;2:953–62.)

clearly demonstrates the danger of not knowing which molecules are circulating in the body. If this type of information is determined early enough in drug development, the metabolite can be selected to replace the parent molecule as the lead development candidate.

There is stunning similarity between the penclomedine story and the history of terfenadine (Seldane), a highly successful antihistamine product that was withdrawn from marketing. In early clinical studies of terfenadines, it was not appreciated that the major source of clinical benefit was its metabolite, fexofenadine (Allegra see structures in Chapter 1, Figure 1.2). It became obvious that the metabolite should have been the lead compound only after cardiotoxicity was subsequently discovered for the parent drug but not the metabolite.

BEYOND TOXICITY

The study of toxicity without consideration of efficacy is inherently unsatisfying. Indeed, when patients paricipate in Phase I trials, there is always therapeutic intent. Realistically, there is only a low probability of success in many settings, but the obligation is to maximize that chance. As it becomes more common to seek "proof-of-concept" or mechanistic evaluations during Phase I, an increased emphasis on demonstrating therapeutic activity, the usual domain for Phase II study, looms on the horizon. By monitoring a target biomarker, both proof-of-concept and dose determination might be achieved simultaneously. Further, by enrolling in the trial those patients who have favorable expression profiles of the target, an "enriched" population is obtained with a higher likelihood of response, if the therapeutic concept has merit.

For "accessible" targets such as blood pressure or heart rate, these concepts are not new. The techniques of external, noninvasive imaging now permit real-time monitoring of targets such as *in situ* regions of the human brain that were previously considered inaccessible. Fowler *et al.* (11) used positron emission tomography (PET) to study inhibition of monoamine oxidase, type B (MAO-B) by lazabemide (Figure 31.6). A dose of 25 mg twice a day inhibited most MAO-B activity, and doubling the dose to 50 mg abolished all detectable activity. Also, brain activity for MAO-B had returned to baseline values within 36 hours of

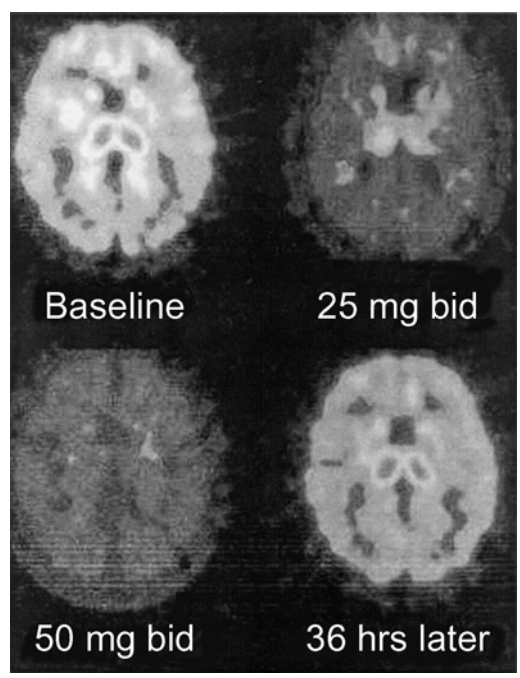

FIGURE 31.6 PET scans showing dose dependency and time dependency of lazabemide inhibition of monoamine oxidase, type B in human brain. (Reproduced with permission from Fowler JS, Volkow ND, Wang G-J, Dewey SL. J Nucl Med 1999;40:1154–63.)

TABLE 31.2 Therapeutic Issues for Drug Development

- Does treatment impact the desired target?
- What is the minimum/maximum dose?
- What dose (therapeutic course) interval is appropriate?

the last dose of lazabemide. This example of MAO-B inhibition demonstrates the successful investigation in early human studies of three areas of fundamental interest in developing drug therapy (Table 31.2): monitoring impact at the desired target, evaluating the dose-response relationship (dose-ranging), and determining an appropriate dose interval from recovery of enzyme activity.

The expansion of Phase I studies to include goals formerly reserved for Phase II evaluation is only one direction of change. Simultaneously, the toxicity goals of Phase I studies are being decoupled from evaluations of absorption, distribution, metabolism, and excretion (ADME). European regulators now permit microdose studies that include both metabolism and excretion components as well as tracer doses for imaging (12, 13). In the United States, a similar regulatory framework has been announced, with an extension to pharmacologic investigations of receptors and other target modulations (14). In both regulatory sectors, the preclinical requirements for first-in-human studies are substantially reduced for situations in which doses are kept low to minimize risk to study participants. This structural change facilitates the type of translational research that has been described as Phase Zero or Pre-Phase I. Re-engineering of the entire drug development pipeline is stimulated by these opportunities to change the goals at early stages.

This blurring of the traditional lines of demarcation between clinical phases of drug development has its pitfalls and disorienting aspects, and not all development organizations will adopt such changes. Indeed, there should always be a place for diversity in approaches to drug development. Nonetheless, the early harvesting of benefits from investments in biomarkers presents exciting new opportunities for clinical pharmacologists and other stakeholders in drug development.

REFERENCES

1. Peck CC, Barr WH, Benet LZ, Collins, J, Desjardins RE, Furst DE *et al.* Opportunities for integration of pharmacokinetics, pharmacodynamics, and toxicokinetics in rational drug development. Clin Pharmacol Ther 1992;51:465–73.
2. Peck CC, Collins JM. First time in man studies: A regulatory perspective — art and science of Phase I trials. J Clin Pharmacol 1990;30:218–22.
3. Cutler NR, Stramek JJ. Scientific and ethical concerns in clinical trials in Alzheimer's patients: The bridging study. Eur J Clin Pharmacol 1995;48:421–8.
4. Rolan P. The contribution of clinical pharmacology surrogates and models to drug development — a critical appraisal. Br J Clin Pharmacol 1997;44:219–25.
5. Simon R, Freidlin B, Rubinstein L, Arbuck SG, Collins J, Christian MC. Accelerated titration designs for Phase I clinical trials in oncology. J Natl Cancer Inst 1997;89:1138–47.
6. Collins JM, Zaharko DS, Dedrick RL, Chabner BA. Potential roles for preclinical pharmacology in Phase I trials. Cancer Treat Rep 1986;70:73–80.
7. Collins JM, Grieshaber CK, Chabner BA. Pharmacologically-guided Phase I trials based upon preclinical development. J Natl Cancer Inst. 1990;82:1321–6.
8. Gianni L, Vigano L, Surbone A, Ballinari D, Casali P, Tarella C, Collins JM, Bonadonna G. Pharmacology and clinical toxicity of 4′-iodo-4′-deoxydoxorubicin: An example of successful application of pharmacokinetics to dose escalation in Phase I trials. J Natl Cancer Inst. 1990;82:469–77.
9. Jamis-Dow CA, Klecker RW, Katki AG, Collins JM. Metabolism of taxol by human and rat liver *in vitro*: A screen for drug interactions and interspecies differences. Cancer Chemother Pharmacol 1995;6:107–14.
10. Hartman NR, O'Reilly S, Rowinsky EK, Collins JM, Strong JM. Murine and human *in vivo* penclomedine metabolism. Clin Cancer Res 1996;2:953–62.
11. Fowler JS, Volkow ND, Wang G-J, Dewey SL. PET and drug research and development. J Nucl Med 1999;40:1154–63.
12. Bergström M, Grahnèn A, Långström B. Positron emission tomography microdosing: A new concept with application in tracer and early clinical development. Eur J Clin Pharmacol 2003;59:357–66.
13. Committee for Medicinal Products for Human Use (CHMP). Position paper on non-clinical safety studies to support clinical trials with a single microdose. London: European Medicines Agency; 2004. (Internet at http:/www.emea.eu.int/pdfs/human/swp/259902en.pdf; accessed August 31, 2005.)
14. CDER. Exploratory IND studies. Draft Guidance for Industry, Investigators and Reviewers. Rockville, MD: FDA; 2005. (Internet at http://www.fda.gov/cder/guidance/6384dft.pdf; accessed August 31, 2005.)

CHAPTER

32

Pharmacokinetic and Pharmacodynamic Considerations in the Development of Biotechnology Products and Large Molecules

PAMELA D. GARZONE
Telik, Inc., Palo Alto, California

INTRODUCTION

In 2004, the FDA approved 36 new medical entitites and 5 new biologics (1). Most notable of these included palifemin (Kepivance), a modified version of a naturally occurring human growth factor, and a number of monoclonal antibodies (mABs) such as cetuximab (Erbitux), erlotinib hydrochloride (Tarceva), and bevacizumab (Avastin) (1). As of 2004, over 300 biotechnology compounds were in clinical development and, of these, 15% are monoclonal antibodies in Phase I or II trials (2). These statistics emphasize how important it is to understand how macromolecules behave in the body, and the special considerations required of researchers and clinicians working with these compounds. For the purpose of this chapter, the definition of macromolecule is a large molecule, with a molecular mass in kilodaltons (kDa), such as a protein or glycoprotein, or a monoclonal antibody, either as an intact immunoglobin or its fragments.

Well-known macromolecules that have been approved and are currently marketed are listed in Table 32.1. This chapter presents information on mABs currently marketed or under investigation and discusses methodology used to assay macromolecules, interspecies scaling of macromolecules, pharmacokinetic (PK) characteristics of macromolecules, and pharmacodynamics (PD) of macromolecules.

Monoclonal Antibodies

Monoclonal antibodies were initially considered "magic bullets" offering, for the first time, targeted therapy against specific tumor surface antigens. The development of mABs as diagnostic aids and as therapy was made possible by advances in hybridoma technology (3). The first murine monoclonal antibody trial was published in 1982 (4). However, in the 1980s and early 1990s, most of the murine mABs failed in clinical trials. The major drawback was the inefficient interaction of the Fc component of the mouse antibody with human effector functions (5). Also, the repeated administration of mouse antibodies to humans resulted in the production of a human anti-mouse antibody (HAMA) response that reduced the effectiveness of the murine antibody or resulted in allergic reactions in humans.

The first murine monoclonal antibody was approved for marketing in 1986, when Orthoclone (CD3-specific antibody), or OKT3, was approved. Now, humanized antibodies, engineered so that HAMA response is mitigated have become mainstream therapy, with such recent successes as Raptiva, Erbitux, and Avastin (Table 32.1). A successful antibody also needs to be potent and specific (6). The following sections describe how engineered antibodies can be produced to meet these requirements.

TABLE 32.1 Examples of Currently Marketed Macromolecules

Macromolecule	Abbreviation	Trade name
Erythropoietin	Epo	Epogen
Growth hormone	GH	Nutropin
Granulocyte colony-stimulating factor	G-CSF	Neupogen
Granulocyte–macrophage colony-stimulating factor	GM-CSF	Leukine
Interleukin-2	IL-2	Proleukin
Interleukin-11	IL-11	Neumega
Factor IX	FIX	BeneFIX
Recombinant tissue plasminogen activator	rt-PA	Activase
Alemtuzumab		Campath
Adalimumab		Humira
Omalizumab		Xolair
Efalizumab		Raptiva
Cetuximab		Erbitux
Bevacizumab		Avastin

Antibody Structure and Production

The basic structure of an immunoglobulin (Ig) antibody is shown in Figure 32.1 (7). The Ig molecule consists of the Fc region, and the Fab region allowing for multivalent high avidity and specificity. It should be noted that immunoglobulin sequences are conserved across species such that considerable homology between mouse and human variable regions exists (8). Mouse antibodies can be further engineered by molecular cloning and expression of the variable region of Ig to be more human (9).

Monoclonal antibodies, by definition, are produced by a single clone of hybridoma cells, i.e., a single species of antibody molecule (Figure 32.2). However, engineered monoclonal antibodies can be chimeras, in which the Fv region from mouse IgG is fused with the variable region of the human IgG. mABs can be humanized so that only the complementarity-determining regions of the murine variable region are combined into the human variable region. They can be single-chain IgG, the simplest fragment being the scFv (single-chain variable fragment). The scFv can be a monomer, dimer, or tetramer; this multivalency results in a significant increase in functional affinity (9).

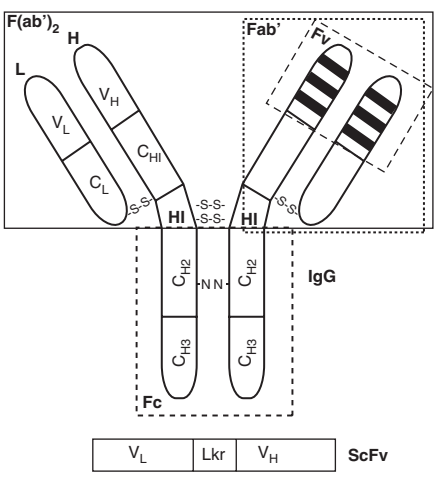

FIGURE 32.1 Structure of prototypical IgG and single-chain Fv (scFv) antibody molecules. The large solid line box encloses the divalent Fab′ molecules, the small dotted line box encloses the Fab′ fragment, the dashed line box encloses the Fc components, and the solid and dashed line box encloses the Fv components, which are the antigen-binding sites. The variable light-chain region is designated V_L and the variable heavy-chain region is designated $V_{H.}$. Other abbreviations: constant region domains, C_{H1}, C_{H2}, C_{H3}; hinge, Hi; constant light region, C_L; linker region, Lkr. Conserved N-linked (-N–N-) carbohydrates are located in the Fc domain; cysteine bonds (-S–S-) join heavy and light chains. (Reproduced with permission from Colcher D *et al.* QJ Nucl Med. 1999; 43:132–9.)

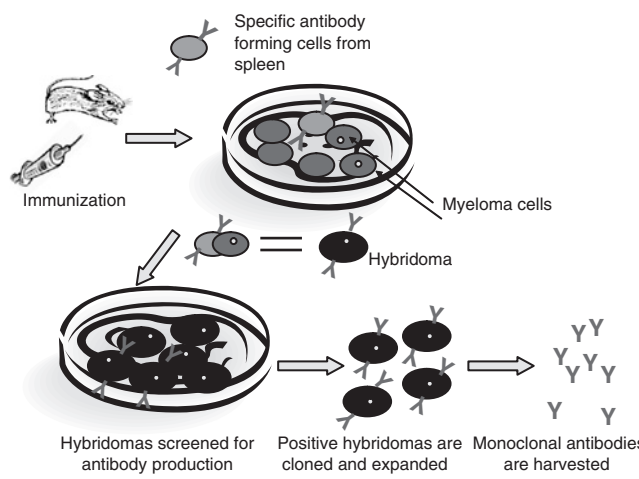

FIGURE 32.2 Schematic depicting monoclonal antibody production. A mouse is immunized by injection of an antigen to stimulate the production of antibodies targeted against the antibody. The antibody-forming cells are isolated from the mouse's spleen. Monoclonal antibodies are produced by fusing single antibody-forming cells to tumyekma cells grown in culture. The resulting cell is called a *hybridoma*. By allowing the hybridoma to multiply in culture, it is possible to produce a population of cells, each of which produces identical antibody molecules. These antibodies are called *monoclonal antibodies* because they are produced by the identical offspring of a single, cloned antibody-producing cell.

Fully human antibodies can be constructed from phage libraries. In addition to the diversity of engineered antibodies, other molecules can be attached to the antibody, such as enzymes, toxins, viruses, radionuclides, and biosensors for targeting, imaging, or diagnosing. These are commonly referred to as "conjugated" monoclonal antibodies.

The production of antibodies appears to be simple (Figure 32.2). However, their commercialization is challenging. The need for specificity makes the market small; thus, the costs of doing clinical trials for small markets are unattractive to most companies. Quality control of the production and manufacture of monoclonal antibodies is another issue since a high degree of purification and low degree of contamination is necessary before approval. Finally, a major limitation is the stability of the mammalian cells expressing the immunoglobulin (7).

TABLE 32.2 Proposed Human Plasma Clearance of Different Antibody Molecules[a]

Antibody molecule	Molecular mass (kDa)	Relative plasma clearance (CL)
Native intact human IgG	150	≈21 days
Fully human/humanized	150	↓
Chimeric human–mouse IgG	150	↓
Whole mouse IgG	150	↓
$F(ab')_2$	110	↓
Fab′	50	↓
Single-chain Fv (scFv)	25	≈1 day

[a] Adapted from Iznaga-Escobar N *et al*. Methods Find Exp Clin Pharmacol 2004;26:123–7.

Pharmacokinetic Properties of Monoclonal Antibodies

Many of the factors affecting the PK of mABs are similar to those affecting other macromolecules, and these principles are explored in the following sections. However, the optimal mAB dose and schedule also are determined by several additional factors, such as the avidity of the antibody and the specific antibody–antigen system, the species being treated with the mAB, and the mAB itself. Dose selection influences mAB distribution into organs and tissues and liver uptake. With increasing dose, saturation of binding sites, including nonspecific binding, is expected to occur, resulting in decreased clearance and greater availability of the antibody to the target. The approved mABs listed in Table 32.1 have diverse pharmacokinetic properties. For example, Avastin claims linear pharmacokinetics in a dose range of 1–10 mg/kg while Erbitux demonstrates nonlinearity at doses greater than 200 mg/m^2.

The most characteristic features of monoclonal antibodies are their low blood clearance and prolonged elimination half-life. It has been demonstrated for both intact mABs and fragments that clearance is inversely related to molecular size (Table 32.2) (10, 11). Detailed investigations have been undertaken to explore the specific Ig structures that may be affect clearance and half-life. In particular, the Fc receptor, FcRn, has been shown to play an important role in determining Ig half-life, and specific sequences in the C_{H2} and C_{H3} regions of IgG regulate clearance rate through their interaction with FcRn (12).

There are disadvantages to the prolonged half-life exhibited by intact mABs. For example, those with the longest half-lives and lowest clearance rates diffuse poorly across tumor membranes. This feature can result in significant exposure to normal tissues and organs when effective antitumor doses are administered. In contrast, scFv fragments, one of the smallest functional modules of antibodies, have more rapid clearance and better penetration of tumor mass than do intact mABs, yet retain high-affinity binding (Table 32.3) (12). Also, tumor-to-blood concentration ratios appear to be higher and less heterogeneous with multivalent scFvs than with intact antibody. $F(ab)_2$ elimination clearance appears to be similar to intact IgG but with a faster distribution to tissues from blood and a higher uptake in kidneys. Other fragments, such as Fab′, $sc(Fv)_2$, $(scFv)_2$, and scFv, have lower uptake in tissues due to their rapid elimination. For example, approximately 90% of scFvs are cleared from body in 24 hours.

As noted earlier, the earliest mABs were derived entirely from mouse proteins and caused highly immunogenic reactions in patients. This reaction, the HAMA response, was against both the constant and the variable regions of the proteins. In addition to the signs and symptoms of the HAMA response that included the classic allergic hallmarks of urticaria, anaphylaxis, and fever, this response resulted in attenuated mAB activity due to the formation of neutralizing antibodies and rapid clearance of the resulting immune complex. Although the HAMA response has been mitigated by the development of humanized or fully human antibodies, these antibodies can elicit antiallotypic or anti-idiotypic antibody responses (11).

TABLE 32.3 Tumor, Kidney, and Blood Distribution, as Percentage of Dose per Gram of Iodinated Antibody Fragments of CC49[a]

Antibody fragment	Tissue	Time (hr)				
		0.5	4.0	24.0	48.0	72.0
scFv	Tumor	4.74	2.93	1.06	0.72	0.27
	Blood	4.66	1.32	0.06	0.04	0.05
	Kidneys	41.24	2.65	0.15	0.07	0.06
$(scFv)_2$	Tumor	5.94	6.91	4.29	2.56	1.92
	Blood	19.27	2.56	0.10	0.07	0.07
	Kidneys	32.83	2.93	0.42	0.13	0.08
$sc(Fv)_2$	Tumor	6.12	6.78	4.29	2.62	1.94
	Blood	18.30	2.17	0.07	0.06	0.07
	Kidneys	27.85	2.32	0.36	0.12	0.07
Fab′	Tumor	4.87	5.91	2.96	2.15	ND[b]
	Blood	9.63	2.38	0.1	0.06	ND
	Kidneys	138.34	21.50	0.37	0.16	ND
$F(ab')_2$	Tumor	14.63	25.82	28.06	19.42	13.11
	Blood	30.15	16.32	1.68	0.36	0.16
	Kidneys	11.48	9.78	2.10	0.52	0.25
IgG	Tumor	8.95	30.66	37.83	42.42	ND
	Blood	28.32	24.20	11.01	5.34	ND
	Kidneys	7.0	5.29	2.19	1.18	ND

[a] Adapted from Colcher D *et al.* Ann NY Acad Sci 1999;880:263–80.
[b] ND, Not determined.

Assay of Macromolecules

The most common types of assays employed to quantitate protein concentrations in biological matrices are listed in Table 32.4. Enzyme-linked immunosorbent assays (ELISAs), radioimmunoassays (RIAs), and immunoradiometric assays (IRMAs) require protein-specific antibodies, labeled proteins, or labeled antibodies as reagents, and are generally competitive inhibition assays. Radioimmunoassays measure concentrations by displacing ligands from cell-bound receptors. The most common assay, the ELISA, is based on antibody recognition of an antigenic epitope (i.e., a molecular region on the surface of a molecule capable of binding to the specific antibody).

TABLE 32.4 Examples of Immunoassays Used to Quantitate Macromolecules

Assay acronym	Assay description
ELISA	Enzyme-linked immunosorbent assay
RIA	Radioimmunoassay
IRMA	Immunoradiometric assay
RRA	Radioreceptor assay

These assays only have a limited ability to quantify proteins. Their limitations include lack of sensitivity of the antibody reagents such that the level of quantitation is near the lower limit of the assay's sensitivity. It is often difficult or impossible to detect fragments of degraded protein. But because immunoassays measure immunoreactivity, they may also detect immunoreactive macromolecule fragments, (i.e., peptides) without providing information on whether or not the fragment is biologically active. In some cases, the fragment containing the epitope is captured but is interpreted as total protein. In determining concentrations of monoclonal antibodies, dilution may be problematic if the assay is measuring free antibody (i.e., the capture and detection antibodies are the same). In this case, dilution may result in dissociation of the antibody.

Interspecies Scaling of Macromolecules: Predictions in Humans

As discussed in Chapter 30 and elsewhere (13), interspecies scaling is based upon allometry (an empirical approach) or physiology. Protein pharmacokinetic parameters such as volume of distribution (V_d), elimination half-life ($t_{1/2}$), and elimination clearance (CL) have been scaled across species using the standard allometric equation (14):

$$Y = aW^b \tag{32.1}$$

In this equation, Y is the parameter of interest, the coefficient a is the value of the parameter at one unit of body weight, W is body weight, and b is the allometric exponent. For convenience, this equation is linearized to

$$\log Y = \log a + b \log W \tag{32.2}$$

In this form, $\log a$ is the y-intercept and b is the slope of the line. In Figure 32.3, representative linearized plots of CL and initial volume of distribution (V_1) are shown for recombinant growth hormone (GH) across four species.

Allometric equations for V_1 and CL for some representative macromolecules are depicted in Table 32.5. The theoretical exponent approximations for V_1 (mL) and CL (mL/min) are $aW^{0.8}$–$aW^{1.0}$ and $aW^{0.6}$–$aW^{0.8}$, respectively. Parameter estimates can be normalized for body weight simply by subtracting 1.0 from the exponent.

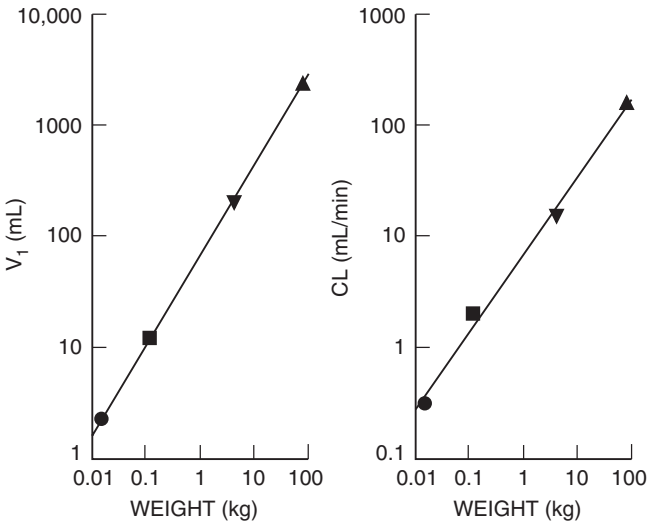

FIGURE 32.3 Log–log plots of V_1 and *CL* versus body weight for recombinant human growth hormone: mouse (●), rat (■), cynomolgus monkey (▼), human (▲). (Reproduced with permission from Mordenti J *et al*. Pharm Res 1991;8:1351–9.)

In Table 32.6 the predicted parameter estimates derived from the allometric equations in Table 32.5 are compared with the corresponding parameter estimates reported in humans. The observed values of V_1 for the macromolecules listed fall within the expected range of observed results. However, the observed clearances of Factor IX (FIX) and interleukin-12 (IL-12) were not predicted from allometry. Factors such as species specificity in the endothelial binding of FIX (22) or saturation of clearance mechanisms may account for the inability to predict these parameters in humans.

Allometric scaling has been applied to mABs (23). Duconge and co-workers conducted PK studies of anti-epidermal growth factor (EGF) receptor in mice, rats, rabbits, and dogs after a single administration of 16, 8, 1.5, and 0.2 mg/kg, respectively, of the murine mAB ior EGF/r[3]. Three female patients with non-small-cell lung cancer were also studied. They were participating in a Phase I trial and received a single IV infusion of 400 mg. EGF concentrations were analyzed either by a radioreceptor assay (mice and rats) or a sandwich ELISA method (rabbits, dogs, and humans). The allometric equations for V_d and *CL* were calculated according to the standard methods and with incorporation of the complex Dedrick plot. The results of the allometric analysis are shown in Table 32.7. A comparison between the predicted and calculated PK parameters in cancer patients is shown in Table 32.8. The actual clearance in patients with cancer was fourfold greater than the predicted value. The authors proposed that variation may suggest that other drug clearance processes occur in patients with cancer but that would not be present in healthy subjects or predicted by studying normal animals. Even with this disparate result, the authors used the scaling factor for clearance (0.85) to assist in the design of dose regimens for a clinical trial (24).

Factors to be considered in deciding whether or not interspecies scaling would be predictive of human PK parameter estimates include (1) binding characteristics, (2) receptor density, (3) size and charge of molecule, (4) end-terminal carbohydrate characteristics, (5) degree of sialylation, and (6) saturation of elimination pathways. These factors are known to influence clearance and distribution volumes, as will be discussed in subsequent sections. For example, clearance may involve several mechanisms, including immune-mediated clearance that results in nonconstant clearance rates. The interspecies predictability of clearance in this situation would be questionable.

In spite of the limitations, interspecies scaling can be used to relate dosages across species in toxicology studies, to predict human PK parameter estimates for macromolecules, and, as discussed in Chapters 30 and 31, to guide dose selection in Phase I clinical trials. An understanding of the characteristics of the macromolecule is important for the interpretation and application of these results.

TABLE 32.5 Allometric Equations for Representative Macromolecules

	Allometric equations		
Macromolecule	**V_1 (mL)**	***CL* (mL/hr)**	**Ref.**
Factor IX[a]	$87W^{1.26}$	$14W^{0.68}$	15, 16[b]
Factor VIII[a]	$44W^{1.04}$	$10W^{0.69}$	17
Interleukin-12[a]	$65W^{0.85}$	$8W^{0.62}$	18, 19[b]
Growth hormone[c]	$68W^{0.83}$	$7W^{0.71}$	14
Tissue plasminogen activator[c]	$91W^{0.93}$	$17W^{0.84}$	14

[a] Based on parameter estimates in at least two species.
[b] Allometric equations determined from pharmacokinetic parameter estimates reported in published literature.
[c] Based on parameter estimates in at least four species.

PHARMACOKINETIC CHARACTERISTICS OF MACROMOLECULES

Endogenous Concentrations

Unlike chemically synthesized molecules, many of the macromolecules currently marketed or under investigation are naturally occurring substances in the body. This presents some unique challenges for

TABLE 32.6 Prediction of Human Pharmacokinetic Parameters Based on Allometric Scaling

	V_1			CL			
Macromolecule	**Predicted (mL)**	**Observed (mL)**	**Expected range[a] (mL/kg)**	**Predicted (mL/hr)**	**Observed (mL/hr)**	**Expected range[a] (mL/hr)**	**Ref.**
FIX	18380	10150[b]	9190–27570	248	434[b]	124–372	20
Factor VIII	3617	3030	1809–5426	195	174	98–293	17
Interleukin-12	2406	3360	1203–3609	113	406	57–170	21
Growth hormone	2243	2432	1122–3365	148	175	74–222	14
Recombinant tissue plasminogen activator	5814	4450	2907–8721	646	620	323–969	14

[a] For comparison with observed results, an expected range is chosen that is 0.5 to 1.5 times the predicted value.
[b] Calculated from Figure 1 of White G *et al*. Semin Hematol 1998;35(suppl 2):33–8.

estimating pharmacokinetic parameters. Most commercially available ELISAs used to quantitate exogenously administered proteins do not distinguish between the native protein in the body and the exogenously administered protein. Clearly, concentrations of endogenous proteins, which can fluctuate because of stimulation or feedback control [e.g. insulin-like growth factor-1 (IGF-1)], can result in erroneous parameter estimates. There are several approaches to deal with the problem posed by detectable endogenous protein concentrations.

In a study by Cheung *et al*. (25), the investigators administered erythropoietin subcutaneously to 30 healthy volunteers. Blood sampling times included a pre-dose sample and samples collected multiple times postadministration. Erythropoietin was detected in all subjects in the pre-dose sample. In general, all detected concentrations were in the physiological range (< 7 to 30 IU/mL) with one exception: an individual whose baseline erythropoietin concentration was 48 IU/mL, exceeding the normal physiologic range. Prior to estimating PK parameters, the investigators subtracted each pre-dose concentration from all concentrations detected postadministration. The underlying assumption for this approach was that the low endogenous concentrations remained relatively stable over the postadministration times. However, data were not presented to confirm or refute this assumption.

Another approach for dealing with this problem is proposed by Veldhuis and colleagues (26) for GH. A deconvolution method is employed to minimize the influence of circulating endogenous GH on PK parameter estimates derived from exogenously administered growth hormone. In this method, the 24-hour secretory rate of GH is estimated by approximating endogenous plasma GH concentration data with cubic spline smoothing controlled by setting a maximum limit for the weighted residual square sum (27). Patient-specific parameters can be estimated from individual endogenous hormone concentrations or from group means. An example of this kind of analysis is shown in Figure 32.4.

Another option is to estimate PK parameters from the sum of exogenous and endogenous protein concentrations detected after the exogenous administration of the protein. The basic assumption is that the PK parameter estimates are not significantly altered by the presence of endogenous protein concentrations. This generally is true in the very early part of the concentration-vs-time profile when the endogenous concentration may represent less than 10% of the total concentration. However, in the example depicted in Figure 32.5 (28), endogenous concentrations are oscillating and pulsatile, reaching peaks during the

TABLE 32.7 Allometric Equations for EGF mAB PK Parameters[a]

Parameter (Y)	**Coefficient (a)**	**Exponent (b)**	**r**
V_d (mL)	219	0.84	0.92
CL (mL/hr)	4.07	0.85	0.94

[a] Adapted from Duconge J *et al*. Biopharm Drug Dispos 2004; 25:177–86.

TABLE 32.8 Comparison between the Predicted EGF PK Parameters from the Allometric Equations and Estimated PK Parameters Determined in Cancer Patients

Parameter (Y)	**Predicted PK parameter estimate[a]**	**Estimated PK parameter in cancer patients**
V_d (L/kg)	0.01	0.04
CL (mL/hr/kg)	0.22	0.98

[a] Determined from the allometric equations in Table 7, Duconge J *et al*. Biopharm Drug Dispos 2004;25:177–86.

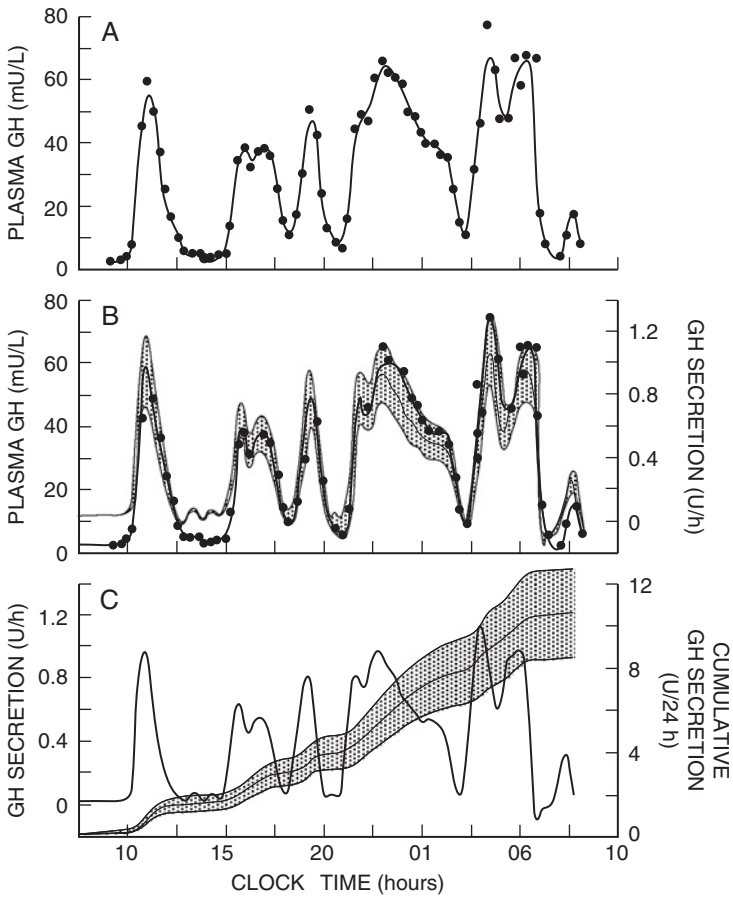

FIGURE 32.4 Analysis of plasma growth hormone (GH) concentration profile by a model-based deconvolution technique. (A) Observed concentrations (●) fitted by a spline approximation curve. (B) Plasma GH concentrations (●) and calculated GH secretory rate with 95% confidence limits (*line and stippled area*). (C) GH secretion (*thin line*) and cumulative secretion with 95% confidence limits (*line and stippled area*). (Reproduced with permission from Albertsson-Wikland K *et al.* Am J Physiol 1989;257:E809–14.)

sampling period that are greater than 100-fold the initial basal values. This illustrates how changes in endogenous protein concentrations over the sampling period can influence model fits and confound PK parameter estimation.

Finally, a crossover study design can be employed such that study participants are randomized to placebo or treatment on one occasion and to the alternate regimen on a second occasion, assuring an adequate washout period between the two occasions. The endogenous concentrations determined in the same persons after placebo administration can be subtracted from the matching sample collected after treatment administration. This design accommodates the intraperson variability and variations in endogenous concentrations due to pulsatile secretion, but assumes that the two separate study days are similar.

Thus, it is important to recognize that current analytical methods cannot distinguish endogenous protein concentrations from exogenous concentrations. Administering radiolabeled proteins would allow for exogenous and endogenous proteins to be distinguished, but there are experimental limitations to the use of radiolabeled proteins. Although the accuracy of PK parameter estimation may be impacted by the presence of endogenous concentrations, study designs and data analysis methods can be employed that take endogenous concentration into consideration.

Absorption

The absolute bioavailability of representative macromolecules following extravascular administration is shown in Table 32.9. It is apparent that

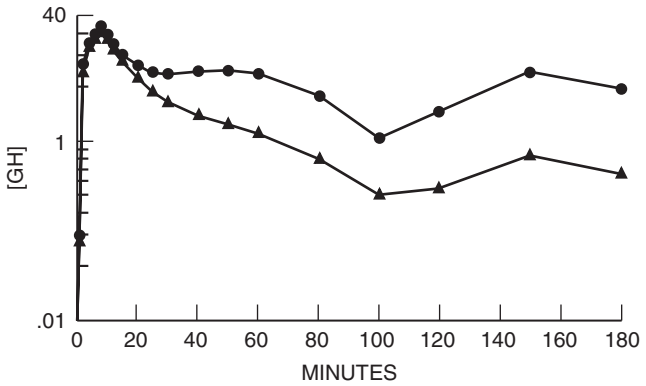

FIGURE 32.5 Simulated effects of increasing basal growth hormone (GH) concentrations on measured total GH concentrations at various times during and after an 8-minute infusion of rhGH using basal concentrations 10 times (▲) and 100 times (●) the observed preinfusion value of 0.042 ng/mL. (Reproduced with permission from Bright GM *et al.* J Clin Endocrinol Metab 1999;84:3301–5.)

bioavailability is variable with the different molecules and with different routes of administration, reflecting individual molecule characteristics. In addition, in one report the bioavailability after subcutaneous (SC) or intramuscular (IM) administration was greater than 100% relative to an intravenous (IV) bolus injection (32). This implausible result may reflect the inability of the immunoradiometric assay to distinguish proteolytic fragments of interferon α (IFNα) from the intact molecule, the slow absorption phase of either the SC or IM routes, or a saturable elimination process. The authors did not elucidate which of these factors might have contributed to their observation.

Flip-flop Pharmacokinetics of Macromolecules

When the absorption rate constant, k_a, is greater than the elimination rate constant, k_e, elimination of the molecule from the body is the rate-limiting step and the terminal portion of the concentration–time curve is primarily determined by the elimination rate. However, as discussed in Chapter 4, if k_a is less than k_e, absorption is rate limiting and the terminal part of the curve reflects the absorption rate. This phenomenon is illustrated for several molecules in Table 32.10.

In the absence of concentration–time profiles after IV administration, it is impossible to estimate the actual elimination rate constant, and the interpretation of absorption and elimination rates after SC administration of macromolecules must be done cautiously. It is for this reason surprising that so few published pharmacokinetic studies include IV administration to assess whether or not the macromolecule follows flip-flop pharmacokinetics.

TABLE 32.9 Bioavailability of Macromolecules after Extravascular Routes of Administration

	Route of administration[a]			
Macromolecule	**SC**	**IP**	**Other**	**Ref.**
Erythropoietin	22.0%	2.9%	—	29
Granulocyte–macrophage colony-stimulating factor	83.0%	—	—	30
Growth hormone	49.5%	—	7.8–9.9%[b]	31
Interferon α_{2b}	>100%	42.0%	>100%[c]	32, 33
Interleukin-11	65%	—	—	34

[a] SC, Subcutaneous; IP, intraperitoneal.
[b] Nasal administration.
[c] Intramuscular administration.

Factors Affecting Absorption from Subcutaneous Sites

Two very important principles on the absorption of macromolecules after SC administration were elucidated by Supersaxo *et al.* (38). First, in the range of the molecular weight (246–19,000) of the various molecules tested, there was a linear relationship between molecular weight and absorption by the lymphatic system (Figure 32.6). Second, the authors concluded that molecules with a molecular weight greater than 16,000 are absorbed mainly by the lymphatic system that drains the SC site of injection, whereas molecules with a molecular weight of less than 1000 are absorbed almost entirely by blood capillaries. The authors hypothesized that macromolecules are absorbed preferentially by lymphatic rather than blood capillaries because lymphatic capillaries lack the subendothelial basement membrane present in continuous blood capillaries, and also may have 20- to 100-nm gaps between adjacent endothelial cells.

In addition to molecular weight, injection site may influence the absorption of macromolecules after SC administration. For example, the absorption half-life was significantly longer, 14.9 vs 12.3 hours, after injection of recombinant human erythropoeitin (rhEPO) into the thigh than after injection into the abdomen (39). Also, the concentration-vs-time profile, after rhEPO injection into the thigh, displayed a double peak that was more pronounced than after the abdominal injection (Figure 32.7). No statistically significant differences were observed in the area under the curve [AUC (5684 vs 6185 U·hr/L)], in the maximum concentration [C_{max} (175 vs 212 U/L)], or in the time of maximum concentration (t_{max} = 10 hr) for thigh vs abdomen, respectively.

TABLE 32.10 Absorption and Apparent Elimination Rates of Macromolecules after SC and IV Administration

Macromolecule	Route of administration	k_a (hr^{-1})	Apparent k_e (hr^{-1})	Ref.
Growth hormone	SC	0.23 ± 0.04	0.43 ± 0.05	35
	IV	—	2.58	28
Interferon α_{2b}	SC	0.24	0.13	32
	IV	—	0.42	
Erythropoietin	SC	0.0403 ± 0.002	0.206 ± 0.004	36
	IV	—	0.077	37

In another study, recombinant human GH was absorbed faster after SC injection into the abdomen compared with the absorption after SC injection into the thigh (40). C_{max} was higher (29.7 ± 4.8 mU/L) and t_{max} was faster (4.3 ± 0.5 hr) after injection into the abdomen than after injection into the thigh (23.2 ± 3.9 mU/L and 5.9 ± 0.4 hr, respectively). However, mean IGF-1 and insulin-like growth factor-binding protein 1 (IGFBP-1) concentrations, a pharmacodynamic marker of GH, were unaffected by the site of injection. Other effects independent of injection site were blood glucose, serum insulin, and glucagon levels. Thus absorption differences may be related to lymphatic drainage of the two injection sites and may depend on differences in lymph flow. However, for both recombinant erythropoeitin and GH, site of injection is clinically irrelevant.

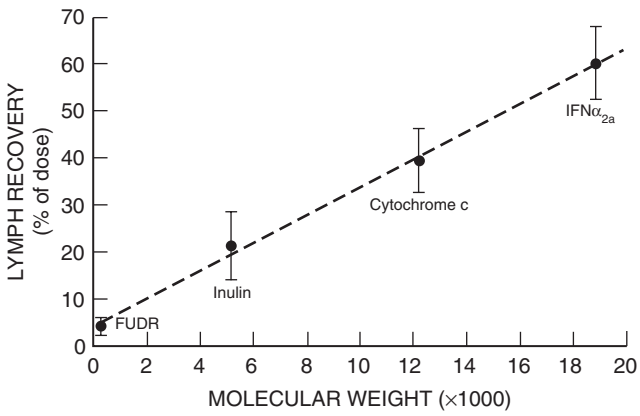

FIGURE 32.6 Correlation between molecular weight (MW) and cumulative recovery of IFNα_{2a} (MW 19,000), cytochrome *c* (MW 12,300), inulin (MW 5200), and 5-fluoro-2′-deoxyuridine (FUDR; MW 246.2) in the efferent lymph from the right popliteal lymph node following SC administration into the lower part of the right hind leg of sheep. Each point and bar show the mean and standard deviation of three experiments performed in three separate sheep. The line drawn represents a least-squares fit of the data ($r = 0.988$, $P < 0.01$). (Reproduced with permission from Supersaxo A *et al.* Pharm Res 1990;7:167–9.)

In summary, molecular weight and site of injection are two factors that may affect the absorption characteristics of macromolecules, and should be considered both in clinical trials and when treating patients.

Distribution

As discussed in Chapter 3, proteins and mABs distribute initially into the plasma volume and then more slowly into the interstitial fluid space. It can be seen from Table 32.11 that the initial distribution volume of interleukin-2 (IL-2) IL-12, granulocyte colony-stimulating factor (G-CSF), and recombinant tissue plasminogen activator (rt-PA) approximates that of plasma volume. In contrast, the initial distribution volume of FIX is approximately twice that of plasma volume. On the other hand, the volumes of distribution at steady state ($V_{d(ss)}$) for IL-12, G-CSF, and rt-PA are considerably smaller than is the $V_{d(ss)}$ of inulin, a marker for extracellular fluid space (ECF). When distribution volume estimates are much less than expected values for ECF, they could reflect the slow transport of large molecules across membranes and the fact that either assay sensitivity or sampling time has been inadequate to characterize the true elimination phase of the compound.

The issue of inadequate sampling time is exemplified by monoclonal antibodies. As shown in Table 32.12, the V_1 and V_{ss} are similar and are similar in size to a vascular space of 2–3 L/m^2. It is also important to note that for the most part, in the studies submitted to support New Drug Application (NDA) approval, V_{ss} was determined with methods assuming linear, first-order kinetics, and clearly this is not the case for the majority of the monoclonal antibodies currently marketed, such as cetuximab (Erbitux). In fact, the use of noncompartmental methods to describe the pharmacokinetics of mABs oversimplifies their complex properties.

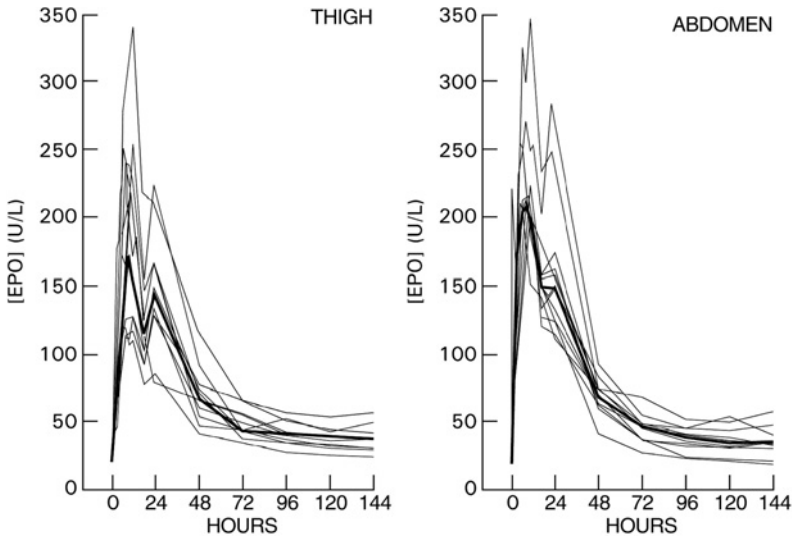

FIGURE 32.7 Serum erythropoietin (EPO) concentrations as a function of time after SC injection of 100 U/kg of recombinant human erythropoietin in the thigh and abdomen of 11 healthy volunteers. The bold curve represents the median. (Reproduced with permission from Jensen JD *et al*. Eur J Clin Pharmacol 1994;46:333–7.)

Binding to α_2-Macroglobulin

α_2-Macroglobulin, one of the major proteins in the serum, is highly conserved across species and can bind many molecules, such as cytokines, enzymes, lipopolysaccharide (LPS), and ions such as zinc and nickel (48). α_2-Macroglobulin is found in extravascular secretions, such as lymph. It exists in two forms, a slow native form and a fast form, the latter being an α_2-Macroglobulin–protease complex that results in a conformational change that increases electrophoretic mobility. This conformational change results in exposure of a hydrophobic region that can bind to cell surface receptors such as those on hepatocytes.

TABLE 32.11 Distribution Volume of Representative Macromolecules

Macromolecule	MW (×1000)	V_1 (mL/kg)	$V_{d(ss)}$ (mL/kg)	Ref.
Inulin	5.2	55	164	41
Factor IX	57	136[a]	271[a]	20
Interleukin-2	15.5	60	112	42, 43
Interleukin-12 (IL-12)	53	52	59	21
Granulocyte colony-stimulating factor	20	44	60	44, 45
Recombinant tissue plasminogen activator	65	59	106	46

[a] Calculated from Figure 1 of White G *et al*. Semin Hematol 1998; 35(suppl 2):33–8.

There is a growing body of evidence suggesting that α_2-Macroglobulin plays an important role in human immune function. Specifically, studies have shown that the fast form can inhibit antibody-dependent cellular toxicity and natural killer (NK) cell-mediated cytolysis (49), as well as superoxide production by activated macrophages (50).

TABLE 32.12 Pharmacokinetics of Marketed Monoclonal Antibodies

mABs	Molecular weight (×1000)	$T^a_{1/2}$ (days)	V^a_1 (L)	V^a_{ss}
Avastin	149	13–15	3	3.5–4.5 L
Erbitux	152	ND[b]	2.7–3.4	2–3 L/m^2
Raptiva	150	6–7.5[c]	NR[d]	9 L[e]
Humira	148	12–18	3	5 L
Campath	150	1–14[f]	NR[d]	7–28 L

[a] All values extracted from the Summary Basis for Approval review posted on http://www.accessdata.fda.gov/scripts/cder/drugsatfda.

[b] Used clearance instead of $T_{1/2}$ since it has nonlinear PK at dosages greater than 200 mg/m^2.

[c] Average $T_{1/2}$ based on noncompartmental methods and after subcutaneous administration [see Ref. (47)].

[d] NR, Not reported.

[e] Calculated as V/F.

[f] Campath has nonlinear PK in the range of 3–30 mg three times weekly.

TABLE 32.13 Binding of Macromolecules to α_2-Macroglobulin

Macromolecule	Physiological effect	Relevance of binding
Nerve growth factor	Stimulates nerve growth	Interferes with assay
Interleukin-1	Regulates proliferation of thymocytes	Regulates cell activity
Interleukin-2	Impairs proliferation of T-cells	Inactivates cytokine
Tissue growth factor-β	Stimulates growth of kidney fibroblasts	Functions as carrier; accelerates clearance

As shown in Table 32.13, α_2-macroglobulin can bind to exogenously administered proteins. Three different mechanisms for this binding have been identified (51). The binding can be noncovalent and reversible. An example of this type of binding is seen with growth factors such as tissue growth factor-β (TGF-β). Second, the binding to α_2-macroglobulin can be covalent, and the third mechanism involves covalent linkages with proteinase reactions. Subsequent to the binding, the pharmacokinetics and pharmacodynamic properties of the macromolecule may be altered. The binding of α_2-macroglobulin is associated with variable results: the α_2-macroglobulin–cytokine complex may interfere with bioassay results (e.g., nerve growth factor) (52), may serve as a carrier (e.g., TGF-β) (51), may prevent proteolytic degradation (e.g., IL-2) (53), or may enhance removal of the protein from the circulation (e.g., tissue necrosis factor-α) (54).

Binding to Other Proteins

Insulin-like growth factor-1 is produced by many tissues in the body and it has approximately 50% structural homology with insulin. In plasma, IGF-1 exists as "free" IGF-1 and "bound" IGF-1. Its physiology is very complex, as depicted in Figure 32.8 and discussed further in the section on pharmacodynamics (55). To date, eight binding proteins (designated IGFBP-1 through -8) have been identified, with IGFBP-3 the most abundant. The binding proteins vary in molecular weight, distribution, concentration in biological fluids, and binding affinity (56). It is important to note that the interactions between the binding proteins and their physiologic role are poorly understood, but probably serve to modulate the clearance of IGF-1.

Metabolism

Table 32.14 summarizes the effects of various cytokines on the cytochrome P450 (CYP) mixed-function oxidase system (57). With the exception of IL-2, these cytokines depress the activity of CYP enzymes. Data on cytokine-mediated depression of drug-metabolizing ability has been obtained primarily in rodents under conditions of inflammation or infection (58). The reduction in drug biotransformation capacity parallels a decrease in total CYP content

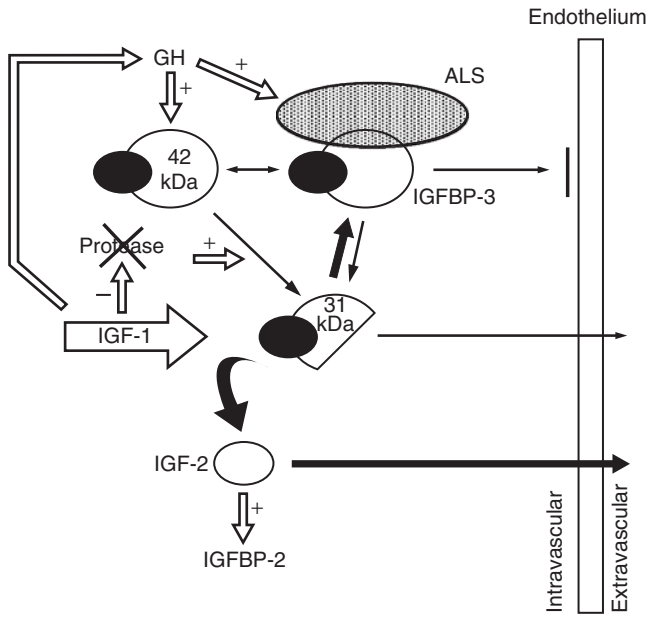

FIGURE 32.8 Hypothetical model of the effects of insulin-like growth factor-1 (IGF-1). Open arrows show regulating influences. Plasma IGF-1 consists of free and bound IGF-1. Insulin-like growth factor-binding protein-3 (IGFBP-3) exists in two forms, a 42-kDa complete form or a 31-kDa fragment. IGF-1 drives the reaction toward binding with the acid-labile subunit (ALS) to form a ternary complex, which is retained in the intravascular space. IFG-1 also suppresses growth hormone (GH) secretion, decreasing the synthesis of IGFBP-3. (Reproduced with permission from Blum WF *et al.* Acta Paediatr Suppl 1993;82(suppl 391):15–9.)

TABLE 32.14 Effect of Various Macromolecules on P450 Isoenzymes

Macromolecule	Isoenzyme	Effects
Interferon α	CYP2C11	Decreased mRNA and enzyme levels
Interleukin-1	CYP2C11	Decreased mRNA and enzyme levels
Interleukin-2	CYP2D	Decreased mRNA and enzyme levels
Interleukin-6	CYP2D1	Increased mRNA and enzyme levels
Tumor necrosis factor	CYP2C11	Decreased mRNA and enzyme levels
	CYP2C11	Decreased enzyme levels

and enzyme activity, and is due primarily to a down-regulation of CYP gene transcription, but modulation of RNA and enzyme inhibition may also be involved (58, 59).

As shown in Table 32.14, the expression of CYP2C11 and CYP2D isoenzymes is frequently suppressed by cytokines. These two CYP gene families are constitutively expressed in male and female rats. In the rat, CYP2C is under developmental and pituitary hormone regulation. Although there is approximately 70% cDNA-deduced amino acid sequence homology with the human CYP2C, caution is needed in extrapolating these observations on CYP2C regulation in rats to humans (59). In both rats and humans, there is polymorphic expression of the CYP2D and CYP2D1 isoenzymes, which exhibit debrisoquine 4-hydroxylase activity. However, this gene family has evolved differently in rats than in humans. Specifically, the rat has four genes that are approximately 73–80% similar while the human has three genes that are 89–95% similar. Thus, results in rat studies may not be predictive of results in humans because of the difference in number of genes, their regulation, and their complexity (60).

In vitro study results have been consistent with those obtained *in vivo*. For example, in primary rat hepatocyte cultures, IL-1, tumor necrosis factor (TNF), and interleukin-6 (IL-6) concentrations ranging from 0.5 to 10.0 ng/mL suppressed the expression of CYP2C11 mRNA (59). It is interesting to note that in rat liver microsomes, IL-2 increased both the amount of immunoreactive CYP2D protein and its mRNA (61). In human primary hepatocytes, IL-1β, Il-6, and TNF-α caused a decrease in all mRNAs and CYP isoenzyme activities. Moreover, interferon γ (IFNγ) was shown to decrease CYP1D2 and CYP2E1 mRNA, but had no effect on CYP2C or CYP3A mRNAs (57).

The clinical significance of the aforementioned findings is unknown. A report by Khakoo *et al.* (62) did not demonstrate a pharmacokinetic interaction between IFNα_{2b} and ribavirin or an additive effect of the combination therapy on safety assessments. In another study, administration of IFNα prior to the administration of cyclophosphamide significantly impaired the metabolism of cyclophosphamide and 4 hydroxycyclophosphamide. In contrast, the administration of IFNα after cyclophosphamide resulted in higher 4-hydroxycyclophosphamide concentrations and produced a significant decrease in leukocyte count (63).

Finally, the interaction between IL-2 and doxorubicin was explored in patients with advanced solid tumors (64). Doxorubicin was given alone, and then 3 weeks later patients received the combination of rhIL-2 (18 mIU/m^2 given SC on days 1–5) and doxorubicin. Doxorubicin pharmacokinetics were assessed for 48 hours after each administration period. SC injections of rhIL-2 did not affect doxorubicin PK. Doxorubicin, given before IL-2, prevented IL-2-induced lymphocyte rebounds but not did not qualitatively alter nonmajor histocompatibility complex-restricted cytotoxicity. Thus, various cytokines have been shown to affect CYP protein content, mRNA, and enzyme activities. However, there are few reports that evaluate the extent and clinical significance of corresponding PK or PD changes.

Little is known regarding the catabolism of proteins that are either currently marketed or under investigation. The absence of suitable biological assays or other analytical methods for identifying and quantitating protein degradation products obviously limits evaluation of this catabolism. Similarly, the catabolism of mABs (in particular, the catabolism of the Ig molecule) is complex and not well understood (65). mAB catabolism reflects the basal metabolic rate of the body as well as the function of phagocytic cells [monocytes, macrophages of the reticuloendothelial system (RES)]. There is also a relationship between IgG concentration and catabolism that is specific for each IgG molecule — the higher the IgG concentration, the shorter the survival time. To explain this characteristic of immunoglobulins, Brambell *et al.* (66) hypothesized, and Junghans and Anderson (67) have confirmed, that there is a specific, saturable receptor for each immunoglobulin that, when bound, protects the IgG from degradation. The IgG subclasses differ from one another in their amino acid sequence and Fc fragment, with survival half-lives of approximately 20 days for IgG_1, IgG_2, and IgG_4, but 7 days for IgG_3(7). The location and mechanism of IgG metabolism is not known but is believed to involve uptake by pinocytic vacuoles, release of proteolytic enzymes, and subsequent degradation of unbound IgG.

Renal Excretion

The renal excretion of proteins is size dependent and glomerular filtration is rate limiting. It has been suggested that the renal clearance rate of macromolecules, relative to the glomerular filtration rate of inulin, decreases with increasing molecular radius (68). The following general conclusions are based on studies using indirect methods to estimate the glomerular sieving coefficients. Small proteins (<25 kDa) cross the glomerular barrier, and filtration accounts for most of their plasma clearance; the degree of sieving is independent of biologic activity and the filtered load of protein is directly related to plasma concentration. The effect of molecular charge

TABLE 32.15 Cell Surface Receptors for the Clearance of Carbohydrates and Monosaccharides

Specificity[a]	Cell type
Gal/Gal/NAc	Liver parenchymal cells (asialoglycoprotein receptor)
Gal/GalNAc	Liver Kupffer and endothelial cells, peritoneal macrophages
Man/GlcNAc	Liver Kupffer and endothelial cells, peritoneal macrophages
Fuc	Liver Kupffer cells

[a] Abbreviations: Gal, D-galactose; Nac, *N*-acetylglucosamine; Glc, D-glucose; Man, D-mannose; Fuc, fucose.

is negligible for these small proteins, whereas charge retards glomerular filtration of anionic proteins as large as albumin (approximately 70 kDa). Subsequent to glomerular filtration, macromolecules may undergo hydrolysis and tubular reabsorption, mainly in endocytotic vesicles located in the apical regions of renal tubular cells (69).

In addition to physical characteristics, the clearance of rt-PA and other glycoproteins is mediated by cell surface receptors for specific terminal carbohydrates and monosaccharides (Table 32.15). There are at least eight such receptors, the most well known of these being the Ashwell or asialoglycoprotein receptor (70). Once the glycoprotein ligand binds to its receptor, it is internalized by endocytosis and degraded. The degrees of glycosylation, sialylation, or fucosylation are all factors that determine the clearance of these glycoproteins.

Clearance of rt-PA appears to mediated by the mannose/*N*-acetylglucosamine (Man-GlcNAc)-specific receptor on hepatic reticuloendothelial cells. To confirm that the mannose receptor is involved, Lucore *et al.* (71) evaluated the clearance of rt-PA from blood circulation in rabbits. Analysis of sequential blood samples by fibrin autography indicated that circulating free tissue plasminogen activator (t-PA) (approximately 55 kDa) was predominant, but that minimal amounts of high molecular weight complexes of approximately 110 and 170 kDa also were present. Competition experiments were conducted to determine the effect of glycosylation on rt-PA clearance. As shown in Figure 32.9, coadministration of rt-PA with *p*-aminophenyl-α-D-mannopyranoside–bovine serum albumin (BSA-Man) prolonged both the α-phase and β-phase half-lives of rt-PA. The fact that BSA-Man inhibits the clearance of rt-PA suggests that the Man-GlcNAc-specific glycoprotein receptor contributes to its clearance. In contrast, coadministration of rt-PA with asialofetuin did not alter the α-phase and

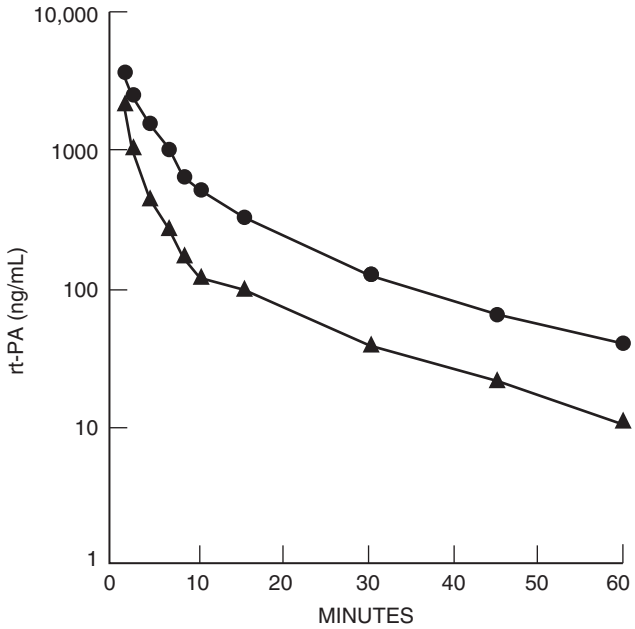

FIGURE 32.9 Clearance of different forms of recombinant tissue plasminogen activator (rt-PA) in rabbits after administration of rt-PA alone (▲) or in combination with *p*-aminophenyl-α-D-mannoside–bovine serum albumin (●). (Reproduced with permission from Lucore CL *et al.* Circulation 1988;77:906–14.)

β-phase half-lives of rt-P, suggesting that the galactose receptor does not mediate clearance. This study demonstrates that the nature and extent of the glycosylation have a direct effect on the clearance of rt-PA and its interaction with the mannose receptors in the liver.

Production of recombinant proteins using Chinese hamster ovary (CHO) cells or other mammalian cells results in a glycosylation pattern that differs from that of recombinant proteins produced by bacteria such as *Escherichia coli* in that CHO-produced proteins are heavily glycosylated whereas those produced by bacteria are not glycosylated. Figure 32.10 depicts the results of an experiment comparing the plasma concentration-vs-time profile of granulocyte–macrophage colony-stimulating factor (GM-CSF) produced by CHO cells with that produced by *E. coli* (72). After intravenous administration, the *E. coli*-produced GM-CSF had a significantly shorter α-phase half-life than did CHO produced GM-CSF, but there was no significant difference in the terminal half-life. The AUC of the glycosylated GM-CSF was approximately four to five times higher (6.3 μg·min/mL) than the AUC of the nonglycosylated product (1.27 μg·min/mL). However, since no difference in neutrophil counts was observed, the choice of one product over the other may only be a theoretical concern.

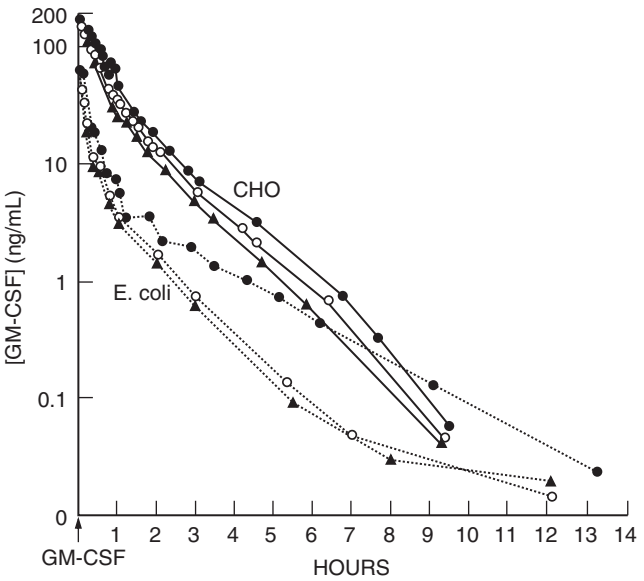

FIGURE 32.10 Granulocyte–macrophage colony-stimulating factor (GM-CSF) serum concentration-vs-time profiles for three patients after IV bolus injection of 8 μg/kg of Chinese hamster ovary (CHO)-produced GM-CSF (*solid lines*), and for three patients who received *E. coli*-produced GM-CSF (*dotted lines*) (one patient received 5.5 μg/kg and two patients received 3 μg/kg). (Reproduced with permission from Hovgaard D *et al.* Eur J Haematol 1993;50:36–6.)

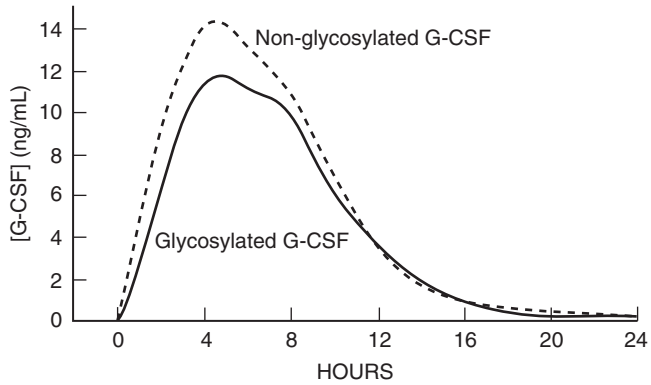

FIGURE 32.11 Comparison of serum concentration-vs-time profiles in healthy volunteers after SC administration of glycosylated granulocyte colony-stimulating factor (G-CSF) (—) and nonglycosylated G-CSF (- - -). (Reproduced with permission from Watts MJ *et al.* Eur J Haematol 1997;98:474–9.)

Similar to GM-CSF, granulocyte colony-stimulating factor (G-CSF) is available as either the glycosylated or nonglycosylated form of the protein. *In vitro* studies suggest that the glycosylated form is more stable and of a higher potency than is the nonglycosylated form (73, 74). The PK of these two forms of G CSF were evaluated in 20 healthy volunteers (75). As shown in Figure 32.11, the nonglycosylated form was more rapidly absorbed after SC administration and produced a higher C_{max} (14.23 vs 11.85 pg/mL), but there was little difference in the elimination-phase half-life (2.75 vs 2.95 hr, respectively). The AUC for the nonglycosylated form was approximately 1.2 times higher than that of the glycosylated form. However, despite these PK differences, the progenitor cell count was significantly higher with the glycosylated product, confirming the *in vitro* potency results.

The results with G-CSF are dissimilar from those produced after IV administration of GM-CSF, where it was found that the C_{max} was higher and the α-phase half-life was longer for the glycosylated than for the nonglycosylated form. The reason for these differences is unknown, but it is apparent that the comparison and subsequent interpretation of study results is dependent on knowing the production source of the protein and the structural features that may influence the potency, PK, and/or PD of individual proteins.

Monoclonal antibody structural features, such as carbohydrate side chains, influence tissue uptake and clearance (11). For example, Morell and colleagues (76) demonstrated that removal of sialic acid residue from the carbohydrate side chain of mouse IgG_1 increased its clearance and shortened its half-life. They also demonstrated increased clearance and liver uptake of asialo-α_2-macroglobulin and asialohaptoglobin.

Finally, clearance may change over time for macromolecules whose clearance is mediated by cell surface receptors and, in the case of mABs, antigens. This is illustrated by an experiment in three patients with metastatic breast cancer who received G-CSF for two consecutive days as a continuous infusion (45). Absolute neutrophil counts were obtained every morning and there was a very strong positive correlation between neutrophil count and G-CSF clearance (Figure 32.12). Clearance on day 2 was 4.6 mL/hr/kg, increasing to 8.3 mL/hr/kg on day 9. Thus, neutrophil production may mediate the clearance of G-CSF.

In summary, there are multiple characteristics of proteins that influence their PK; some of these are listed in Table 32.16.

Application of Sparse Sampling and Population Kinetic Methods

There have been attempts to study the pharmacokinetics of macromolecules by applying the sparse sampling strategy and population kinetic methods described in Chapter 10 (36, 77). In one study, erythropoietin was administered SC to 48 healthy adult male

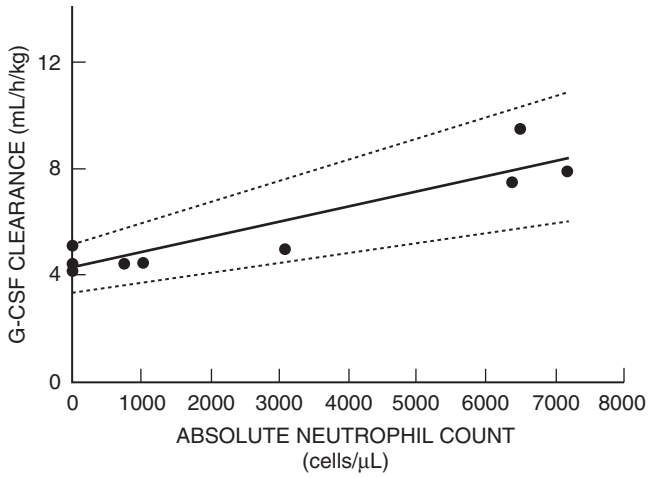

FIGURE 32.12 Relationship between G-CSF clearance and absolute neutrophil count (r = 0.85, P = 0.00025). The dotted lines represent the 95% confidence intervals of the regression. (Reproduced with permission from Ericson SG *et al.* Exp Hematol 1997;25:1313–25.)

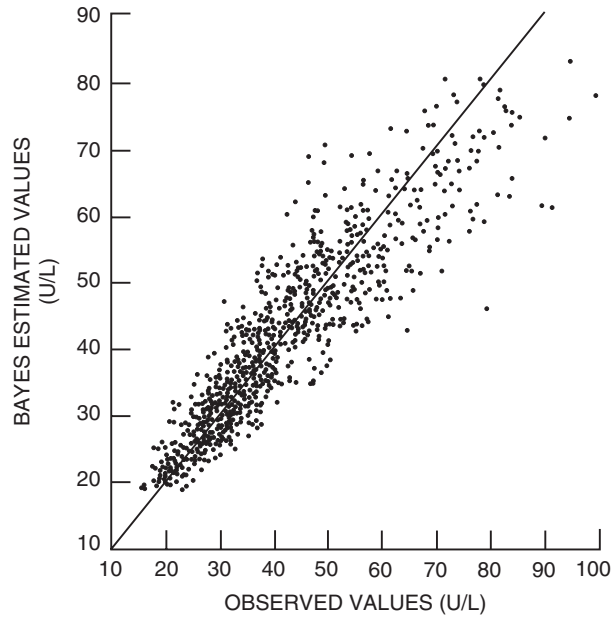

FIGURE 32.13 Correlation between observed and predicted erythropoietin concentration values analyzing sparse sampling data with a population pharmacokinetic model (no r value given). (Reproduced with permission from Hayashi W *et al.* Br J Clin Pharmacol 1998;46:11–9.)

Japanese volunteers (36). The analysis estimated the population mean values of k_a, k_e, V_d, and the endogenous erythropoietin production rate to be 0.043 hr^{-1}, 0.206 hr^{-1}, 3.14 L, and 15.7 IU hr^{-1}, respectively. The good correlation between predicted and observed concentration values shown in Figure 32.13 supports the choice of model, as does the fact that the values for k_e and V_d determined by this analysis were similar to those reported for intravenous erythropoietin with the standard two-stage method of determining population PK parameters (see Chapter 10). However, given the flip-flop PK characteristics of erythropoietin (Table 32.10), the comparison to the IV parameter estimates may be misleading. In fact, the values for k_e estimated by the population PK are dissimilar to those obtained by other authors after SC administration of erythropoietin (25).

Population PK methods also were used to analyze the concentration-vs-time profiles of IFNα in 27 patients with chronic hepatitis C virus infection who received an SC injection of this macromolecule (77). The investigators reported that the absorption rate was best described by two processes: an initial zero-order process, accounting for 24% of net absorption, followed by a first-order process that had a rate constant of 0.18 hr^{-1}. The authors noted that this value for k_a is consistent with the 0.13 hr^{-1}reported by Radwanski *et al.* (33). Both results confirm that IFNα is only slowly absorbed after SC administration.

Last, population pharmacokinetics of sibrotuzumab, a humanized monoclonal antibody directed against fibroblast activation protein (FAP), which is expressed in the stromal fibroblasts in >90% of malignant epithelial tumors, were analzyed in patients with advanced or metastatic carcinoma after multiple IV infusions of doses ranging from 5 mg/m^2 to a maximum of 100 mg (78). The PK model consisted of two distribution compartments with parallel first-order and Michaelis–Menten elimination pathways from the central compartment. Body weight was significantly correlated with both central and peripheral distribution volumes, the first-order elimination clearance, and V_{max} of the Michaelis–Menten pathway. Of interest was the observation that body surface area was inferior to body weight as a covariate in explaining interpatient variability.

TABLE 32.16 Characteristics That Affect the Pharmacokinetics of Macromolecules

Physical characteristics	Size, structure, net charge
Post-translational modifications	Degree of glycosylation, sialylation, fucosylation
Protein binding	Plasma proteins, induced proteins
Route of administration	Transient peaks and troughs, sustained concentrations
Duration of administration	Time-dependent changes in elimination clearance
Frequency of administration	Up- or down-regulation of receptors

PHARMACODYNAMICS

The relationship between circulating protein concentrations following exogenous administration and pharmacodynamic endpoints, either for efficacy or for safety, has been explored for a number of molecules, such as growth hormone, IGF-1, recombinant Factor VIII, interleukins (IL-2, IL-12), and mABs (24). Several conclusions emerge from the currently published data: these relationships are complex and not easily explained by a simple E_{max} model, the endpoints are not clear cut (except for those macromolecules intended to substitute for endogenous proteins that are deficient), and there is a high likelihood of regimen dependency.

Models

Several of the PK/PD models described in Chapter 19 have been employed to explore the relationship between circulating protein concentrations and pharmacodynamic endpoints. For example, a dog model of hemophilia was used to study the activity of recombinant FIX (79). Activity was determined in a bioassay, a modified one-stage partial thromboplastin time assay with pooled human plasma as the internal standard. As shown in Figure 32.14, the relationship between activity and recombinant FIX (BeneFIX) concentration was linear ($r^2 = 0.86$), suggesting that for every 34.5 ng/mL of FIX, there would be a corresponding 1% increase in FIX activity. In 11 males with hemophilia B, it was necessary to use a sigmoid E_{max} model to describe the relationship between FIX activity and concentration (unpublished observations). In this study, FIX serum concentrations of approximately 46 ng/mL were necessary to obtain a 1% increase in FIX activity. This translates into a 20% increase in the dosage of recombinant FIX necessary to achieve the same efficacy.

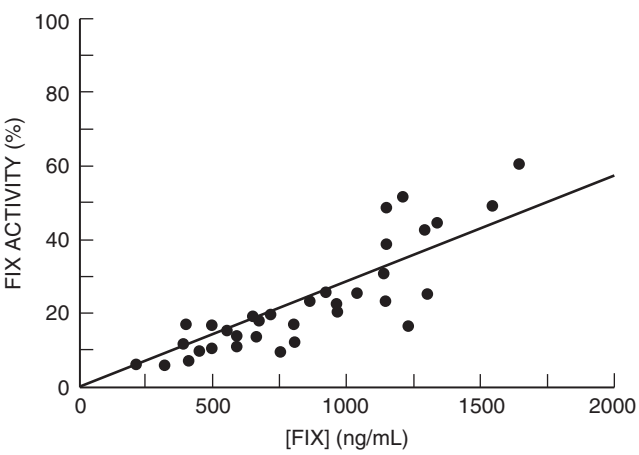

FIGURE 32.14 The relationship between Factor IX (FIX) activity (determined by a modified one-stage partial thromboplastin assay) and FIX concentration in hemophilia B dogs after an infusion of 50 μg/kg FIX over 10 minutes. (Reproduced with permission from Schaub R *et al*. Semin Hematol 1998;35(suppl 2):28–32.)

Figure 32.15 represents a theoretical model of IGF-1 and IGFBPs after intravenous infusion (80). The IGFBPs have a significant role in controlling circulating IGF-1. As shown in Figure 32.8 and Table 32.17, there are three components to the IGFBP complex, which consists of α (acid-labile), β (binding), and γ (growth factor) subunits (81). In addition, GH is involved in regulating IGF-1 (82). The major circulating IGF-1 binding protein, IGFBP3, combines with a glycoprotein known as the acid-labile subunit (ALS) to form a ternary complex of approximately 150 kDa. This complex is retained within the intravascular space, which in turn decreases the clearance of IGFBP-3. IGF-1 also decreases GH secretion thereby reducing the synthesis of IGFBP-3 and the ALS.

Fourteen differential equations were needed to describe the PK and PD interactions of IGF-1 and its binding proteins that are depicted in Figure 32.15. The assumptions were as follows: (1) all IGFBPs exhibit first-order elimination kinetics, (2) binding to the receptor is a first-order process, (3) IGFPBs act as reservoirs for the retention of IGF-1 in the vascular compartment, (4) IGF-1 bound to IGFBPs is excluded from the interstitial fluid space, and (5) the production rates of the IGBPs are invariant over time. There was fairly good agreement between the predicted and observed concentrations of free and bound IGF-1 in plasma. However, there was not good agreement between the predicted and observed concentrations of total IGFBPs in either the 150-kDa or 50-kDa plasma fractions. This disagreement probably is the result of two wrong assumptions: that IGFBPs exhibit first-order elimination kinetics and that IGBP production rates do not vary over time, which only would be the case if IGF-1 did not alter the production rates or if the influence of growth hormone secretion on the production rate of IGFBP-3 was negligible.

To establish the relationship between free IGF-1, binding proteins, and insulin sensitivity, 11 healthy volunteers were given IV glucose (0.3 g/kg) and insulin (0.05 U/kg) at two times, with each administration separated by 20 minutes (83). Blood samples were collected for measurement of free IGF-1, total IGF-1, IGFBP-1, and IGFBP-3. Free IGF-1 decreased by 20% 20 minutes after the first insulin administration and by 35% 20 minutes after the second administration. IFGBP-3 increased to 20% above the basal level,

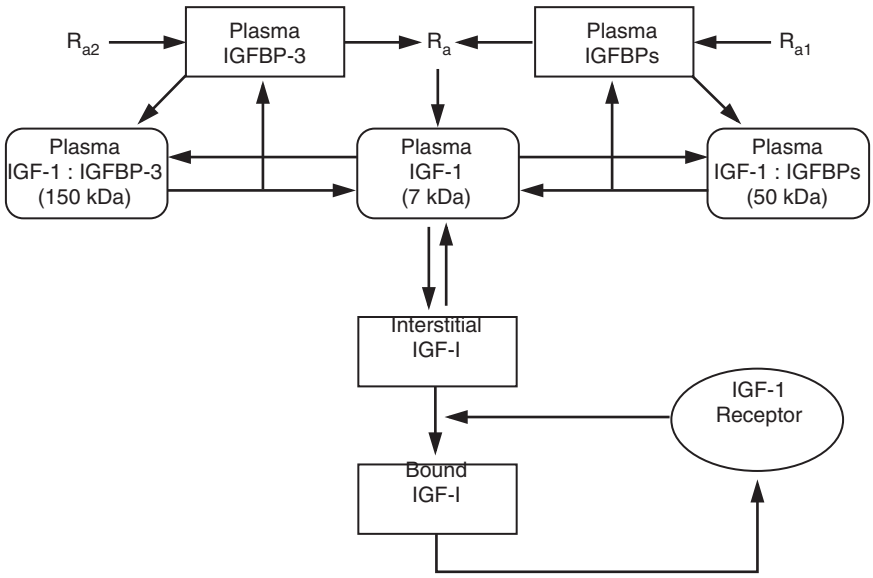

FIGURE 32.15 Theoretical model of IGF-1 pharmacokinetics. Abbreviations: $R_{a,1}$, IGFBPs, 50-kDa production rate; $R_{a,2}$, IGFBPs, 150-kDa production rate, R_a, IGF-1 production rate. The 150-kDa compartment represents bound IGF-1/IGFBP3 in a tenary complex with the acid-labile subunit. The 50-kDa compartment includes fractions of IGF-1 bound to IGFBP-1 through -6. IGF-1 and IGFBPs are the substrates for their degradation, i.e., the binding proteins inhibit the transfer of IGF-1 to their tissue sites of action. (Reproduced with permission from Boroujerdi MA *et al.* Am J Physiol 1997;273:E438–47.)

mirroring the decline in free IFG-1. Insulin sensitivity was positively correlated with free IGF-1 ($r = 0.52$, $P < 0.005$) and inversely correlated with IGFBP-1 ($r = -0.65$; $P < 0.001$) and glucose ($r = 0.51$, $P < 0.005$).

Other investigators have reported that the exogenous administration of IGF-1 increased IGFBP-2 concentrations but had no effects on IGFBP-1 and IGFBP-3 concentrations in patients with type 1 diabetes mellitus (84) or in adolescent patients with GH receptor deficiency (85). In contrast, Cheetham *et al.* (86) showed that IGF-1, administered as a single 40-μg/kg SC dose, increased IGFBP-3 concentrations.

Mandel *et al.* (87) administered GH to GH-deficient children and found that IGFBP-3 increased 76%, IGFBP-2 decreased by 56%, and ALS increased by 41%. The response to GH therapy was correlated with the percentage change in total IGFBP-3 ($r = 0.72$), intact IGFBP-3 ($r = 0.845$), proteolyzed IGFBP-3 ($r = 0.703$), and ALS ($r = 0.813$). There was a significant percentage increase of IGF-1 in the ternary complex and a significant percentage decrease in uncomplexed IGF-1.

In contrast to the aforementioned direct relationships, the indirect response model shown in Figure 32.16 was used to describe the relationship between the administration of GH and IGF-1 in nonhuman primates (88). It was assumed in this model that the production of IGF-1 varied over time, a reasonable assumption. As shown in Figure 32.17, the indirect model provided a reasonable characterization of the induction of IGF-1 after both single and multiple GH doses. However, one limitation to this simple model is its inability to account for the role of the IGFBPs in both GH and IGF-1 responses.

Taken together, these observations suggest a complex, internal, multiple-level control of glucose metabolism, insulin sensitivity, and growth. The binding proteins may not only alter the PK of exogenously administered IGF-1, but ultimately its efficacy and/or safety in patients.

TABLE 32.17 Role of Different Molecules in the Hypothetical Model of IGF-1 Physiology

Molecule	Role
IGFBP-3	Exists in a 42-kDa "complete" form and a 31-kDa "fragment"
IGF-1	Displaces IGF-2 from IGFBP-3; drives reaction toward forming a ternary complex with ALS; formed complex is retained within the intravascular space; suppresses GH secretion
IGF-2	Induces IGFBP-2
GH	Increases synthesis of IGFBP-3 and acid-labile subunit

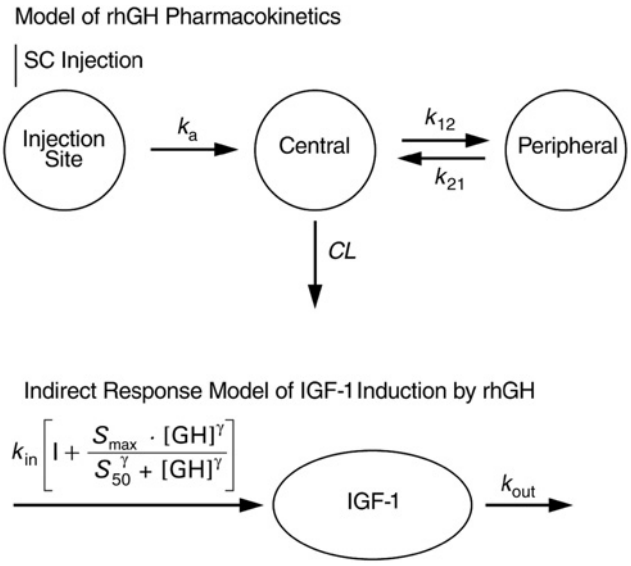

FIGURE 32.16 Pharmacokinetic model for recombinant human growth hormone (rhGH) coupled with an indirect response model for IGF-1 induction by rhGH. The Hill equation was used to model IGF-1 induction by rhGH. Abbreviations: k_a = absorption rate of rhGH after SC injection; CL = elimination clearance of rhGH; k_{12} and k_{21} = intercompartmental transfer rates of rhGH; IGF-1 = total IGF concentration; k_{in} = basal formation rate of IGF-1. Stimulation of IGF-1 production is modeled by the Hill function shown in brackets, where S_{max} = maximum IGF stimulation of k_{in} by rhGH, S_{50} = rhGH concentration for 50% maximal stimulation of k_{in}, [GH] = rhGH concentration, γ = the Hill coefficient, and k_{out} = elimination rate of IGF-1. (Modified from Sun YN *et al.* J Pharmacol Exp Ther 1999;289:1523–32.)

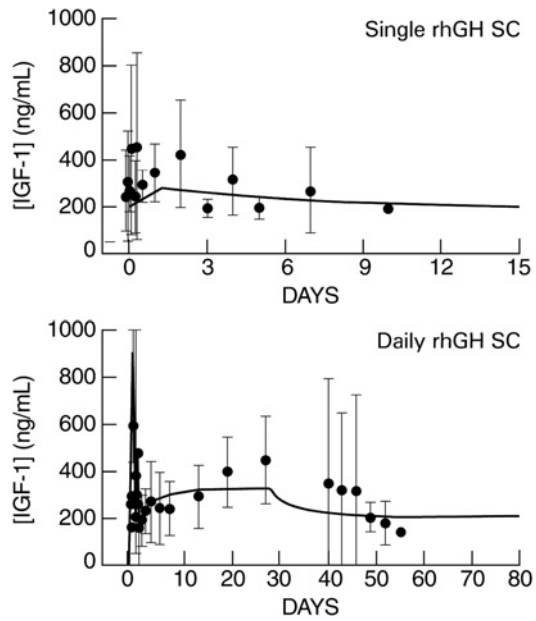

FIGURE 32.17 Total IGF-1 concentrations resulting from single (upper panel) and daily (lower panel) SC injections of rhGH. Data points and bars represent the mean and standard deviation of results from four monkeys. Solid lines are the values that were simulated from the model shown in Figure 32.16. (Reproduced with permission from Sun YN *et al.* J Pharmacol Exp Ther 1999;289:1523–32.)

Regimen Dependency

Regimen dependency was first shown for the antitumor efficacy of IL-2. Mice given 12 injections of a 1500-unit dose of this cytokine showed greater tumor inhibition than did those mice that received two doses of 9000 units (89). Similar results were obtained in a Phase I clinical trial in which patients with renal cell carcinoma were given one of three schedules of IL-2 at an IV dosage of either 1.0 or 3.0×10^6 U/m^2/day: a 24-hour continuous infusion, a single daily bolus injection, and a combination of one-half of the dosage by bolus and the remaining one-half by 24-hour infusion (90). At least three patients received each schedule. Two of the 23 patients with renal cell carcinoma had a partial response and acceptable toxicity with the combined bolus and continuous infusion regimen of 3.0×10^6 U/m^2/day. On the other hand, disease progressed in the patients that received 3.0×10^6 U/m^2/day as a daily bolus injection.

Other investigators have also described regimen dependency for IL-12 given IV (91) and SC (92). For example, Motzer and colleagues (92) treated patients

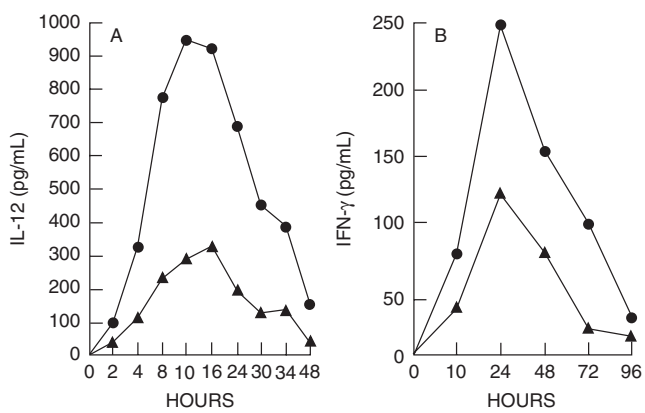

FIGURE 32.18 Regimen dependency of IL-12 pharmacokinetics and IFNγ stimulating effects. In the left panel, IL-12 serum concentrations are compared in patients who received a subcutaneous dose of 1.0 g/mL IL-12 on day 1 of their therapy (•) with levels obtained in other patients who received the same dose on day 15 of an escalating-dose scheme (▲). In the right panel, the IFNγ responses of these two patient groups are compared. (Reproduced with permission from Motzer RJ *et al.* Clin Cancer Res 1998;4:1183–91.)

with renal cell carcinoma with IL-12, administered on days 1, 8, and 15 either as a fixed dose of 1.0 μg/kg or as a series of escalating doses. As shown in Figure 32.18, IL-12 concentrations and IFNγ response were greater after patients received their initial 1.0-μg/kg dose on the fixed-dose regimen than after they received the same dose on day 15 as part of the dose-escalation scheme. However, more severe toxicity was encountered with the single, fixed-dose regimen and the maximum tolerated dose was lower (1.0 μg/kg) than that achievable with the escalation scheme (1.5 μg/kg). As a result, Phase II trials with this cytokine were begun with a regimen in which doses were escalated to 1.25 μg/kg.

REFERENCES

1. CDER. 2004 report to the nation: Improving health through human drugs. Rockville, MD: FDA; 2005. (Internet at http://www.fda.gov/cder/reports/rtn/2004/rtn2004.htm.)
2. PhRMA. 2004 survey. Medicines in development for biotechnology, 2004. Washington, D.C.: PhRMA; 2004. (Internet at http://www.phrma.org/newmedicines/surveys.cfm?newmedsrindex=76.)
3. Cote RJ, Morrissey DM, Houghtone AN, Beattie EJ, Oettgen HF, Old LJ. Generation of human monoclonal antibodies reactive with cellular antigens. Proc Natl Acad Sci USA 1983; 80:2026–30.
4. Sears HF, Atkinson B, Mattis J, Ernst C, Herlyn D, Steplewski A *et al.* Phase-1 clinical trial of monoclonal antibody in treatment of gastrointestinal tumours. Lancet 1982;1:762–5.
5. Mellstedt H. Monoclonal antibodies in human cancer. Drugs Today (Barc) 2003;39(suppl C):1–16.
6. Hoet RM, Cohen EH, Kent RB, Rookey K, Schoonbroodt S, Hogan S *et al.* Generation of high-affinity human antibodies by combining donor-derived and synthetic complementarity-determining-region diversity. Nat Biotechnol 2005;23:344–8.
7. Colcher D, Goel A, Pavlinkova G, Beresford G, Booth B, Batra SK. Effects of genetic engineering on the pharmacokinetics of antibodies. QJ Nucl Med 1999;43:132–9.
8. Clark M. Antibody humanisation for therapeutic applications. Cambridge, UK: Cambridge University; 2000. (Internet at www.path.cam.ac.uk/~mrc7/humanisation/index.html.)
9. Batra SK, Jain M, Wittel UA, Chauhan SC, Colcher D. Pharmacokinetics and biodistribution of genetically engineered antibodies. Curr Opin Biotechnol 2002;13:603–8.
10. Miller K, Meng G, Liu J, Hurst A, Hsei V, Wong WL *et al.* Design, construction, and *in vitro* analysis of multivalent antibodies. J Immunol 2003;170:4854–61.
11. Iznaga-Escobar N, Mishra Ak, Perez-Rodriguez R. Factors affecting the pharmacokinetics of monoclonal antibodies: A review article. Methods Find Exp Clin Pharmacol 2004;26:123–7.
12. Colcher D, Pavlinkova G, Beresford G, Booth BJ, Batra SK. Single-chain antibodies in pancreatic cancer. Ann NY Acad Sci 1999;880:263–80.
13. Chappell WR, Mordenti J. Extrapolation of toxicological and pharmacological data from animals to humans. In: Testa B, editor. Advances in drug research. New York: Academic Press; 1991;20:1–116.
14. Mordenti J, Chen SA, Moore JA, Ferraiolo BL, Green JD. Interspecies scaling of clearance and volume of distribution data for five therapeutic proteins. Pharm Res 1991;8:1351–9.
15. Schaub R, Garzone P, Bouchard P, Rup B, Keith J, Brinkhous K *et al.* Preclinical studies of recombinant factor IX. Semin Hematol 1998;35(suppl 2):28–32.
16. Brinkhouse KM, Sigman JL, Read MS, Stewart PF, McCarthy KP, Timony GA *et al.* Recombinant human Factor IX: Replacement therapy, prophylaxis, and pharmacokinetics in canine hemophilia B. Blood 1996;88:2603–10.
17. Mordenti J, Osaka G, Garcia K, Thomsen K, Licko V, Meng G. Pharmacokinetics and interspecies scaling of recombinant human factor VIII. Toxicol Appl Pharmacol 1996;136:75–8.
18. Nadeau RR, Ostrowski C, Ni-Wu G, Liberator DJ. Pharmacokinetics and pharmacodynamics of recombinant human interleukin-12 in male rhesus monkeys. J Pharmacol Exp Ther 1995;274:78–83.
19. Rakhit A, Yeon MM, Ferrante J, Fettner S, Nadeau R, Motzer R *et al.* Down-regulation of the pharmacokinetic–pharmacodynamic response to interleukin-12 during long-term administration to patients with renal cell carcinoma and evaluation of the mechanism of this 'adaptive response' in mice. Clin Pharmacol Ther 1999;65:615–29.
20. White G, Shapiro A, Ragni M, Garzone P, Goodfellow J, Tubridy K *et al.* Clinical evaluation of recombinant factor IX. Semin Hematol 1998;35(suppl 2):33–8.
21. Atkins MB, Robertson MJ, Gordon M, Lotze MT, DeCoste M, DuBois JS *et al.* Phase 1 evaluation of intravenous recombinant human interleukin 12 (rhIL-12) in patients with advanced malignancies. Clin Cancer Res 1997;3:409–17.
22. Wolberg AS, Stafford DW, Erie DA. Human factor IX binds to specific sites on the collagenous domain of collagen IV. J Biol Chem 1997;272:16717–20.
23. Duconge J, Fernandez-Sanchez E, Alvarez D. Interspecies scaling of the monoclonal anti-EGF receptor ior EGF/r^{3}antibody disposition using allometric paradigm: Is it really suitable? Biopharm Drug Dispos 2004;25:177–86.
24. Duconge J, Castillo R, Crombet T, Alvarez D, Matheu J, Vecino G, Alsonso K, Beausoleil I *et al.* Integrated pharmacokinetic-pharmacodynamic modeling and allometric scaling for optimizing the dosage regimen of the monoclonal ior EGF/r^3 antibody. Eur J Pharm Sci 2004;21:261–70.
25. Cheung WK, Goon BL, Guilfoyle MC, Wacholtz MC. Pharmacokinetics and pharmacodynamics of recombinant human erythropoietin after single and multiple subcutaneous doses to healthy subjects. Clin Pharmacol Ther 1998;64:412–23.

26. Veldhuis JD, Evans WS, Johnson ML. Complicating effects of highly correlated model variables on nonlinear least-squares estimates of unique parameter values and their statistical confidence intervals: Estimating basal secretion and neurohormone half-life by deconvolution analysis. Methods Neurosci 1995;28:130–8.
27. Albertsson-Wikland K, Rosberg S, Libre E, Lundberg LO, Groth T. Growth hormone secretory rates in children as estimated by deconvolution analysis of 24-h plasma concentration profiles. Am J Physiol 1989;257:E809–14.
28. Bright GM, Veldhuis JD, Iranmanesh A, Baumann G, Maheshwari H, Lima J. Appraisal of growth hormone (GH) secretion: Evaluation of a composite pharmacokinetic model that discriminates multiple components of GH input. J Clin Endocrinol Metab 1999;84:3301–8.
29. Macdougall IC, Roberts DE, Neubert P, Dharmasena AD, Coles GA, Williams JD. Pharmacokinetics of intravenous, intraperitoneal, and subcutaneous recombinant erythropoietin in patients on CAPD. A rationale for treatment. Contrib Nephrol 1989;76:112–21.
30. Cetron JS, Bury RW, Lieschke GJ, Morstyn G. The effects of dose and route of administration on the pharmacokinetics of granulocyte–macrophage colony stimulating factor. Eur J Cancer 1990;26:1064–9.
31. Lauresen T, Grardjean B, Jørgensen JOL, Christiansen JS. Bioavailability and bioactivity of three different doses of nasal growth hormone (GH) administered to GH-deficient patients: Comparison with intravenous and subcutaneous administration. Eur J Endocrinol 1996;135:309–15.
32. Radwanski E, Perentisis G, Jacobs S, Oden E, Affrime M, Symchowicz S *et al.* Pharmacokinetics of interferon alpha-2b in healthy volunteers. J Clin Pharmacol 1987;27:432–5
33. Schuller J, Czejka MJ, Schernthaner G, Wirth M, Bosse C, Jager W *et al.* Pharmacokinetics of interferon-alpha-2b after intrahepatic or intraperitoneal administration. Semin Oncol 1992;19(suppl 3):98–104.
34. Aoyama K, UchidaT, Takanuki F, Usui T, Watanabe T, Higuchi S *et.al.* Pharmacokinetics of recombinant human interleukin-11 (rhIL-11) in healthy male subjects. Br J Clin Pharmacol 1997;43:571–8.
35. Kearns GL, Kemp SF, Frindik JP. Single and multiple dose pharmacokinetics of methionyl growth hormone in children with idiopathic growth hormone deficiency. J Clin Endocrin Metabol 1991;72:1148-56.
36. Hayashi W, Kinoshita H, Yukawa E, Higuchi S. Pharmacokinetic analysis of subcutaneous erythropoietin administration with non-linear mixed effect model including endogenous production. Br J Clin Pharmacol 1998;46:11–9.
37. Kindler J, Eckardt KU, Ehmer B, Jandeleit K, Kurtz A, Schreiber A *et al.* Single-dose pharmacokinetics of recombinant human erythropoietin in patients with various degrees of renal failure. Nephrol Dial Transplant 1989;4:345–9.
38. Supersaxo A, Hein WR, Steffen H. Effect of molecular weight on the lymphatic absorption of water-soluble compounds following subcutaneous administration. Pharm Res 1990;7:167–9.
39. Jensen JD, Jensen LW, Madsen JK. The pharmacokinetics of recombinant human erythropoietin after subcutaneous injection at different sites. Eur J Clin Pharmacol 1994;46:333-7.
40. Laursen T, Jørgensen JOL, Christiansen JS. Pharmacokinetics and metabolic effects of growth hormone injected subcutaneously in growth hormone deficient patients: Thigh versus abdomen. Clin Endocrinol 1994;40:373–8.
41. Odeh YK, Wang Z, Ruo TI, Wang T, Frederiksen MC, Pospisil PA *et al.* Simultaneous analysis of inulin and $^{15}N_2$-urea kinetics in humans. Clin Pharmacol Ther 1993;53:419–25.
42. Sculier JP, Body JJ, Donnadieu N, Nejai S, Glibert F, Raymakers N *et al.* Pharmacokinetics of repeated i.v. bolus administration of high doses of r-met-Hu interleukin-2 in advanced cancer patients. Cancer Chemother Pharmacol 1990;26:355–8.
43. Konrad MW, Hemstreet G, Hersch EM, Mansell PW, Mertelsmann R, Kolitz JE *et al.* Pharmacokinetics of recombinant interleukin-2 in humans. Cancer Res 1990;50:2009–17.
44. Watari K, Ozawa K, Takahashi S, Tojo A, Tani K, Kamachi S *et al.* Pharmacokinetic studies of intravenous glycosylated recombinant human granulocyte colony-stimulating factor in various hematological disorders: Inverse correlation between the half-life and bone marrow myeloid cell pool. Int J Hematol 1997;66:57–67.
45. Ericson SG, Gao H, Gericke GH, Lewis LD. The role of PMNs in clearance of granulocyte colony-stimulating factor (G-CSF) *in vivo* and *in vitro*. Exp Hematol 1997;25:1313–25.
46. Tanswell P, Seifried E, Su PCAF, Feuerer W, Rijken DC. Pharmacokinetics and systemic effects of tissue-type plasminogen activator in normal subjects. Clin Pharmacol Ther 1989;46;155–62.
47. Mortensen DL, Walicke PA, Wang X, Kwan P *et al.* Pharmacokinetics and pharmacodynamics of multiple weekly subcutaneous efalizumab doses in patients with plaque psoriasis. J Clin Pharmacol 2005;45:286-8.
48. James K. Interactions between cytokines and alpha-2 macroglobulin. Immunol Today 1990;11:163–6.
49. Dickinson AM, Shenton BK, Alomran AH, Donnelly PK, Proctor SJ. Inhibition of natural killing and antibody-dependent cell-mediated cytotoxicity by the plasma protease inhibitor alpha 2-macroglobulin (alpha 2M) and alpha 2M protease complexes. Clin Immunol Immunopathol 1985;36:259–5.
50. Hoffman M, Feldman SR, Pizzo SV. α_2-Macroglobulin 'fast' forms inhibit superoxide production by activated macrophages. Biochim Biophys Acta 1983;760:421–3.
51. Feige JJ, Negoescu A, Keramidas M, Souchelnitskiy S, Chambaz EM. Alpha 2-macroglobulin: A binding protein for transforming growth factor-beta and various cytokines. Horm Res 1996;45:227–32.
52. Huang JS, Huang SS, Deuel TF. Specific covalent binding of platelet-derived growth factor to human plasma alpha 2-macroglobulin. Proc Natl Acad Sci USA 1984;81:342–6.
53. Legrès LG, Pochon F, Barray M, Gay F, Chouaib S, Delain E. Evidence for the binding of a biologically active interleukin-2 to human alpha 2-macroglobulin. J Biol Chem 1995;8381–4.
54. LaMarre J, Wollenberg GK, Gonias SL, Hayes MA. Cytokine binding and clearance properties of

proteinase-activated alpha 2-macroglobulin. Lab Invest 1991;65:3–14.

55. Blum WF, Hall K, Ranke MB, Wilton P. Growth hormone insensitivity syndromes: A preliminary report on changes in insulin-like growth factors and their binding proteins during treatment with recombinant insulin-like growth factor I. Kabi Pharmacia Study Group on Insulin-like Growth Factor I Treatment in Growth Hormone Insensitivity Syndromes. Acta Paediatr Suppl 1993;82(suppl 391):15–9.
56. Kostecka Y, Blahovec J. Insulin-like growth factor binding proteins and their functions. Endocr Regul 1999;33:90–4.
57. Abdel-Razzak ZA, Loyer P, Fautrel A, Gautier JC, Corcos L, Turlin B *et al.* Cytokines down-regulate expression of major cytochrome P-450 enzymes in adult human hepatocytes in primary culture. Mol Pharmacol 1993;44:707–15.
58. Morgan ET. Regulation of cytochrome P450 during inflammation and infection. Drug Metab Rev 1997;9:1129–88
59. Chen JQ, Ström A, Gustafsson JA, Morgan ET. Suppression of the constitutive expression of cytochrome P-450 2C11 by cytokines and interferons in primary cultures of rat hepatocytes: Comparison with induction of acute-phase genes and demonstration that CYP2C11 promoter sequences are involved in the suppressive response to interleukins 1 and 6. Mol Pharmacol 1995;47:940–7.
60. Gonzalez FJ. Molecular biology of cytochrome P450s. Pharmacol Rev 1989;40:243–87.
61. Kurokohchi K, Matsuo Y, Yoneyama H, Nishioka M, Ichikawa Y. Interleukin-2 induction of cytochrome P450-linked monooxygenase systems of rat liver microsomes. Biochem Pharmacol 1993;45:585–92.
62. Khakoo S, Glue P, Grellier L, Wells B, Bell A, Dash C *et al.* Ribivarin and interferon alpha-2b in chronic hepatitis C: Assessment of possible pharmacokinetic and pharmacodynamic interactions. Br J Clin Pharmacol 1998;46:563–70.
63. Hassan M, Nilsson C, Olsson H, Lundin J, Osterborg A. The influence of interferon-alpha on the pharmacokinetics of cyclophosphamide and its 4-hydroxy metabolite in patients with multiple myeloma. Eur J Haematol 1999;63:163–70.
64. Le Cesne A, Vassal G, Farace F, Spielmann M, Le Chevalier T, Angevin E *et al.* Combination interleukin-2 and doxorubicin in advanced adult solid tumors: Circumvention of doxorubicin resistance in soft-tissue sarcoma? J Immunother 1999;22:268–77.
65. Morell A, Terry WD, Waldmann TA. Metabolic properties of IgG subclasses in man. J Clin Invest 1970;49:673–80.
66. Brambell FWR, Hemmings WA, Morris LG. A Theoretical model of τ-globulin catabolism. Nature 1964;1352–5.
67. Junghans RP, Anderson CL. The protection receptor for IgG catabolism is the β_2-microglobulin-containing neonatal intestinal transport receptor. Proc Natl Acad Sci USA 1996;93;5512–6.
68. Venkatachalam MA, Rennke HG. The structural and molecular basis of glomerular filtration. Circ Res 1978;43:337–47.
69. Maack T, Johnson V, Kau ST, Figueiredo J, Sigulem D. Renal filtration, transport, and metabolism of low-molecular-weight proteins: A review. Kidney Int 1979;16:251–70.
70. Ashwell G, Harford J. Carbohydrate-specific receptors of the liver. Annu Rev Biochem 1982;51:531–54.
71. Lucore CL, Fry ETA, Nachowiak DA, Sobel BE. Biochemical determinants of clearance of tissue-type plasminogen activator from the circulation. Circulation 1988;77:906–14.
72. Hovgaard D, Mortensen BT, Schifter S, Nissen NI. Comparative pharmacokinetics of single dose administration of mammalian and bacterially-derived recombinant human granulocyte-macrophage colony stimulating factor. Eur J Haematol 1993;50:32–6.
73. Moonen P, Mermod JJ, Ernst JF, Hirschi M, DeLamarter JF. Increased biological activity of deglycosylated recombinant human granulocyte-macrophage colony stimulating factor produced by yeast or animal cells. Proc Natl Acad Sci USA 1987;84:4428–31.
74. Kauskansky K. Role of carbohydrate in the function of human granulocyte-macrophage colony stimulating factor. Biochemistry 1987;26:4861–7.
75. Watts MJ, Addison L, Long SG, Hartley S, Warrington S, Boyce M *et al.* Crossover study of the haematological effects and pharmacokinetics of glycosylated and nonglycosylated G-CSF in healthy volunteers. Br J Haematol 1997;98:474–9.
76. Morell AG, Gregoriadis G, Scheinberg HI, Hickman J, Ashwell G. The role of sialic acid in determining the survival of glycoproteins in the circulation. J Biol Chem 1971;246:1461–7.
77. Chatelut E, Rostaing L, Grégoire N, Payen JL, Pujol A, Izopet J *et al.* A pharmacokinetic model for alpha interferon administered subcutaneously. Br J Clin Pharmacol 1999;47:365–7.
78. Kloft C, Graefe E-U, Tanswell P, Scott AM, Hofheinz R, Amelsberg A, Karlsson MO. Population pharmacokinetics of sibrotuzumab, a novel therapeutic monoclonal antibody, in cancer patients. Invest New Drugs 2004;22:39–52
79. Evans JP, Brinkhouse KM, Brayer GD, Reisner HM, High KA. Canine hemophilia B resulting from a point mutation with unusual consequences. Proc Natl Acad Sci USA 1989;86:10095–9.
80. Boroujerdi MA, Jones RH, Sönkesen PH, Russell-Jones DL. Simulation of IGF-1 pharmacokinetics after infusion of recombinant IGF-1 in human subjects. Am J Physiol 1997;273:E438–47.
81. Baxter RC. Insulin-like growth factor (IGF) binding proteins: The role of serum IGFBPs in regulating IGF availability. Acta Paediatr Scand Suppl 1991;372:107–14.
82. Hartman ML, Clayton PE, Johnson ML, Celniker A, Perlman AJ, Alberti KG *et al.* A low dose euglycemic infusion of recombinant human insulin-like growth factor 1 rapidly suppresses fasting-enhanced pulsatile growth hormone secretion in humans. J Clin Invest 1993;91:2453–62.

83. Nyomba BL, Berard L, Murphy LJ. Free insulin-like growth factor I (IGF-I) in healthy subjects: Relationship with IGF-binding proteins and insulin sensitivity. J Clin Endocrinol Metab 1997;82:2177–81.
84. Carroll PV, Umpleby M, Alexander EL, Egel VA, Callison KV, Sonksen PH *et al.* Recombinant human insulin-like growth factor-I (rhIGF-I) therapy in adults with type 1 diabetes mellitus: Effects on IGFs, IGF-binding proteins, glucose levels and insulin treatment. Clin Endocrinol 1998;49:739–46.
85. Wilson KF, Fielder PJ, Guevara-Aguirre J, Cohen P, Vasconez O, Martinez V *et al.* Long-term effects of insulin-like growth factor (IGF)-I treatment on serum IGFs and IGF binding proteins in adolescent patients with growth hormone receptor deficiency. Clin Endocrinol 1995;42:399–407.
86. Cheetham TD, Holly JM, Baxter RC, Meadows K, Jones J, Taylor AM *et al.* The effects of recombinant human IGF-I administration on concentrations of acid labile subunit, IGF binding protein-3, IGF-I, IGF-II and proteolysis of IGF binding protein-3 in adolescents with insulin-dependent diabetes mellitus. J Endocrinol 1998;157:81–7.
87. Mandel SH, Moreland E, Rosenfeld RG, Gargosky SE. The effect of GH therapy on the immunoreactive forms and distribution of IGFBP-3, IGF-I, the acid-labile subunit, and growth rate in GH-deficient children. Endocrine 1997;7:351–60.
88. Sun YN, Lee JH, Almon RR, Jusko WJ. A pharmacokinetic/pharmacodynamic model for recombinant human growth hormone. Effects on induction of insulin-like growth factor 1 in monkeys. J Pharmacol Exp Ther 1999;89:1523–32.
89. Vaage J, Pauly JL, Harlos JP. Influence of the administration schedule on the therapeutic effect of interleukin-2. Int J Cancer 1987;39:530–3.
90. Sosman JA, Kohler PC, Hank J, Moore KH, Bechhofer R, Storer B *et al*. Repetitive weekly cycles of recombinant human interleukin-2: Responses of renal carcinoma with acceptable toxicity. J Natl Cancer Inst 1988;80:60–3
91. Leonard JP, Sherman ML, Fisher GL, Buchanan LJ, Larsen G, Atkins MB *et al.* Effects of single dose interleukin-12 exposure on interleukin-12-associated toxicity and interferon-gamma production. Blood 1997;90:2541–8
92. Motzer RJ, Rakhit A, Schwartz LH , Olencki T, Malone TM, Sandstrom K *et al.* Phase 1 trial of subcutaneous human interleukin-12 in patients with advanced renal cell carcinoma. Clin Cancer Res 1998; 4:1183–91.

CHAPTER

33

Design of Clinical Development Programs

CHARLES GRUDZINSKAS
NDA Partners LLC, Annapolis, Maryland, and University of California, San Francisco, Center for Drug Development Science, Washington, D.C.

INTRODUCTION

This chapter provides an overview of the clinical drug development process, which includes the clinical proof of mechanism (POM), clinical proof of concept (POC), the characterization of clinical safety, the characterization clinical activity, and the generation of evidence of safety and effectiveness to support regulatory review and, ultimately, marketing approval. The clinical trials that are conducted to generate the safety and effectiveness database, to meet the regulatory standard of "evidence," are referred to as "confirming clinical trials." It is this understanding of the clinical effectiveness and safety of a new drug that provides the knowledge for informed decision-making regarding the clinical development, approval, marketing, prescribing, and proper use of a new drug. The clinical development process consists of (a) clinical trials for scientific development, (b) clinical trials for scientific regulatory purposes, and (c) clinical trials that are pharmacoeconomically motivated (1). This chapter covers the clinical drug development process with a focus on *critical decision points* and the use of the *learning and confirming* and the *label-driven question-based* approaches to designing, developing, and planning clinical development strategies.

This chapter is intended to provide the reader with a strategic overview of the manner in which an effective and efficient contemporary clinical development program is created. It is beyond the scope of a single chapter to be able to adequately cover all aspects of a clinical development program. More comprehensive overviews of the operational aspects of clinical plans and clinical trial design are provided by texts written by Spilker (2) and Friedman (3). For a comprehensive overview of clinical trial design and analysis, the reader is referred to *Studying a Study and Testing a Test* by Riegelman (4). Information about the new drug regulatory review process and how it relates to new drug development is presented in Chapter 34 and at the Center for Drug Evaluation and Research (CDER) Handbook web site (5). Another valuable resource for the design and conduct of clinical trials is a comprehensive glossary of clinical drug development terminology (6). In addition, the U.S. Food and Drug Administration (FDA) announced a Critical Path Initiative in 2004 and this provides insight into several areas of focus for streamlining the drug development process (7).

PHASES, SIZE, AND SCOPE OF CLINICAL DEVELOPMENT PROGRAMS

The FDA broadly defines *drugs* as those compounds that are synthesized and *biologics* as those that are produced by living organisms. However, for the purposes of this chapter, we will use the term "drug" to represent both drugs and biologics.

Global Development

Within the past decade, international guidelines and regulations have become more uniform through

the efforts of the International Conference on Harmonization (ICH) (8). The efforts of the ICH, which included participation of regulatory agencies, industry, and academia from the United States, Europe, and Japan, have resulted in a series of comprehensive ICH Guidances. These guidances address effectiveness (E), safety (S), and manufacturing (M), and develop a Common Technical Document.

Clinical Drug Development Phases

Traditionally, the clinical development process has been divided into four phases.

Phase I

As described in Chapter 31, Phase I includes first-in-human (FIH) trials to provide information about the safety (tolerability) and pharmacokinetics of a new drug. These trials are usually conducted in healthy volunteers unless the trials involve certain cytotoxic drugs such those used in cancer and HIV treatments. It should be noted that Phase I-type clinical pharmacology trials, such as those to study pharmacokinetics in special populations, can and do occur throughout the clinical drug development process (see Chapter 1, Figure 1.1).

Phase II

Phase II consists of small trials in individuals with the illness to be treated (usually trials of 24 to 300 persons). The goals of Phase II trials are to provide either a proof of mechanism or a proof of the hypothesized therapeutic concept, identify the patient population(s) in which the new drug appears to work, and determine an appropriate dose regimen for subsequent large-scale trials. Dose regimen includes the loading dose, maintenance dose, dose frequency, dose duration, and dose adjustments for special populations and for coadministration with other drugs.

Phase III

Phase III trials are trials conducted to confirm the effectiveness of a new drug in a broad patient population in order to establish clinical settings in which the drug works or does not work. These trials also are designed to provide an evaluation of the frequency and intensity of adverse drug events that are likely to be encountered in subsequent clinical use. These trials are large (250 to >1000 patients) so as to provide information that can reasonably be extrapolated to the general population. After successful completion of Phase III trials that meet U.S. requirements, the sponsor of the development program generally files a New Drug Application (NDA) or Biologics License Application (BLA) with the Food and Drug Administration. FDA approval of these applications is required before the product can be marketed in the United States. Similar procedures are in place in other countries (i.e., a Marketing Authorization Application in Europe and/or the equivalent regulatory submission in Japan and other parts of Asia); here the focus is primarily on U.S. regulatory review processes and requirements.

Phase IV

Phase IV trials are conducted as postmarketing efforts to further evaluate the characteristics of the new drug with regard to safety, efficacy, new indications for additional patient populations, and new formulations. Phase IV is generally used to characterize all post-NDA/BLA clinical development programs. However, some organizations use Phase IV to describe only FDA-requested clinical trials and use Phase V to describe internally motivated market expansion trials (e.g., new indications, new formulations, updated safety databases).

It is noteworthy that in an attempt to better characterize the types of information and knowledge that are developed during each phase, terms such as early-Phase II or late-Phase III (or Phase IIa and Phase IIIb, respectively) have crept into the clinical development lexicon. Although the traditional four phases are helpful in broadly defining a clinical drug development program, the use of these phases in a strict chronological sense or as milestones would be misleading. A strict chronological interpretation would infer that pharmacokinetic determinations are very limited and only occur in the early (Phase I) part of the clinical drug development process, and that Phase IV market expansion trials are started only after the new drug has been approved. Therefore, instead of thinking of drug development as a series of consecutive phases, it is preferable to think of the drug development process as a series of interactive knowledge-building efforts, like the expanding layers of an onion, that allow us to make cogent scientific drug development decisions.

Drug Development Time and Cost — A Changing Picture

Clinical drug development is a complex, expensive, and lengthy process that can be thought of as having several main objectives in support of the ultimate goal — marketing approval with the desired indications and claims. The average cost of bringing one new medicine to market cited by the Pharmaceutical

Research and Manufacturers of America (PhRMA) (9, 10) is $799 million, and a report by Bain & Company (11) estimates the cost for a new drug at $1.7 billion. These cost estimates take the following factors into consideration:

- The actual cost of the successful drug discovery and development programs.
- The cost of money [the financial return that would be realized if the money spent on research and development (R&D) were invested in long-term notes].
- The cost of unsuccessful discovery and development projects ("dry holes").

The actual "out-of-pocket" expense for a single new drug varies, depending on the number of indications, formulations, and study participants needed to obtain regulatory approval, but is probably in the neighborhood of $200 million to more than $300 million. It is noteworthy that if one divides the total R&D spent for the year 2004, ~$38.8 billion (12), by 34, the number of new molecular entities (NMEs) that were approved by the FDA during 2004 (13), one arrives at an estimate of ~$1.14 billion per NME. It also should be noted that since large pharmaceutical companies expend approximately one-half of their R&D funds on line extensions, the average cost per new drug approved for marketing may indeed approach an average cost of approximately $500–700 million, which, of course, includes funding for the 11 out of the 12 drugs that enter clinical trials but never achieve marketing approval (14).

Estimates for the cost per participant in a clinical trial range from less than $2,000/person for a short treatment, to as much as $15,000/person for lengthy or complex treatments. In addition to the clinical grants to investigators, the full clinical costs include development of the protocol and of the clinical investigators' brochure, clinical investigator meetings, monitoring and site visits, clinical data collection, data quality resolution, data management and analysis, and report preparation. If the clinical database needed to achieve approval requires 4,000 to 8,000 study participants, one can see how the cost of the clinical portion of drug development can quickly approach $150 million.

Clinical drug development requires the integration of many disciplines, including discovery research, nonclinical and clinical development, pharmacometrics, statistics and bioinformatics, regulatory science, and marketing to identify, evaluate, develop, and achieve regulatory approval for the successful marketing of new drugs.

In the recent past, the overall time from the initiation of a drug discovery program to regulatory approval was 10 to 15 years, but this has been reduced so that development timelines now range from 4 to 6 years. Much of the time and expense of drug development is related to the large numbers of individuals who need to be studied in clinical trials. Clinical development programs with large numbers of individuals are needed for therapies such as broad-spectrum antibiotics, which usually are developed for many indications. Similarly, large clinical programs are needed for a vaccine or flu treatment. In these cases the incidence of the disease is small and many individuals are needed to demonstrate a clinically significant difference in disease incidence between test-drug-treated and placebo-treated study participants. As a result, contemporary clinical development plans usually include a minimum of 1,500 participants, the ICH default minimum, and often exceed 6,000 participants.

The drivers that determine the size of a clinical development program include what is referred to as the "treatment effect size" and the intended level of differentiation that is being sought by the developer. The treatment effect is determined by the underlying population event rate and the expected event rate in the treated population (3). The level of differentiation impacts the trial size in that if developers want to provide evidence that their drug is as safe as an already marketed drug that has an adverse event rate in the range of 4%, it has been estimated that an 80,000-patient trial would be need to provide convincing evidence that the new drug is "equivalent" with regard to the incidence of the adverse event being studied. Likewise, there have been recent occurrences in which the incidence of certain adverse events for an already marketed drug was in the range of 30–40% and the developer of a new drug wanted to demonstrate that the new drug had an adverse event rate of one-half that of the already marketed drug. Although convincing evidence of a clinically significant decrease in the adverse event rate might be generated with 250–500 patients, it may require much larger trials to demonstrate that the new drug has the same level of effectiveness as the existing drug ("noninferiority" of the new drug). Otherwise, the argument could be made that the new drug may be safer, but may also be less effective (e.g., 50% safer, but also 50% less effective).

Although the cost of drug development is likely to remain high, contemporary drug development technologies, the availability of high-quality contract research organizations (CROs) for the outsourcing of key efforts, and the emergence of online clinical trial data collection and management ("e-R&D") have reduced the average time from drug discovery to NDA/BLA submission to a new benchmark of

4 to 6 years. In addition, regulatory review procedures have been streamlined, further shortening the time required to bring new drugs to market. For instance, the FDA is increasingly requesting that INDs be submitted in electronic format using the ICH Common Technical Document format (15).

Impact of Regulation on Clinical Development Programs

As described in Chapter 34, the Kefauver–Harris Drug Amendments (16) were passed by Congress in 1962 to ensure drug efficacy and greater drug safety. For the first time, drug manufacturers were required to prove to FDA the clinical effectiveness of their products before marketing them. This legislation led to the corresponding development at the FDA of a formalized process of regulatory review. This process is needed to determine whether there is adequate knowledge to be able to make an informed evaluation about the benefit-to-risk profile of the new drug, and to then decide whether the proposed product should be approved for use by certain segments of the nation's population. The regulatory review process requires the integration of many of the same disciplines required for drug development, including basic pharmacology, pharmacometrics, toxicology, chemistry, clinical medicine, statistics, and regulatory science. As will be emphasized subsequently, the ultimate "product" of the drug development and drug review process is the *package insert (PI)* or *label* that contains the information regarding the approved indication(s) and the expressed and implied basis that a prescriber uses to decide what drug to prescribe for which patients, and in what dose, dose interval, and duration.

The statement that the proof of effectiveness would be derived from "well-controlled investigations" has been the cornerstone of the FDA's position for the requirement of two positive adequate and well-controlled clinical trials, both of which must demonstrate effectiveness at the $P < 0.05$ level (16). However, in practice, most clinical development plans include more than just two studies to document efficacy and evaluate safety. In a pilot study reported by Peck (1) of a cohort of 12 of the 51 NDAs that were approved by the FDA in 1994–1995, the total number of clinical trials in each submission ranged from 23 to 150. In those trials that were designed to establish efficacy and evaluate safety, the number of study participants ranged from 1,000 to 13,000. Peck has pointed out that these NDAs probably reflect clinical plans that were designed in the mid-1980s.

A retrospective review of five recent NDAs and BLAs was conducted by research fellows at the Center for Drug Development Science (CDDS) using information found on the CDER and Center for Biologics Evaluation and Research (CBER) web sites (17). This review is summarized in Table 33.1 and indicates that the size of the clinical development plans for these five diverse products ranged from a total of 10 to 68 clinical trials and included between 1,069 and 8,528 participants. The large number of participants in some clinical development programs may reflect the intensity with which sponsors focus on demonstrating a clinically significant differentiation. For example, the sildenafil NDA for treating erectile dysfunction included population subgroups to demonstrate efficacy regardless of baseline severity, race, and etiology. Patient etiology subgroups included specific trials in patients whose erectile dysfunction was psychogenic, due to spinal cord injury, or a result of diabetes (18). The rofecoxib NDA supported both an indication for osteoarthritis and an indication for pain management, requiring demonstration of effectiveness in three distinct pain models as well as the demonstration of differentiation in improved gastrointestinal safety when compared with multiple traditional nonsteroidal anti-inflammatory drugs (NSAIDs). Similar retrospective analyses can be made for both NDAs (19) and BLAs (20) by downloading the reviews prepared by the FDA medical officers, chemists, pharmacologists, and clinical pharmacologists. These reviews provide an excellent starting place for understanding the design of a clinical drug development program.

In several of the clinical development programs analyzed in Table 33.1, there is a substantial reduction in the number of clinical trials from that reported in the pilot study of 1994–1995 NDA approvals. This reduction is seen as a positive move in shortening the time and expense of drug development. Even more impressive speed records are being set for drug development that uses structure-based drug discovery approaches and effective and efficient clinical development programs based on critical label-driven question-based decision-making. The development of a protease inhibitor may hold the speed record with the following metrics (21):

- The first-in-human dose was 18 weeks after the start of the nonclinical safety program.
- Phase II started 9.5 months after the start of the nonclinical safety program.
- The NDA was submitted 3.5 years after the discovery of the drug.

In the 1999 annual report from Monsanto, it was stated that the development and NDA submission

TABLE 33.1 Retrospective Reviews of Recently Approved NDAs and BLAs[a]

Drug	Indication	FIH[b] to NDA filing (years)	Phase I		Phase II		Phase III		Total	
			Trials[c]	Participants	Trials	Participants	Trials	Participants	Trials[d]	Participants[e]
Trastuzumab (Herceptin®)	Breast cancer	6–10	3	48	6	532	1	489	10	1,069
Etanercept (Enbrel®)	Rheumatoid arthritis	6–7	8	163	3	503	23	1,381	34	2,048
Zanamivir (Relenza®)	Treatment of influenza	4–5	18	446	7	3,275	3	1,588	28	5,309
Sildenafil (Viagra®)	Erectile dysfunction	5	42	905	13	498	13	4,679	68	6,082
Rofecoxib (Vioxx®)	Osteoarthritis, pain	4–5	31	940	2	1,855	13	5,733	46	8,528

[a]The assignment of trials and study participants was not always straightforward based on the source documents and should be used as only semiquantitative estimates of the size of each phase. For instance, in the etanercept BLA there were 3 efficacy and 23 safety studies. We have categorized the efficacy studies as Phase II and the safety studies as Phase III.

[b]Time of FIH trial for the approved indication was derived from sources in addition to those on the FDA web sites and in several cases represents an educated estimate.

[c]Phase I includes all of the clinical pharmacology studies that in many cases were conducted within 12 months of the NDA\BLA submission.

[d]The total number of trials indicated is the number of trials included in the NDA\BLA and might not include certain trials ongoing at the time of the NDA\BLA submission.

[e]The total number of study participants indicated is the number of participants in the NDA/BLA and might not include participants in certain trials ongoing at the time of the NDA\BLA submission.

of the COX-2 inhibitor celecoxib was completed in 39 months from the FIH dose. This is even more remarkable when one takes into account that the celecoxib NDA contained data from over 9,000 patients with osteoarthritis, rheumatoid arthritis, and surgical pain. These data were used by the FDA to approve celecoxib for the indications of osteoarthritis and rheumatoid arthritis.

Another important development that may help reduce the time and cost of drug development is found in the May 1998 FDA "Guidance for Industry: Providing Clinical Evidence of Effectiveness for Human Drug and Biological Products" (22). This guidance points out that in section 115(a) of the FDA Modernization Act (FDAMA), Congress amended section 505(d) of the Food Drug and Cosmetic Act to indicate that the FDA may consider "data from one adequate and well-controlled clinical investigation and confirmatory evidence" to constitute substantial evidence if FDA determines that such data and evidence are sufficient to establish effectiveness (22). In making this clarification, Congress raised the possibility that fewer clinical trials may be needed than in the past. This appears to reflect the fact that contemporary multicenter clinical trials typically enroll more patients than do single-center trials that were conducted in the past, as well as the substantial progress in drug development science that has resulted in higher quality clinical trial data.

GOAL AND OBJECTIVES OF CLINICAL DRUG DEVELOPMENT

The ultimate goal of the clinical drug development process is to achieve approval to market a new drug for the desired indications, based on an effective and efficient clinical plan that fully characterizes the differentiating features of the new drug. Target product profiles (TPPs) and target package inserts (TPIs), described in Chapter 27, are valuable design and planning tools for the design of effective and efficient clinical development plans and are consonant with the presentation in this chapter (23, 24). An important development that was intended to promote the use of these tools is that the CDER Division of Cardio-Renal Drug Products in 1999 launched a pilot program for working with sponsors to develop a label-driven approach to drug development. As anticipated, this program has been extended to other FDA divisions.

Two key resources for input into the design of a successful clinical development program are the corresponding therapeutic FDA Guidance (25, 26) and the publicly available reviews by FDA reviewers for

previously approved drugs (27). Additional input may be gained by interactions with the Study Endpoint and Label Development (SEALD) division within the Office of New Drugs/CDER.

The goal of an effective and efficient clinical drug development process is met by achieving seven objectives that generate an understanding of the intrinsic and extrinsic characteristics of the new drug being developed.

Objective 1 — Clinical Pharmacology and Pharmacometrics

Objective 1 of clinical development focuses on understanding the factors that influence the absorption, distribution, metabolism, and elimination (ADME) of a new drug, as well as the relationship between drug concentrations in various body fluids or organs and the observed pharmacological effects. This understanding includes how different and special patient populations handle the drug, the potential for drug–drug interactions, as well as how patients might handle the drug differently in short-term treatments vs long-term treatments. "Pharmacometrics" can be thought of as a quantitative description of pharmacology that includes the design and analysis of protocols and studies related to drug therapy questions and that provides insights into the processes controlling the time course of drug concentrations and therapeutic and toxic responses (28). Thus, clinical pharmacology and pharmacometrics underlie the entire clinical drug development process, but deserve particularly heavy emphasis at the beginning and at the end of the clinical drug development program.

Objective 2 — Safety

Objective 2 entails the assessment of a new drug to determine what types of clinical side effects can be expected and in which patient populations, at what doses and dose durations, and whether the side effects are reversible and, if so, after how long. This knowledge is summarized in the Integrated Summary of Safety (ISS) portion of the NDA/BLA submission and is used by regulatory authorities to decide what should be included in the precautions or warnings sections of the drug label.

Although safety is identified as the second objective, the highest priority needs to be given to gathering relevant safety information throughout the drug development process. In light of the withdrawal of Vioxx in September 2004 (29, 30) and the subsequent congressional hearings, the FDA is reorganizing to strengthen its preapproval safety reviews (31).

Objective 3 — Activity

Objective 3 is to characterize as early as possible the dose regimen (e.g., dose, dose frequency, dose duration) and patient populations in which the new drug is active, in order to be able to select the dose regimen to be used in subsequent large confirming trials.

Objective 4 — Effectiveness

Objective 4 is to confirm drug effectiveness in large-scale clinical trials. The results of these trials are summarized in the Integrated Summary of Efficacy (ISE) portion of the NDA/BLA submission and play an important role in determining appropriate therapeutic indications, dose regimens, and benefit/risk ratios for various patient populations.

Objective 5 — Differentiation

Objective 5 is to provide evidence that the new drug will provide enhanced value to patients over other available drugs with regard to effectiveness and patient safety and adherence (compliance).

Objective 6 — Preparation of a Successful NDA/BLA Submission

Objective 6 centers on the preparation of a reviewer-friendly submission that regulatory authorities will use to determine whether to permit marketing of the new drug for the indications and dose regimens being sought.

Objective 7 — Market Expansion and Postmarketing Surveillance

Objective 7 underscores the fact that clinical development efforts do not stop with the regulatory approval of an NDA or BLA but continue throughout the life cycle of the product. Market expansion is accomplished by demonstrating effectiveness, safety, and value of the drug in new patient populations, by demonstrating its use in combination with another product, or by introducing new formulations to improve patient adherence or simply to increase market share. Planning for this expansion process begins far in advance of the submission of the drug dossier to a regulatory agency for a review. Likewise, it is increasingly common for sponsors to initiate a post-marketing surveillance program to track the emergence and severity of any adverse events that were or were not observed during the pre-NDA clinical development program.

CRITICAL DRUG DEVELOPMENT PARADIGMS

Six critical paradigms that have evolved within the last decade are valuable tools in ensuring the rapid and successful clinical development of new drugs.

Label-Driven Question-Based Clinical Development Plan Paradigm

It is appropriate that we begin with the label-driven question-based focus, since the ultimate product that is "produced" from a clinical drug development program is the descriptive drug label that is approved by a regulatory agency (32). The label-driven question-based paradigm is one in which the entire drug development program is designed with a focus on generating the knowledge about the new drug that is needed to be able to address the elements that make up the drug label or package insert (PI). The objective of a well-written PI is to provide prescribers with the information that is needed to make informed decisions regarding the clinical use of the drug.

A PI includes the following information: Who should receive the new drug? How much drug should be given? How frequently should the drug be given? For how long does the drug need to be given to be effective? And, of course, the PI must include much additional important prescribing information regarding drug–drug interactions, the effect of the patient's age on the drug's activity, how to administer the drug, potential adverse effects of which the prescriber and patient need to be aware, and the contraindications, precautions, and warnings. One way to remember the "label-driven question-based" drug development concept is to think: "We sell only the package insert, we give away the product!"

An appropriate analogy is the purchase of a computer program on a compact disk (CD). The CD itself probably costs pennies to manufacture. What we purchase is the value of the knowledge that is on the CD and the effort that went into producing that knowledge. The costs of medicines are very much the same as the costs associated with these software products. We are, of course, paying for the research and development costs associated with bringing the new product to market, plus the manufacturing, advertising, and distribution costs of the medicine, but a majority of the costs are associated with the value of the product to our health.

Differentiation Paradigm

Differentiation is the term used to describe how the new product being developed will be unique from the products currently marketed or under development. Differentiation could be based on the following constructs:

- A better prevention-of-relapse profile, such as a proton pump inhibitor for duodenal ulcers.
- A better gastrointestinal safety profile, such as the COX-2 inhibitors vs traditional NSAIDs.
- Better patient compliance, such as a weekly transdermal patch.
- A formulation that is easier to use, such as oral or inhaled insulin vs injected insulin.

Whatever the differentiating feature is, both the drug discovery and the clinical development programs need to be designed to demonstrate the specific differentiation(s) that can be incorporated in the drug label and in product advertising.

One of the most valuable educational tools in developing an understanding of differentiation for a clinical trial program is to study the PIs and advertisements for approved drugs. Serious students of clinical drug development would be well advised to take a few minutes, when they see a journal advertisement for a drug, to read the entire PI, which is found on the back of the advertisement. Based on the information found in the PI, one can reasonably reconstruct the elements of a clinical development plan for that drug, or design a clinical drug development plan for a drug with similar indications.

Indeed, the starting point for the development of a clinical plan to demonstrate the differentiation of a new drug could be the creation of a spreadsheet, with the rows consisting of all drugs (marketed and in development) for the same or similar indications. The spreadsheet columns might include indications, special indications, dose, dose regimen, dose duration, warnings, precautions, contraindications, adverse events, serious adverse events, life-threatening events, drug–drug interactions, elimination half-life, C_{max}, t_{max}, V_d, CL, food effect, compatible drugs, noncompatible drugs, how supplied, and so on. This type of spreadsheet would be invaluable in identifying specific areas for differentiation.

The selected areas of differentiation become the points of focus in designing a clinical development plan that is able to demonstrate advantages of a new drug over existing and pending drugs. One precautionary note: it is never too early to develop a draft PI that incorporates the target elements. Indeed, the very best drug discovery programs use a *target PI* to define the criteria for selecting promising clinical leads, and to guide the selection and design of subsequent clinical trials. To facilitate this approach, the Pharmaceutical Research Manufacturers Association and the

FDA's Office of Drug Evaluation IV have collaborated in drawing up a Targeted Product Information template (23).

Of course, the contents of the target PI will evolve over time as knowledge about the new drug is generated. The target PI not only serves as an effective means of establishing initial consensus goals that are shared by all stakeholders in the drug development process (e.g., discovery, development, and marketing), but also provides metrics to determine whether the development process is subsequently yielding the essential differentiating features that were the original basis for undertaking the project.

Drug Action → Response → Outcome → Benefit Paradigm

The usefulness of a new drug is based on a cascade of pharmacological events, which result in both desired (effectiveness) and undesired (side effects) pharmacological outcomes. As described by Holford *et al*. (33), we can think of this cascade as having four levels. The first level is the *action* of the drug at a pharmacologically active site in humans (e.g., binding to a receptor). The second level is the *effect* that the drug produces as a result of that binding (e.g., the up-regulation of a protein). The third level is the *patient response* observed (e.g., the lowering of blood pressure). And the fourth level is the resulting *clinical outcome* (e.g., a lowering in the risk of stroke due to elevated blood pressure).

What distinguishes contemporary clinical drug development from traditional approaches is the important role that pharmacometrics plays in our understanding of the relationships between drug action, drug effect, patient response, and clinical outcome. The value of this understanding is not just in the definitive nature of the specific knowledge gained, but rather in its predictive utility that allows us, as clinical drug developers, to use knowledge that we have just learned to enhance the effectiveness and efficiency of the overall clinical development program. An extension of this paradigm can be found in the report by Shiener (34) that illustrates the usefulness of the "learning vs confirming" paradigm in contemporary drug development.

Learning vs Confirming Paradigm

In 1997, Sheiner (34) proposed the formal use of the learning vs confirming paradigm for clinical drug development. *Learning* trials address an essentially infinite set of quantitative questions concerning the functional relationship between prognostic variables, dosage, and outcomes. On the other hand, *confirming* trials must answer only a single yes/no question: Is the null hypothesis falsified or not? An important distinction is that detailed knowledge regarding protocol compliance is imperative if valid conclusions are to be drawn from learning trials. Clearly, the introduction of the learning vs confirming paradigm into a clinical development program has the potential to provide for more efficient, effective, and rapid decision-making.

Decision-Making Paradigm

Well-designed clinical development programs support effective decision-making. In this context, a *decision* can be defined as a commitment of resources toward a prespecified target. Unfortunately, the resource portion of the definition is frequently missing in a clinical development plan. Many "decisions" are often made that involve the need for a resource change, yet no resource change occurs. Therefore, these become "hollow"decisions. The successful implementation of a decision in a clinical project may entail the following considerations:

- Resources may need to be added.
- Resources may need to be taken away.
- There might be no need to change the resources allocated to a project.

A clinical development plan cannot be considered complete until the required resources (people, funds, equipment, sites, clinical supplies, etc.) are identified for each major objective.

For those who design, track, and make decisions regarding the progress of clinical development programs, the inclusion within the development plan of critical decision points, with prespecified go/no-go criteria, provides a focus for the clinical development team. The key clinical drug development decisions are identified in Table 33.2, with the critical go/no-go decisions being shown in boldface. These critical decisions will be expanded on later in this chapter. It is important to note that the driver for these decisions is our question-based label-driven clinical development plan. Indeed, the creation of a label-driven question-based clinical development plan not only increases the efficiency and speed of the clinical development process, but also supports the question-based review by the FDA of an NDA, as described by Lesko and Williams (35).

Fail Early/Fail Cheaply Paradigm

As discussed in detail in Chapter 27, a critically important point is that, on average, only 1 out of 12

TABLE 33.2 Label-Driven Question-Based Clinical Development Decision Points[a]

1.	**What is the intended clinical disease model (prevention, treatment, cure, or diagnosis)?**
2.	**Are animal safety and activity data adequate to justify human clinical trials?**
3.	**What are the efficacy and safety differentiation targets and respective success criteria?**
4.	What starting dose should be used for the first-in-humans trial?
5.	What dose escalation scheme should be used for the early clinical safety trials?
6.	Is there dose proportionality such that if the dose of the drug is doubled, the blood levels also will double?
7.	What are the appropriate primary and secondary clinical outcome metrics for determination of drug effect?
8.	What are the appropriate patient population subgroups for clinical determination of drug effect?
9.	**Has "proof of concept" been achieved using either a biomarker or a clinical outcome?**
10.	**Based on the safety and pharmacometric profile observed from the early clinical trials, what starting dose and dose escalation scheme are appropriate for patient population subgroups to be studied for the determination of drug effect?**
11.	Is there a clinical advantage to using the new drug in combination with an already marketed drug?
12.	Do the formulations being developed (oral, parenteral, transdermal, etc.) release the drug at the desired rate?
13.	What dose adjustments are needed for special patient populations (age, sex, and ethnicity; renal and hepatic impairments)?
14.	For how long should one take the drug?
15.	Should the same dose be used for different levels of disease progression?
16.	What are the right times of day for dosing?
17.	What is the clinical significance of any observed food effect upon bioavailability?
18.	What is the clinical significance of any observed drug–drug interactions?
19.	What are the appropriate primary and secondary clinical outcome metrics for determination of clinical efficacy?
20.	**Have the patient populations, dose and dose regimen, and benefit/safety ratio been adequately characterized to support the conduct of the large trials that are needed to confirm efficacy and to achieve the intended clinical differentiation?**
21.	**Have the frequency and severity of any side effects been adequately characterized, and the reversibility established of any severe or life-threatening side effects?**
22.	Are there any patients who should not take this drug?
23.	**Do some individuals metabolize the new drug differently such that those individuals could have serious and life-threatening adverse reactions?**
24.	**Does the route of metabolism of this drug, or of an already marketed drug, pose a risk of important drug–drug interactions?**
25.	Is the drug highly protein bound? Will medical conditions or other drugs compete and increase this drug's unbound blood levels, or will this drug compete for plasma protein binding sites of another drug the patient is taking?
26.	What happens when the patient suddenly stops taking the drug or misses a few doses? Is there a rebound?
27.	Is the drug addictive? How addictive?
28.	**Have adequate clinical efficacy and safety data been generated to support the proposed indications and labeling that will be submitted to a regulatory agency for marketing approval?**
29.	**Have adequate clinical efficacy and safety data been generated to differentiate this drug from those that are already marketed?**

[a] Critical decisions are in bold type.

compounds selected for FIH clinical trials will make it to the market (7). Based on this average, most companies are adopting the "fail early/fail cheaply" paradigm. The intent here is to conduct "killer experiments" early in the drug development process in order to identify as soon as possible those projects that, by their intrinsic properties, have a low probability of success later in the clinical development process. Successful implementation of this paradigm entails identifying potential failures:

- Before the compound even gets into the pre-FIH development process.
- Early in the clinical development process for those compounds that pass the preclinical screens.

With an understanding of the six clinical development paradigms, we are ready to move forward to the critical issues in clinical drug development.

CRITICAL CLINICAL DRUG DEVELOPMENT DECISION POINTS

Once one recognizes that the end product of clinical drug development is the knowledge and

the information needed to permit the informed peer review, approval (including approved labeling), and use of the new drug, one can then establish prespecified criteria for each of the critical clinical drug decision points. The decision-making criteria outlined here are guided by evolving clinical knowledge about the drug, particularly during the learning and confirming development cycle, and are supported by label-driven question-based clinical development plan concepts.

Which Disease State?

At least four approaches to drug development can be targeted:

- Dx = Diagnosis to identify potential drug responders.
- Px = Prevention of the illness.
- Tx = Treatment to relieve signs and symptoms of illness.
- Cr = Treatment to arrests or cure the illness.

Of course, subsets exist within each of these four approaches. For example, within each category there can be patients with mild, moderate, or severe disease states and symptoms. Although one drug may work well for patients with mild or moderate disease, that same drug might not be effective for patients with the most severe conditions.

A Priori Identification of Potential Drug Responders and Nonresponders

The Human Genome Project has laid the foundation for not only finding both new Cr and Tx drugs, but also for new methods to be able to identify which patient subgroups will respond to which drugs. An excellent overview of the impact of the Human Genome Project can be found in the article entitled "The Genome Gold Rush" (36).

The results of the Human Genome Project will provide breakthroughs in three major areas:

- The identification of differences among patients, explaining why some respond in clinical trials, while others do not.
- The development of new drugs that will be able to treat specific patient populations.
- The identification of which patients are more prone to serious or life-threatening side effects from a particular drug so that the prescriber will avoid that drug in these vulnerable individuals.

In the past, the need to include a plan for the codevelopment of a corresponding diagnostic method to indicate whether a drug would be useful was mainly limited to the domain of antibiotics. With the advent of the powerful tools that the Human Genome Project has introduced, many of the future clinical development programs will need to include a companion development and validation component for an FDA-approved diagnostic test. The FDA, having recognized the potential for *a priori* identification of patients who might or might not respond to a drug, is developing guidelines for the codevelopment of drugs and diagnostic tests to guide patient selection. A white paper on this topic has been published by Frueh (37).

The future for the identification and clinical development of diagnostic tests to determine whether an individual will respond to a certain medication is already a reality with drugs such as trastuzumab for first-line use in treating breast cancer in patients who overexpress human epidermal growth factor receptor 2 (HER2). Because approximately one-third of all breast cancer patients overexpress the HER2 protein (and, likewise, two-thirds do not overexpress the HER2 protein), it is important to be able to identify which patients overexpress HER2 before prescribing trastuzumab. Shortly after the FDA approval of trastuzumab and the corresponding diagnostic test, it was reported that 90% of newly diagnosed stage IV metastatic breast cancer patients were being tested for HER2 and that 67% of metastatic breast cancer patients were aware of their HER2 status (38). It is noteworthy that the BLA clinical program for the approval of trastuzumab consisted of 10 clinical trials and 1,069 study participants (see Table 33.1).

Another example of the clinical usefulness of genomics in the clinical development of both a Dx and a Tx product is the investigation of the contribution of interleukin-9 (IL-9) to the pathogenesis of asthma. It has been was reported that expression of IL-9 was significantly increased ($P > 0.001$) in the airways of asthmatics compared to normal individuals or those with other lung diseases (39). Likewise, there are significant programs under way to identify *a priori* which subjects might have an unusually high probability of experiencing adverse events or even serious adverse events with drugs that are either marketed or in development.

Preventive Therapy

The next great breakthough in new drugs will be those that can prevent or reduce the probability of the first occurrence, or of a relapse, of a serious and life-threatening disease. A recent example is the supplemental approval in December 1999 by the FDA for the use of the COX-2 inhibitor celecoxib to reduce the number of adenomatous colorectal polyps in

patients with familial adenomatous polyposis (FAP). This is intended as an adjunct to usual care of these patients (e.g., endoscopic surveillance, surgery). Similarly, tamoxifen has been approved for the "reduction of risk" of breast cancer. A major portion of the September 1998 FDA Oncologic Advisory Committee meeting was dedicated to a discussion of how the general practitioner would be able to predict the benefit/risk ratio for various patient populations from the clinical data that made up the NDA.

A major challenge for clinicians will be the design of clinical development programs that can answer the benefit-to-risk profile questions for both prevention and risk reduction drugs. Px drug development will require new animal models and a new way of thinking about the conduct of clinical trials, especially in cases in which the incidence of the disease to be prevented is low and the new drug might also produce undesirable side effects, albeit at a low rate. Clinically relevant biomarkers and surrogate endpoints will play a major role in the decision-making and development of Px-type drugs (40)

Relief of Signs and Symptoms

Drugs that treat the signs and symptoms of an illness can range in diversity, from sildenafil for erectile dysfunction to drugs that reduce blood pressure, lower cholesterol levels, help control diabetes, or relieve acute or chronic pain. These Tx drugs, by definition, provide relief from the signs and symptoms, but do not slow down or treat the underlying disease state. Outcomes in clinical development programs for Tx drugs can range from demonstrating a reduction in the signs and symptoms of the disease, such as stiffness and swollen joints for an arthritis drug, to an improvement in exercise tolerance for a drug that treats congestive heart failure.

Treatment That Arrests or Cures Disease

Therapy for patients with rheumatoid arthritis provides an example of the distinction between Cr and Tx drugs. Tx treatment drugs, such as the traditional NSAIDs and COX-2 inhibitors, relieve the signs and symptoms of pain and stiffness, but do little or nothing to arrest the disease progression. However, Cr drugs, such as entanercept, leflunomide, and infliximab, have been designed to actually arrest disease progression, as demonstrated by serial radiographic assessment of a patient's joints. Additional examples of Cr drugs include antibiotics that eradicate bacteria and drugs that restore bone density. In some cases, the "cure" might end if the patient no longer takes the drug. However, the future looks particularly bright for the development of drugs that not only correct presently untreatable diseases but also do not have to be taken for the remainder of a patient's life. The challenge for those who design the clinical development programs for these drugs will be to demonstrate that disease progression has been arrested (or ideally even reversed), by using innovative methods and assessments that do not require clinical trials that could not be completed within the patent life of the test drug.

What Are the Differentiation Targets?

Differentiation targets and quantified metrics will need to be clearly defined in order for a new drug to be "first in class" or "best in class." This can be illustrated by examining the development of the COX-2 inhibitor celecoxib. The hoped-for differentiating features for this drug were to maintain the anti-inflammatory effectiveness of the traditional NSAIDs, while at the same time significantly reducing the potential for gastrointestinal bleeding and avoiding loss of normal platelet aggregation inhibition and nephrotoxicity. The candidate compounds selected for clinical trials had to pass rigorous *in vitro* and *in vivo* preclinical tests to demonstrate a high probability that they would possess the desired differentiation when they were tested in humans. This was accomplished for gastrointestinal and platelet side effects, but there was no reduction in the potential for nephrotoxicity. It is noteworthy that at the FDA Advisory Committee meeting for celecoxib, the office director for anti-inflammatory drugs at CDER pointed out that the sponsor could have demonstrated anti-inflammatory activity by studying only 1,500 persons. But in order to demonstrate a lower potential for gastrointestinal adverse events, the sponsor needed to conduct a clinical development program that included more than 9,000 persons. This illustrates the point that clinical trials designed to demonstrate an enhanced safety profile compared to an already marketed product will have to be designed with more power than would normally be needed to demonstrate a statistically and clinically meaningful efficacy difference from placebo.

An additional cautionary note needs to be considered in planning a clinical program to differentiate a product on the basis of improved safety. Clinical trials in general have been sized to be able to demonstrate either an increase in effectiveness vs an active comparator or a placebo, or designed to demonstrate "no different than" an active comparator. To demonstrate that a new drug is safer than a comparator, the FDA has rightly established the precedent with oxybutynin that one must also demonstrate equivalent efficacy

before being able to make a claim with regard to an enhanced safety profile (41).

Is the Drug "Reasonably Safe" for FIH Trials?

The topic of preclinical assessment of a clinical candidate has been reviewed in Chapter 29. The topic is mentioned here because the decision as to whether it is safe to take a candidate drug into humans is ultimately a medical judgment that can only be made by individuals responsible for clinical drug development. Preclinical safety assessments are designed to provide the knowledge needed to decide whether it is reasonably safe to study a drug candidate in humans. The term *reasonably safe* is used in this context because that is what an FDA reviewer must answer when reviewing an IND application.

Two simple questions can be asked to help decide if a candidate drug is ready to be studied in Phase I FIH trials:

1. Based on the preclinical data we have, would I be willing to roll up my sleeve and be the first to receive this drug?
2. Would I be willing to let my son or daughter be the first to receive this drug?

If the answer is "yes" to both questions, the development team is ready to prepare an IND or a CTA (Clinical Trial Application) application, the European equivalent of an IND, to request permission to begin a clinical trial program.

Starting Dose for the FIH Trial

This topic has been covered in Chapters 30 and 31. Additional information regarding allometric scaling is available in "Man versus Beast: Pharmacometric Scaling in Mammals" (42).

Have Clinical Proof of Mechanism and Proof of Concept Been Obtained?

Once the human safety and pharmacokinetic profiles are established, the focus shifts to the design and conduct of early clinical trials that will confirm the hypothesized mechanism of drug action and characterize the differentiating features of the drug. These trials to establish mechanism of action and differentiation profile are the "killer experiments" that need to be conducted early in the program to provide the data to support a critically important Go/No-Go decision. It is essential to have answered the following four questions before proceeding to more extensive clinical trials in patients with the illness to be treated:

1. What is the mechanism of action in humans?
2. Does the clinical activity profile meet the prespecified safety criteria?
3. Are the bioavailability, half-life, and other features of the pharmacokinetic profile within the prespecified criteria?
4. Can the new drug be administered safely together with expected concomitant medications?

Mechanism of action

Typical mechanism of action and POC questions:

- Has the hypothesized mechanism of action been demonstrated in humans (POM)?
- Is the dose within the projected dose range using the intended route of administration?
- Is the size of the diseased patient population that is responding to the drug large enough to justify continued development?
- How many individuals were screened to find those who qualified for our trials? Does this indicate that there will be enough patients that meet the entry criteria to justify continuing this clinical program?

Safety

Typical safety questions:

- Is the safety adequate at the active dose and corresponding blood levels? Was any unusual toxicity that was observed in animals either observed or ruled out in humans?
- What do we know about human safety at several times the therapeutically active dose or blood level?
- Have we "stressed" the conditions to ensure that toxicity observed with currently marketed products will not occur with our candidate?

Pharmacokinetics

Typical questions regarding drug absorption, distribution, metabolism, and excretion:

- Does the drug have the bioavailability, elimination half-life, and other pharmacologic properties needed to support the desired dosing regimen?
- Will a special formulation be able to overcome any deficiencies in the pharmacokinetic profile?
- What are the sources of interindividual and intraindividual variability in pharmacokinetics?

Drug Interactions

Typical questions regarding interactions resulting from concurrent administration of other drugs:

- If this drug is to be given in combination with another drug, have therapeutic activity and safety

been demonstrated with combination dosing?
- Is the dose for combination therapy different (higher or lower) than the single-agent dose?
- Have clinically significant gut and liver cytochrome P450 drug interactions (inhibition or induction) been identified or ruled out by *in vitro* or *in vivo* studies?

Have the Dose, Dose Regimen, and Patient Population Been Characterized?

The goal of a Phase II learning program is to provide three essential pieces of information that are critical to the success of subsequent long-term confirmatory Phase III trials:

1. Dose: The dose needed for effectiveness of each of the various disease states (early-, mid-, and late-stage disease).
2. Dose regimen: The regimen (frequency or interval) at which the dose needs to be given (once daily, twice a day, every other day, weekly) and the dose duration (for how long?).
3. Patient population: The patient population that will respond to the drug:
   - Mild, moderate, severe disease?
   - Refractory to existing therapies?
   - Old, young, male, female?

Because Phase III is in actuality the confirmation of Phase II observations, it is likely that the Phase III program will be successful only if the answers to these questions are known with a high degree of certainty and the design of the Phase III program does not deviate from a design to confirm the Phase II learnings. Many times when a Phase III program is not successful, the reason for failure is either that the patient population for Phase III was not the same as the Phase II population or that the dose and dose regimen were not appropriately based on the Phase II experience.

Within the past decade there has been significant interest in determining whether the use of clinical modeling and simulation software would increase the probability of conducting successful clinical trials (43). This approach incorporates the technique of pharmacokinetic–pharmacodynamic modeling that was discussed in Chapter 19 with the disease progression models described in Chapter 20. Although this type of a clinical development tool has considerable potential, the outcomes to date have been mixed. For example, this approach has identified the placebo-response rate for various disease states as an area requiring better understanding. If the placebo-response rate observed in a large clinical trial is significantly higher than what was projected in the preliminary simulations, the size of the actual trial might not be adequate to distinguish the new drug from placebo, even if the new drug is active at the doses tested.

Will the Product Grow in the Postmarketing Environment?

To maximize the value of a new drug, project teams are charged with ensuring that there is a full life-cycle global development and regulatory plan that includes postmarketing growth. Clinical trials to support new indications and new formulation development must therefore begin even before the NDA/BLA is submitted. In some cases, clinical trials that demonstrate synergism of the new drug in combination with other drugs can provide information that will expand the market. The exploration of this synergism has been the subject of several alliances between pharmaceutical manufacturers, such as the joint development by Merck and Schering of a combination of an asthma product, montelukast, with an allergy product, loratidine.

Will the Clinical Development Program Be Adequate for Regulatory Approval?

It is important to establish a global clinical development and regulatory strategy early in the development program. Most organizations require a draft of a global clinical development and regulatory strategy at the time of clinical lead selection. The regulatory strategy, along with the label-driven question-based development plan, establishes the framework for a comprehensive FIH-to-market-expansion clinical development program.

An important consideration is to determine whether the development program is global or regional. If the program is global, then a global clinical development plan will need to be drafted at the beginning of the development project. Most drug development conducted today is of a global nature, designed to meet the regulatory requirements of the United States, Europe, and Asia. The task of achieving global drug approvals has been greatly simplified with the advent of International Conference on Harmonization guidelines for the development and registration of new medicines (44). Critical global clinical development considerations include the following parameters:

- Ensuring the inclusion of local populations with all the disease states that are needed to support the package insert indications.

- Ensuring the inclusion of individuals who are taking the types of concomitant drugs that these patient populations usually take in individual countries.

Until 1990, sponsors essentially had to conduct three parallel development programs in the United States, in Europe, and in Asia. However, the ICH was started in 1990 and finalized in 2000 with the goal of producing a Common Technical Document that could be used by sponsors to file for marketing approval in any country in the world. The ICH is a joint initiative that involves both regulators and industry as equal partners in scientific and technical discussions of the testing procedures that are required to ensure and assess the safety, quality, and efficacy of medicines. Despite the progress that has been made by the ICH, it is critical to establish the intended filing strategy for Europe as early as possible, since there still are multiple ways to proceed in this region. Until recently, drug development programs in Japan generally ran considerably longer than did the U.S./European counterparts. However, there have been recent regulatory changes in Japan that are intended to speed up the process. Nevertheless, Phase I and Phase II studies will need to be repeated in Japan before the Phase III trials can be started in that country.

In addition, the following clinical/regulatory questions are representative of those that need to be considered in designing a clinical development plan to meet U.S. regulatory requirements:

- ***Does the drug qualify for fast-track and accelerated approval?*** *Fast track* is a regulatory status that is granted by the FDA for certain drugs that will address an unmet medical need. Advantages of obtaining fast-track status include the opportunity for an increased number of FDA–sponsor meetings and Special Protocol Assessments (SPAs) that provide the sponsor with FDA input into the design of clinical trials that will meet FDA expectations and accelerate the review and approval process.

  Accelerated approval enables the FDA, under 21 CFR 314 (Subpart H), to provide marketing approval for a drug on the basis of efficacy based on a surrogate endpoint, with the understanding the sponsor will continue trials to provide evidence of efficacy based on a clinical endpoint. Accelerated approval is usually granted for drugs, (such as HIV antiretroviral agents, anticancer agents, and other agents) that address an unmet medical need.
- ***Does the drug qualify for priority review?*** *Priority review* is designated by the FDA shortly after the NDA/BLA is filed. Priority reviews are to be reviewed within 6 months of the filing date.
- ***Does the drug qualify for a continuous marketing application NDA/BLA review?*** The continuous marketing NDA/BLA *application* (CMA "*Rolling NDA/BLA*") describes a process in which the FDA works with the sponsor during the phases of clinical development and accepts for review parts of the NDA/BLA before a complete NDA can be filed. In 1993, the Rolling NDA/BLA was pioneered by the FDA Pilot Drug Division and the Medications Development Division of NIDA/NIH for the NDA filing for L-α-acetylmethadol, an alternative to methadone for the treatment of heroin addiction. This process enabled the FDA to approve L-α-acetylmethadol 18 days after the complete NDA was submitted (45). Subsequent Rolling NDA/BLA approvals have been made for HIV antiretroviral drugs by the CDER Anti-Viral Division.
- ***Does the drug meet the FDA requirement to develop pediatric labeling?*** As discussed in Chapter 23, sponsors now are required either to develop pediatric dosing information or to request a waiver of this requirement if the drug is not expected to be used in pediatric populations.

LEARNING CONTEMPORARY CLINICAL DRUG DEVELOPMENT

Drug development is as much an art as a science. We are trained in various professions such as biology, pharmacology, chemistry, medicine, biostatistics, computer science, etc., but rarely does a university offer a course, yet alone a curriculum, in drug development.

Courses and Other Educational Opportunities

Courses, workshops, and meetings are offered by the Pharmaceutical Education and Research Institute (PERI) (46), Drug Information Association (DIA) (47), Center for Drug Development Science (CDDS) at the University of California, San Francisco, Washington, D.C. Center (48), Tufts Center for the Study of Drug Development (CSDD-Tufts) (49), the National Institutes of Health (50), the FDA's Center for Drug Evaluation and Research (CDER), and other organizations.

In addition to courses and workshops, instructive drug development case studies are provided by attending FDA Advisory Committee meetings, or

viewing the video tapes, or reading the transcripts of these informative meetings (51); by reading FDC Reports "Pink Sheets" and "Pharmaceutical Approvals Monthly" (52); and by attending the annual meetings of DIA (47), Regulatory Affairs Professionals Society (RAPS) (53), American Association of Pharmaceutical Scientists (AAPS) (54), American College of Clinical Pharmacology (ACCP) (55), American Society for Clinical Pharmacology and Therapeutics (ASCPT) (56), and other professional organizations associated with drug development.

Failed Clinical Drug Development Programs as Teaching Examples

One way to learn how to avoid the pitfalls of drug discovery and development is to examine examples of failed programs. We will examine three cases:

1. Tasosartan, which the sponsor withdrew from FDA review during the NDA/BLA review since it was likely not to be approved.
2. Cisapride, for which the FDA requested revised labeling, leading the sponsor to withdraw the drug from U.S. marketing.
3. Mibefradil, which was withdrawn from the marketplace.

Safety NDA Withdrawal during the NDA Review Process

On March 3, 1998, the tasosartan application was withdrawn from FDA consideration by the sponsor, who stated that the "action was the result of an unresolved question [with FDA] regarding the safety profile" of the product (57). The product had been found to be associated with liver enzyme elevations during clinical trials. The sponsor is reanalyzing the safety data for this angiotensin II inhibitor in hopes of resubmitting the NDA.

Drug–Drug Interactions — Revised Labeling and Removal from the Market

Cisapride underwent significant PI changes, which reserved the drug for second-line use for patients with gastroesophageal reflux before it eventually was removed from the market in mid-2000 (58). Following reports of cardiac adverse events and deaths associated with cisapride use, the FDA instructed the sponsor to revise the labeling to include a "black box" warning that "serious cardiac arrhythmias including ventricular tachycardia, ventricular fibrillation, *torsades de pointes*, and QT prolongation have been reported" in patients taking cisapride with other drugs that inhibit CYP3A4. The new labeling contraindicated the use of cisapride with at least 20 different drugs, including antibiotics (erythromycin, clarithromycin, and troleandomyacin), antifungals (fluconazole, itraconazole, and ketoconazole), protease inhibitors (indinavir and ritonavir), and the antidepressant nefazodone. Additional labeled contraindications were concomitant use of cisapride with certain medications known to prolong the QT interval: antiarrhythmics, such as quinidine, procainamide, and sotalol; antidepressants, such as amitryptiline and maprotiline; and phenothiazines.

Safety NDA Removal from the Market

The calcium channel blocker mibefradil (Posicor®) was removed from the market in 1998. The headline for the Pink Sheets article describing this action was "Posicor® Withdrawal Reflects 'Complexity' of Interaction Profile" (59). Products identified as potentially dangerous in combination with mibefradil included cardiac drugs, such as amiodarone, flecainide, and propafenone; oncologic products, such as tamoxifen, cyclophosphamide, etoposide, ifosfamide, and vinblastine; and the immunosuppressant medications cyclosporine and tacrolimus. The sponsor's decision to withdraw mibefradil was based on the complexity of the drug interaction information that would have to be communicated to ensure safe usage.

REFERENCES

1. Peck CC. Drug development: Improving the process. Food Drug Law J 1997;52:163–7.
2. Spilker B. Guide to clinical trials. Philadelphia: Lippincott-Raven; 1996. p. 1156.
3. Friedman LM, Furberg C, Demets DL. Fundamentals of clinical trials, 3rd ed. New York: Springer Verlag; 1998. p. 384.
4. Riegelman RK. Studying a study and testing a test — how to read the medical literature (with CD-ROM for Windows & Macintosh). Baltimore: Lippincott Williams & Wilkins; 2004.
5. U.S. Food and Drug Administration. (Internet at http://www.fda.gov/cder/handbook/index.htm.)
6. Clinical Research Terminology. Appl Clin Trials 1998;4:28–50.
7. U.S. Food and Drug Administration. (Internet at http://www.fda.gov/oc/initiatives/criticalpath.)
8. International Conference on Harmonization of Technical Requirements for Registration of Pharmaceuticals for Human Use. (Internet at www.ich.org.)
9. PhRMA Annual Report 2000–2001. Washington, D.C.: Pharmaceutical Research and Manufacturers of America. (Internet at http://www.phrma.org/.)

10. The pharmaceutical industry's R&D investment — the rising cost of R&D. PhRMA Annual Report 2000–2001, Washington, D.C.: Pharmaceutical Research and Manufacturers of America. (Internet at http://www.phrma.org/.)
11. Gilbert J, Henske P, Singh A. Rebuilding big pharma's business model. In Vivo, November 2003. (Internet at http://www.bain.com/bainweb/PDFs/cms/Marketing/rebuilding_big_pharma.pdf.)
12. Pharmaceutical Research and Manufacturers of America. (Internet at http://www.phrma.org/mediaroom/press/releases/18.02.2005.1128.cfm.)
13. U.S. Food and Drug Administration. (Internet at http://www.fda.gov/bbs/topics/answers/2005/ans01346.html.)
14. DiMasi J. Risks in new drug development: Approval success rates for investigational drugs. Clin Pharmacol Ther 2001;69:297–307.
15. Regulatory Affairs Professional Society. (Internet at http://www.raps.org/s_raps/event_session.asp?TRACKID=&CID=1912&DID=23891.)
16. Federal Register. Title 21 CRF 310, Kefauver–Harris Drug Amendments of the Food, Drug and Cosmetic Act, 1962.
17. Personal communications from Rob Bies (sildenafil, Viagra®), Jianguo Li (zanamivir, Relenza®), Mike Staschen (trastuzumab, Herceptin®), Theo Jang (rofecoxib, Vioxx®), and Agnes Westelinck (etanercept, Enbrel®), Center for Drug Development Science, University of California, San Francisco, Washington, D.C.
18. The Pink Sheet, March 30, 1998. Chevy Chase, MD: F-D-C Reports, Inc.; p. 4. (Internet at http//www.fdcreports.com/.)
19. U.S. Food and Drug Administration. (Internet at http://www.fda.gov/cder/approval.)
20. U.S. Food and Drug Administration. (Internet at http://www.fda.gov/cber/cberac.htm.)
21. Clemento A. New and integrated approaches to successful accelerated drug development. Drug Inf J 1999;33:699–710.
22. CDER, CBER. Guidance for Industry: Providing clinical evidence of effectiveness for human drug and biological products. Rockville, MD: FDA; 1998. (Internet at http://www.fda.gov/cder/guidance/index.htm.)
23. CDER ODE IV. Pilot targeted product information. Rockville, MD: FDA;2000. (Internet at http://www.fda.gov/cder/tpi/default.htm.)
24. U.S. Food and Drug Administration. (Internet at http://www.fda.gov/cder/present/DIA2005/delasko.pdf.)
25. For available FDA/CDER approved and draft guidances, see Internet at http://www.fda.gov/cder/guidance/index.htm.
26. For available FDA/CBER approved and draft guidances, see Internet at http://www.fda.gov/cber/guidelines.htm.
27. For access to NDA/BLA reviews, see Internet at http://www.accessdata.fda.gov/scripts/cder/drugsatfda.
28. Holford NH. Personal communication.
29. Kolata G. A widely used arthritis drug is withdrawn. The New York Times, October 1, 2004. (Internet at http://www.nytimes.com.)
30. Kaufman M. FDA officer suggests strict curbs on 5 drugs: Makers dispute claims about health risks. The Washington Post, November 19, 2004. (Internet at http://www.washingtonpost.com.)
31. Kaufman M. FDA plans new board to monitor drug safety: Independent panel to be more open to the public. The Washington Post, February 16, 2005.
32. Grudzinskas C. Change + communication = challenge — management of new drug development. Clin Res Pract Drug Regul Affairs 1988;6:87–111.
33. Holford NHG, Peck CC. Population pharmacodynamics and drug development. In: Van Boxtel C, Holford NHG, Danhof M, editors. The *in vivo* study of drug action. Amsterdam: Elsevier; 1992. p. 401–13.
34. Sheiner LB. Learning versus confirming in clinical drug development. Clin Pharmacol Ther 1997; 61:275–91.
35. Lesko L, Williams R. Early clinical development: The question based review. Appl Clin Trials 1999;8:56–62.
36. Carey J. The genome gold rush. Business Week June 13, 2000;147–58.
37. CDER Preliminary Concept Paper. Drug-diagnostic co-development concept paper. Rockville, MD: FDA; 2005. (Internet at http://www.fda.gov/cder/genomics/pharmacoconceptfn.pdf.)
38. The Pink Sheet, January 31, 2000. Chevy Chase, MD: F-D-C Reports, Inc.; p. 30. (Internet at http//www.fdcreports.com/.)
39. Gounni AS. Nutku E. Koussih L, Aris F. Louahed J. Levitt RC. Nicolaides NC, Hamid Q. IL9 expression by human eosinophils: Regulation by IL-1 beta and TNF-alpha. J Allergy Clin Immunol 2000; 106:460–6.
40. Lesko LJ, Atkinson AJ Jr. Use of biomarkers and surrogate endpoints in drug development and decision making: Criteria, validation, strategies. Annu Rev Pharmacol Toxicol 2001;41:347–66.
41. Pharmaceutical Approvals Monthly. April 1999. Chevy Chase, MD: F-D-C Reports, Inc.; p. 26–30. (Internet at http//www.fdcreports.com/.)
42. Mordenti J. Man versus beast: Pharmacokinetic scaling in mammals. J Pharm Sci 1986;75:1028–40.
43. Holford NHG, Kimko HC, Monteleone JPR, Peck, CC. Simulation of clinical trials. Annu Rev Pharmacol Toxicol 2000;40:209–34.
44. International Conference on Harmonization of Technical Requirements for Registration of Pharmaceuticals for Human Use. (Internet at http://www.ifpma.org/ich1.html.)
45. Grudzinskas CV, Wright C. Reshaping the drug development and review process — a case study of an 18-day approval. Pharmaceutical Executive. October 1994;14:74–80.
46. Pharmaceutical Education and Research Institute. (Internet at http://www.peri.org).
47. Drug Information Association. (Internet at http://www.diahome.org.)
48. Center for Drug Development Science at University of California, San Francisco — Washington, D.C. Center. (Internet at http://cdds.ucsf.edu.)
49. Tufts Center for the Study of Drug Development. (Internet at http://www.tufts.edu/med/research/csdd/.)

50. National Institutes for Health clinical pharmacology web site. (Internet at http://www.cc.nih.gov/researchers/training/principles.html.)
51. CDER list of advisory committee meetings and workshops. (Internet at http://www.fda.gov/cder/calendar/default.htm.)
52. Transcripts, videotapes, and subscriptions to the Pink Sheet can be obtained from the FDC Reports web site. (Internet at http://www.fdcreports.com/.)
53. Regulatory Affairs Professionals Society. (Internet at http://www.raps.org/.)
54. American Association of Pharmaceutical Scientists. (Internet at http://www.aaps.org/.)
55. American College of Clinical Pharmacology. (Internet at http://www.accp1.org/.)
56. American Society for Clinical Pharmacology and Therapeutics. (Internet at http://www.ascpt.org/.)
57. The Pink Sheet, March 9, 1998. Chevy Chase, MD: F-D-C Reports, Inc.; p. 22. (Internet at http//www.fdcreports.com/.)
58. The Pink Sheet, July 6, 1998. Chevy Chase, MD: F-D-C Reports, Inc.; p. 5. (Internet at http//www.fdcreports.com/.)
59. The Pink Sheet, June 15, 1998. Chevy Chase, MD: F-D-C Reports, Inc.; p. 5. (Internet at http//www.fdcreports.com/.)

This page intentionally left blank

CHAPTER

34

Role of the FDA in Guiding Drug Development

LAWRENCE J. LESKO AND CHANDRA G. SAHAJWALLA
Center for Drug Evaluation and Research, Food and Drug Administration, Rockville, Maryland

The drug development process is defined here as a process that includes the preclinical and clinical phases of drug development following the selection of a lead molecule by the sponsor, and includes the regulatory review phase that is intended to lead to marketing authorization. As discussed in Chapter 33, this process is complex, time-consuming, and costly. A typical new molecular entity (NME), if approved for marketing, has gone through time-consuming preclinical discovery and evaluation periods, followed by a clinical evaluation stage that lasts, on average, 5 to 7 years. With an average of 6 to 10 months required for traditional regulatory review, the entire process, from preclinical discovery to marketing, may take up to 15 years, with a cost that may exceed $800 million (1–3). Given the current high failure rate of drugs that enter into clinical testing (~50% in Phase III), the need for efficient and informative drug development is obvious.

A goal of the drug development process, which includes regulatory review, is to get effective drugs to patients as quickly as possible and to manage the risks associated with these drugs in the best way possible. Another goal is to make sure that ineffective drugs, unsafe drugs, drugs with inappropriate benefit/risk ratios, or drugs for which risk management after marketing authorization is a problem do not get to the marketplace. Another goal of drug development is to obtain data to achieve individualization of dose and dosing regimen for specific special patient populations (e.g., pediatric patients), and, where appropriate and needed, tailoring of dose and dosing to individual patients. To achieve these goals, there needs to be a transparent and accountable review process. The Food and Drug Administration (FDA) not only reviews the results of studies submitted by the sponsor (pharmaceutical firm) in a submitted New Drug Application (NDA), but also plays a critical role in guiding drug development decisions by providing sponsors with advice, insights, and credible knowledge gleaned from past experiences regarding the science of drug development in conformance with applicable regulations regarding the investigational new drug phase of drug development. Effective communication and mutual trust between the FDA and sponsors is essential to achieving the goals of the drug development process in an efficient, successful, and informative manner. Meetings held face-to-face between sponsor representatives and FDA staff are a key part of direct communication. However, less direct but useful communication can also occur through domestic and international guidances, telephone conferences, FDA presentations at public meetings (including advisory committee meetings), and the FDA web site. These sources of information combine to provide transparency and accountability that should facilitate drug development and reduce uncertainty about the regulatory review process by enabling sponsors to learn about the FDA's thinking.

This chapter reviews the various ways that the FDA gets involved in guiding drug development

and communicating with sponsors. This chapter is written from the perspective of the NDAs that are the responsibility of the Center for Drug Evaluation and Research (CDER) in FDA. However, similar considerations apply to the development of new biologic products, which have additional unique attributes associated with the drug development process.

WHY DOES THE FDA GET INVOLVED IN DRUG DEVELOPMENT?

In the United States, the development and marketing of drug products for human use are regulated by legislation enacted by the U.S. Congress in 1962. The FDA is responsible for interpreting and enforcing these legislations. To facilitate that process, the FDA implements rules and regulations, which are published in the Federal Register and coded in the U.S. Code of Federal Regulations (CFR). According to 21 CFR 393, the FDA has a dual mission of promoting the public health by promptly and efficiently reviewing clinical research and taking appropriate action on the marketing of regulated products in a timely way.

The 2004 FDA Critical Path White Paper ("Innovation/Stagnation: Challenge and Opportunity on the Critical Path to New Medical Products") addressed the recent slowdown in innovative medical therapies submitted to the FDA for approval. The report describes the urgent need to modernize the medical product development process, the "critical path", to make product development more predictable and less costly. In this regard, the FDA and the pharmaceutical industry have basically the same goals — namely, to promote public health by getting safe and effective drugs to patients as quickly as possible and to protect public health by assuring that drugs with inadequate benefit/risk attributes do not get into the marketplace. In addition, both the FDA and the industry maintain pharmacovigilance programs to monitor adverse drug reactions after a new drug is marketed, and risk management strategies have been a part of the FDA's 5-year plan that is outlined in the 1992 Prescription Drug User Fee Act III (PDUFA III).

The chronology of legislation regulating drug development is summarized in Table 34.1. Beginning with the Food and Drugs Act in 1906 that prohibited interstate commerce in misbranded and adulterated foods, drinks, and drugs, the FDA has had an important role in protecting the public health. Over the years, public health safety disasters have contributed to the evolution of drug regulations that currently impact drug development. For example, the sulfanilamide elixir disaster in 1937, in which the sulfanilamide was dissolved in the poisonous solvent diethylene glycol, killed 107 persons and dramatized the need to establish drug safety before marketing. The Federal Food, Drug and Cosmetic Act of 1938, which contained provisions to require sponsors to show that new drugs were safe before marketing, ushered in a new system of drug regulation. The thalidomide tragedy of 1962, in which the drug caused birth defects in thousands of babies, aroused public support for stronger drug regulations. As a result, the 1962 Kefauver–Harris Drug Amendments were passed to ensure drug efficacy and greater drug safety. The bioavailability problems with digoxin reported in 1974, which included substantial variability in bioavailability between different manufacturers and between different lots of the same manufacturer, led to a greater awareness of need for better regulatory standards in manufacturing to assure high-quality drug products for the American public (4). Dissolution-rate testing requirements for digoxin tablets initiated by the FDA in 1974 improved the uniformity of performance of digoxin tablets from various manufacturers. More recently, drug regulations have focused on the individualization of drug therapy in patient subsets defined by age, sex, and race. With the pharmacogenomic advances in molecular biology, the next stage in the evolution of drug regulations may well focus on individualization of drug therapy (5). With the recent safety issues associated with postmarketing use of the COX-2 inhibitors, there has been a new call to strengthen postmarketing surveillance. Further, the FDA has been proactive in implementing a framework for collecting DNA samples from individual patients who experience a rare and serious adverse event. The intent is to identify genomic biomarkers that provide a better understanding of safety risks, such as prolongation of the electrocardiographic QT interval.

TABLE 34.1 Chronology of Pharmaceutical Legislation

Date	Legislation
1906	Food and Drugs Act
1938	Federal Food, Drug and Cosmetic Act (FD&C Act)
1962	Kefauver–Harris Amendments
1974	Dissolution Rate Testing Requirements
1992	Prescription Drug User Fee Act III (PDUFA III)
1997	FDA Modernization Act (FDAMA)

WHEN DOES THE FDA GET INVOLVED IN DRUG DEVELOPMENT?

For over 25 years, the FDA has had a formal process for holding meetings with sponsors to discuss

scientific and clinical issues related to drug development. These formal meetings are consistent with the FDA's goal of facilitating drug development by providing advice and assuring a transparent review process. Although these meetings are voluntary, they are quite common and generally helpful. The meetings are referred to by the time frame in which they occur during the drug development process, and meetings at different times have different purposes and goals. Examples are meetings held before submission of an Investigational New Drug application (IND) or at the end-of-Phase I (EOP I), end-of-Phase IIA (EOP IIA), end-of-Phase II (EOP II), and pre-NDA submission.

Each of these meetings can have a major impact on the drug development process, including regulatory review of an NDA. The questions that are raised and discussed at each of these meetings are appropriate for the stage of development. For example, pre-IND meetings that are held early in the drug development process are extremely valuable to both the FDA and the sponsor because they routinely focus on critical issues (e.g., drug safety) in the drug development program, before the sponsor has expended substantial resources in the conduct of clinical trials. A major goal for sponsors also is to avoid the occurrence of, if at all possible, any issues that might lead to an FDA order to halt clinical trials, i.e., a *clinical hold*.

Because of great interest on the part of sponsors to get early advice and FDA's goal of facilitating drug development, EOP IIA meetings were recently introduced and are being promoted by the Agency. These meetings are held at the request of the sponsor when the sponsor is seeking advice or nonbinding consultations at a time when there is uncertainty related to the limited data that are available at that point in drug development. Primary objectives of the FDA are to help optimize the drug development process by reducing the potential of Phase II or Phase III clinical trial failures and improving dose selection for pivotal trials. At this meeting, sponsor plans for Phase II and/or Phase III trial designs are reviewed and recommendations are made based on available preclinical, clinical, and literature data, and on the experience that FDA staff may have with the same class of compounds. Often, the FDA, in conjunction with sponsors, develops disease-state models that can be used to simulate different clinical trials designs. These models allow for calculations of the probability of a favorable outcome when variables in the study design are tested. Strategies on conducting studies in special populations are also discussed, which could provide the knowledge and the basis for subsequent package insert recommendations for individualizing drug dose and dosing regimen. At any of the meetings held during the drug development phase, the sponsor could seek advice on the utility or acceptability of emerging science such as pharmacogenetics and pharmacogenomics, advice on designing an enrichment trail to demonstrate proof of efficacy and/or proof of concept, or advice on designing studies to look at drug toxicity (for example, the effect of the drug on the electrocardiographic QT interval).

During the clinical development phase, the EOP II meeting is critical to discuss any remaining product development issues, safety risks, and the efficiency and appropriateness of the study design, especially with respect to the endpoints of the pivotal Phase III efficacy studies. Acceptable statistical analysis approaches to provide evidence of efficacy that should be specified in advance are also discussed. These meetings also play an important role in resolving any outstanding manufacturing issues, or questions regarding dose, dose regimen selection, or major modifications to the drug development plan that are contemplated to support anticipated label claims. Pre-NDA meetings are intended to focus on the content and format of the sponsor's marketing application, and to familiarize the reviewers from various disciplines with the NDA that will be submitted. Any issues that remain to be resolved [e.g., chemistry, manufacturing, and control (CMC) problems or questions] may also be discussed at this meeting. Pre-NDA meetings serve as a means to identify any other pending issues that may result in refuse-to-file (RTF) action when an NDA is submitted for review to the Agency.

Important interactions between a pharmaceutical company and the FDA occur at the end of the marketing application review process, when meetings and discussions take place to sort out the content and language of the label or package insert. Risk management plans may also be further discussed at this point. Following market authorization, the FDA continues to be involved with the development and approval of new uses or new dosage forms for an approved product and maintains the MedWatch postmarketing surveillance program of adverse drug reactions (6).

HOW DOES THE FDA GUIDE DRUG DEVELOPMENT?

As previously indicated, the FDA guides drug development in many different ways, such as by interpreting laws, rules, and regulations, by disseminating policy statements that may otherwise be vague or unclear, by providing advice and sharing experiences and expertise in face-to-face meetings, via written agreements and letters, by domestic and international guidances, by planned telephone conferences and/or scheduled videoconferences, and via the

FDA web site (7). Communicating with the FDA is sometimes confusing for sponsors who are uncertain about what to ask, whom to ask, and what to do with the answers. Conversely, communicating with sponsors is sometimes a challenge for the FDA staff, who must balance FDA advice and guidance to sponsors with the need to remain objective when the sponsor's application is being reviewed later on. FDA also has to be cautious in what to communicate and cannot divulge any proprietary information. To help with these situations, there are regulatory requirements for the various types of meetings with the FDA. Policies and procedures for requesting, scheduling, and conducting formal meetings between the Center for Drug Evaluation and Research (CDER) and a sponsor are described in the FDA Guidance for Industry entitled "Formal Meetings with Sponsors and Applicants for PDUFA Products" (8).

Since CDER added review divisions from the Center for Biologics Evaluation and Research (CBER), it now receives over 2000 meeting requests annually, and must balance its review responsibility with its obligation to respond to meeting requests. Prior to this change, in 2004, for example, the CDER had over 1400 formal meetings with sponsors, and, depending on the type of meeting, these meetings occurred within 30 to 75 days following a meeting request. The FDA prepares official minutes for these meetings within 4 weeks after the meeting. According to the formal meeting guidance, sponsors have the option to contact the appropriate FDA project manager to arrange discussion of any differences of opinion expressed in the minutes of the meeting. There is also a formal pathway described in the guidance for dispute resolution if this is necessary.

One or more formal meetings with the FDA generally occur for every development plan for a new chemical entity. Given the relatively short time available for meetings, the quality of these meetings is an important determinant of their impact on the drug development process. Both sponsors and the FDA review division that is involved in the meeting share the responsibility for planning and conducting these meetings in an optimally productive way. To assure a high-quality meeting with substantive agreements or understanding about issues, the meetings should be focused, designed with a specific purpose in mind, have necessary background data appropriate for the agenda or any questions, and have a well-defined agenda. Timing is important if the meeting involves a discussion of drug development plans. For example, in planning a meeting to discuss a clinical trial protocol, the sponsor should allow sufficient time so that the meeting is held before the study is begun, otherwise the meeting and the sponsor's resources may be wasted. The EOP IIA meetings, for example, are extremely resource intensive for the FDA and the sponsor, sometimes taking the equivalent of four or five full-time reviewers from 2 to 5 weeks to prepare. The FDA may conduct substantial data analysis, including modeling and simulation, on data received from the sponsor in order to provide recommendations on options for the drug development plan. In order to maximize the value of the dialogue, the preplanning for these meetings may entail substantial expenditure of time and money on both the sponsor's and the FDA's part. Meetings that are expected to have a significant impact on drug development or approval are attended by many consultants or investigators representing the sponsor, and sponsors should request attendance by discipline-specific reviewers from the FDA review divisions that are appropriate for the agenda. This ensures that the expertise needed for the meeting is on hand.

In the past 15 years, the FDA has implemented regulatory initiatives that have impacted the drug development process, and sponsors should be quite familiar with their regulatory options. As discussed in Chapter 33, these include fast-track drug development programs, accelerated approvals (21 CFR 314.500–560), and priority reviews. The Subpart E (21 CFR 312.80–88) and fast-track regulations (21 CFR 356), respectively, have expedited the drug development process and market access for new drugs for severely debilitating and serious conditions or life-threatening diseases without approved alternative treatments. An additional requirement for fast-track status is that there is an unmet medical need. In these instances, multiple meetings between sponsors and the FDA early in the development process are recommended to gain agreement on the development plan, and it is imperative for the sponsor to stay in close contact with the responsible FDA review division. It is also possible under Subpart E to gain approval with less safety data than normal. The accelerated approval regulations were developed as a complementary program to the Subpart E initiative, and encourage the use of surrogate endpoints as a basis for accelerated approval. Applications designated for fast-track approvals can be submitted as continuous marketing applications (CMAs) whereby the FDA will even accept and review only certain sections (e.g., preclinical, chemistry, clinical pharmacology) of the NDA prior to submission of full application.

Two pilot programs for CMAs also have been undertaken by the FDA. The first pilot (Pilot 1) provides for the review of a limited number of presubmitted portions of a sponsor's marketing application (*reviewable units*) based on the terms and conditions agreed upon

by the applicant and the FDA. Under the second pilot (Pilot 2), the FDA and sponsor can enter into agreements to engage in frequent scientific feedback and interactions during the IND phase of product development. Pilot 2 will be limited to a maximum of one drug per clinical review division. More recently, the FDA has offered a regulatory pathway for voluntary and required genomic data submissions for which guidance, along with related information on genomics, is available on the FDA web site (9). The Prescription Drug User Fee Act (PDUFA) of 1992 has allowed CDER to increase the number of reviewers as the workload has increased, and CDER has made a commitment to schedule the planned meetings that sponsors request in a reasonable time, so that the drug development process can be advanced expeditiously (10). However, the newer meetings, such as the EOP IIA and the voluntary genomics submission meetings, require much more forward planning and resources.

The FDA also guides drug development by holding closed or open advisory committee meetings. These meetings facilitate the regulatory review and FDA approval process by bringing together external experts to assess data, to recommend need for new studies, and to address specific questions formulated by the FDA to help resolve scientific or clinical problems related to the drug development process or a specific product approval. Podium presentations by senior FDA personnel are another way that the FDA attempts to guide drug development by informing participants in meetings and workshops about the current thinking on a scientific or clinical topic. It is advantageous to sponsors to pay attention to these talks and interact with the FDA speakers on any qualifying questions. Slides and handouts presented in these public meetings generally are available to anyone who requests them and are placed on an FDA web site (e.g., http://www.fda.gov/cder/genomics/default.htm).

WHAT ARE FDA GUIDANCES?

Perhaps the most widespread, effective, and important way that the FDA communicates with sponsors and guides drug development is through guidances issued either by the FDA or by the International Conference on Harmonization (ICH). Guidances represent a wealth of knowledge, consensus, and experience, generally drawn collectively from academia, industry, and FDA. The FDA published the first guidance to industry in 1949, and this guidance was related to procedures for the appraisal of the toxicity of chemicals in food. Information on over 400 final or draft guidances can be found on the Internet (11).

The development of guidances proceeds by a process known as Good Guidance Practices, which is intended to assure that there is the appropriate level of meaningful public participation in the guidance development process (12, 13). Recent guidance development was motivated, in part, by the Food and Drug Administration Modernization Act of 1997 (FDAMA) that reauthorized the PDUFA of 1992 and mandated the most wide-ranging reforms in FDA practices since 1938 (14). Since 1997, significant numbers of final or draft guidances have been published on the FDA guidance web site (11). For example, under FDAMA, Section 111, guidance has been developed that deals with the important application of "bridging studies" for pediatric drug approval, in which a pharmacokinetic study can serve to bridge to children the efficacy and safety database that has been established in adults. Another key provision of FDAMA, Section 115, deals with clinical investigations in which data from *one* adequate and well-controlled clinical investigation, and *confirmatory evidence*, are sufficient to establish effectiveness. Much speculation has focused on the meaning of "confirmatory" evidence (e.g., if a relevant and well-designed pharmacokinetic/pharmacodynamic study would serve as confirmatory evidence), and further discussion of this issue is needed in a public forum.

The FDA recognizes the value to sponsors of transparency, consistency, and predictability in regulatory decision-making, and guidances for industry are developed as good faith efforts to share with sponsors the current thinking on a scientific topic. Guidances are intended to provide sponsors with assurances that FDA staff will interpret statutes and regulations in a consistent manner across its various divisions. However, on occasion, inconsistent interpretation of guidances does occur. This is not surprising given that CDER has 15 different therapeutic review divisions. However, guidances, in contrast to regulations that are substantive and binding, do not legally bind the FDA or sponsors. Sponsors are not required to follow guidances, and with appropriate rationale may propose alternative approaches to an issue. Likewise, the FDA may not accept data that is generated by following guidance if there is a valid scientific reason. So if any inconsistencies in interpretation are detected, it is advisable to contact the review division. Although the rate of guidance development is slowing down, many more guidances are being planned by the FDA. The additional burden of maintaining and updating existing guidances will be a challenge in the future.

Guidances cover a wide range of topics that focus on standards of quality, such as CMC, preclinical animal toxicology requirements, ethical standards for the conduct of clinical trials, and documentary requirements for INDs, Abbreviated New Drug Applications (ANDAs), and NDAs. Other guidances focus on the clinical phase of drug development, including biopharmaceutics, clinical pharmacology, and clinical trial design. Many of the newer guidances issued by the FDA are based on the principles of risk management in clinical pharmacology. These include guidances related to *in vitro* and *in vivo* drug metabolism–drug interaction studies, to the design and conduct of pharmacokinetic studies in special populations (renal disease, hepatic disease, and pediatrics), and to the use of clinical pharmacology tools in drug development (e.g., population pharmacokinetics, exposure response, voluntary submission of pharmacogenomics/pharmacogenetic data). All of the clinical pharmacology guidances are intended to provide sponsors with ways to streamline the drug development process, gather and analyze important information, and submit it to the FDA efficiently.

One of the most important guidances, issued by the FDA in 1998, is entitled "Providing Clinical Evidence of Effectiveness for Human Drug and Biological Products." This guidance puts forth advice and experience in drawing evidence of effectiveness from all clinical phases of drug development. In particular, it provides examples to demonstrate how exposure-response relationships may be used provide the primary evidence of efficacy in drug development. Among these examples are recommendations regarding requests for approval of new formulations and new doses or dosing regimens of approved drug products. Other noteworthy guidances include those relating to exposure response, which can be found on the FDA web site (11).

Through its guidances, the FDA also facilitates and encourages the use of emerging scientific technology and knowledge. For example, to enable scientific progress in the field of pharmacogenomics and to facilitate the use of pharmacogenomic data in informing regulatory decisions, FDA recently issued a final guidance on when pharmacogenomic data are to be submitted, the format of the data, and how the data will be used (15). This guidance states that pharmacogenomics data submission for NDAs is required if it is used to support scientific/clinical arguments or for labeling purposes. Otherwise, data submission is voluntary and will not be utilized for regulatory decision-making.

In the area of biopharmaceutics, two guidances are noteworthy because they are the culmination of a decade of public discussion of scientific principles related to the documentation of product quality. The General Bioavailability (BA) and Bioequivalence (BE) Guidance (16) statement provides guidance on the design, analysis, and utility of BA and BE studies in new and generic drug development, including the use of replicate design studies. The so-called biopharmaceutical classification system (BCS) guidance (17) offers advice on when BA and BE studies may be waived on sound scientific principles of drug absorption as it relates to the solubility and permeability of drug substances, and the dissolution of drug products (see Chapter 4). Together, these guidances, along with the Scale-Up and Post Approval Changes (SUPAC), provide a framework for the biopharmaceutical development of new and generic drug dosage forms.

In short, the FDA attempts to communicate extensively with industry via guidances and encourages and facilitates the application of new technology and science in the drug development process. Because of its unique vantage point, the FDA can work with companies, patient groups, academic researchers, and other stakeholders to coordinate, develop, and/or disseminate solutions to scientific hurdles that are impairing the efficiency of product development industry-wide. The FDA should and will take the lead in developing a national Critical Path Opportunities List to bring concrete focus to these tasks, and prepare for the challenges in drug development in the future. The ultimate value of these efforts will be reflected in the quality of the data and of the NDA and ANDA submissions provided by sponsors.

REFERENCES

1. Pharmaceutical Research and Manufacturers of America. (Internet at http://www.phrma.org.)
2. PhRMA 2005: An industrial revolution in R&D. London: PricewaterhouseCoopers; 1998. p. 11.
3. DiMasi JA, Hansen RW, Grabowski HG. The price of innovation: New estimates of drug development costs. J Health Econ 2003;22: 151–85.
4. Lindenbaum J, Mellow MH, Blackstone MO, Butler VP Jr. Variation in biologic availability of digoxin from four preparations. N Engl J Med 1971;285:1344–7.
5. Lesko LJ, Sahajwalla C. Introduction to drug development and regulatory-decision making. In: Sahajwalla CG, editor. New drug development, regulatory paradigms for clinical pharmacology and biopharmaceutics. New York: Marcel Dekker; 2004. p. 1–12.
6. MedWatch: The FDA medical products reporting program. Rockville, MD: FDA; 2005. (Internet at http://www.fda.gov/medwatch.)

7. U.S. Food and Drug Administration. (Internet at http://www.fda.cder.gov.)
8. CDER, CBER. Formal meetings with sponsors and applicants for PDUFA products. Guidance for industry, Rockville, MD: FDA; 2000. (Internet at http://www.fda.gov/cder/guidance/index.htm.)
9. CDER. Genomics at FDA, Rockville, MD: FDA; 2005. (Internet at http://www.fda.gov/cder/genomics/default.htm.)
10. Prescription Drug User Fee Act of 1992. Public Law 102-571. In the U.S. Code of Federal Regulations 21 CFR 379.106 Stat 4491; Oct 29, 1992.
11. CDER. Guidance documents. Rockville, MD: FDA; 2005. (Internet at http://www.fda.gov/cder/guidance/index.htm.)
12. Good guidance practices (Notice): The FDA's development, issuance, and use of guidance documents. Federal Register 62 FR 8961; February 17, 1977.
13. Good guidance practices (Final Rule). Federal Register 65FR182; September 29, 2000.
14. Food and Drug Cost of Administration Modernization Act of 1997. Public Law 105-115. In the U.S. Code of Federal Regulations 21 CFR 355a.111 Stat 2296, Nov 21, 1997. (Internet at http://www.fda.gov/cber/fdama.htm.)
15. CDER, CBER, CDRH. Guidance for Industry. Pharmacogenomic data submissions. Rockville, MD: FDA; 2005. (Internet at http://www.fda.gov/cder/guidance/6400fnl.htm.)
16. CDER. Guidance for Industry. Bioavailability and bioequivalence studies for orally administered drug products — general considerations. Rockville, MD: FDA; 2003. (Internet at http://www.fda.gov/cder/guidance/index.htm.)
17. CDER. Guidance for Industry. Waiver of *in vivo* bioavailability and bioequivalence studies for immediate-release solid oral dosage forms based on a biopharmaceutics classification system. Rockville, MD: FDA; 2000. (Internet at http://www.fda.gov/cder/guidance/index.htm.)

This page intentionally left blank

APPENDIX

I

Abbreviated Tables of Laplace Transforms

TABLE I.1 Table of Operations ($\mathcal{L}$)

Time domain	Laplace domain
$F(t)$	$f(s) = \int_0^\infty F(t)e^{-st}dt$
1	$1/s$
A	A/s
$F'(t)$	$s\,f(s) - F(0)$
$F''(t)$	$s^2 f(s) - s\,F(0) - F'(0)$

TABLE I.2 Table of Inverse Operations ($\mathcal{L}^{-1}$)

Laplace domain	Time domain
$\frac{1}{s}$	1
$\frac{1}{s-a}$	e^{at}
$\frac{1}{(s-a)^2}$	te^{at}
$\frac{1}{s(s-a)}$	$\frac{1}{a}\left(e^{at} - 1\right)$
$\frac{1}{(s-a)(s-b)}, \quad a \neq b$	$\frac{1}{a-b}\left(e^{at} - e^{bt}\right)$

This page intentionally left blank

APPENDIX

II

Answers to Study Problems

ARTHUR J. ATKINSON, JR.
Clinical Center, National Institutes of Health, Bethesda, Maryland

ANSWERS TO STUDY PROBLEMS — CHAPTER 2

Note how dimensional analysis has been performed by including units in the calculations.

Problem 1: Answer — E

$$V_d = \frac{\text{Dose}}{C_0} = \frac{80\,\text{mg}}{4\,\text{mg/L}} = 20\,\text{L}$$

Problem 2: Answer — A

$$V_d = 2.0\,\text{L/kg} \cdot 80\,\text{kg} = 160\,\text{L}; \qquad t_{1/2} = 3\,\text{hr}$$

Therefore,

$$CL_E = \frac{\ln 2 \cdot V_d}{t_{1/2}} = \frac{\ln 2 \cdot 160\,\text{L}}{3\,\text{hr}} = 37\,\text{L/hr}$$

and the infusion rate should be

$$I = C_{ss} \cdot CL = 4\,\text{mg/L} \cdot 37\,\text{L/hr} = 148\,\text{mg/hr}$$

$$= 2.5\,\text{mg/min}$$

Problem 3: Answer — C

The gentamicin plasma level fell to half of its previous value in the 5-hour interval between blood draws. Therefore, $t_{1/2} = 5\,\text{hr}$ and $k = \ln 2 / t_{1/2} = 0.139\,\text{hr}^{-1}$

$$CF = \frac{1}{(1 - e^{-k\tau})}$$

since $\tau = 8\,\text{hr}$.

$$CF = \frac{1}{\left(1 - e^{-1.11}\right)} = \frac{1}{0.67} = 1.49$$

therefore, the expected steady-state peak level is $1.49 \cdot 10\,\mu\text{g/mL} = 15\,\mu\text{g/mL}$

Problem 4: Answer — C

Target level of 12 μg/mL = one-half the toxic level of 24 μg/mL. Therefore, one should wait one half-life before restarting aminophylline.

$$t_{1/2} = \frac{0.693 V_d}{CL}, \qquad V_d = 60\,\text{kg} \cdot 0.45\ \text{L/kg} = 27\,\text{L}$$

$$CL = \frac{I}{C_{ss}} = \frac{\left(0.5\,\text{mg/kg} \cdot \text{hr}\right) \cdot \left(60\,\text{kg}\right)}{24\,\text{mg/L}} = 1.25\,\text{L/hr}$$

Therefore,

$$t_{1/2} = \frac{0.693 \cdot 27\,\text{L}}{1.25\,\text{L/hr}} = 15\,\text{hr}$$

Problem 5: Answer — D

It requires 3.3 half-lives to reach 90% of the eventual steady-state level:

$$3.3 \cdot 7\ \text{days} = 23\ \text{days}$$

Problem 6: Answer — B

On admission, the digoxin plasma level was 3.2 ng/mL and it fell to 2.7 ng/mL 24 hours later. Hence, the daily excretion fraction is 0.5/3.2 = 0.156 (the excretion fraction with normal renal function = 1/3). Therefore, levels can be expected to fall by 0.156 every 24 hours as follows:

Hospital day:	0	1	2	3	4
Digoxin level:	3.2 ng/mL	2.7 ng/mL	2.28 ng/mL	1.92 ng/mL	1.62 ng/mL
"More days":	—	—	1	2	3

We can see that levels can be expected to reach the 1.6-ng/mL target on the fourth hospital day, or *three more days after the level of 2.7 ng/mL was measured*.

Problem 7: Answer — E

Three half-lives are needed for plasma levels to fall from 8 μg/mL to 1 μg/mL:

Level:	8 μg/mL	→	4 μg/mL	→	2 μg/Ml	→	1 μg/mL
Half-lives:	0		1		2		3

Since the elimination-phase half-life is given as 2 hours, three half-lives would require 6 hours. However, the question asks for a dosing interval that would allow peak levels *to exceed 8 μg/mL and fall below 1 μg/mL*. The only dosing interval offered that is longer than 6 hours is 8 hours.

Problem 8: Answer — D

Since phenytoin is eliminated by Michaelis–Menten kinetics, Equation 2.6 applies:

$$\text{Dose}/\tau = \frac{V_{max}}{K_m + \overline{C}_{ss}} \cdot \overline{C}_{ss} \qquad \text{(II.1)}$$

Rearranging:

$$(\text{Dose}/\tau)K_m + (\text{Dose}/\tau)\,\overline{C}_{ss} = V_{max}\overline{C}_{ss}$$

Two simultaneous equations can be set up one for the concentration measured at each previously administered dose.

$$300\,\text{mg/day} \cdot K_m + 300\,\text{mg/day} \cdot 5\,\mu\text{g/mL} = 5\,\mu\text{g/mL} \cdot V_{max} \qquad \text{(II.2)}$$

$$600\,\text{mg/day} \cdot K_m + 600\,\text{mg/day} \cdot 30\,\mu\text{g/mL} = 30\,\mu\text{g/mL} \cdot V_{max} \qquad \text{(II.3)}$$

These can be simplified to

$$300\,\text{mg/day} \cdot K_m + 1500\,\text{mg}^2/\text{L} \cdot \text{day} = 5\,\text{mg/L} \cdot V_{max} \qquad \text{(II.4)}$$

$$600\,\text{mg/day} \cdot K_m + 18,000\,\text{mg}^2/\text{L} \cdot \text{day} = 30\,\text{mg/L} \cdot V_{max} \qquad \text{(II.5)}$$

By multiplying Equation II.2 by 2 and subtracting it from Equation II.3 we obtain:

$$15,000\,\text{mg}^2/\text{L} \cdot \text{day} = 20\,\text{mg/L} \cdot V_{max}$$

Therefore,

$$V_{max} = 750\,\text{mg/day}$$

Substituting this value for V_{max} into Equation II.4 yields

$$300\,\text{mg/day} \cdot K_m + 1500\,\text{mg}^2/\text{L} \cdot \text{day} = 5\,\text{mg/L} \cdot 750\,\text{mg/day}$$

$$300\,\text{mg/day} \cdot K_m = 2250\,\text{mg}^2/\text{L} \cdot \text{day}$$

$$K_m = 7.5\,\text{mg/L}$$

We can now substitute these parameters into Equation II.1 to estimate the dose that will provide a phenytoin level of 15 μg/mL:

$$\text{Dose}/\tau = \frac{750\,\text{mg/day}}{7.5\,\text{mg/L} + 15.0\,\text{mg/L}} \cdot 15\,\text{mg/L}$$

$$\text{Dose}/\tau = 500\,\text{mg/day}$$

ANSWERS TO STUDY PROBLEMS — CHAPTER 3

Problem 1

We are given that $CF_{obs} = 1.29$ and $\tau = 12$ hr. Since

$$k_{eff} = \frac{1}{\tau} \ln\left[\frac{CF_{obs}}{CF_{obs} - 1}\right]$$

$$k_{eff} = \frac{1}{12} \ln\left[\frac{1.29}{0.29}\right] = 0.124$$

Therefore,

$$t_{1/2eff} = \frac{\ln 2}{0.124} = 5.6\,\text{hr}$$

Problem 2

Part a

Although a number of software packages of this types are available to facilitate analysis of these types of data, most of the software requires the kineticist to provide initial estimates of parameter values. The technique of "curve peeling" is widely used for this purpose, and also provides an initial evaluation of data quality.

The first step is to graph the experimental data (●) in the semilogarithmic plot of drug concentration-vs.-time as shown in Figure II.1. Then draw a line through the terminal exponential phase and back-extrapolate it to the y-axis. Read the y-intercept (B') and half-life of this line ($\beta_{t1/2}$) from the graph. Next, as shown in Table II.1, obtain the difference (alpha values in the table) between the experimental data points lying above the back-extrapolated line and the corresponding values on the back-extrapolated line (beta values in the table).

The alpha values (○) are then plotted on the graph (Figure II.1) and are used to draw an alpha line from which the y-intercept (A') and $\alpha_{t1/2}$ are obtained. Criteria that can be used to assess data quality at this point are: (1) the number of points that lie on each of the exponential lines and (2) the scatter of the points about the alpha and beta lines.

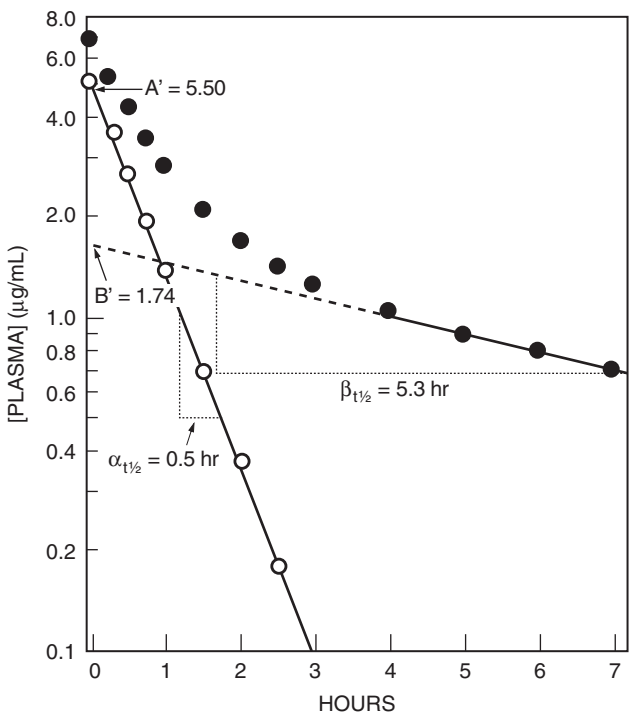

FIGURE II.1 Curve peel of the data (●) that are plotted on semilogarithmic coordinates. The points for the α-curve (○) are obtained by subtracting back-extrapolated β-curve values from the experimental data, as shown in Table II.1.

TABLE II.1 Results of Curve Peel

Time (hr)	[Plasma] (μg/mL)	Beta value (μg/mL)	Alpha value (μg/mL)
0.10	6.3	1.7	4.6
0.25	5.4	1.7	3.7
0.50	4.3	1.6	2.7
0.75	3.5	1.6	1.9
1.0	2.9	1.5	1.4
1.5	2.1	1.43	0.67
2.0	1.7	1.34	0.36
2.5	1.4	1.25	0.15

The values for α and β are obtained from their half-life estimates as follows:

$$\alpha = \frac{\ln 2}{\alpha_{t1/2}} = \frac{\ln 2}{0.5\,\text{hr}} = 1.39\,\text{hr}^{-1}$$

$$\beta = \frac{\ln 2}{\beta_{t1/2}} = \frac{\ln 2}{5.3\,\text{hr}} = 0.131\,\text{hr}^{-1}$$

Please note: Although it might seem easier to calculate α and β directly from the graph as slopes, this is complicated by the fact that this semilogarithmic graph paper uses a $\log_{10}$ scale rather than a natural log scale on the y-axis. A simple way to circumvent this difficulty is to calculate the values of α and β from their respective half-lives.

The intercept values of $A' = 5.50$ μg/mL and $B' = 1.74$ μg/mL are normalized as follows:

$$A = \frac{A'}{A' + B'} = \frac{5.50}{5.50 + 1.74} = 0.76$$

$$B = \frac{B'}{A' + B'} = \frac{1.74}{5.50 + 1.74} = 0.24$$

As shown here, normalization is a technique for converting the sum of A and B to 1 and is required because we have stipulated that the administered dose is 1 in our derivation of the equations for calculating the model parameters.

Part b

From Equation 3.11:

$$k_{01} = \frac{1}{A/\alpha + B/\beta} = \frac{1}{\frac{0.76}{1.39} + \frac{0.24}{0.131}} = 0.42\,\text{hr}^{-1}$$

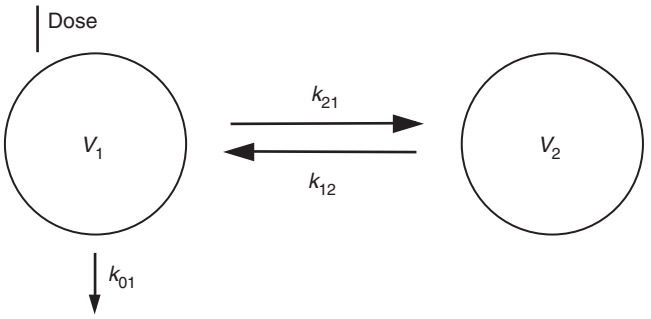

FIGURE II.2 Diagram of the two-compartment model used to analyze the experimental data.

From Equation 3.14:

$$k_{12} = \beta A + \alpha\beta = (0.131)(0.76) + (1.39)(0.24)$$
$$= 0.43\,\text{hr}^{-1}$$

From Equation 3.15:

$$k_{21} = \frac{AB(\alpha - \beta)^2}{k_{12}} = \frac{(0.76)(0.24)(1.39 - 0.13)^2}{0.43}$$
$$= 0.67\,\text{hr}^{-1}$$

Part c

$$V_1 = \frac{\text{Dose}}{A' + B'} = \frac{100\,\text{mg}}{(5.50 + 1.74)\,\text{mg/L}} = 13.8\,\text{L}$$

The elimination clearance is

$$CL_E = k_{01} \cdot V_1 = (0.42\,\text{hr}^{-1})(13.8\,\text{L}) = 5.8\,\text{L/hr}$$

Similarly,

$$CL_I = k_{21} \cdot V_1 = (0.67\,\text{hr}^{-1})(13.8\,\text{L}) = 9.25\,\text{L/hr}$$

Part d

$$V_2 = \frac{CL_I}{k_{12}} = \frac{9.25\,\text{L/hr}}{0.43\,\text{hr}^{-1}} = 21.5\,\text{L}$$

$$V_{d(SS)} = V_1 + V_2 = 13.8\,\text{L} + 21.5\,\text{L} = 35.3\,\text{L}$$

Compare this value with

$$V_{d(area)} = \frac{CL_E \cdot t_{1/2\beta}}{\ln 2} = \frac{5.8\,\text{L/hr} \cdot 5.3\,\text{hr}}{\ln 2} = 44\,\text{L}$$

and

$$V_{d(extrap)} = \frac{\text{Dose}}{B'} = \frac{100\,\text{mg}}{1.74\,\text{mg/L}} = 57.5\,\text{L}$$

The reason that $V_{d(ss)}$ is smaller than either of these two estimates is that neither the half-life equation used to calculate $V_{d(area)}$ nor the single-compartment model implied in calculating $V_{d(extrap)}$ makes any provision for the contribution of intercompartmental clearance to the prolongation of the elimination-phase half-life. Therefore, these estimates must compensate for this by increasing the estimate of distribution volume, which in these approaches is the only way that half-life can be prolonged without affecting elimination clearance.

ANSWERS TO STUDY PROBLEMS — CHAPTER 4

Problem 1

*AUC **after a Single Intravenous Drug Dose***

We have shown that after a single drug dose,

$$F \cdot D = CL \cdot AUC$$

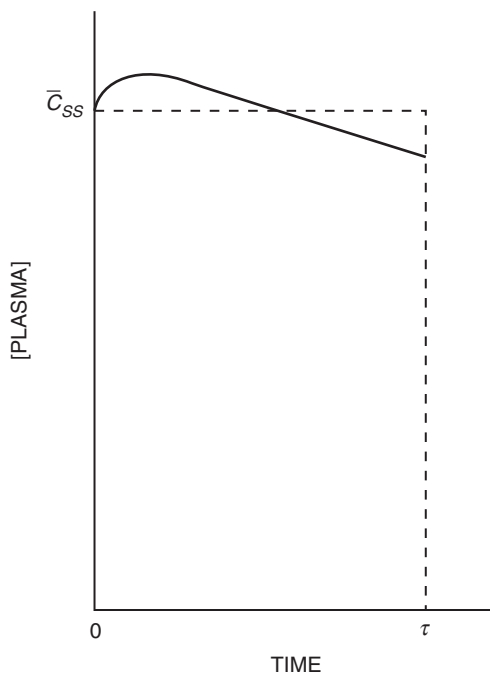

FIGURE II.3 Diagram of a plasma level-vs-time curve during a dosing interval at steady state. $\overline{C}_{ss}$ is the average plasma concentration during the dosing interval τ. $AUC_{0\to\tau}$ is equal to the area given by the product $\overline{C}_{ss} \cdot \tau$.

When the dose is administered intravenously it is completely absorbed, so $F = 1$, and

$$AUC_{IV} = \frac{D_{IV}}{CL}$$

$AUC_{0\rightarrow\tau}$ after an Oral Dose at Steady State

The mean steady-state concentration ($\overline{C}_{ss}$) with oral dosing is

$$\overline{C}_{ss} = \frac{F \cdot D_{oral}/\tau}{CL}$$

where the dose (D_{oral}) divided by the dosing interval (τ) is the dosing rate. As shown in Figure II.3, the area under the plasma-level-vs.-time curve during a steady-state dosing interval is equivalent to the area of a rectangle whose height equals $\overline{C}_{ss}$ and whose base equals τ. In other words,

$$AUC_{0\rightarrow\tau\,(oral)} = \overline{C}_{ss} \cdot \tau$$

Substituting for $\overline{C}_{ss}$,

$$AUC_{0\rightarrow\tau\,(oral)} = \frac{F \cdot D_{oral}/\tau}{CL} \cdot \tau = \frac{F \cdot D_{oral}}{CL}$$

Therefore, it can be seen by inspection that

$$\frac{AUC_{0\rightarrow\tau\,(oral)}}{D_{oral}} = F \cdot \frac{AUC_{IV}}{D_{IV}}$$

and that the extent of absorption of the oral dose formulation is

$$\%\ \text{Absorption} = \frac{D_{IV} \cdot AUC_{0\rightarrow\tau\,(oral)}}{D_{oral} \cdot AUC_{IV}} \times 100$$

Problem 2

We are asked to obtain *X(t)* from the convolution of *G(t)* and the disposition function *H(t)*, where the input function *G(t)* is a constant intravenous drug infusion:

$$X(t) = G(t) * H(t)$$

Since the operation of convolution in the time domain corresponds to multiplication in the domain of the subsidiary algebraic equation given by Laplace transformation, we can write the subsidiary equation as

$$x(s) = g(s) \cdot h(s)$$

The intravenous infusion provides a constant rate of drug appearance in plasma (I), so

$$G(t) = I$$

Since $\mathcal{L}\,1 = 1/s$

$$g(s) = \frac{I}{s}$$

We have shown previously (see Chapter 4, derivation of Equation 4.3) that the Laplace transform of the disposition function is

$$h(s) = \frac{1}{s+k}$$

Therefore, the subsidiary equation for the output function is

$$x(s) = \frac{I}{s} \cdot \frac{1}{s+k}$$

and $\mathcal{L}^{-1}\,x(s)$ is

$$X(t) = \frac{I}{k}\left(1 - e^{-kt}\right)$$

Problem 3

Part a

From the equation derived above for *X(t)*, we see that steady state is only reached when $t = 8$. At infinite time

$$X_{\infty} = I/k$$

Since $C_{ss} = X_{\infty}/V_d$ and $k = CL_E/V_d$,

$$C_{ss} = I/CL_E$$

Note that this is Equation 2.2 that we presented in Chapter 2. In the problem that we are given, I = 2 mg/min, and $V_{d(area)}$ = 1.9 L/kg · 70 *kg* = 133 *L*.

Therefore,

$$CL_E = \frac{\ln 2 \cdot V_{d(area)}}{t_{1/2}} = \frac{0.693 \cdot 133\ \text{L}}{90\ \text{min}} = 1.02\ \text{L/min}$$

and

$$C_{ss} = \frac{2\ \text{mg/min}}{1.02\ \text{L/min}} = 2.0\ \mu\text{g/mL}$$

Note: Many nurses who work in cardiac intensive care units know that the expected steady-state lidocaine level in μg/mL simply equals the infusion rate in mg/min (usual therapeutic range: 2–5 μg/mL). Somewhat higher levels occur in patients with congestive heart failure or severe hepatic dysfunction.

Part b

Since

$$X(t) = \frac{I}{k}\left(1 - e^{-kt}\right)$$

when $t = \infty$,

$$X_\infty = \frac{I}{k}$$

Therefore, for any fraction of the eventual steady state,

$$X(t)/X_\infty = \left(1 - e^{-kt}\right)$$

When 90% of the eventual steady-state level is reached,

$$0.90 = \left(1 - e^{-kt_{0.90}}\right)$$

$$e^{-kt_{0.90}} = 0.10$$

$$kt_{0.90} = \ln 10 = 2.30$$

Since

$$k = \frac{\ln 2}{90\ \text{min}} = 0.0077\ \text{min}^{-1}$$

it follows that

$$t_{0.90} = \frac{2.30}{0.0077\ \text{min}^{-1}} = 299\ \text{min}$$

Note: Because it takes so long for an infusion to provide stable therapeutic drug concentrations, lidocaine therapy of life-threatening cardiac arrhythmias is usually begun by administering an intravenous loading dose together with an infusion.

Part c

Since $t_{1/2} = 90$ minutes, this corresponds to 3.3 half-lives. *Note:* This result for a continuous intravenous infusion is equivalent to Equation 2.17 (Chapter 2) that was derived for intermittent dosing.

ANSWER TO STUDY PROBLEMS — CHAPTER 5

Part a

$t_{1/2} = 6.2$ hr; $CL_E = 233$ mL/min $= 14.0$ L/hr; % renal excretion = 85.5%

$$CL_R = 0.855 CL_E = 12.0\ \text{L/hr}$$

$$CL_{NR} = 0.145 CL_E = 2.03\ \text{L/hr}$$

$$V_{d(area)} = \frac{CL_E \cdot t_{1/2}}{\ln 2} = \frac{(14.0\ \text{L/hr})\,(6.2\ \text{hr})}{\ln 2} = 125\ \text{L}$$

Therefore, if CL_{NR} is unchanged in functionally anephric patients, the expected elimination-phase half-life would be

$$t_{1/2} = \frac{(\ln 2)\ V_{d(area)}}{CL_{NR}} = \frac{(\ln 2)(125\ \text{L})}{2.03\ \text{L/hr}} = 42.7\ \text{hr}$$

Note: The mean elimination half-life measured in six functionally anephric patients was 41.9 hours (Stec GP, Atkinson AJ Jr, Nevin MJ, Thenot J-P, Ruo TI, Gibson TP, Ivanovich P, del Greco F. *N*-Acetylprocainamide pharmacokinetics in functionally anephric patients before and after perturbation by hemodialysis. Clin Pharmacol Ther 1979;26:618–28).

Part b

From Figure II.4, when $CL_{CR} = 50$ mL/min, expected $CL_E = 8.0$ L/hr.

By direct calculation, when $CL_{CR} = 50$ mL/min,

$$CL_R = (50/100)\,(12\ \text{L/hr}) = 6.0\ \text{L/hr}$$

Since $CL_{NR} = 2.0$ L/hr,

$$CL_E = CL_R + CL_{NR} = 8.0\ \text{L/hr}$$

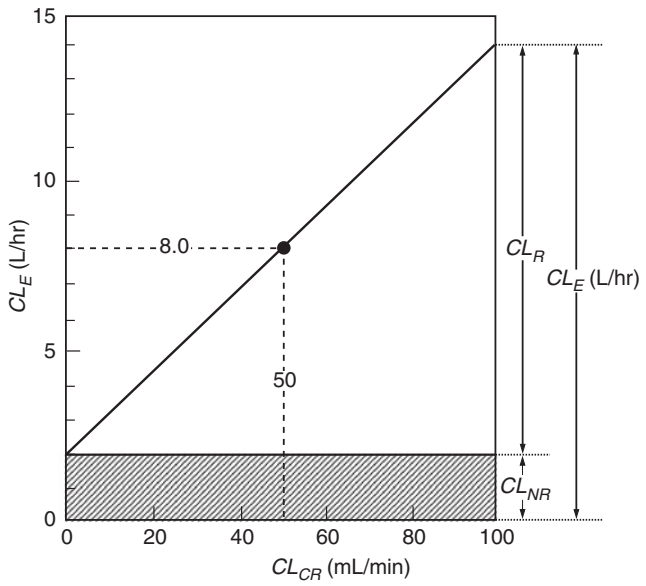

FIGURE II.4 Nomogram for estimating *N*-acetylprocainamide elimination clearance in patients with impaired renal function. The hypothetical patient described in Part b of the problem has a creatinine clearance of 50 mL/min and would be expected to have an *N*-acetylprocainamide elimination clearance of 8.0 L/hr.

Part c

The 8-hour dosing interval is maintained.

$$\text{Adjusted dose} = (8/14)(1\,\text{g}) = 0.57\,\text{g}$$

This would reduce fluctuation between peak and trough levels but would be awkward if only 0.5-g tablets were available.

Part d

The 1-g dose is maintained and the interval is adjusted. The usual 8-hour interval corresponds to 8 hr/6.2 hr = 1.3 half-lives when renal function is normal.

Expected half-life when $CL_{CR} = 50$ mL/min:

$$t_{1/2} = \frac{(\ln 2)\, V_{d(area)}}{CL_E} = \frac{(\ln 2)(125\,\text{L})}{8.0\,\text{L/hr}} = 10.8\,\text{hr}$$

$$\text{Adjusted dose interval} = (1.3)(10.8\,\text{hr}) = 14\,\text{hr}$$

In practice, a 12-hour dose interval would be selected to increase patient convenience.

This page intentionally left blank

Index

NOTE: The italicized *t* or *f* following a page number indicates a table or figure will be found on that page, respectively. Multiple tables or figures on a page will be indicated by *tt* or *ff*, respectively.

This page intentionally left blank